A WELL PERFORMANCE STUDY OF EAGLE FORD SHALE GAS WELLS INTEGRATING EMPIRICAL TIME-RATE AND ANALYTICAL TIME-RATE-PRESSURE ANALYSIS

A Thesis

by

AVERY SUTTON DAVIS

Submitted to the Office of Graduate and Professional Studies of
Texas A&M University
in partial fulfillment of the requirements for the degree of

MASTER OF SCIENCE

Chair of Committee,	Thomas A. Blasingame
Co-Chair of Committee,	Peter P. Valkó
Committee Member,	Francisco Olivera
Head of Department,	A. Daniel Hill

August 2015

Major Subject: Petroleum Engineering

ABSTRACT

In this work, our purpose is to create a "performance-based reservoir characterization" using production data (measured rates and pressures) from a selected gas condensate region within the Eagle Ford Shale (S. Texas). We use modern time-rate ("decline curve") analysis and time-rate-pressure ("model-based") analysis methods to analyze/interpret/diagnose gas condensate well production data. We estimate reservoir and completion properties — specifically: formation permeability, fracture-face skin effect, fracture half-length, and fracture conductivity. We correlate these results with known completion variables — specifically: completed lateral length, total proppant, total water used, and type of hydraulic fracturing fluid. We use the time-rate and time-rate-pressure analyses to forecast future production and to estimate ultimate recovery. Finally, we apply pressure transient analysis methods to those cases where the production history contains shut-in periods of sufficient duration to provide resolution in the pressure build-up data to identify reservoir features and qualitatively validate completion effectiveness. It is noted that ONLY surface pressures are available for the wells considered in this study.

We utilize industry-standard software to perform single well rate-time "decline curve" analyses. The traditional "modified-hyperbolic" time-rate model was used as the "basis" relation and the "power-law exponential" time-rate model was used as a check/validation (the power-law exponential model tends to be a more conservative relation for generating forecasts and estimating ultimate recovery). We also utilize industry-standard software to perform single well time-rate-pressure "model-based" analyses --- this methodology is also known as Rate Transient Analysis (RTA). In this work we used the full analytical model for the performance of a Multi-Fracture Horizontal Well (as opposed to a proxy or numerical model). We use Microsoft Excel and a commercial statistical software package to correlate the production analysis results with the measured completion parameters to create "design" relations for well completions — specifically correlations of estimated ultimate recovery with completion variables (completed lateral length, total proppant, total water used, and type of hydraulic fracturing fluid). Finally, we utilize industry-standard software to perform pressure transient analysis on the cases where the quality and relevance of the shut-in pressure data warranted such analyses.

In this work, we "cross-validate" the estimated ultimate recovery results by comparison of the time-rate and time-rate-pressure analysis results. The correlation of EUR with completion variables, we propose, is shown to be statistically relevant for almost all combinations of variables, and the correlation relation should be applicable for creating completion designs. The analysis of surface-derived pressure transient data is successfully demonstrated for several cases taken from the gas condensate region of the Eagle Ford Shale (S. Texas). The work we perform in this thesis clearly demonstrates the validity of using empirical (time-rate) and analytical (time-rate-pressure) analysis methods for the purpose of characterizing well performance for wells in the gas condensate region of the Eagle Ford Shale (S. Texas).

DEDICATION

This work is dedicated to my wife and daughter who have selflessly loved and supported me throughout my graduate studies and thesis research.

ACKNOWLEDGEMENTS

I would like to thank my committee chair, Dr. Thomas A. Blasingame, for his guidance and support throughout the course of this research; and to Dr. Peter P. Valkó and Dr. Francisco Olivera for their support and service as committee members.

Thanks also go to my family and friends for their encouragement, as well as to my wife for her patience, love and support during my graduate studies.

TABLE OF CONTENTS

Page

LIST OF FIGURES

FIGURE Page

FIGURE Page

FIGURE Page

FIGURE Page

FIGURE Page

FIGURE Page

FIGURE Page

FIGURE Page

FIGURE Page

LIST OF TABLES

CHAPTER I

INTRODUCTION

1.1 Statement of the Problem

Conventional time-rate relations, or decline curve analysis, were first summarized by Arps (1945). The use of the Arps "decline curves" has become a common tool for forecasting well production and estimating reserves in the oil and gas industry. Arps presented the exponential and hyperbolic production rate decline curves assuming the loss-ratio function proposed by Johnson and Bollens (1927), Eq. 1.1, and the loss-ratio derivative function, Eq. 1.2, to be constant and then solving both equations for the flowrate, $q(t)$, term.

$$\frac{1}{D(t)} = -\frac{q(t)}{dq(t)/dt} \qquad \text{(loss-ratio)} \quad (1.1)$$

$$b(t) = \frac{d}{dt}\left[\frac{1}{D(t)}\right] = -\frac{d}{dt}\left[\frac{q(t)}{dq(t)/dt}\right] \qquad \text{(loss-ratio derivative)} \quad (1.2)$$

Eq. 1.3 and Eq. 1.4 give the resulting exponential and hyperbolic rate decline relations, respectfully. The Arps time-rate relations are empirical in nature and applicable for oil and gas wells under constant operating conditions *during boundary-dominated flow*. In addition, Arps stated that the loss-ratio derivative parameter, $b(t)$, should range strictly between values of zero and one.

$$q(t) = q_i \exp[-D_i t] \qquad \text{(exponential decline relation)} \quad (1.3)$$

$$q(t) = \frac{q_i}{(1+bD_i t)^{1/b}} \qquad \text{(hyperbolic decline relation)} \quad (1.4)$$

Another diagnostic function is the constant flowing pressure β-derivative function developed by Blasingame et al. (2007). The β-derivative function multiplies the decline parameter, $D(t)$, by the production time as shown in Eq. 1.5.

$$\beta(t) = tD(t) = -\frac{t}{q(t)}\left[\frac{dq(t)}{dt}\right] \quad (1.5)$$

Idorenyin et al. (2011) discuss the diagnostic value the β-derivative function possesses in identifying the flow regime(s) and wellbore storage for a well. A summary of β-derivative values for different types of flow regimes is shown in **Table 1.1**.

Table 1.1 — β-derivative values for different flow regimes (Idorenyin et al., 2011)

Flow Regime	Flow Equation*	β-Derivative
Linear Flow	$p_D = \sqrt{\pi t_{Dx_f}}$	$\frac{1}{2}$
Bilinear Flow	$p_D = \frac{2.541}{\sqrt{F_{CD}}} t_{Dx_f}{}^{1/4}$	$\frac{1}{4}$
Infinite Acting Radial Flow	$p_D = \frac{1}{2}\ln t_D + 0.80908$	NA
Pseudo-Steady-State Flow	$p_D = 2\pi t_{DA} + \ln r_{eD} - \frac{3}{4}$	1
Steady State Flow	$p_D = \ln r_{eD}$	0
Wellbore Storage	$p_D = \frac{t_D}{C_D}$	1

* The equations shown here are for constant-rate oil flow; the equivalent equations for gas, written in terms of pseudopressure, have the same β-derivative values.

Within the last decade, the trend in onshore exploration and development has been in unconventional (low/ultra-low permeability) tight sand or shale reservoirs. The wells producing from these unconventional reservoirs exhibit extended periods of transient flow due to the low permeability nature of the reservoir rock. The extended transient flow behavior is a direct violation of the Arps decline curve assumption of boundary-dominated flow, and leads to significant over-estimation of reserves when using the model (Rushing et al., 2007). Therefore, development in unconventional reservoirs, such as the Eagle Ford Shale, has required the industry to recalibrate the methodology used to evaluate oil and gas production data for reserves estimates.

In this work, we develop a systematic production analysis workflow, as seen in **Figure 1.1**, for the diagnosis, analysis and interpretation of shale gas well production data. The data required for the completion of the proposed methodology are:

- Well History Files
- Daily Rate and Flowing Pressure Measurements
- Lab PVT and Fluid Analysis Reports

We use the diagnostic plots listed below to identify potential errors in the production data and abnormalities observed in the production history plot, as well as to verify the correlation between gas flowrate and calculated flowing bottomhole pressure data:

- Rate-Pressure-Time Plot [Semi-log] — $\log(q_g)$ and p_{wf} vs. t
- Productivity Index – Time Plot [Semi-log] — $\log(q_g/\Delta m(p))$ vs. t
- Productivity Index – Time Plot [Log-log] — $\log(q_g/\Delta m(p))$ vs. $\log(t)$
- Rate-Cumulative Production – Time Plot [Log-log] — $\log(q_g)$ and $\log(G_p)$ vs. $\log(t)$
- Pressure-Rate Correlation Plot [Cartesian] — p_{wf} vs. q_g
- Rate-Pressure-Cumulative Production Plot [Semi-log] — $\log(q_g)$ and p_{wf} vs. G_p

In addition to checking the integrity and correlation of production data, we also use the following diagnostic plots to establish the reservoir model and flow regimes:

- "Log-Log" Plot [Log-log] — $\log(\Delta m(p)/q_g)$ and $\log(\Delta m(p)/q_g)_{id}$ vs. $\log(G_p/q_g)$
- Blasingame Plot [Log-log] — $\log(q_g/\Delta m(p))$, $\log(q_g/\Delta m(p))_i$ and $\log(q_g/\Delta m(p))_{id}$ vs. $\log(G_p/q_g)$
- *PI* – Normalized G_p Plot [Log-log] — $\log(q_g/\Delta m(p))$ vs. $\log(G_p/\Delta m(p))$

As comment, for the diagnostic plots described above, an incorrect estimate of the initial reservoir pressure will yield plots that show skewed trends, and/or "clumping" or scattering of data points, particularly at early production times.

Based on the information gathered from the diagnostic plots and well history files, we then proceed to filter non-representative production data points that are likely the result of non-reservoir effects or operational changes such as well cleanup effects, liquid loading, well recompletions, well workovers, and/or choke changes.

We prepare the diagnostic plots listed below using the filtered production data to identify the flow regime(s) experienced by a given well. It is of primary importance to recognize if the well is still in transient flow or has already entered boundary-dominated flow, because it allows us to determine which of the time-rate relation models is appropriate for the given production data:

- $q\beta Db$ – Time Plot [Log-log] — $\log(q_g)$, $\log(b)$, $\log(D)$ and $\log(\beta)$ vs. $\log(t)$
- Inverse Rate – *MBT* Plot [Log-log] — $\log(1/q_g)$ vs. $\log(G_p/q_g)$
- Inverse PI – $\sqrt{t}$ Plot [Semi-log] — $\log(\Delta m(p)/q_g)$ vs. $\sqrt{t}$
- Time Plot [Semi-log] — $\log(\Delta m(p)/q_g)$ and $\log(\Delta m(p)/q_g)_d$ vs. $\log(t)$
- "Log-Log" Plot [Log-log] — $\log(\Delta m(p)/q_g)$ and $\log(\Delta m(p)/q_g)_{id}$ vs. $\log(G_p/q_g)$
- Blasingame Plot [Log-log] — $\log(q_g/\Delta m(p))$, $\log(q_g/\Delta m(p))_i$ and $\log(q_g/\Delta m(p))_{id}$ vs. $\log(G_p/q_g)$
- PI – G_p Plot [Log-log] — $\log(q_g/\Delta m(p))$ vs. $\log(G_p/\Delta m(p))$

The models/techniques given below can be used for the direct estimation of reserves:

- Modified Hyperbolic and Power-Law Exponential Time-Rate Relations: (*time-rate* data)
  - Arps Modified Hyperbolic Rate Relation (Robertson, 1988)
  - Power-Law Exponential Rate Relation (Ilk et al., 2008)
- Flowing Material Balance Techniques for Boundary-Dominated Flow: (*time-rate-pressure* data)
  - Agarwal-Gardner (Agarwal et al., 1998)
  - Flowing $\bar{p}/z$ (Mattar and McNeil, 1998)

We have elected to focus on the modified hyperbolic and power-law exponential relations as our primary "time-rate" analysis relations as these provide reasonable estimates when properly calibrated. Both relations have some constraining (or terminal) decline mechanism. For the modified hyperbolic an "exponential tail" is "spliced" to the typical Arps hyperbolic relation. For the power-law exponential relation there is also an a terminal exponential decline component (but this term is often not used as the form of the "power-law" (time) term has an implicit terminal decline as well). For reference, of the two methods, the power-law exponential is almost always the more conservative reserves estimator.

The so-called "flowing material balance" methods (Agarwal et al. and Mattar and McNeil) utilize a combination of the gas material balance relation and the boundary-dominated flow relation for gas flow — which implicitly require that pseudosteady-state/boundary-dominated flow behavior exists for these

relations to be valid. There are a few software implementations of these relations in the industry, and care must be exercised when using these methods for unconventional reservoirs. Utilizing the latest performance data it is possible to use the "flowing material balance" methods to establish a "minimum" reservoir volume, but this can be (and often) is quite arbitrary. Strong caution is urged if/when "flowing material balance" methods are applied to unconventional oil or gas reservoirs.

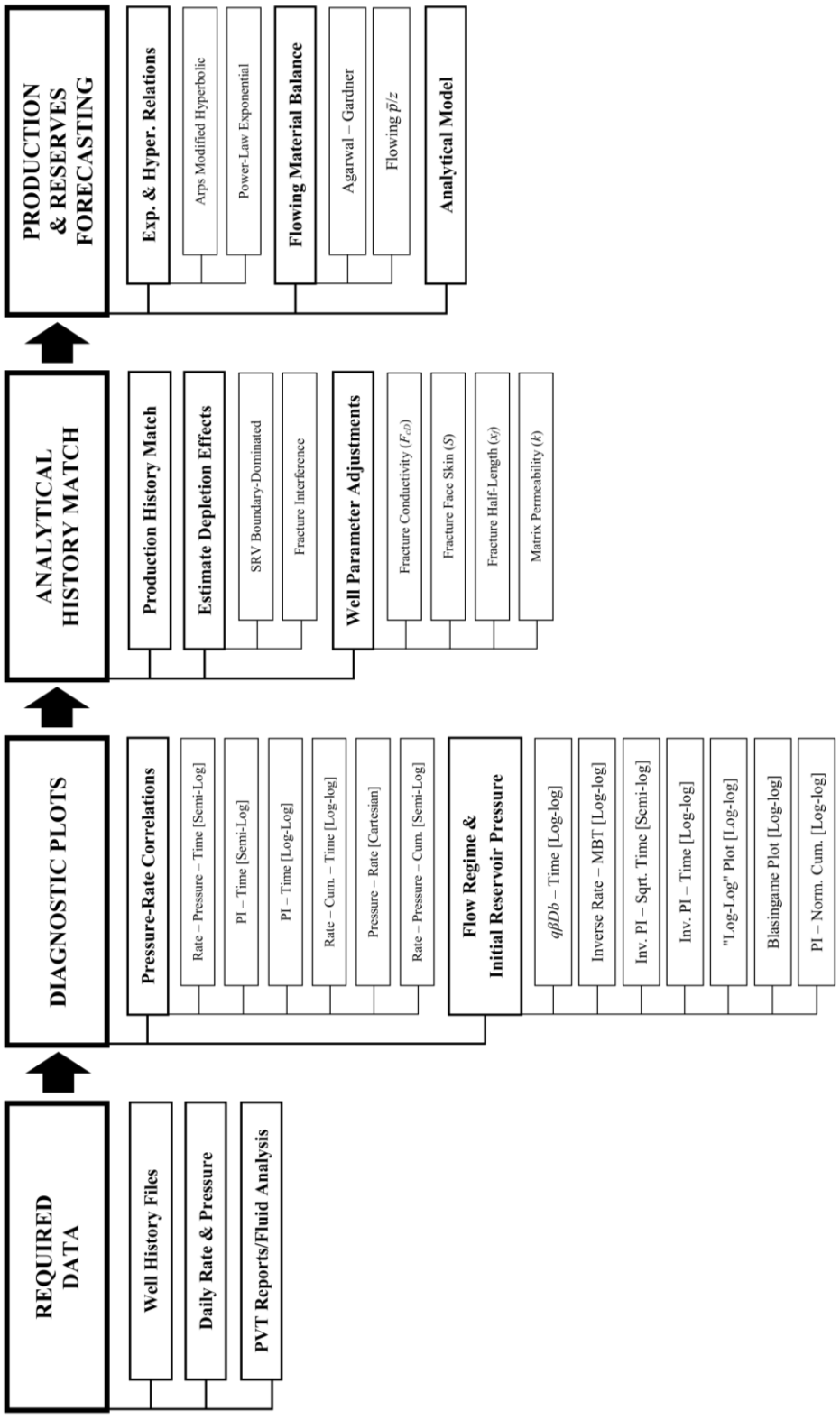

Figure 1.1 — (Diagram): Proposed production analysis workflow.

1.2 Objectives

The objectives of this work are to:

- *Provide* a production analysis workflow that consists of production data diagnostics, empirical time-rate relations and analytical time-rate-pressure model-based production analysis to estimate reserves and reservoir properties in shale gas reservoirs.
- *Demonstrate* the applicability of the proposed workflow by applying this workflow to field production data obtained from thirty Eagle Ford Shale gas wells.
- *Compare* the reserves estimates generated by the time-rate-pressure analytical models to those of the time-rate relation models utilizing the pre-analysis diagnostics and production data editing.
- *Develop* a regression model to predict the 30-year estimated cumulative production volume for a given well based on hydraulic fracture completion design parameters.

1.3 Validation and Application of Study — Field Example 1

In this section, we demonstrate the proposed production analysis workflow by applying this workflow to the following shale gas well field example. We also apply the proposed workflow to twenty-nine (29) additional field examples cases with the results included in **Appendix C**.

In this case, we consider a field dataset for a multiple, hydraulically fractured horizontal shale gas well. The well has been producing for approximately two years, and the gas flowrate and calculated flowing bottomhole pressure data are shown in **Figure 1.2**. We review the flowrate and pressure history for instances of shut-in periods, evidence of liquid loading, or obvious surface operational changes. We observe no major shut-in periods, but do see varied flowrate and pressure data after approximately 400 days of production.

In addition, if boundary-dominated flow is established as the current flow regime for the well, then the plot identifies the nature of the gas flowrate decline. During boundary-dominated flow, a linearly declining production rate represents exponential decline, and any upward concavity signifies either a hyperbolic or harmonic decline. In **Figure 1.2**, we observe a slight upward concavity in the gas flowrate, therefore, if the well is determined to be in boundary-dominated flow, then we can conclude that the well is likely experiencing a hyperbolic, rather than exponential decline.

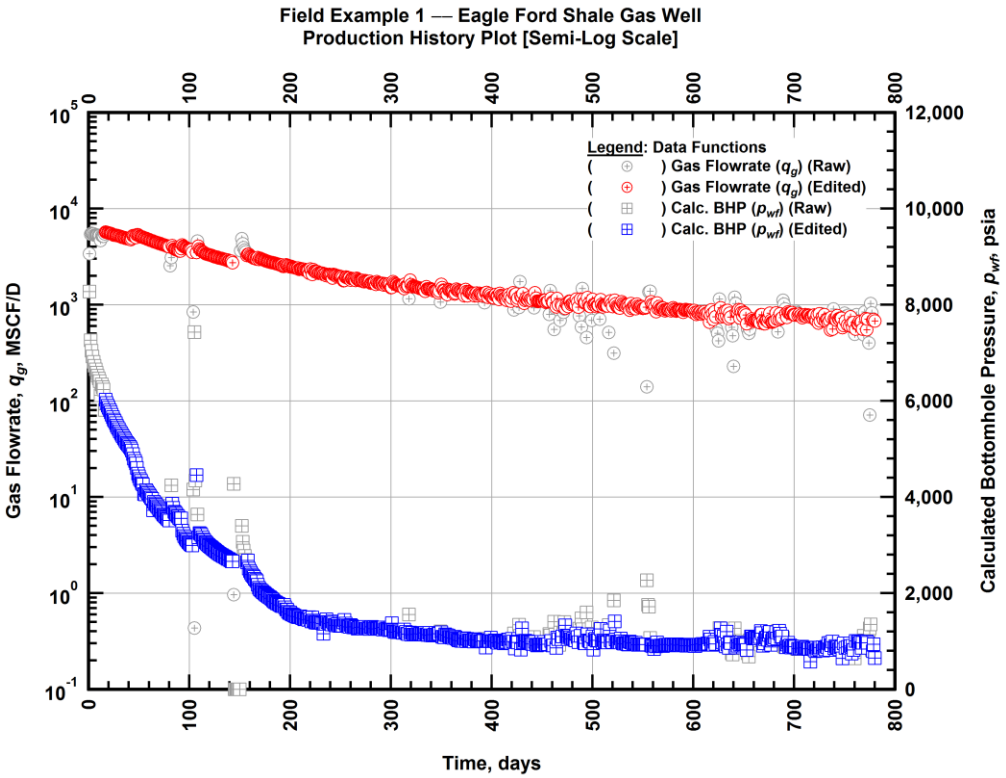

Figure 1.2 — (Semi-log Plot): Filtered production history plot — flowrate (q_g) and calculated bottomhole pressure (p_{wf}) versus production time.

In **Figure 1.3**, we plot the pseudopressure drop-normalized rate (or *productivity index*) for this well versus production time. The scatter present in the pseudopressure drop-normalized rate plot correlates directly to the scatter present in the gas flowrate values. As seen in the figure below, we filter the same data points as the production history plot, **Figure 1.2**, thus removing the data points affected by the initial well cleanup, the data points directly following the shut-in of the well, as well as the data points showing the operational scatter present in the data after approximately 400 days of production.

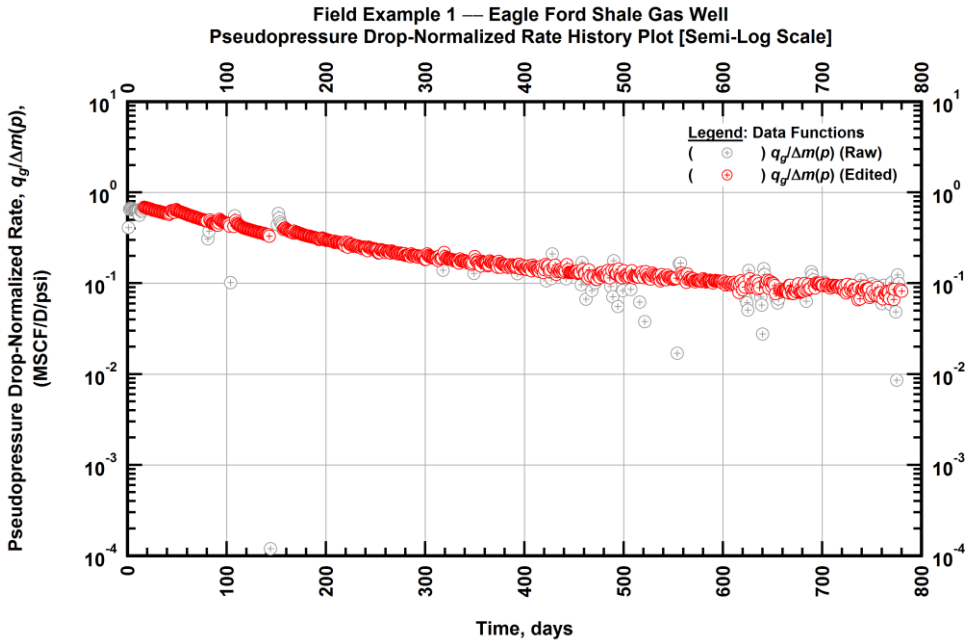

Figure 1.3 — (Semi-log Plot): Filtered normalized rate production history plot — pseudopressure drop-normalized gas flowrate ($q_g/\Delta m(p)$) versus production time.

In **Figure 1.4**, we prepare a log-log plot of pseudopressure drop-normalized gas flowrate versus production time. Diagnostically, this plot is one of several plots that help us identify the flow regimes encountered by the well. We overlay the flow regime lines, described below, on the data plotted in **Figure 1.4** to aid in the flow regime determination (Houzé et al., 2012):

- A line with a negative quarter-slope suggests a bi-linear flow regime.
- A line with a negative half-slope suggests a linear flow regime.
- A line with a negative unit-slope suggests a depletion, or boundary-dominated flow regime.

Theoretically, a well early in its production history will produce from a linear or bi-linear flow regime, then after a period of time, the well will progress into a transitional flow period, before finally entering depletion or boundary-dominated flow.

When reviewing **Figure 1.4**, we recognize from the shape of the data that the early production data shows the presence of linear flow before entering into what appears to be a depletion or boundary-dominated flow regime.

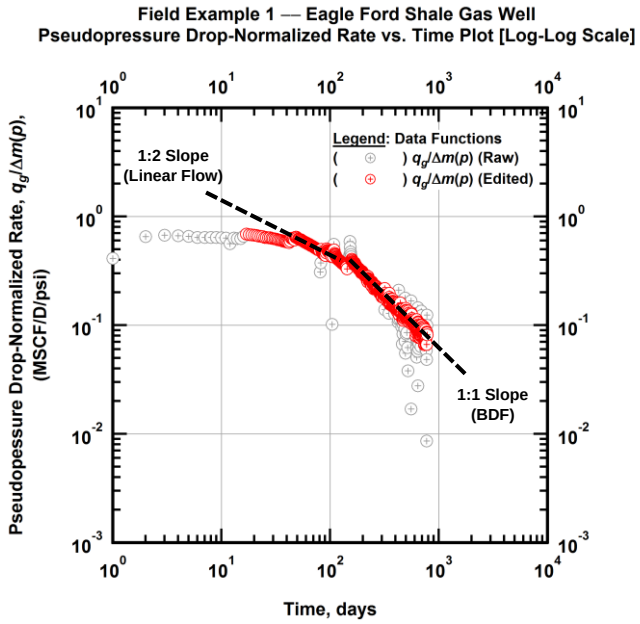

Figure 1.4 — (Log-log Plot): Filtered normalized rate production history plot — pseudopressure drop-normalized gas flowrate ($q_g/\Delta m(p)$) versus production time.

In **Figure 1.5**, we concurrently plot the gas flowrate and cumulative gas production for the known producing life of the well. In this plot, we look for sharp or drastic changes in the slopes of both sets of data, which is generally symptomatic of a mechanical or surface operations change (*not* a reservoir effect). Although not drastic, we observe a slope change in the cumulative gas production at approximately 150 days into the production of the well. We also see the same negative half-slope and unit-slope lines in the production history as **Figure 1.4**, which implies linear and boundary-dominated flow regimes, respectfully.

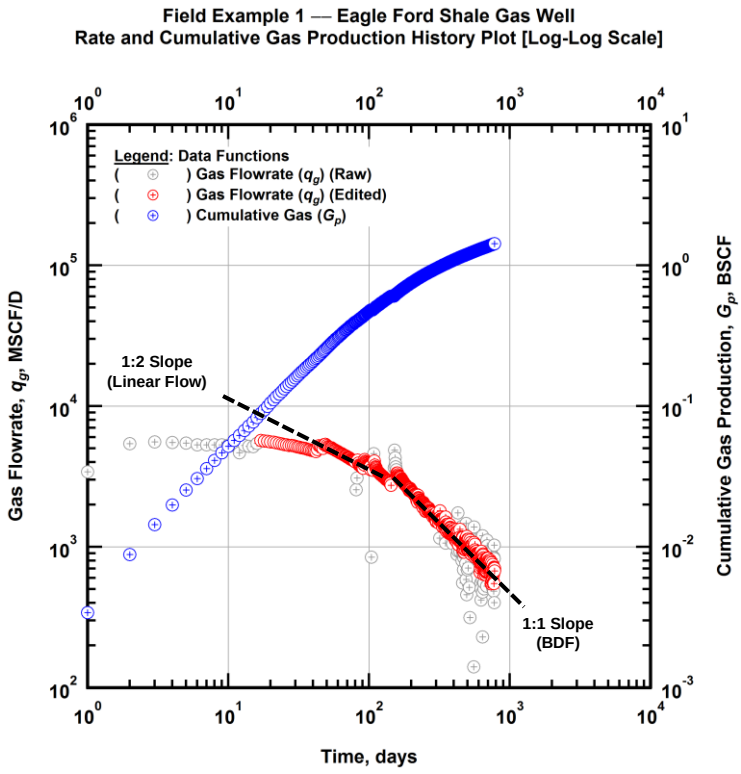

Figure 1.5 — (Log-log Plot): Filtered rate and unfiltered cumulative gas production history plot — flowrate (q_g) and cumulative production (G_p) versus production time.

In **Figure 1.6**, we plot the (filtered) calculated flowing bottomhole pressure data against the (filtered) gas flowrate, which provides a direct correlation between flowrate and pressure for the well (Kabir and Izgec, 2006). The figure shows three distinct areas of interest for the data correlation. First, we observe high rate and pressure data points are likely the result of well cleanup effects and initial production operational adjustments. Therefore, we filter these points as these data are not representative of reservoir performance for this well.

Second, we observe several similarly sloped, correlated transient responses, which imply similar decline trends and operational conditions. The discontinuity seen with the last transient response, as well as its change in slope are indicative of modified surface production operations and a possible change in flow regime. Third, the lower rates and pressures do not display a definitive correlation and suggest inaccurate data acquisition or the presence of liquid loading. We filter the same data points as the production history

plot (**Figure 1.2**) thus, we generally filter from our analysis any of the scattered or non-correlating gas flowrate and pressure data points, as seen in **Figure 1.6** below.

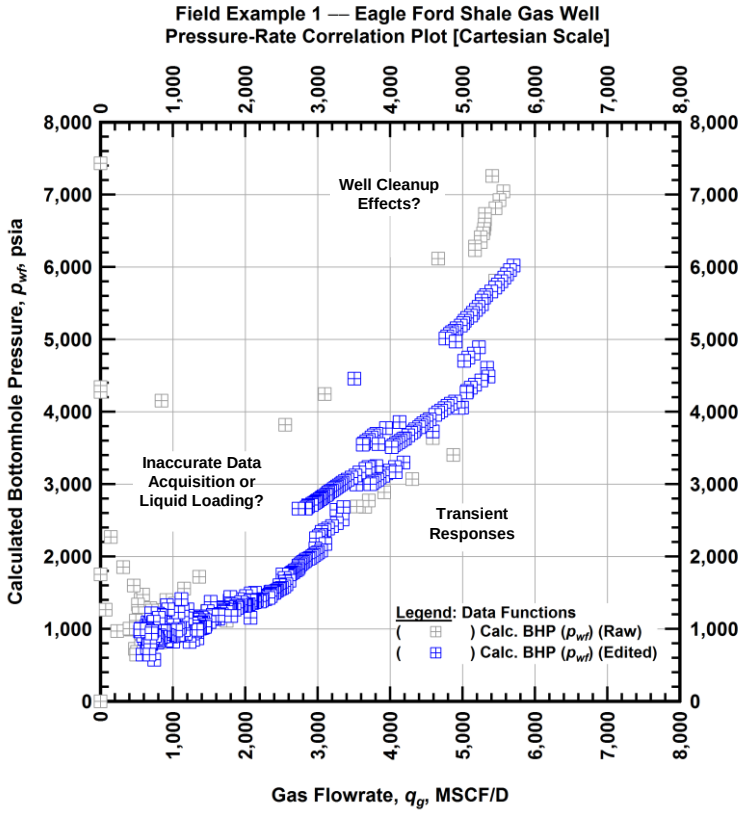

Figure 1.6 — (Cartesian Plot): Filtered pressure-rate correlation plot — calculated bottomhole pressure (p_{wf}) versus flowrate (q_g).

In **Figure 1.7**, we plot the filtered (or edited) gas flowrate and calculated flowing bottomhole pressure data with respect to the cumulative gas production. This plot is diagnostically similar to the flowrate and pressure history plot (**Figure 1.2**) because we evaluate for instances of shut-in periods, evidence of liquid loading, or obvious surface operational changes, as well as to identify the type of the gas flowrate decline once the well exhibits depletion, or boundary-dominated flow regime. From our observations, we draw the same conclusions as from the production history plot regarding no major shut-in periods, varied flowrate

beginning at approximately 1 BSCF of cumulative production (or at approximately 400 days of production), and a non-exponential flowrate decline trend.

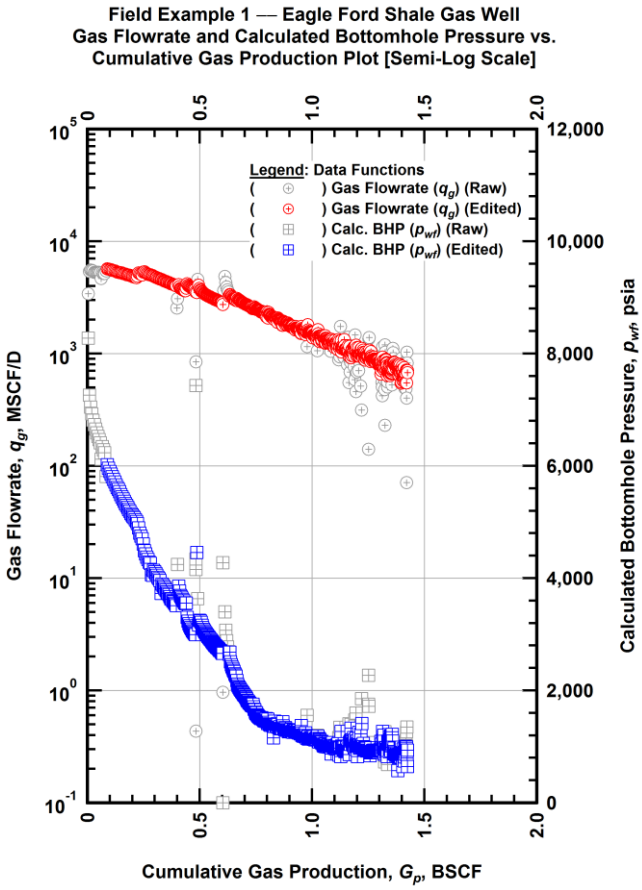

Figure 1.7 — (Semi-log Plot): Filtered rate-pressure-cumulative production history plot — flowrate (q_g) and calculated bottomhole pressure (p_{wf}) versus cumulative production (G_p).

We use the diagnostic plots shown in **Figure 1.8** through **Figure 1.10** to determine the various flow regimes experienced by the well, as well as to verify the initial reservoir pressure of the well.

Listed below is the diagnostic value for the observed trends of the loss-ratio derivative (b), reciprocal of the loss-ratio (D), and beta derivative (β) data functions represented in the figure above:

- Loss-ratio derivative (b):
  - Relatively constant value of approximately 2 represents linear flow.

- Relatively constant value of approximately 4 represents bi-linear flow.
- A decreasing value represents depletion flow as presented by Ilk et al. (2008).
- Relatively constant value between 0 and 1 represents depletion flow as presented by Arps.

- Reciprocal of the loss-ratio (D):
  - A log-log linear decline of $D(t)$ represents power-law, or transient, flow behavior (Ilk et al., 2008).
  - Relatively constant value during early-time production before transitioning to a log-log linear decline represents the hyperbolic decline (boundary-dominated flow) (Arps, 1945).
  - A constant D-value represents the exponential decline (boundary-dominated flow) (Arps, 1945).
- Beta derivative (β):
  - Relatively constant value less than one suggests power-law flow behavior (Ilk et al., 2008).
  - A log-log linear increase represents depletion, or boundary-dominated, flow (Ilk et al., 2008).

In **Figure 1.8**, we plot the filtered (edited) loss-ratio derivative (b), reciprocal of the loss-ratio (D) and beta derivative (β) versus production time. We observe highly scattered unfiltered (or raw) data points due to the gas flowrate variability from the early production well cleanup effects and also after approximately 400 days of production. We conclude the following from the trends shown in **Figure 1.8**:

- The loss-ratio derivative, although scattered during later production time appears to maintain a "relatively constant" value between 0 and 1. Thus, this can be interpreted as representing a hyperbolic decline (depletion flow) as presented by Arps (1945).
- The reciprocal of the loss-ratio appears to be relatively flat during early-time production before transitioning to a log-log linear decline. Thus, this can be interpreted as representing a hyperbolic decline (depletion flow) as presented by Arps (1945).
- The beta derivative function appears to be asymptotic to a constant value of 1 which suggests a hyperbolic decline (boundary-dominated flow) as documented by Ilk et al. (2008) and Idorenyin et al. (2011).

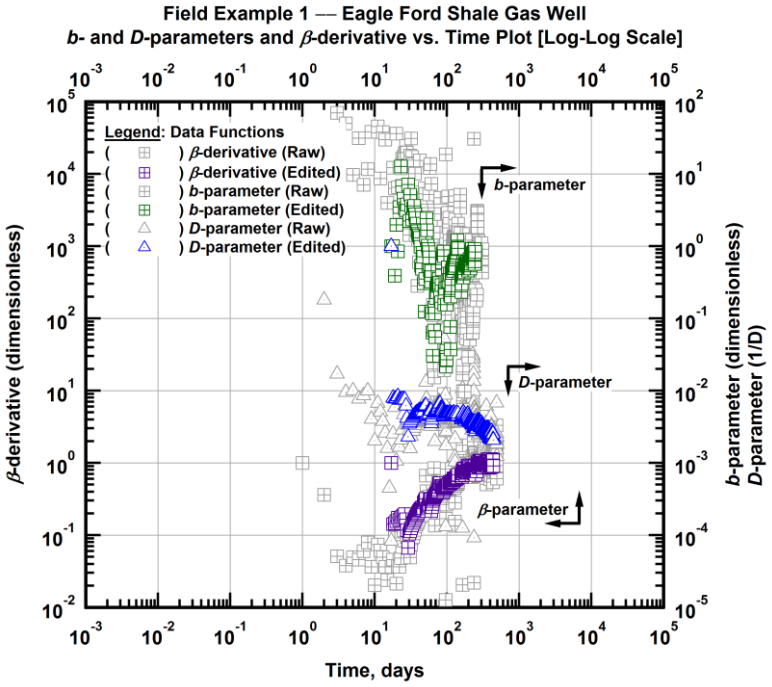

Figure 1.8 — (Log-Log Plot): Filtered *b*, *D* and *β* production history plot — *b*- and *D*-parameters and *β*-derivative versus production time.

In **Figure 1.9**, we plot the filtered gas flowrate versus production time on a log-log scale to identify the current and previous flow regimes experienced by the well. We overlay the flow regime lines (described in our workflow (**Figure 1.4**)) and we observe that *both* a half-slope line, representing a linear flow regime, and a unit slope line, representing depletion or boundary-dominated flow regime, fit portions of the data. Therefore, we determine that the well appears to be exhibiting depletion or boundary-dominated flow at late times, which implies that the Arps modified hyperbolic rate decline relation is applicable for this well.

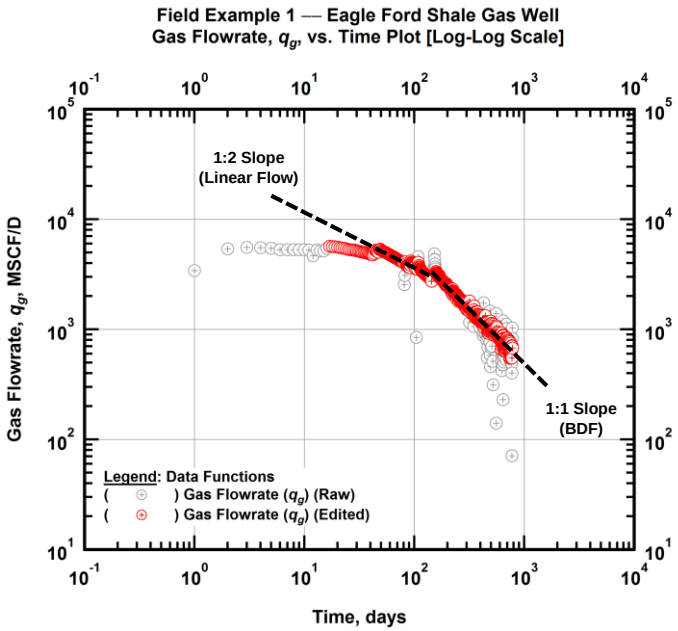

Figure 1.9 — (Log-Log Plot): Filtered gas flowrate production history and flow regime identification plot — gas flowrate (q_g) versus production time.

In **Figure 1.10**, we plot the inverse of the gas flowrate versus material balance time on a log-log scale to identify the current and previous flow regimes experienced by the well. We overlay the inverse of the flow regime lines (described in our workflow (**Figure 1.4**)) on the data plot to aid in the flow regime determination (Houzé et al., 2012). We observe both a half-slope line, representing a linear flow regime, and a unit slope line, representing depletion or boundary-dominated flow regime, fit portions of the data. Therefore, once again, we determine that the well appears to be exhibiting depletion or boundary-dominated flow at late times.

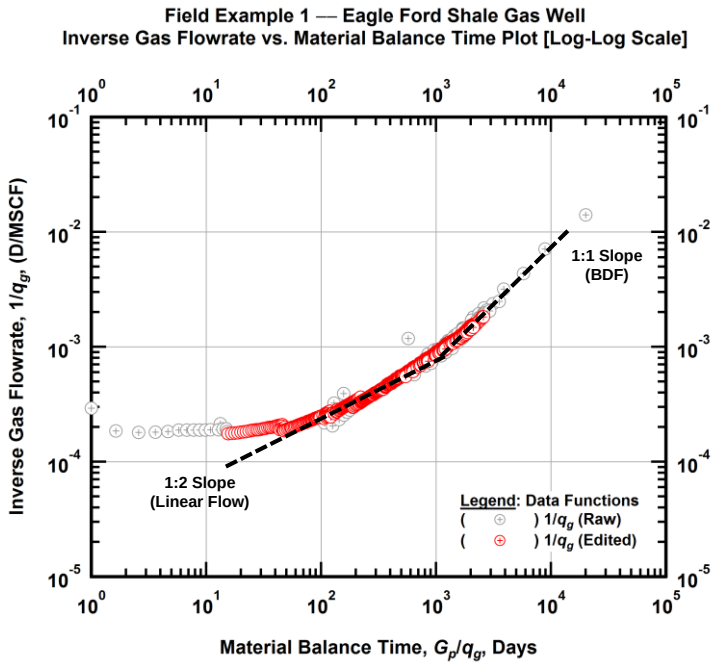

Figure 1.10 — (Log-log Plot): Filtered inverse rate with material balance time plot — inverse gas flowrate ($1/q_g$) versus material balance time (G_p/q_g).

In **Figure 1.11**, we plot the filtered gas flowrate-normalized pseudopressure drop, or inverse productivity index, versus the square root of production time. By taking the square root of the production time, a linear trend of the gas flowrate-normalized pseudopressure drop data represents the time when the well is experiencing a linear flow regime. The upward trending curve following the straight-line portion represents a flow regime other than linear flow. We note in **Figure 1.11** that the initial trend is linear and can be interpreted as being the linear flow regime, and is then followed by an upward trending curve. This upward trend corresponds to the production data identified in **Figure 1.9** and **Figure 1.10** to be experiencing a boundary-dominated or depletion flow regime.

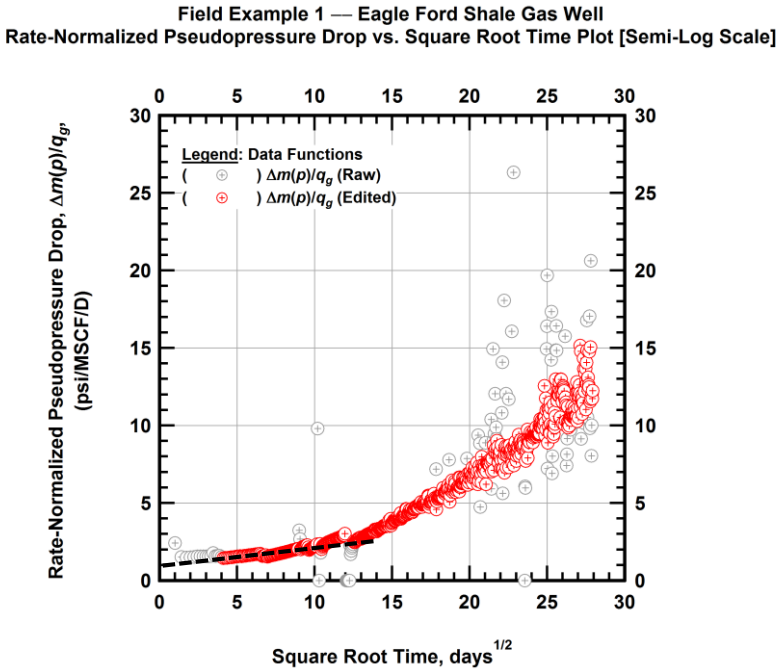

Figure 1.11 — (Semi-log Plot): Filtered normalized pseudopressure drop production history plot — rate-normalized pseudopressure drop ($\Delta m(p)/q_g$) versus square root production time ($\sqrt{t}$).

In **Figure 1.12**, we plot the inverse of the productivity index versus production time on a log-log scale to identify the current and previous flow regimes experienced by the well. We overlay the inverse of the flow regime lines (described in our workflow (**Figure 1.4**)) on the data plotted to aid in the flow regime determination (Houzé et al., 2012). We observe both a half-slope line, representing a linear flow regime, and a unit slope line, representing depletion or boundary-dominated flow regime, fit portions of the data. Therefore, once again, we determine that the well appears to be exhibiting depletion or boundary-dominated flow.

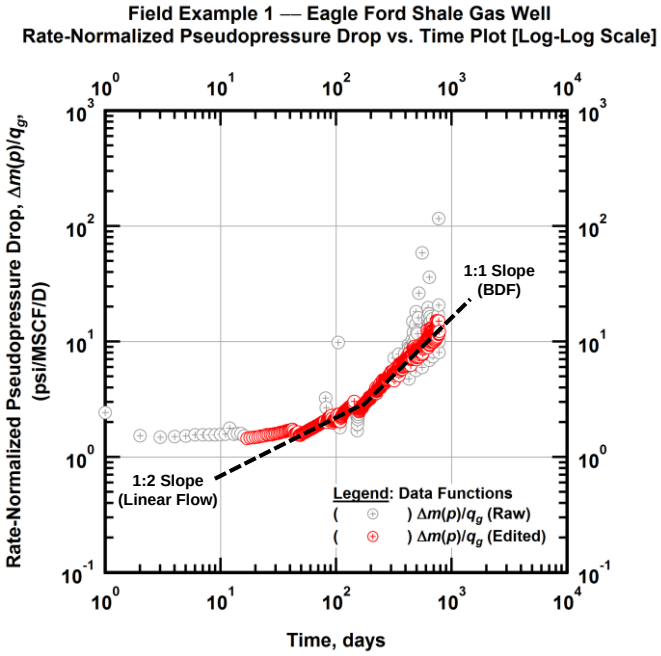

Figure 1.12 — (Log-log Plot): Filtered normalized pseudopressure drop production history plot — rate-normalized pseudopressure drop ($\Delta m(p)/q_g$) versus production time.

Ilk et al. (2010) presented a schematic of the rate normalized-pseudopressure drop integral-derivative function $(\Delta m(p)/q_g)_{id}$ in terms of material balance time, as shown in **Figure 1.13**, and provides well-test equivalent behavior of increasing rate functions with time. Both the location and angle of the slope(s) represented by the pressure integral-derivative function provide qualitative information regarding the flow regime(s) of the well, as well as properties of the well completion and reservoir. Including the inverse of the productivity index to the rate normalized-pseudopressure drop integral-derivative function plot, creates the diagnostic plot commonly referred to as the "log-log" plot.

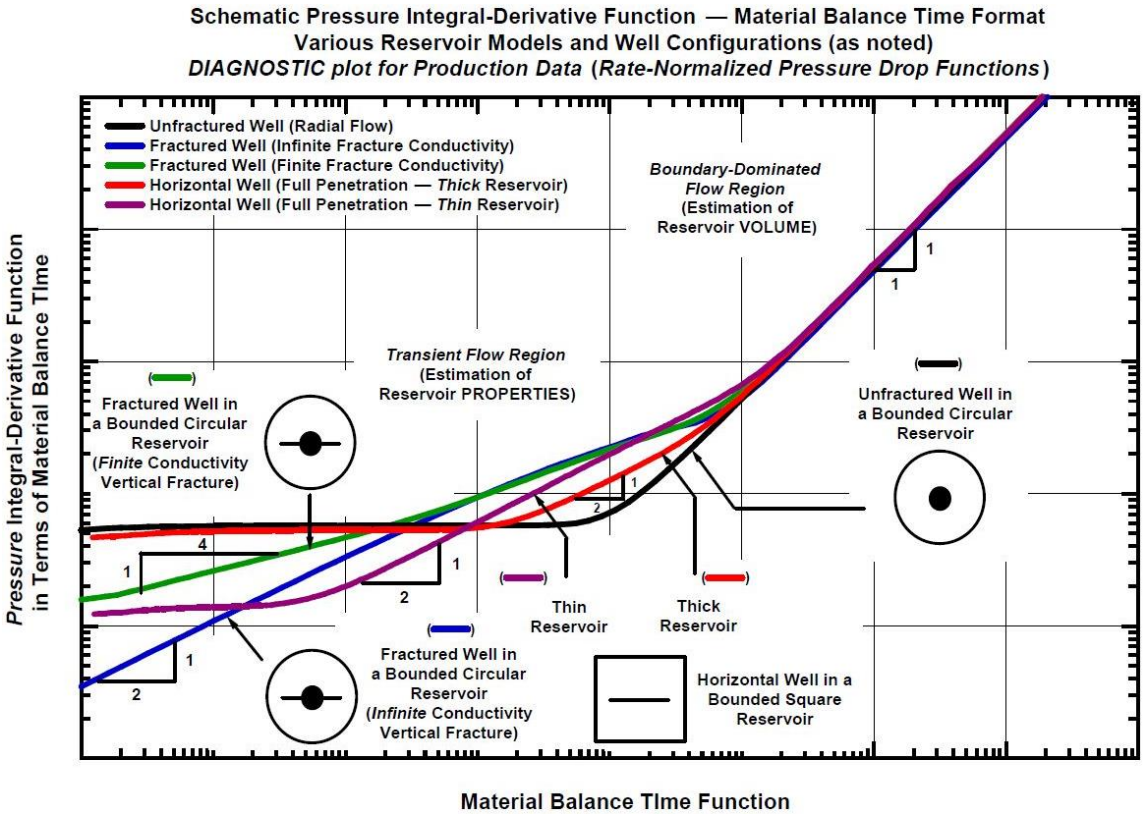

Figure 1.13 — (Log-log Plot): Schematic/diagnostic plot for production-data analysis — rate-normalized pseudopressure drop integral-derivative $(\Delta m(p)/q_g)_{id}$ versus material balance time (G_p/q_g) (Ilk et al., 2010).

In **Figure 1.14**, we plot the "log-log" diagnostic plot for the filtered production data. We then overlay both a one-half slope and a unit slope line on the rate-normalized pseudopressure drop integral-derivative data. When qualitatively comparing the slopes and shape of the data from **Figure 1.14** with the schematic plot in **Figure 1.13**, we conclude that the well appears to match the line representing a fully penetrated horizontal well in a thin bounded square reservoir.

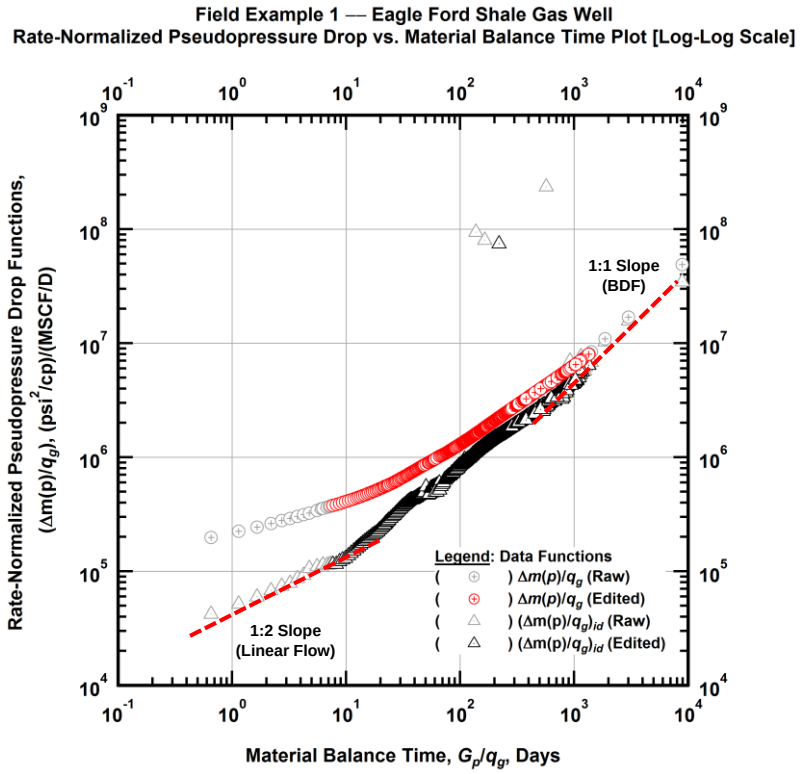

Figure 1.14 — (Log-log Plot): "Log-log" diagnostic plot of the filtered production data — rate-normalized pseudopressure drop ($\Delta m(p)/q_g$) and the rate-normalized pseudopressure drop integral-derivative $(\Delta m(p)/q_g)_{id}$ versus material balance time (G_p/q_g).

Ilk et al. (2010) also presented a schematic of the pseudopressure drop normalized-rate integral-derivative function $(\Delta m(p)/q_g)_{id}$ in terms of material balance time, as shown in **Figure 1.15**, and provides a decline type curve equivalent behavior of decreasing rate functions with time. Both the location and angle of the slope(s) represented by the pseudopressure integral-derivative function provide qualitative information regarding the flow regime(s) of the well, as well as properties of the well completion and reservoir. Including the productivity index and the pseudopressure drop normalized-rate integral to the pseudopressure drop normalized-rate integral-derivative function plot, creates the diagnostic plot commonly referred to as the Blasingame plot.

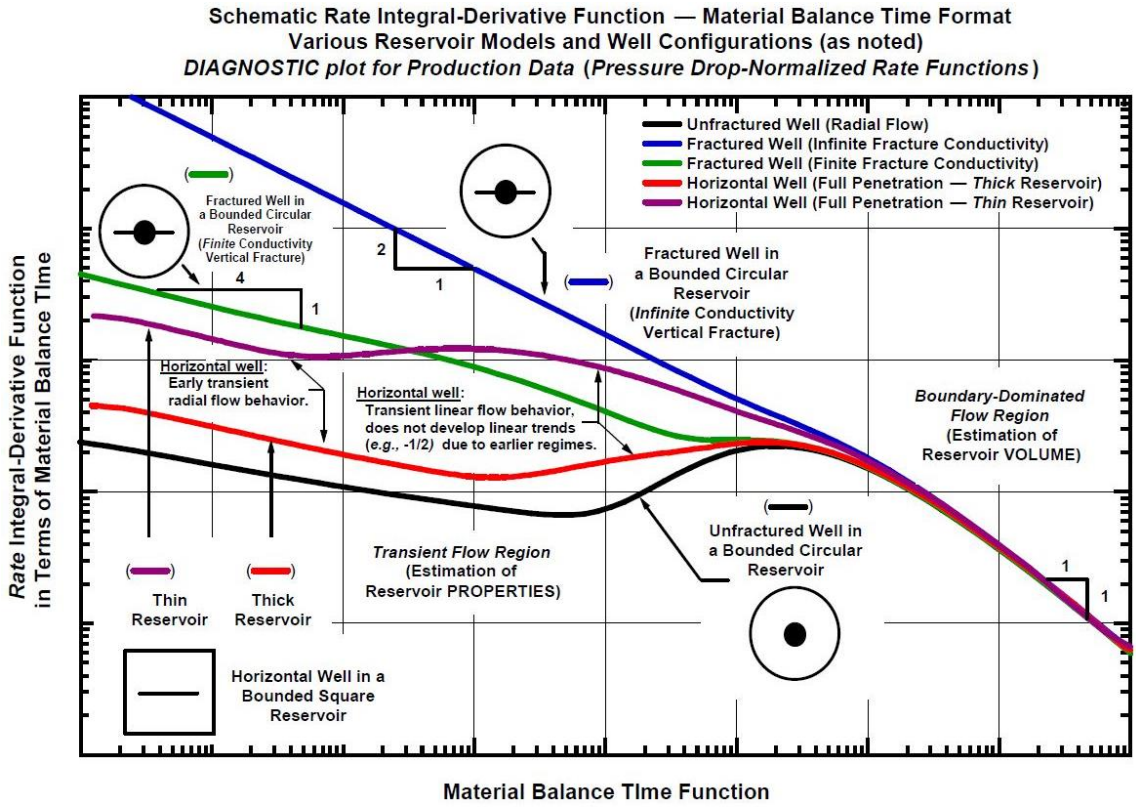

Figure 1.15 — (Log-log Plot): Schematic/diagnostic plot for production-data analysis — pseudopressure drop-normalized gas flowrate integral-derivative $(q_g/\Delta m(p))_{id}$ versus material balance time (G_p/q_g) (Ilk et al., 2010).

In **Figure 1.16**, we plot the Blasingame diagnostic plot for the filtered production data. We then attempt to overlay both a one-half slope and a unit slope line on the rate-normalized pseudopressure drop integral-derivative data, however, neither of the slopes fit the pseudopressure drop-normalized gas flowrate integral-derivative data. When qualitatively comparing the shape of the data from **Figure 1.16** with the schematic plot in **Figure 1.15** although not a strong signature, we conclude that the well appears to match the fully penetrated horizontal well in a thin bounded square reservoir.

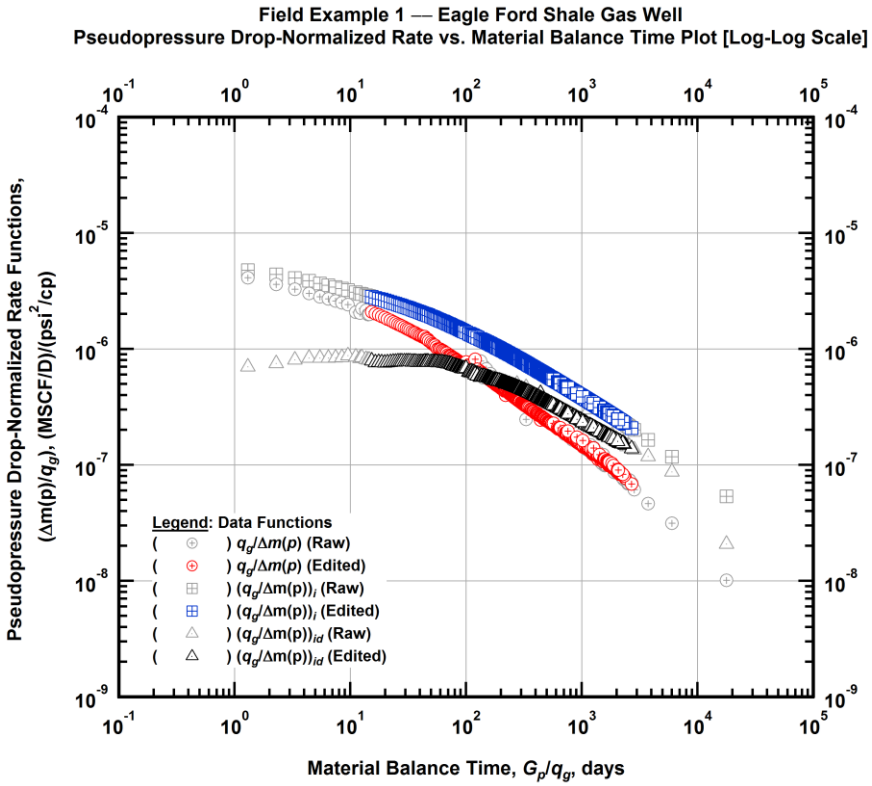

Figure 1.16 — (Log-log Plot): "Blasingame" diagnostic plot of the filtered production data — pseudopressure drop-normalized gas flowrate ($q_g/\Delta m(p)$), pseudopressure drop-normalized gas flowrate integral $(q_g/\Delta m(p))_i$ and pseudopressure drop-normalized gas flowrate integral-derivative $(q_g/\Delta m(p))_{id}$ versus material balance time (G_p/q_g).

In **Figure 1.17**, we plot the filtered pseudopressure drop-normalized gas flowrate ($q_g/\Delta m(p)$) versus pseudopressure drop-normalized cumulative gas production ($G_p/\Delta m(p)$). The plot is a qualitative assessment of the initial reservoir pressure estimate. A correct estimation of the initial reservoir pressure will produce a plot similarly to **Figure 1.17**. In the instance of an underestimated initial reservoir pressure, the early-time data will not be near-horizontal, but rather, almost vertical in nature and producing an apparent log-log linear decline with the late-time data.

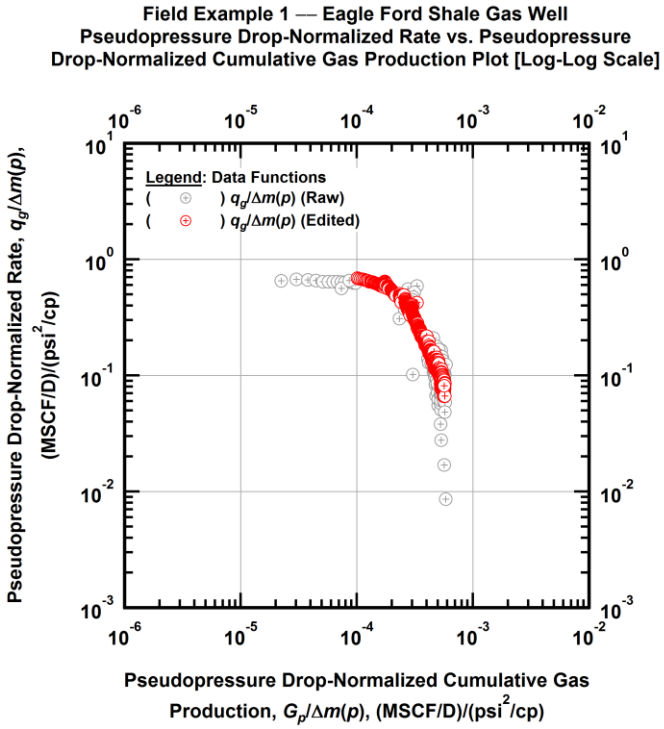

Figure 1.17 — (Log-log Plot): Filtered normalized rate with normalized cumulative production plot — pseudopressure drop-normalized gas flowrate ($q_g/\Delta m(p)$) versus pseudopressure drop-normalized cumulative gas production ($G_p/\Delta m(p)$).

After completing the initial diagnostic analysis and filtering of the non-representative production data, we then apply empirically based time-rate decline model analysis to the dataset. We fit the Arps modified hyperbolic (**Figure 1.18**) and power-law exponential (**Figure 1.19**) time-rate decline relations to the loss-ratio (b), reciprocal of the loss-ratio (D), beta derivative (β), and gas flowrate (q_g).

In **Figure 1.18**, we observe a close match of the Arps modified hyperbolic model with the filtered gas flowrate, the loss-ratio (b), reciprocal of the loss-ratio (D) and beta derivative (β) data. The closeness of match by the model is consistent with our assertion that the well has entered a depletion or boundary-dominated flow regime, which is a primary assumption of the Arps modified hyperbolic decline model.

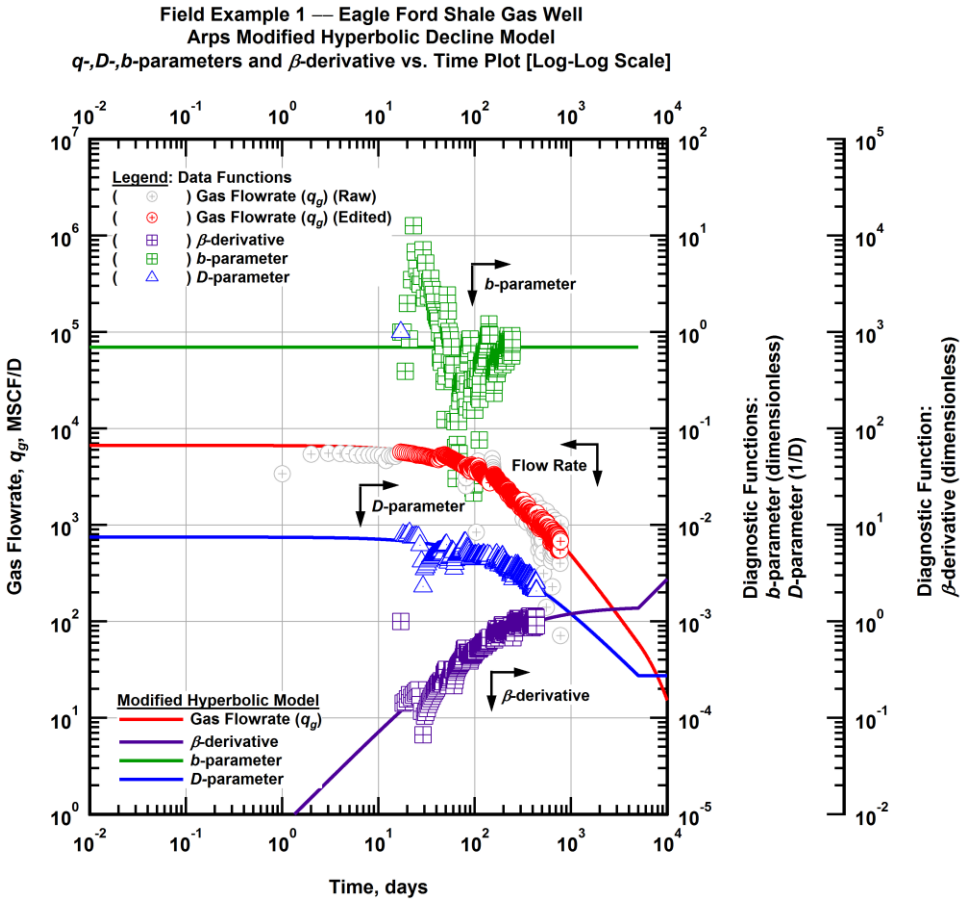

Figure 1.18 — (Log-Log Plot): Arps Modified hyperbolic decline model plot — time-rate model and data gas flowrate (q_g), *D*- and *b*-parameters and β-derivative versus production time.

In **Figure 1.19**, we observe that the power-law exponential model also generally matches the filtered gas flowrate, the loss-ratio (*b*), reciprocal of the loss-ratio (*D*) and beta derivative (β) data. There appears to be a fair amount of scatter with the loss-ratio derivative function for this well, which makes it difficult to assert if the Arps modified hyperbolic constant loss-ratio or the power-law exponential declining loss-ratio assumption is the more accurate representation of the production decline.

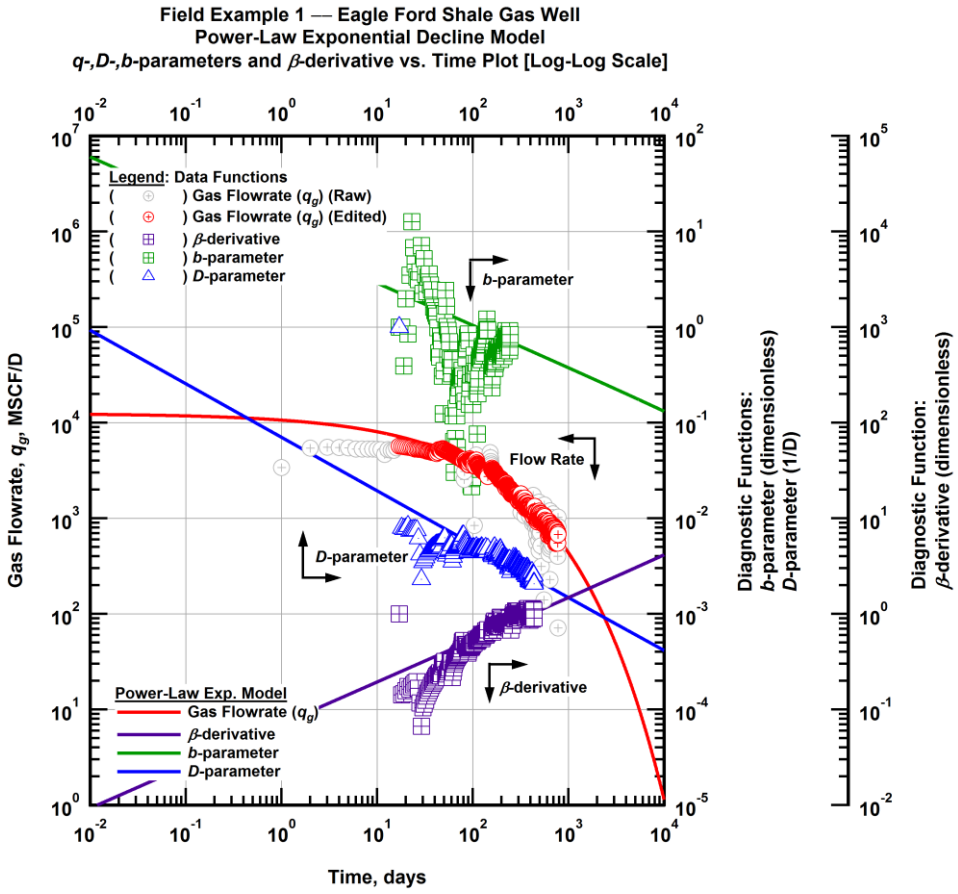

Figure 1.19 — (Log-Log Plot): Power-law exponential decline model plot — time-rate model and data gas flowrate (q_g), *D*- and *b*-parameters and β-derivative versus production time.

Upon the completion of the time-rate production analysis, we conduct analytical (time-rate-pressure) model-based production analysis of the well and history match the gas flowrate, the calculated flowing bottomhole pressure, and the cumulative gas production by calibrating the fracture conductivity (F_c), fracture face skin (s), fracture half-length (x_f) and formation permeability (k) parameters.

We demonstrate in **Figure 1.22** through **Figure 1.33** the issue of non-uniqueness in the solution when generating an analytical model for a multi-fracture horizontal well (MFHW) to history match the production data for an ultra-low permeability, shale gas reservoir. To illustrate this point, we prepare four scenarios that assume differing percentage efficiencies of the fracture clusters generating a successful fracture, and use either the original gas flowrate or an equivalent, PVT transformed "total" gas flowrate.

In **Figure 1.20**, we present the schematic design for a multi-fracture horizontal well assuming that the perforation clusters during the well completion had only a 50 percent efficiency in successfully forming propagated fractures (*i.e.*, every other perforation cluster produced a single vertical fracture).

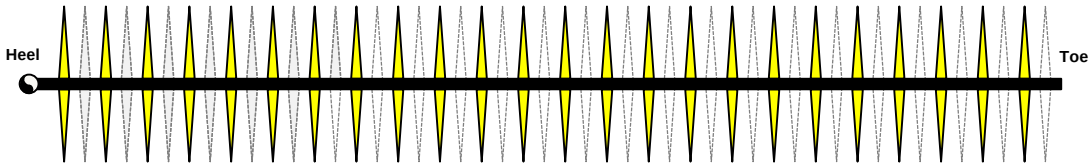

Figure 1.20 — (Diagram): 50 percent efficiency that the perforation clusters during the well completion succeeded in forming a propagated fracture.

In **Figure 1.21**, we present the schematic design for a multi-fracture horizontal well assuming that the perforation clusters during the well completion had a 100 percent efficiency in successfully forming propagated fractures (*i.e.*, every perforation cluster produced a single vertical fracture).

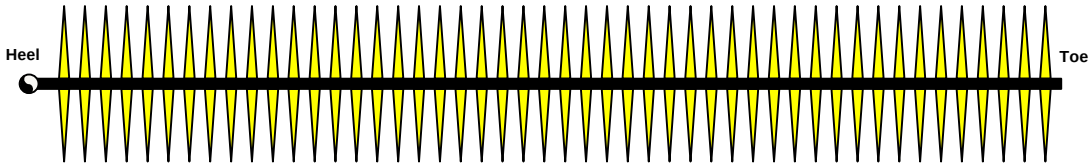

Figure 1.21 — (Diagram): 100 percent efficiency that the perforation clusters during the well completion succeeded in forming a propagated fracture.

In the first model scenario, we use the original gas flowrate data and assume a 50 percent efficiency that the perforation clusters during the well completion succeeded in forming a propagated fracture (**Figure 1.20**) (*i.e.*, the model contains 64 fractures). In **Figure 1.22**, we plot the original gas flowrate (q_g), the cumulative gas production (G_p) and the calculated bottomhole pressure (p_{wf}) production history with the model matches overlaid.

The model shows generally good agreement with the production data except for the first 50 days of production. In **Figure 1.23**, we plot the "Log-log" diagnostic plot of both the production data and model to check for agreement, and found that the model fits the late production time data, but did not follow the shape of the early-time data. In **Figure 1.24**, we plot the Blasingame diagnostic plot of both the production data and model to check for agreement, and once again found the model fit the late production time data, but did not adhere to the curvature of the early-time data.

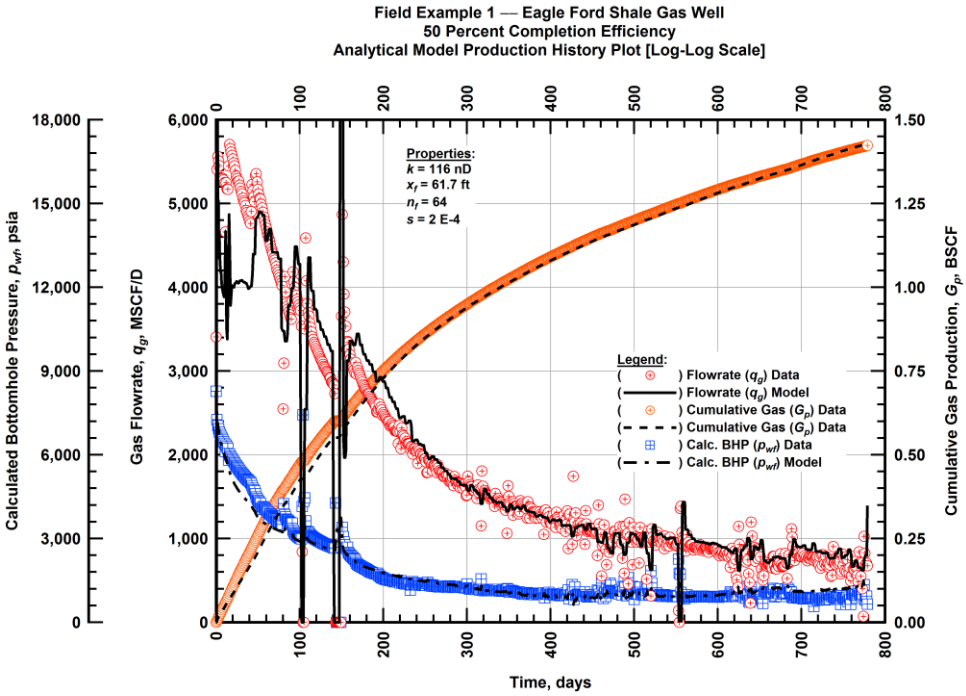

Figure 1.22 — (Cartesian Plot): Production history plot — original gas flowrate (q_g), cumulative gas production (G_p), calculated bottomhole pressure (p_{wf}) and 50 percent completion efficiency model matches versus production time.

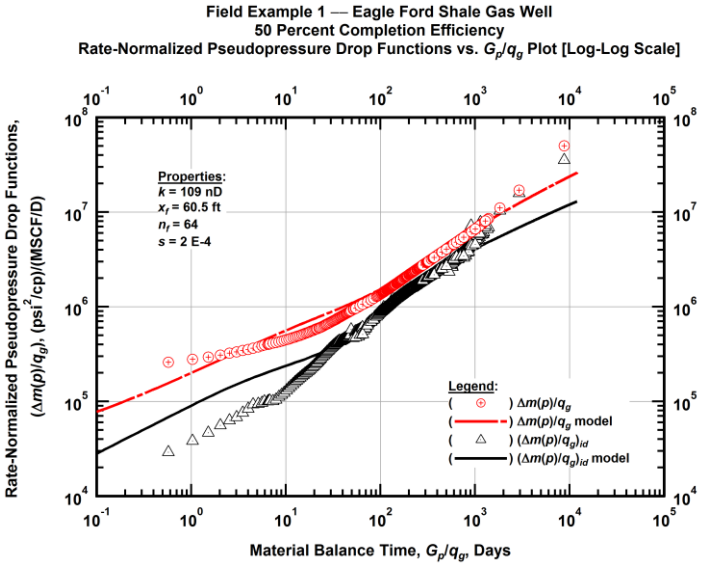

Figure 1.23 — (Log-log Plot): "Log-log" diagnostic plot of the original production data — rate-normalized pseudopressure drop ($\Delta m(p)/q_g$), rate-normalized pseudopressure drop integral-derivative $(\Delta m(p)/q_g)_{id}$ and 50 percent completion efficiency model matches versus material balance time (G_p/q_g).

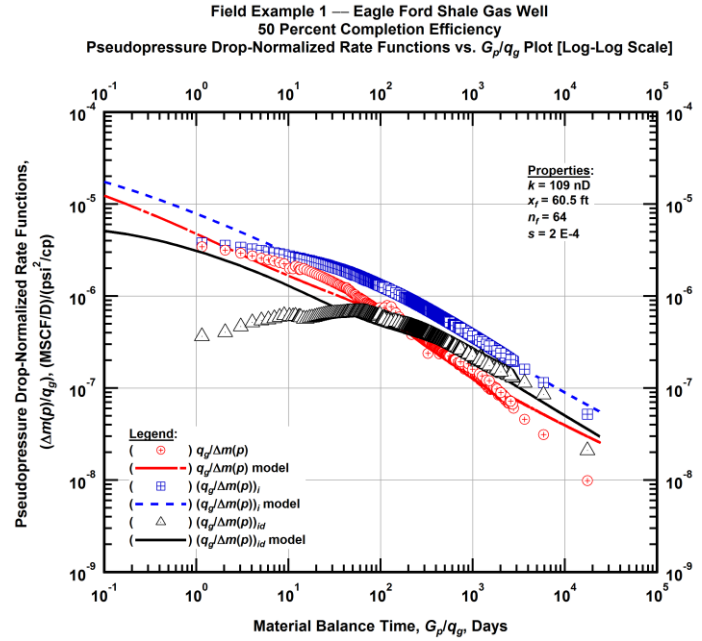

Figure 1.24 — (Log-log Plot): "Blasingame" diagnostic plot of the original production data — pseudopressure drop-normalized gas flowrate ($q_g/\Delta m(p)$), pseudopressure drop-normalized gas flowrate integral $(q_g/\Delta m(p))_i$, pseudopressure drop-normalized gas flowrate integral-derivative $(q_g/\Delta m(p))_{id}$ and 50 percent completion efficiency model matches versus material balance time (G_p/q_g).

In the second model scenario, we use the original gas flowrate data and we assume a 100 percent efficiency that the perforation clusters during the well completion succeeded in forming a propagated fracture (**Figure 1.21**) (*i.e.*, the model contains 128 fractures). In **Figure 1.25**, we plot the original gas flowrate (q_g), the cumulative gas production (G_p) and the calculated bottomhole pressure (p_{wf}) histories with the model matches overlaid. The model has good agreement with the production data, and although not a perfect match, this model fits the first 50 days of production better than the model of the previous scenario. In **Figure 1.26**, we plot the "Log-log" diagnostic plot of both the production data and model to check for agreement, and found the model closely fit the data. In **Figure 1.27**, we plot the Blasingame diagnostic plot of both the production data and model to check for agreement, and once more found the model closely adhered to the shape of the data.

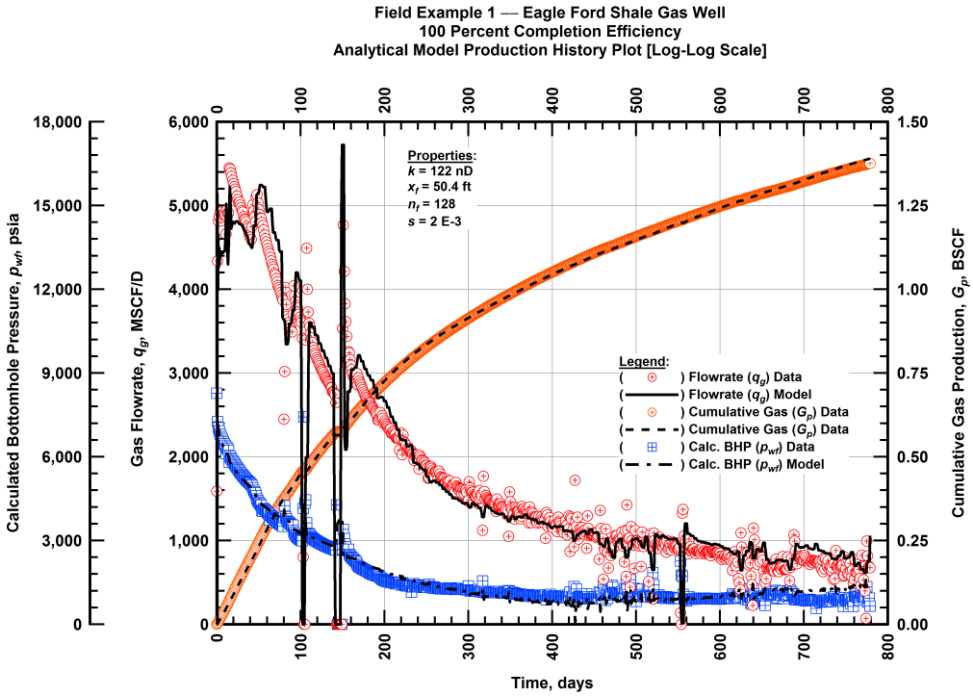

Figure 1.25 — (Cartesian Plot): Production history plot — original gas flowrate (q_g), cumulative gas production (G_p), calculated bottomhole pressure (p_{wf}) and 100 percent completion efficiency model matches versus production time.

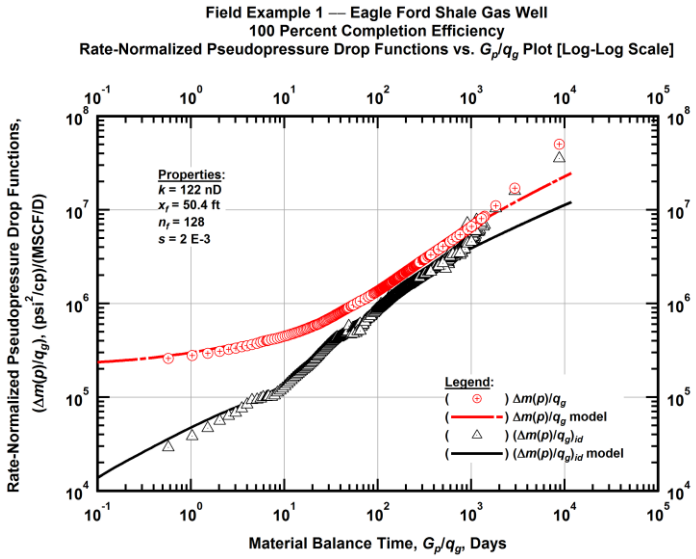

Figure 1.26 — (Log-log Plot): "Log-log" diagnostic plot of the original production data — rate-normalized pseudopressure drop $(\Delta m(p)/q_g)$, rate-normalized pseudopressure drop integral-derivative $(\Delta m(p)/q_g)_{id}$ and 100 percent completion efficiency model matches versus material balance time (G_p/q_g).

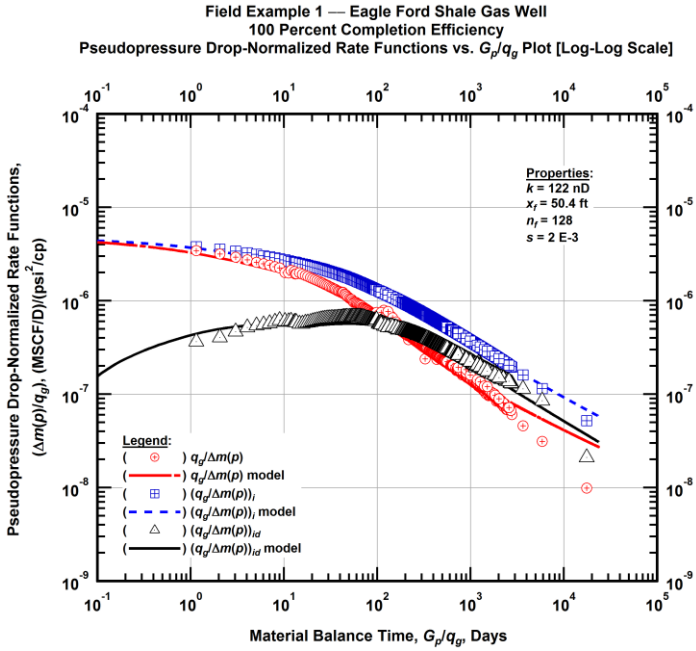

Figure 1.27 — (Log-log Plot): "Blasingame" diagnostic plot of the original production data — pseudopressure drop-normalized gas flowrate $(q_g/\Delta m(p))$, pseudopressure drop-normalized gas flowrate integral $(q_g/\Delta m(p))_i$, pseudopressure drop-normalized gas flowrate integral-derivative $(q_g/\Delta m(p))_{id}$ and 100 percent completion efficiency model matches versus material balance time (G_p/q_g).

In the third model scenario, we use the PVT data for this well to transform the water and condensate rates into equivalent gas flowrates in order to generate an equivalent dry gas flowrate (essentially on a molar basis). Additionally, we assume a 50 percent efficiency that the perforation clusters during the well completion succeeded in forming a propagated fracture (**Figure 1.20**) (*i.e.*, the model contains 64 fractures).

In **Figure 1.28**, we plot the PVT revised gas flowrate (q_g), the cumulative gas production (G_p) and the calculated bottomhole pressure (p_{wf}) production history with the model matches overlaid. Similar to the first scenario, the model has good agreement with the production data except for the first 50 days of production. In **Figure 1.29**, we plot the "Log-log" diagnostic plot of both the production data and model to check for agreement, and found the model fit the late production time data, but did not follow the shape of the early-time data. In **Figure 1.30**, we plot the Blasingame diagnostic plot of both the production data and model to check for agreement, and once again found the model fit the late production time data, but did not adhere to the curvature of the early-time data.

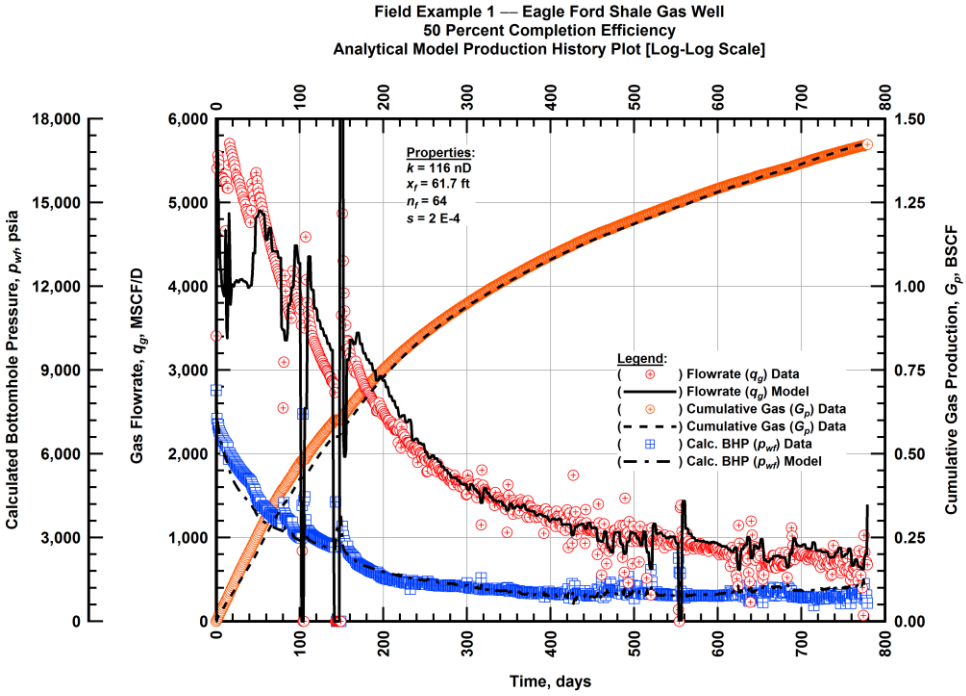

Figure 1.28 — (Cartesian Plot): Production history plot — revised gas flowrate (q_g), cumulative gas production (G_p), calculated bottomhole pressure (p_{wf}) and 50 percent completion efficiency model matches versus production time.

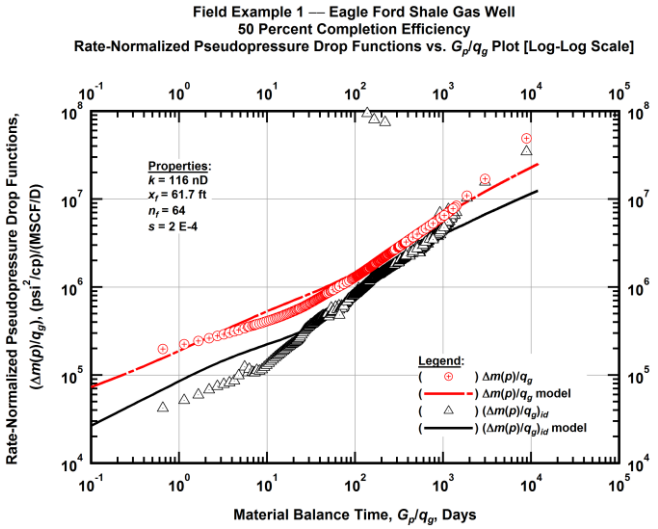

Figure 1.29 — (Log-log Plot): "Log-log" diagnostic plot of the revised production data — rate-normalized pseudopressure drop ($\Delta m(p)/q_g$), rate-normalized pseudopressure drop integral-derivative $(\Delta m(p)/q_g)_{id}$ and 50 percent completion efficiency model matches versus material balance time (G_p/q_g).

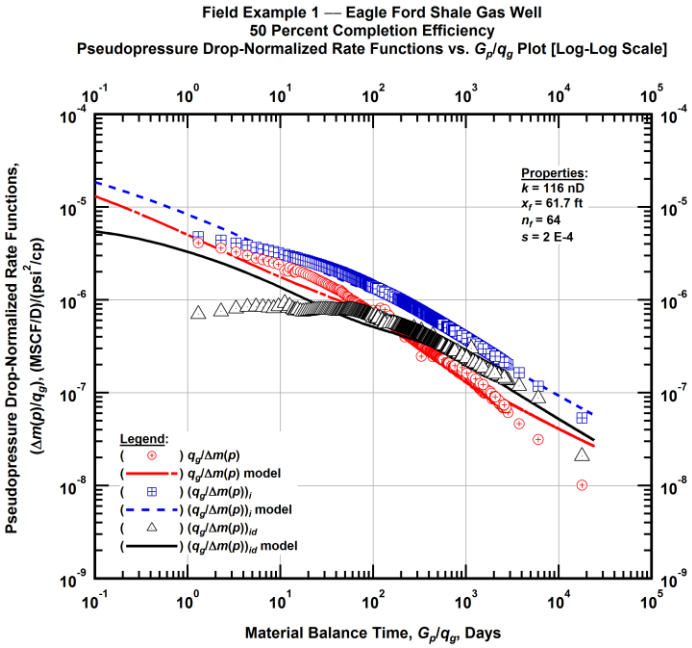

Figure 1.30 — (Log-log Plot): "Blasingame" diagnostic plot of the revised production data — pseudopressure drop-normalized gas flowrate ($q_g/\Delta m(p)$), pseudopressure drop-normalized gas flowrate integral $(q_g/\Delta m(p))_i$, pseudopressure drop-normalized gas flowrate integral-derivative $(q_g/\Delta m(p))_{id}$ and 50 percent completion efficiency model matches versus material balance time (G_p/q_g).

In the fourth model scenario, we use the PVT data of the well to transform the water and condensate rates into equivalent gas flowrates in order to generate an equivalent dry gas flowrate (essentially on a molar basis). In addition, we assume a 100 percent efficiency that the perforation clusters during the well completion succeeded in forming a propagated fracture (**Figure 1.21**) (*i.e.*, the model contains 128 fractures). In **Figure 1.31**, we plot the PVT revised gas flowrate (q_g), the cumulative gas production (G_p) and the calculated bottomhole pressure (p_{wf}) histories with the model matches overlaid. Similar to the second scenario, the model has good agreement with the production data, and although not a perfect match, this model fits the first 50 days of production better than the model of the previous scenario. In **Figure 1.32**, we plot the "Log-log" diagnostic plot of both the production data and model to check for agreement, and found the model closely fit the data. In **Figure 1.33**, we plot the Blasingame diagnostic plot of both the production data and model to check for agreement, and once more found the model closely adhered to the shape of the data.

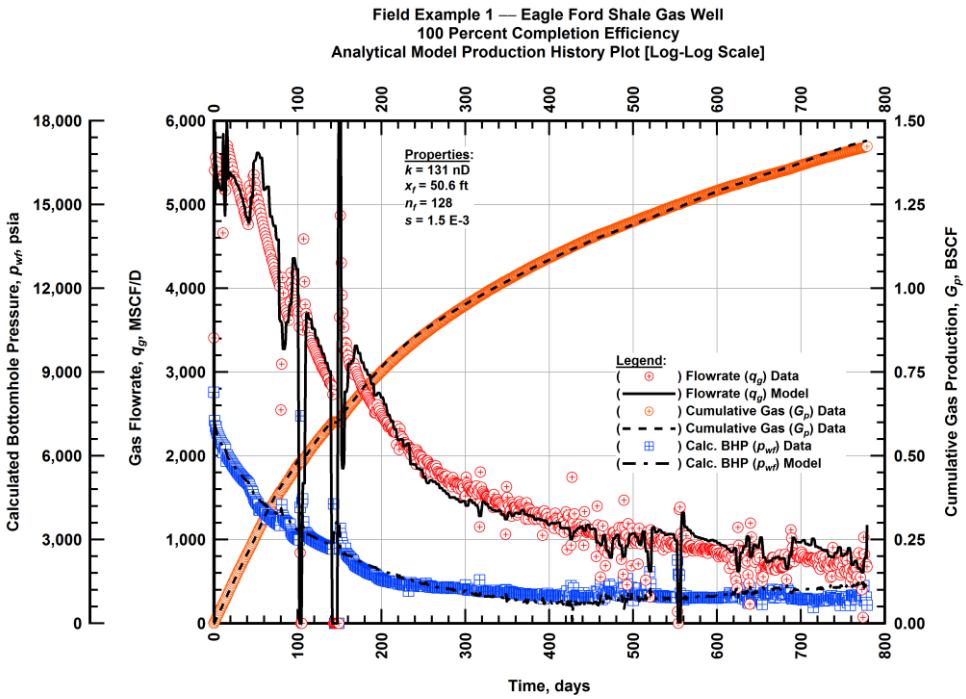

Figure 1.31 — (Cartesian Plot): Production history plot — revised gas flowrate (q_g), cumulative gas production (G_p), calculated bottomhole pressure (p_{wf}) and 100 percent completion efficiency model matches versus production time.

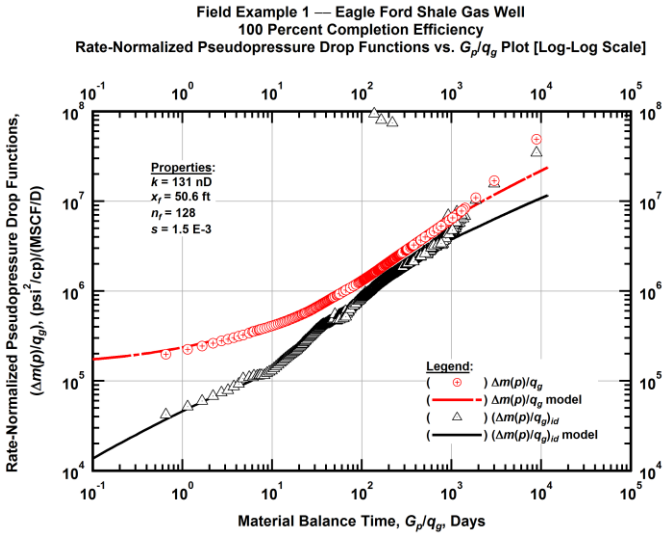

Figure 1.32 — (Log-log Plot): "Log-log" diagnostic plot of the revised production data — rate-normalized pseudopressure drop ($\Delta m(p)/q_g$), rate-normalized pseudopressure drop integral-derivative $(\Delta m(p)/q_g)_{id}$ and 100 percent completion efficiency model matches versus material balance time (G_p/q_g).

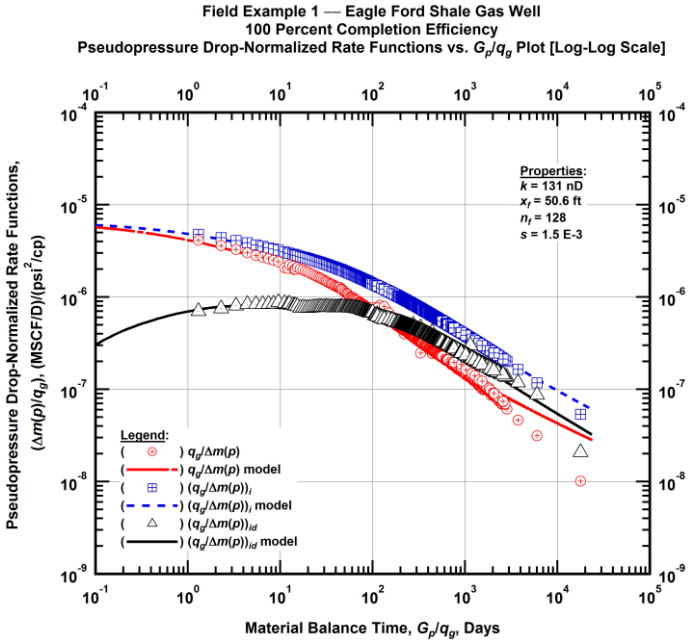

Figure 1.33 — (Log-log Plot): "Blasingame" diagnostic plot of the revised production data — pseudopressure drop-normalized gas flowrate ($q_g/\Delta m(p)$), pseudopressure drop-normalized gas flowrate integral $(q_g/\Delta m(p))_i$, pseudopressure drop-normalized gas flowrate integral-derivative $(q_g/\Delta m(p))_{id}$ and 100 percent completion efficiency model matches versus material balance time (G_p/q_g).

As seen above, the analytical models generated for each of the scenarios fit the production history data almost identically, however, it is not until we evaluate the "Log-Log" and Blasingame diagnostic plots that differences in the fit of the model to the well production data becomes apparent. In the field example above, all four scenarios fit the late-time data, but the two scenarios for the higher number of fractures clearly match the early-time data better in the diagnostic plots.

In **Figure 1.34**, we plot the PVT revised gas 30-year estimated flowrate forecast of the Arps modified hyperbolic decline model, power-law exponential decline model, and the 50 and 100 percent completion efficiency time-rate-pressure analytical models along with the historic gas flowrate data (q_g) versus production time. We observe a marked difference in the projected forecast estimates between the empirical and analytical models. The power-law exponential model demonstrated the sharpest gas flowrate decline trend, and almost identically, the 50 percent and the 100 percent completion efficiency time-rate-pressure models had the most gradual decline with highest final gas flowrate values.

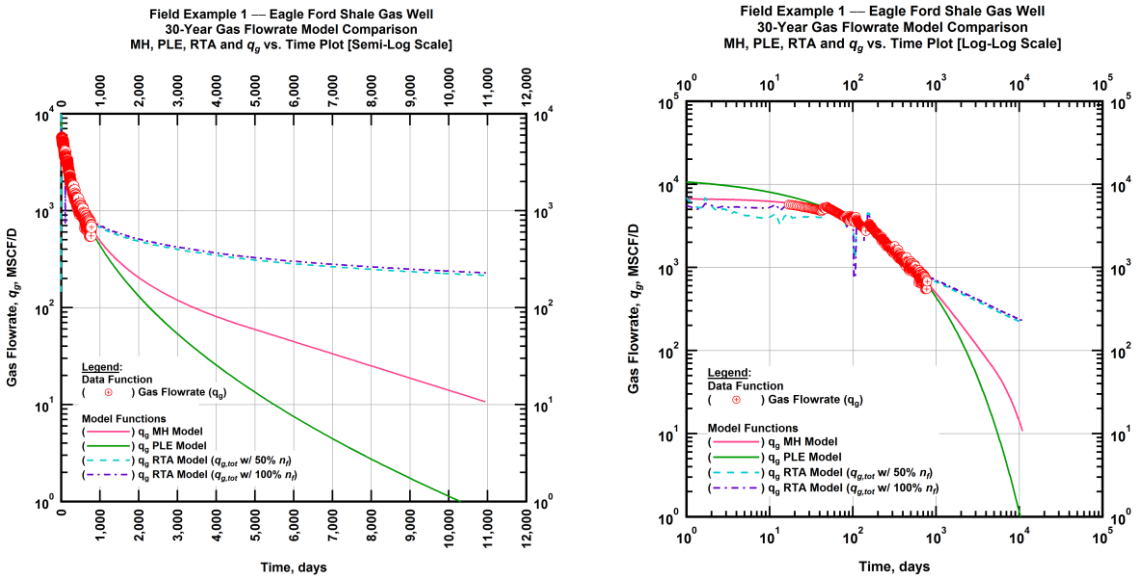

A **B**

Figure 1.34 — (A — Semi-Log Plot) and (B — Log-Log Plot): Revised gas 30-year estimated flowrate model comparison — Arps modified hyperbolic decline model, power-law exponential decline model, and 50 percent and 100 percent completion efficiency RTA models revised gas 30-year estimated flowrate decline and historic gas flowrate data (q_g) versus production time.

In **Figure 1.35**, we plot the PVT revised gas 30-year estimated cumulative gas production volume forecast of the Arps modified hyperbolic decline model, power-law exponential decline model, and the 50 percent and 100 percent completion efficiency time-rate-pressure analytical models along with the historic cumulative gas production volume data (q_g) versus production time. We observe a substantial difference in the projected forecast estimates between the empirical and analytical models. The power-law exponential model estimated the lowest cumulative gas production volume, and the 50 percent and 100 percent completion efficiency time-rate-pressure models, almost identically, estimated the highest cumulative gas production volume.

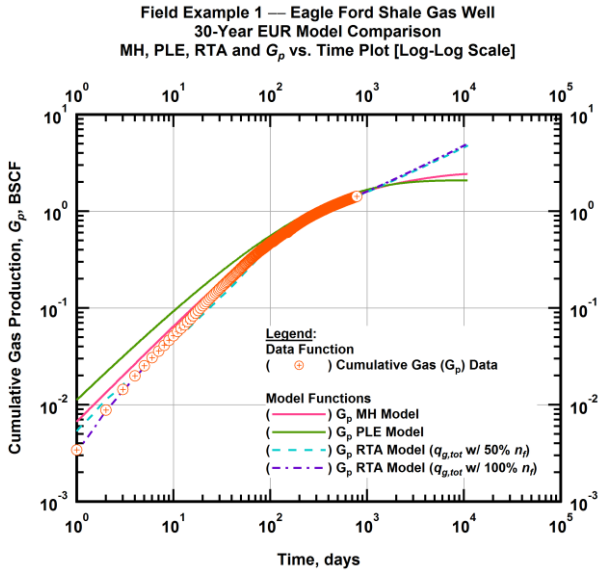

Figure 1.35 — (Log-log Plot): Estimated 30-year cumulative gas production volume model comparison — Arps modified hyperbolic decline model, power-law exponential decline model, and 50 percent and 100 percent completion efficiency RTA models estimated 30-year cumulative gas production volumes and historic cumulative gas production (G_p) versus production time.

In **Table 1.2**, we show the final 30-year estimated cumulative gas production volumes for both the empirical time-rate relations and the 50 percent and 100 percent completion efficiency time-rate-pressure analytical models for the field example.

Table 1.2 — 30-year estimated cumulative production (EUR), in units of BSCF, for the Arps modified hyperbolic, power-law exponential, and analytical time-rate-pressure decline models.

Arps Modified Hyperbolic (BSCF)	Power-Law Exponential (BSCF)	(gas only) Analytical Model ($q_{g,orig}$ w/ 50% n_f) (BSCF)	(gas only) Analytical Model ($q_{g,orig}$ w/ 100% n_f) (BSCF)	(total rate) Analytical Model ($q_{g,tot}$ w/ 50% n_f) (BSCF)	(total rate) Analytical Model ($q_{g,tot}$ w/ 100% n_f) (BSCF)
2.36	1.95	4.77	4.98	4.95	5.16

CHAPTER II

LITERATURE REVIEW

2.1 Historic Time-Rate Analysis

Arnold and Anderson (1908) introduced the use of geometric series to calculate oil and gas well production decline trends. Lewis and Beal (1918) then expanded the work of Arnold and Anderson by introducing the use of percentage decline curves in order to make well data comparable for analysis purposes. The most basic definitions of the decline parameter functions (*i.e.*, the loss-ratio and the loss-ratio derivative functions) were first presented by Johnson and Bollens (1927) and are given as:

$$\frac{1}{D(t)} = -\frac{q(t)}{dq(t)/dt} \qquad \text{(loss-ratio)} \qquad (2.1)$$

$$b(t) = \frac{d}{dt}\left[\frac{1}{D(t)}\right] = -\frac{d}{dt}\left[\frac{q(t)}{dq(t)/dt}\right] \qquad \text{(loss-ratio derivative)} \qquad (2.2)$$

In the summary article by Arps (1945) the basic decline curve variables and models were presented and applied. It should be noted that the Arps time-rate relations are strictly empirical (although later efforts have shown that the exponential decline relation can be derived under some fairly strong constraints/assumptions and that hyperbolic decline can be partially derived assuming certain behavior of the compressibility and mobility functions). The original "Arps" relations are given as:

$$q(t) = q_i \exp[-D_i t] \qquad \text{(exponential decline relation)} \qquad (2.3)$$

$$q(t) = \frac{q_i}{(1+bD_i t)^{1/b}} \qquad \text{(hyperbolic decline relation)} \qquad (2.4)$$

As a means to directly estimate the decline curve parameters (q_i, D_i, b) from data, Fetkovich (1980) developed "type curves" using the hyperbolic and exponential decline relations. Fetkovich (1980) also provided a "type curve" that combined the analytical solutions for the transient flow regime(s) experienced at early time with Arps relations for late-time behavior as a means of estimating reservoir properties and to construct graphical extrapolations of time-rate performance.

2.2 Modern Time-Rate Analysis

The work of Gentry and McCray (1978) and Maley (1985) showed that the loss-ratio derivative (*b*) exceeded the assumed constraint value of one for the production decline trends of layered or heterogeneous reservoirs as well as tight gas wells that have been hydraulically fractured. Maley (1985) extended the work of Gentry and McCray to show that this phenomena also applied to other types of reservoirs where wells exhibited extended transient flow behavior. Therefore, it was recognized that *new rate-time relations were needed to forecast the production decline behavior of wells experiencing long periods of transient flow,* such as low/ultra-low permeability, unconventional tight gas and shale wells.

Robertson (1988) presented the Arps "modified hyperbolic" model by combining the traditional Arps hyperbolic and exponential time-rate decline relations into a single equation. He also modified one of Arps' fundamental assumptions by allowing the hyperbolic decline exponent, or loss-ratio derivative, parameter (*b*) applied to early-time data to exceed a value of 1 (Fulford and Blasingame, 2013), whereas, the traditional Arps hyperbolic loss-ratio equation constrains the loss-ratio parameter to values between 0 and 1 (Arps, 1945).

Ilk et al. (2008) developed the "power-law exponential" model to capture the "non-hyperbolic" production rate behavior (non-constant *b*-parameter and *D*-parameter values) experienced during early production times. In the "power-law exponential" model the *D*-parameter behaves as a decaying power law function at early times, and transitions to a constant value at later production times by use of a terminal decline coefficient. This behavior contrasts the hyperbolic nature of the *D*-parameter found in the Arps modified hyperbolic decline model, which remains approximately constant at very early times, and then becomes a unit-slope decaying power law relation at later times. Ilk et al. observed that the power-law exponential model fit tight gas and shale gas production data during early-time transient, transition, and late-time boundary-dominated flow regimes.

Other models such as the stretched exponential production decline model proposed by Valkó (2009) and the Duong model (Duong, 2011) are also models which capture transient flow regime models. The stretched

exponential model and the power-law exponential are the same base model, but the power-law exponential model deploys a terminal decline coefficient to provide more flexibility and constraint. It is also worth noting that the Duong model typically over-extrapolates the production performance, primary due to the power-law (time-rate) nature of this model, the Duong model can be constrained, but in doing so one is left with a mode similar to the modified hyperbolic relation.

In **Figure 2.1**, Blasingame (2011) summarizes, in a simplified graphical form, the typical flow regimes experienced for a multi-fracture horizontal well (MFHW) in a low/ultra-low permeability reservoir.

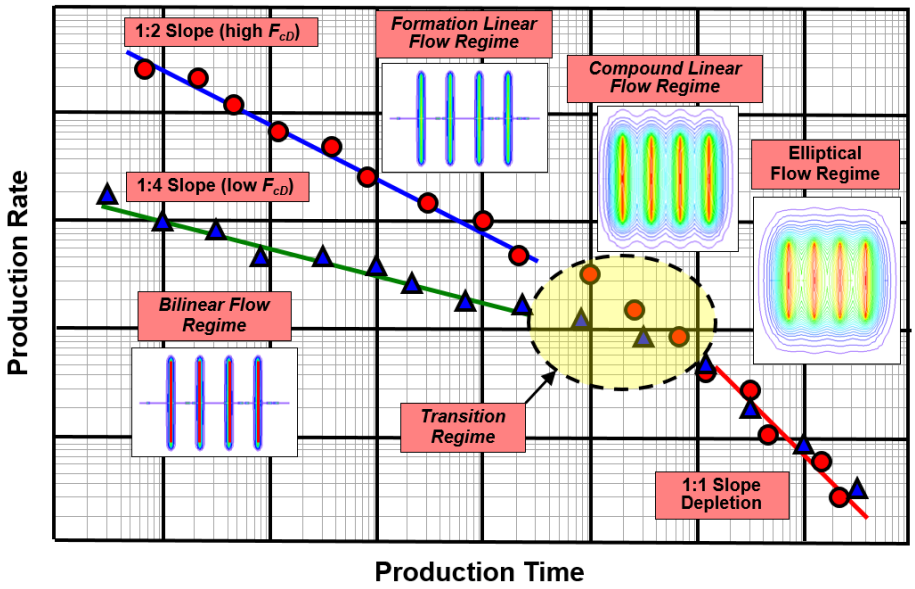

Figure 2.1 — (Log-log Plot): Multiple, hydraulically fractured horizontal well flow regime schematic — flowrate (q) versus production time (Blasingame, 2011).

2.3 Modern Model-Based (Time-Rate-Pressure) Production Analysis

Fraim and Wattenbarger (1987) developed a real gas-normalized time function to linearize the gas flowrate decline for a well experiencing a boundary-dominated flow regime. The proposed method estimated values of the original-gas-in-place, formation permeability and porosity. Palacio and Blasingame (1993) developed decline type curves for production data analysis that incorporate flowrate, flowrate integral and flowrate

integral-derivative functions versus material balance time on a log-log scale. These plots, when combined, are commonly referred to as the Blasingame plot. Callard and Schenewerk (1995) presented a reservoir characterization technique that pressure-normalized both the production rate and cumulative production data using the flowing bottomhole pressure data. They then developed diagnostic type curves from the pressure-normalized solution with applicability to most wellbore configurations and reservoir types.

Ansah et al. (1996) developed a semi-analytical model, utilizing the relationship between the viscosity-compressibility product and reservoir pressure, for matching gas production data during the boundary-dominated flow regime. The model enables the estimation or calculation of original-gas-in-place, formation permeability and reservoir drive mechanism(s). Agarwal et al. (1999) developed, using concepts derived from pressure transient analysis, a set of rate-time and rate-cumulative and cumulative-time production decline type curves along with their associated derivatives. The type curves were developed for radial flow geometries and vertically fractured wells.

Anderson and Mattar (2004) presented diagnostic procedures to be applied to production data for identifying liquid loading, wellbore skin, and well productivity changes, as well as diagnosing production interference and external pressure support. Al-Ahmadi et al. (2010) presented a procedure for choosing a dual porosity fracture pattern model used to calculate the analytical linear flow solution needed to history match well production data. Aboaba and Cheng (2010) developed a method for estimating fracture half-length and formation permeability for a multiple hydraulic fracture, horizontal well using the daily production and pressure data for a well. Ilk et al. (2011a) conducted a study of several existing production analysis and diagnostic techniques to identify inherent pitfalls in unconventional well production analysis and proposed a workflow for evaluating unconventional well production data. Ilk et al. (2011b) presented the use of the constant-pressure "beta derivative" function for use in identifying production behavior characteristics for unconventional shale wells.

2.4 Pressure Transient Analysis of Fractured Wells

Muskat (1937) observed a linear trend when plotting the shut-in pressure drop versus the logarithm of shut-in time. Arps and Smith (1949) developed a semi-log linear extrapolation method to determine the static bottomhole pressure for low productivity index wells using the pressure and pressure derivative functions. Miller, Dyes and Hutchinson (1950) developed a method for estimating the effective permeability and reservoir pressure from the early portion of a pressure build-up curve, for instances of a stabilized well prior to shut-in. Horner (1951) presented a plot, commonly referred to as the Horner plot, of shut-in bottomhole pressure versus the logarithm of his proposed superposition time function. Horner presented relationships from the linear trend in the plot to estimate the initial reservoir pressure and permeability for an infinite acting, radial flow in a homogeneous reservoir with slightly compressible, single-phase fluid.

Perrine (1956) developed a pressure build-up data analysis procedure to measure the static reservoir pressure, near wellbore damage or skin, and effective reservoir permeability. Cinco-Ley et al. (1978) developed a mathematical model to study the transient behavior for a well containing a single, finite-conductivity vertical fracture in an infinite slab reservoir. In their work, they also developed a type-curve matching procedure based upon their correlation of the dimensionless fracture storage capacity, dimensionless hydraulic diffusivity, and dimensionless fracture conductivity with reservoir and other fracture characteristics. Additionally, they also demonstrated that a finite-conductivity vertical fracture in an infinite-acting homogeneous reservoir could be considered infinite-conductivity once the dimensionless fracture conductivity was equal to or greater than a value of 300.

Agarwal (1980) developed new pressure change and superposition time functions for application with pressure build-up data for analysis with existing pressure drawdown type curves. Cinco-Ley and Samaniego (1981) developed a technique for analyzing pressure transient data for wells with a finite-conductivity vertical fracture based on bi-linear flow theory, which accounts for linear flow in both the vertical fracture and reservoir. Cinco-Ley and Samaniego demonstrated that the bi-linear flow regime yields a quarter-root time signature when plotted against pressure, and is inversely proportional to the product of the fracture height and the square-root of fracture conductivity.

For use in evaluating pressure build-up test information, Bourdet et al. (1983) developed type curves of the dimensionless pressure derivative solution versus dimensionless time on a log-log scale (initially only for the case of infinite-acting radial flow). Bourdet et al. (1989) provided a well-test interpretation methodology based on the analysis of the pressure derivative function. Larson and Hegre (1994) conducted a study of the pressure transient behavior of horizontal wells with single or multiple vertical fractures and concluded that fracture performance is dependent on both the fracture conductivity and hydraulic fracture spacing. Al-Kobaisi et al. (2006) conducted a simulation study to assess the impact of hydraulic fracture properties on early-time flow regimes, as well as the identify pressure transient characteristics particular to hydraulically fractured, horizontal wells. From the study, Al-Kobaisi et al. concluded that the fracture geometry, fracture properties and non-Darcy flow greatly impact the flow regimes as well as the analysis of the pressure build-up data.

Cheng (2011) conducted a sensitivity study on pressure transient characteristics for a hydraulically fractured, horizontal shale gas well. The study concluded that matrix permeability, fracture conductivity, fracture spacing, and the existence of a stimulated zone impacted the pressure transient behavior of a well. However, the permeability of the stimulated zone, gas desorption and stress-dependent fracture conductivity appear to have only minor or even negligible effects on the pressure transient behavior of a well. Mayerhofer et al. (2011) conducted a field study of Marcellus Shale hydraulically fractured, horizontal gas wells and concluded that the pressure build-up analysis did not provide a clear interpretation of reservoir quality and stimulation effectiveness because for these cases, significant pressure communication was observed between wells.

CHAPTER III

TIME-RATE ANALYSIS

In this chapter, we demonstrate the applicability of the proposed production analysis workflow by applying the methodology (see **Figure 1.4**) to the two field examples from a shale gas reservoir. We selected these wells because they are representative of either linear or boundary-dominated flow regimes experienced by the other wells in the field. We also apply an expanded form of the proposed workflow to all thirty wells provided for this work, and the results for these additional wells are included in **Appendix C**.

3.1 Field Example 10 — Apparent Boundary-Dominated Flow Regime

In this case, the well has been producing for more than a year and a half, and the gas flowrate and calculated flowing bottomhole pressure data are shown in **Figure 3.1**. We reviewed the flowrate and pressure history for data which show the effects of shut-in periods, evidence of liquid loading, or obvious surface operational changes; and we have filtered (edited) the data accordingly. We observe that the well has almost continuous production with very little scatter in the data except for a one-month shut-in period beginning around 220 days of production.

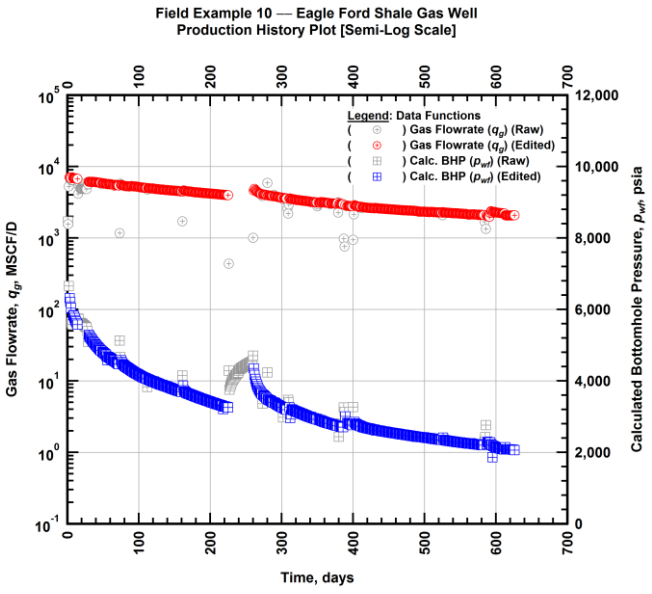

Figure 3.1 — (Semi-log Plot): Filtered production history plot — flowrate (q_g) and calculated bottomhole pressure (p_{wf}) versus production time.

In **Figure 3.2** through **Figure 3.5**, we plot the gas flowrate versus production time, the inverse of the gas flowrate versus material balance time, the pseudopressure drop-normalized gas flowrate versus production time, and the rate-normalized pseudopressure drop versus production time respectfully on a log-log scale to identify the current and previous flow regimes experienced by the well. We overlay the flow regime lines, described below, on the data plotted in the figures to aid in the flow regime determination (Houzé et al., 2012):

- A linear trend with a positive/negative quarter-slope suggests a bi-linear flow regime.
- A linear trend with a positive/negative half-slope suggests a linear flow regime.
- A linear trend with a positive/negative unit-slope suggests a boundary-dominated flow regime.

We observe both a quarter-slope line, representing a bi-linear flow regime, and a unit slope line, representing depletion or boundary-dominated flow regime, fit portions of the data. Therefore, we determine that the well appears to be exhibiting depletion or boundary-dominated flow beginning at approximately 300 days of production.

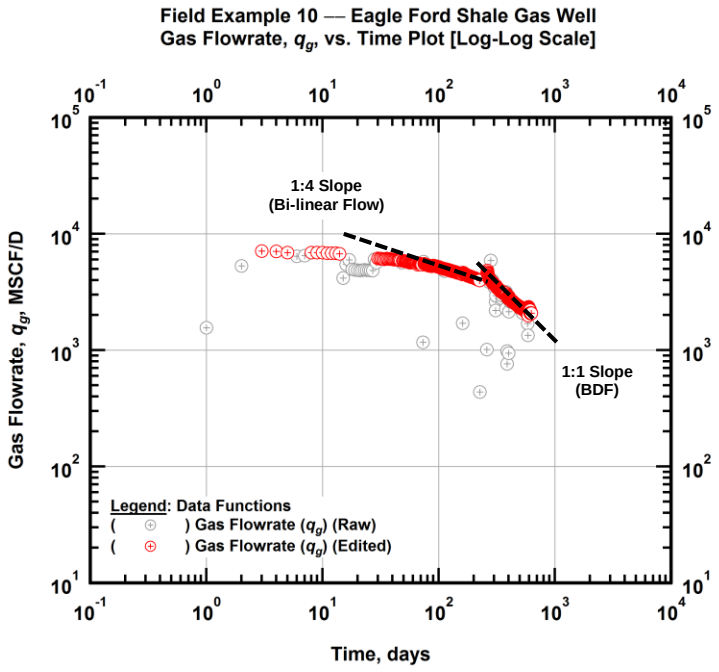

Figure 3.2 — (Log-Log Plot): Filtered gas flowrate production history and flow regime identification plot — gas flowrate (q_g) versus production time.

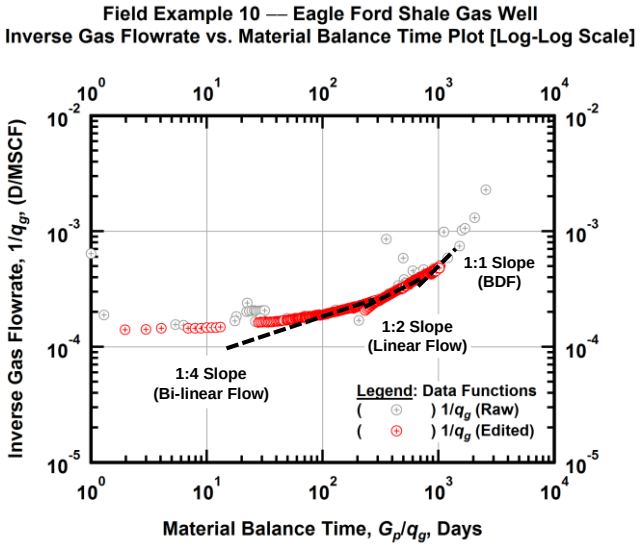

Figure 3.3 — (Log-log Plot): Filtered inverse rate with material balance time plot — inverse gas flowrate ($1/q_g$) versus material balance time (G_p/q_g).

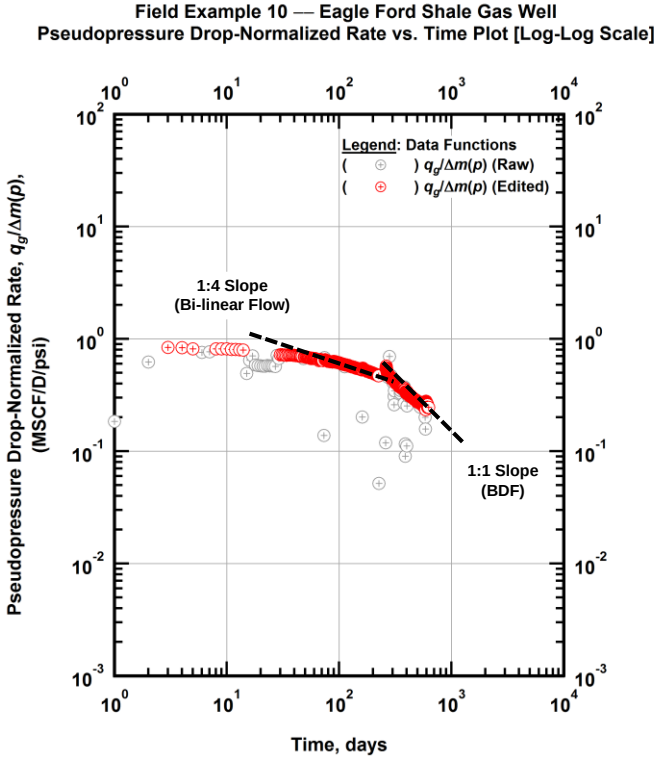

Figure 3.4 — (Log-log Plot): Filtered normalized rate production history plot — pseudopressure drop-normalized gas flowrate ($q_g/\Delta m(p)$) versus production time.

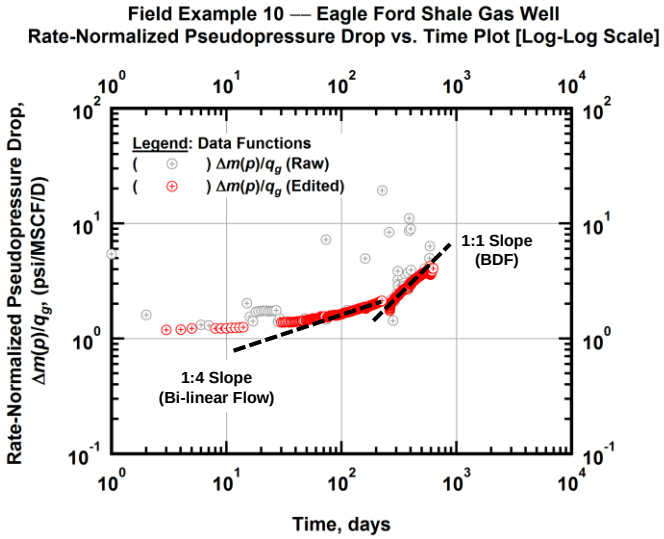

Figure 3.5 — (Log-log Plot): Filtered normalized pseudopressure drop production history plot — rate-normalized pseudopressure drop ($\Delta m(p)/q_g$) versus production time.

In **Figure 3.6**, we plot the filtered (*i.e.*, edited) calculated flowing bottomhole pressure data against the gas flowrate to establish a pressure-rate correlation for this well (Kabir and Izgec, 2006). The figure shows three primary areas of interest for the data correlation. First, we observe high rate and pressure data points that are likely the result of well cleanup effects and initial production operational adjustments. Several of these high data points are not representative production data for the well and are therefore filtered. Second, we observe several correlated transient responses that have similar slopes, which imply similar decline trends. The discontinuities seen with the middle and last transient responses are indicative of surface operations. Third, the lower rates and pressures do not display a definitive correlation and suggests inaccurate data acquisition and/or the presence of liquid loading. In **Figure 3.6** we apply present the same data points as the production history plot, **Figure 3.1**.

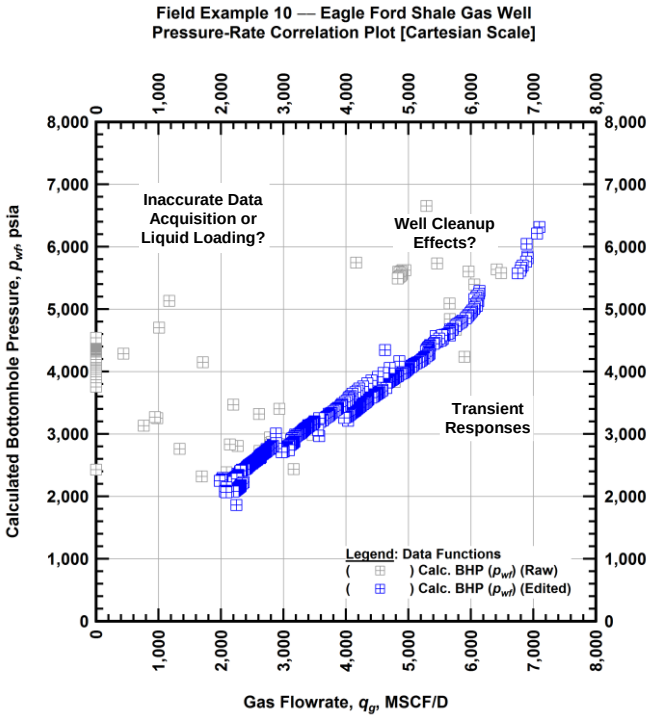

Figure 3.6 — (Cartesian Plot): Filtered rate-pressure correlation plot — calculated bottomhole pressure (p_{wf}) versus flowrate (q_g).

After completing our initial diagnostic analysis and filtering of the non-representative production data, we then fitted the Arps modified hyperbolic (**Figure 3.7**) and power-law exponential (**Figure 3.8**) time-rate decline relations to the loss-ratio (b), reciprocal of the loss-ratio (D), beta derivative (β), and gas flowrate (q_g).

In **Figure 3.7**, we observe a general match of the Arps modified hyperbolic model with the filtered gas flowrate, the loss-ratio (b), reciprocal of the loss-ratio (D) and beta derivative (β) data. The closeness of match by the model is consistent with the assertion that the well may have entered a depletion/boundary-dominated flow regime — which is a primary assumption of the Arps modified hyperbolic decline model.

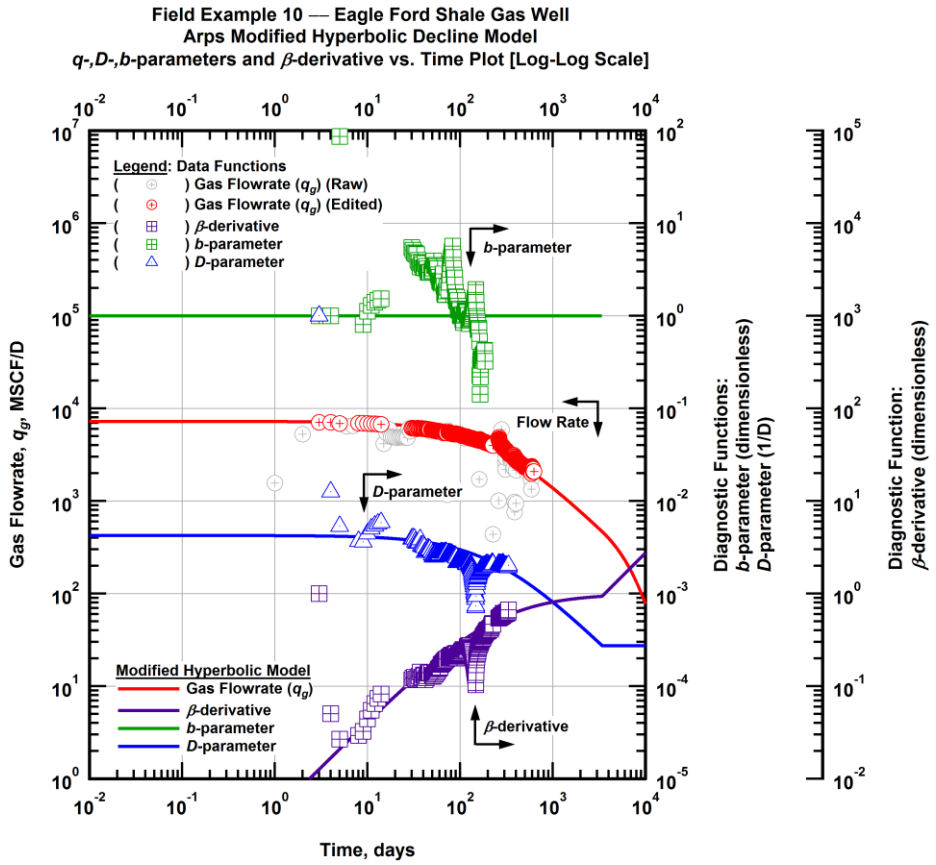

Figure 3.7 — (Log-Log Plot): Arps modified hyperbolic decline model plot — time-rate model and data gas flowrate (q_g), *D*- and *b*-parameters and β-derivative versus production time.

In **Figure 3.8**, we observe that the power-law exponential model closely matches the filtered gas flowrate, the loss-ratio (*b*), reciprocal of the loss-ratio (*D*) and beta derivative (β) data. Although both models fit the gas flowrate data, we observe that the power-law exponential decline model is better able to fit the loss-ratio, the derivative of the reciprocal of the loss-ratio, and the beta derivative data functions.

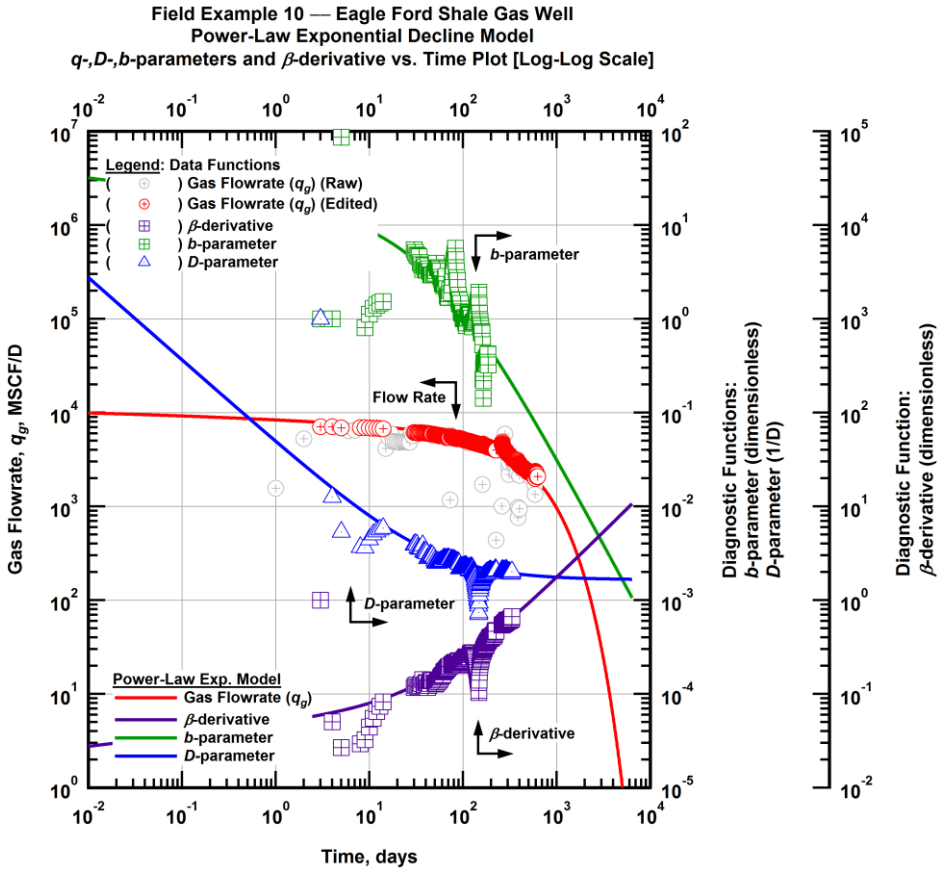

Figure 3.8 — (Log-Log Plot): Power-law exponential decline model plot — time-rate model and data gas flowrate (q_g), *D*- and *b*-parameters and β-derivative versus production time.

3.2 Field Example 24 — Linear Flow Regime

In this case, the well has been producing for a little more than a year, and the gas flowrate and calculated flowing bottomhole pressure data are shown in **Figure 3.9**. We observe no extended shut-in periods or extensive scatter in the production data and we only provide minimal data editing, generally for points at or near an operational shut-in of the well.

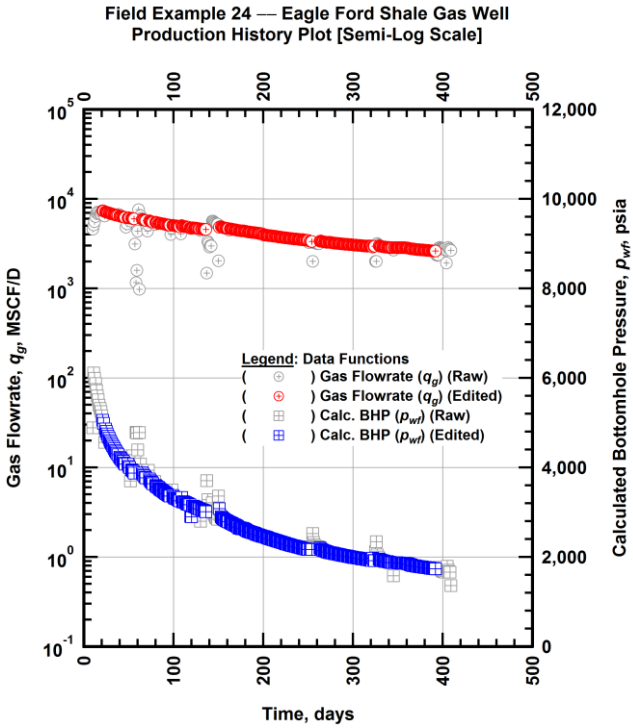

Figure 3.9 — (Semi-log Plot): Filtered production history plot — flowrate (q_g) and calculated bottomhole pressure (p_{wf}) versus production time.

In **Figure 3.10** through **Figure 3.13**, we plot the gas flowrate versus production time, the inverse of the gas flowrate versus material balance time, the pseudopressure drop-normalized gas flowrate versus production time, and the rate-normalized pseudopressure drop versus production time, respectfully on a log-log scale to identify the current and previous flow regimes experienced by the well. In this case we observe both a quarter-slope line representing a bi-linear flow regime at early times and a half-slope line representing linear flow behavior at later times. This well does not appear to exhibit depletion/boundary-dominated flow throughout its production history.

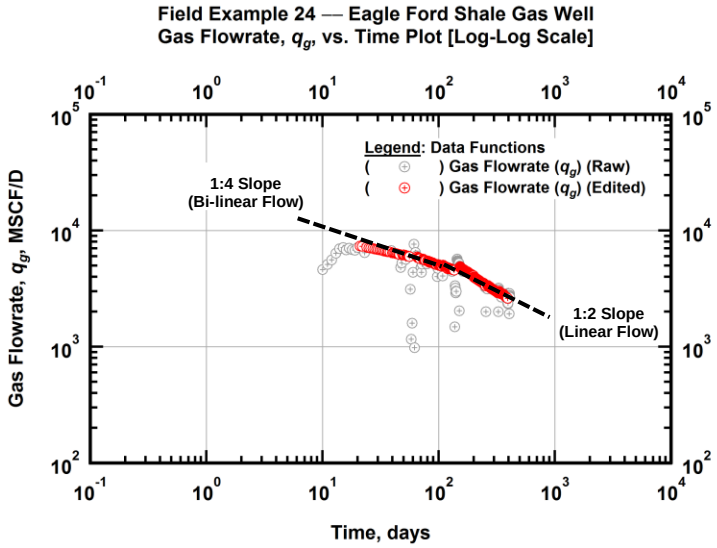

Figure 3.10 — (Log-Log Plot): Filtered gas flowrate production history and flow regime identification plot — gas flowrate (q_g) versus production time.

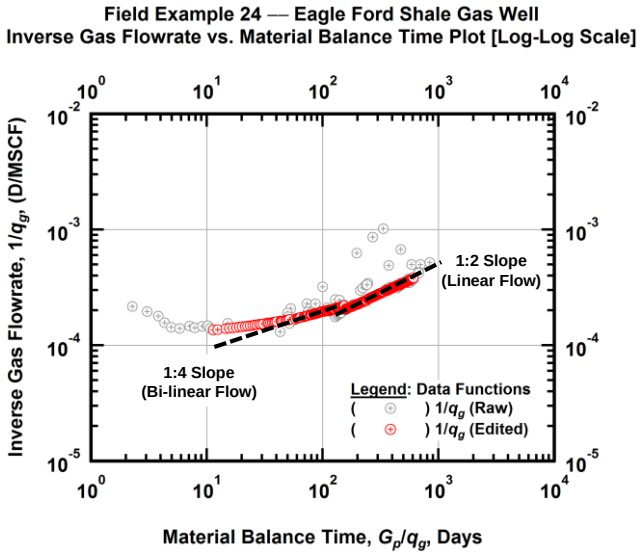

Figure 3.11 — (Log-log Plot): Filtered inverse rate with material balance time plot — inverse gas flowrate ($1/q_g$) versus material balance time (G_p/q_g).

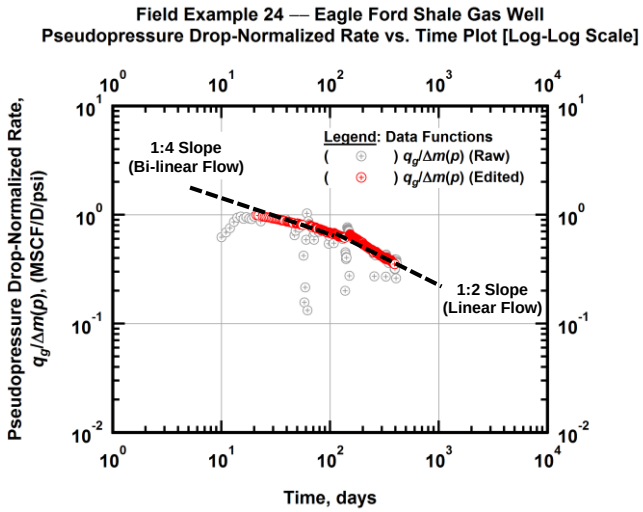

Figure 3.12 — (Log-log Plot): Filtered normalized rate production history plot — pseudopressure drop-normalized gas flowrate ($q_g/\Delta m(p)$) versus production time.

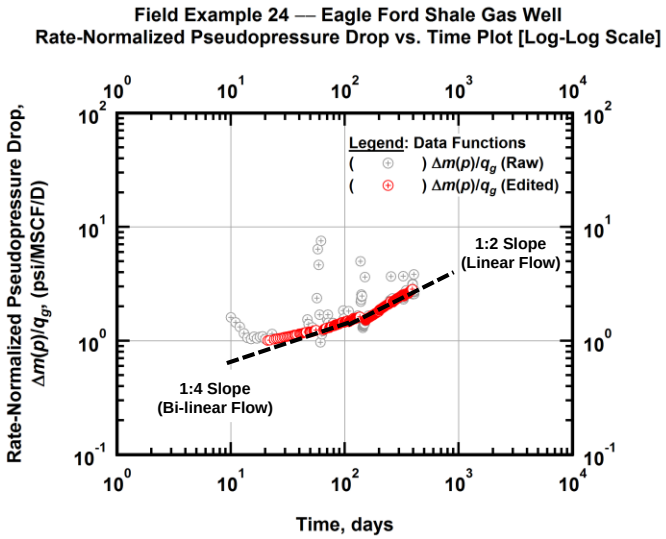

Figure 3.13 — (Log-log Plot): Filtered normalized pseudopressure drop production history plot — rate-normalized pseudopressure drop ($\Delta m(p)/q_g$) versus production time.

In **Figure 3.14**, we plot the filtered (*i.e.*, edited) calculated flowing bottomhole pressure data against the gas flowrate. As noted previously for this case, most of the spurious data are caused by the pressure and rate responses in the time vicinity of an operational shut-in. The overall trend illustrated in **Figure 3.14** suggests very good correlation of well performance and minimal analysis/interpretation issues.

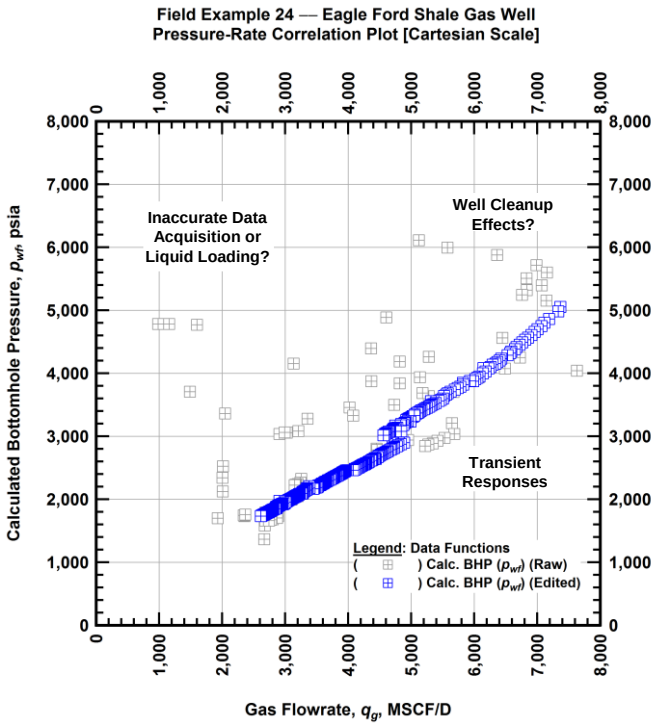

Figure 3.14 — (Cartesian Plot): Filtered rate-pressure correlation plot — calculated bottomhole pressure (p_{wf}) versus flowrate (q_g).

After the initial diagnostic analysis and data filtering, we then fit the Arps modified hyperbolic model to the data (**Figure 3.15**) as well as the power-law exponential (**Figure 3.16**). As done previously, we attempt to apply the time-rate relations simultaneously to the data trends for the loss-ratio (b), reciprocal of the loss-ratio (D), beta derivative (β), and gas flowrate (q_g). In **Figure 3.15**, we observe a (generally) good match of the Arps modified hyperbolic model various rate data functions, but in **Figure 3.16** we observe a somewhat better match of the power-law exponential time-rate model, particularly for the auxiliary data function (*i.e.*, the loss-ratio, the derivative of the reciprocal of the loss-ratio, and the beta derivative).

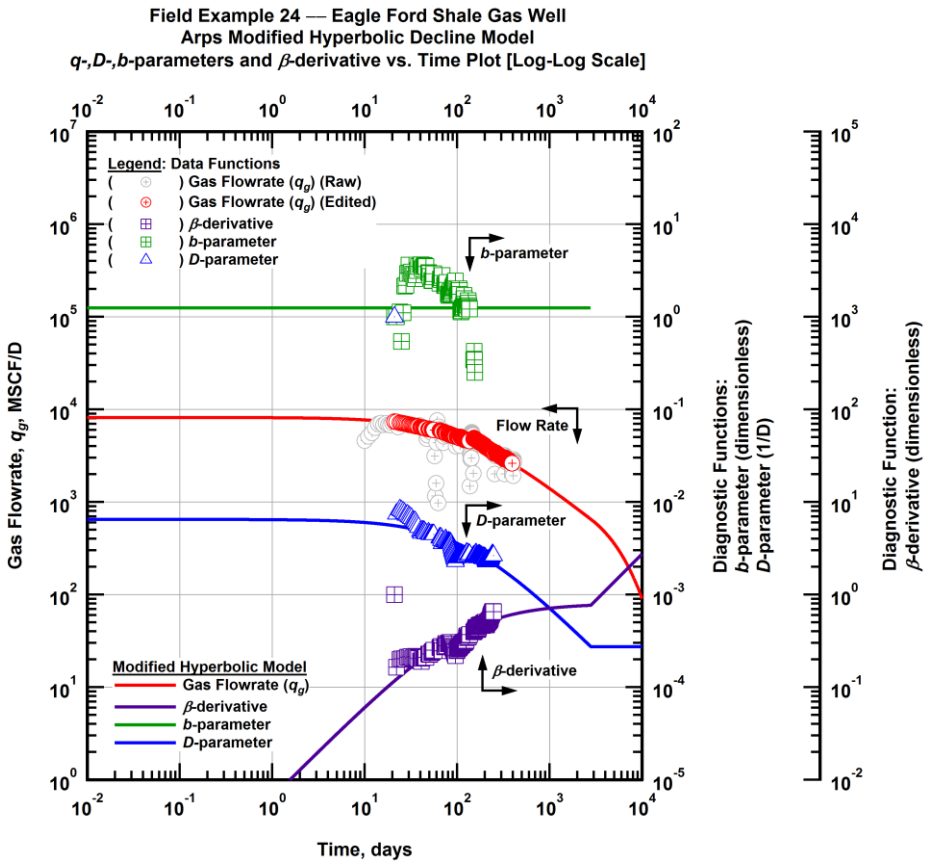

Figure 3.15 — (Log-Log Plot): Arps modified hyperbolic decline model plot — time-rate model and data gas flowrate (q_g), *D*- and *b*-parameters and β-derivative versus production time.

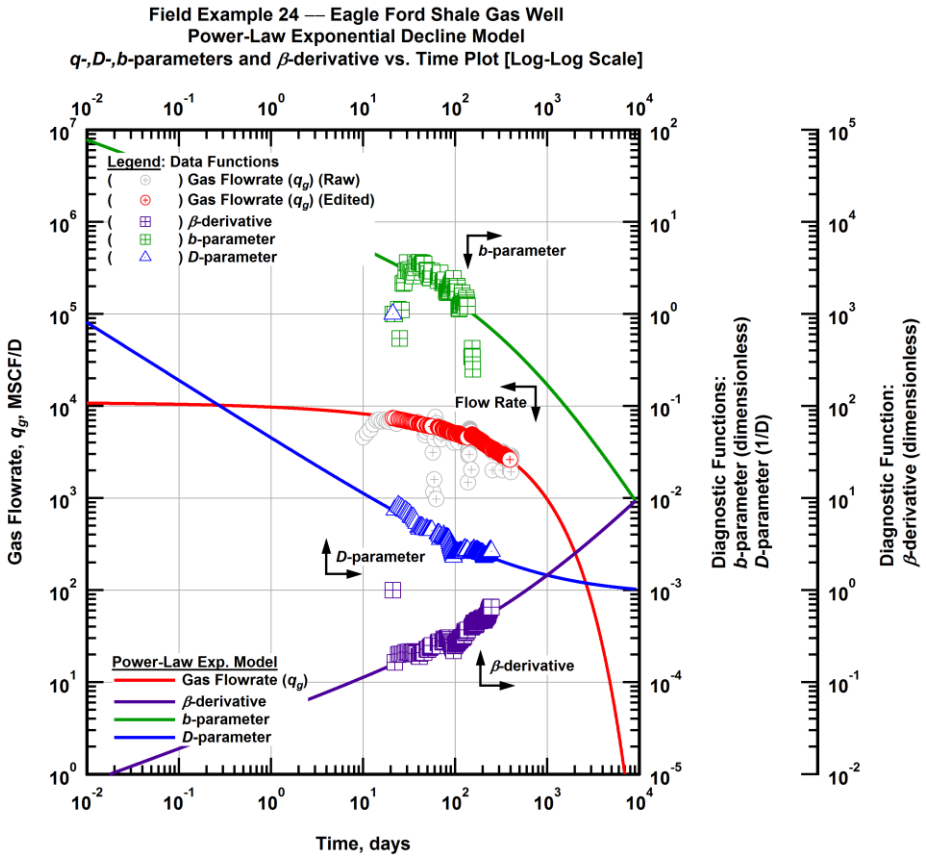

Figure 3.16 — (Log-Log Plot): Power-law exponential decline model plot — time-rate model and data gas flowrate (q_g), *D*- and *b*-parameters and β-derivative versus production time.

In **Table 3.1**, we show the current flow regime and the 30-year estimated ultimate recovery (EUR) calculated using the Arps modified hyperbolic rate model and the power-law exponential rate model, as well as the absolute percentage difference between the 30-year EUR-values calculated by the 2 decline models for each shale gas well field examples. We observe that the Arps modified hyperbolic rate model consistently calculates higher estimates of the 30-year EUR compared to the power-law exponential decline model. The difference in estimates range from 7 to 170 percent, with the average difference being 62.3 percent. The relatively high average difference suggests that some cases are more "modified hyperbolic" while others are more "power-law exponential." Comparison of EUR values in isolation, without knowledge of the governing flow regime can (and will) lead to inaccurate conclusions regarding performance.

Table 3.1 — 30-year estimated ultimate recovery (EUR) for the Arps modified hyperbolic and power-law exponential decline models.

Field Example	Current Flow Regime	Arps Modified Hyperbolic (BSCF)	Power-Law Exponential (BSCF)	30-yr EUR Absolute Difference (%)
1	BDF	2.36	1.95	21.0
2	BDF	3.81	2.56	48.8
3	Linear Flow	5.17	3.56	45.2
4	Linear Flow	6.16	3.61	70.6
5	Linear Flow	5.41	3.36	61.0
6	Linear Flow	5.92	4.51	31.3
7	Linear Flow	11.12	5.43	104.8
8	Linear Flow	6.01	5.61	7.1
9	Linear Flow	7.28	4.07	78.9
10	BDF	6.09	3.18	91.5
11	BDF	5.19	3.71	39.9
12	BDF	3.21	2.83	13.4
13	BDF	4.94	3.41	44.9
14	Linear Flow	6.89	3.98	73.1
15	Linear Flow	5.87	4.11	42.8
16	Linear Flow	8.43	4.27	97.4
17	Linear Flow	5.32	4.04	31.7
18	Linear Flow	4.80	2.98	61.1
19	Linear Flow	4.83	4.24	13.9
20	Linear Flow	3.09	4.04	23.5
21	Linear Flow	3.20	2.85	12.3
22	Bi-linear Flow	14.96	7.85	90.6
23	Linear Flow	11.89	7.87	51.1
24	Linear Flow	6.51	3.30	97.3
25	Linear Flow	15.82	10.13	56.2
26	Linear Flow	12.20	6.84	78.4
27	Linear Flow	11.79	5.44	116.7
28	Linear Flow	11.87	4.40	169.8
29	Linear Flow	12.08	5.23	131.0
30	Linear Flow	13.36	8.09	65.1

In **Figure 3.17**, we plot the EUR results estimated using the Arps modified hyperbolic rate model versus the EUR results estimated using the power-law exponential decline model on a log-log scale. This plot is a visual representation of the data contained in **Table 3.1**, and better illustrates the higher 30-year EUR values computed by the Arps modified hyperbolic decline model. A somewhat qualitative conclusion that could be stated based on the behavior shown in **Figure 3.17** is that for cases of lower EUR, the power-law exponential model is more appropriate, and for cases of higher EUR, the modified hyperbolic is more appropriate. We will continue to investigate the estimation of EUR in the remaining work provided in this thesis.

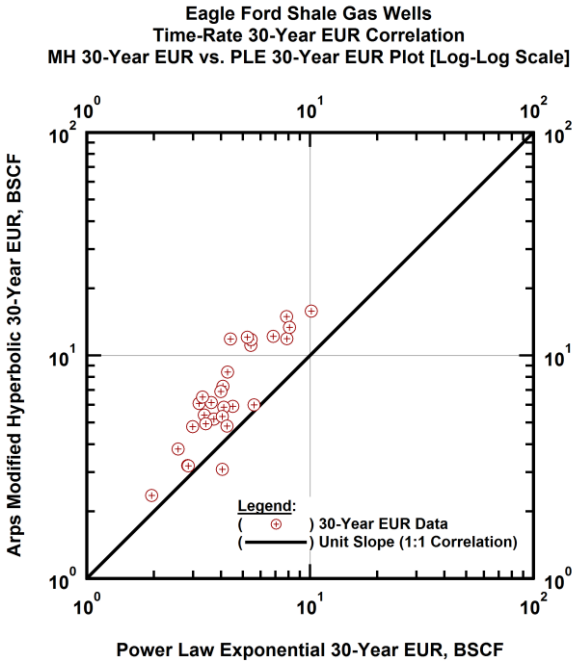

Figure 3.17 — (Log-Log Plot): Time-rate decline model 30-year estimated cumulative production volumes comparison plot — Arps modified hyperbolic decline model 30-year estimated cumulative production volumes versus power-law exponential decline model 30-year estimated cumulative production volumes.

CHAPTER IV

MODEL-BASED (TIME-RATE-PRESSURE) PRODUCTION ANALYSIS

In this chapter, we conduct analytical (time-rate-pressure) model-based production analysis for a given well and history match the gas flowrate, the calculated flowing bottomhole pressure, and the cumulative gas production by adjusting the fracture conductivity (F_c), fracture face skin (s), fracture half-length (x_f) and formation permeability (k) parameters. This is a standard practice in the industry, often referred to as "PA" (Production Analysis) or "RTA" (Rate-Transient Analysis). As caution, this methodology is quite robust and while the solutions/methods are well-documented, there are often challenges with being able to match only "part of the data" — we believe this is due to the nature of the reservoir/completion interface. For example, we can often match months or even years of production performance quite well, but after say, an extended shut-in, the character of the well performance changes (but the reservoir/completion model does not). We believe this "mismatch" could be related to the degradation of the completion as well as other factors. In this particular application, most if not all of the wells are matched will little obvious uncertainty.

We demonstrate this methodology using the two field example cases we have analyzed before. As with the example presented in **Chapter I**, we prepare four scenarios for each well where for two cases we assume differing percentage efficiencies of the perforation clusters generating a successful fracture, and for another two cases we assume only gas flow or a "total gas" flow computed from the gas, water, and condensate flowrates using a molar-equivalent calculation. We have also applied this approach to the remaining 28 field examples, and the results for all cases are included in **Appendix C**.

4.1 Field Example 10 — Apparent Boundary-Dominated Flow Regime

In the first model scenario, we use the original gas flowrate data and assume a 50 percent completion efficiency (*i.e.*, that the perforation clusters during the well completion succeeded in forming a propagated fracture (**Figure 1.20**)) — for this case it is assumed that there are 64 fractures for this well.

In **Figure 4.1**, we plot the original gas flowrate (q_g), the cumulative gas production (G_p) and the calculated bottomhole pressure (p_{wf}) production history with the model matches overlaid. The model has good agreement with the production data. In **Figure 4.2**, we plot the "Log-log" diagnostic plot of both the production data and model to check for agreement, and found the model closely fit the data except for the early-time data. In **Figure 4.3**, we plot the Blasingame diagnostic plot of both the production data and model to check for agreement, and once again found the model fit the closely fit the data except for the early-time data. It is also worth noting that the summary plot in **Figure 4.1** indicates that the pressure model match even captures the shape and magnitude of the approximately month-long shut in (from 220 to 260 days). The rate match is after the shut-in is less well-matched, but directionally also has the same shape (just not the same magnitude for the first 10-12 days).

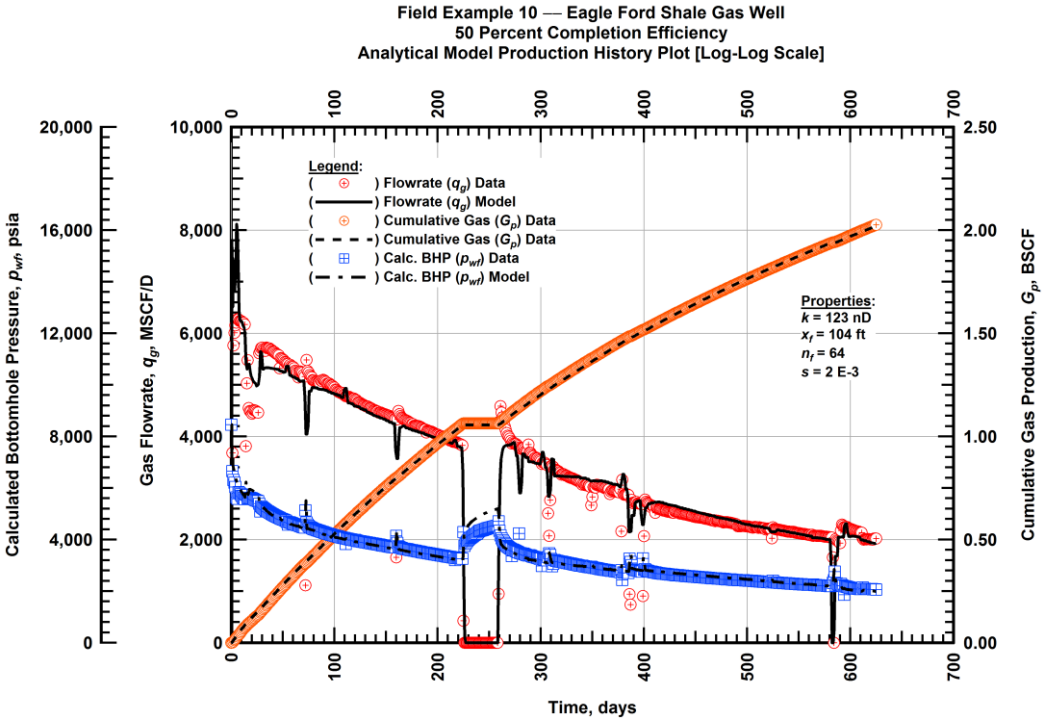

Figure 4.1 — (Cartesian Plot): Production history plot — original gas flowrate (q_g), cumulative gas production (G_p), calculated bottomhole pressure (p_{wf}) and 50 percent completion efficiency model matches versus production time.

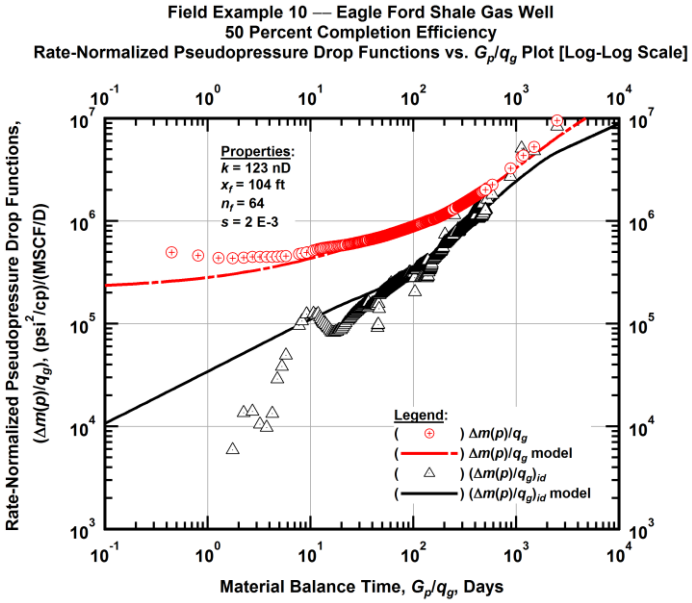

Figure 4.2 — (Log-log Plot): "Log-log" diagnostic plot of the original production data — rate-normalized pseudopressure drop ($\Delta m(p)/q_g$), rate-normalized pseudopressure drop integral-derivative $(\Delta m(p)/q_g)_{id}$ and 50 percent completion efficiency model matches versus material balance time (G_p/q_g).

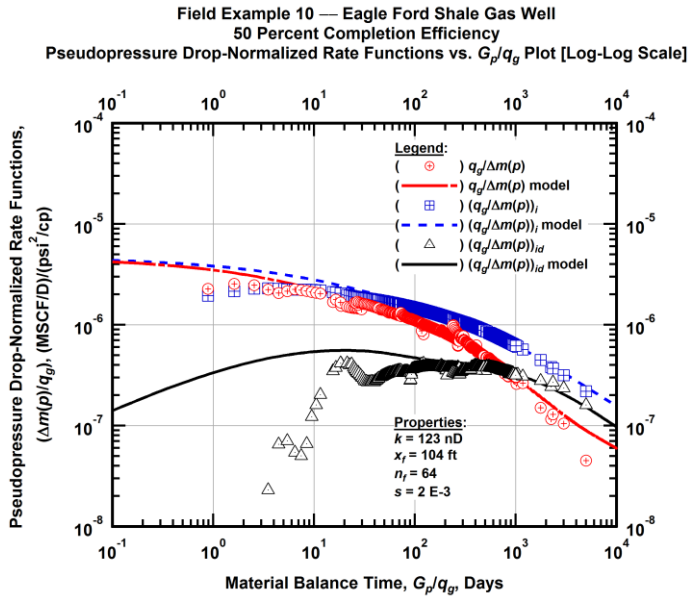

Figure 4.3 — (Log-log Plot): "Blasingame" diagnostic plot of the original production data — pseudopressure drop-normalized gas flowrate ($q_g/\Delta m(p)$), pseudopressure drop-normalized gas flowrate integral $(q_g/\Delta m(p))_i$, pseudopressure drop-normalized gas flowrate integral-derivative $(q_g/\Delta m(p))_{id}$ and 50 percent completion efficiency model matches versus material balance time (G_p/q_g).

In the second model scenario, we again use the original gas flowrate data but we now assume a 100 percent completion efficiency (*i.e.*, 128 fractures for the well). In **Figure 4.4**, we plot the original gas flowrate (q_g), the cumulative gas production (G_p) and the calculated bottomhole pressure (p_{wf}) production history with the model matches overlaid. The model has good agreement with the production data and is, in fact, difficult to distinguish from **Figure 4.1**. In **Figure 4.5**, we plot the "Log-log" diagnostic plot and in **Figure 4.6** we plot the Blasingame diagnostic plot — found the model fits the given data functions somewhat better than the 50 percent efficiency cases (*i.e.*, the 64 fracture case versus the 128 fracture case).

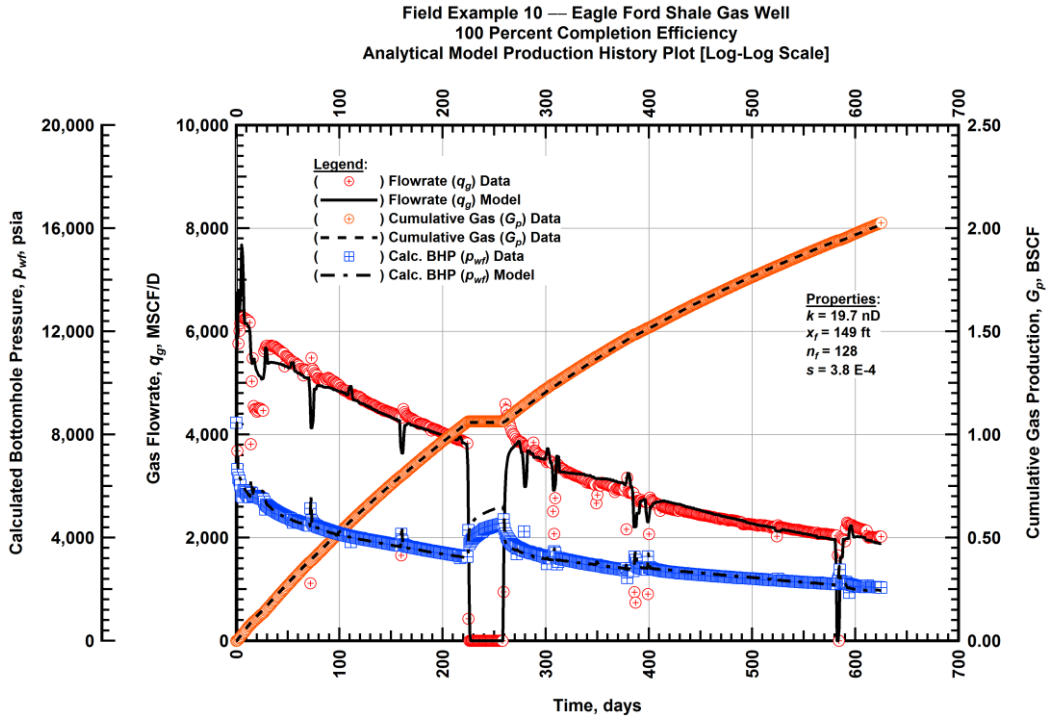

Figure 4.4 — (Cartesian Plot): Production history plot — original gas flowrate (q_g), cumulative gas production (G_p), calculated bottomhole pressure (p_{wf}) and 100 percent completion efficiency model matches versus production time.

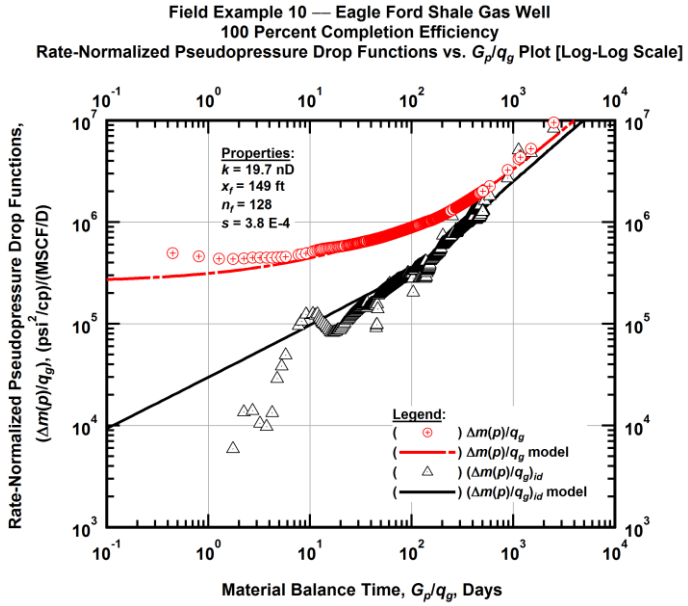

Figure 4.5 — (Log-log Plot): "Log-log" diagnostic plot of the original production data — rate-normalized pseudopressure drop ($\Delta m(p)/q_g$), rate-normalized pseudopressure drop integral-derivative $(\Delta m(p)/q_g)_{id}$ and 100 percent completion efficiency model matches versus material balance time (G_p/q_g).

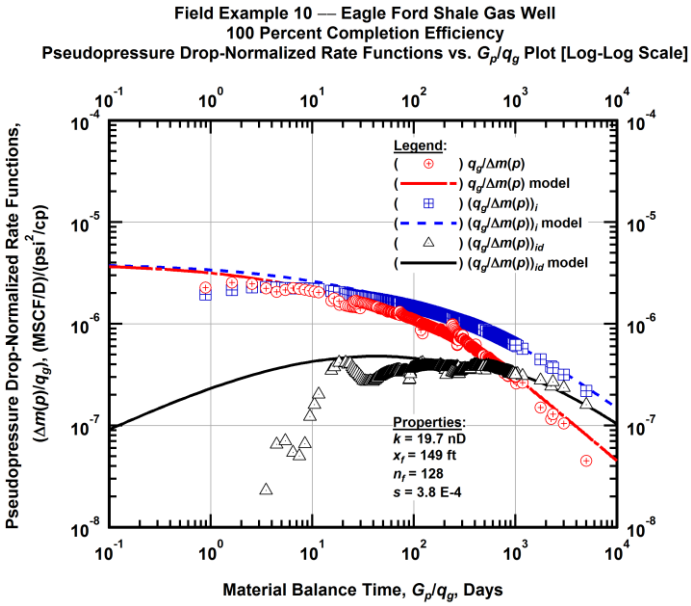

Figure 4.6 — (Log-log Plot): "Blasingame" diagnostic plot of the original production data — pseudopressure drop-normalized gas flowrate ($q_g/\Delta m(p)$), pseudopressure drop-normalized gas flowrate integral $(q_g/\Delta m(p))_i$, pseudopressure drop-normalized gas flowrate integral-derivative $(q_g/\Delta m(p))_{id}$ and 100 percent completion efficiency model matches versus material balance time (G_p/q_g).

In the third scenario, we use the PVT data and the gas, water, and condensate rates to estimate the "total" gas flowrate (on a molar basis). In this scenario we also assume a 50 percent completion efficiency (*i.e.*, 64 fractures for this well). In **Figure 4.7**, we plot the "total" gas flowrate (q_g), the cumulative gas production (G_p) and the calculated bottomhole pressure (p_{wf}) production history with the model matches overlain, and we again find a very good match (with similarly observations that the recovery of the total gas rate after a shut-in is less than expected). In **Figure 4.8** (the "log-log" diagnostic plot) and in **Figure 4.9** (the Blasingame diagnostic plot) we find essentially the same data match as for the "gas rate only" version of this case (*i.e.*, **Figure 4.2** and **Figure 4.3**). Qualitatively and quantitatively, the use of the "total gas rate" does not yield a significantly different match for this case over the "gas rate only" case.

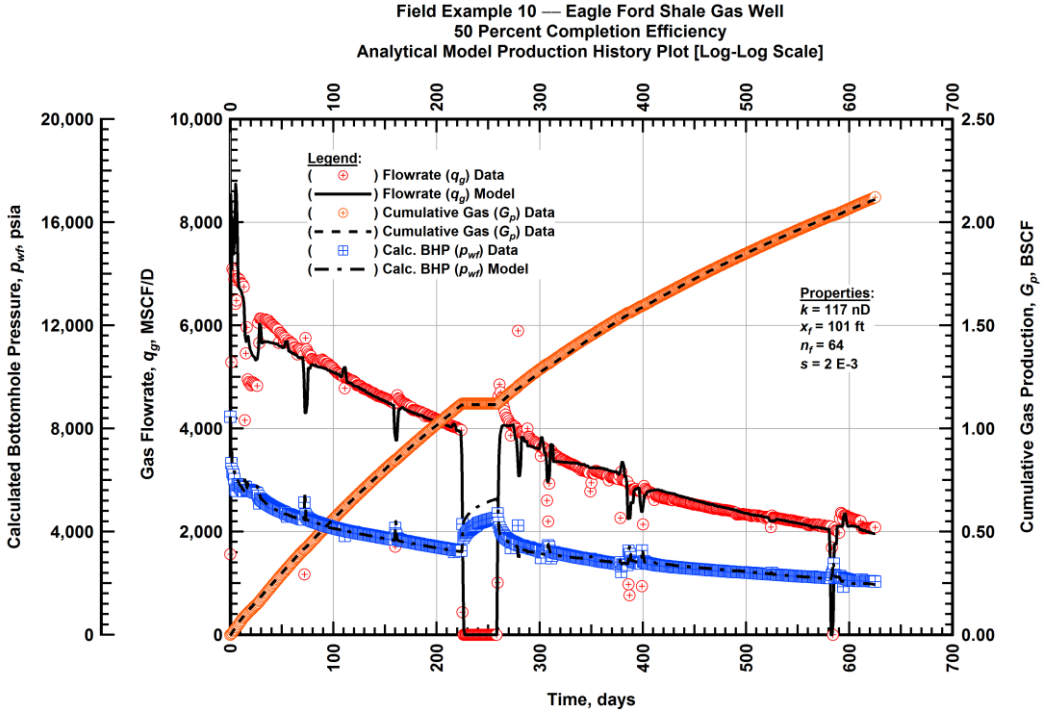

Figure 4.7 — (Cartesian Plot): Production history plot — revised gas flowrate (q_g), cumulative gas production (G_p), calculated bottomhole pressure (p_{wf}) and 50 percent completion efficiency model matches versus production time.

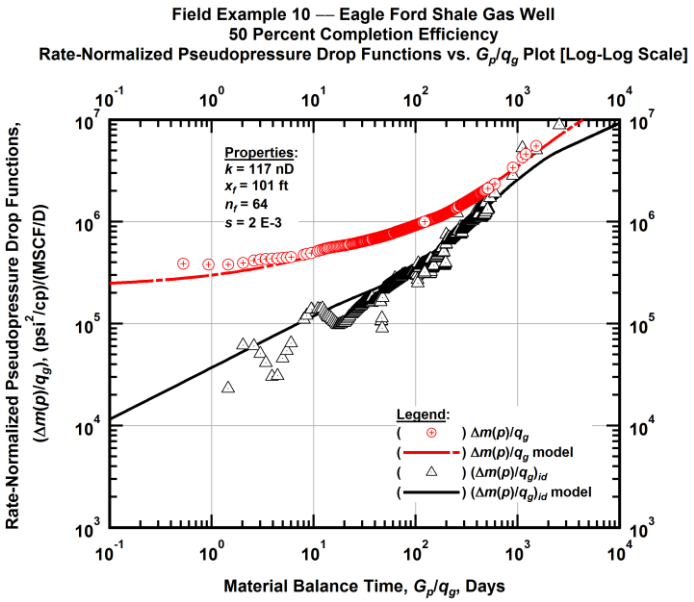

Figure 4.8 — (Log-log Plot): "Log-log" diagnostic plot of the revised production data — rate-normalized pseudopressure drop ($\Delta m(p)/q_g$), rate-normalized pseudopressure drop integral-derivative $(\Delta m(p)/q_g)_{id}$ and 50 percent completion efficiency model matches versus material balance time (G_p/q_g).

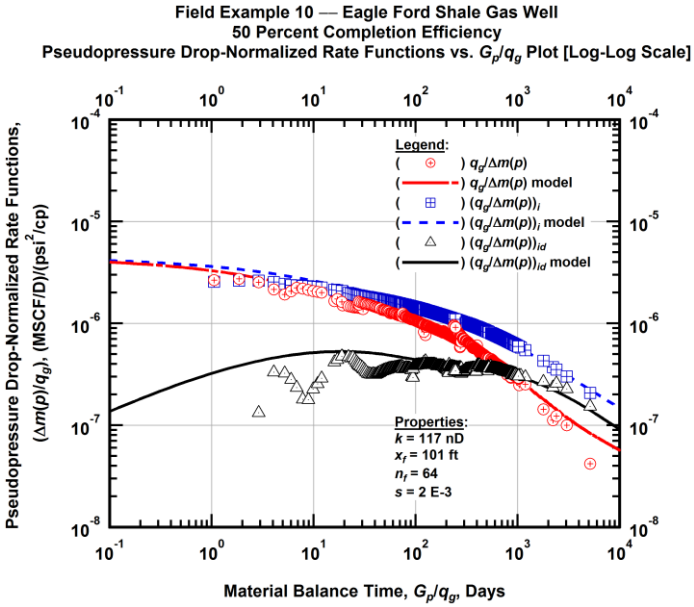

Figure 4.9 — (Log-log Plot): "Blasingame" diagnostic plot of the revised production data — pseudopressure drop-normalized gas flowrate ($q_g/\Delta m(p)$), pseudopressure drop-normalized gas flowrate integral $(q_g/\Delta m(p))_i$, pseudopressure drop-normalized gas flowrate integral-derivative $(q_g/\Delta m(p))_{id}$ and 50 percent completion efficiency model matches versus material balance time (G_p/q_g).

In the fourth scenario, we again use the total gas flowrate (computed essentially on a molar basis). In this case we assume a 100 percent completion efficiency (*i.e.*, 128 fractures for this well). **Figure 4.10** presents the "total gas" flowrate (q_g), the cumulative gas production (G_p) and the calculated bottomhole pressure (p_{wf}) production history with the model matches overlaid and in comparison to the match is approximately equivalent (the match in **Figure 4.10** has a slightly better match of the "total gas" flowrate, but the match in **Figure 4.10** appears to have a bit better match of the cumulative gas production). The diagnostic plots shown in **Figure 4.11** and **Figure 4.12** (*i.e.*, "log-log" and Blasingame plots, respectively) show very good matches, but these matches are not distinctly different than the "gas rate only" versions of these plots (**Figure 4.5** and **Figure 4.6**, respectively).

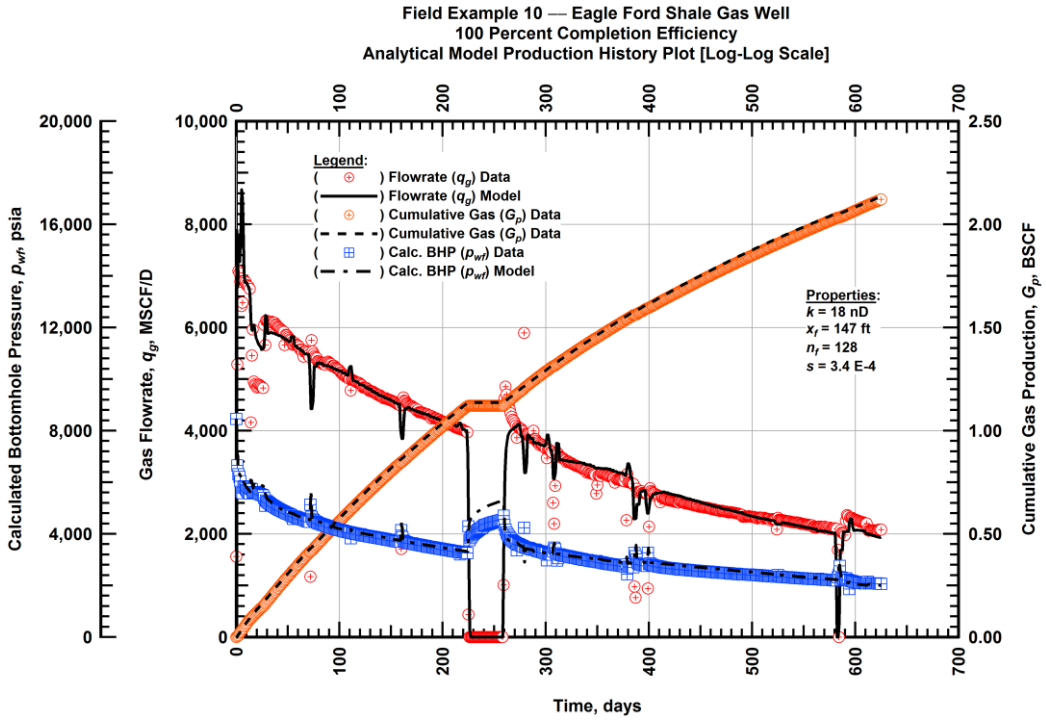

Figure 4.10 — (Cartesian Plot): Production history plot — revised gas flowrate (q_g), cumulative gas production (G_p), calculated bottomhole pressure (p_{wf}) and 100 percent completion efficiency model matches versus production time.

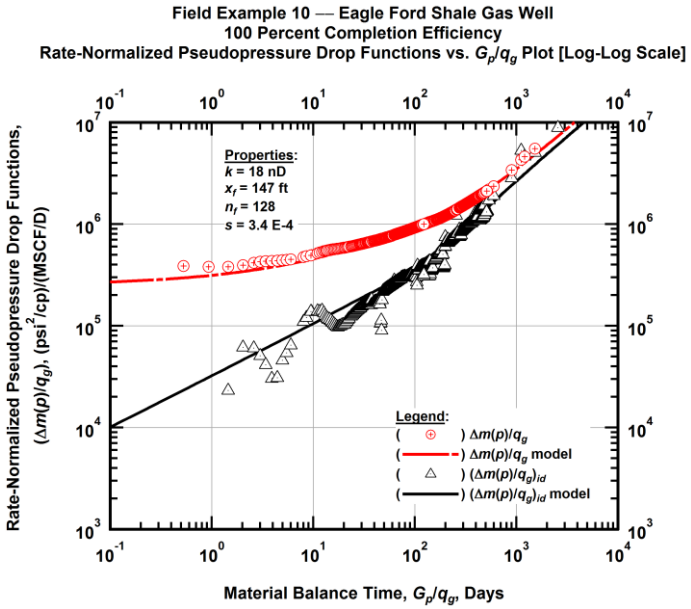

Figure 4.11 — (Log-log Plot): "Log-log" diagnostic plot of the revised production data — rate-normalized pseudopressure drop ($\Delta m(p)/q_g$), rate-normalized pseudopressure drop integral-derivative $(\Delta m(p)/q_g)_{id}$ and 100 percent completion efficiency model matches versus material balance time (G_p/q_g).

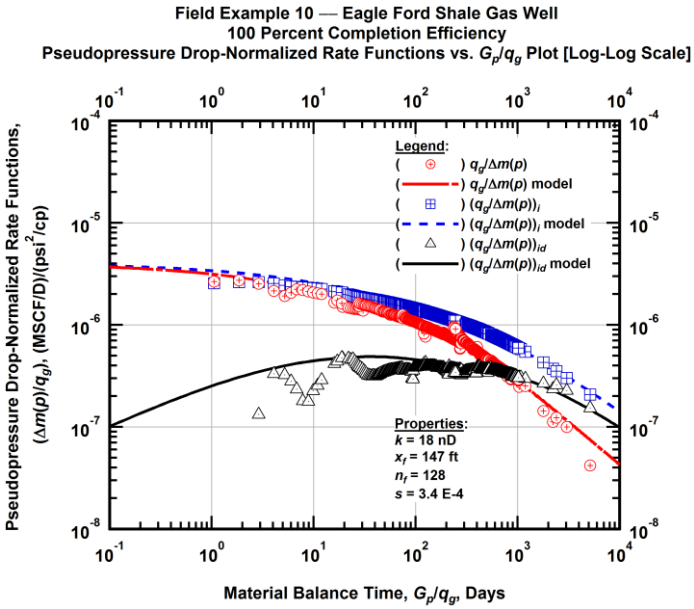

Figure 4.12 — (Log-log Plot): "Blasingame" diagnostic plot of the revised production data — pseudopressure drop-normalized gas flowrate ($q_g/\Delta m(p)$), pseudopressure drop-normalized gas flowrate integral $(q_g/\Delta m(p))_i$, pseudopressure drop-normalized gas flowrate integral-derivative $(q_g/\Delta m(p))_{id}$ and 100 percent completion efficiency model matches versus material balance time (G_p/q_g).

In **Figure 4.13**, we plot the semi-log "total gas rate" versus time profiles estimated using the Arps modified hyperbolic and the power-law exponential rate model, as well as the profiles for the analytical reservoir models computed using 50 and 100 percent completion efficiencies. For these cases we note substantive differences in the forecasted total gas flowrates — in particular, the power-law exponential model demonstrates the most aggressive rate (decline) trend. By comparison, the modified hyperbolic trend is comparable to the analytical reservoir models, but the 50 percent completion efficiency case is actually the highest recovery case (most likely because the estimated permeability for this case is more than 6 times higher than the estimated permeability for the 100 percent completion efficiency case).

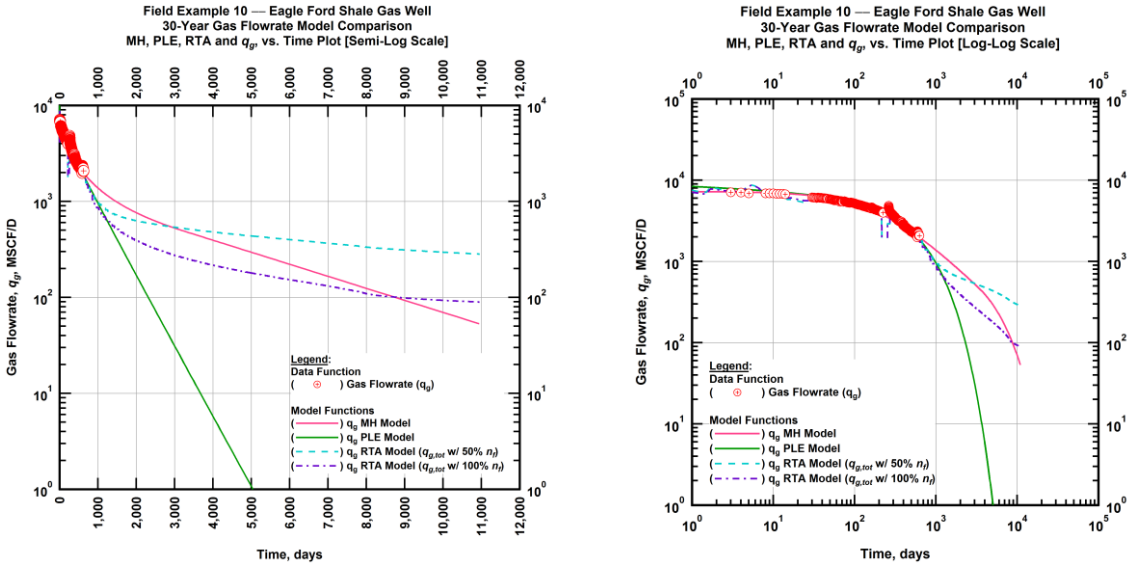

A **B**

Figure 4.13 — (A — Semi-Log Plot) and (B — Log-Log Plot): Estimated 30-year revised gas flowrate model comparison — Arps modified hyperbolic decline model, power-law exponential decline model, and 50 percent and 100 percent completion efficiency RTA models revised gas 30-year estimated flowrate decline and historic gas flowrate data (q_g) versus production time.

In **Figure 4.14**, we 30-year estimated ultimate cumulative production estimated using the Arps modified hyperbolic and the power-law exponential rate model, as well as the profiles for the analytical reservoir models computed using 50 and 100 percent completion efficiencies. As with the comparison of the rate

profiles (**Figure 4.13**) discussed earlier, we see significant contrast in the forecasted cumulative production volumes as well. In particular, the trend computed using the power-law exponential relation shows significantly lower total recovery at 30 years (recall this is our proxy for the estimated ultimate recovery (EUR). The analytical model with 50 percent completion efficiency has the highest recovery — again, most likely due to the substantially higher permeability for this case (more than 6 times higher than the 100 percent completion efficiency case).

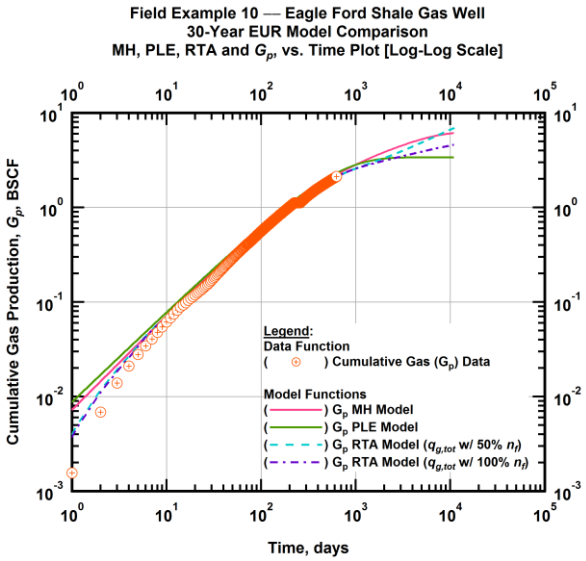

Figure 4.14 — (Log-log Plot): PVT revised gas 30-year estimated cumulative production volume model comparison — Arps modified hyperbolic decline model, power-law exponential decline model, and 50 percent and 100 percent completion efficiency RTA model estimated 30-year cumulative gas production volumes and historic cumulative gas production (G_p) versus production time.

In **Table 4.1**, we present the 30-year estimated cumulative gas production volumes (volumes are based on "gas only" and total gas rates) for both the empirical time-rate relations and the analytical model using 50 percent and 100 percent completion efficiencies — these volumes are thought of as proxies for the estimated ultimate recovery (or EUR).

Table 4.1 — 30-year estimated cumulative production (EUR), in units of BSCF, for the Arps modified hyperbolic, power-law exponential, and analytical time-rate-pressure decline models.

Arps Modified Hyperbolic (BSCF)	Power-Law Exponential (BSCF)	(gas only) Analytical Model ($q_{g,orig}$ w/ 50% n_f) (BSCF)	(gas only) Analytical Model ($q_{g,orig}$ w/ 100% n_f) (BSCF)	(total rate) Analytical Model ($q_{g,tot}$ w/ 50% n_f) (BSCF)	(total rate) Analytical Model ($q_{g,tot}$ w/ 100% n_f) (BSCF)
6.09	3.18	6.79	4.47	7.09	4.65

4.2 Field Example 24 — Linear Flow Regime

Based on our prior review, in this case our expectation is that the well performance will be dominated by the "linear flow" regime where the pressure profiles for the individual vertical fractures do not interfere, and we assume that these vertical fractures are of infinite fracture conductivity. In the first scenario, we use the original "gas only" flowrate data and we assume a 50 percent completion (i.e., 72 fractures for this case). In **Figure 4.15**, we provide the "summary" plot where the gas flowrate (q_g), the cumulative gas production (G_p) and the calculated bottomhole pressure (p_{wf}) production history are plotted along with the model match for each function is overlaid.

The model yields good agreement with the production data for the first 125 days of production, and slightly overestimates the production rate from approximately 200 to 320 days of production (this overestimation is also manifested in the cumulative gas production profile). In contrast, the match of the calculated flowing bottomhole pressure is excellent.

In **Figure 4.16** and **Figure 4.17**, we plot the "log-log" and Blasingame diagnostic plots, respectively — and we note that the matches for each function are very good, with a minor mismatch at early times. We would comment that these early time features are most likely due to the effects of data "extraction" (the process whereby the data functions are computed in the commercial software), this is a fairly well-known artifact of the point in time where the extraction is begun. Otherwise, the matches for this case are very good to excellent.

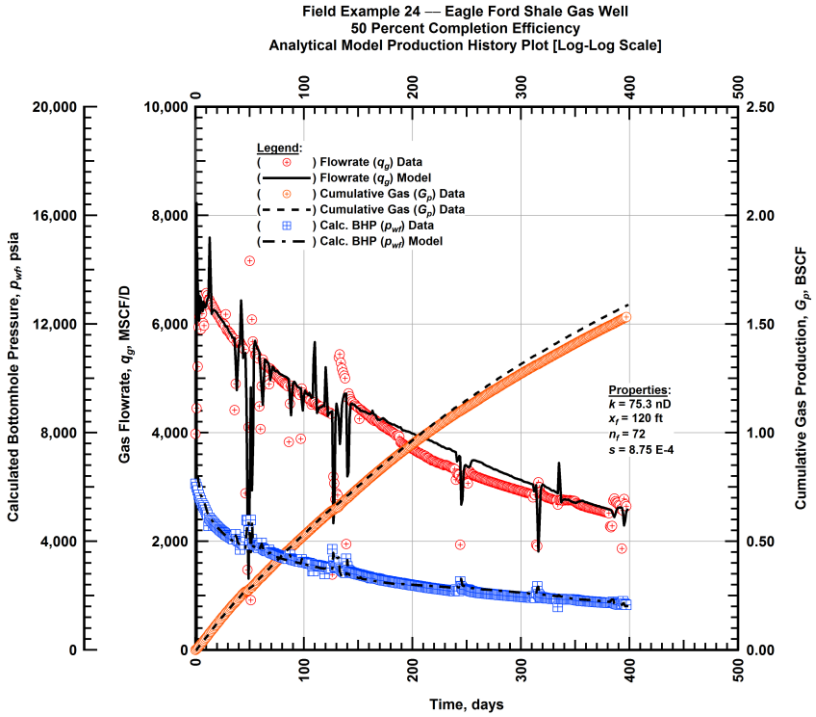

Figure 4.15 — (Cartesian Plot): Production history plot — original gas flowrate (q_g), cumulative gas production (G_p), calculated bottomhole pressure (p_{wf}) and 50 percent completion efficiency model matches versus production time.

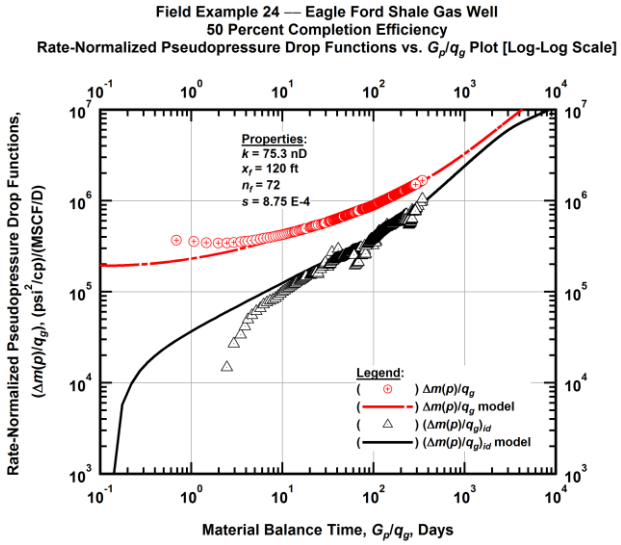

Figure 4.16 — (Log-log Plot): "Log-log" diagnostic plot of the original production data — rate-normalized pseudopressure drop ($\Delta m(p)/q_g$), rate-normalized pseudopressure drop integral-derivative $(\Delta m(p)/q_g)_{id}$ and 50 percent completion efficiency model matches versus material balance time (G_p/q_g).

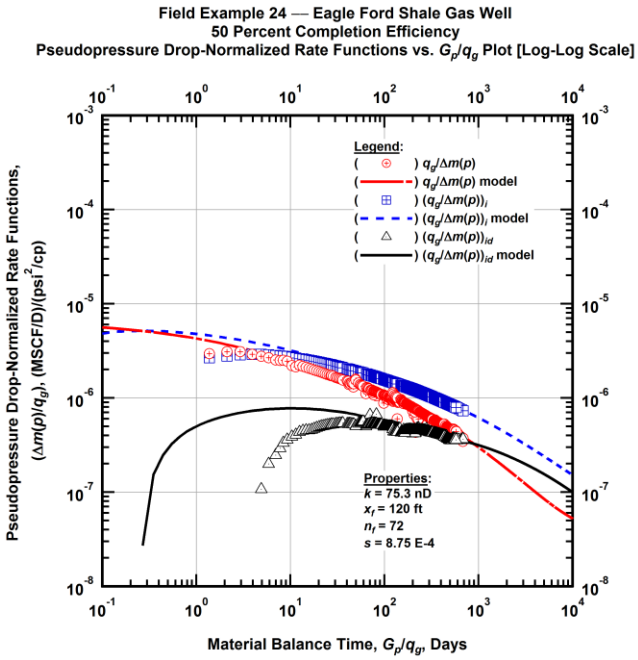

Figure 4.17 — (Log-log Plot): "Blasingame" diagnostic plot of the original production data — pseudopressure drop-normalized gas flowrate ($q_g/\Delta m(p)$), pseudopressure drop-normalized gas flowrate integral $(q_g/\Delta m(p))_i$, pseudopressure drop-normalized gas flowrate integral-derivative $(q_g/\Delta m(p))_{id}$ and 50 percent completion efficiency model matches versus material balance time (G_p/q_g).

In the second scenario, we again use the "gas only" flowrate data and we assume a 100 percent completion efficiency (*e.g.*, 144 fractures for this well). In **Figure 4.18** provide a summary plot of the data and model functions for the gas rate, cumulative gas production, and calculated flowing bottomhole pressures. The matches shown in **Figure 4.18** (100 percent completion efficiency) are essentially identical to the matches shown in **Figure 4.15** (50 percent completion efficiency) — the most significant difference (other than the number of fractures which varies by a multiple of 2) is the permeability estimates for these 2 cases which vary by a factor of more than 6.

We review the "log-log" and Blasingame plots for this case (**Figure 4.19** and **Figure 4.20**) and note extra-ordinary similarity (essentially identical matches) when we compare these plots for the 50 percent completion efficiency case (*i.e.*, **Figure 4.16** and **Figure 4.17**), again suggesting that there is an inter-

dependence of the permeability and the number of fractures (as well as a slight dependence on fracture half-length).

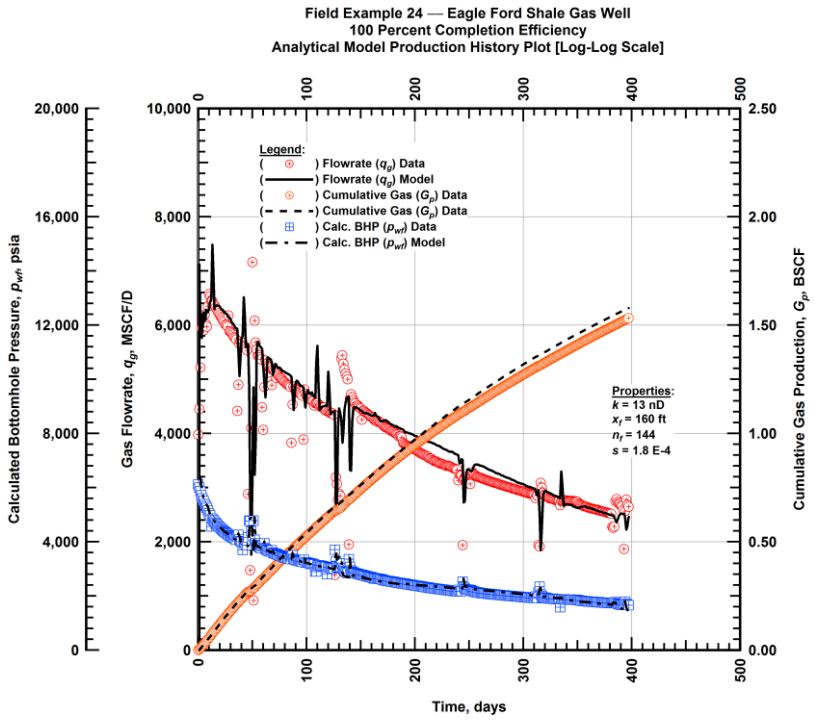

Figure 4.18 — (Cartesian Plot): Production history plot — original gas flowrate (q_g), cumulative gas production (G_p), calculated bottomhole pressure (p_{wf}) and 100 percent completion efficiency model matches versus production time.

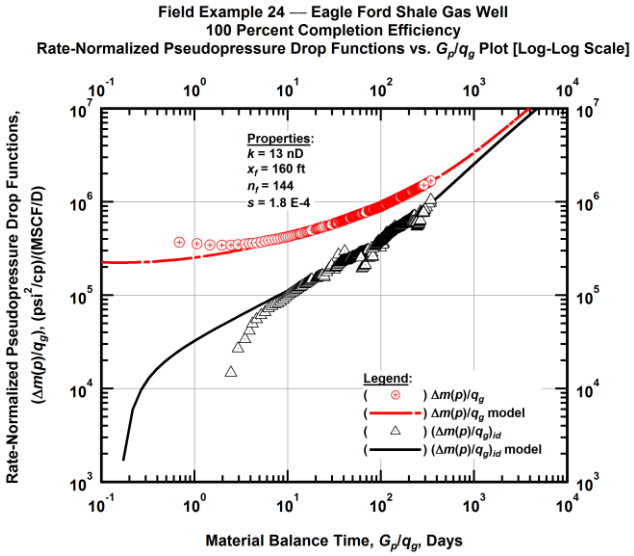

Figure 4.19 — (Log-log Plot): "Log-log" diagnostic plot of the original production data — rate-normalized pseudopressure drop ($\Delta m(p)/q_g$), rate-normalized pseudopressure drop integral-derivative $(\Delta m(p)/q_g)_{id}$ and 100 percent completion efficiency model matches versus material balance time (G_p/q_g).

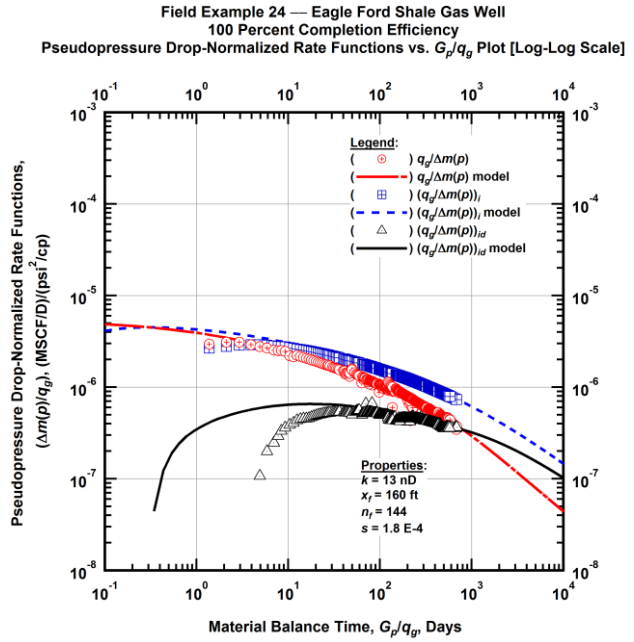

Figure 4.20 — (Log-log Plot): "Blasingame" diagnostic plot of the original production data — pseudopressure drop-normalized gas flowrate ($q_g/\Delta m(p)$), pseudopressure drop-normalized gas flowrate integral $(q_g/\Delta m(p))_i$, pseudopressure drop-normalized gas flowrate integral-derivative $(q_g/\Delta m(p))_{id}$ and 100 percent completion efficiency model matches versus material balance time (G_p/q_g).

In the next scenarios, we use "total gas" rate computed from the gas, water, and condensate rates, converted on an approximate molar basis into an equivalent gas flowrate. The expectation is that the "total gas" flowrate may capture more character than the "gas only" performance data. As we have done before, our first scenario assumes a 50 percent completion efficiency (or approximately 72 fractures for this well).

The summary (or history) plot with all data and model functions is shown in **Figure 4.21** — we note a somewhat better match of the rate and cumulative production functions compared to the original "gas only" case (**Figure 4.15**), but this observation is not definitive in that there are slight changes in parameters for this case (most notably, estimates of a somewhat shorter fracture half-length).

The "log-log" and Blasingame diagnostic plots (**Figure 4.22** and **Figure 4.23**, respectively) show essentially the same matches as were obtained for the "gas only" version of this case (*i.e.*, **Figure 4.16** and **Figure 4.17**). As with the discussion of the history plot for this case, the results for this case may be a bit non-unique given the interdependence of permeability, fracture half-length, and the number of fractures.

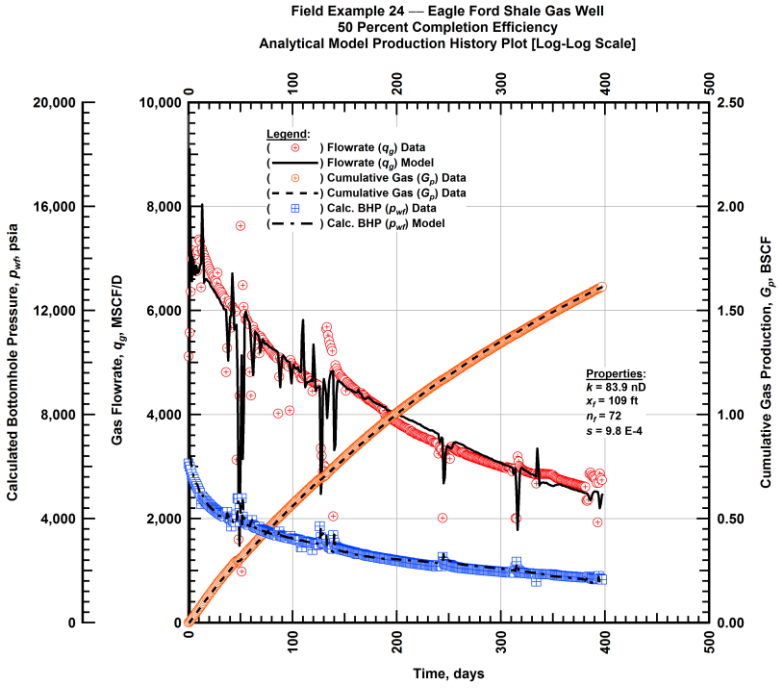

Figure 4.21 — (Cartesian Plot): Production history plot — revised gas flowrate (q_g), cumulative gas production (G_p), calculated bottomhole pressure (p_{wf}) and 50 percent completion efficiency model matches versus production time.

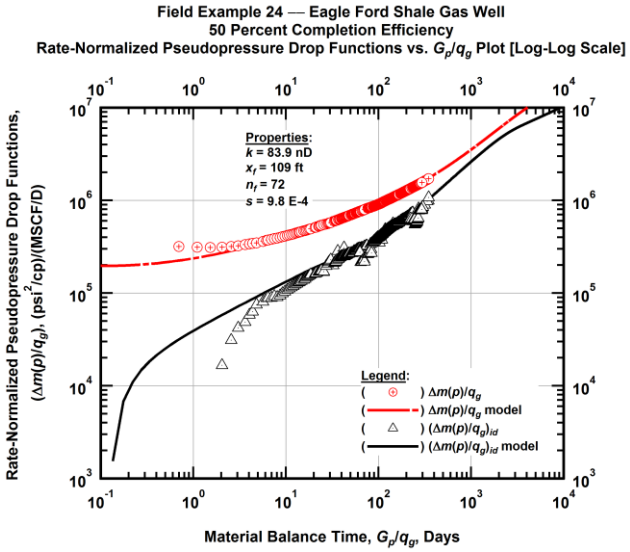

Figure 4.22 — (Log-log Plot): "Log-log" diagnostic plot of the revised production data — rate-normalized pseudopressure drop ($\Delta m(p)/q_g$), rate-normalized pseudopressure drop integral-derivative $(\Delta m(p)/q_g)_{id}$ and 50 percent completion efficiency model matches versus material balance time (G_p/q_g).

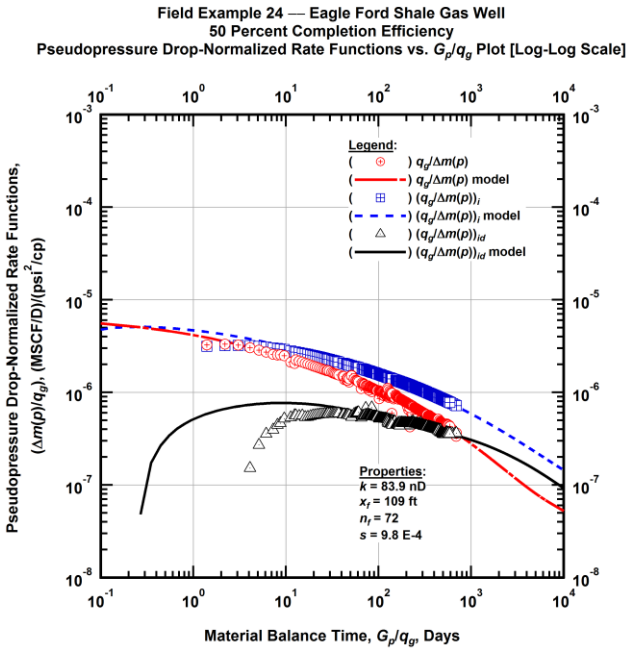

Figure 4.23 — (Log-log Plot): "Blasingame" diagnostic plot of the revised production data — pseudopressure drop-normalized gas flowrate ($q_g/\Delta m(p)$), pseudopressure drop-normalized gas flowrate integral $(q_g/\Delta m(p))_i$, pseudopressure drop-normalized gas flowrate integral-derivative $(q_g/\Delta m(p))_{id}$ and 50 percent completion efficiency model matches versus material balance time (G_p/q_g).

For the final scenario in this sequence we again use the "total gas" rates and volumes and we now assume a 100 percent completion efficiency (*i.e.*, 144 fractures for this well). The base "history match" plot is shown in **Figure 4.24** (rate, cumulative, and pressure functions) and the trends in this plot are *somewhat* better than those in the "gas only" version of this work (*i.e.*, **Figure 4.18**), using essentially the same model parameters, suggesting that the "total gas" variable may be more appropriate in this particular case. The "log-log" and Blasingame diagnostic plots (**Figure 4.25** and **Figure 4.26**) are, for all intents and purposes, identical to the "gas only" plots for this case (**Figure 4.19** and **Figure 4.20**), suggesting that the use of the "total gas" variables does not add substantively to the interpretation(s) for this case.

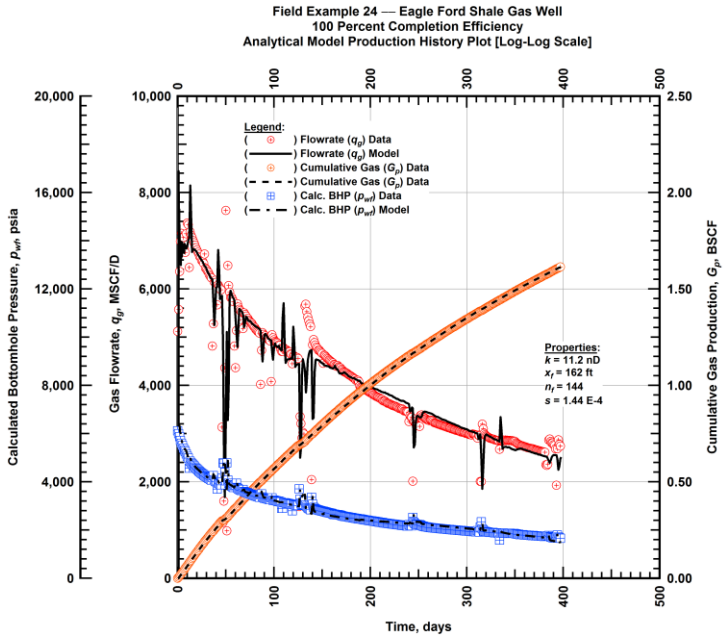

Figure 4.24 — (Cartesian Plot): Production history plot — revised gas flowrate (q_g), cumulative gas production (G_p), calculated bottomhole pressure (p_{wf}) and 100 percent completion efficiency model matches versus production time.

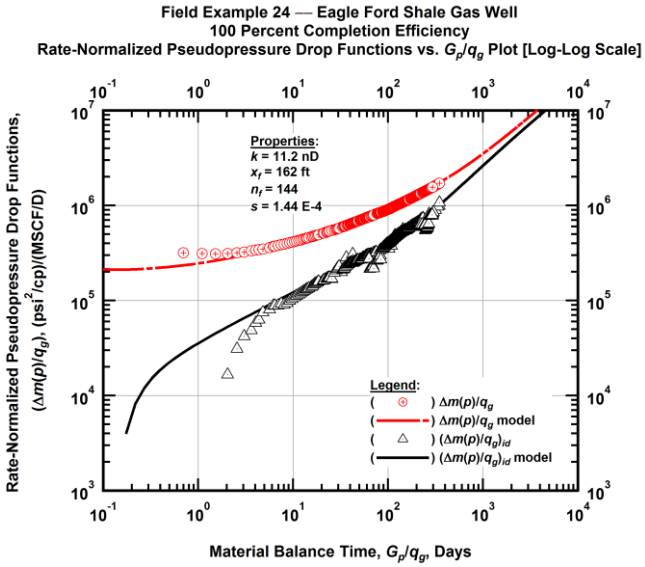

Figure 4.25 — (Log-log Plot): "Log-log" diagnostic plot of the revised production data — rate-normalized pseudopressure drop ($\Delta m(p)/q_g$), rate-normalized pseudopressure drop integral-derivative $(\Delta m(p)/q_g)_{id}$ and 100 percent completion efficiency model matches versus material balance time (G_p/q_g).

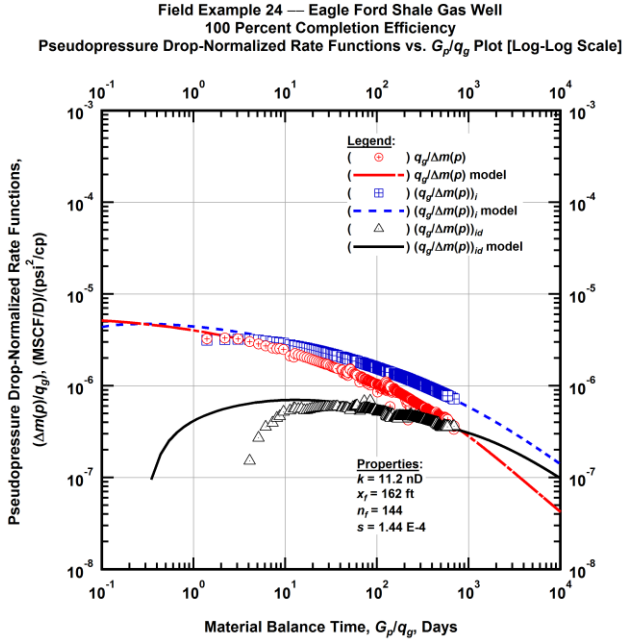

Figure 4.26 — (Log-log Plot): "Blasingame" diagnostic plot of the revised production data — pseudopressure drop-normalized gas flowrate ($q_g/\Delta m(p)$), pseudopressure drop-normalized gas flowrate integral $(q_g/\Delta m(p))_i$, pseudopressure drop-normalized gas flowrate integral-derivative $(q_g/\Delta m(p))_{id}$ and 100 percent completion efficiency model matches versus material balance time (G_p/q_g).

The forecasted production rate trends are presented in **Figure 4.27** and we note that the power-law exponential time-rate model is (by far) the most conservative estimator, and that the modified hyperbolic rate-time relation is the most liberal estimator, followed closely by the analytical model match for the case of a 50 percent completion efficiency (where this case actually overtakes the modified hyperbolic case at about 15 years). We note that the "total gas" functions are used for calibrating the empirical (time-rate) and analytical (time-rate-pressure) models

The forecasted cumulative production trends are shown with the "total gas" cumulative production data in **Figure 4.28**, and, as with the forecasted rate trends we note that the power-law exponential time-rate model is the low-end estimator and the modified hyperbolic is the high-end estimator. Recall that the cumulative production value at 30 years is taken to be our proxy for the estimated ultimate recovery (EUR). As with previous cases, it is our contention that the reason that the 50 percent completion efficiency time-rate-pressure model has the highest potential EUR is because of the permeability for this case is almost 8 times higher than the permeability for the 100 percent completion efficiency case.

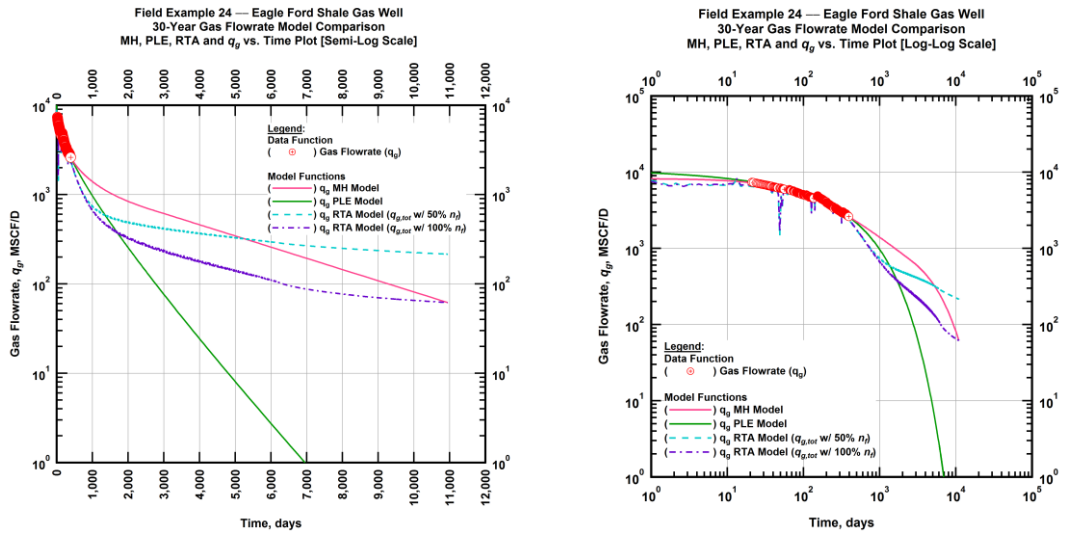

A **B**

Figure 4.27 — (A — Semi-Log Plot) and (B — Log-Log Plot): Estimated 30-year revised gas flowrate model comparison — Arps modified hyperbolic decline model, power-law exponential decline model, and 50 percent and 100 percent completion efficiency RTA models estimated 30-year revised gas flowrate decline and historic revised gas flowrate data (q_g) versus production time.

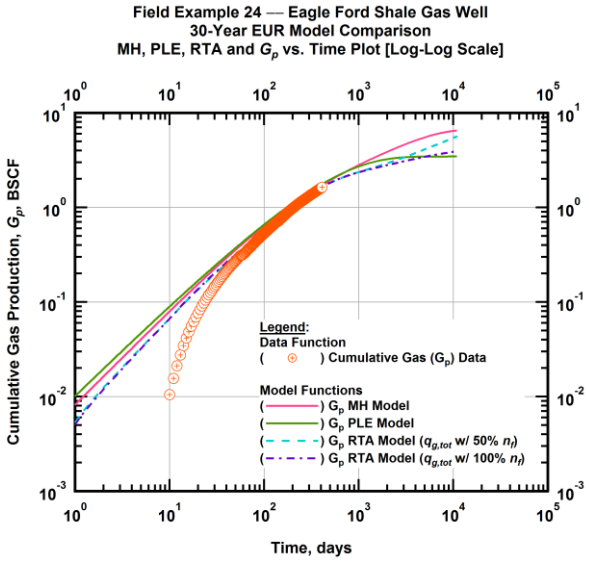

Figure 4.28 — (Log-log Plot): PVT revised gas 30-year estimated cumulative production volume model comparison — Arps modified hyperbolic decline model, power-law exponential decline model, and 50 percent and 100 percent completion efficiency RTA model estimated 30-year cumulative gas production volumes and historic cumulative gas production (G_p) versus production time.

The 30-year cumulative production values (*i.e.*, the proxies for EUR) are shown in **Table 4.2**.

Table 4.2 — 30-year estimated cumulative "gas only" and "total gas" production (EUR), in units of BSCF, for the Arps modified hyperbolic, power-law exponential, and analytical time-rate-pressure decline models. (Field Examples 10 and 24)

30-yr EUR Arps Modified Hyperbolic BSCF)	30-yr EUR Power-Law Exponential (BSCF)	(gas only) 30-yr EUR Analytical Model ($q_{g,orig}$ w/ 50% n_f) (BSCF)	(gas only) 30-yr EUR Analytical Model ($q_{g,orig}$ w/ 100% n_f) (BSCF)	(total rate) 30-yr EUR Analytical Model ($q_{g,tot}$ w/ 50% n_f) (BSCF)	(total rate) 30-yr EUR Analytical Model ($q_{g,tot}$ w/ 100% n_f) (BSCF)
7.28	4.07	6.91	4.87	6.85	5.02

In **Table 4.3** we present the table of results for the analytical models extrapolated to 30-year cumulative production for all 30 cases considered in this thesis. The difference in the 30-year cumulative production volumes ranges 4 percent to 63.5 percent, with the average and median difference being 29.6 percent and

26.3 percent respectively. The disparity in these results is most likely due to controlling factors such as permeability, fracture half-length, and the number of fractures.

A quick scan of Table 3 comparing the "gas only" and "total gas" results suggests only a minor deviations in these values, with the "total gas" results almost always being slightly higher. In **Figure 4.29** and **Figure 4.30**, we provide a log-log validation (cross-plot) of the data provided in **Table 4.3**. The results are plotted as the "gas only" results on the x-axis and the "total gas" results on the y-axis. As mentioned earlier, these results are typically very close (such that there is very little deviation seen on **Figure 4.29** and **Figure 4.30**).

Table 4.3 — 30-year estimated cumulative "gas only" and "total gas" production (EUR), in units of BSCF, for the analytical time-rate-pressure decline models. (all cases)

Field Example	(gas only) 30-yr EUR Analytical Model ($q_{g,orig}$ w/ 50% n_f) (BSCF)	(gas only) 30-yr EUR Analytical Model ($q_{g,orig}$ w/ 100% n_f) (BSCF)	(gas only) 30-yr EUR Absolute Difference (%)	(total rate) 30-yr EUR Analytical Model ($q_{g,tot}$ w/ 50% n_f) (BSCF)	(total rate) 30-yr EUR Analytical Model ($q_{g,tot}$ w/ 100% n_f) (BSCF)	(total rate) 30-yr EUR Absolute Difference (%)
1	4.77	4.98	4.2	4.95	5.16	4.1
2	3.72	3.06	21.6	3.74	3.10	20.6
3	6.41	4.28	49.8	5.79	4.30	34.7
4	4.48	3.59	24.8	4.70	3.73	26.0
5	5.03	4.14	21.5	5.06	5.08	0.4
6	6.96	5.17	34.6	7.11	5.14	38.3
7	8.97	6.75	32.9	8.54	6.76	26.3
8	4.56	3.82	19.4	4.76	3.93	21.1
9	6.91	4.87	41.9	6.85	5.02	36.5
10	6.79	4.47	51.9	7.09	4.65	52.5
11	4.63	4.04	14.6	4.81	4.21	14.3
12	2.62	2.16	21.3	2.70	2.27	18.9
13	4.13	3.53	17.0	4.18	3.62	15.5
14	6.58	4.75	38.5	6.68	4.89	36.6
15	8.02	5.24	53.1	8.22	5.35	53.6
16	5.65	4.85	16.5	5.98	5.04	18.7
17	3.60	3.12	15.4	3.79	3.15	20.3
18	3.71	3.20	15.9	3.82	3.37	13.4
19	3.64	3.28	11.0	3.85	3.49	10.3
20	3.12	1.94	60.8	3.19	2.13	49.8

Table 4.3 — Continued

Field Example	(gas only) 30-yr EUR Analytical Model ($q_{g,orig}$ w/ 50% n_f) (BSCF)	(gas only) 30-yr EUR Analytical Model ($q_{g,orig}$ w/ 100% n_f) (BSCF)	(gas only) 30-yr EUR Absolute Difference (%)	(total rate) 30-yr EUR Analytical Model ($q_{g,tot}$ w/ 50% n_f) (BSCF)	(total rate) 30-yr EUR Analytical Model ($q_{g,tot}$ w/ 100% n_f) (BSCF)	(total rate) 30-yr EUR Absolute Difference (%)
21	3.56	2.69	32.3	3.72	2.81	32.4
22	12.70	8.55	48.5	12.10	8.30	45.8
23	6.91	5.62	23.0	6.84	5.70	20.0
24	5.46	3.90	40.0	5.73	3.96	44.7
25	8.52	6.75	26.2	8.71	6.73	29.4
26	9.14	5.59	63.5	8.17	5.55	47.2
27	8.08	5.56	45.3	7.90	5.56	42.1
28	8.57	5.91	45.0	8.57	5.79	48.0
29	18.08	16.64	8.7	18.53	18.34	1.0
30	7.78	6.14	26.7	7.70	6.15	25.2

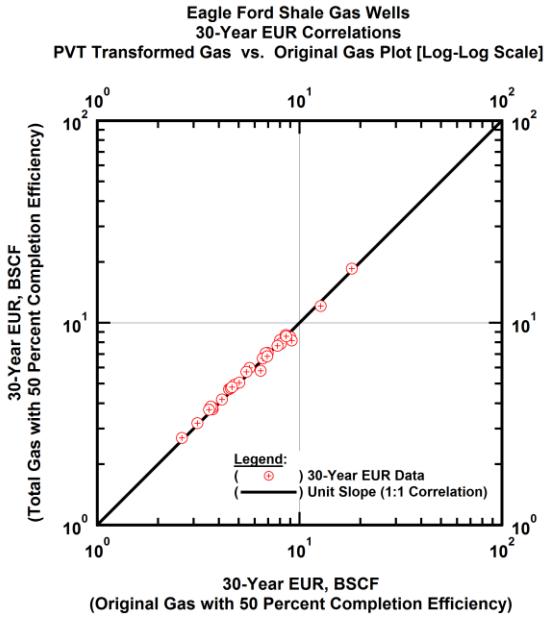

Figure 4.29 — (Log-log Plot): 30-year cumulative gas production correlation plot — PVT transformed gas flowrate with 50 percent completion efficiency 30-year estimated cumulative production versus original gas flowrate with 50 percent completion efficiency 30-year estimated cumulative production.

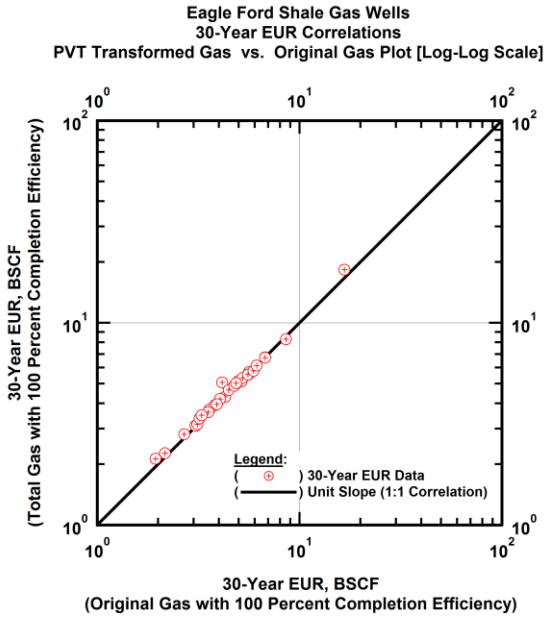

Figure 4.30 — (Log-log Plot): 30-year cumulative gas production correlation plot — PVT transformed gas flowrate with 100 percent completion efficiency 30-year estimated cumulative production versus original gas flowrate with 100 percent completion efficiency 30-year estimated cumulative production.

Figure 4.31 presents a validation cross-plot for case of the 50 percent completion efficiency results versus the 100 percent completion efficiency results given in **Table 4.3**, using both the "gas only" (or original gas flowrate data) and the "total gas" (or revised rate data). We believe that the difference in these cases is almost wholly due to the fact that the permeabilities for the 50 percent completion efficiency cases are 6-8 times *higher* than the permeabilities for the 100 percent completion efficiency cases.

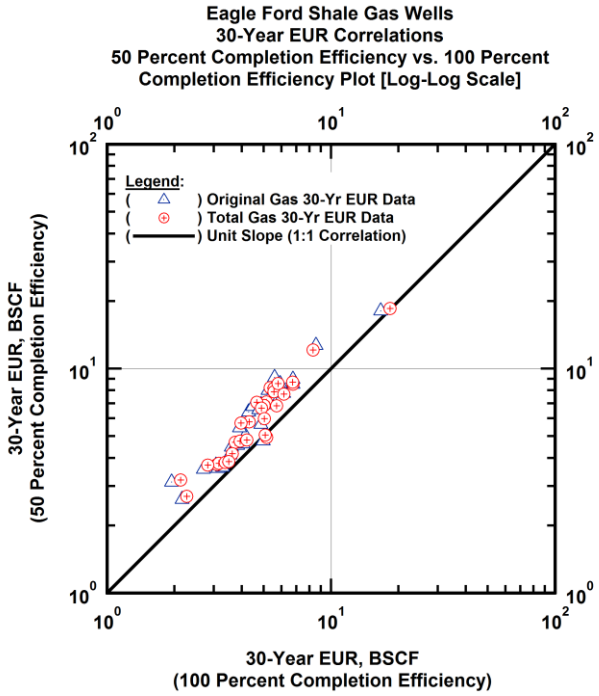

Figure 4.31 — (Log-log Plot): 30-year cumulative gas production correlation plot — PVT transformed or original gas flowrate with 50 percent completion efficiency 30-year estimated cumulative production versus PVT transformed or original gas flowrate with 100 percent completion efficiency 30-year estimated cumulative production.

In **Figure 4.32** we compare the EUR estimated using the modified hyperbolic and power-law exponential cases versus the model results for the 50 percent completion efficiency scenario. Similarly, in **Figure 4.33**, we compare the EUR estimated using the modified hyperbolic and power-law exponential cases versus the model results for the 100 percent completion efficiency scenario. In **Figure 4.32** we note the results for the modified hyperbolic case are almost always too high and the results for the power-law exponential case are almost always too low with compared to the model results for the 50 percent completion efficiency scenario. This is not unexpected given our earlier discussion that the modified hyperbolic model tends to be a liberal predictor and the power-law exponential model tends to be a conservative predictor. We would prefer to have a "tighter" band of data about the 1:1 correlation trend, but the results are somewhat as predicted.

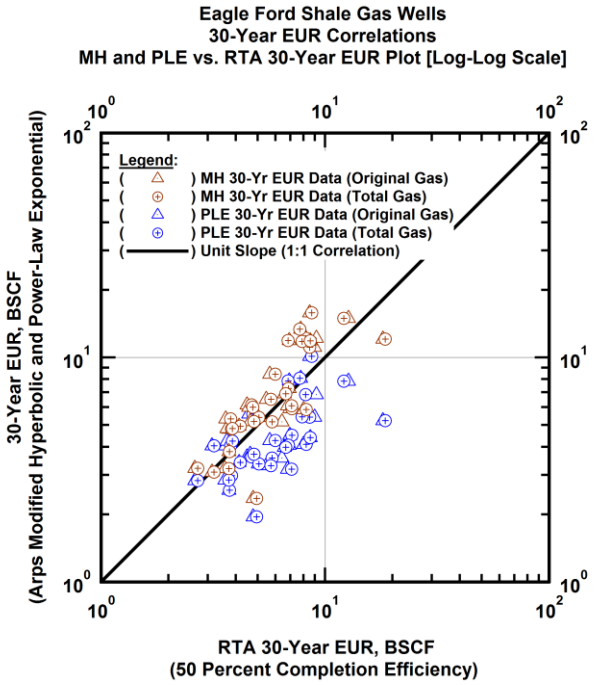

Figure 4.32 — (Log-log Plot): 30-year cumulative gas production correlation plot — Arps modified hyperbolic decline model calculated 30-year estimated cumulative production or power-law exponential decline model calculated 30-year estimated cumulative production versus PVT transformed or original gas flowrate with 50 percent completion efficiency 30-year estimated cumulative production.

Similarly, in **Figure 4.32** we note the results for the modified hyperbolic case are almost always too high when compared to the model results for the 100 percent completion efficiency scenario. However; the results for the power-law exponential case lie along the 1:1 correlation trend, indicating that the power-law exponential results are consistent with the model results for the 100 percent completion efficiency scenario. This is also (somewhat) not unexpected as the 100 percent completion efficiency scenario should provide the "best case results" and the power-law exponential case is most often thought to be representative of the actual reservoir behavior for tight gas and shale gas reservoir cases.

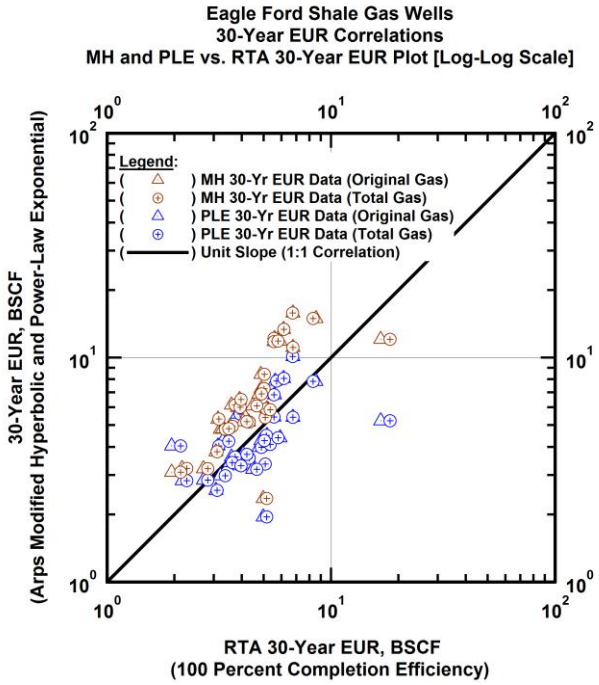

Figure 4.33 — (Log-log Plot): 30-year cumulative gas production correlation plot — Arps modified hyperbolic decline model calculated 30-year estimated cumulative production or power-law exponential decline model calculated 30-year estimated cumulative production versus PVT transformed or original gas flowrate with 100 percent completion efficiency 30-year estimated cumulative production.

CHAPTER V

RELATIONSHIP OF WELL PERFORMANCE WITH WELL AND RESERVOIR CHARACTERISTICS

5.1 Full Regression Model

In this chapter, we develop a regression model to predict the 30-year estimated cumulative production volume (EUR) for a given well. To assist in our analysis, we use the statistical computing and graphics software *R* (2015). We begin our work by stating the full regression model:

$$Y = \beta_0 + \beta_1 x_1 + \beta_2 x_2 + \beta_3 x_3 + \beta_4 x_4 + \beta_5 x_5 \quad \text{.....(5.1)}$$

For Eq. 5.1, the "dependent" variable for this work is the 30-year EUR and the "independent" variables (correlation parameters) are the completion parameters for a multi-fracture horizontal well:

Y = EUR30_RTA = 30-year EUR for the "total gas" flowrate (100 percent completion efficiency)
x_1 = StgWtr = Water/fracturing fluid pumped per fracture stage (bbl).
x_2 = StmLatLen = Stimulated well lateral length (ft).
x_3 = StgPrp = Proppant pumped per fracture stage(lb).
x_4 = NumFrcStg = Number of fracture stages.
x_5 = FrcDsgn = Well fracture design

In **Figure 5.1**, we provide a "scatter plot matrix" for the data used in the regression model as an attempt to observe relationships between the response ("dependent") and predictor ("independent") variables.

After creating the initial model, we perform a multivariate Box-Cox transformation analysis and conclude that the 30-year EUR (EUR30_RTA) should be transformed using the natural logartithm, the water pumped per fracture stage (StgWtr), the stimulated well lateral length (StmLatLen), and the proppant per fracture stage (StgPrp) variables. Also, we take the square-root of the number of fracture stages (NumFrcStg) variable. Therefore, we define the transformed full model is given as Eq. 5.2.

$$\log(Y) = \beta_0 + \beta_1 \log(x_1) + \beta_2 \log(x_2) + \beta_3 \log(x_3) + \beta_4 \sqrt{x_4} + \beta_5 x_5 \quad \text{.....(5.2)}$$

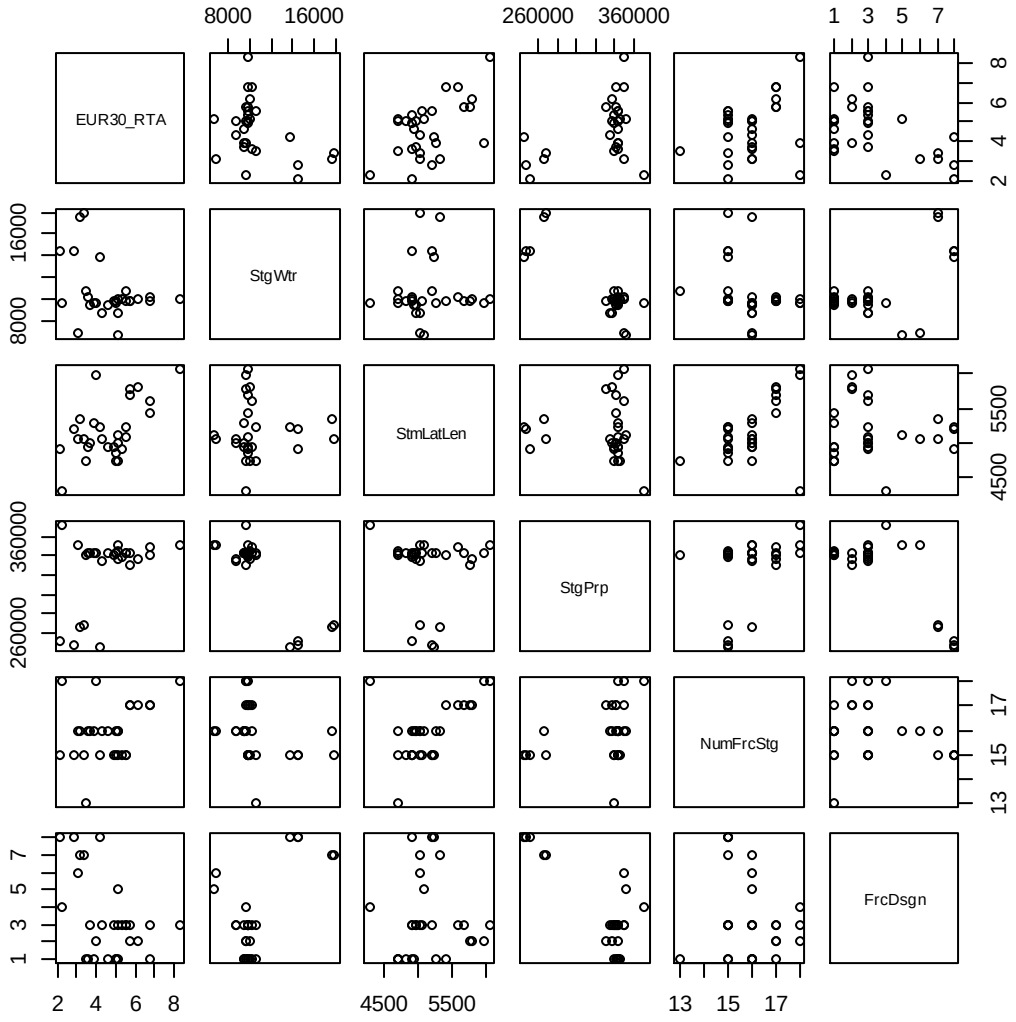

Figure 5.1 — (Cartesian Plot): Scatter plot matrix of the original data used in the regression model defined by Eq. 5.1.

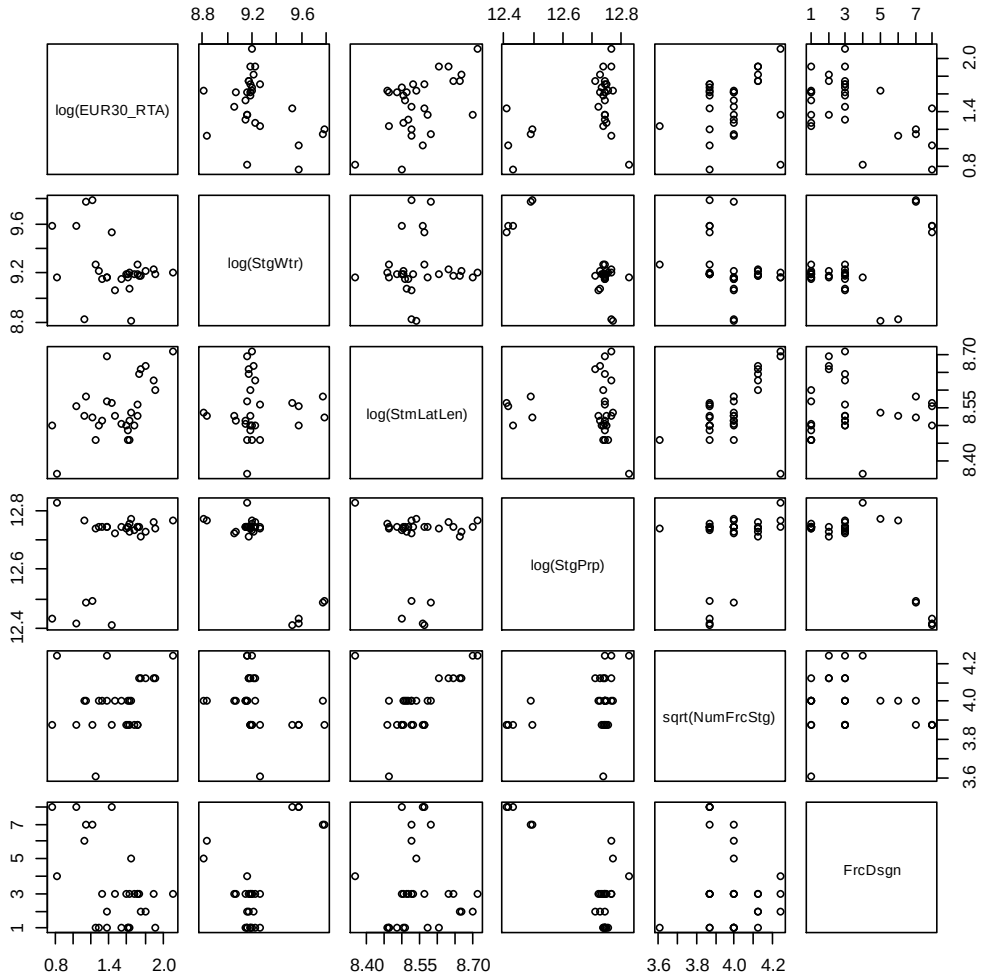

Figure 5.2 — (Cartesian Plot): Scatter plot matrix of the transformed data used in the regression model defined by Eq. 5.2.

In **Figure 5.3** and **Figure 5.4**, we plot, on a Cartesian and log-log scales respectfully, the model "calculated" 30-year EUR versus the actual 30-year EUR.

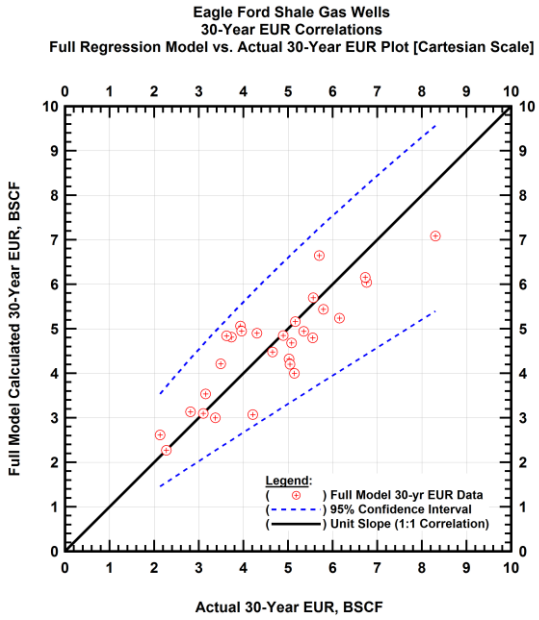

Figure 5.3 — (Cartesian Plot): 30-year cumulative gas production correlation plot — model "calculated" 30-year EUR versus the actual 30-year EUR (based on Eq. 5.2).

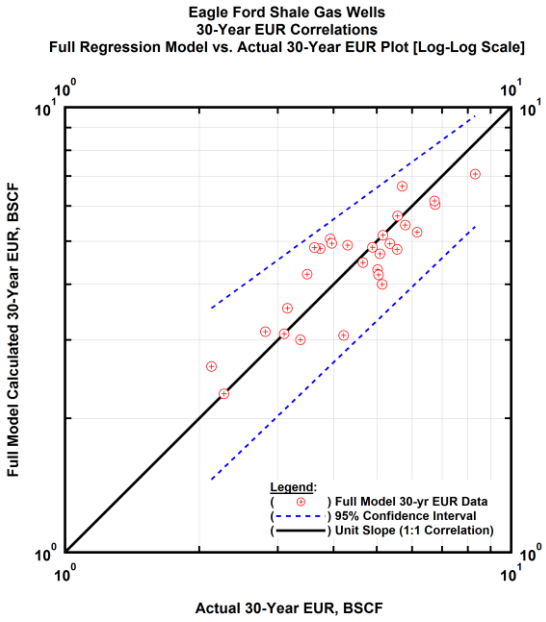

Figure 5.4 — (Log-log Plot): 30-year cumulative gas production correlation plot — model "calculated" 30-year EUR versus the actual 30-year EUR (based on Eq. 5.2).

We observe a general agreement between the fitted values from the regression model and the actual 30-year EUR values, as well as observe that all of the points fall inside the 95 percent confidence interval range for the model. By initial inspection, the model appears to be valid, but we conduct diagnostic plots to check its validity. In **Figure 5.5**, we generate scatter plots of the standardized residuals against each predictor variable and the fitted values for the regression model. Each of the plots, except for the proppant per fracture stage predictor, show a fairly randomized pattern, and none of the standardized residual values appear to be greater than the absolute value of two. These factors help to confirm the validity of the model to the data.

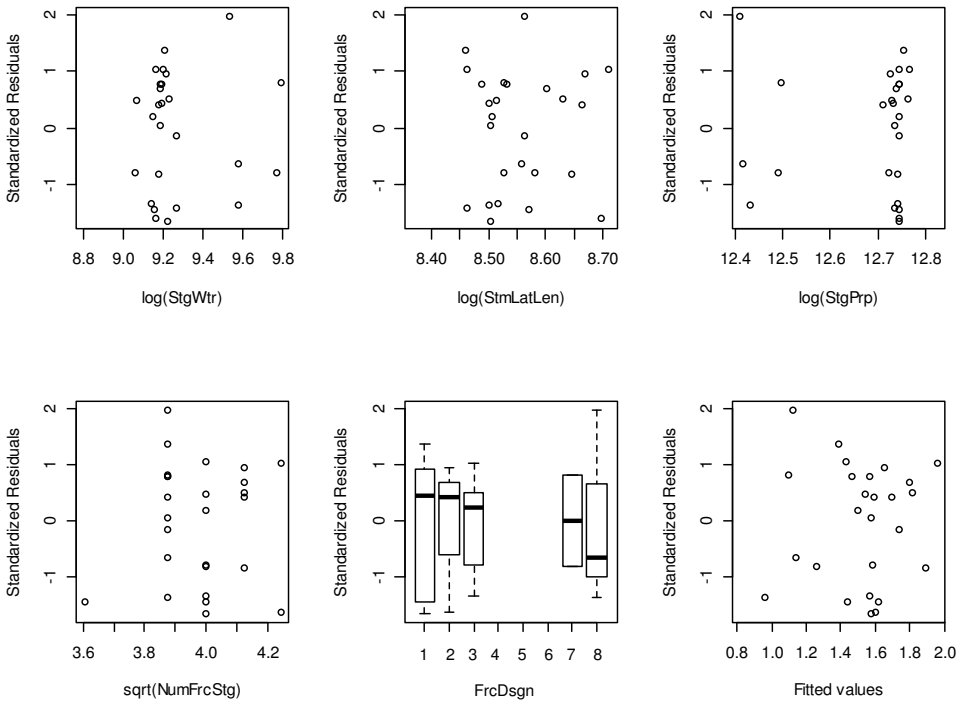

Figure 5.5 — (Cartesian Plot): Standardized residual plots for the model defined by Eq. 5.2.

In **Figure 5.6**, we plot "diagnostic plots" produced by *R* for the regression model (Eq. 5.2). The top left is a plot of the residuals plot versus fitted values, and we see that the model variance appears to be fairly constant. The top right is a plot of the standardized residuals versus theoretical quantiles, or commonly referred to as a "normal Q-Q" plot, and we observe that the points generally follow the dashed line and

maintain standardized residual values less than an absolute value of two. The bottom left is a plot of the square root of the standardized residuals versus fitted values, and also qualitatively illustrates the constant nature of the error term variance for the model. The bottom right is a plot of the standardized residuals versus leverage, and we do not observe any "bad" leverage points present with high leverage and standardized residual values with an absolute value of two or higher. All of these observations confirm that the model is valid and relevant.

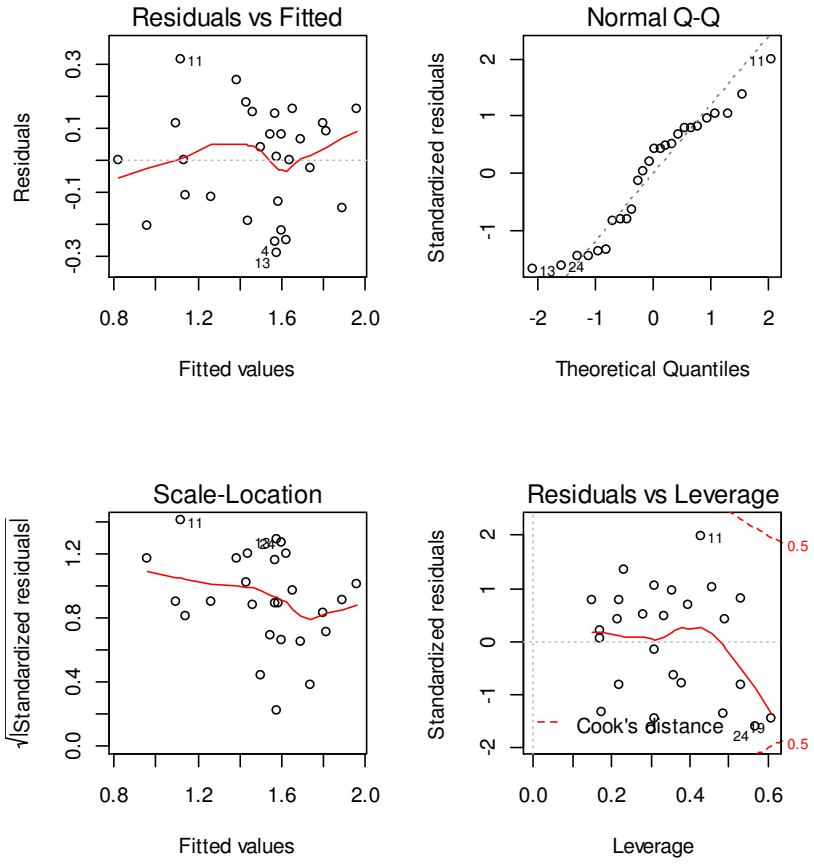

Figure 5.6 — (Cartesian Plot): Diagnostic plots generated by *R* for the model defined by Eq. 5.2.

In **Figure 5.7**, we present the "marginal model plots" for the full regression model. The solid, blue lines represent the loess (or locally weighted polynomial regression) estimate of the data, whereas the red, dashed lines represent the loess estimate of the regression model. We find good agreement between the data and

regression model loess curves (except for the marginal model plot for the number of fracture stages). Even with the discrepancies seen in the number of fracture stages plot, the agreement of the model with the data in the other four plots lends validity to the model.

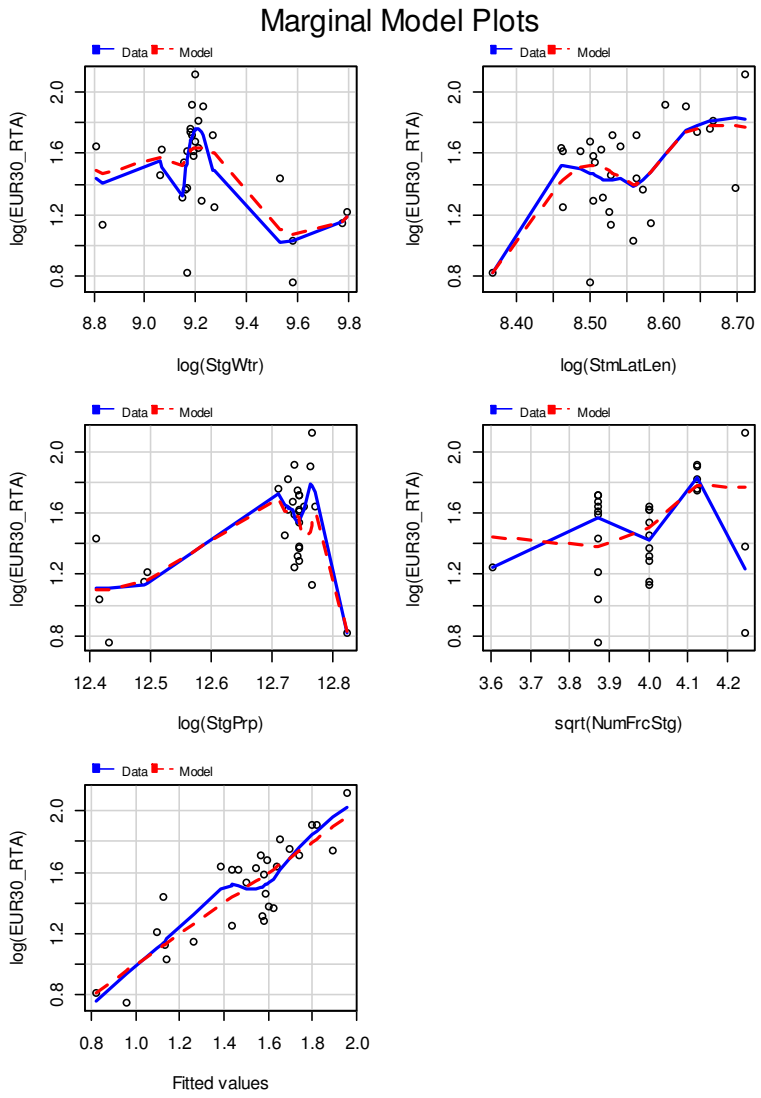

Figure 5.7 — (Cartesian Plot): Marginal model plots for the model defined by Eq. 5.2.

In **Table 5.1**, we present the regression output for the transformed model. We observe that none of the predictor variables are considered statistically significant since their associated p-values are not less than a

value of 0.05. Statistical significance of a variable means that a predictor variable independently affects the regression model when all other predictor variables are held constant. Therefore, *we cannot infer the direct impact or influence of any one predictor in the model*. The lack of statistical significance in the model signifies that there are either *too many or too few predictor variables* in the model to adequately describe the behavior of the dataset.

Table 5.1 — Regression output for the transformed full model defined by Eq. 5.2.

Coefficients	Estimate	Standard Error	t-value	Pr (>|t|)
Intercept	43.17	68.14	0.63	0.54
log(StgWtr)	1.29	1.54	0.84	0.41
log(StmLatLen)	1.74	1.48	1.17	0.26
log(StgPrp)	-5.50	5.92	-0.93	0.37
Sqrt(NumFrcStg)	0.45	0.83	0.55	0.59
FrcDsgn #1	-0.36	0.24	-1.46	0.16
FrcDsgn #2	0.05	0.12	0.42	0.68
FrcDsgn #3	-0.12	0.55	-0.22	0.83
FrcDsgn #4	0.67	0.73	0.92	0.37
FrcDsgn #5	0.13	0.67	0.19	0.85
FrcDsgn #6	-2.58	2.17	-1.19	0.25
FrcDsgn #7	-2.75	2.29	-1.20	0.25

Residual standard error: 0.2099 on 17 degrees of freedom
Multiple R-squared: 0.742
Adjusted R-squared: 0.575
F-statistic: 4.444 on 11 and 17 DF
p-value: 0.003079

A limitation of **Figure 5.2** is that each insert plot considers the effect of a specific predictor on the explanatory variable; while ignoring the effects that other predictors may have the explanatory variable. Therefore in **Figure 5.8**, we create added-variable plots for our proposed model. The added-variable plots, also known as partial regression plots, are designed to show the effects of adding a specified variable to the existing model, which already contains the other predictor variables.

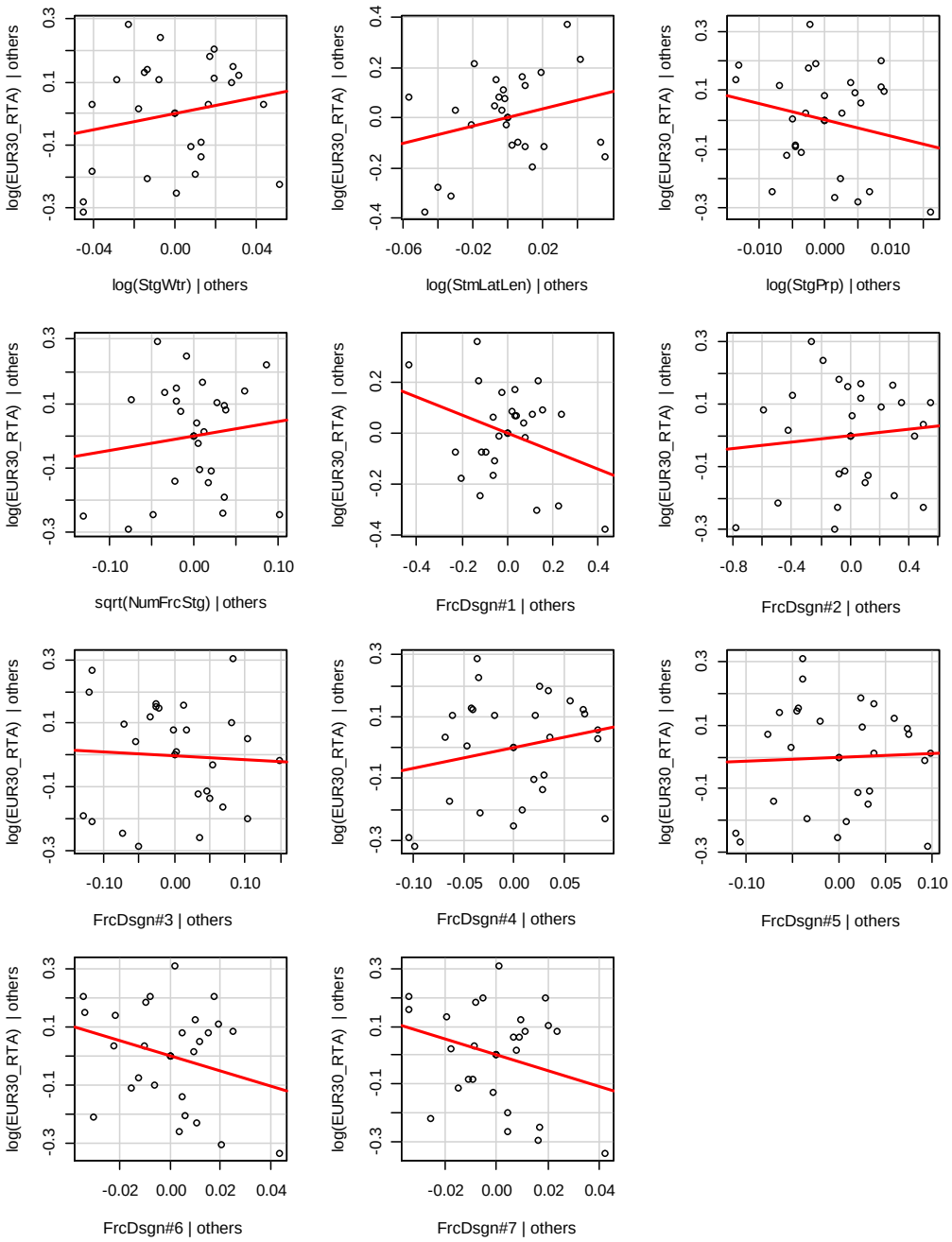

Figure 5.8 — (Cartesian Plot): Added-variable plots for the model defined by Eq. 5.2.

We observe from the added-variable plots that each of the predictors impacts the model — even though the model regression output indicate that none of the predictors are statistically significant. Thus, we proceed to select and evaluate alternative models using the following selection criteria to find, if possible, both a valid and statistically significant model. Our process is to:

- Reduce the full model by *eliminating the well fracture design predictor variable.*
- Forward predictor variable selection based on the Akaike's Information Criterion (AIC).
- Forward predictor variable selection based on the Bayesian Information Criterion (BIC).
- Backward predictor variable elimination based on the Akaike's Information Criterion (AIC).
- Backward predictor variable elimination based on the Bayesian Information Criterion (BIC).

5.2 Reduced Regression Model Removing Well Fracture Design Predictor Variable

We develop a reduced regression model to predict the 30-year EUR for a given well by reducing the full regression model, Eq. 5.2, by eliminating the well fracture design predictor variable:

$$\log(Y) = \beta_0 + \beta_1 \log(x_1) + \beta_2 \log(x_2) + \beta_3 \log(x_3) + \beta_4 \sqrt{x_4} \quad \text{.....(5.3)}$$

Where, the variables used in Eq. 5.3 are defined as follows:

Y = EUR30_RTA = 30-year EUR for the "total gas" flowrate (100 percent completion efficiency)
x_1 = StgWtr = Water/fracturing fluid pumped per fracture stage (bbl).
x_2 = StmLatLen = Stimulated well lateral length (ft).
x_3 = StgPrp = Proppant pumped per fracture stage(lb).
x_4 = NumFrcStg = Number of fracture stages.

In **Figure 5.9**, we provide a "scatter plot matrix" of the transformed data used in the reduced regression model as a means of assessing relationships between the response and predictor variables.

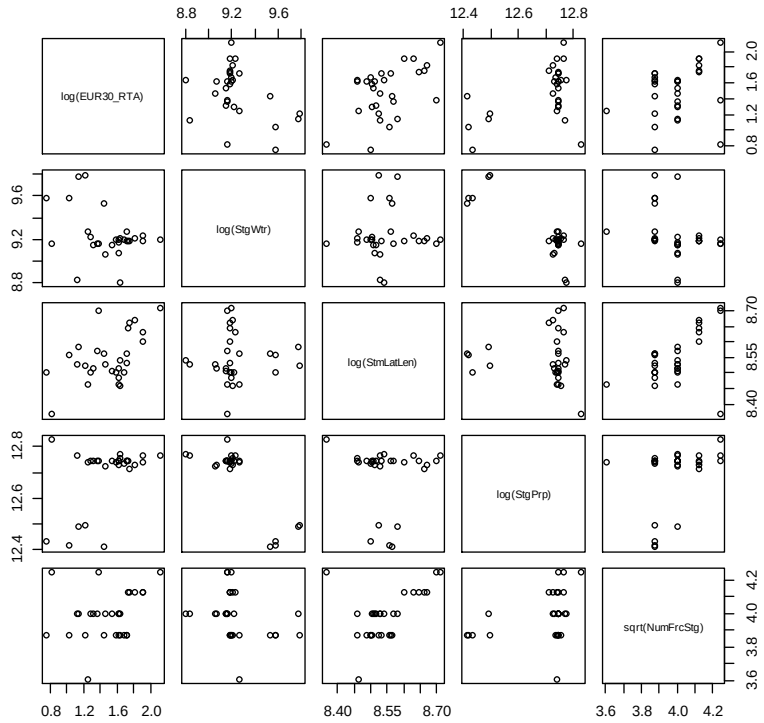

Figure 5.9 — (Cartesian Plot): Scatter plot matrix of the transformed data used in the regression model defined by Eq. 5.3.

In **Figure 5.10** and **Figure 5.11**, we plot the 30-year EUR calculated using the reduced regression model versus the actual 30-year EUR values and we observe a general agreement between these plots. However, for this regression model we identify that points lie outside the 95 percent confidence interval range for the model, which suggests that the model may not be valid for the given dataset.

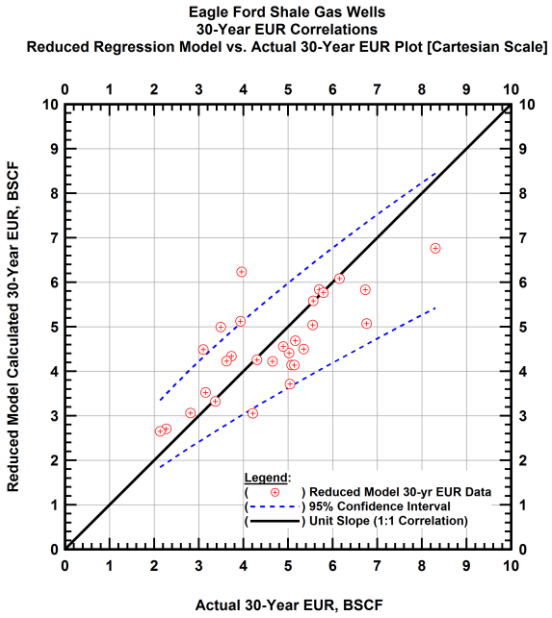

Figure 5.10 — (Cartesian Plot): 30-year cumulative gas production correlation plot — model "calculated" 30-year EUR versus the actual 30-year EUR (based on Eq. 5.3).

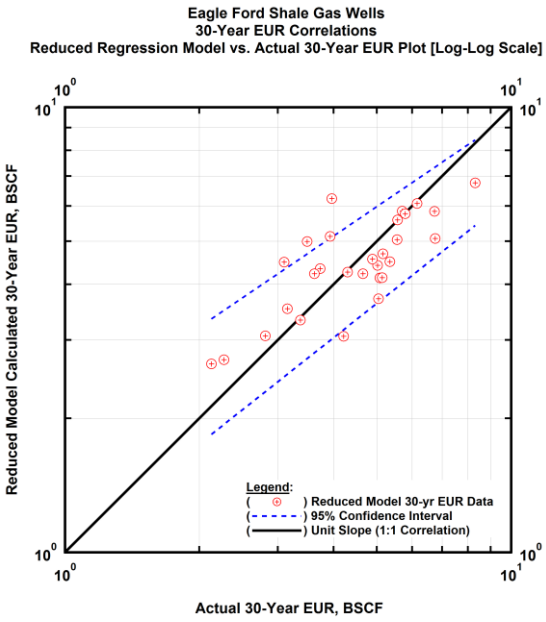

Figure 5.11 — (Log-log Plot): 30-year cumulative gas production correlation plot — model "calculated" 30-year EUR versus the actual 30-year EUR (based on Eq. 5.2).

In **Figure 5.12** we provide a series of scatter plots of the standardized residuals plotted against each predictor variable and the fitted values for the regression model. Each of the cases (except for the proppant per fracture stage predictor), show a fairly randomized pattern, which is indicative of a valid model. However, several of the standardized residual values appear to be greater than the absolute value of two, which is generally an indication of an invalid model.

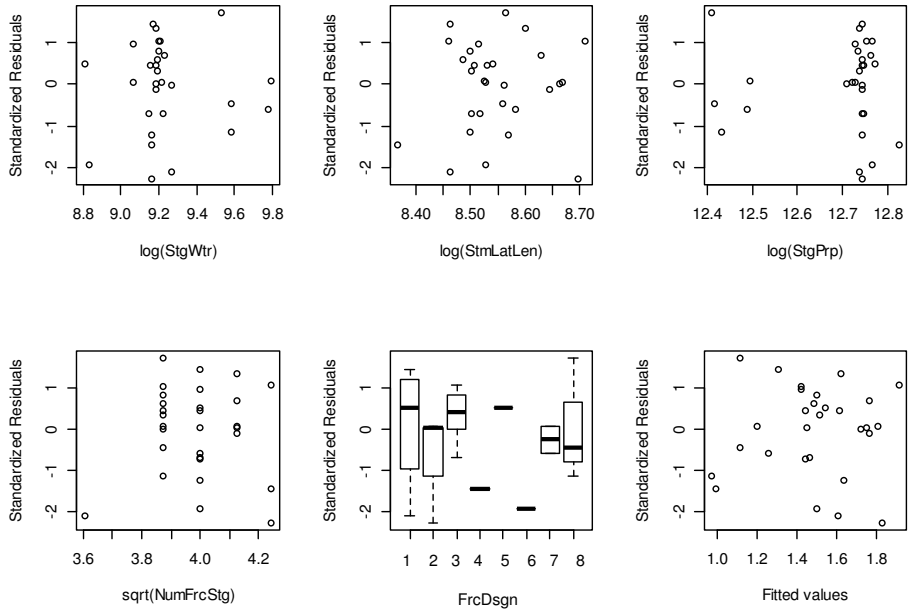

Figure 5.12 — (Cartesian Plot): Standardized residual plots for the model defined by Eq. 5.3.

In **Figure 5.13**, we plot "diagnostic plots" and see that the model variance appears to be fairly constant. However, we observe several "bad" leverage points present with high leverage and standardized residual values with an absolute value of two or higher.

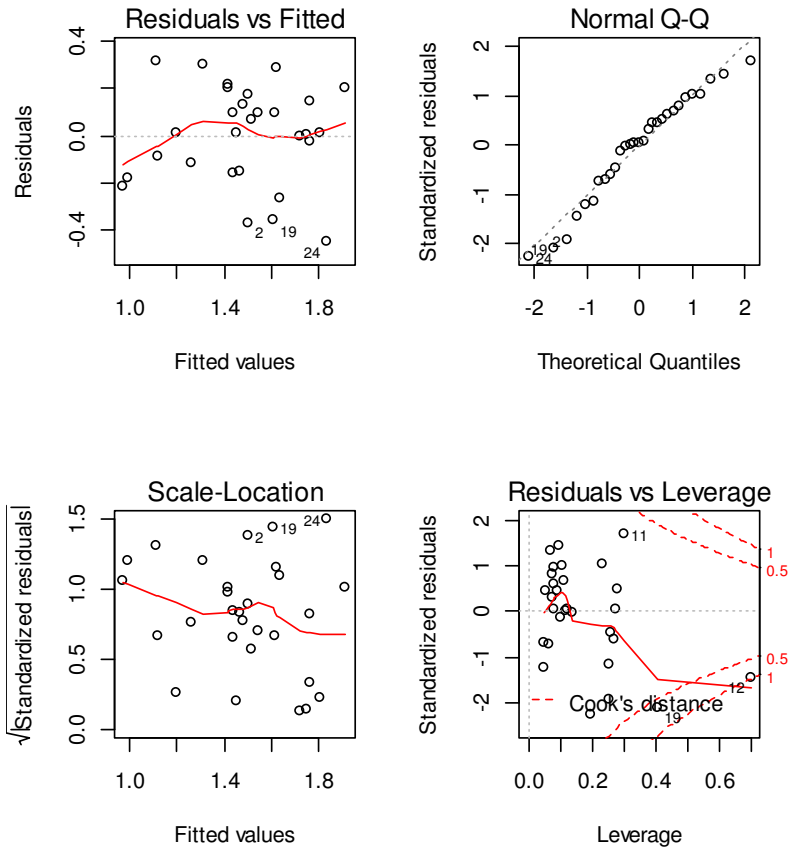

Figure 5.13 — (Cartesian Plot): Diagnostic plots generated by R for the model defined by Eq. 5.3.

In **Figure 5.14**, we plot the "marginal model" plots for the reduced regression model and find that there is marginal agreement between the data and regression model loess curves, especially since the model does match well on three of the five plots.

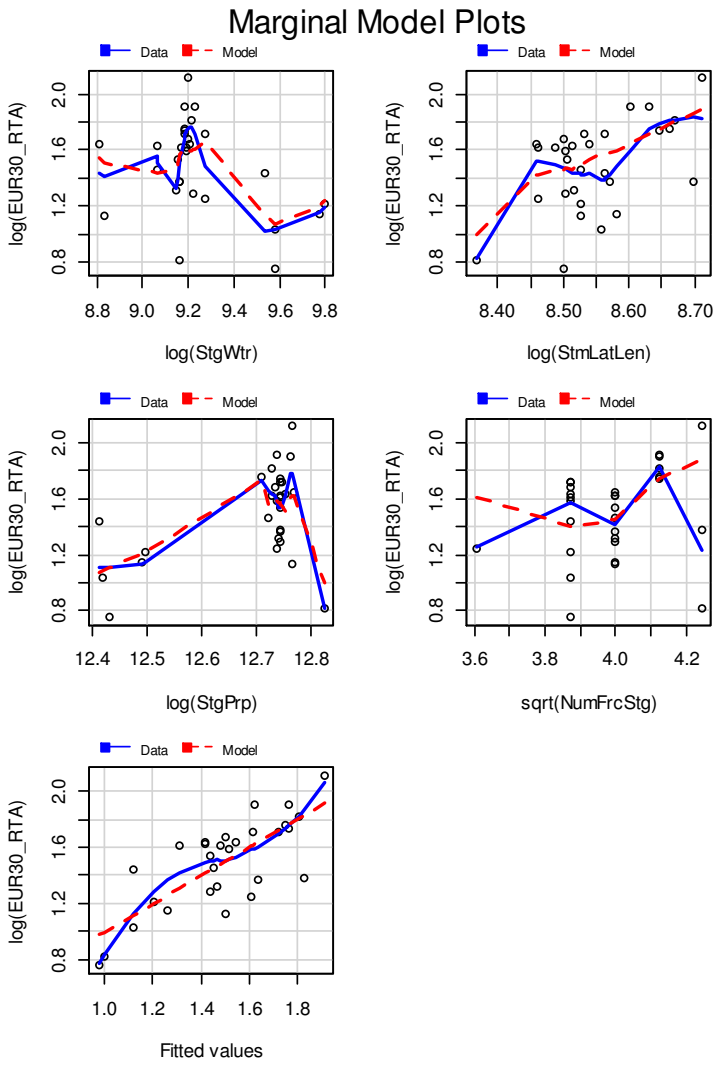

Figure 5.14 — (Cartesian Plot): Marginal model plots for the model defined by Eq. 5.3.

In **Table 5.2** we present the regression output for the reduced model. We observe from the results that all of the predictor variables can be considered statistically significant (except for the water per fracture stage predictor variable), as the p-values are approximately less than or equal to 0.05. Therefore, we can infer the direct impact or influence of the predictors in the model.

Table 5.2 — Regression output for the reduced model defined by Eq. 5.3.

Coefficients	Estimate	Standard Error	t-value	Pr (>|t|)
Intercept	-46.56	12.77	-3.65	1.28 E-3
log(StgWtr)	0.14	0.34	0.40	0.70
log(StmLatLen)	2.98	0.66	4.54	1.33 E-4
log(StgPrp)	1.92	0.68	2.83	9.23 E-3
sqrt(NumFrcStg)	-0.76	0.39	-1.97	0.06

Residual standard error: 0.2234 on 24 degrees of freedom
Multiple R-squared: 0.5876
Adjusted R-squared: 0.5189
F-statistic: 8.551 on 4 and 24 DF
p-value: 1.946 E-4

In **Figure 5.15** provide the added-variable plots for this model (Eq. 5.3). We observe from the added-variable plots that each of the predictors directly impacts the model, with minimal impact evident in the water per fracture stage plot, which substantiates the statistical significance (or lack thereof), for each of the predictors per the model regression output.

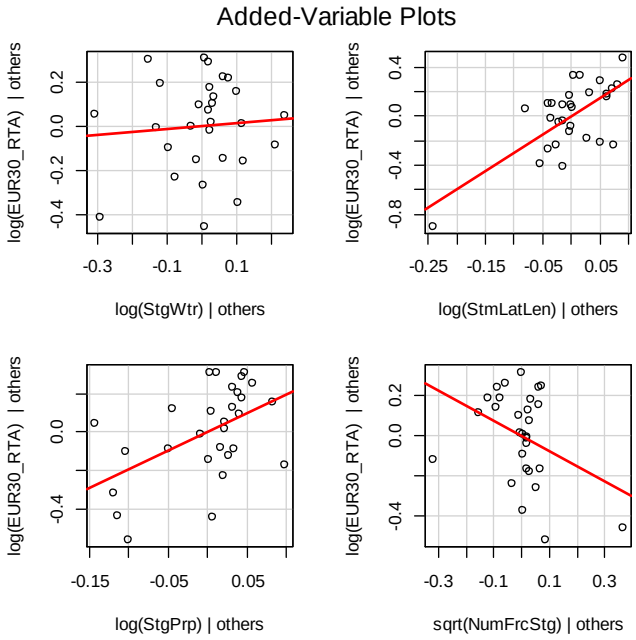

Figure 5.15 — (Cartesian Plot): Added-variable plots for the model defined by Eq. 5.3.

5.3 Reduced Regression Model using the Akaike's Information Criterion (AIC)

Using the forward predictor variable selection and backward predictor variable elimination based upon the Akaike's Information Criterion (AIC) we develop another reduced regression model to predict the 30-year EUR. This model is given by:

$$\log(Y) = \beta_0 + \beta_2 \log(x_2) + \beta_5 x_5 \quad \text{.....(5.4)}$$

Where, the variables used in Eq. 5.4 are defined as follows:

Y = EUR30_RTA = 30-year EUR for the "total gas" flowrate (100 percent completion efficiency)

x_2 = StmLatLen = Stimulated well lateral length (ft).

x_5 = FrcDsgn = Well fracture design

In **Figure 5.16**, we present a scatter plot matrix of the transformed data used in the AIC reduced regression model to establish relationships between the response and predictor variables.

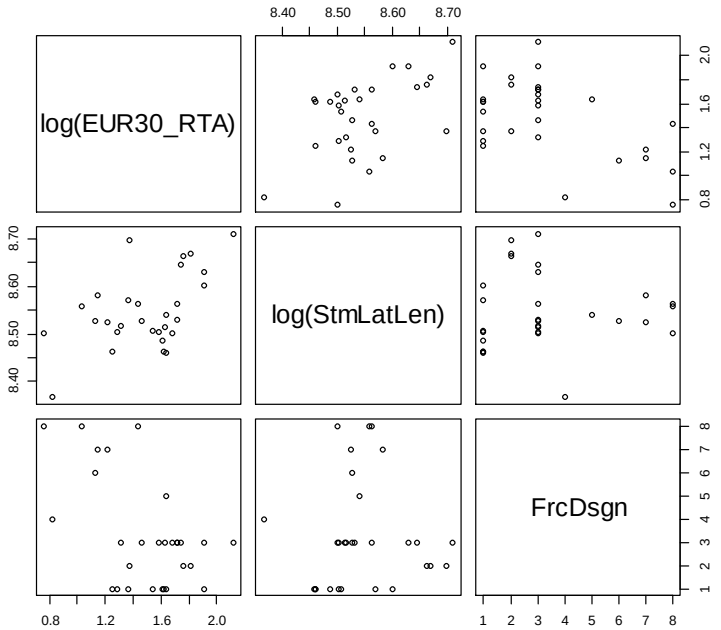

Figure 5.16 — (Cartesian Plot): Scatter plot matrix of the transformed data used in the regression model defined by Eq. 5.4.

In **Figure 5.17** and **Figure 5.18**, we plot 30-year EUR calculated using the AIC reduced regression model versus the actual 30-year EUR values. We observe a general agreement between the model and the data, as well as observing that all of the data points fall inside the 95 percent confidence interval range for the model. Given the trends in **Figure 5.17** and **Figure 5.18**, we conclude that the model appears to be valid.

In **Figure 5.19**, we provide scatter plots of the standardized residuals against each predictor variable and the fitted values for the regression model. Each of the plots (except for the proppant per fracture stage predictor), show a random pattern; and none of the standardized residual values appear to be greater than the absolute value of two. Both these factors help to substantiate the validity of the model relative to the data.

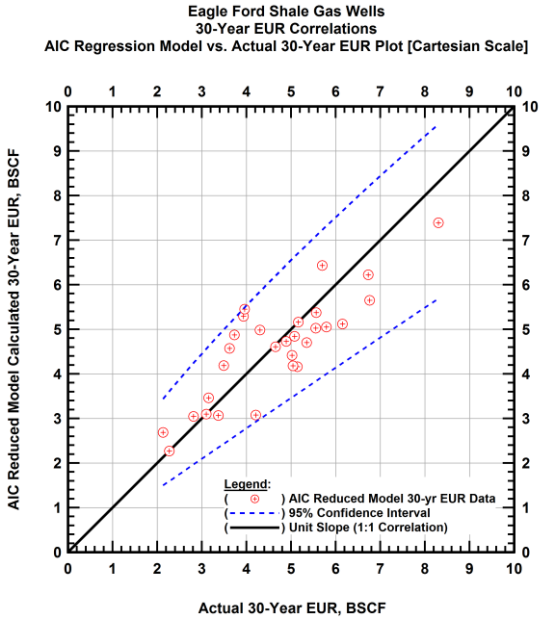

Figure 5.17 — (Cartesian Plot): 30-year cumulative gas production correlation plot — model "calculated" 30-year EUR versus the actual 30-year EUR (based on Eq. 5.4).

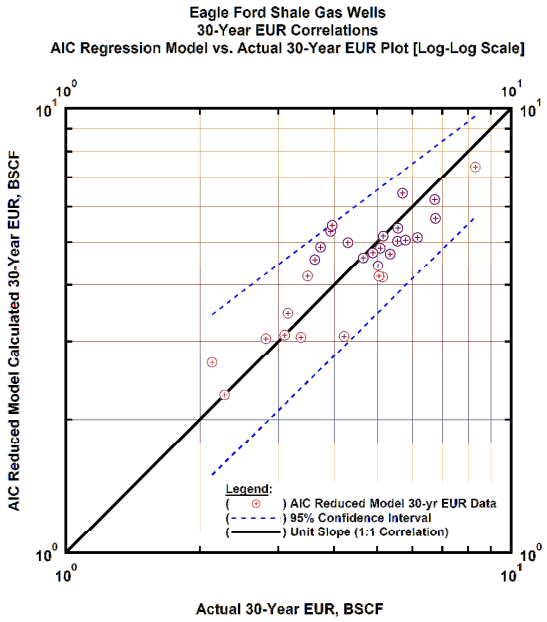

Figure 5.18 — (Log-log Plot): 30-year cumulative gas production correlation plot — model "calculated" 30-year EUR versus the actual 30-year EUR (based on Eq. 5.4).

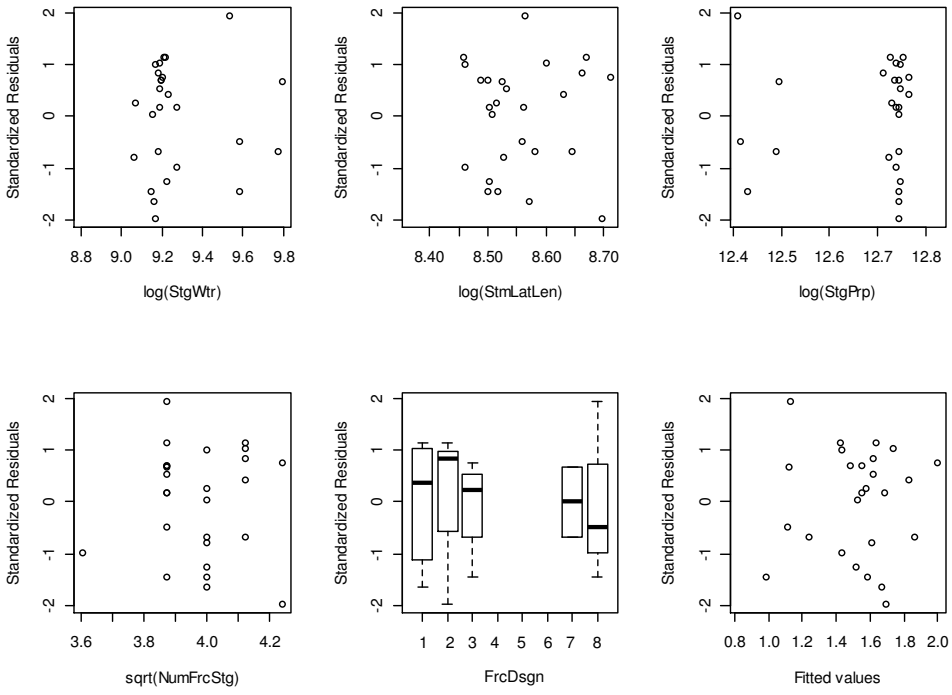

Figure 5.19 — (Cartesian Plot): Standardized residual plots for the model defined by Eq. 5.4.

In **Figure 5.20**, we plot "diagnostic plots" and observe that the model variance appears to be fairly constant. In addition, we observe that the points generally follow the "normal Q-Q" plot dashed line and maintain standardized residual values less than an absolute value of two. Lastly, the standardized residuals versus leverage plot does not contain any "bad" leverage points present with high leverage and standardized residual values with an absolute value of two or higher. As noted earlier, this model appears to be valid.

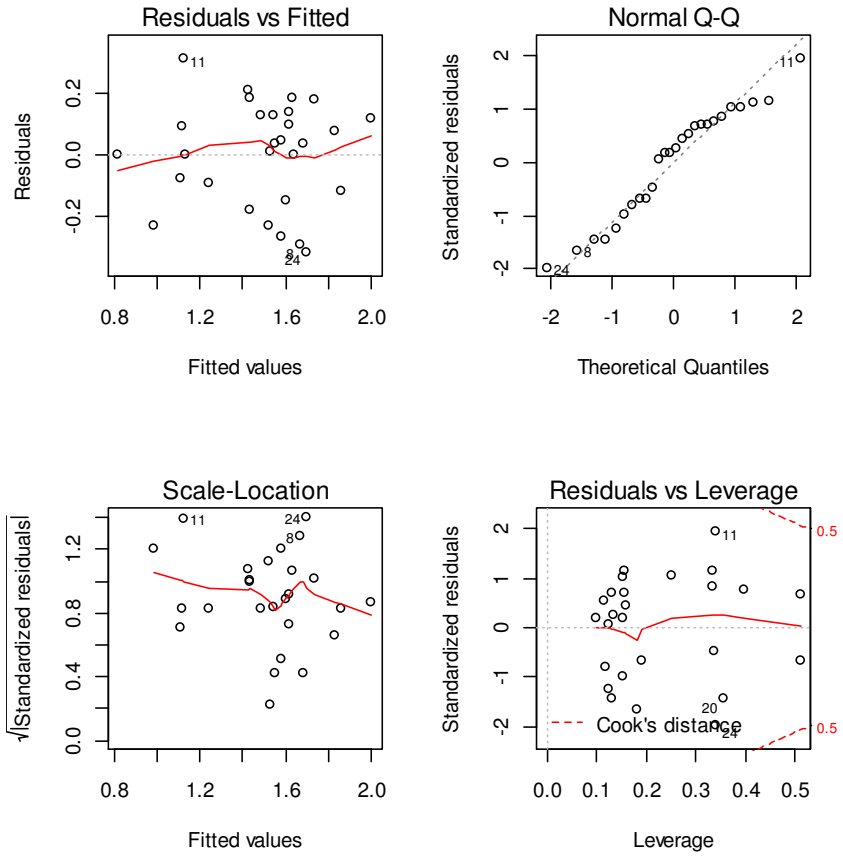

Figure 5.20 — (Cartesian Plot): Diagnostic plots generated by *R* for the model defined by Eq. 5.4.

In **Figure 5.21** we provide the marginal model plots for the AIC reduced regression model and observe good agreement — based on these observations, the model appears to be valid.

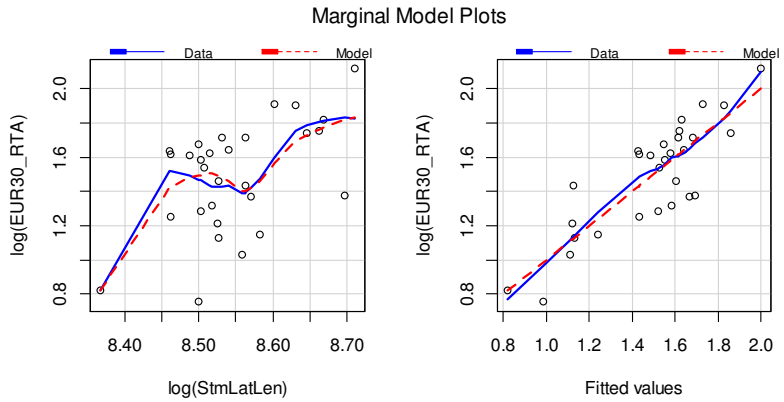

Figure 5.21 — (Cartesian Plot): Marginal model plots for the model defined by Eq. 5.4.

In **Table 5.3**, we present the regression output for the AIC reduced regression model. We observe that two-thirds of the predictor variables are considered statistically significant since their p-values are approximately equal to or less than 0.05. This means that the majority of the variables appear to independently affect the regression model when all other predictor variables are held constant.

Table 5.3 — Regression output for the AIC reduced model defined by Eq. 5.4.

Coefficients	Estimate	Standard Error	t-value	Pr (>|t|)
Intercept	-16.75	6.31	-2.66	1.5 E-2
log(StmLatLen)	2.14	0.74	2.90	8.9 E-3
FrcDsgn #1	-0.24	0.18	-1.32	0.20
FrcDsgn #2	0.03	0.10	0.33	0.75
FrcDsgn #3	-0.41	0.24	-1.73	9.8 E-2
FrcDsgn #4	0.04	0.21	0.19	0.85
FrcDsgn #5	-0.44	0.21	-2.08	0.05
FrcDsgn #6	-0.45	0.16	-2.78	0.01
FrcDsgn #7	-0.53	0.14	-3.83	1.1 E-3

Residual standard error: 0.1991 on 20 degrees of freedom
Multiple R-squared: 0.7269
Adjusted R-squared: 0.6177
F-statistic: 6.654 on 8 and 20 DF
p-value: 0.003079

In **Figure 5.22**, we create added-variable plots for the model. We see from the added-variable plots that each of the predictors impacts the model, with minimal impact evident in three of the well fracture design plots, which substantiates the statistical significance, or lack thereof, for each of the predictors per the model regression output.

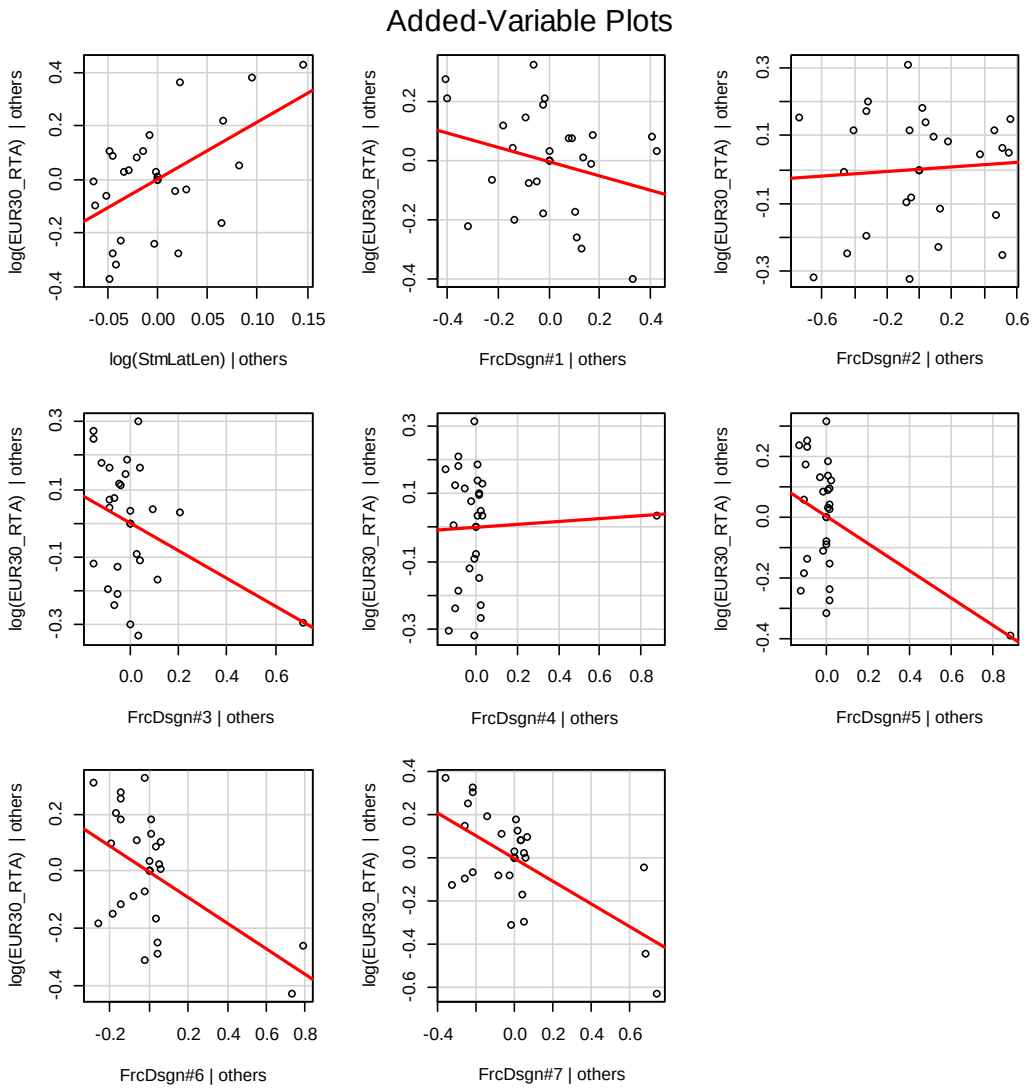

Figure 5.22 — (Cartesian Plot): Added-variable plots for the model defined by Eq. 5.4.

5.4 Reduced Regression Model using the Bayesian Information Criterion (BIC)

Using the forward predictor variable selection and backward predictor variable elimination based upon the Bayesian Information Criterion (BIC), we developed a third reduced regression model for 30-year EUR. This model is given as:

$$\log(Y) = \beta_0 + \beta_2 \log(x_2) + \beta_3 \log(x_3) + \beta_4 \sqrt{x_4} \quad \text{.....(5.5)}$$

The variables used in Eq. 5.5 are defined as follows:

Y = EUR30_RTA = 30-year EUR for the "total gas" flowrate (100 percent completion efficiency)

x_2 = StmLatLen = Stimulated well lateral length (ft).

x_3 = StgPrp = Proppant pumped per fracture stage(lb).

x_4 = NumFrcStg = Number of fracture stages.

In **Figure 5.23**, we provide a scatter plot matrix of the transformed data used in the BIC reduced regression model to establish relationships between the response and predictor variables.

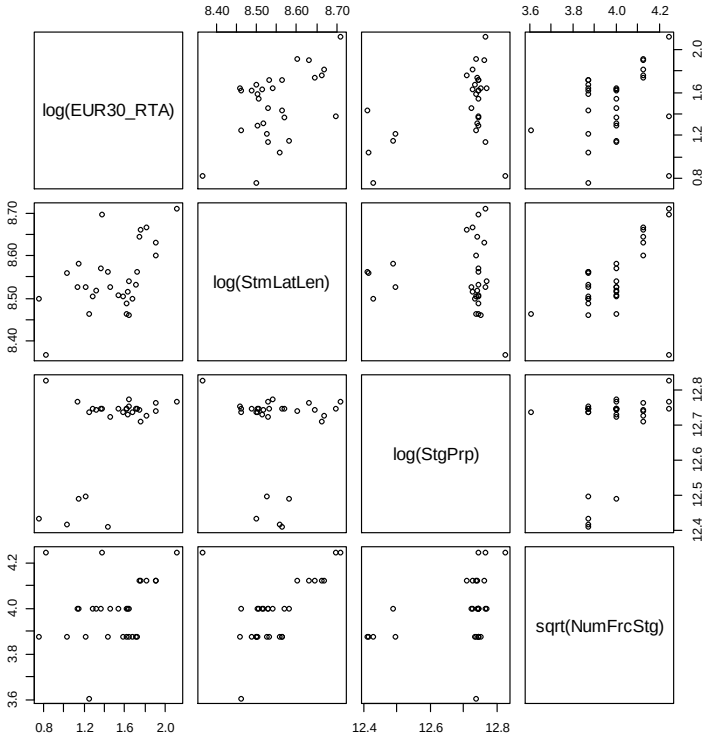

Figure 5.23 — (Cartesian Plot): Scatter plot matrix of the transformed data used in the regression model defined by Eq. 5.5.

In **Figure 5.24** and **Figure 5.25** we plot the 30-year EUR calculated using the BIC reduced regression model versus the actual 30-year EUR values and observe general agreement. However, as with some of the other "reduced" models, we do observe several of the data points fall outside the 95 percent confidence interval range for the model. Thus, the model does not appear to be valid for the given dataset — however, we have prepared diagnostic plots to verify the validity of this model.

In **Figure 5.26**, we provide scatter plots of the standardized residuals against each predictor variable and the fitted values for the regression model. Each of the plots (except for the proppant per fracture stage predictor), show a fairly randomized pattern, which is indicative of a valid model. However, several of the standardized residual values appear to be greater than the absolute value of two, which may be an indication of an invalid model.

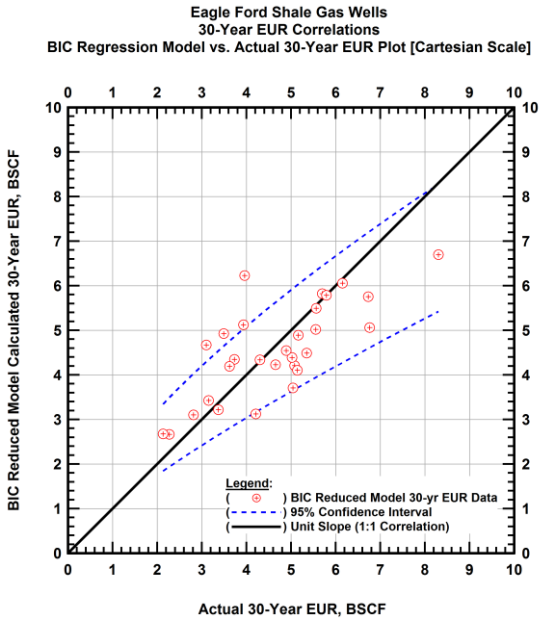

Figure 5.24 — (Cartesian Plot): 30-year cumulative gas production correlation plot — model "calculated" 30-year EUR versus the actual 30-year EUR (based on Eq. 5.5).

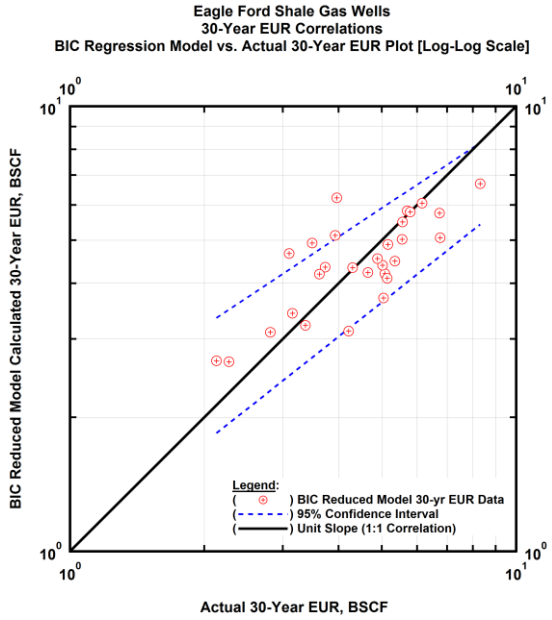

Figure 5.25 — (Log-log Plot): production correlation plot — model "calculated" 30-year EUR versus the actual 30-year EUR (based on Eq. 5.5).

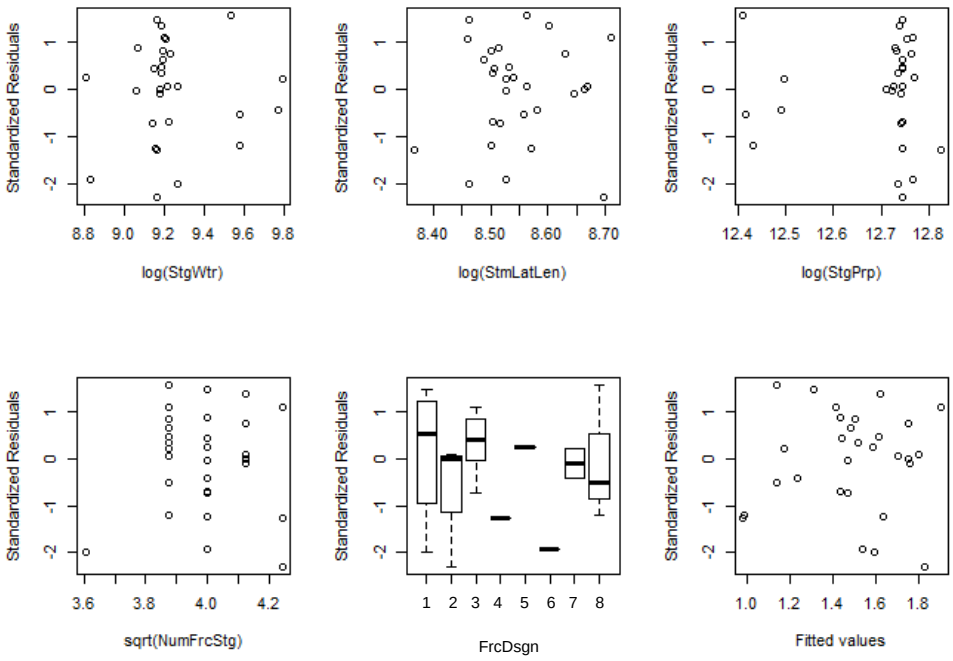

Figure 5.26 — (Cartesian Plot): Standardized residual plots for the model defined by Eq. 5.5.

In **Figure 5.27**, we present the "diagnostic plots" and we observe that the model variance appears to be fairly constant. However, several of the standardized residual values are greater than an absolute value of two, and the standardized residuals versus leverage plot contains several "bad" leverage points with high leverage and standardized residual values with an absolute value of two or higher. As we have noted in other cases, the results of the diagnostic plots question the validity of the model.

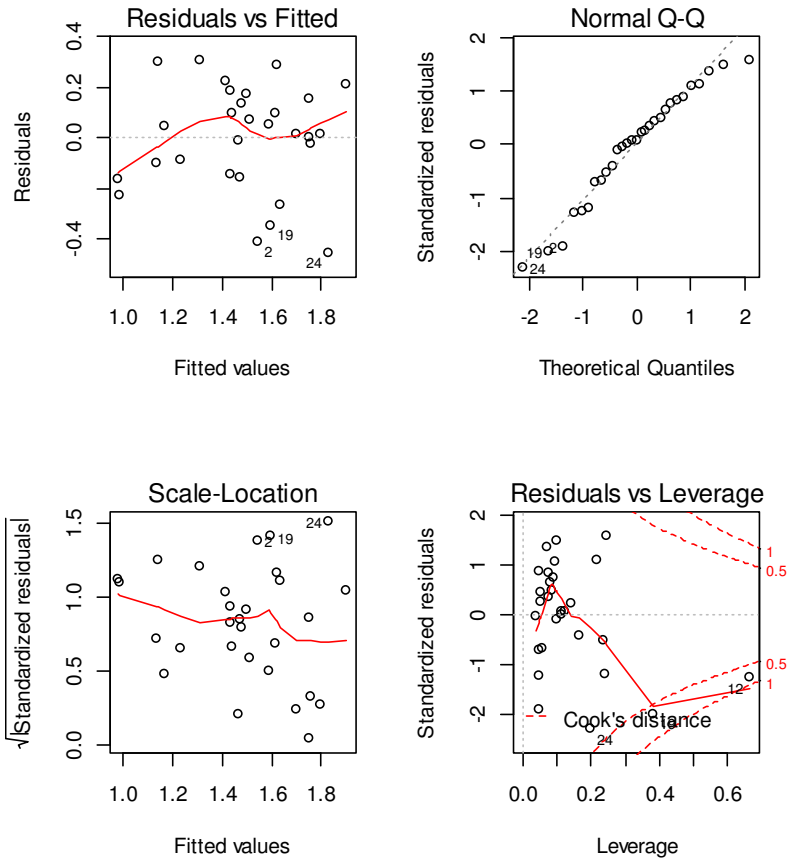

Figure 5.27 — (Cartesian Plot): Diagnostic plots generated by *R* for the model defined by Eq. 5.5.

In **Figure 5.28** we plot the "marginal model" plots for the BIC reduced regression model and we find marginal agreement between the data and regression model loess curves, especially since the model does not match on three of the four plots.

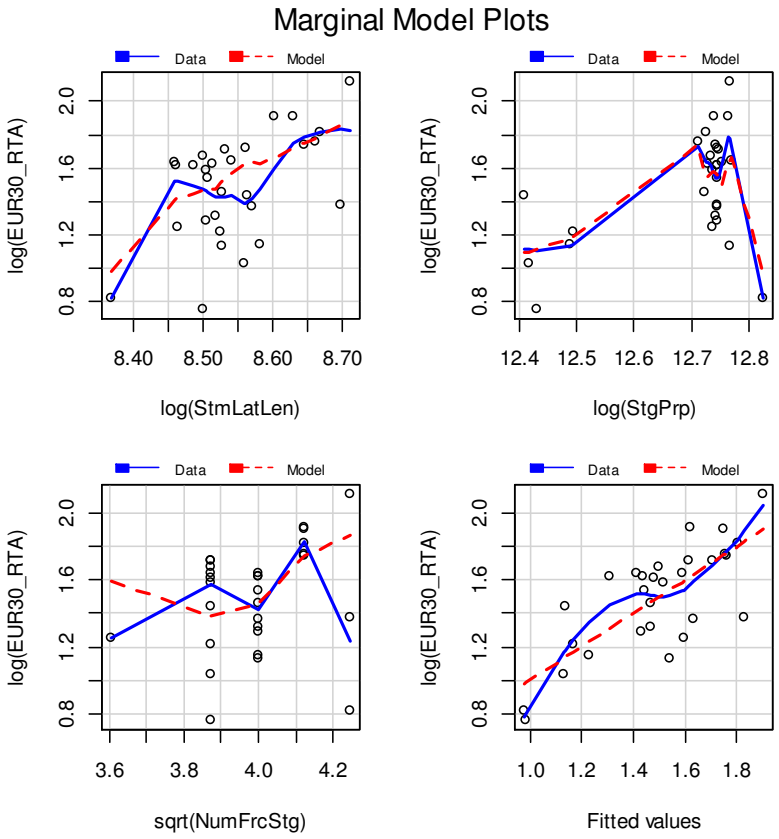

Figure 5.28 — (Cartesian Plot): Marginal model plots for the model defined by Eq. 5.5.

In **Table 5.4**, we show the regression output for the BIC reduced model. We observe that all of the predictor variables can be considered statistically significant since their p-values are approximately less than or equal to 0.05. This means that all of the variables appear to independently affect the regression model when all other predictor variables are held constant.

Table 5.4 — Regression output for the BIC reduced model defined by Eq. 5.5.

Coefficients	Estimate	Standard Error	t-value	Pr (>|t|)
Intercept	-42.53	7.55	-5.63	7.31 E-6
log(StmLatLen)	2.97	0.64	4.61	1.01 E-4
log(StgPrp)	1.70	0.39	4.33	2.11 E-4
sqrt(NumFrcStg)	-0.75	0.38	-1.99	5.7 E-2

Residual standard error: 0.2196 on 25 degrees of freedom
Multiple R-squared: 0.585
Adjusted R-squared: 0.5352
F-statistic: 11.75 on 3 and 25 DF
p-value: 5.423 E-5

In **Figure 5.29** we provide added-variable plots for the model. We see from the added-variable plots that each of the predictors impacts the model, which substantiates the statistical significance of the predictor variables per the model regression output.

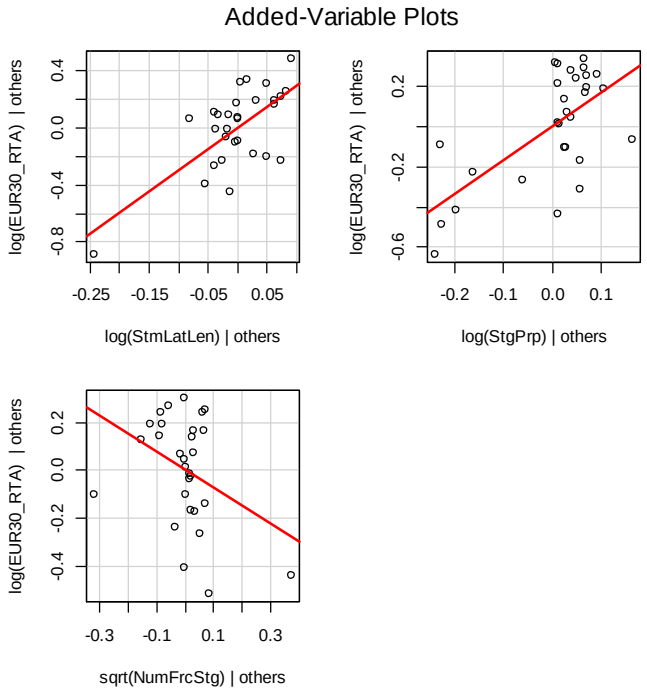

Figure 5.29 — (Cartesian Plot): Added-variable plots for the model defined by Eq. 5.5.

5.5 Regression Model Analysis of Variance (ANOVA)

In **Table 5.5** we present the results of the regression model analysis of variance (ANOVA) between the full model and three reduced models. We use this statistical diagnostic tool to check the statistical equivalence between the means of the full model against each of the reduced models. If the means for the compared models are similar, then the models themselves are similar, and the resulting p-value will have a value close to one. However, if the means for the compared models are different, then the resulting p-value will have a value close to zero.

Upon review of the ANOVA results, we observe that the reduced regression model formed by removing well fracture design predictor variable from the full model, Eq. 5.3, and the BIC reduced regression model, Eq. 5.5, have lower p-values, and therefore, do not adequately explain the full model, Eq. 5.2. The AIC reduced regression model, Eq. 5.4, has a relatively high p-value, and may be considered adequate for replacing the full model. However, we refrain from advocating the AIC reduced regression model, because it over simplifies the model and does not provide any hydraulic fracture completion parameters as predictor variables.

Table 5.5 — Analysis of variance (ANOVA) table between the full and reduced regression models.

Full Model	Reduced Model	Sum of Squares	F-value	Pr (>F)
Eq. 5.2	Eq. 5.3	0.448	1.45	0.25
Eq. 5.2	Eq. 5.4	0.044	0.33	0.80
Eq. 5.2	Eq. 5.5	0.456	1.29	0.31

The results of the ANOVA table reveals two primary items regarding the aforementioned models. First, the well fracture design predictor variable significantly impacts the model. Second, there are likely additional well fracture design parameters (other than the parameters considered in this work), that should be included in future regression analyses.

CHAPTER VI

SUMMARY, CONCLUSIONS AND RECOMMENDATIONS

6.1 Summary

In this work, we propose a workflow for production data analysis in order to reduce the uncertainty in reserves estimation for shale gas reservoirs by accounting for the following items:

- We create rate-pressure diagnostic plots that can be used to identify spurious data points as well as inconsistent flowrate-pressure trends so that these data points can be removed prior to analysis.
- For time-rate diagnostics, we use the $qDb\beta$ log-log plot (gas flowrate (q_g), decline parameter (D), loss-ratio parameter (b) and β-derivative versus production time) as our primary diagnostic plot.
- For time-rate-pressure diagnostics, we plot the pseudopressure drop-normalized gas flowrate ($q_g/\Delta m(p)$) and gas flowrate-normalized pseudopressure drop ($\Delta m(p)/q_g$) versus material balance time (G_p/q_g) diagnostic functions to identify the various flow regime(s) experienced by the well during production. These plots are also used qualitatively to identify possible incorrect initial reservoir pressure estimates.
- We select and regress the applicable time-rate model(s), based on the flow regime(s) observed/ identified using the filtered gas flowrate data (DeGolyer and MacNaughton, 2014).
- We create a history match of the gas flowrate, the calculated flowing bottomhole pressure, and the cumulative gas production data using an analytical time-rate-pressure (RTA) reservoir model (Ecrin — Topaze, 2013).
- We estimate the 30-year cumulative gas production volume as a proxy for the estimated ultimate recovery (EUR) using the empirical time-rate (DCA) models, as well as the more rigorous analytical time-rate-pressure analytical reservoir models tuned using production data.
- We use the "total gas" flowrate (computed on essentially a molar basis) along with the 100 percent completion efficiency to estimate the 30-year estimated cumulative production (EUR proxy) to create a regression model for reservoir and completion variables.

6.2 Conclusions

Based on this work, we state the following conclusions:

- It is essential to begin the analysis of production data with a thorough review of the well history to identify specific instances of well stimulation, workovers, recompletions, and/or significant mechanical and/or operational changes.
- Production data analysis is sensitive to both the quality and frequency of the production and pressure data. Diagnostic plots are an efficient means of assessing the integrity of the production and pressure data because spurious/outlier data are easily seen on these plots.

- The $qDb\beta$ log-log plot (gas flowrate (q_g), decline parameter (D), loss-ratio parameter (b) and β-derivative versus production time) should be used as both a diagnostic plot and a presentation plot for time-rate model analyses as the entire spectrum of data can be observed and interpreted using this plot.
- The number of fractures used in the "time-rate-pressure" analytical models has some impact on the goodness of fit for the "log-log" and Blasingame plots, but we would note that permeability and the number of fractures have a strong correlation, so a prior estimate of the number of "productive" fractures is essential for unique matches using analytical (and/or numerical) reservoir models.

6.3 Recommendations for Future Work

This work should be continued as follows:

- The proposed workflow for production data analysis should be applied to other shale gas plays for further validation of production forecasting and reserves estimation approaches used in this work.
- In order to create statistically significant regression model, additional well design and completion parameters should be integrated into the correlation(s).

NOMENCLATURE

Field Variables:

b	=	Arps model parameter (derivative of the loss ratio), dimensionless
D	=	Arps model parameter (reciprocal of the loss-ratio), D^{-1}
D_i	=	Decline parameter used in the Arps modified hyperbolic time-rate relation, D^{-1}
$\hat{D}_i$	=	Decline parameter used in the power-law exponential time-rate relation, D^{-1}
D_{lim}	=	Terminal decline parameter in the Arps modified hyperbolic time-rate relation, D^{-1}
D_∞	=	Terminal decline parameter in the power-law exponential time-rate relation, D^{-1}
F_c	=	Fracture conductivity, md-ft
G_p	=	Cumulative gas production, MSCF or BSCF
k	=	Formation permeability, nD
$m(p)$	=	Real gas pseudopressure, psi^2/cp
$\Delta m(p)$	=	Real gas pseudopressure drop ($m(p_i) - m(p_{wf})$), $psia^2/cp$
n	=	Power-law exponential time exponent, dimensionless
n_f	=	Number of fractures, dimensionless
p	=	Pressure, psia
p_i	=	Initial reservoir pressure, psia
p_p	=	Real gas pseudopressure, psia
p_{wf}	=	Flowing bottomhole pressure, psia
Δp	=	Pressure drop ($p_i - p_{wf}$), psi
q_g	=	Gas flowrate, MSCF/D
$q_{i,hyp}$	=	Initial gas flowrate for hyperbolic relations, MSCF/D
q_{lim}	=	Initial gas flowrate for exponential relations, MSCF/D
$\hat{q}_i$	=	Initial rate parameter in the power-law exponential time-rate relation, MSCF/D
s	=	Fracture face skin, dimensionless
t	=	Production time, D
t_{lim}	=	Switch time for when Arps relation switches from hyperbolic to exponential decline, D
x_f	=	Fracture half-length, ft
z	=	Gas compressibility factor, dimensionless

Greek Variables:

β	=	Beta-derivative function, dimensionless
μ	=	Gas viscosity, cp

Acronyms:

DCA = Decline curve analysis

EUR = Estimated ultimate recovery

MBT = Material balance time (G_p/q_g), days

PI = Productivity Index [$q_g/(m(p_i) - m(p_{wf}))$], MSCF/D/psia^2/cp

RTA = Rate transient analysis

PTA = Pressure transient analysis

Subscripts:

d = Derivative

g = Gas

i = Initial or integral

id = Integral-derivative

Gas Pseudofunctions:

$m(p) = \frac{1}{2}\int_{p_{base}}^{p}\frac{p}{\mu z}dp$ (Pseudopressure — "psia^2/cp" form)

$p_p = \frac{\mu_i z_i}{p_i}\int_{p_{base}}^{p}\frac{p}{\mu z}dp$ (Pseudopressure — "psia" form)

Arps Definitions:

$\frac{1}{D(t)} = -\frac{q(t)}{dq(t)/dt}$ (loss-ratio)

$b(t) = \frac{d}{dt}\left[\frac{1}{D(t)}\right] = -\frac{d}{dt}\left[\frac{q(t)}{dq(t)/dt}\right]$ (loss-ratio derivative)

REFERENCES

Aboaba, A. and Cheng, Y. 2010. Estimation of Fracture Properties For a Horizontal Well With Multiple Hydraulic Fractures in Gas Shale. Paper SPE 138524 presented at the SPE Eastern Regional Meeting, Morgantown, West Virginia, 12-14 October. http://dx.doi.org/10.2118/138524-MS.

Agarwal, R. 1980. A New Method To Account For Producing Time Effects When Drawdown Type Curves Are Used To Analyze Pressure Buildup And Other Test Data. Paper SPE 9289 presented at the SPE Annual Technical Conference and Exhibition, Dallas, Texas, September 21-24. http://dx.doi.org/10.2118/9289-MS.

Agarwal, R., Gardner, D., Kleinsteiber, S., et al. 1998. Analyzing Well Production Data Using Combined Type Curve and Decline Curve Analysis Concepts. Paper SPE 49222 presented at the SPE Annual Technical Conference and Exhibition, New Orleans, Louisiana, 27-30 September. http://dx.doi.org/10.2118/49222-MS.

Agarwal, R., Gardner, D., Kleinsteiber, S., et al. 1999. Analyzing Well Production Data Using Combined-Type-Curve and Decline-Curve Analysis Concepts. *SPE Res Eval & Eng*. **2** (5): 478-486. SPE 57916-PA. http://dx.doi.org/10.2118/57916-PA.

Al-Ahmadi, H. A., Almarzooq, A. M. and Wattenbarger, R. A. 2010. Application of Linear Flow Analysis to Shale Gas Wells - Field Cases. Paper SPE 130370 presented at the SPE Unconventional Gas Conference, Pittsburgh, Pennsylvania, 23-25 February. http://dx.doi.org/10.2118/130370-MS.

Al-Kobaisi, M., Ozkan, E., Kazemi, H., et al. 2006. Pressure-Transient-Analysis of Horizontal Wells with Transverse, Finite-Conductivity Fractures. Paper PETSOC 2006-162 presented at the Canadian International Petroleum Conference, Calgary, Alberta, Canada, 13-15 June. http://dx.doi.org/10.2118/2006-162.

Anderson, D. and Mattar, L. 2004. Practical Diagnostics Using Production Data and Flowing Pressures. Paper SPE 89939 presented at the SPE Annual Technical Conference and Exhibition, Houston, Texas, 26-29 September. http://dx.doi.org/10.2118/89939-MS.

Ansah, J., Knowles, R. S. and Blasingame, T. A. 1996. A Semi-Analytic (p/z) Rate-Time Relation for the Analysis and Prediction of Gas Well Performance. Paper SPE 35268 presented at the SPE Mid-Continent Gas Symposium, Amarillo, Texas, 28-30 April. http://dx.doi.org/10.2118/35268-MS.

Arnold, R. and Anderson, R. 1908. Preliminary Report on the Coalinga Oil District: Fresno and Kings Counties, California. *U. S. Geol. Survey*. **357**: 1-142.

Arps, J. J. 1945. Analysis of Decline Curves. *Trans.* **160** (1): 228-247. SPE 945228. http://dx.doi.org/10.2118/945228-G.

Arps, J. J. and Smith, A. E. 1949. Practical Use of Bottom-hole Pressure Buildup curves. Paper API 49-155 presented at the Mid-Continent District Meeting, Tulsa, Oklahoma, March.

Blasingame, T. A., Ilk, D. and Hosseinpour-Zonoozi, N. 2007. Application of the B-Derivative Function to Production Analysis. Paper SPE 107967 presented at the 2007 SPE Rocky Mountain Oil & Gas Technology Symposium, Denver, Colorado, 16-18 April. http://dx.doi.org/10.2118/107967-MS.

Blasingame, T. A. 2011. Reservoir Engineering Aspects of Unconventional Reservoirs. Presented at the SPE GCS Reservoir Study Group, Houston, Texas, 27 October.

Bourdet, D., Ayoub, J. and Pirard, Y. 1989. Use of Pressure Derivative in Well Test Interpretation. *SPE Form Eval*. **4** (2): 293-302. SPE 12777-PA. http://dx.doi.org/10.2118/12777-PA.

Bourdet, D., Whittle, T., Douglas, A., et al. 1983. *A New Set of Type Curves Simplifies Well Test Analysis*. Houston, Texas, Gulf Publishing Co.

Callard, J. and Schenewerk, P. 1995. Reservoir Performance History Matching Using Rate/Cumulative Type-Curves. Paper SPE 30793 presented at the SPE Annual Technical Conference and Exhibition, Dallas, Texas, 22-25 October. http://dx.doi.org/10.2118/30793-MS.

Cheng, Y. 2011. Pressure Transient Characteristics of Hydraulically Fractured Horizontal Shale Gas Wells. Paper SPE 149311 presented at the SPE Eastern Regional Meeting, Columbus, Ohio, 17-19 August. http://dx.doi.org/10.2118/149311-MS.

Cinco-Ley, H., Samaniego-V, F. and Dominguez, A. 1978. Transient Pressure Behavior for a Well With a Finite-Conductivity Vertical Fracture. *SPE J.* **18** (4): 253-264. SPE 6014-PA. http://dx.doi.org/10.2118/6014-PA.

Cinco-Ley, H. and Samaniego-V, F. 1981. Transient Pressure Analysis for Fractured Wells. *J. Pet Tech*. **33** (9): 1749-1766. SPE 7490-PA. http://dx.doi.org/10.2118/7490-PA.

DeGolyer and MacNaughton. 2014. Citrine, version 1.00.02. 2014. Paris, France: KAPPA Engineering.

Duong, A. 2011. Rate-Decline Analysis for Fracture-Dominated Shale Reservoirs. *SPE Res Eval & Eng*. **14** (3): SPE-137748-PA. http://dx.doi.org/10.2118/137748-PA.

Ecrin ─ Topaze, version 4.30.05. 2013. Paris, France: KAPPA.

Fetkovich, M. J. 1980. Decline Curve Analysis Using Type Curves. *J. Pet Tech*. **32** (6): 1065-1077. http://dx.doi.org/10.2118/4629-PA.

Fraim, M. L. and Wattenbarger, R. A. 1987. Gas Reservoir Decline-Curve Analysis Using Type Curves With Real Gas Pseudopressure and Normalized Time. *SPE Form Eval*. **2** (4): 671-682. SPE 14238-PA. http://dx.doi.org/10.2118/14238-PA.

Fulford, D. and Blasingame, T.A. 2013. Evaluation of Time-Rate Performance of Shale Wells using the Transient Hyperbolic Relation. Paper SPE 167242 presented at the SPE Unconventional Resources Conference-Canada, Calgary, Alberta, Canada, 5-7 November. http://dx.doi.org/10.2118/167242-MS.

Gentry, R. W. and McCray, A. W. 1978. The Effect of Reservoir and Fluid Properties on Production Decline Curves. *J. Pet Tech*. **30** (9): 1327-1341. SPE 6341-PA. http://dx.doi.org/10.2118/6341-PA.

Horner, D. R. 1951. Pressure Build-up in Wells. Paper WPC 4135 presented at the Third World Petroleum Congress, The Hague, The Netherlands, 28 May-6 June.

Houzé, O., Viturat, D., Fjaere, O., et al. 2012. *Dynamic Data Analysis: The theory and practice of Pressure Transient, Production Analysis, Well Performance Analysis, Production Logging and the use of Permanent Downhole Gauge data.*, Vol. 4.12.03. Paris, France, KAPPA Engineering.

Idorenyin, E., Okouma, V. and Mattar, L. 2011. Analysis of Production Data Using the Beta-Derivative. Paper SPE 149361 presented at the Canadian Unconventional Resources Conference, Calgary, Alberta, Canada, 15-17 November. http://dx.doi.org/10.2118/149361-MS.

Ilk, D., Perego, A., Rushing, J., et al. 2008. Integrating Multiple Production Analysis Techniques To Assess Tight Gas Sand Reserves: Defining a New Paradigm for Industry Best Practices. Paper SPE 114947 presented at the CIPC/SPE Gas Technology Symposium 2008 Joint Conference, Calgary, Alberta, Canada, 16-19 June. http://dx.doi.org/10.2118/114947-MS.

Ilk, D., Anderson, D., Stotts, G., et al. 2010. Production Data Analysis--Challenges, Pitfalls, Diagnostics. *SPE Res Eval & Eng*. **13** (3): 538-552. SPE 102048. http://dx.doi.org/10.2118/102048-PA.

Ilk, D., Jenkins, C. D. and Blasingame, T. A. 2011a. Production Analysis in Unconventional Reservoirs - Diagnostics, Challenges, and Methodologies. Paper SPE 144376 presented at the SPE North American Unconventional Gas Conference and Exhibition, The Woodlands, 14-16 June. http://dx.doi.org/10.2118/144376-MS.

Ilk, D., Okouma, V. and Blasingame, T. A. 2011b. Characterization of Well Performance in Unconventional Reservoirs using Production Data Diagnostics. Paper SPE 147604 presented at the SPE Annual Technical Conference and Exhibition, Denver, Colorado, 30 October - 2 November. http://dx.doi.org/10.2118/147604-MS.

Johnson, R. and Bollens, A. 1927. The Loss Ratio Method of Extrapolating Oil Well Decline Curves. *Trans.* **77** (1): 771-778. SPE 927771. http://dx.doi.org/10.2118/927771-G.

Kabir, C. and Izgec, B. 2006. Diagnosis of Reservoir Behavior From Measured Pressure/Rate Data. Paper SPE 100384 presented at the SPE Gas Technology Symposium, Calgary, Alberta, Canada, 15-17 May. http://dx.doi.org/10.2118/100384-MS.

Larsen, L. and Hegre, T. M. 1994. Pressure Transient Analysis of Multifractured Horizontal Wells. Paper SPE 28389 presented at the SPE Annual Technical Conference and Exhibition, New Orleans, Louisiana, 25-28 September. http://dx.doi.org/10.2118/28389-MS.

Lewis, J. and Beal, C. 1918. Some New Methods for Estimating the Future Production of Oil Wells. *Trans.* **59** (1): 492-525. SPE 918492-G. http://dx.doi.org/10.2118/918492-G.

Maley, S. 1985. The Use of Conventional Decline Curve Analysis in Tight Gas Well Applications. Paper SPE 13898 presented at the SPE/DOE 1985 Low Permeability Gas Reservoirs, Denver, Colorado, May 19-22. http://dx.doi.org/10.2118/13898-MS.

Mattar, L. and McNeil, R. 1998. The "Flowing"Gas Material Balance. *The Journal of Canadian Petroleum Technology*. **37** (02): 52-55. PETSOC 98-02-06. http://dx.doi.org/10.2118/98-02-06.

Mayerhofer, M., Stegent, N., Barth, J., et al. 2011. Integrating Fracture Diagnostics and Engineering Data in the Marcellus Shale. Paper SPE 145463 presented at the SPE Annual Technical Conference and Exhibition, Denver, Colorado, 30 October-2 November. http://dx.doi.org/10.2118/145463-MS.

Miller, C. C., Dyes, A. B. and Hutchinson, C. A., Jr. 1950. The Estimation of Permeability and Reservoir Pressure From Bottom Hole Pressure Build-Up Characteristics. *J. Pet Tech*. **2** (4): 91-104. SPE 950091-G. http://dx.doi.org/10.2118/950091-G.

Muskat, M. 1937. Use of Data Oil the Build-up of Bottom-hole Pressures. *Trans.* **123** (1): 44-48. SPE 937044-G. http://dx.doi.org/10.2118/937044-G.

Palacio, J. and Blasingame, T. A. 1993. Decline Curve Analysis Using Type Curves: Analysis of Gas Well Production Data. Paper SPE 25909 presented at the SPE Joint Rocky Mountain and Low Permeability Symposium, Denver, Colorado, 12-13 April. http://dx.doi.org/10.2118/25909-MS.

Perrine, R. L. 1956. Analysis of Pressure-buildup Curves. *Drill. & Prod. Prac. J*. 482-509. API 56-482.

R: A Language and Environment for Statistical Computing, version 3.1.3. 2015. Vienna, Austria: R Foundation for Statistical Computing.

Robertson, S. 1988. *Generalized Hyperbolic Equation*. Paper SPE 18731 available from SPE, Richardson, Texas.

Rushing, J., Perego, A., Sullivan, R., et al. 2007. Estimating Reserves in Tight Gas Sands at HP/HT Reservoir Conditions: Use and Misuse of an Arps Decline Curve Methodology. Paper SPE 109625 presented at the 2007 SPE Annual Technical Conference and Exhibition, Anaheim, California, 11–14 November. http://dx.doi.org/10.2118/109625-MS.

Valkó, P. 2009. Assigning Value to Stimulation in the Barnett Shale: A Simultaneous Analysis of 7000 Plus Production Histories and Well Completion Records. Paper SPE 119369 presented at the 2009 SPE Hydraulic Fracturing Technology Conference, The Woodlands, Texas, 19-21 January. http://dx.doi.org/10.2118/119369-MS.

APPENDIX A

EAGLE FORD SHALE GAS FIELD EXAMPLES

Field Example 1 — Time-Rate Analysis

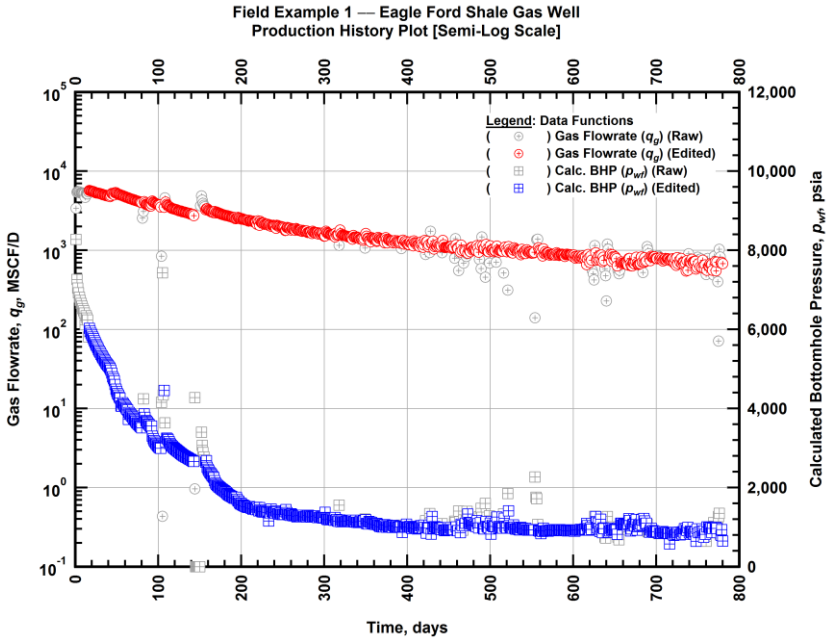

Figure A.1 — (Semi-log Plot): Filtered production history plot — flowrate (q_g) and calculated bottomhole pressure (p_{wf}) versus production time.

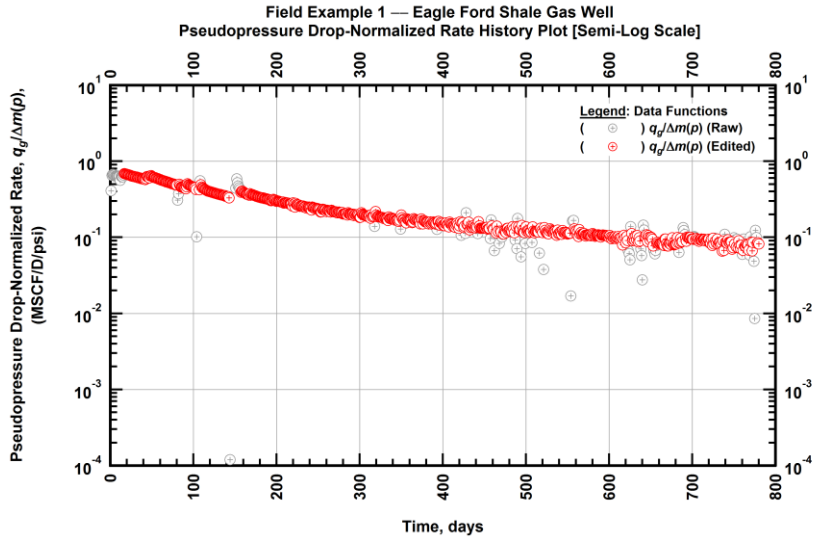

Figure A.2 — (Semi-log Plot): Filtered normalized rate production history plot — pseudopseudopressure drop-normalized gas flowrate ($q_g/\Delta m(p)$) versus production time.

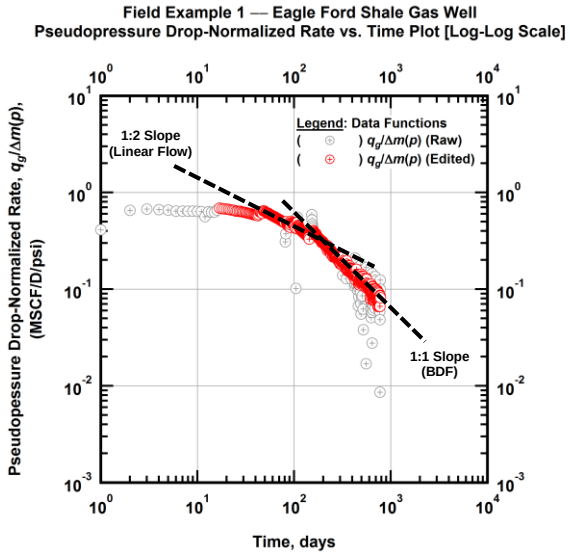

Figure A.3 — (Log-log Plot): Filtered normalized rate production history plot — pseudopseudopressure drop-normalized gas flowrate ($q_g/\Delta m(p)$) versus production time.

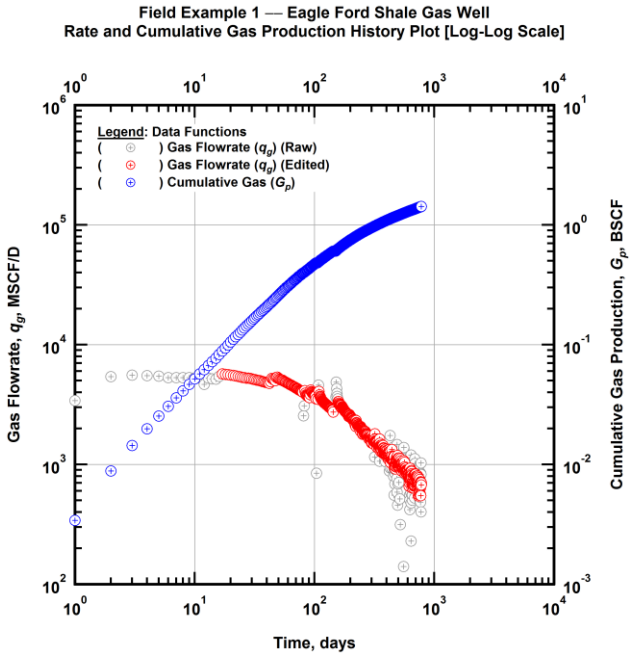

Figure A.4 — (Log-log Plot): Filtered rate and unfiltered cumulative gas production history plot — flowrate (q_g) and cumulative production (G_p) versus production time.

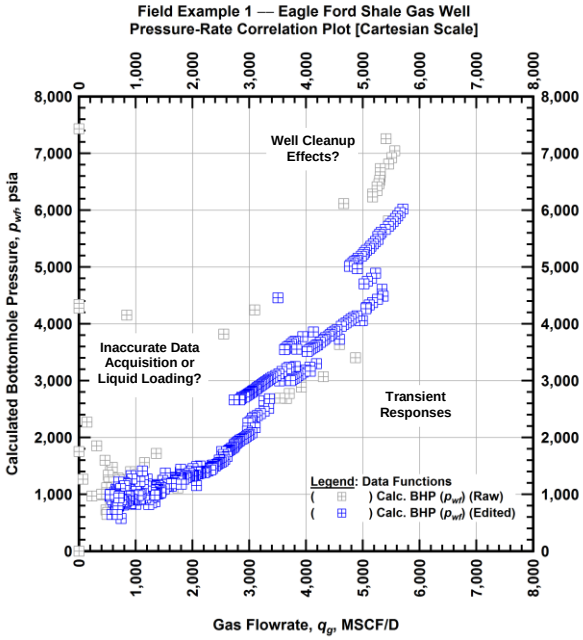

Figure A.5 — (Cartesian Plot): Filtered rate-pressure correlation plot — calculated bottomhole pressure (p_{wf}) versus flowrate (q_g).

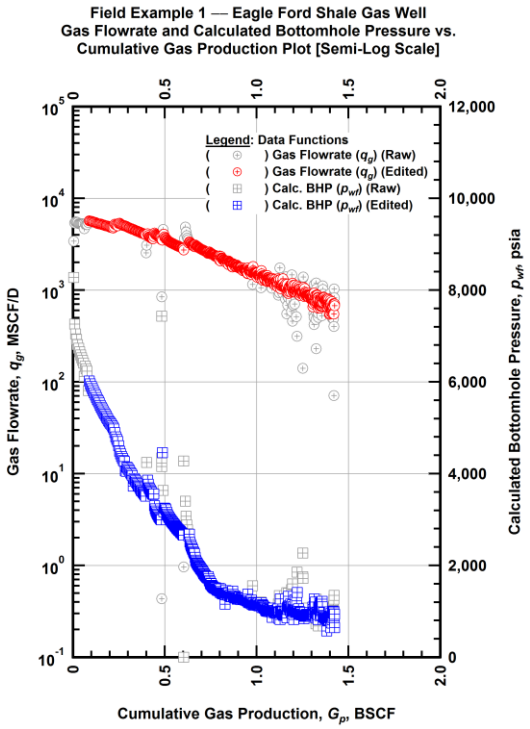

Figure A.6 — (Semi-log Plot): Filtered rate-pressure-cumulative production history plot — flowrate (q_g) and calculated bottomhole pressure (p_{wf}) versus cumulative production (G_p).

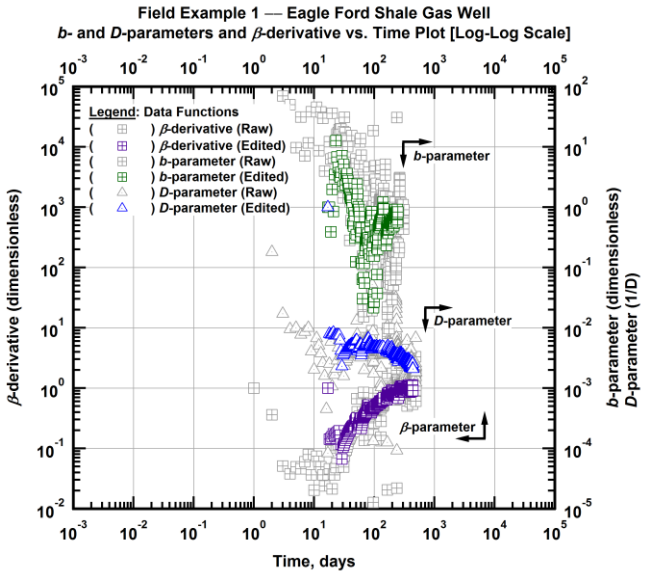

Figure A.7 — (Log-Log Plot): Filtered b, D and β production history plot — b- and D-parameters and β-derivative versus production time.

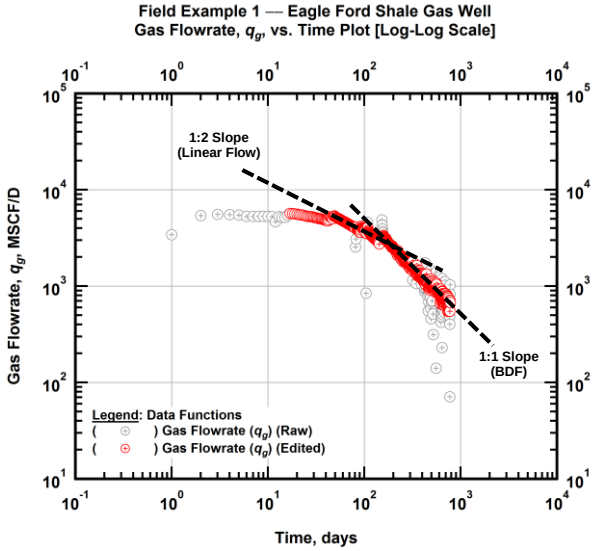

Figure A.8 — (Log-Log Plot): Filtered gas flowrate production history and flow regime identification plot — gas flowrate (q_g) versus production time.

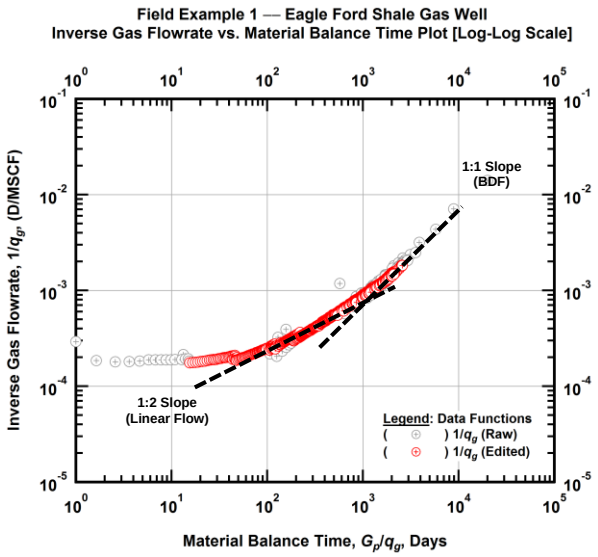

Figure A.9 — (Log-log Plot): Filtered inverse rate with material balance time plot — inverse gas flowrate ($1/q_g$) versus material balance time (G_p/q_g).

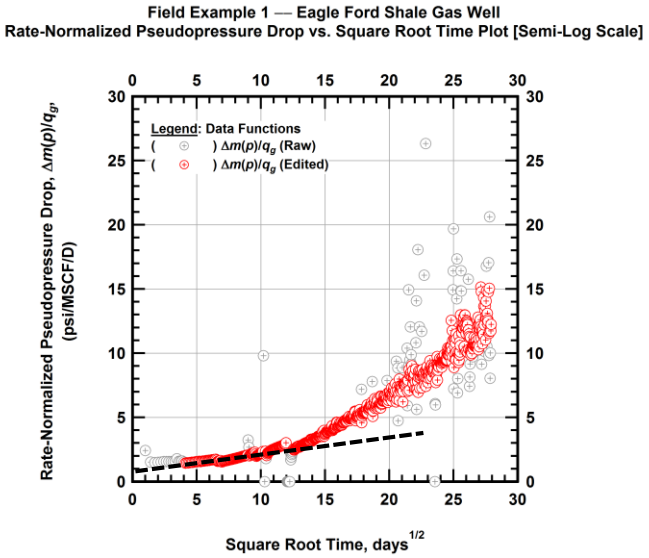

Figure A.10 — (Semi-log Plot): Filtered normalized pseudopressure drop production history plot — rate-normalized pseudopressure drop ($\Delta m(p)/q_g$) versus square root production time ($\sqrt{t}$).

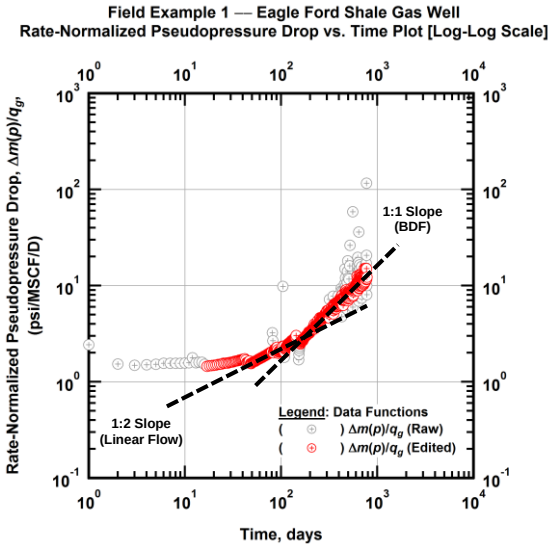

Figure A.11 — (Log-log Plot): Filtered normalized pseudopressure drop production history plot — rate-normalized pseudopressure drop ($\Delta m(p)/q_g$) versus production time.

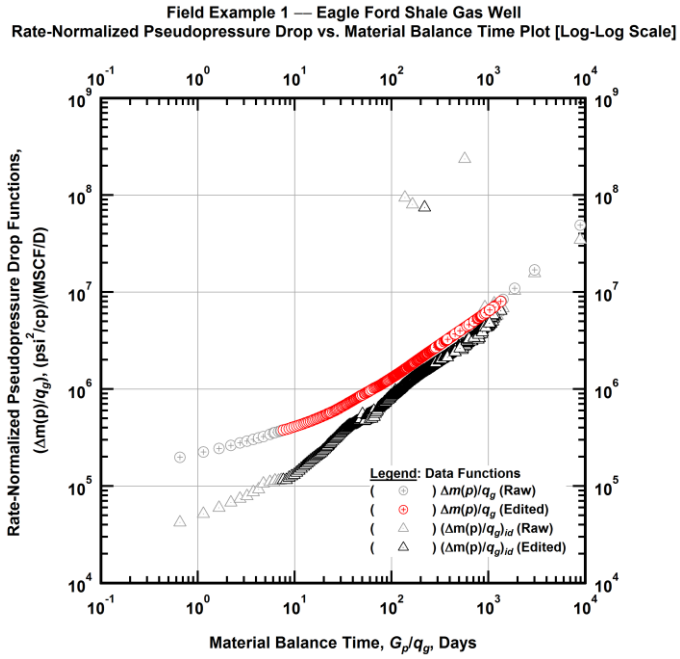

Figure A.12 — (Log-log Plot): "Log-log" diagnostic plot of the filtered production data — rate-normalized pseudopressure drop ($\Delta m(p)/q_g$) and rate-normalized pseudopressure drop integral-derivative $(\Delta m(p)/q_g)_{id}$ versus material balance time (G_p/q_g).

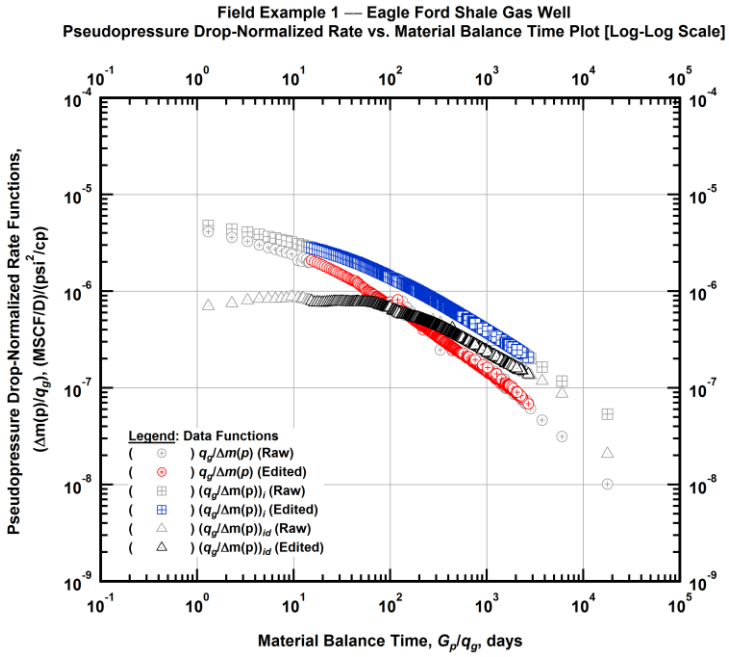

Figure A.13 — (Log-log Plot): "Blasingame" diagnostic plot of the filtered production data — pseudopressure drop-normalized gas flowrate ($q_g/\Delta m(p)$), pseudopressure drop-normalized gas flowrate integral $(q_g/\Delta m(p))_i$ and pseudopressure drop-normalized gas flowrate integral-derivative $(q_g/\Delta m(p))_{id}$ versus material balance time (G_p/q_g).

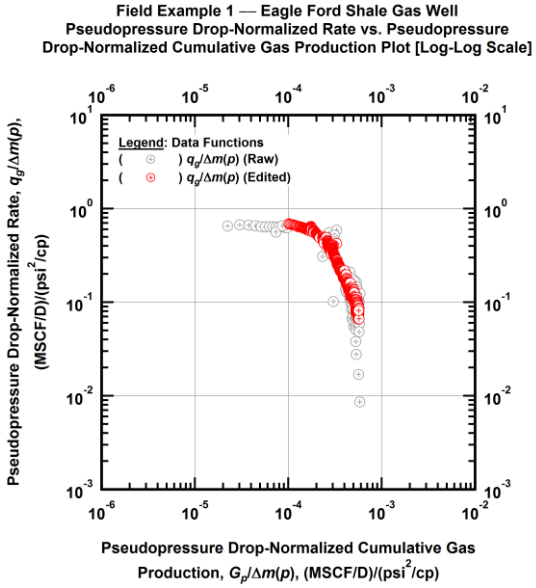

Figure A.14 — (Log-log Plot): Filtered normalized rate with normalized cumulative production plot — pseudopressure drop-normalized gas flowrate ($q_g/\Delta m(p)$) versus pseudopressure drop-normalized cumulative gas production ($G_p/\Delta m(p)$).

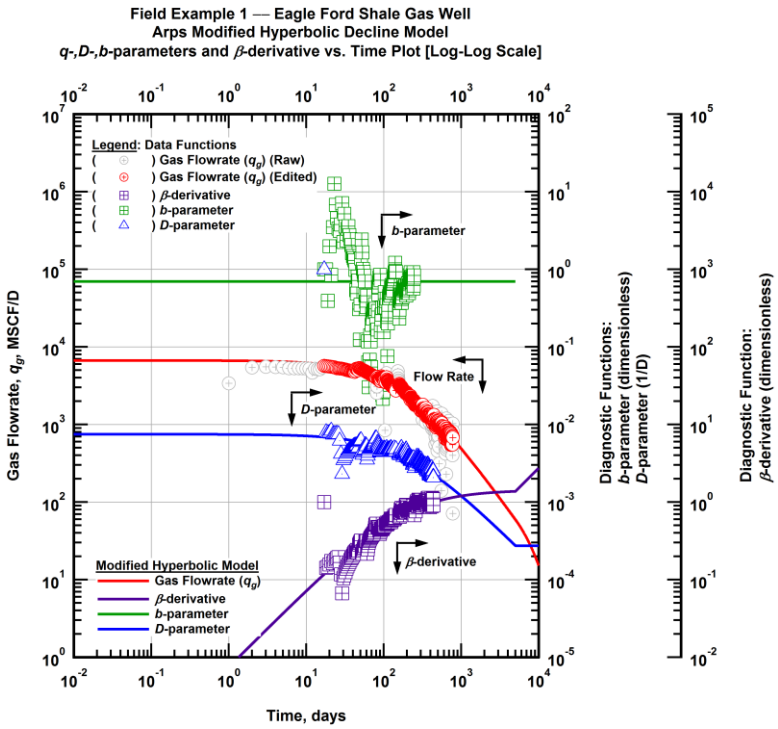

Figure A.15— (Log-Log Plot): Arps modified hyperbolic decline model plot — time-rate model and data gas flowrate (q_g), *D*- and *b*-parameters and β-derivative versus production time.

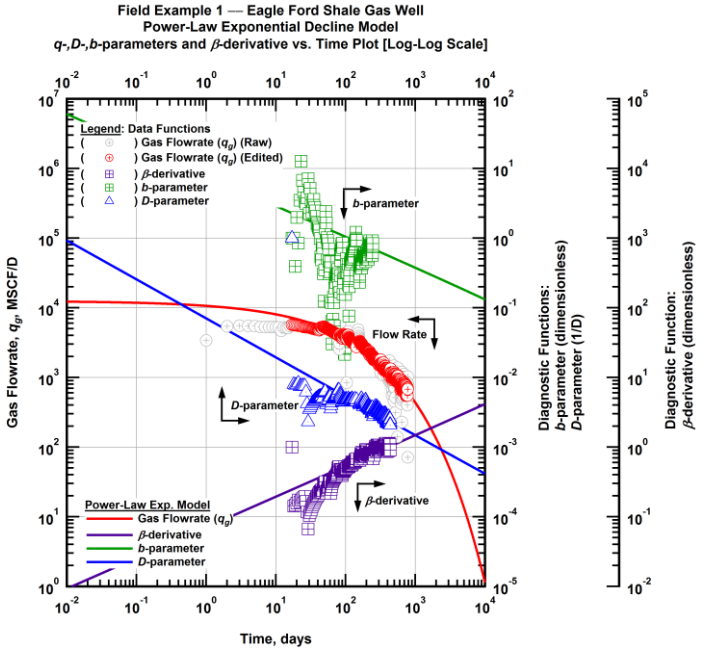

Figure A.16 — (Log-Log Plot): Power-law exponential decline model plot — time-rate model and data gas flowrate (q_g), *D*- and *b*-parameters and β-derivative versus production time.

Field Example 1 — Model-Based (Time-Rate-Pressure) Production Analysis

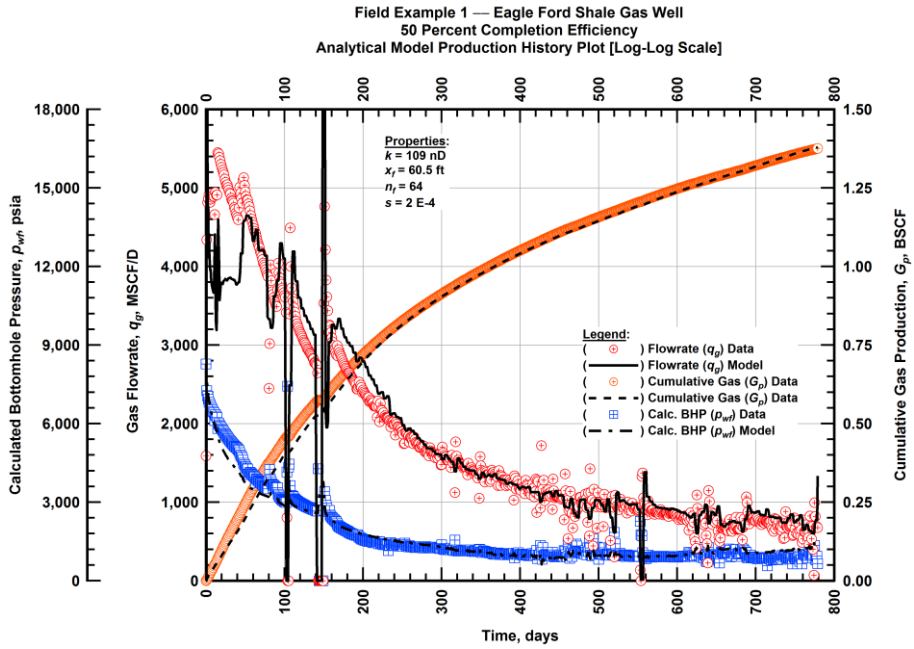

Figure A.17 — (Cartesian Plot): Production history plot — original gas flowrate (q_g), cumulative gas production (G_p), calculated bottomhole pressure (p_{wf}) and 50 percent completion efficiency model matches versus production time.

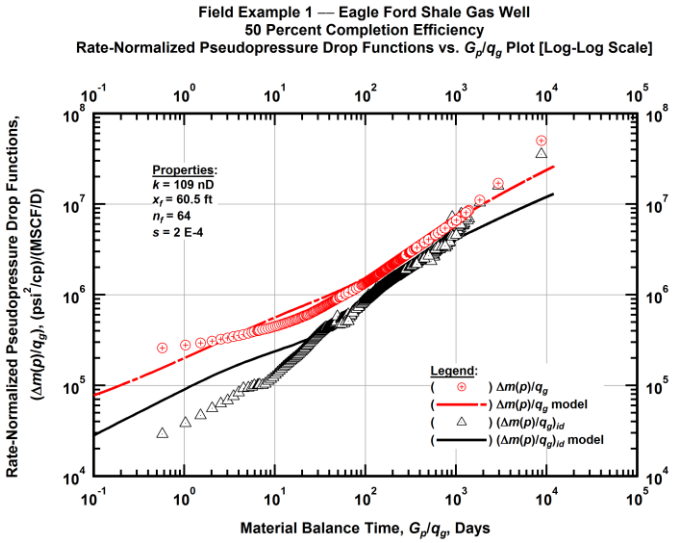

Figure A.18 — (Log-log Plot): "Log-log" diagnostic plot of the original production data — rate-normalized pseudopressure drop ($\Delta m(p)/q_g$), rate-normalized pseudopressure drop integral-derivative $(\Delta m(p)/q_g)_{id}$ and 50 percent completion efficiency model matches versus material balance time (G_p/q_g).

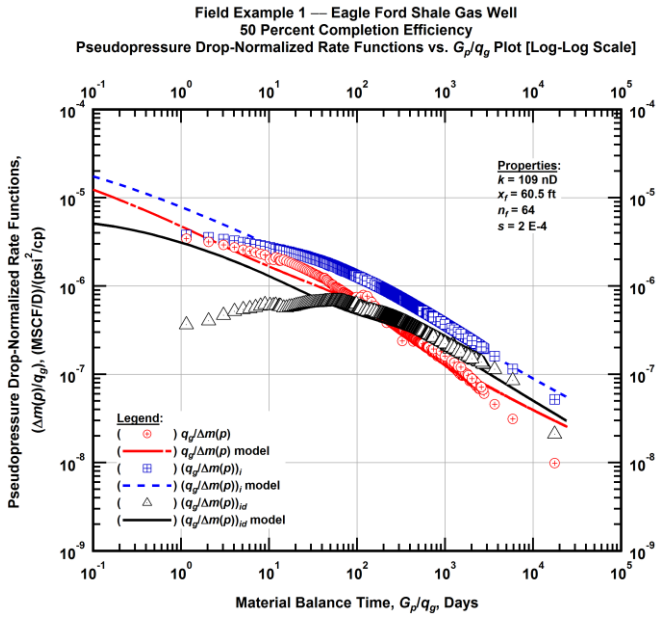

Figure A.19 — (Log-log Plot): "Blasingame" diagnostic plot of the original production data — pseudopressure drop-normalized gas flowrate ($q_g/\Delta m(p)$), pseudopressure drop-normalized gas flowrate integral $(q_g/\Delta m(p))_i$, pseudopressure drop-normalized gas flowrate integral-derivative $(q_g/\Delta m(p))_{id}$ and 50 percent completion efficiency model matches versus material balance time (G_p/q_g).

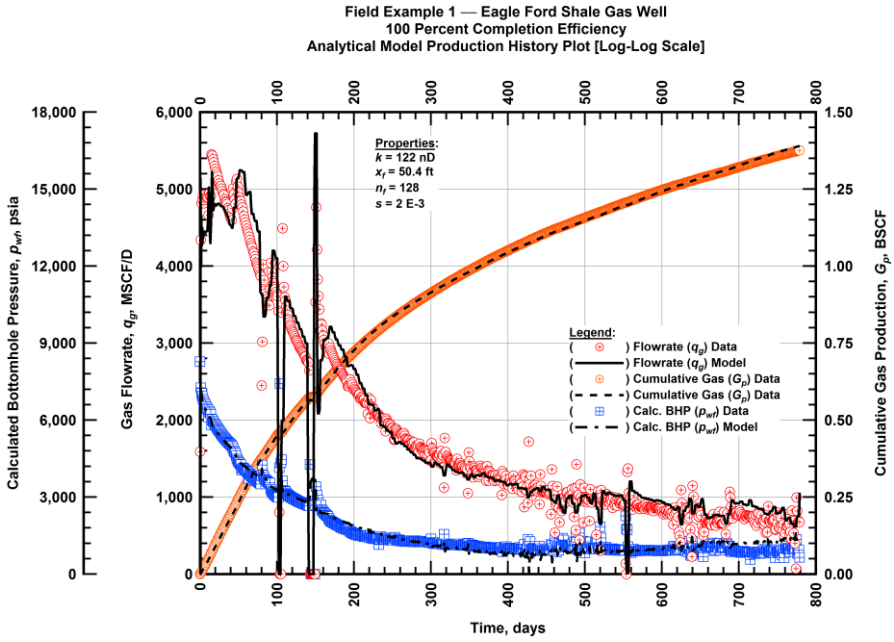

Figure A.20 — (Cartesian Plot): Production history plot — original gas flowrate (q_g), cumulative gas production (G_p), calculated bottomhole pressure (p_{wf}) and 100 percent completion efficiency model matches versus production time.

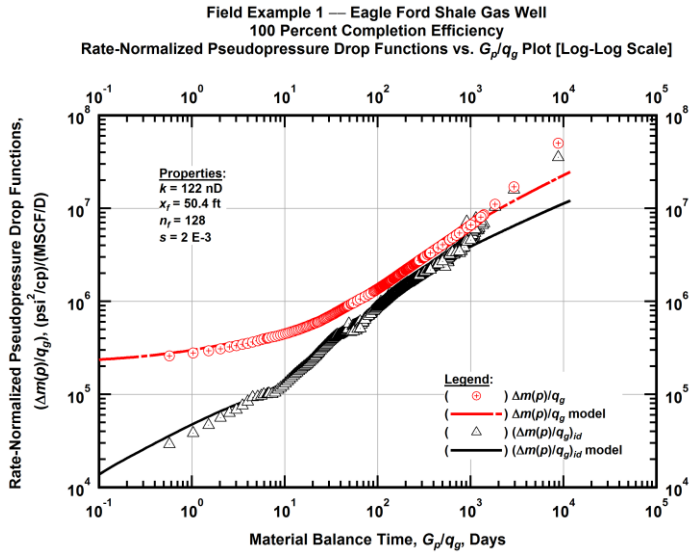

Figure A.21 — (Log-log Plot): "Log-log" diagnostic plot of the original production data — rate-normalized pseudopressure drop ($\Delta m(p)/q_g$), rate-normalized pseudopressure drop integral-derivative $(\Delta m(p)/q_g)_{id}$ and 100 percent completion efficiency model matches versus material balance time (G_p/q_g).

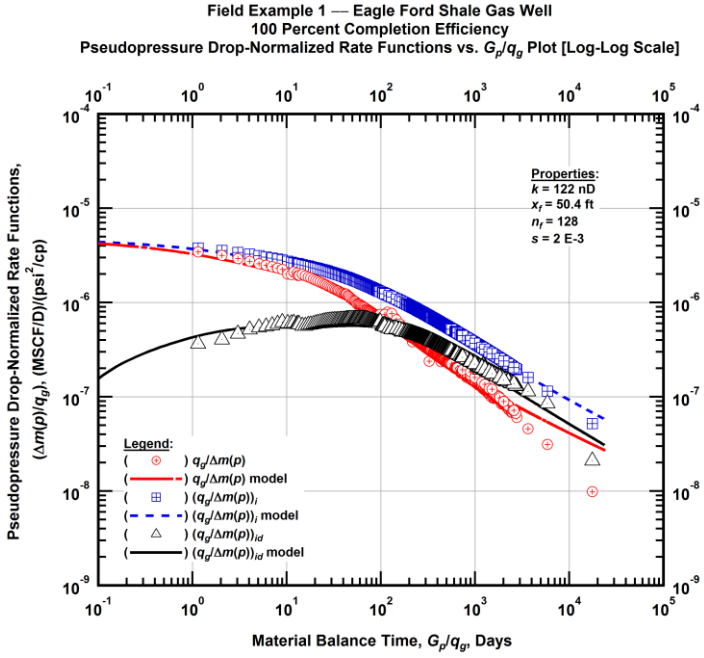

Figure A.22 — (Log-log Plot): "Blasingame" diagnostic plot of the original production data — pseudopressure drop-normalized gas flowrate ($q_g/\Delta m(p)$), pseudopressure drop-normalized gas flowrate integral $(q_g/\Delta m(p))_i$, pseudopressure drop-normalized gas flowrate integral-derivative $(q_g/\Delta m(p))_{id}$ and 100 percent completion efficiency model matches versus material balance time (G_p/q_g).

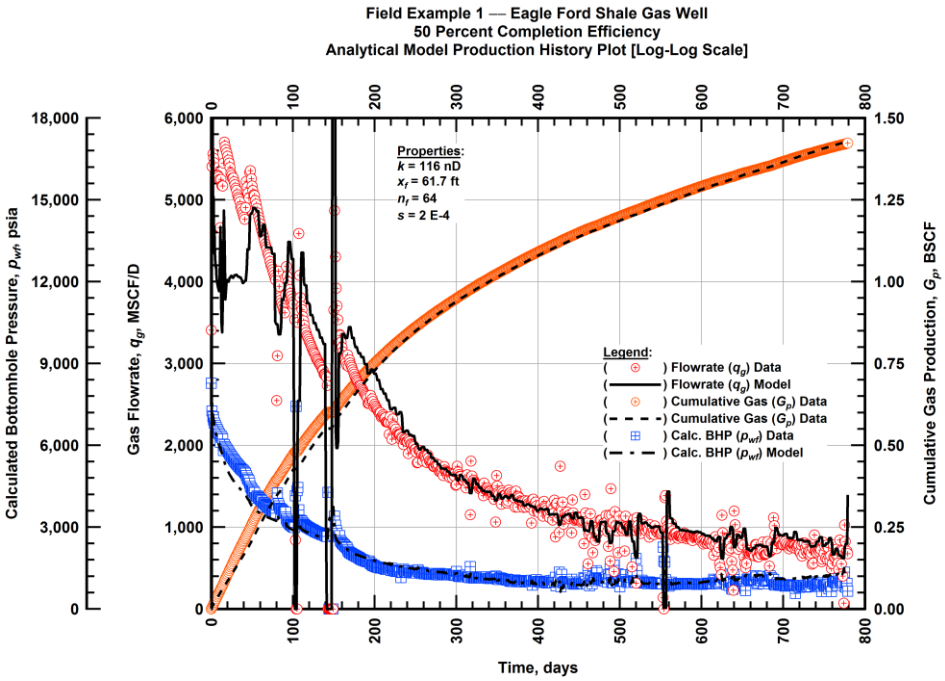

Figure A.23 — (Cartesian Plot): Production history plot — revised gas flowrate (q_g), cumulative gas production (G_p), calculated bottomhole pressure (p_{wf}) and 50 percent completion efficiency model matches versus production time.

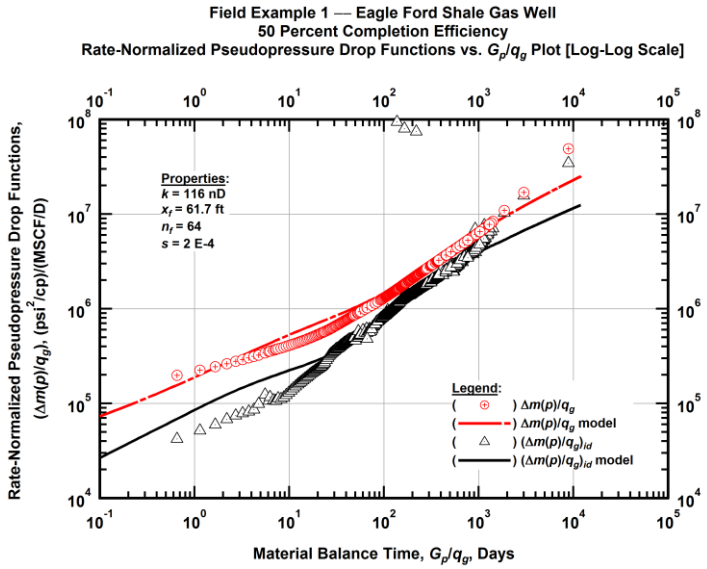

Figure A.24 — (Log-log Plot): "Log-log" diagnostic plot of the revised production data — rate-normalized pseudopressure drop ($\Delta m(p)/q_g$), rate-normalized pseudopressure drop integral-derivative $(\Delta m(p)/q_g)_{id}$ and 50 percent completion efficiency model matches versus material balance time (G_p/q_g).

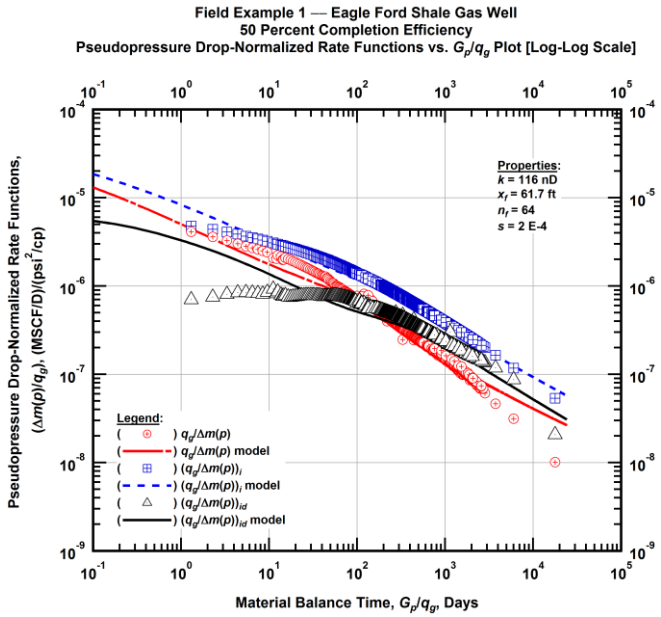

Figure A.25 — (Log-log Plot): "Blasingame" diagnostic plot of the revised production data — pseudopressure drop-normalized gas flowrate ($q_g/\Delta m(p)$), pseudopressure drop-normalized gas flowrate integral $(q_g/\Delta m(p))_i$, pseudopressure drop-normalized gas flowrate integral-derivative $(q_g/\Delta m(p))_{id}$ and 50 percent completion efficiency model matches versus material balance time (G_p/q_g).

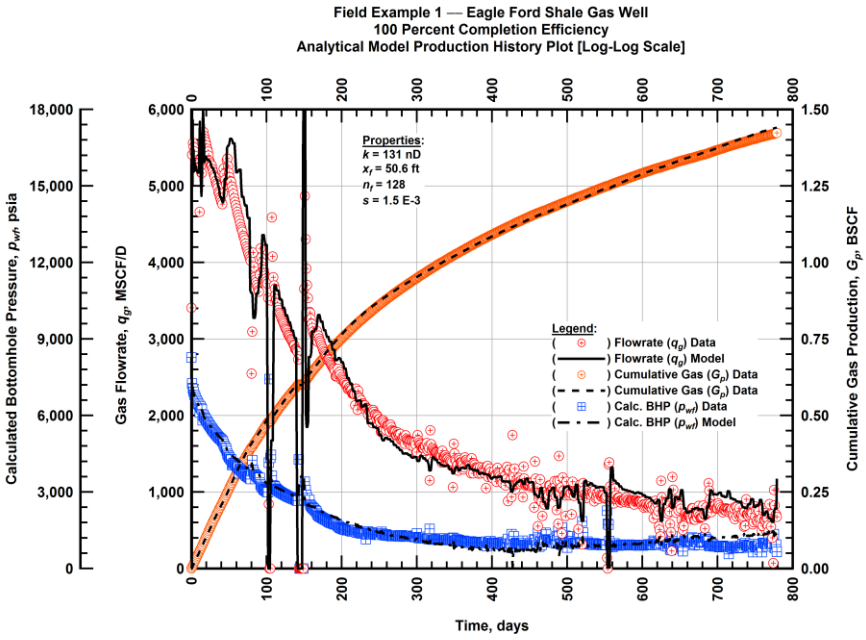

Figure A.26 — (Cartesian Plot): Production history plot — revised gas flowrate (q_g), cumulative gas production (G_p), calculated bottomhole pressure (p_{wf}) and 100 percent completion efficiency model matches versus production time.

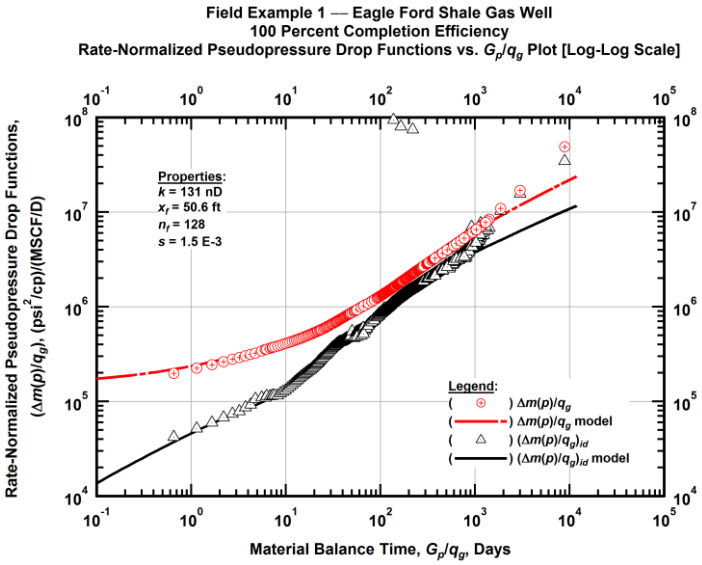

Figure A.27 — (Log-log Plot): "Log-log" diagnostic plot of the revised production data — rate-normalized pseudopressure drop ($\Delta m(p)/q_g$), rate-normalized pseudopressure drop integral-derivative $(\Delta m(p)/q_g)_{id}$ and 100 percent completion efficiency model matches versus material balance time (G_p/q_g).

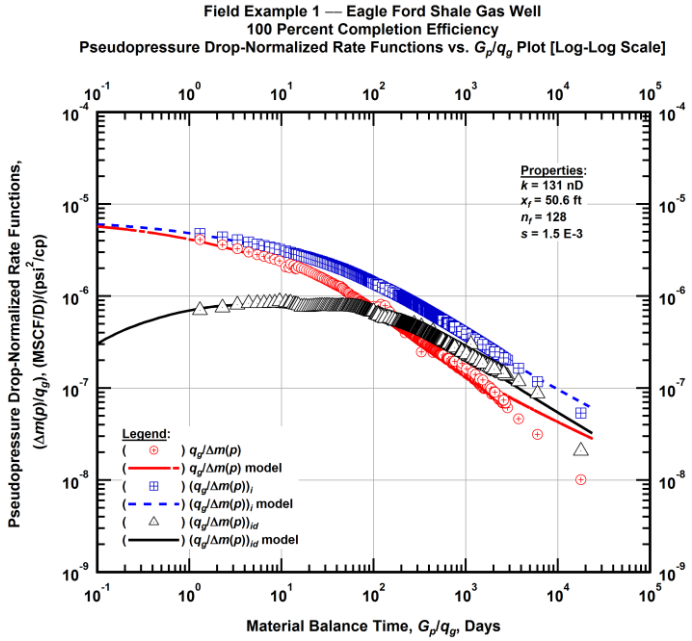

Figure A.28 — (Log-log Plot): "Blasingame" diagnostic plot of the revised production data — pseudopressure drop-normalized gas flowrate ($q_g/\Delta m(p)$), pseudopressure drop-normalized gas flowrate integral $(q_g/\Delta m(p))_i$, pseudopressure drop-normalized gas flowrate integral-derivative $(q_g/\Delta m(p))_{id}$ and 100 percent completion efficiency model matches versus material balance time (G_p/q_g).

Field Example 1 — 30-Year EUR Model Comparison

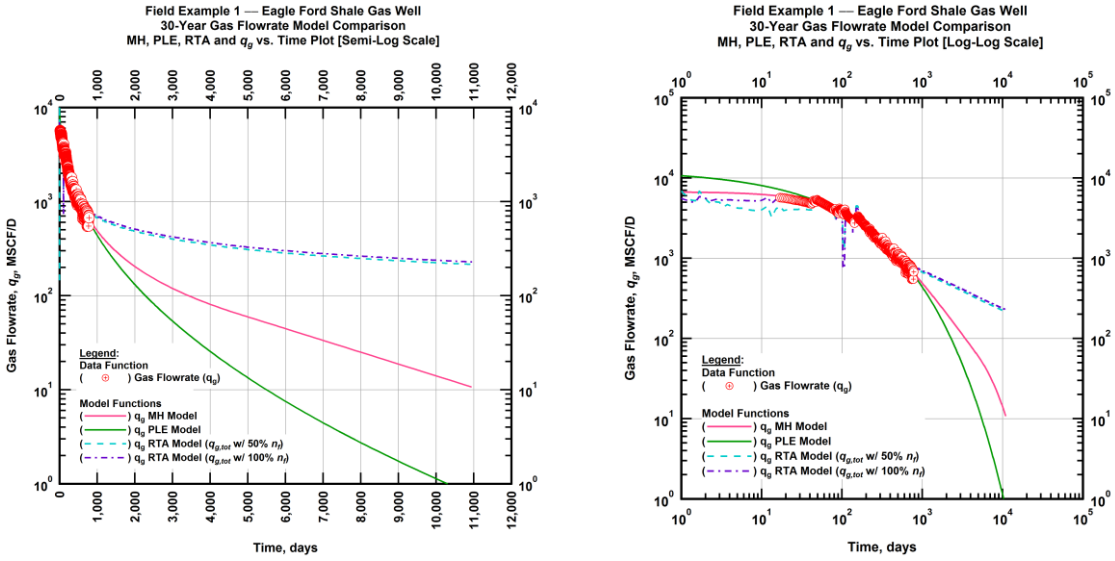

A **B**

Figure A.29 — (A — Semi-Log Plot) and (B — Log-Log Plot): Estimated 30-year revised gas flowrate model comparison — Arps modified hyperbolic decline model, power-law exponential decline model, and 50 percent and 100 percent completion efficiency RTA models estimated 30-year revised gas flowrate decline and historic revised gas flowrate data (q_g) versus production time.

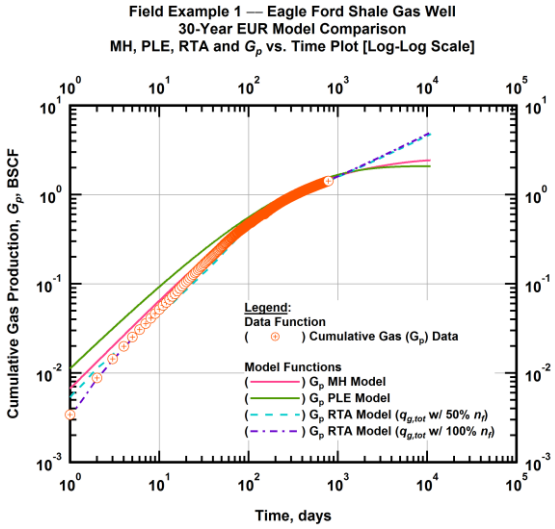

Figure A.30 — (Log-log Plot): Estimated 30-year cumulative gas production volume model comparison — Arps modified hyperbolic decline model, power-law exponential decline model, and 50 percent and 100 percent completion efficiency RTA models estimated 30-year cumulative gas production volumes and historic cumulative gas production (Gp) versus production time.

Table A.1 — 30-year estimated cumulative revised gas production (EUR), in units of BSCF, for the Arps modified hyperbolic, power-law exponential and analytical time-rate-pressure decline models.

Arps Modified Hyperbolic (BSCF)	Power-Law Exponential (BSCF)	RTA Analytical Model ($q_{g,tot}$ w/ 50% n_f) (BSCF)	RTA Analytical Model ($q_{g,tot}$ w/ 100% n_f) (BSCF)
2.36	1.95	4.95	5.16

Field Example 2 — Time-Rate Analysis

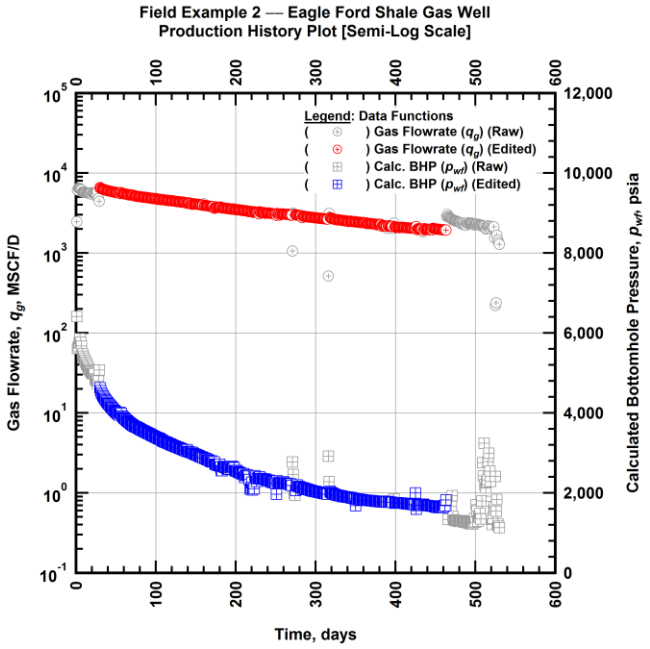

Figure A.31 — (Semi-log Plot): Filtered production history plot — flowrate (q_g) and calculated bottomhole pressure (p_{wf}) versus production time.

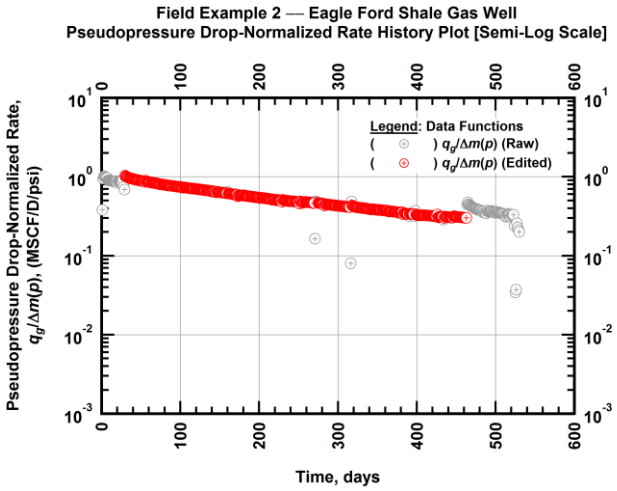

Figure A.32 — (Semi-log Plot): Filtered normalized rate production history plot — pseudopseudopressure drop-normalized gas flowrate ($q_g/\Delta m(p)$) versus production time.

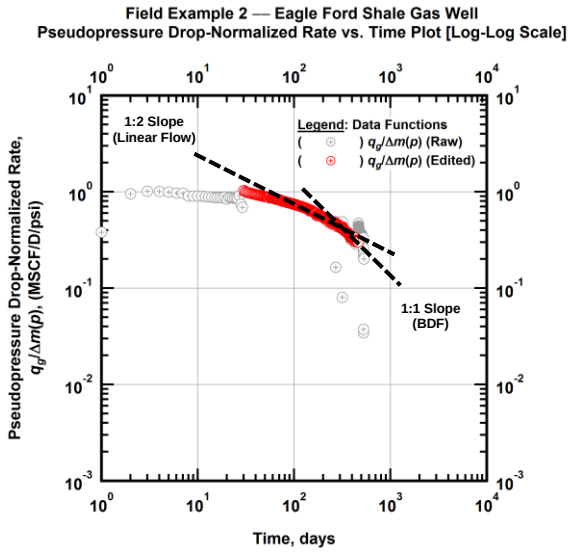

Figure A.33 — (Log-log Plot): Filtered normalized rate production history plot — pseudopseudopressure drop-normalized gas flowrate ($q_g/\Delta m(p)$) versus production time.

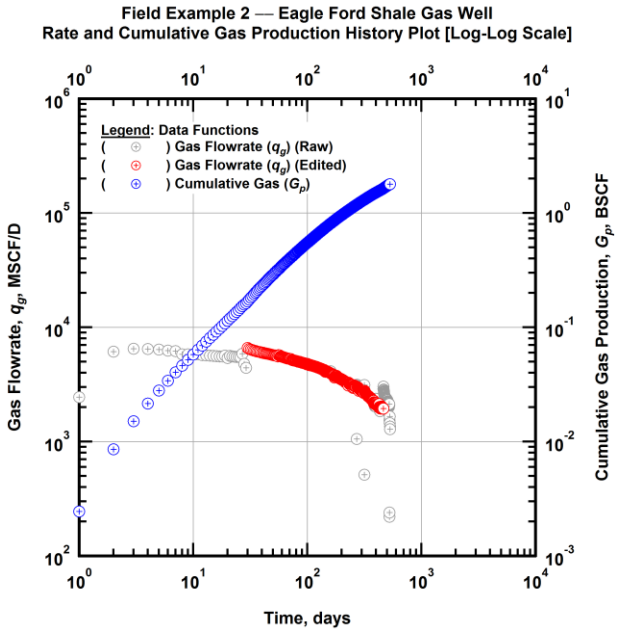

Figure A.34 — (Log-log Plot): Filtered rate and unfiltered cumulative gas production history plot — flowrate (q_g) and cumulative production (G_p) versus production time.

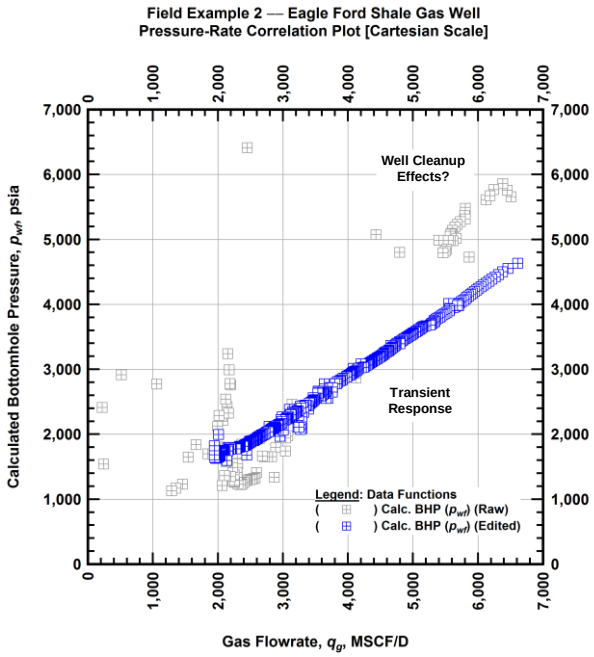

Figure A.35 — (Cartesian Plot): Filtered rate-pressure correlation plot — calculated bottomhole pressure (p_{wf}) versus flowrate (q_g).

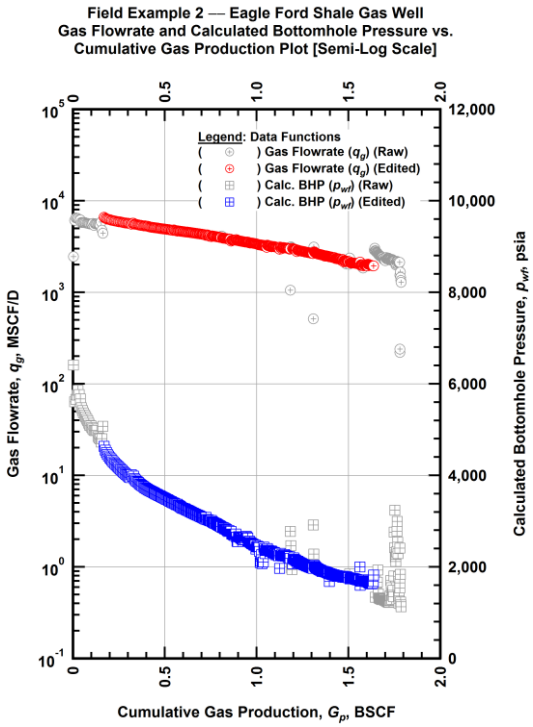

Figure A.36 — (Semi-log Plot): Filtered rate-pressure-cumulative production history plot — flowrate (q_g) and calculated bottomhole pressure (p_{wf}) versus cumulative production (G_p).

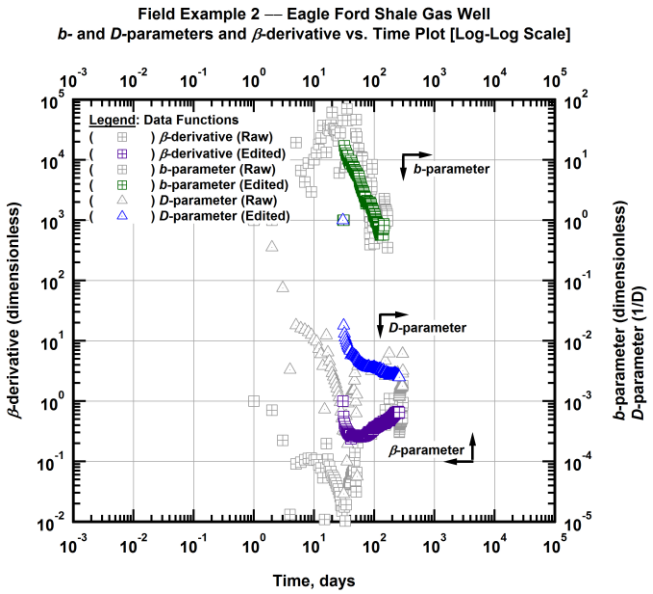

Figure A.37 — (Log-Log Plot): Filtered b, D and β production history plot — b- and D-parameters and β-derivative versus production time.

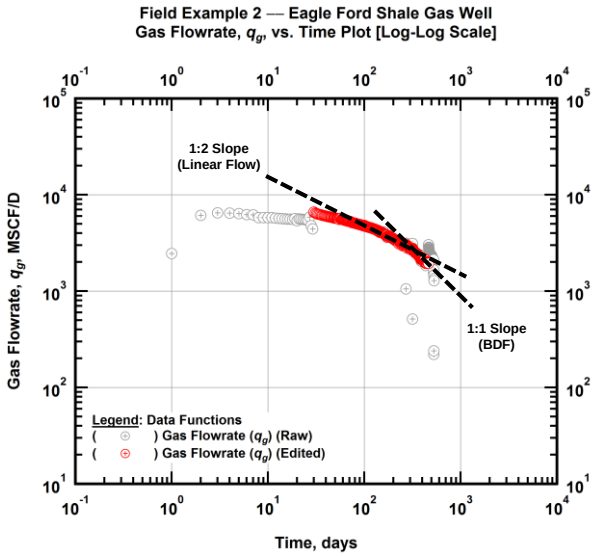

Figure A.38 — (Log-Log Plot): Filtered gas flowrate production history and flow regime identification plot — gas flowrate (q_g) versus production time.

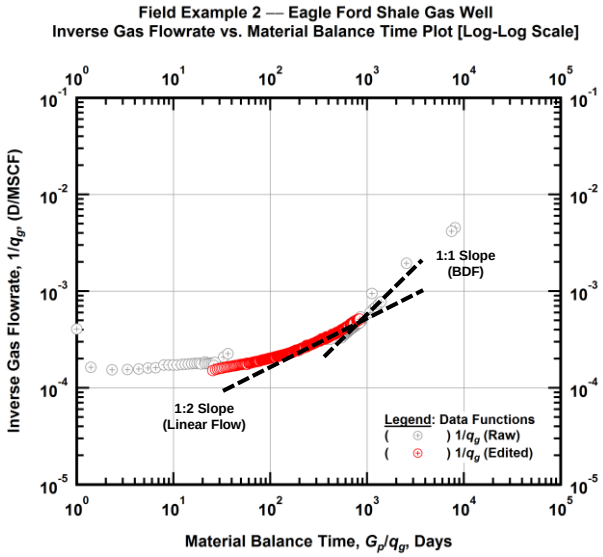

Figure A.39 — (Log-log Plot): Filtered inverse rate with material balance time plot — inverse gas flowrate ($1/q_g$) versus material balance time (G_p/q_g).

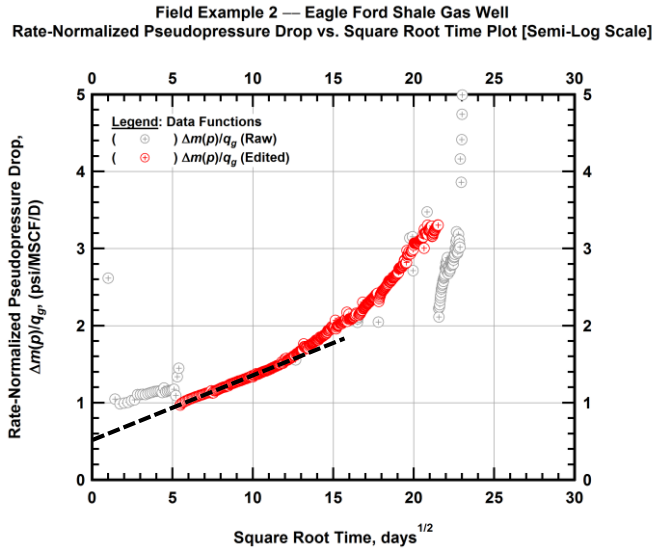

Figure A.40 — (Semi-log Plot): Filtered normalized pseudopressure drop production history plot — rate-normalized pseudopressure drop ($\Delta m(p)/q_g$) versus square root production time ($\sqrt{t}$).

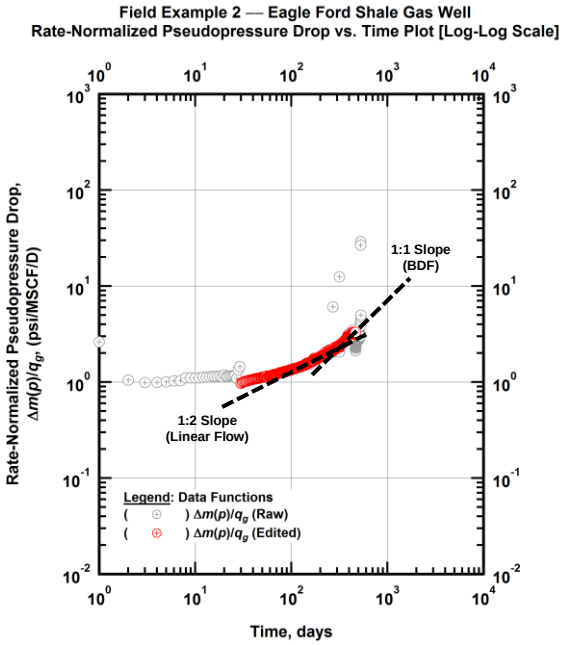

Figure A.41 — (Log-log Plot): Filtered normalized pseudopressure drop production history plot — rate-normalized pseudopressure drop ($\Delta m(p)/q_g$) versus production time.

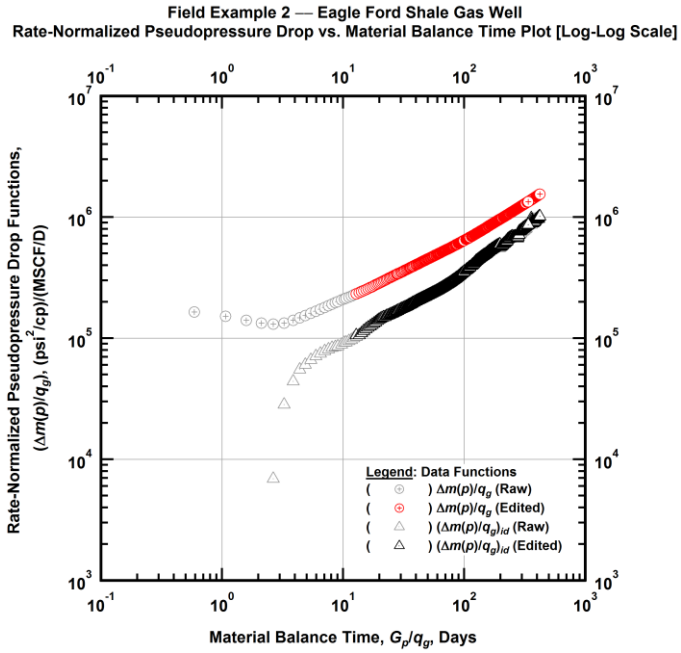

Figure A.42 — (Log-log Plot): "Log-log" diagnostic plot of filtered production data — rate-normalized pseudopressure drop ($\Delta m(p)/q_g$) and rate-normalized pseudopressure drop integral-derivative $(\Delta m(p)/q_g)_{id}$ versus material balance time (G_p/q_g).

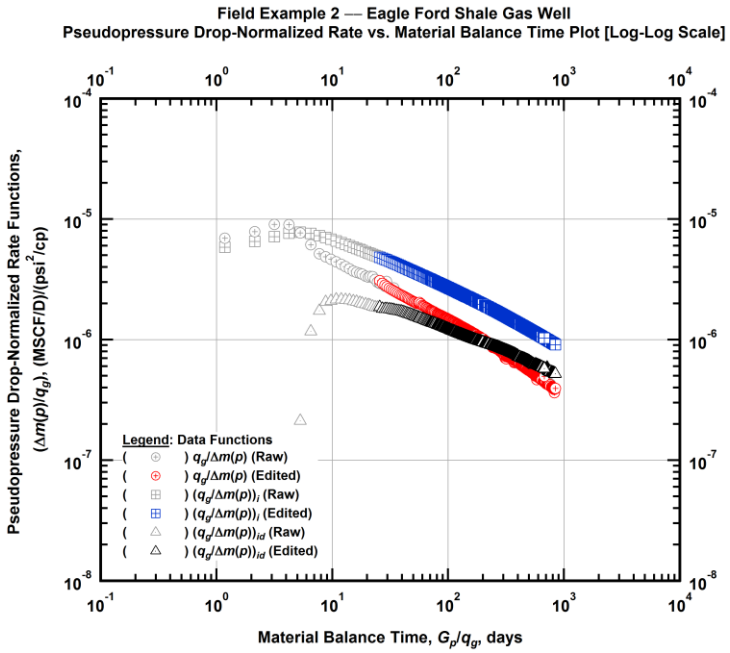

Figure A.43 — (Log-log Plot): "Blasingame" diagnostic plot of filtered production data — pseudopressure drop-normalized gas flowrate ($q_g/\Delta m(p)$), pseudopressure drop-normalized gas flowrate integral $(q_g/\Delta m(p))_i$ and pseudopressure drop-normalized gas flowrate integral-derivative $(q_g/\Delta m(p))_{id}$ versus material balance time (G_p/q_g).

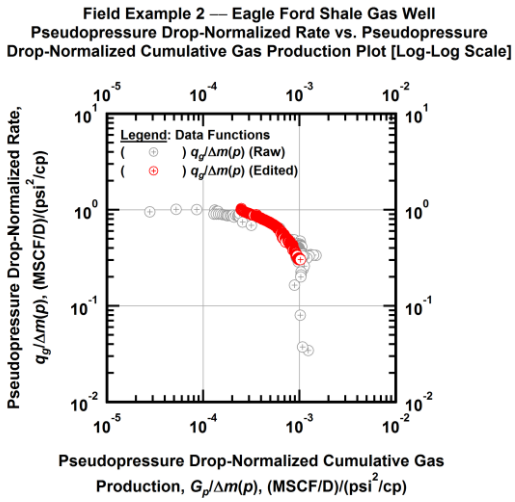

Figure A.44 — (Log-log Plot): Filtered normalized rate with normalized cumulative production plot — pseudopressure drop-normalized gas flowrate ($q_g/\Delta m(p)$) versus pseudopressure drop-normalized cumulative gas production ($G_p/\Delta m(p)$).

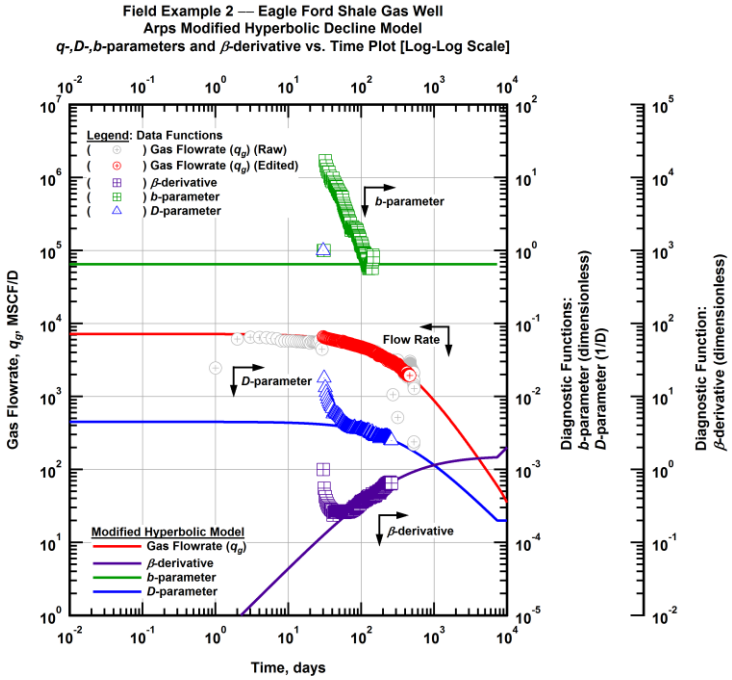

Figure A.45 — (Log-Log Plot): Arps modified hyperbolic decline model plot — time-rate model and data gas flowrate (q_g), *D*- and *b*-parameters and β-derivative versus production time.

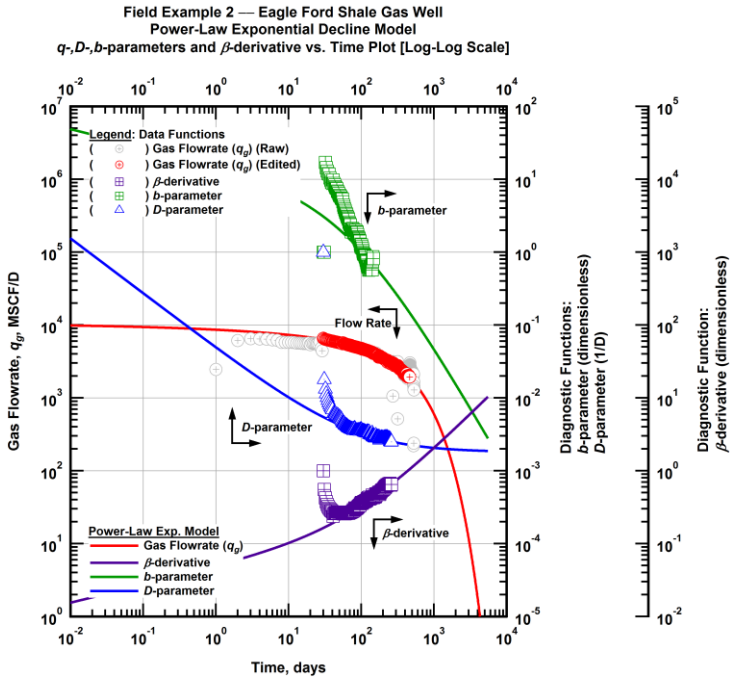

Figure A.46 — (Log-Log Plot): Power-law exponential decline model plot — time-rate model and data gas flowrate (q_g), *D*- and *b*-parameters and β-derivative versus production time.

Field Example 2 — Model-Based (Time-Rate-Pressure) Production Analysis

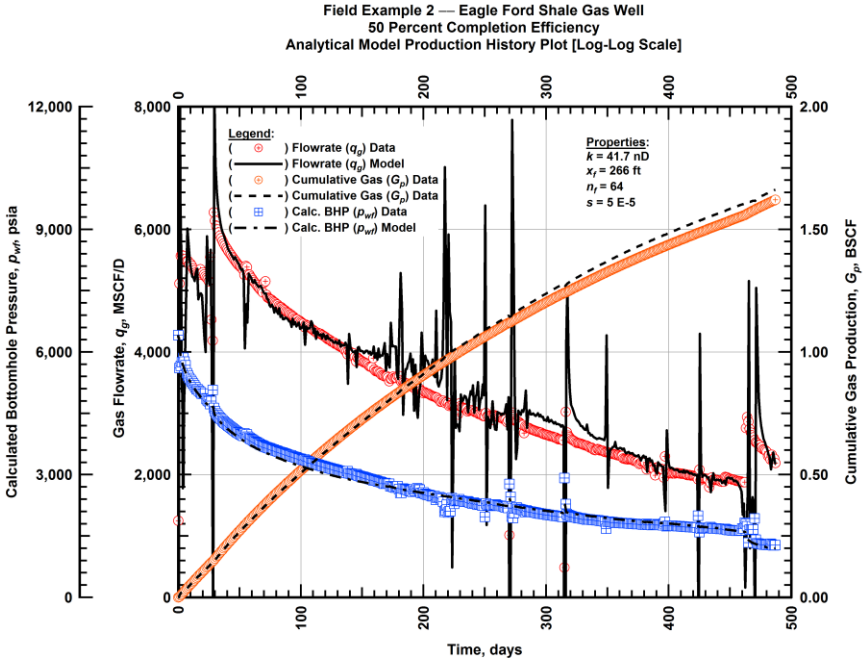

Figure A.47 — (Cartesian Plot): Production history plot — original gas flowrate (q_g), cumulative gas production (G_p), calculated bottomhole pressure (p_{wf}) and 50 percent completion efficiency model matches versus production time.

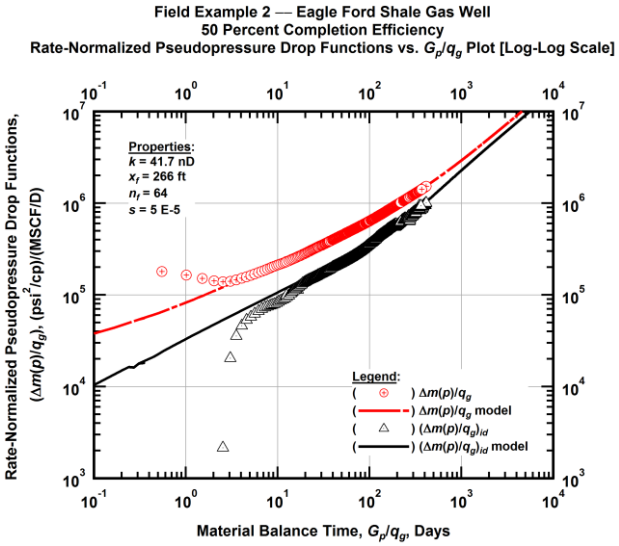

Figure A.48 — (Log-log Plot): "Log-log" diagnostic plot of the original production data — rate-normalized pseudopressure drop ($\Delta m(p)/q_g$), rate-normalized pseudopressure drop integral-derivative $(\Delta m(p)/q_g)_{id}$ and 50 percent completion efficiency model matches versus material balance time (G_p/q_g).

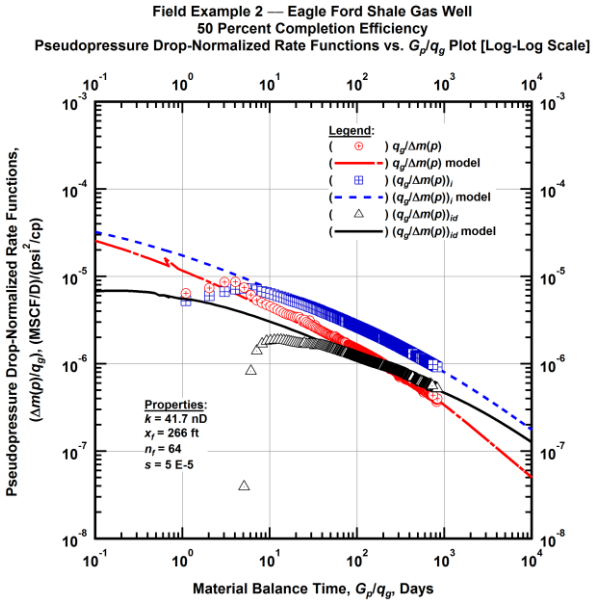

Figure A.49 — (Log-log Plot): "Blasingame" diagnostic plot of the original production data — pseudopressure drop-normalized gas flowrate ($q_g/\Delta m(p)$), pseudopressure drop-normalized gas flowrate integral $(q_g/\Delta m(p))_i$, pseudopressure drop-normalized gas flowrate integral-derivative $(q_g/\Delta m(p))_{id}$ and 50 percent completion efficiency model matches versus material balance time (G_p/q_g).

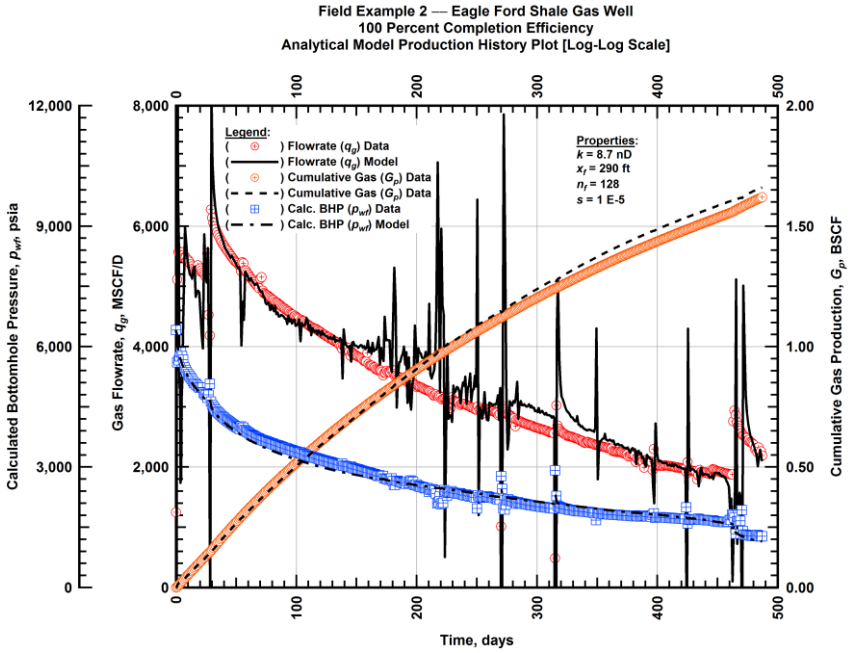

Figure A.50 — (Cartesian Plot): Production history plot — original gas flowrate (q_g), cumulative gas production (G_p), calculated bottomhole pressure (p_{wf}) and 100 percent completion efficiency model matches versus production time.

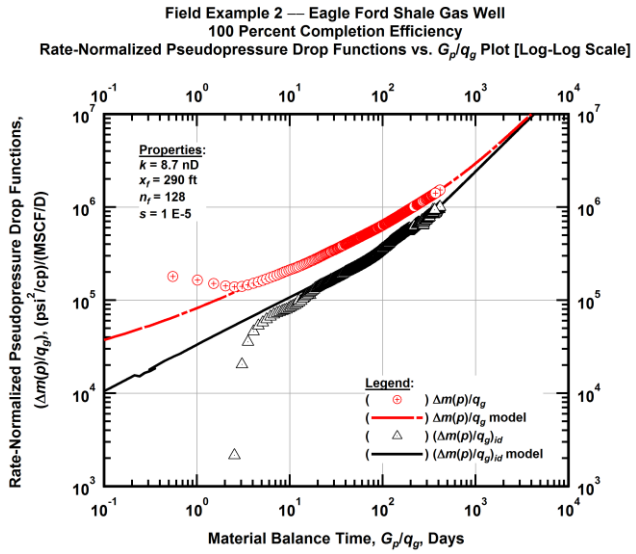

Figure A.51 — (Log-log Plot): "Log-log" diagnostic plot of the original production data — rate-normalized pseudopressure drop ($\Delta m(p)/q_g$), rate-normalized pseudopressure drop integral-derivative $(\Delta m(p)/q_g)_{id}$ and 100 percent completion efficiency model matches versus material balance time (G_p/q_g).

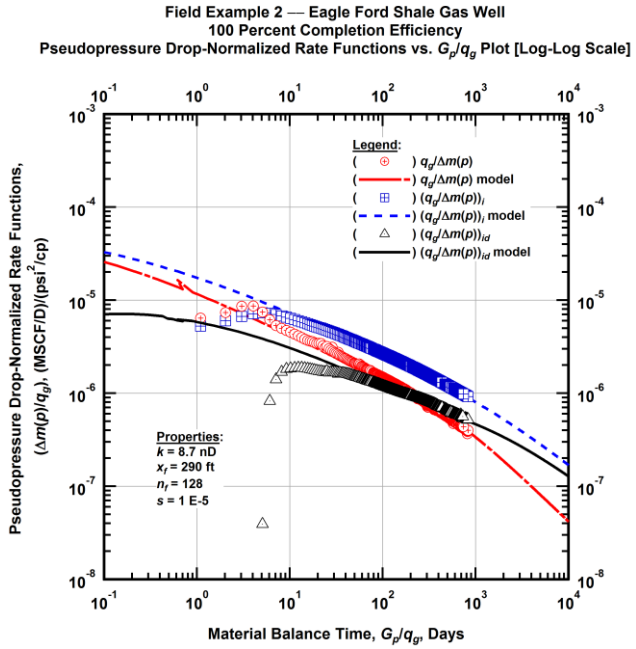

Figure A.52 — (Log-log Plot): "Blasingame" diagnostic plot of the original production data — pseudopressure drop-normalized gas flowrate ($q_g/\Delta m(p)$), pseudopressure drop-normalized gas flowrate integral $(q_g/\Delta m(p))_i$, pseudopressure drop-normalized gas flowrate integral-derivative $(q_g/\Delta m(p))_{id}$ and 100 percent completion efficiency model matches versus material balance time (G_p/q_g).

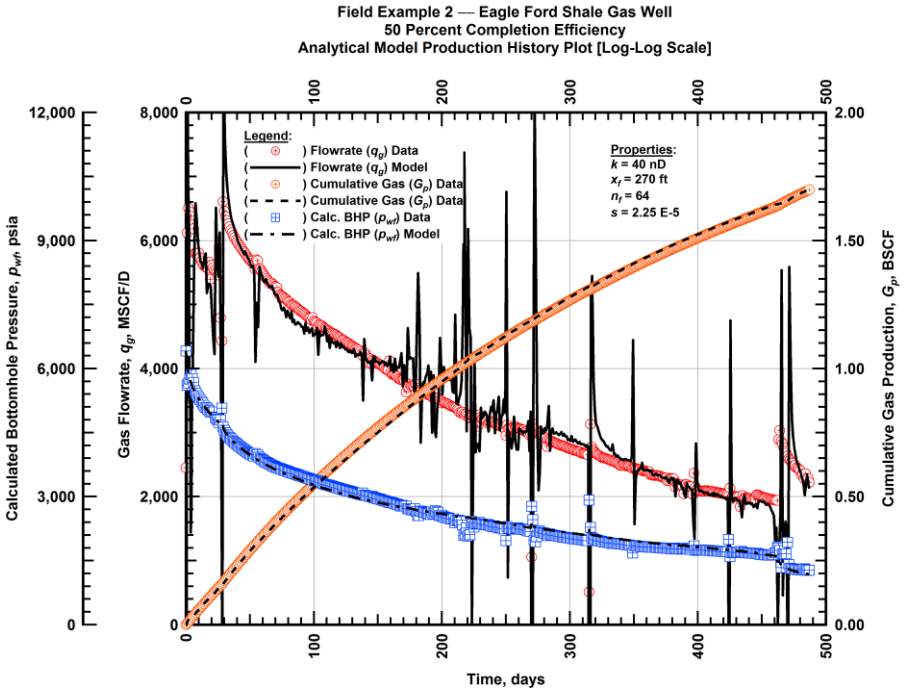

Figure A.53 — (Cartesian Plot): Production history plot — revised gas flowrate (q_g), cumulative gas production (G_p), calculated bottomhole pressure (p_{wf}) and 50 percent completion efficiency model matches versus production time.

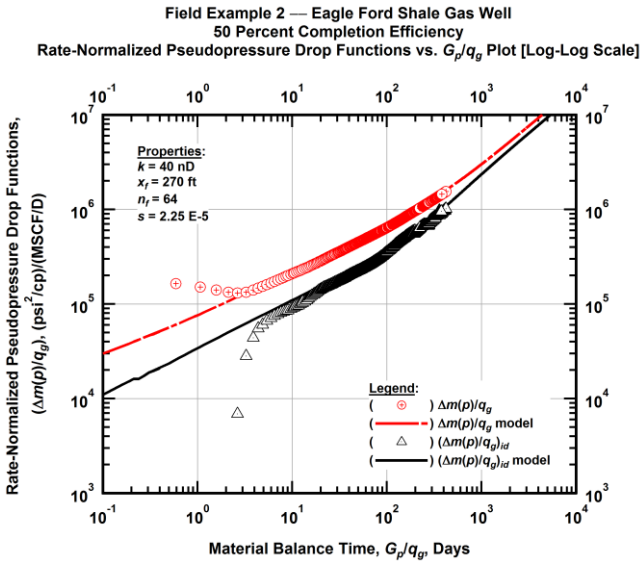

Figure A.54 — (Log-log Plot): "Log-log" diagnostic plot of the revised production data — rate-normalized pseudopressure drop ($\Delta m(p)/q_g$), rate-normalized pseudopressure drop integral-derivative $(\Delta m(p)/q_g)_{id}$ and 50 percent completion efficiency model matches versus material balance time (G_p/q_g).

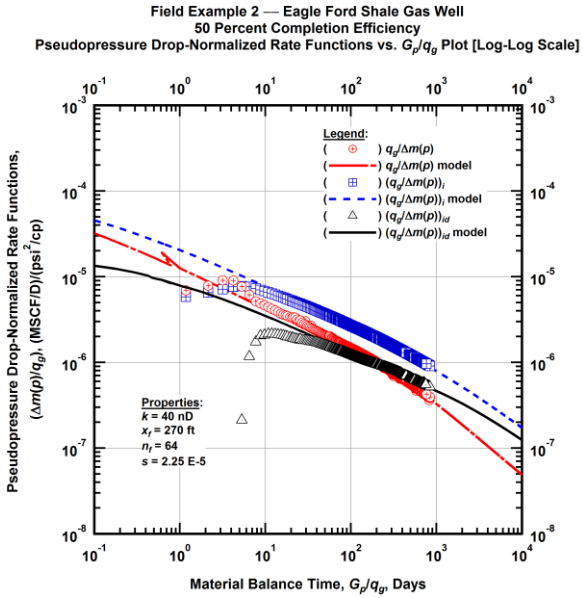

Figure A.55 — (Log-log Plot): "Blasingame" diagnostic plot of the revised production data — pseudopressure drop-normalized gas flowrate ($q_g/\Delta m(p)$), pseudopressure drop-normalized gas flowrate integral $(q_g/\Delta m(p))_i$, pseudopressure drop-normalized gas flowrate integral-derivative $(q_g/\Delta m(p))_{id}$ and 50 percent completion efficiency model matches versus material balance time (G_p/q_g).

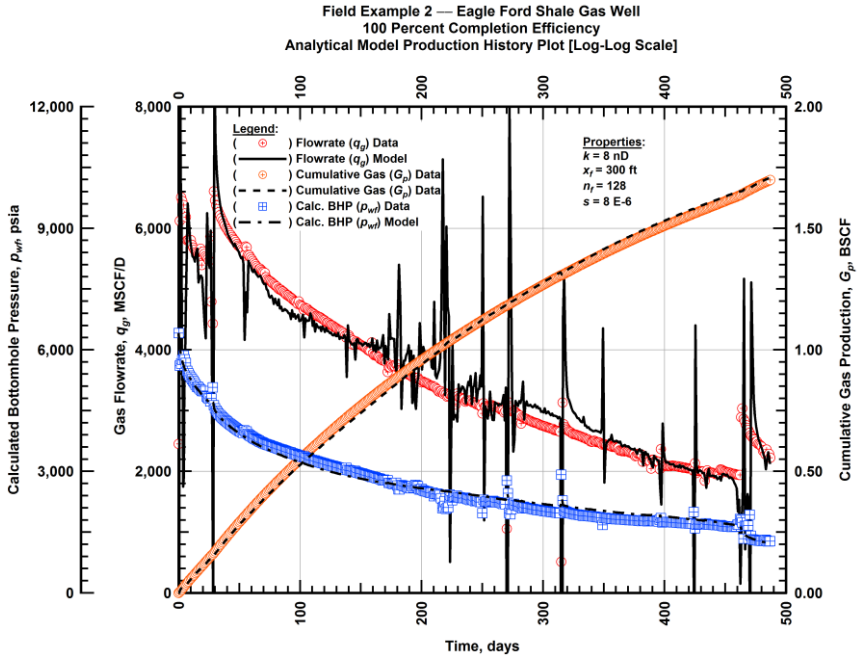

Figure A.56 — (Cartesian Plot): Production history plot — revised gas flowrate (q_g), cumulative gas production (G_p), calculated bottomhole pressure (p_{wf}) and 100 percent completion efficiency model matches versus production time.

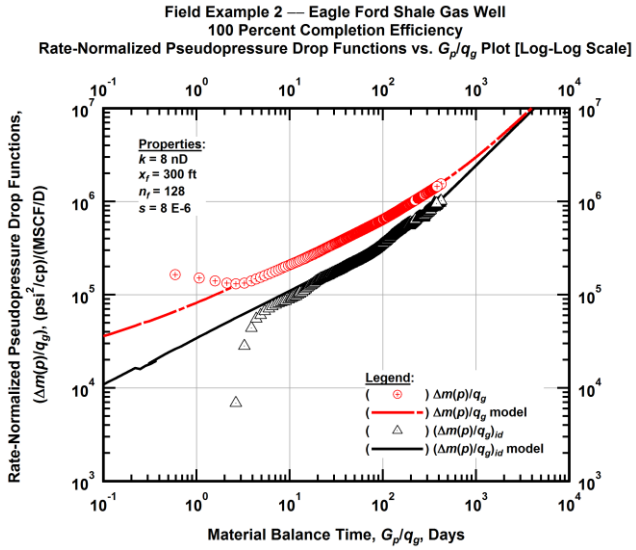

Figure A.57 — (Log-log Plot): "Log-log" diagnostic plot of the revised production data — rate-normalized pseudopressure drop ($\Delta m(p)/q_g$), rate-normalized pseudopressure drop integral-derivative $(\Delta m(p)/q_g)_{id}$ and 100 percent completion efficiency model matches versus material balance time (G_p/q_g).

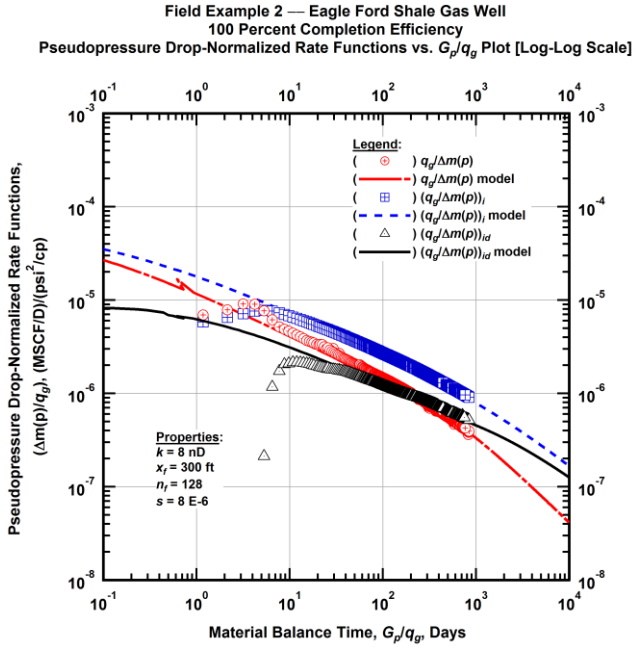

Figure A.58 — (Log-log Plot): "Blasingame" diagnostic plot of the revised production data — pseudopressure drop-normalized gas flowrate ($q_g/\Delta m(p)$), pseudopressure drop-normalized gas flowrate integral $(q_g/\Delta m(p))_i$, pseudopressure drop-normalized gas flowrate integral-derivative $(q_g/\Delta m(p))_{id}$ and 100 percent completion efficiency model matches versus material balance time (G_p/q_g).

Field Example 2 — 30-Year EUR Model Comparison

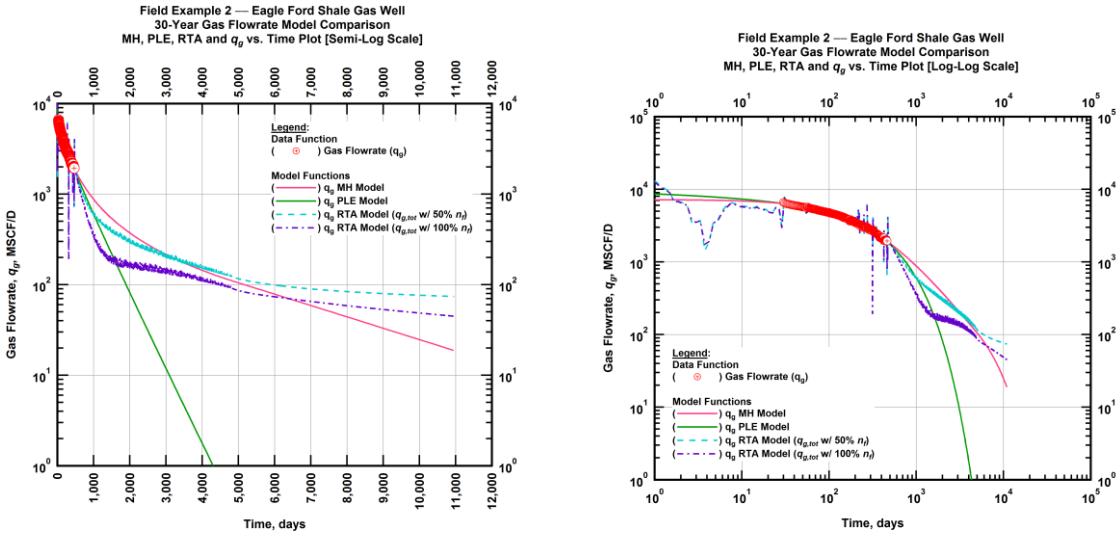

A **B**

Figure A.59 — (A — Semi-Log Plot) and (B — Log-Log Plot): Estimated 30-year revised gas flowrate model comparison — Arps modified hyperbolic decline model, power-law exponential decline model, and 50 percent and 100 percent completion efficiency RTA models revised gas 30-year estimated flowrate decline and historic gas flowrate data (q_g) versus production time.

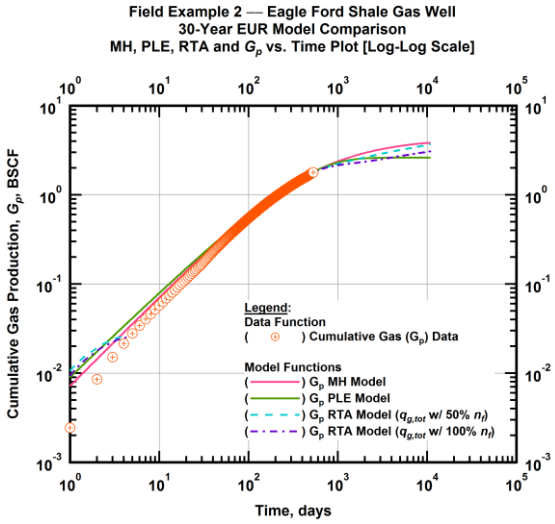

Figure A.60 — (Log-log Plot): Estimated 30-year cumulative gas production volume model comparison — Arps modified hyperbolic decline model, power-law exponential decline model, and 50 percent and 100 percent completion efficiency RTA models estimated 30-year cumulative gas production volumes and historic cumulative gas production (Gp) versus production time.

Table A.2 — 30-year estimated cumulative revised gas production (EUR), in units of BSCF, for the Arps modified hyperbolic, power-law exponential and analytical time-rate-pressure decline models.

Arps Modified Hyperbolic (BSCF)	Power-Law Exponential (BSCF)	RTA Analytical Model ($q_{g,tot}$ w/ 50% n_f) (BSCF)	RTA Analytical Model ($q_{g,tot}$ w/ 100% n_f) (BSCF)
3.81	2.56	3.74	3.10

Field Example 3 — Time-Rate Analysis

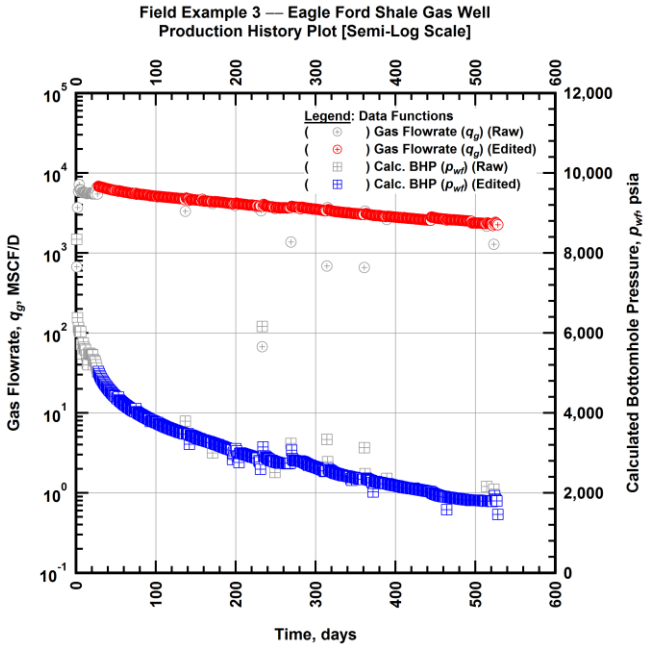

Figure A.61 — (Semi-log Plot): Filtered production history plot — flowrate (q_g) and calculated bottomhole pressure (p_{wf}) versus production time.

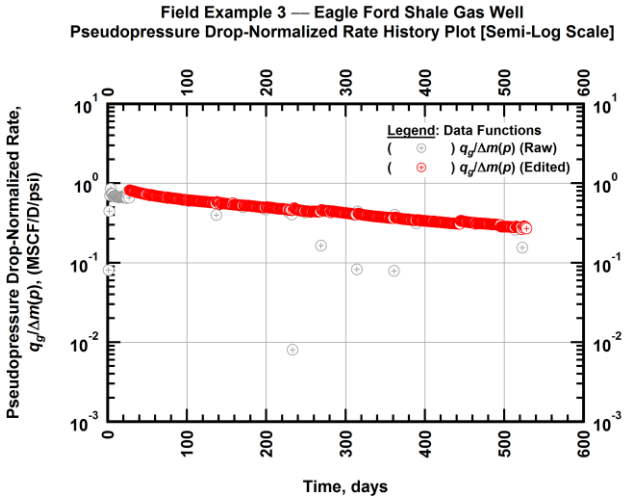

Figure A.62 — (Semi-log Plot): Filtered normalized rate production history plot — pseudopseudopressure drop-normalized gas flowrate ($q_g/\Delta m(p)$) versus production time.

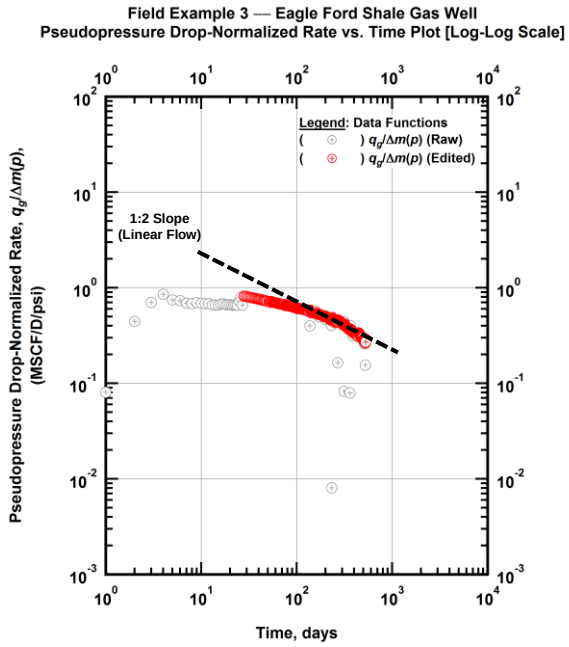

Figure A.63 — (Log-log Plot): Filtered normalized rate production history plot — pseudopseudopressure drop-normalized gas flowrate ($q_g/\Delta m(p)$) versus production time.

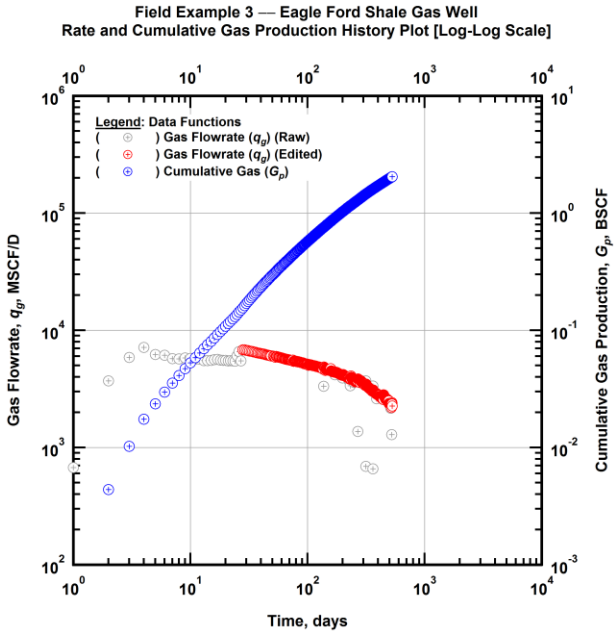

Figure A.64 — (Log-log Plot): Filtered rate and unfiltered cumulative gas production history plot — flowrate (q_g) and cumulative production (G_p) versus production time.

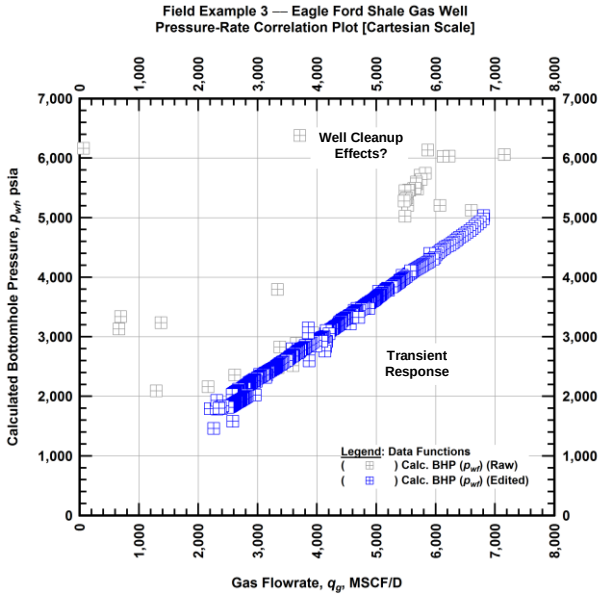

Figure A.65 — (Cartesian Plot): Filtered rate-pressure correlation plot — calculated bottomhole pressure (p_{wf}) versus flowrate (q_g).

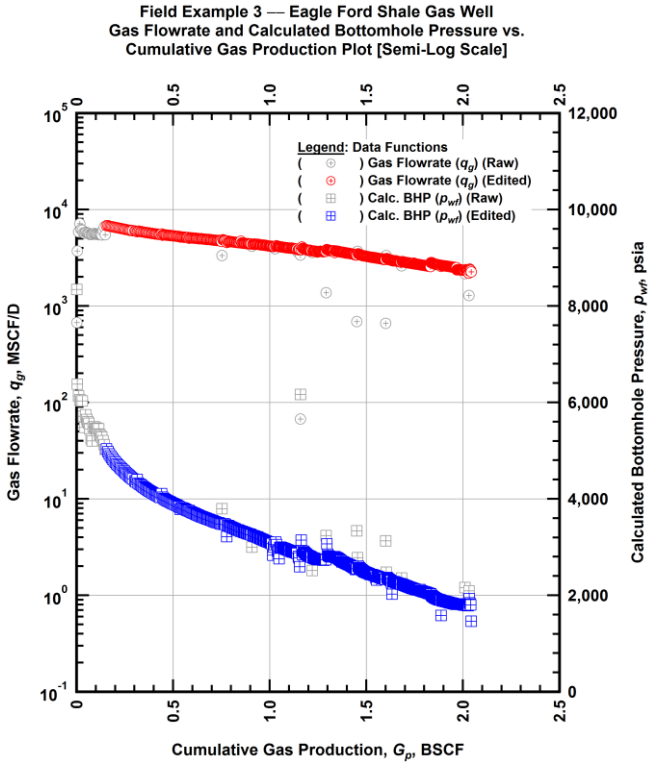

Figure A.66 — (Semi-log Plot): Filtered rate-pressure-cumulative production history plot — flowrate (q_g) and calculated bottomhole pressure (p_{wf}) versus cumulative production (G_p).

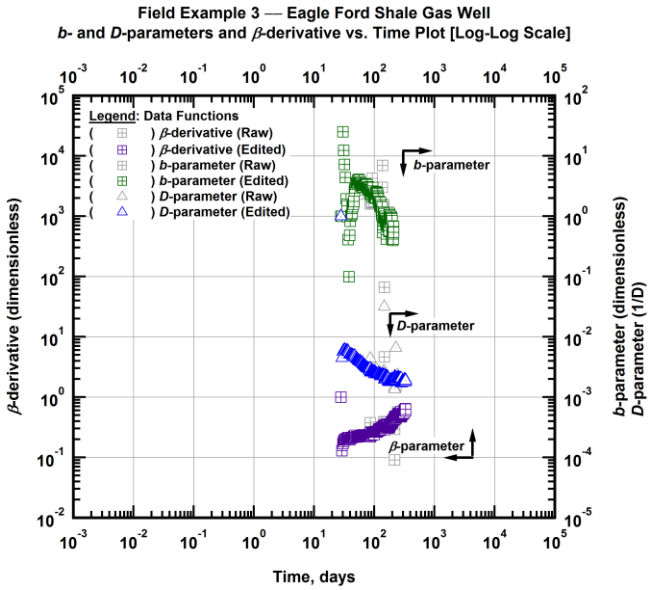

Figure A.67 — (Log-Log Plot): Filtered b, D and β production history plot — b- and D-parameters and β-derivative versus production time.

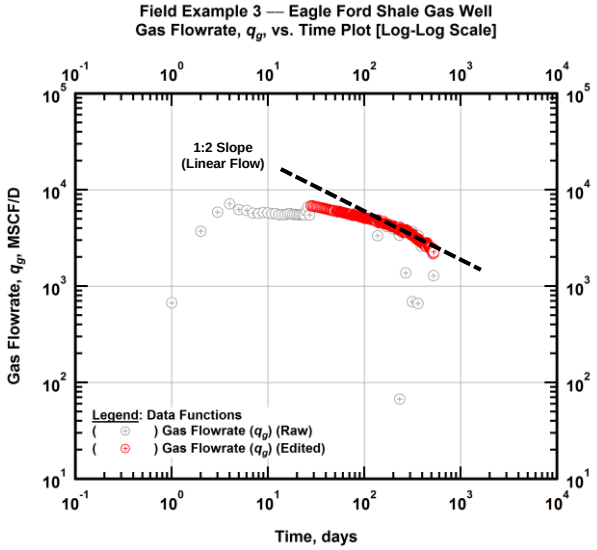

Figure A.68 — (Log-Log Plot): Filtered gas flowrate production history and flow regime identification plot — gas flowrate (q_g) versus production time.

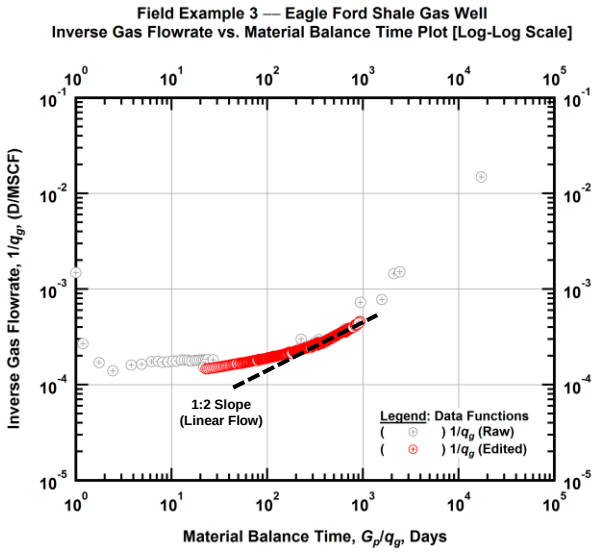

Figure A.69 — (Log-log Plot): Filtered inverse rate with material balance time plot — inverse gas flowrate ($1/q_g$) versus material balance time (G_p/q_g).

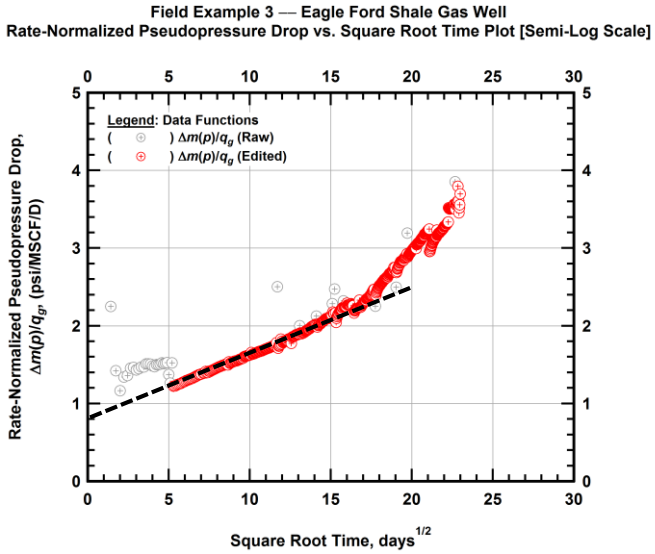

Figure A.70 — (Semi-log Plot): Filtered normalized pseudopressure drop production history plot — rate-normalized pseudopressure drop ($\Delta m(p)/q_g$) versus square root production time ($\sqrt{t}$).

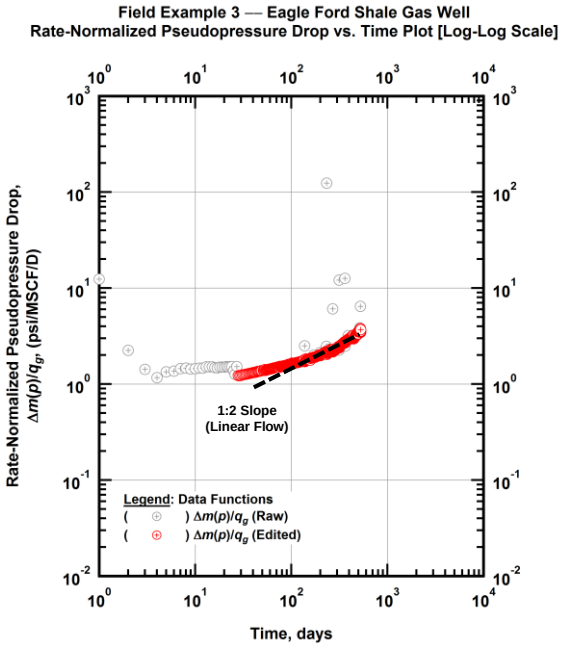

Figure A.71 — (Log-log Plot): Filtered normalized pseudopressure drop production history plot — rate-normalized pseudopressure drop ($\Delta m(p)/q_g$) versus production time.

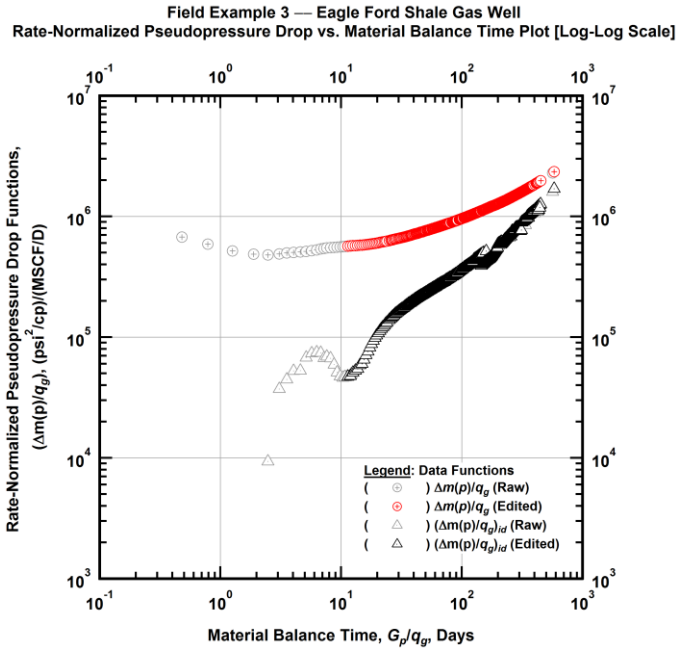

Figure A.72 — (Log-log Plot): "Log-log" diagnostic plot of the filtered production data — rate-normalized pseudopressure drop ($\Delta m(p)/q_g$) and rate-normalized pseudopressure drop integral-derivative $(\Delta m(p)/q_g)_{id}$ versus material balance time (G_p/q_g).

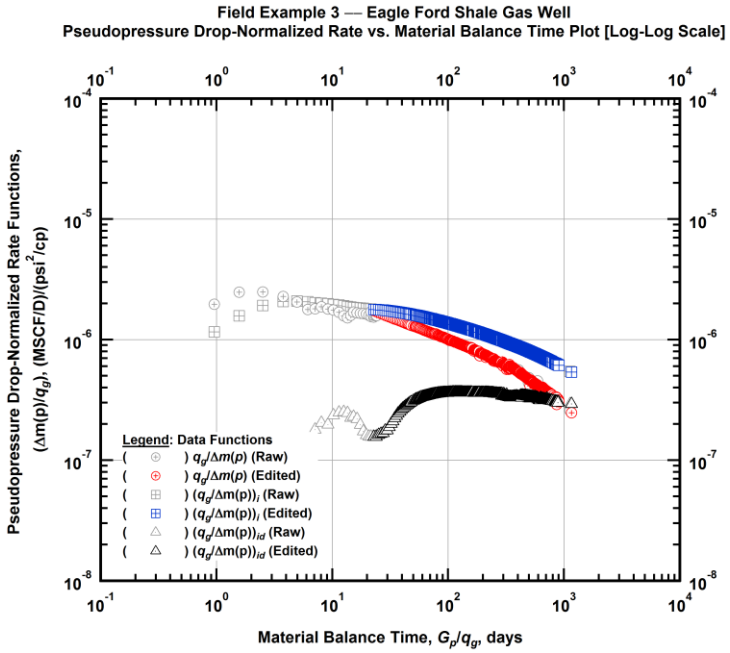

Figure A.73 — (Log-log Plot): "Blasingame" diagnostic plot of the filtered production data — pseudopressure drop-normalized gas flowrate ($q_g/\Delta m(p)$), pseudopressure drop-normalized gas flowrate integral $(q_g/\Delta m(p))_i$ and pseudopressure drop-normalized gas flowrate integral-derivative $(q_g/\Delta m(p))_{id}$ versus material balance time (G_p/q_g).

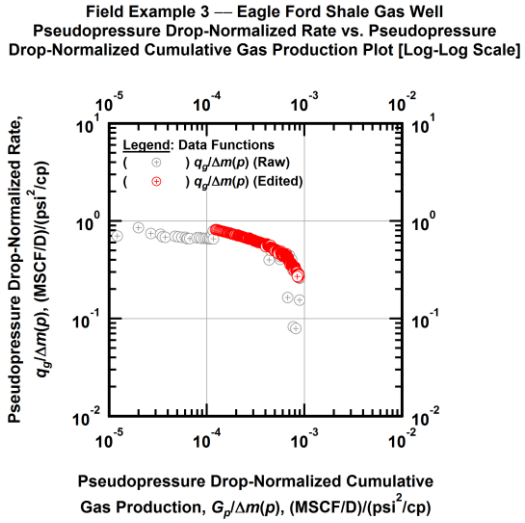

Figure A.74 — (Log-log Plot): Filtered normalized rate with normalized cumulative production plot — pseudopressure drop-normalized gas flowrate ($q_g/\Delta m(p)$) versus pseudopressure drop-normalized cumulative gas production ($G_p/\Delta m(p)$).

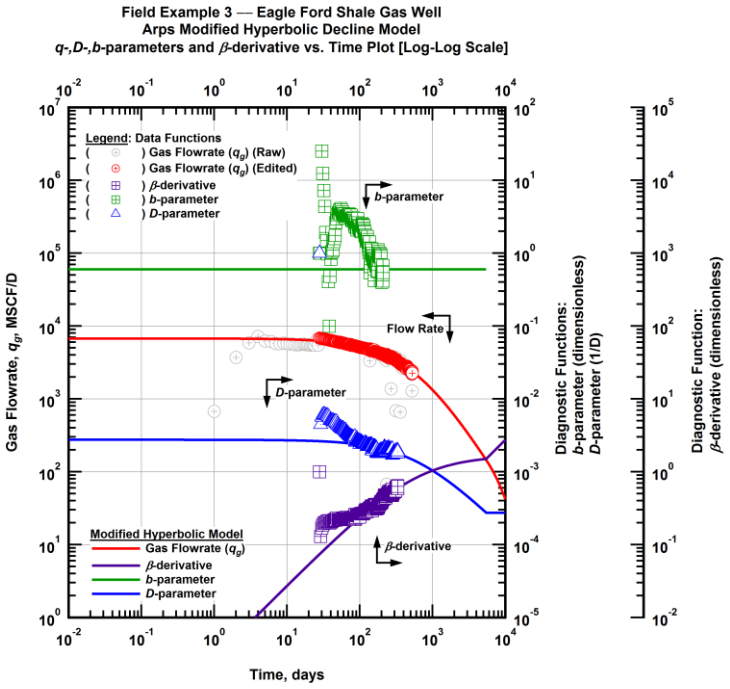

Figure A.75 — (Log-Log Plot): Arps modified hyperbolic decline model plot — time-rate model and data gas flowrate (q_g), *D*- and *b*-parameters and β-derivative versus production time.

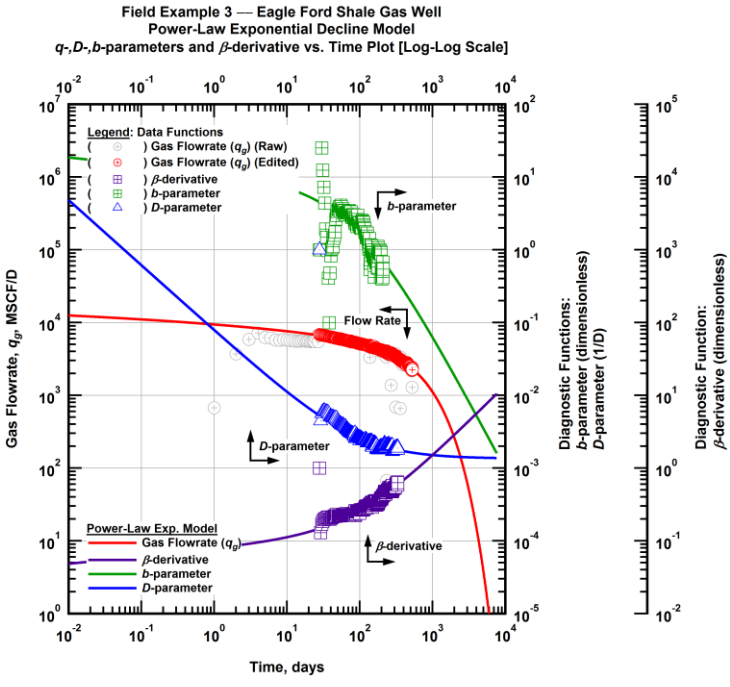

Figure A.76 — (Log-Log Plot): Power-law exponential decline model plot — time-rate model and data gas flowrate (q_g), *D*- and *b*-parameters and β-derivative versus production time.

Field Example 3 — Model-Based (Time-Rate-Pressure) Production Analysis

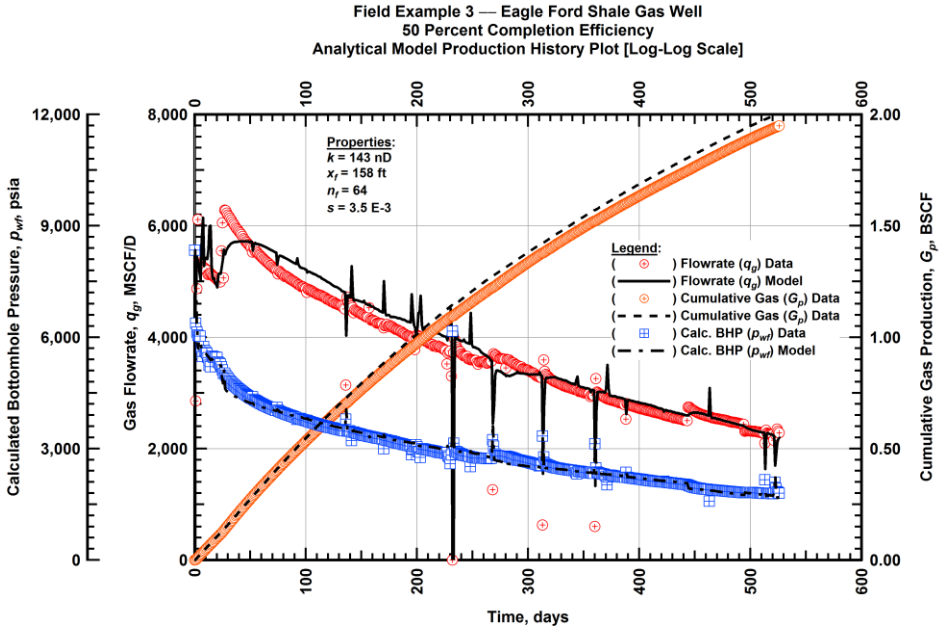

Figure A.77 — (Cartesian Plot): Production history plot — original gas flowrate (q_g), cumulative gas production (G_p), calculated bottomhole pressure (p_{wf}) and 50 percent completion efficiency model matches versus production time.

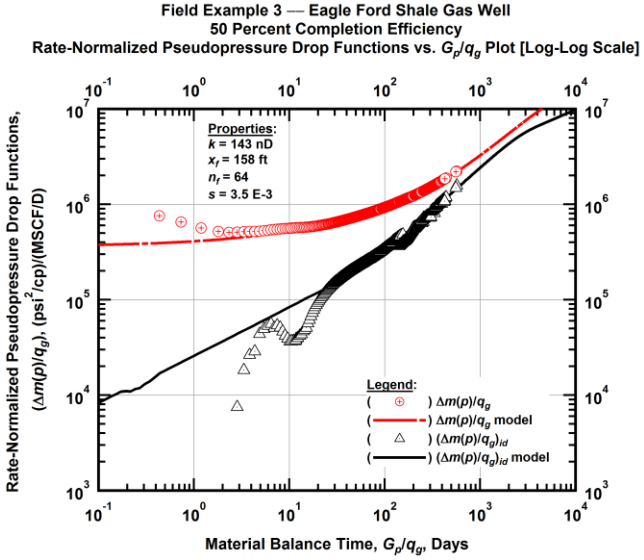

Figure A.78 — (Log-log Plot): "Log-log" diagnostic plot of the original production data — rate-normalized pseudopressure drop ($\Delta m(p)/q_g$), rate-normalized pseudopressure drop integral-derivative $(\Delta m(p)/q_g)_{id}$ and 50 percent completion efficiency model matches versus material balance time (G_p/q_g).

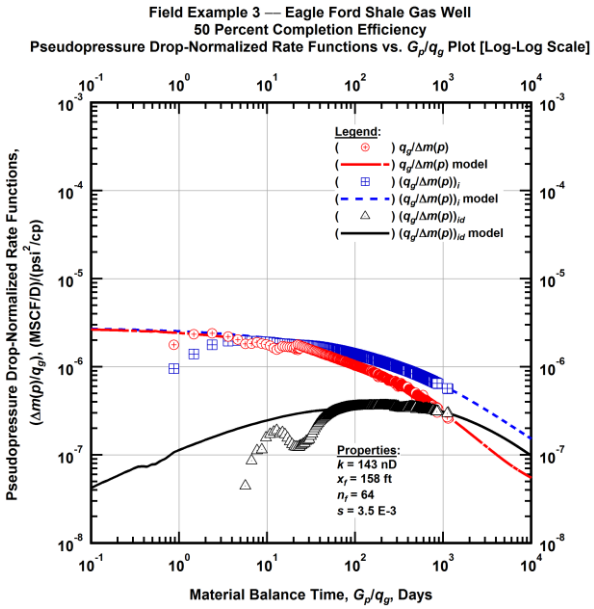

Figure A.79 — (Log-log Plot): "Blasingame" diagnostic plot of the original production data — pseudopressure drop-normalized gas flowrate ($q_g/\Delta m(p)$), pseudopressure drop-normalized gas flowrate integral $(q_g/\Delta m(p))_i$, pseudopressure drop-normalized gas flowrate integral-derivative $(q_g/\Delta m(p))_{id}$ and 50 percent completion efficiency model matches versus material balance time (G_p/q_g).

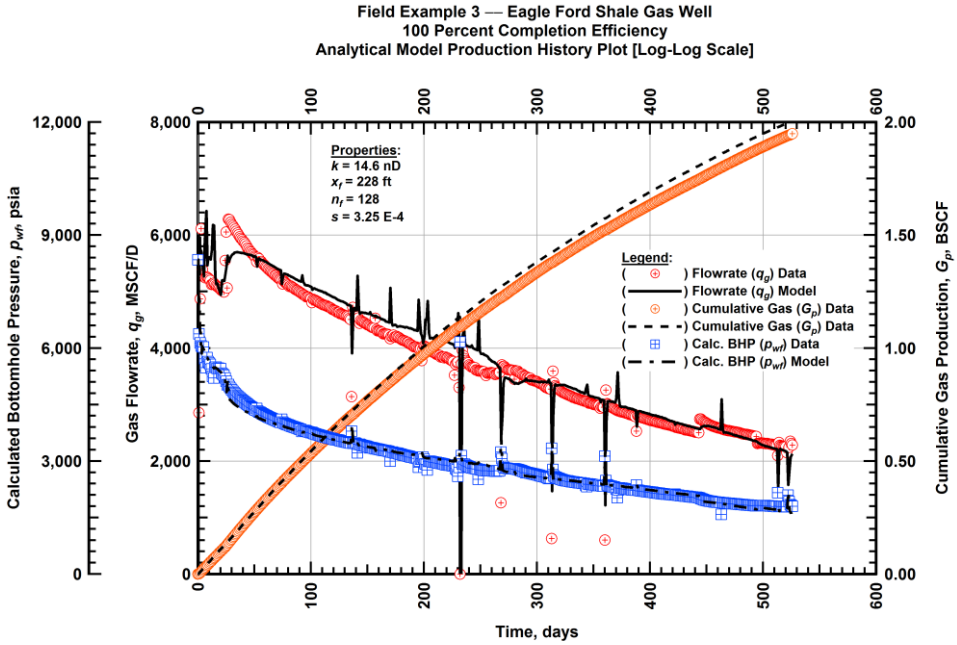

Figure A.80 — (Cartesian Plot): Production history plot — original gas flowrate (q_g), cumulative gas production (G_p), calculated bottomhole pressure (p_{wf}) and 100 percent completion efficiency model matches versus production time.

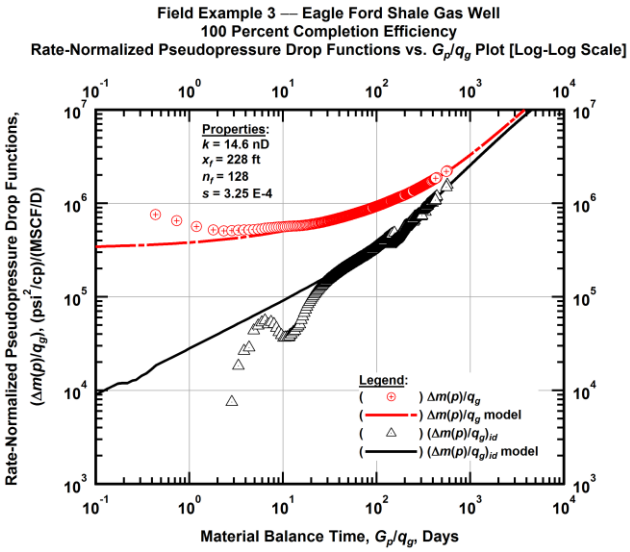

Figure A.81 — (Log-log Plot): "Log-log" diagnostic plot of the original production data — rate-normalized pseudopressure drop ($\Delta m(p)/q_g$), rate-normalized pseudopressure drop integral-derivative $(\Delta m(p)/q_g)_{id}$ and 100 percent completion efficiency model matches versus material balance time (G_p/q_g).

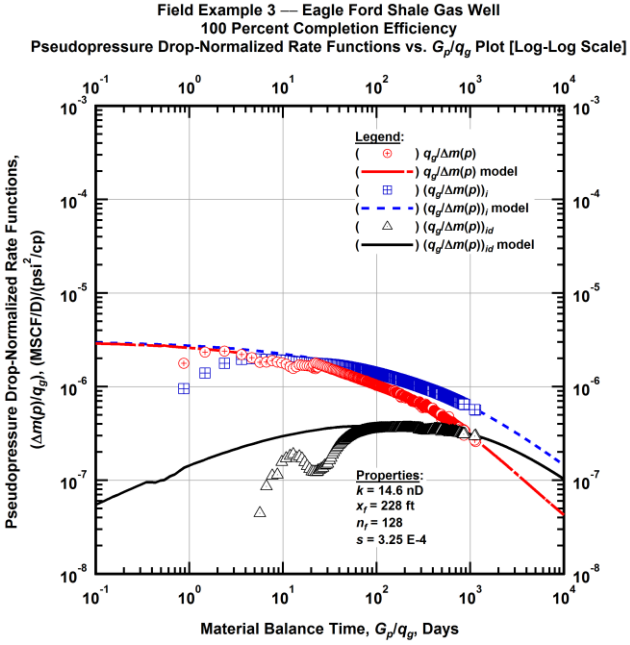

Figure A.82 — (Log-log Plot): "Blasingame" diagnostic plot of the original production data — pseudopressure drop-normalized gas flowrate ($q_g/\Delta m(p)$), pseudopressure drop-normalized gas flowrate integral $(q_g/\Delta m(p))_i$, pseudopressure drop-normalized gas flowrate integral-derivative $(q_g/\Delta m(p))_{id}$ and 100 percent completion efficiency model matches versus material balance time (G_p/q_g).

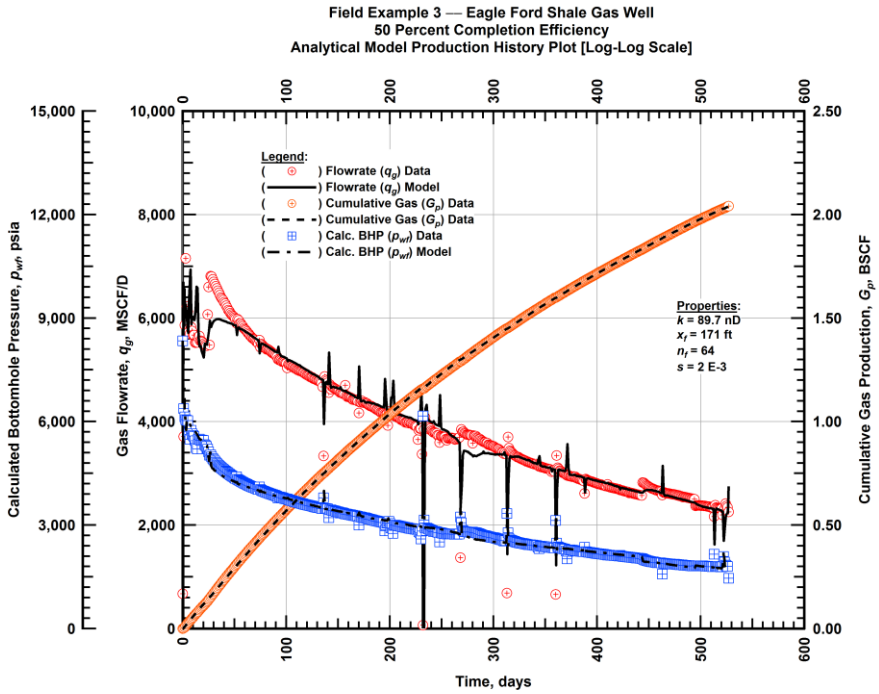

Figure A.83 — (Cartesian Plot): Production history plot — revised gas flowrate (q_g), cumulative gas production (G_p), calculated bottomhole pressure (p_{wf}) and 50 percent completion efficiency model matches versus production time.

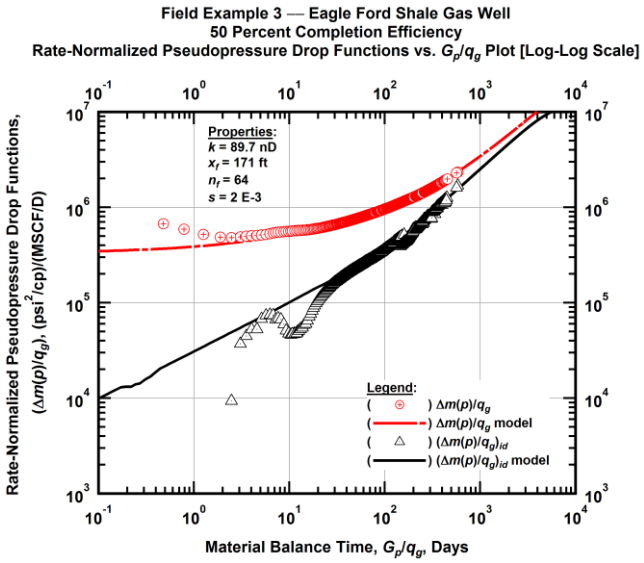

Figure A.84 — (Log-log Plot): "Log-log" diagnostic plot of the revised production data — rate-normalized pseudopressure drop ($\Delta m(p)/q_g$), rate-normalized pseudopressure drop integral-derivative $(\Delta m(p)/q_g)_{id}$ and 50 percent completion efficiency model matches versus material balance time (G_p/q_g).

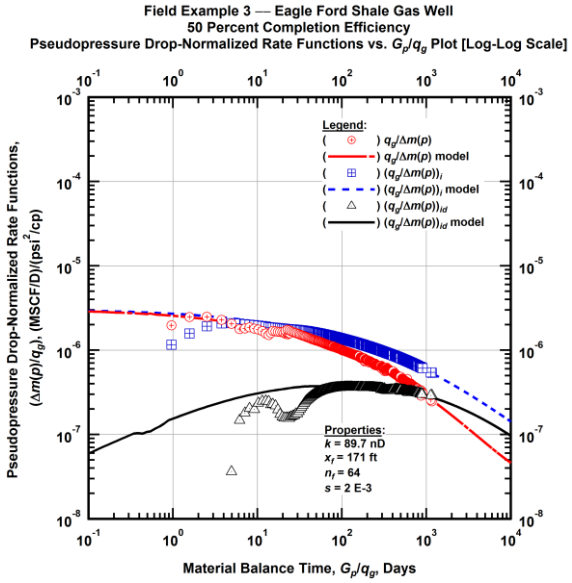

Figure A.85 — (Log-log Plot): "Blasingame" diagnostic plot of the revised production data — pseudopressure drop-normalized gas flowrate ($q_g/\Delta m(p)$), pseudopressure drop-normalized gas flowrate integral $(q_g/\Delta m(p))_i$, pseudopressure drop-normalized gas flowrate integral-derivative $(q_g/\Delta m(p))_{id}$ and 50 percent completion efficiency model matches versus material balance time (G_p/q_g).

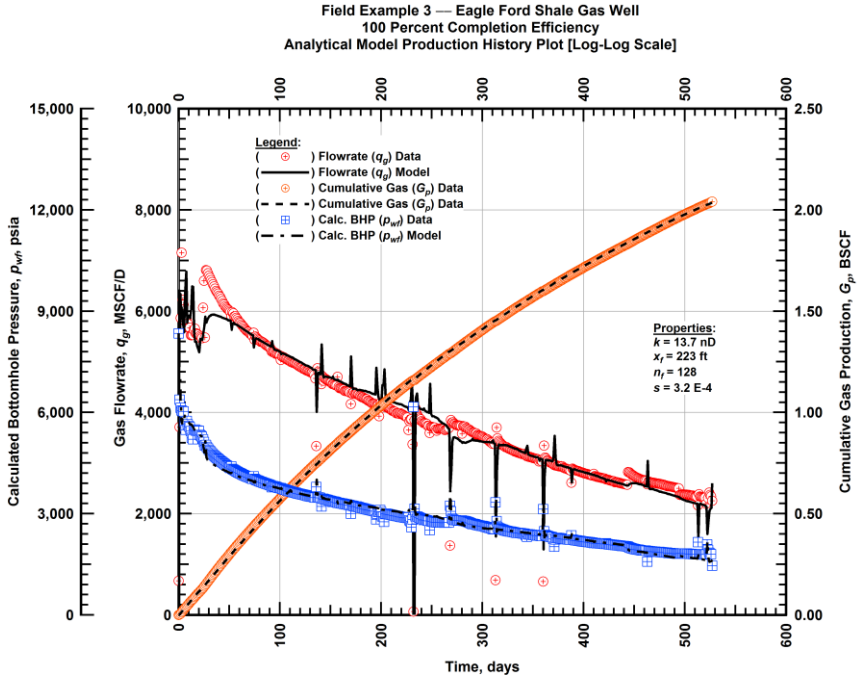

Figure A.86 — (Cartesian Plot): Production history plot — revised gas flowrate (q_g), cumulative gas production (G_p), calculated bottomhole pressure (p_{wf}) and 100 percent completion efficiency model matches versus production time.

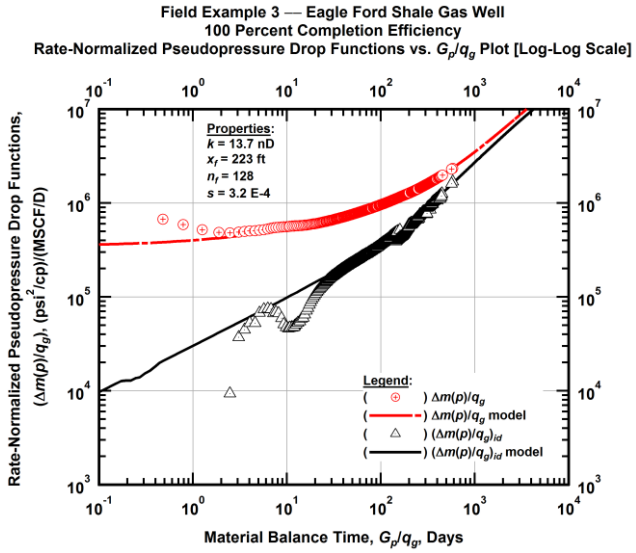

Figure A.87 — (Log-log Plot): "Log-log" diagnostic plot of the revised production data — rate-normalized pseudopressure drop ($\Delta m(p)/q_g$), rate-normalized pseudopressure drop integral-derivative $(\Delta m(p)/q_g)_{id}$ and 100 percent completion efficiency model matches versus material balance time (G_p/q_g).

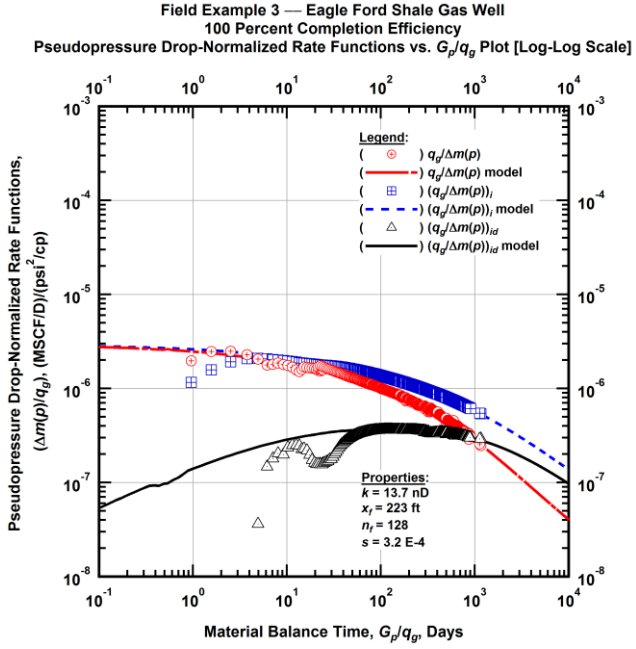

Figure A.88 — (Log-log Plot): "Blasingame" diagnostic plot of the revised production data — pseudopressure drop-normalized gas flowrate ($q_g/\Delta m(p)$), pseudopressure drop-normalized gas flowrate integral $(q_g/\Delta m(p))_i$, pseudopressure drop-normalized gas flowrate integral-derivative $(q_g/\Delta m(p))_{id}$ and 100 percent completion efficiency model matches versus material balance time (G_p/q_g).

Field Example 3 — 30-Year EUR Model Comparison

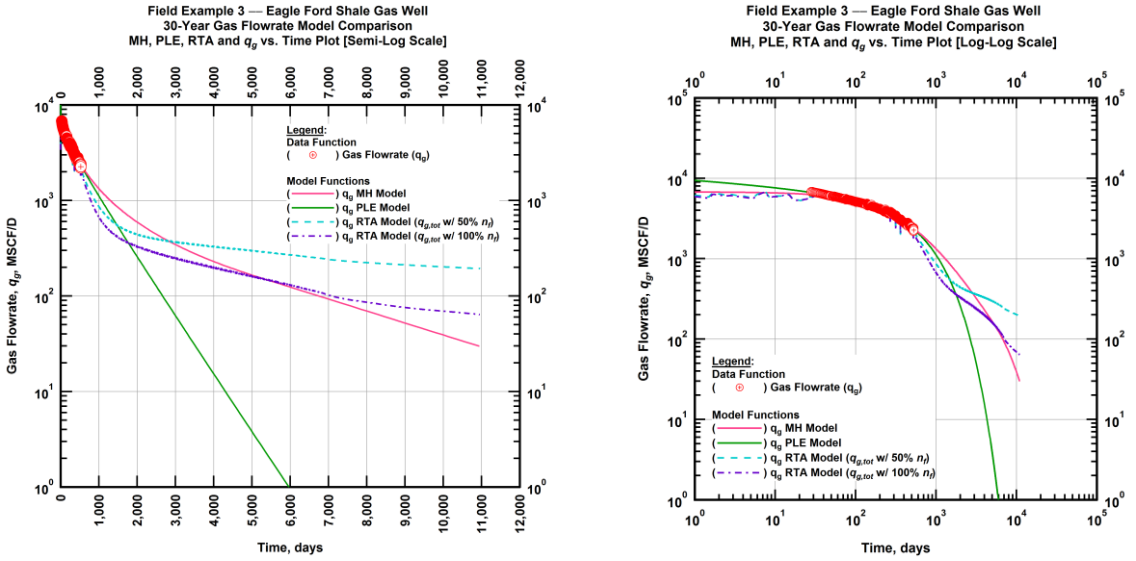

A **B**

Figure A.89 — (A — Semi-Log Plot) and (B — Log-Log Plot): Estimated 30-year revised gas flowrate model comparison — Arps modified hyperbolic decline model, power-law exponential decline model, and 50 percent and 100 percent completion efficiency RTA models revised gas 30-year estimated flowrate decline and historic gas flowrate data (q_g) versus production time.

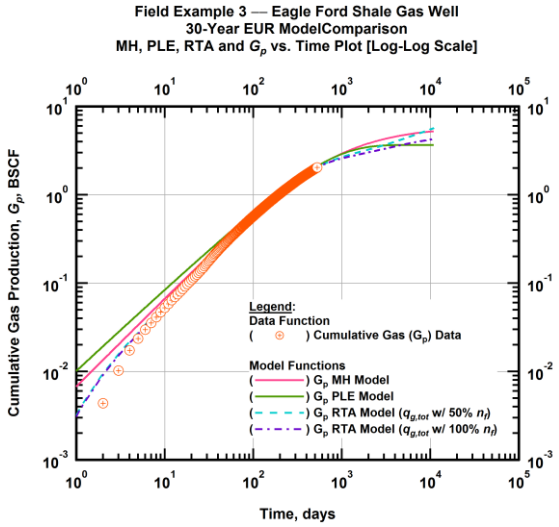

Figure A.90 — (Log-log Plot): Estimated 30-year cumulative gas production volume model comparison — Arps modified hyperbolic decline model, power-law exponential decline model, and 50 percent and 100 percent completion efficiency RTA models estimated 30-year cumulative gas production volumes and historic cumulative gas production (Gp) versus production time.

Table A.3 — 30-year estimated cumulative revised gas production (EUR), in units of BSCF, for the Arps modified hyperbolic, power-law exponential and analytical time-rate-pressure decline models.

Arps Modified Hyperbolic (BSCF)	Power-Law Exponential (BSCF)	RTA Analytical Model ($q_{g,tot}$ w/ 50% n_f) (BSCF)	RTA Analytical Model ($q_{g,tot}$ w/ 100% n_f) (BSCF)
5.17	3.56	5.79	4.30

Field Example 4 — Time-Rate Analysis

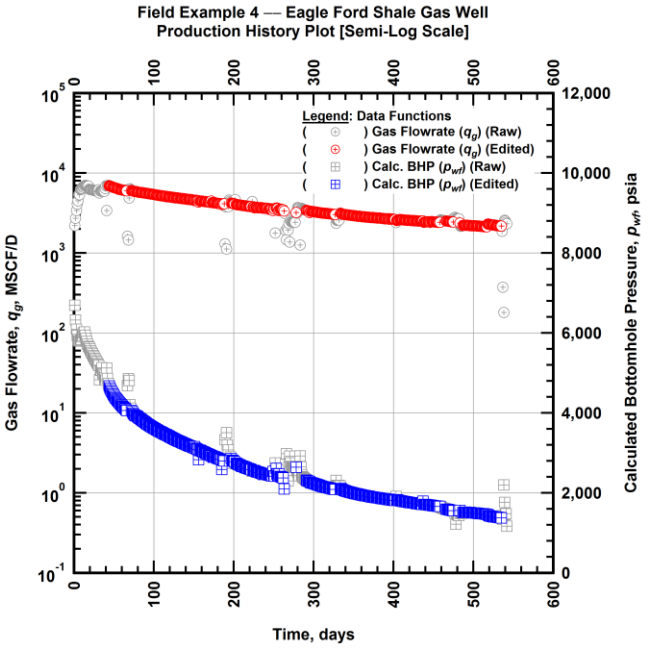

Figure A.91 — (Semi-log Plot): Filtered production history plot — flowrate (q_g) and calculated bottomhole pressure (p_{wf}) versus production time.

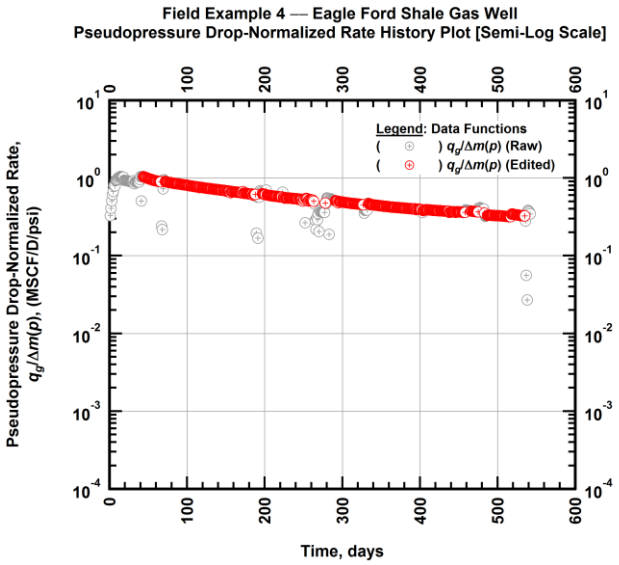

Figure A.92 — (Semi-log Plot): Filtered normalized rate production history plot — pseudopseudopressure drop-normalized gas flowrate ($q_g/\Delta m(p)$) versus production time.

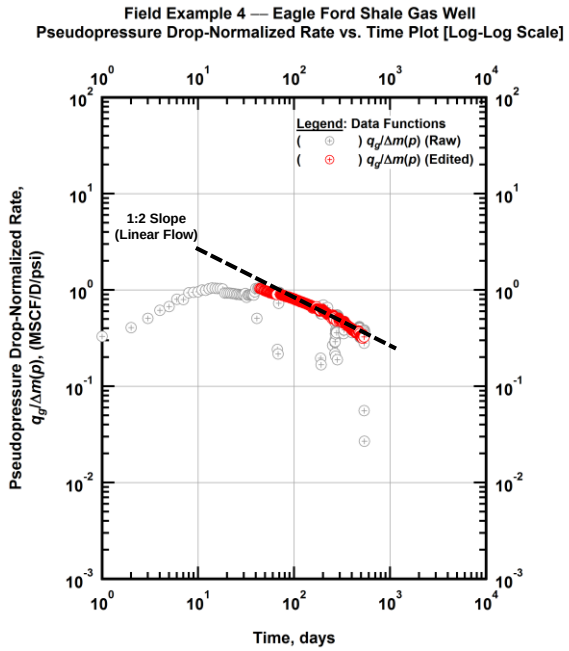

Figure A.93 — (Log-log Plot): Filtered normalized rate production history plot — pseudopseudopressure drop-normalized gas flowrate ($q_g/\Delta m(p)$) versus production time.

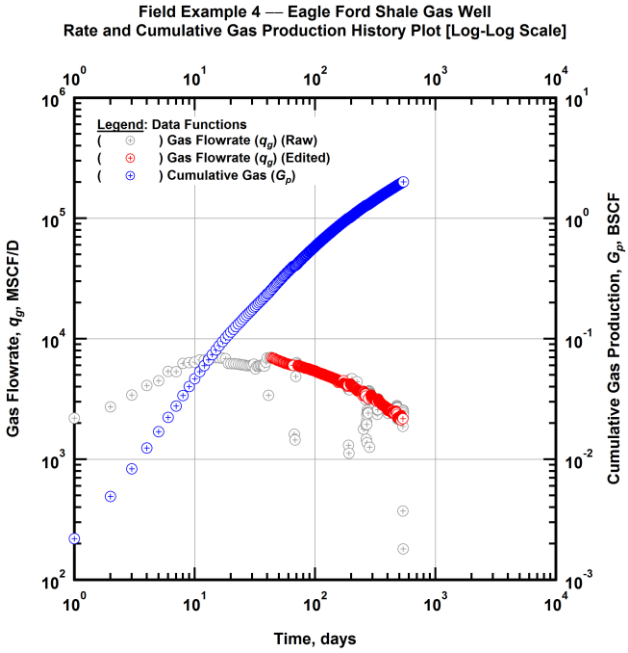

Figure A.94 — (Log-log Plot): Filtered rate and unfiltered cumulative gas production history plot — flowrate (q_g) and cumulative production (G_p) versus production time.

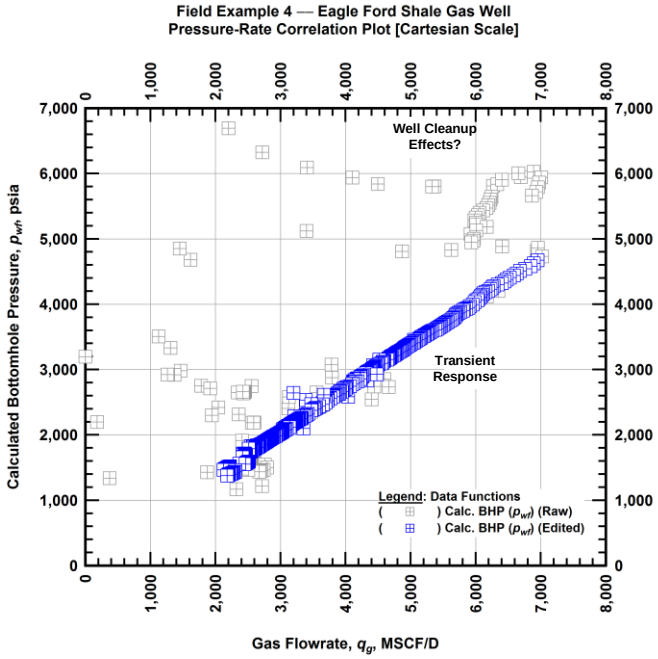

Figure A.95 — (Cartesian Plot): Filtered rate-pressure correlation plot — calculated bottomhole pressure (p_{wf}) versus flowrate (q_g).

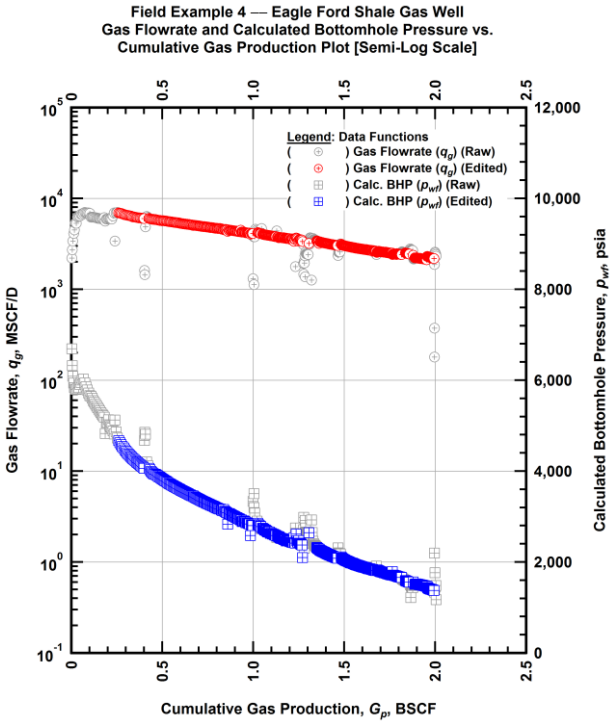

Figure A.96 — (Semi-log Plot): Filtered rate-pressure-cumulative production history plot — flowrate (q_g) and calculated bottomhole pressure (p_{wf}) versus cumulative production (G_p).

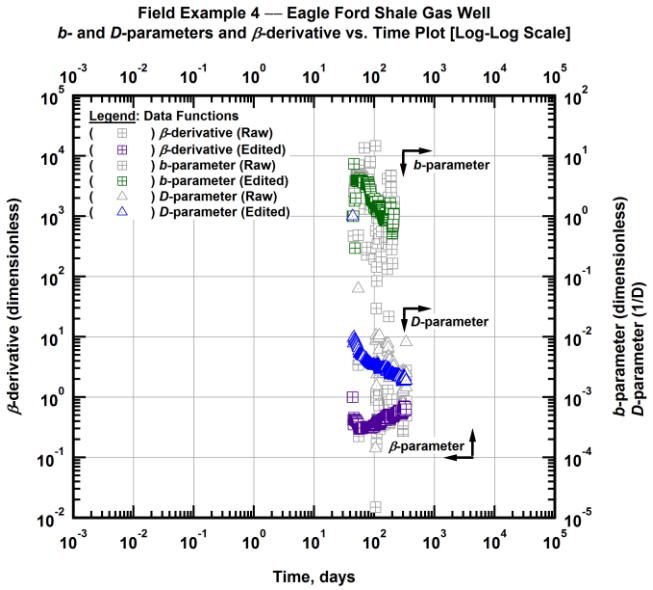

Figure A.97 — (Log-Log Plot): Filtered b, D and β production history plot — b- and D-parameters and β-derivative versus production time.

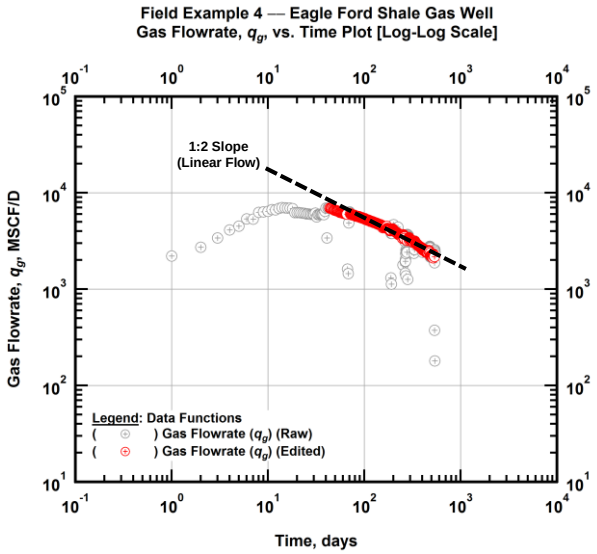

Figure A.98 — (Log-Log Plot): Filtered gas flowrate production history and flow regime identification plot — gas flowrate (q_g) versus production time.

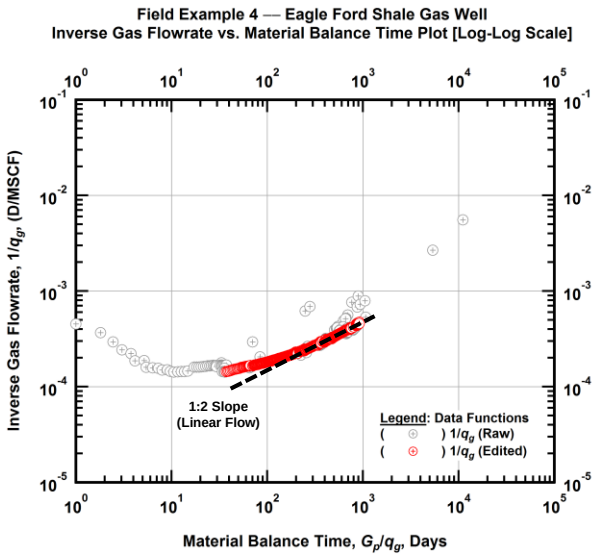

Figure A.99 — (Log-log Plot): Filtered inverse rate with material balance time plot — inverse gas flowrate ($1/q_g$) versus material balance time (G_p/q_g).

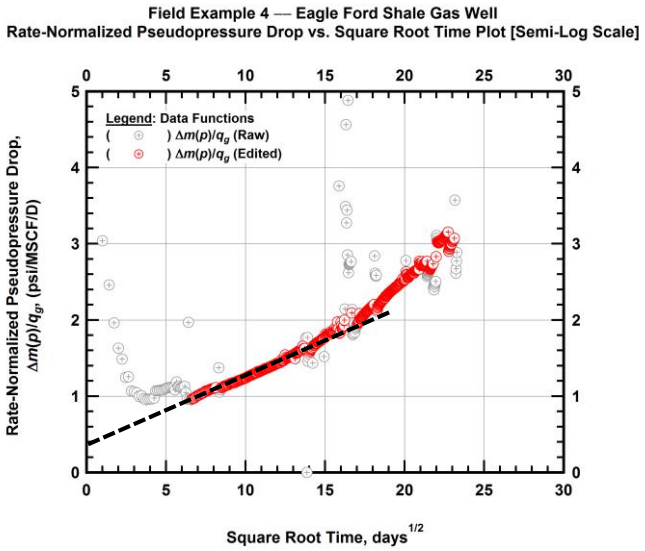

Figure A.100 — (Semi-log Plot): Filtered normalized pseudopressure drop production history plot — rate-normalized pseudopressure drop ($\Delta m(p)/q_g$) versus square root production time ($\sqrt{t}$).

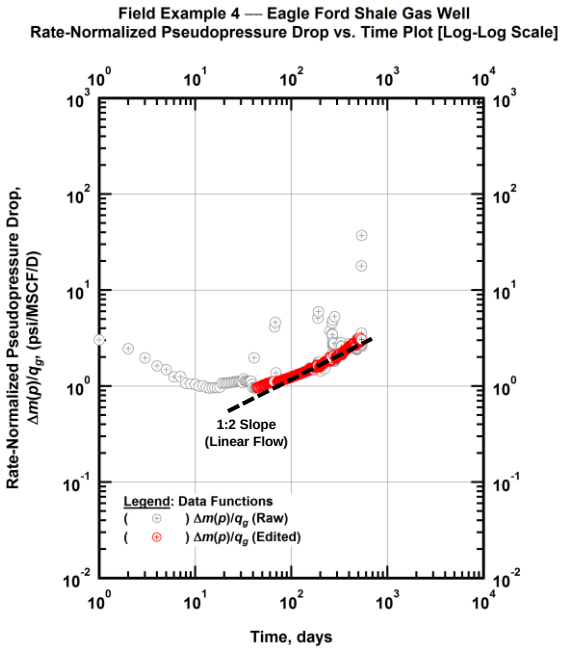

Figure A.101 — (Log-log Plot): Filtered normalized pseudopressure drop production history plot — rate-normalized pseudopressure drop ($\Delta m(p)/q_g$) versus production time.

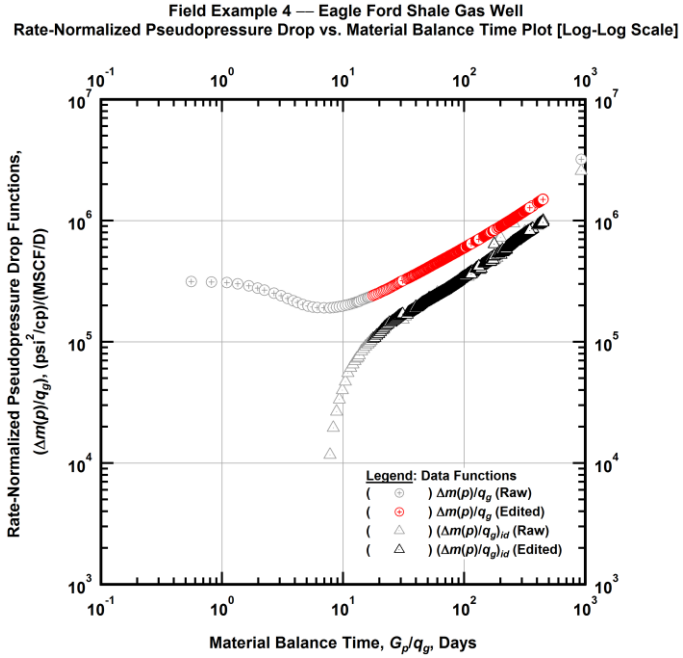

Figure A.102 — (Log-log Plot): "Log-log" diagnostic plot of the filtered production data — rate-normalized pseudopressure drop ($\Delta m(p)/q_g$) and rate-normalized pseudopressure drop integral-derivative $(\Delta m(p)/q_g)_{id}$ versus material balance time (G_p/q_g).

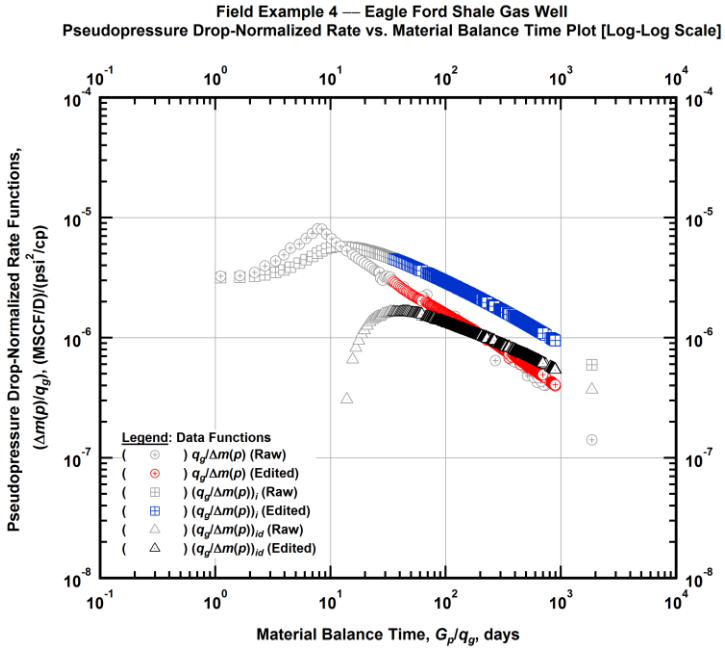

Figure A.103 — (Log-log Plot): "Blasingame" diagnostic plot of the filtered production data — pseudopressure drop-normalized gas flowrate ($q_g/\Delta m(p)$), pseudopressure drop-normalized gas flowrate integral $(q_g/\Delta m(p))_i$ and pseudopressure drop-normalized gas flowrate integral-derivative $(q_g/\Delta m(p))_{id}$ versus material balance time (G_p/q_g).

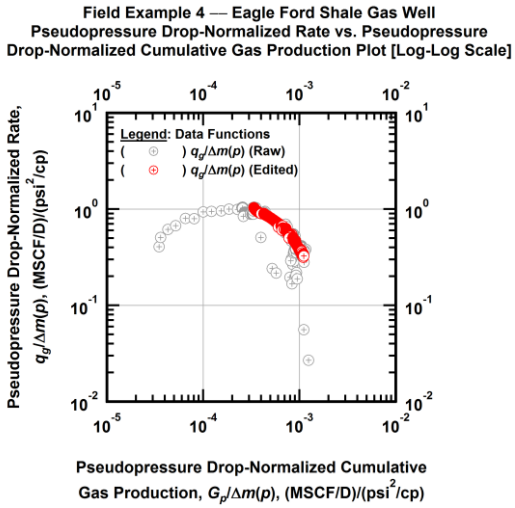

Figure A.104 — (Log-log Plot): Filtered normalized rate with normalized cumulative production plot — pseudopressure drop-normalized gas flowrate ($q_g/\Delta m(p)$) versus pseudopressure drop-normalized cumulative gas production ($G_p/\Delta m(p)$).

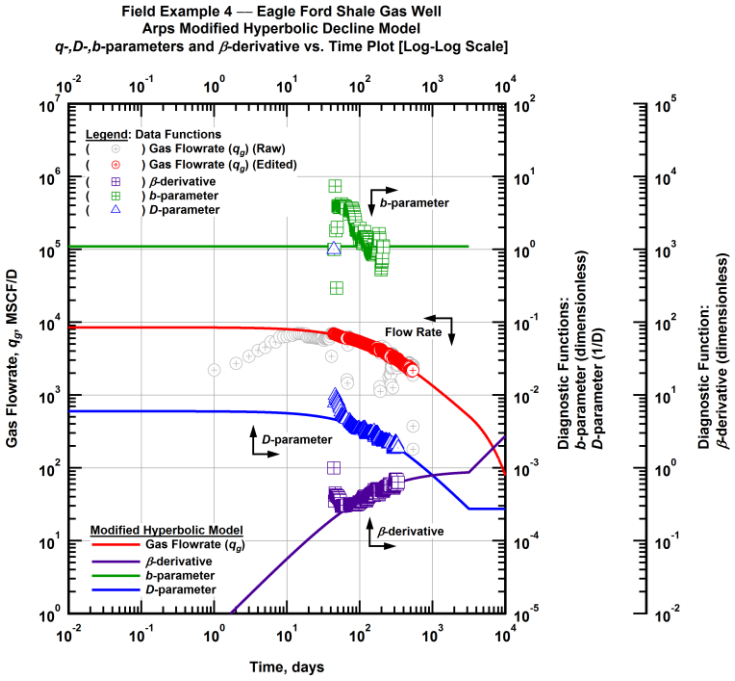

Figure A.105 — (Log-Log Plot): Arps modified hyperbolic decline model plot — time-rate model and data gas flowrate (q_g), D- and b-parameters and β-derivative versus production time.

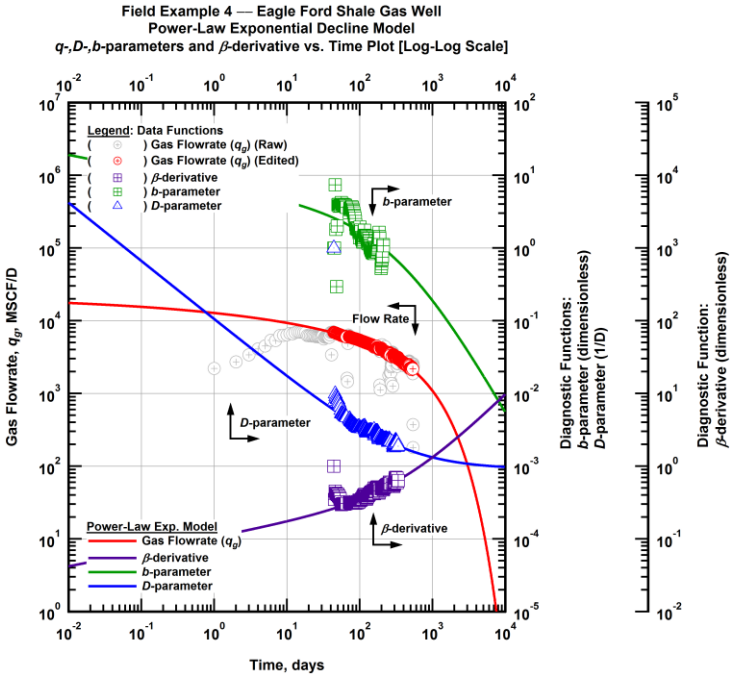

Figure A.106 — (Log-Log Plot): Power-law exponential decline model plot — time-rate model and data gas flowrate (q_g), D- and b-parameters and β-derivative versus production time.

Field Example 4 — Model-Based (Time-Rate-Pressure) Production Analysis

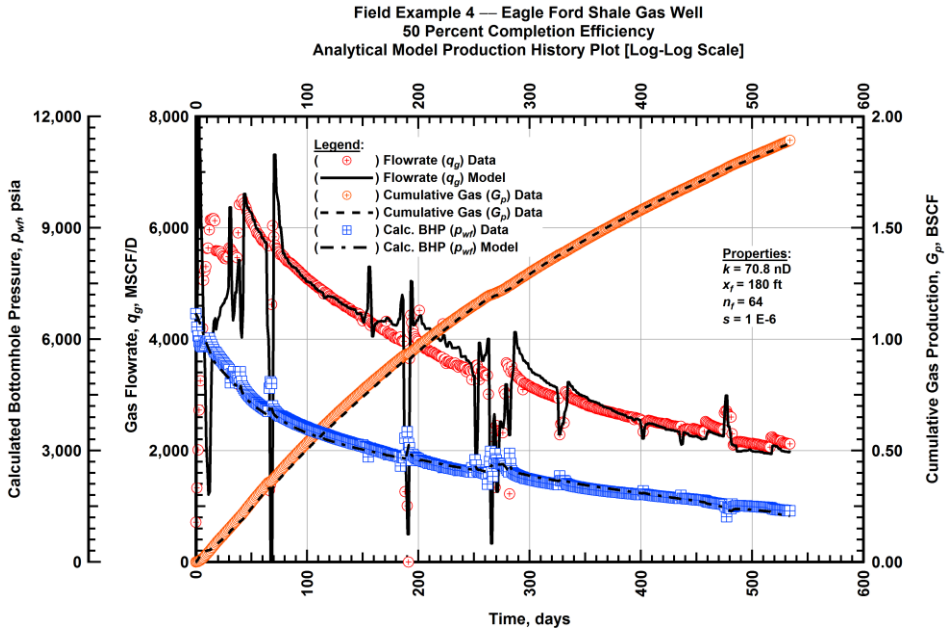

Figure A.107 — (Cartesian Plot): Production history plot — original gas flowrate (q_g), cumulative gas production (G_p), calculated bottomhole pressure (p_{wf}) and 50 percent completion efficiency model matches versus production time.

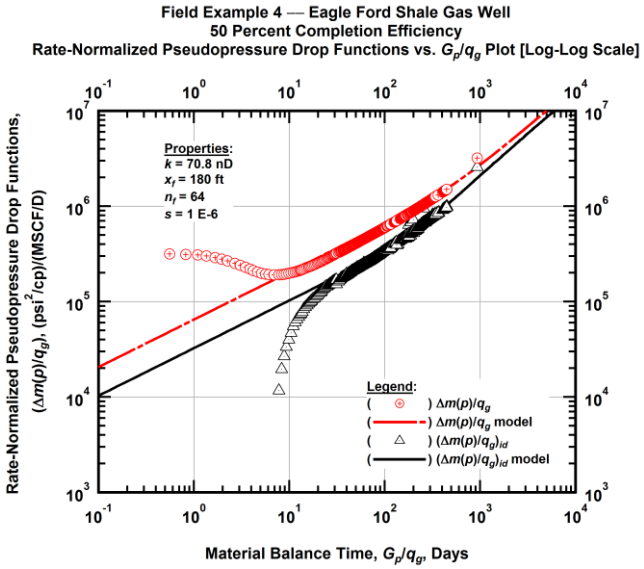

Figure A.108 — (Log-log Plot): "Log-log" diagnostic plot of the original production data — rate-normalized pseudopressure drop ($\Delta m(p)/q_g$), rate-normalized pseudopressure drop integral-derivative $(\Delta m(p)/q_g)_{id}$ and 50 percent completion efficiency model matches versus material balance time (G_p/q_g).

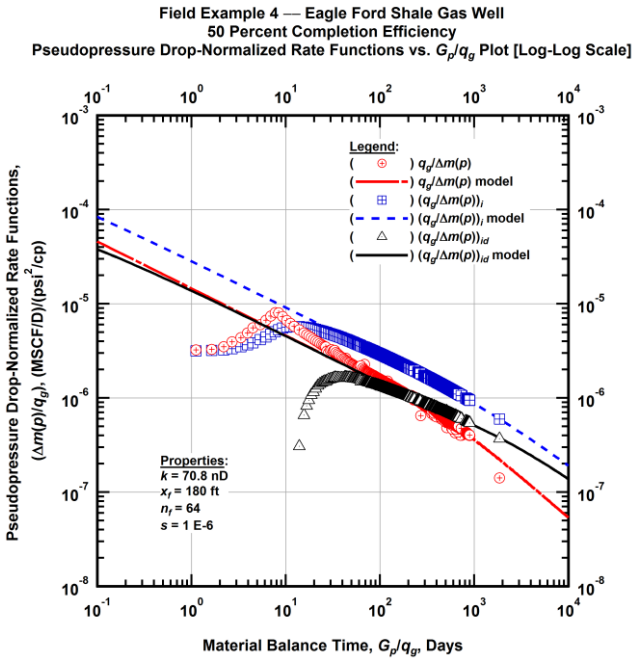

Figure A.109 — (Log-log Plot): "Blasingame" diagnostic plot of the original production data — pseudopressure drop-normalized gas flowrate ($q_g/\Delta m(p)$), pseudopressure drop-normalized gas flowrate integral ($q_g/\Delta m(p))_i$, pseudopressure drop-normalized gas flowrate integral-derivative ($q_g/\Delta m(p))_{id}$ and 50 percent completion efficiency model matches versus material balance time (G_p/q_g).

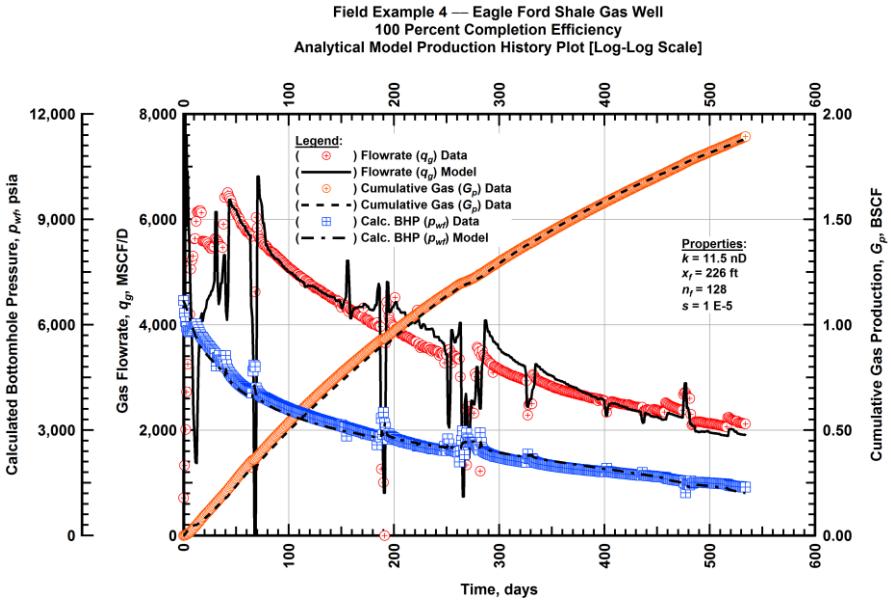

Figure A.110 — (Cartesian Plot): Production history plot — original gas flowrate (q_g), cumulative gas production (G_p), calculated bottomhole pressure (p_{wf}) and 100 percent completion efficiency model matches versus production time.

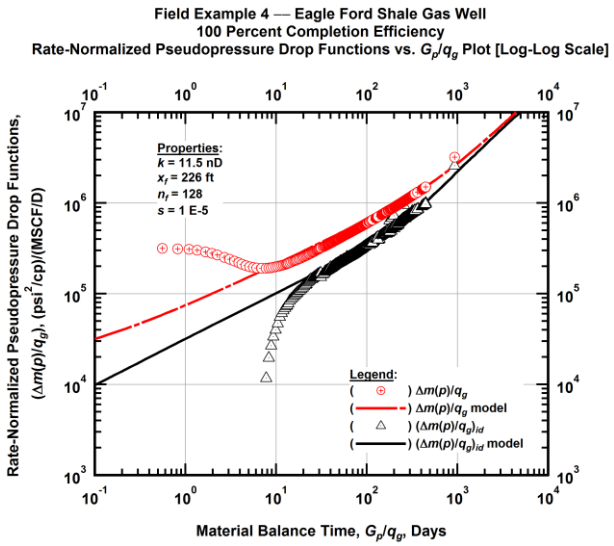

Figure A.111 — (Log-log Plot): "Log-log" diagnostic plot of the original production data — rate-normalized pseudopressure drop ($\Delta m(p)/q_g$), rate-normalized pseudopressure drop integral-derivative $(\Delta m(p)/q_g)_{id}$ and 100 percent completion efficiency model matches versus material balance time (G_p/q_g).

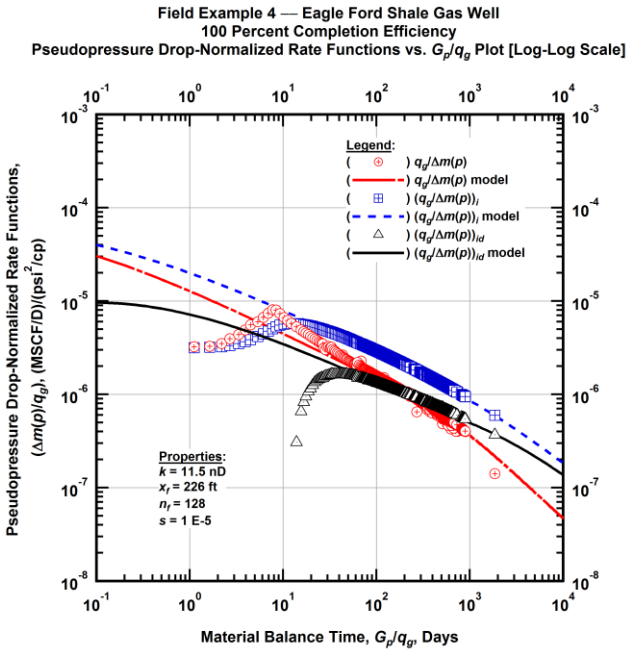

Figure A.112 — (Log-log Plot): "Blasingame" diagnostic plot of the original production data — pseudopressure drop-normalized gas flowrate ($q_g/\Delta m(p)$), pseudopressure drop-normalized gas flowrate integral $(q_g/\Delta m(p))_i$, pseudopressure drop-normalized gas flowrate integral-derivative $(q_g/\Delta m(p))_{id}$ and 100 percent completion efficiency model matches versus material balance time (G_p/q_g).

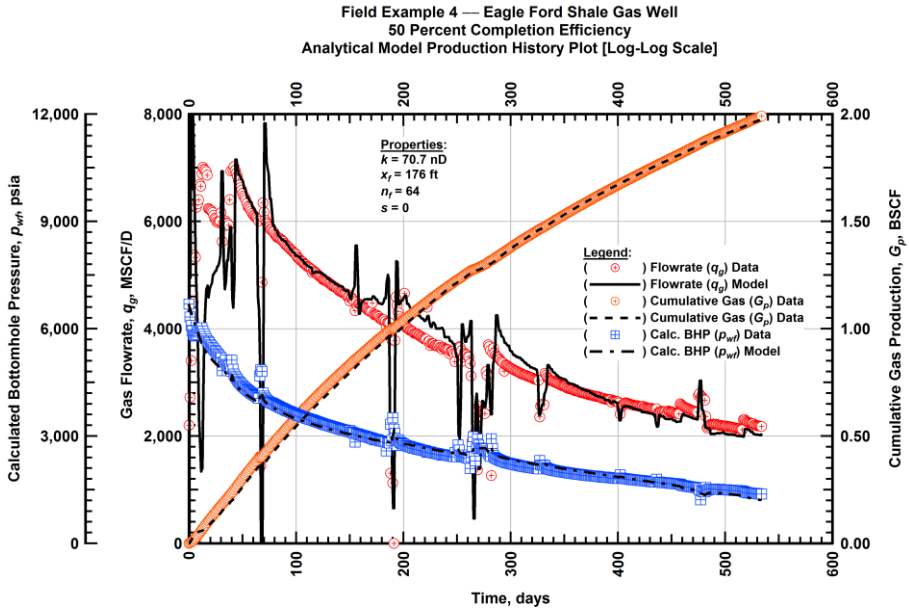

Figure A.113 — (Cartesian Plot): Production history plot — revised gas flowrate (q_g), cumulative gas production (G_p), calculated bottomhole pressure (p_{wf}) and 50 percent completion efficiency model matches versus production time.

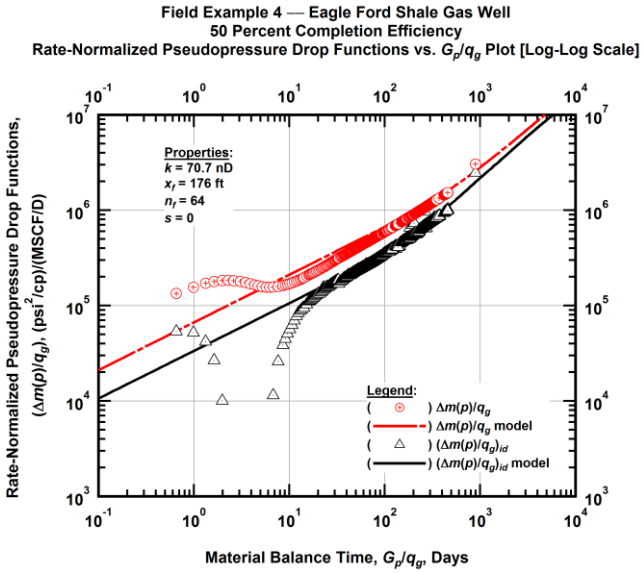

Figure A.114 — (Log-log Plot): "Log-log" diagnostic plot of the revised production data — rate-normalized pseudopressure drop ($\Delta m(p)/q_g$), rate-normalized pseudopressure drop integral-derivative $(\Delta m(p)/q_g)_{id}$ and 50 percent completion efficiency model matches versus material balance time (G_p/q_g).

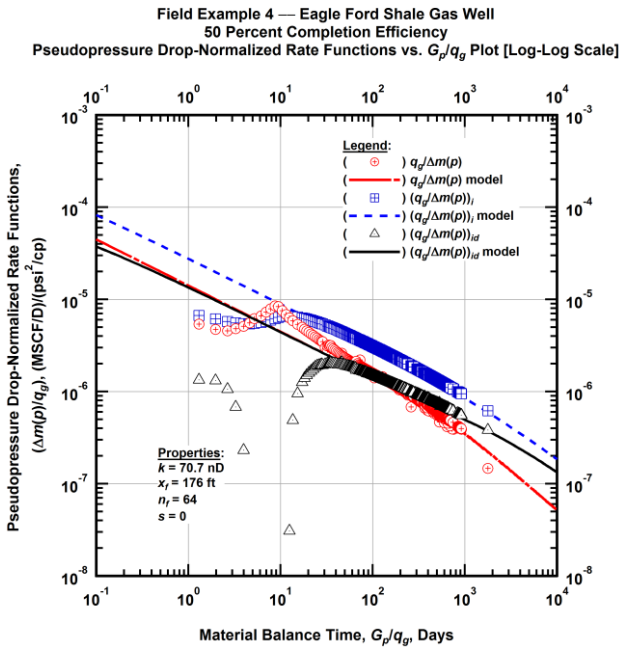

Figure A.115 — (Log-log Plot): "Blasingame" diagnostic plot of the revised production data — pseudopressure drop-normalized gas flowrate ($q_g/\Delta m(p)$), pseudopressure drop-normalized gas flowrate integral $(q_g/\Delta m(p))_i$, pseudopressure drop-normalized gas flowrate integral-derivative $(q_g/\Delta m(p))_{id}$ and 50 percent completion efficiency model matches versus material balance time (G_p/q_g).

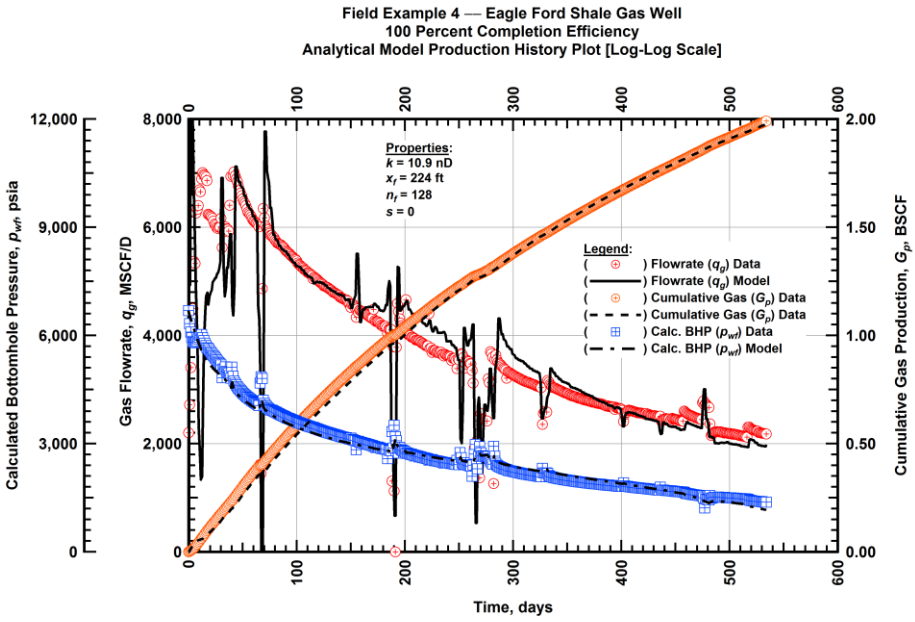

Figure A.116 — (Cartesian Plot): Production history plot — revised gas flowrate (q_g), cumulative gas production (G_p), calculated bottomhole pressure (p_{wf}) and 100 percent completion efficiency model matches versus production time.

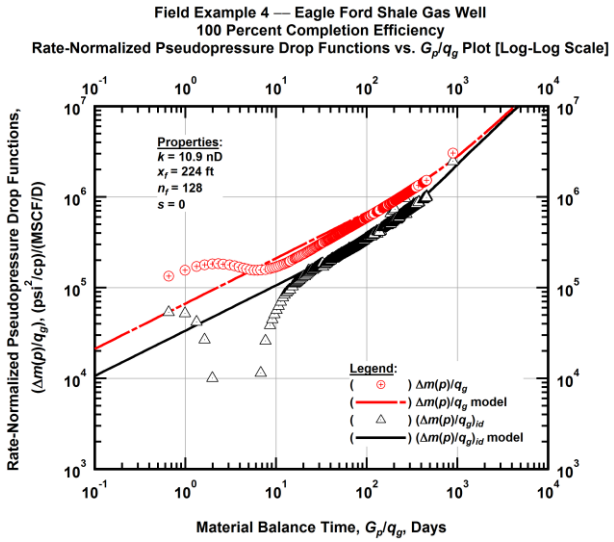

Figure A.117 — (Log-log Plot): "Log-log" diagnostic plot of the revised production data — rate-normalized pseudopressure drop ($\Delta m(p)/q_g$), rate-normalized pseudopressure drop integral-derivative $(\Delta m(p)/q_g)_{id}$ and 100 percent completion efficiency model matches versus material balance time (G_p/q_g).

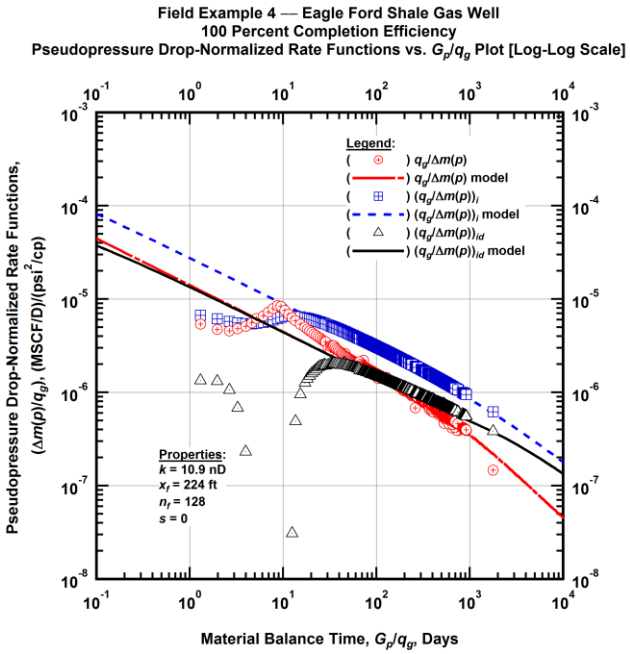

Figure A.118 — (Log-log Plot): "Blasingame" diagnostic plot of the revised production data — pseudopressure drop-normalized gas flowrate ($q_g/\Delta m(p)$), pseudopressure drop-normalized gas flowrate integral $(q_g/\Delta m(p))_i$, pseudopressure drop-normalized gas flowrate integral-derivative $(q_g/\Delta m(p))_{id}$ and 100 percent completion efficiency model matches versus material balance time (G_p/q_g).

Field Example 4 — 30-Year EUR Model Comparison

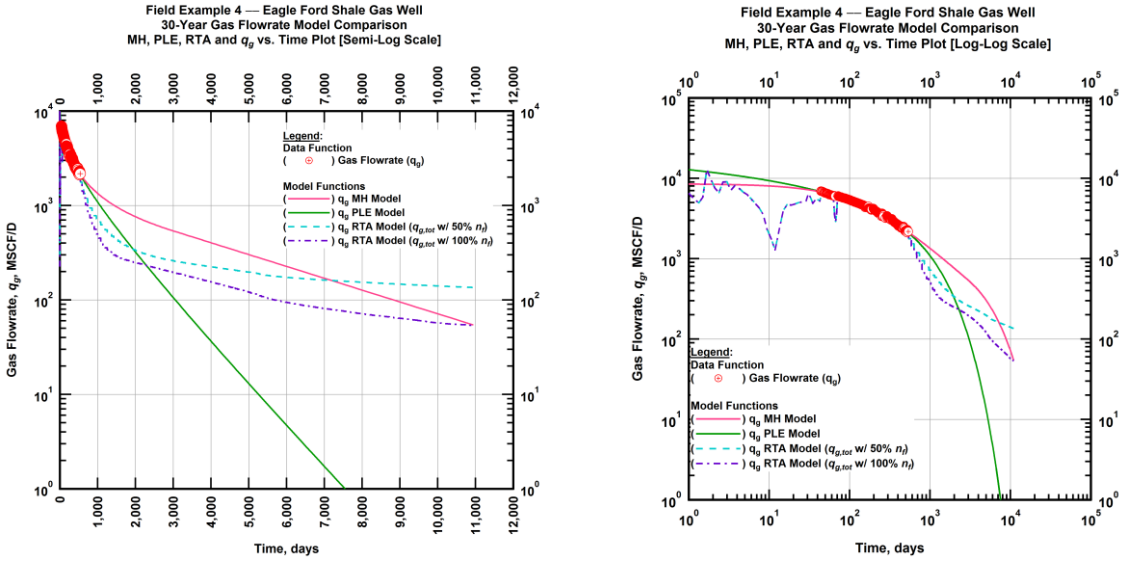

A **B**

Figure A.119 — (A — Semi-Log Plot) and (B — Log-Log Plot): Estimated 30-year revised gas flowrate model comparison — Arps modified hyperbolic decline model, power-law exponential decline model, and 50 percent and 100 percent completion efficiency RTA models revised gas 30-year estimated flowrate decline and historic gas flowrate data (q_g) versus production time.

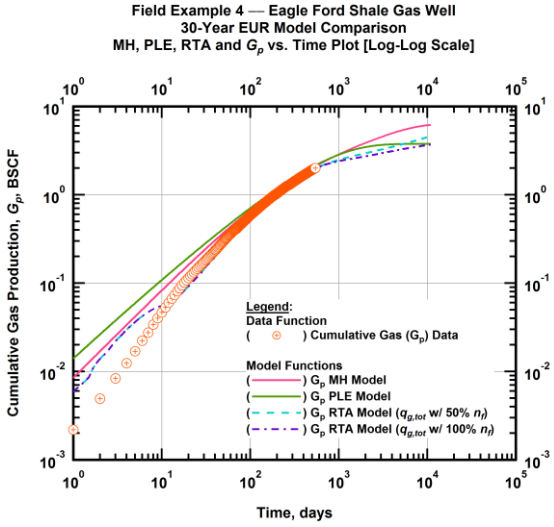

Figure A.120 — (Log-log Plot): Estimated 30-year cumulative gas production volume model comparison — Arps modified hyperbolic decline model, power-law exponential decline model, and 50 percent and 100 percent completion efficiency RTA models estimated 30-year cumulative gas production volumes and historic cumulative gas production (G_p) versus production time.

Table A.4 — 30-year estimated cumulative revised gas production (EUR), in units of BSCF, for the Arps modified hyperbolic, power-law exponential and analytical time-rate-pressure decline models.

Arps Modified Hyperbolic (BSCF)	Power-Law Exponential (BSCF)	RTA Analytical Model ($q_{g,tot}$ w/ 50% n_f) (BSCF)	RTA Analytical Model ($q_{g,tot}$ w/ 100% n_f) (BSCF)
6.16	3.61	4.70	3.73

Field Example 5 — Time-Rate Analysis

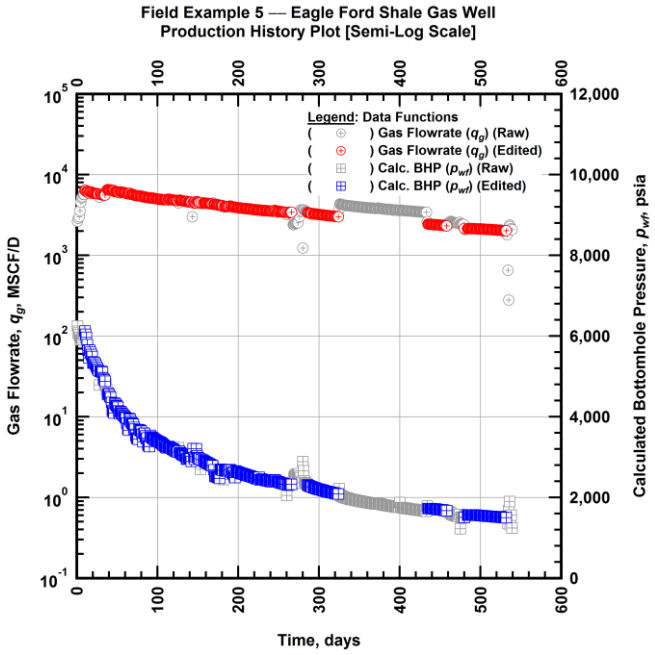

Figure A.121 — (Semi-log Plot): Filtered production history plot — flowrate (q_g) and calculated bottomhole pressure (p_{wf}) versus production time.

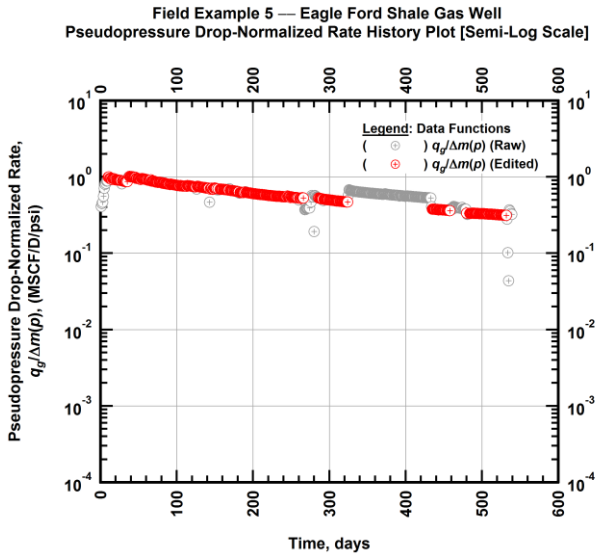

Figure A.122 — (Semi-log Plot): Filtered normalized rate production history plot — pseudopressure drop-normalized gas flowrate ($q_g/\Delta m(p)$) versus production time.

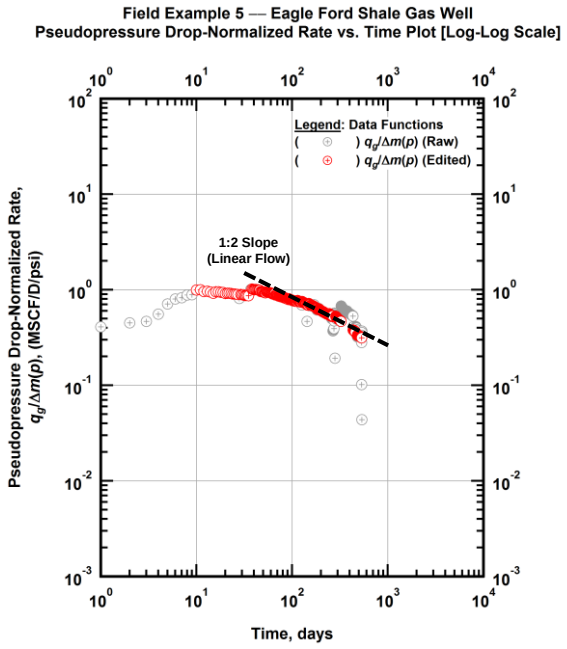

Figure A.123 — (Log-log Plot): Filtered normalized rate production history plot — pseudopressure drop-normalized gas flowrate ($q_g/\Delta m(p)$) versus production time.

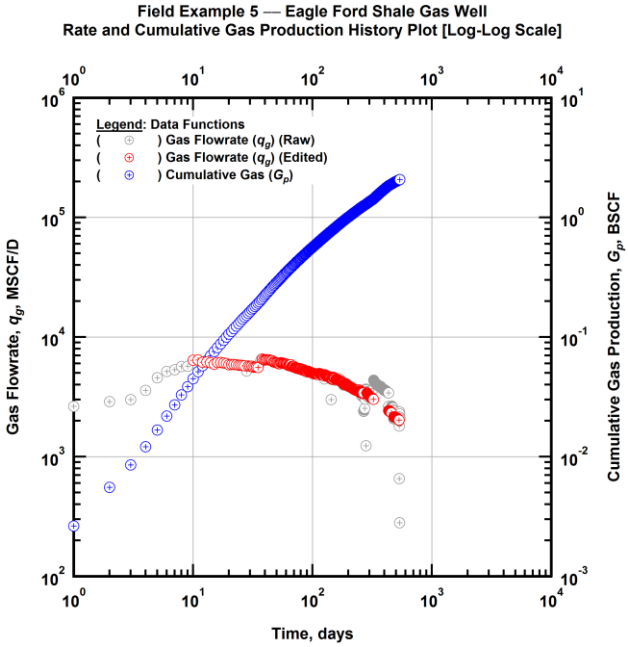

Figure A.124 — (Log-log Plot): Filtered rate and unfiltered cumulative gas production history plot — flowrate (q_g) and cumulative production (G_p) versus production time.

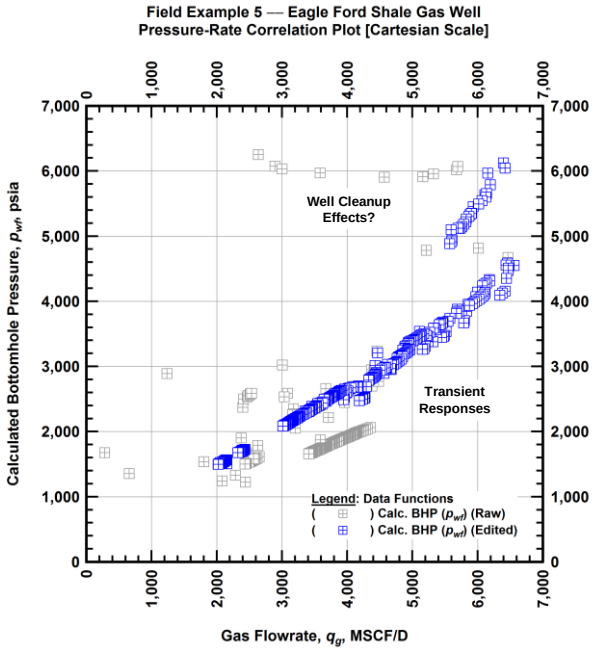

Figure A.125 — (Cartesian Plot): Filtered rate-pressure correlation plot — calculated bottomhole pressure (p_{wf}) versus flowrate (q_g).

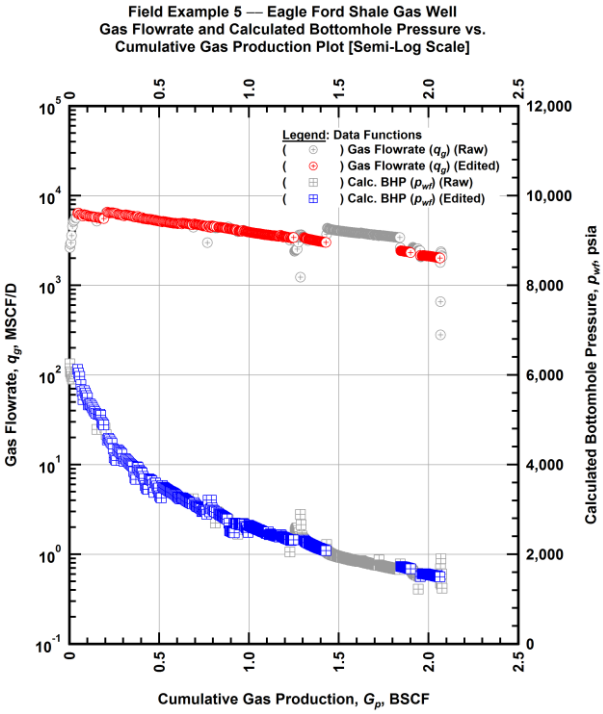

Figure A.126 — (Semi-log Plot): Filtered rate-pressure-cumulative production history plot — flowrate (q_g) and calculated bottomhole pressure (p_{wf}) versus cumulative production (G_p).

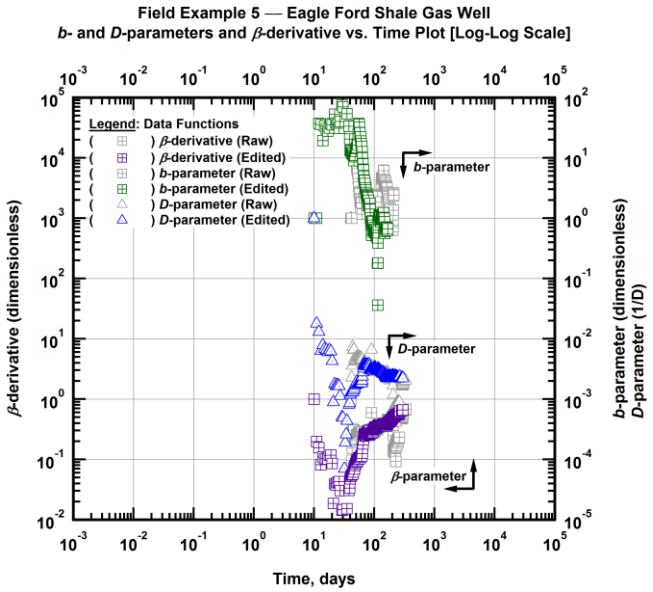

Figure A.127 — (Log-Log Plot): Filtered b, D and β production history plot — b- and D-parameters and β-derivative versus production time.

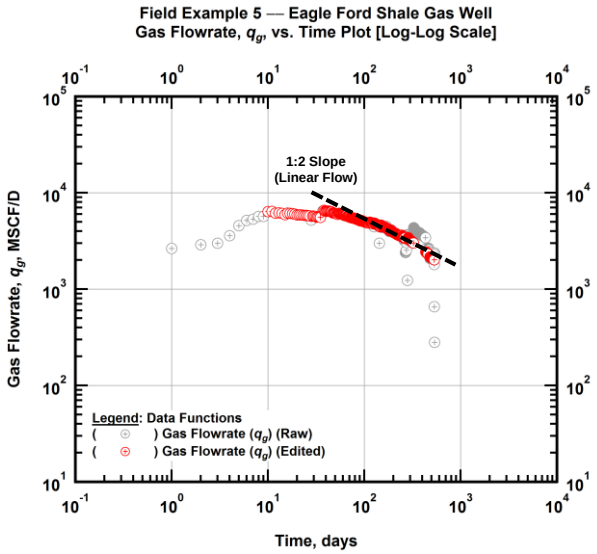

Figure A.128 — (Log-Log Plot): Filtered gas flowrate production history and flow regime identification plot — gas flowrate (q_g) versus production time.

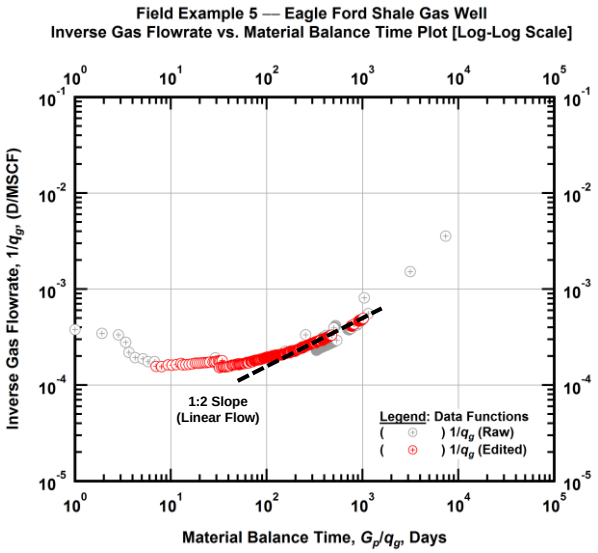

Figure A.129 — (Log-log Plot): Filtered inverse rate with material balance time plot — inverse gas flowrate ($1/q_g$) versus material balance time (G_p/q_g).

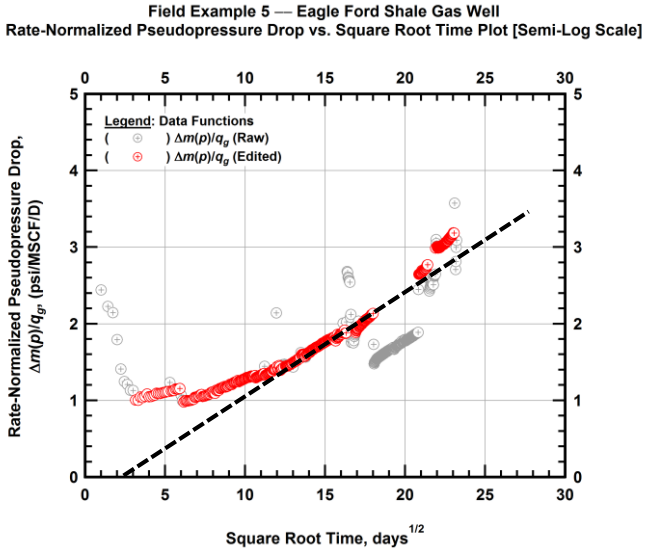

Figure A.130 — (Semi-log Plot): Filtered normalized pseudopressure drop production history plot — rate-normalized pseudopressure drop ($\Delta m(p)/q_g$) versus square root production time ($\sqrt{t}$).

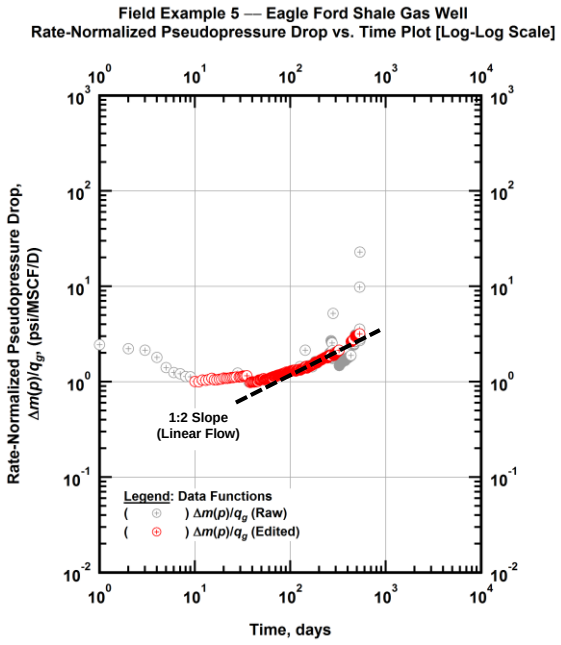

Figure A.131 — (Log-log Plot): Filtered normalized pseudopressure drop production history plot — rate-normalized pseudopressure drop ($\Delta m(p)/q_g$) versus production time.

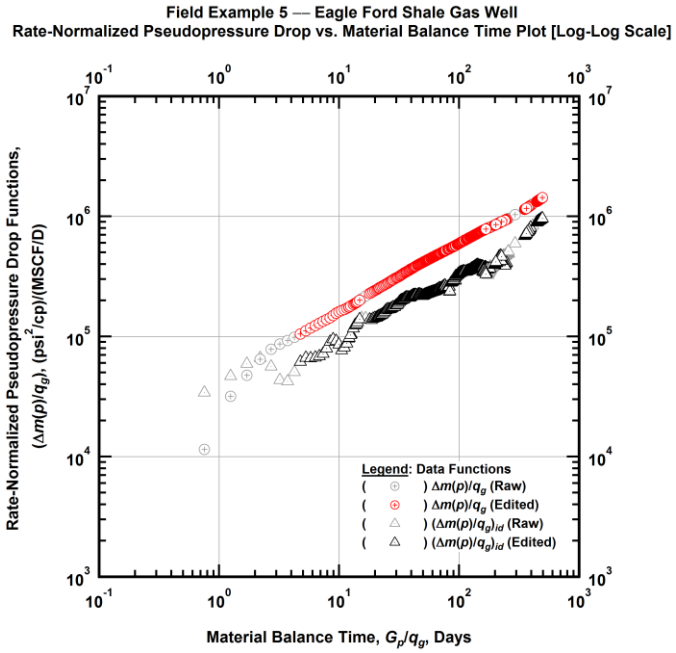

Figure A.132 — (Log-log Plot): "Log-log" diagnostic plot of the filtered production data — rate-normalized pseudopressure drop ($\Delta m(p)/q_g$) and rate-normalized pseudopressure drop integral-derivative $(\Delta m(p)/q_g)_{id}$ versus material balance time (G_p/q_g).

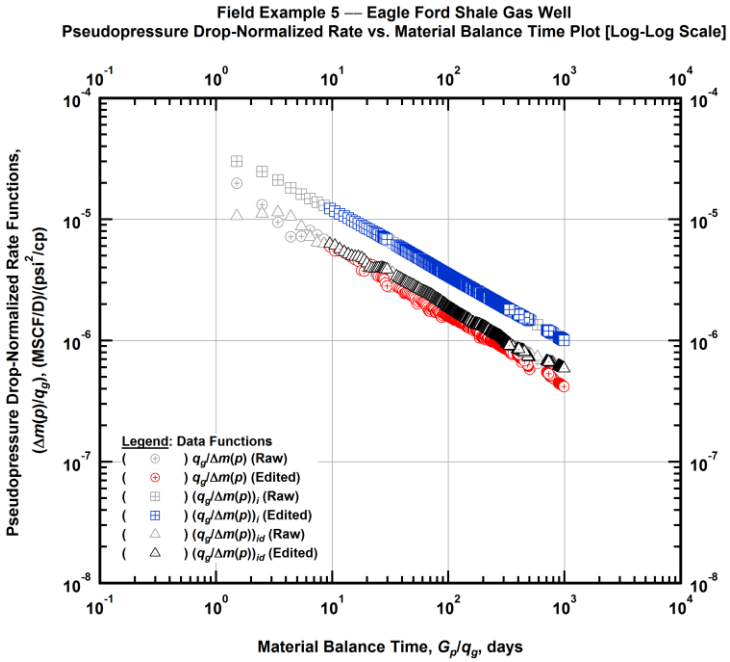

Figure A.133 — (Log-log Plot): "Blasingame" diagnostic plot of the filtered production data — pseudopressure drop-normalized gas flowrate ($q_g/\Delta m(p)$), pseudopressure drop-normalized gas flowrate integral $(q_g/\Delta m(p))_i$ and pseudopressure drop-normalized gas flowrate integral-derivative $(q_g/\Delta m(p))_{id}$ versus material balance time (G_p/q_g).

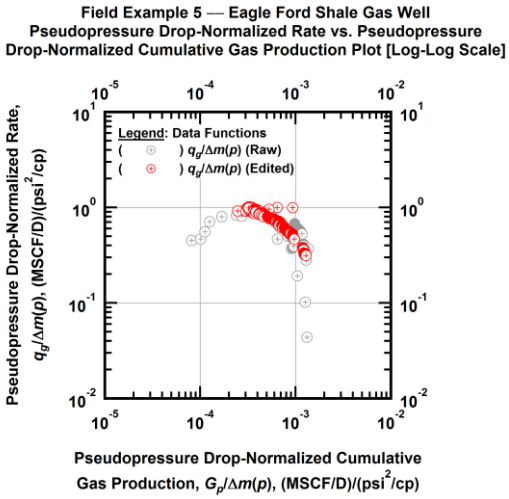

Figure A.134 — (Log-log Plot): Filtered normalized rate with normalized cumulative production plot — pseudopressure drop-normalized gas flowrate ($q_g/\Delta m(p)$) versus pseudopressure drop-normalized cumulative gas production ($G_p/\Delta m(p)$).

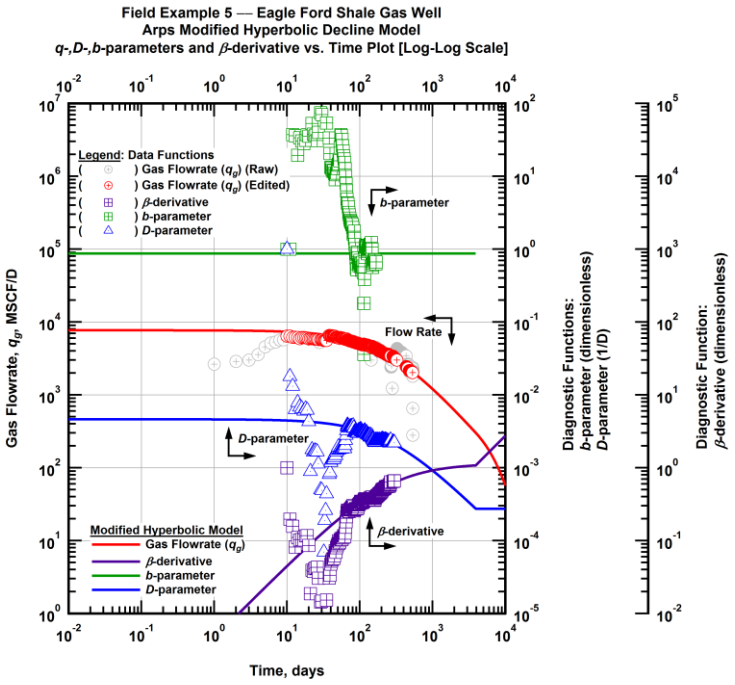

Figure A.135 — (Log-Log Plot): Arps modified hyperbolic decline model plot — time-rate model and data gas flowrate (q_g), *D*- and *b*-parameters and β-derivative versus production time.

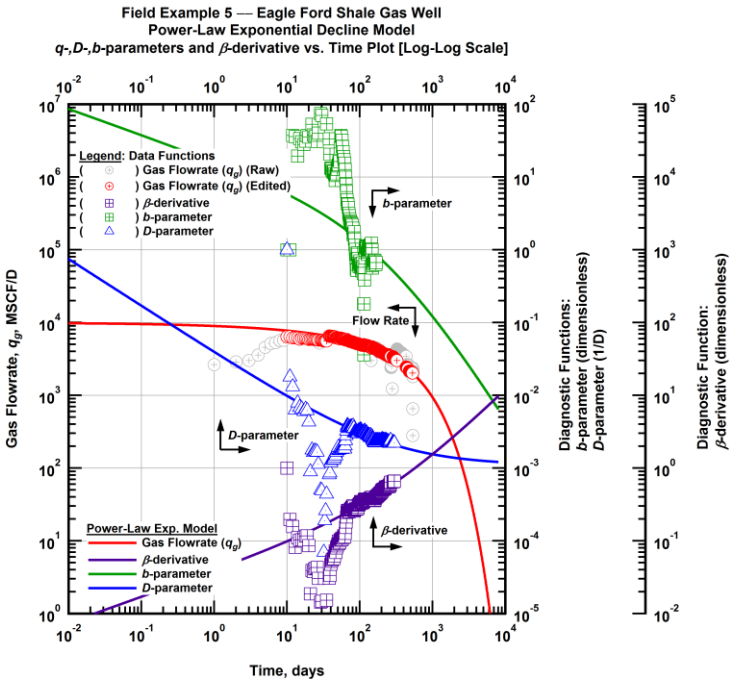

Figure A.136 — (Log-Log Plot): Power-law exponential decline model plot — time-rate model and data gas flowrate (q_g), *D*- and *b*-parameters and β-derivative versus production time.

Field Example 5 — Model-Based (Time-Rate-Pressure) Production Analysis

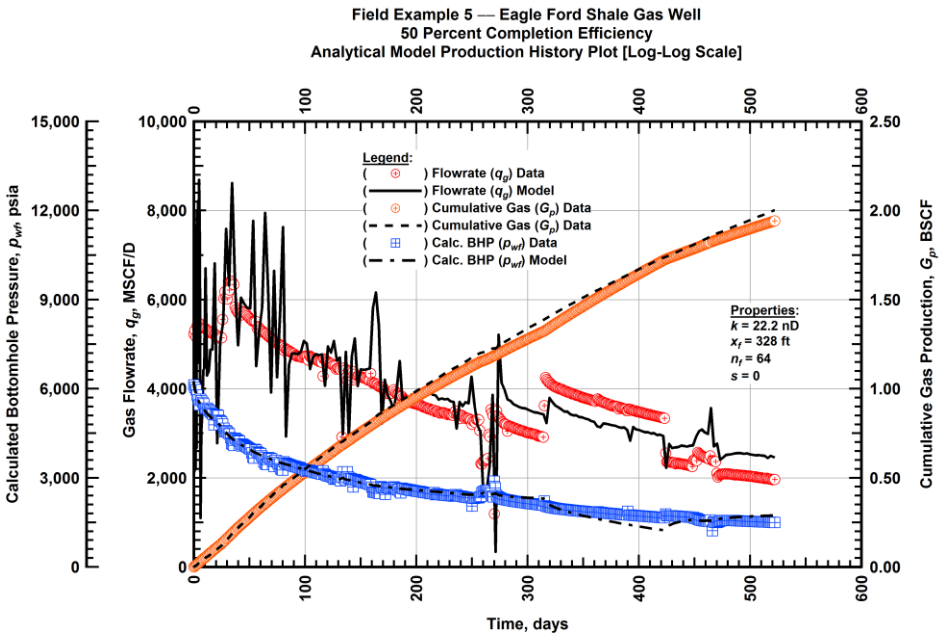

Figure A.137 — (Cartesian Plot): Production history plot — original gas flowrate (q_g), cumulative gas production (G_p), calculated bottomhole pressure (p_{wf}) and 50 percent completion efficiency model matches versus production time.

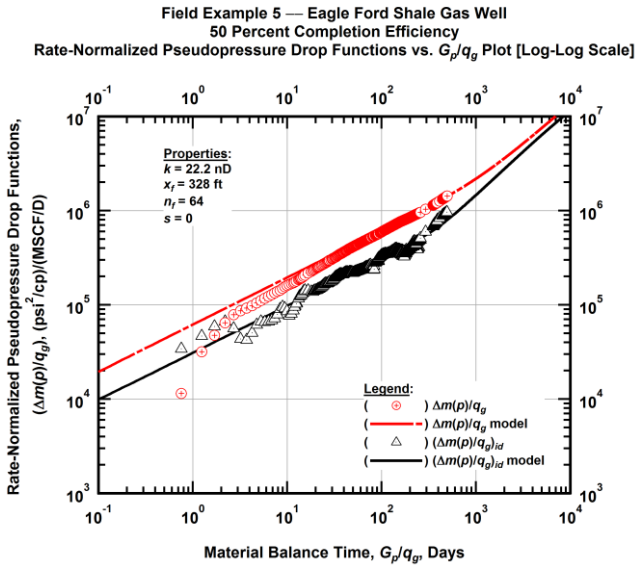

Figure A.138 — (Log-log Plot): "Log-log" diagnostic plot of the original production data — rate-normalized pseudopressure drop ($\Delta m(p)/q_g$), rate-normalized pseudopressure drop integral-derivative $(\Delta m(p)/q_g)_{id}$ and 50 percent completion efficiency model matches versus material balance time (G_p/q_g).

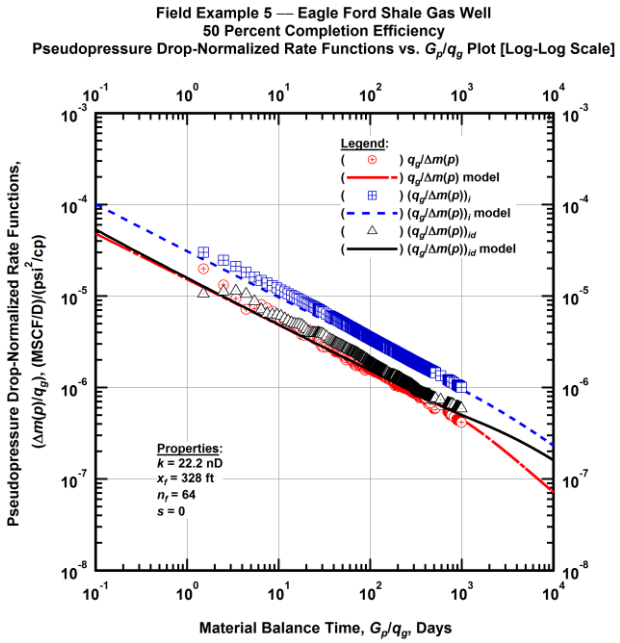

Figure A.139 — (Log-log Plot): "Blasingame" diagnostic plot of the original production data — pseudopressure drop-normalized gas flowrate ($q_g/\Delta m(p)$), pseudopressure drop-normalized gas flowrate integral $(q_g/\Delta m(p))_i$, pseudopressure drop-normalized gas flowrate integral-derivative $(q_g/\Delta m(p))_{id}$ and 50 percent completion efficiency model matches versus material balance time (G_p/q_g).

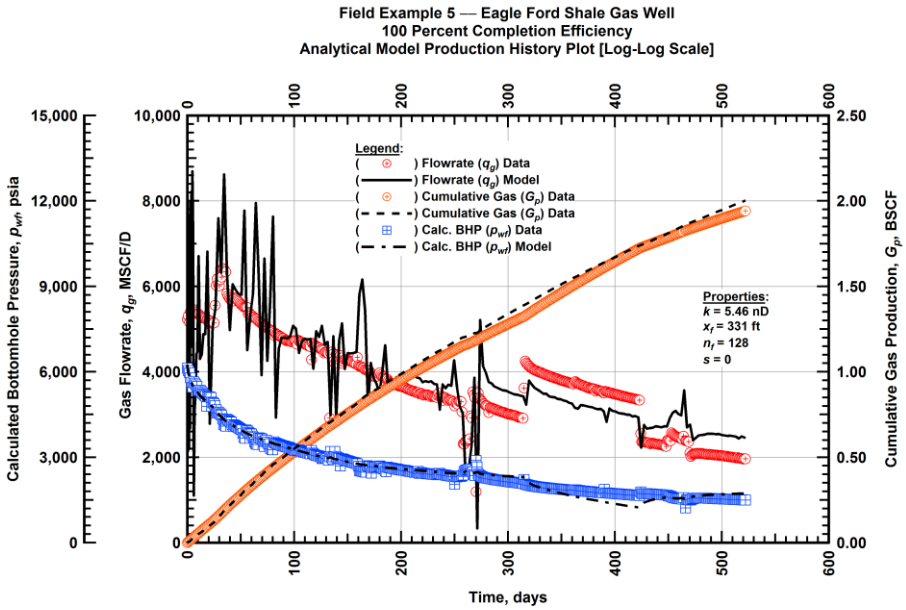

Figure A.140 — (Cartesian Plot): Production history plot — original gas flowrate (q_g), cumulative gas production (G_p), calculated bottomhole pressure (p_{wf}) and 100 percent completion efficiency model matches versus production time.

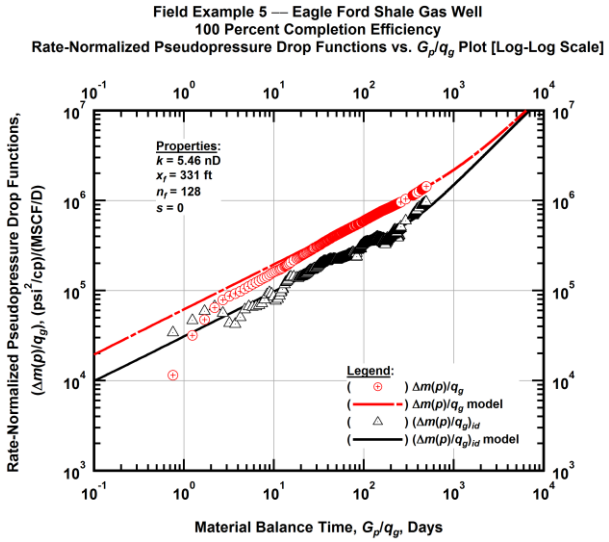

Figure A.141 — (Log-log Plot): "Log-log" diagnostic plot of the original production data — rate-normalized pseudopressure drop ($\Delta m(p)/q_g$), rate-normalized pseudopressure drop integral-derivative $(\Delta m(p)/q_g)_{id}$ and 100 percent completion efficiency model matches versus material balance time (G_p/q_g).

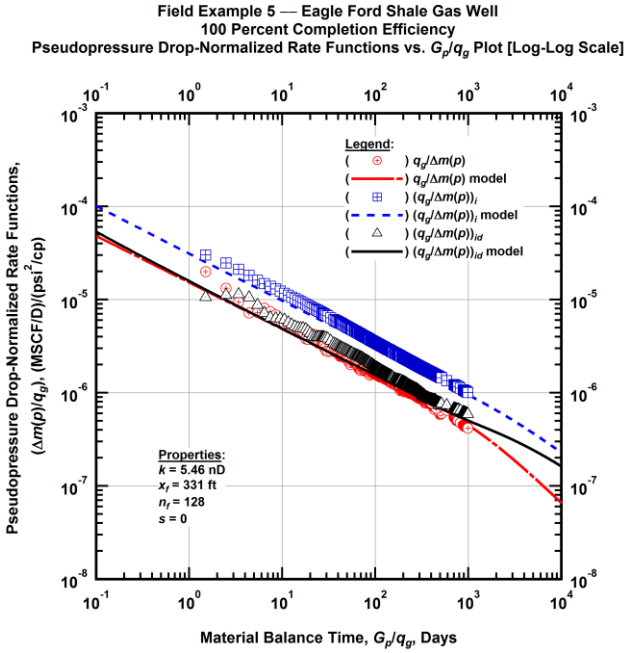

Figure A.142 — (Log-log Plot): "Blasingame" diagnostic plot of the original production data — pseudopressure drop-normalized gas flowrate ($q_g/\Delta m(p)$), pseudopressure drop-normalized gas flowrate integral $(q_g/\Delta m(p))_i$, pseudopressure drop-normalized gas flowrate integral-derivative $(q_g/\Delta m(p))_{id}$ and 100 percent completion efficiency model matches versus material balance time (G_p/q_g).

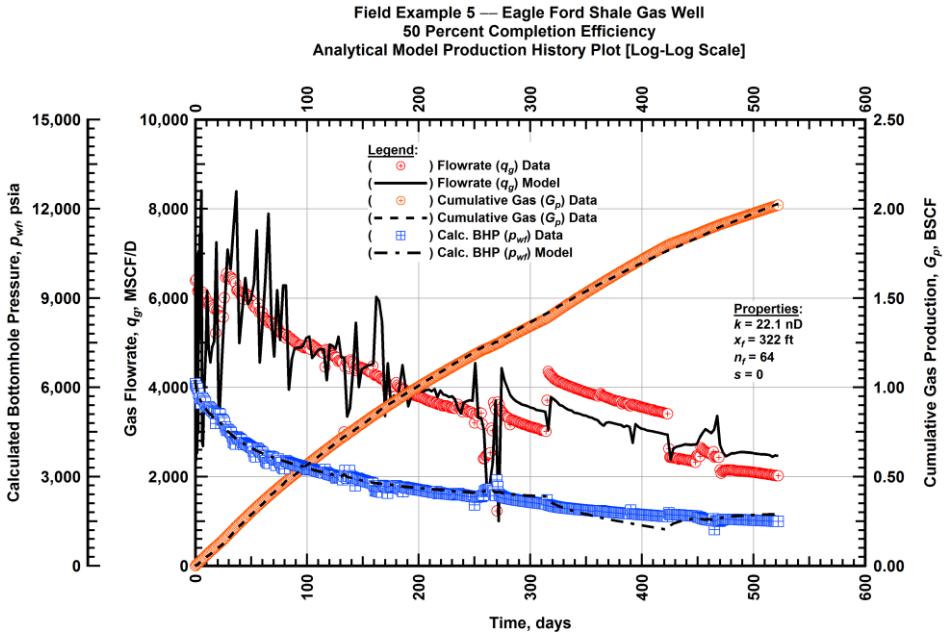

Figure A.143 — (Cartesian Plot): Production history plot — revised gas flowrate (q_g), cumulative gas production (G_p), calculated bottomhole pressure (p_{wf}) and 50 percent completion efficiency model matches versus production time.

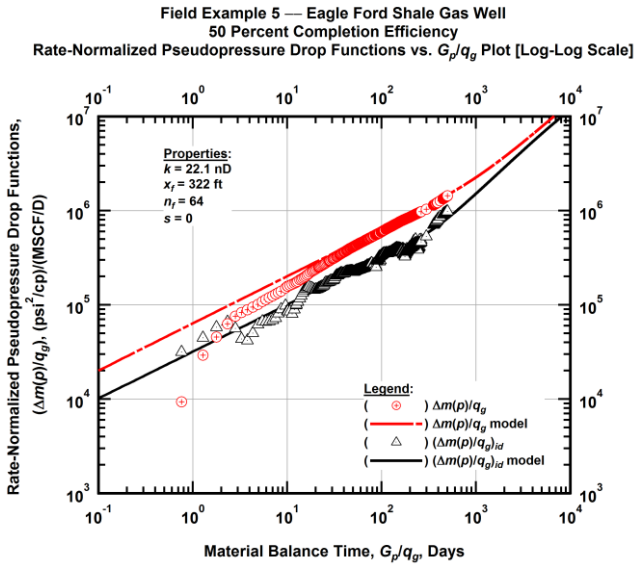

Figure A.144 — (Log-log Plot): "Log-log" diagnostic plot of the revised production data — rate-normalized pseudopressure drop ($\Delta m(p)/q_g$), rate-normalized pseudopressure drop integral-derivative $(\Delta m(p)/q_g)_{id}$ and 50 percent completion efficiency model matches versus material balance time (G_p/q_g).

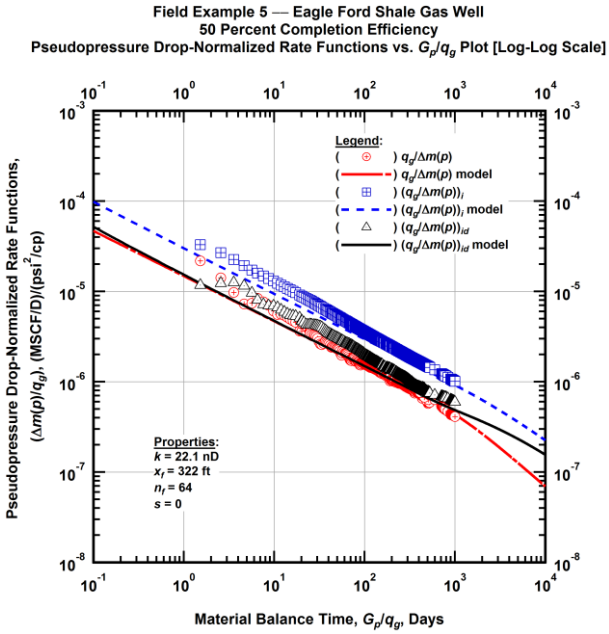

Figure A.145 — (Log-log Plot): "Blasingame" diagnostic plot of the revised production data — pseudopressure drop-normalized gas flowrate ($q_g/\Delta m(p)$), pseudopressure drop-normalized gas flowrate integral ($q_g/\Delta m(p))_i$, pseudopressure drop-normalized gas flowrate integral-derivative ($q_g/\Delta m(p))_{id}$ and 50 percent completion efficiency model matches versus material balance time (G_p/q_g).

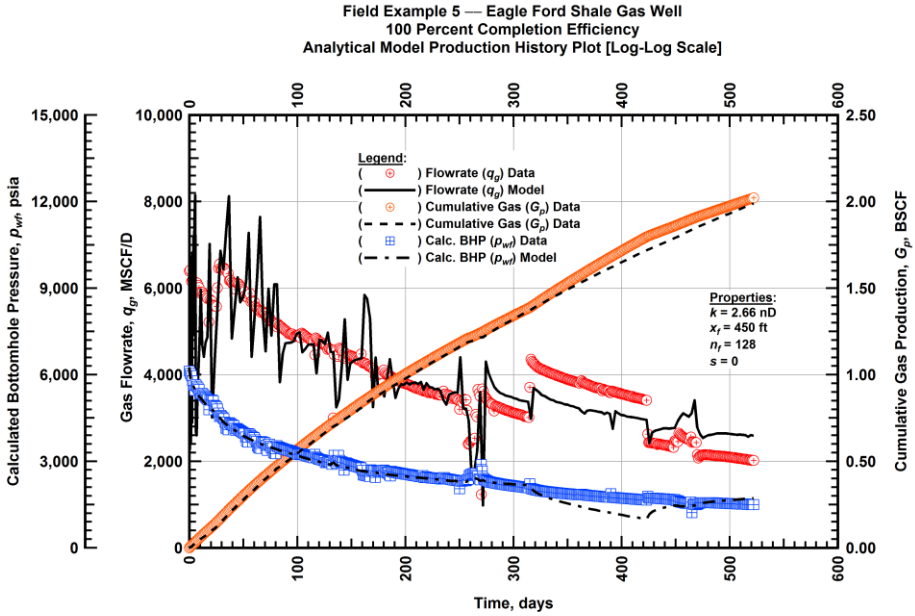

Figure A.146 — (Cartesian Plot): Production history plot — revised gas flowrate (q_g), cumulative gas production (G_p), calculated bottomhole pressure (p_{wf}) and 100 percent completion efficiency model matches versus production time.

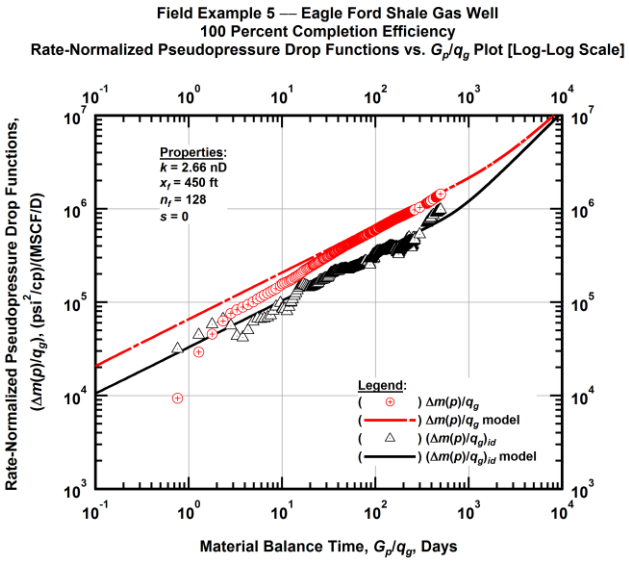

Figure A.147 — (Log-log Plot): "Log-log" diagnostic plot of the revised production data — rate-normalized pseudopressure drop ($\Delta m(p)/q_g$), rate-normalized pseudopressure drop integral-derivative $(\Delta m(p)/q_g)_{id}$ and 100 percent completion efficiency model matches versus material balance time (G_p/q_g).

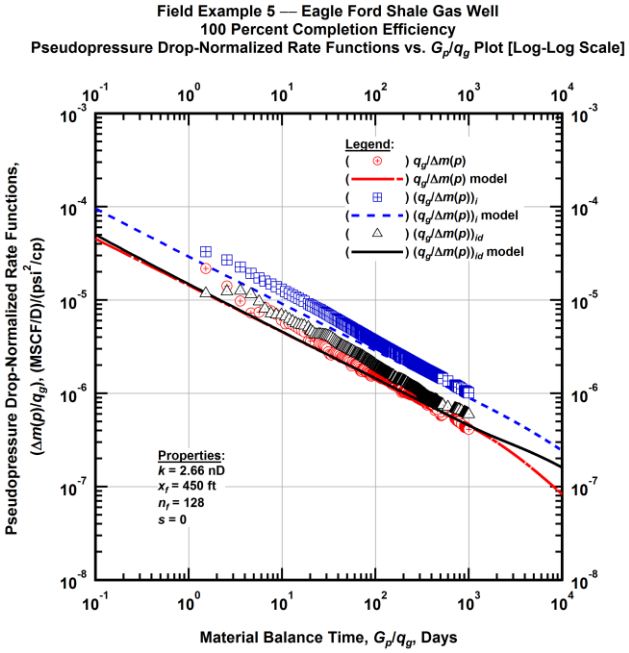

Figure A.148 — (Log-log Plot): "Blasingame" diagnostic plot of the revised production data — pseudopressure drop-normalized gas flowrate ($q_g/\Delta m(p)$), pseudopressure drop-normalized gas flowrate integral $(q_g/\Delta m(p))_i$, pseudopressure drop-normalized gas flowrate integral-derivative $(q_g/\Delta m(p))_{id}$ and 100 percent completion efficiency model matches versus material balance time (G_p/q_g).

Field Example 5 — 30-Year EUR Model Comparison

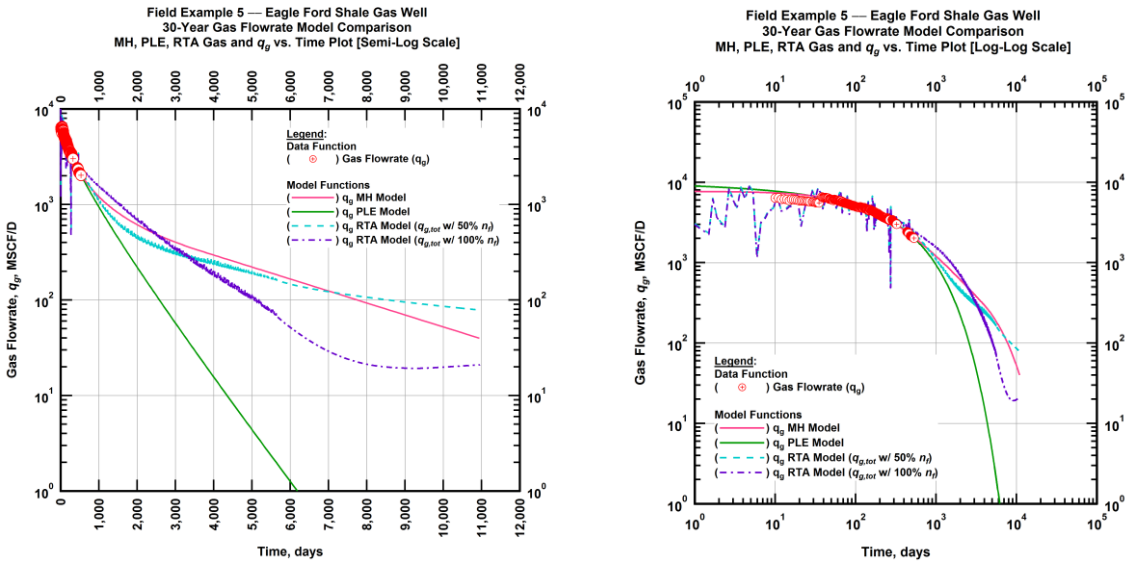

A **B**

Figure A.149 — (A — Semi-Log Plot) and (B — Log-Log Plot): Estimated 30-year revised gas flowrate model comparison — Arps modified hyperbolic decline model, power-law exponential decline model, and 50 percent and 100 percent completion efficiency RTA models revised gas 30-year estimated flowrate decline and historic gas flowrate data (q_g) versus production time.

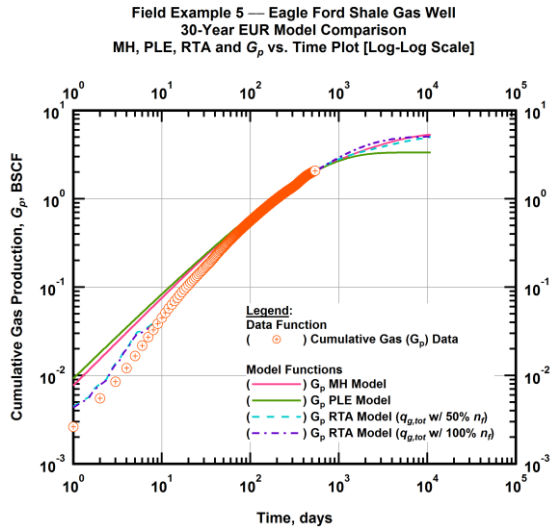

Figure A.150 — (Log-log Plot): Estimated 30-year cumulative gas production volume model comparison — Arps modified hyperbolic decline model, power-law exponential decline model, and 50 percent and 100 percent completion efficiency RTA models estimated 30-year cumulative gas production volumes and historic cumulative gas production (Gp) versus production time.

Table A.5 — 30-year estimated cumulative revised gas production (EUR), in units of BSCF, for the Arps modified hyperbolic, power-law exponential and analytical time-rate-pressure decline models.

Arps Modified Hyperbolic (BSCF)	Power-Law Exponential (BSCF)	RTA Analytical Model ($q_{g,tot}$ w/ 50% n_f) (BSCF)	RTA Analytical Model ($q_{g,tot}$ w/ 100% n_f) (BSCF)
5.41	3.36	5.06	5.08

Field Example 6 — Time-Rate Analysis

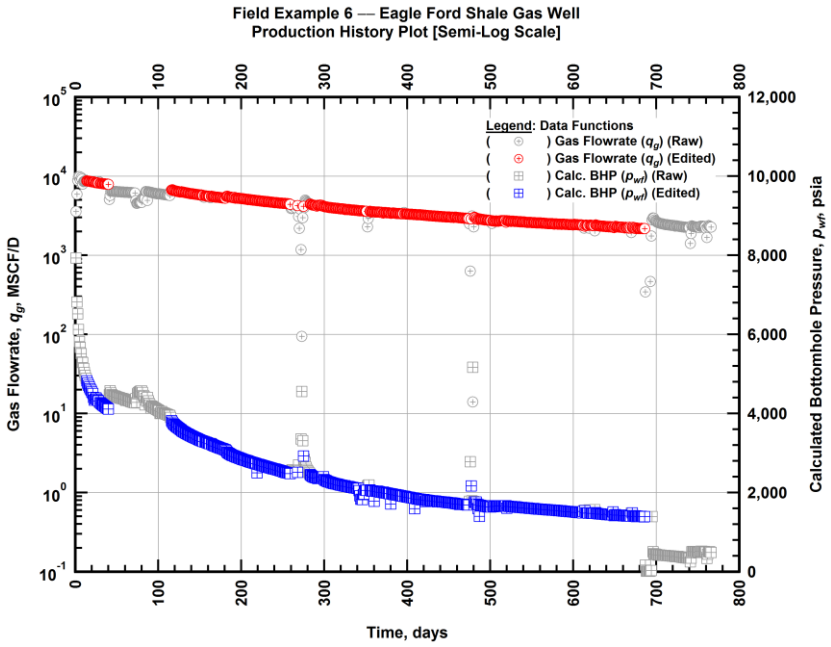

Figure A.151 — (Semi-log Plot): Filtered production history plot — flowrate (q_g) and calculated bottomhole pressure (p_{wf}) versus production time.

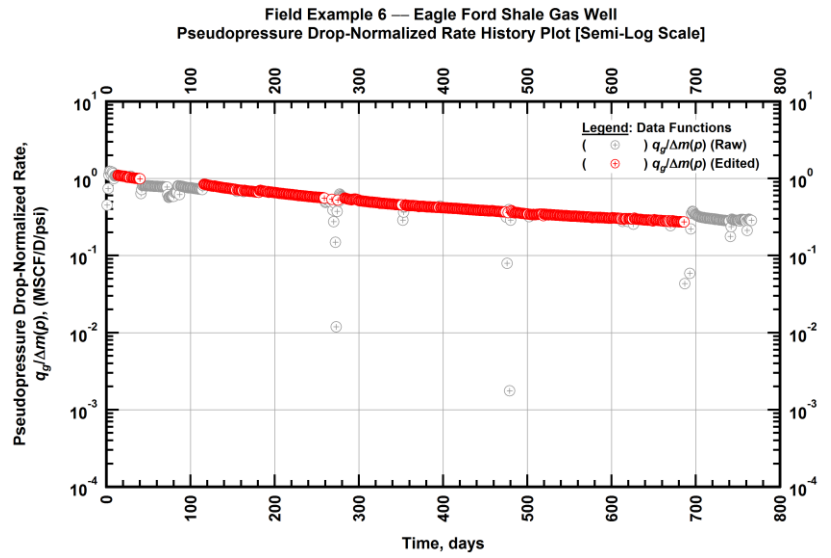

Figure A.152 — (Semi-log Plot): Filtered normalized rate production history plot — pseudopressure drop-normalized gas flowrate ($q_g/\Delta m(p)$) versus production time.

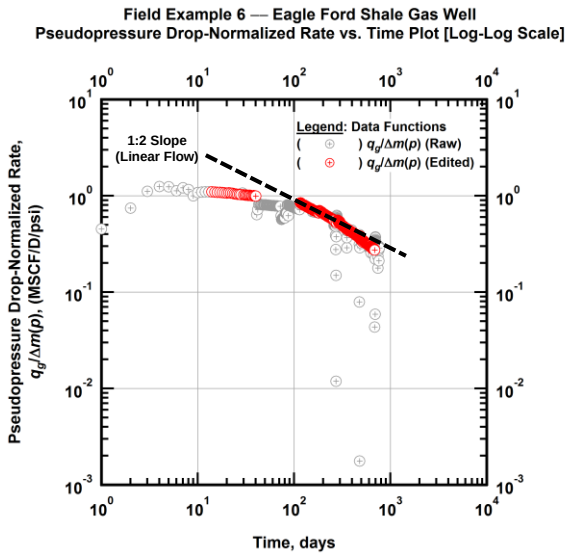

Figure A.153 — (Log-log Plot): Filtered normalized rate production history plot — pseudopressure drop-normalized gas flowrate ($q_g/\Delta m(p)$) versus production time.

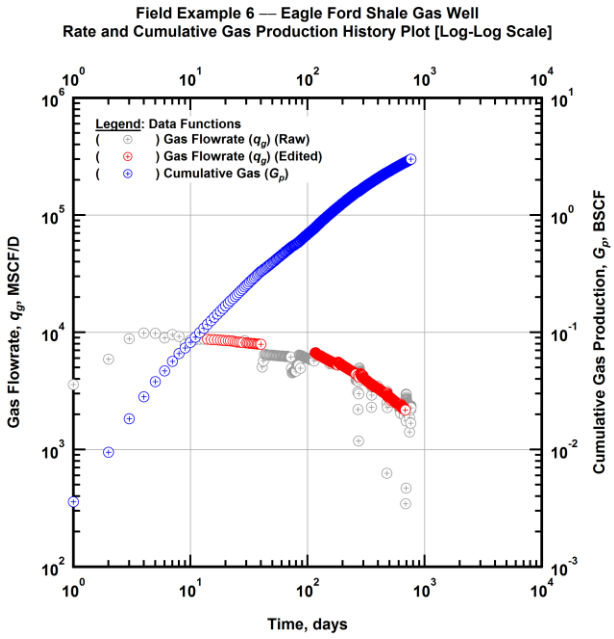

Figure A.154 — (Log-log Plot): Filtered rate and unfiltered cumulative gas production history plot — flowrate (q_g) and cumulative production (G_p) versus production time.

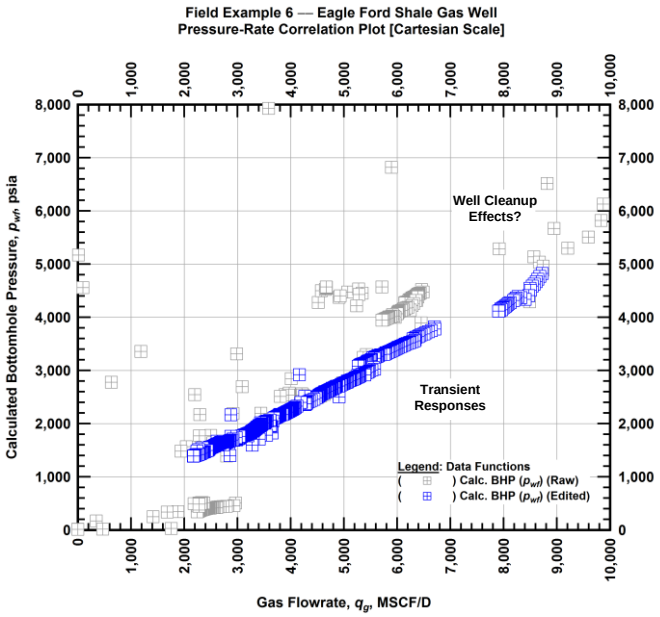

Figure A.155 — (Cartesian Plot): Filtered rate-pressure correlation plot — calculated bottomhole pressure (p_{wf}) versus flowrate (q_g).

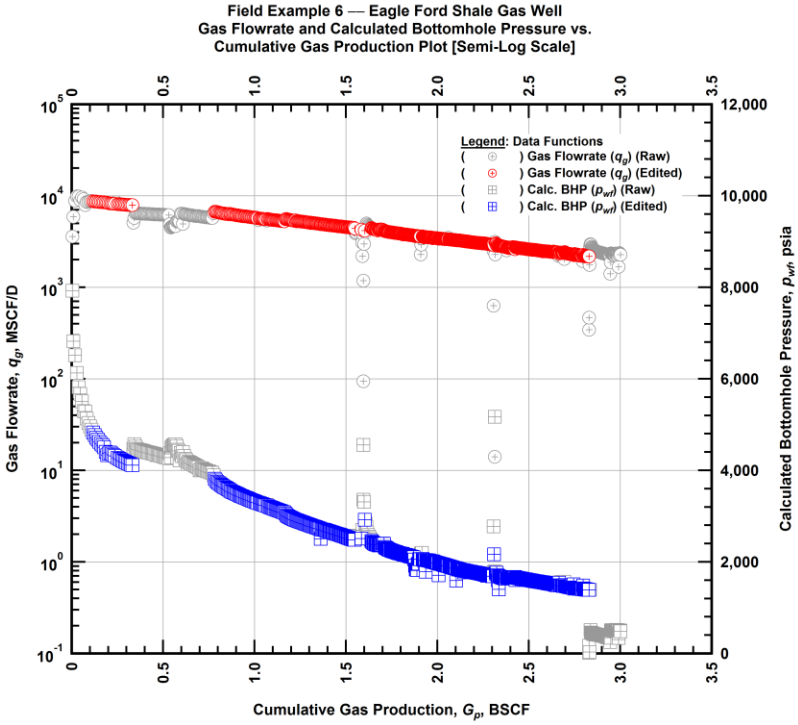

Figure A.156 — (Semi-log Plot): Filtered rate-pressure-cumulative production history plot — flowrate (q_g) and calculated bottomhole pressure (p_{wf}) versus cumulative production (G_p).

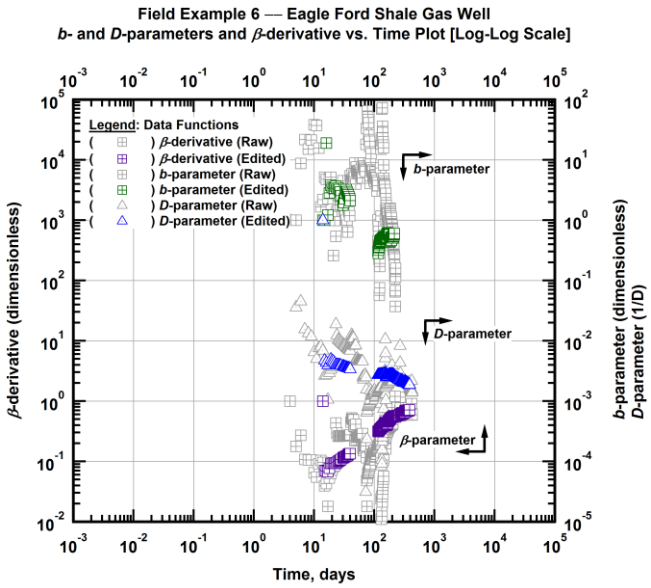

Figure A.157 — (Log-Log Plot): Filtered b, D and β production history plot — b- and D-parameters and β-derivative versus production time.

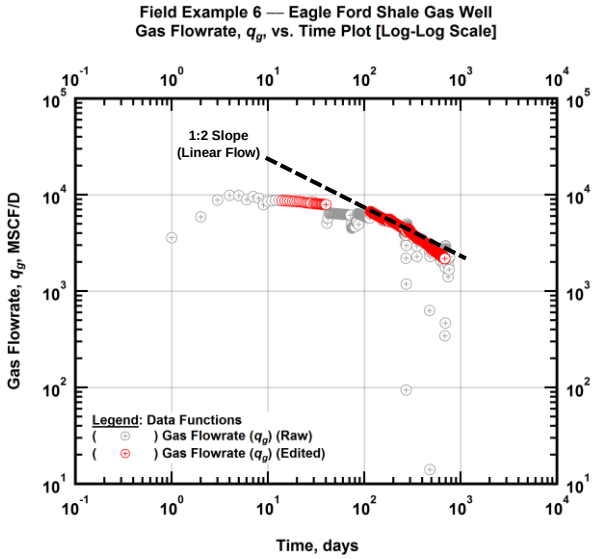

Figure A.158 — (Log-Log Plot): Filtered gas flowrate production history and flow regime identification plot — gas flowrate (q_g) versus production time.

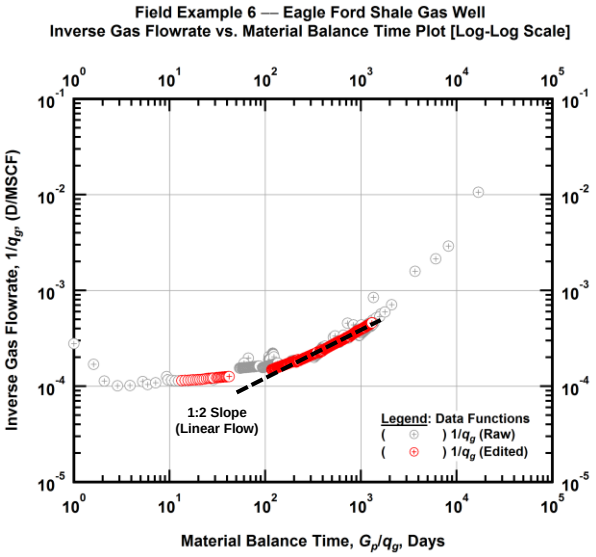

Figure A.159 — (Log-log Plot): Filtered inverse rate with material balance time plot — inverse gas flowrate ($1/q_g$) versus material balance time (G_p/q_g).

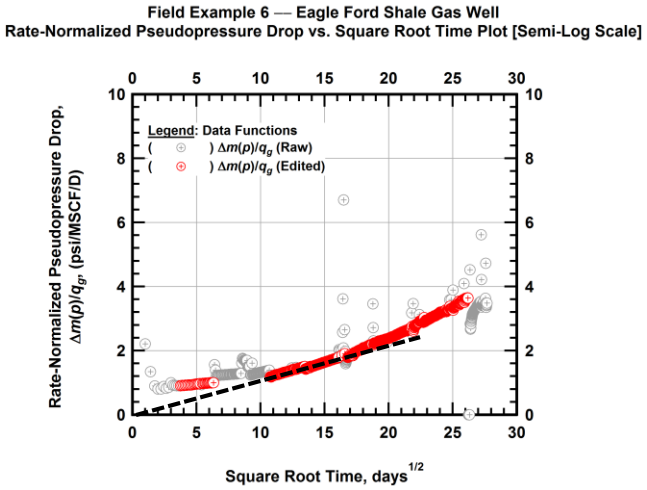

Figure A.160 — (Semi-log Plot): Filtered normalized pseudopressure drop production history plot — rate-normalized pseudopressure drop ($\Delta m(p)/q_g$) versus square root production time ($\sqrt{t}$).

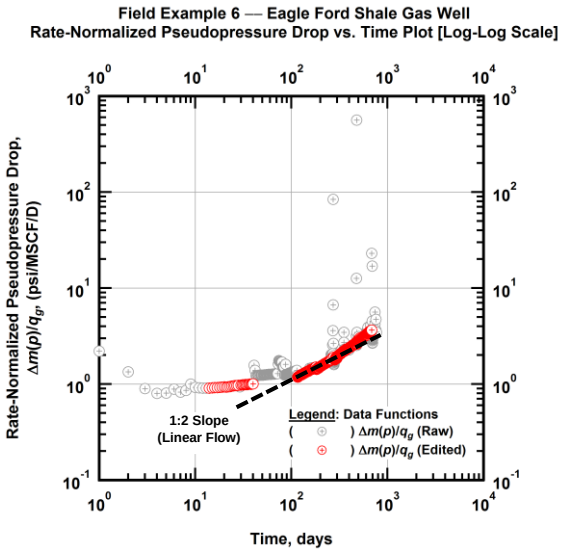

Figure A.161 — (Log-log Plot): Filtered normalized pseudopressure drop production history plot — rate-normalized pseudopressure drop ($\Delta m(p)/q_g$) versus production time.

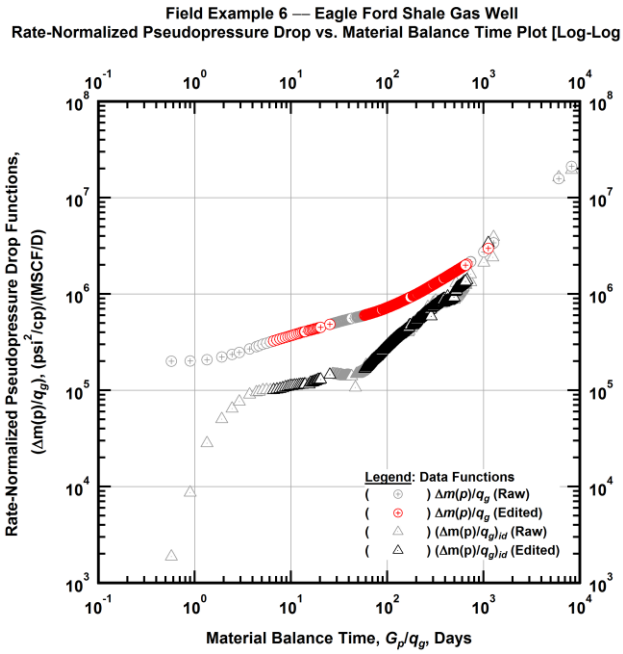

Figure A.162 — (Log-log Plot): "Log-log" diagnostic plot of the filtered production data — rate-normalized pseudopressure drop ($\Delta m(p)/q_g$) and rate-normalized pseudopressure drop integral-derivative $(\Delta m(p)/q_g)_{id}$ versus material balance time (G_p/q_g).

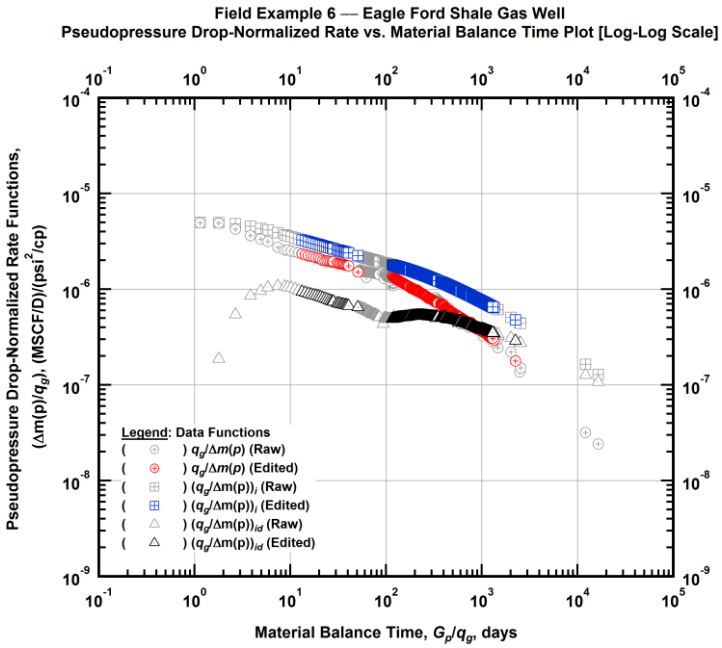

Figure A.163 — (Log-log Plot): "Blasingame" diagnostic plot of the filtered production data — pseudopressure drop-normalized gas flowrate ($q_g/\Delta m(p)$), pseudopressure drop-normalized gas flowrate integral $(q_g/\Delta m(p))_i$ and pseudopressure drop-normalized gas flowrate integral-derivative $(q_g/\Delta m(p))_{id}$ versus material balance time (G_p/q_g).

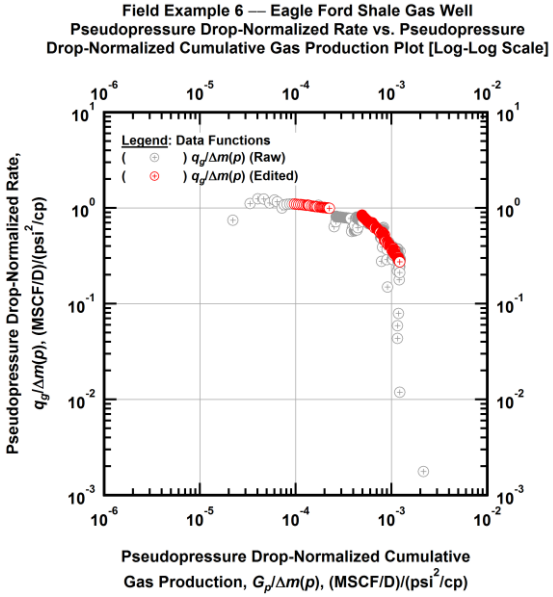

Figure A.164 — (Log-log Plot): Filtered normalized rate with normalized cumulative production plot — pseudopressure drop-normalized gas flowrate ($q_g/\Delta m(p)$) versus pseudopressure drop-normalized cumulative gas production ($G_p/\Delta m(p)$).

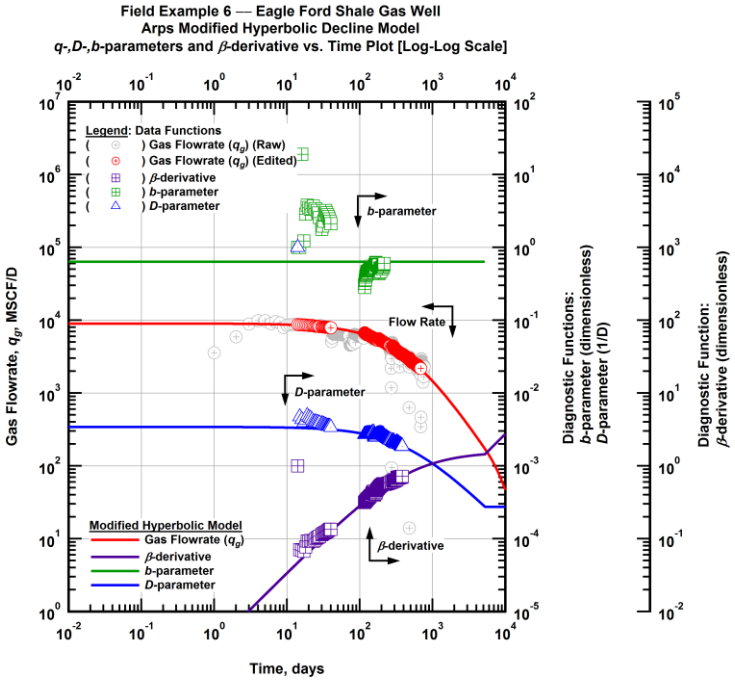

Figure A.165 — (Log-Log Plot): Arps modified hyperbolic decline model plot — time-rate model and data gas flowrate (q_g), *D*- and *b*-parameters and β-derivative versus production time.

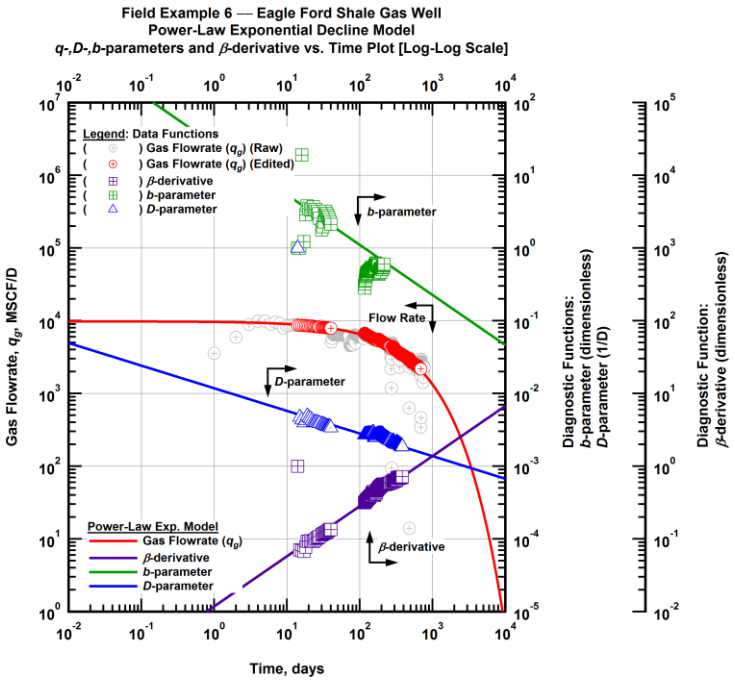

Figure A.166 — (Log-Log Plot): Power-law exponential decline model plot — time-rate model and data gas flowrate (q_g), *D*- and *b*-parameters and β-derivative versus production time.

Field Example 6 — Model-Based (Time-Rate-Pressure) Production Analysis

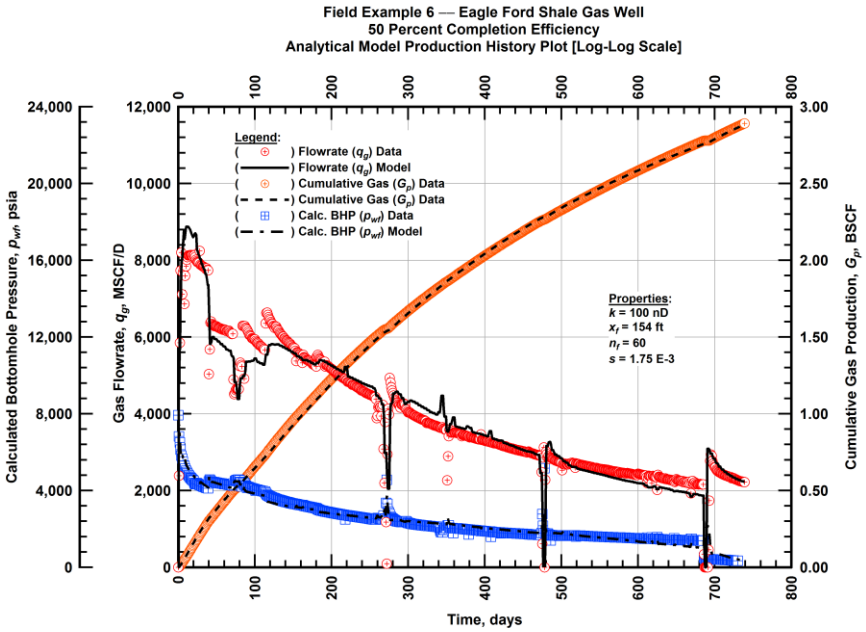

Figure A.167 — (Cartesian Plot): Production history plot — original gas flowrate (q_g), cumulative gas production (G_p), calculated bottomhole pressure (p_{wf}) and 50 percent completion efficiency model matches versus production time.

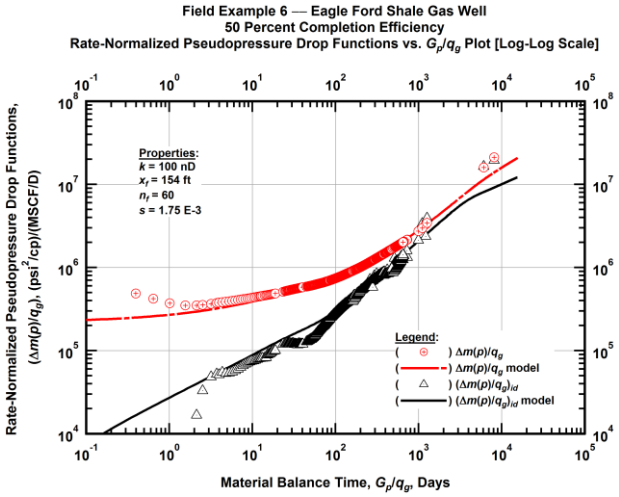

Figure A.168 — (Log-log Plot): "Log-log" diagnostic plot of the original production data — rate-normalized pseudopressure drop ($\Delta m(p)/q_g$), rate-normalized pseudopressure drop integral-derivative $(\Delta m(p)/q_g)_{id}$ and 50 percent completion efficiency model matches versus material balance time (G_p/q_g).

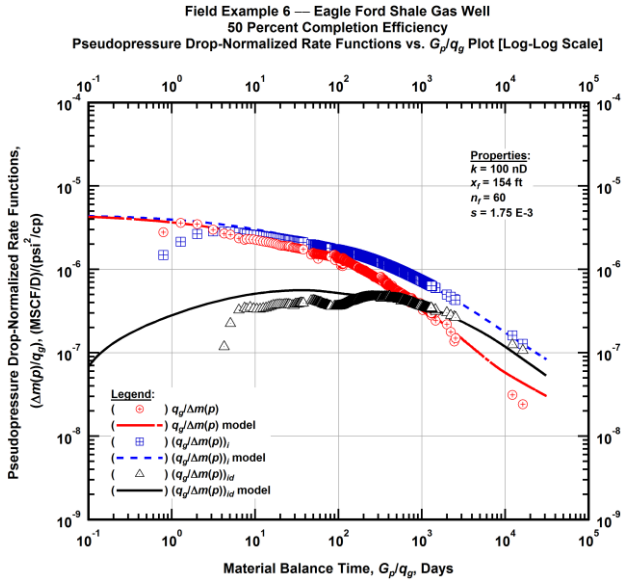

Figure A.169 — (Log-log Plot): "Blasingame" diagnostic plot of the original production data — pseudopressure drop-normalized gas flowrate ($q_g/\Delta m(p)$), pseudopressure drop-normalized gas flowrate integral $(q_g/\Delta m(p))_i$, pseudopressure drop-normalized gas flowrate integral-derivative $(q_g/\Delta m(p))_{id}$ and 50 percent completion efficiency model matches versus material balance time (G_p/q_g).

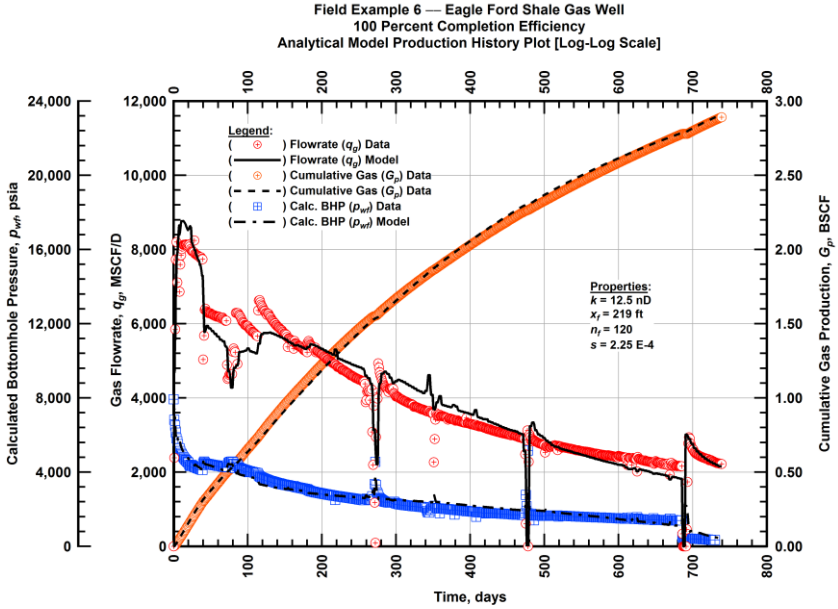

Figure A.170 — (Cartesian Plot): Production history plot — original gas flowrate (q_g), cumulative gas production (G_p), calculated bottomhole pressure (p_{wf}) and 100 percent completion efficiency model matches versus production time.

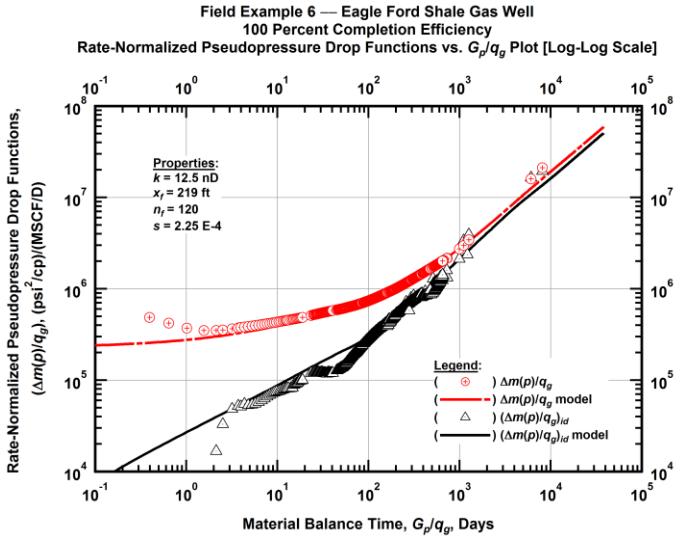

Figure A.171 — (Log-log Plot): "Log-log" diagnostic plot of the original production data — rate-normalized pseudopressure drop ($\Delta m(p)/q_g$), rate-normalized pseudopressure drop integral-derivative $(\Delta m(p)/q_g)_{id}$ and 100 percent completion efficiency model matches versus material balance time (G_p/q_g).

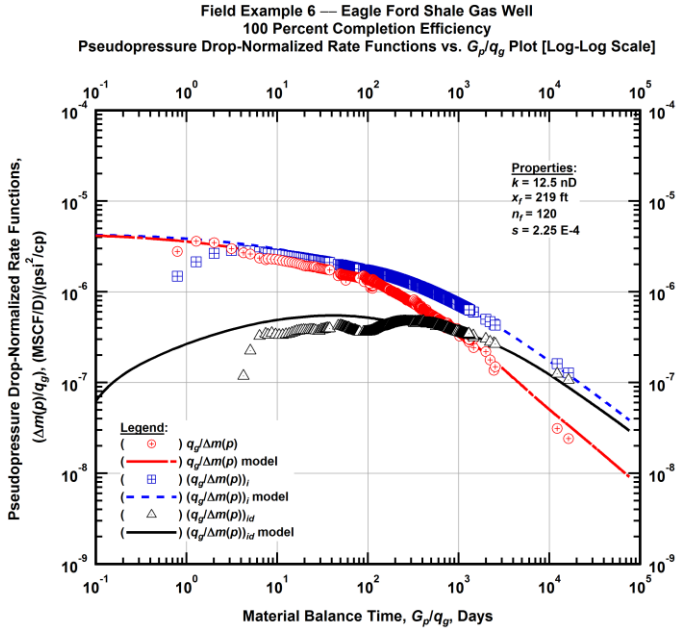

Figure A.172 — (Log-log Plot): "Blasingame" diagnostic plot of the original production data — pseudopressure drop-normalized gas flowrate ($q_g/\Delta m(p)$), pseudopressure drop-normalized gas flowrate integral $(q_g/\Delta m(p))_i$, pseudopressure drop-normalized gas flowrate integral-derivative $(q_g/\Delta m(p))_{id}$ and 100 percent completion efficiency model matches versus material balance time (G_p/q_g).

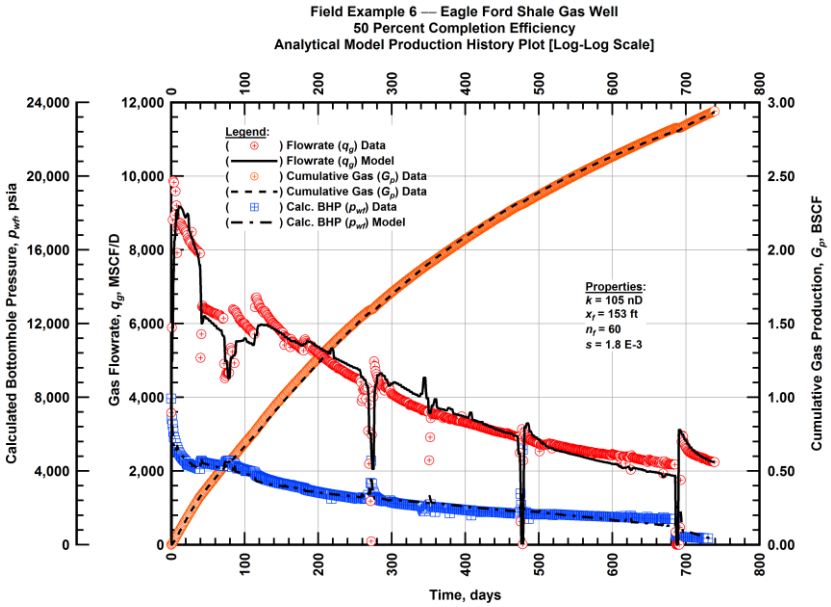

Figure A.173 — (Cartesian Plot): Production history plot — revised gas flowrate (q_g), cumulative gas production (G_p), calculated bottomhole pressure (p_{wf}) and 50 percent completion efficiency model matches versus production time.

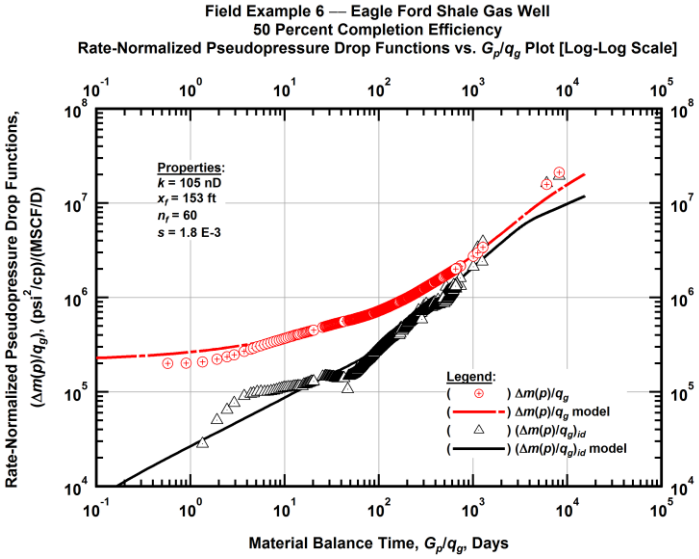

Figure A.174 — (Log-log Plot): "Log-log" diagnostic plot of the revised production data — rate-normalized pseudopressure drop ($\Delta m(p)/q_g$), rate-normalized pseudopressure drop integral-derivative $(\Delta m(p)/q_g)_{id}$ and 50 percent completion efficiency model matches versus material balance time (G_p/q_g).

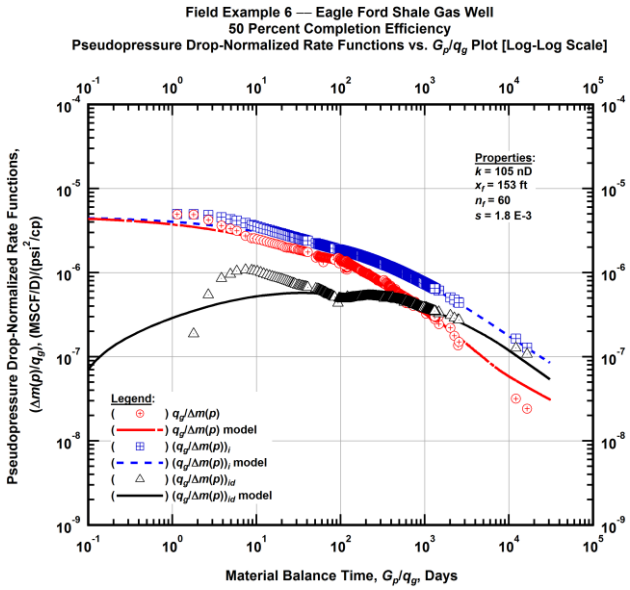

Figure A.175 — (Log-log Plot): "Blasingame" diagnostic plot of the revised production data — pseudopressure drop-normalized gas flowrate ($q_g/\Delta m(p)$), pseudopressure drop-normalized gas flowrate integral $(q_g/\Delta m(p))_i$, pseudopressure drop-normalized gas flowrate integral-derivative $(q_g/\Delta m(p))_{id}$ and 50 percent completion efficiency model matches versus material balance time (G_p/q_g).

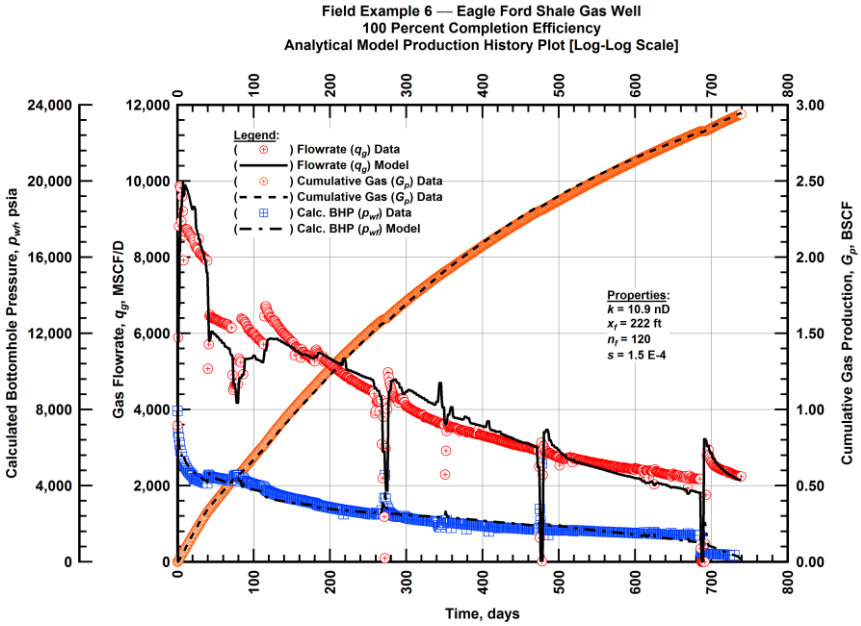

Figure A.176 — (Cartesian Plot): Production history plot — revised gas flowrate (q_g), cumulative gas production (G_p), calculated bottomhole pressure (p_{wf}) and 100 percent completion efficiency model matches versus production time.

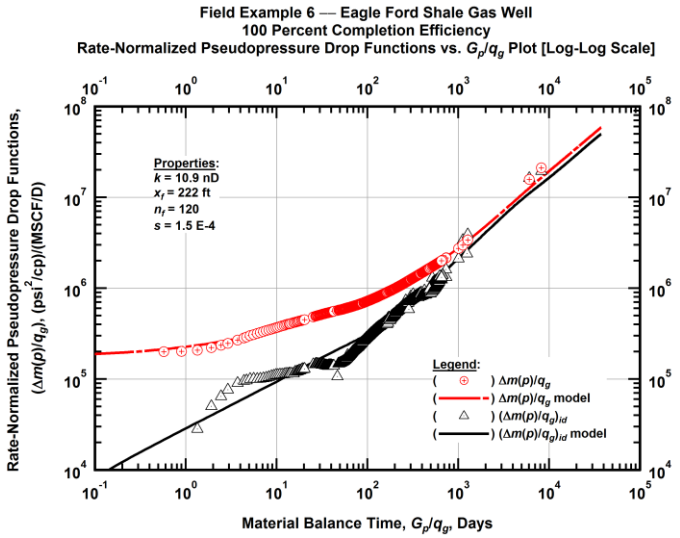

Figure A.177 — (Log-log Plot): "Log-log" diagnostic plot of the revised production data — rate-normalized pseudopressure drop ($\Delta m(p)/q_g$), rate-normalized pseudopressure drop integral-derivative $(\Delta m(p)/q_g)_{id}$ and 100 percent completion efficiency model matches versus material balance time (G_p/q_g).

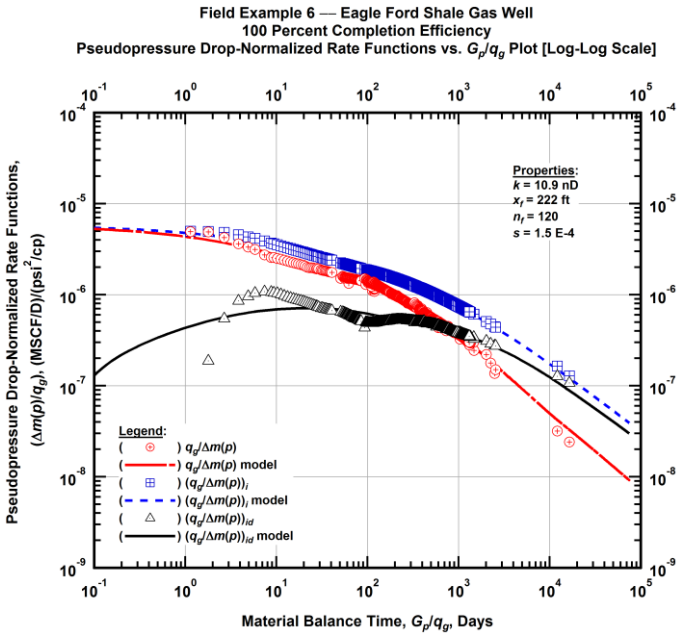

Figure A.178 — (Log-log Plot): "Blasingame" diagnostic plot of the revised production data — pseudopressure drop-normalized gas flowrate ($q_g/\Delta m(p)$), pseudopressure drop-normalized gas flowrate integral $(q_g/\Delta m(p))_i$, pseudopressure drop-normalized gas flowrate integral-derivative $(q_g/\Delta m(p))_{id}$ and 100 percent completion efficiency model matches versus material balance time (G_p/q_g).

Field Example 6 — 30-Year EUR Model Comparison

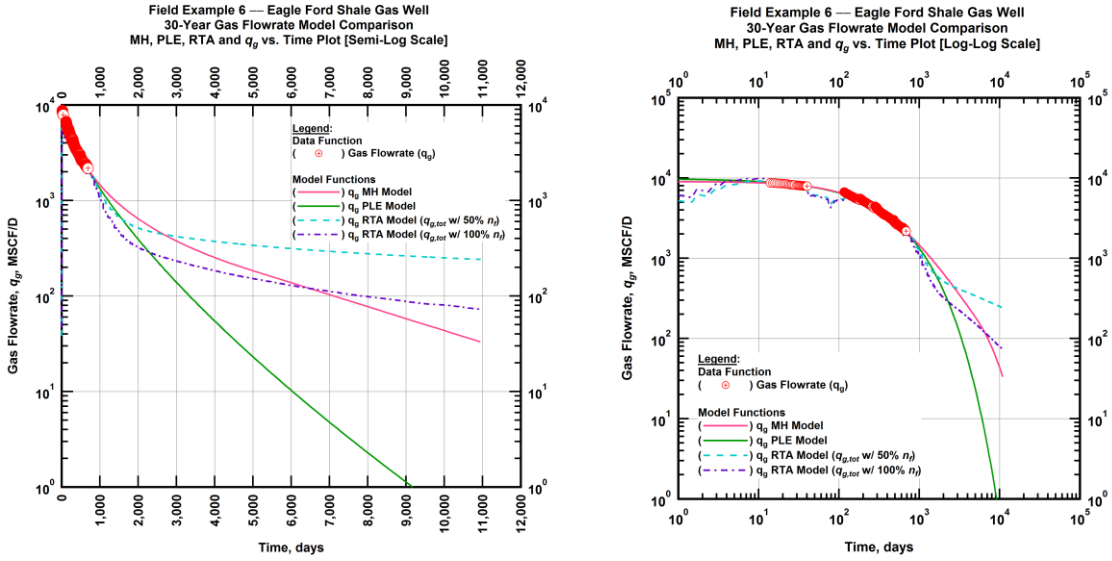

A **B**

Figure A.179 — (A — Semi-Log Plot) and (B — Log-Log Plot): Revised gas 30-year estimated flowrate model comparison — Arps modified hyperbolic decline model, power-law exponential decline model, and 50 percent and 100 percent completion efficiency RTA models revised gas 30-year estimated flowrate decline and historic gas flowrate data (q_g) versus production time.

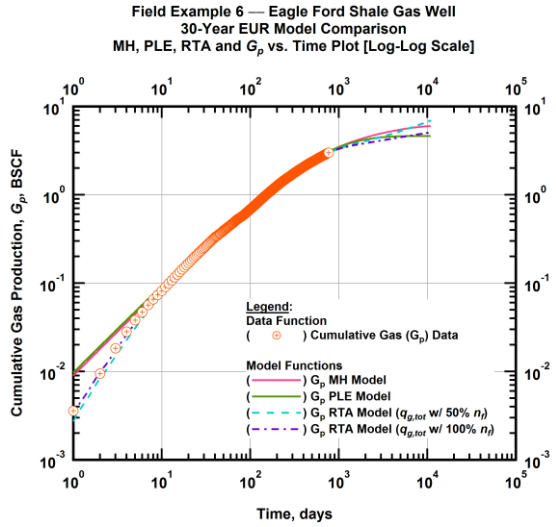

Figure A.180 — (Log-log Plot): Estimated 30-year cumulative gas production volume model comparison — Arps modified hyperbolic decline model, power-law exponential decline model, and 50 percent and 100 percent completion efficiency RTA models estimated 30-year cumulative gas production volumes and historic cumulative gas production (Gp) versus production time.

Table A.6 — 30-year estimated cumulative revised gas production (EUR), in units of BSCF, for the Arps modified hyperbolic, power-law exponential and analytical time-rate-pressure decline models.

Arps Modified Hyperbolic (BSCF)	Power-Law Exponential (BSCF)	RTA Analytical Model ($q_{g,tot}$ w/ 50% n_f) (BSCF)	RTA Analytical Model ($q_{g,tot}$ w/ 100% n_f) (BSCF)
5.92	4.51	7.11	5.14

Field Example 7 — Time-Rate Analysis

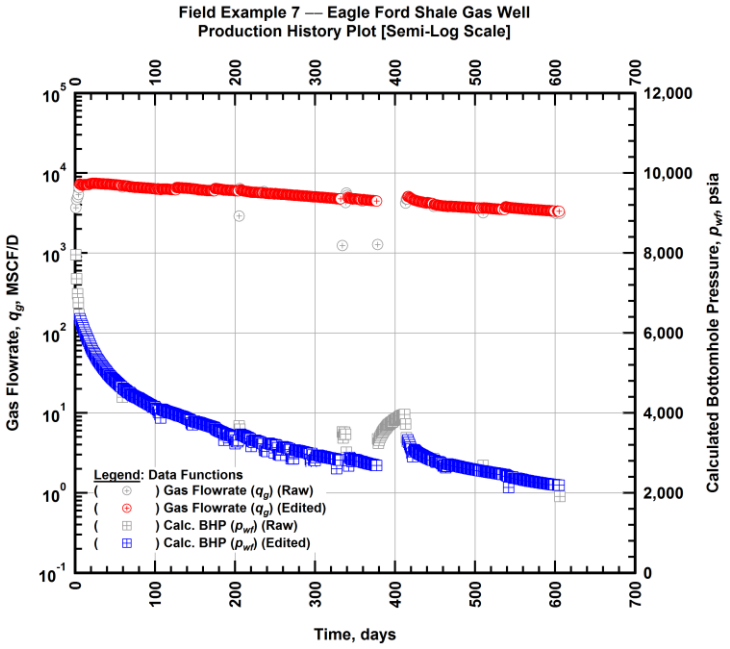

Figure A.181 — (Semi-log Plot): Filtered production history plot — flowrate (q_g) and calculated bottomhole pressure (p_{wf}) versus production time.

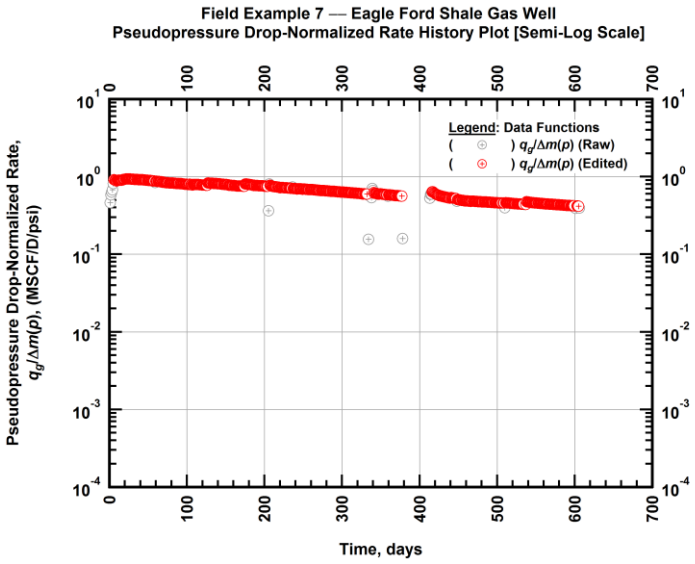

Figure A.182 — (Semi-log Plot): Filtered normalized rate production history plot — pseudopressure drop-normalized gas flowrate ($q_g/\Delta m(p)$) versus production time.

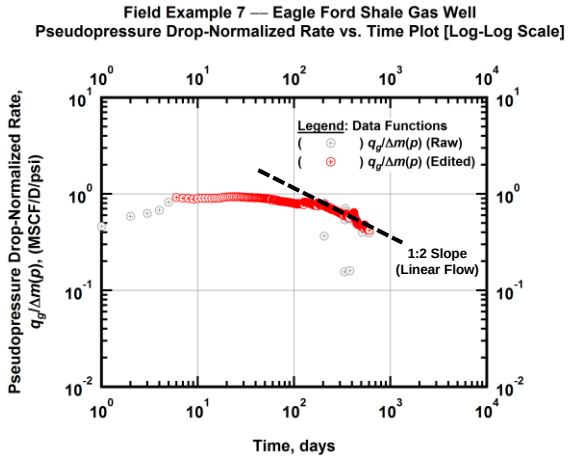

Figure A.183 — (Log-log Plot): Filtered normalized rate production history plot — pseudopressure drop-normalized gas flowrate ($q_g/\Delta m(p)$) versus production time.

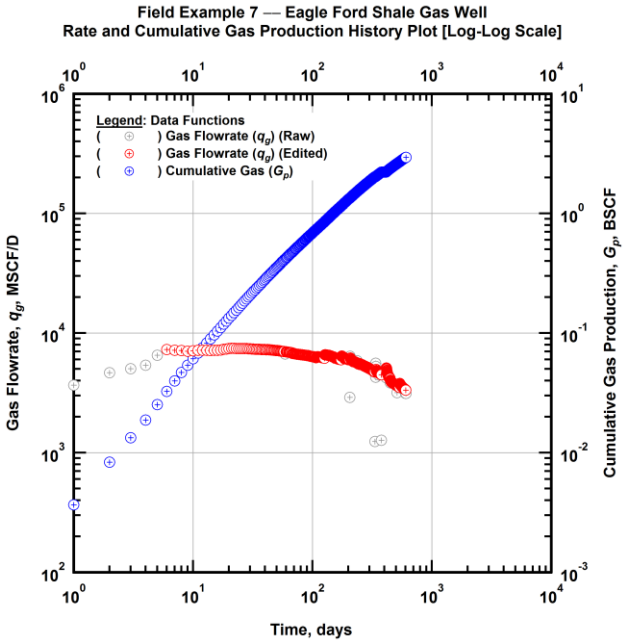

Figure A.184 — (Log-log Plot): Filtered rate and unfiltered cumulative gas production history plot — flowrate (q_g) and cumulative production (G_p) versus production time.

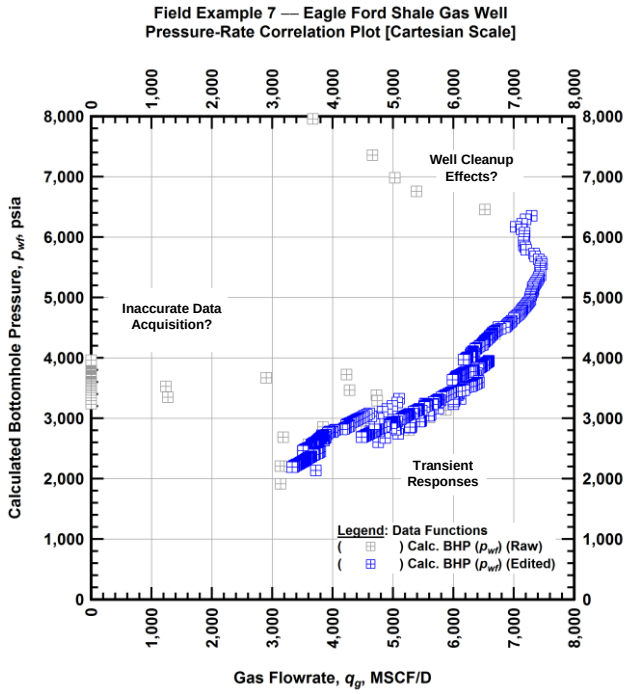

Figure A.185 — (Cartesian Plot): Filtered rate-pressure correlation plot — calculated bottomhole pressure (p_{wf}) versus flowrate (q_g).

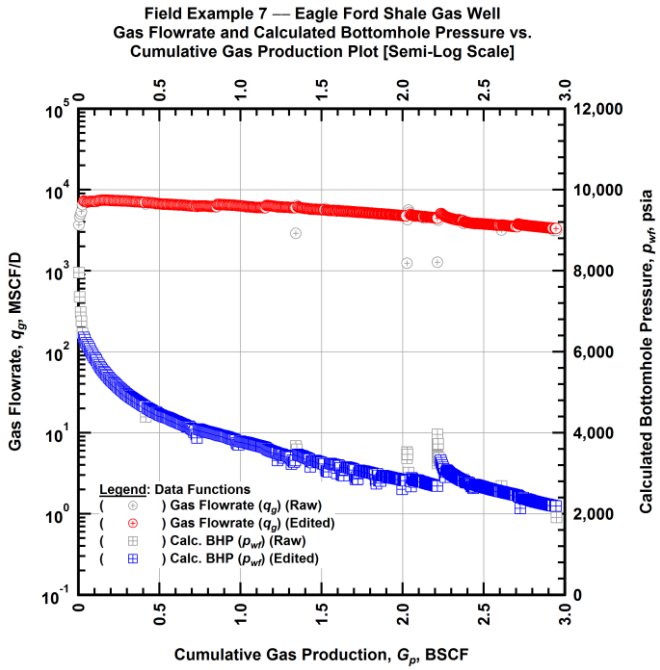

Figure A.186 — (Semi-log Plot): Filtered rate-pressure-cumulative production history plot — flowrate (q_g) and calculated bottomhole pressure (p_{wf}) versus cumulative production (G_p).

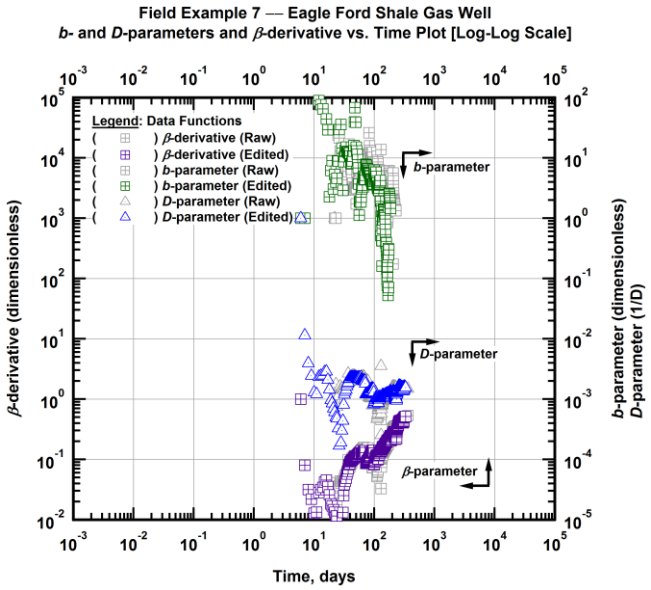

Figure A.187 — (Log-Log Plot): Filtered b, D and β production history plot — b- and D-parameters and β-derivative versus production time.

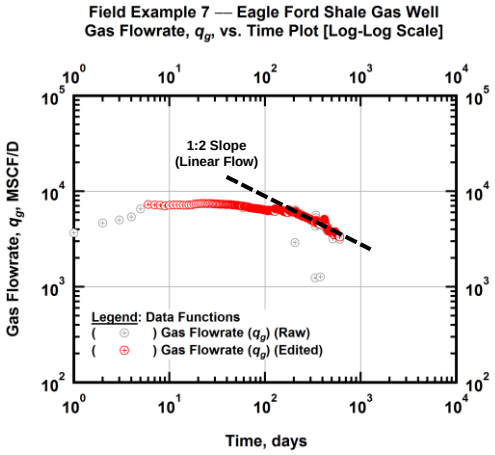

Figure A.188 — (Log-Log Plot): Filtered gas flowrate production history and flow regime identification plot — gas flowrate (q_g) versus production time.

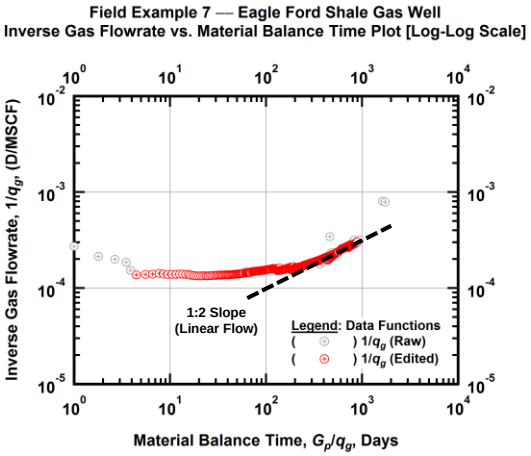

Figure A.189 — (Log-log Plot): Filtered inverse rate with material balance time plot — inverse gas flowrate ($1/q_g$) versus material balance time (G_p/q_g).

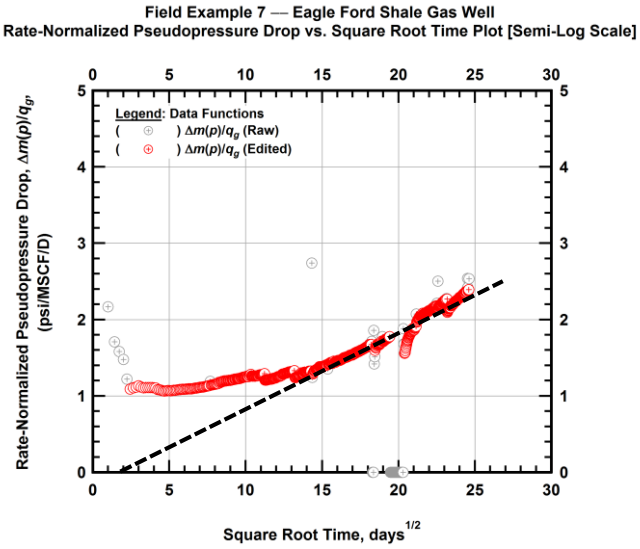

Figure A.190 — (Semi-log Plot): Filtered normalized pseudopressure drop production history plot — rate-normalized pseudopressure drop ($\Delta m(p)/q_g$) versus square root production time ($\sqrt{t}$).

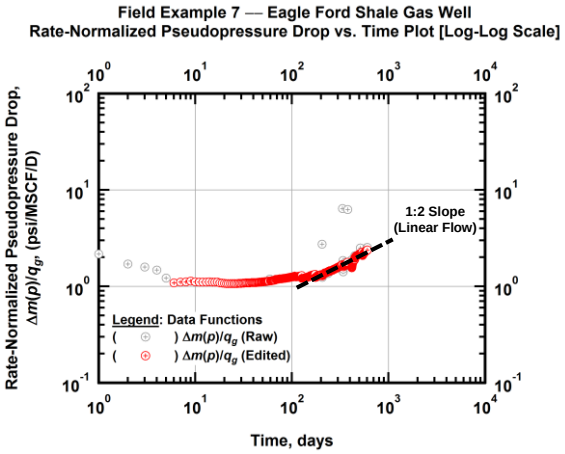

Figure A.191 — (Log-log Plot): Filtered normalized pseudopressure drop production history plot — rate-normalized pseudopressure drop ($\Delta m(p)/q_g$) versus production time.

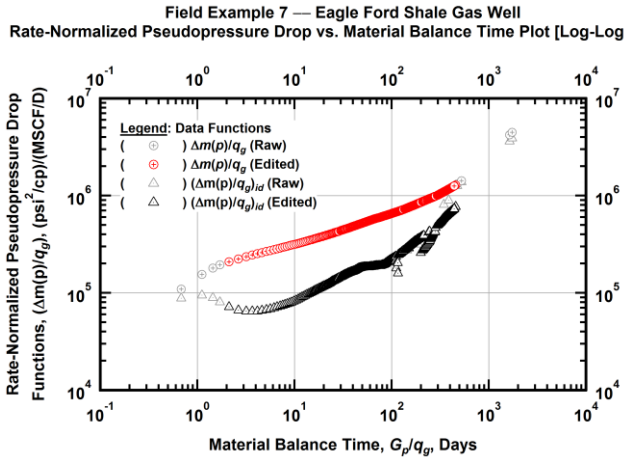

Figure A.192 — (Log-log Plot): "Log-log" diagnostic plot of the filtered production data — rate-normalized pseudopressure drop ($\Delta m(p)/q_g$) and rate-normalized pseudopressure drop integral-derivative $(\Delta m(p)/q_g)_{id}$ versus material balance time (G_p/q_g).

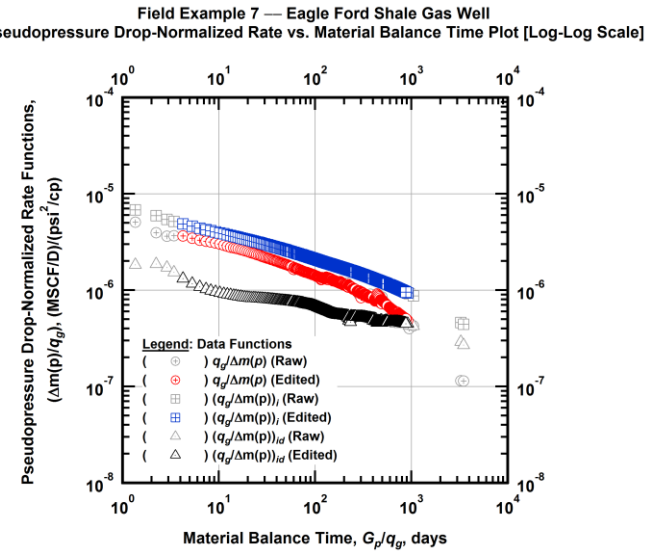

Figure A.193 — (Log-log Plot): "Blasingame" diagnostic plot of the filtered production data — pseudopressure drop-normalized gas flowrate ($q_g/\Delta m(p)$), pseudopressure drop-normalized gas flowrate integral $(q_g/\Delta m(p))_i$ and pseudopressure drop-normalized gas flowrate integral-derivative $(q_g/\Delta m(p))_{id}$ versus material balance time (G_p/q_g).

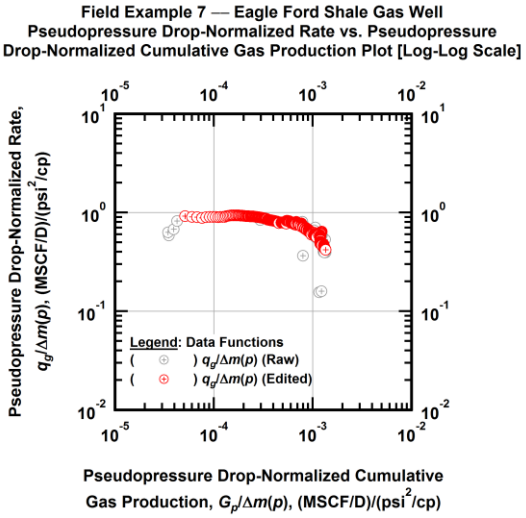

Figure A.194 — (Log-log Plot): Filtered normalized rate with normalized cumulative production plot — pseudopressure drop-normalized gas flowrate ($q_g/\Delta m(p)$) versus pseudopressure drop-normalized cumulative gas production ($G_p/\Delta m(p)$).

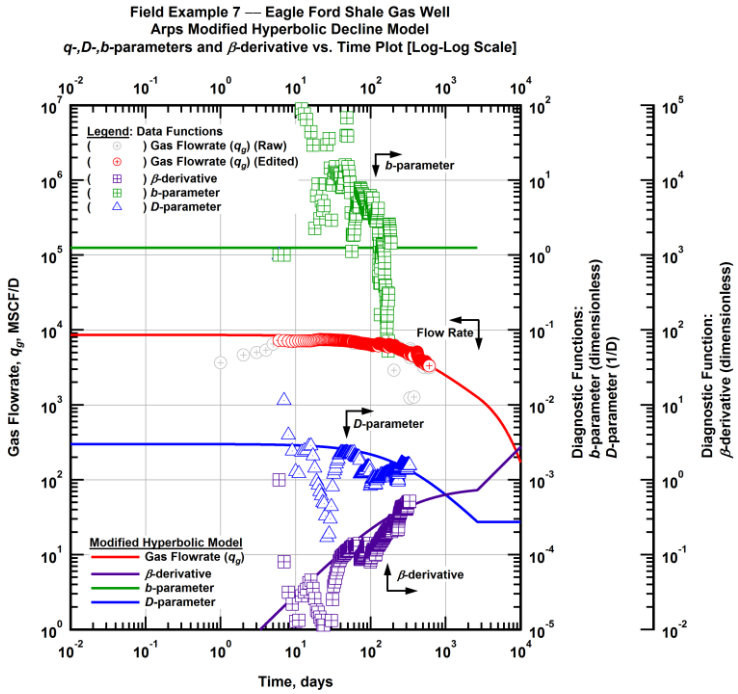

Figure A.195 — (Log-Log Plot): Arps modified hyperbolic decline model plot — time-rate model and data gas flowrate (q_g), *D*- and *b*-parameters and β-derivative versus production time.

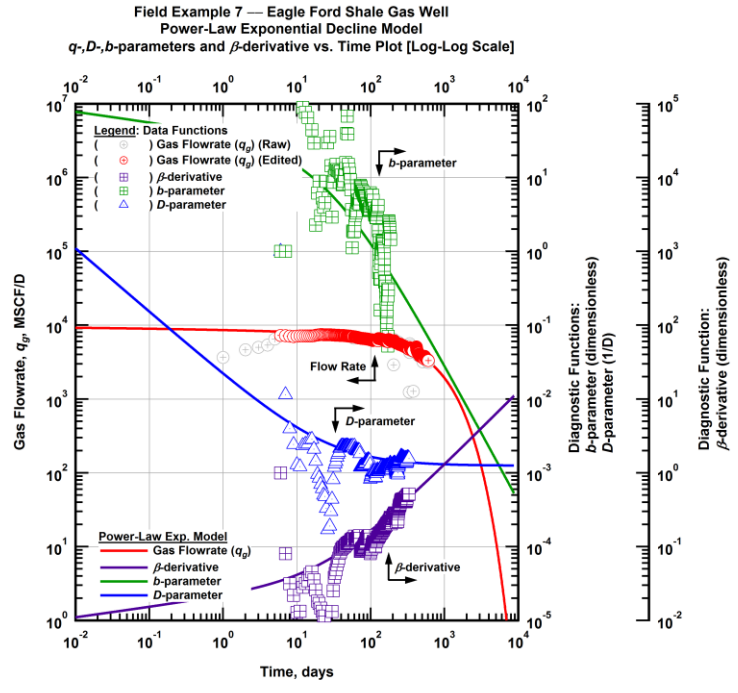

Figure A.196 — (Log-Log Plot): Power-law exponential decline model plot — time-rate model and data gas flowrate (q_g), *D*- and *b*-parameters and β-derivative versus production time.

Field Example 7 — Model-Based (Time-Rate-Pressure) Production Analysis

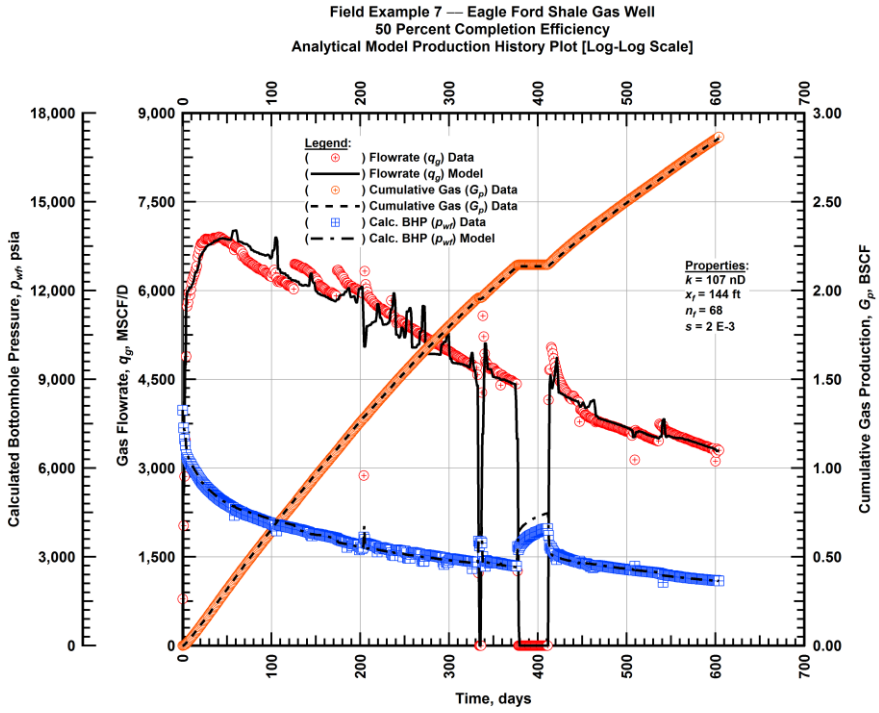

Figure A.197 — (Cartesian Plot): Production history plot — original gas flowrate (q_g), cumulative gas production (G_p), calculated bottomhole pressure (p_{wf}) and 50 percent completion efficiency model matches versus production time.

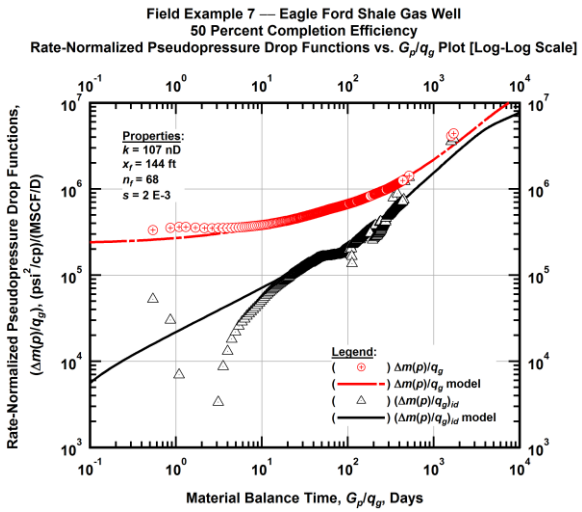

Figure A.198 — (Log-log Plot): "Log-log" diagnostic plot of the original production data — rate-normalized pseudopressure drop ($\Delta m(p)/q_g$), rate-normalized pseudopressure drop integral-derivative $(\Delta m(p)/q_g)_{id}$ and 50 percent completion efficiency model matches versus material balance time (G_p/q_g).

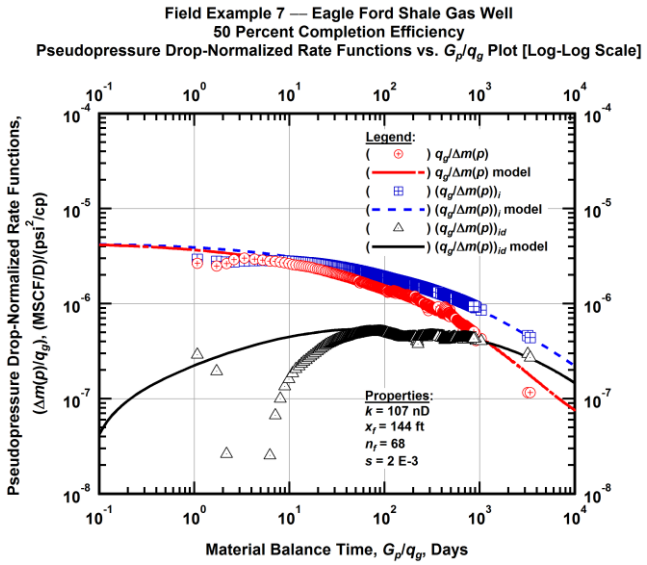

Figure A.199 — (Log-log Plot): "Blasingame" diagnostic plot of the original production data — pseudopressure drop-normalized gas flowrate ($q_g/\Delta m(p)$), pseudopressure drop-normalized gas flowrate integral $(q_g/\Delta m(p))_i$, pseudopressure drop-normalized gas flowrate integral-derivative $(q_g/\Delta m(p))_{id}$ and 50 percent completion efficiency model matches versus material balance time (G_p/q_g).

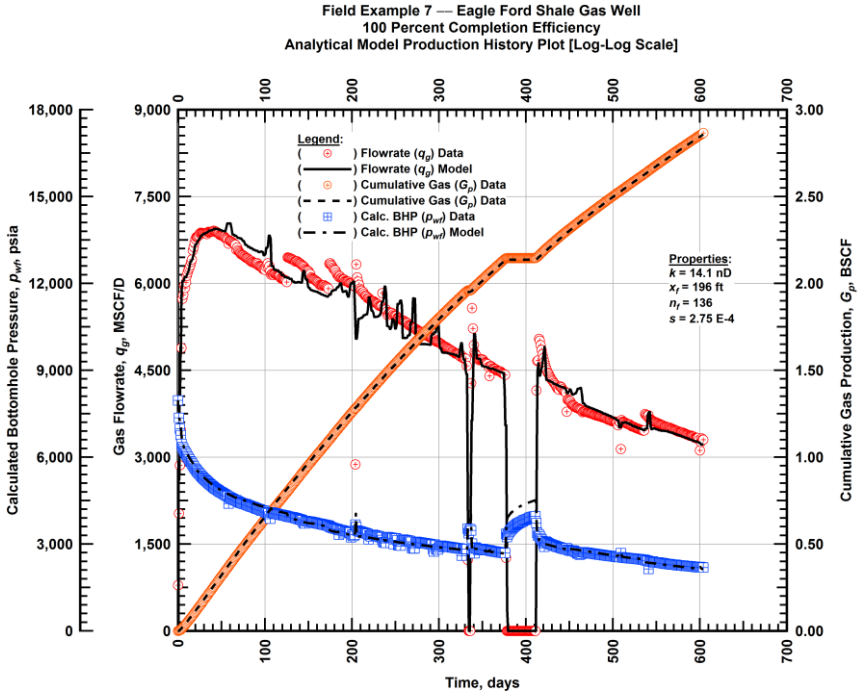

Figure A.200 — (Cartesian Plot): Production history plot — original gas flowrate (q_g), cumulative gas production (G_p), calculated bottomhole pressure (p_{wf}) and 100 percent completion efficiency model matches versus production time.

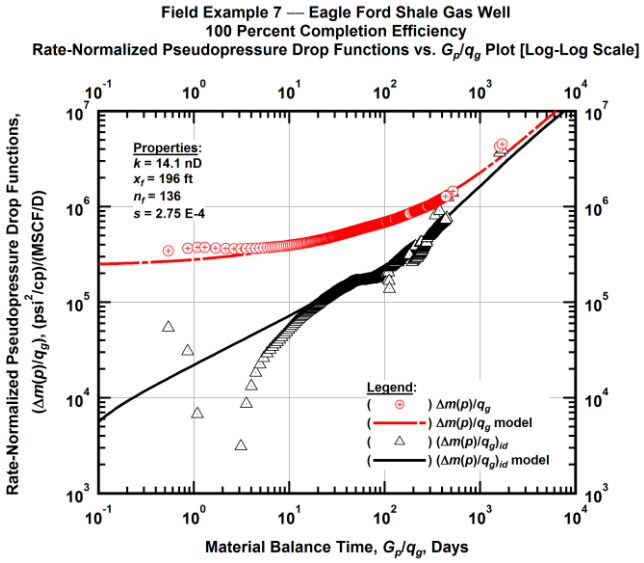

Figure A.201 — (Log-log Plot): "Log-log" diagnostic plot of the original production data — rate-normalized pseudopressure drop ($\Delta m(p)/q_g$), rate-normalized pseudopressure drop integral-derivative $(\Delta m(p)/q_g)_{id}$ and 100 percent completion efficiency model matches versus material balance time (G_p/q_g).

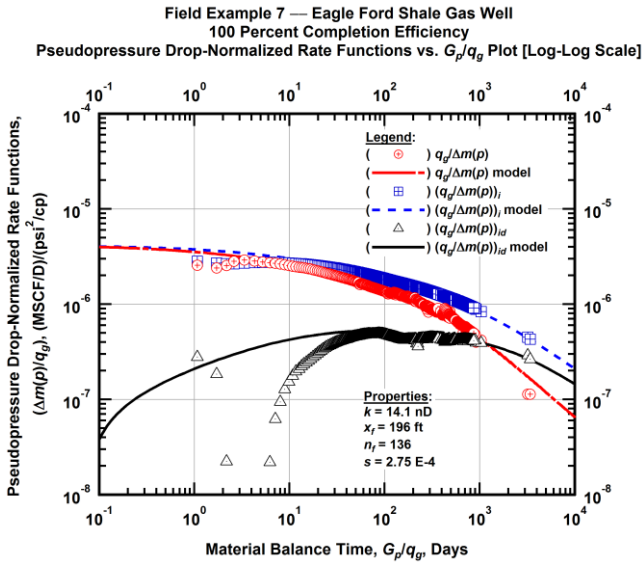

Figure A.202 — (Log-log Plot): "Blasingame" diagnostic plot of the original production data — pseudopressure drop-normalized gas flowrate ($q_g/\Delta m(p)$), pseudopressure drop-normalized gas flowrate integral $(q_g/\Delta m(p))_i$, pseudopressure drop-normalized gas flowrate integral-derivative $(q_g/\Delta m(p))_{id}$ and 100 percent completion efficiency model matches versus material balance time (G_p/q_g).

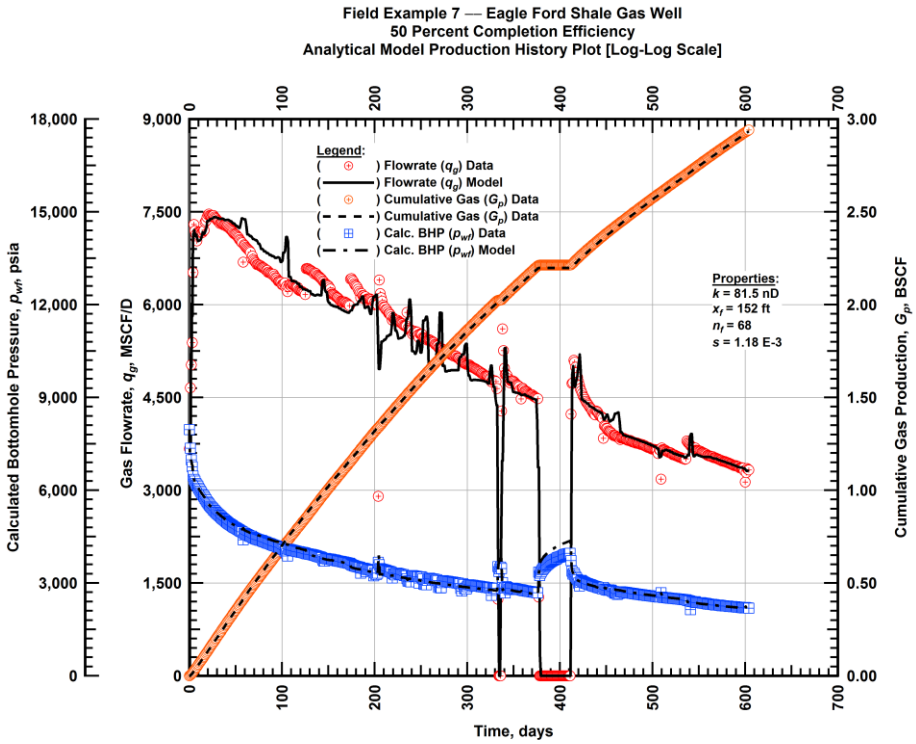

Figure A.203 — (Cartesian Plot): Production history plot — revised gas flowrate (q_g), cumulative gas production (G_p), calculated bottomhole pressure (p_{wf}) and 50 percent completion efficiency model matches versus production time.

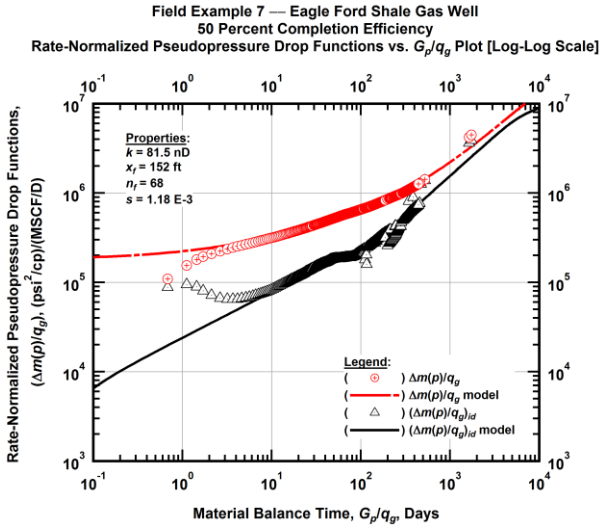

Figure A.204 — (Log-log Plot): "Log-log" diagnostic plot of the revised production data — rate-normalized pseudopressure drop ($\Delta m(p)/q_g$), rate-normalized pseudopressure drop integral-derivative $(\Delta m(p)/q_g)_{id}$ and 50 percent completion efficiency model matches versus material balance time (G_p/q_g).

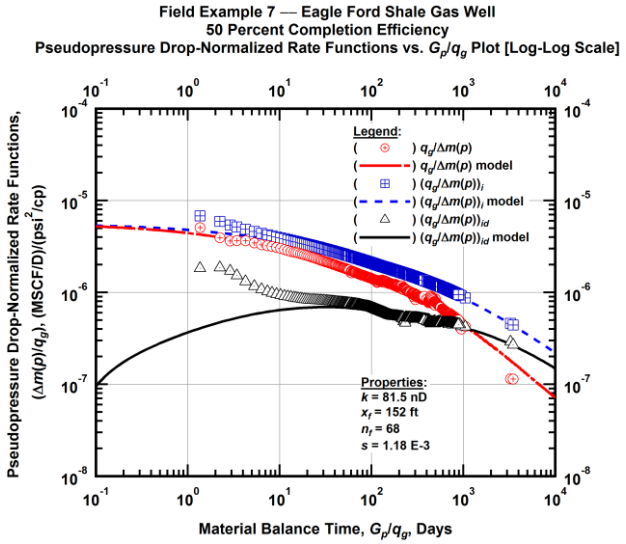

Figure A.205 — (Log-log Plot): "Blasingame" diagnostic plot of the revised production data — pseudopressure drop-normalized gas flowrate ($q_g/\Delta m(p)$), pseudopressure drop-normalized gas flowrate integral $(q_g/\Delta m(p))_i$, pseudopressure drop-normalized gas flowrate integral-derivative $(q_g/\Delta m(p))_{id}$ and 50 percent completion efficiency model matches versus material balance time (G_p/q_g).

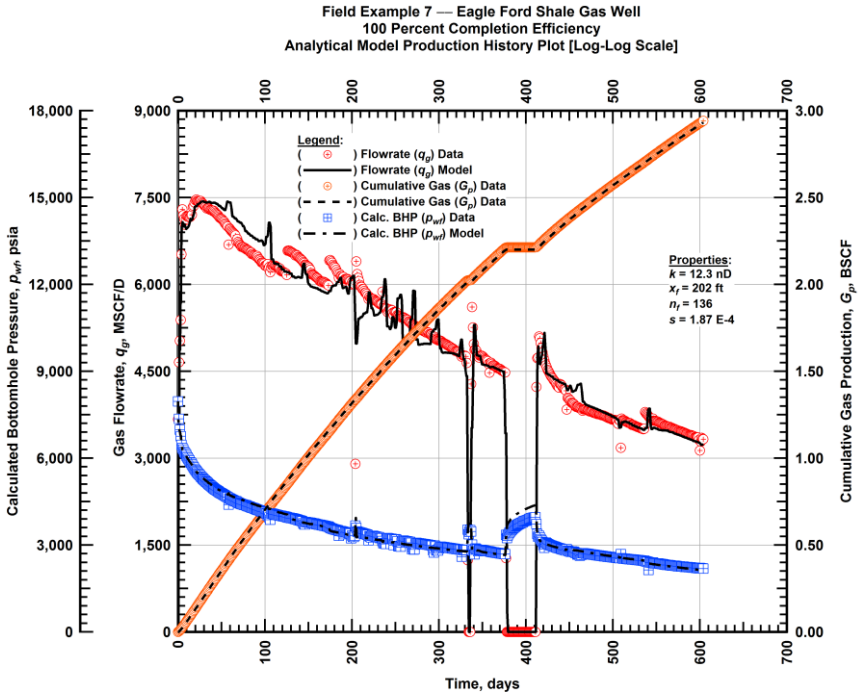

Figure A.206 — (Cartesian Plot): Production history plot — revised gas flowrate (q_g), cumulative gas production (G_p), calculated bottomhole pressure (p_{wf}) and 100 percent completion efficiency model matches versus production time.

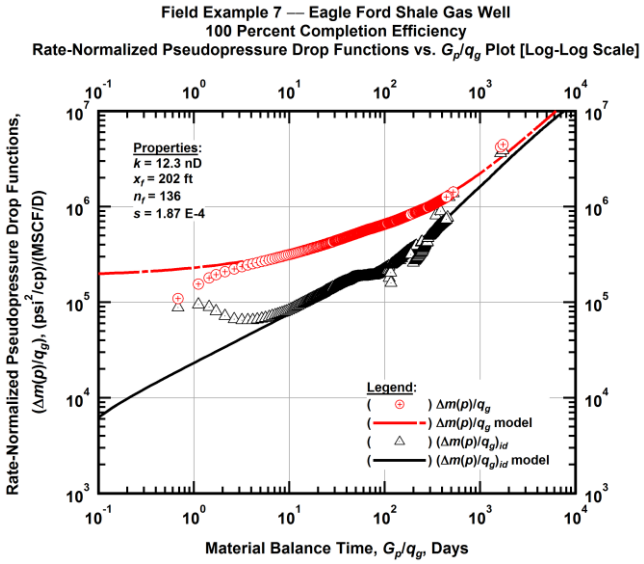

Figure A.207 — (Log-log Plot): "Log-log" diagnostic plot of the revised production data — rate-normalized pseudopressure drop ($\Delta m(p)/q_g$), rate-normalized pseudopressure drop integral-derivative $(\Delta m(p)/q_g)_{id}$ and 100 percent completion efficiency model matches versus material balance time (G_p/q_g).

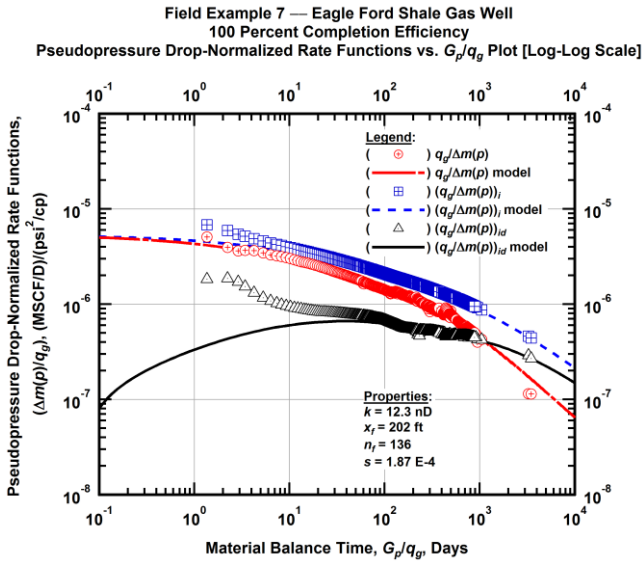

Figure A.208 — (Log-log Plot): "Blasingame" diagnostic plot of the revised production data — pseudopressure drop-normalized gas flowrate ($q_g/\Delta m(p)$), pseudopressure drop-normalized gas flowrate integral $(q_g/\Delta m(p))_i$, pseudopressure drop-normalized gas flowrate integral-derivative $(q_g/\Delta m(p))_{id}$ and 100 percent completion efficiency model matches versus material balance time (G_p/q_g).

Field Example 7 — 30-Year EUR Model Comparison

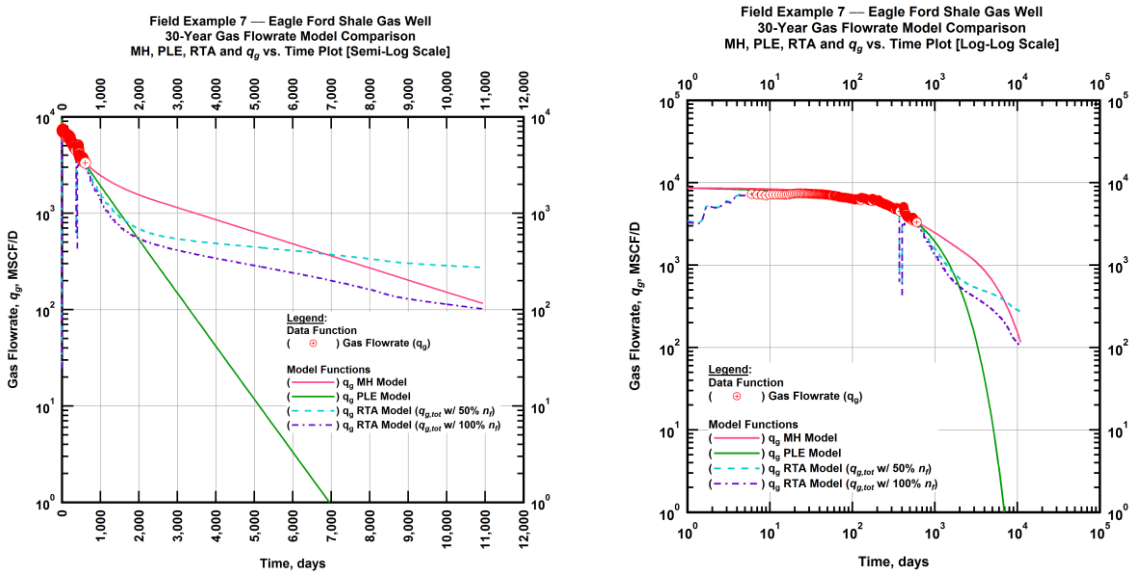

A **B**

Figure A.209 — (A — Semi-Log Plot) and (B — Log-Log Plot): Revised gas 30-year estimated flowrate model comparison — Arps modified hyperbolic decline model, power-law exponential decline model, and 50 percent and 100 percent completion efficiency RTA models revised gas 30-year estimated flowrate decline and historic gas flowrate data (q_g) versus production time.

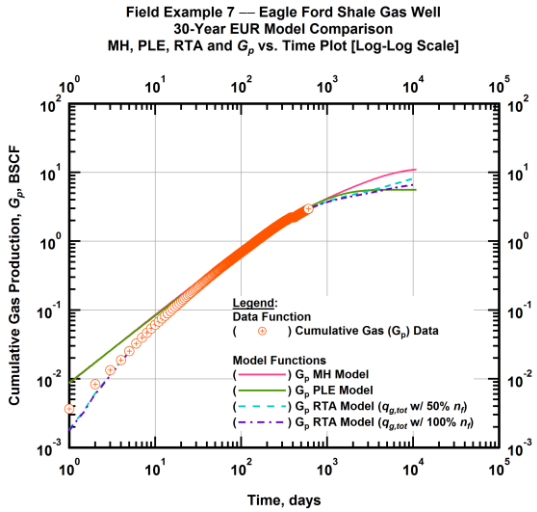

Figure A.210 — (Log-log Plot): Estimated 30-year cumulative gas production volume model comparison — Arps modified hyperbolic decline model, power-law exponential decline model, and 50 percent and 100 percent completion efficiency RTA models estimated 30-year cumulative gas production volumes and historic cumulative gas production (G_p) versus production time.

Table A.7 — 30-year estimated cumulative revised gas production (EUR), in units of BSCF, for the Arps modified hyperbolic, power-law exponential and analytical time-rate-pressure decline models.

Arps Modified Hyperbolic BSCF)	Power-Law Exponential (BSCF)	RTA Analytical Model ($q_{g,tot}$ w/ 50% n_f) (BSCF)	RTA Analytical Model ($q_{g,tot}$ w/ 100% n_f) (BSCF)
11.12	5.43	8.54	6.76

Field Example 8 — Time-Rate Analysis

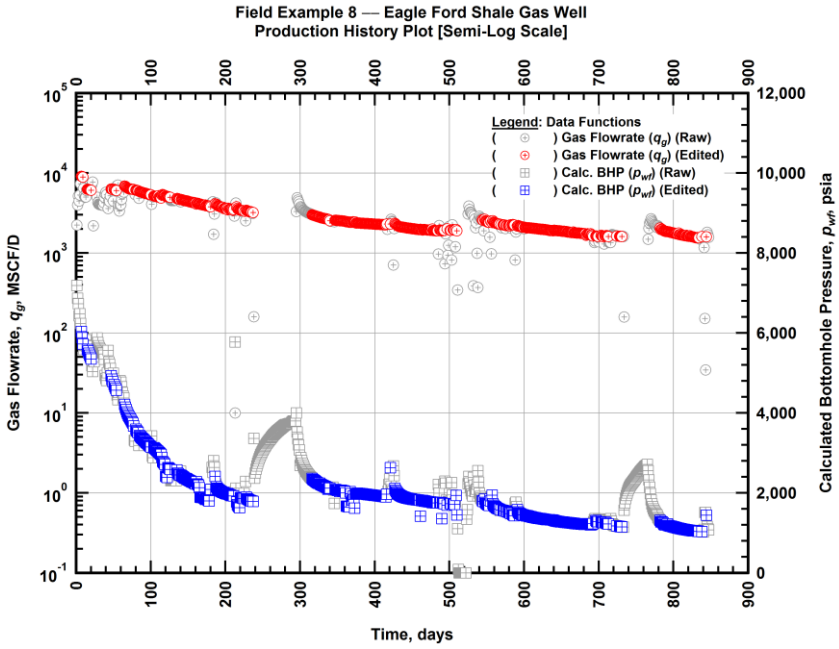

Figure A.211 — (Semi-log Plot): Filtered production history plot — flowrate (q_g) and calculated bottomhole pressure (p_{wf}) versus production time.

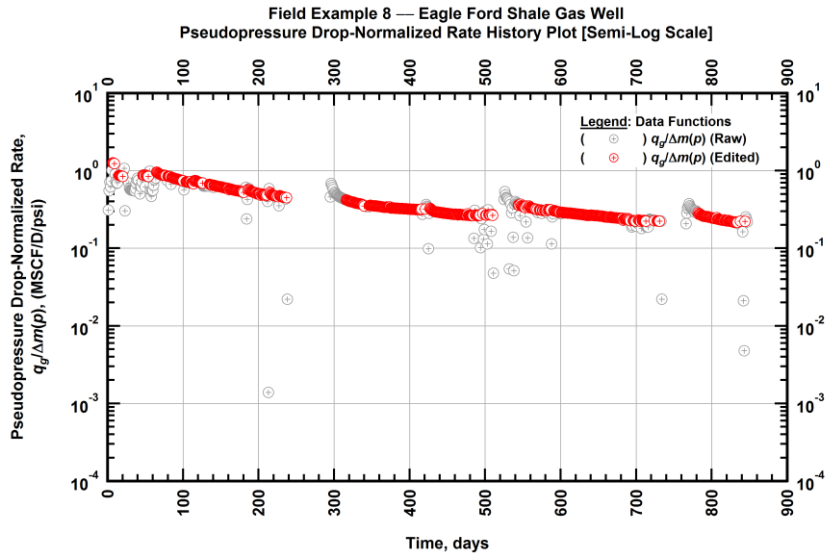

Figure A.212 — (Semi-log Plot): Filtered normalized rate production history plot — pseudopressure drop-normalized gas flowrate ($q_g/\Delta m(p)$) versus production time.

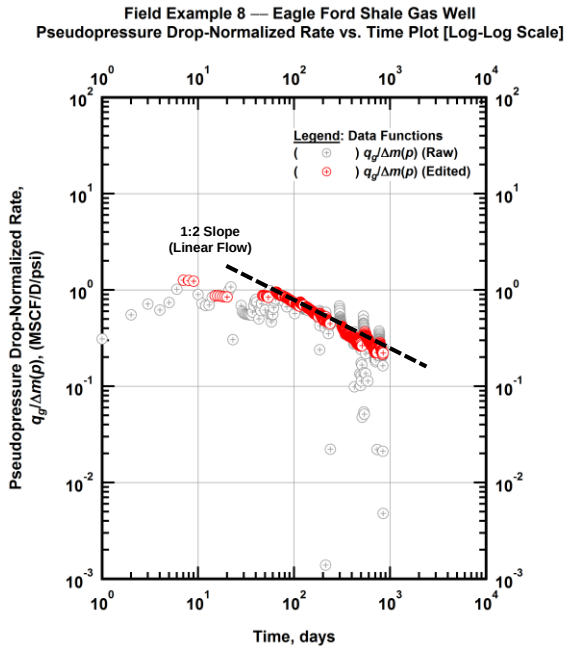

Figure A.213 — (Log-log Plot): Filtered normalized rate production history plot — pseudopressure drop-normalized gas flowrate ($q_g/\Delta m(p)$) versus production time.

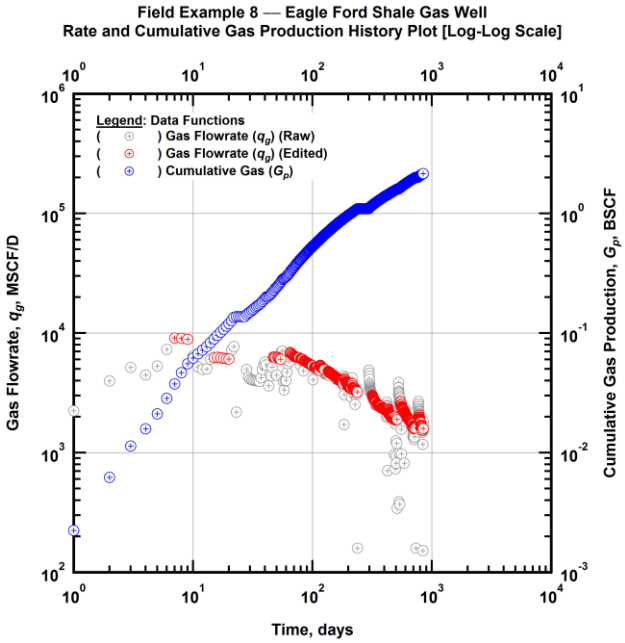

Figure A.214 — (Log-log Plot): Filtered rate and unfiltered cumulative gas production history plot — flowrate (q_g) and cumulative production (G_p) versus production time.

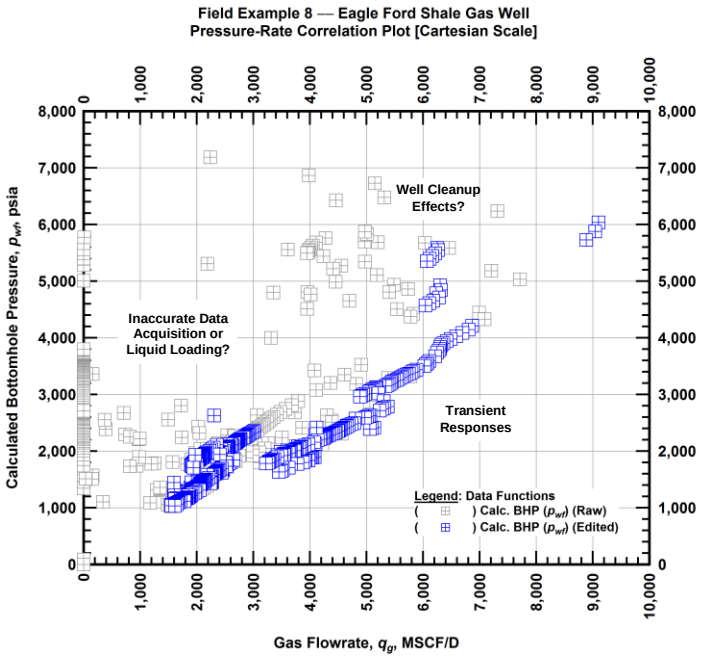

Figure A.215 — (Cartesian Plot): Filtered rate-pressure correlation plot — calculated bottomhole pressure (p_{wf}) versus flowrate (q_g).

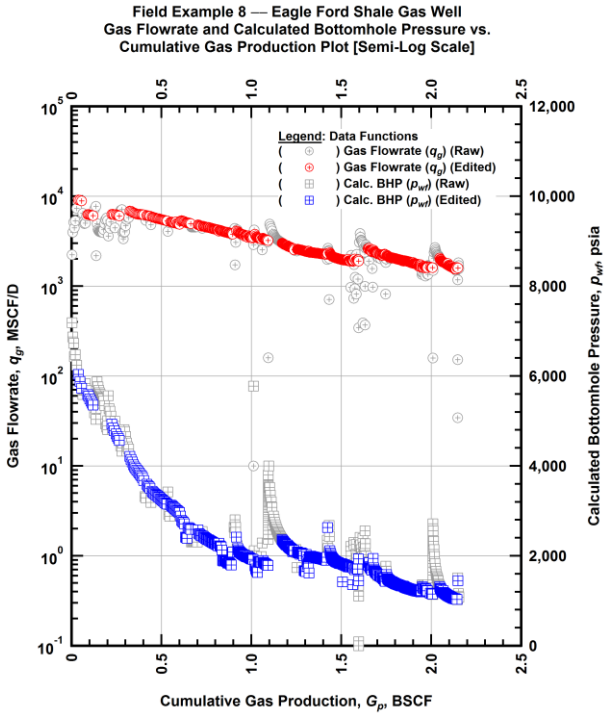

Figure A.216 — (Semi-log Plot): Filtered rate-pressure-cumulative production history plot — flowrate (q_g) and calculated bottomhole pressure (p_{wf}) versus cumulative production (G_p).

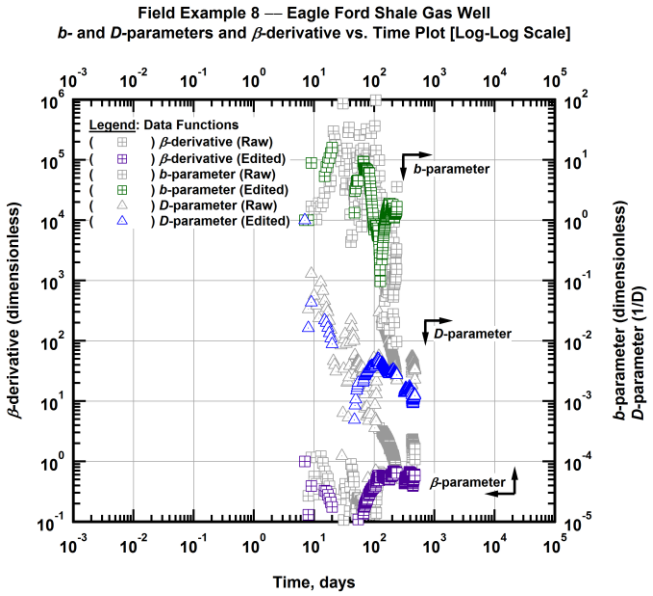

Figure A.217 — (Log-Log Plot): Filtered b, D and β production history plot — b- and D-parameters and β-derivative versus production time.

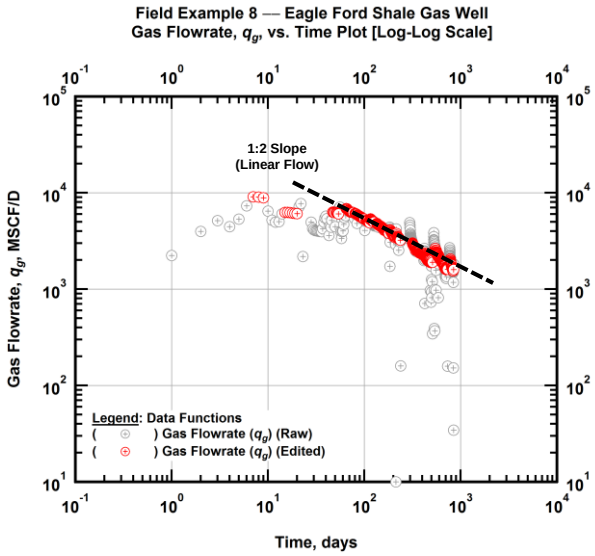

Figure A.218 — (Log-Log Plot): Filtered gas flowrate production history and flow regime identification plot — gas flowrate (q_g) versus production time.

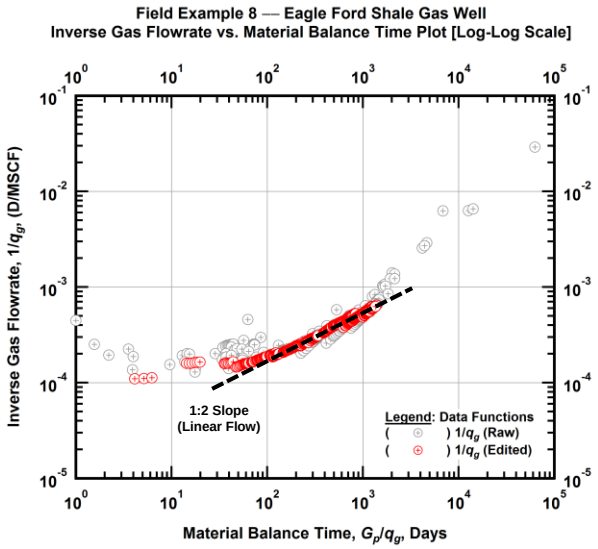

Figure A.219 — (Log-log Plot): Filtered inverse rate with material balance time plot — inverse gas flowrate ($1/q_g$) versus material balance time (G_p/q_g).

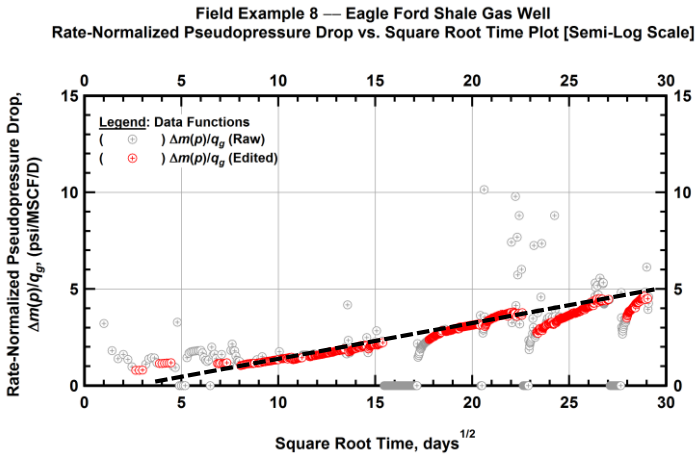

Figure A.220 — (Semi-log Plot): Filtered normalized pseudopressure drop production history plot — rate-normalized pseudopressure drop ($\Delta m(p)/q_g$) versus square root production time ($\sqrt{t}$).

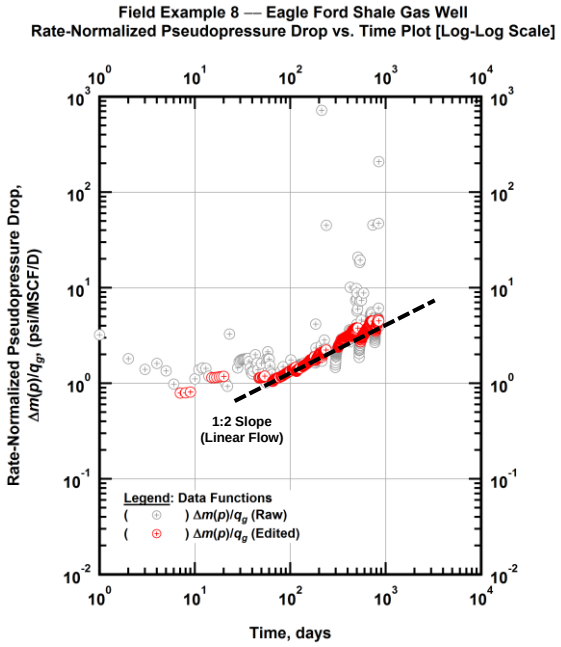

Figure A.221 — (Log-log Plot): Filtered normalized pseudopressure drop production history plot — rate-normalized pseudopressure drop ($\Delta m(p)/q_g$) versus production time.

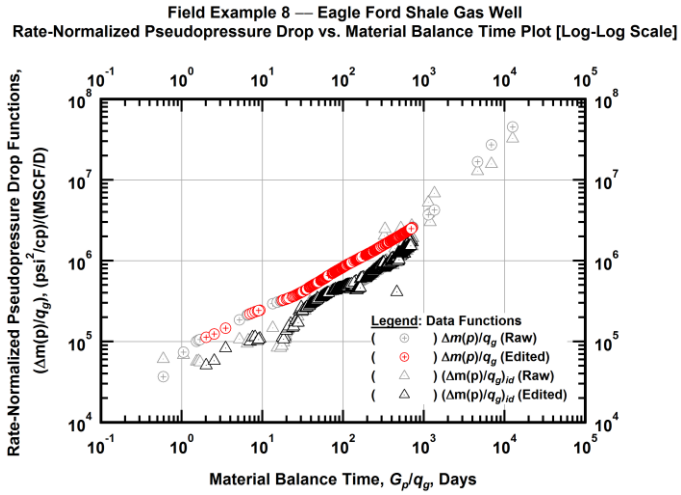

Figure A.222 — (Log-log Plot): "Log-log" diagnostic plot of the filtered production data — rate-normalized pseudopressure drop ($\Delta m(p)/q_g$) and rate-normalized pseudopressure drop integral-derivative $(\Delta m(p)/q_g)_{id}$ versus material balance time (G_p/q_g).

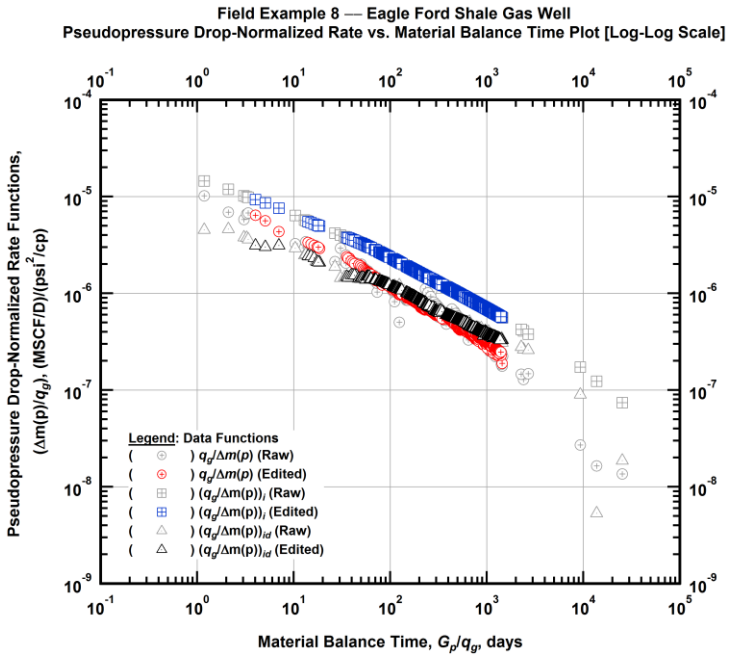

Figure A.223 — (Log-log Plot): "Blasingame" diagnostic plot of the filtered production data — pseudopressure drop-normalized gas flowrate ($q_g/\Delta m(p)$), pseudopressure drop-normalized gas flowrate integral $(q_g/\Delta m(p))_i$ and pseudopressure drop-normalized gas flowrate integral-derivative $(q_g/\Delta m(p))_{id}$ versus material balance time (G_p/q_g).

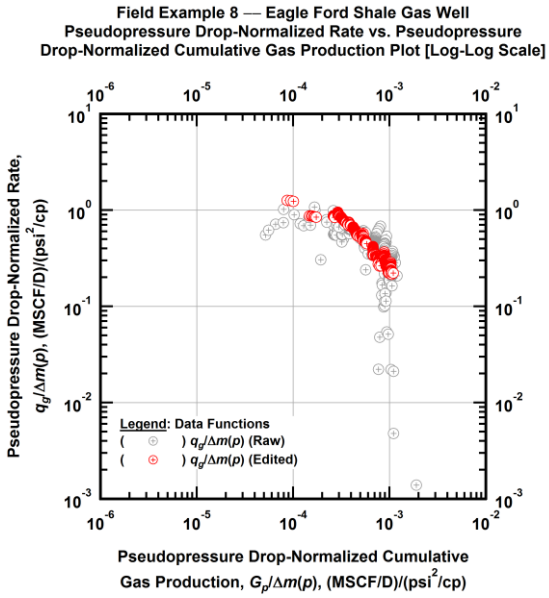

Figure A.224 — (Log-log Plot): Filtered normalized rate with normalized cumulative production plot — pseudopressure drop-normalized gas flowrate ($q_g/\Delta m(p)$) versus pseudopressure drop-normalized cumulative gas production ($G_p/\Delta m(p)$).

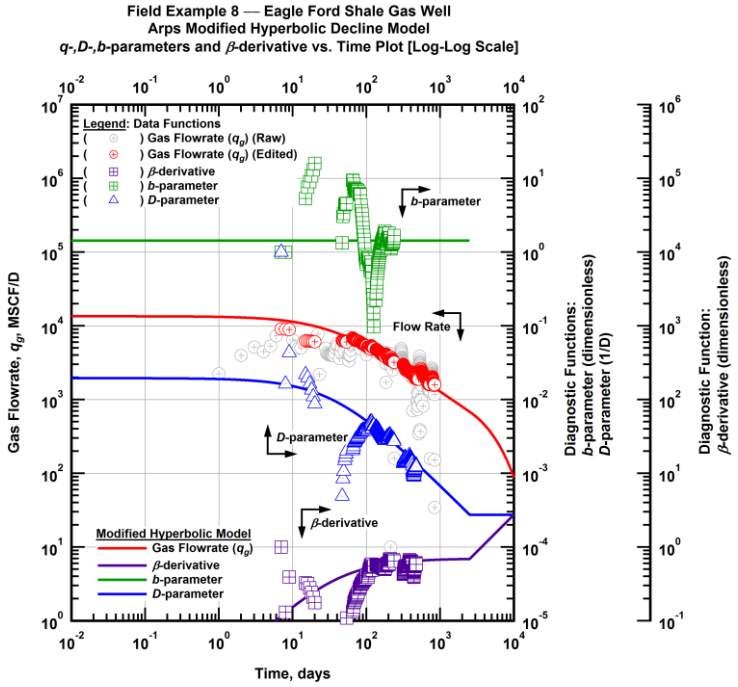

Figure A.225 — (Log-Log Plot): Arps modified hyperbolic decline model plot — time-rate model and data gas flowrate (q_g), *D*- and *b*-parameters and β-derivative versus production time.

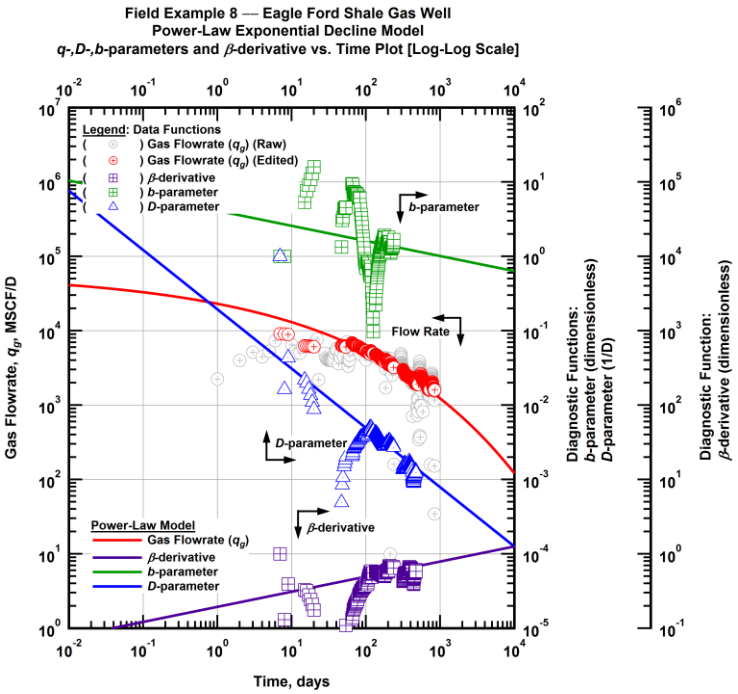

Figure A.226 — (Log-Log Plot): Power-law exponential decline model plot — time-rate model and data gas flowrate (q_g), *D*- and *b*-parameters and β-derivative versus production time.

Field Example 8 — Model-Based (Time-Rate-Pressure) Production Analysis

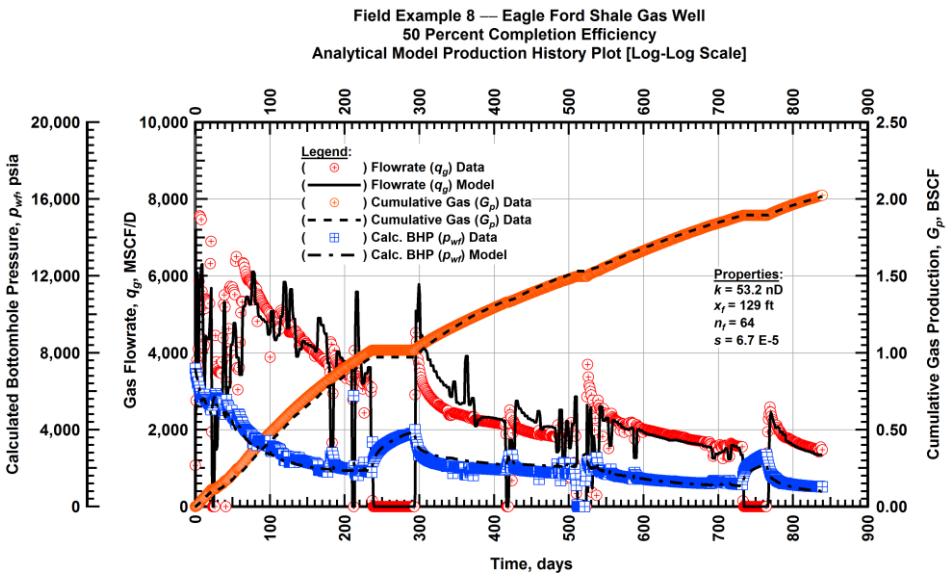

Figure A.227 — (Cartesian Plot): Production history plot — original gas flowrate (q_g), cumulative gas production (G_p), calculated bottomhole pressure (p_{wf}) and 50 percent completion efficiency model matches versus production time.

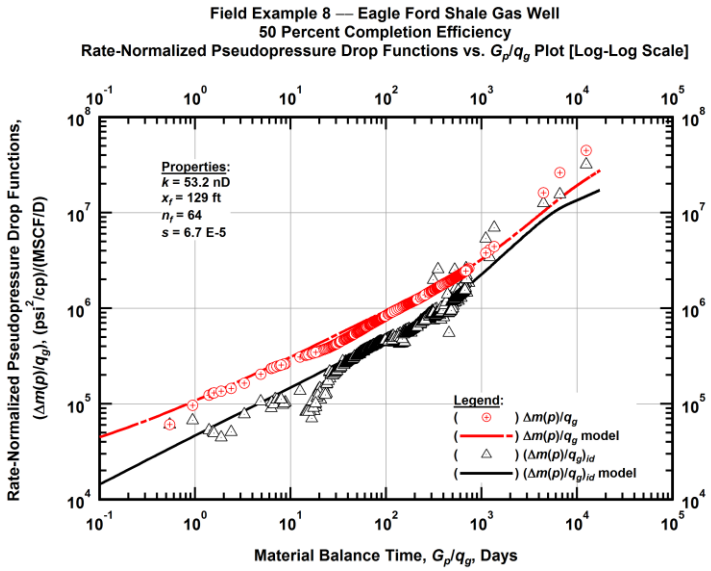

Figure A.228 — (Log-log Plot): "Log-log" diagnostic plot of the original production data — rate-normalized pseudopressure drop ($\Delta m(p)/q_g$), rate-normalized pseudopressure drop integral-derivative $(\Delta m(p)/q_g)_{id}$ and 50 percent completion efficiency model matches versus material balance time (G_p/q_g).

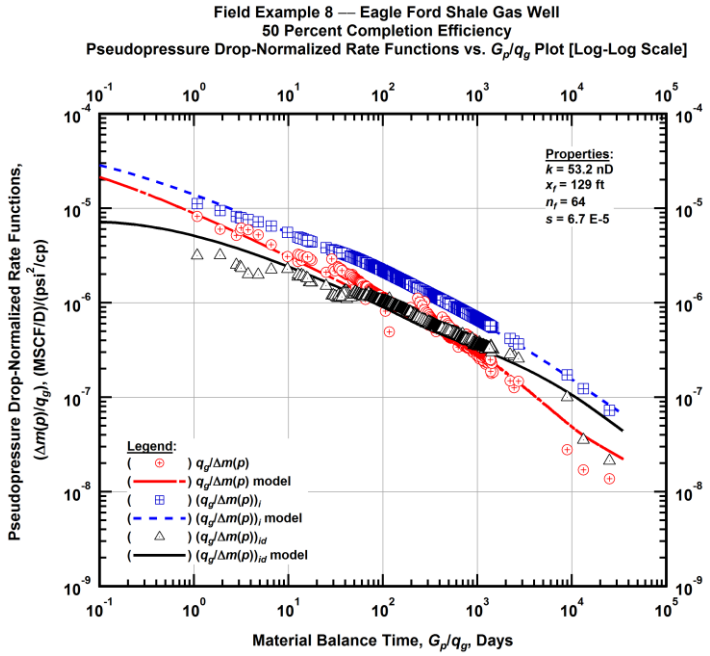

Figure A.229 — (Log-log Plot): "Blasingame" diagnostic plot of the original production data — pseudopressure drop-normalized gas flowrate ($q_g/\Delta m(p)$), pseudopressure drop-normalized gas flowrate integral $(q_g/\Delta m(p))_i$, pseudopressure drop-normalized gas flowrate integral-derivative $(q_g/\Delta m(p))_{id}$ and 50 percent completion efficiency model matches versus material balance time (G_p/q_g).

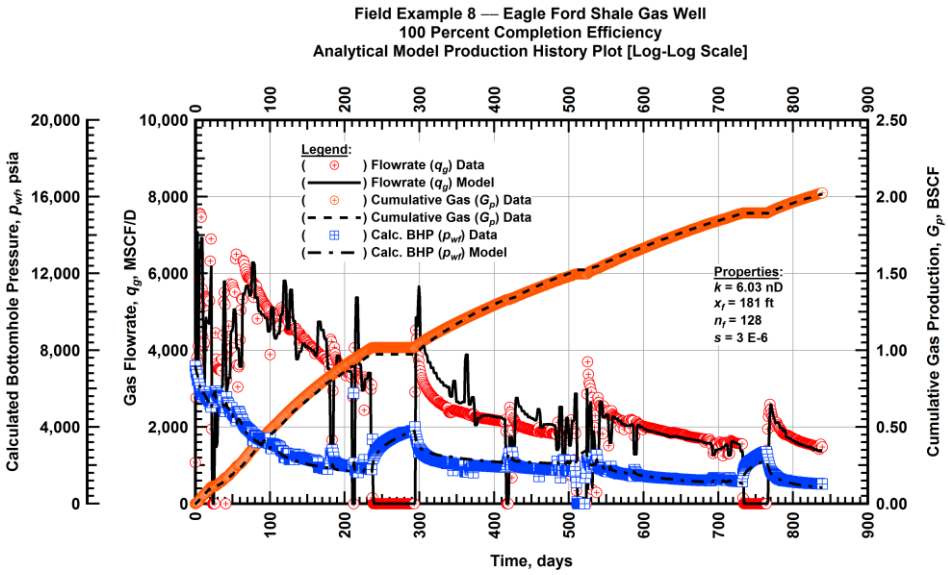

Figure A.230 — (Cartesian Plot): Production history plot — original gas flowrate (q_g), cumulative gas production (G_p), calculated bottomhole pressure (p_{wf}) and 100 percent completion efficiency model matches versus production time.

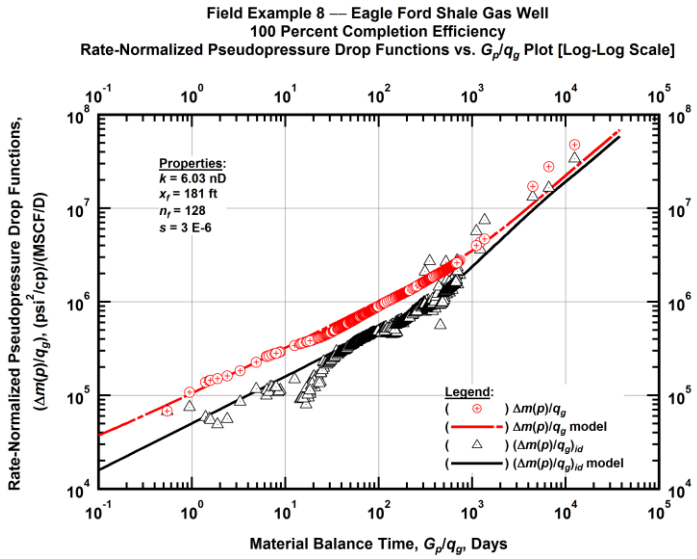

Figure A.231 — (Log-log Plot): "Log-log" diagnostic plot of the original production data — rate-normalized pseudopressure drop ($\Delta m(p)/q_g$), rate-normalized pseudopressure drop integral-derivative $(\Delta m(p)/q_g)_{id}$ and 100 percent completion efficiency model matches versus material balance time (G_p/q_g).

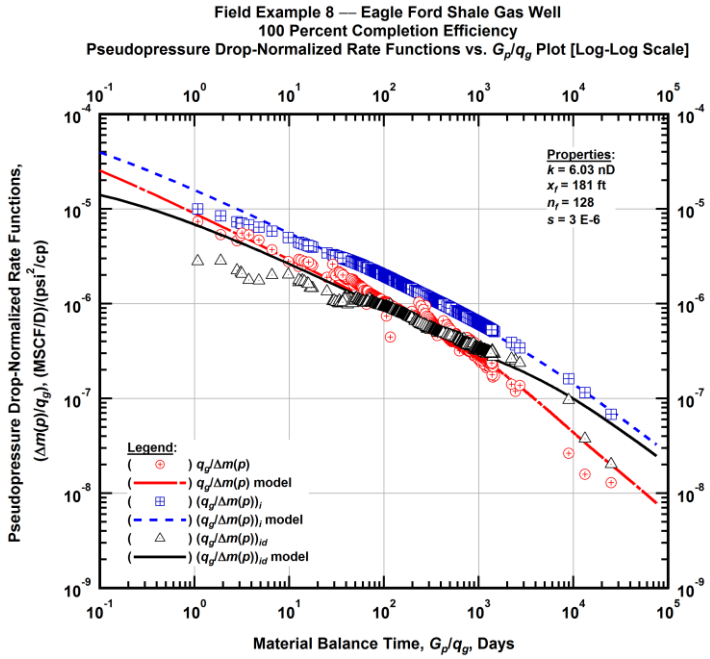

Figure A.232 — (Log-log Plot): "Blasingame" diagnostic plot of the original production data — pseudopressure drop-normalized gas flowrate ($q_g/\Delta m(p)$), pseudopressure drop-normalized gas flowrate integral $(q_g/\Delta m(p))_i$, pseudopressure drop-normalized gas flowrate integral-derivative $(q_g/\Delta m(p))_{id}$ and 100 percent completion efficiency model matches versus material balance time (G_p/q_g).

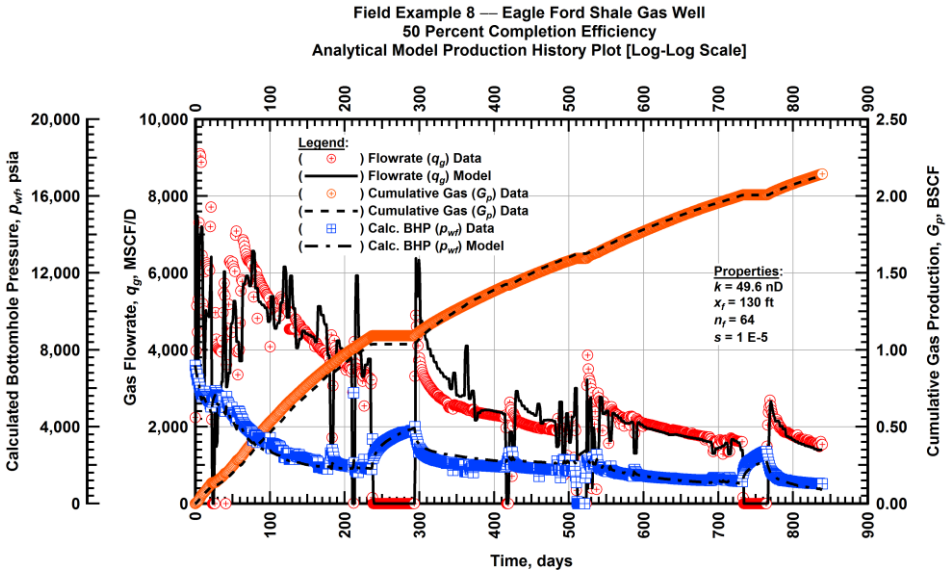

Figure A.233 — (Cartesian Plot): Production history plot — revised gas flowrate (q_g), cumulative gas production (G_p), calculated bottomhole pressure (p_{wf}) and 50 percent completion efficiency model matches versus production time.

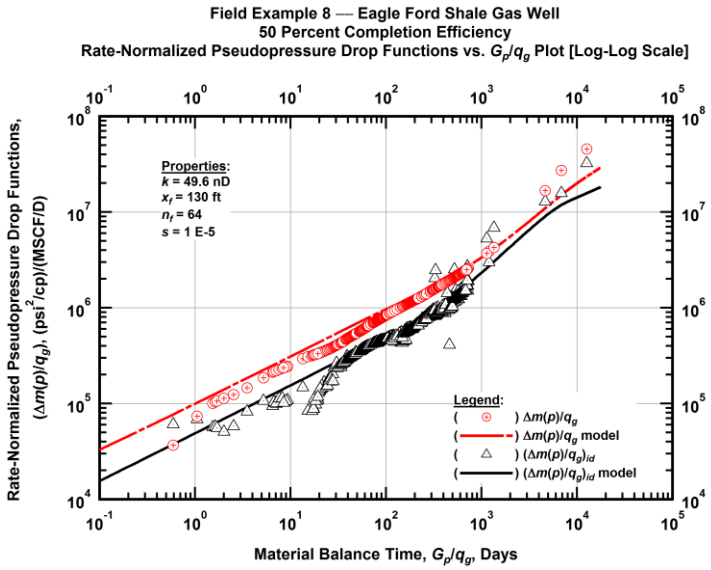

Figure A.234 — (Log-log Plot): "Log-log" diagnostic plot of the revised production data — rate-normalized pseudopressure drop ($\Delta m(p)/q_g$), rate-normalized pseudopressure drop integral-derivative $(\Delta m(p)/q_g)_{id}$ and 50 percent completion efficiency model matches versus material balance time (G_p/q_g).

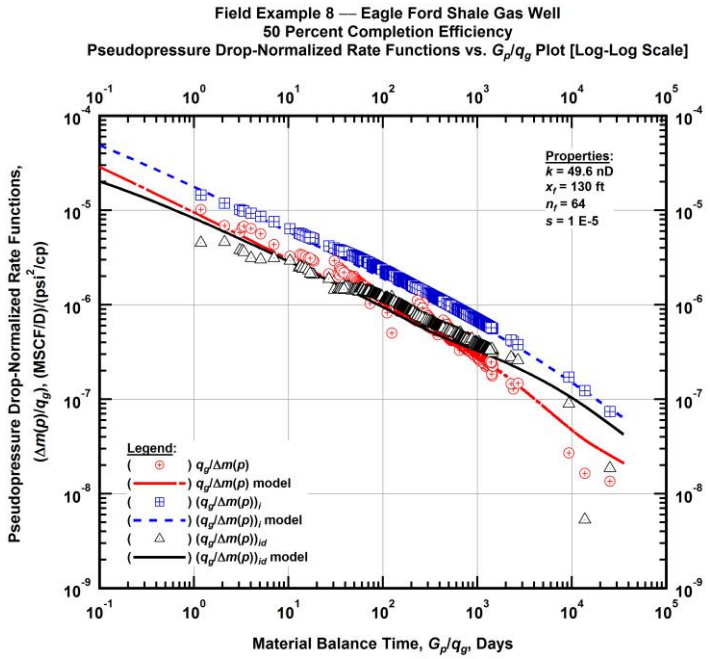

Figure A.235 — (Log-log Plot): "Blasingame" diagnostic plot of the revised production data — pseudopressure drop-normalized gas flowrate ($q_g/\Delta m(p)$), pseudopressure drop-normalized gas flowrate integral $(q_g/\Delta m(p))_i$, pseudopressure drop-normalized gas flowrate integral-derivative $(q_g/\Delta m(p))_{id}$ and 50 percent completion efficiency model matches versus material balance time (G_p/q_g).

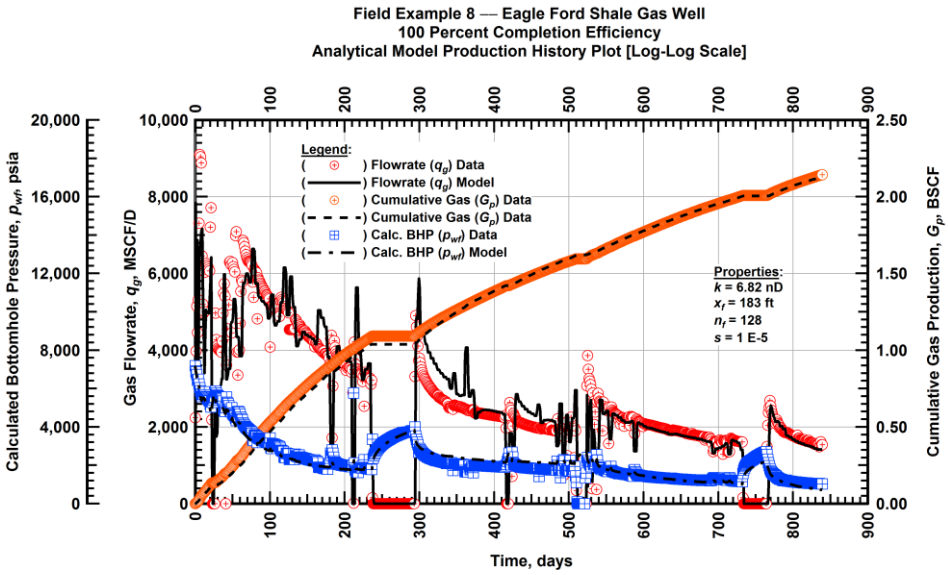

Figure A.236 — (Cartesian Plot): Production history plot — revised gas flowrate (q_g), cumulative gas production (G_p), calculated bottomhole pressure (p_{wf}) and 100 percent completion efficiency model matches versus production time.

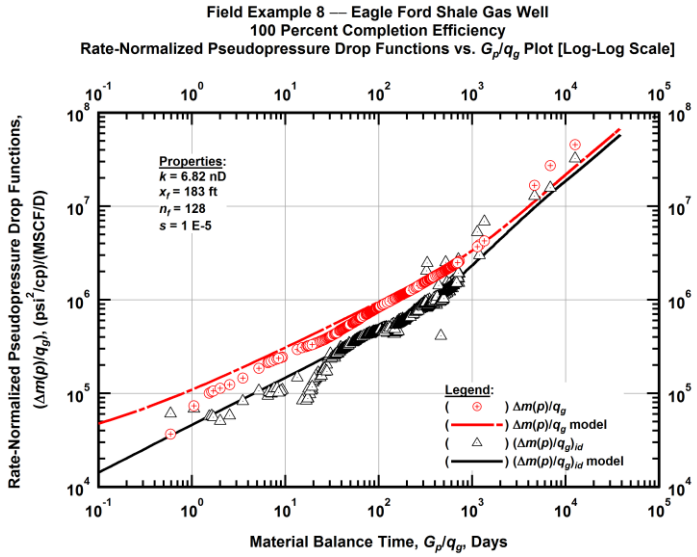

Figure A.237 — (Log-log Plot): "Log-log" diagnostic plot of the revised production data — rate-normalized pseudopressure drop ($\Delta m(p)/q_g$), rate-normalized pseudopressure drop integral-derivative $(\Delta m(p)/q_g)_{id}$ and 100 percent completion efficiency model matches versus material balance time (G_p/q_g).

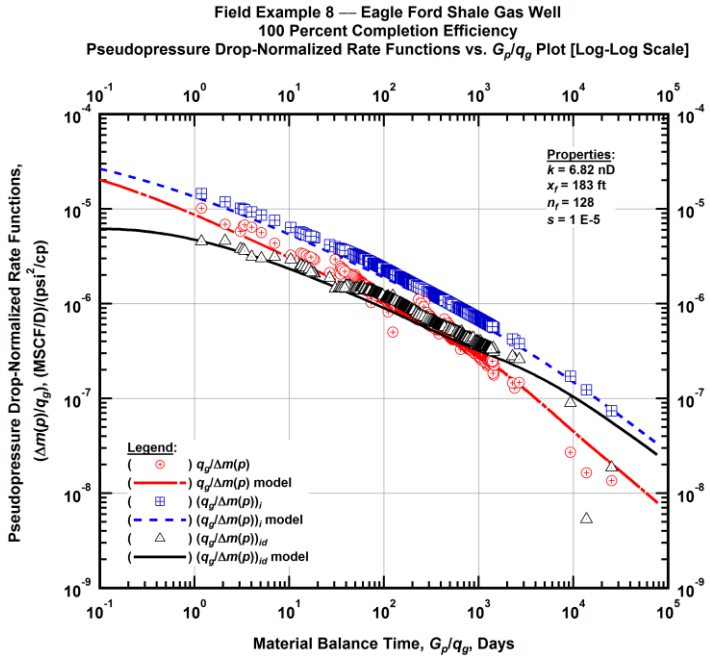

Figure A.238 — (Log-log Plot): "Blasingame" diagnostic plot of the revised production data — pseudopressure drop-normalized gas flowrate ($q_g/\Delta m(p)$), pseudopressure drop-normalized gas flowrate integral $(q_g/\Delta m(p))_i$, pseudopressure drop-normalized gas flowrate integral-derivative $(q_g/\Delta m(p))_{id}$ and 100 percent completion efficiency model matches versus material balance time (G_p/q_g).

Field Example 8 — 30-Year EUR Model Comparison

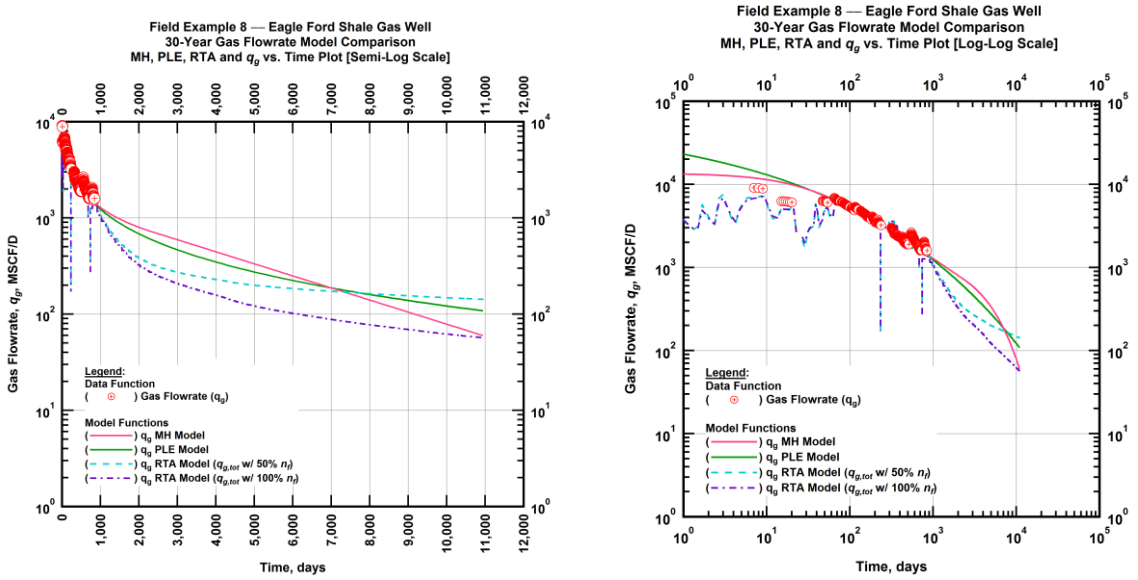

A **B**

Figure A.239 — (A — Semi-Log Plot) and (B — Log-Log Plot): Revised gas 30-year estimated flowrate model comparison — Arps modified hyperbolic decline model, power-law exponential decline model, and 50 percent and 100 percent completion efficiency RTA models revised gas 30-year estimated flowrate decline and historic gas flowrate data (q_g) versus production time.

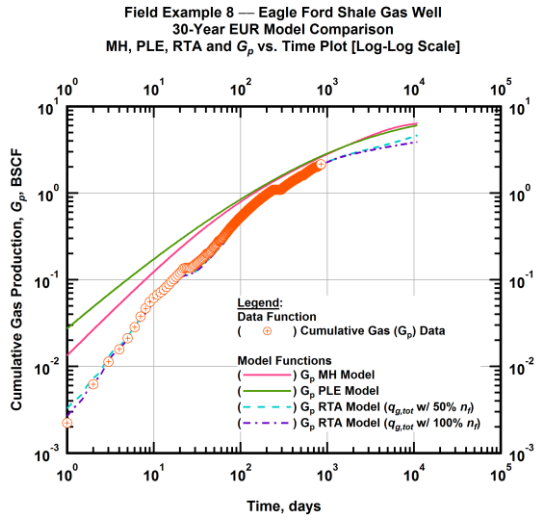

Figure A.240 — (Log-log Plot): Estimated 30-year cumulative gas production volume model comparison — Arps modified hyperbolic decline model, power-law exponential decline model, and 50 percent and 100 percent completion efficiency RTA models estimated 30-year cumulative gas production volumes and historic cumulative gas production (G_p) versus production time.

Table A.8 — 30-year estimated cumulative revised gas production (EUR), in units of BSCF, for the Arps modified hyperbolic, power-law exponential and analytical time-rate-pressure decline models.

Arps Modified Hyperbolic BSCF)	Power-Law Exponential (BSCF)	RTA Analytical Model ($q_{g,tot}$ w/ 50% n_f) (BSCF)	RTA Analytical Model ($q_{g,tot}$ w/ 100% n_f) (BSCF)
6.01	5.61	4.76	3.93

Field Example 9 — Time-Rate Analysis

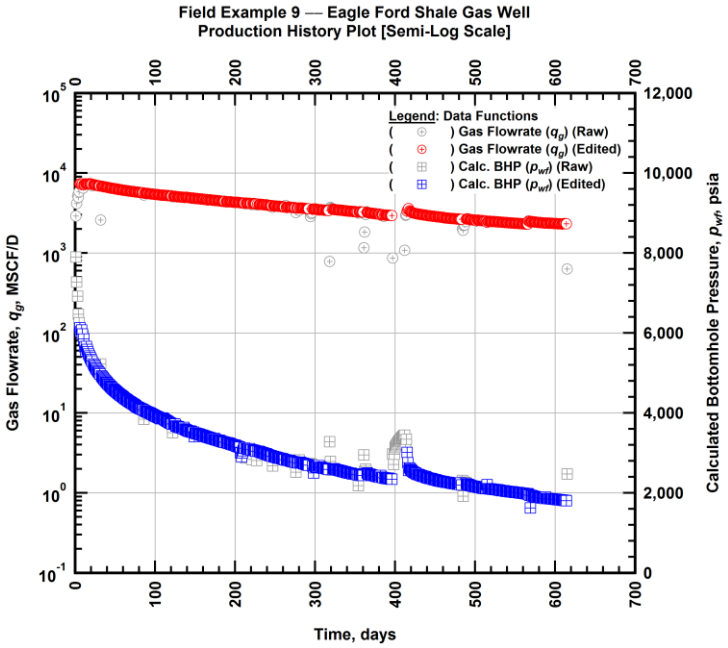

Figure A.241 — (Semi-log Plot): Filtered production history plot — flowrate (q_g) and calculated bottomhole pressure (p_{wf}) versus production time.

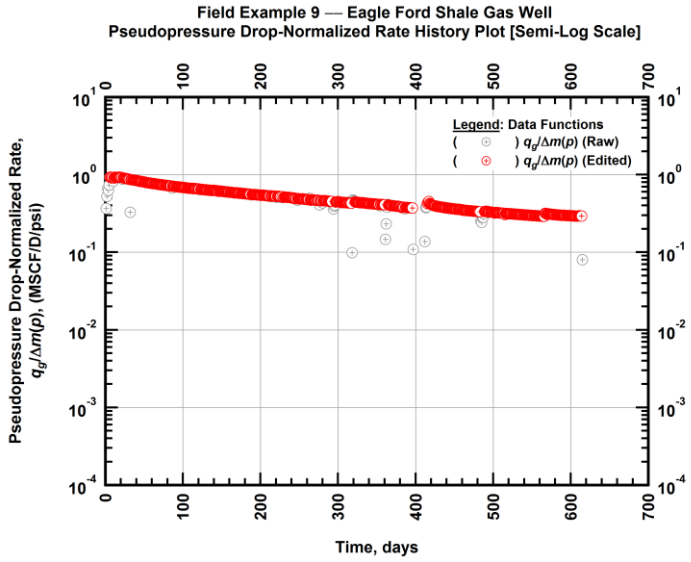

Figure A.242 — (Semi-log Plot): Filtered normalized rate production history plot — pseudopressure drop-normalized gas flowrate ($q_g/\Delta m(p)$) versus production time.

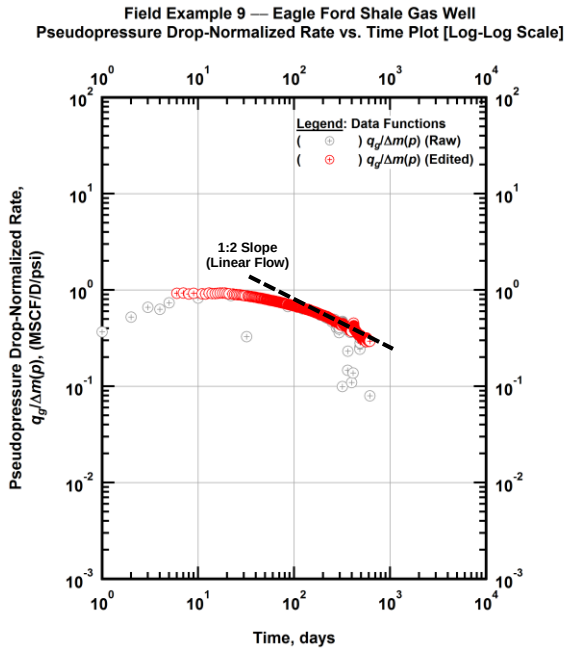

Figure A.243 — (Log-log Plot): Filtered normalized rate production history plot — pseudopressure drop-normalized gas flowrate ($q_g/\Delta m(p)$) versus production time.

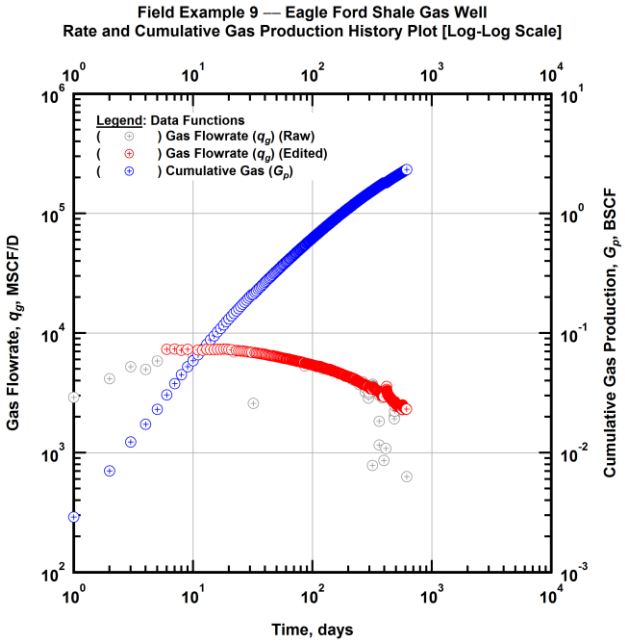

Figure A.244 — (Log-log Plot): Filtered rate and unfiltered cumulative gas production history plot — flowrate (q_g) and cumulative production (G_p) versus production time.

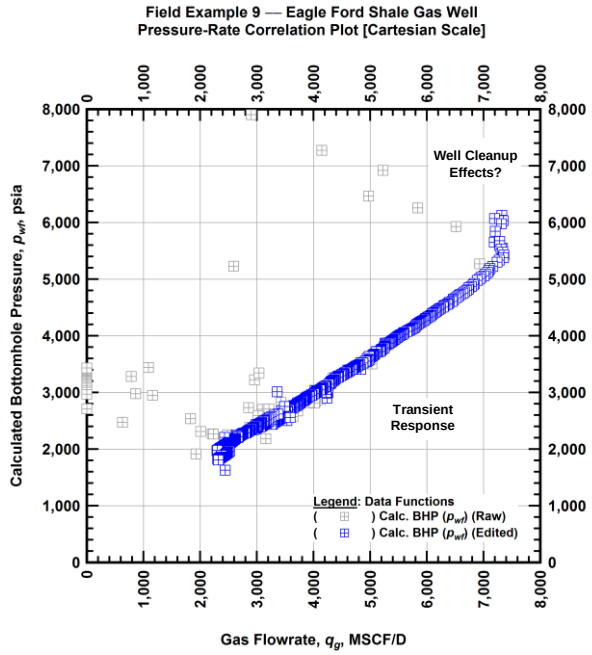

Figure A.245 — (Cartesian Plot): Filtered rate-pressure correlation plot — calculated bottomhole pressure (p_{wf}) versus flowrate (q_g).

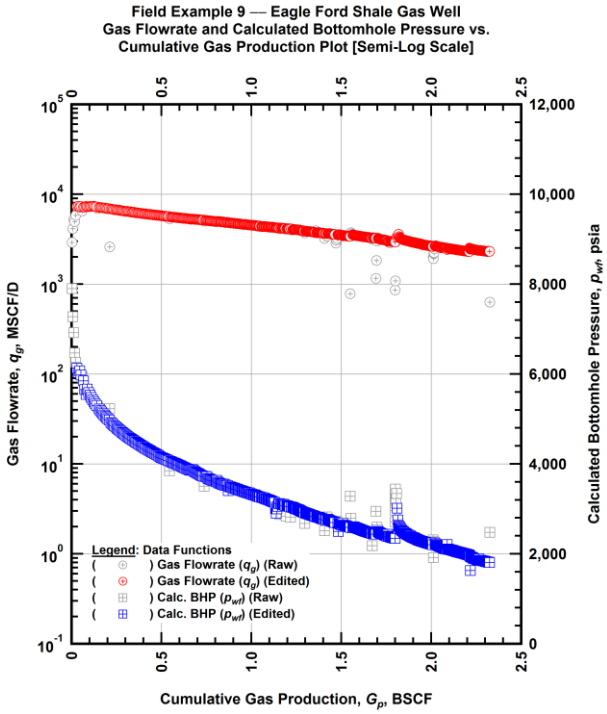

Figure A.246 — (Semi-log Plot): Filtered rate-pressure-cumulative production history plot — flowrate (q_g) and calculated bottomhole pressure (p_{wf}) versus cumulative production (G_p).

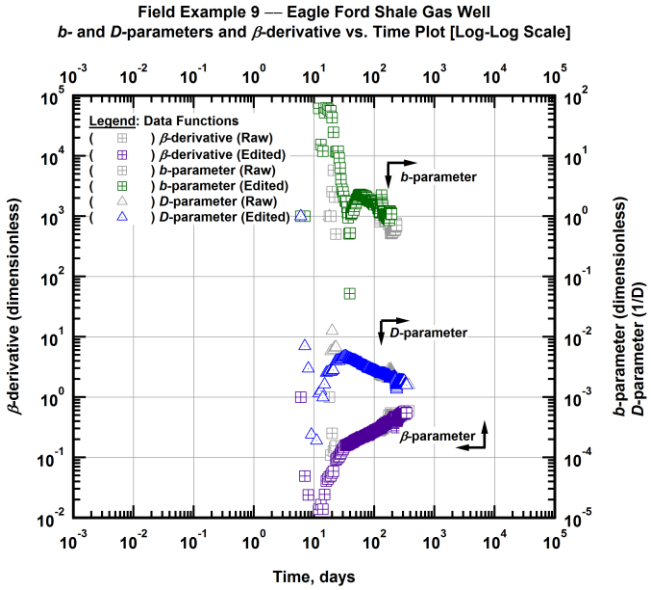

Figure A.247 — (Log-Log Plot): Filtered b, D and β production history plot — b- and D-parameters and β-derivative versus production time.

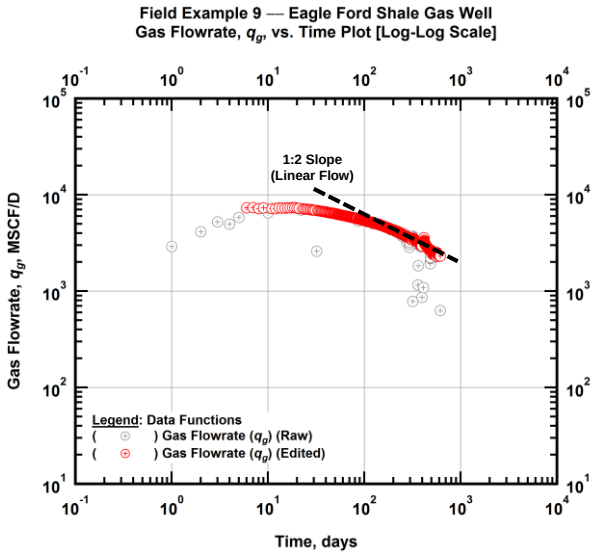

Figure A.248 — (Log-Log Plot): Filtered gas flowrate production history and flow regime identification plot — gas flowrate (q_g) versus production time.

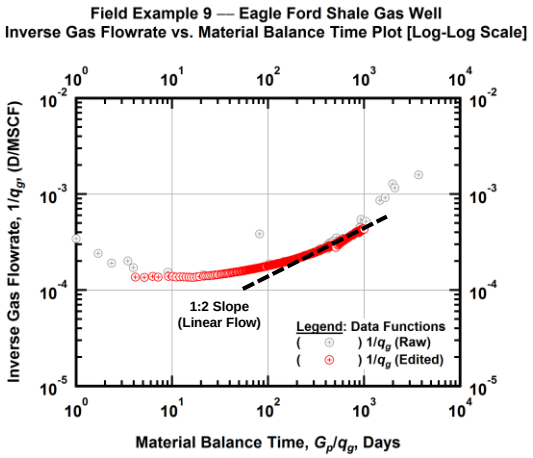

Figure A.249 — (Log-log Plot): Filtered inverse rate with material balance time plot — inverse gas flowrate ($1/q_g$) versus material balance time (G_p/q_g).

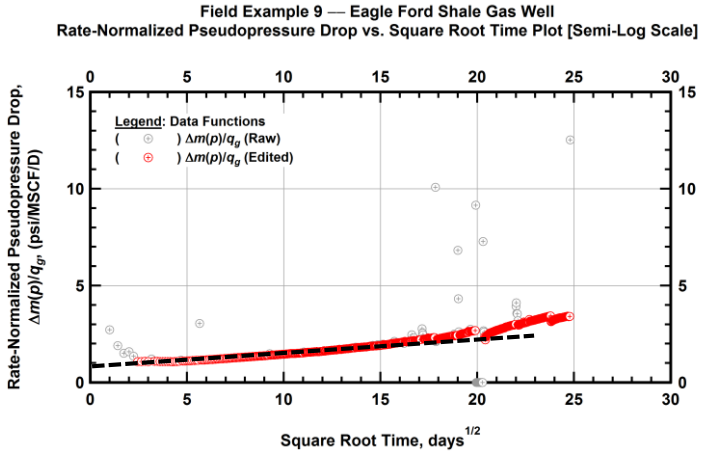

Figure A.250 — (Semi-log Plot): Filtered normalized pseudopressure drop production history plot — rate-normalized pseudopressure drop ($\Delta m(p)/q_g$) versus square root production time ($\sqrt{t}$).

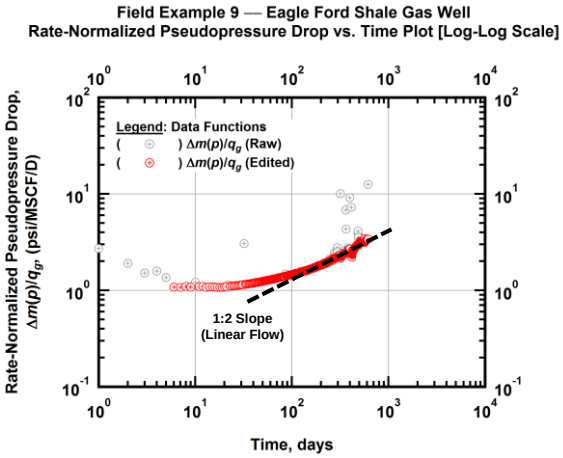

Figure A.251 — (Log-log Plot): Filtered normalized pseudopressure drop production history plot — rate-normalized pseudopressure drop ($\Delta m(p)/q_g$) versus production time.

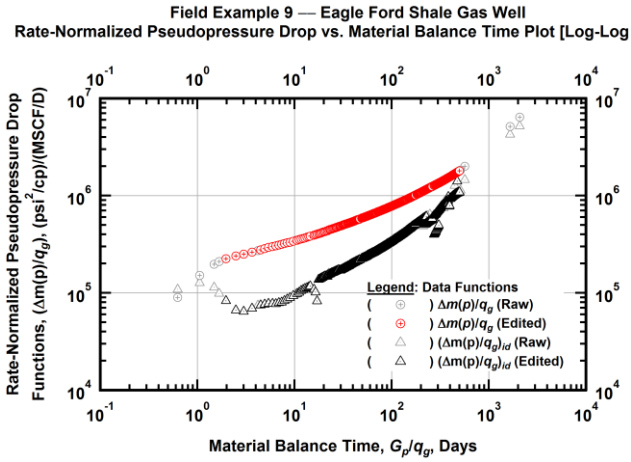

Figure A.252 — (Log-log Plot): "Log-log" diagnostic plot of the filtered production data — rate-normalized pseudopressure drop ($\Delta m(p)/q_g$) and rate-normalized pseudopressure drop integral-derivative ($\Delta m(p)/q_g)_{id}$ versus material balance time (G_p/q_g).

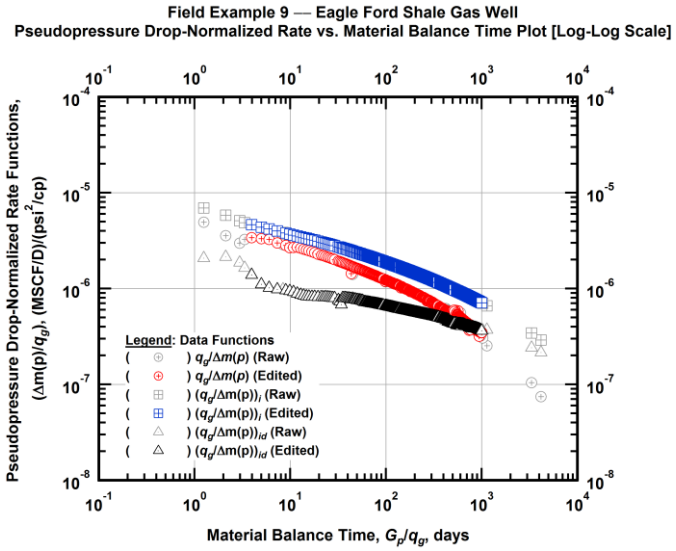

Figure A.253 — (Log-log Plot): "Blasingame" diagnostic plot of the filtered production data — pseudopressure drop-normalized gas flowrate ($q_g/\Delta m(p)$), pseudopressure drop-normalized gas flowrate integral $(q_g/\Delta m(p))_i$ and pseudopressure drop-normalized gas flowrate integral-derivative $(q_g/\Delta m(p))_{id}$ versus material balance time (G_p/q_g).

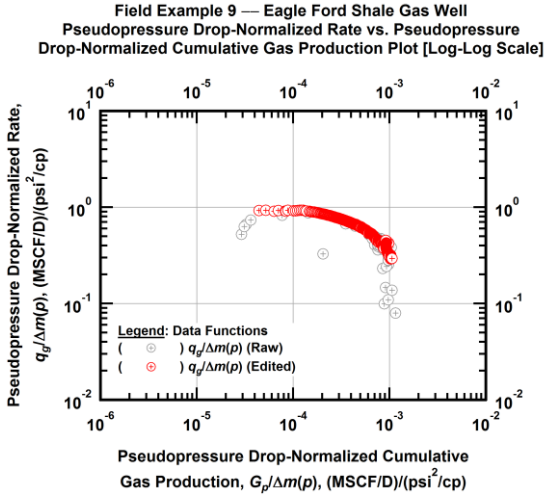

Figure A.254 — (Log-log Plot): Filtered normalized rate with normalized cumulative production plot — pseudopressure drop-normalized gas flowrate ($q_g/\Delta m(p)$) versus pseudopressure drop-normalized cumulative gas production ($G_p/\Delta m(p)$).

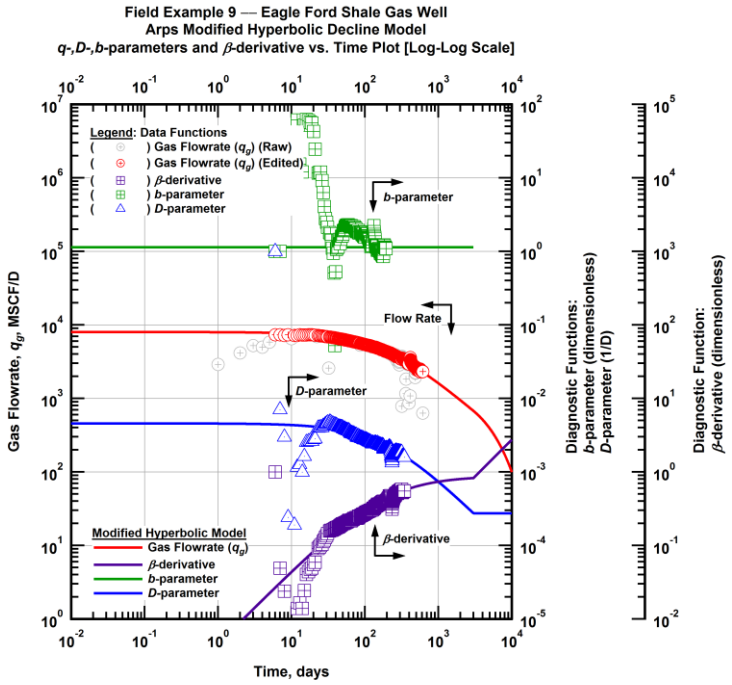

Figure A.255 — (Log-Log Plot): Arps modified hyperbolic decline model plot — time-rate model and data gas flowrate (q_g), *D*- and *b*-parameters and β-derivative versus production time.

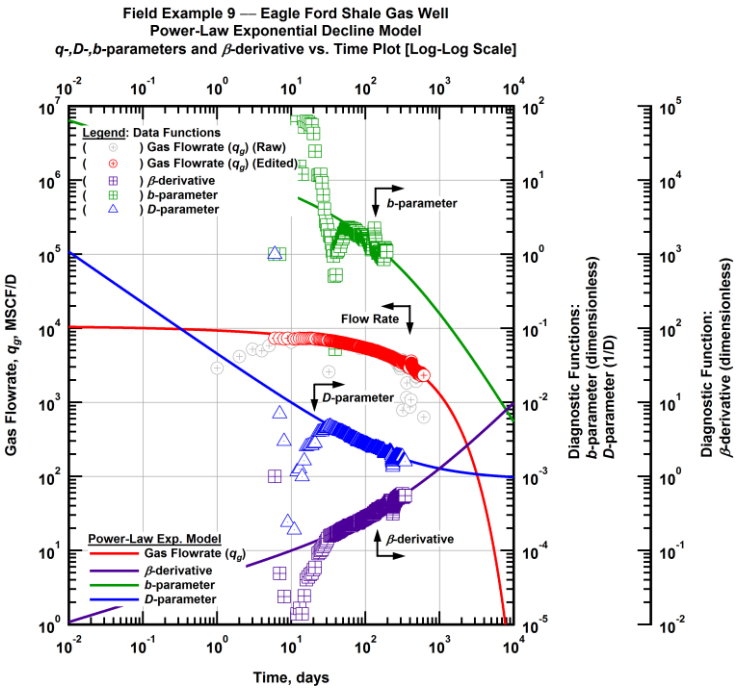

Figure A.256 — (Log-Log Plot): Power-law exponential decline model plot — time-rate model and data gas flowrate (q_g), *D*- and *b*-parameters and β-derivative versus production time.

Field Example 9 — Model-Based (Time-Rate-Pressure) Production Analysis

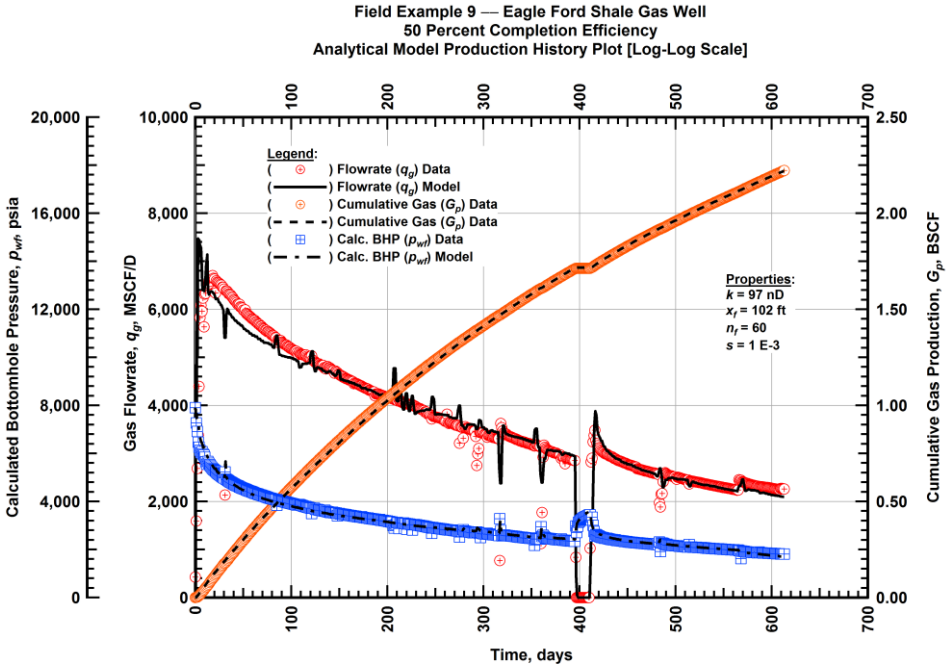

Figure A.257 — (Cartesian Plot): Production history plot — original gas flowrate (q_g), cumulative gas production (G_p), calculated bottomhole pressure (p_{wf}) and 50 percent completion efficiency model matches versus production time.

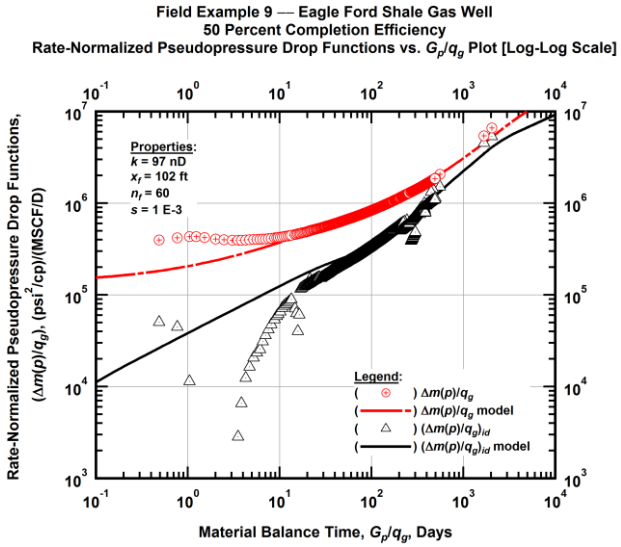

Figure A.258 — (Log-log Plot): "Log-log" diagnostic plot of the original production data — rate-normalized pseudopressure drop ($\Delta m(p)/q_g$), rate-normalized pseudopressure drop integral-derivative $(\Delta m(p)/q_g)_{id}$ and 50 percent completion efficiency model matches versus material balance time (G_p/q_g).

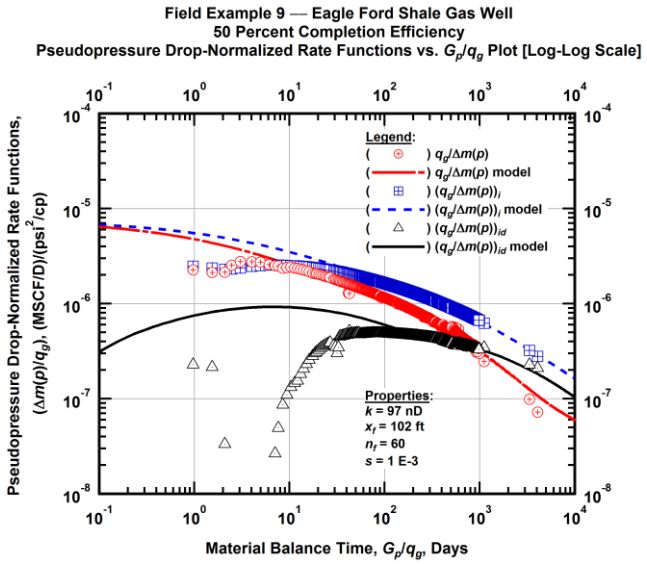

Figure A.259 — (Log-log Plot): "Blasingame" diagnostic plot of the original production data — pseudopressure drop-normalized gas flowrate ($q_g/\Delta m(p)$), pseudopressure drop-normalized gas flowrate integral $(q_g/\Delta m(p))_i$, pseudopressure drop-normalized gas flowrate integral-derivative $(q_g/\Delta m(p))_{id}$ and 50 percent completion efficiency model matches versus material balance time (G_p/q_g).

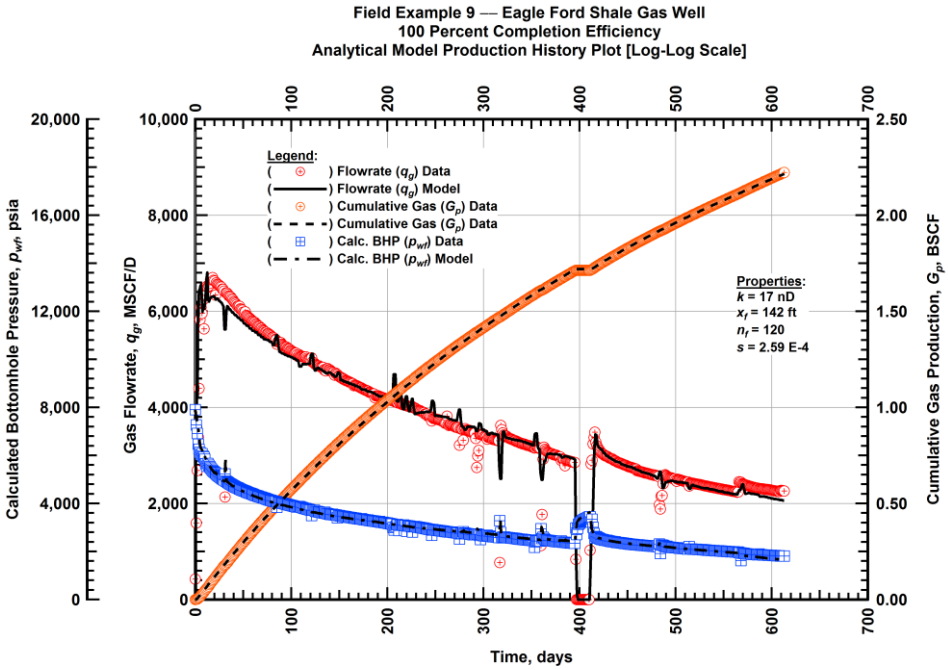

Figure A.260 — (Cartesian Plot): Production history plot — original gas flowrate (q_g), cumulative gas production (G_p), calculated bottomhole pressure (p_{wf}) and 100 percent completion efficiency model matches versus production time.

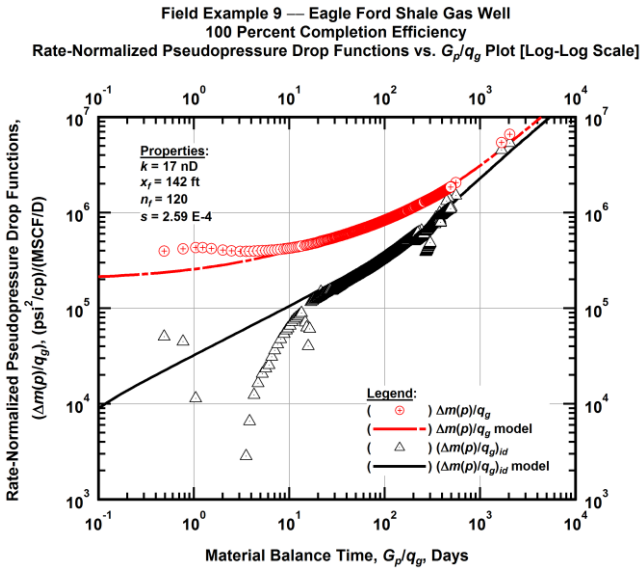

Figure A.261 — (Log-log Plot): "Log-log" diagnostic plot of the original production data — rate-normalized pseudopressure drop ($\Delta m(p)/q_g$), rate-normalized pseudopressure drop integral-derivative $(\Delta m(p)/q_g)_{id}$ and 100 percent completion efficiency model matches versus material balance time (G_p/q_g).

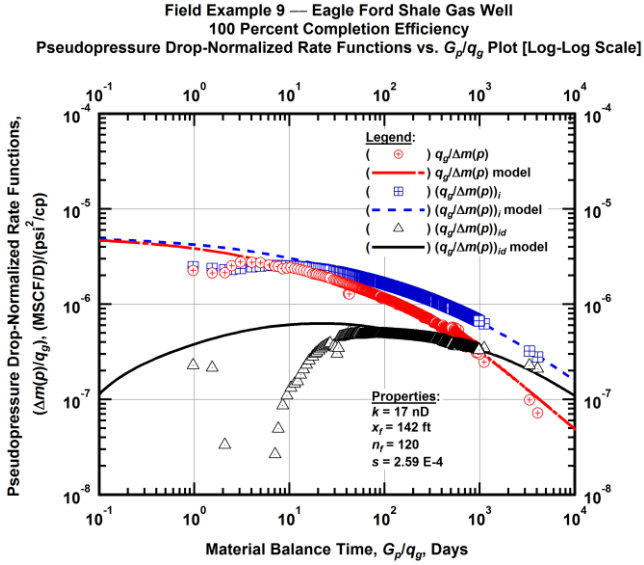

Figure A.262 — (Log-log Plot): "Blasingame" diagnostic plot of the original production data — pseudopressure drop-normalized gas flowrate ($q_g/\Delta m(p)$), pseudopressure drop-normalized gas flowrate integral $(q_g/\Delta m(p))_i$, pseudopressure drop-normalized gas flowrate integral-derivative $(q_g/\Delta m(p))_{id}$ and 100 percent completion efficiency model matches versus material balance time (G_p/q_g).

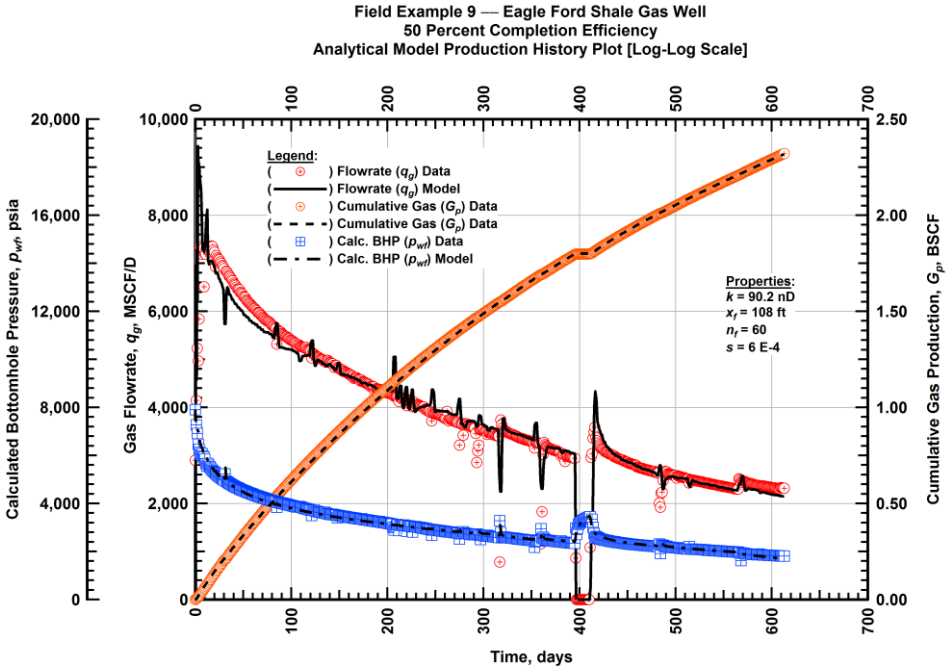

Figure A.263 — (Cartesian Plot): Production history plot — revised gas flowrate (q_g), cumulative gas production (G_p), calculated bottomhole pressure (p_{wf}) and 50 percent completion efficiency model matches versus production time.

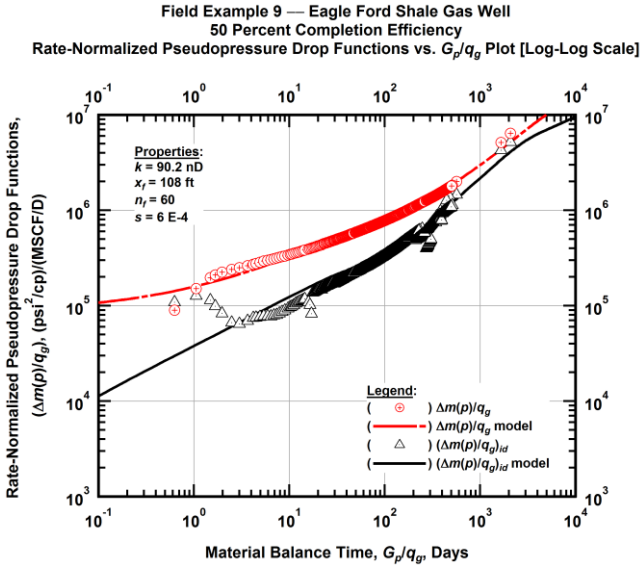

Figure A.264 — (Log-log Plot): "Log-log" diagnostic plot of the revised production data — rate-normalized pseudopressure drop ($\Delta m(p)/q_g$), rate-normalized pseudopressure drop integral-derivative $(\Delta m(p)/q_g)_{id}$ and 50 percent completion efficiency model matches versus material balance time (G_p/q_g).

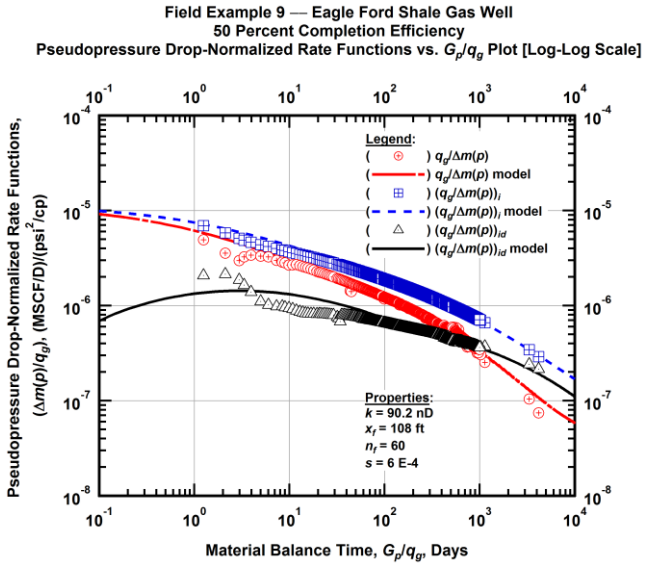

Figure A.265 — (Log-log Plot): "Blasingame" diagnostic plot of the revised production data — pseudopressure drop-normalized gas flowrate ($q_g/\Delta m(p)$), pseudopressure drop-normalized gas flowrate integral $(q_g/\Delta m(p))_i$, pseudopressure drop-normalized gas flowrate integral-derivative $(q_g/\Delta m(p))_{id}$ and 50 percent completion efficiency model matches versus material balance time (G_p/q_g).

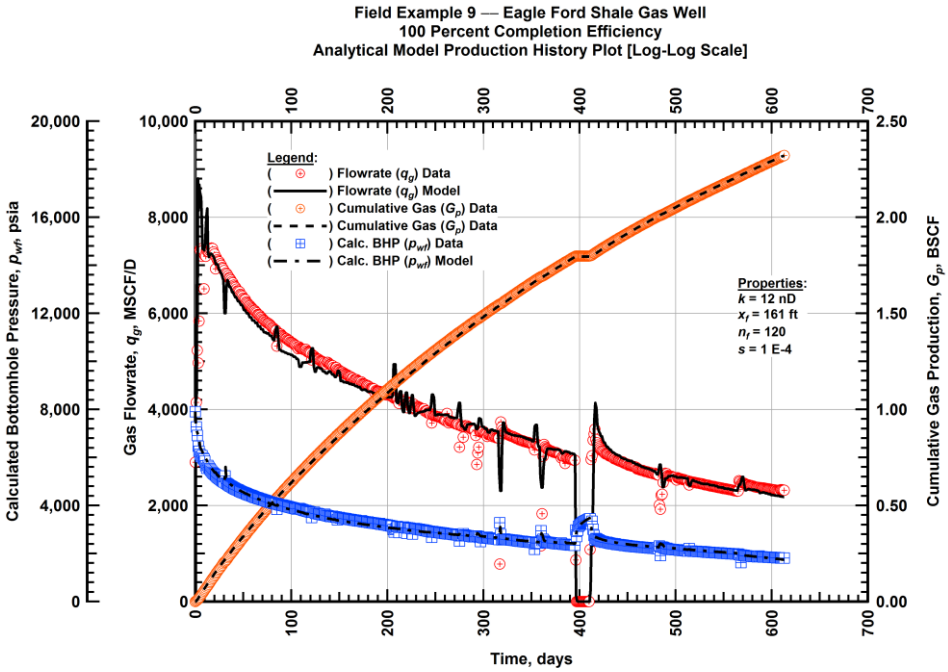

Figure A.266 — (Cartesian Plot): Production history plot — revised gas flowrate (q_g), cumulative gas production (G_p), calculated bottomhole pressure (p_{wf}) and 100 percent completion efficiency model matches versus production time.

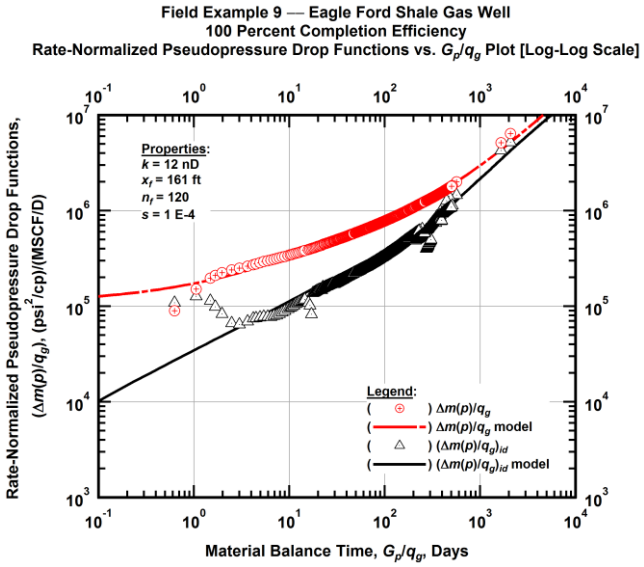

Figure A.267 — (Log-log Plot): "Log-log" diagnostic plot of the revised production data — rate-normalized pseudopressure drop ($\Delta m(p)/q_g$), rate-normalized pseudopressure drop integral-derivative $(\Delta m(p)/q_g)_{id}$ and 100 percent completion efficiency model matches versus material balance time (G_p/q_g).

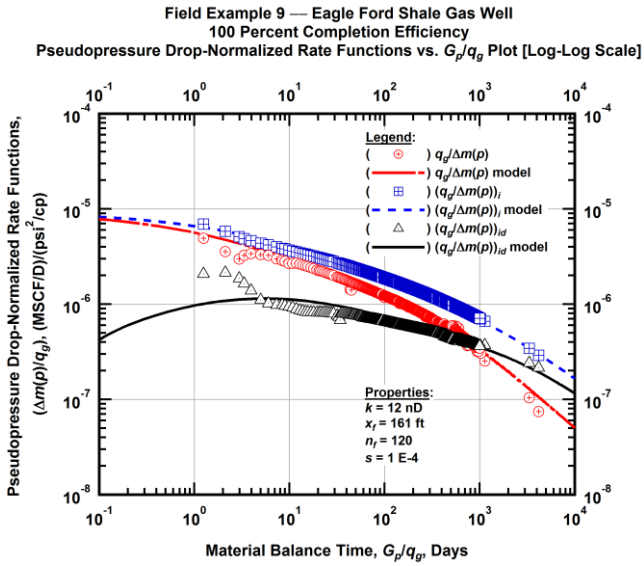

Figure A.268 — (Log-log Plot): "Blasingame" diagnostic plot of the revised production data — pseudopressure drop-normalized gas flowrate ($q_g/\Delta m(p)$), pseudopressure drop-normalized gas flowrate integral $(q_g/\Delta m(p))_i$, pseudopressure drop-normalized gas flowrate integral-derivative $(q_g/\Delta m(p))_{id}$ and 100 percent completion efficiency model matches versus material balance time (G_p/q_g).

Field Example 9 — 30-Year EUR Model Comparison

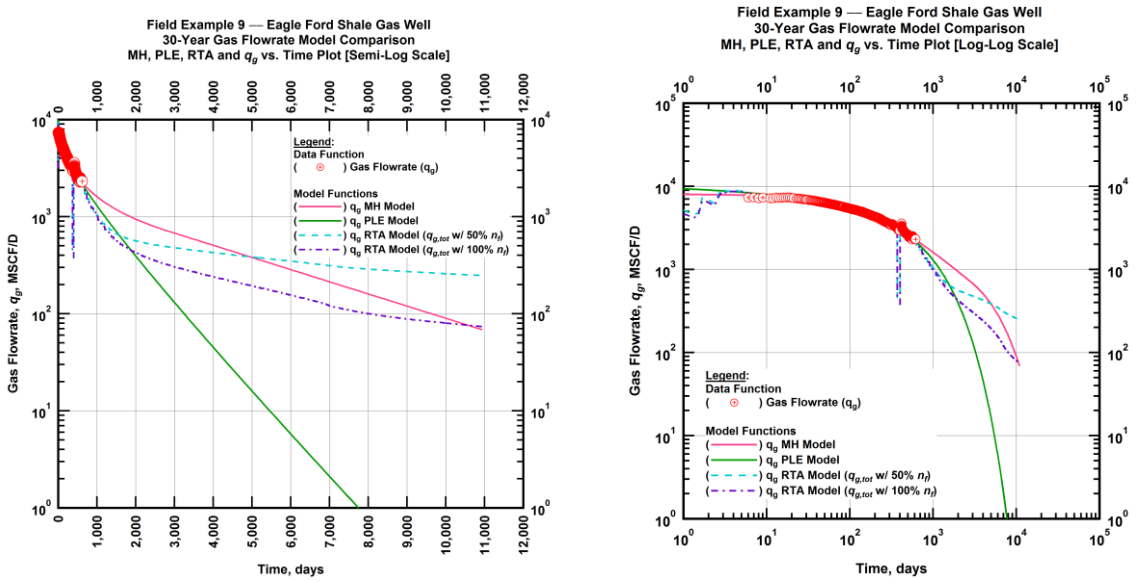

A **B**

Figure A.269 — (A — Semi-Log Plot) and (B — Log-Log Plot): Revised gas 30-year estimated flowrate model comparison — Arps modified hyperbolic decline model, power-law exponential decline model, and 50 percent and 100 percent completion efficiency RTA models revised gas 30-year estimated flowrate decline and historic gas flowrate data (q_g) versus production time.

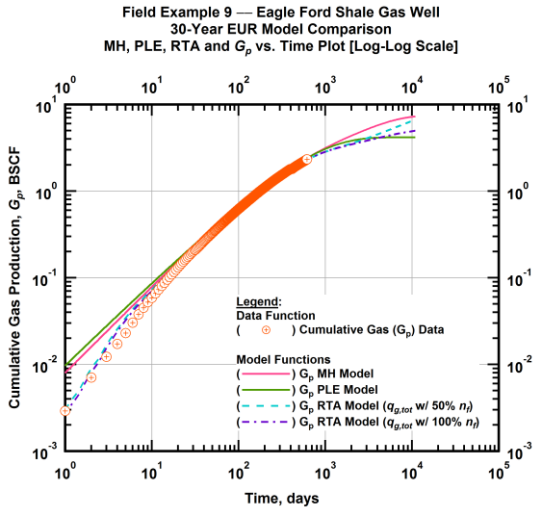

Figure A.270 — (Log-log Plot): Estimated 30-year cumulative gas production volume model comparison — Arps modified hyperbolic decline model, power-law exponential decline model, and 50 percent and 100 percent completion efficiency RTA models estimated 30-year cumulative gas production volumes and historic cumulative gas production (G_p) versus production time.

Table A.9 — 30-year estimated cumulative revised gas production (EUR), in units of BSCF, for the Arps modified hyperbolic, power-law exponential and analytical time-rate-pressure decline models.

Arps Modified Hyperbolic BSCF)	Power-Law Exponential (BSCF)	RTA Analytical Model ($q_{g,tot}$ w/ 50% n_f) (BSCF)	RTA Analytical Model ($q_{g,tot}$ w/ 100% n_f) (BSCF)
7.28	4.07	6.85	5.02

Field Example 10 — Time-Rate Analysis

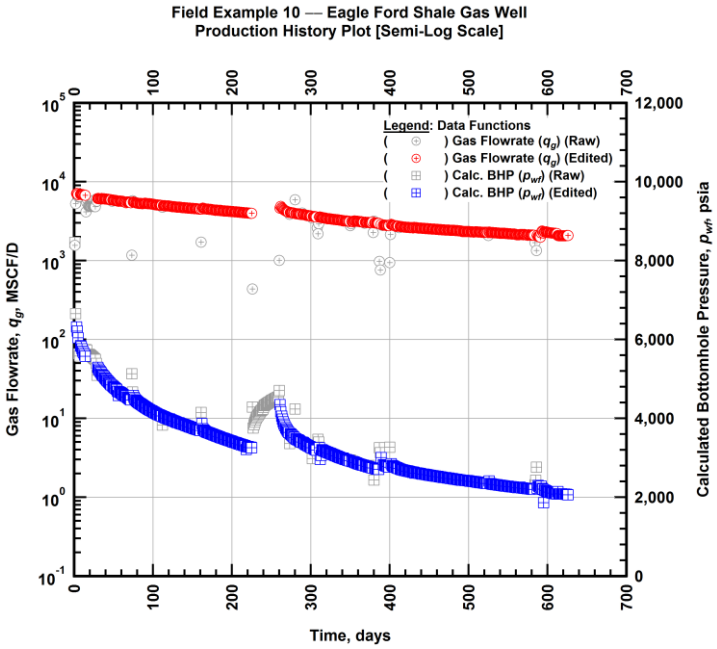

Figure A.271 — (Semi-log Plot): Filtered production history plot — flowrate (q_g) and calculated bottomhole pressure (p_{wf}) versus production time.

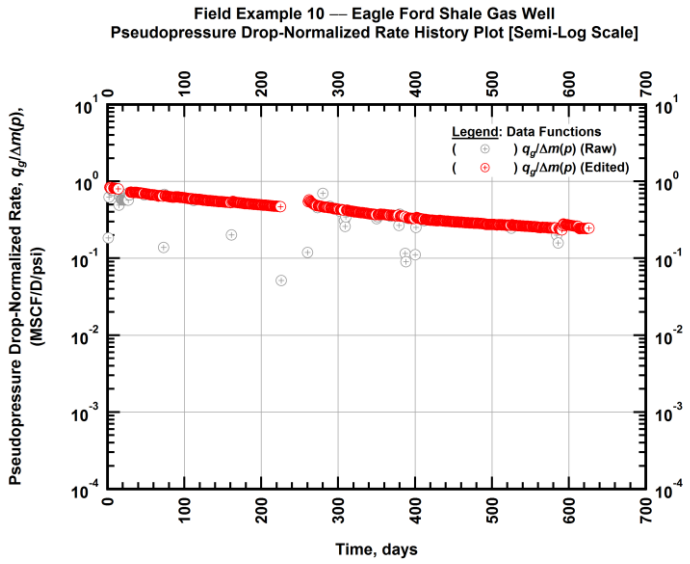

Figure A.272 — (Semi-log Plot): Filtered normalized rate production history plot — pseudopressure drop-normalized gas flowrate ($q_g/\Delta m(p)$) versus production time.

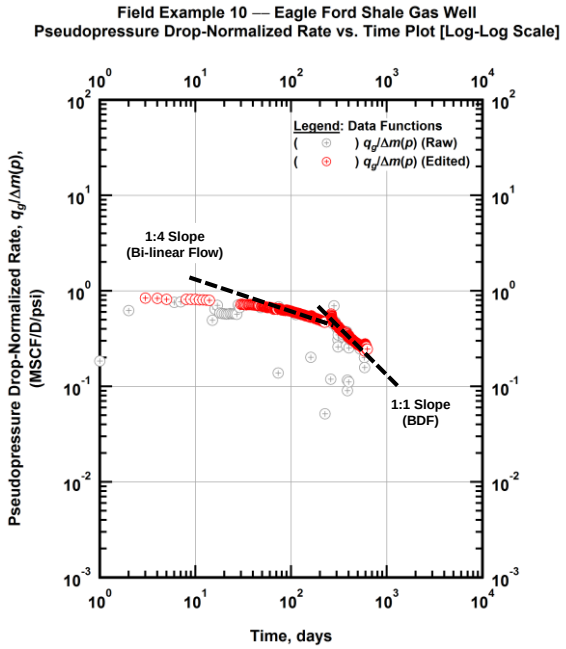

Figure A.273 — (Log-log Plot): Filtered normalized rate production history plot — pseudopressure drop-normalized gas flowrate ($q_g/\Delta m(p)$) versus production time.

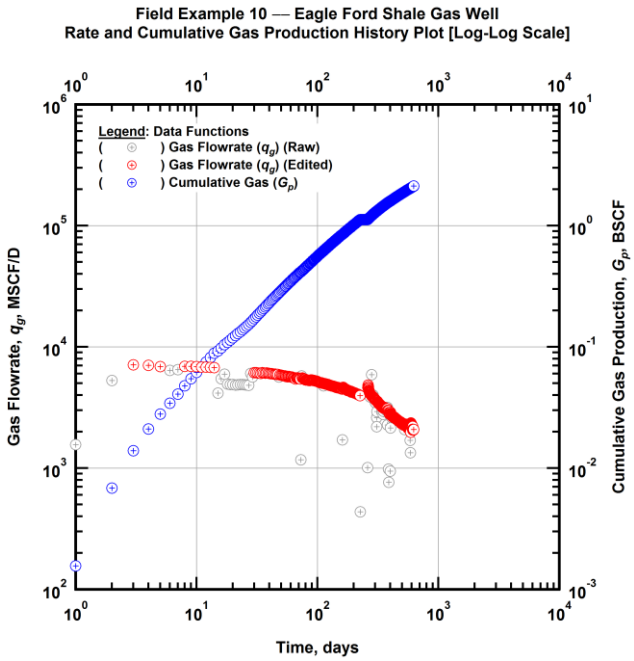

Figure A.274 — (Log-log Plot): Filtered rate and unfiltered cumulative gas production history plot — flowrate (q_g) and cumulative production (G_p) versus production time.

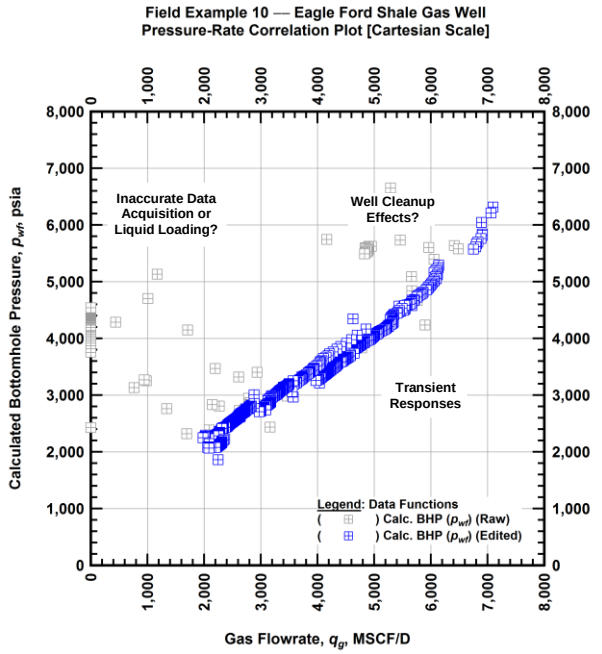

Figure A.275 — (Cartesian Plot): Filtered rate-pressure correlation plot — calculated bottomhole pressure (p_{wf}) versus flowrate (q_g).

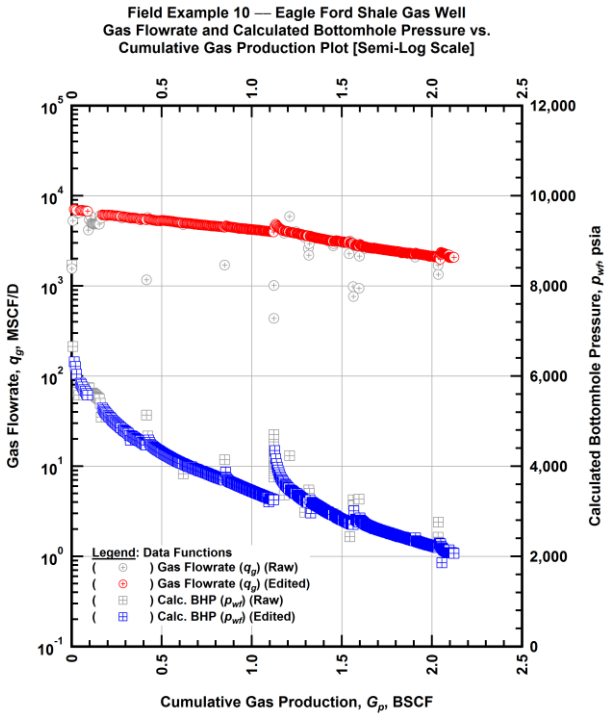

Figure A.276 — (Semi-log Plot): Filtered rate-pressure-cumulative production history plot — flowrate (q_g) and calculated bottomhole pressure (p_{wf}) versus cumulative production (G_p).

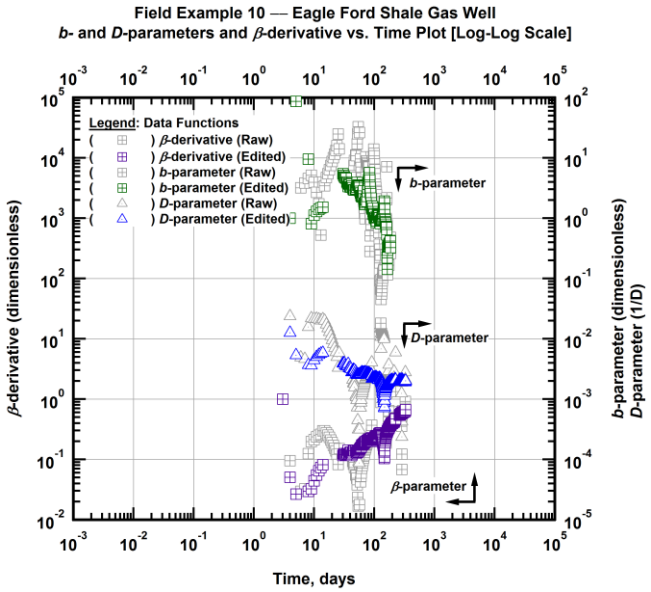

Figure A.277 — (Log-Log Plot): Filtered b, D and β production history plot — b- and D-parameters and β-derivative versus production time.

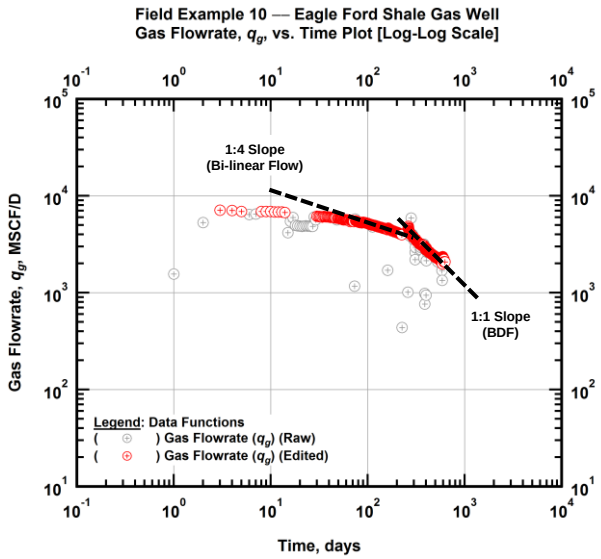

Figure A.278 — (Log-Log Plot): Filtered gas flowrate production history and flow regime identification plot — gas flowrate (q_g) versus production time.

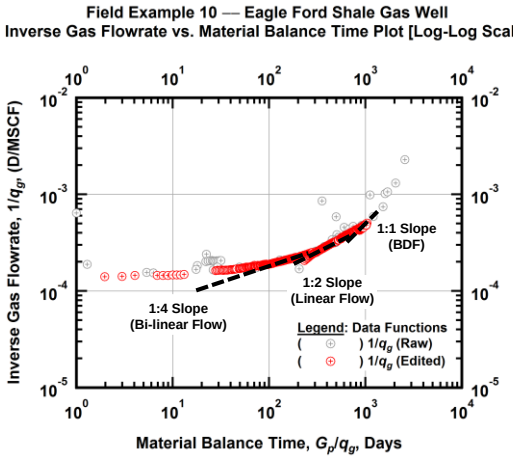

Figure A.279 — (Log-log Plot): Filtered inverse rate with material balance time plot — inverse gas flowrate ($1/q_g$) versus material balance time (G_p/q_g).

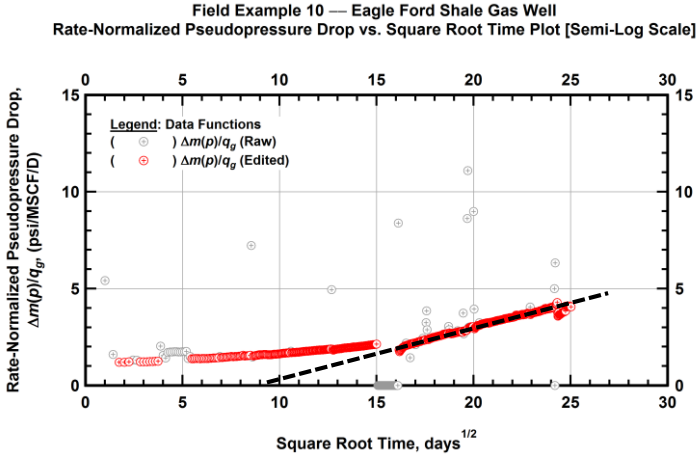

Figure A.280 — (Semi-log Plot): Filtered normalized pseudopressure drop production history plot — rate-normalized pseudopressure drop ($\Delta m(p)/q_g$) versus square root production time ($\sqrt{t}$).

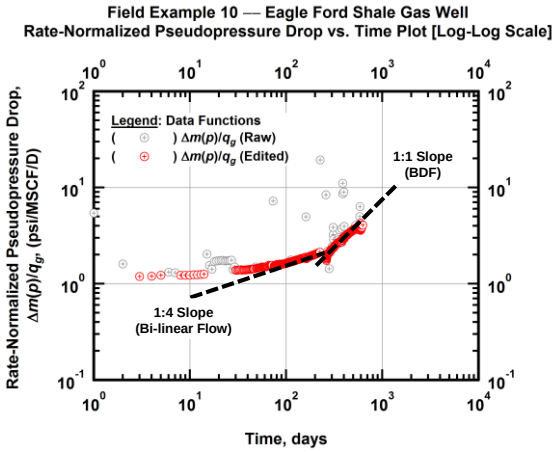

Figure A.281 — (Log-log Plot): Filtered normalized pseudopressure drop production history plot — rate-normalized pseudopressure drop ($\Delta m(p)/q_g$) versus production time.

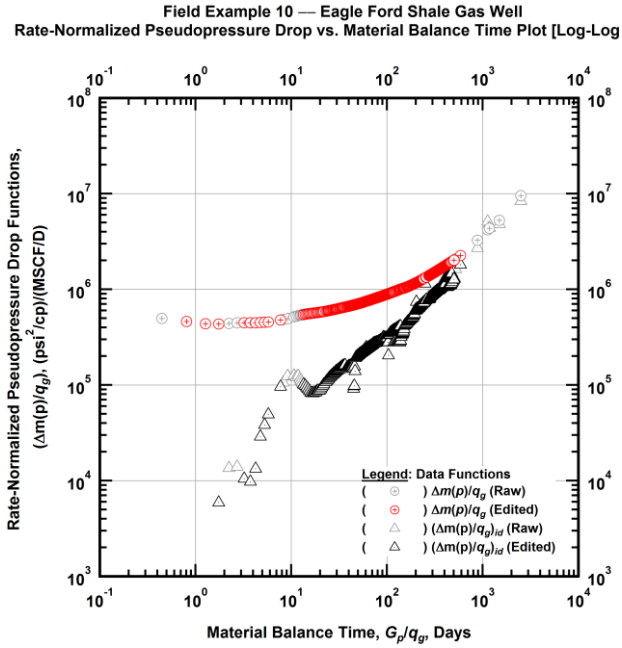

Figure A.282 — (Log-log Plot): "Log-log" diagnostic plot of the filtered production data — rate-normalized pseudopressure drop ($\Delta m(p)/q_g$) and rate-normalized pseudopressure drop integral-derivative $(\Delta m(p)/q_g)_{id}$ versus material balance time (G_p/q_g).

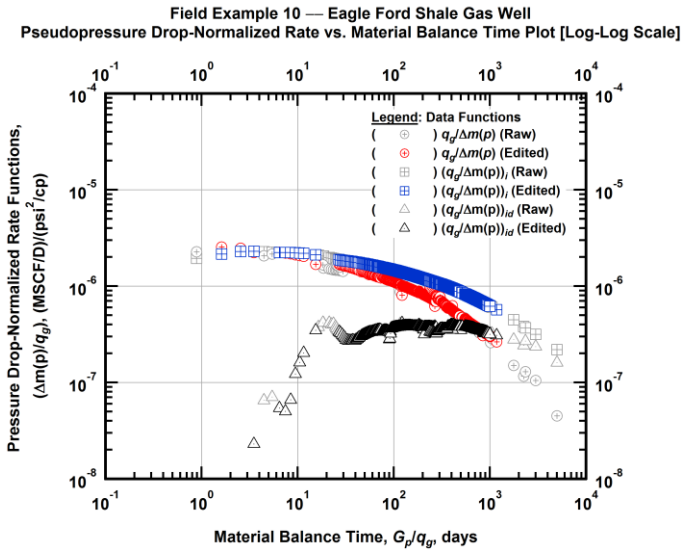

Figure A.283 — (Log-log Plot): "Blasingame" diagnostic plot of the filtered production data — pseudopressure drop-normalized gas flowrate ($q_g/\Delta m(p)$), pseudopressure drop-normalized gas flowrate integral $(q_g/\Delta m(p))_i$ and pseudopressure drop-normalized gas flowrate integral-derivative $(q_g/\Delta m(p))_{id}$ versus material balance time (G_p/q_g).

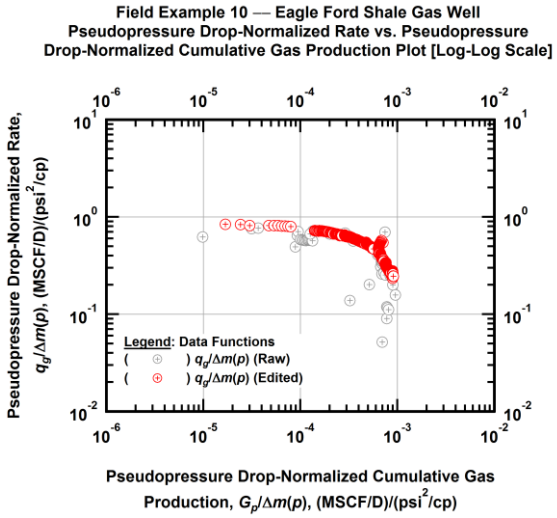

Figure A.284 — (Log-log Plot): Filtered normalized rate with normalized cumulative production plot — pseudopressure drop-normalized gas flowrate ($q_g/\Delta m(p)$) versus pseudopressure drop-normalized cumulative gas production ($G_p/\Delta m(p)$).

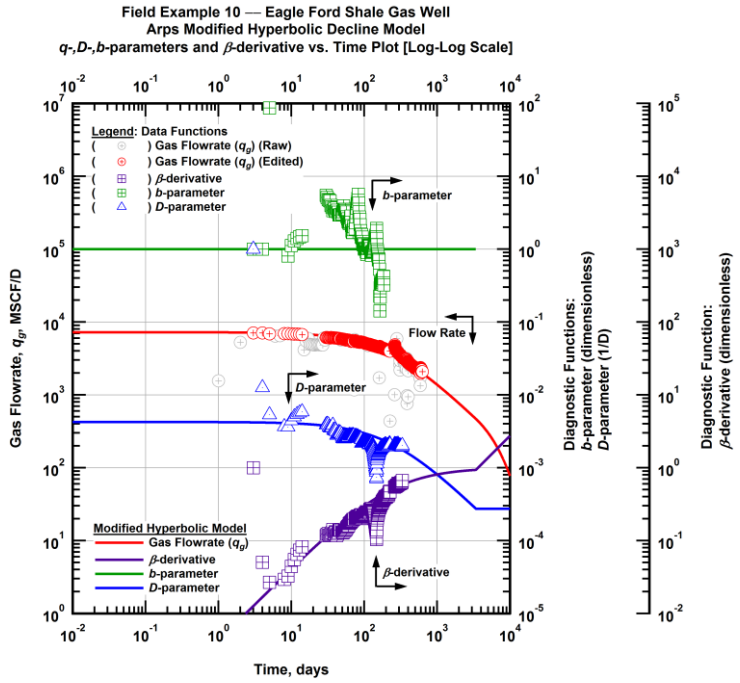

Figure A.285 — (Log-Log Plot): Arps modified hyperbolic decline model plot — time-rate model and data gas flowrate (q_g), *D*- and *b*-parameters and β-derivative versus production time.

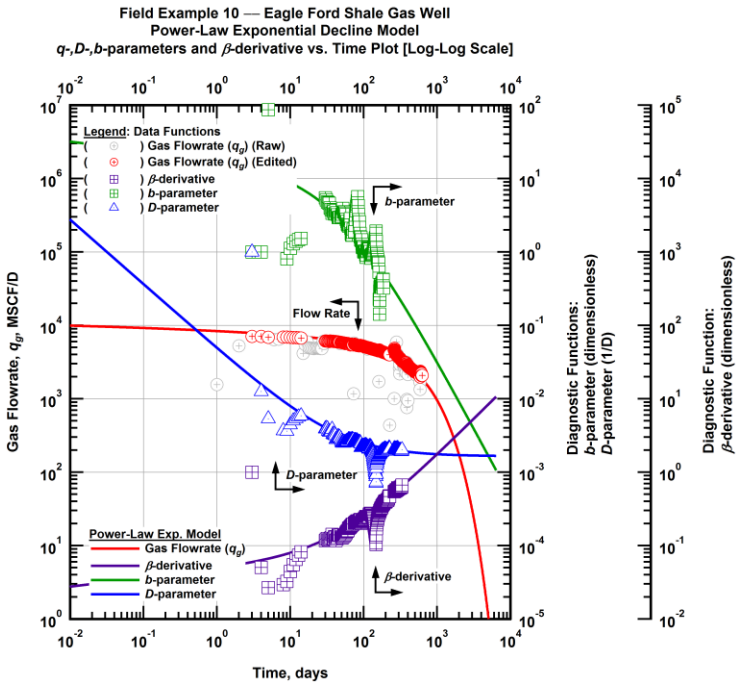

Figure A.286 — (Log-Log Plot): Power-law exponential decline model plot — time-rate model and data gas flowrate (q_g), *D*- and *b*-parameters and β-derivative versus production time.

Field Example 10 — Model-Based (Time-Rate-Pressure) Production Analysis

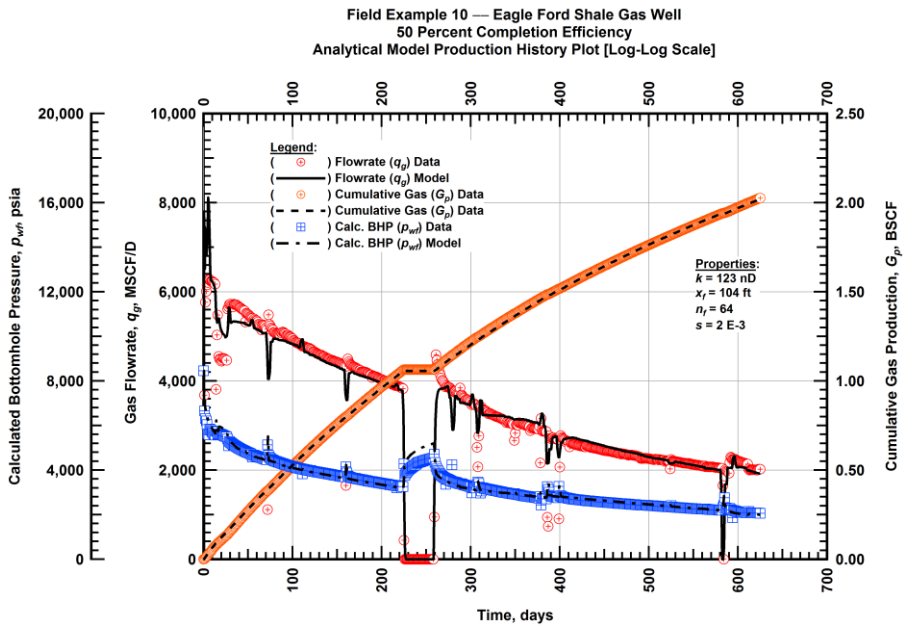

Figure A.287 — (Cartesian Plot): Production history plot — original gas flowrate (q_g), cumulative gas production (G_p), calculated bottomhole pressure (p_{wf}) and 50 percent completion efficiency model matches versus production time.

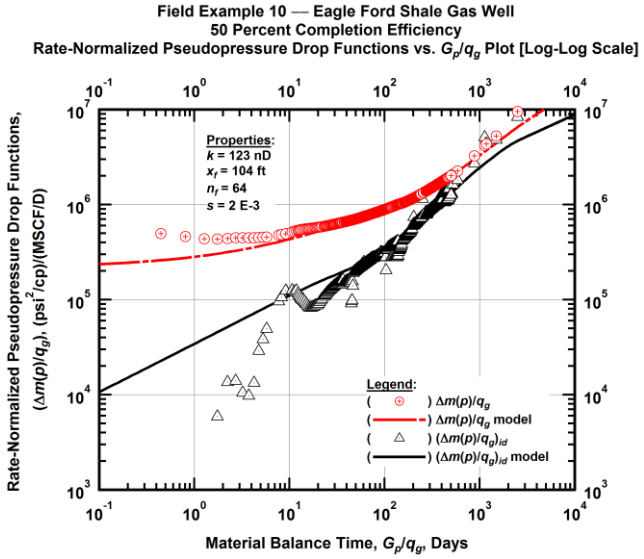

Figure A.288 — (Log-log Plot): "Log-log" diagnostic plot of the original production data — rate-normalized pseudopressure drop ($\Delta m(p)/q_g$), rate-normalized pseudopressure drop integral-derivative $(\Delta m(p)/q_g)_{id}$ and 50 percent completion efficiency model matches versus material balance time (G_p/q_g).

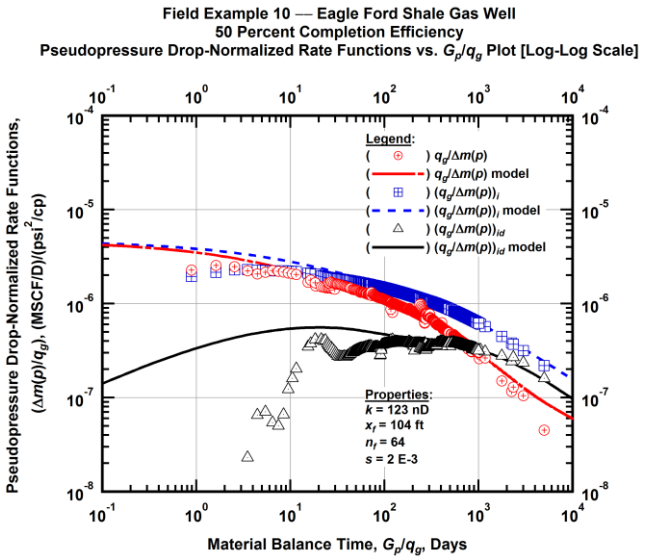

Figure A.289 — (Log-log Plot): "Blasingame" diagnostic plot of the original production data — pseudopressure drop-normalized gas flowrate ($q_g/\Delta m(p)$), pseudopressure drop-normalized gas flowrate integral $(q_g/\Delta m(p))_i$, pseudopressure drop-normalized gas flowrate integral-derivative $(q_g/\Delta m(p))_{id}$ and 50 percent completion efficiency model matches versus material balance time (G_p/q_g).

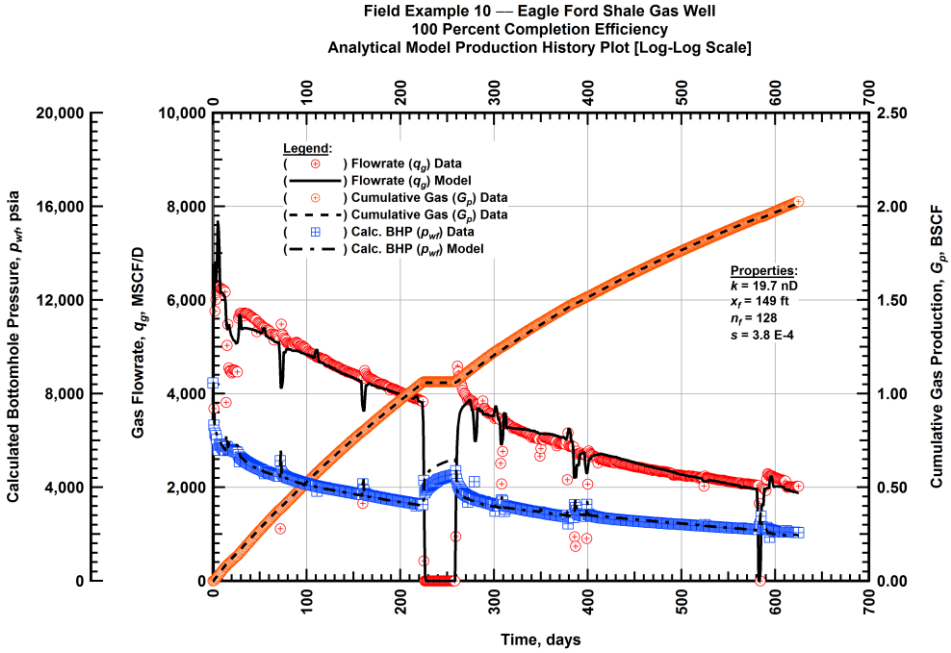

Figure A.290 — (Cartesian Plot): Production history plot — original gas flowrate (q_g), cumulative gas production (G_p), calculated bottomhole pressure (p_{wf}) and 100 percent completion efficiency model matches versus production time.

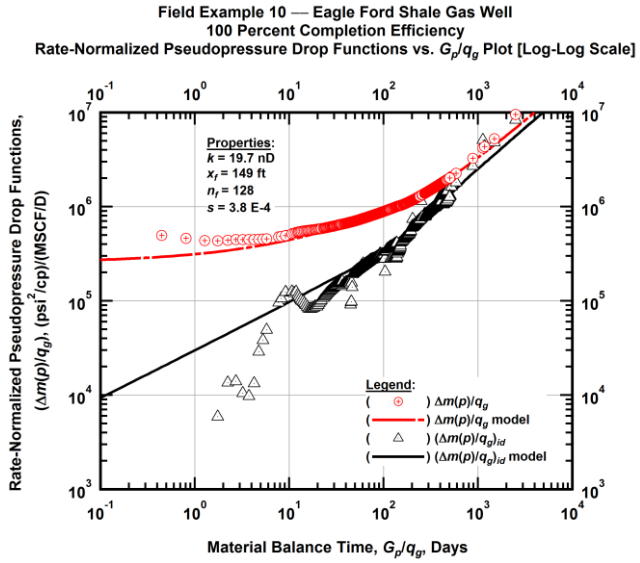

Figure A.291 — (Log-log Plot): "Log-log" diagnostic plot of the original production data — rate-normalized pseudopressure drop ($\Delta m(p)/q_g$), rate-normalized pseudopressure drop integral-derivative $(\Delta m(p)/q_g)_{id}$ and 100 percent completion efficiency model matches versus material balance time (G_p/q_g).

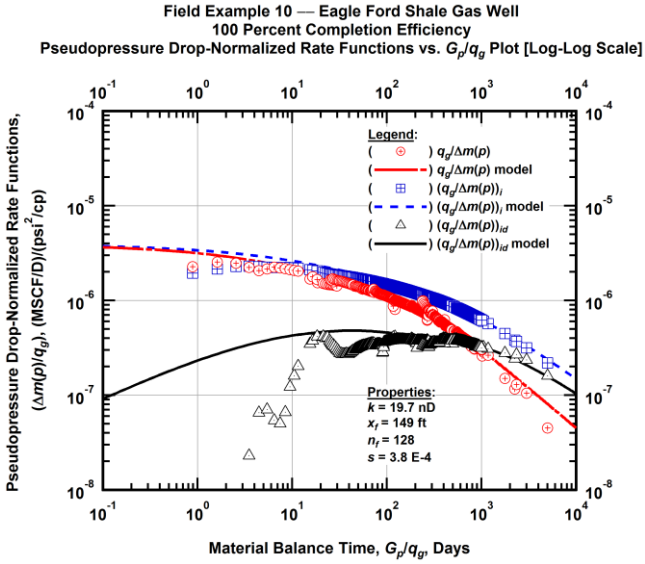

Figure A.292 — (Log-log Plot): "Blasingame" diagnostic plot of the original production data — pseudopressure drop-normalized gas flowrate ($q_g/\Delta m(p)$), pseudopressure drop-normalized gas flowrate integral $(q_g/\Delta m(p))_i$, pseudopressure drop-normalized gas flowrate integral-derivative $(q_g/\Delta m(p))_{id}$ and 100 percent completion efficiency model matches versus material balance time (G_p/q_g).

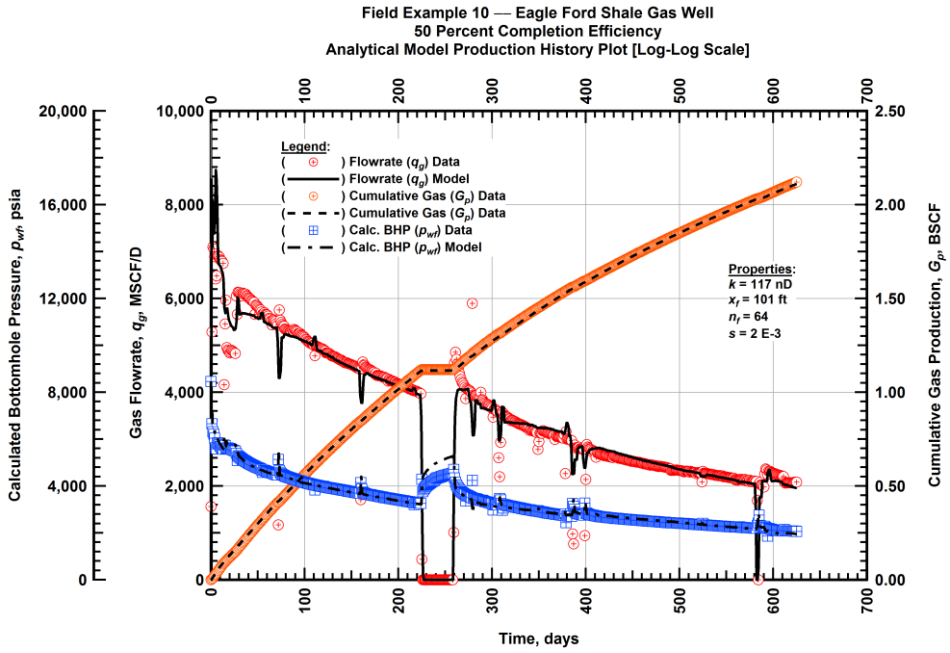

Figure A.293 — (Cartesian Plot): Production history plot — revised gas flowrate (q_g), cumulative gas production (G_p), calculated bottomhole pressure (p_{wf}) and 50 percent completion efficiency model matches versus production time.

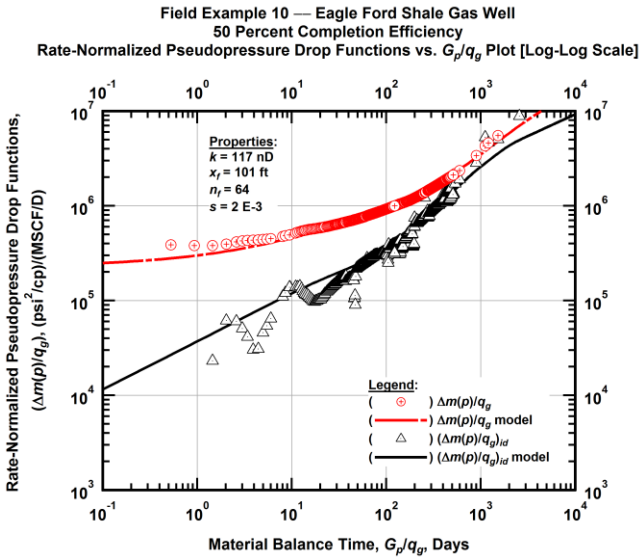

Figure A.294— (Log-log Plot): "Log-log" diagnostic plot of the revised production data — rate-normalized pseudopressure drop ($\Delta m(p)/q_g$), rate-normalized pseudopressure drop integral-derivative $(\Delta m(p)/q_g)_{id}$ and 50 percent completion efficiency model matches versus material balance time (G_p/q_g).

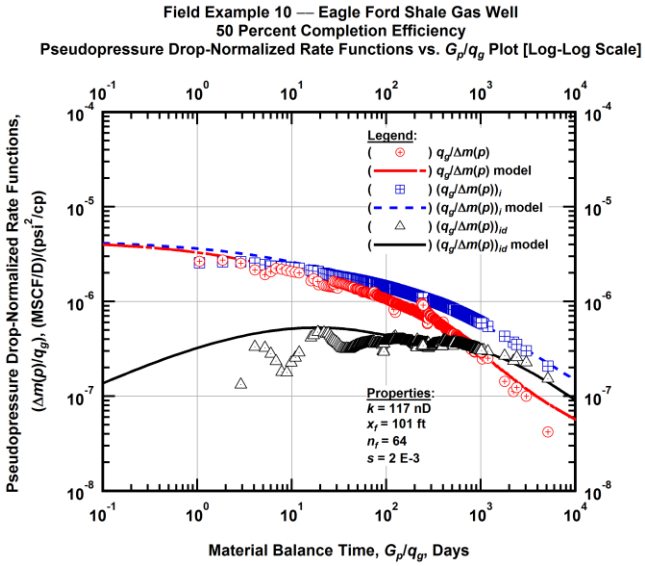

Figure A.295 — (Log-log Plot): "Blasingame" diagnostic plot of the revised production data — pseudopressure drop-normalized gas flowrate ($q_g/\Delta m(p)$), pseudopressure drop-normalized gas flowrate integral $(q_g/\Delta m(p))_i$, pseudopressure drop-normalized gas flowrate integral-derivative $(q_g/\Delta m(p))_{id}$ and 50 percent completion efficiency model matches versus material balance time (G_p/q_g).

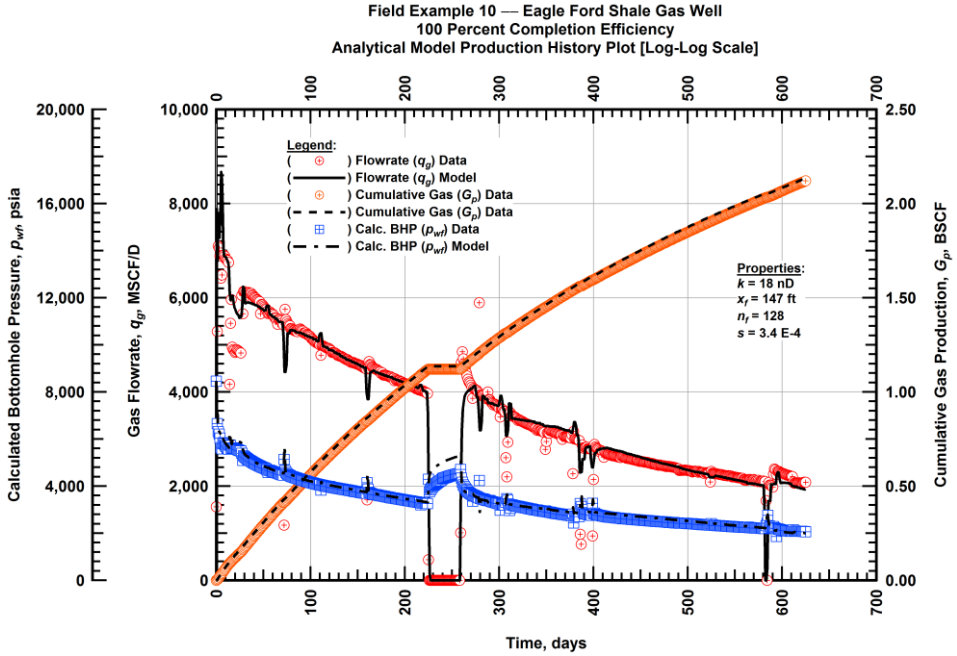

Figure A.296 — (Cartesian Plot): Production history plot — revised gas flowrate (q_g), cumulative gas production (G_p), calculated bottomhole pressure (p_{wf}) and 100 percent completion efficiency model matches versus production time.

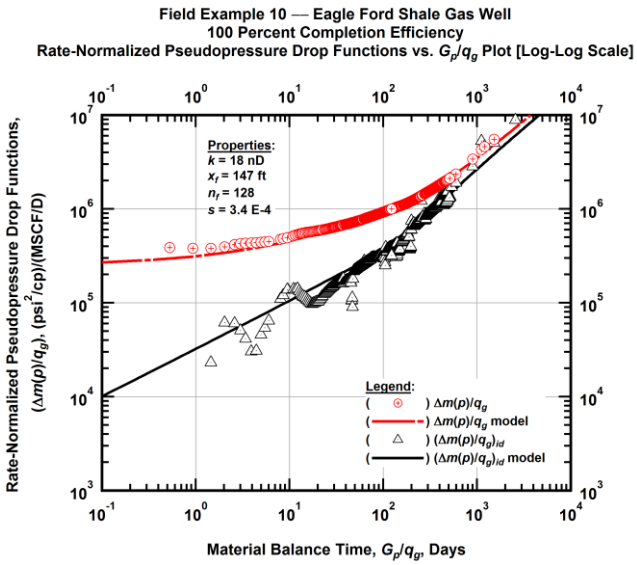

Figure A.297 — (Log-log Plot): "Log-log" diagnostic plot of the revised production data — rate-normalized pseudopressure drop ($\Delta m(p)/q_g$), rate-normalized pseudopressure drop integral-derivative $(\Delta m(p)/q_g)_{id}$ and 100 percent completion efficiency model matches versus material balance time (G_p/q_g).

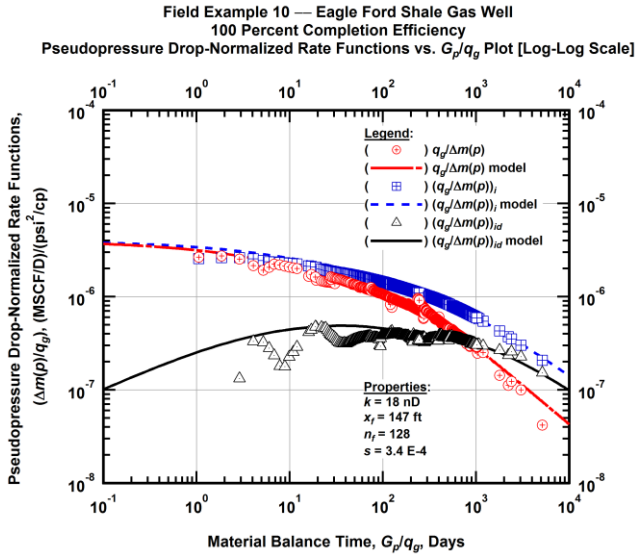

Figure A.298 — (Log-log Plot): "Blasingame" diagnostic plot of the revised production data — pseudopressure drop-normalized gas flowrate ($q_g/\Delta m(p)$), pseudopressure drop-normalized gas flowrate integral $(q_g/\Delta m(p))_i$, pseudopressure drop-normalized gas flowrate integral-derivative $(q_g/\Delta m(p))_{id}$ and 100 percent completion efficiency model matches versus material balance time (G_p/q_g).

Field Example 10 — 30-Year EUR Model Comparison

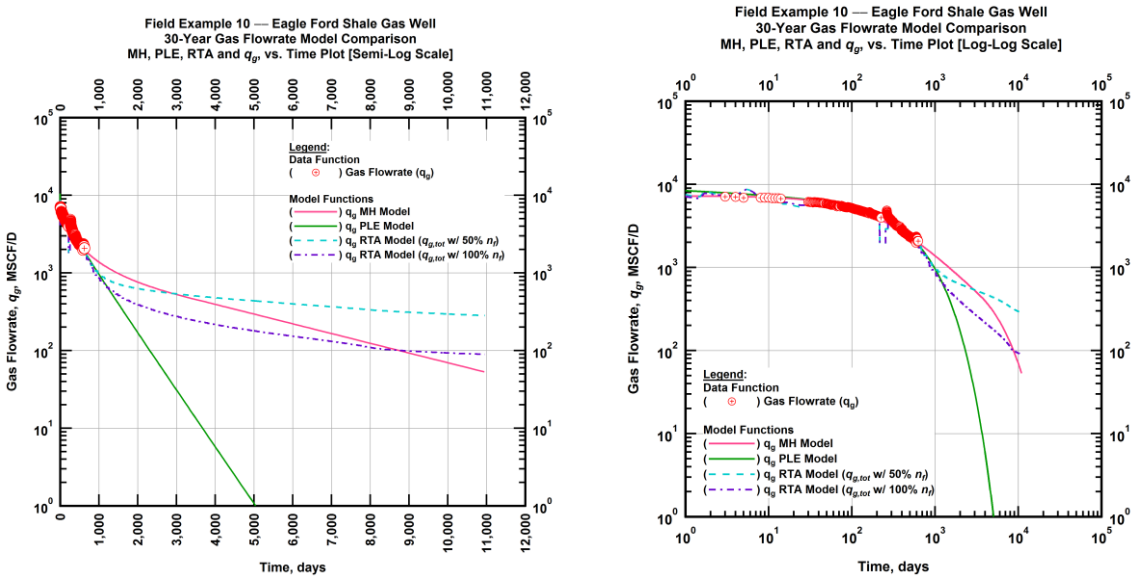

A **B**

Figure A.299 — (A — Semi-Log Plot) and (B — Log-Log Plot): Revised gas 30-year estimated flowrate model comparison — Arps modified hyperbolic decline model, power-law exponential decline model, and 50 percent and 100 percent completion efficiency RTA models revised gas 30-year estimated flowrate decline and historic gas flowrate data (q_g) versus production time.

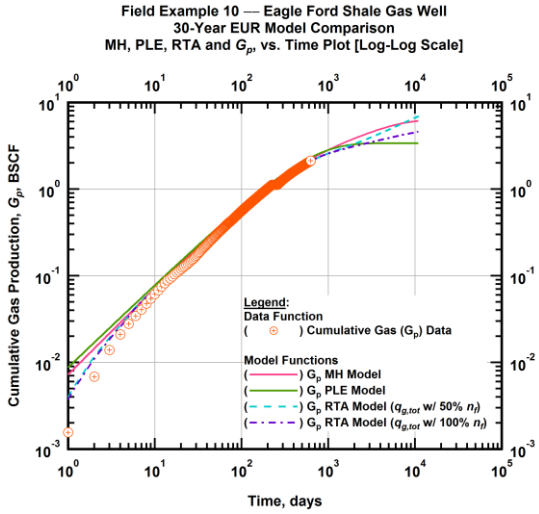

Figure A.300 — (Log-log Plot): Estimated 30-year cumulative gas production volume model comparison — Arps modified hyperbolic decline model, power-law exponential decline model, and 50 percent and 100 percent completion efficiency RTA models estimated 30-year cumulative gas production volumes and historic cumulative gas production (G_p) versus production time.

Table A.10 — 30-year estimated cumulative revised gas production (EUR), in units of BSCF, for the Arps modified hyperbolic, power-law exponential and analytical time-rate-pressure decline models.

Arps Modified Hyperbolic BSCF)	Power-Law Exponential (BSCF)	RTA Analytical Model ($q_{g,tot}$ w/ 50% n_f) (BSCF)	RTA Analytical Model ($q_{g,tot}$ w/ 100% n_f) (BSCF)
6.09	3.18	7.09	4.65

Field Example 11 — Time-Rate Analysis

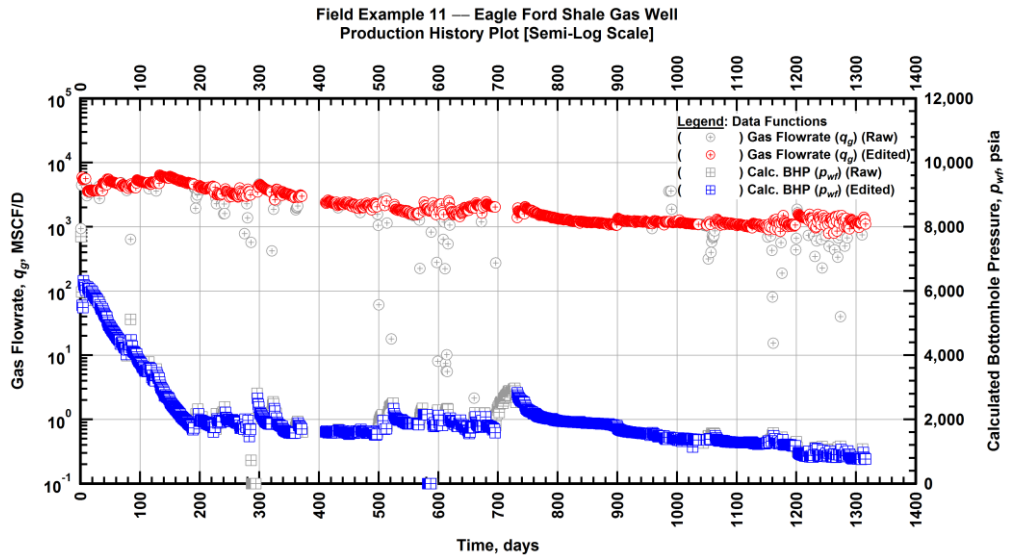

Figure A.301 — (Semi-log Plot): Filtered production history plot — flowrate (q_g) and calculated bottomhole pressure (p_{wf}) versus production time.

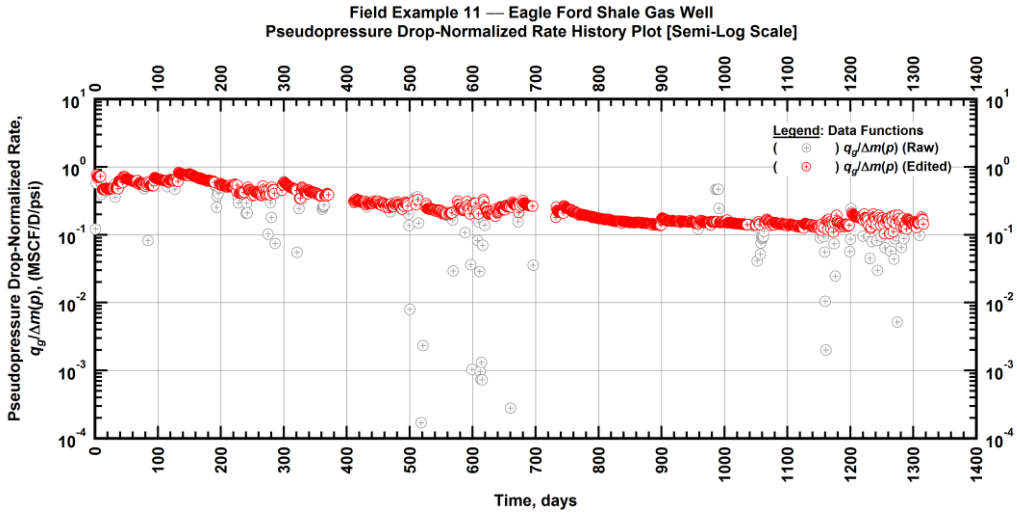

Figure A.302 — (Semi-log Plot): Filtered normalized rate production history plot — pseudopressure drop-normalized gas flowrate ($q_g/\Delta m(p)$) versus production time.

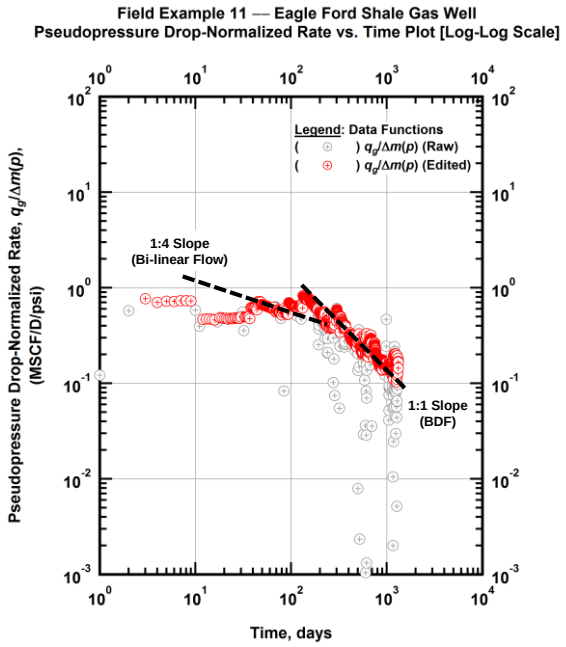

Figure A.303 — (Log-log Plot): Filtered normalized rate production history plot — pseudopressure drop-normalized gas flowrate ($q_g/\Delta m(p)$) versus production time.

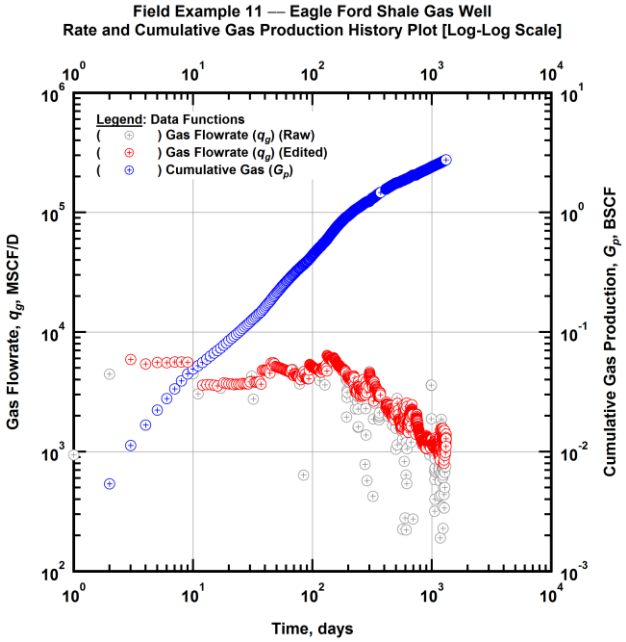

Figure A.304 — (Log-log Plot): Filtered rate and unfiltered cumulative gas production history plot — flowrate (q_g) and cumulative production (G_p) versus production time.

Transient

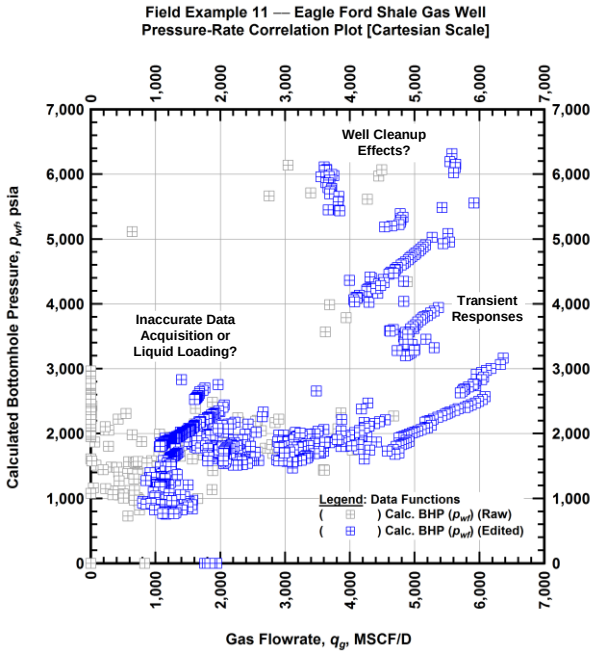

Figure A.305 — (Cartesian Plot): Filtered rate-pressure correlation plot — calculated bottomhole pressure (p_{wf}) versus flowrate (q_g).

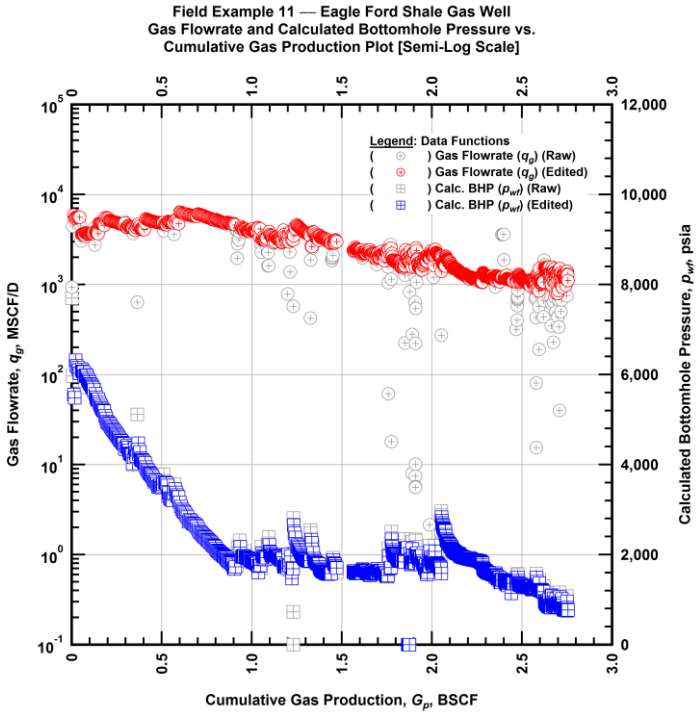

Figure A.306 — (Semi-log Plot): Filtered rate-pressure-cumulative production history plot — flowrate (q_g) and calculated bottomhole pressure (p_{wf}) versus cumulative production (G_p).

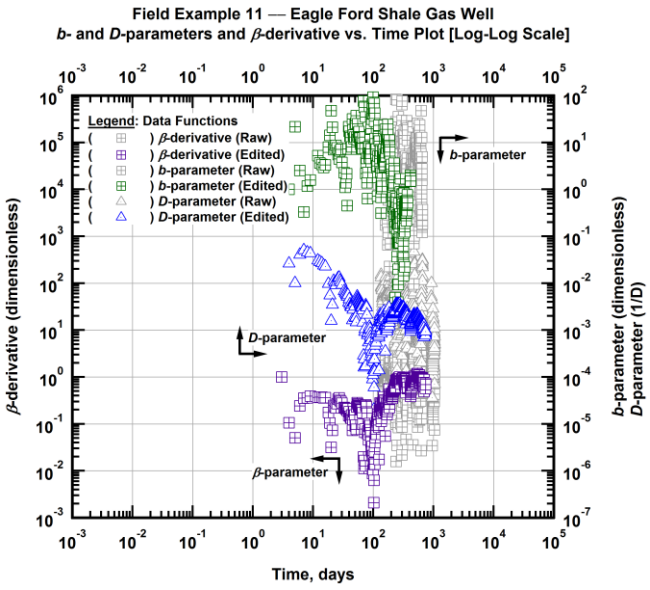

Figure A.307 — (Log-Log Plot): Filtered b, D and β production history plot — b- and D-parameters and β-derivative versus production time.

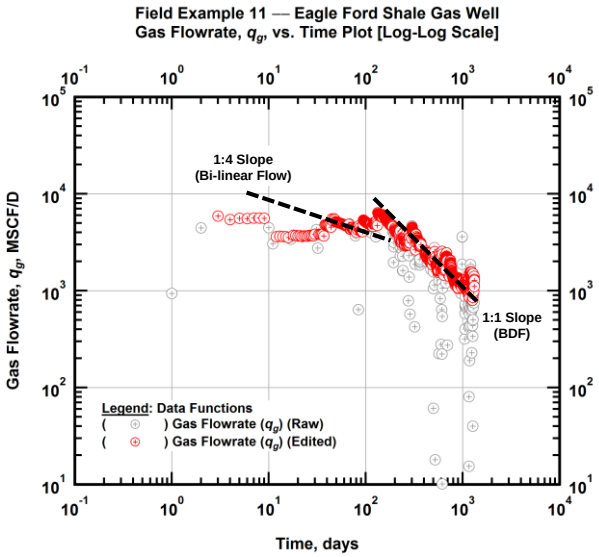

Figure A.308 — (Log-Log Plot): Filtered gas flowrate production history and flow regime identification plot — gas flowrate (q_g) versus production time.

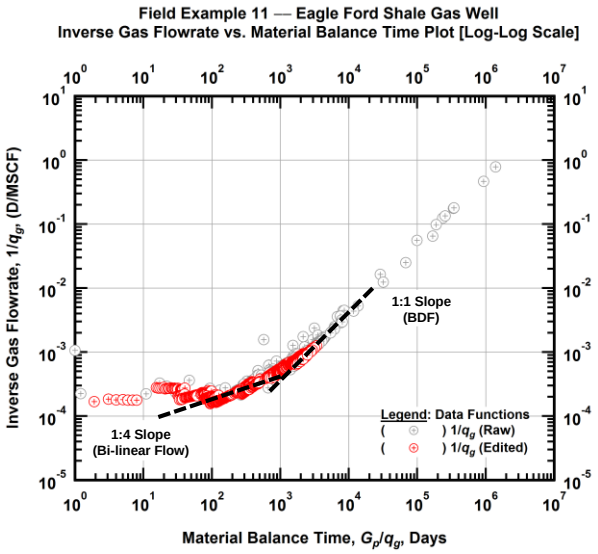

Figure A.309 — (Log-log Plot): Filtered inverse rate with material balance time plot — inverse gas flowrate ($1/q_g$) versus material balance time (G_p/q_g).

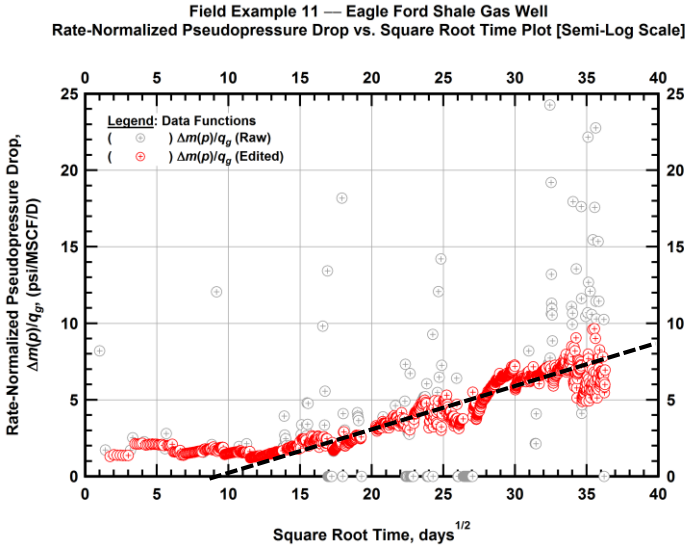

Figure A.310 — (Semi-log Plot): Filtered normalized pseudopressure drop production history plot — rate-normalized pseudopressure drop ($\Delta m(p)/q_g$) versus square root production time ($\sqrt{t}$).

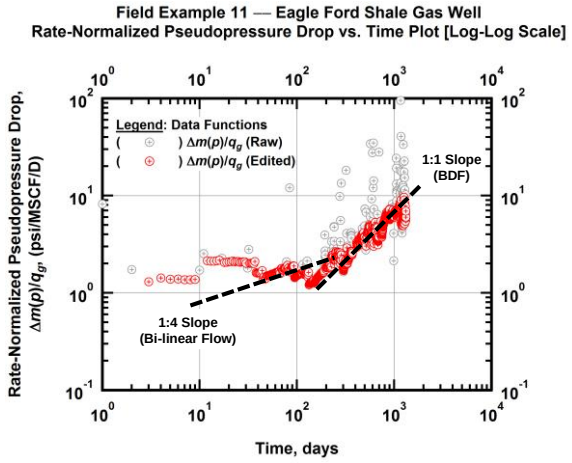

Figure A.311 — (Log-log Plot): Filtered normalized pseudopressure drop production history plot — rate-normalized pseudopressure drop ($\Delta m(p)/q_g$) versus production time.

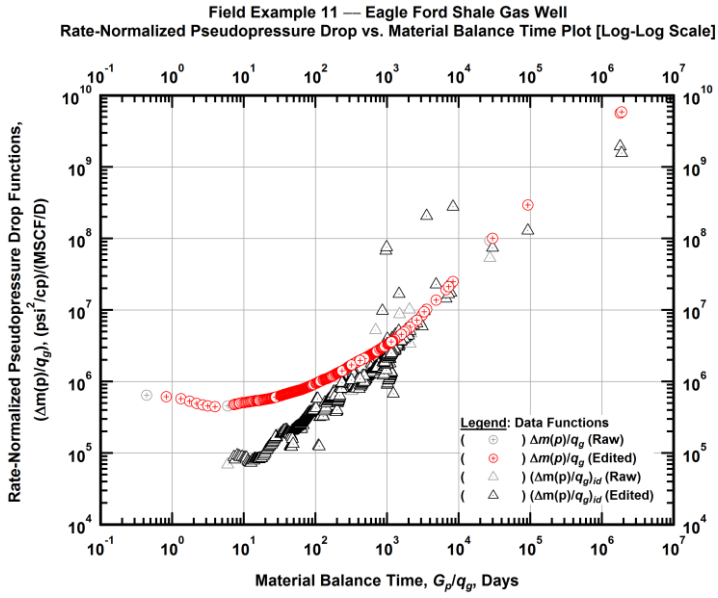

Figure A.312 — (Log-log Plot): "Log-log" diagnostic plot of the filtered production data — rate-normalized pseudopressure drop ($\Delta m(p)/q_g$) and rate-normalized pseudopressure drop integral-derivative $(\Delta m(p)/q_g)_{id}$ versus material balance time (G_p/q_g).

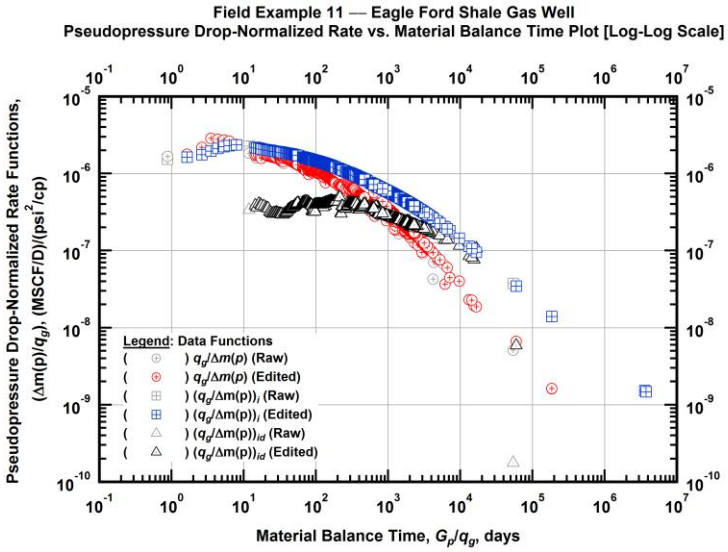

Figure A.313 — (Log-log Plot): "Blasingame" diagnostic plot of the filtered production data — pseudopressure drop-normalized gas flowrate ($q_g/\Delta m(p)$), pseudopressure drop-normalized gas flowrate integral $(q_g/\Delta m(p))_i$ and pseudopressure drop-normalized gas flowrate integral-derivative $(q_g/\Delta m(p))_{id}$ versus material balance time (G_p/q_g).

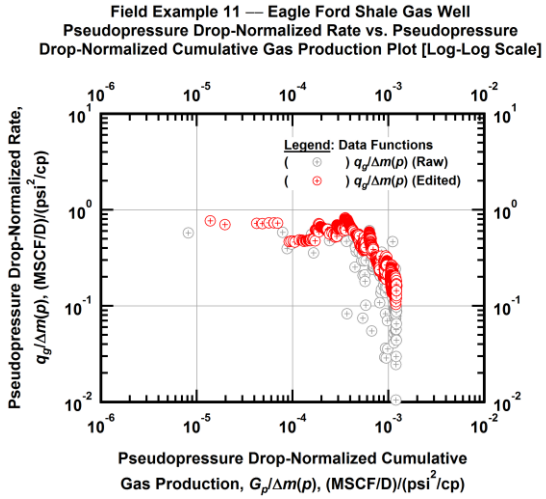

Figure A.314 — (Log-log Plot): Filtered normalized rate with normalized cumulative production plot — pseudopressure drop-normalized gas flowrate ($q_g/\Delta m(p)$) versus pseudopressure drop-normalized cumulative gas production ($G_p/\Delta m(p)$).

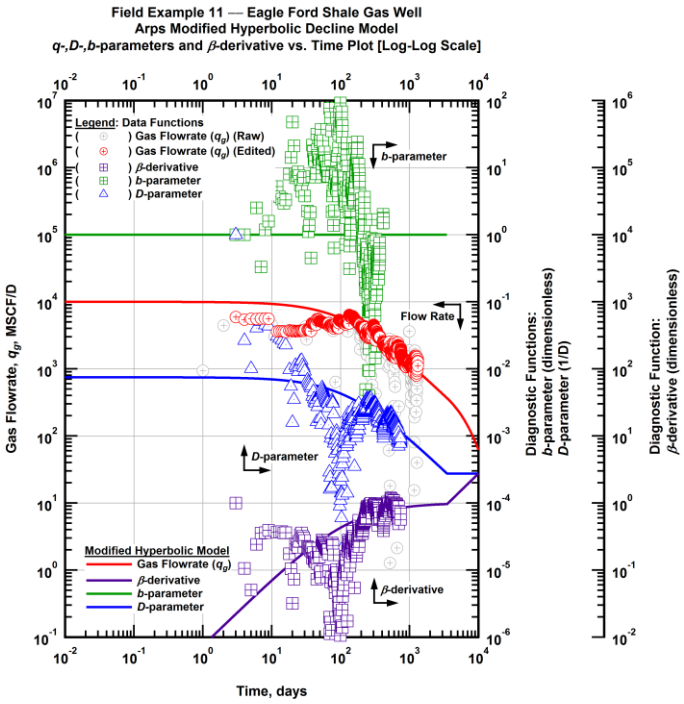

Figure A.315 — (Log-Log Plot): Arps modified hyperbolic decline model plot — time-rate model and data gas flowrate (q_g), *D*- and *b*-parameters and β-derivative versus production time.

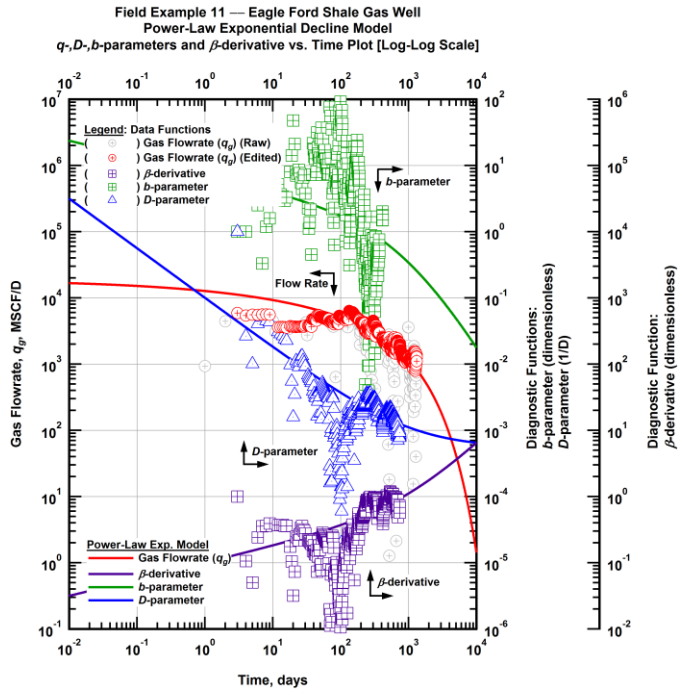

Figure A.316 — (Log-Log Plot): Power-law exponential decline model plot — time-rate model and data gas flowrate (q_g), *D*- and *b*-parameters and β-derivative versus production time.

Field Example 11 — Model-Based (Time-Rate-Pressure) Production Analysis

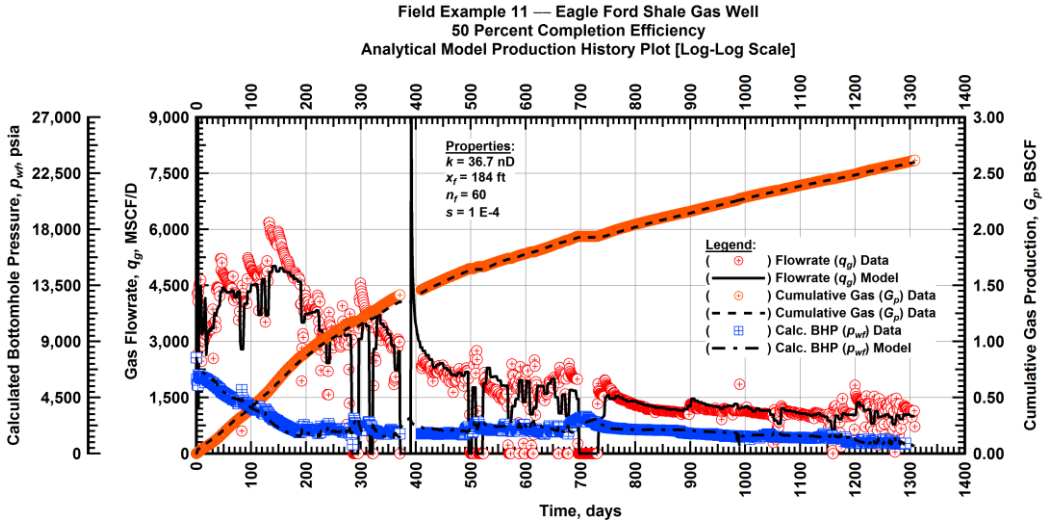

Figure A.317 — (Cartesian Plot): Production history plot — original gas flowrate (q_g), cumulative gas production (G_p), calculated bottomhole pressure (p_{wf}) and 50 percent completion efficiency model matches versus production time.

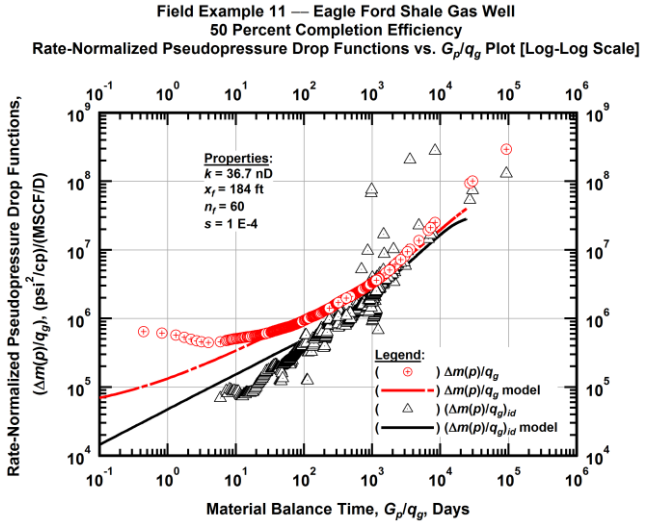

Figure A.318 — (Log-log Plot): "Log-log" diagnostic plot of the original production data — rate-normalized pseudopressure drop ($\Delta m(p)/q_g$), rate-normalized pseudopressure drop integral-derivative $(\Delta m(p)/q_g)_{id}$ and 50 percent completion efficiency model matches versus material balance time (G_p/q_g).

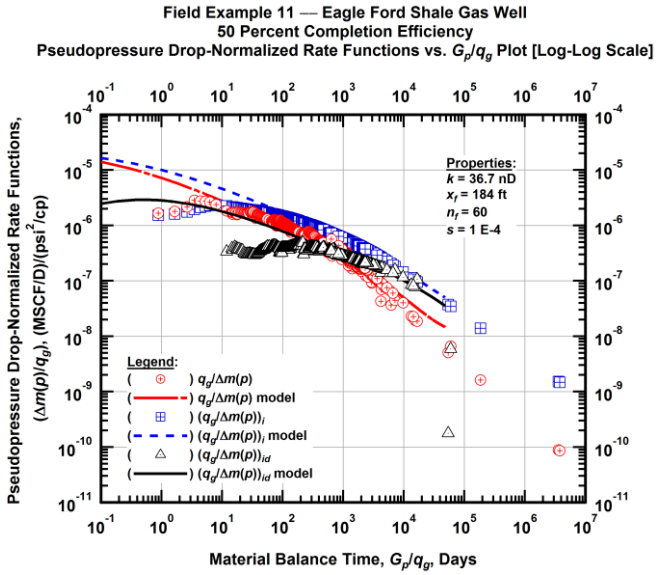

Figure A.319 — (Log-log Plot): "Blasingame" diagnostic plot of the original production data — pseudopressure drop-normalized gas flowrate ($q_g/\Delta m(p)$), pseudopressure drop-normalized gas flowrate integral $(q_g/\Delta m(p))_i$, pseudopressure drop-normalized gas flowrate integral-derivative $(q_g/\Delta m(p))_{id}$ and 50 percent completion efficiency model matches versus material balance time (G_p/q_g).

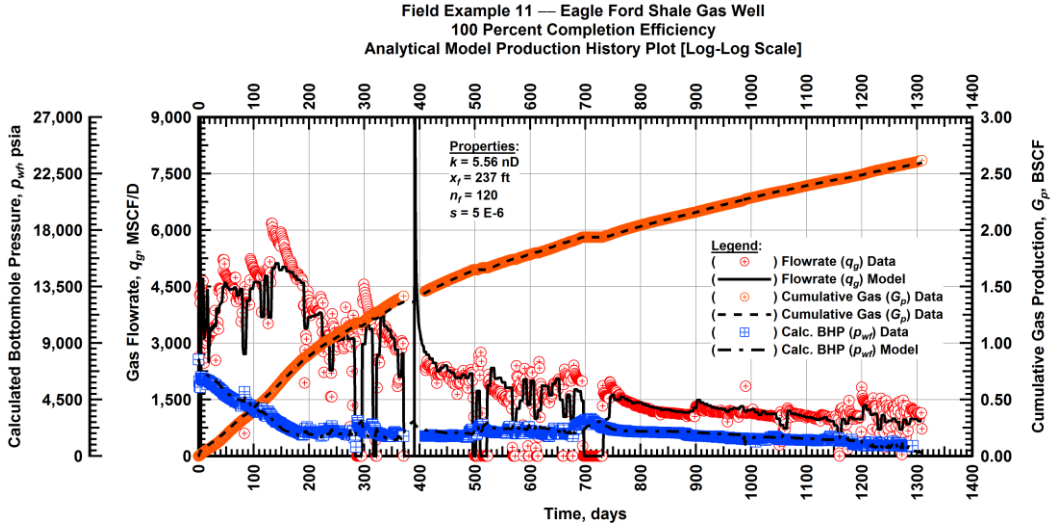

Figure A.320 — (Cartesian Plot): Production history plot — original gas flowrate (q_g), cumulative gas production (G_p), calculated bottomhole pressure (p_{wf}) and 100 percent completion efficiency model matches versus production time.

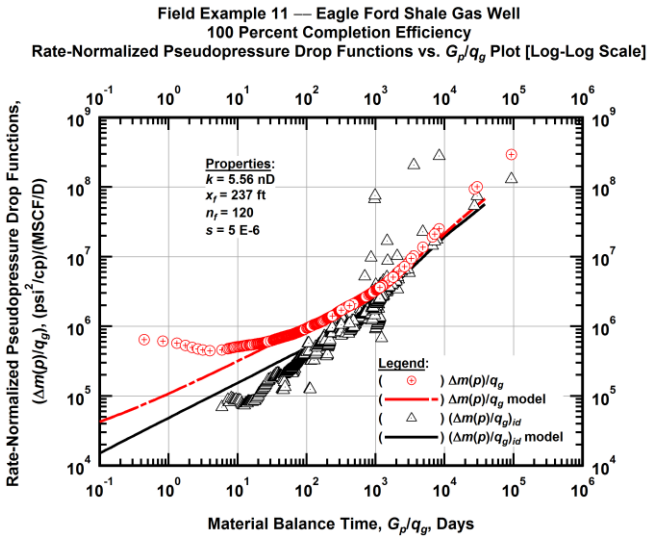

Figure A.321 — (Log-log Plot): "Log-log" diagnostic plot of the original production data — rate-normalized pseudopressure drop ($\Delta m(p)/q_g$), rate-normalized pseudopressure drop integral-derivative $(\Delta m(p)/q_g)_{id}$ and 100 percent completion efficiency model matches versus material balance time (G_p/q_g).

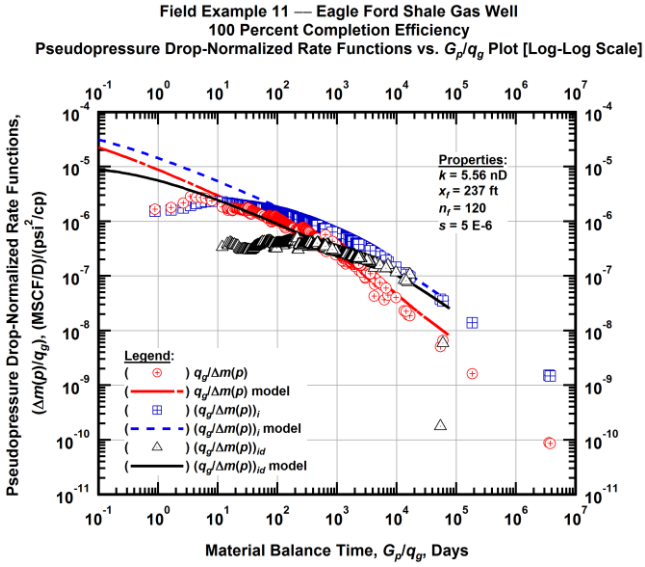

Figure A.322 — (Log-log Plot): "Blasingame" diagnostic plot of the original production data — pseudopressure drop-normalized gas flowrate ($q_g/\Delta m(p)$), pseudopressure drop-normalized gas flowrate integral $(q_g/\Delta m(p))_i$, pseudopressure drop-normalized gas flowrate integral-derivative $(q_g/\Delta m(p))_{id}$ and 100 percent completion efficiency model matches versus material balance time (G_p/q_g).

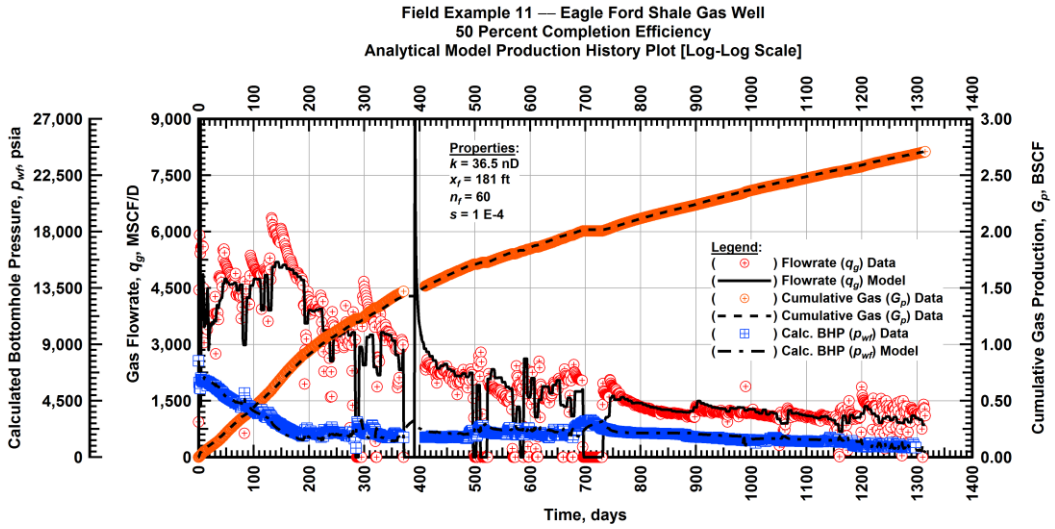

Figure A.323 — (Cartesian Plot): Production history plot — revised gas flowrate (q_g), cumulative gas production (G_p), calculated bottomhole pressure (p_{wf}) and 50 percent completion efficiency model matches versus production time.

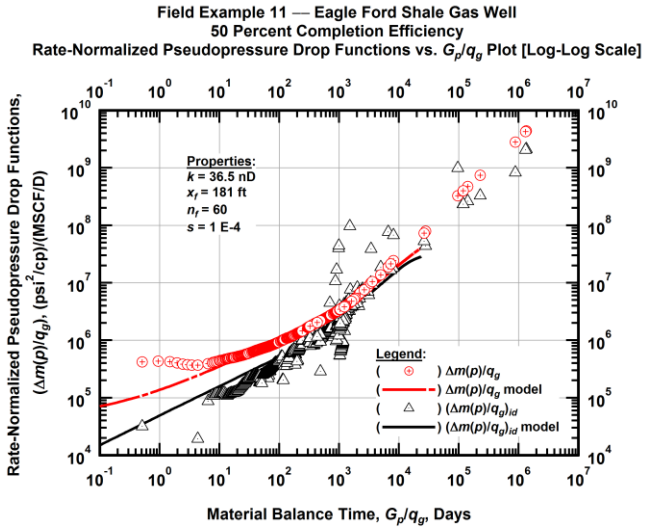

Figure A.324— (Log-log Plot): "Log-log" diagnostic plot of the revised production data — rate-normalized pseudopressure drop ($\Delta m(p)/q_g$), rate-normalized pseudopressure drop integral-derivative $(\Delta m(p)/q_g)_{id}$ and 50 percent completion efficiency model matches versus material balance time (G_p/q_g).

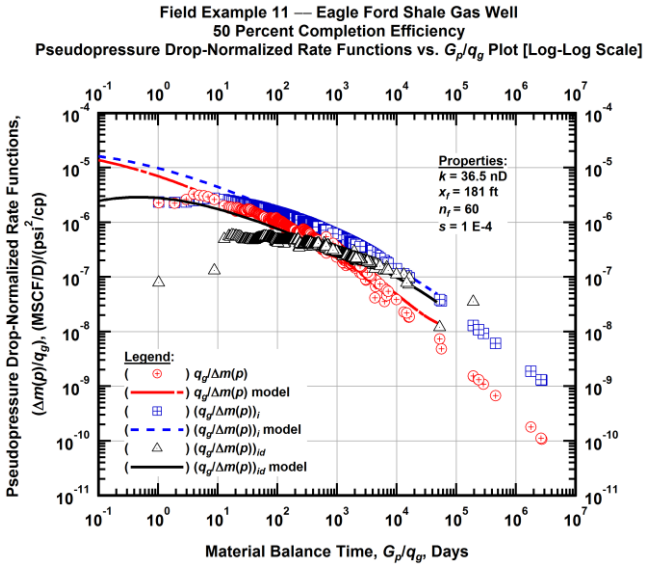

Figure A.325 — (Log-log Plot): "Blasingame" diagnostic plot of the revised production data — pseudopressure drop-normalized gas flowrate ($q_g/\Delta m(p)$), pseudopressure drop-normalized gas flowrate integral $(q_g/\Delta m(p))_i$, pseudopressure drop-normalized gas flowrate integral-derivative $(q_g/\Delta m(p))_{id}$ and 50 percent completion efficiency model matches versus material balance time (G_p/q_g).

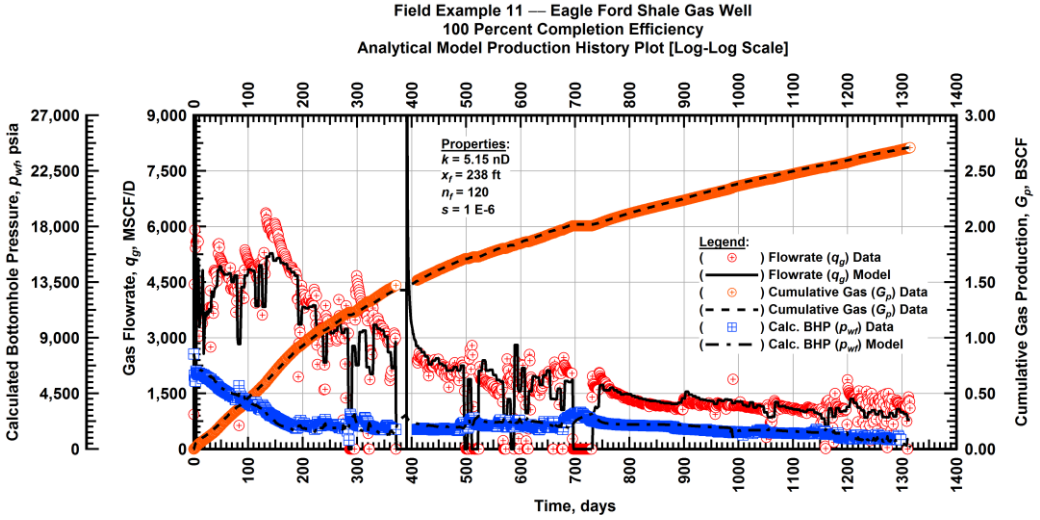

Figure A.326 — (Cartesian Plot): Production history plot — revised gas flowrate (q_g), cumulative gas production (G_p), calculated bottomhole pressure (p_{wf}) and 100 percent completion efficiency model matches versus production time.

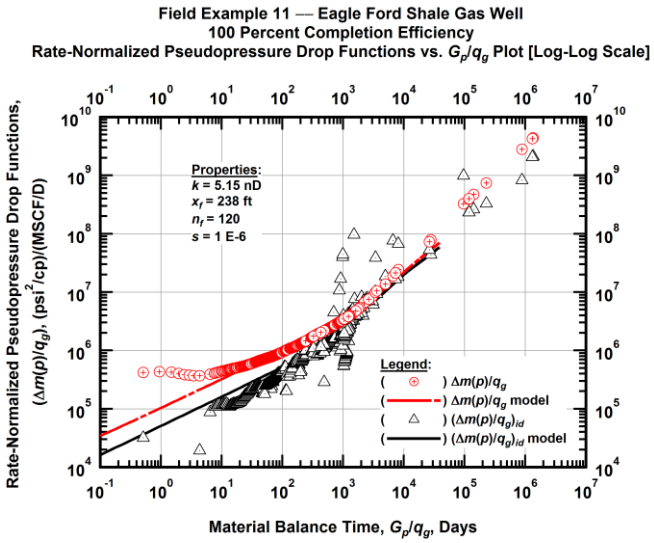

Figure A.327 — (Log-log Plot): "Log-log" diagnostic plot of the revised production data — rate-normalized pseudopressure drop ($\Delta m(p)/q_g$), rate-normalized pseudopressure drop integral-derivative $(\Delta m(p)/q_g)_{id}$ and 100 percent completion efficiency model matches versus material balance time (G_p/q_g).

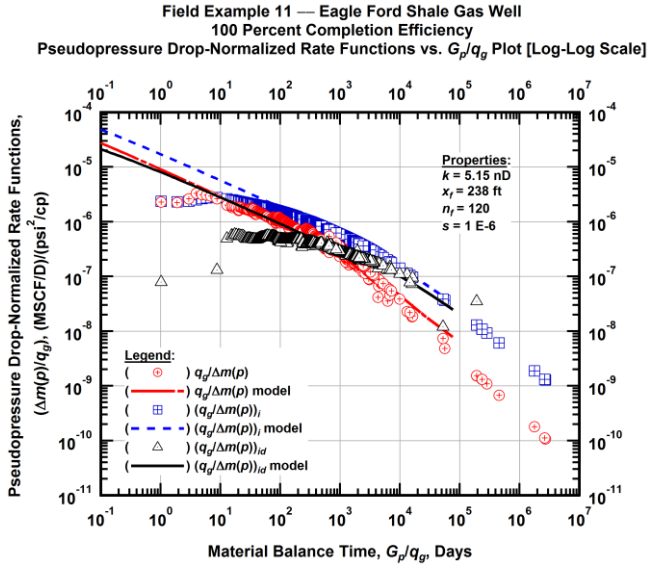

Figure A.328 — (Log-log Plot): "Blasingame" diagnostic plot of the revised production data — pseudopressure drop-normalized gas flowrate ($q_g/\Delta m(p)$), pseudopressure drop-normalized gas flowrate integral $(q_g/\Delta m(p))_i$, pseudopressure drop-normalized gas flowrate integral-derivative $(q_g/\Delta m(p))_{id}$ and 100 percent completion efficiency model matches versus material balance time (G_p/q_g).

Field Example 11 — 30-Year EUR Model Comparison

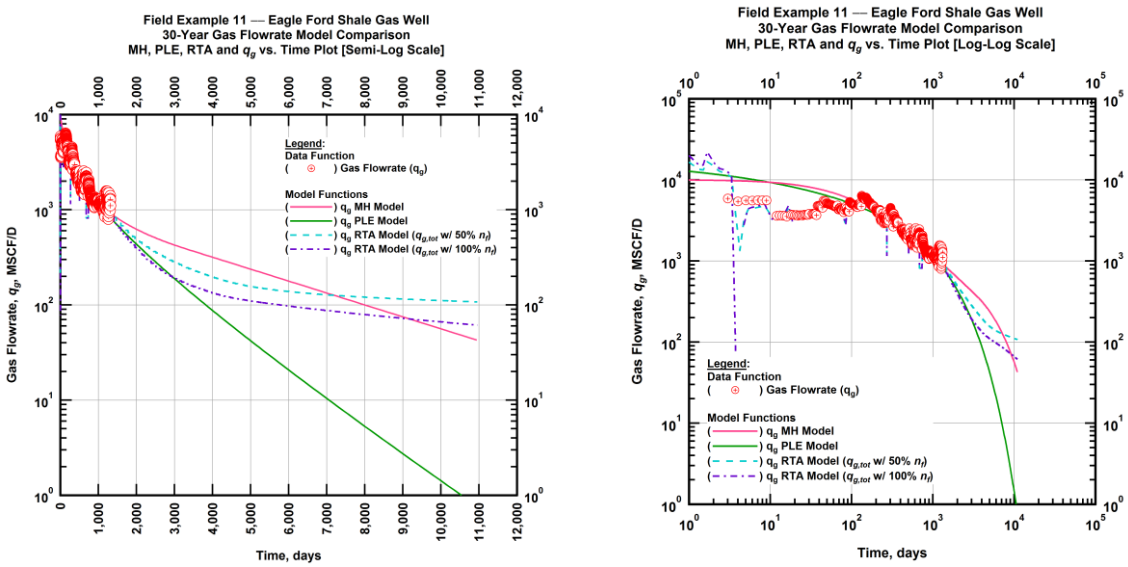

A **B**

Figure A.329 — (A — Semi-Log Plot) and (B — Log-Log Plot): Estimated 30-year revised gas flowrate model comparison — Arps modified hyperbolic decline model, power-law exponential decline model, and 50 percent and 100 percent completion efficiency RTA models revised gas 30-year estimated flowrate decline and historic gas flowrate data (q_g) versus production time.

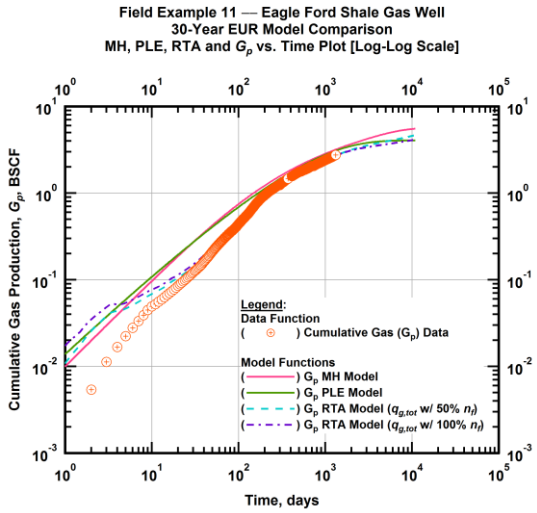

Figure A.330 — (Log-log Plot): PVT revised gas 30-year estimated cumulative production volume model comparison — Arps modified hyperbolic decline model, power-law exponential decline model, and 50 percent and 100 percent completion efficiency RTA model estimated 30-year cumulative gas production volumes and historic cumulative gas production (G_p) versus production time.

Table A.11 — 30-year estimated cumulative revised gas production (EUR), in units of BSCF, for the Arps modified hyperbolic, power-law exponential and analytical time-rate-pressure decline models.

Arps Modified Hyperbolic BSCF)	Power-Law Exponential (BSCF)	RTA Analytical Model ($q_{g,tot}$ w/ 50% n_f) (BSCF)	RTA Analytical Model ($q_{g,tot}$ w/ 100% n_f) (BSCF)
5.19	3.71	4.81	4.21

Field Example 12 — Time-Rate Analysis

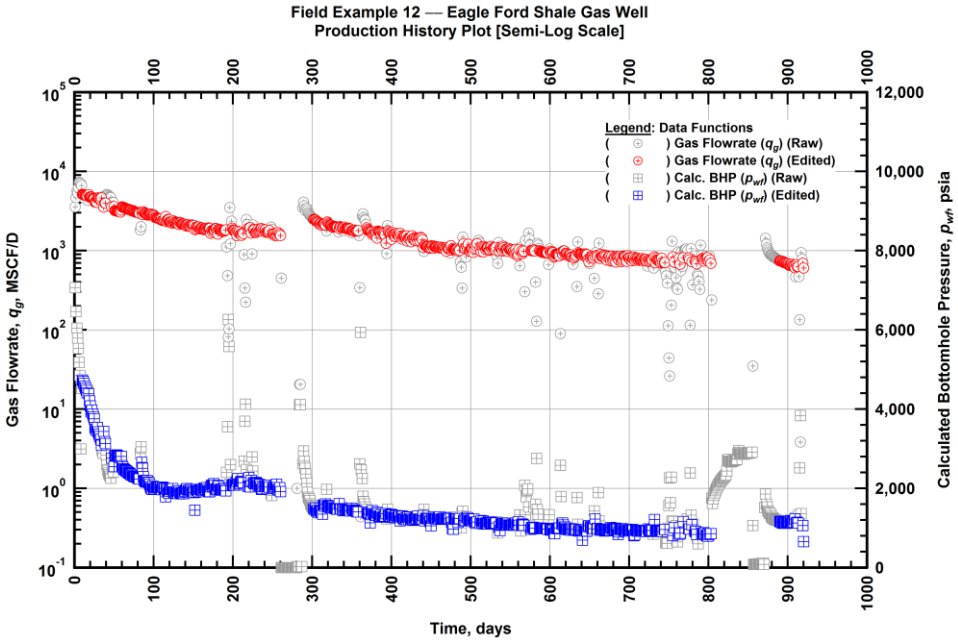

Figure A.331 — (Semi-log Plot): Filtered production history plot — flowrate (q_g) and calculated bottomhole pressure (p_{wf}) versus production time.

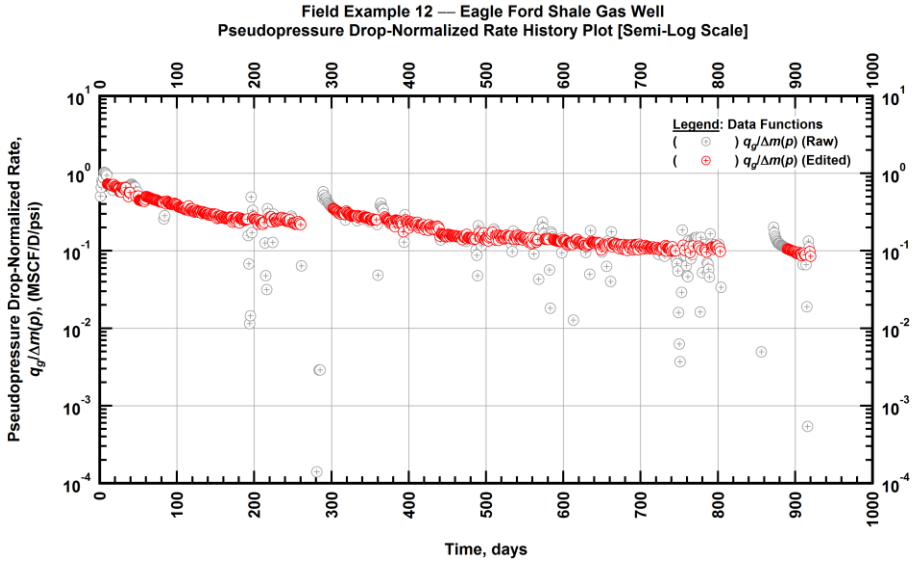

Figure A.332 — (Semi-log Plot): Filtered normalized rate production history plot — pseudopressure drop-normalized gas flowrate ($q_g/\Delta m(p)$) versus production time.

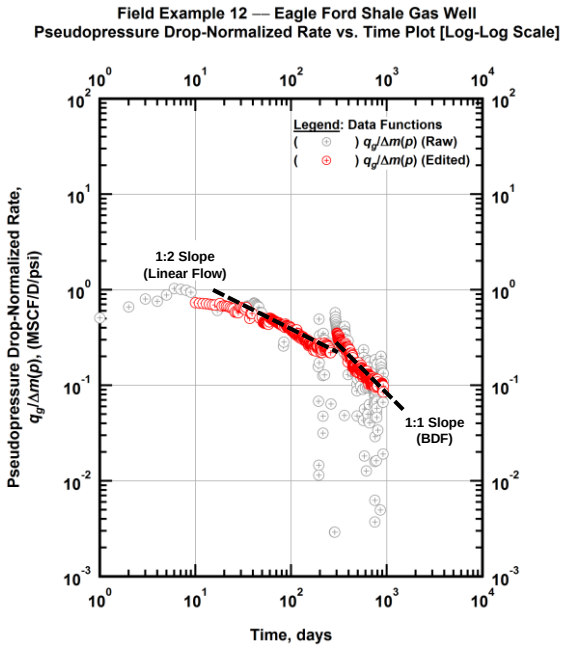

Figure A.333 — (Log-log Plot): Filtered normalized rate production history plot — pseudopressure drop-normalized gas flowrate ($q_g/\Delta m(p)$) versus production time.

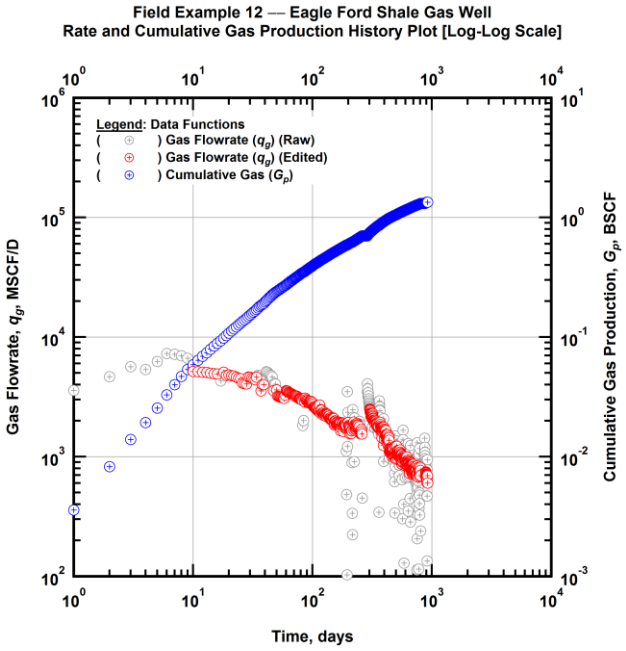

Figure A.334 — (Log-log Plot): Filtered rate and unfiltered cumulative gas production history plot — flowrate (q_g) and cumulative production (G_p) versus production time.

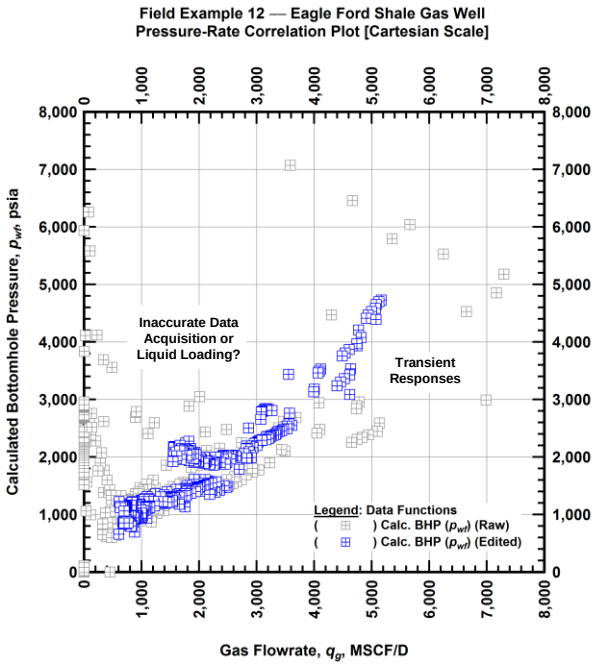

Figure A.335 — (Cartesian Plot): Filtered rate-pressure correlation plot — calculated bottomhole pressure (p_{wf}) versus flowrate (q_g).

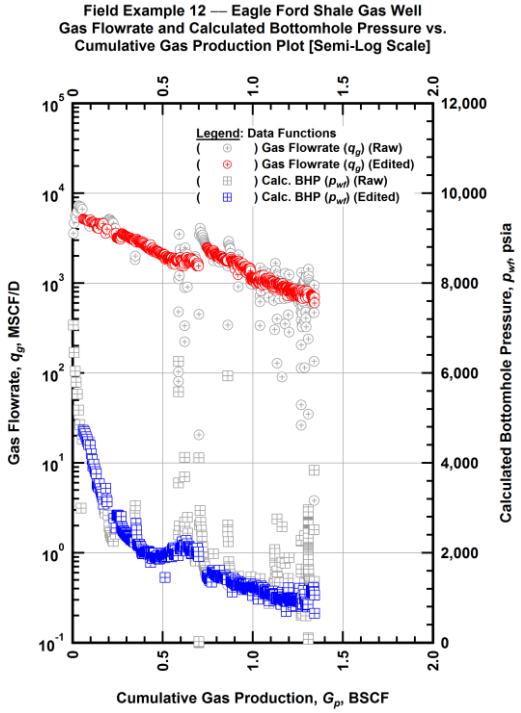

Figure A.336 — (Semi-log Plot): Filtered rate-pressure-cumulative production history plot — flowrate (q_g) and calculated bottomhole pressure (p_{wf}) versus cumulative production (G_p).

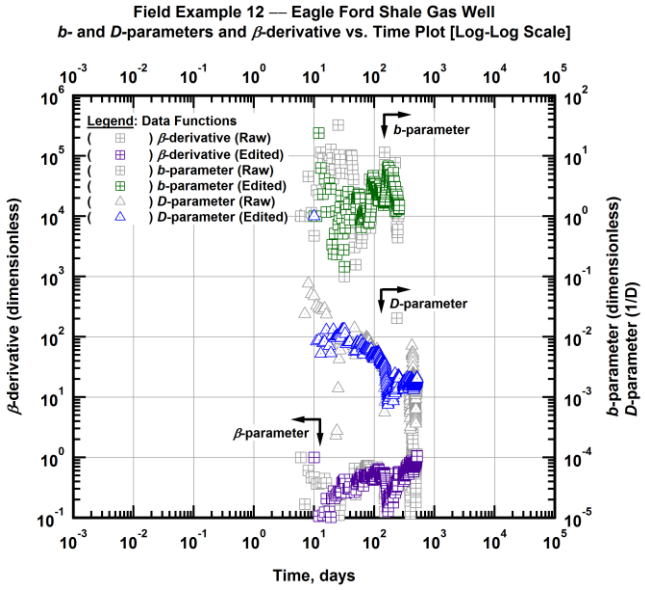

Figure A.337 — (Log-Log Plot): Filtered b, D and β production history plot — b- and D-parameters and β-derivative versus production time.

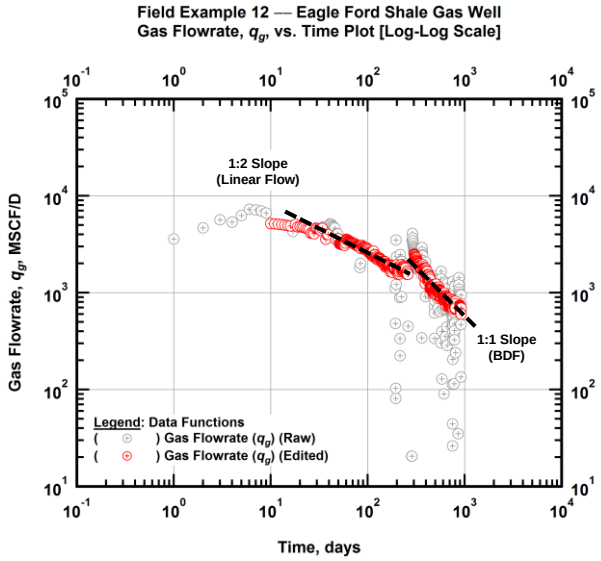

Figure A.338 — (Log-Log Plot): Filtered gas flowrate production history and flow regime identification plot — gas flowrate (q_g) versus production time.

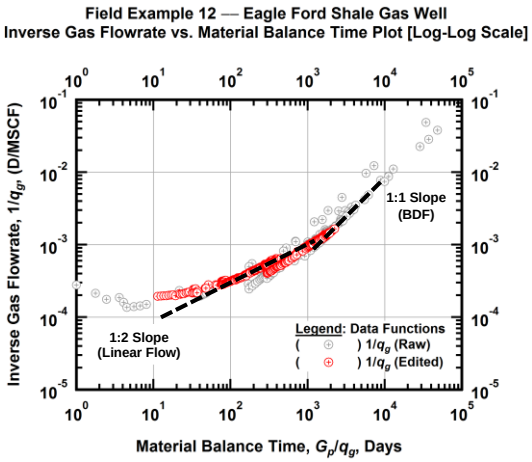

Figure A.339 — (Log-log Plot): Filtered inverse rate with material balance time plot — inverse gas flowrate ($1/q_g$) versus material balance time (G_p/q_g).

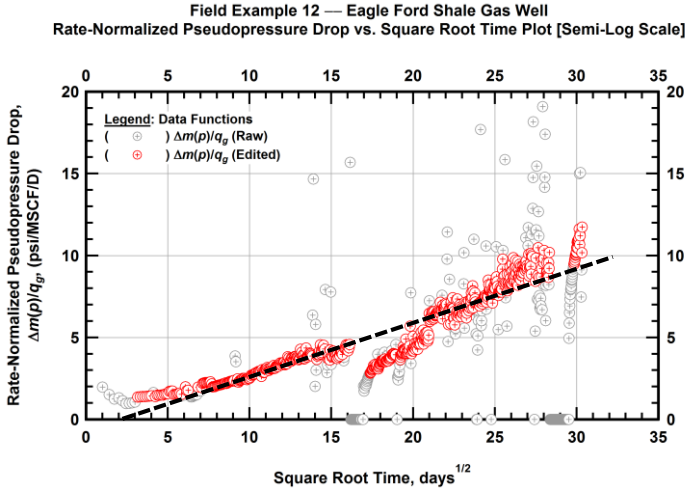

Figure A.340 — (Semi-log Plot): Filtered normalized pseudopressure drop production history plot — rate-normalized pseudopressure drop ($\Delta m(p)/q_g$) versus square root production time ($\sqrt{t}$).

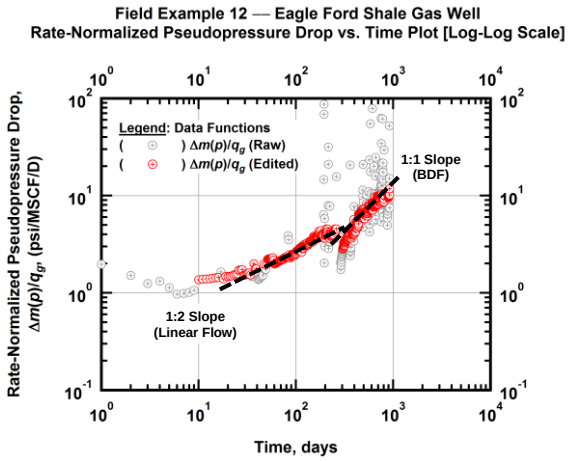

Figure A.341 — (Log-log Plot): Filtered normalized pseudopressure drop production history plot — rate-normalized pseudopressure drop ($\Delta m(p)/q_g$) versus production time.

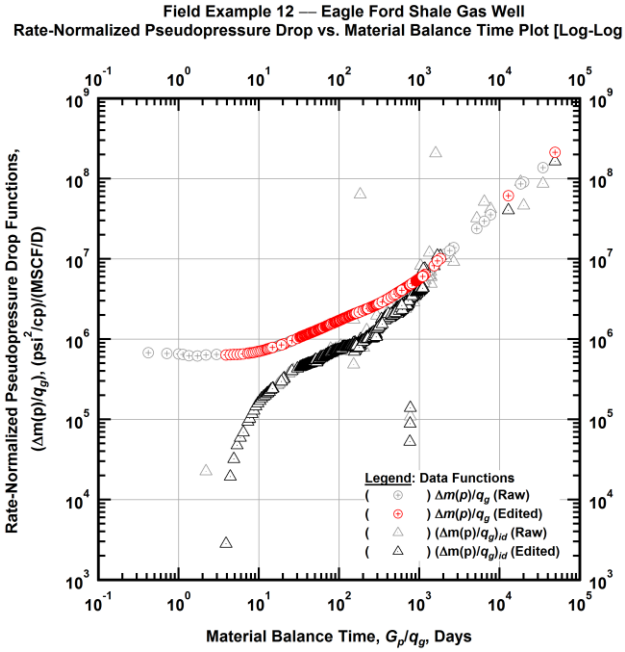

Figure A.342 — (Log-log Plot): "Log-log" diagnostic plot of the filtered production data — rate-normalized pseudopressure drop ($\Delta m(p)/q_g$) and rate-normalized pseudopressure drop integral-derivative $(\Delta m(p)/q_g)_{id}$ versus material balance time (G_p/q_g).

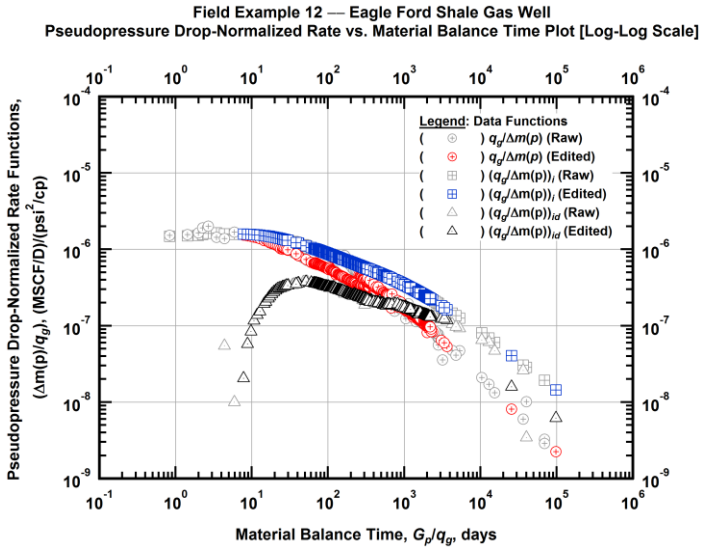

Figure A.343 — (Log-log Plot): "Blasingame" diagnostic plot of the filtered production data — pseudopressure drop-normalized gas flowrate ($q_g/\Delta m(p)$), pseudopressure drop-normalized gas flowrate integral $(q_g/\Delta m(p))_i$ and pseudopressure drop-normalized gas flowrate integral-derivative $(q_g/\Delta m(p))_{id}$ versus material balance time (G_p/q_g).

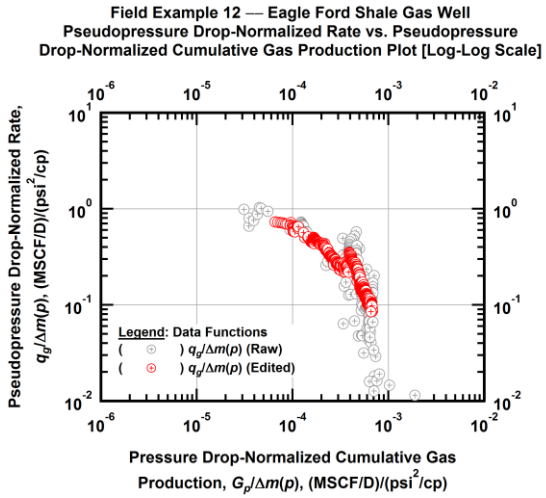

Figure A.344 — (Log-log Plot): Filtered normalized rate with normalized cumulative production plot — pseudopressure drop-normalized gas flowrate ($q_g/\Delta m(p)$) versus pseudopressure drop-normalized cumulative gas production ($G_p/\Delta m(p)$).

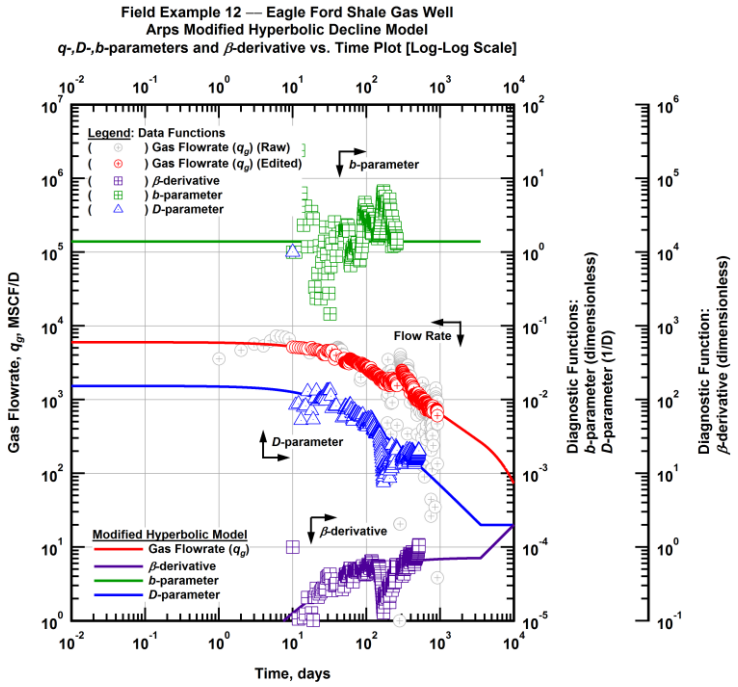

Figure A.345 — (Log-Log Plot): Arps modified hyperbolic decline model plot — time-rate model and data gas flowrate (q_g), *D*- and *b*-parameters and β-derivative versus production time.

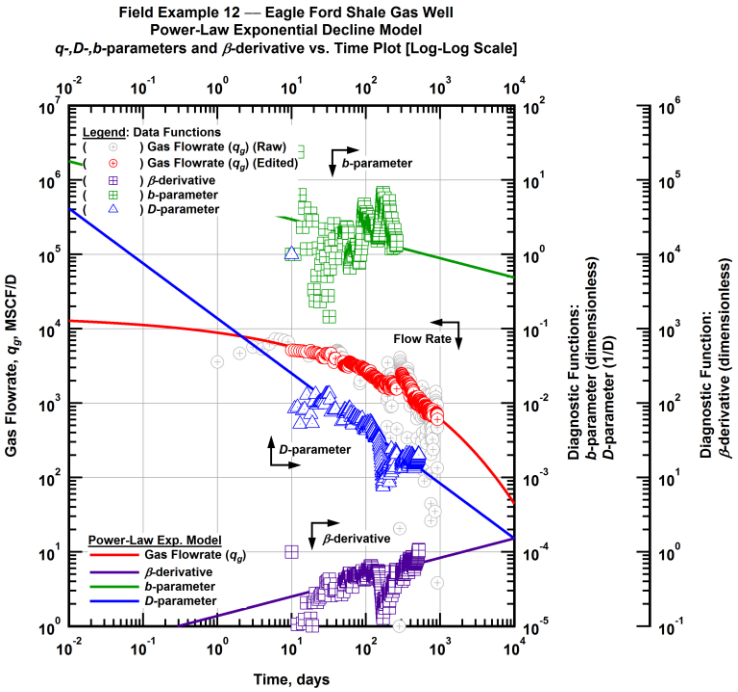

Figure A.346 — (Log-Log Plot): Power-law exponential decline model plot — time-rate model and data gas flowrate (q_g), *D*- and *b*-parameters and β-derivative versus production time.

Field Example 12 — Model-Based (Time-Rate-Pressure) Production Analysis

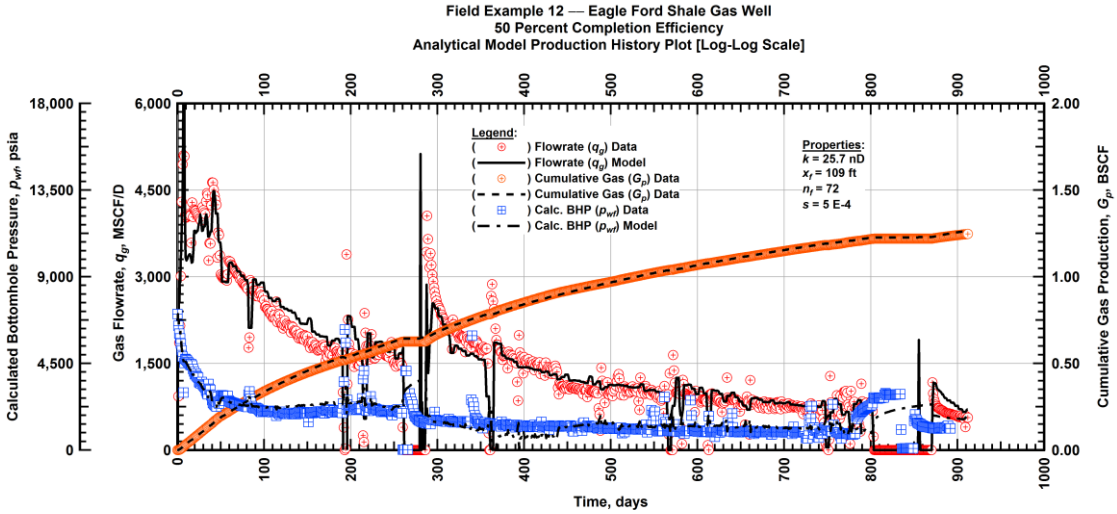

Figure A.347 — (Cartesian Plot): Production history plot — original gas flowrate (q_g), cumulative gas production (G_p), calculated bottomhole pressure (p_{wf}) and 50 percent completion efficiency model matches versus production time.

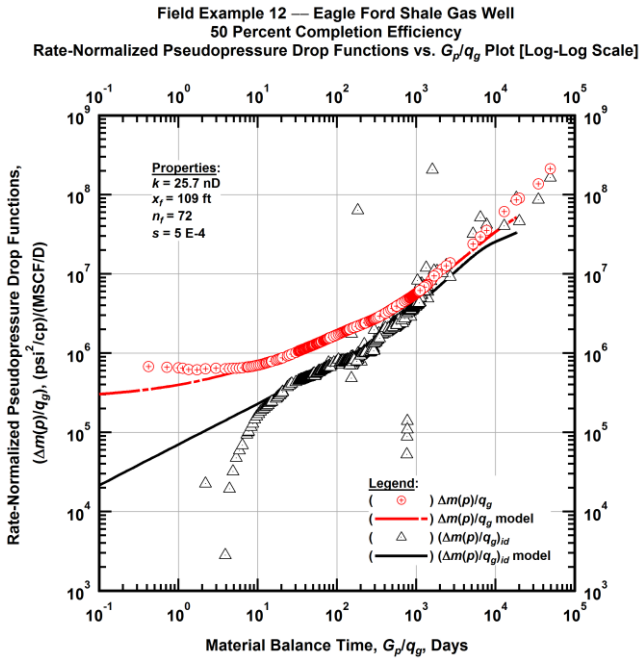

Figure A.348 — (Log-log Plot): "Log-log" diagnostic plot of the original production data — rate-normalized pseudopressure drop ($\Delta m(p)/q_g$), rate-normalized pseudopressure drop integral-derivative $(\Delta m(p)/q_g)_{id}$ and 50 percent completion efficiency model matches versus material balance time (G_p/q_g).

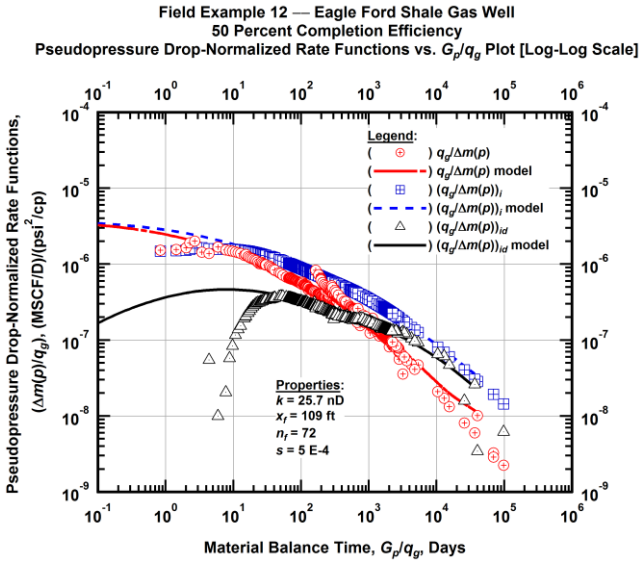

Figure A.349 — (Log-log Plot): "Blasingame" diagnostic plot of the original production data — pseudopressure drop-normalized gas flowrate ($q_g/\Delta m(p)$), pseudopressure drop-normalized gas flowrate integral $(q_g/\Delta m(p))_i$, pseudopressure drop-normalized gas flowrate integral-derivative $(q_g/\Delta m(p))_{id}$ and 50 percent completion efficiency model matches versus material balance time (G_p/q_g).

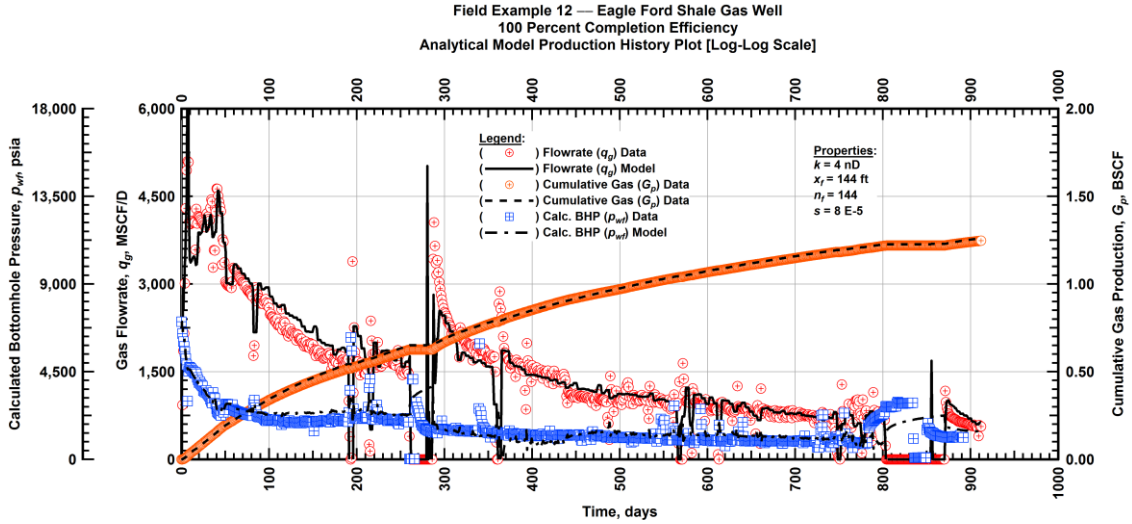

Figure A.350 — (Cartesian Plot): Production history plot — original gas flowrate (q_g), cumulative gas production (G_p), calculated bottomhole pressure (p_{wf}) and 100 percent completion efficiency model matches versus production time.

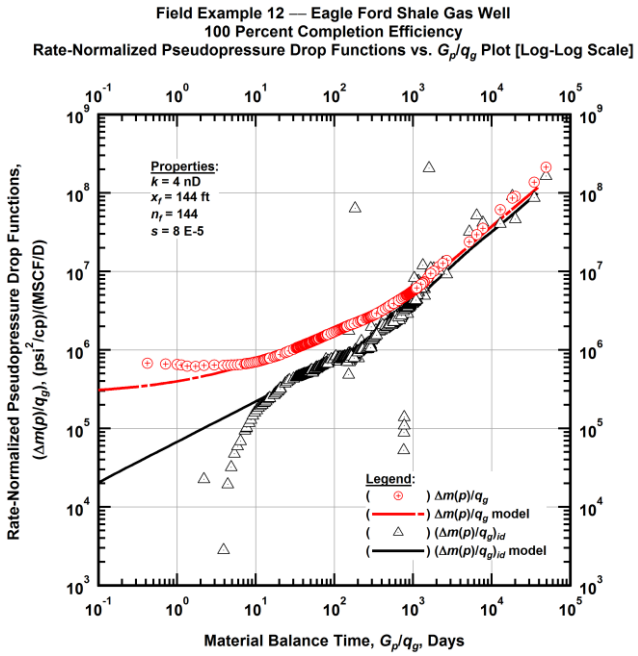

Figure A.351 — (Log-log Plot): "Log-log" diagnostic plot of the original production data — rate-normalized pseudopressure drop ($\Delta m(p)/q_g$), rate-normalized pseudopressure drop integral-derivative $(\Delta m(p)/q_g)_{id}$ and 100 percent completion efficiency model matches versus material balance time (G_p/q_g).

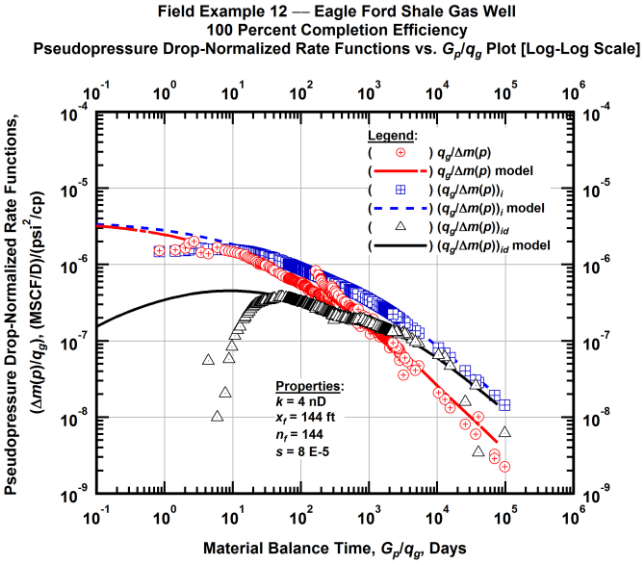

Figure A.352 — (Log-log Plot): "Blasingame" diagnostic plot of the original production data — pseudopressure drop-normalized gas flowrate ($q_g/\Delta m(p)$), pseudopressure drop-normalized gas flowrate integral $(q_g/\Delta m(p))_i$, pseudopressure drop-normalized gas flowrate integral-derivative $(q_g/\Delta m(p))_{id}$ and 100 percent completion efficiency model matches versus material balance time (G_p/q_g).

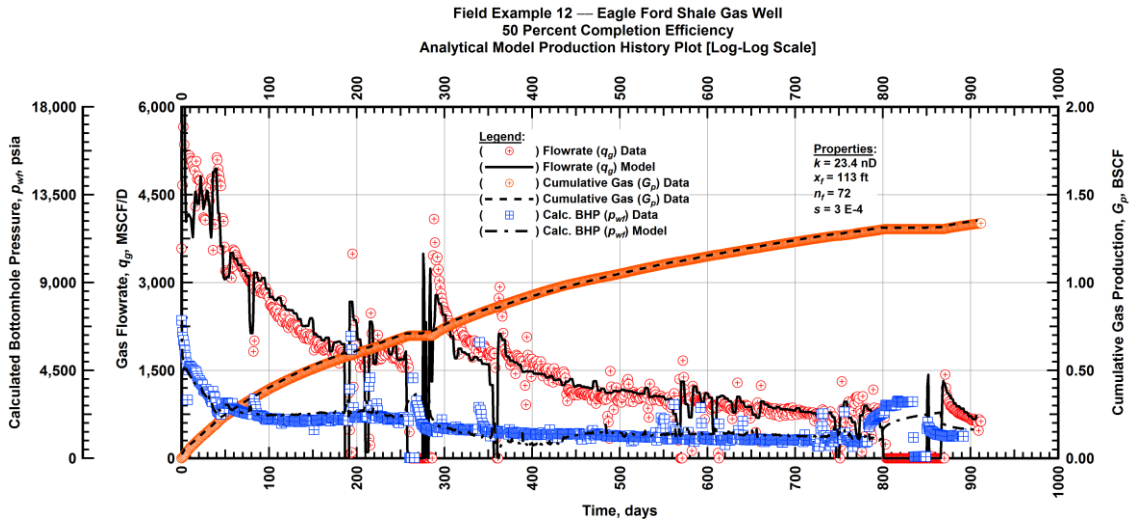

Figure A.353 — (Cartesian Plot): Production history plot — revised gas flowrate (q_g), cumulative gas production (G_p), calculated bottomhole pressure (p_{wf}) and 50 percent completion efficiency model matches versus production time.

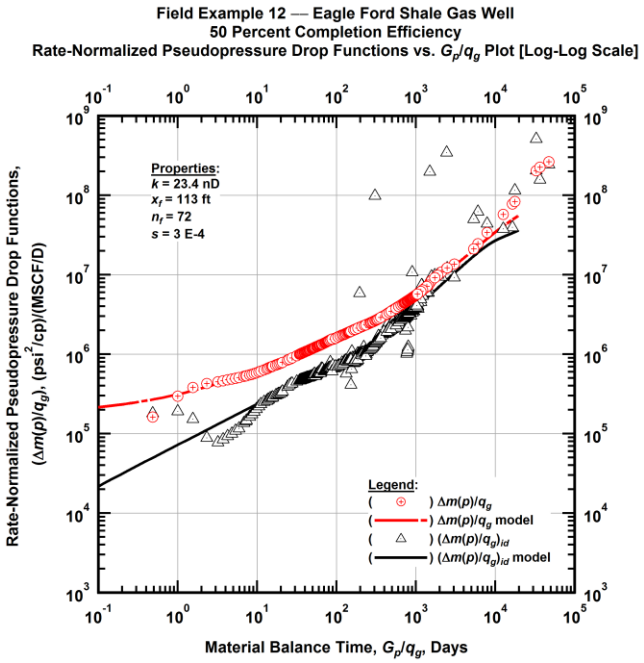

Figure A.354— (Log-log Plot): "Log-log" diagnostic plot of the revised production data — rate-normalized pseudopressure drop ($\Delta m(p)/q_g$), rate-normalized pseudopressure drop integral-derivative $(\Delta m(p)/q_g)_{id}$ and 50 percent completion efficiency model matches versus material balance time (G_p/q_g).

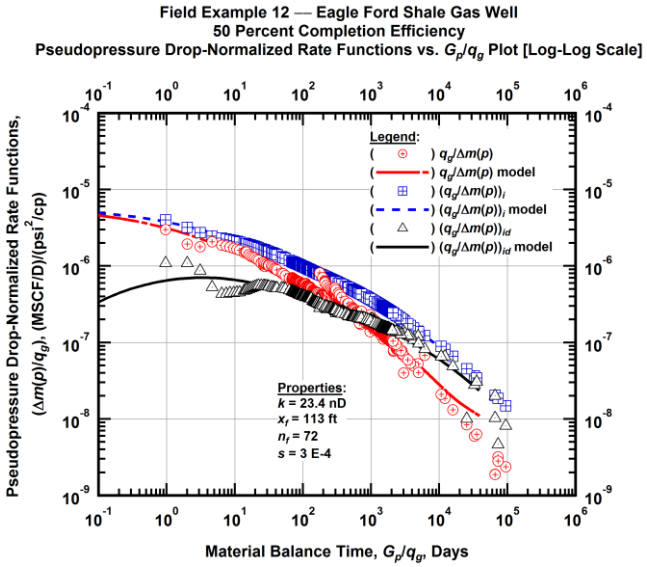

Figure A.355 — (Log-log Plot): "Blasingame" diagnostic plot of the revised production data — pseudopressure drop-normalized gas flowrate ($q_g/\Delta m(p)$), pseudopressure drop-normalized gas flowrate integral $(q_g/\Delta m(p))_i$, pseudopressure drop-normalized gas flowrate integral-derivative $(q_g/\Delta m(p))_{id}$ and 50 percent completion efficiency model matches versus material balance time (G_p/q_g).

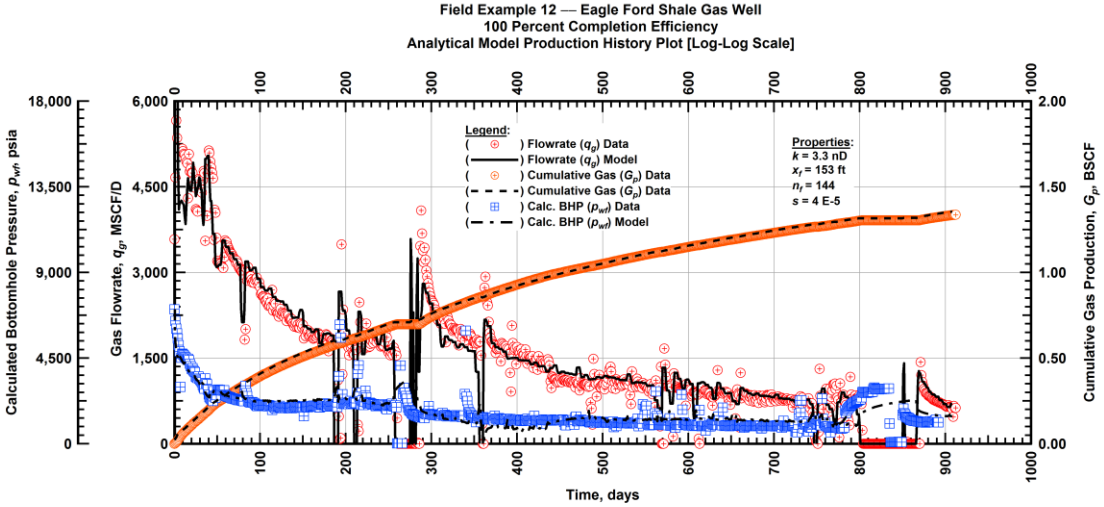

Figure A.356 — (Cartesian Plot): Production history plot — revised gas flowrate (q_g), cumulative gas production (G_p), calculated bottomhole pressure (p_{wf}) and 100 percent completion efficiency model matches versus production time.

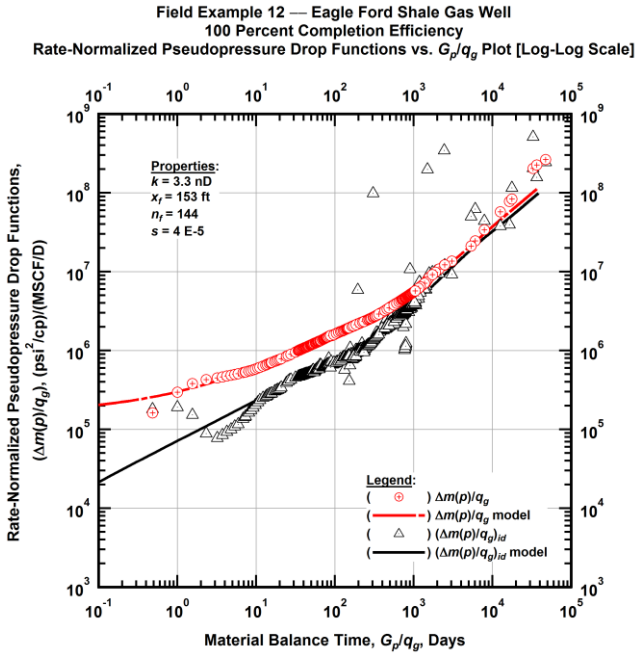

Figure A.357 — (Log-log Plot): "Log-log" diagnostic plot of the revised production data — rate-normalized pseudopressure drop ($\Delta m(p)/q_g$), rate-normalized pseudopressure drop integral-derivative $(\Delta m(p)/q_g)_{id}$ and 100 percent completion efficiency model matches versus material balance time (G_p/q_g).

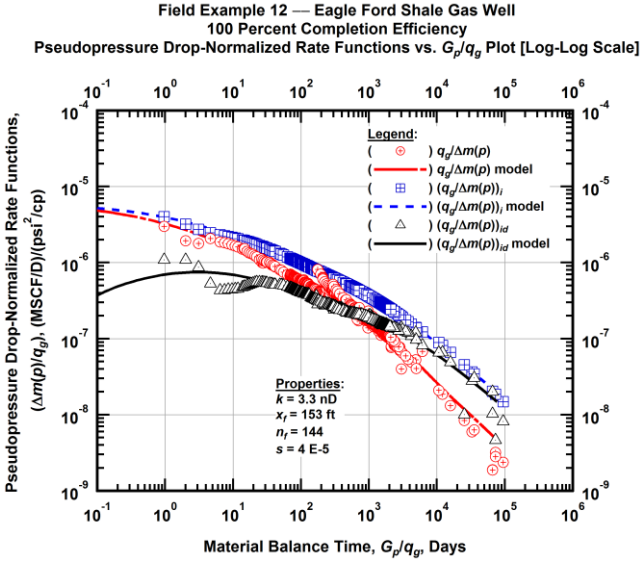

Figure A.358 — (Log-log Plot): "Blasingame" diagnostic plot of the revised production data — pseudopressure drop-normalized gas flowrate ($q_g/\Delta m(p)$), pseudopressure drop-normalized gas flowrate integral $(q_g/\Delta m(p))_i$, pseudopressure drop-normalized gas flowrate integral-derivative $(q_g/\Delta m(p))_{id}$ and 100 percent completion efficiency model matches versus material balance time (G_p/q_g).

Field Example 12 — 30-Year EUR Model Comparison

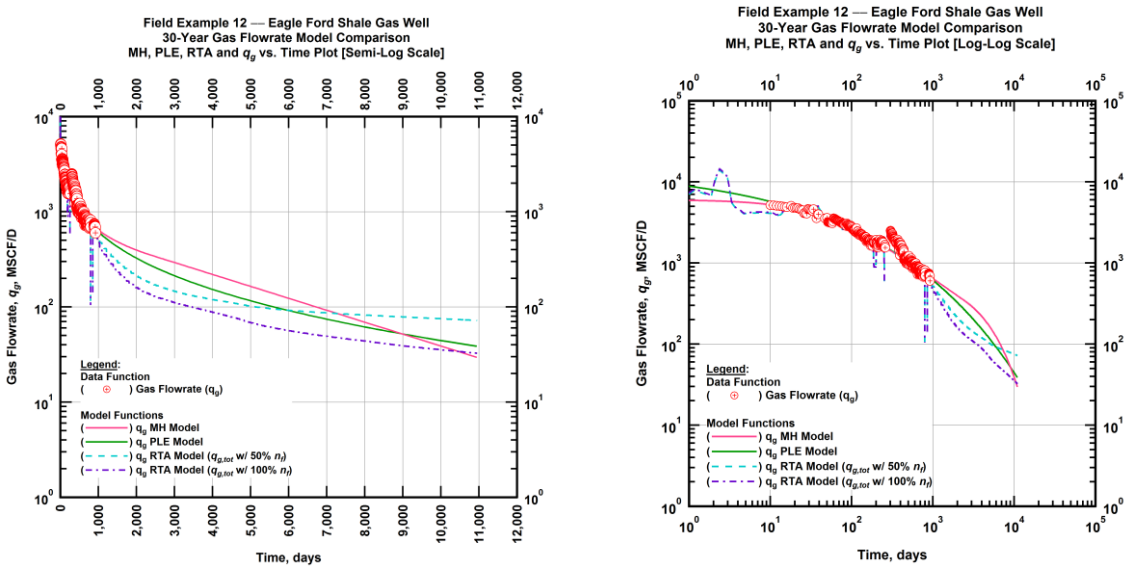

A **B**

Figure A.359 — (A — Semi-Log Plot) and (B — Log-Log Plot): Estimated 30-year revised gas flowrate model comparison — Arps modified hyperbolic decline model, power-law exponential decline model, and 50 percent and 100 percent completion efficiency RTA models revised gas 30-year estimated flowrate decline and historic gas flowrate data (q_g) versus production time.

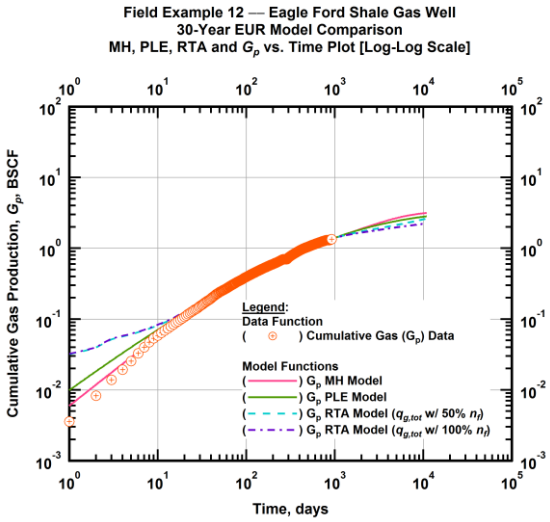

Figure A.360 — (Log-log Plot): PVT revised gas 30-year estimated cumulative production volume model comparison — Arps modified hyperbolic decline model, power-law exponential decline model, and 50 percent and 100 percent completion efficiency RTA model estimated 30-year cumulative gas production volumes and historic cumulative gas production (G_p) versus production time.

Table A.12 — 30-year estimated cumulative revised gas production (EUR), in units of BSCF, for the Arps modified hyperbolic, power-law exponential and analytical time-rate-pressure decline models.

Arps Modified Hyperbolic (BSCF)	Power-Law Exponential (BSCF)	RTA Analytical Model ($q_{g,tot}$ w/ 50% n_f) (BSCF)	RTA Analytical Model ($q_{g,tot}$ w/ 100% n_f) (BSCF)
3.21	2.83	2.70	2.27

Field Example 13 — Time-Rate Analysis

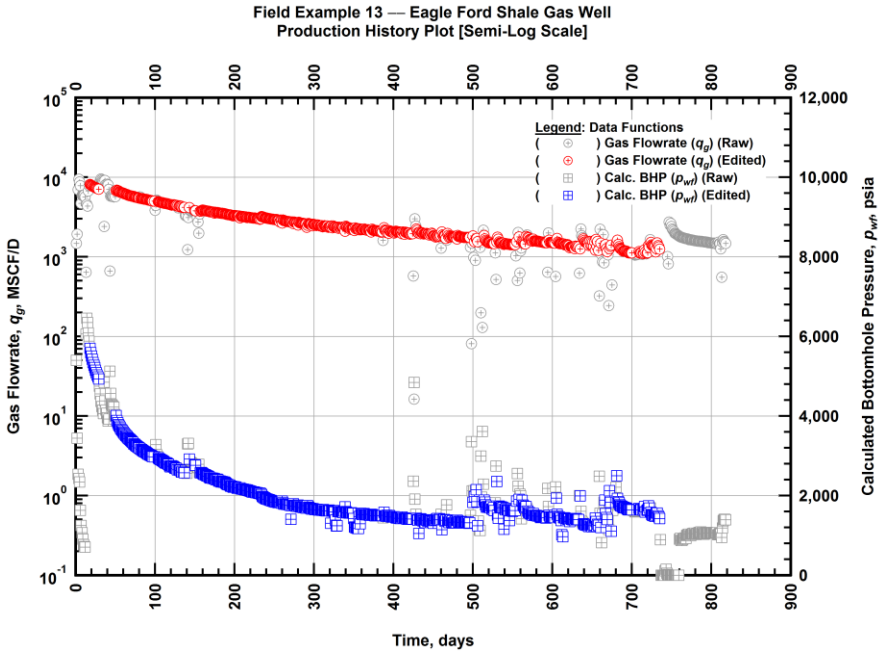

Figure A.361 — (Semi-log Plot): Filtered production history plot — flowrate (q_g) and calculated bottomhole pressure (p_{wf}) versus production time.

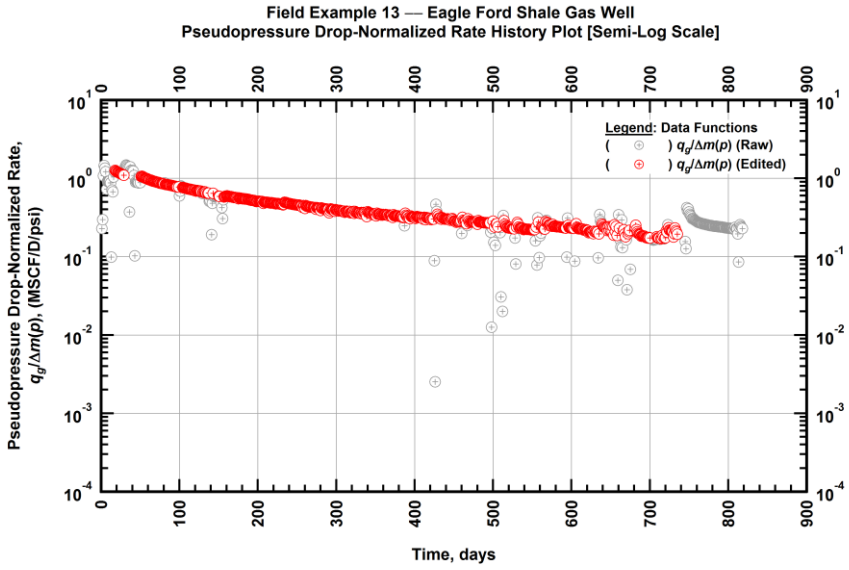

Figure A.362 — (Semi-log Plot): Filtered normalized rate production history plot — pseudopressure drop-normalized gas flowrate ($q_g/\Delta m(p)$) versus production time.

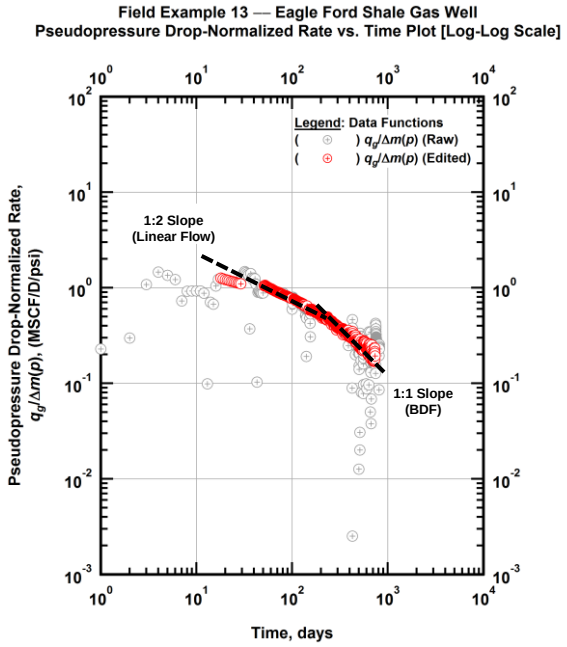

Figure A.363 — (Log-log Plot): Filtered normalized rate production history plot — pseudopressure drop-normalized gas flowrate ($q_g/\Delta m(p)$) versus production time.

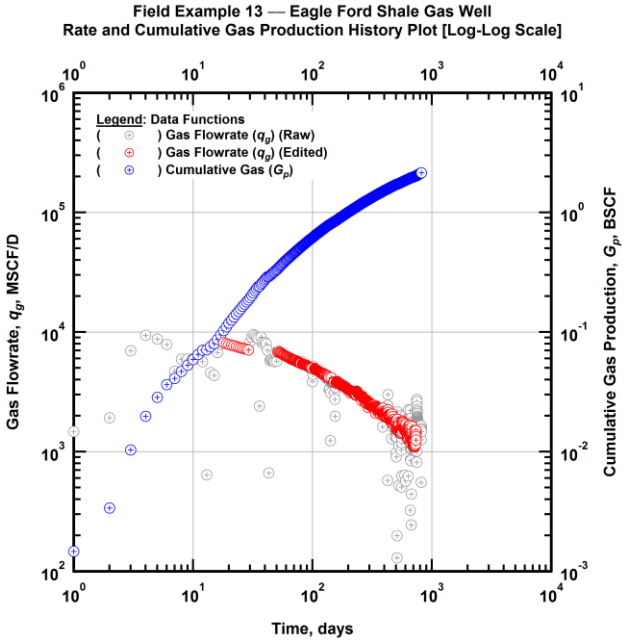

Figure A.364 — (Log-log Plot): Filtered rate and unfiltered cumulative gas production history plot — flowrate (q_g) and cumulative production (G_p) versus production time.

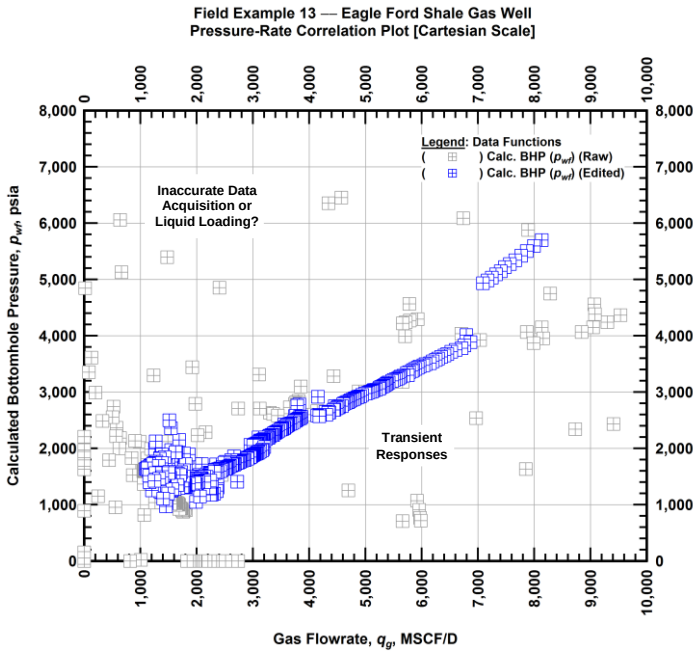

Figure A.365 — (Cartesian Plot): Filtered rate-pressure correlation plot — calculated bottomhole pressure (p_{wf}) versus flowrate (q_g).

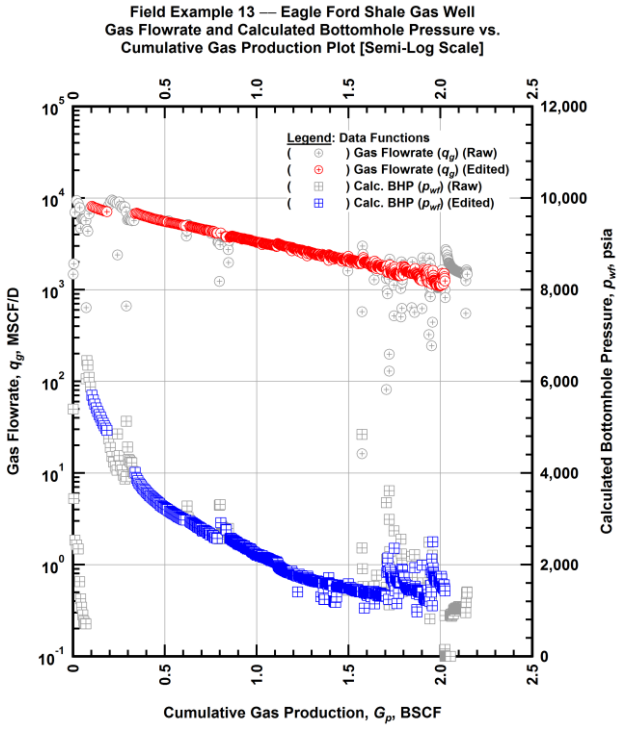

Figure A.366 — (Semi-log Plot): Filtered rate-pressure-cumulative production history plot — flowrate (q_g) and calculated bottomhole pressure (p_{wf}) versus cumulative production (G_p).

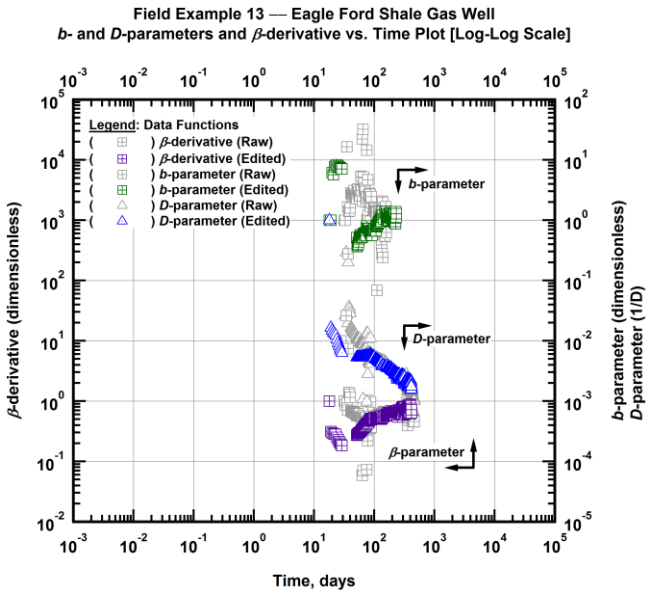

Figure A.367 — (Log-Log Plot): Filtered b, D and β production history plot — b- and D-parameters and β-derivative versus production time.

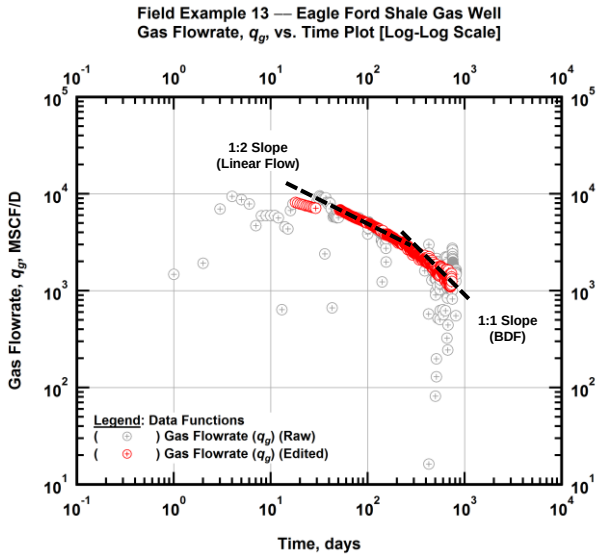

Figure A.368 — (Log-Log Plot): Filtered gas flowrate production history and flow regime identification plot — gas flowrate (q_g) versus production time.

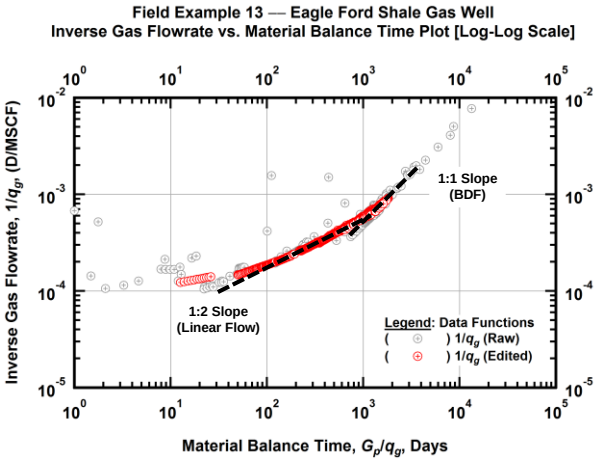

Figure A.369 — (Log-log Plot): Filtered inverse rate with material balance time plot — inverse gas flowrate ($1/q_g$) versus material balance time (G_p/q_g).

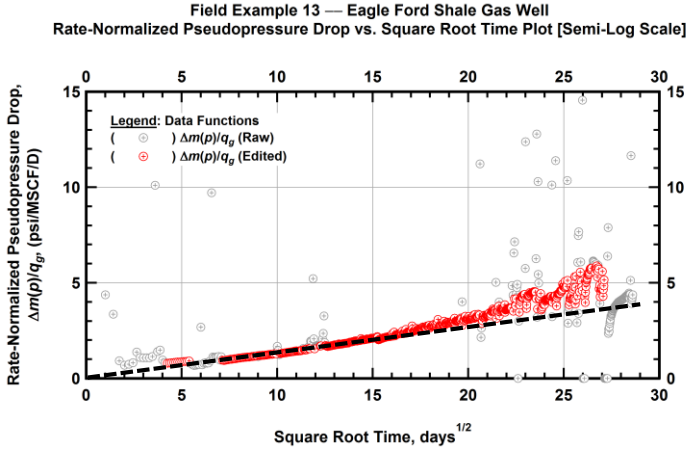

Figure A.370 — (Semi-log Plot): Filtered normalized pseudopressure drop production history plot — rate-normalized pseudopressure drop ($\Delta m(p)/q_g$) versus square root production time ($\sqrt{t}$).

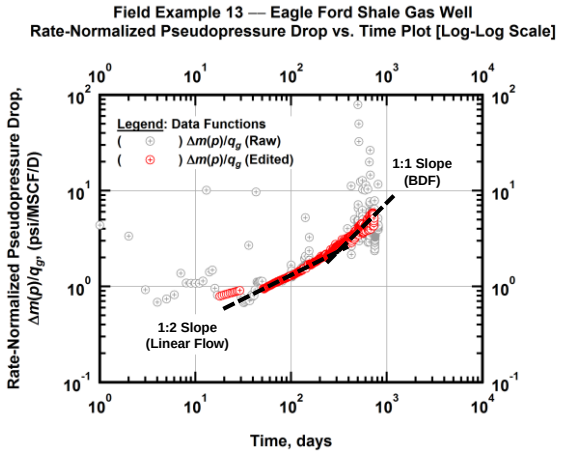

Figure A.371 — (Log-log Plot): Filtered normalized pseudopressure drop production history plot — rate-normalized pseudopressure drop ($\Delta m(p)/q_g$) versus production time.

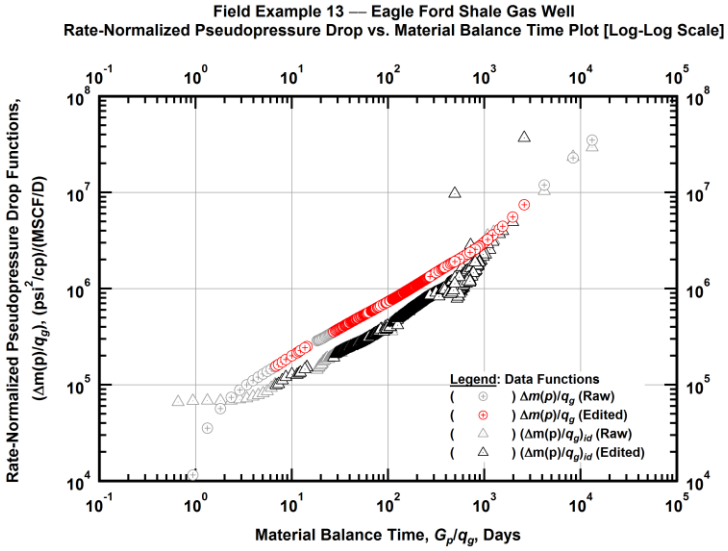

Figure A.372 — (Log-log Plot): "Log-log" diagnostic plot of the filtered production data — rate-normalized pseudopressure drop ($\Delta m(p)/q_g$) and rate-normalized pseudopressure drop integral-derivative $(\Delta m(p)/q_g)_{id}$ versus material balance time (G_p/q_g).

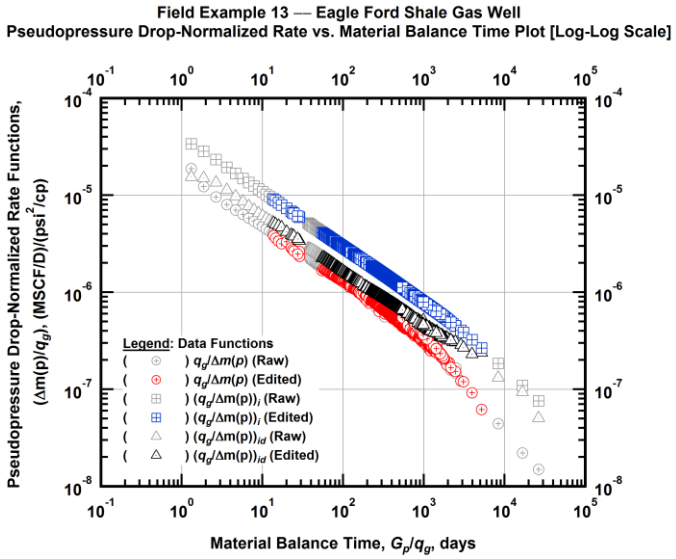

Figure A.373 — (Log-log Plot): "Blasingame" diagnostic plot of the filtered production data — pseudopressure drop-normalized gas flowrate ($q_g/\Delta m(p)$), pseudopressure drop-normalized gas flowrate integral $(q_g/\Delta m(p))_i$ and pseudopressure drop-normalized gas flowrate integral-derivative $(q_g/\Delta m(p))_{id}$ versus material balance time (G_p/q_g).

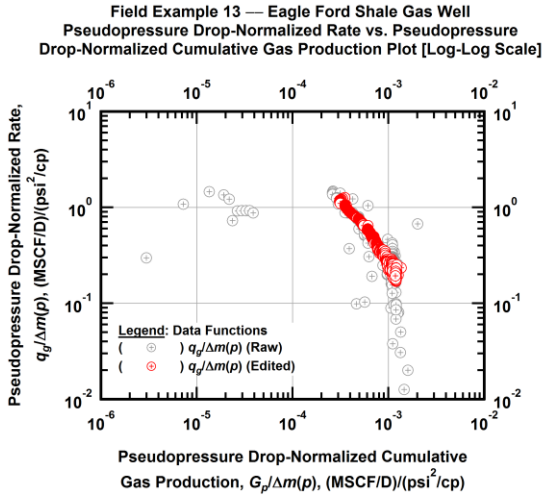

Figure A.374 — (Log-log Plot): Filtered normalized rate with normalized cumulative production plot — pseudopressure drop-normalized gas flowrate ($q_g/\Delta m(p)$) versus pseudopressure drop-normalized cumulative gas production ($G_p/\Delta m(p)$).

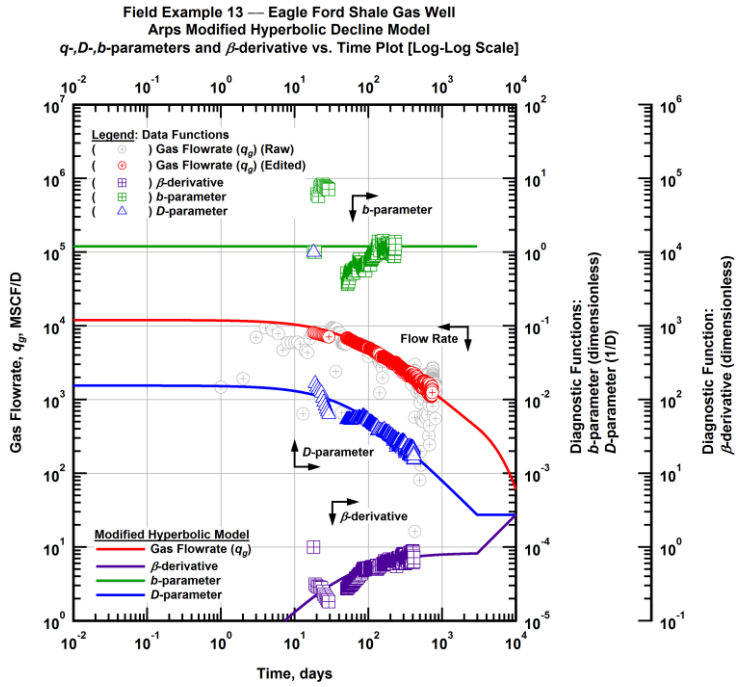

Figure A.375 — (Log-Log Plot): Arps modified hyperbolic decline model plot — time-rate model and data gas flowrate (q_g), *D*- and *b*-parameters and β-derivative versus production time.

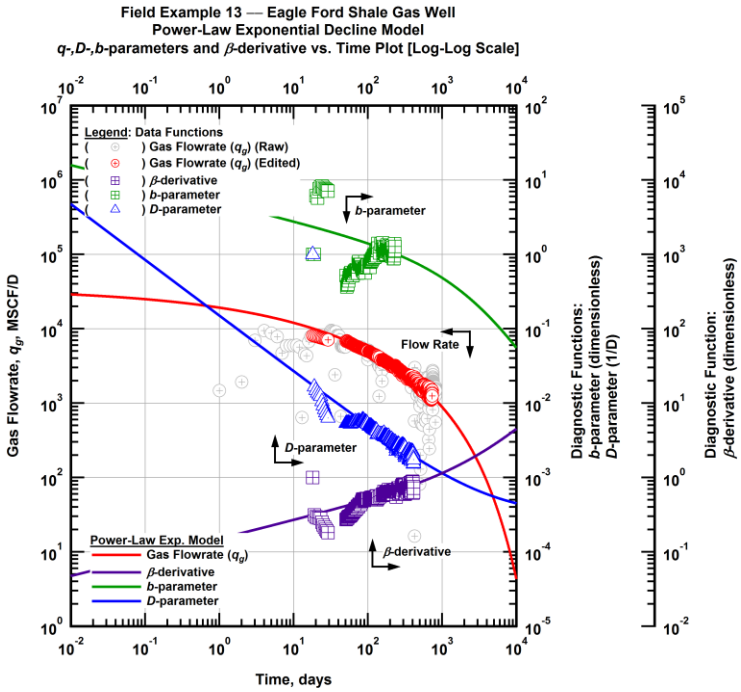

Figure A.376 — (Log-Log Plot): Power-law exponential decline model plot — time-rate model and data gas flowrate (q_g), *D*- and *b*-parameters and β-derivative versus production time.

Field Example 13 — Model-Based (Time-Rate-Pressure) Production Analysis

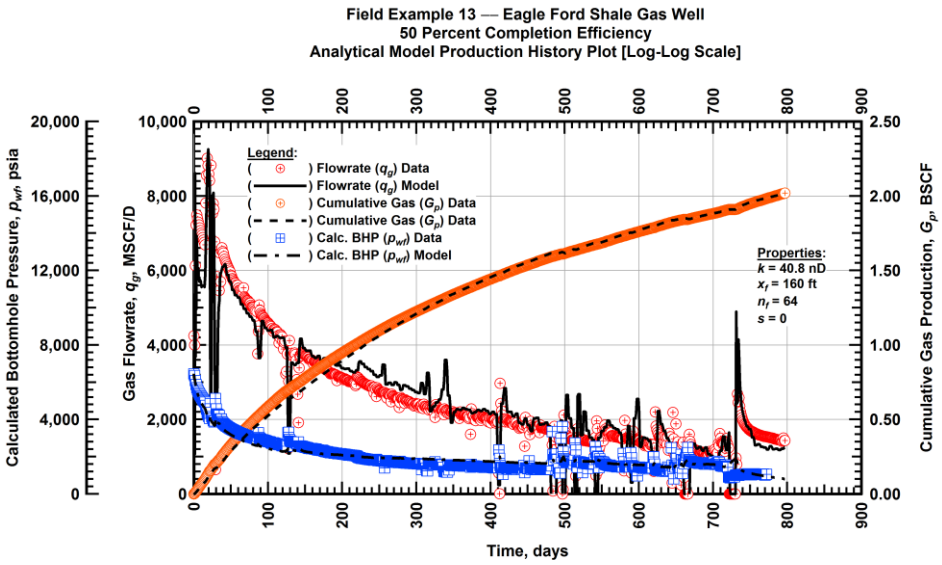

Figure A.377 — (Cartesian Plot): Production history plot — original gas flowrate (q_g), cumulative gas production (G_p), calculated bottomhole pressure (p_{wf}) and 50 percent completion efficiency model matches versus production time.

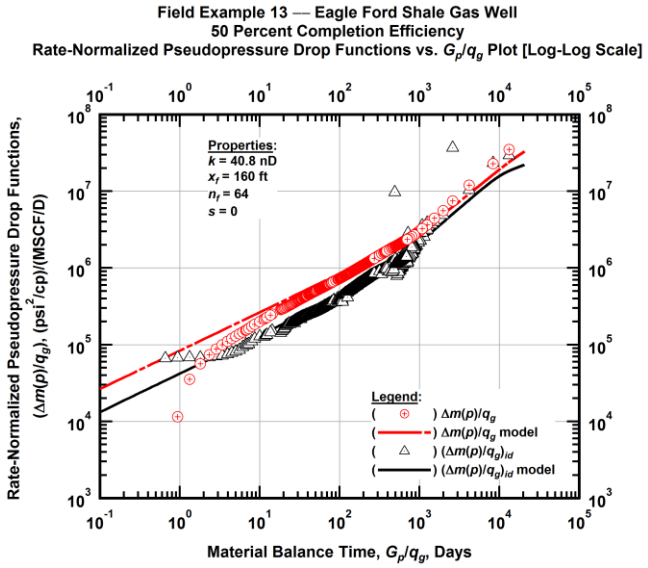

Figure A.378 — (Log-log Plot): "Log-log" diagnostic plot of the original production data — rate-normalized pseudopressure drop ($\Delta m(p)/q_g$), rate-normalized pseudopressure drop integral-derivative $(\Delta m(p)/q_g)_{id}$ and 50 percent completion efficiency model matches versus material balance time (G_p/q_g).

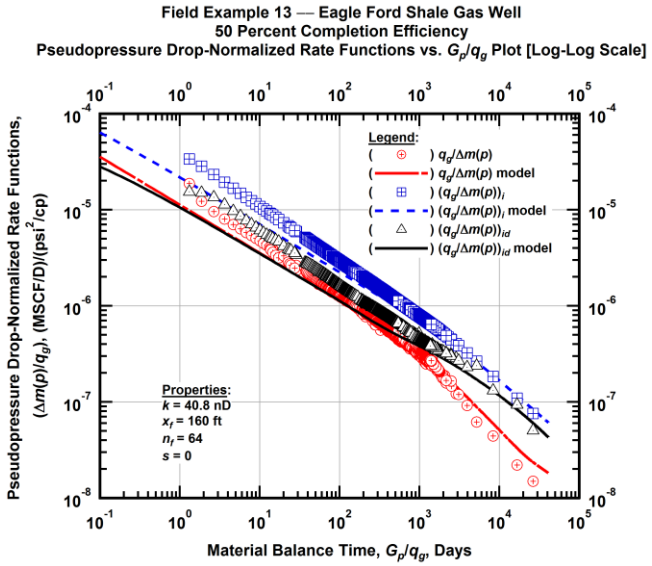

Figure A.379 — (Log-log Plot): "Blasingame" diagnostic plot of the original production data — pseudopressure drop-normalized gas flowrate ($q_g/\Delta m(p)$), pseudopressure drop-normalized gas flowrate integral $(q_g/\Delta m(p))_i$, pseudopressure drop-normalized gas flowrate integral-derivative $(q_g/\Delta m(p))_{id}$ and 50 percent completion efficiency model matches versus material balance time (G_p/q_g).

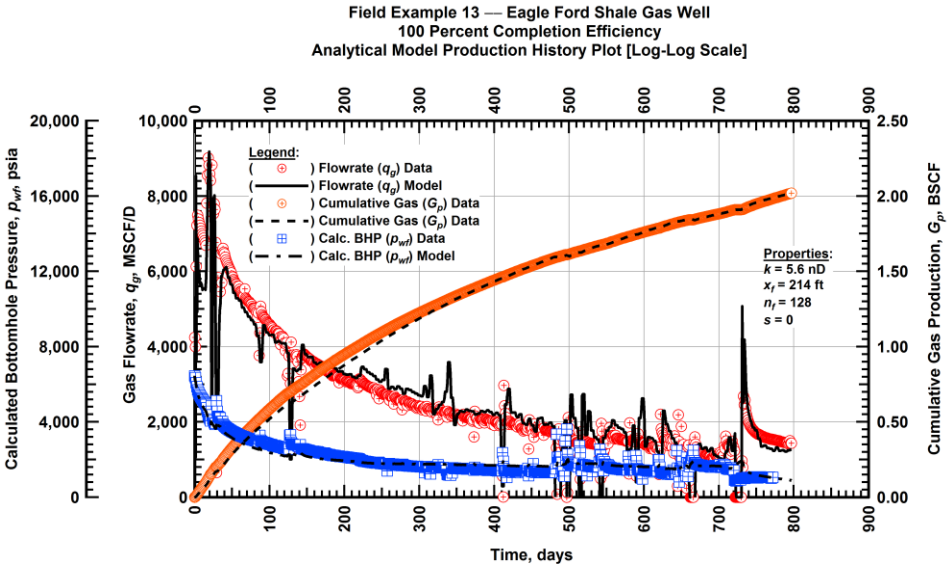

Figure A.380 — (Cartesian Plot): Production history plot — original gas flowrate (q_g), cumulative gas production (G_p), calculated bottomhole pressure (p_{wf}) and 100 percent completion efficiency model matches versus production time.

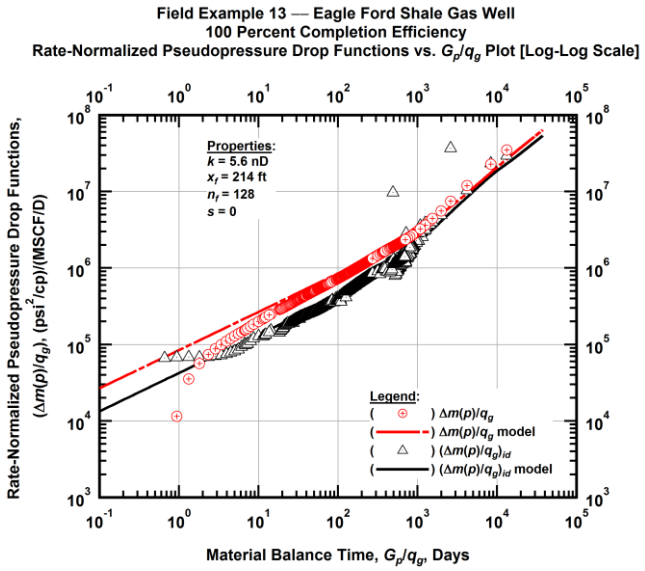

Figure A.381 — (Log-log Plot): "Log-log" diagnostic plot of the original production data — rate-normalized pseudopressure drop ($\Delta m(p)/q_g$), rate-normalized pseudopressure drop integral-derivative $(\Delta m(p)/q_g)_{id}$ and 100 percent completion efficiency model matches versus material balance time (G_p/q_g).

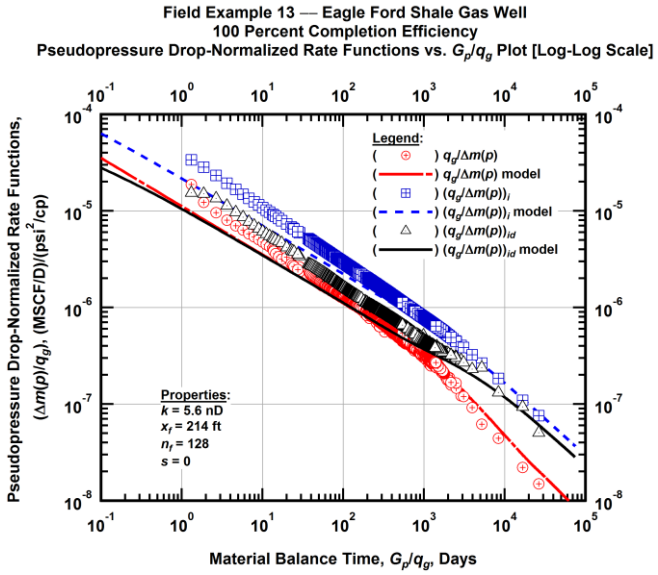

Figure A.382 — (Log-log Plot): "Blasingame" diagnostic plot of the original production data — pseudopressure drop-normalized gas flowrate ($q_g/\Delta m(p)$), pseudopressure drop-normalized gas flowrate integral $(q_g/\Delta m(p))_i$, pseudopressure drop-normalized gas flowrate integral-derivative $(q_g/\Delta m(p))_{id}$ and 100 percent completion efficiency model matches versus material balance time (G_p/q_g).

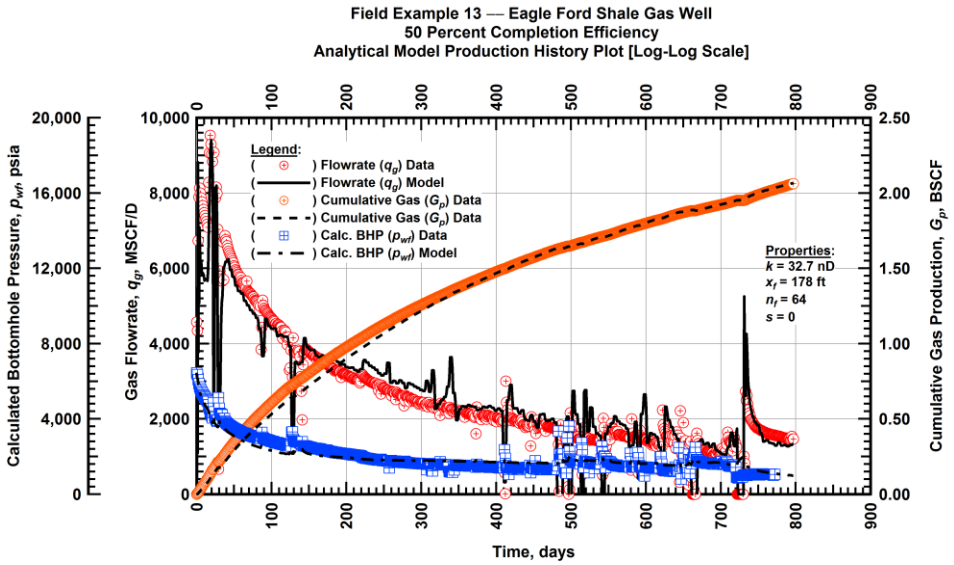

Figure A.383 — (Cartesian Plot): Production history plot — revised gas flowrate (q_g), cumulative gas production (G_p), calculated bottomhole pressure (p_{wf}) and 50 percent completion efficiency model matches versus production time.

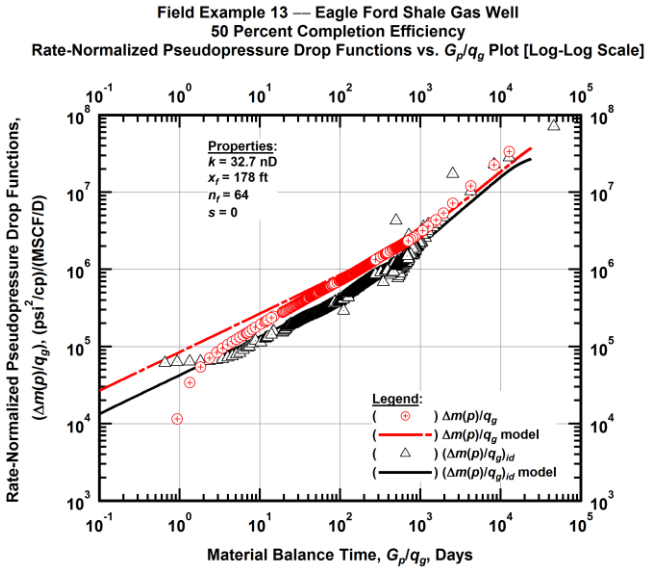

Figure A.384— (Log-log Plot): "Log-log" diagnostic plot of the revised production data — rate-normalized pseudopressure drop ($\Delta m(p)/q_g$), rate-normalized pseudopressure drop integral-derivative $(\Delta m(p)/q_g)_{id}$ and 50 percent completion efficiency model matches versus material balance time (G_p/q_g).

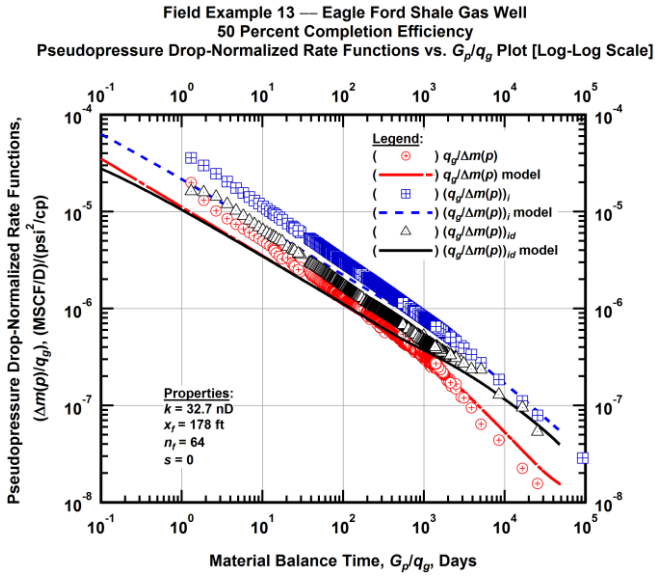

Figure A.385 — (Log-log Plot): "Blasingame" diagnostic plot of the revised production data — pseudopressure drop-normalized gas flowrate ($q_g/\Delta m(p)$), pseudopressure drop-normalized gas flowrate integral $(q_g/\Delta m(p))_i$, pseudopressure drop-normalized gas flowrate integral-derivative $(q_g/\Delta m(p))_{id}$ and 50 percent completion efficiency model matches versus material balance time (G_p/q_g).

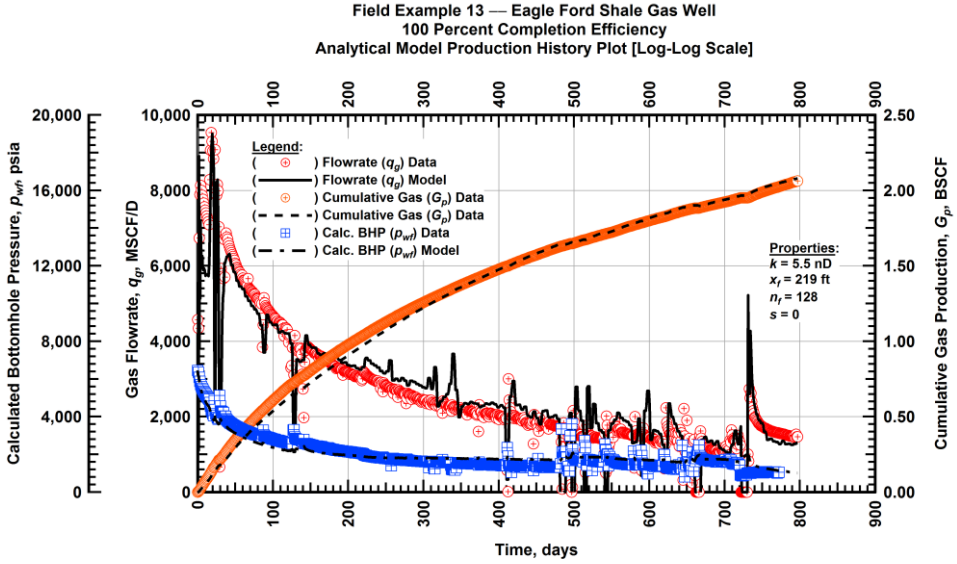

Figure A.386 — (Cartesian Plot): Production history plot — revised gas flowrate (q_g), cumulative gas production (G_p), calculated bottomhole pressure (p_{wf}) and 100 percent completion efficiency model matches versus production time.

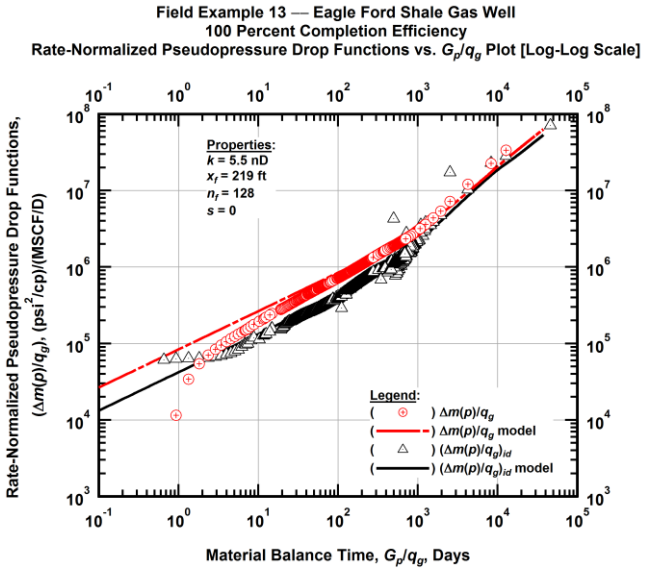

Figure A.387 — (Log-log Plot): "Log-log" diagnostic plot of the revised production data — rate-normalized pseudopressure drop ($\Delta m(p)/q_g$), rate-normalized pseudopressure drop integral-derivative $(\Delta m(p)/q_g)_{id}$ and 100 percent completion efficiency model matches versus material balance time (G_p/q_g).

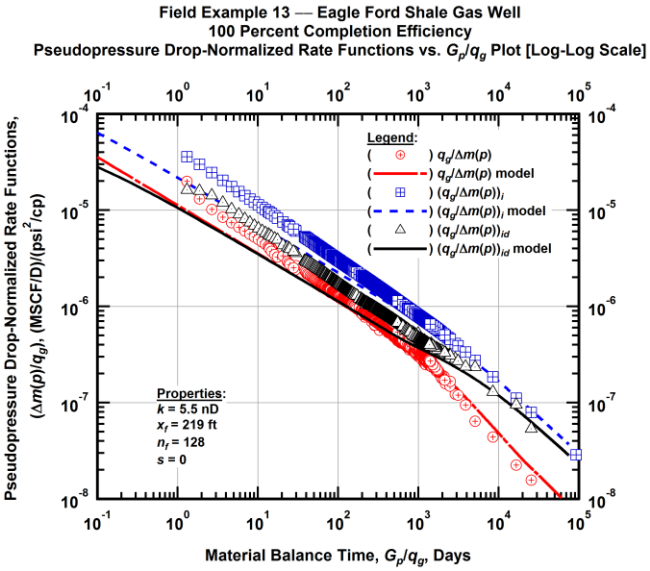

Figure A.388 — (Log-log Plot): "Blasingame" diagnostic plot of the revised production data — pseudopressure drop-normalized gas flowrate ($q_g/\Delta m(p)$), pseudopressure drop-normalized gas flowrate integral $(q_g/\Delta m(p))_i$, pseudopressure drop-normalized gas flowrate integral-derivative $(q_g/\Delta m(p))_{id}$ and 100 percent completion efficiency model matches versus material balance time (G_p/q_g).

Field Example 13 — 30-Year EUR Model Comparison

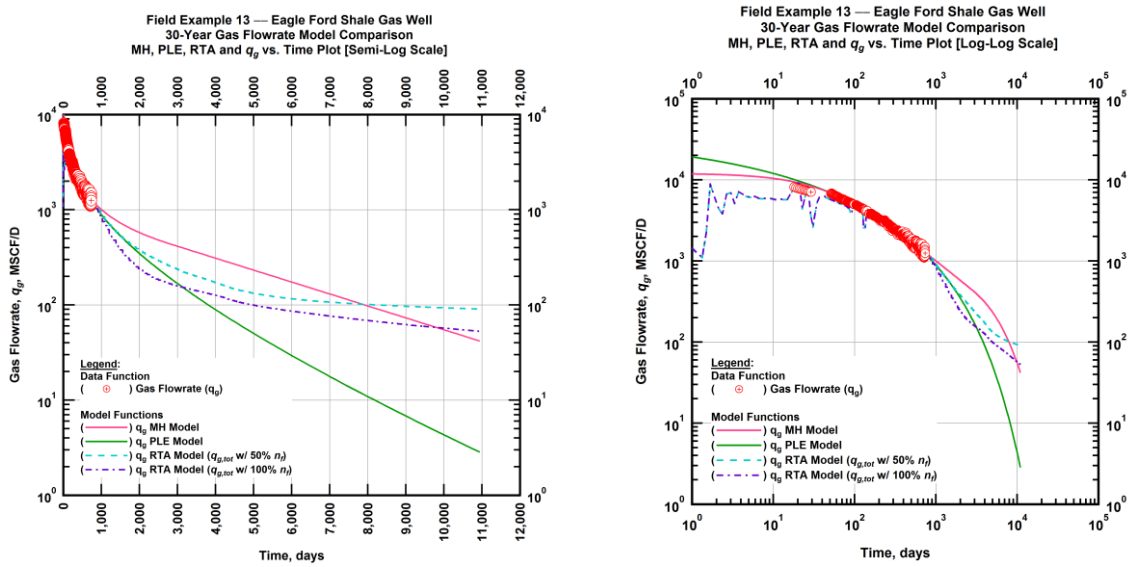

A **B**

Figure A.389 — (A — Semi-Log Plot) and (B — Log-Log Plot): Estimated 30-year revised gas flowrate model comparison — Arps modified hyperbolic decline model, power-law exponential decline model, and 50 percent and 100 percent completion efficiency RTA models revised gas 30-year estimated flowrate decline and historic gas flowrate data (q_g) versus production time.

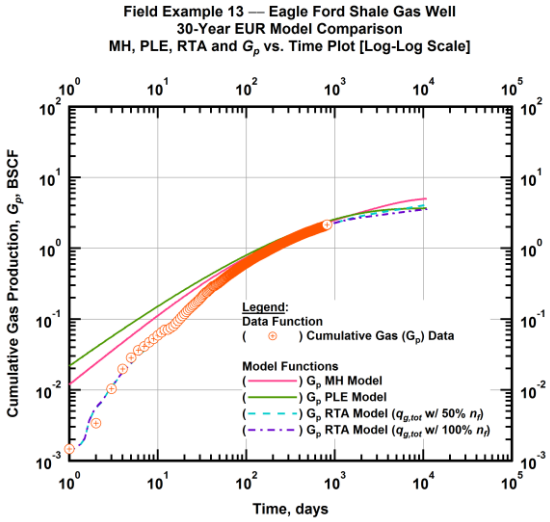

Figure A.390 — (Log-log Plot): PVT revised gas 30-year estimated cumulative production volume model comparison — Arps modified hyperbolic decline model, power-law exponential decline model, and 50 percent and 100 percent completion efficiency RTA model estimated 30-year cumulative gas production volumes and historic cumulative gas production (G_p) versus production time.

Table A.13 — 30-year estimated cumulative revised gas production (EUR), in units of BSCF, for the Arps modified hyperbolic, power-law exponential and analytical time-rate-pressure decline models.

Arps Modified Hyperbolic (BSCF)	Power-Law Exponential (BSCF)	RTA Analytical Model ($q_{g,tot}$ w/ 50% n_f) (BSCF)	RTA Analytical Model ($q_{g,tot}$ w/ 100% n_f) (BSCF)
4.94	3.41	4.18	3.62

Field Example 14 — Time-Rate Analysis

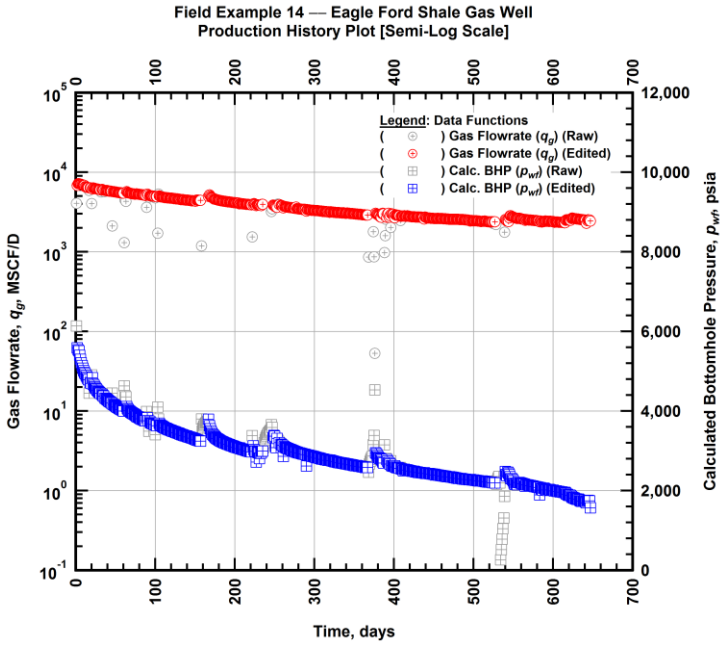

Figure A.391 — (Semi-log Plot): Filtered production history plot — flowrate (q_g) and calculated bottomhole pressure (p_{wf}) versus production time.

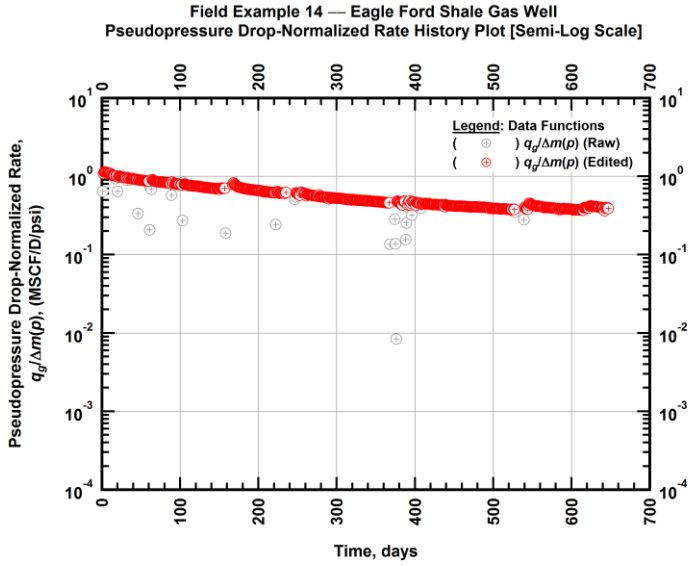

Figure A.392 — (Semi-log Plot): Filtered normalized rate production history plot — pseudopressure drop-normalized gas flowrate ($q_g/\Delta m(p)$) versus production time.

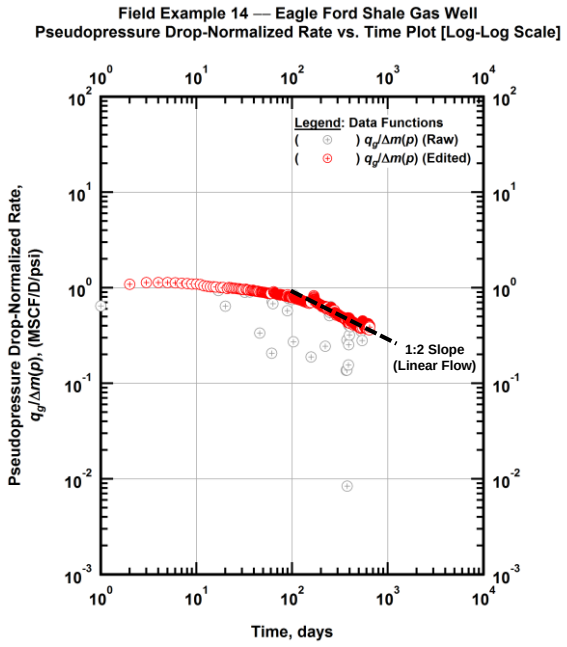

Figure A.393 — (Log-log Plot): Filtered normalized rate production history plot — pseudopressure drop-normalized gas flowrate ($q_g/\Delta m(p)$) versus production time.

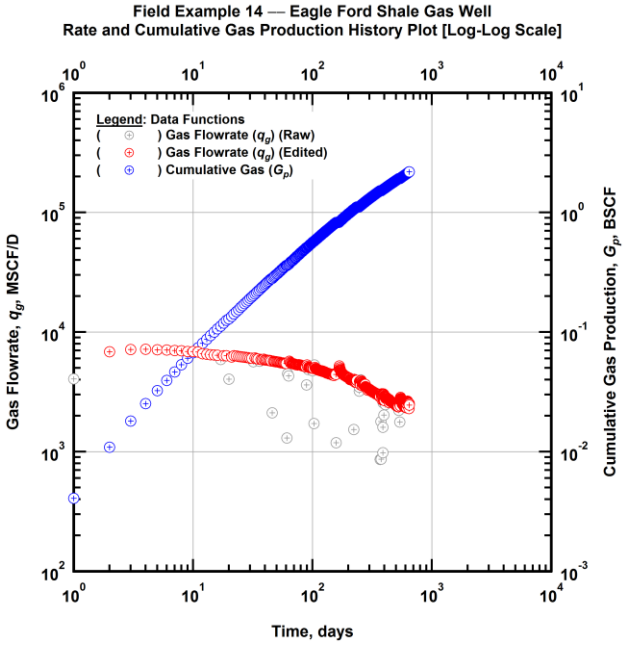

Figure A.394 — (Log-log Plot): Filtered rate and unfiltered cumulative gas production history plot — flowrate (q_g) and cumulative production (G_p) versus production time.

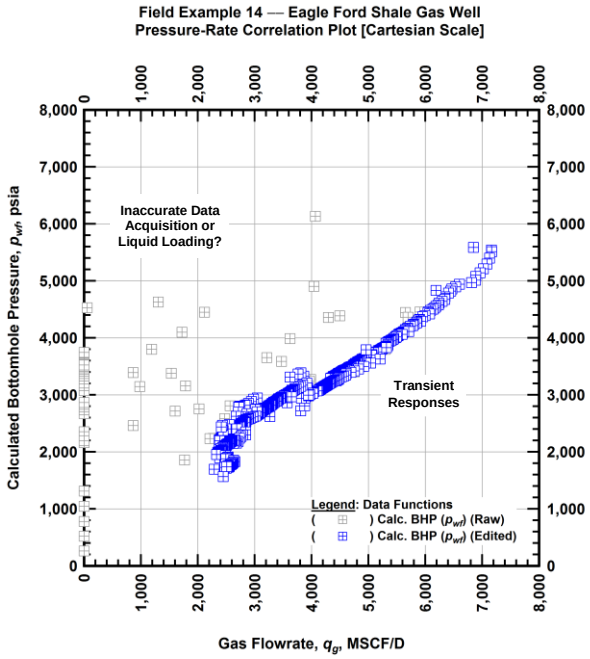

Figure A.395 — (Cartesian Plot): Filtered rate-pressure correlation plot — calculated bottomhole pressure (p_{wf}) versus flowrate (q_g).

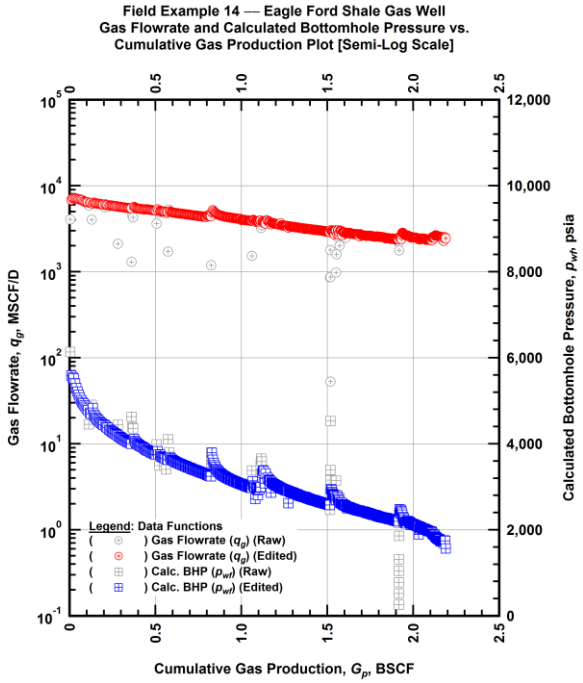

Figure A.396 — (Semi-log Plot): Filtered rate-pressure-cumulative production history plot — flowrate (q_g) and calculated bottomhole pressure (p_{wf}) versus cumulative production (G_p).

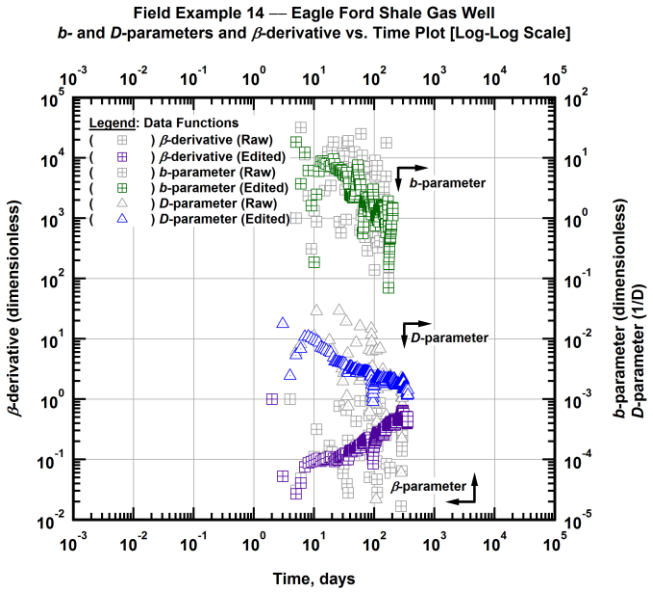

Figure A.397 — (Log-Log Plot): Filtered b, D and β production history plot — b- and D-parameters and β-derivative versus production time.

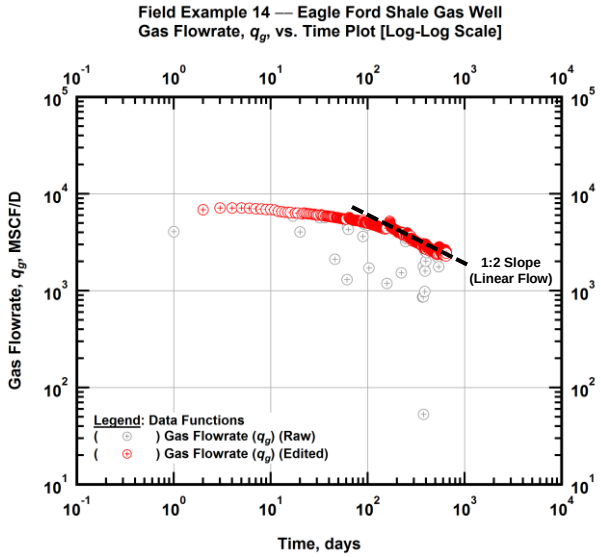

Figure A.398 — (Log-Log Plot): Filtered gas flowrate production history and flow regime identification plot — gas flowrate (q_g) versus production time.

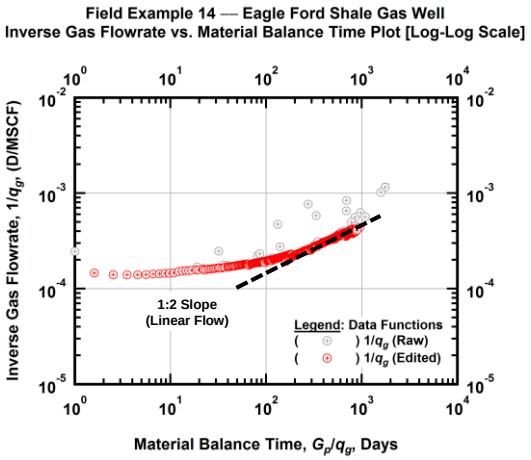

Figure A.399 — (Log-log Plot): Filtered inverse rate with material balance time plot — inverse gas flowrate ($1/q_g$) versus material balance time (G_p/q_g).

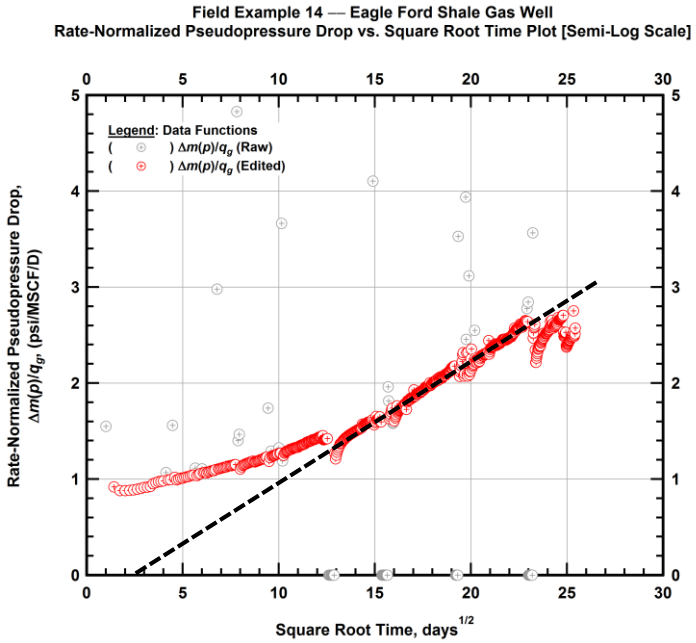

Figure A.400 — (Semi-log Plot): Filtered normalized pseudopressure drop production history plot — rate-normalized pseudopressure drop ($\Delta m(p)/q_g$) versus square root production time ($\sqrt{t}$).

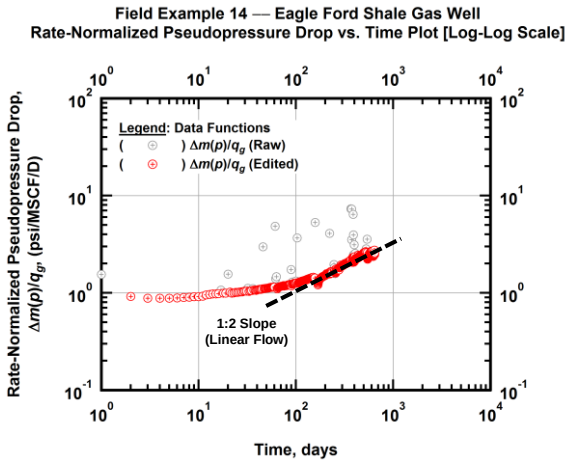

Figure A.401 — (Log-log Plot): Filtered normalized pseudopressure drop production history plot — rate-normalized pseudopressure drop ($\Delta m(p)/q_g$) versus production time.

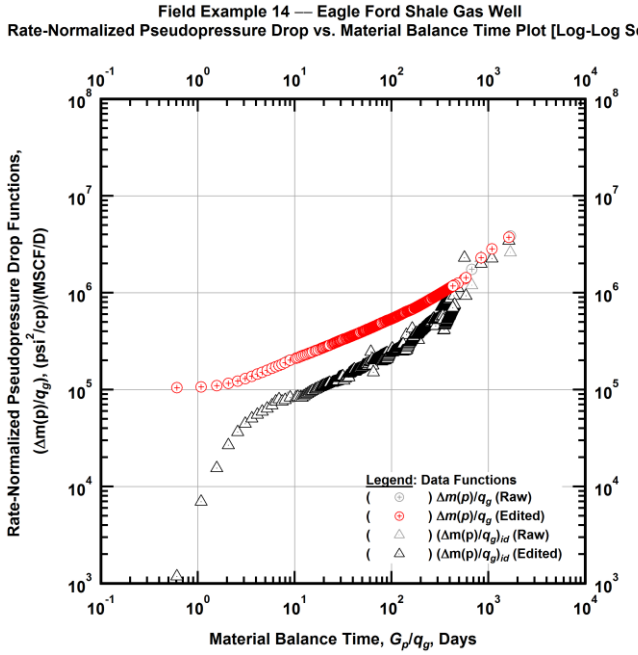

Figure A.402 — (Log-log Plot): "Log-log" diagnostic plot of the filtered production data — rate-normalized pseudopressure drop ($\Delta m(p)/q_g$) and rate-normalized pseudopressure drop integral-derivative $(\Delta m(p)/q_g)_{id}$ versus material balance time (G_p/q_g).

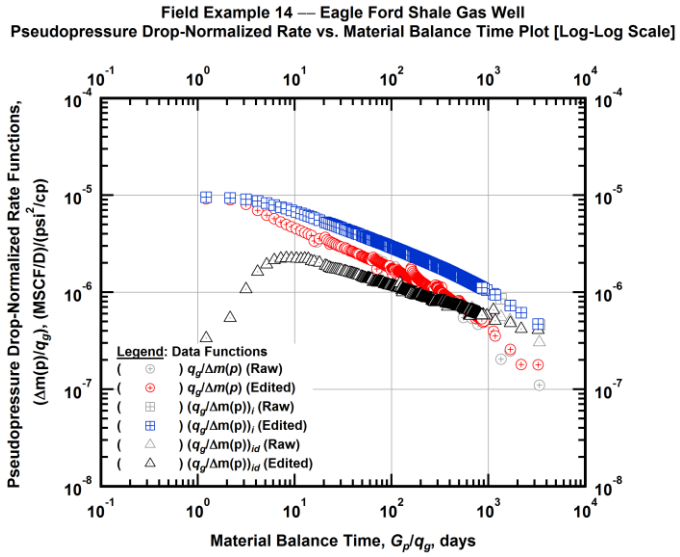

Figure A.403 — (Log-log Plot): "Blasingame" diagnostic plot of the filtered production data — pseudopressure drop-normalized gas flowrate ($q_g/\Delta m(p)$), pseudopressure drop-normalized gas flowrate integral $(q_g/\Delta m(p))_i$ and pseudopressure drop-normalized gas flowrate integral-derivative $(q_g/\Delta m(p))_{id}$ versus material balance time (G_p/q_g).

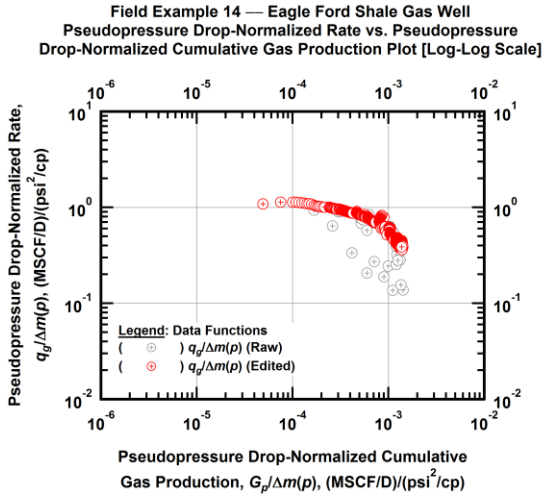

Figure A.404 — (Log-log Plot): Filtered normalized rate with normalized cumulative production plot — pseudopressure drop-normalized gas flowrate ($q_g/\Delta m(p)$) versus pseudopressure drop-normalized cumulative gas production ($G_p/\Delta m(p)$).

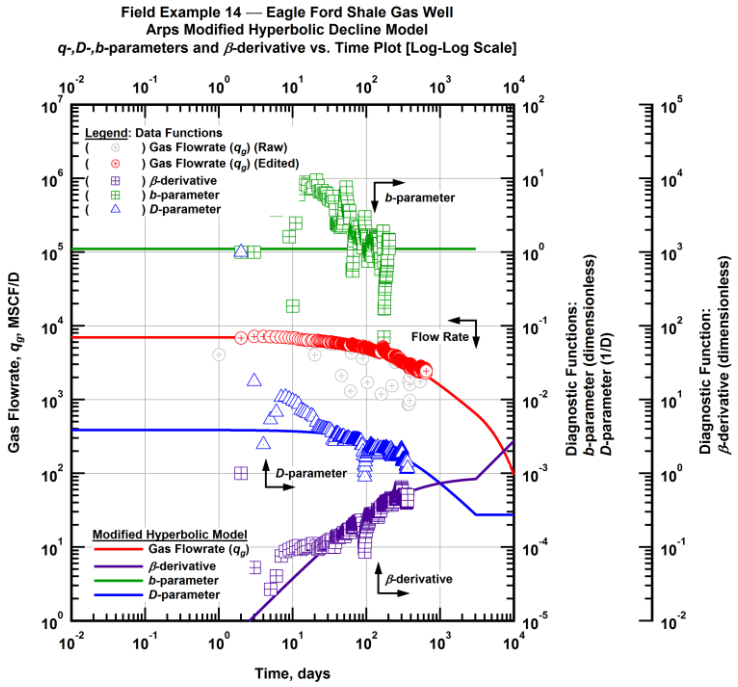

Figure A.405 — (Log-Log Plot): Arps modified hyperbolic decline model plot — time-rate model and data gas flowrate (q_g), *D*- and *b*-parameters and β-derivative versus production time.

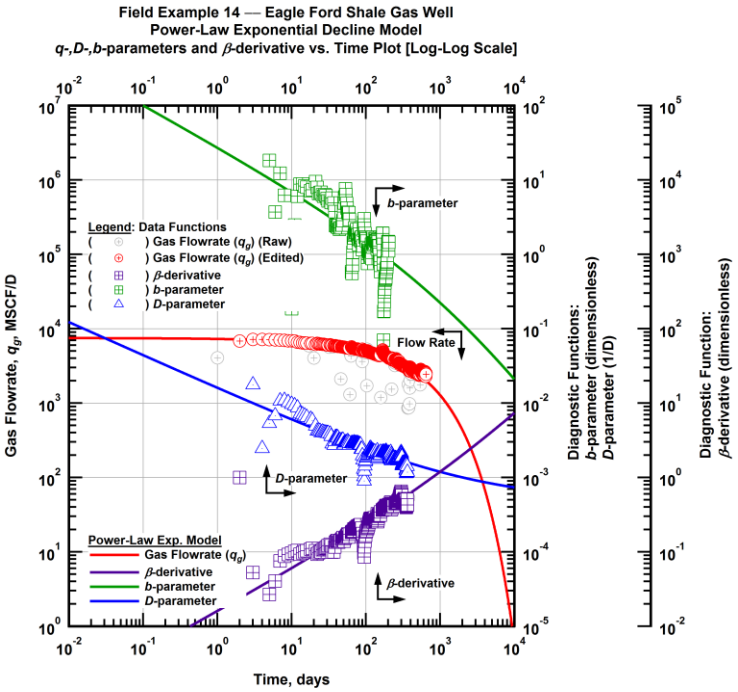

Figure A.406 — (Log-Log Plot): Power-law exponential decline model plot — time-rate model and data gas flowrate (q_g), *D*- and *b*-parameters and β-derivative versus production time.

Field Example 14 — Model-Based (Time-Rate-Pressure) Production Analysis

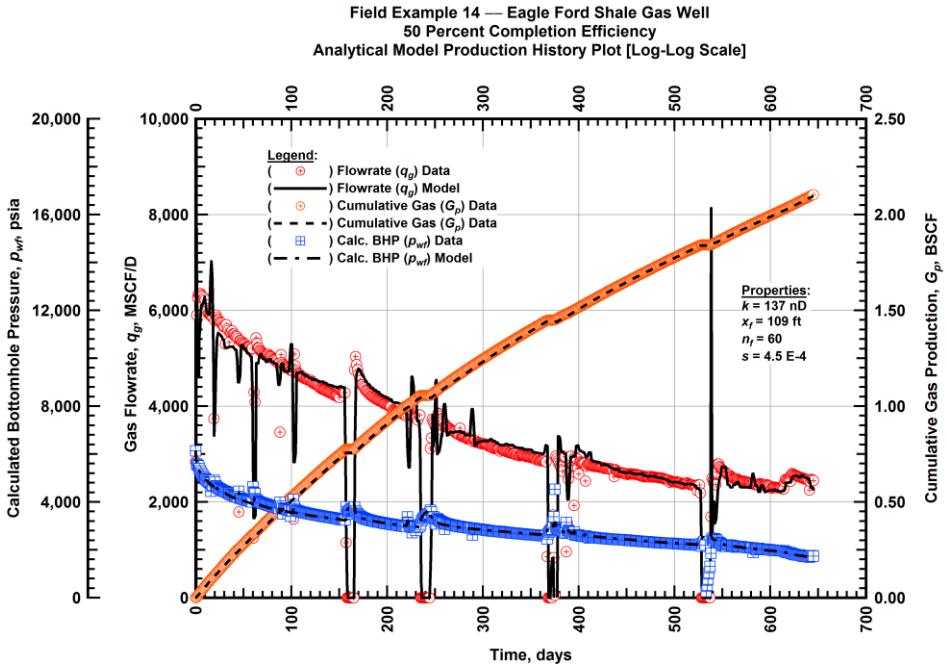

Figure A.407 — (Cartesian Plot): Production history plot — original gas flowrate (q_g), cumulative gas production (G_p), calculated bottomhole pressure (p_{wf}) and 50 percent completion efficiency model matches versus production time.

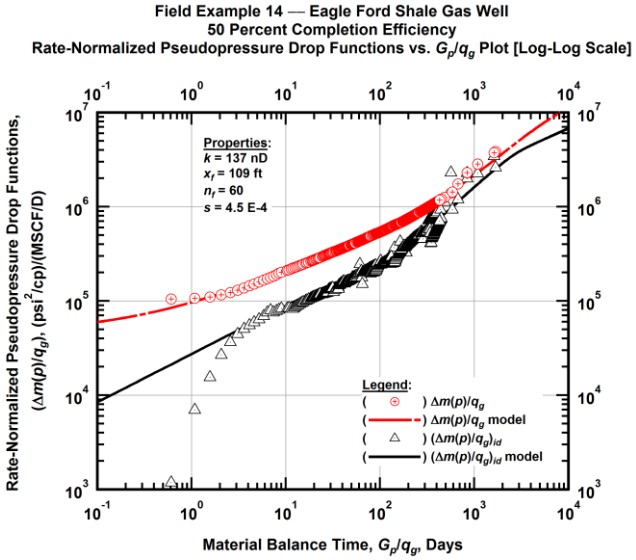

Figure A.408 — (Log-log Plot): "Log-log" diagnostic plot of the original production data — rate-normalized pseudopressure drop ($\Delta m(p)/q_g$), rate-normalized pseudopressure drop integral-derivative $(\Delta m(p)/q_g)_{id}$ and 50 percent completion efficiency model matches versus material balance time (G_p/q_g).

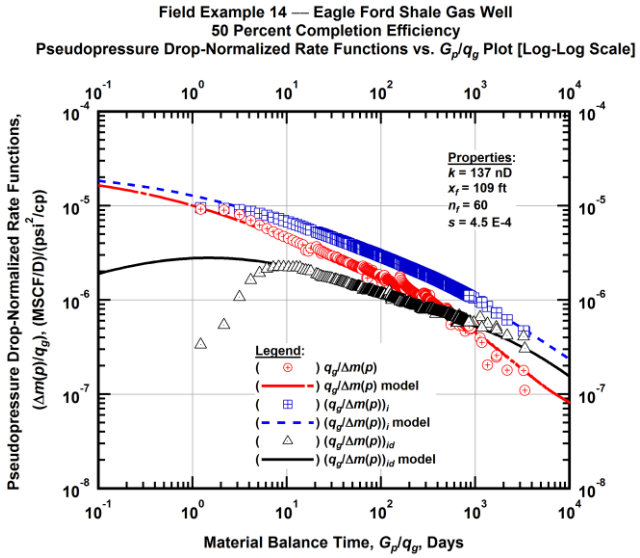

Figure A.409 — (Log-log Plot): "Blasingame" diagnostic plot of the original production data — pseudopressure drop-normalized gas flowrate ($q_g/\Delta m(p)$), pseudopressure drop-normalized gas flowrate integral $(q_g/\Delta m(p))_i$, pseudopressure drop-normalized gas flowrate integral-derivative $(q_g/\Delta m(p))_{id}$ and 50 percent completion efficiency model matches versus material balance time (G_p/q_g).

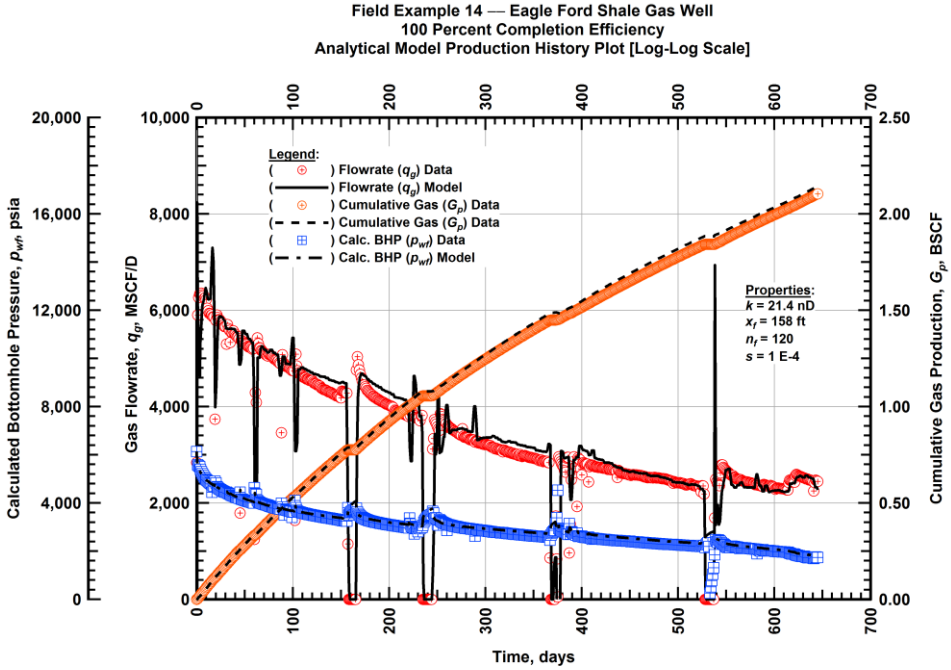

Figure A.410 — (Cartesian Plot): Production history plot — original gas flowrate (q_g), cumulative gas production (G_p), calculated bottomhole pressure (p_{wf}) and 100 percent completion efficiency model matches versus production time.

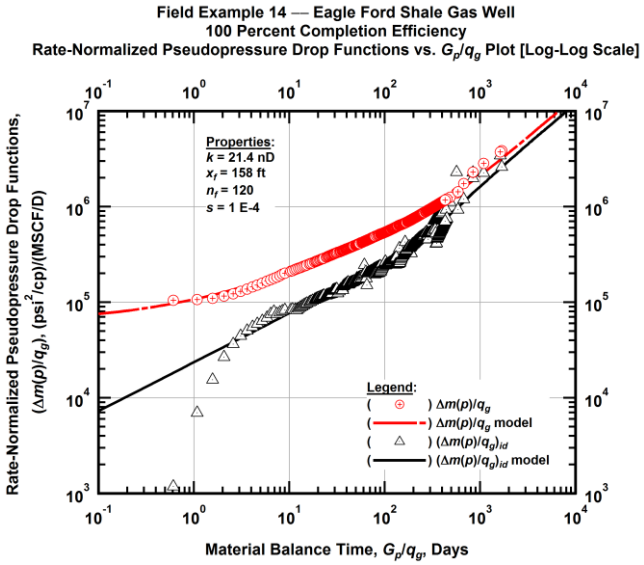

Figure A.411 — (Log-log Plot): "Log-log" diagnostic plot of the original production data — rate-normalized pseudopressure drop ($\Delta m(p)/q_g$), rate-normalized pseudopressure drop integral-derivative $(\Delta m(p)/q_g)_{id}$ and 100 percent completion efficiency model matches versus material balance time (G_p/q_g).

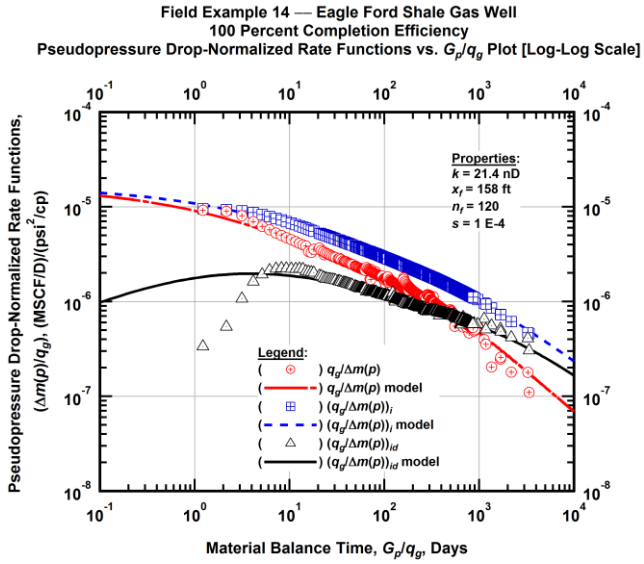

Figure A.412 — (Log-log Plot): "Blasingame" diagnostic plot of the original production data — pseudopressure drop-normalized gas flowrate ($q_g/\Delta m(p)$), pseudopressure drop-normalized gas flowrate integral $(q_g/\Delta m(p))_i$, pseudopressure drop-normalized gas flowrate integral-derivative $(q_g/\Delta m(p))_{id}$ and 100 percent completion efficiency model matches versus material balance time (G_p/q_g).

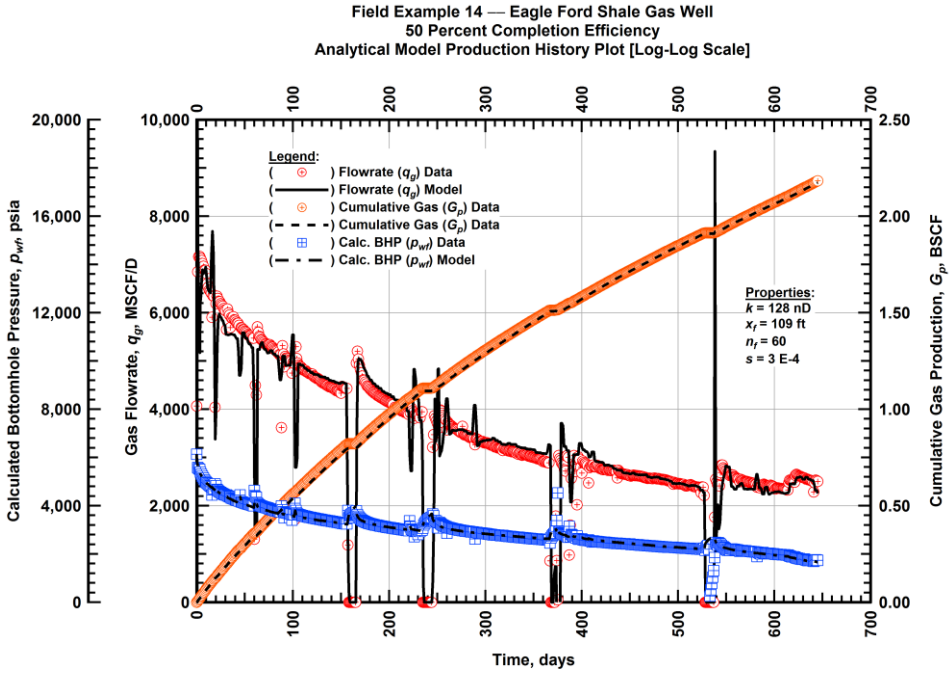

Figure A.413 — (Cartesian Plot): Production history plot — revised gas flowrate (q_g), cumulative gas production (G_p), calculated bottomhole pressure (p_{wf}) and 50 percent completion efficiency model matches versus production time.

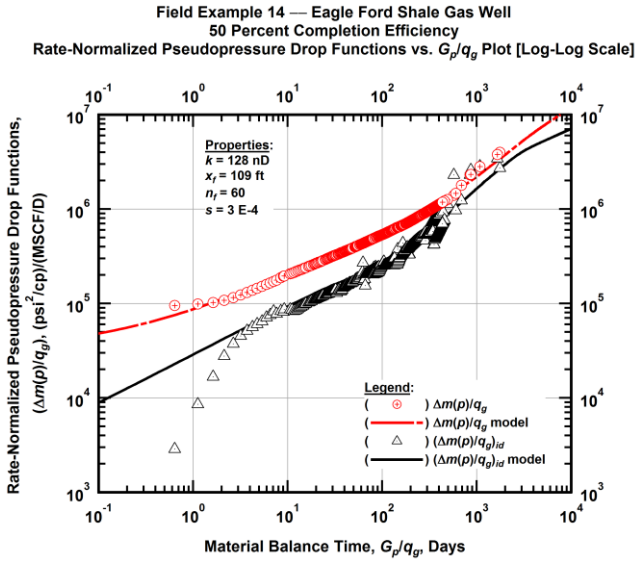

Figure A.414— (Log-log Plot): "Log-log" diagnostic plot of the revised production data — rate-normalized pseudopressure drop ($\Delta m(p)/q_g$), rate-normalized pseudopressure drop integral-derivative $(\Delta m(p)/q_g)_{id}$ and 50 percent completion efficiency model matches versus material balance time (G_p/q_g).

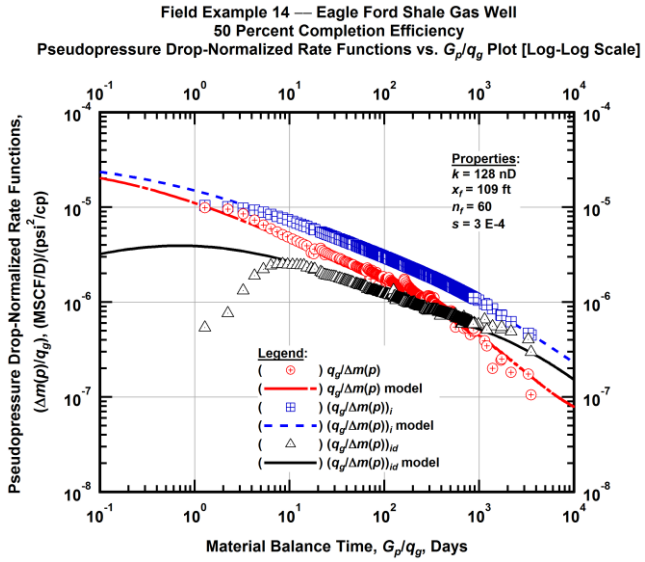

Figure A.415 — (Log-log Plot): "Blasingame" diagnostic plot of the revised production data — pseudopressure drop-normalized gas flowrate ($q_g/\Delta m(p)$), pseudopressure drop-normalized gas flowrate integral $(q_g/\Delta m(p))_i$, pseudopressure drop-normalized gas flowrate integral-derivative $(q_g/\Delta m(p))_{id}$ and 50 percent completion efficiency model matches versus material balance time (G_p/q_g).

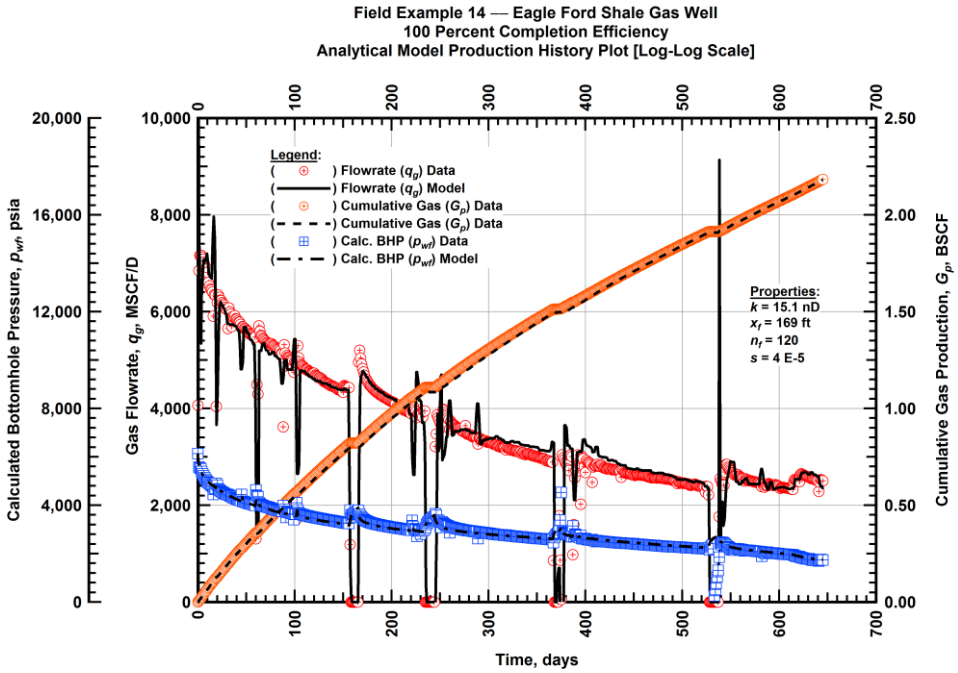

Figure A.416 — (Cartesian Plot): Production history plot — revised gas flowrate (q_g), cumulative gas production (G_p), calculated bottomhole pressure (p_{wf}) and 100 percent completion efficiency model matches versus production time.

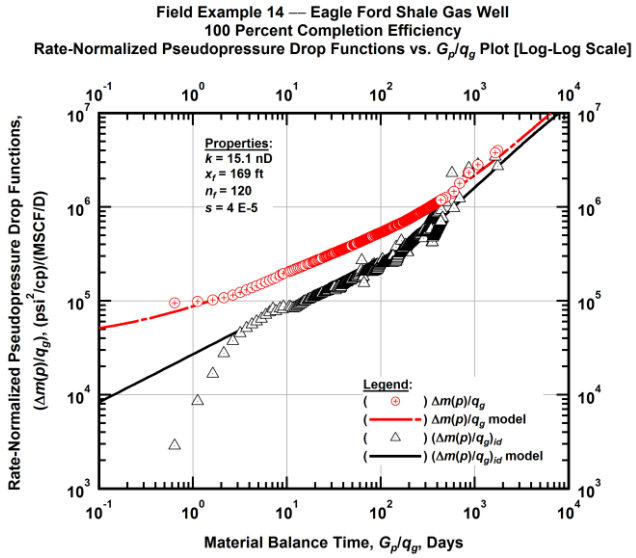

Figure A.417 — (Log-log Plot): "Log-log" diagnostic plot of the revised production data — rate-normalized pseudopressure drop ($\Delta m(p)/q_g$), rate-normalized pseudopressure drop integral-derivative $(\Delta m(p)/q_g)_{id}$ and 100 percent completion efficiency model matches versus material balance time (G_p/q_g).

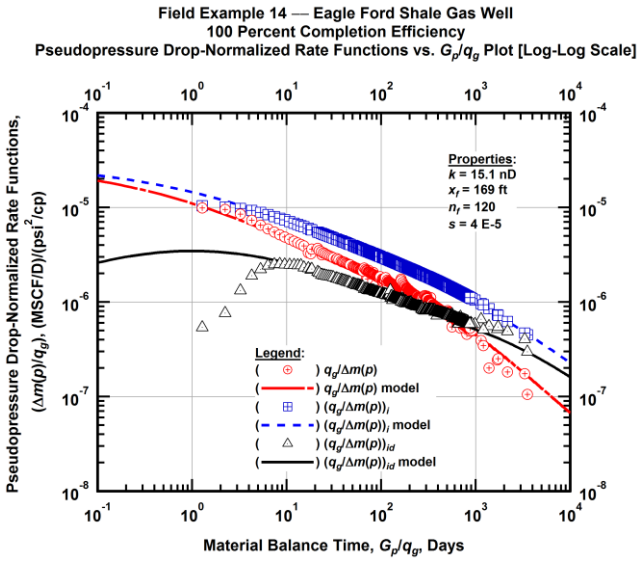

Figure A.418 — (Log-log Plot): "Blasingame" diagnostic plot of the revised production data — pseudopressure drop-normalized gas flowrate ($q_g/\Delta m(p)$), pseudopressure drop-normalized gas flowrate integral $(q_g/\Delta m(p))_i$, pseudopressure drop-normalized gas flowrate integral-derivative $(q_g/\Delta m(p))_{id}$ and 100 percent completion efficiency model matches versus material balance time (G_p/q_g).

Field Example 14 — 30-Year EUR Model Comparison

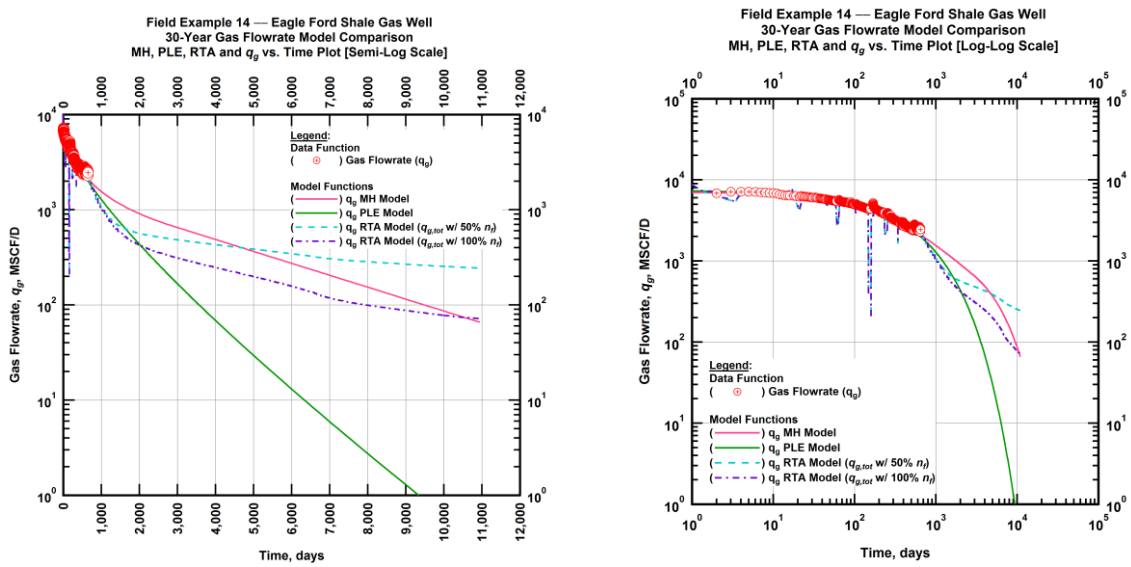

A **B**

Figure A.419 — (A — Semi-Log Plot) and (B — Log-Log Plot): Estimated 30-year revised gas flowrate model comparison — Arps modified hyperbolic decline model, power-law exponential decline model, and 50 percent and 100 percent completion efficiency RTA models revised gas 30-year estimated flowrate decline and historic gas flowrate data (q_g) versus production time.

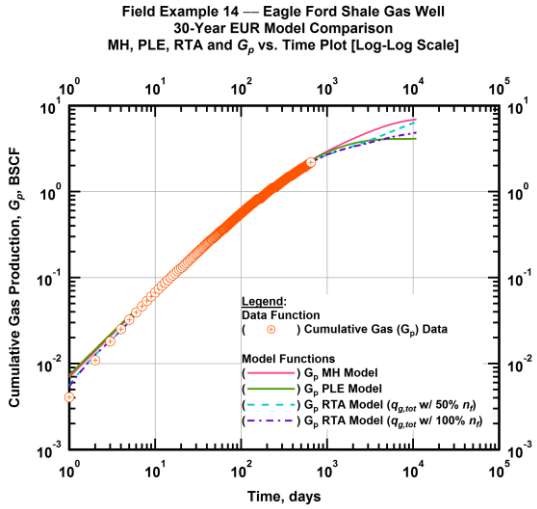

Figure A.420 — (Log-log Plot): PVT revised gas 30-year estimated cumulative production volume model comparison — Arps modified hyperbolic decline model, power-law exponential decline model, and 50 percent and 100 percent completion efficiency RTA model estimated 30-year cumulative gas production volumes and historic cumulative gas production (G_p) versus production time.

Table A.14 — 30-year estimated cumulative revised gas production (EUR), in units of BSCF, for the Arps modified hyperbolic, power-law exponential and analytical time-rate-pressure decline models.

Arps Modified Hyperbolic BSCF)	Power-Law Exponential (BSCF)	RTA Analytical Model ($q_{g,tot}$ w/ 50% n_f) (BSCF)	RTA Analytical Model ($q_{g,tot}$ w/ 100% n_f) (BSCF)
6.89	3.98	6.68	4.89

Field Example 15 — Time-Rate Analysis

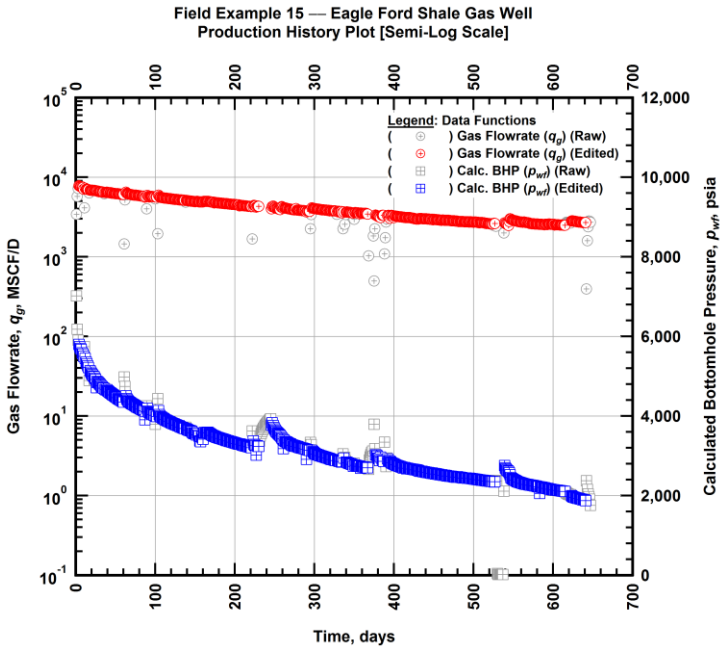

Figure A.421 — (Semi-log Plot): Filtered production history plot — flowrate (q_g) and calculated bottomhole pressure (p_{wf}) versus production time.

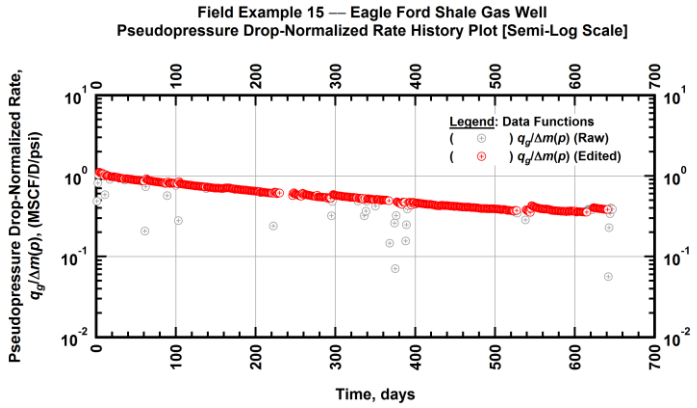

Figure A.422 — (Semi-log Plot): Filtered normalized rate production history plot — pseudopressure drop-normalized gas flowrate ($q_g/\Delta m(p)$) versus production time.

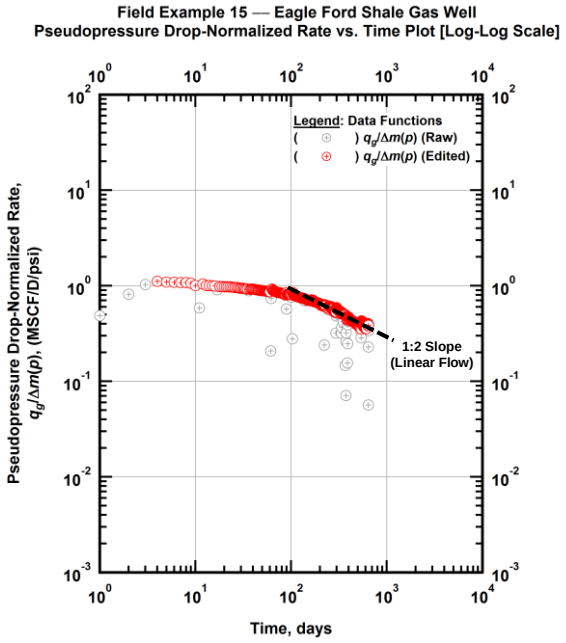

Figure A.423 — (Log-log Plot): Filtered normalized rate production history plot — pseudopressure drop-normalized gas flowrate ($q_g/\Delta m(p)$) versus production time.

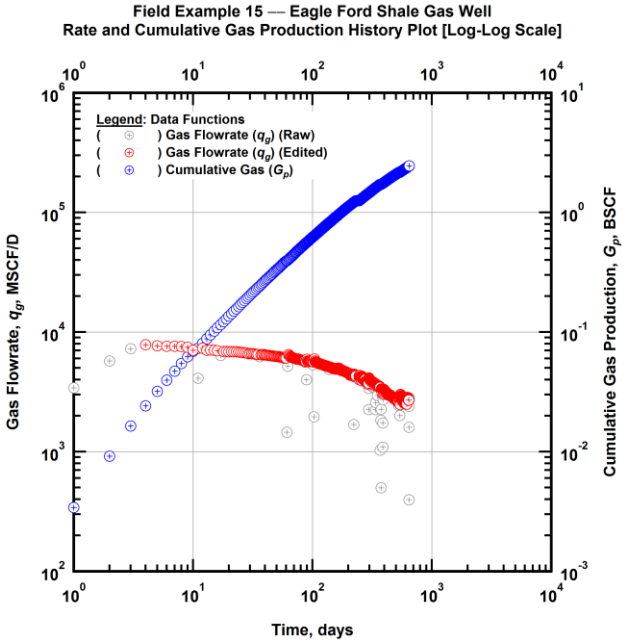

Figure A.424 — (Log-log Plot): Filtered rate and unfiltered cumulative gas production history plot — flowrate (q_g) and cumulative production (G_p) versus production time.

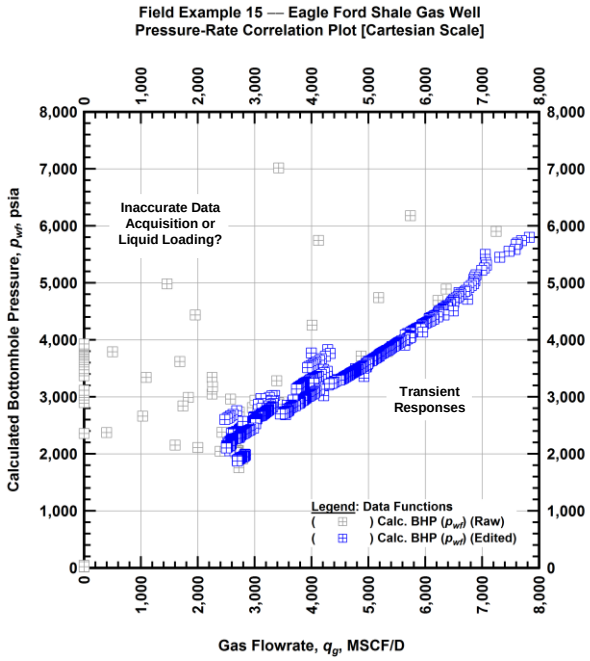

Figure A.425 — (Cartesian Plot): Filtered rate-pressure correlation plot — calculated bottomhole pressure (p_{wf}) versus flowrate (q_g).

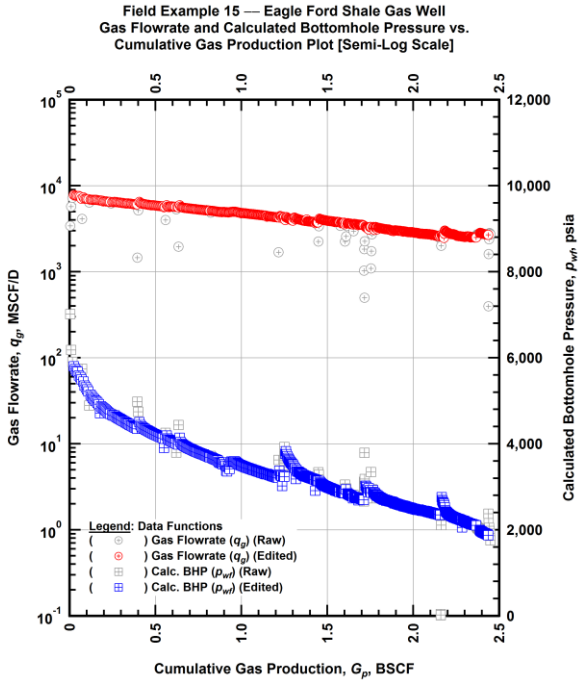

Figure A.426 — (Semi-log Plot): Filtered rate-pressure-cumulative production history plot — flowrate (q_g) and calculated bottomhole pressure (p_{wf}) versus cumulative production (G_p).

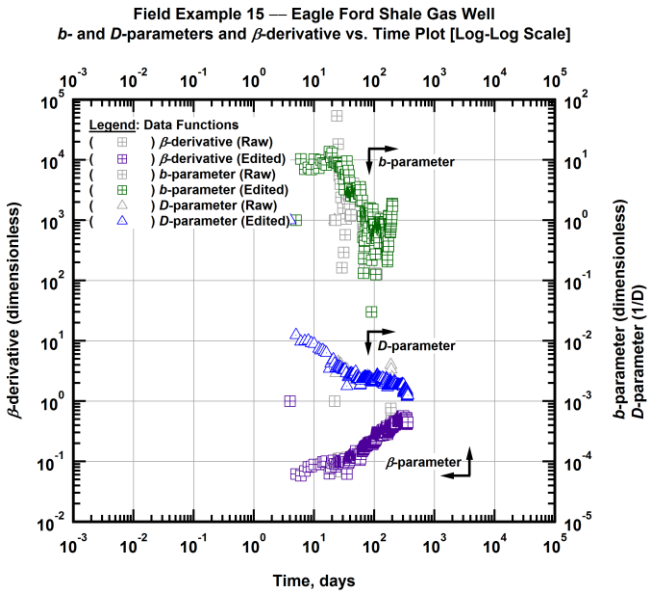

Figure A.427 — (Log-Log Plot): Filtered b, D and β production history plot — b- and D-parameters and β-derivative versus production time.

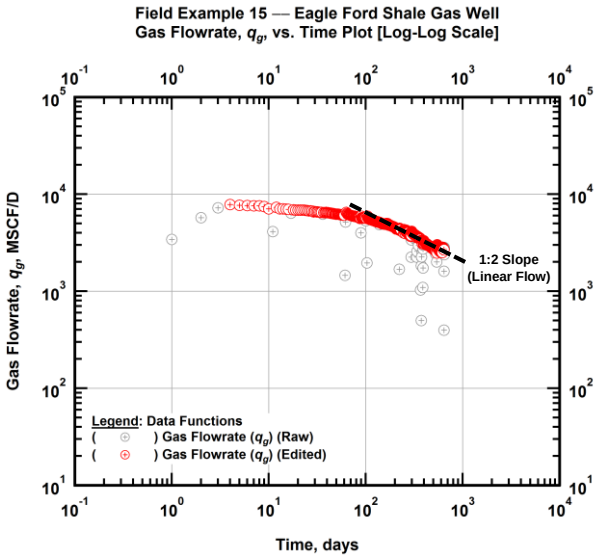

Figure A.428 — (Log-Log Plot): Filtered gas flowrate production history and flow regime identification plot — gas flowrate (q_g) versus production time.

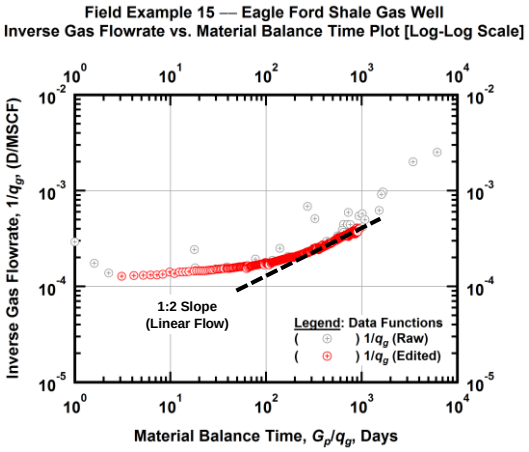

Figure A.429 — (Log-log Plot): Filtered inverse rate with material balance time plot — inverse gas flowrate ($1/q_g$) versus material balance time (G_p/q_g).

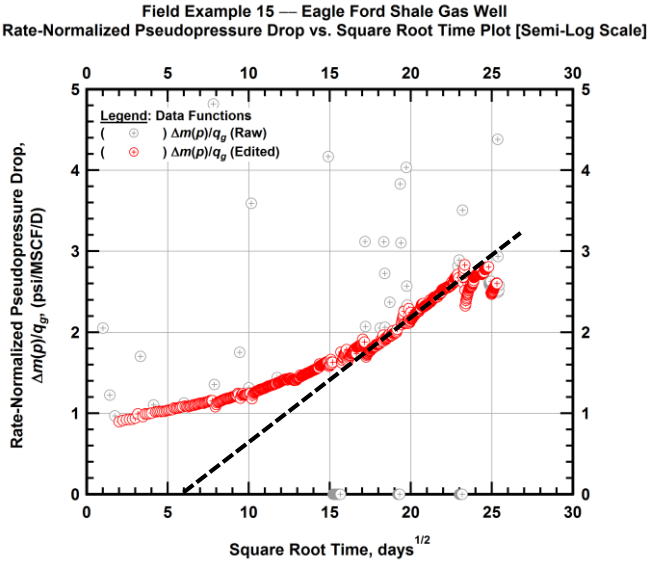

Figure A.430 — (Semi-log Plot): Filtered normalized pseudopressure drop production history plot — rate-normalized pseudopressure drop ($\Delta m(p)/q_g$) versus square root production time ($\sqrt{t}$).

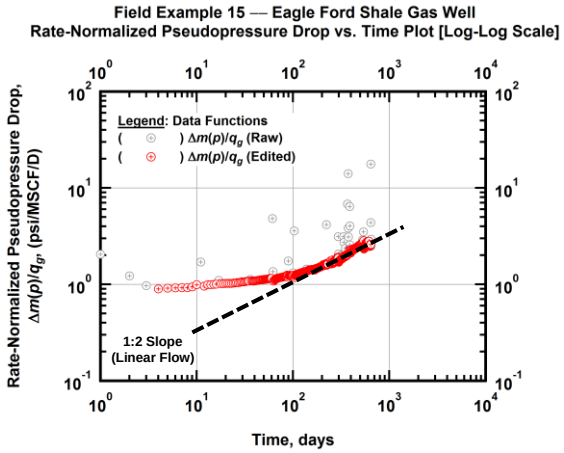

Figure A.431 — (Log-log Plot): Filtered normalized pseudopressure drop production history plot — rate-normalized pseudopressure drop ($\Delta m(p)/q_g$) versus production time.

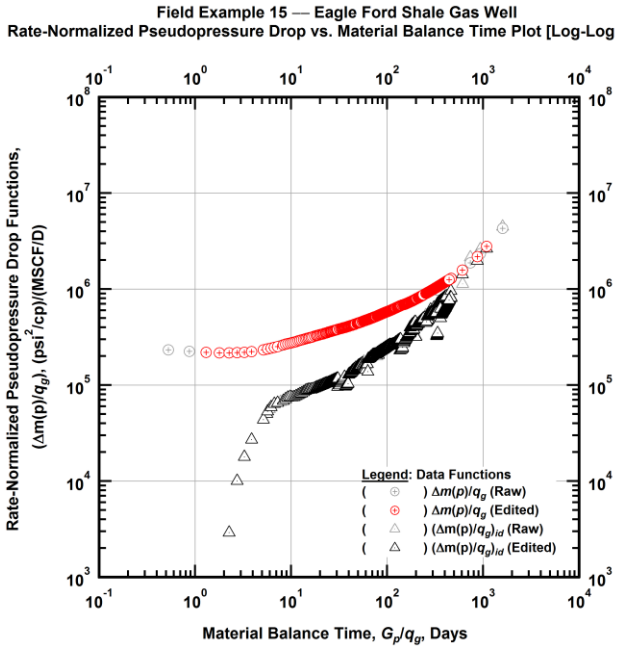

Figure A.432 — (Log-log Plot): "Log-log" diagnostic plot of the filtered production data — rate-normalized pseudopressure drop ($\Delta m(p)/q_g$) and rate-normalized pseudopressure drop integral-derivative $(\Delta m(p)/q_g)_{id}$ versus material balance time (G_p/q_g).

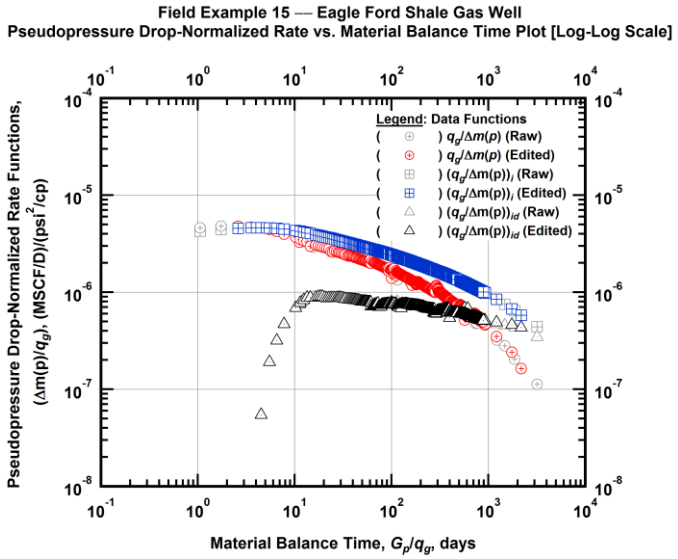

Figure A.433 — (Log-log Plot): "Blasingame" diagnostic plot of the filtered production data — pseudopressure drop-normalized gas flowrate ($q_g/\Delta m(p)$), pseudopressure drop-normalized gas flowrate integral $(q_g/\Delta m(p))_i$ and pseudopressure drop-normalized gas flowrate integral-derivative $(q_g/\Delta m(p))_{id}$ versus material balance time (G_p/q_g).

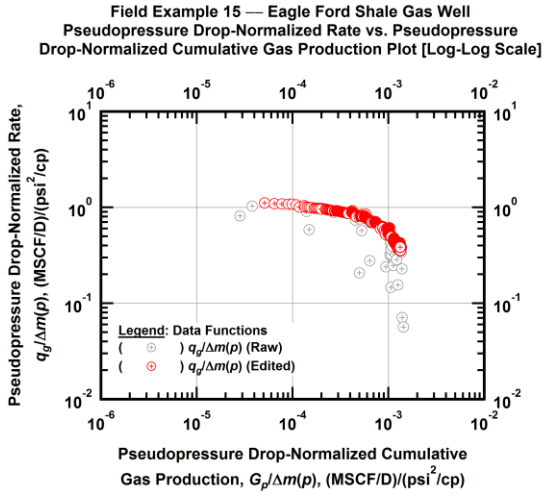

Figure A.434 — (Log-log Plot): Filtered normalized rate with normalized cumulative production plot — pseudopressure drop-normalized gas flowrate ($q_g/\Delta m(p)$) versus pseudopressure drop-normalized cumulative gas production ($G_p/\Delta m(p)$).

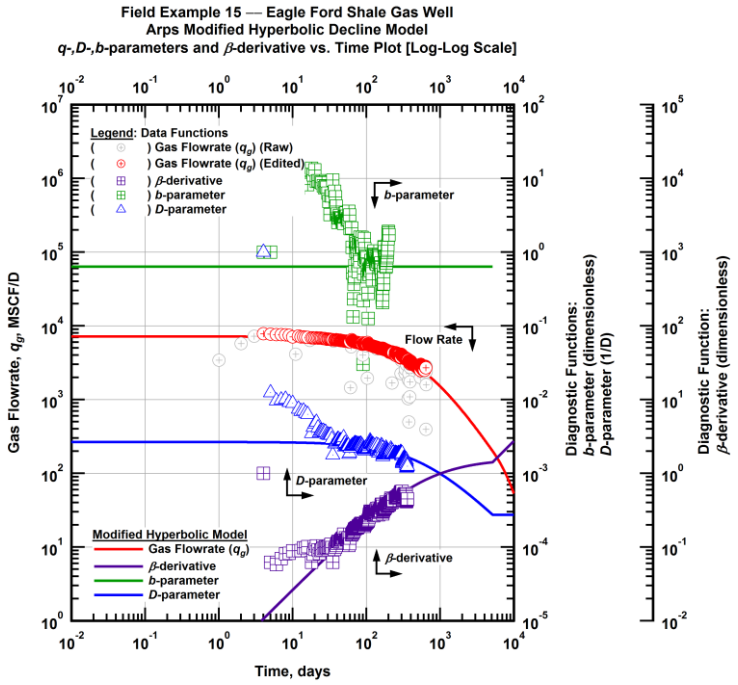

Figure A.435 — (Log-Log Plot): Arps modified hyperbolic decline model plot — time-rate model and data gas flowrate (q_g), *D*- and *b*-parameters and β-derivative versus production time.

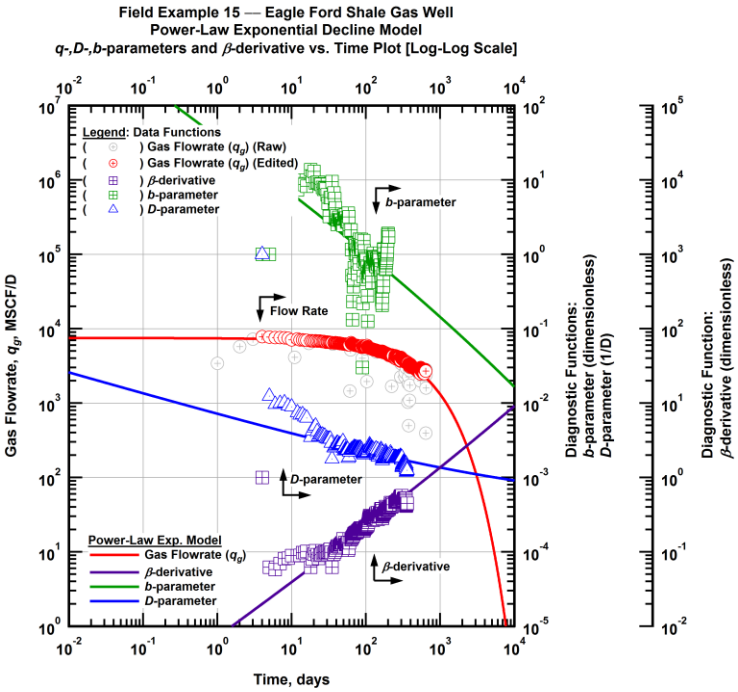

Figure A.436 — (Log-Log Plot): Power-law exponential decline model plot — time-rate model and data gas flowrate (q_g), *D*- and *b*-parameters and β-derivative versus production time.

Field Example 15 — Model-Based (Time-Rate-Pressure) Production Analysis

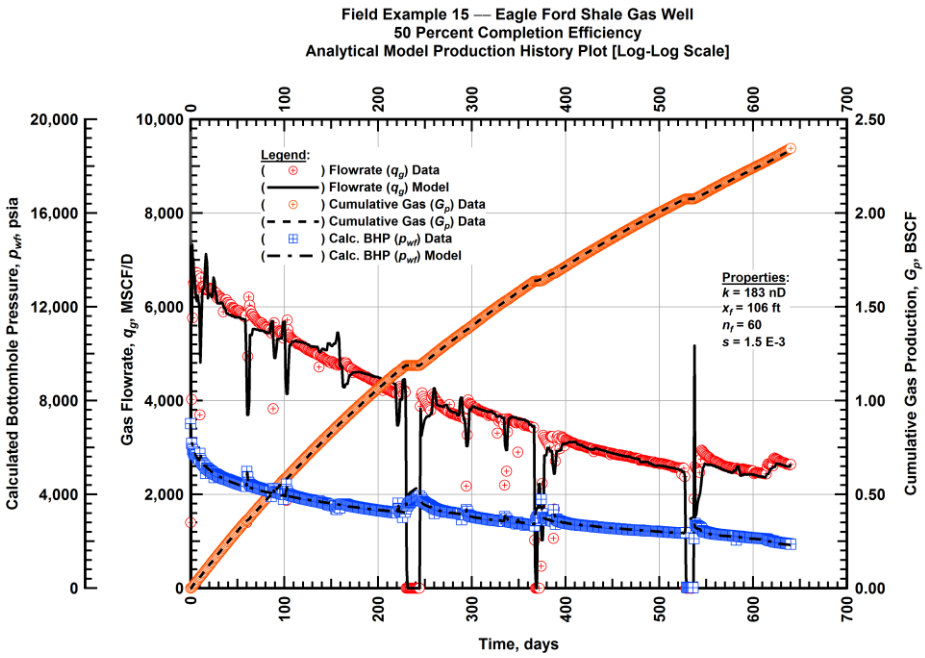

Figure A.437 — (Cartesian Plot): Production history plot — original gas flowrate (q_g), cumulative gas production (G_p), calculated bottomhole pressure (p_{wf}) and 50 percent completion efficiency model matches versus production time.

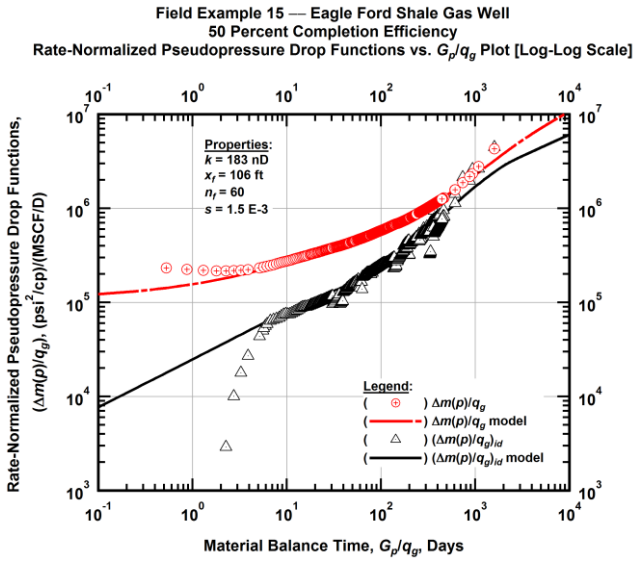

Figure A.438 — (Log-log Plot): "Log-log" diagnostic plot of the original production data — rate-normalized pseudopressure drop ($\Delta m(p)/q_g$), rate-normalized pseudopressure drop integral-derivative $(\Delta m(p)/q_g)_{id}$ and 50 percent completion efficiency model matches versus material balance time (G_p/q_g).

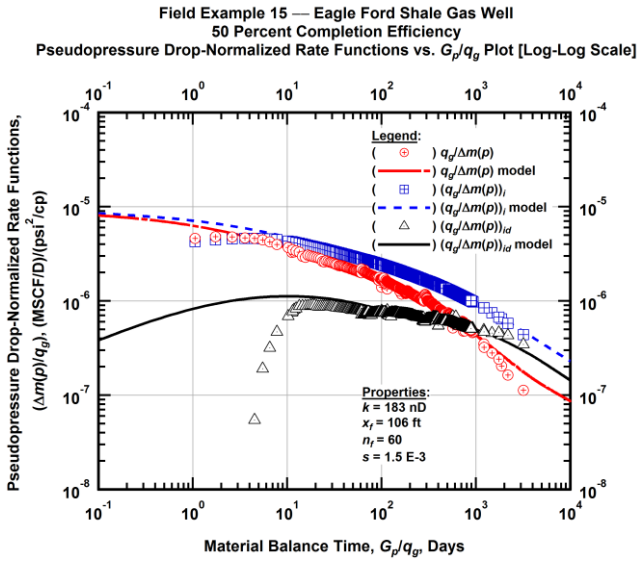

Figure A.439 — (Log-log Plot): "Blasingame" diagnostic plot of the original production data — pseudopressure drop-normalized gas flowrate ($q_g/\Delta m(p)$), pseudopressure drop-normalized gas flowrate integral $(q_g/\Delta m(p))_i$, pseudopressure drop-normalized gas flowrate integral-derivative $(q_g/\Delta m(p))_{id}$ and 50 percent completion efficiency model matches versus material balance time (G_p/q_g).

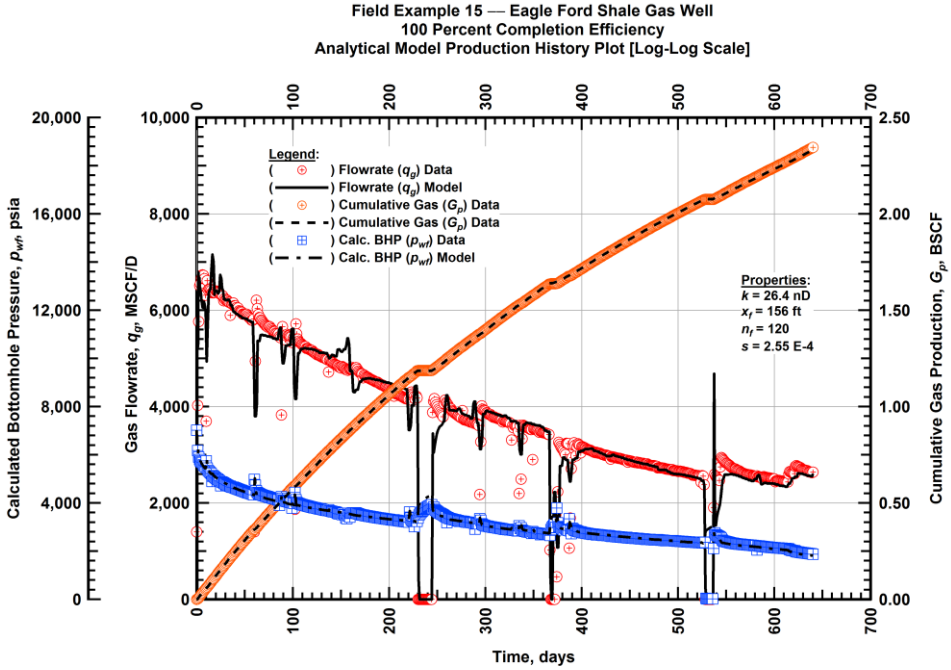

Figure A.440 — (Cartesian Plot): Production history plot — original gas flowrate (q_g), cumulative gas production (G_p), calculated bottomhole pressure (p_{wf}) and 100 percent completion efficiency model matches versus production time.

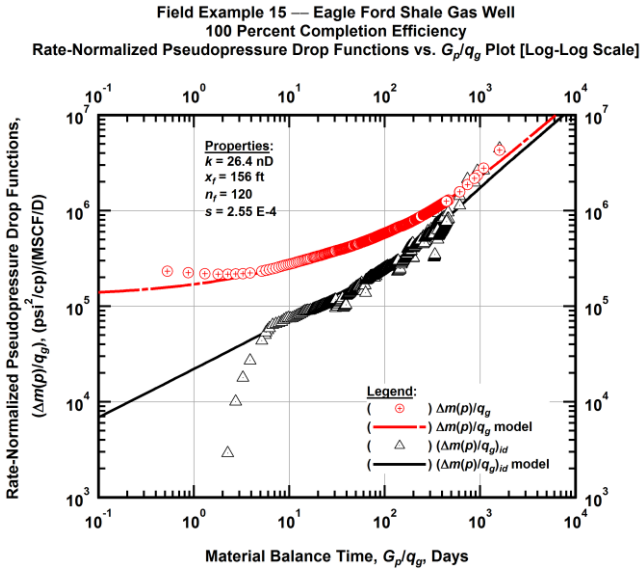

Figure A.441 — (Log-log Plot): "Log-log" diagnostic plot of the original production data — rate-normalized pseudopressure drop ($\Delta m(p)/q_g$), rate-normalized pseudopressure drop integral-derivative $(\Delta m(p)/q_g)_{id}$ and 100 percent completion efficiency model matches versus material balance time (G_p/q_g).

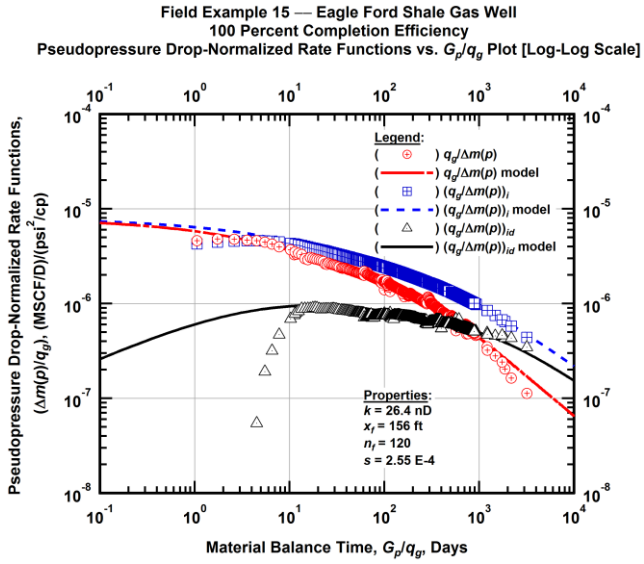

Figure A.442 — (Log-log Plot): "Blasingame" diagnostic plot of the original production data — pseudopressure drop-normalized gas flowrate ($q_g/\Delta m(p)$), pseudopressure drop-normalized gas flowrate integral $(q_g/\Delta m(p))_i$, pseudopressure drop-normalized gas flowrate integral-derivative $(q_g/\Delta m(p))_{id}$ and 100 percent completion efficiency model matches versus material balance time (G_p/q_g).

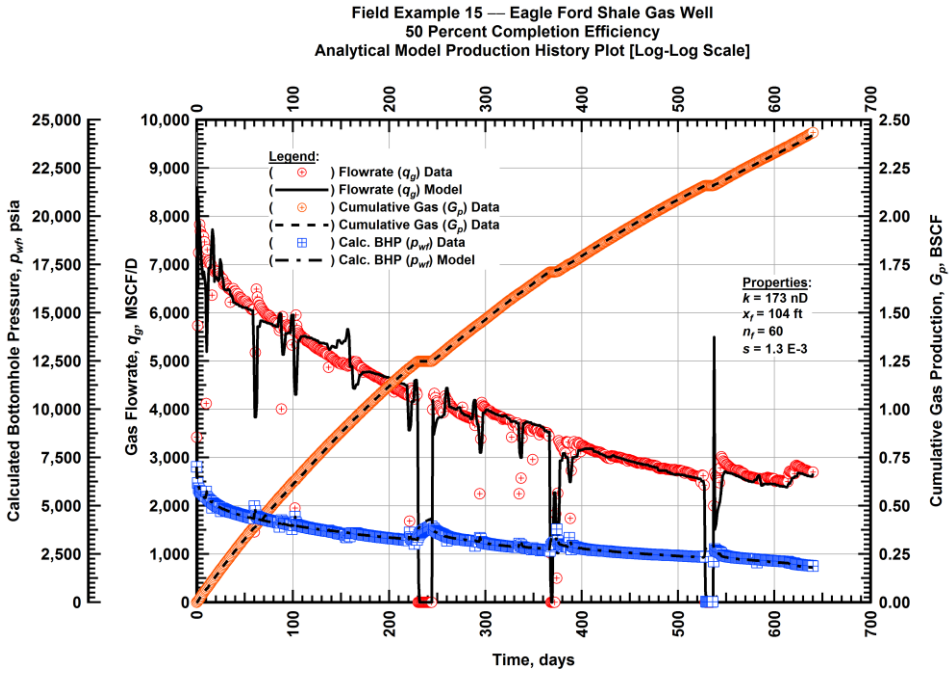

Figure A.443 — (Cartesian Plot): Production history plot — revised gas flowrate (q_g), cumulative gas production (G_p), calculated bottomhole pressure (p_{wf}) and 50 percent completion efficiency model matches versus production time.

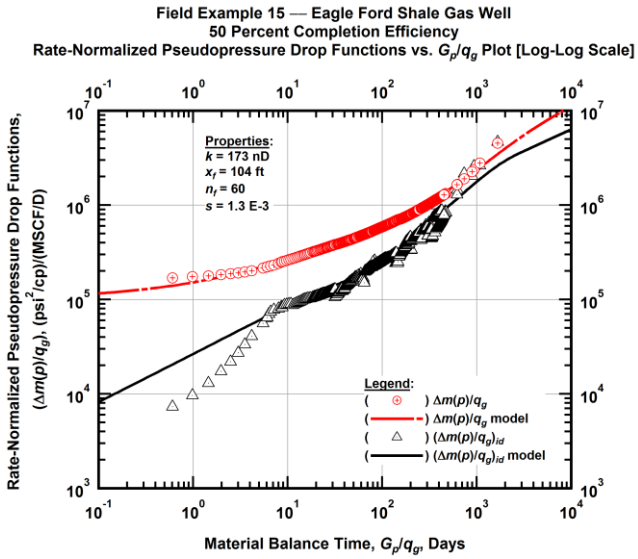

Figure A.444— (Log-log Plot): "Log-log" diagnostic plot of the revised production data — rate-normalized pseudopressure drop ($\Delta m(p)/q_g$), rate-normalized pseudopressure drop integral-derivative $(\Delta m(p)/q_g)_{id}$ and 50 percent completion efficiency model matches versus material balance time (G_p/q_g).

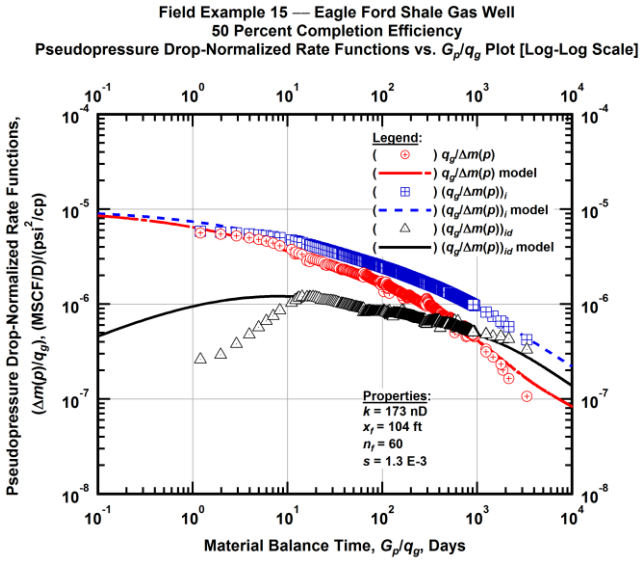

Figure A.445 — (Log-log Plot): "Blasingame" diagnostic plot of the revised production data — pseudopressure drop-normalized gas flowrate ($q_g/\Delta m(p)$), pseudopressure drop-normalized gas flowrate integral $(q_g/\Delta m(p))_i$, pseudopressure drop-normalized gas flowrate integral-derivative $(q_g/\Delta m(p))_{id}$ and 50 percent completion efficiency model matches versus material balance time (G_p/q_g).

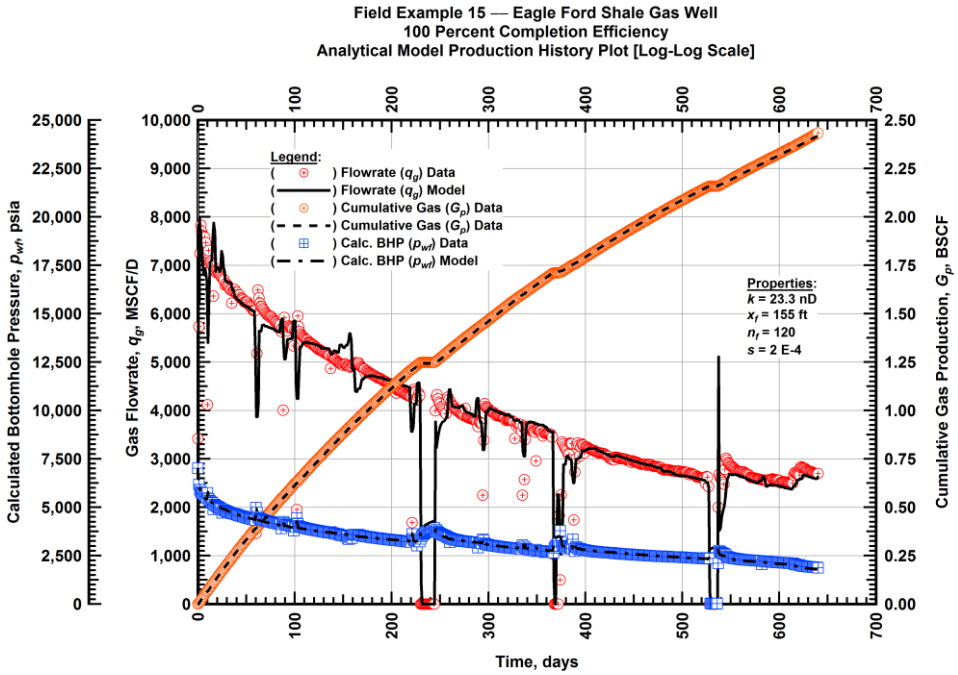

Figure A.446 — (Cartesian Plot): Production history plot — revised gas flowrate (q_g), cumulative gas production (G_p), calculated bottomhole pressure (p_{wf}) and 100 percent completion efficiency model matches versus production time.

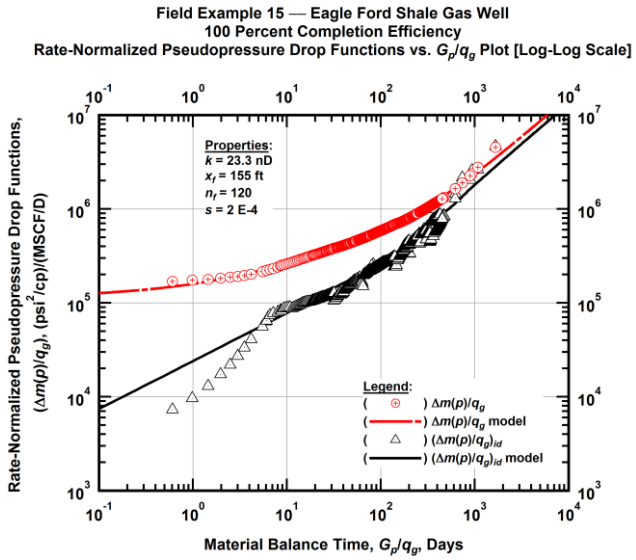

Figure A.447 — (Log-log Plot): "Log-log" diagnostic plot of the revised production data — rate-normalized pseudopressure drop ($\Delta m(p)/q_g$), rate-normalized pseudopressure drop integral-derivative $(\Delta m(p)/q_g)_{id}$ and 100 percent completion efficiency model matches versus material balance time (G_p/q_g).

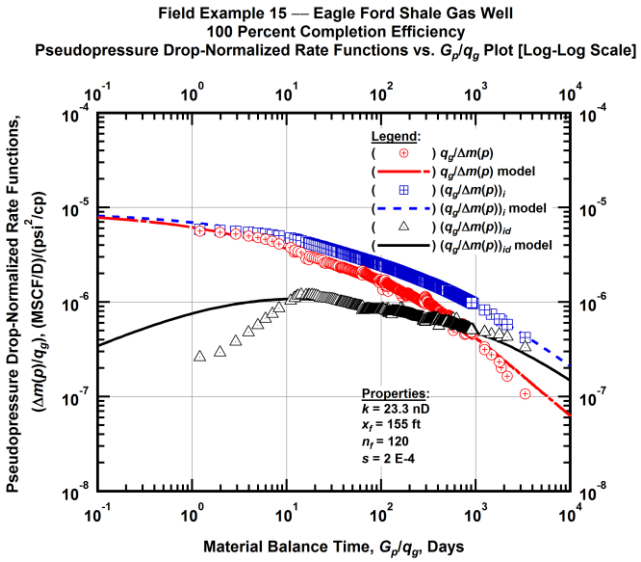

Figure A.448 — (Log-log Plot): "Blasingame" diagnostic plot of the revised production data — pseudopressure drop-normalized gas flowrate ($q_g/\Delta m(p)$), pseudopressure drop-normalized gas flowrate integral $(q_g/\Delta m(p))_i$, pseudopressure drop-normalized gas flowrate integral-derivative $(q_g/\Delta m(p))_{id}$ and 100 percent completion efficiency model matches versus material balance time (G_p/q_g).

Field Example 15 — 30-Year EUR Model Comparison

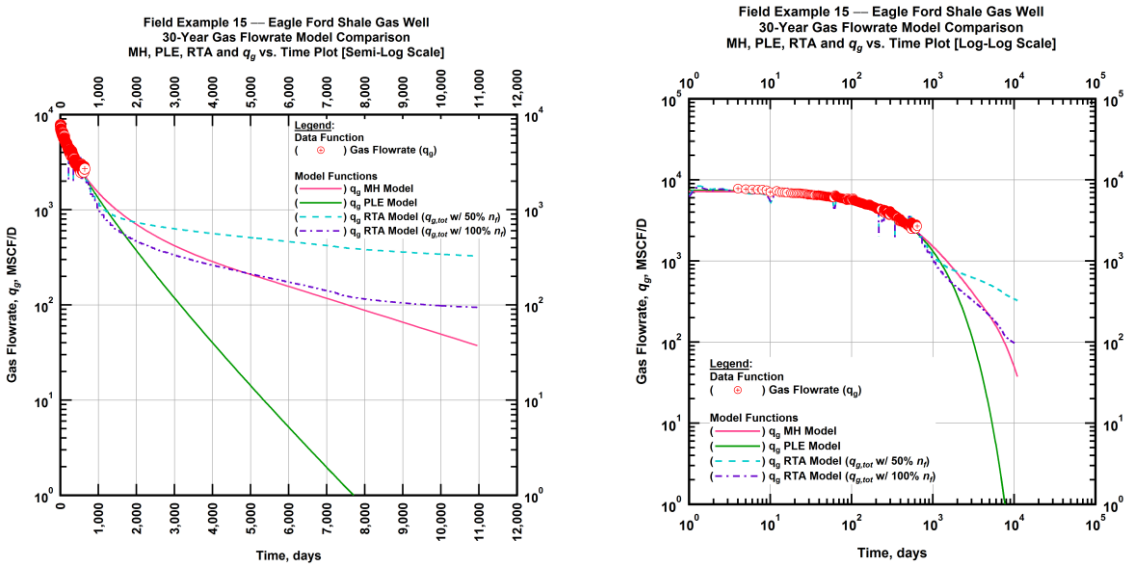

A **B**

Figure A.449 — (A — Semi-Log Plot) and (B — Log-Log Plot): Estimated 30-year revised gas flowrate model comparison — Arps modified hyperbolic decline model, power-law exponential decline model, and 50 percent and 100 percent completion efficiency RTA models revised gas 30-year estimated flowrate decline and historic gas flowrate data (q_g) versus production time.

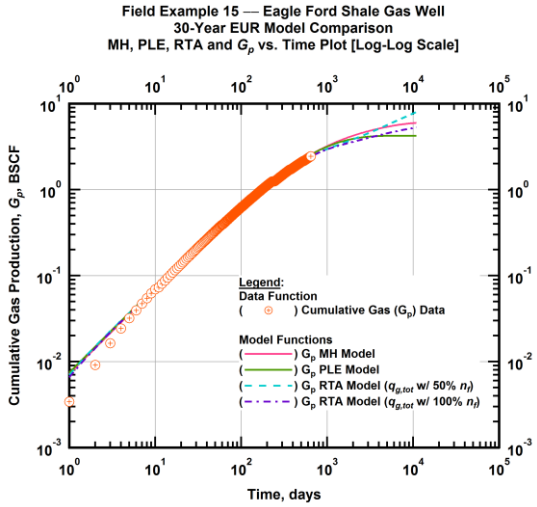

Figure A.450 — (Log-log Plot): PVT revised gas 30-year estimated cumulative production volume model comparison — Arps modified hyperbolic decline model, power-law exponential decline model, and 50 percent and 100 percent completion efficiency RTA model estimated 30-year cumulative gas production volumes and historic cumulative gas production (G_p) versus production time.

Table A.15 — 30-year estimated cumulative revised gas production (EUR), in units of BSCF, for the Arps modified hyperbolic, power-law exponential and analytical time-rate-pressure decline models.

Arps Modified Hyperbolic BSCF)	Power-Law Exponential (BSCF)	RTA Analytical Model ($q_{g,tot}$ w/ 50% n_f) (BSCF)	RTA Analytical Model ($q_{g,tot}$ w/ 100% n_f) (BSCF)
5.87	4.11	8.22	5.35

Field Example 16 — Time-Rate Analysis

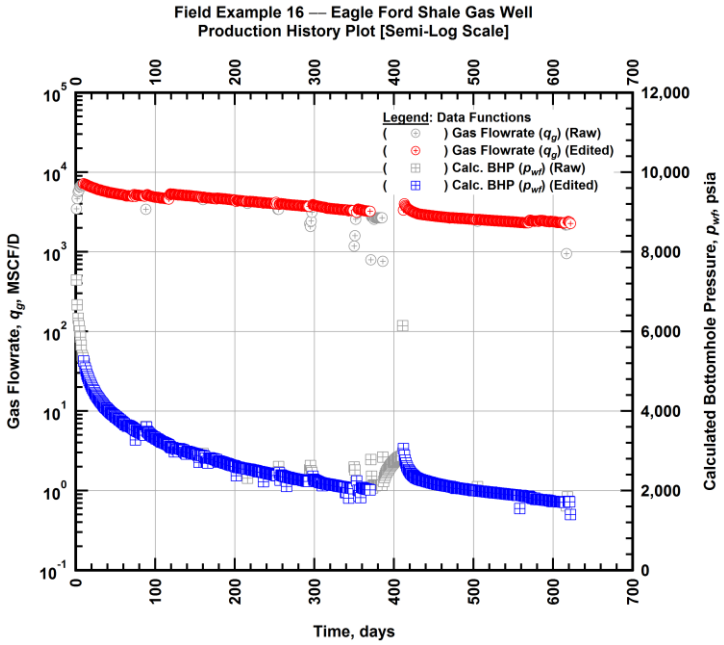

Figure A.451 — (Semi-log Plot): Filtered production history plot — flowrate (q_g) and calculated bottomhole pressure (p_{wf}) versus production time.

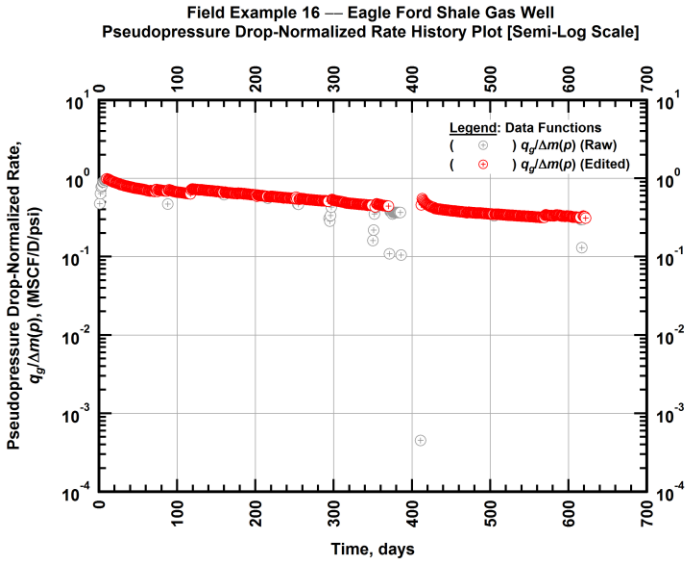

Figure A.452 — (Semi-log Plot): Filtered normalized rate production history plot — pseudopressure drop-normalized gas flowrate ($q_g/\Delta m(p)$) versus production time.

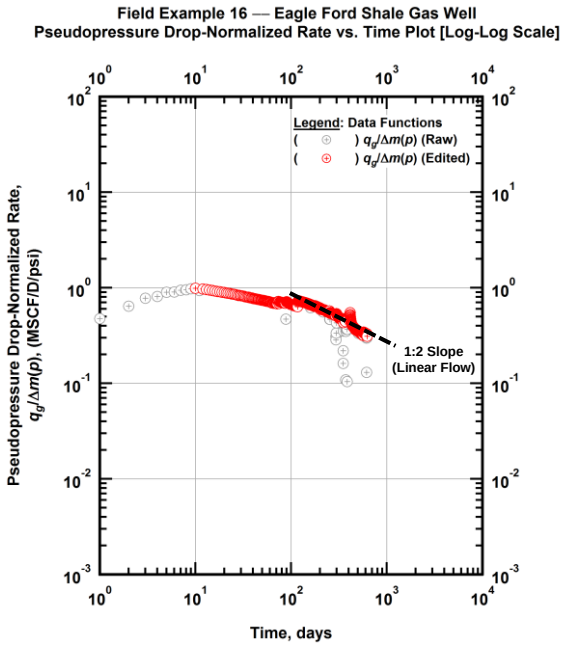

Figure A.453 — (Log-log Plot): Filtered normalized rate production history plot — pseudopressure drop-normalized gas flowrate ($q_g/\Delta m(p)$) versus production time.

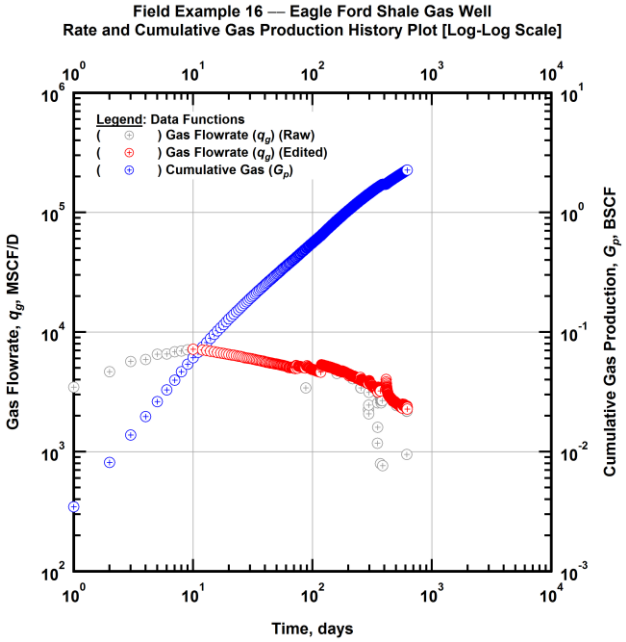

Figure A.454 — (Log-log Plot): Filtered rate and unfiltered cumulative gas production history plot — flowrate (q_g) and cumulative production (G_p) versus production time.

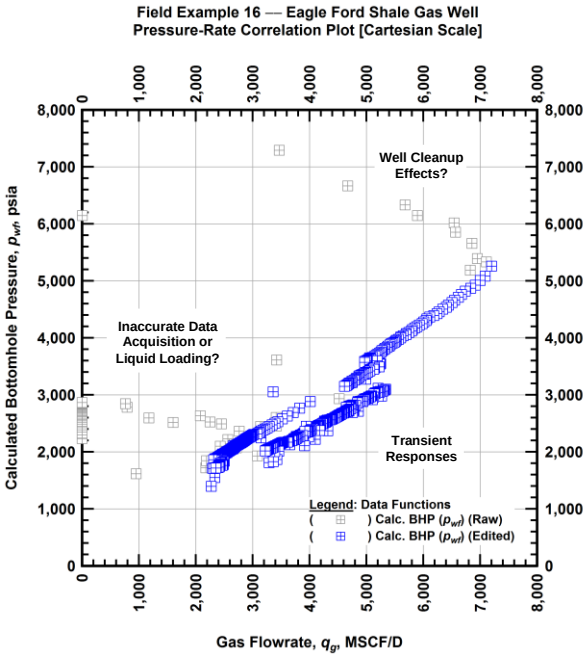

Figure A.455 — (Cartesian Plot): Filtered rate-pressure correlation plot — calculated bottomhole pressure (p_{wf}) versus flowrate (q_g).

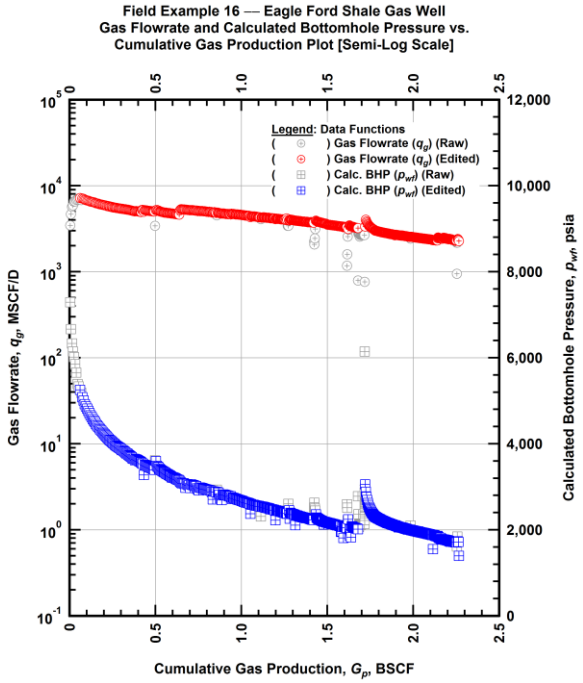

Figure A.456 — (Semi-log Plot): Filtered rate-pressure-cumulative production history plot — flowrate (q_g) and calculated bottomhole pressure (p_{wf}) versus cumulative production (G_p).

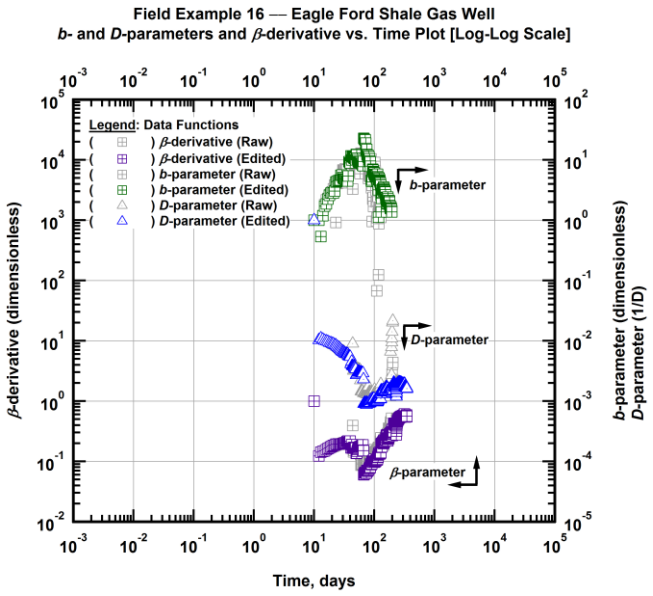

Figure A.457 — (Log-Log Plot): Filtered b, D and β production history plot — b- and D-parameters and β-derivative versus production time.

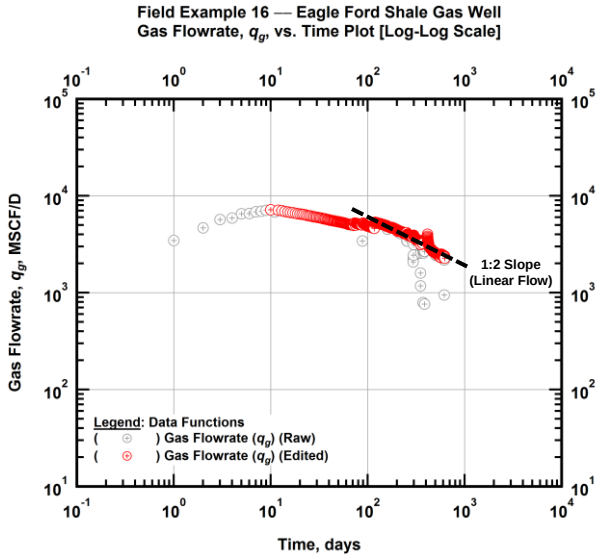

Figure A.458 — (Log-Log Plot): Filtered gas flowrate production history and flow regime identification plot — gas flowrate (q_g) versus production time.

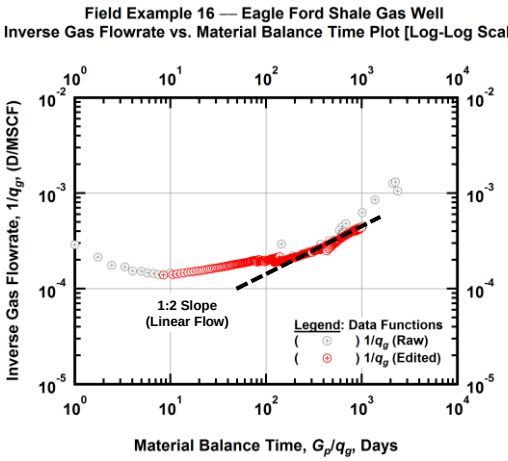

Figure A.459 — (Log-log Plot): Filtered inverse rate with material balance time plot — inverse gas flowrate ($1/q_g$) versus material balance time (G_p/q_g).

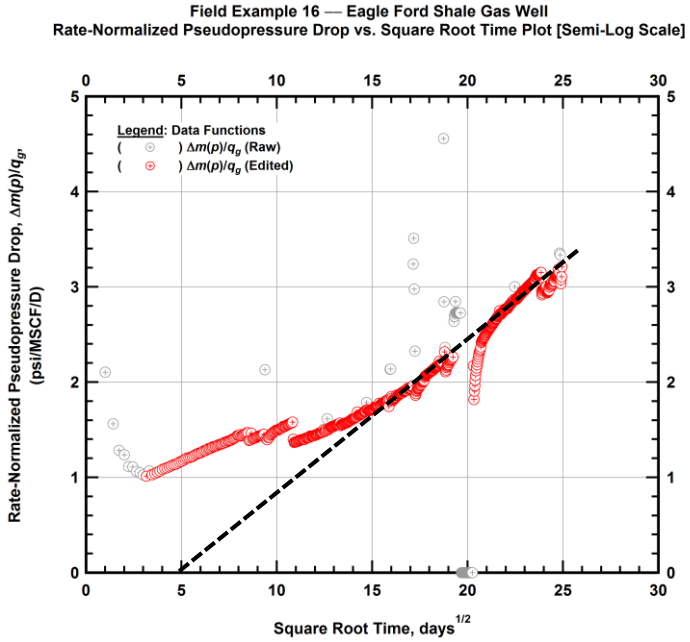

Figure A.460 — (Semi-log Plot): Filtered normalized pseudopressure drop production history plot — rate-normalized pseudopressure drop ($\Delta m(p)/q_g$) versus square root production time ($\sqrt{t}$).

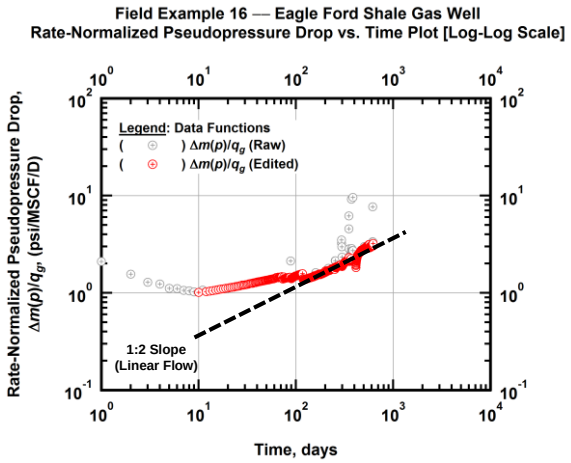

Figure A.461 — (Log-log Plot): Filtered normalized pseudopressure drop production history plot — rate-normalized pseudopressure drop ($\Delta m(p)/q_g$) versus production time.

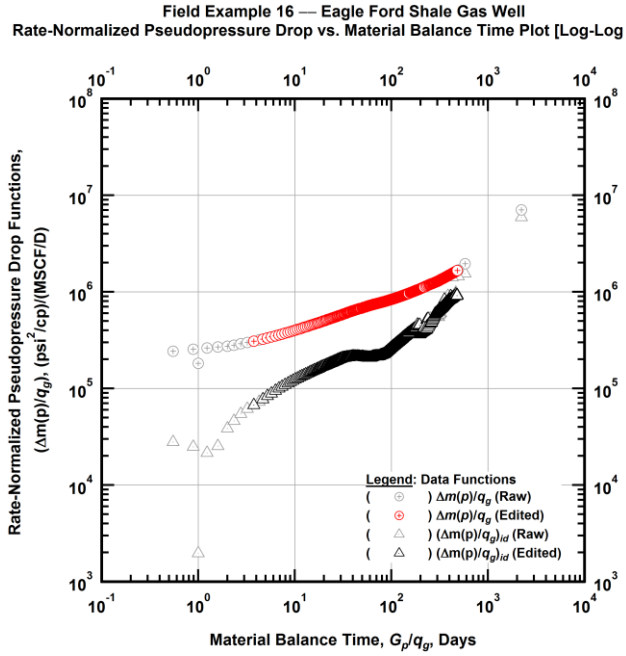

Figure A.462 — (Log-log Plot): "Log-log" diagnostic plot of the filtered production data — rate-normalized pseudopressure drop ($\Delta m(p)/q_g$) and rate-normalized pseudopressure drop integral-derivative $(\Delta m(p)/q_g)_{id}$ versus material balance time (G_p/q_g).

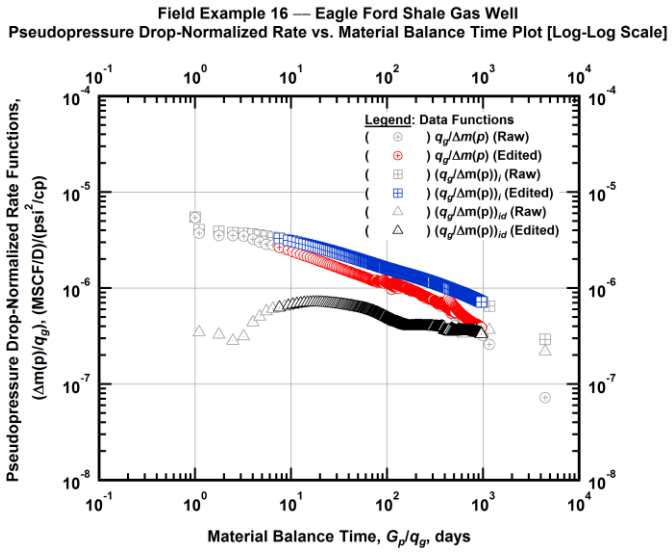

Figure A.463 — (Log-log Plot): "Blasingame" diagnostic plot of the filtered production data — pseudopressure drop-normalized gas flowrate ($q_g/\Delta m(p)$), pseudopressure drop-normalized gas flowrate integral $(q_g/\Delta m(p))_i$ and pseudopressure drop-normalized gas flowrate integral-derivative $(q_g/\Delta m(p))_{id}$ versus material balance time (G_p/q_g).

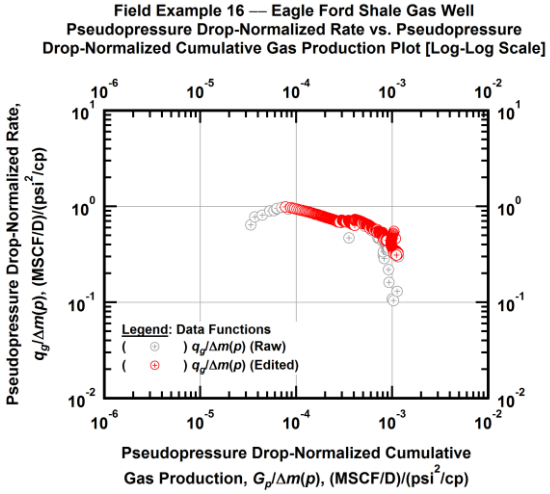

Figure A.464 — (Log-log Plot): Filtered normalized rate with normalized cumulative production plot — pseudopressure drop-normalized gas flowrate ($q_g/\Delta m(p)$) versus pseudopressure drop-normalized cumulative gas production ($G_p/\Delta m(p)$).

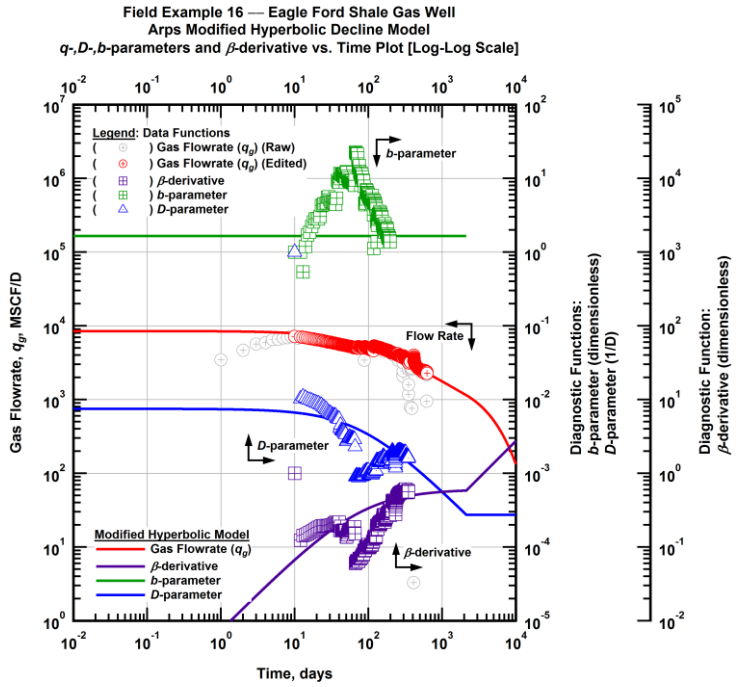

Figure A.465 — (Log-Log Plot): Arps modified hyperbolic decline model plot — time-rate model and data gas flowrate (q_g), *D*- and *b*-parameters and β-derivative versus production time.

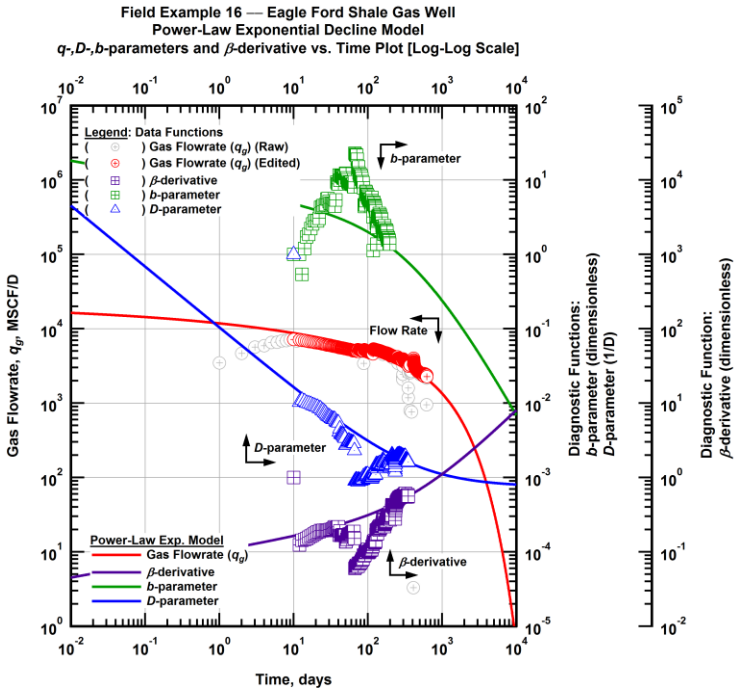

Figure A.466 — (Log-Log Plot): Power-law exponential decline model plot — time-rate model and data gas flowrate (q_g), *D*- and *b*-parameters and β-derivative versus production time.

Field Example 16 — Model-Based (Time-Rate-Pressure) Production Analysis

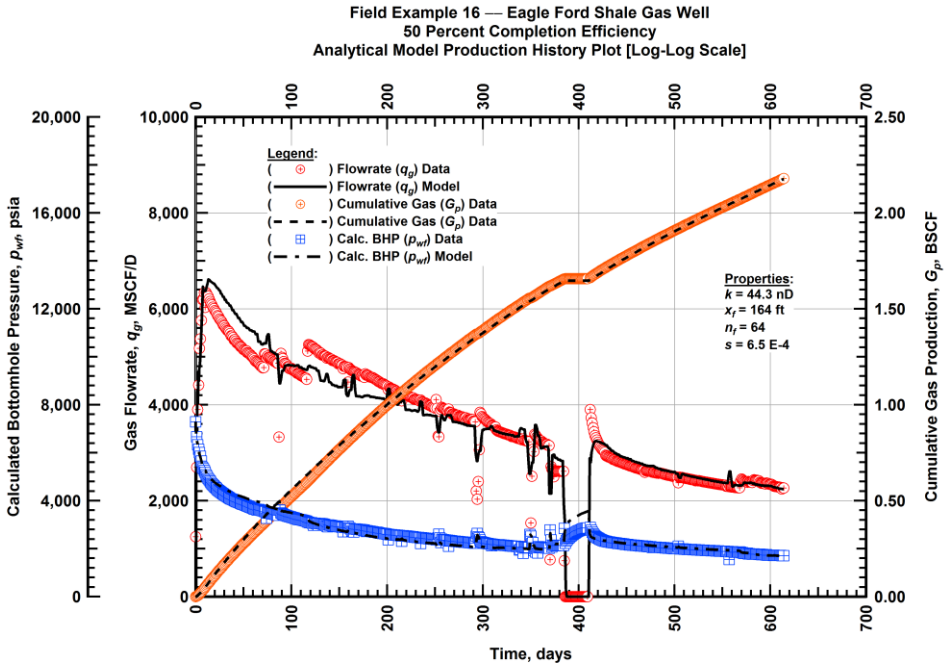

Figure A.467 — (Cartesian Plot): Production history plot — original gas flowrate (q_g), cumulative gas production (G_p), calculated bottomhole pressure (p_{wf}) and 50 percent completion efficiency model matches versus production time.

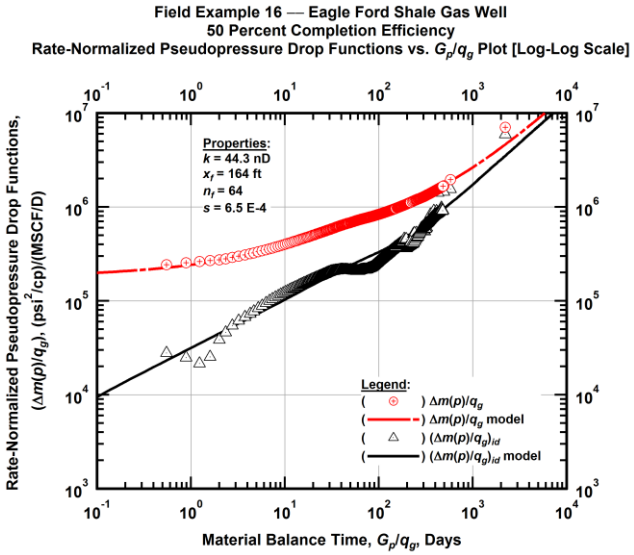

Figure A.468 — (Log-log Plot): "Log-log" diagnostic plot of the original production data — rate-normalized pseudopressure drop ($\Delta m(p)/q_g$), rate-normalized pseudopressure drop integral-derivative $(\Delta m(p)/q_g)_{id}$ and 50 percent completion efficiency model matches versus material balance time (G_p/q_g).

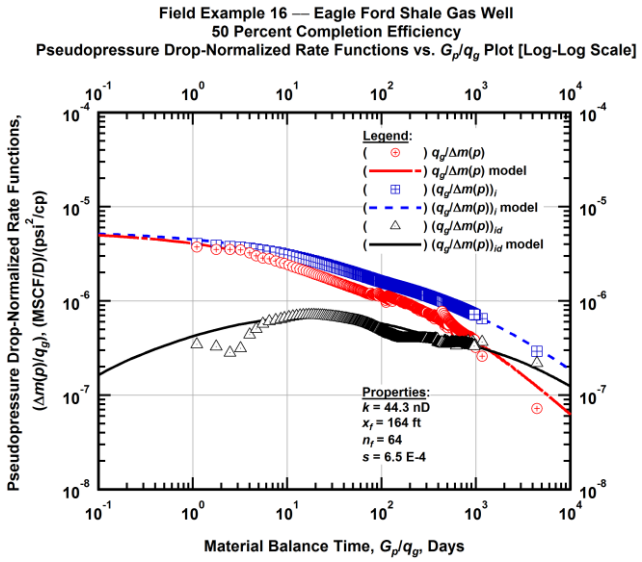

Figure A.469 — (Log-log Plot): "Blasingame" diagnostic plot of the original production data — pseudopressure drop-normalized gas flowrate ($q_g/\Delta m(p)$), pseudopressure drop-normalized gas flowrate integral $(q_g/\Delta m(p))_i$, pseudopressure drop-normalized gas flowrate integral-derivative $(q_g/\Delta m(p))_{id}$ and 50 percent completion efficiency model matches versus material balance time (G_p/q_g).

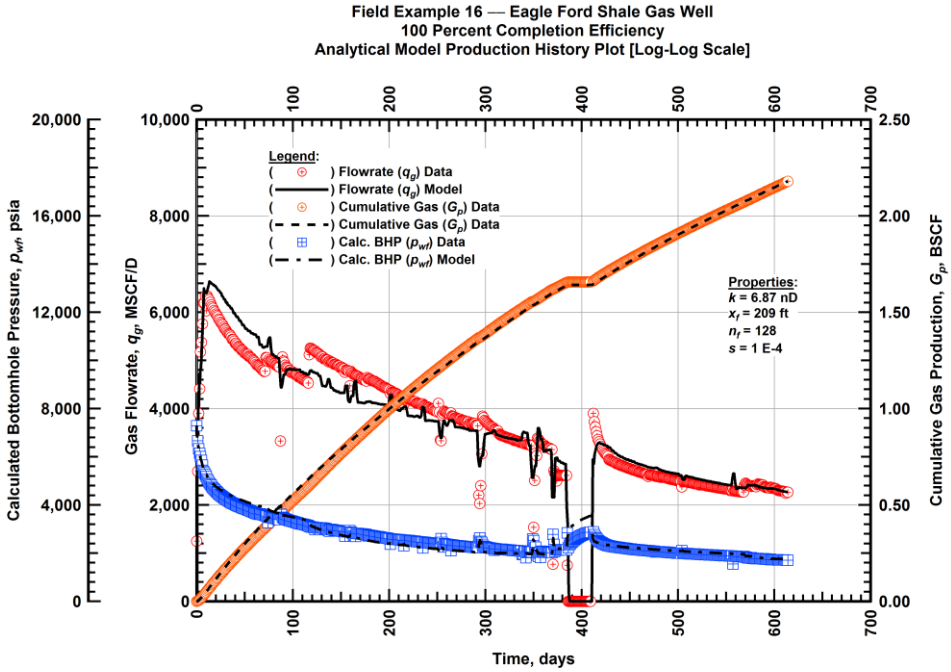

Figure A.470 — (Cartesian Plot): Production history plot — original gas flowrate (q_g), cumulative gas production (G_p), calculated bottomhole pressure (p_{wf}) and 100 percent completion efficiency model matches versus production time.

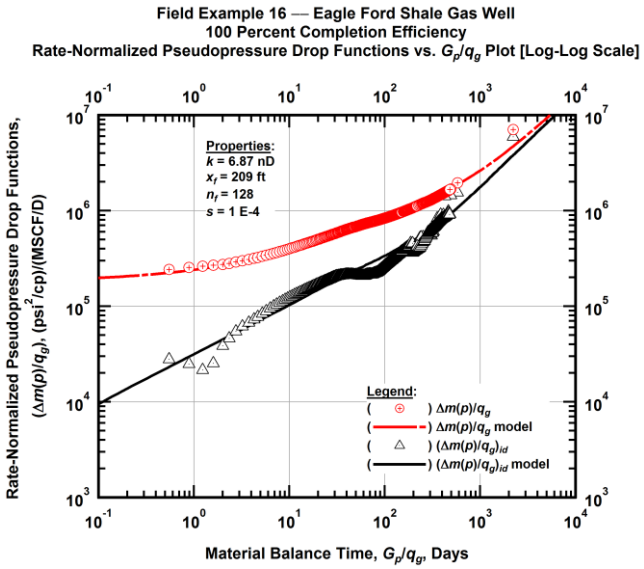

Figure A.471 — (Log-log Plot): "Log-log" diagnostic plot of the original production data — rate-normalized pseudopressure drop ($\Delta m(p)/q_g$), rate-normalized pseudopressure drop integral-derivative $(\Delta m(p)/q_g)_{id}$ and 100 percent completion efficiency model matches versus material balance time (G_p/q_g).

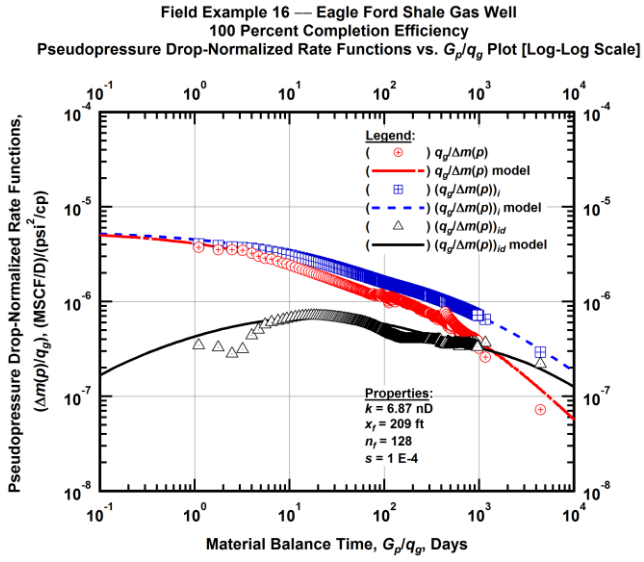

Figure A.472 — (Log-log Plot): "Blasingame" diagnostic plot of the original production data — pseudopressure drop-normalized gas flowrate ($q_g/\Delta m(p)$), pseudopressure drop-normalized gas flowrate integral $(q_g/\Delta m(p))_i$, pseudopressure drop-normalized gas flowrate integral-derivative $(q_g/\Delta m(p))_{id}$ and 100 percent completion efficiency model matches versus material balance time (G_p/q_g).

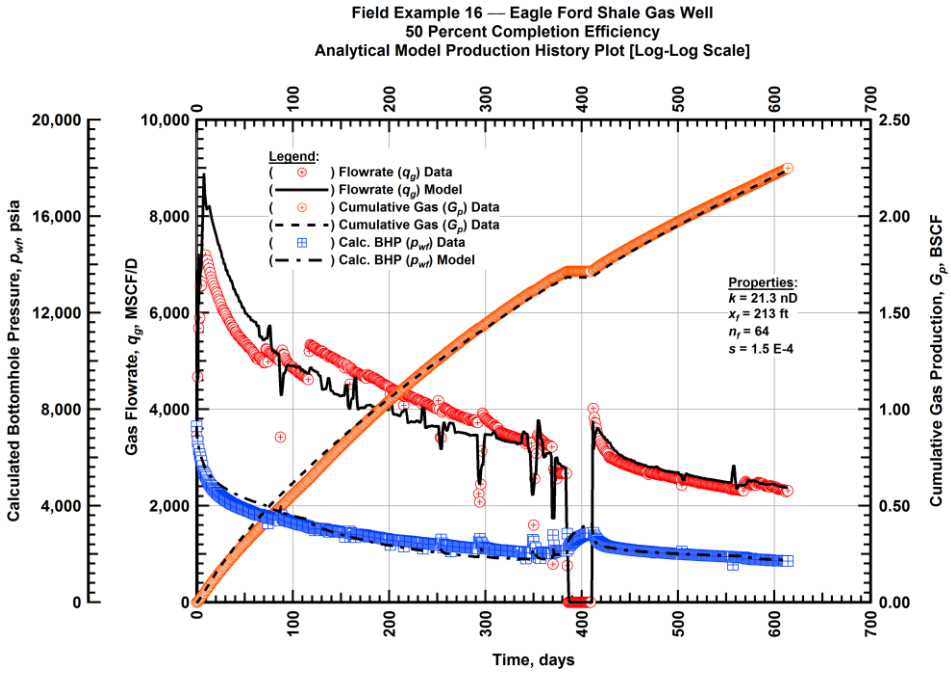

Figure A.473 — (Cartesian Plot): Production history plot — revised gas flowrate (q_g), cumulative gas production (G_p), calculated bottomhole pressure (p_{wf}) and 50 percent completion efficiency model matches versus production time.

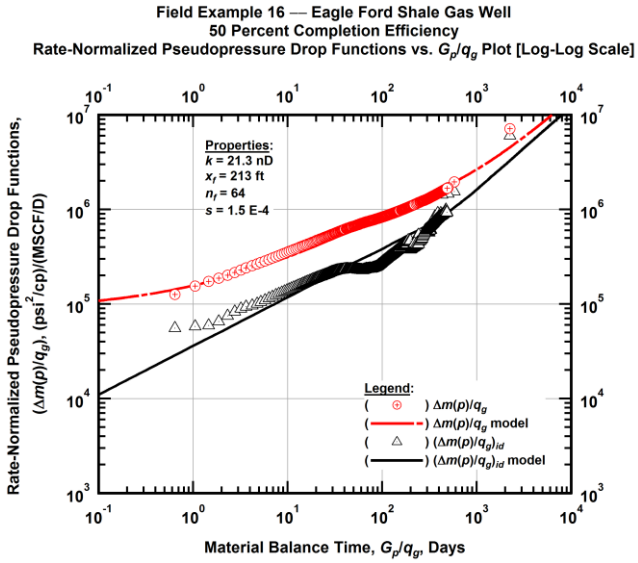

Figure A.474— (Log-log Plot): "Log-log" diagnostic plot of the revised production data — rate-normalized pseudopressure drop ($\Delta m(p)/q_g$), rate-normalized pseudopressure drop integral-derivative $(\Delta m(p)/q_g)_{id}$ and 50 percent completion efficiency model matches versus material balance time (G_p/q_g).

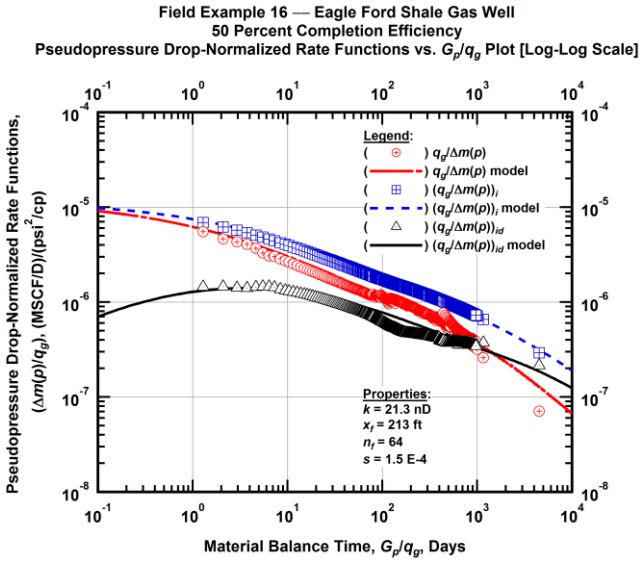

Figure A.475 — (Log-log Plot): "Blasingame" diagnostic plot of the revised production data — pseudopressure drop-normalized gas flowrate ($q_g/\Delta m(p)$), pseudopressure drop-normalized gas flowrate integral $(q_g/\Delta m(p))_i$, pseudopressure drop-normalized gas flowrate integral-derivative $(q_g/\Delta m(p))_{id}$ and 50 percent completion efficiency model matches versus material balance time (G_p/q_g).

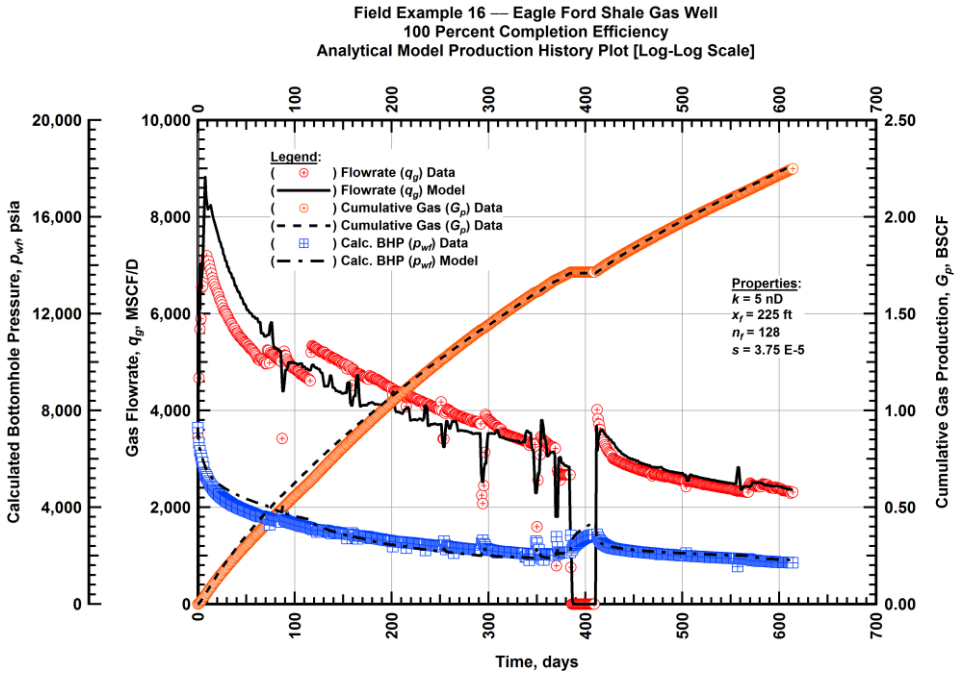

Figure A.476 — (Cartesian Plot): Production history plot — revised gas flowrate (q_g), cumulative gas production (G_p), calculated bottomhole pressure (p_{wf}) and 100 percent completion efficiency model matches versus production time.

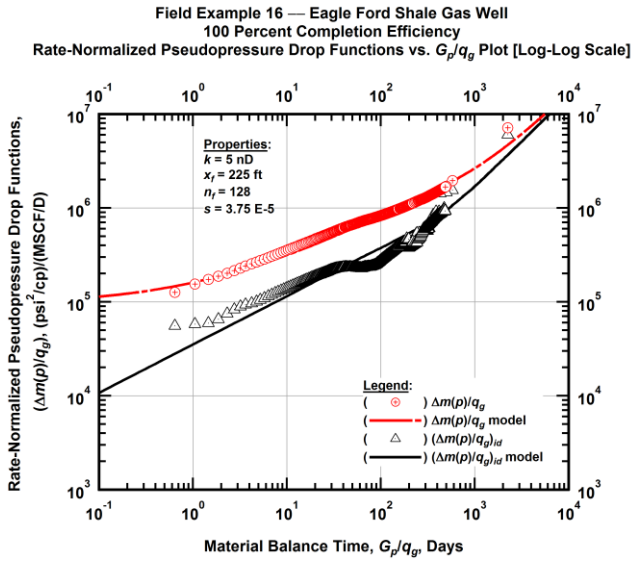

Figure A.477 — (Log-log Plot): "Log-log" diagnostic plot of the revised production data — rate-normalized pseudopressure drop ($\Delta m(p)/q_g$), rate-normalized pseudopressure drop integral-derivative $(\Delta m(p)/q_g)_{id}$ and 100 percent completion efficiency model matches versus material balance time (G_p/q_g).

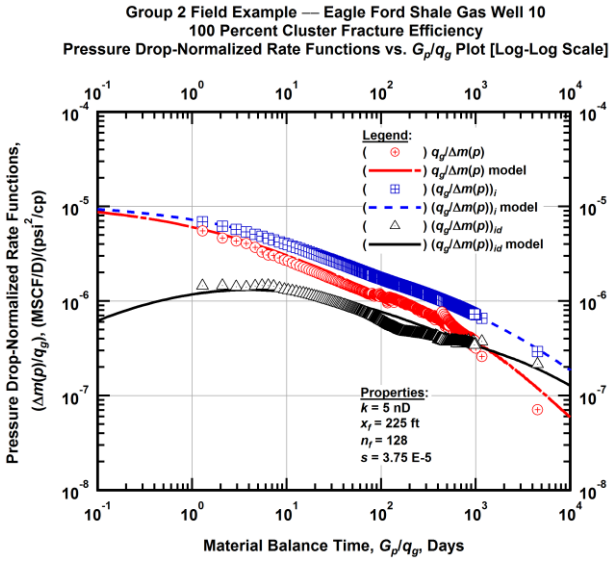

Figure A.478 — (Log-log Plot): "Blasingame" diagnostic plot of the revised production data — pseudopressure drop-normalized gas flowrate ($q_g/\Delta m(p)$), pseudopressure drop-normalized gas flowrate integral $(q_g/\Delta m(p))_i$, pseudopressure drop-normalized gas flowrate integral-derivative $(q_g/\Delta m(p))_{id}$ and 100 percent completion efficiency model matches versus material balance time (G_p/q_g).

Field Example 16 — 30-Year EUR Model Comparison

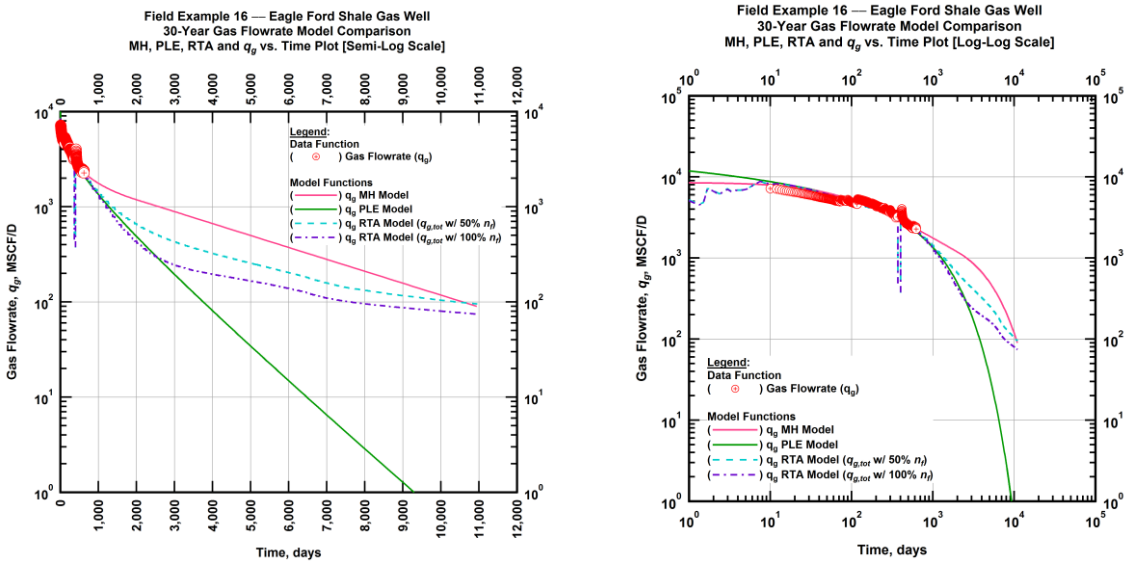

A **B**

Figure A.479 — (A — Semi-Log Plot) and (B — Log-Log Plot): Estimated 30-year revised gas flowrate model comparison — Arps modified hyperbolic decline model, power-law exponential decline model, and 50 percent and 100 percent completion efficiency RTA models revised gas 30-year estimated flowrate decline and historic gas flowrate data (q_g) versus production time.

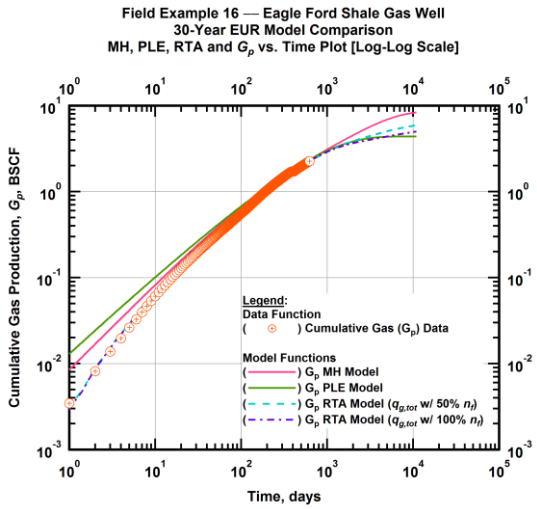

Figure A.480 — (Log-log Plot): PVT revised gas 30-year estimated cumulative production volume model comparison — Arps modified hyperbolic decline model, power-law exponential decline model, and 50 percent and 100 percent completion efficiency RTA model estimated 30-year cumulative gas production volumes and historic cumulative gas production (G_p) versus production time.

Table A.16 — 30-year estimated cumulative revised gas production (EUR), in units of BSCF, for the Arps modified hyperbolic, power-law exponential and analytical time-rate-pressure decline models.

Arps Modified Hyperbolic BSCF)	Power-Law Exponential (BSCF)	RTA Analytical Model ($q_{g,tot}$ w/ 50% n_f) (BSCF)	RTA Analytical Model ($q_{g,tot}$ w/ 100% n_f) (BSCF)
8.43	4.27	5.98	5.04

Field Example 17 — Time-Rate Analysis

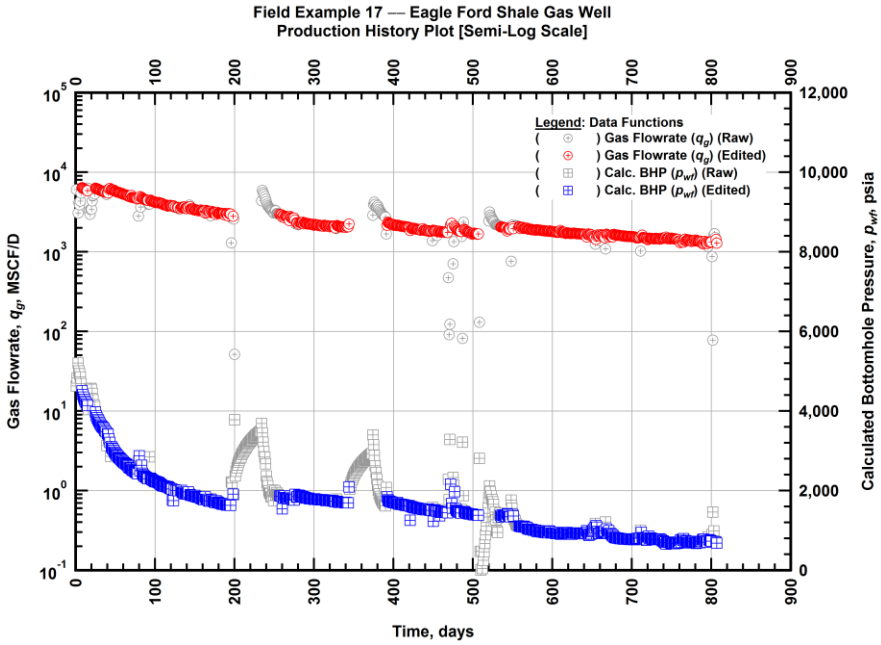

Figure A.481 — (Semi-log Plot): Filtered production history plot — flowrate (q_g) and calculated bottomhole pressure (p_{wf}) versus production time.

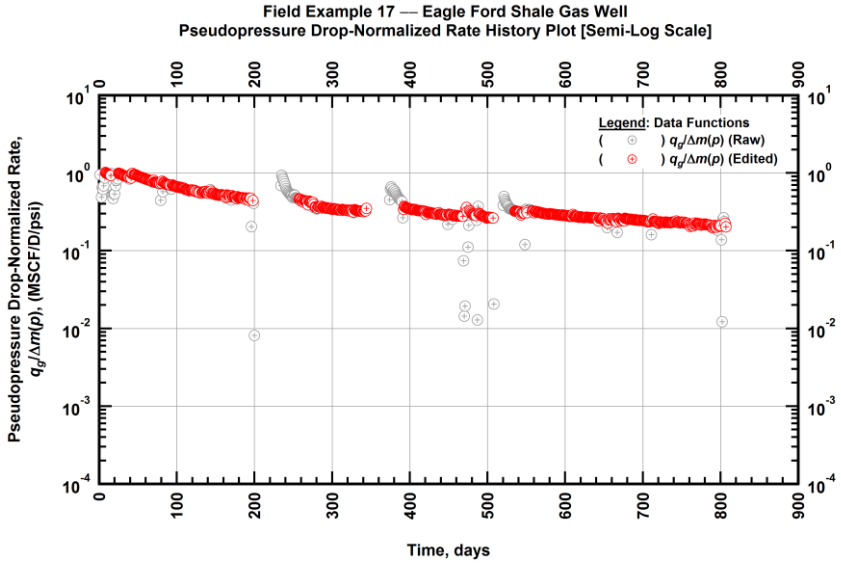

Figure A.482 — (Semi-log Plot): Filtered normalized rate production history plot — pseudopressure drop-normalized gas flowrate ($q_g/\Delta m(p)$) versus production time.

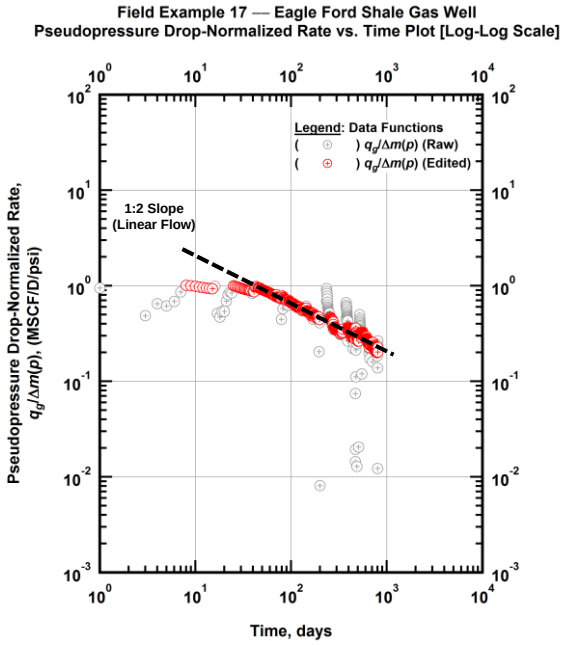

Figure A.483 — (Log-log Plot): Filtered normalized rate production history plot — pseudopressure drop-normalized gas flowrate ($q_g/\Delta m(p)$) versus production time.

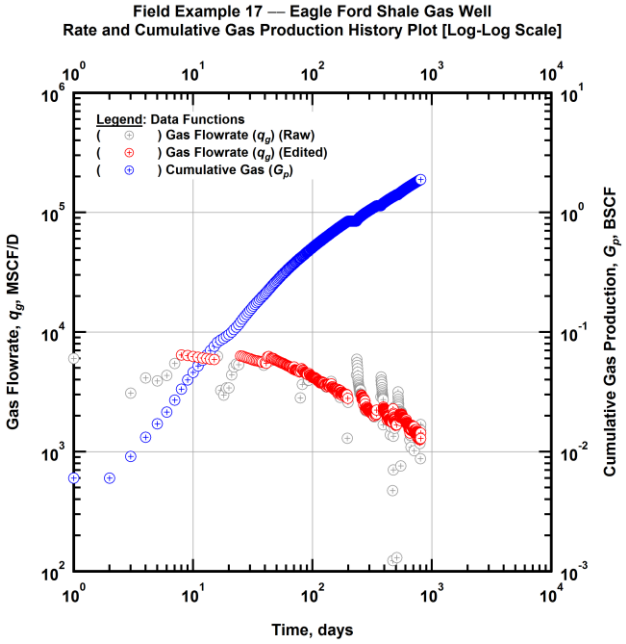

Figure A.484 — (Log-log Plot): Filtered rate and unfiltered cumulative gas production history plot — flowrate (q_g) and cumulative production (G_p) versus production time.

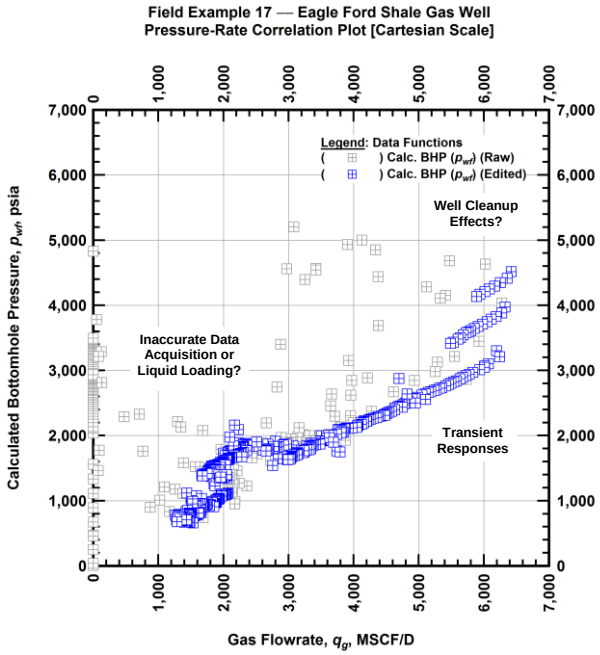

Figure A.485 — (Cartesian Plot): Filtered rate-pressure correlation plot — calculated bottomhole pressure (p_{wf}) versus flowrate (q_g).

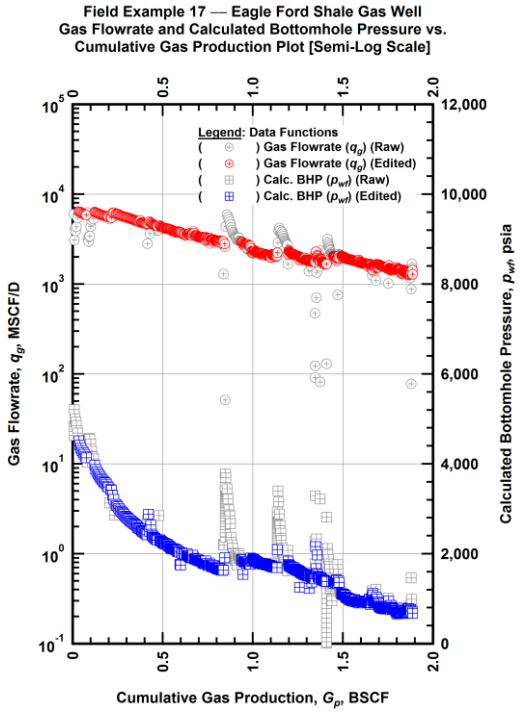

Figure A.486 — (Semi-log Plot): Filtered rate-pressure-cumulative production history plot — flowrate (q_g) and calculated bottomhole pressure (p_{wf}) versus cumulative production (G_p).

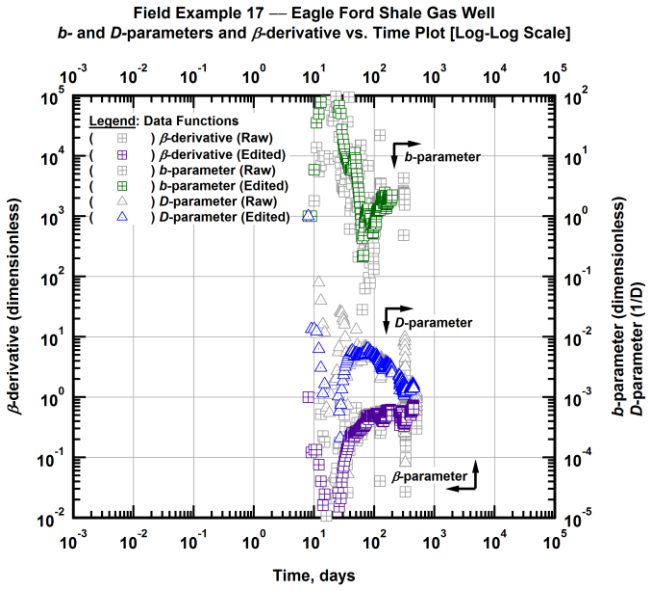

Figure A.487 — (Log-Log Plot): Filtered b, D and β production history plot — b- and D-parameters and β-derivative versus production time.

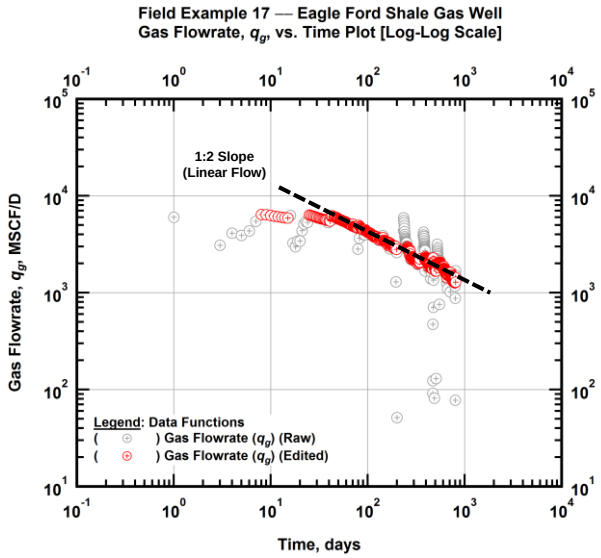

Figure A.488 — (Log-Log Plot): Filtered gas flowrate production history and flow regime identification plot — gas flowrate (q_g) versus production time.

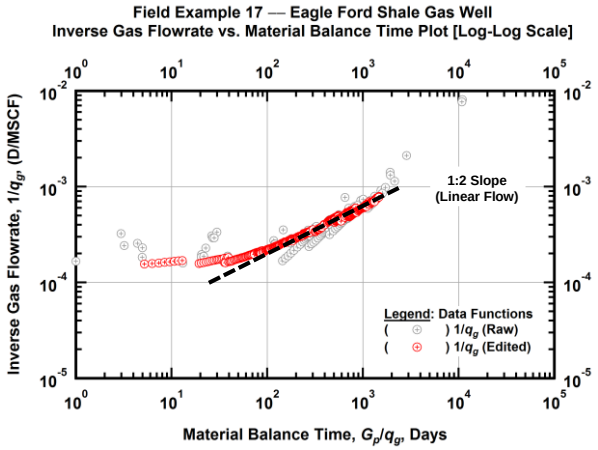

Figure A.489 — (Log-log Plot): Filtered inverse rate with material balance time plot — inverse gas flowrate ($1/q_g$) versus material balance time (G_p/q_g).

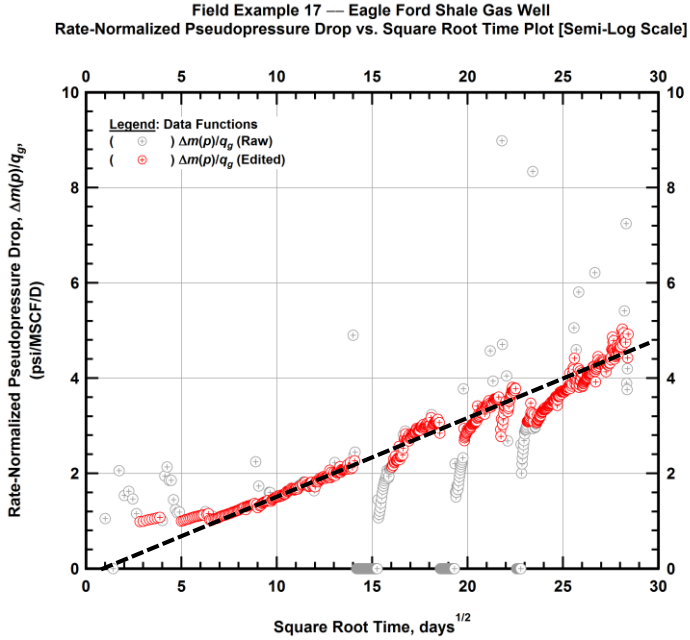

Figure A.490 — (Semi-log Plot): Filtered normalized pseudopressure drop production history plot — rate-normalized pseudopressure drop ($\Delta m(p)/q_g$) versus square root production time ($\sqrt{t}$).

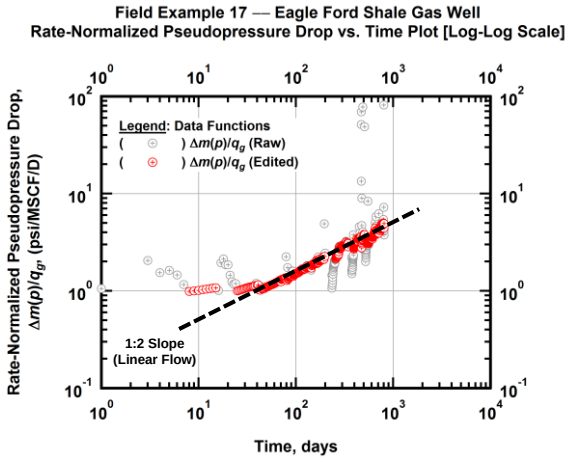

Figure A.491 — (Log-log Plot): Filtered normalized pseudopressure drop production history plot — rate-normalized pseudopressure drop ($\Delta m(p)/q_g$) versus production time.

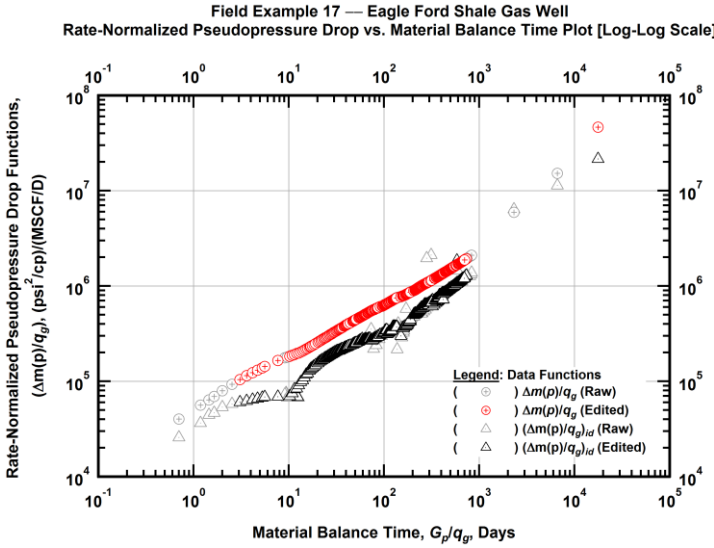

Figure A.492 — (Log-log Plot): "Log-log" diagnostic plot of the filtered production data — rate-normalized pseudopressure drop ($\Delta m(p)/q_g$) and rate-normalized pseudopressure drop integral-derivative $(\Delta m(p)/q_g)_{id}$ versus material balance time (G_p/q_g).

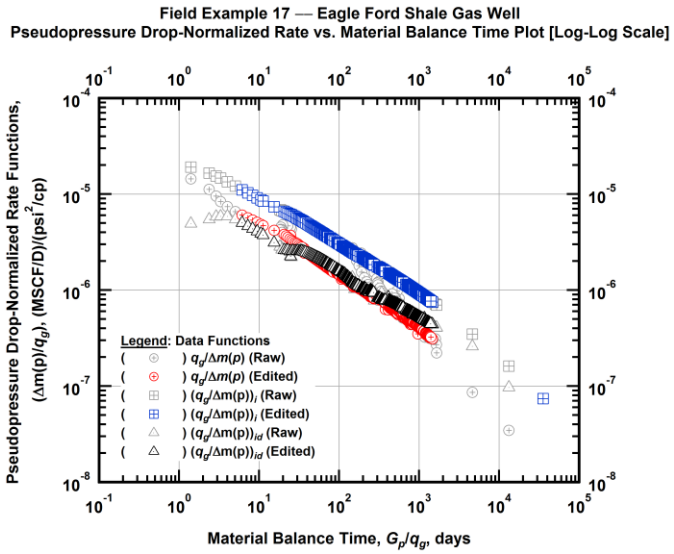

Figure A.493 — (Log-log Plot): "Blasingame" diagnostic plot of the filtered production data — pseudopressure drop-normalized gas flowrate ($q_g/\Delta m(p)$), pseudopressure drop-normalized gas flowrate integral $(q_g/\Delta m(p))_i$ and pseudopressure drop-normalized gas flowrate integral-derivative $(q_g/\Delta m(p))_{id}$ versus material balance time (G_p/q_g).

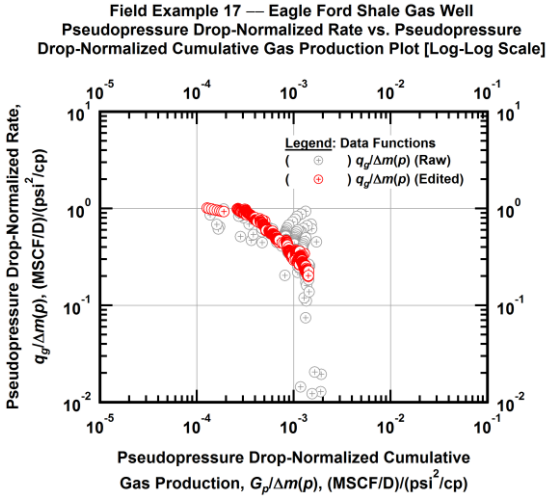

Figure A.494 — (Log-log Plot): Filtered normalized rate with normalized cumulative production plot — pseudopressure drop-normalized gas flowrate ($q_g/\Delta m(p)$) versus pseudopressure drop-normalized cumulative gas production ($G_p/\Delta m(p)$).

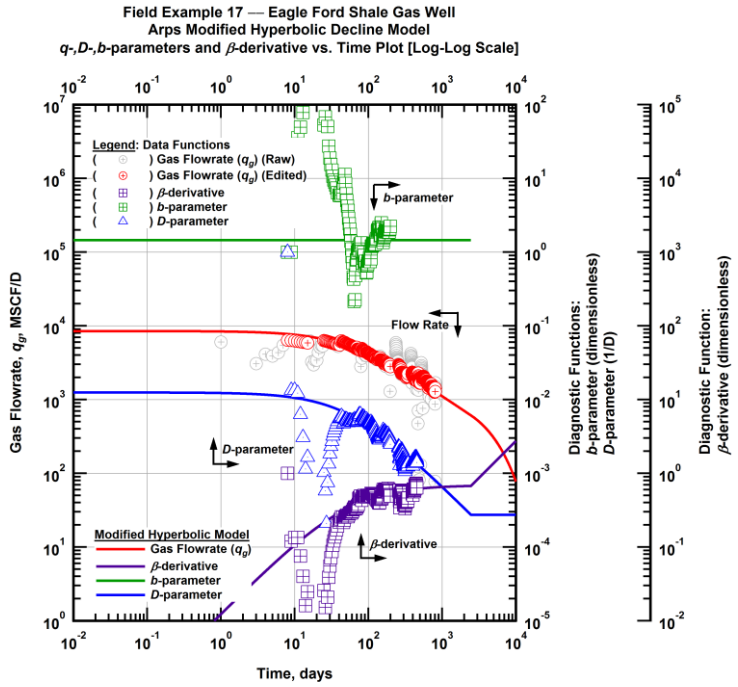

Figure A.495 — (Log-Log Plot): Arps modified hyperbolic decline model plot — time-rate model and data gas flowrate (q_g), *D*- and *b*-parameters and β-derivative versus production time.

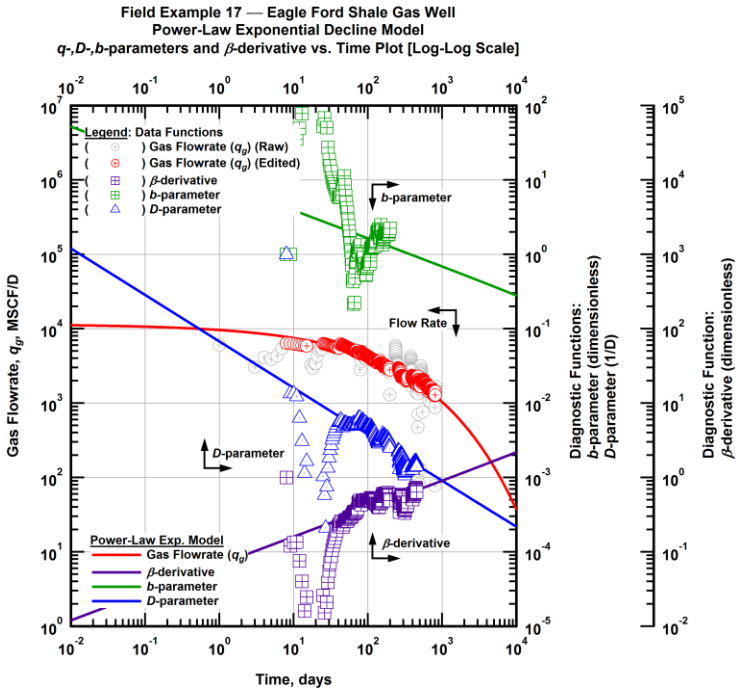

Figure A.496 — (Log-Log Plot): Power-law exponential decline model plot — time-rate model and data gas flowrate (q_g), *D*- and *b*-parameters and β-derivative versus production time.

Field Example 17 — Model-Based (Time-Rate-Pressure) Production Analysis

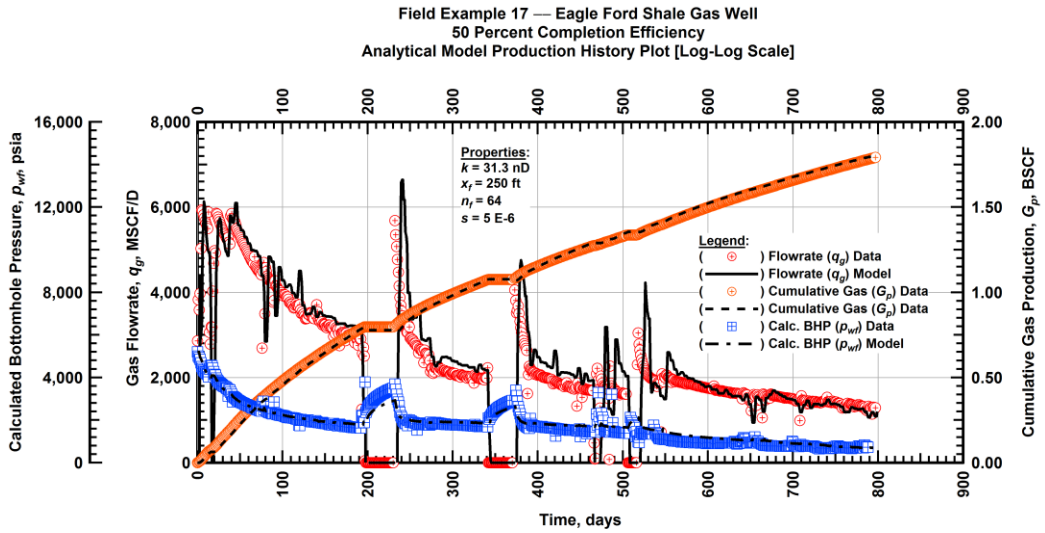

Figure A.497 — (Cartesian Plot): Production history plot — original gas flowrate (q_g), cumulative gas production (G_p), calculated bottomhole pressure (p_{wf}) and 50 percent completion efficiency model matches versus production time.

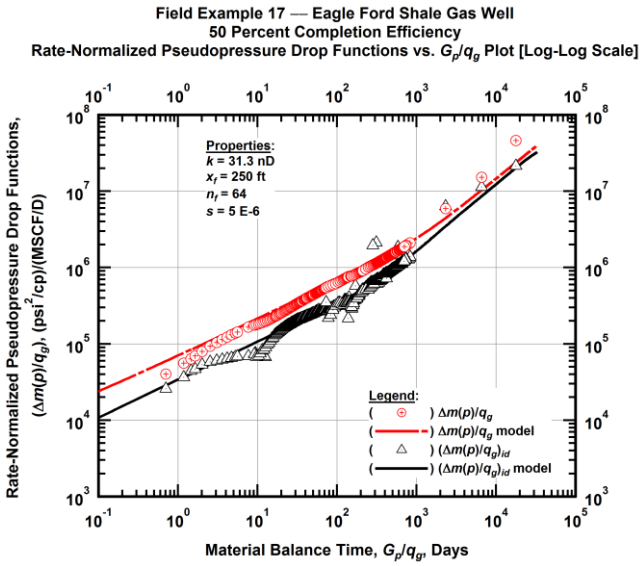

Figure A.498 — (Log-log Plot): "Log-log" diagnostic plot of the original production data — rate-normalized pseudopressure drop ($\Delta m(p)/q_g$), rate-normalized pseudopressure drop integral-derivative $(\Delta m(p)/q_g)_{id}$ and 50 percent completion efficiency model matches versus material balance time (G_p/q_g).

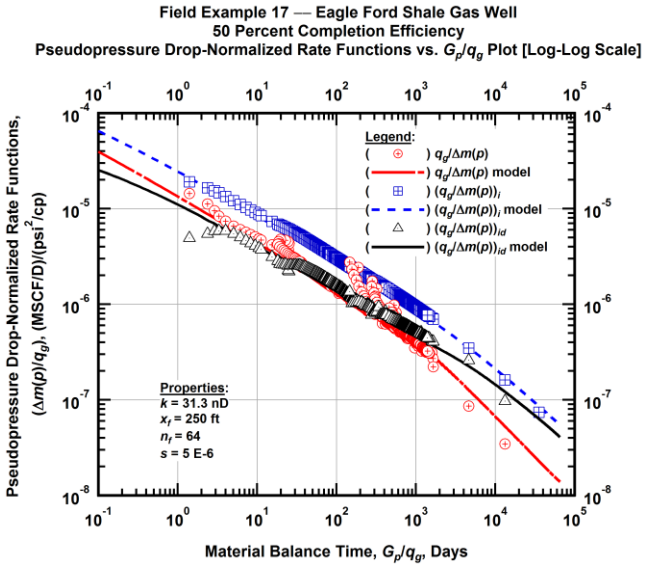

Figure A.499 — (Log-log Plot): "Blasingame" diagnostic plot of the original production data — pseudopressure drop-normalized gas flowrate ($q_g/\Delta m(p)$), pseudopressure drop-normalized gas flowrate integral $(q_g/\Delta m(p))_i$, pseudopressure drop-normalized gas flowrate integral-derivative $(q_g/\Delta m(p))_{id}$ and 50 percent completion efficiency model matches versus material balance time (G_p/q_g).

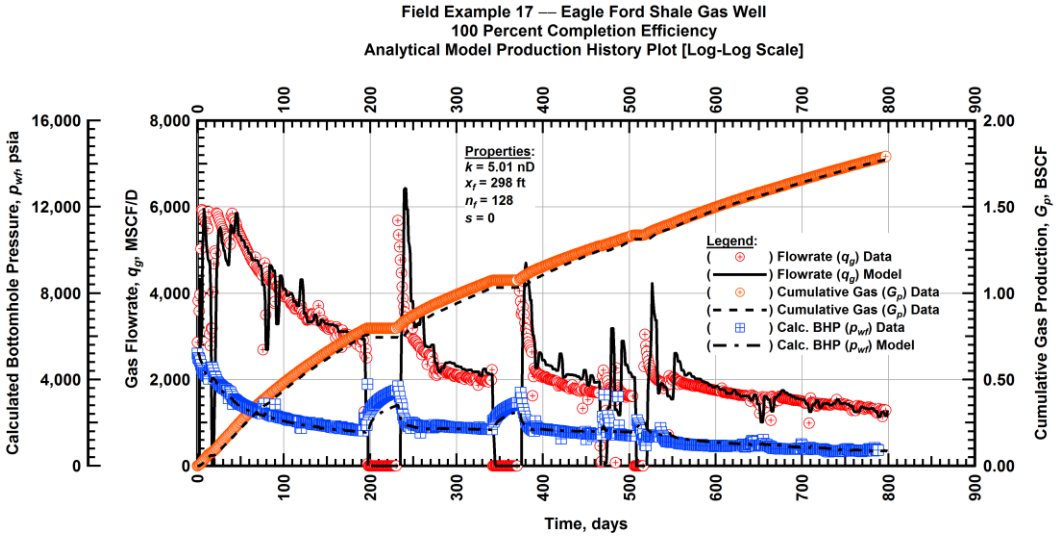

Figure A.500 — (Cartesian Plot): Production history plot — original gas flowrate (q_g), cumulative gas production (G_p), calculated bottomhole pressure (p_{wf}) and 100 percent completion efficiency model matches versus production time.

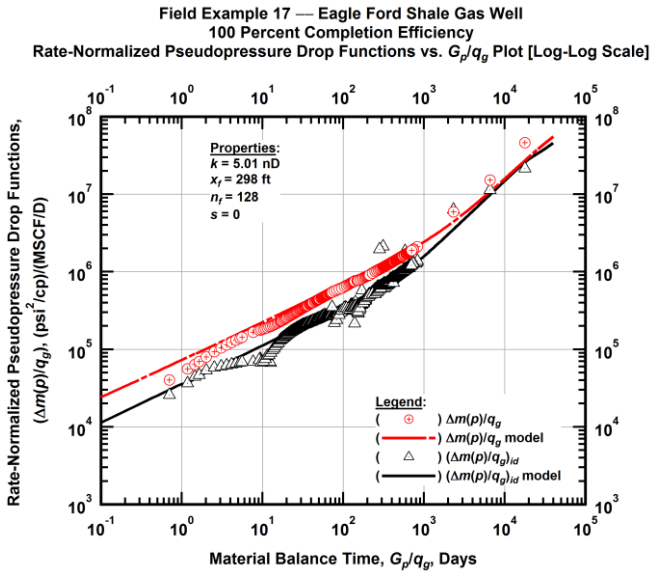

Figure A.501 — (Log-log Plot): "Log-log" diagnostic plot of the original production data — rate-normalized pseudopressure drop ($\Delta m(p)/q_g$), rate-normalized pseudopressure drop integral-derivative $(\Delta m(p)/q_g)_{id}$ and 100 percent completion efficiency model matches versus material balance time (G_p/q_g).

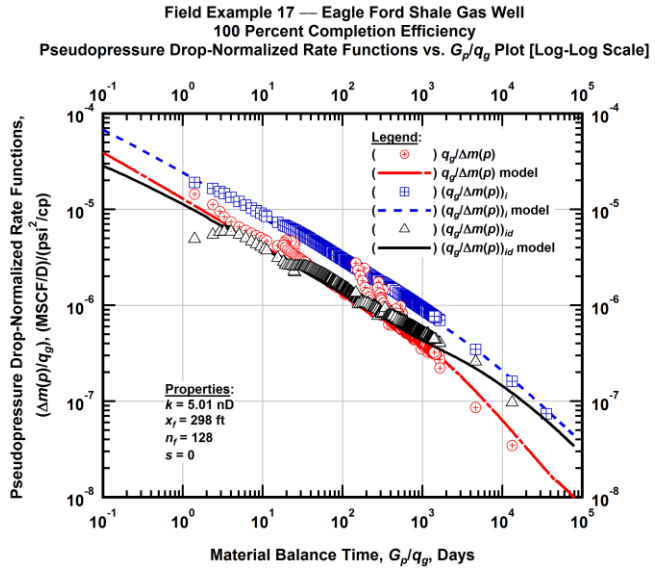

Figure A.502 — (Log-log Plot): "Blasingame" diagnostic plot of the original production data — pseudopressure drop-normalized gas flowrate ($q_g/\Delta m(p)$), pseudopressure drop-normalized gas flowrate integral $(q_g/\Delta m(p))_i$, pseudopressure drop-normalized gas flowrate integral-derivative $(q_g/\Delta m(p))_{id}$ and 100 percent completion efficiency model matches versus material balance time (G_p/q_g).

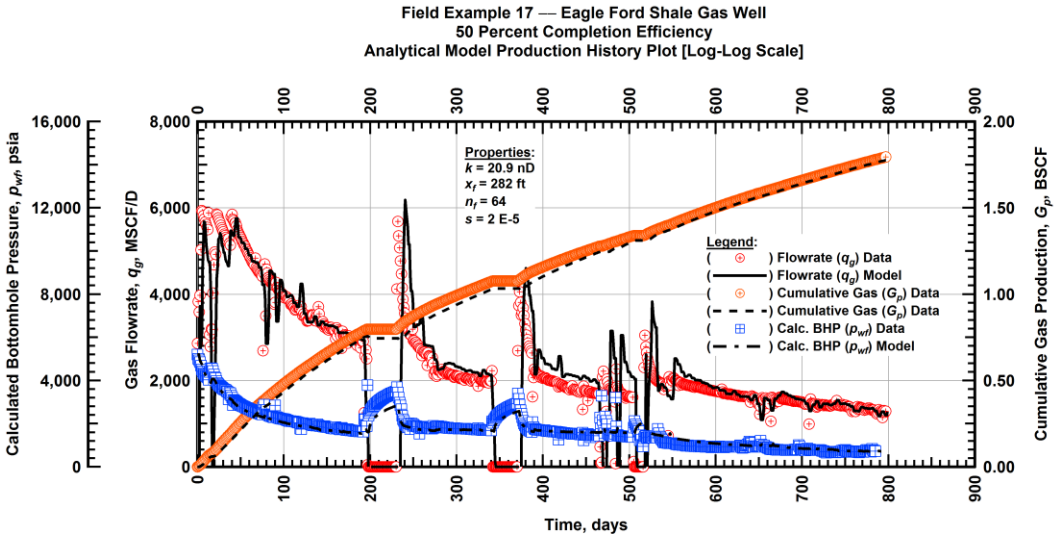

Figure A.503 — (Cartesian Plot): Production history plot — revised gas flowrate (q_g), cumulative gas production (G_p), calculated bottomhole pressure (p_{wf}) and 50 percent completion efficiency model matches versus production time.

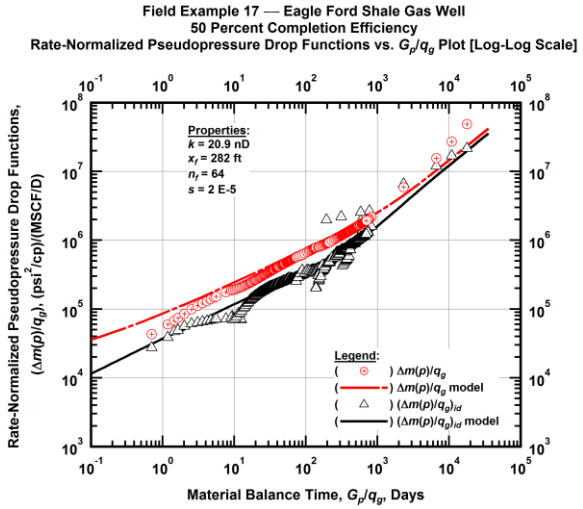

Figure A.504— (Log-log Plot): "Log-log" diagnostic plot of the revised production data — rate-normalized pseudopressure drop ($\Delta m(p)/q_g$), rate-normalized pseudopressure drop integral-derivative $(\Delta m(p)/q_g)_{id}$ and 50 percent completion efficiency model matches versus material balance time (G_p/q_g).

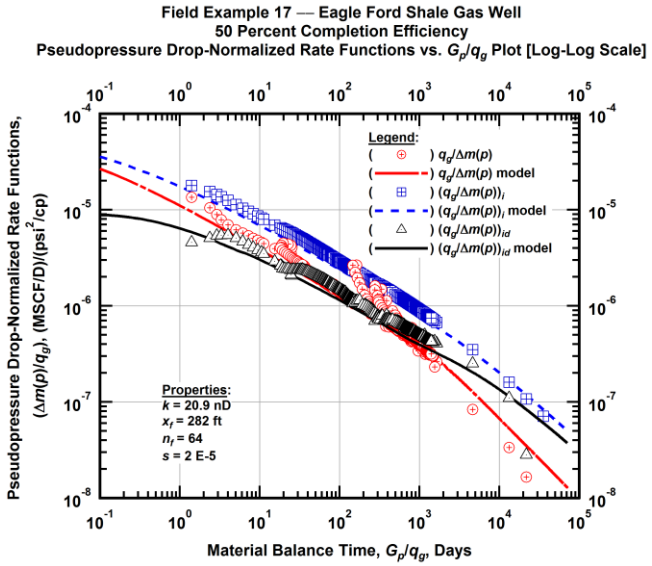

Figure A.505 — (Log-log Plot): "Blasingame" diagnostic plot of the revised production data — pseudopressure drop-normalized gas flowrate ($q_g/\Delta m(p)$), pseudopressure drop-normalized gas flowrate integral $(q_g/\Delta m(p))_i$, pseudopressure drop-normalized gas flowrate integral-derivative $(q_g/\Delta m(p))_{id}$ and 50 percent completion efficiency model matches versus material balance time (G_p/q_g).

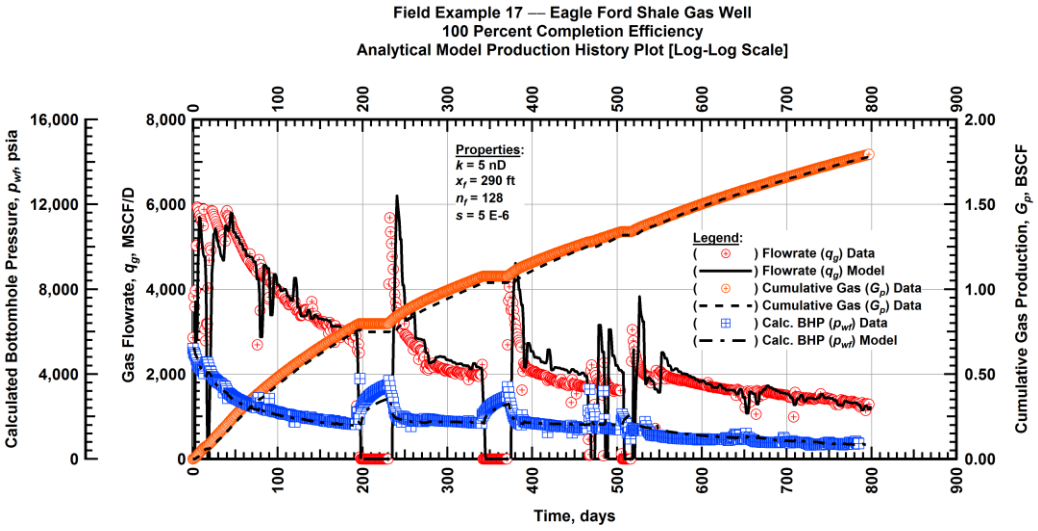

Figure A.506 — (Cartesian Plot): Production history plot — revised gas flowrate (q_g), cumulative gas production (G_p), calculated bottomhole pressure (p_{wf}) and 100 percent completion efficiency model matches versus production time.

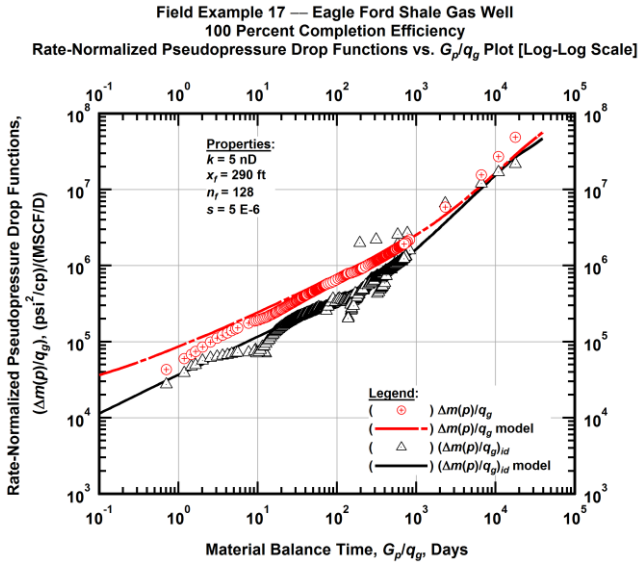

Figure A.507 — (Log-log Plot): "Log-log" diagnostic plot of the revised production data — rate-normalized pseudopressure drop ($\Delta m(p)/q_g$), rate-normalized pseudopressure drop integral-derivative $(\Delta m(p)/q_g)_{id}$ and 100 percent completion efficiency model matches versus material balance time (G_p/q_g).

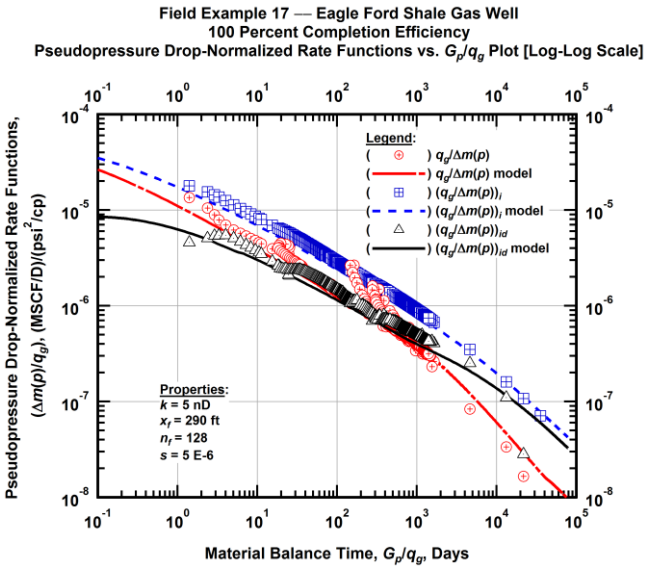

Figure A.508 — (Log-log Plot): "Blasingame" diagnostic plot of the revised production data — pseudopressure drop-normalized gas flowrate ($q_g/\Delta m(p)$), pseudopressure drop-normalized gas flowrate integral $(q_g/\Delta m(p))_i$, pseudopressure drop-normalized gas flowrate integral-derivative $(q_g/\Delta m(p))_{id}$ and 100 percent completion efficiency model matches versus material balance time (G_p/q_g).

Field Example 17 — 30-Year EUR Model Comparison

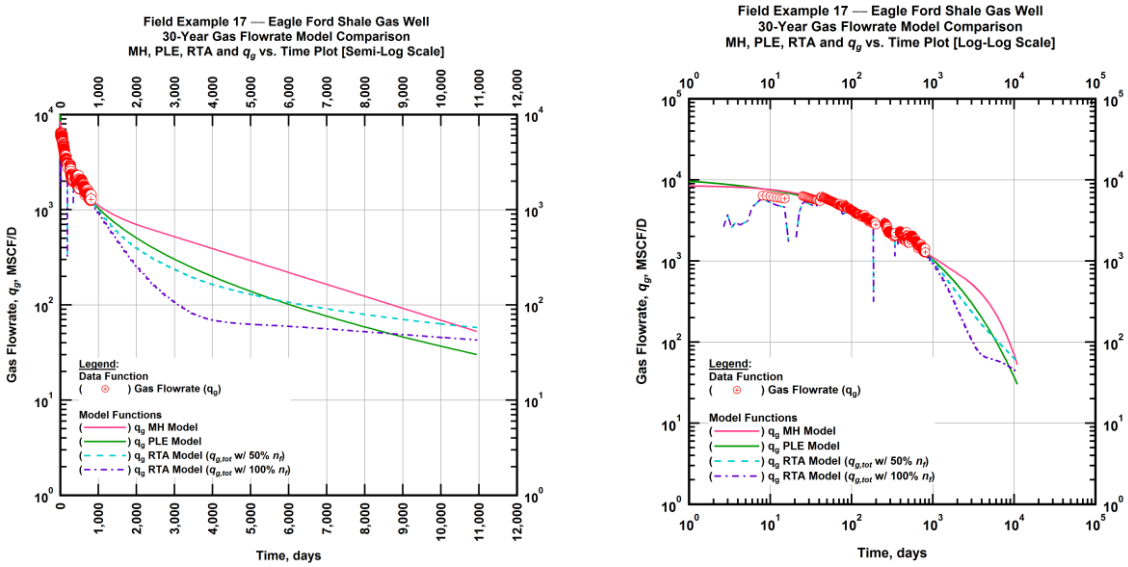

A **B**

Figure A.509 — (A — Semi-Log Plot) and (B — Log-Log Plot): Estimated 30-year revised gas flowrate model comparison — Arps modified hyperbolic decline model, power-law exponential decline model, and 50 percent and 100 percent completion efficiency RTA models revised gas 30-year estimated flowrate decline and historic gas flowrate data (q_g) versus production time.

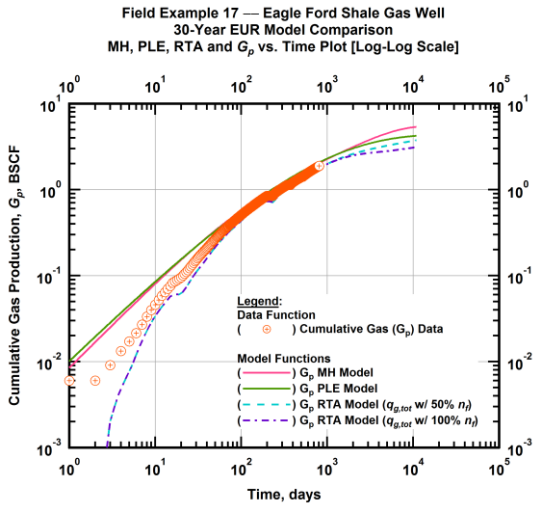

Figure A.510 — (Log-log Plot): PVT revised gas 30-year estimated cumulative production volume model comparison — Arps modified hyperbolic decline model, power-law exponential decline model, and 50 percent and 100 percent completion efficiency RTA model estimated 30-year cumulative gas production volumes and historic cumulative gas production (G_p) versus production time.

Table A.17 — 30-year estimated cumulative revised gas production (EUR), in units of BSCF, for the Arps modified hyperbolic, power-law exponential and analytical time-rate-pressure decline models.

Arps Modified Hyperbolic BSCF)	Power-Law Exponential (BSCF)	RTA Analytical Model ($q_{g,tot}$ w/ 50% n_f) (BSCF)	RTA Analytical Model ($q_{g,tot}$ w/ 100% n_f) (BSCF)
5.32	4.04	3.79	3.15

Field Example 18 — Time-Rate Analysis

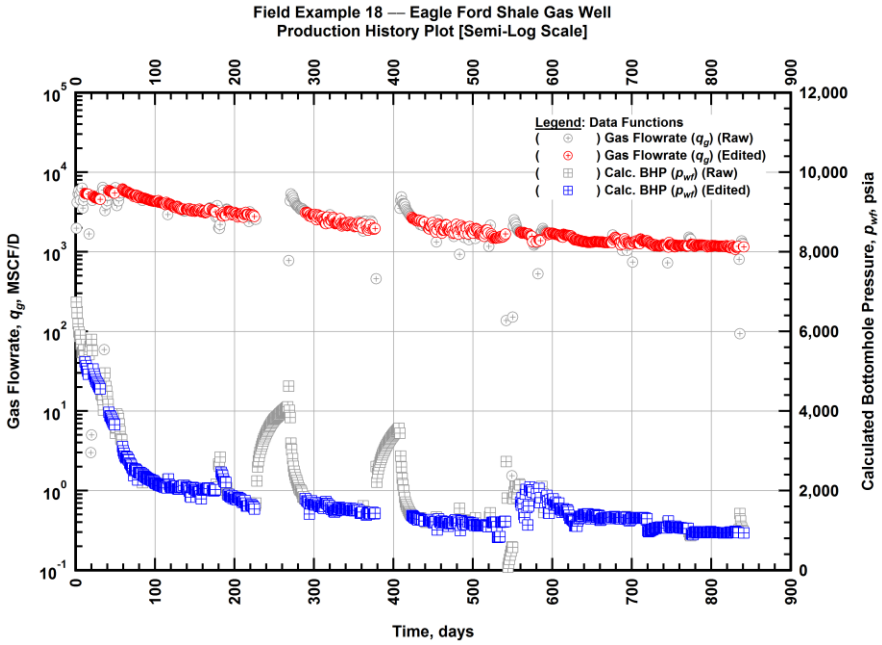

Figure A.511 — (Semi-log Plot): Filtered production history plot — flowrate (q_g) and calculated bottomhole pressure (p_{wf}) versus production time.

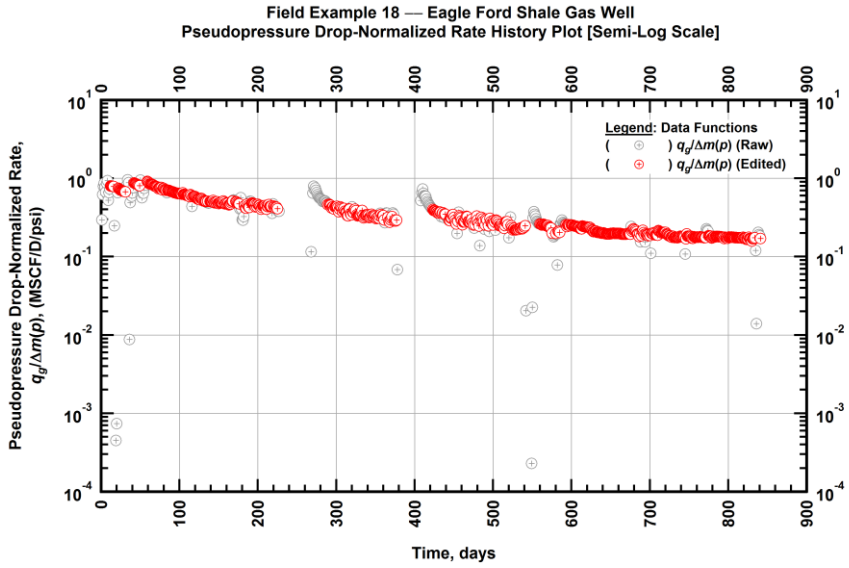

Figure A.512 — (Semi-log Plot): Filtered normalized rate production history plot — pseudopressure drop-normalized gas flowrate ($q_g/\Delta m(p)$) versus production time.

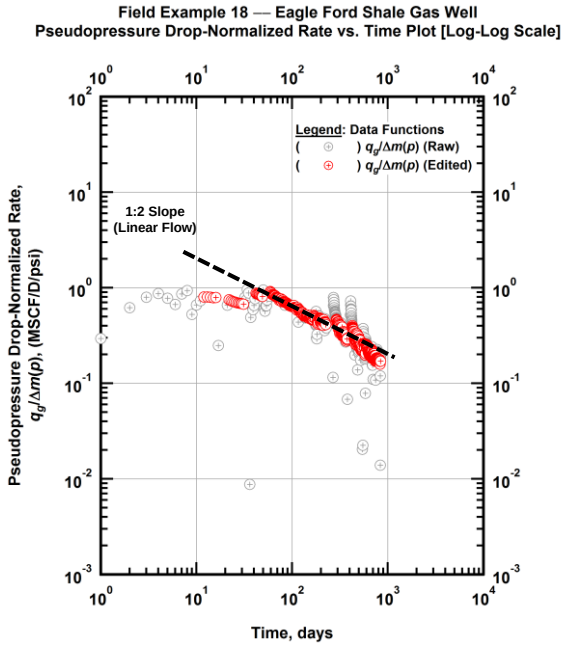

Figure A.513 — (Log-log Plot): Filtered normalized rate production history plot — pseudopressure drop-normalized gas flowrate ($q_g/\Delta m(p)$) versus production time.

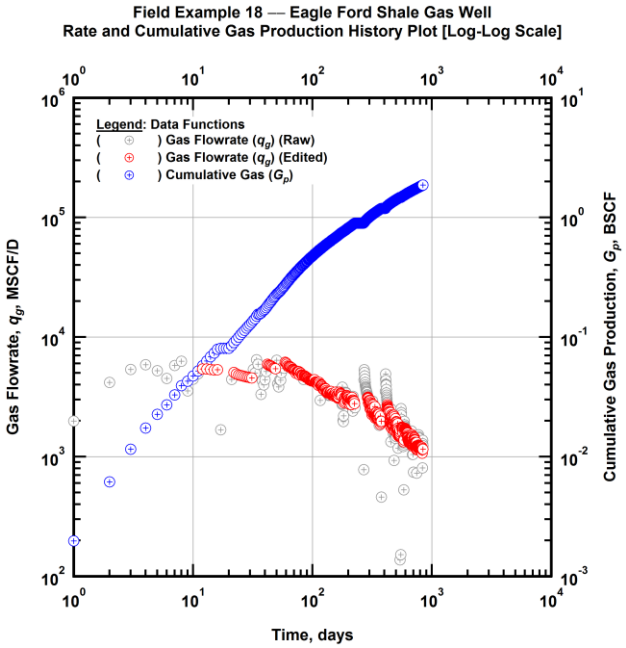

Figure A.514 — (Log-log Plot): Filtered rate and unfiltered cumulative gas production history plot — flowrate (q_g) and cumulative production (G_p) versus production time.

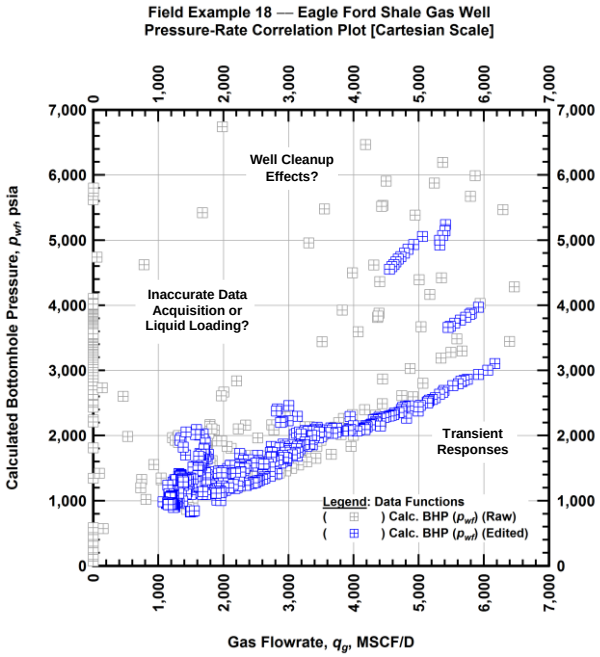

Figure A.515 — (Cartesian Plot): Filtered rate-pressure correlation plot — calculated bottomhole pressure (p_{wf}) versus flowrate (q_g).

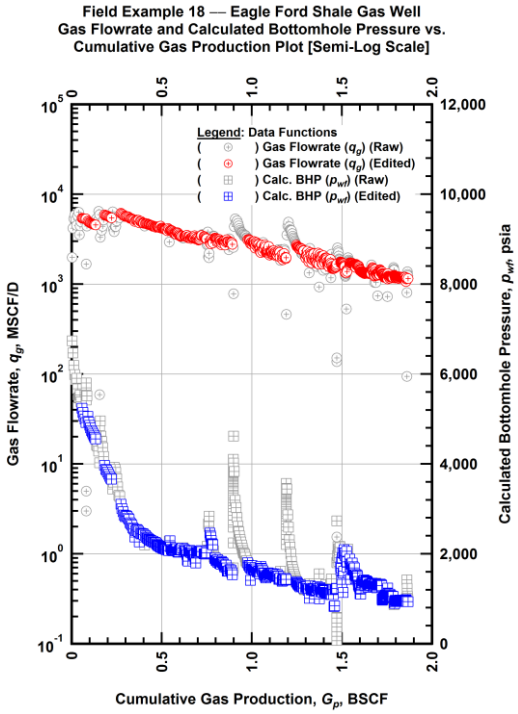

Figure A.516 — (Semi-log Plot): Filtered rate-pressure-cumulative production history plot — flowrate (q_g) and calculated bottomhole pressure (p_{wf}) versus cumulative production (G_p).

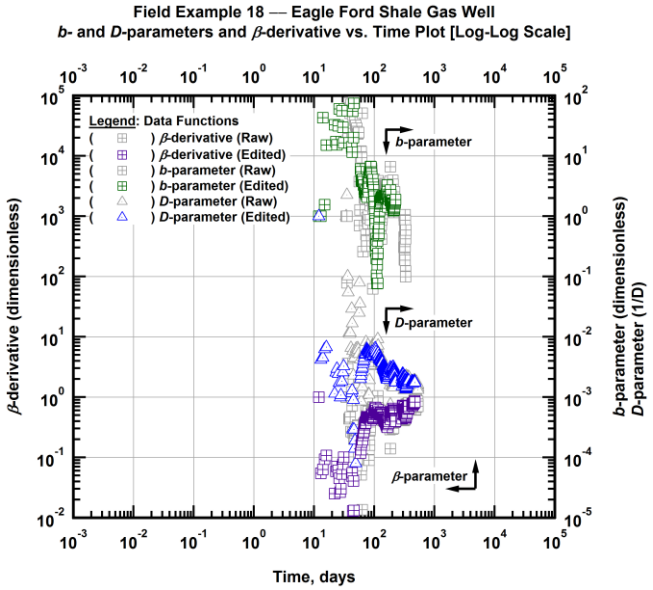

Figure A.517 — (Log-Log Plot): Filtered b, D and β production history plot — b- and D-parameters and β-derivative versus production time.

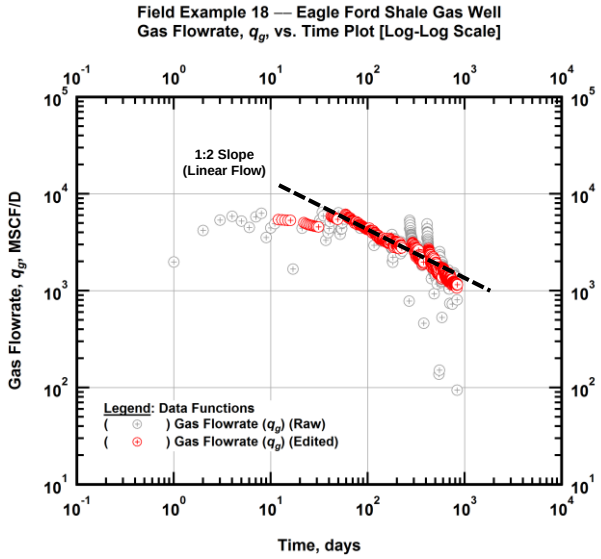

Figure A.518 — (Log-Log Plot): Filtered gas flowrate production history and flow regime identification plot — gas flowrate (q_g) versus production time.

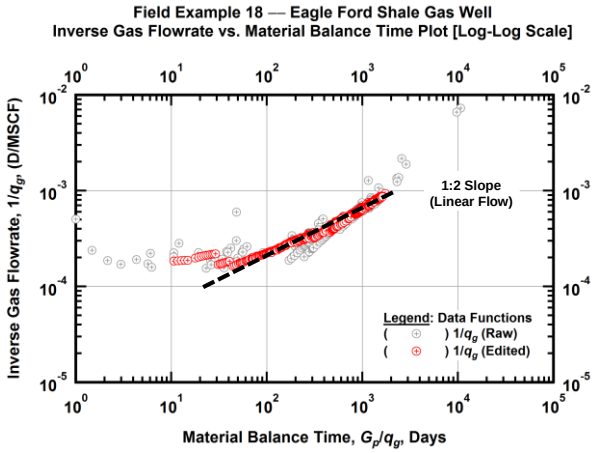

Figure A.519 — (Log-log Plot): Filtered inverse rate with material balance time plot — inverse gas flowrate ($1/q_g$) versus material balance time (G_p/q_g).

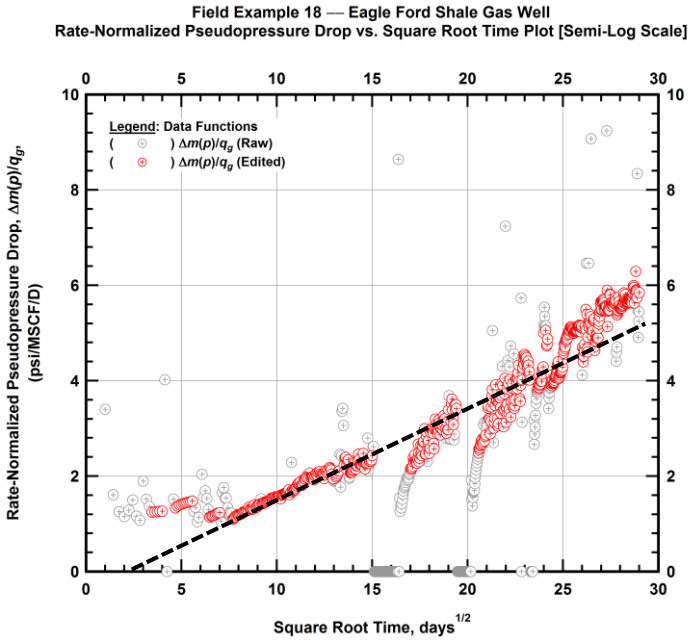

Figure A.520 — (Semi-log Plot): Filtered normalized pseudopressure drop production history plot — rate-normalized pseudopressure drop ($\Delta m(p)/q_g$) versus square root production time ($\sqrt{t}$).

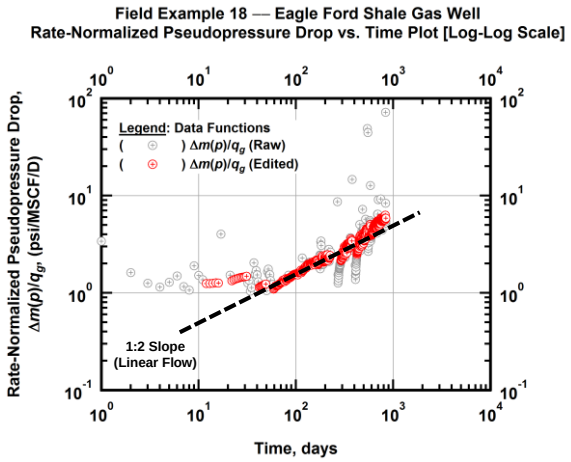

Figure A.521 — (Log-log Plot): Filtered normalized pseudopressure drop production history plot — rate-normalized pseudopressure drop ($\Delta m(p)/q_g$) versus production time.

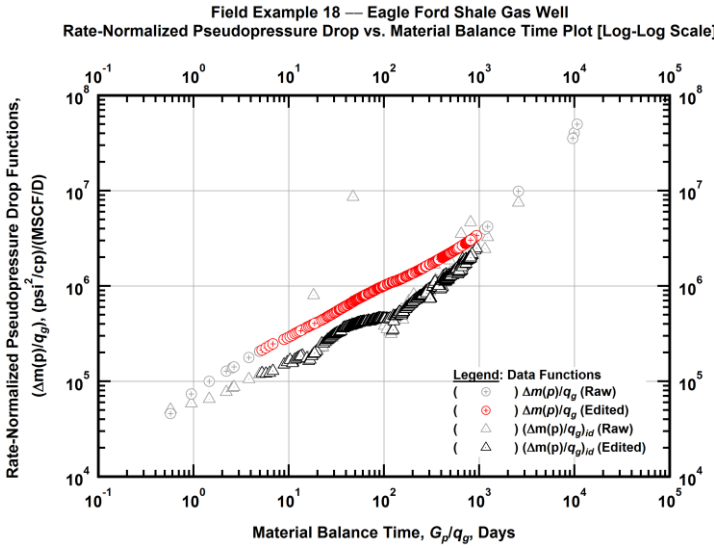

Figure A.522 — (Log-log Plot): "Log-log" diagnostic plot of the filtered production data — rate-normalized pseudopressure drop ($\Delta m(p)/q_g$) and rate-normalized pseudopressure drop integral-derivative $(\Delta m(p)/q_g)_{id}$ versus material balance time (G_p/q_g).

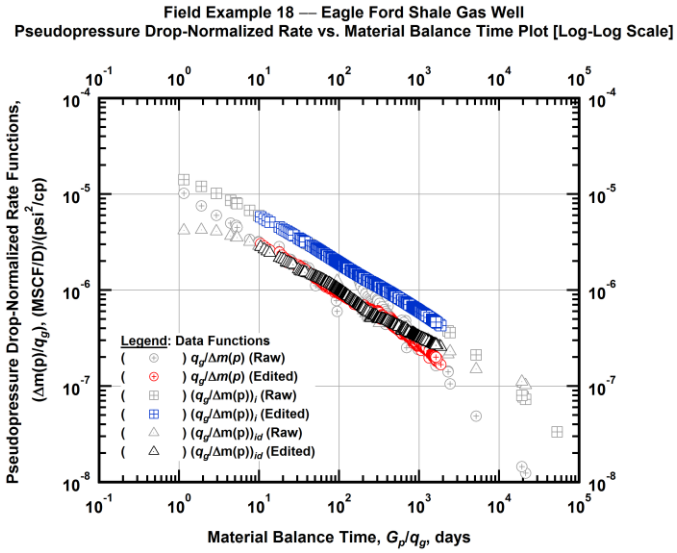

Figure A.523 — (Log-log Plot): "Blasingame" diagnostic plot of the filtered production data — pseudopressure drop-normalized gas flowrate ($q_g/\Delta m(p)$), pseudopressure drop-normalized gas flowrate integral $(q_g/\Delta m(p))_i$ and pseudopressure drop-normalized gas flowrate integral-derivative $(q_g/\Delta m(p))_{id}$ versus material balance time (G_p/q_g).

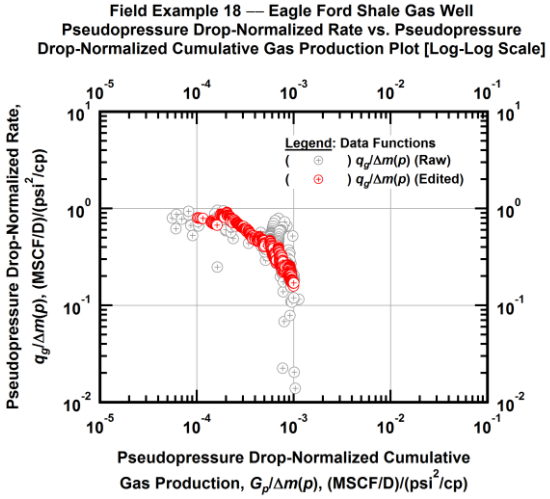

Figure A.524 — (Log-log Plot): Filtered normalized rate with normalized cumulative production plot — pseudopressure drop-normalized gas flowrate ($q_g/\Delta m(p)$) versus pseudopressure drop-normalized cumulative gas production ($G_p/\Delta m(p)$).

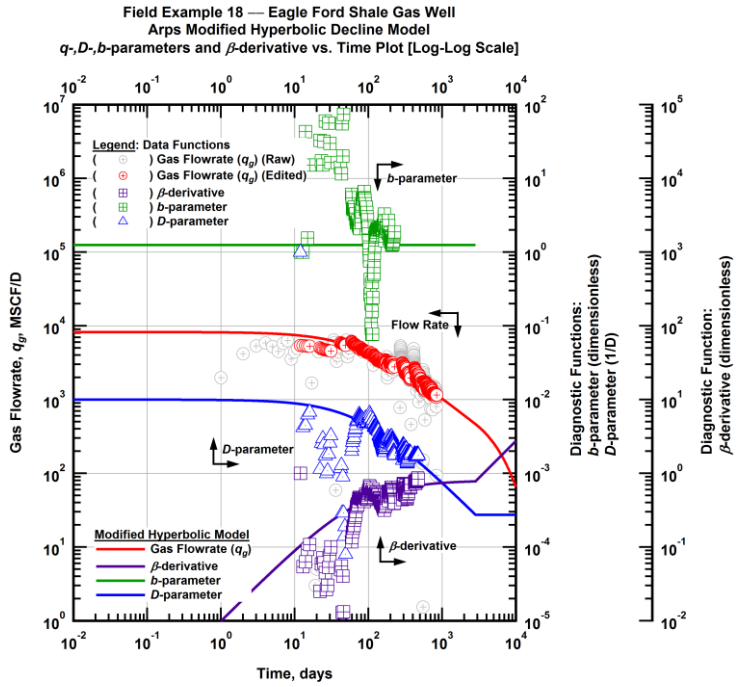

Figure A.525 — (Log-Log Plot): Arps modified hyperbolic decline model plot — time-rate model and data gas flowrate (q_g), *D*- and *b*-parameters and β-derivative versus production time.

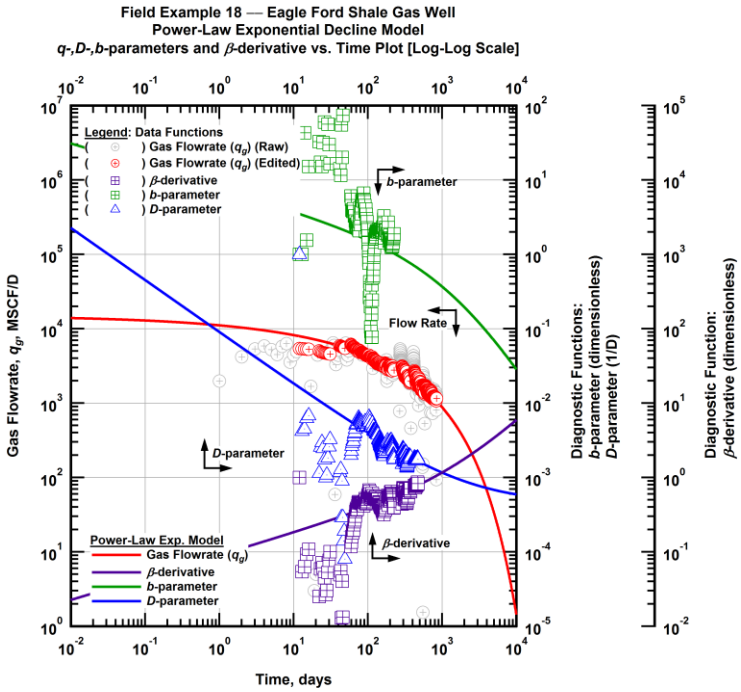

Figure A.526 — (Log-Log Plot): Power-law exponential decline model plot — time-rate model and data gas flowrate (q_g), *D*- and *b*-parameters and β-derivative versus production time.

Field Example 18 — Model-Based (Time-Rate-Pressure) Production Analysis

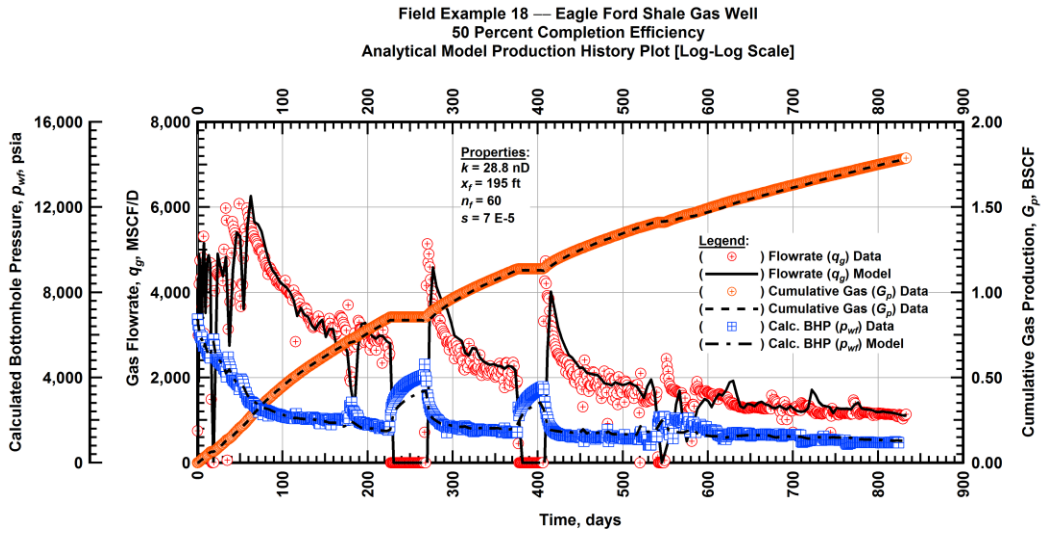

Figure A.527 — (Cartesian Plot): Production history plot — original gas flowrate (q_g), cumulative gas production (G_p), calculated bottomhole pressure (p_{wf}) and 50 percent completion efficiency model matches versus production time.

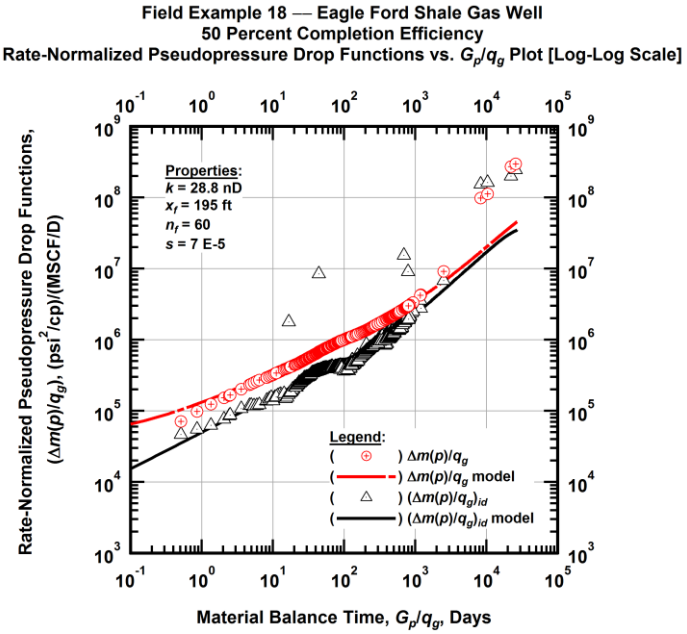

Figure A.528 — (Log-log Plot): "Log-log" diagnostic plot of the original production data — rate-normalized pseudopressure drop ($\Delta m(p)/q_g$), rate-normalized pseudopressure drop integral-derivative $(\Delta m(p)/q_g)_{id}$ and 50 percent completion efficiency model matches versus material balance time (G_p/q_g).

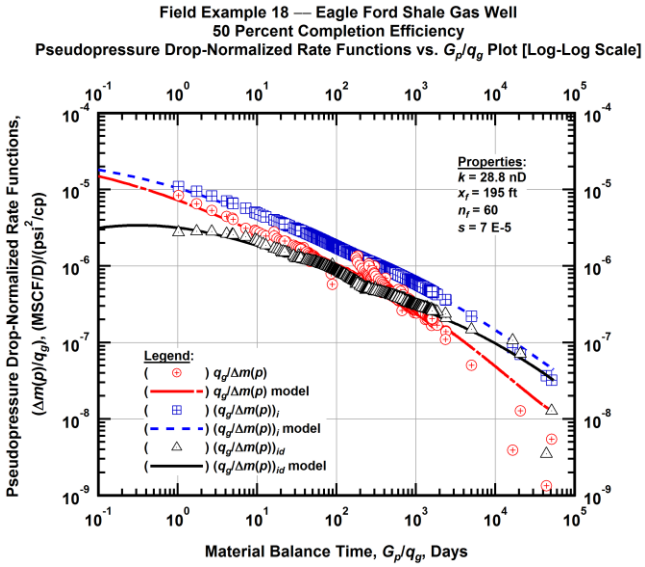

Figure A.529 — (Log-log Plot): "Blasingame" diagnostic plot of the original production data — pseudopressure drop-normalized gas flowrate ($q_g/\Delta m(p)$), pseudopressure drop-normalized gas flowrate integral $(q_g/\Delta m(p))_i$, pseudopressure drop-normalized gas flowrate integral-derivative $(q_g/\Delta m(p))_{id}$ and 50 percent completion efficiency model matches versus material balance time (G_p/q_g).

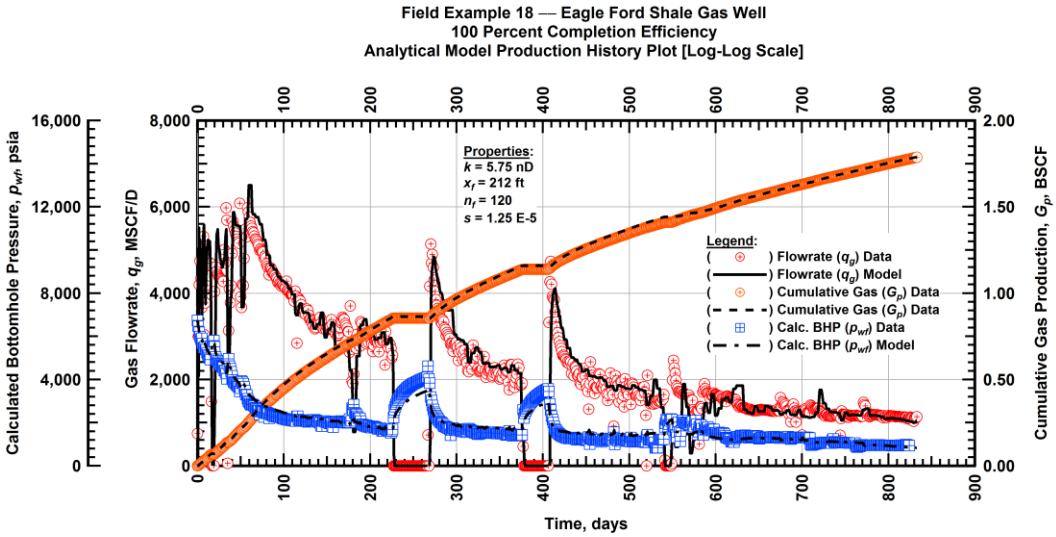

Figure A.530 — (Cartesian Plot): Production history plot — original gas flowrate (q_g), cumulative gas production (G_p), calculated bottomhole pressure (p_{wf}) and 100 percent completion efficiency model matches versus production time.

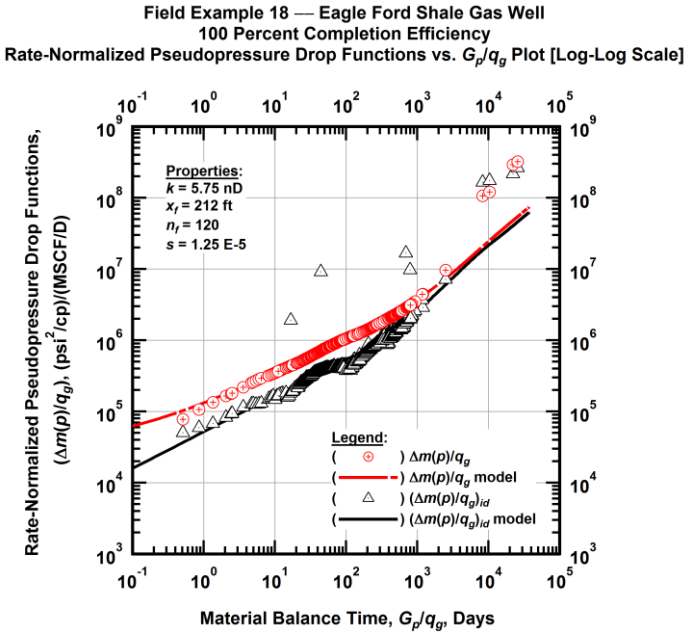

Figure A.531 — (Log-log Plot): "Log-log" diagnostic plot of the original production data — rate-normalized pseudopressure drop ($\Delta m(p)/q_g$), rate-normalized pseudopressure drop integral-derivative $(\Delta m(p)/q_g)_{id}$ and 100 percent completion efficiency model matches versus material balance time (G_p/q_g).

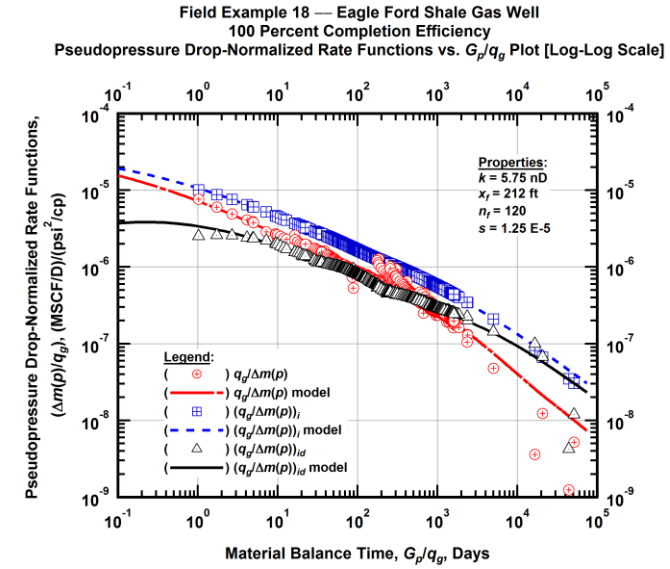

Figure A.532 — (Log-log Plot): "Blasingame" diagnostic plot of the original production data — pseudopressure drop-normalized gas flowrate ($q_g/\Delta m(p)$), pseudopressure drop-normalized gas flowrate integral $(q_g/\Delta m(p))_i$, pseudopressure drop-normalized gas flowrate integral-derivative $(q_g/\Delta m(p))_{id}$ and 100 percent completion efficiency model matches versus material balance time (G_p/q_g).

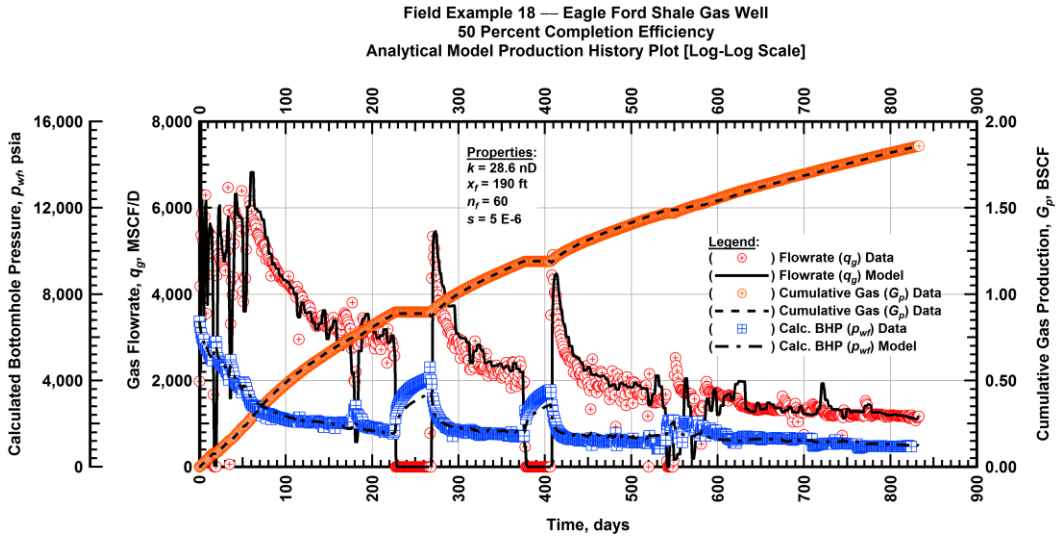

Figure A.533 — (Cartesian Plot): Production history plot — revised gas flowrate (q_g), cumulative gas production (G_p), calculated bottomhole pressure (p_{wf}) and 50 percent completion efficiency model matches versus production time.

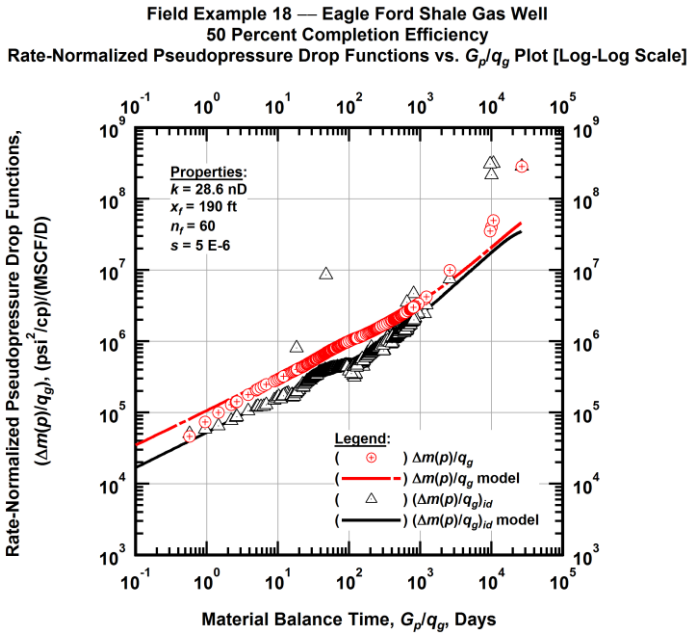

Figure A.534— (Log-log Plot): "Log-log" diagnostic plot of the revised production data — rate-normalized pseudopressure drop ($\Delta m(p)/q_g$), rate-normalized pseudopressure drop integral-derivative $(\Delta m(p)/q_g)_{id}$ and 50 percent completion efficiency model matches versus material balance time (G_p/q_g).

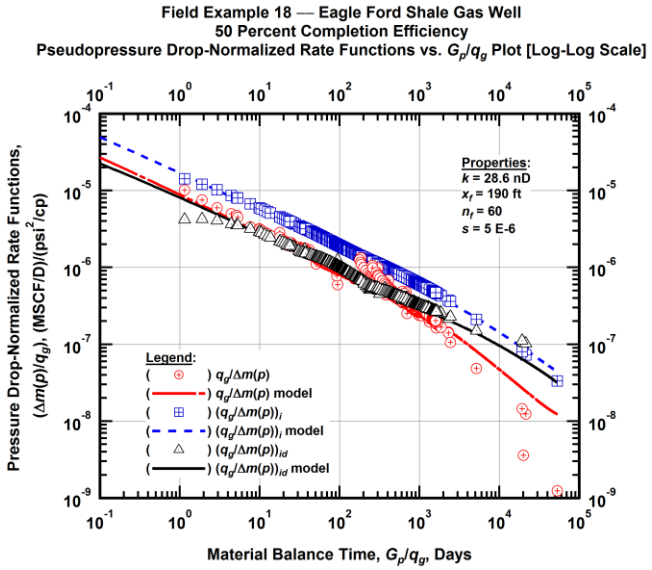

Figure A.535 — (Log-log Plot): "Blasingame" diagnostic plot of the revised production data — pseudopressure drop-normalized gas flowrate ($q_g/\Delta m(p)$), pseudopressure drop-normalized gas flowrate integral $(q_g/\Delta m(p))_i$, pseudopressure drop-normalized gas flowrate integral-derivative $(q_g/\Delta m(p))_{id}$ and 50 percent completion efficiency model matches versus material balance time (G_p/q_g).

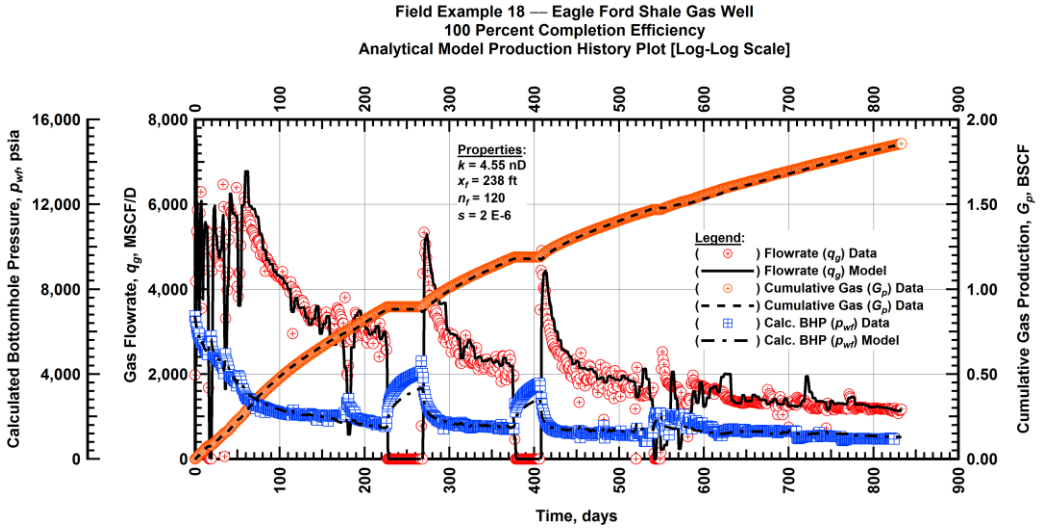

Figure A.536 — (Cartesian Plot): Production history plot — revised gas flowrate (q_g), cumulative gas production (G_p), calculated bottomhole pressure (p_{wf}) and 100 percent completion efficiency model matches versus production time.

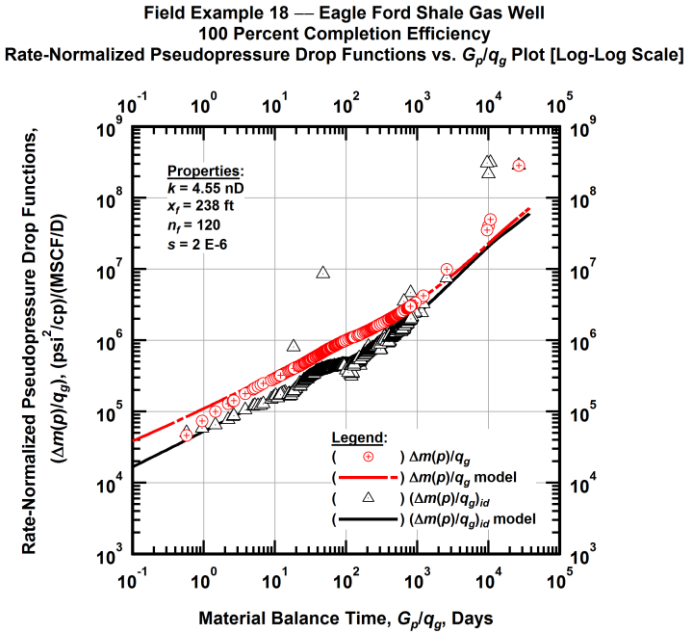

Figure A.537 — (Log-log Plot): "Log-log" diagnostic plot of the revised production data — rate-normalized pseudopressure drop ($\Delta m(p)/q_g$), rate-normalized pseudopressure drop integral-derivative $(\Delta m(p)/q_g)_{id}$ and 100 percent completion efficiency model matches versus material balance time (G_p/q_g).

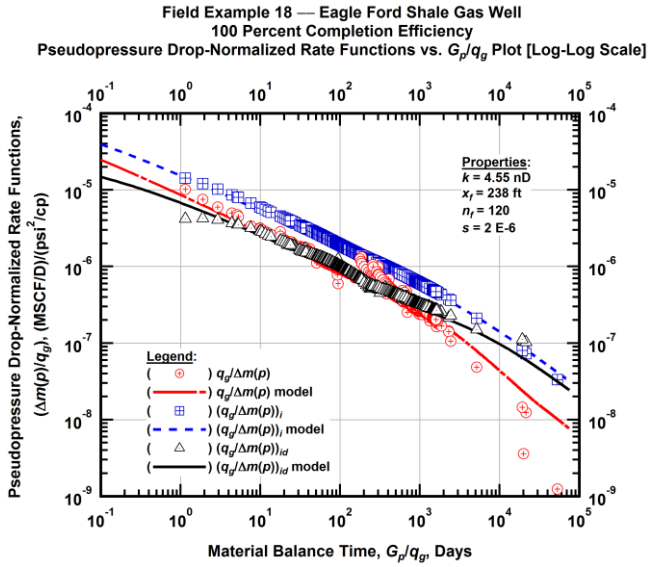

Figure A.538 — (Log-log Plot): "Blasingame" diagnostic plot of the revised production data — pseudopressure drop-normalized gas flowrate ($q_g/\Delta m(p)$), pseudopressure drop-normalized gas flowrate integral $(q_g/\Delta m(p))_i$, pseudopressure drop-normalized gas flowrate integral-derivative $(q_g/\Delta m(p))_{id}$ and 100 percent completion efficiency model matches versus material balance time (G_p/q_g).

Field Example 18 — 30-Year EUR Model Comparison

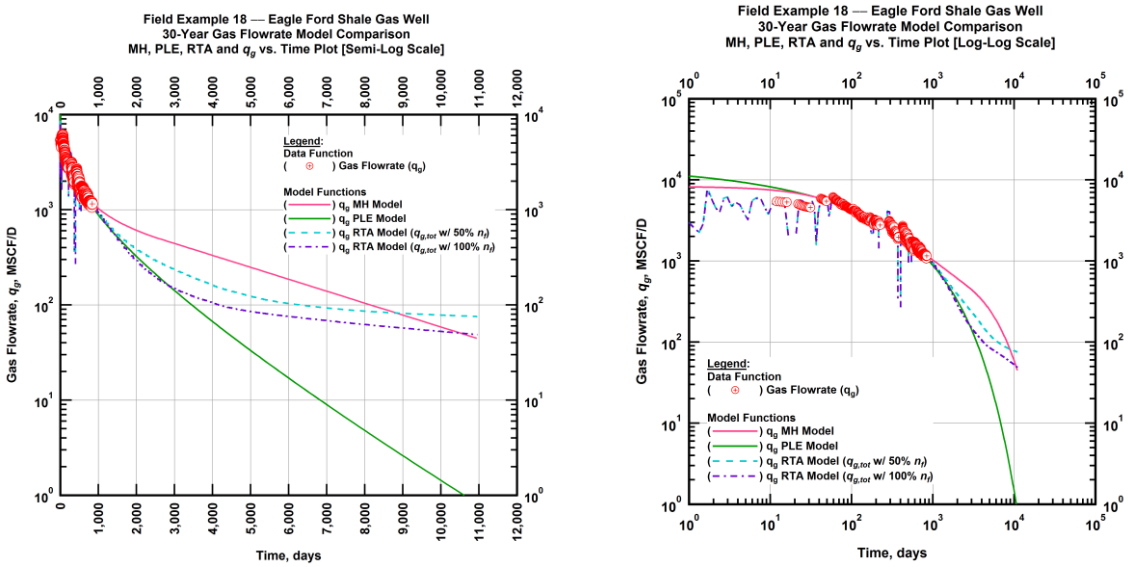

A **B**

Figure A.539 — (A — Semi-Log Plot) and (B — Log-Log Plot): Estimated 30-year revised gas flowrate model comparison — Arps modified hyperbolic decline model, power-law exponential decline model, and 50 percent and 100 percent completion efficiency RTA models revised gas 30-year estimated flowrate decline and historic gas flowrate data (q_g) versus production time.

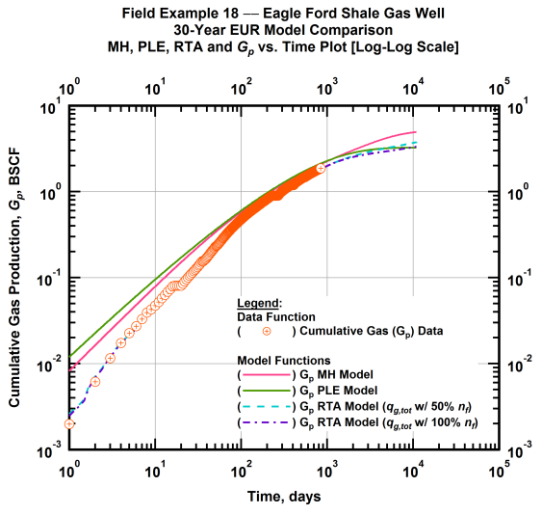

Figure A.540 — (Log-log Plot): PVT revised gas 30-year estimated cumulative production volume model comparison — Arps modified hyperbolic decline model, power-law exponential decline model, and 50 percent and 100 percent completion efficiency RTA model estimated 30-year cumulative gas production volumes and historic cumulative gas production (G_p) versus production time.

Table A.18 — 30-year estimated cumulative revised gas production (EUR), in units of BSCF, for the Arps modified hyperbolic, power-law exponential and analytical time-rate-pressure decline models.

Arps Modified Hyperbolic BSCF)	Power-Law Exponential (BSCF)	RTA Analytical Model ($q_{g,tot}$ w/ 50% n_f) (BSCF)	RTA Analytical Model ($q_{g,tot}$ w/ 100% n_f) (BSCF)
4.80	2.98	3.82	3.37

Field Example 19 — Time-Rate Analysis

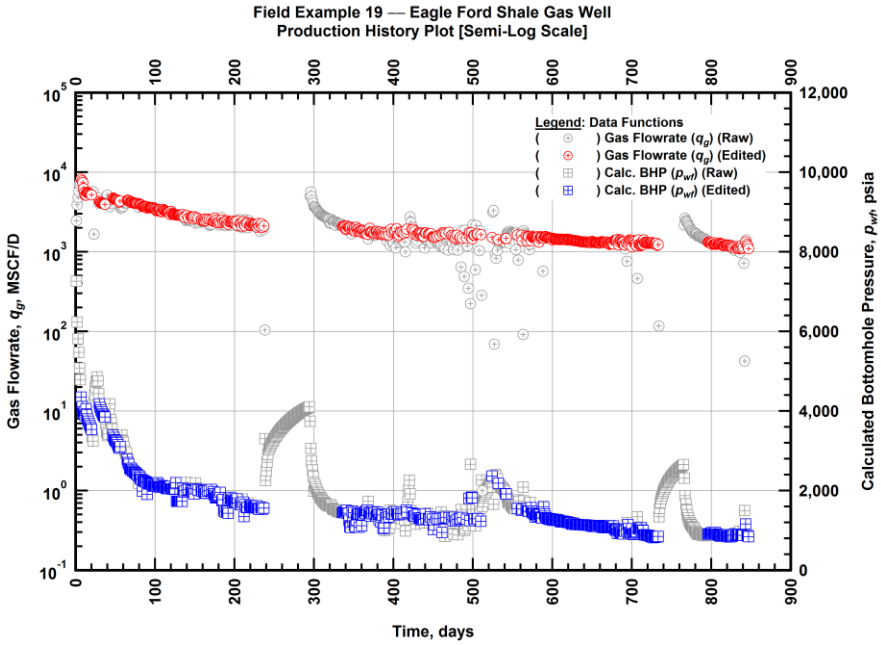

Figure A.541 — (Semi-log Plot): Filtered production history plot — flowrate (q_g) and calculated bottomhole pressure (p_{wf}) versus production time.

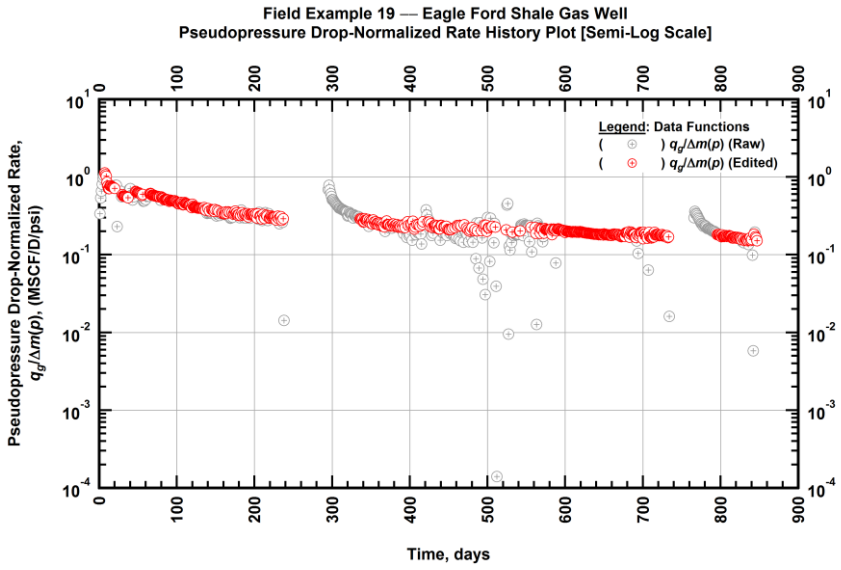

Figure A.542 — (Semi-log Plot): Filtered normalized rate production history plot — pseudopressure drop-normalized gas flowrate ($q_g/\Delta m(p)$) versus production time.

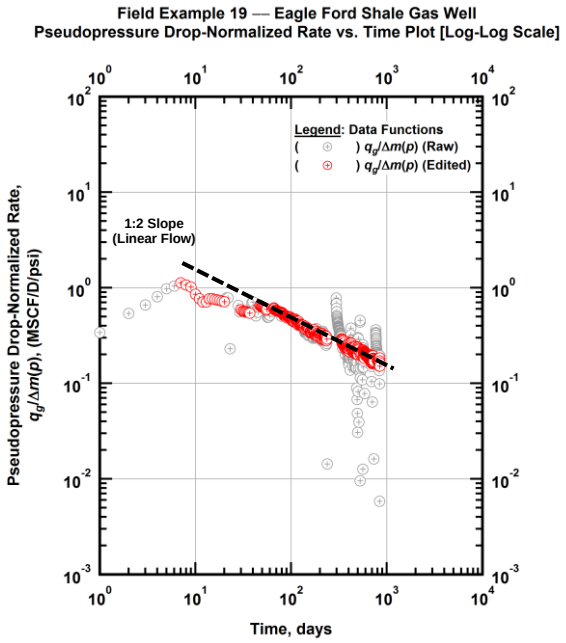

Figure A.543 — (Log-log Plot): Filtered normalized rate production history plot — pseudopressure drop-normalized gas flowrate ($q_g/\Delta m(p)$) versus production time.

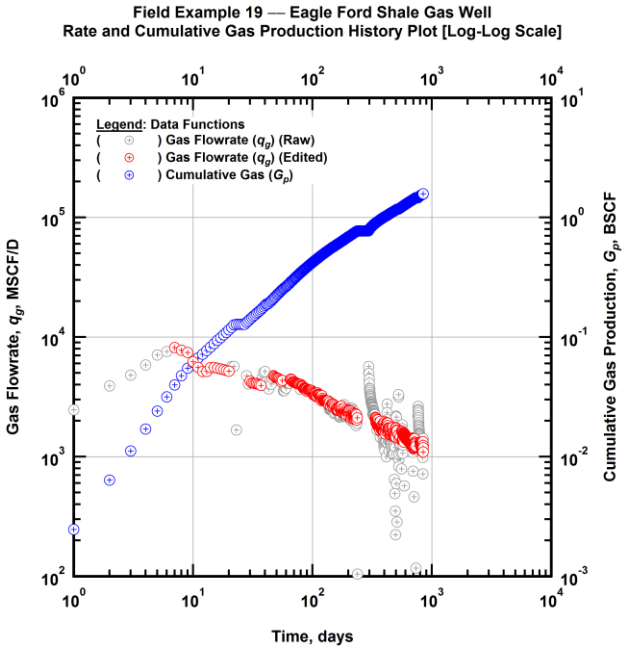

Figure A.544 — (Log-log Plot): Filtered rate and unfiltered cumulative gas production history plot — flowrate (q_g) and cumulative production (G_p) versus production time.

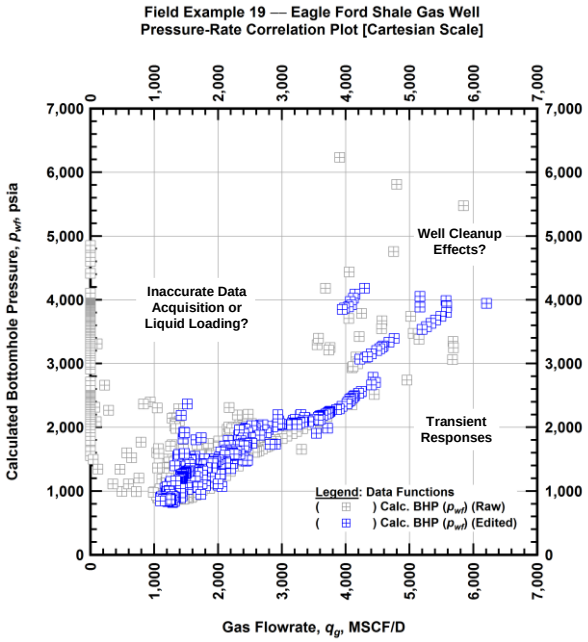

Figure A.545 — (Cartesian Plot): Filtered rate-pressure correlation plot — calculated bottomhole pressure (p_{wf}) versus flowrate (q_g).

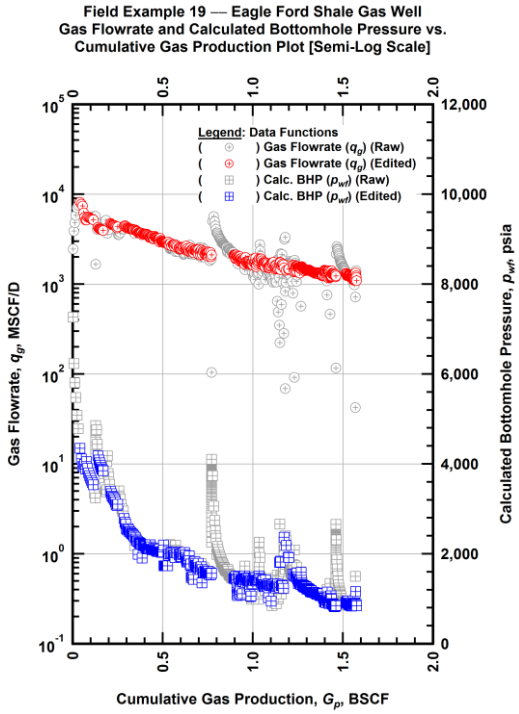

Figure A.546 — (Semi-log Plot): Filtered rate-pressure-cumulative production history plot — flowrate (q_g) and calculated bottomhole pressure (p_{wf}) versus cumulative production (G_p).

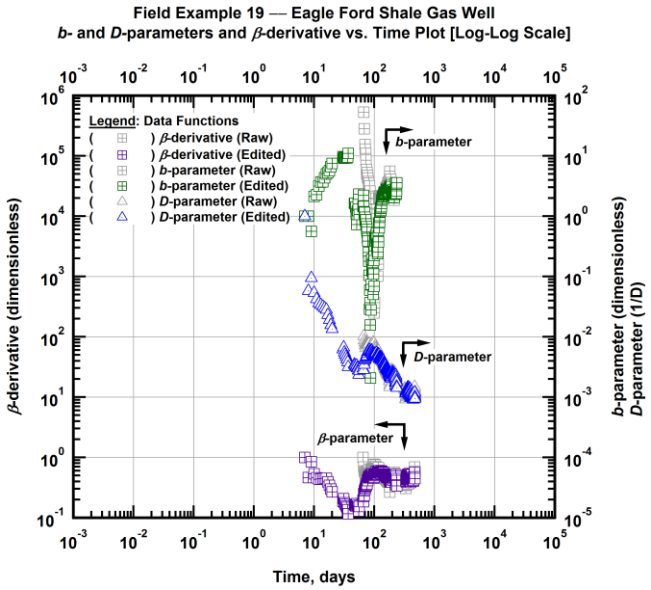

Figure A.547 — (Log-Log Plot): Filtered b, D and β production history plot — b- and D-parameters and β-derivative versus production time.

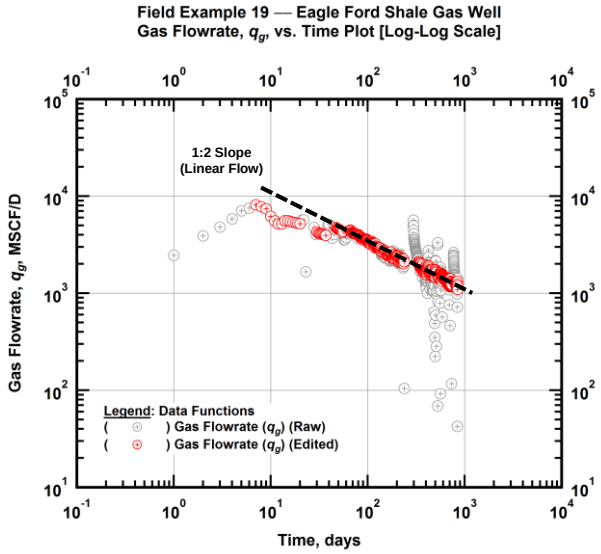

Figure A.548 — (Log-Log Plot): Filtered gas flowrate production history and flow regime identification plot — gas flowrate (q_g) versus production time.

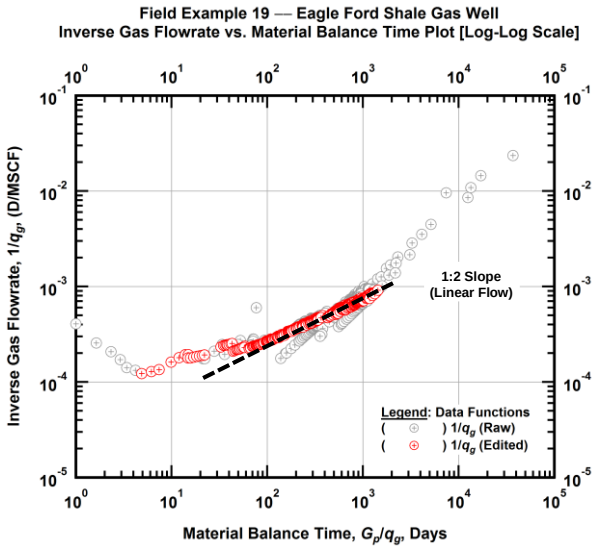

Figure A.549 — (Log-log Plot): Filtered inverse rate with material balance time plot — inverse gas flowrate ($1/q_g$) versus material balance time (G_p/q_g).

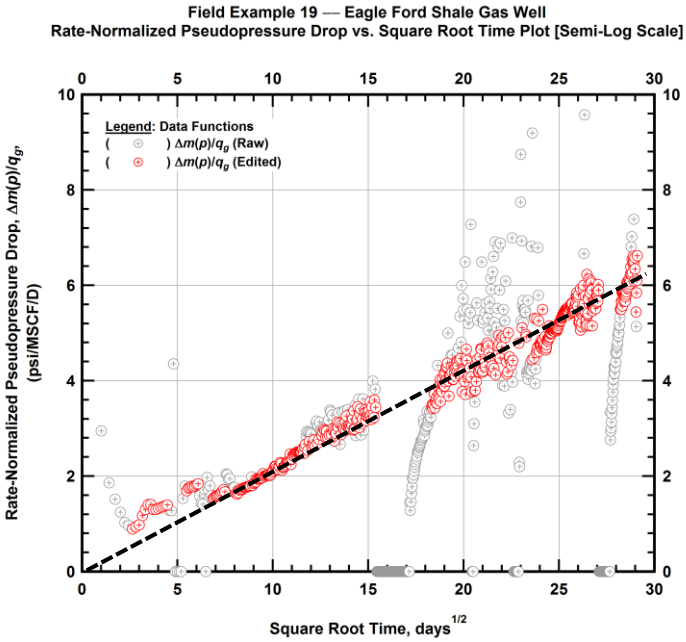

Figure A.550 — (Semi-log Plot): Filtered normalized pseudopressure drop production history plot — rate-normalized pseudopressure drop ($\Delta m(p)/q_g$) versus square root production time ($\sqrt{t}$).

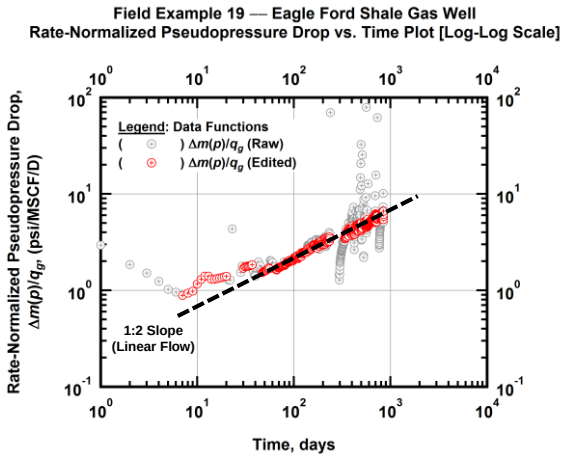

Figure A.551 — (Log-log Plot): Filtered normalized pseudopressure drop production history plot — rate-normalized pseudopressure drop ($\Delta m(p)/q_g$) versus production time.

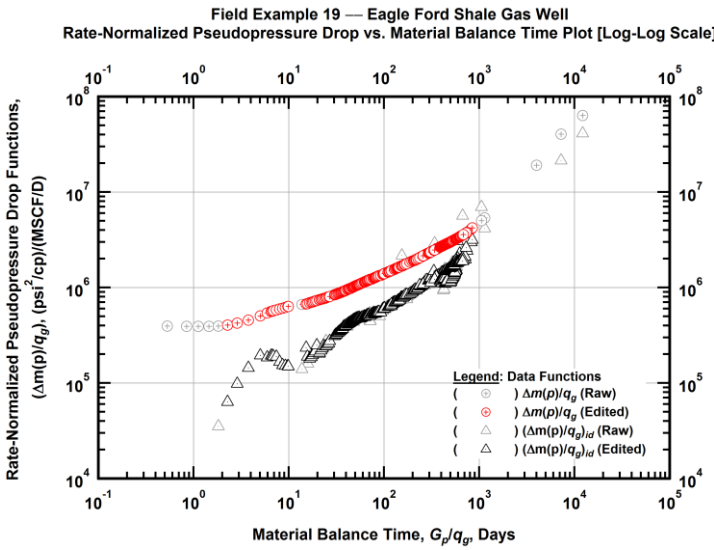

Figure A.552 — (Log-log Plot): "Log-log" diagnostic plot of the filtered production data — rate-normalized pseudopressure drop ($\Delta m(p)/q_g$) and rate-normalized pseudopressure drop integral-derivative $(\Delta m(p)/q_g)_{id}$ versus material balance time (G_p/q_g).

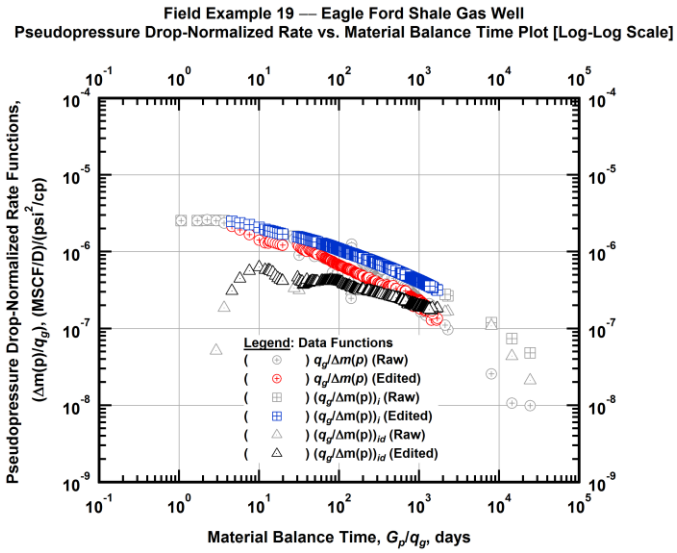

Figure A.553 — (Log-log Plot): "Blasingame" diagnostic plot of the filtered production data — pseudopressure drop-normalized gas flowrate ($q_g/\Delta m(p)$), pseudopressure drop-normalized gas flowrate integral $(q_g/\Delta m(p))_i$ and pseudopressure drop-normalized gas flowrate integral-derivative $(q_g/\Delta m(p))_{id}$ versus material balance time (G_p/q_g).

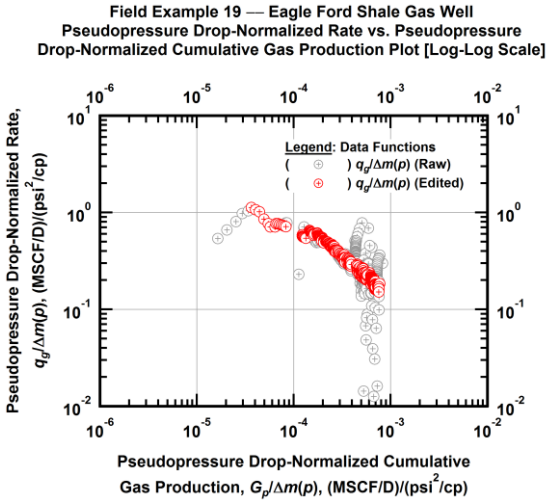

Figure A.554 — (Log-log Plot): Filtered normalized rate with normalized cumulative production plot — pseudopressure drop-normalized gas flowrate ($q_g/\Delta m(p)$) versus pseudopressure drop-normalized cumulative gas production ($G_p/\Delta m(p)$).

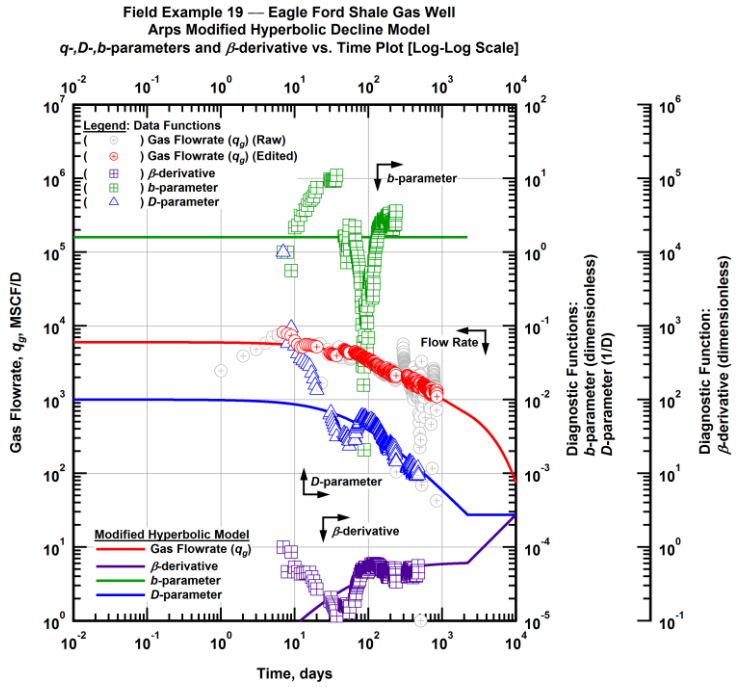

Figure A.555 — (Log-Log Plot): Arps modified hyperbolic decline model plot — time-rate model and data gas flowrate (q_g), *D*- and *b*-parameters and β-derivative versus production time.

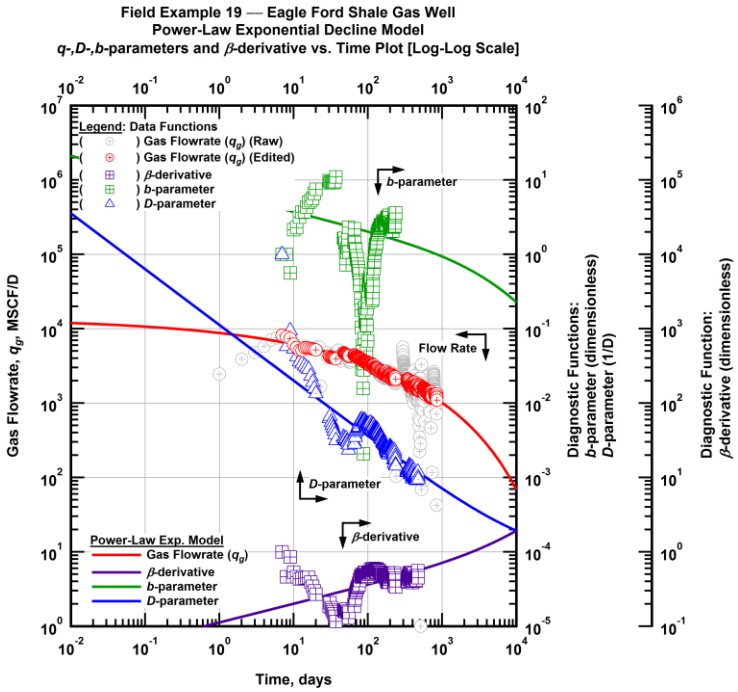

Figure A.556 — (Log-Log Plot): Power-law exponential decline model plot — time-rate model and data gas flowrate (q_g), *D*- and *b*-parameters and β-derivative versus production time.

Field Example 19 — Model-Based (Time-Rate-Pressure) Production Analysis

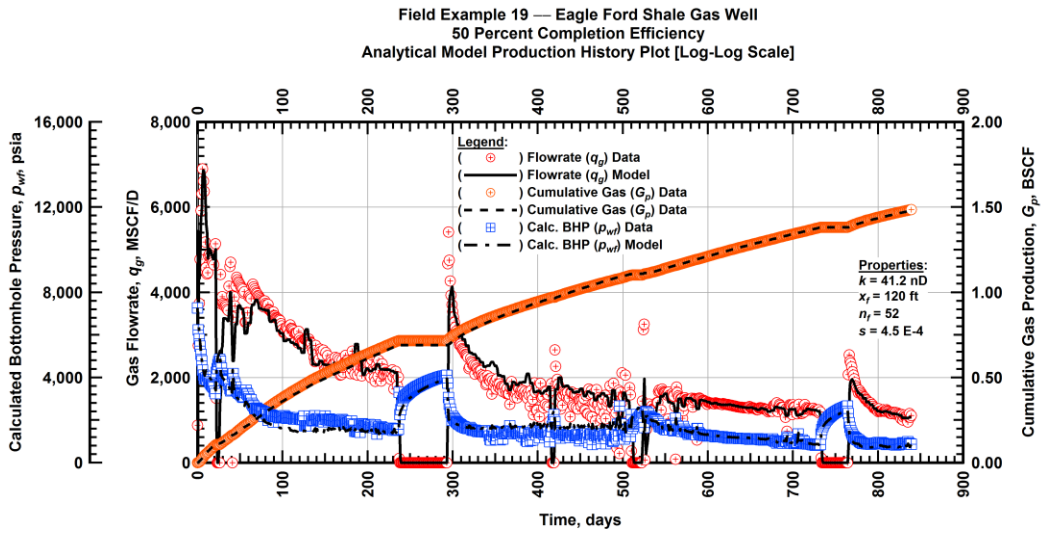

Figure A.557 — (Cartesian Plot): Production history plot — original gas flowrate (q_g), cumulative gas production (G_p), calculated bottomhole pressure (p_{wf}) and 50 percent completion efficiency model matches versus production time.

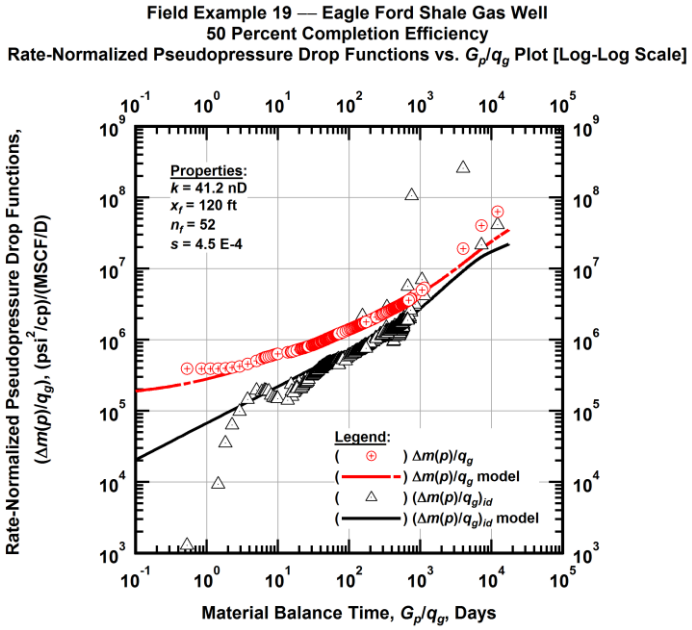

Figure A.558 — (Log-log Plot): "Log-log" diagnostic plot of the original production data — rate-normalized pseudopressure drop ($\Delta m(p)/q_g$), rate-normalized pseudopressure drop integral-derivative $(\Delta m(p)/q_g)_{id}$ and 50 percent completion efficiency model matches versus material balance time (G_p/q_g).

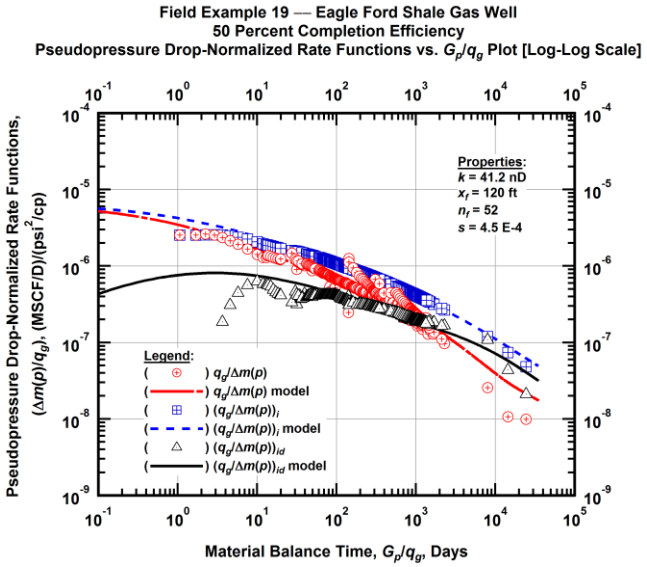

Figure A.559 — (Log-log Plot): "Blasingame" diagnostic plot of the original production data — pseudopressure drop-normalized gas flowrate ($q_g/\Delta m(p)$), pseudopressure drop-normalized gas flowrate integral $(q_g/\Delta m(p))_i$, pseudopressure drop-normalized gas flowrate integral-derivative $(q_g/\Delta m(p))_{id}$ and 50 percent completion efficiency model matches versus material balance time (G_p/q_g).

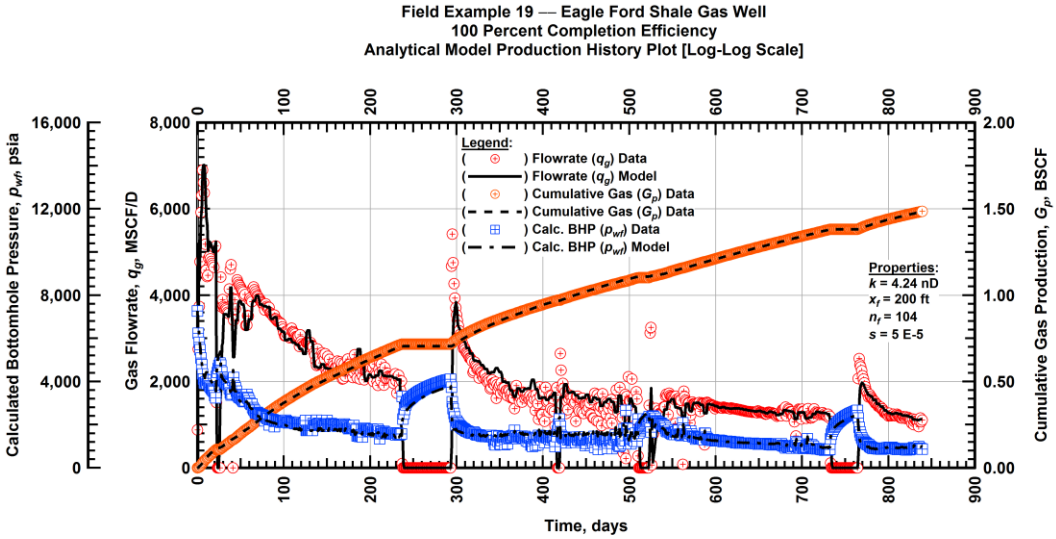

Figure A.560 — (Cartesian Plot): Production history plot — original gas flowrate (q_g), cumulative gas production (G_p), calculated bottomhole pressure (p_{wf}) and 100 percent completion efficiency model matches versus production time.

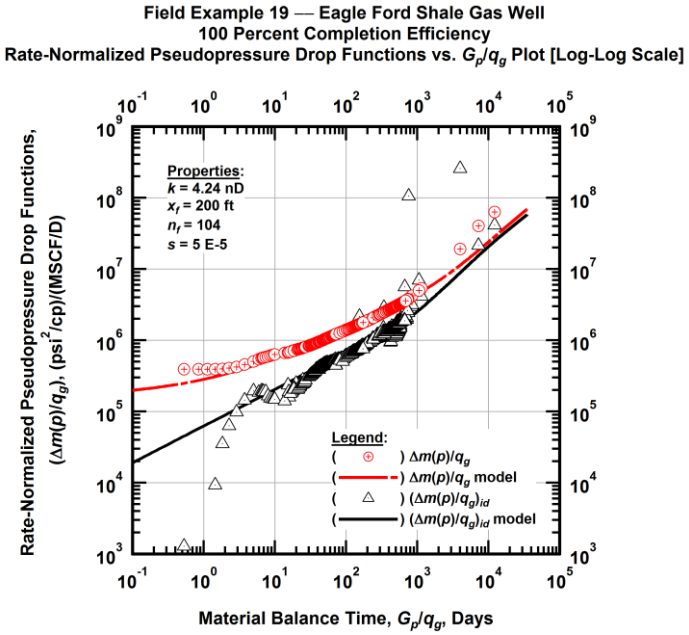

Figure A.561 — (Log-log Plot): "Log-log" diagnostic plot of the original production data — rate-normalized pseudopressure drop ($\Delta m(p)/q_g$), rate-normalized pseudopressure drop integral-derivative $(\Delta m(p)/q_g)_{id}$ and 100 percent completion efficiency model matches versus material balance time (G_p/q_g).

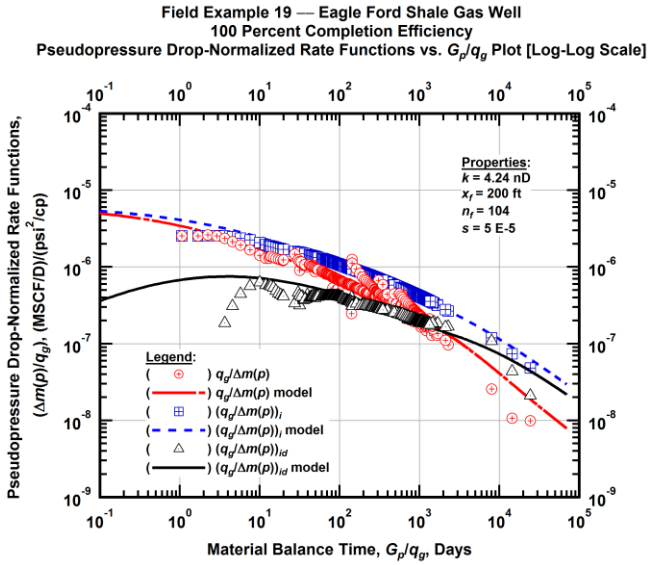

Figure A.562 — (Log-log Plot): "Blasingame" diagnostic plot of the original production data — pseudopressure drop-normalized gas flowrate ($q_g/\Delta m(p)$), pseudopressure drop-normalized gas flowrate integral $(q_g/\Delta m(p))_i$, pseudopressure drop-normalized gas flowrate integral-derivative $(q_g/\Delta m(p))_{id}$ and 100 percent completion efficiency model matches versus material balance time (G_p/q_g).

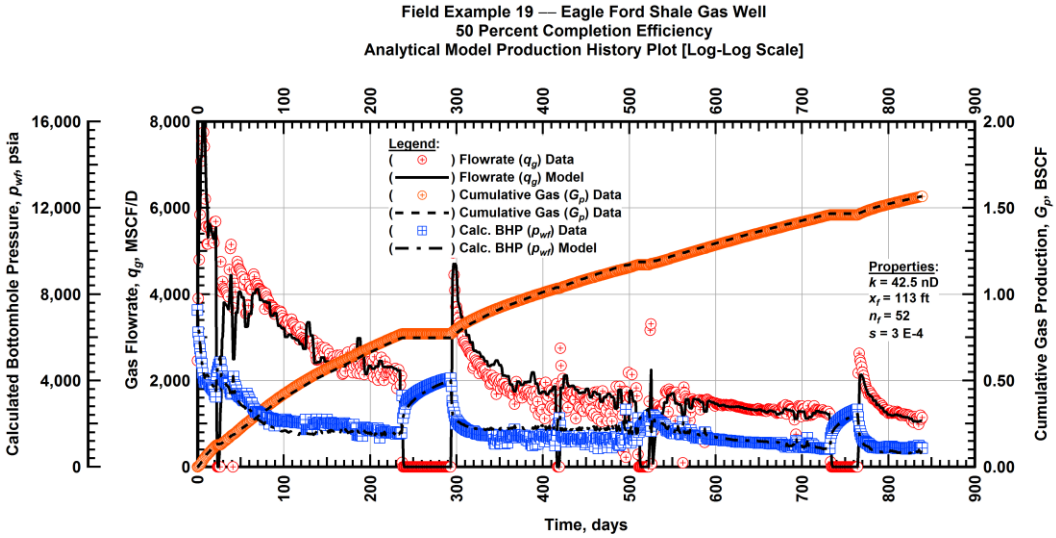

Figure A.563 — (Cartesian Plot): Production history plot — revised gas flowrate (q_g), cumulative gas production (G_p), calculated bottomhole pressure (p_{wf}) and 50 percent completion efficiency model matches versus production time.

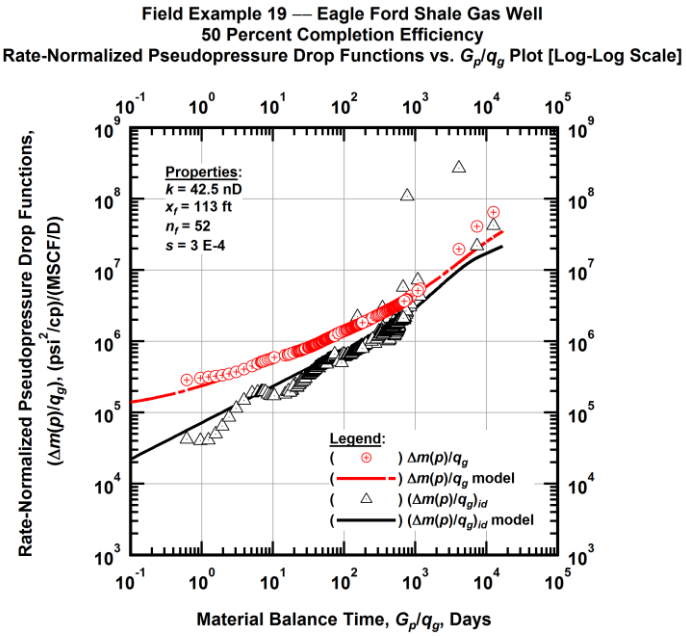

Figure A.564— (Log-log Plot): "Log-log" diagnostic plot of the revised production data — rate-normalized pseudopressure drop ($\Delta m(p)/q_g$), rate-normalized pseudopressure drop integral-derivative $(\Delta m(p)/q_g)_{id}$ and 50 percent completion efficiency model matches versus material balance time (G_p/q_g).

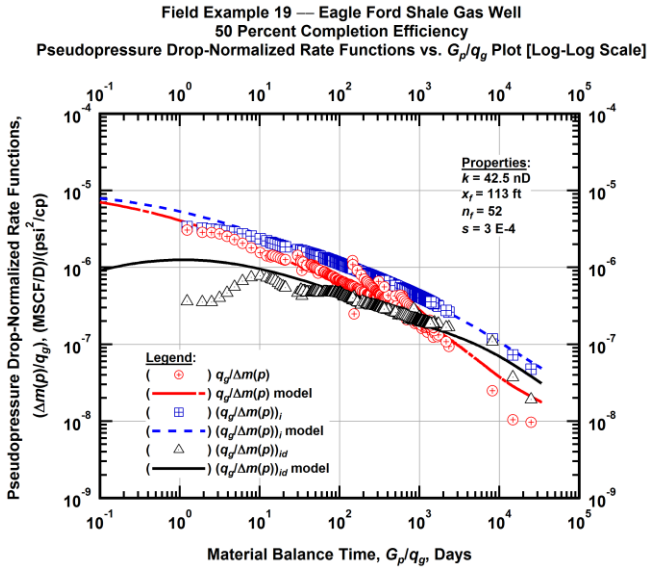

Figure A.565 — (Log-log Plot): "Blasingame" diagnostic plot of the revised production data — pseudopressure drop-normalized gas flowrate ($q_g/\Delta m(p)$), pseudopressure drop-normalized gas flowrate integral $(q_g/\Delta m(p))_i$, pseudopressure drop-normalized gas flowrate integral-derivative $(q_g/\Delta m(p))_{id}$ and 50 percent completion efficiency model matches versus material balance time (G_p/q_g).

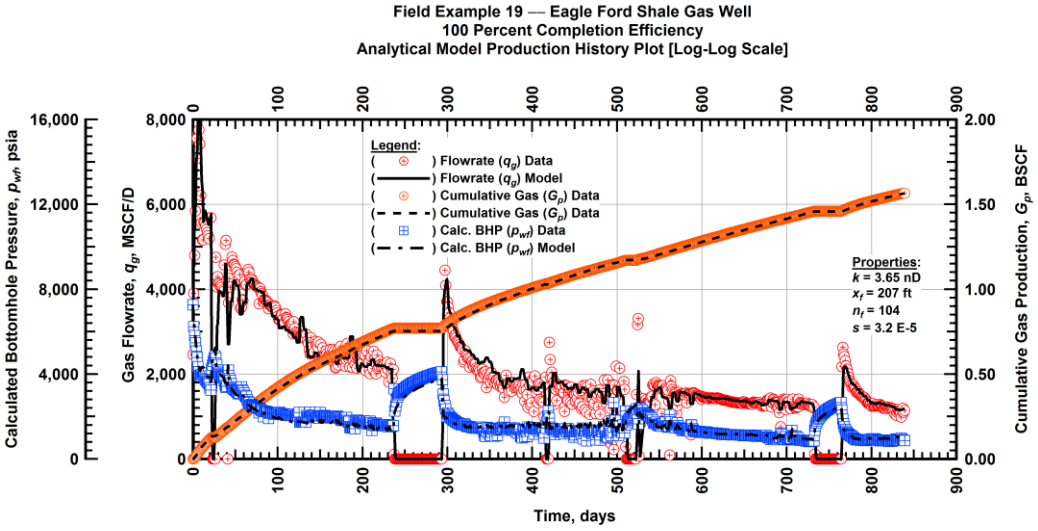

Figure A.566 — (Cartesian Plot): Production history plot — revised gas flowrate (q_g), cumulative gas production (G_p), calculated bottomhole pressure (p_{wf}) and 100 percent completion efficiency model matches versus production time.

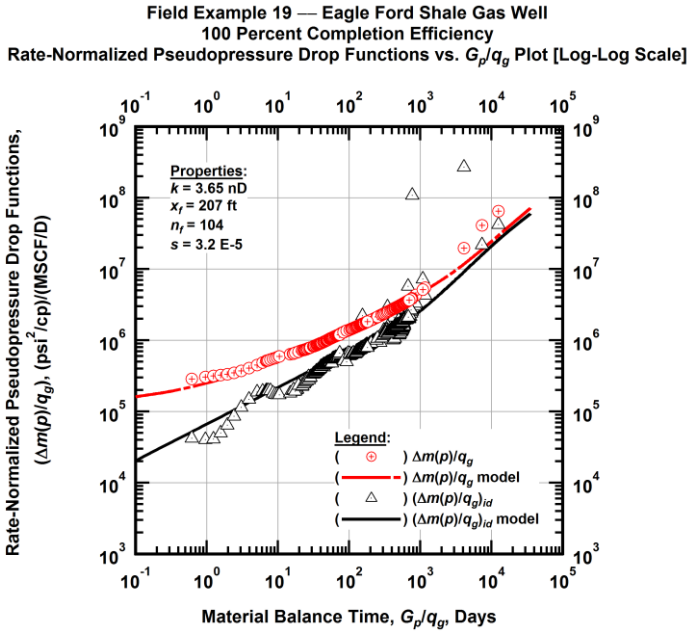

Figure A.567 — (Log-log Plot): "Log-log" diagnostic plot of the revised production data — rate-normalized pseudopressure drop ($\Delta m(p)/q_g$), rate-normalized pseudopressure drop integral-derivative $(\Delta m(p)/q_g)_{id}$ and 100 percent completion efficiency model matches versus material balance time (G_p/q_g).

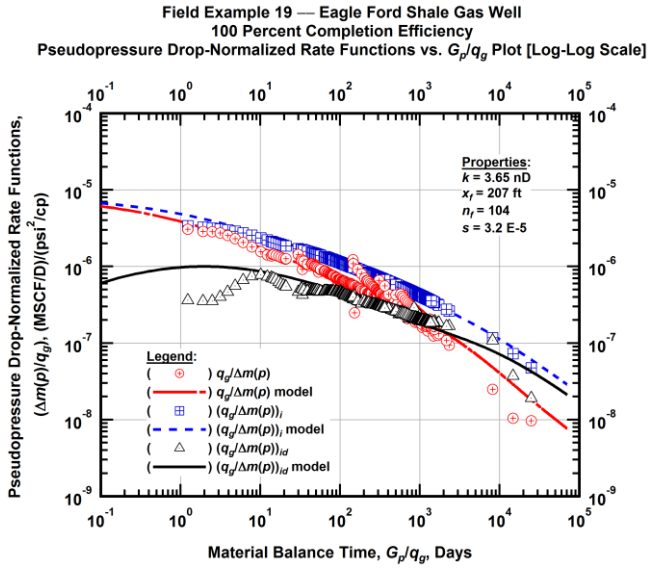

Figure A.568 — (Log-log Plot): "Blasingame" diagnostic plot of the revised production data — pseudopressure drop-normalized gas flowrate ($q_g/\Delta m(p)$), pseudopressure drop-normalized gas flowrate integral $(q_g/\Delta m(p))_i$, pseudopressure drop-normalized gas flowrate integral-derivative $(q_g/\Delta m(p))_{id}$ and 100 percent completion efficiency model matches versus material balance time (G_p/q_g).

Field Example 19 — 30-Year EUR Model Comparison

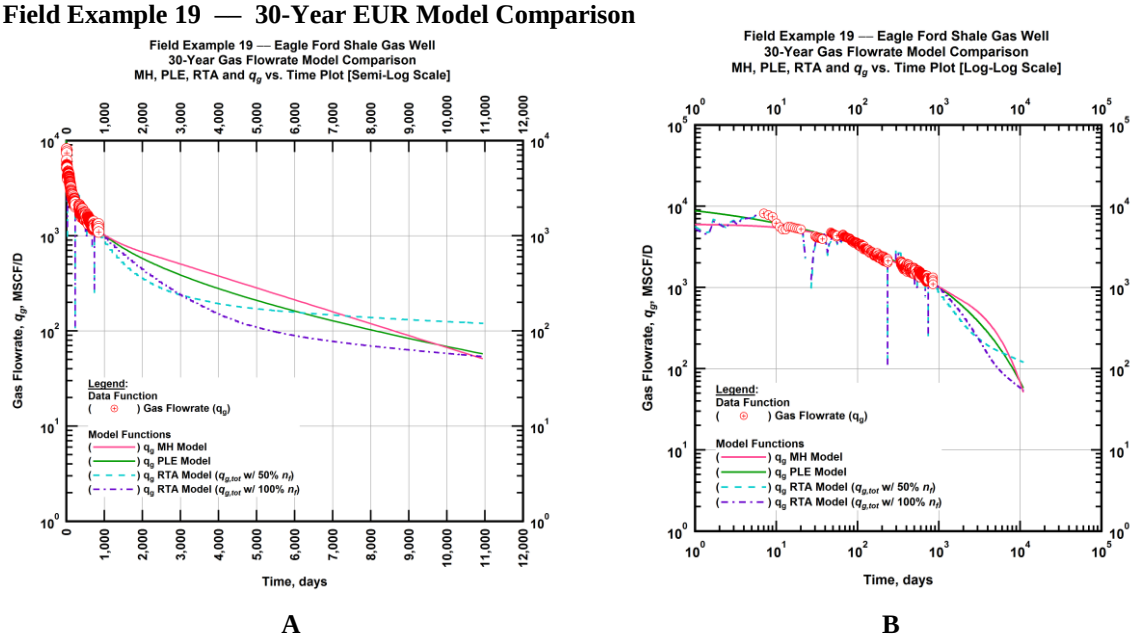

A **B**

Figure A.569 — (A — Semi-Log Plot) and (B — Log-Log Plot): Estimated 30-year revised gas flowrate model comparison — Arps modified hyperbolic decline model, power-law exponential decline model, and 50 percent and 100 percent completion efficiency RTA models revised gas 30-year estimated flowrate decline and historic gas flowrate data (q_g) versus production time.

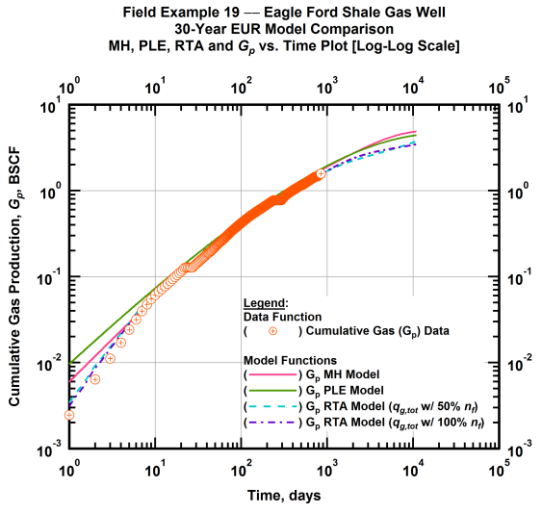

Figure A.570 — (Log-log Plot): PVT revised gas 30-year estimated cumulative production volume model comparison — Arps modified hyperbolic decline model, power-law exponential decline model, and 50 percent and 100 percent completion efficiency RTA model estimated 30-year cumulative gas production volumes and historic cumulative gas production (G_p) versus production time.

Table A.19 — 30-year estimated cumulative revised gas production (EUR), in units of BSCF, for the Arps modified hyperbolic, power-law exponential and analytical time-rate-pressure decline models.

Arps Modified Hyperbolic BSCF)	Power-Law Exponential (BSCF)	RTA Analytical Model ($q_{g,tot}$ w/ 50% n_f) (BSCF)	RTA Analytical Model ($q_{g,tot}$ w/ 100% n_f) (BSCF)
4.83	4.24	3.85	3.49

Field Example 20 — Time-Rate Analysis

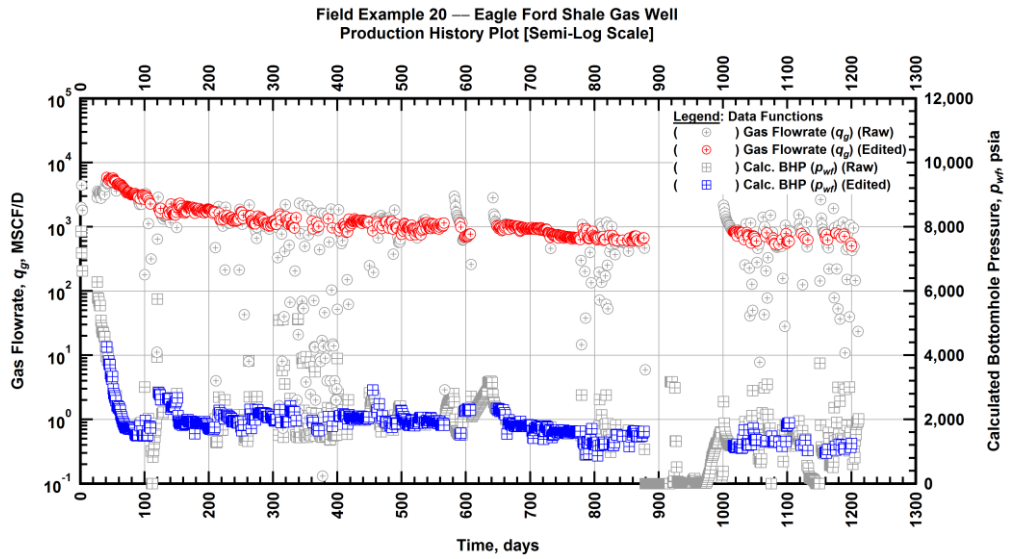

Figure A.571 — (Semi-log Plot): Filtered production history plot — flowrate (q_g) and calculated bottomhole pressure (p_{wf}) versus production time.

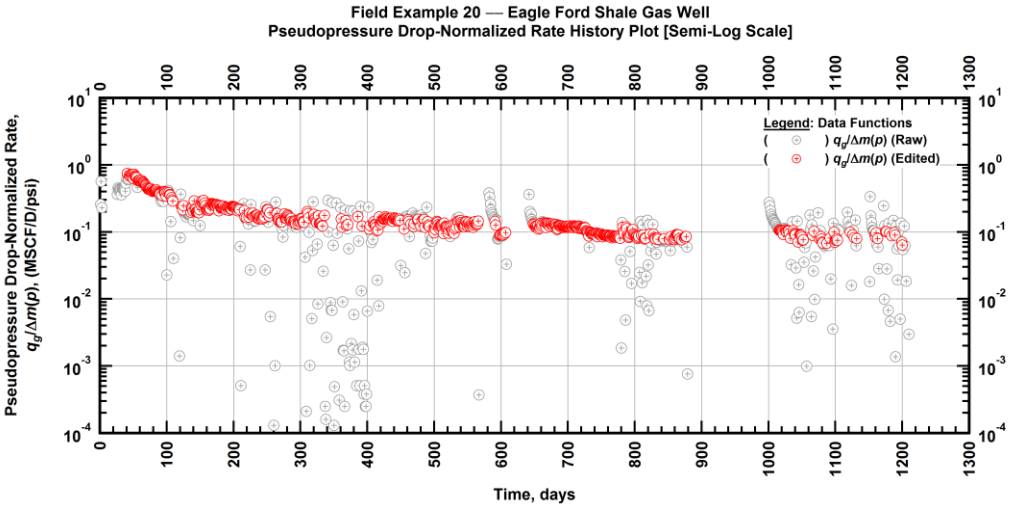

Figure A.572 — (Semi-log Plot): Filtered normalized rate production history plot — pseudopressure drop-normalized gas flowrate ($q_g/\Delta m(p)$) versus production time.

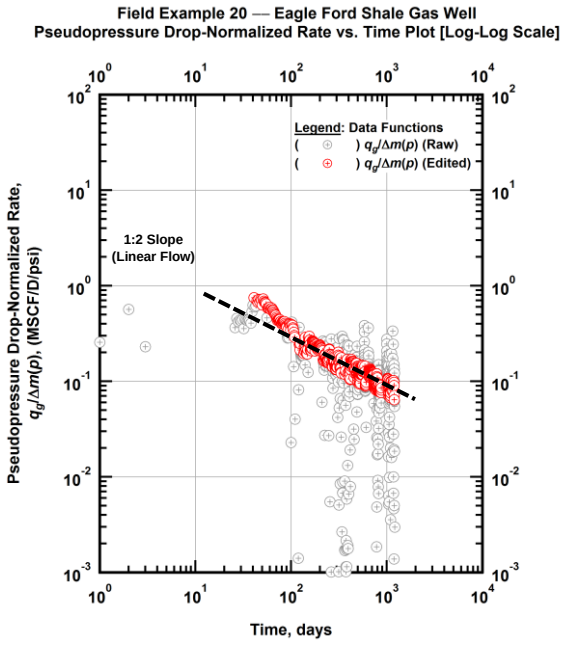

Figure A.573 — (Log-log Plot): Filtered normalized rate production history plot — pseudopressure drop-normalized gas flowrate ($q_g/\Delta m(p)$) versus production time.

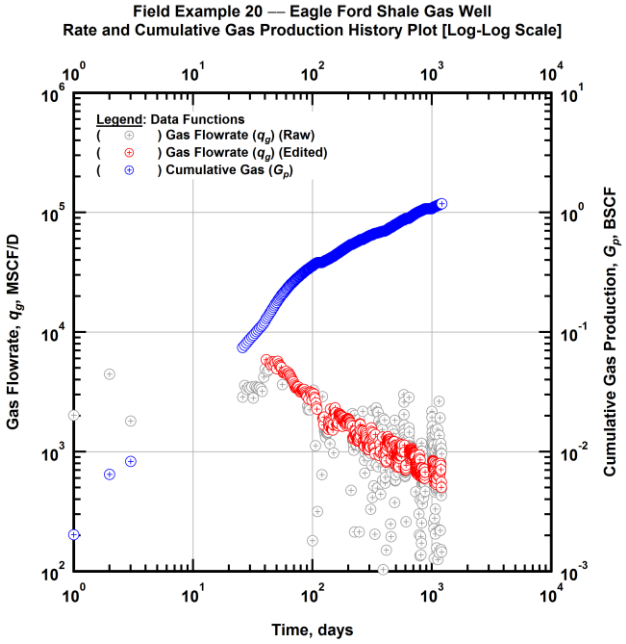

Figure A.574 — (Log-log Plot): Filtered rate and unfiltered cumulative gas production history plot — flowrate (q_g) and cumulative production (G_p) versus production time.

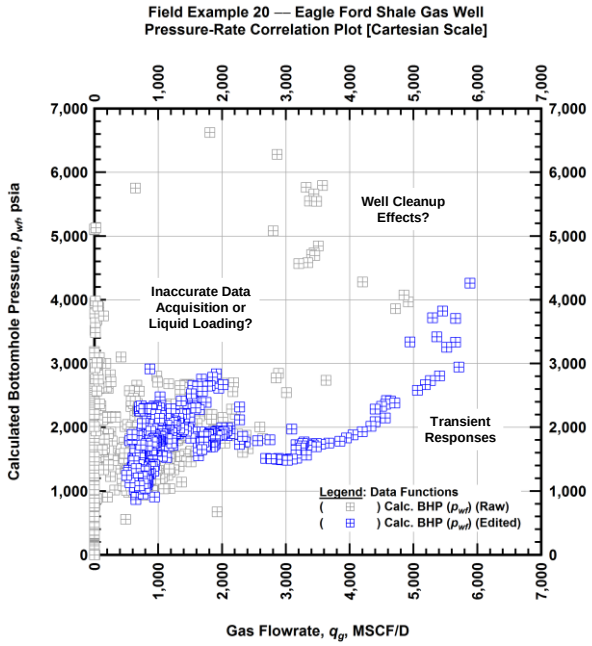

Figure A.575 — (Cartesian Plot): Filtered rate-pressure correlation plot — calculated bottomhole pressure (p_{wf}) versus flowrate (q_g).

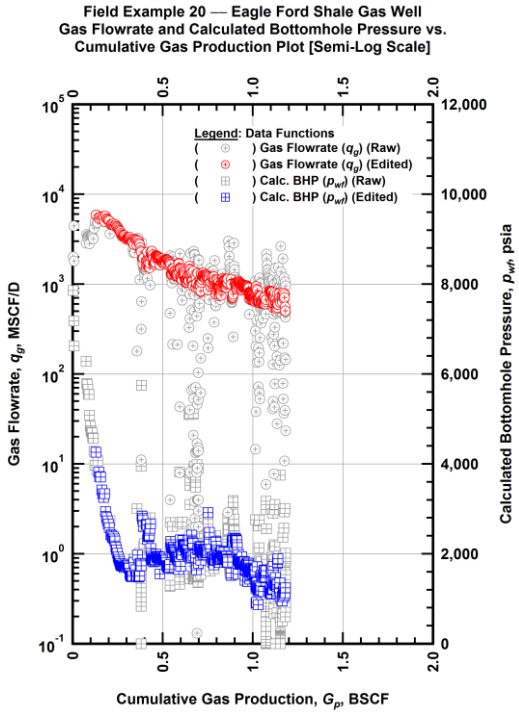

Figure A.576 — (Semi-log Plot): Filtered rate-pressure-cumulative production history plot — flowrate (q_g) and calculated bottomhole pressure (p_{wf}) versus cumulative production (G_p).

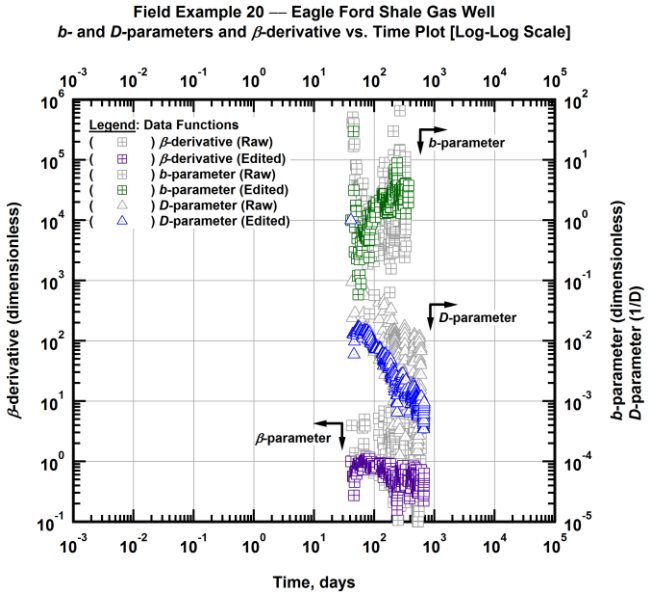

Figure A.577 — (Log-Log Plot): Filtered b, D and β production history plot — b- and D-parameters and β-derivative versus production time.

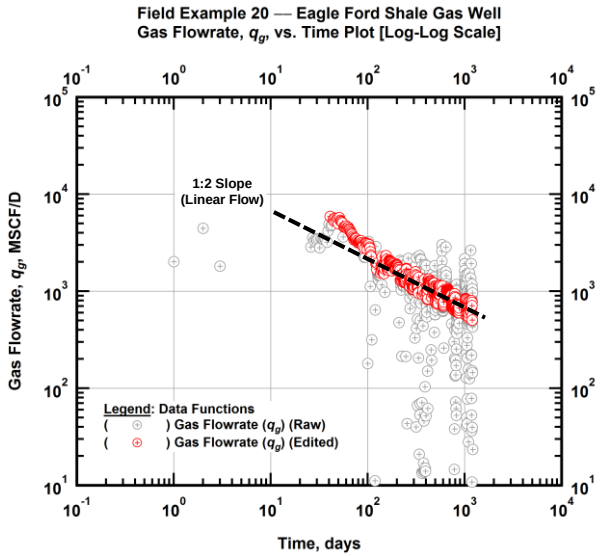

Figure A.578 — (Log-Log Plot): Filtered gas flowrate production history and flow regime identification plot — gas flowrate (q_g) versus production time.

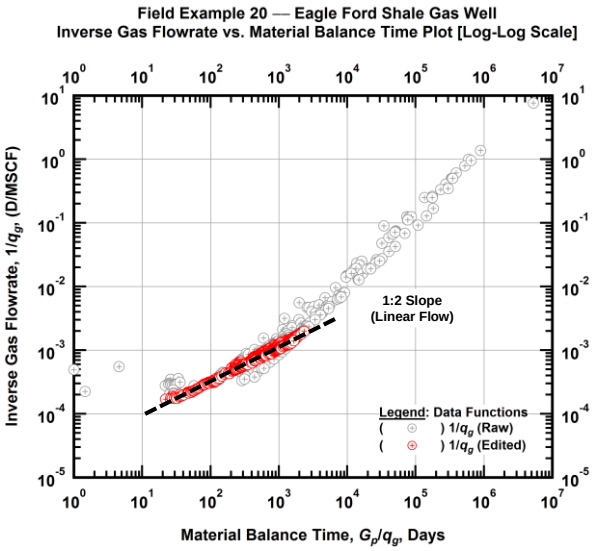

Figure A.579 — (Log-log Plot): Filtered inverse rate with material balance time plot — inverse gas flowrate ($1/q_g$) versus material balance time (G_p/q_g).

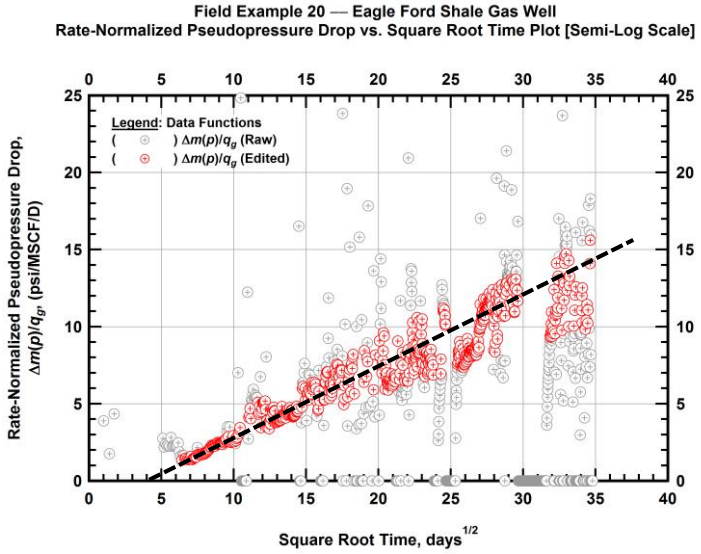

Figure A.580 — (Semi-log Plot): Filtered normalized pseudopressure drop production history plot — rate-normalized pseudopressure drop ($\Delta m(p)/q_g$) versus square root production time ($\sqrt{t}$).

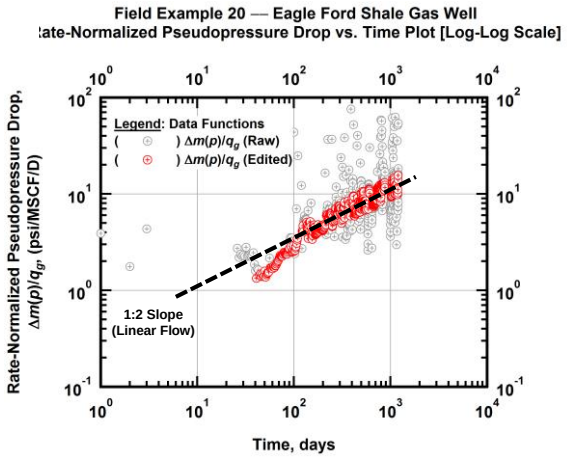

Figure A.581 — (Log-log Plot): Filtered normalized pseudopressure drop production history plot — rate-normalized pseudopressure drop ($\Delta m(p)/q_g$) versus production time.

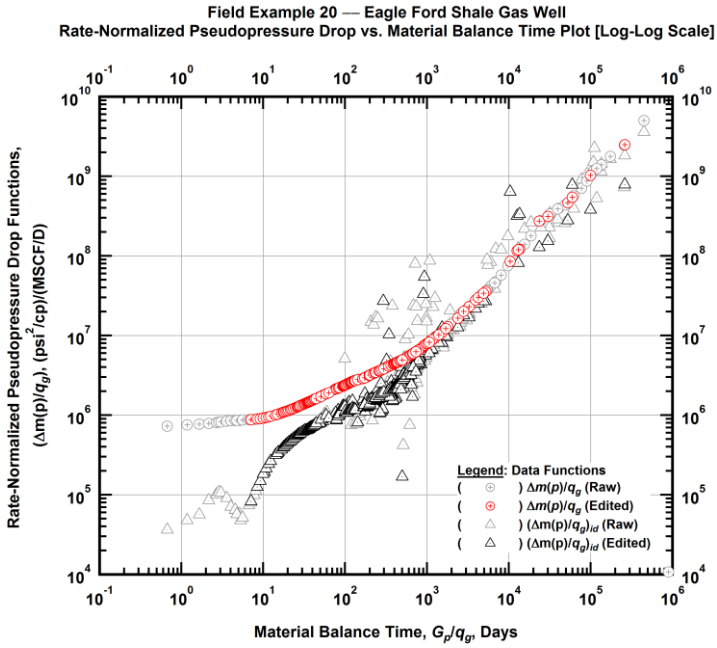

Figure A.582 — (Log-log Plot): "Log-log" diagnostic plot of the filtered production data — rate-normalized pseudopressure drop ($\Delta m(p)/q_g$) and rate-normalized pseudopressure drop integral-derivative $(\Delta m(p)/q_g)_{id}$ versus material balance time (G_p/q_g).

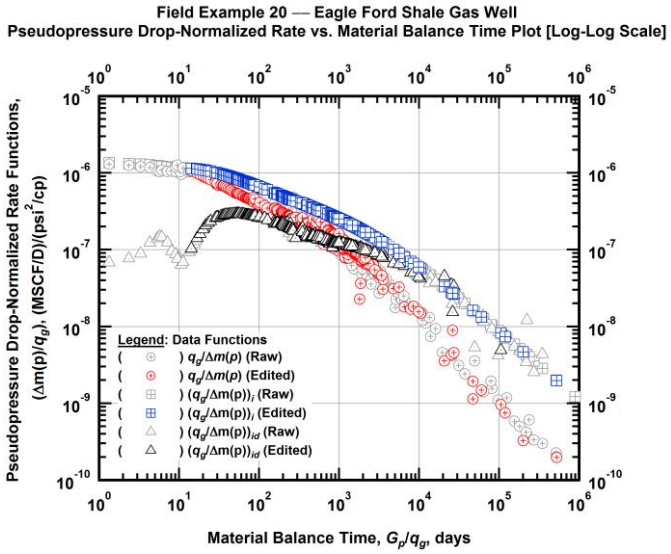

Figure A.583 — (Log-log Plot): "Blasingame" diagnostic plot of the filtered production data — pseudopressure drop-normalized gas flowrate ($q_g/\Delta m(p)$), pseudopressure drop-normalized gas flowrate integral $(q_g/\Delta m(p))_i$ and pseudopressure drop-normalized gas flowrate integral-derivative $(q_g/\Delta m(p))_{id}$ versus material balance time (G_p/q_g).

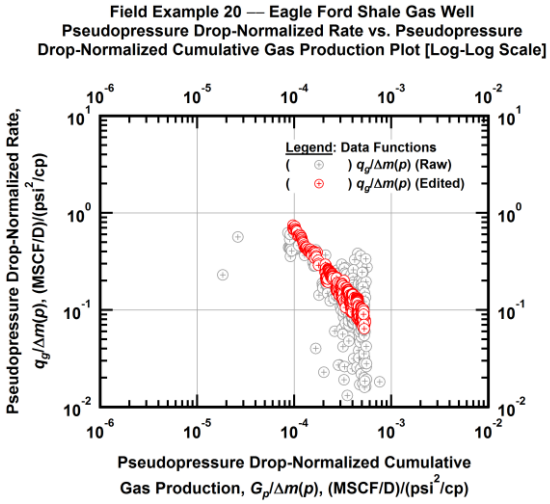

Figure A.584 — (Log-log Plot): Filtered normalized rate with normalized cumulative production plot — pseudopressure drop-normalized gas flowrate ($q_g/\Delta m(p)$) versus pseudopressure drop-normalized cumulative gas production ($G_p/\Delta m(p)$).

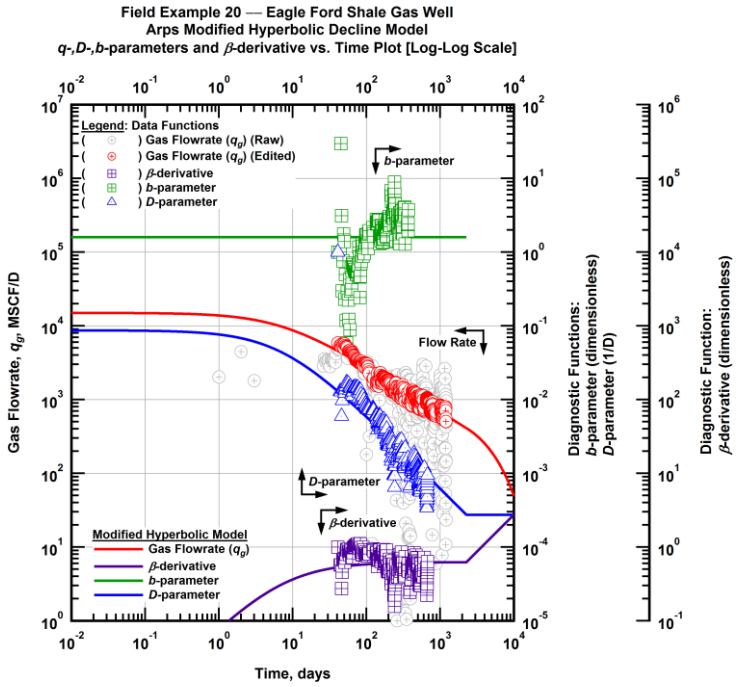

Figure A.585 — (Log-Log Plot): Arps modified hyperbolic decline model plot — time-rate model and data gas flowrate (q_g), *D*- and *b*-parameters and β-derivative versus production time.

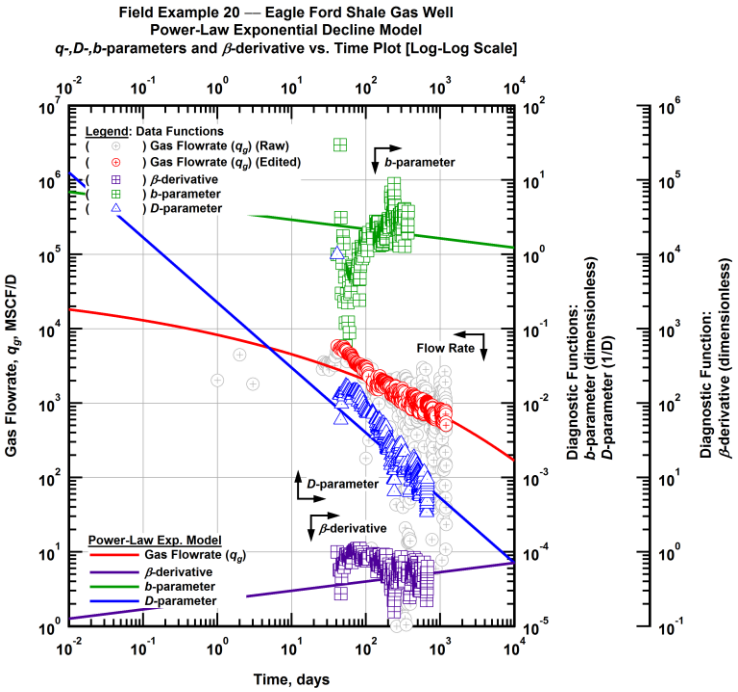

Figure A.586 — (Log-Log Plot): Power-law exponential decline model plot — time-rate model and data gas flowrate (q_g), *D*- and *b*-parameters and β-derivative versus production time.

Field Example 20 — Model-Based (Time-Rate-Pressure) Production Analysis

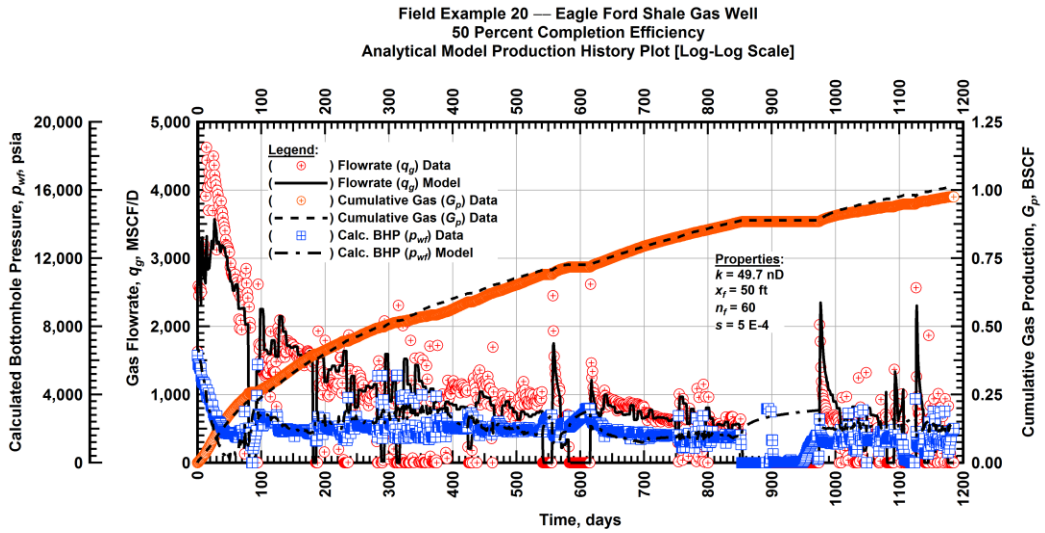

Figure A.587 — (Cartesian Plot): Production history plot — original gas flowrate (q_g), cumulative gas production (G_p), calculated bottomhole pressure (p_{wf}) and 50 percent completion efficiency model matches versus production time.

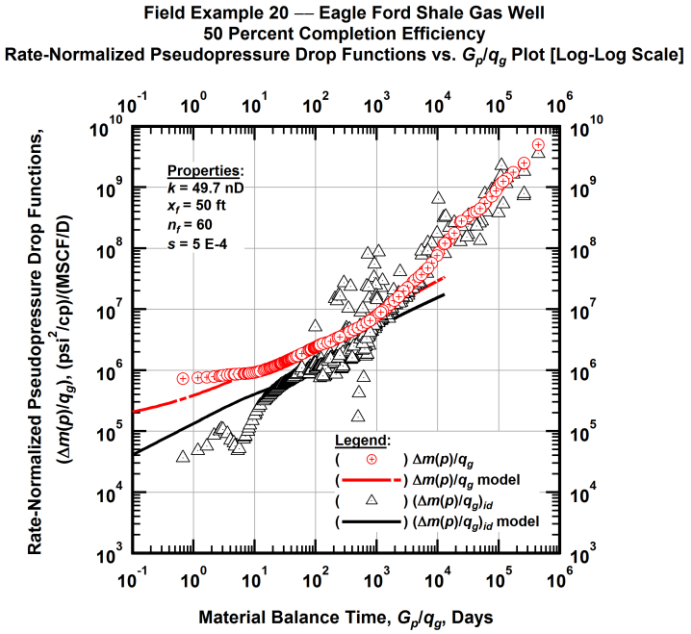

Figure A.588 — (Log-log Plot): "Log-log" diagnostic plot of the original production data — rate-normalized pseudopressure drop ($\Delta m(p)/q_g$), rate-normalized pseudopressure drop integral-derivative $(\Delta m(p)/q_g)_{id}$ and 50 percent completion efficiency model matches versus material balance time (G_p/q_g).

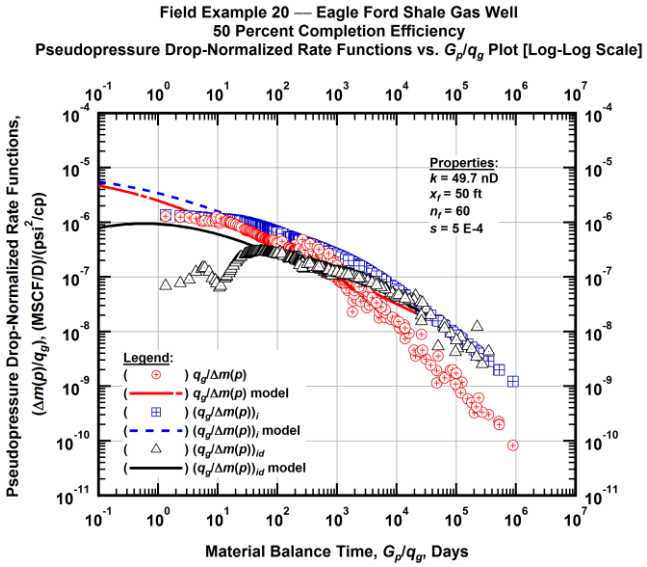

Figure A.589 — (Log-log Plot): "Blasingame" diagnostic plot of the original production data — pseudopressure drop-normalized gas flowrate ($q_g/\Delta m(p)$), pseudopressure drop-normalized gas flowrate integral $(q_g/\Delta m(p))_i$, pseudopressure drop-normalized gas flowrate integral-derivative $(q_g/\Delta m(p))_{id}$ and 50 percent completion efficiency model matches versus material balance time (G_p/q_g).

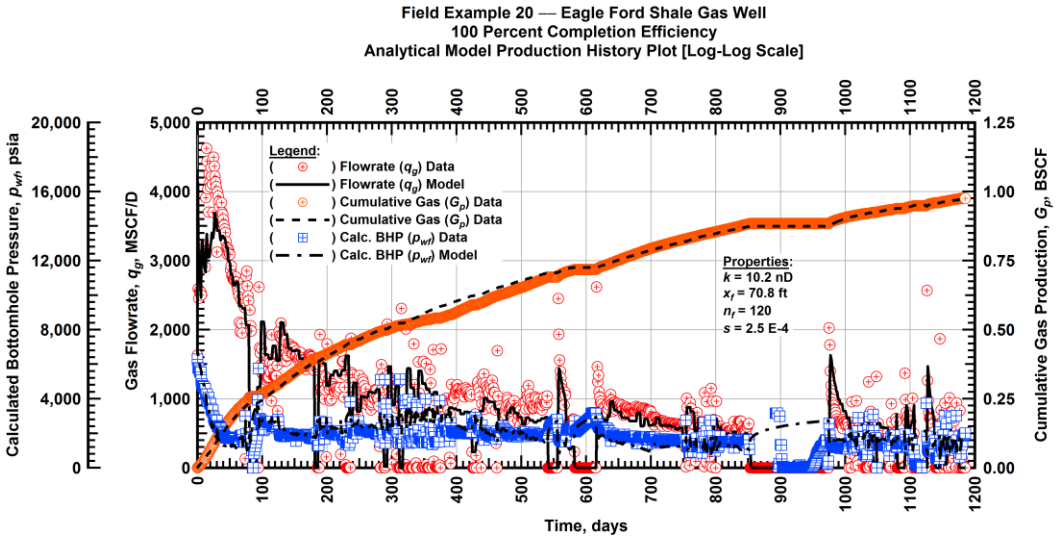

Figure A.590 — (Cartesian Plot): Production history plot — original gas flowrate (q_g), cumulative gas production (G_p), calculated bottomhole pressure (p_{wf}) and 100 percent completion efficiency model matches versus production time.

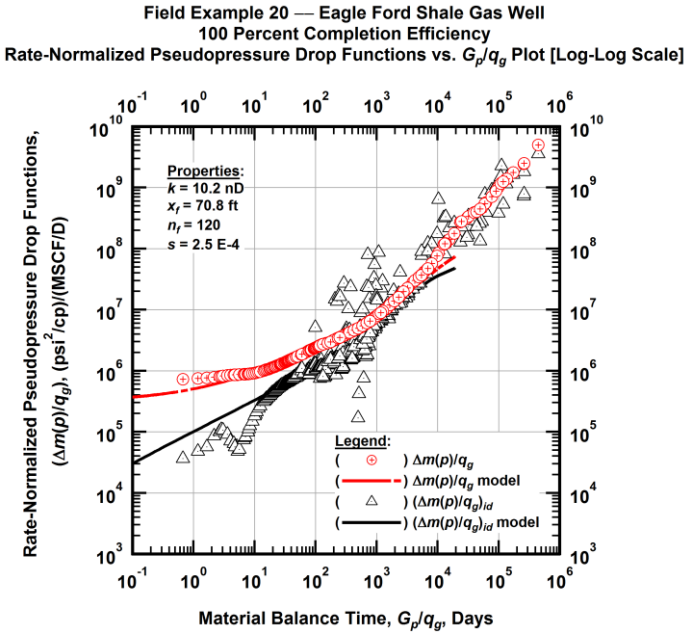

Figure A.591 — (Log-log Plot): "Log-log" diagnostic plot of the original production data — rate-normalized pseudopressure drop ($\Delta m(p)/q_g$), rate-normalized pseudopressure drop integral-derivative $(\Delta m(p)/q_g)_{id}$ and 100 percent completion efficiency model matches versus material balance time (G_p/q_g).

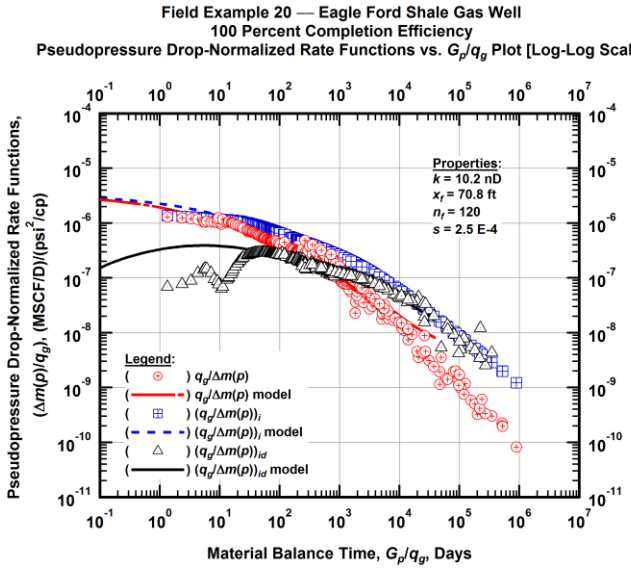

Figure A.592 — (Log-log Plot): "Blasingame" diagnostic plot of the original production data — pseudopressure drop-normalized gas flowrate ($q_g/\Delta m(p)$), pseudopressure drop-normalized gas flowrate integral $(q_g/\Delta m(p))_i$, pseudopressure drop-normalized gas flowrate integral-derivative $(q_g/\Delta m(p))_{id}$ and 100 percent completion efficiency model matches versus material balance time (G_p/q_g).

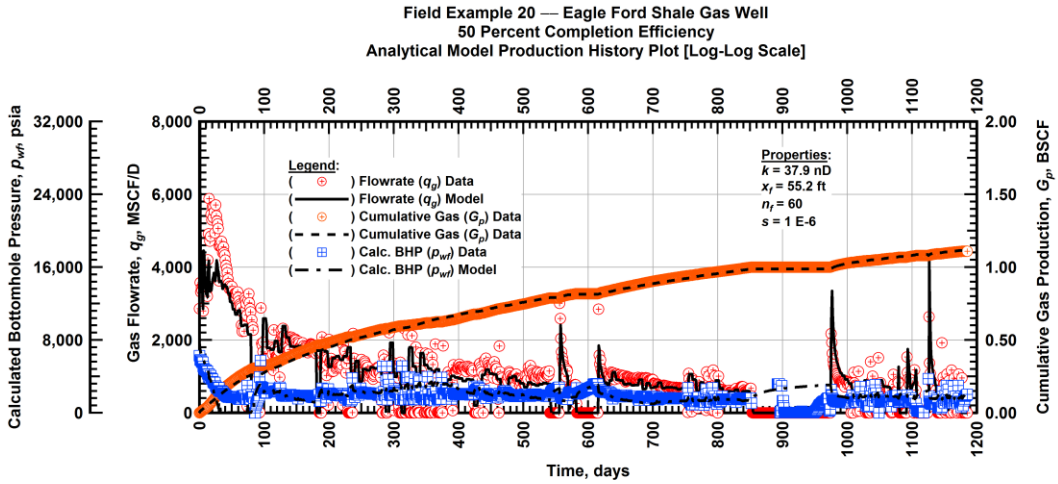

Figure A.593 — (Cartesian Plot): Production history plot — revised gas flowrate (q_g), cumulative gas production (G_p), calculated bottomhole pressure (p_{wf}) and 50 percent completion efficiency model matches versus production time.

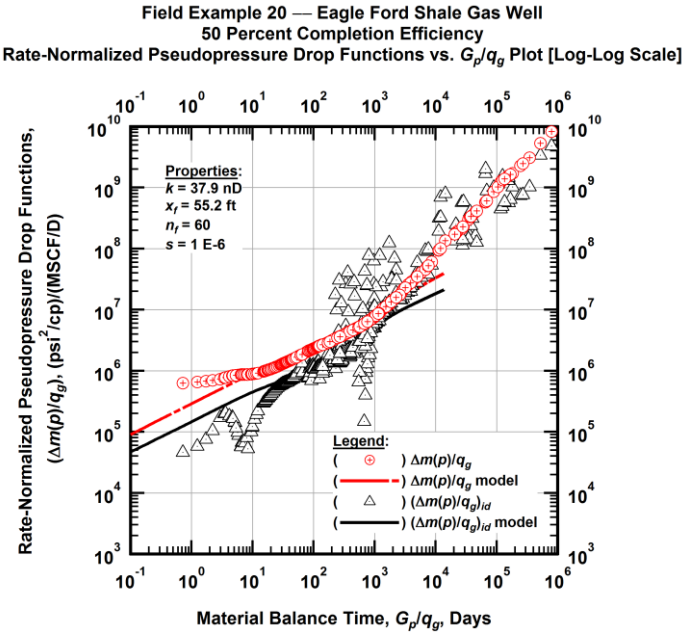

Figure A.594— (Log-log Plot): "Log-log" diagnostic plot of the revised production data — rate-normalized pseudopressure drop ($\Delta m(p)/q_g$), rate-normalized pseudopressure drop integral-derivative $(\Delta m(p)/q_g)_{id}$ and 50 percent completion efficiency model matches versus material balance time (G_p/q_g).

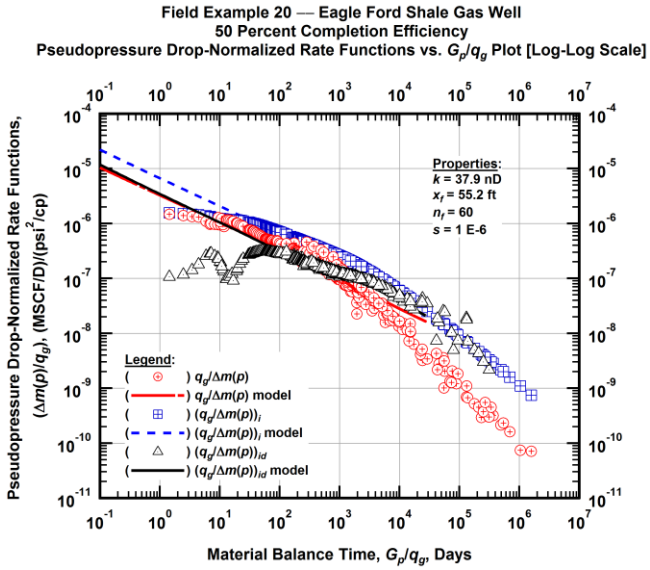

Figure A.595 — (Log-log Plot): "Blasingame" diagnostic plot of the revised production data — pseudopressure drop-normalized gas flowrate ($q_g/\Delta m(p)$), pseudopressure drop-normalized gas flowrate integral $(q_g/\Delta m(p))_i$, pseudopressure drop-normalized gas flowrate integral-derivative $(q_g/\Delta m(p))_{id}$ and 50 percent completion efficiency model matches versus material balance time (G_p/q_g).

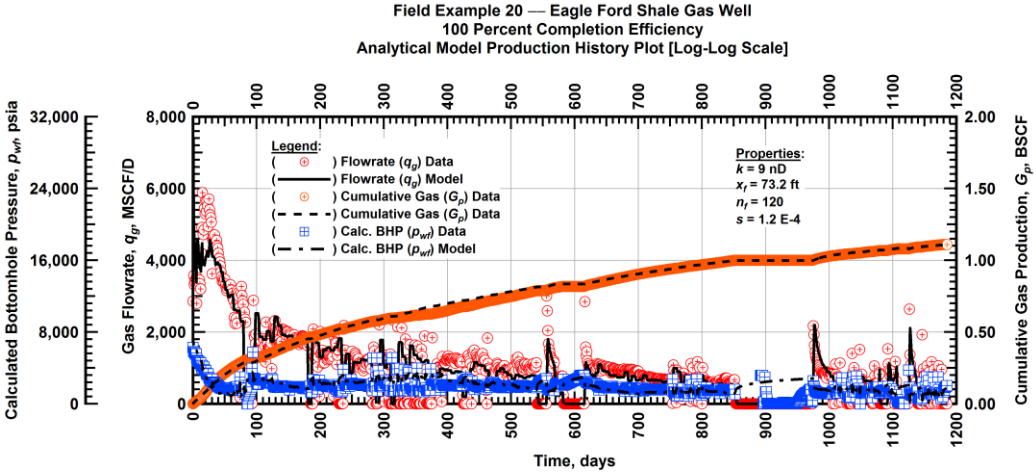

Figure A.596 — (Cartesian Plot): Production history plot — revised gas flowrate (q_g), cumulative gas production (G_p), calculated bottomhole pressure (p_{wf}) and 100 percent completion efficiency model matches versus production time.

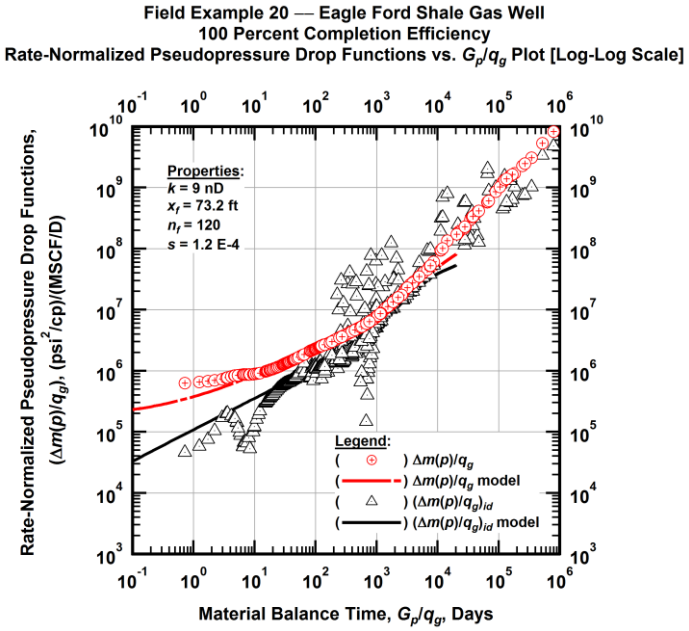

Figure A.597 — (Log-log Plot): "Log-log" diagnostic plot of the revised production data — rate-normalized pseudopressure drop ($\Delta m(p)/q_g$), rate-normalized pseudopressure drop integral-derivative $(\Delta m(p)/q_g)_{id}$ and 100 percent completion efficiency model matches versus material balance time (G_p/q_g).

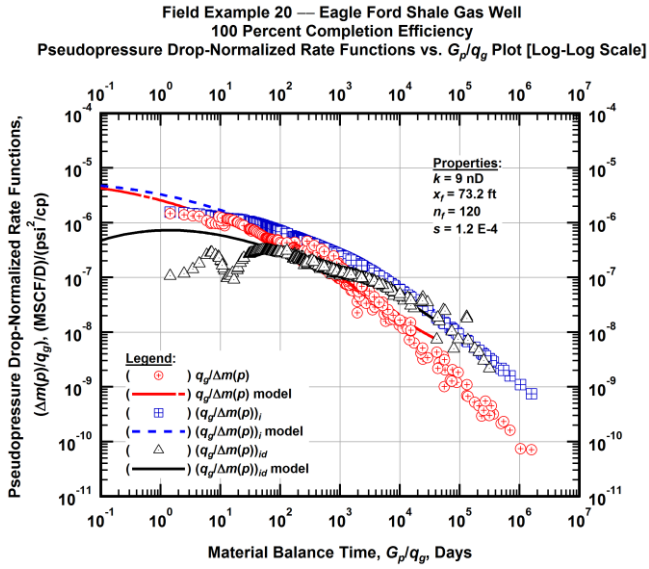

Figure A.598 — (Log-log Plot): "Blasingame" diagnostic plot of the revised production data — pseudopressure drop-normalized gas flowrate ($q_g/\Delta m(p)$), pseudopressure drop-normalized gas flowrate integral $(q_g/\Delta m(p))_i$, pseudopressure drop-normalized gas flowrate integral-derivative $(q_g/\Delta m(p))_{id}$ and 100 percent completion efficiency model matches versus material balance time (G_p/q_g).

Field Example 20 — 30-Year EUR Model Comparison

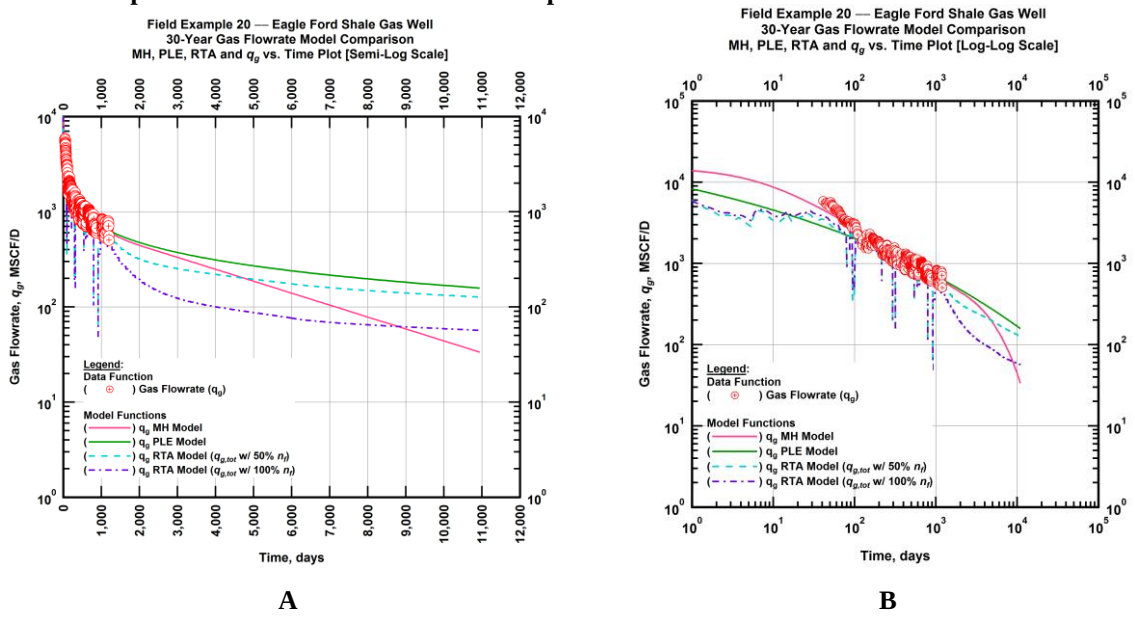

A **B**

Figure A.599 — (A — Semi-Log Plot) and (B — Log-Log Plot): Estimated 30-year revised gas flowrate model comparison — Arps modified hyperbolic decline model, power-law exponential decline model, and 50 percent and 100 percent completion efficiency RTA models revised gas 30-year estimated flowrate decline and historic gas flowrate data (q_g) versus production time.

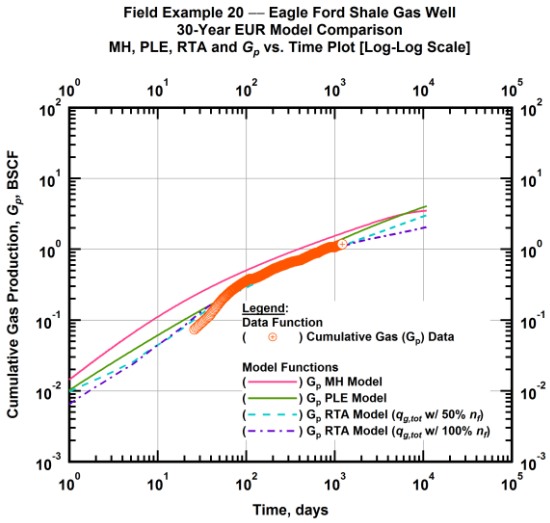

Figure A.600 — (Log-log Plot): PVT revised gas 30-year estimated cumulative production volume model comparison — Arps modified hyperbolic decline model, power-law exponential decline model, and 50 percent and 100 percent completion efficiency RTA model estimated 30-year cumulative gas production volumes and historic cumulative gas production (G_p) versus production time.

Table A.20 — 30-year estimated cumulative revised gas production (EUR), in units of BSCF, for the Arps modified hyperbolic, power-law exponential and analytical time-rate-pressure decline models.

Arps Modified Hyperbolic (BSCF)	Power-Law Exponential (BSCF)	RTA Analytical Model ($q_{g,tot}$ w/ 50% n_f) (BSCF)	RTA Analytical Model ($q_{g,tot}$ w/ 100% n_f) (BSCF)
3.09	4.04	3.19	2.13

Field Example 21 — Time-Rate Analysis

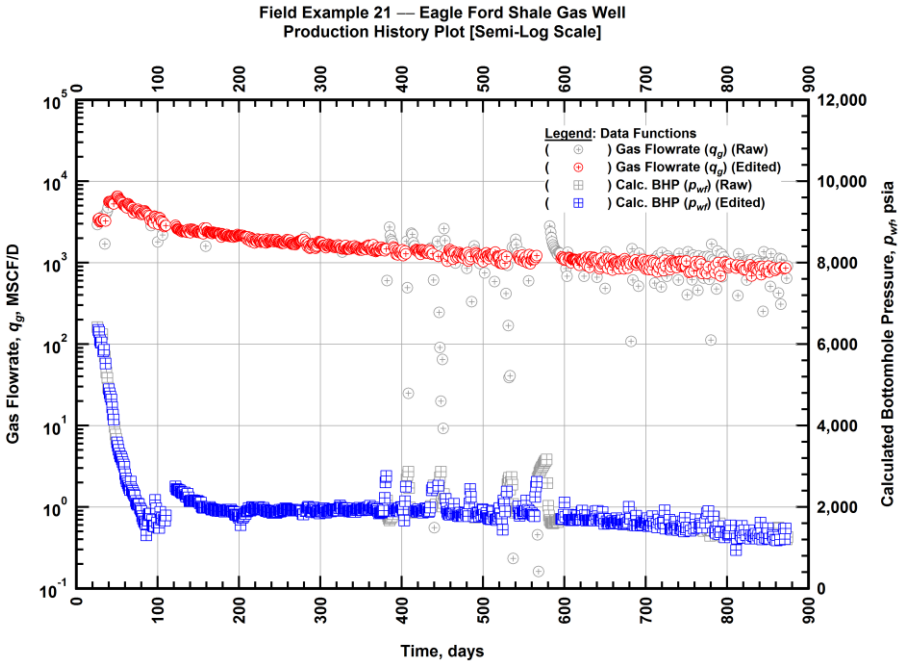

Figure A.601 — (Semi-log Plot): Filtered production history plot — flowrate (q_g) and calculated bottomhole pressure (p_{wf}) versus production time.

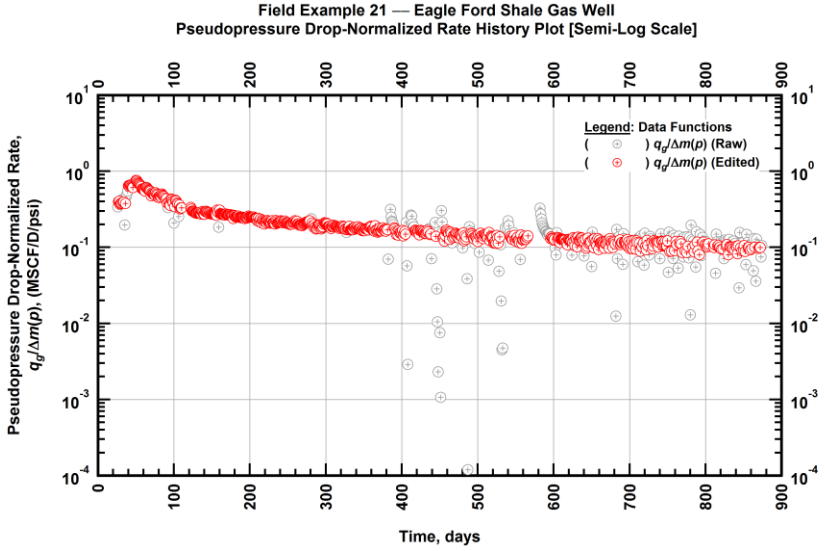

Figure A.602 — (Semi-log Plot): Filtered normalized rate production history plot — pseudopressure drop-normalized gas flowrate ($q_g/\Delta m(p)$) versus production time.

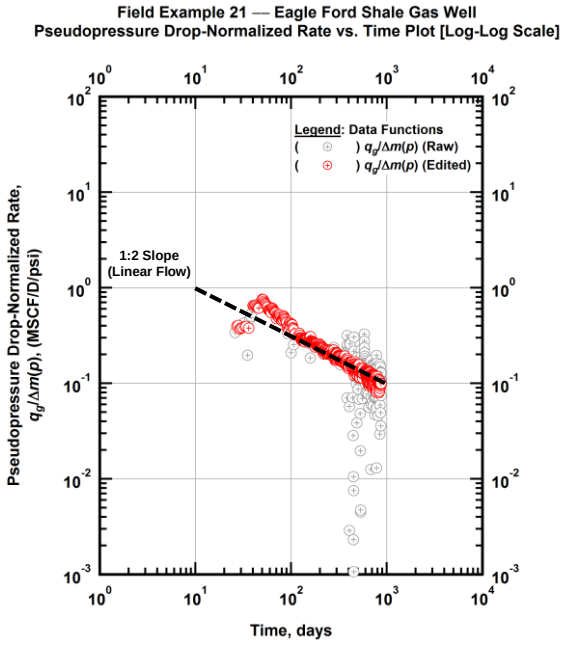

Figure A.603 — (Log-log Plot): Filtered normalized rate production history plot — pseudopressure drop-normalized gas flowrate ($q_g/\Delta m(p)$) versus production time.

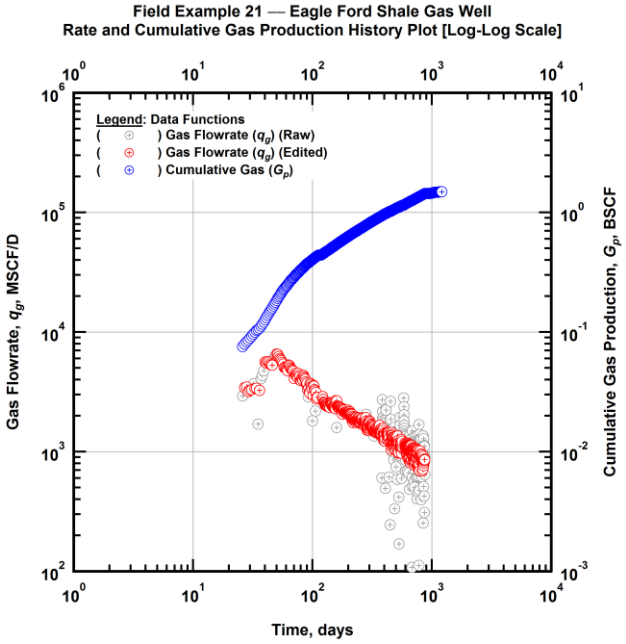

Figure A.604 — (Log-log Plot): Filtered rate and unfiltered cumulative gas production history plot — flowrate (q_g) and cumulative production (G_p) versus production time.

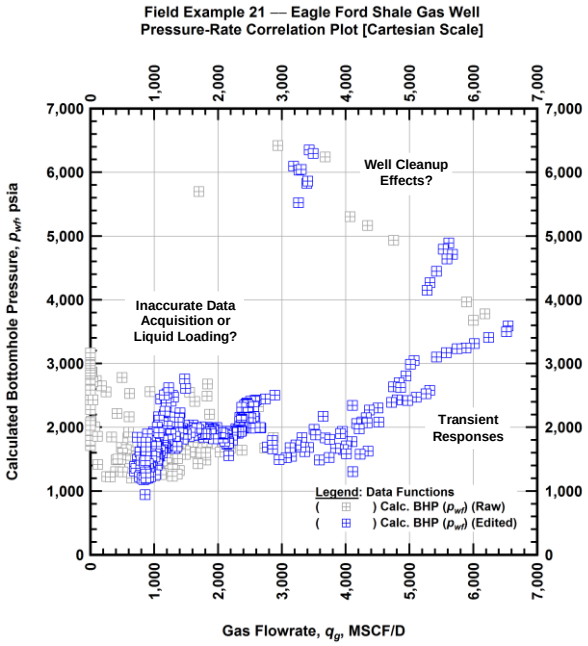

Figure A.605 — (Cartesian Plot): Filtered rate-pressure correlation plot — calculated bottomhole pressure (p_{wf}) versus flowrate (q_g).

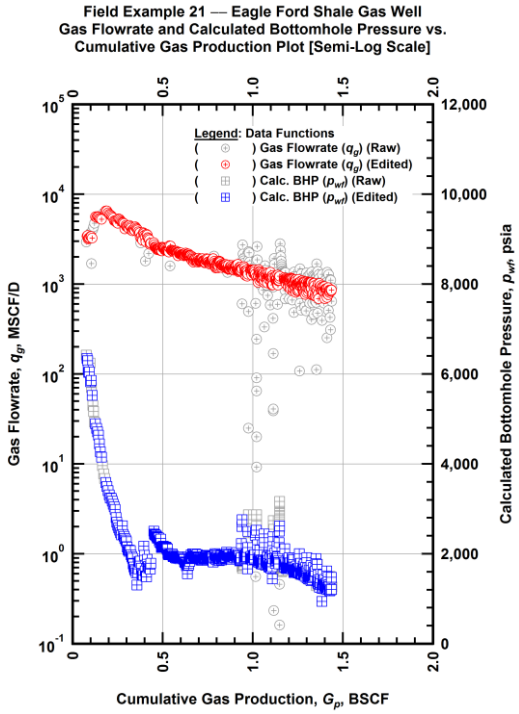

Figure A.606 — (Semi-log Plot): Filtered rate-pressure-cumulative production history plot — flowrate (q_g) and calculated bottomhole pressure (p_{wf}) versus cumulative production (G_p).

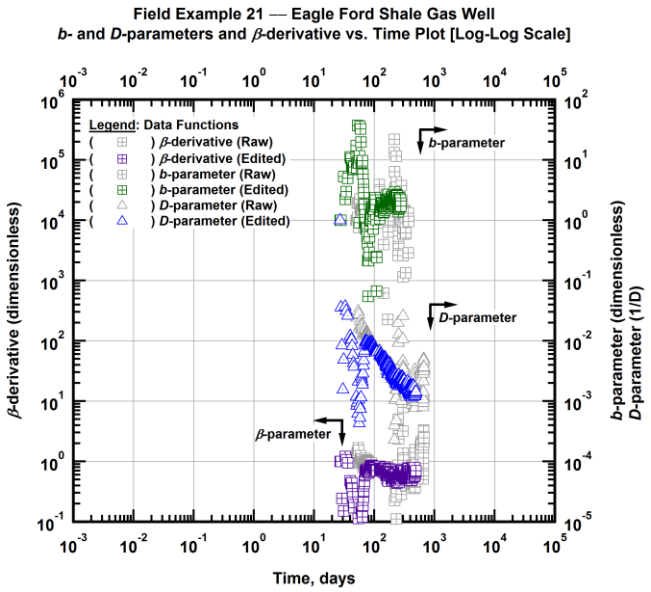

Figure A.607 — (Log-Log Plot): Filtered b, D and β production history plot — b- and D-parameters and β-derivative versus production time.

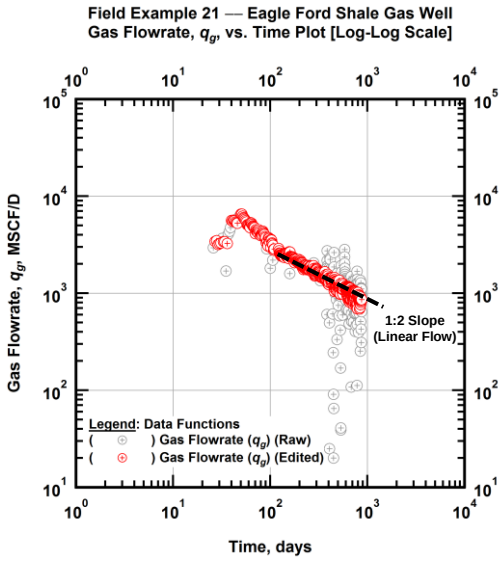

Figure A.608 — (Log-Log Plot): Filtered gas flowrate production history and flow regime identification plot — gas flowrate (q_g) versus production time.

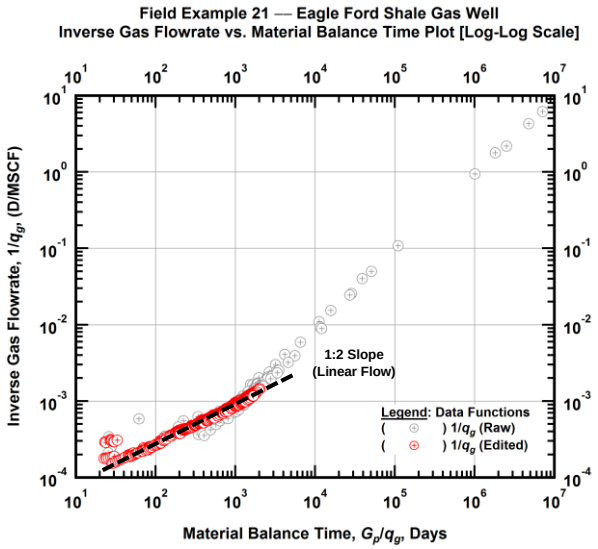

Figure A.609 — (Log-log Plot): Filtered inverse rate with material balance time plot — inverse gas flowrate ($1/q_g$) versus material balance time (G_p/q_g).

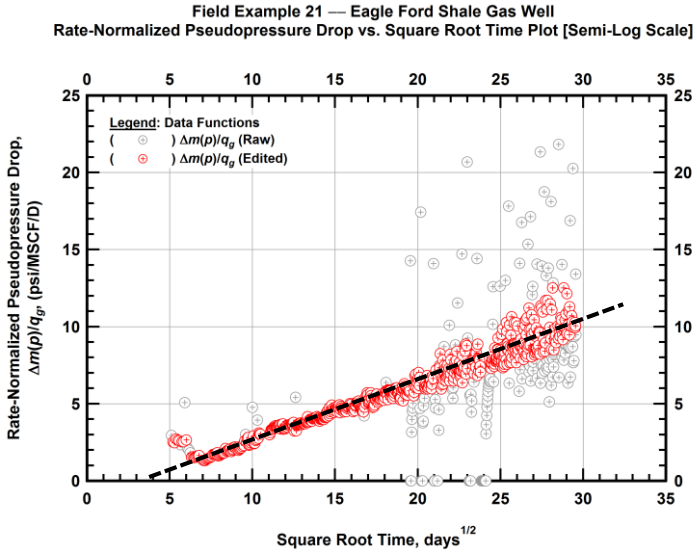

Figure A.610 — (Semi-log Plot): Filtered normalized pseudopressure drop production history plot — rate-normalized pseudopressure drop ($\Delta m(p)/q_g$) versus square root production time ($\sqrt{t}$).

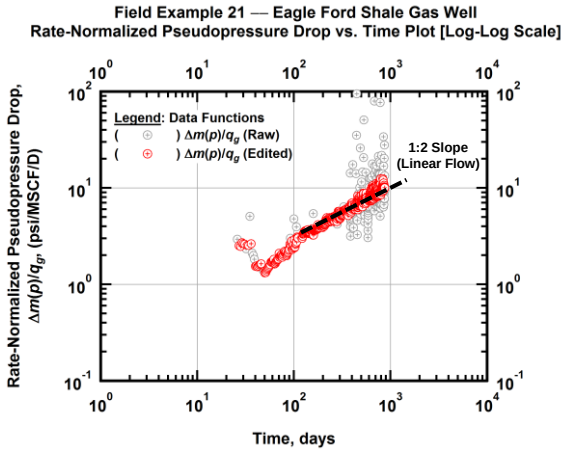

Figure A.611 — (Log-log Plot): Filtered normalized pseudopressure drop production history plot — rate-normalized pseudopressure drop ($\Delta m(p)/q_g$) versus production time.

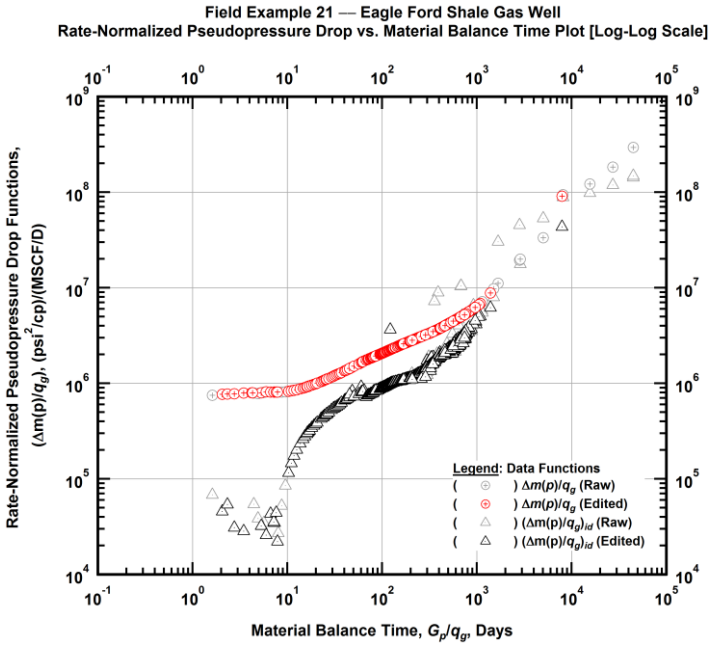

Figure A.612 — (Log-log Plot): "Log-log" diagnostic plot of the filtered production data — rate-normalized pseudopressure drop ($\Delta m(p)/q_g$) and rate-normalized pseudopressure drop integral-derivative $(\Delta m(p)/q_g)_{id}$ versus material balance time (G_p/q_g).

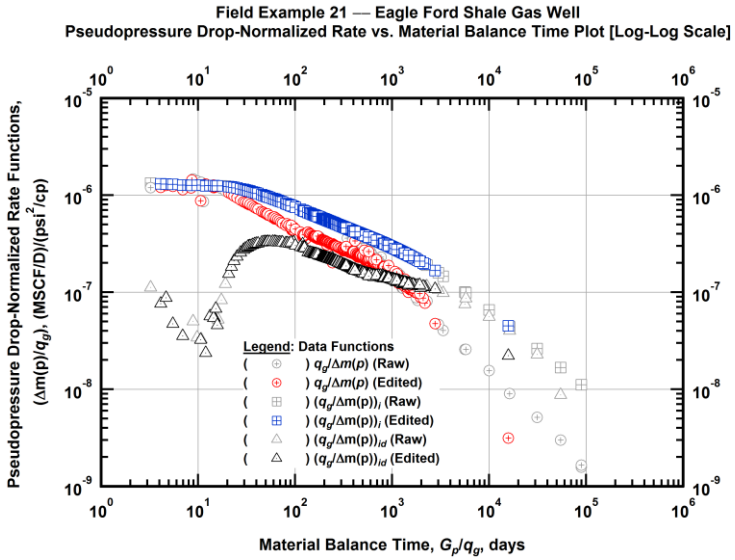

Figure A.613 — (Log-log Plot): "Blasingame" diagnostic plot of the filtered production data — pseudopressure drop-normalized gas flowrate ($q_g/\Delta m(p)$), pseudopressure drop-normalized gas flowrate integral $(q_g/\Delta m(p))_i$ and pseudopressure drop-normalized gas flowrate integral-derivative $(q_g/\Delta m(p))_{id}$ versus material balance time (G_p/q_g).

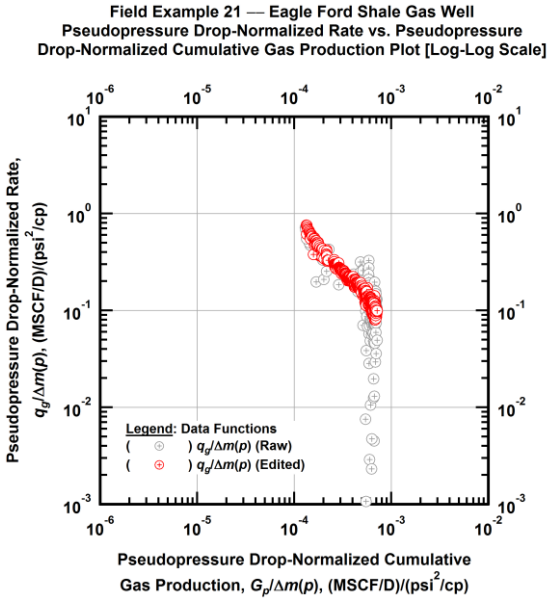

Figure A.614 — (Log-log Plot): Filtered normalized rate with normalized cumulative production plot — pseudopressure drop-normalized gas flowrate ($q_g/\Delta m(p)$) versus pseudopressure drop-normalized cumulative gas production ($G_p/\Delta m(p)$).

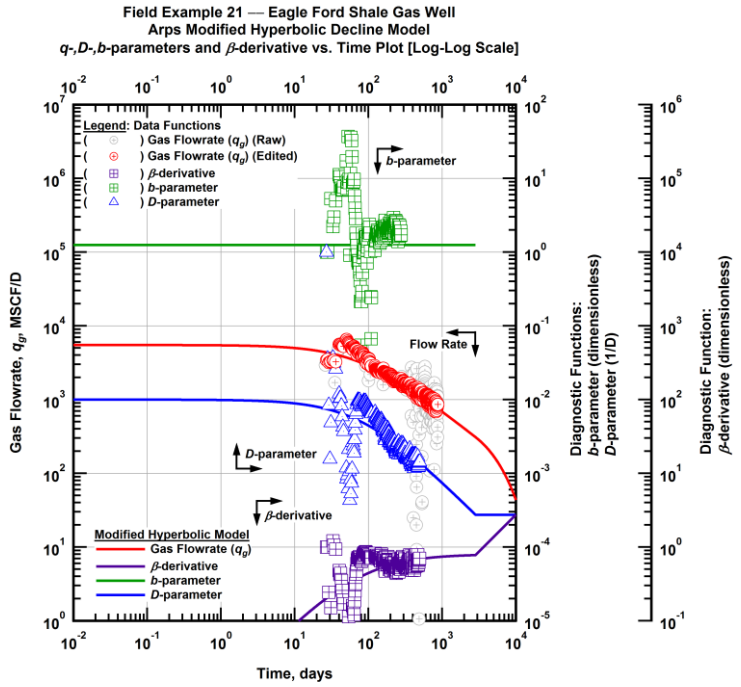

Figure A.615 — (Log-Log Plot): Arps modified hyperbolic decline model plot — time-rate model and data gas flowrate (q_g), *D*- and *b*-parameters and β-derivative versus production time.

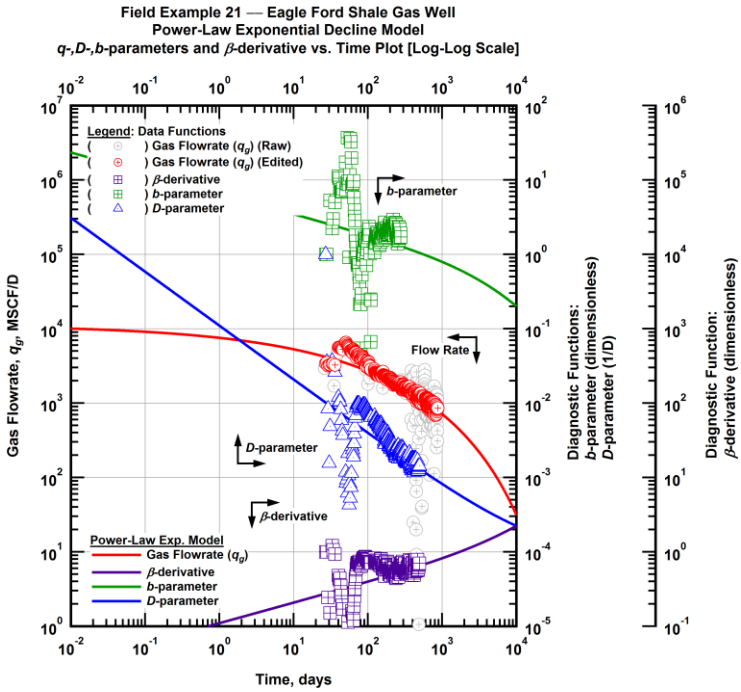

Figure A.616 — (Log-Log Plot): Power-law exponential decline model plot — time-rate model and data gas flowrate (q_g), *D*- and *b*-parameters and β-derivative versus production time.

Field Example 21 — Model-Based (Time-Rate-Pressure) Production Analysis

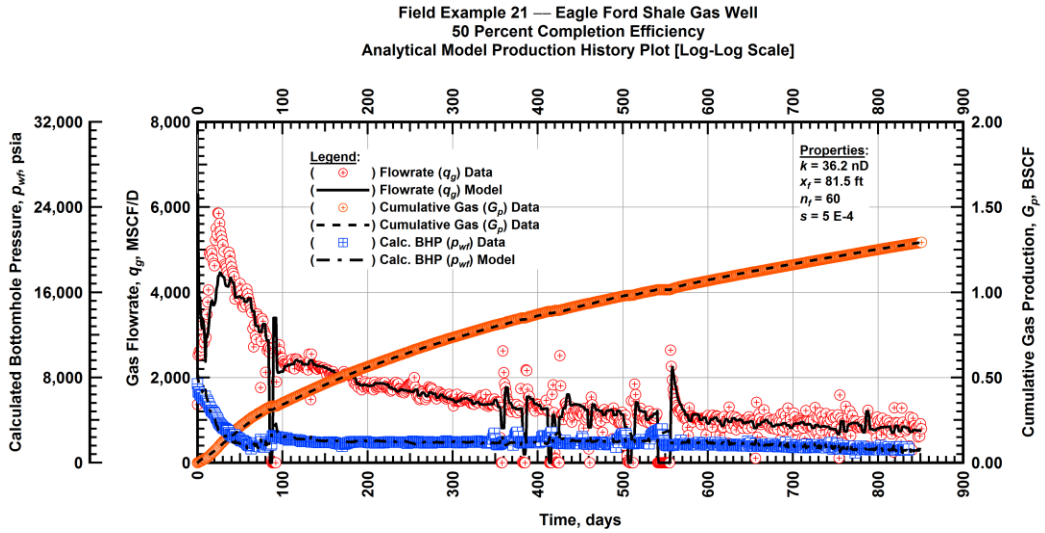

Figure A.617 — (Cartesian Plot): Production history plot — original gas flowrate (q_g), cumulative gas production (G_p), calculated bottomhole pressure (p_{wf}) and 50 percent completion efficiency model matches versus production time.

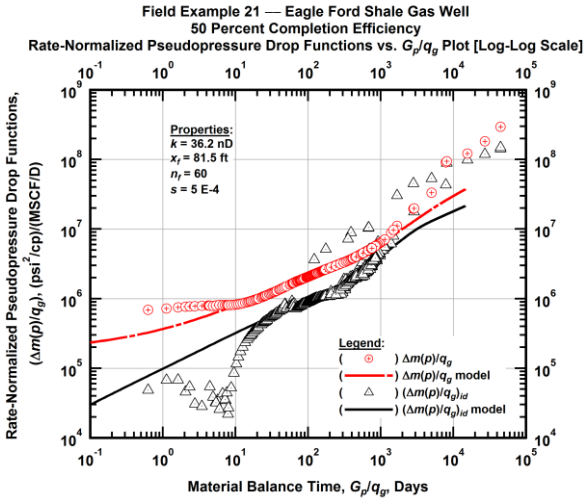

Figure A.618 — (Log-log Plot): "Log-log" diagnostic plot of the original production data — rate-normalized pseudopressure drop ($\Delta m(p)/q_g$), rate-normalized pseudopressure drop integral-derivative $(\Delta m(p)/q_g)_{id}$ and 50 percent completion efficiency model matches versus material balance time (G_p/q_g).

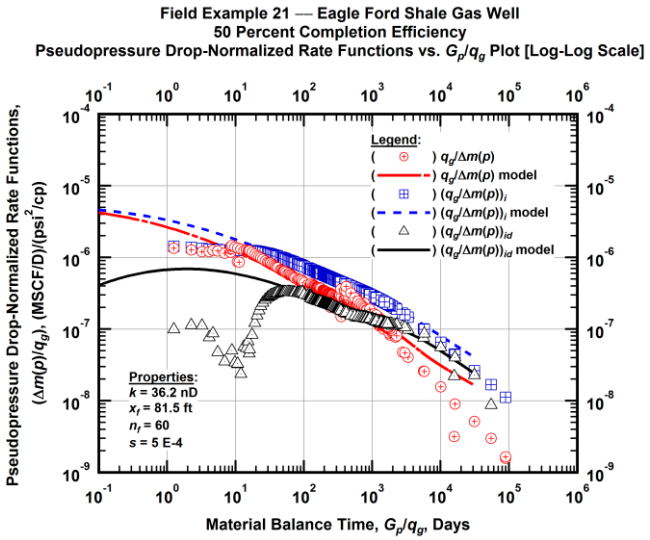

Figure A.619 — (Log-log Plot): "Blasingame" diagnostic plot of the original production data — pseudopressure drop-normalized gas flowrate ($q_g/\Delta m(p)$), pseudopressure drop-normalized gas flowrate integral $(q_g/\Delta m(p))_i$, pseudopressure drop-normalized gas flowrate integral-derivative $(q_g/\Delta m(p))_{id}$ and 50 percent completion efficiency model matches versus material balance time (G_p/q_g).

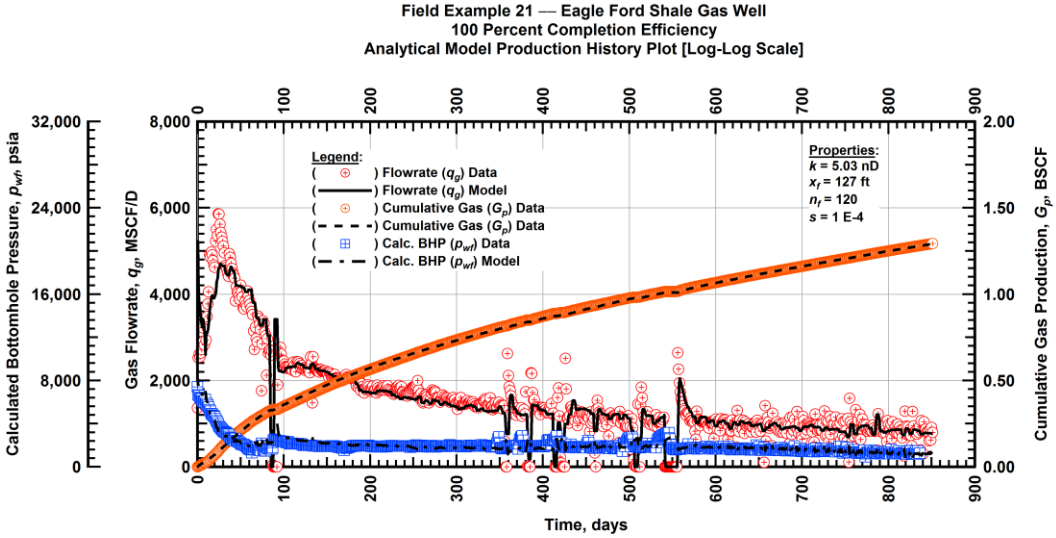

Figure A.620 — (Cartesian Plot): Production history plot — original gas flowrate (q_g), cumulative gas production (G_p), calculated bottomhole pressure (p_{wf}) and 100 percent completion efficiency model matches versus production time.

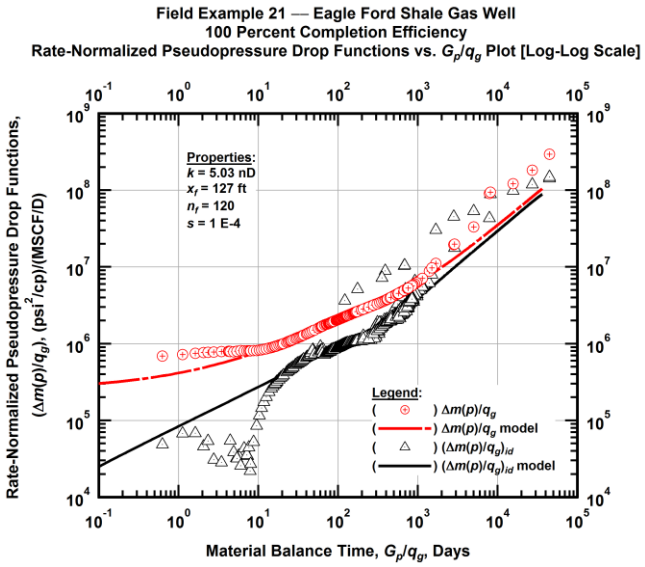

Figure A.621 — (Log-log Plot): "Log-log" diagnostic plot of the original production data — rate-normalized pseudopressure drop ($\Delta m(p)/q_g$), rate-normalized pseudopressure drop integral-derivative $(\Delta m(p)/q_g)_{id}$ and 100 percent completion efficiency model matches versus material balance time (G_p/q_g).

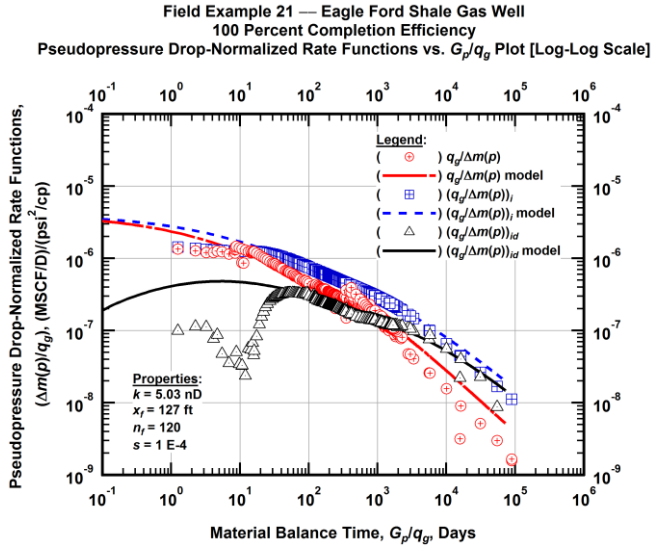

Figure A.622 — (Log-log Plot): "Blasingame" diagnostic plot of the original production data — pseudopressure drop-normalized gas flowrate ($q_g/\Delta m(p)$), pseudopressure drop-normalized gas flowrate integral $(q_g/\Delta m(p))_i$, pseudopressure drop-normalized gas flowrate integral-derivative $(q_g/\Delta m(p))_{id}$ and 100 percent completion efficiency model matches versus material balance time (G_p/q_g).

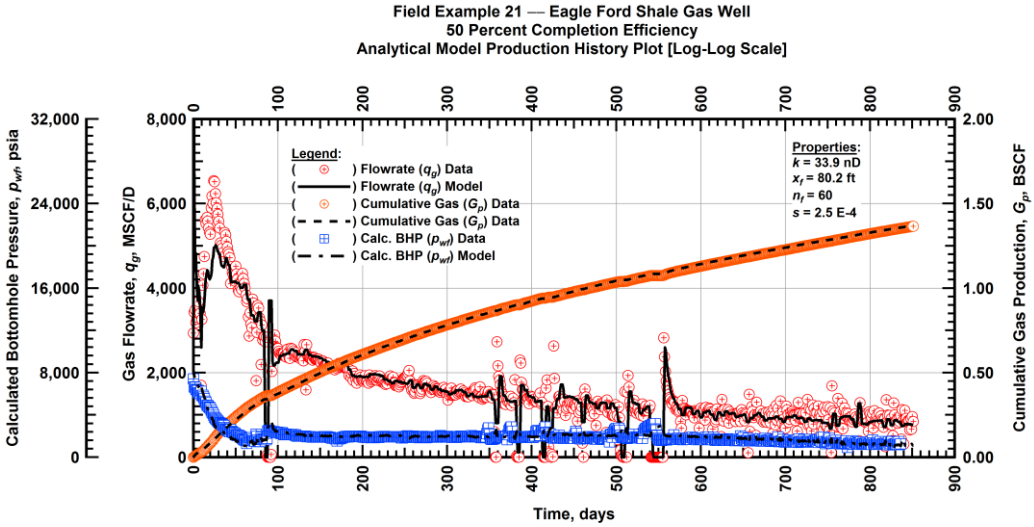

Figure A.623 — (Cartesian Plot): Production history plot — revised gas flowrate (q_g), cumulative gas production (G_p), calculated bottomhole pressure (p_{wf}) and 50 percent completion efficiency model matches versus production time.

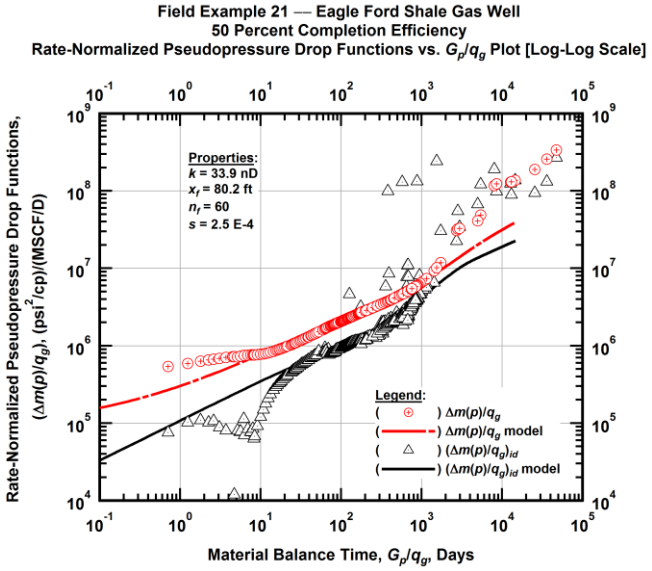

Figure A.624— (Log-log Plot): "Log-log" diagnostic plot of the revised production data — rate-normalized pseudopressure drop ($\Delta m(p)/q_g$), rate-normalized pseudopressure drop integral-derivative $(\Delta m(p)/q_g)_{id}$ and 50 percent completion efficiency model matches versus material balance time (G_p/q_g).

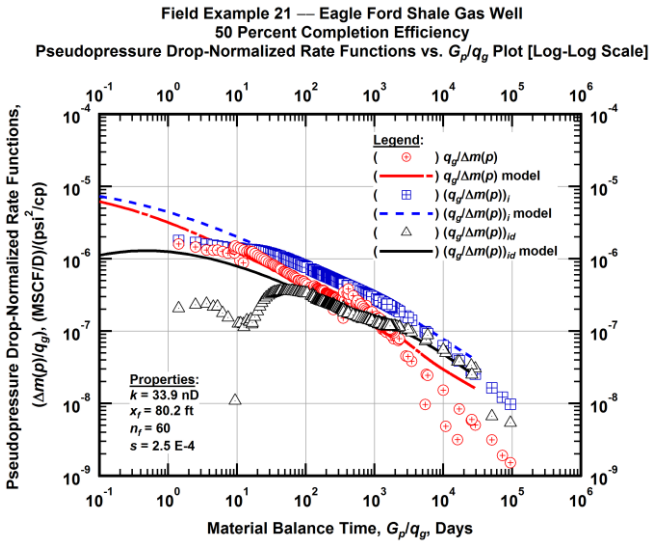

Figure A.625 — (Log-log Plot): "Blasingame" diagnostic plot of the revised production data — pseudopressure drop-normalized gas flowrate ($q_g/\Delta m(p)$), pseudopressure drop-normalized gas flowrate integral $(q_g/\Delta m(p))_i$, pseudopressure drop-normalized gas flowrate integral-derivative $(q_g/\Delta m(p))_{id}$ and 50 percent completion efficiency model matches versus material balance time (G_p/q_g).

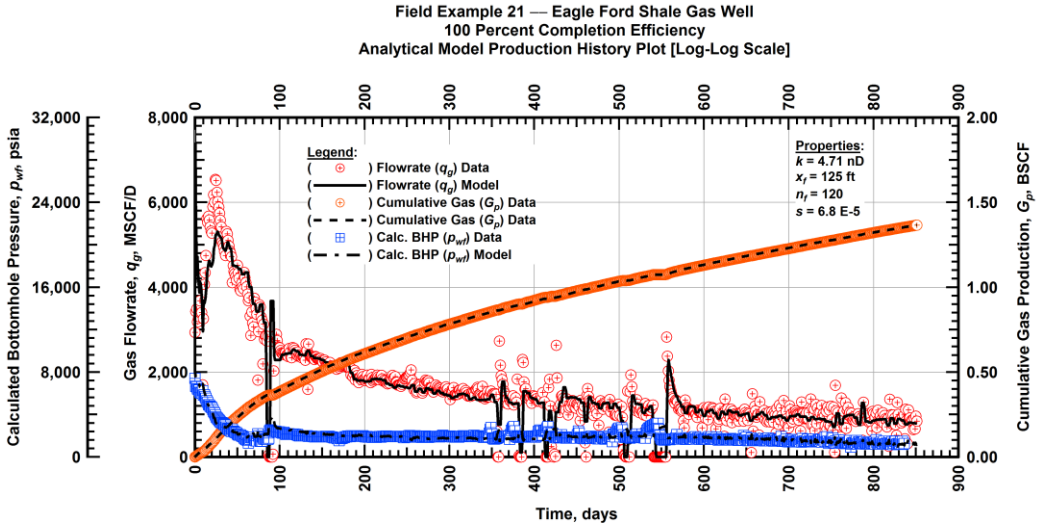

Figure A.626 — (Cartesian Plot): Production history plot — revised gas flowrate (q_g), cumulative gas production (G_p), calculated bottomhole pressure (p_{wf}) and 100 percent completion efficiency model matches versus production time.

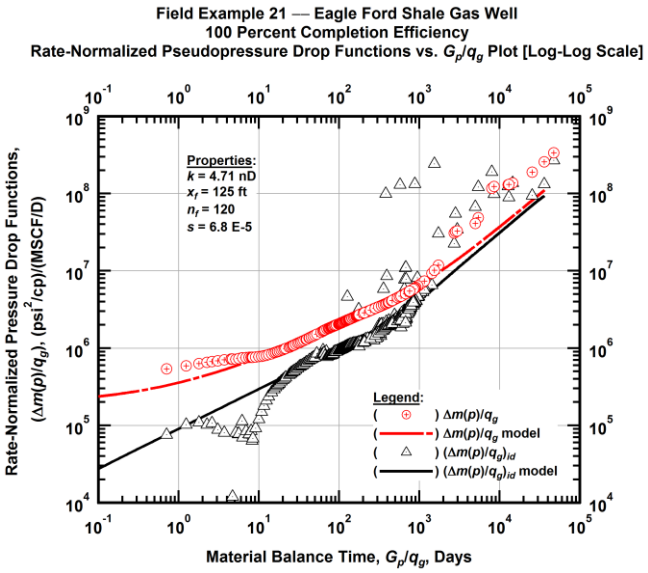

Figure A.627 — (Log-log Plot): "Log-log" diagnostic plot of the revised production data — rate-normalized pseudopressure drop ($\Delta m(p)/q_g$), rate-normalized pseudopressure drop integral-derivative $(\Delta m(p)/q_g)_{id}$ and 100 percent completion efficiency model matches versus material balance time (G_p/q_g).

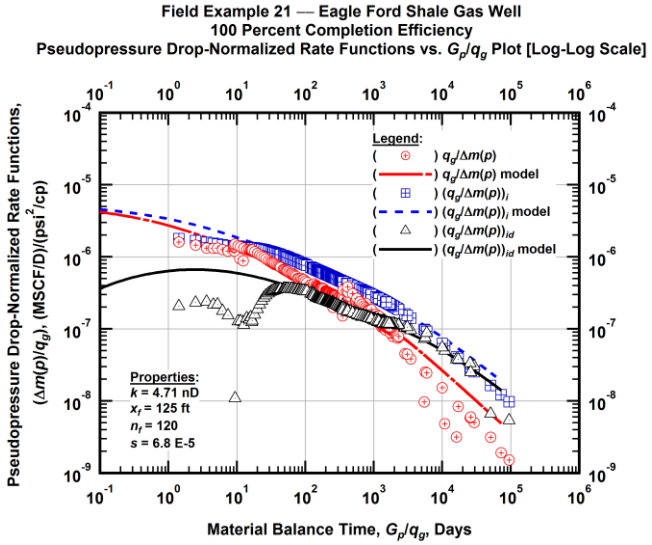

Figure A.628 — (Log-log Plot): "Blasingame" diagnostic plot of the revised production data — pseudopressure drop-normalized gas flowrate ($q_g/\Delta m(p)$), pseudopressure drop-normalized gas flowrate integral $(q_g/\Delta m(p))_i$, pseudopressure drop-normalized gas flowrate integral-derivative $(q_g/\Delta m(p))_{id}$ and 100 percent completion efficiency model matches versus material balance time (G_p/q_g).

Field Example 21 — 30-Year EUR Model Comparison

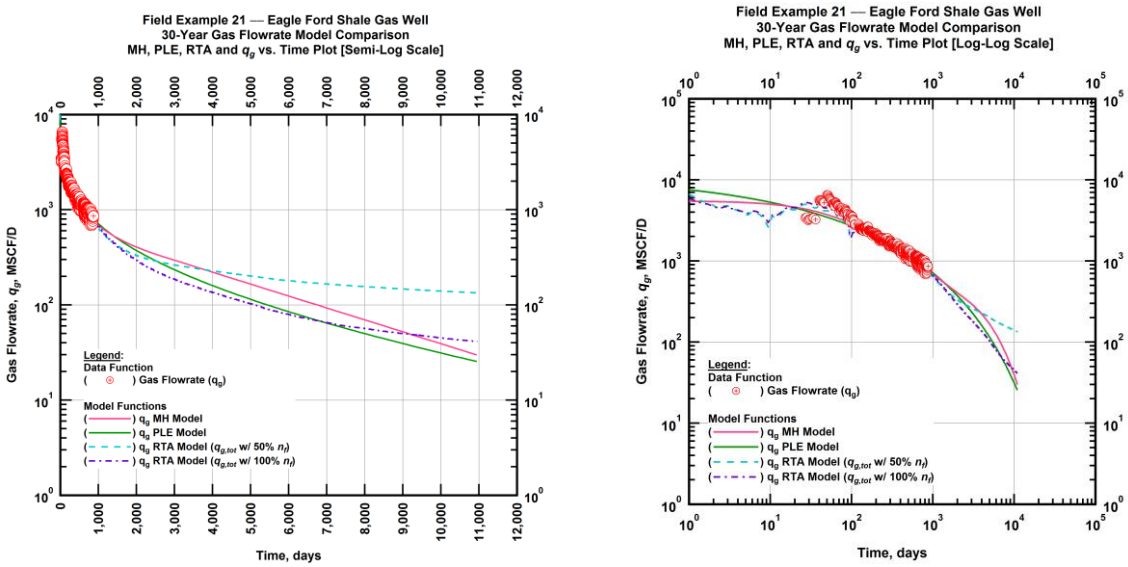

A **B**

Figure A.629 — (A — Semi-Log Plot) and (B — Log-Log Plot): Estimated 30-year revised gas flowrate model comparison — Arps modified hyperbolic decline model, power-law exponential decline model, and 50 percent and 100 percent completion efficiency RTA models revised gas 30-year estimated flowrate decline and historic gas flowrate data (q_g) versus production time.

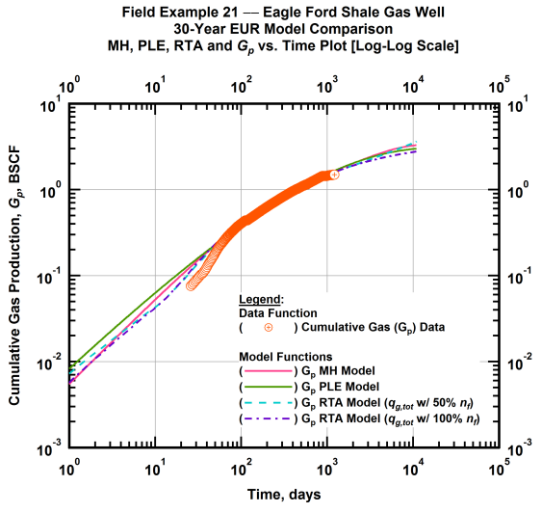

Figure A.630 — (Log-log Plot): PVT revised gas 30-year estimated cumulative production volume model comparison — Arps modified hyperbolic decline model, power-law exponential decline model, and 50 percent and 100 percent completion efficiency RTA model estimated 30-year cumulative gas production volumes and historic cumulative gas production (G_p) versus production time.

Table A.21 — 30-year estimated cumulative revised gas production (EUR), in units of BSCF, for the Arps modified hyperbolic, power-law exponential and analytical time-rate-pressure decline models.

Arps Modified Hyperbolic BSCF)	Power-Law Exponential (BSCF)	RTA Analytical Model ($q_{g,tot}$ w/ 50% n_f) (BSCF)	RTA Analytical Model ($q_{g,tot}$ w/ 100% n_f) (BSCF)
3.20	2.85	3.72	2.81

Field Example 22 — Time-Rate Analysis

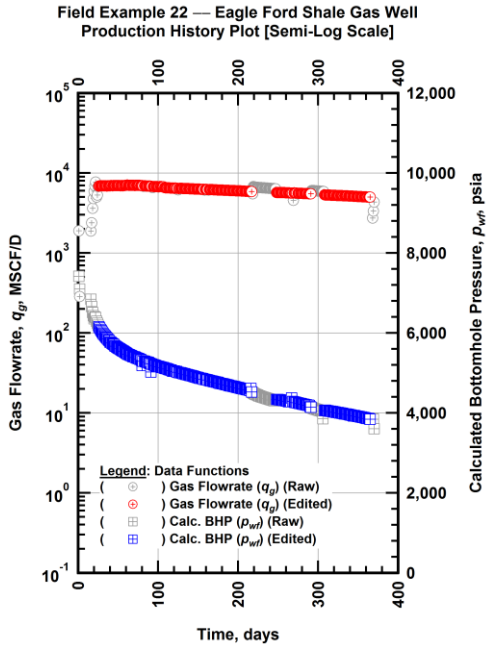

Figure A.631 — (Semi-log Plot): Filtered production history plot — flowrate (q_g) and calculated bottomhole pressure (p_{wf}) versus production time.

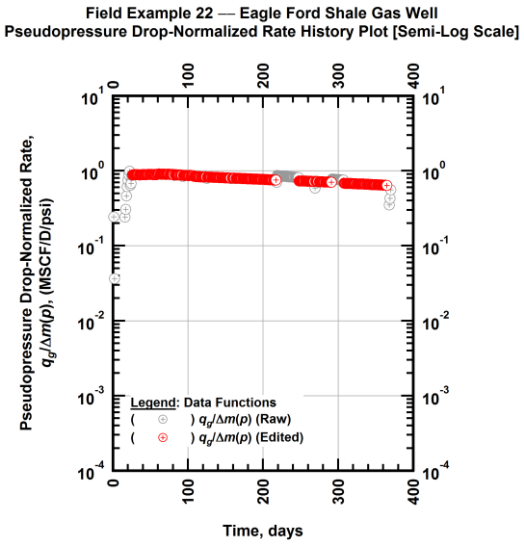

Figure A.632 — (Semi-log Plot): Filtered normalized rate production history plot — pseudopressure drop-normalized gas flowrate ($q_g/\Delta m(p)$) versus production time.

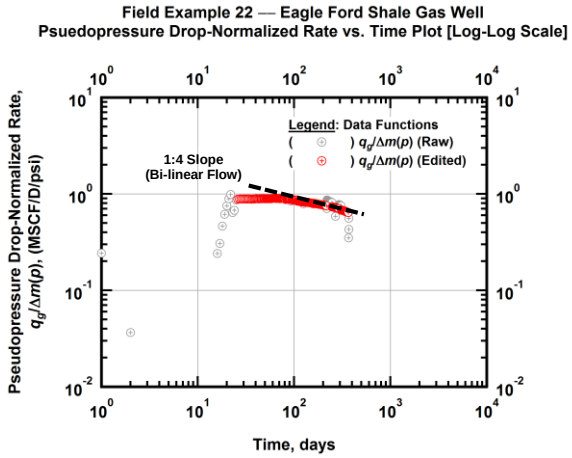

Figure A.633 — (Log-log Plot): Filtered normalized rate production history plot — pseudopressure drop-normalized gas flowrate ($q_g/\Delta m(p)$) versus production time.

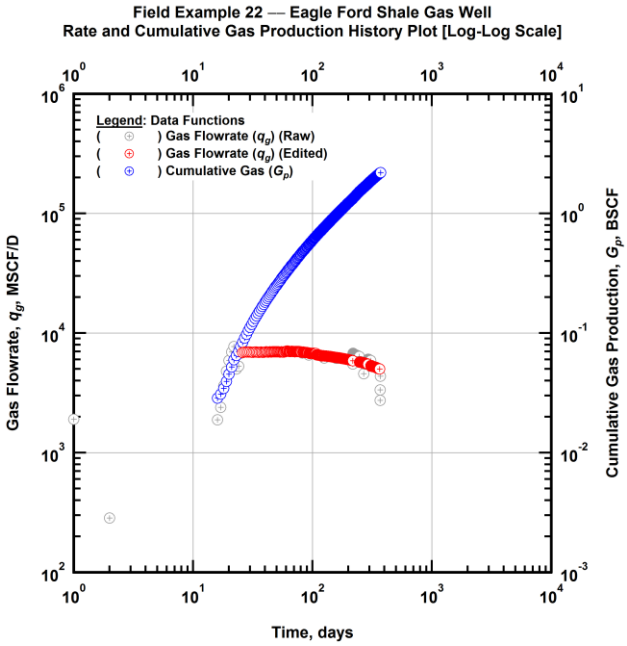

Figure A.634 — (Log-log Plot): Filtered rate and unfiltered cumulative gas production history plot — flowrate (q_g) and cumulative production (G_p) versus production time.

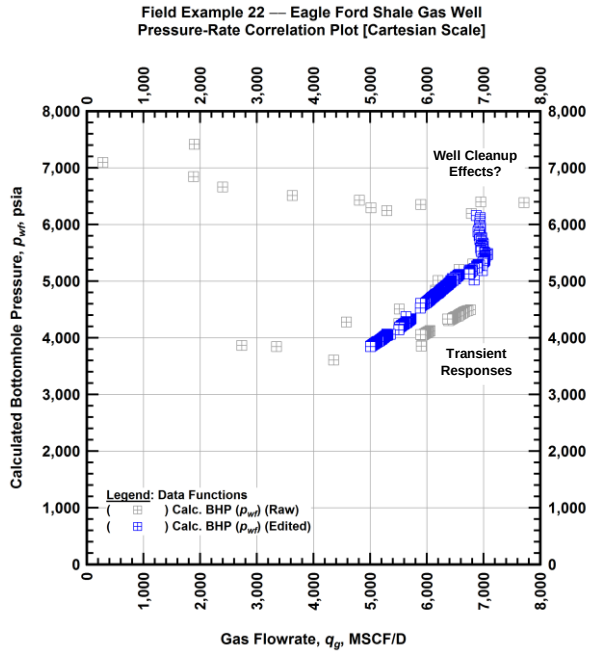

Figure A.635 — (Cartesian Plot): Filtered rate-pressure correlation plot — calculated bottomhole pressure (p_{wf}) versus flowrate (q_g).

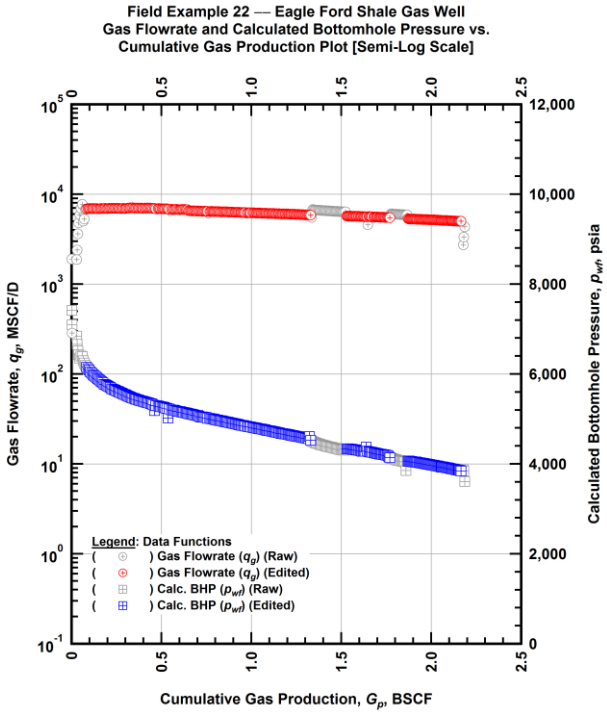

Figure A.636 — (Semi-log Plot): Filtered rate-pressure-cumulative production history plot — flowrate (q_g) and calculated bottomhole pressure (p_{wf}) versus cumulative production (G_p).

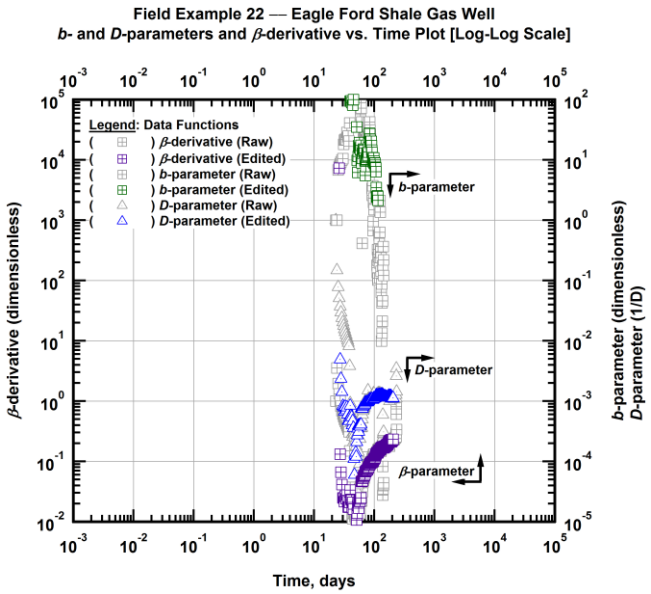

Figure A.637 — (Log-Log Plot): Filtered b, D and β production history plot — b- and D-parameters and β-derivative versus production time.

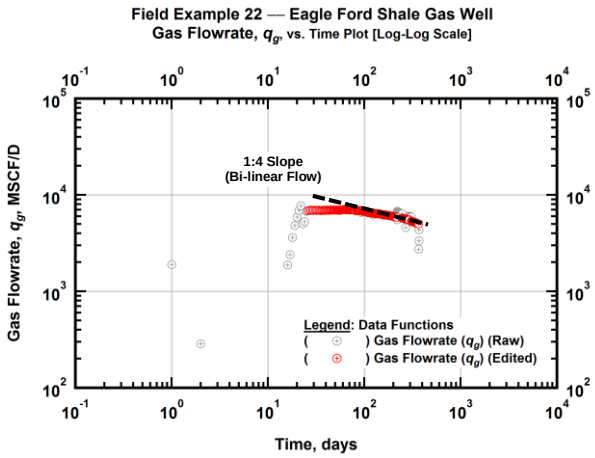

Figure A.638 — (Log-Log Plot): Filtered gas flowrate production history and flow regime identification plot — gas flowrate (q_g) versus production time.

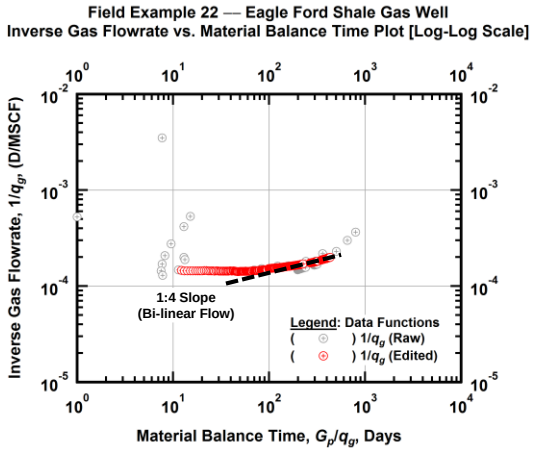

Figure A.639 — (Log-log Plot): Filtered inverse rate with material balance time plot — inverse gas flowrate ($1/q_g$) versus material balance time (G_p/q_g).

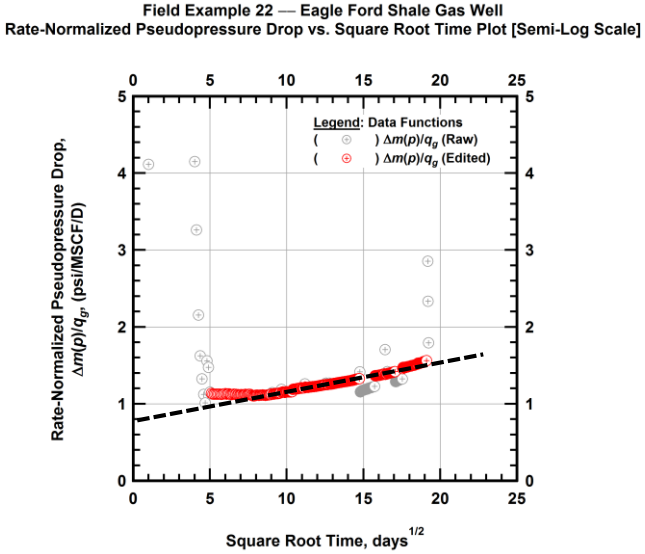

Figure A.640 — (Semi-log Plot): Filtered normalized pseudopressure drop production history plot — rate-normalized pseudopressure drop ($\Delta m(p)/q_g$) versus square root production time ($\sqrt{t}$).

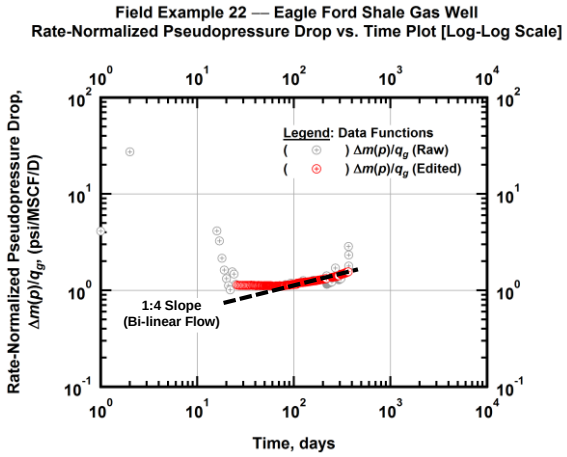

Figure A.641 — (Log-log Plot): Filtered normalized pseudopressure drop production history plot — rate-normalized pseudopressure drop ($\Delta m(p)/q_g$) versus production time.

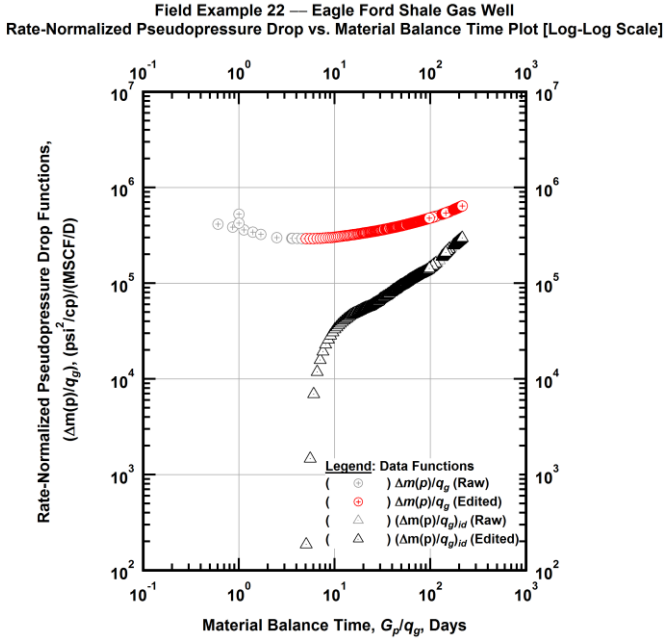

Figure A.642 — (Log-log Plot): "Log-log" diagnostic plot of the filtered production data — rate-normalized pseudopressure drop ($\Delta m(p)/q_g$) and rate-normalized pseudopressure drop integral-derivative $(\Delta m(p)/q_g)_{id}$ versus material balance time (G_p/q_g).

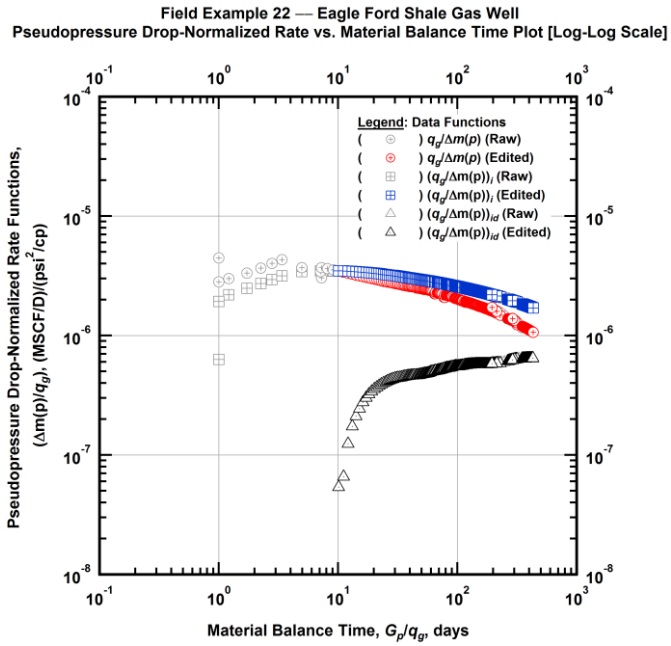

Figure A.643 — (Log-log Plot): "Blasingame" diagnostic plot of the filtered production data — pseudopressure drop-normalized gas flowrate ($q_g/\Delta m(p)$), pseudopressure drop-normalized gas flowrate integral $(q_g/\Delta m(p))_i$ and pseudopressure drop-normalized gas flowrate integral-derivative $(q_g/\Delta m(p))_{id}$ versus material balance time (G_p/q_g).

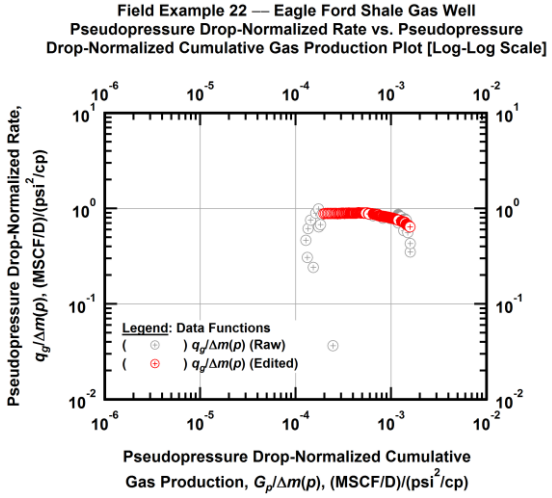

Figure A.644 — (Log-log Plot): Filtered normalized rate with normalized cumulative production plot — pseudopressure drop-normalized gas flowrate ($q_g/\Delta m(p)$) versus pseudopressure drop-normalized cumulative gas production ($G_p/\Delta m(p)$).

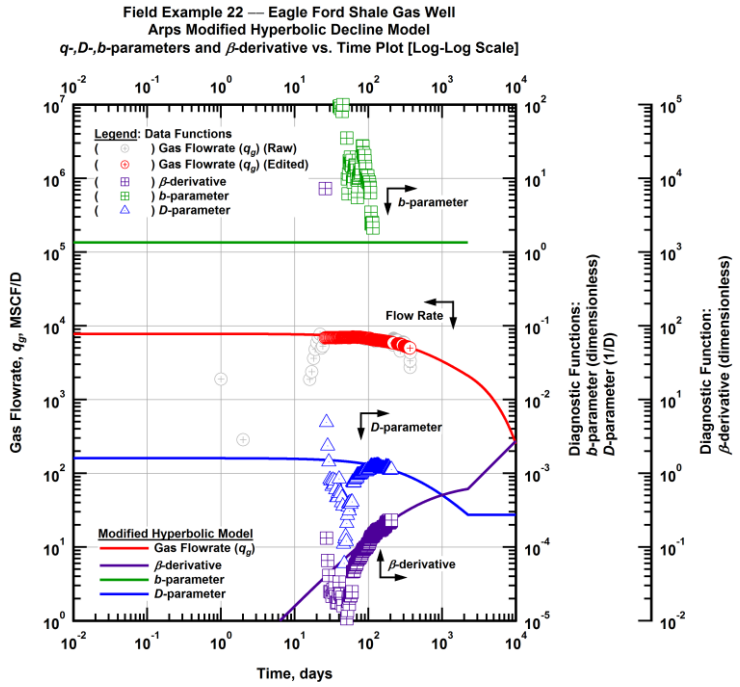

Figure A.645 — (Log-Log Plot): Arps modified hyperbolic decline model plot — time-rate model and data gas flowrate (q_g), *D*- and *b*-parameters and β-derivative versus production time.

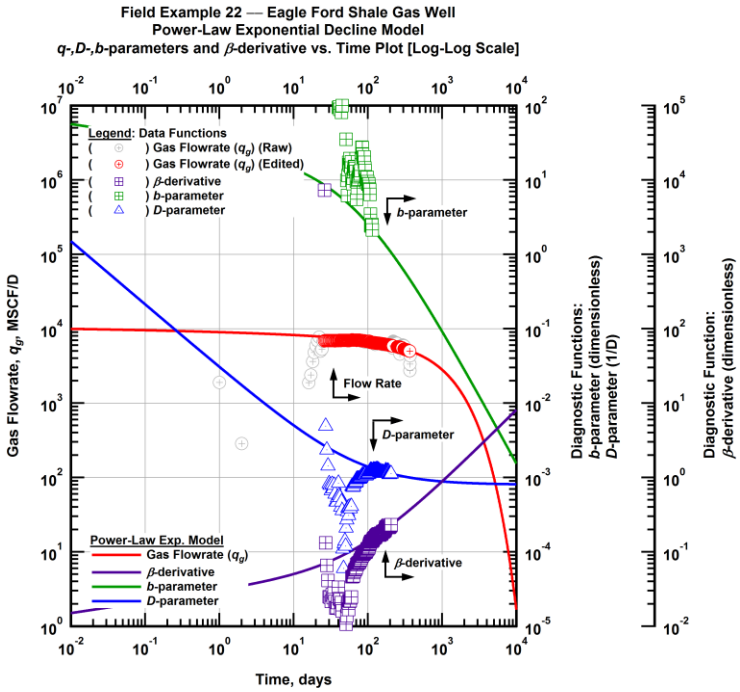

Figure A.646 — (Log-Log Plot): Power-law exponential decline model plot — time-rate model and data gas flowrate (q_g), *D*- and *b*-parameters and β-derivative versus production time.

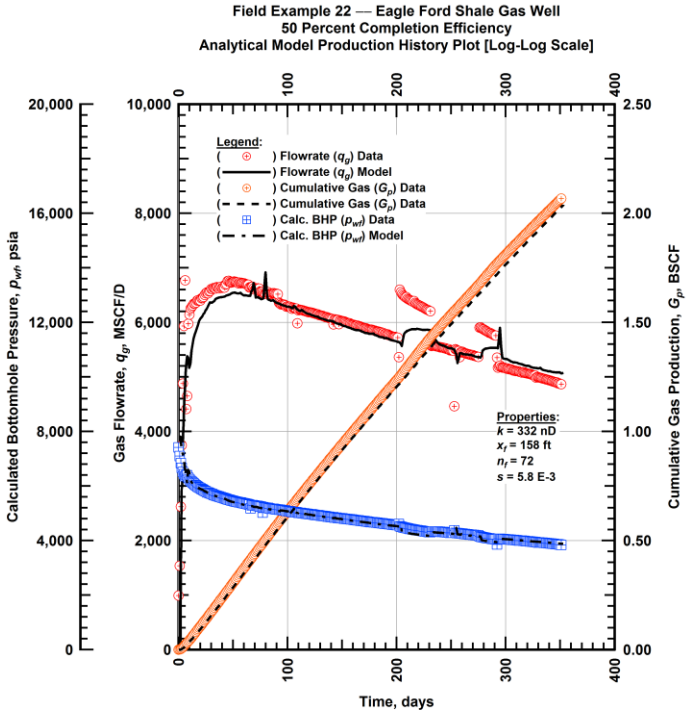

Figure A.647 — (Cartesian Plot): Production history plot — original gas flowrate (q_g), cumulative gas production (G_p), calculated bottomhole pressure (p_{wf}) and 50 percent completion efficiency model matches versus production time.

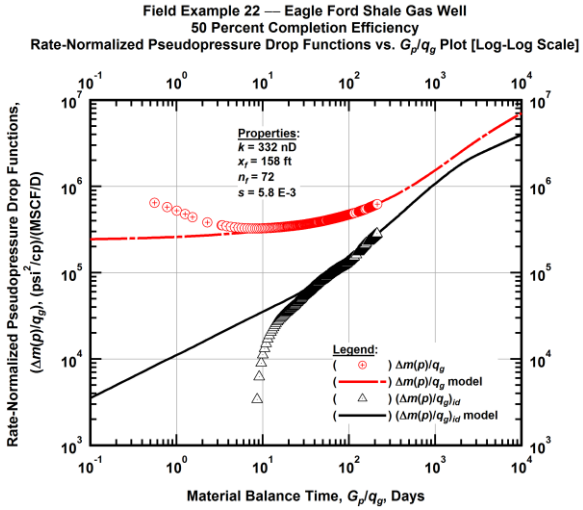

Figure A.648 — (Log-log Plot): "Log-log" diagnostic plot of the original production data — rate-normalized pseudopressure drop ($\Delta m(p)/q_g$), rate-normalized pseudopressure drop integral-derivative $(\Delta m(p)/q_g)_{id}$ and 50 percent completion efficiency model matches versus material balance time (G_p/q_g).

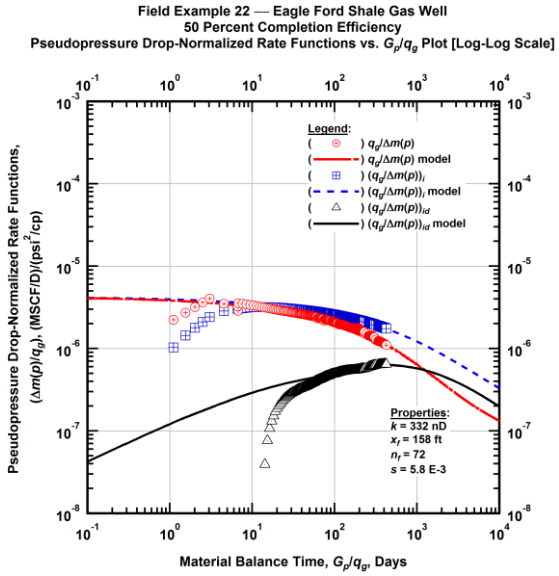

Figure A.649 — (Log-log Plot): "Blasingame" diagnostic plot of the original production data — pseudopressure drop-normalized gas flowrate ($q_g/\Delta m(p)$), pseudopressure drop-normalized gas flowrate integral ($q_g/\Delta m(p))_i$, pseudopressure drop-normalized gas flowrate integral-derivative ($q_g/\Delta m(p))_{id}$ and 50 percent completion efficiency model matches versus material balance time (G_p/q_g).

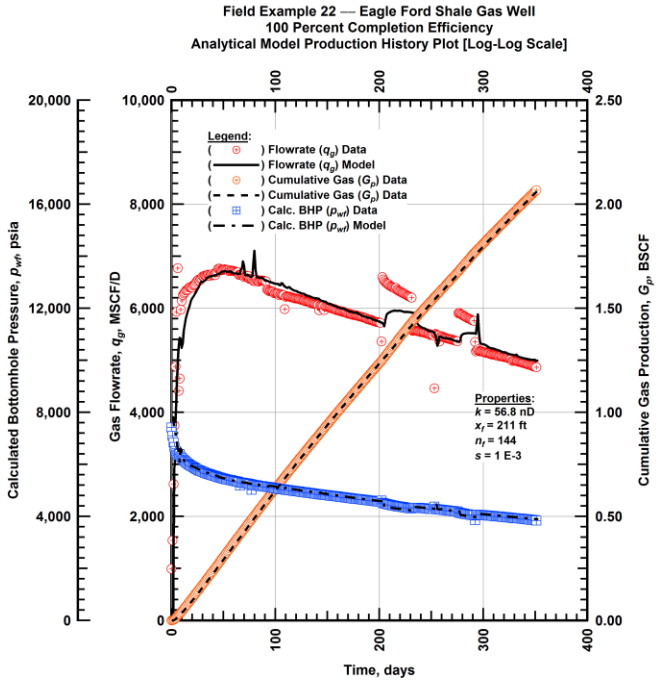

Figure A.650 — (Cartesian Plot): Production history plot — original gas flowrate (q_g), cumulative gas production (G_p), calculated bottomhole pressure (p_{wf}) and 100 percent completion efficiency model matches versus production time.

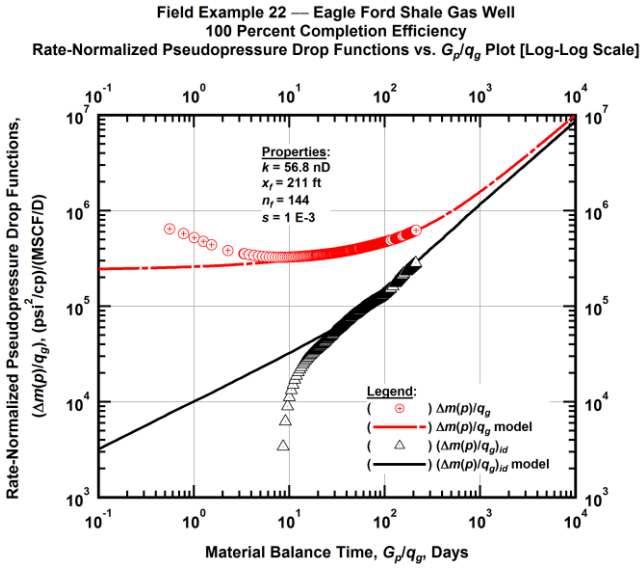

Figure A.651 — (Log-log Plot): "Log-log" diagnostic plot of the original production data — rate-normalized pseudopressure drop ($\Delta m(p)/q_g$), rate-normalized pseudopressure drop integral-derivative $(\Delta m(p)/q_g)_{id}$ and 100 percent completion efficiency model matches versus material balance time (G_p/q_g).

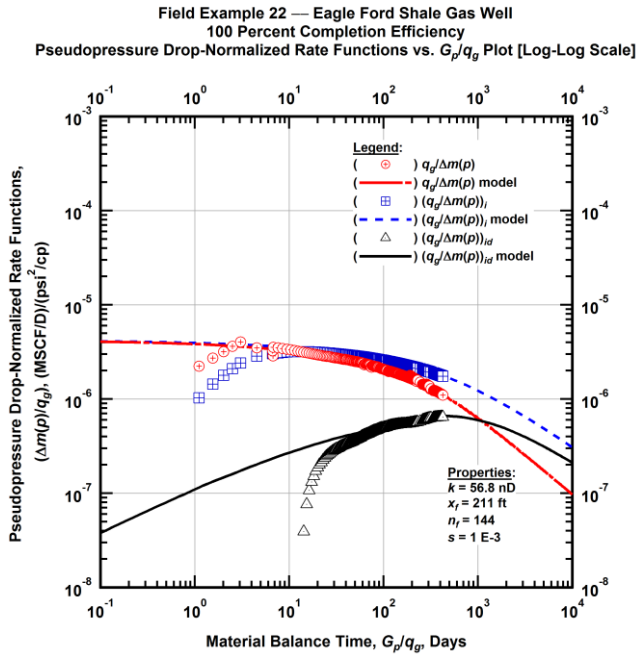

Figure A.652 — (Log-log Plot): "Blasingame" diagnostic plot of the original production data — pseudopressure drop-normalized gas flowrate ($q_g/\Delta m(p)$), pseudopressure drop-normalized gas flowrate integral $(q_g/\Delta m(p))_i$, pseudopressure drop-normalized gas flowrate integral-derivative $(q_g/\Delta m(p))_{id}$ and 100 percent completion efficiency model matches versus material balance time (G_p/q_g).

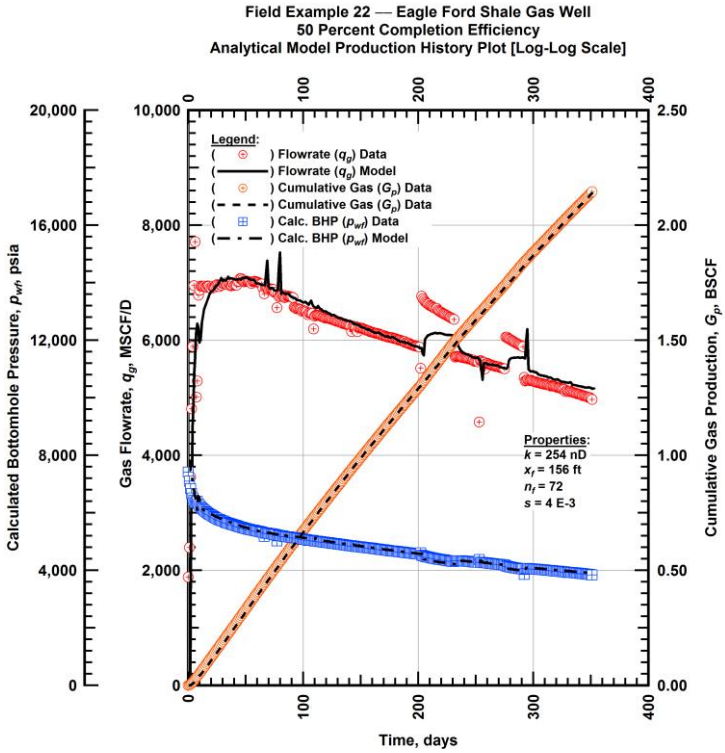

Figure A.653 — (Cartesian Plot): Production history plot — revised gas flowrate (q_g), cumulative gas production (G_p), calculated bottomhole pressure (p_{wf}) and 50 percent completion efficiency model matches versus production time.

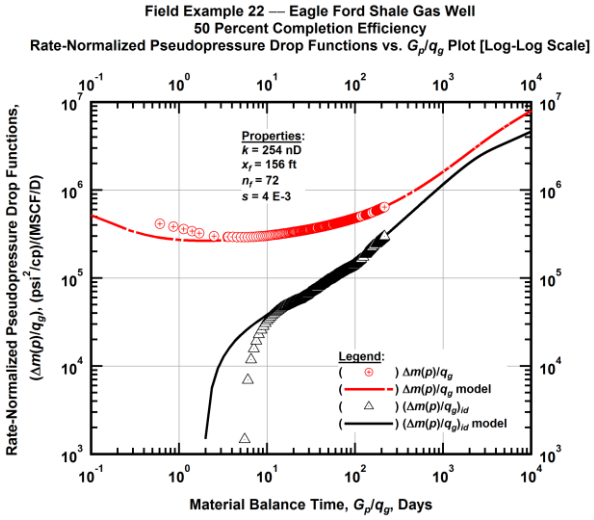

Figure A.654— (Log-log Plot): "Log-log" diagnostic plot of the revised production data — rate-normalized pseudopressure drop ($\Delta m(p)/q_g$), rate-normalized pseudopressure drop integral-derivative $(\Delta m(p)/q_g)_{id}$ and 50 percent completion efficiency model matches versus material balance time (G_p/q_g).

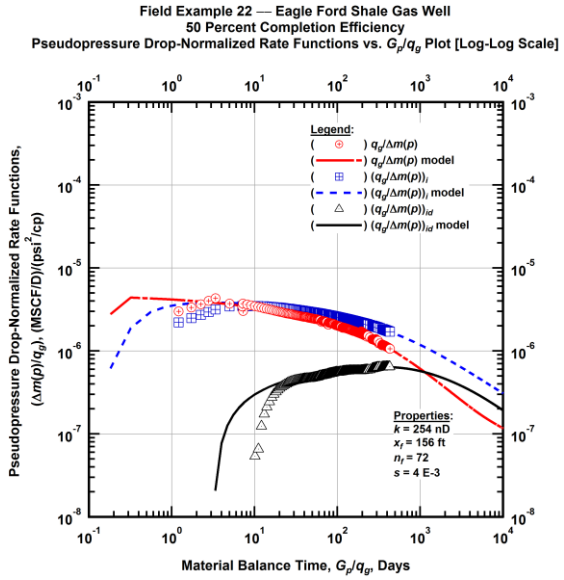

Figure A.655 — (Log-log Plot): "Blasingame" diagnostic plot of the revised production data — pseudopressure drop-normalized gas flowrate ($q_g/\Delta m(p)$), pseudopressure drop-normalized gas flowrate integral $(q_g/\Delta m(p))_i$, pseudopressure drop-normalized gas flowrate integral-derivative $(q_g/\Delta m(p))_{id}$ and 50 percent completion efficiency model matches versus material balance time (G_p/q_g).

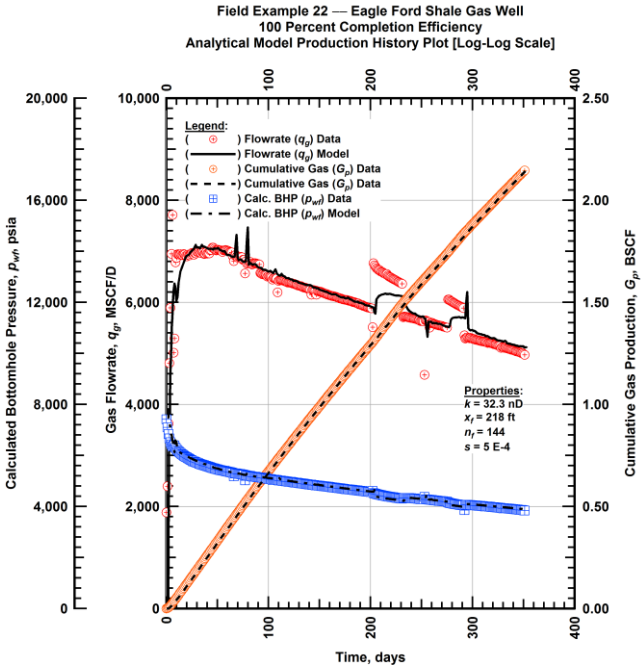

Figure A.656 — (Cartesian Plot): Production history plot — revised gas flowrate (q_g), cumulative gas production (G_p), calculated bottomhole pressure (p_{wf}) and 100 percent completion efficiency model matches versus production time.

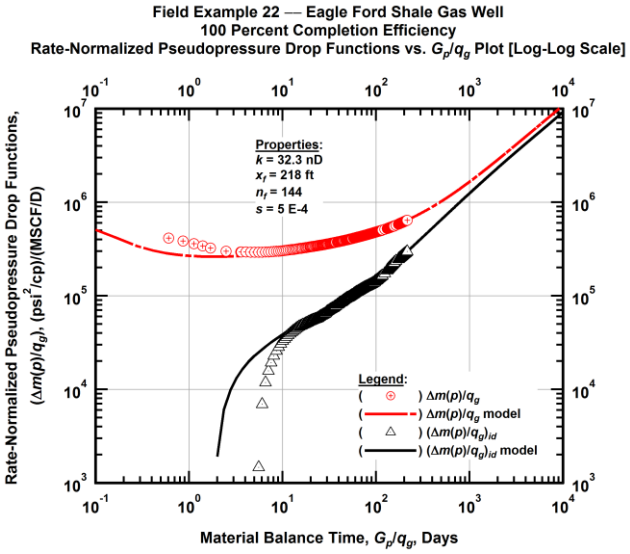

Figure A.657 — (Log-log Plot): "Log-log" diagnostic plot of the revised production data — rate-normalized pseudopressure drop ($\Delta m(p)/q_g$), rate-normalized pseudopressure drop integral-derivative $(\Delta m(p)/q_g)_{id}$ and 100 percent completion efficiency model matches versus material balance time (G_p/q_g).

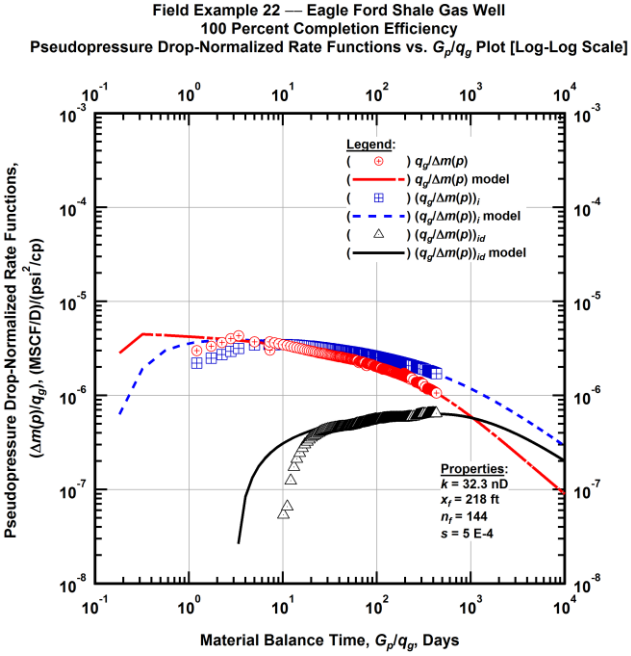

Figure A.658 — (Log-log Plot): "Blasingame" diagnostic plot of the revised production data — pseudopressure drop-normalized gas flowrate ($q_g/\Delta m(p)$), pseudopressure drop-normalized gas flowrate integral $(q_g/\Delta m(p))_i$, pseudopressure drop-normalized gas flowrate integral-derivative $(q_g/\Delta m(p))_{id}$ and 100 percent completion efficiency model matches versus material balance time (G_p/q_g).

Field Example 22 — 30-Year EUR Model Comparison

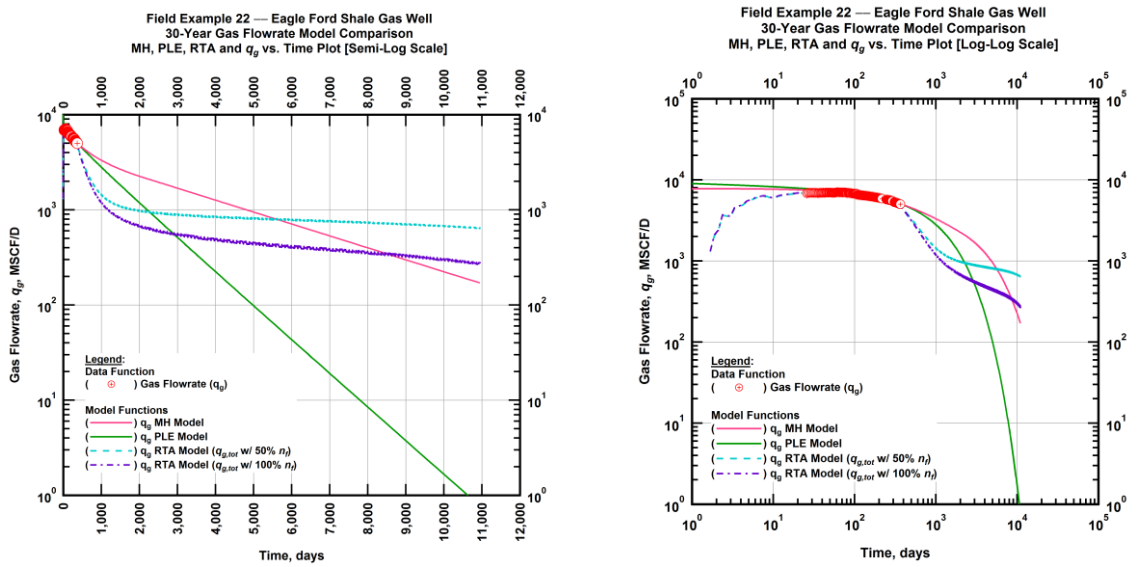

A **B**

Figure A.659 — (A — Semi-Log Plot) and (B — Log-Log Plot): Estimated 30-year revised gas flowrate model comparison — Arps modified hyperbolic decline model, power-law exponential decline model, and 50 percent and 100 percent completion efficiency RTA models revised gas 30-year estimated flowrate decline and historic gas flowrate data (q_g) versus production time.

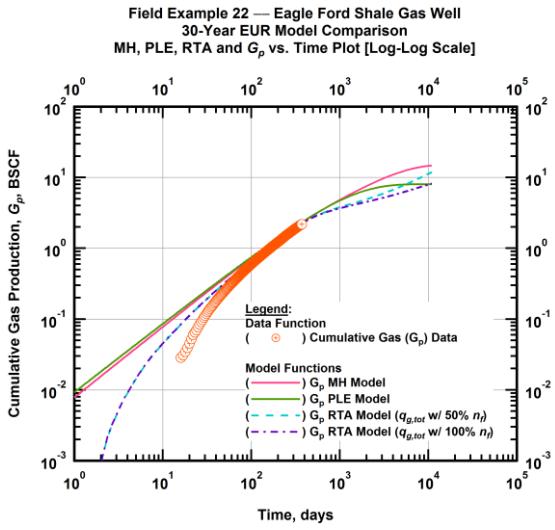

Figure A.660 — (Log-log Plot): PVT revised gas 30-year estimated cumulative production volume model comparison — Arps modified hyperbolic decline model, power-law exponential decline model, and 50 percent and 100 percent completion efficiency RTA model estimated 30-year cumulative gas production volumes and historic cumulative gas production (G_p) versus production time.

Table A.22 — 30-year estimated cumulative revised gas production (EUR), in units of BSCF, for the Arps modified hyperbolic, power-law exponential and analytical time-rate-pressure decline models.

Arps Modified Hyperbolic (BSCF)	Power-Law Exponential (BSCF)	RTA Analytical Model ($q_{g,tot}$ w/ 50% n_f) (BSCF)	RTA Analytical Model ($q_{g,tot}$ w/ 100% n_f) (BSCF)
14.96	7.85	12.10	8.30

Field Example 23 — Time-Rate Analysis

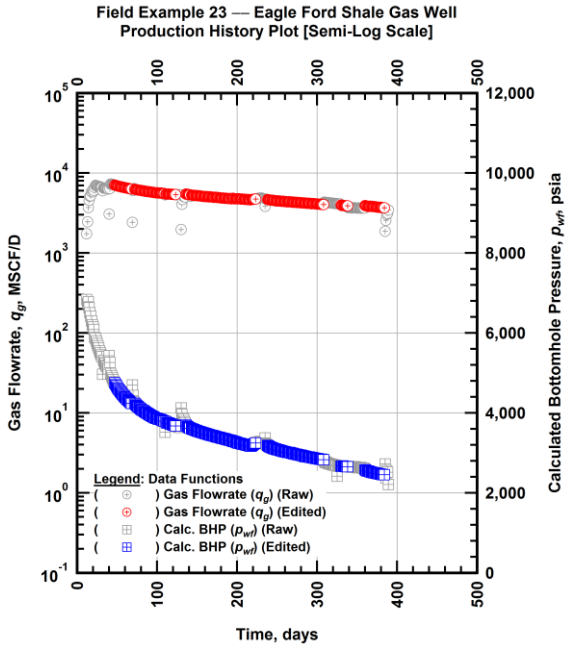

Figure A.661 — (Semi-log Plot): Filtered production history plot — flowrate (q_g) and calculated bottomhole pressure (p_{wf}) versus production time.

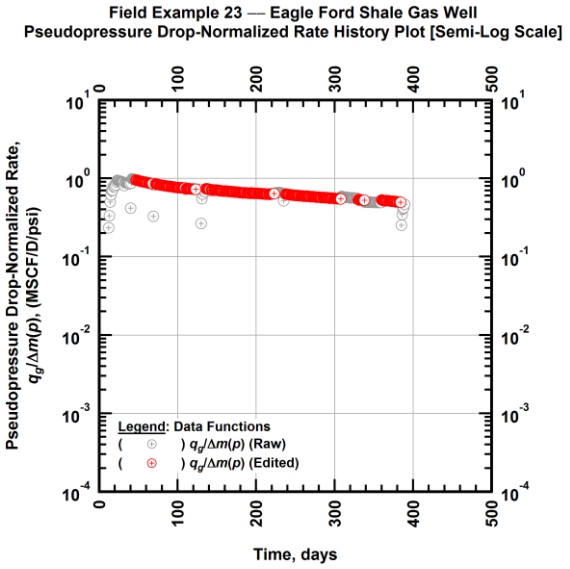

Figure A.662 — (Semi-log Plot): Filtered normalized rate production history plot — pseudopressure drop-normalized gas flowrate ($q_g/\Delta m(p)$) versus production time.

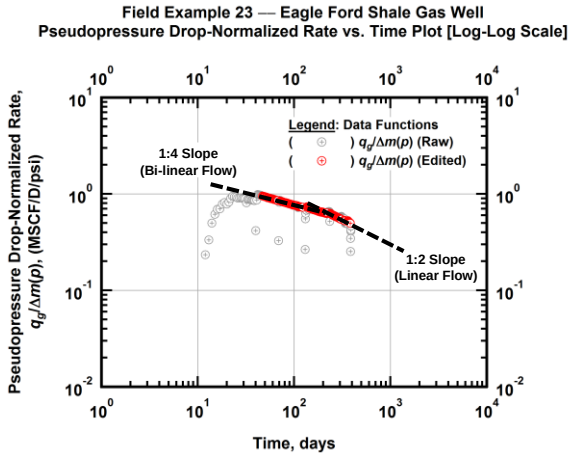

Figure A.663 — (Log-log Plot): Filtered normalized rate production history plot — pseudopressure drop-normalized gas flowrate ($q_g/\Delta m(p)$) versus production time.

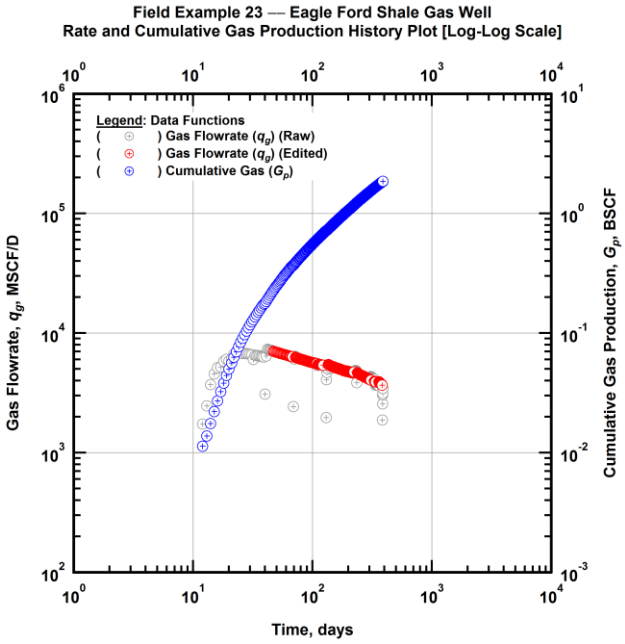

Figure A.664 — (Log-log Plot): Filtered rate and unfiltered cumulative gas production history plot — flowrate (q_g) and cumulative production (G_p) versus production time.

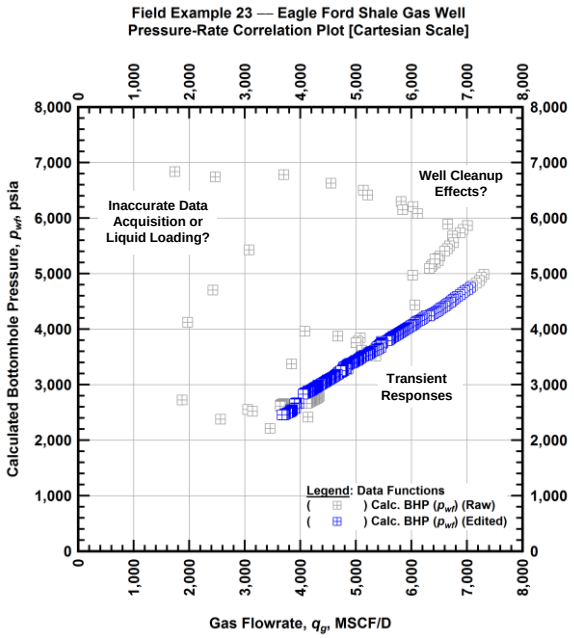

Figure A.665 — (Cartesian Plot): Filtered rate-pressure correlation plot — calculated bottomhole pressure (p_{wf}) versus flowrate (q_g).

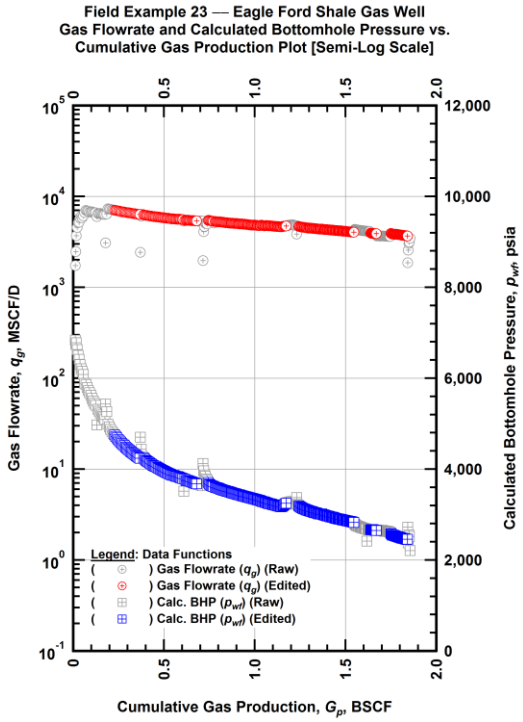

Figure A.666 — (Semi-log Plot): Filtered rate-pressure-cumulative production history plot — flowrate (q_g) and calculated bottomhole pressure (p_{wf}) versus cumulative production (G_p).

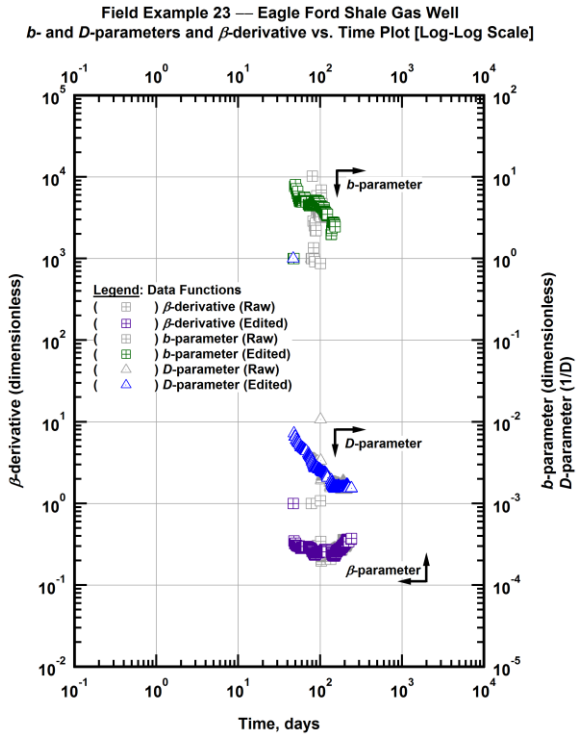

Figure A.667 — (Log-Log Plot): Filtered b, D and β production history plot — b- and D-parameters and β-derivative versus production time.

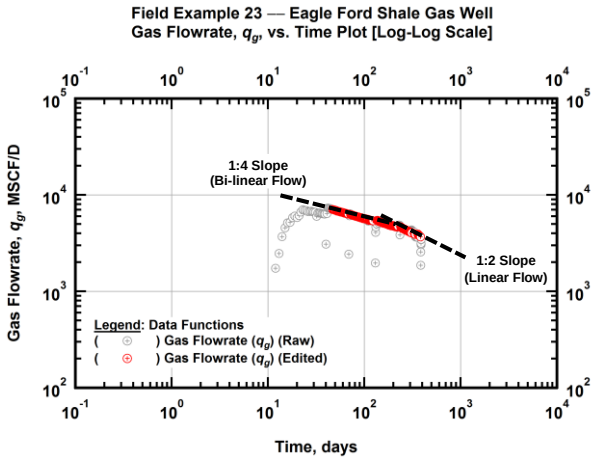

Figure A.668 — (Log-Log Plot): Filtered gas flowrate production history and flow regime identification plot — gas flowrate (q_g) versus production time.

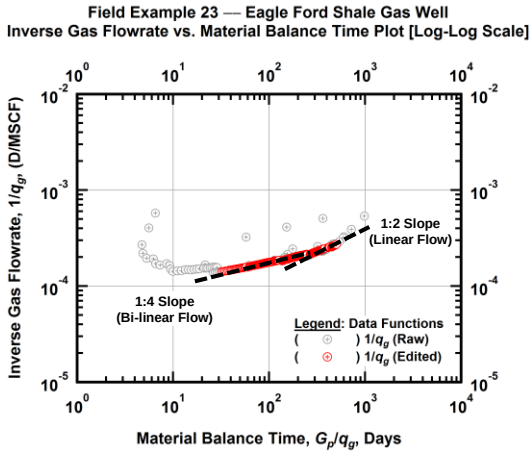

Figure A.669 — (Log-log Plot): Filtered inverse rate with material balance time plot — inverse gas flowrate ($1/q_g$) versus material balance time (G_p/q_g).

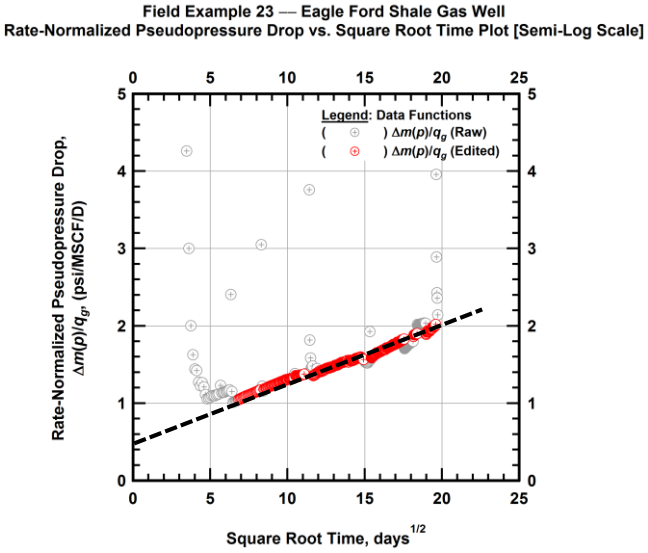

Figure A.670 — (Semi-log Plot): Filtered normalized pseudopressure drop production history plot — rate-normalized pseudopressure drop ($\Delta m(p)/q_g$) versus square root production time ($\sqrt{t}$).

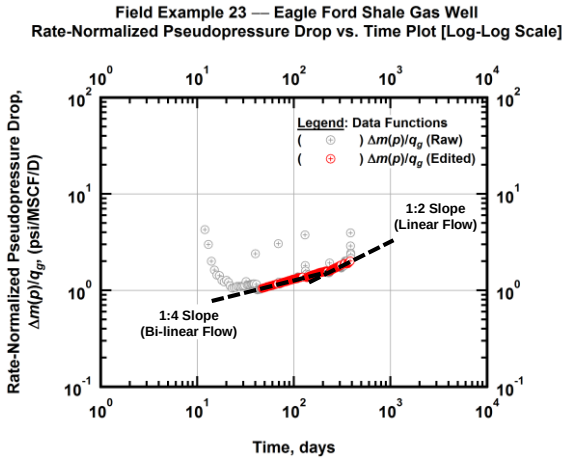

Figure A.671 — (Log-log Plot): Filtered normalized pseudopressure drop production history plot — rate-normalized pseudopressure drop ($\Delta m(p)/q_g$) versus production time.

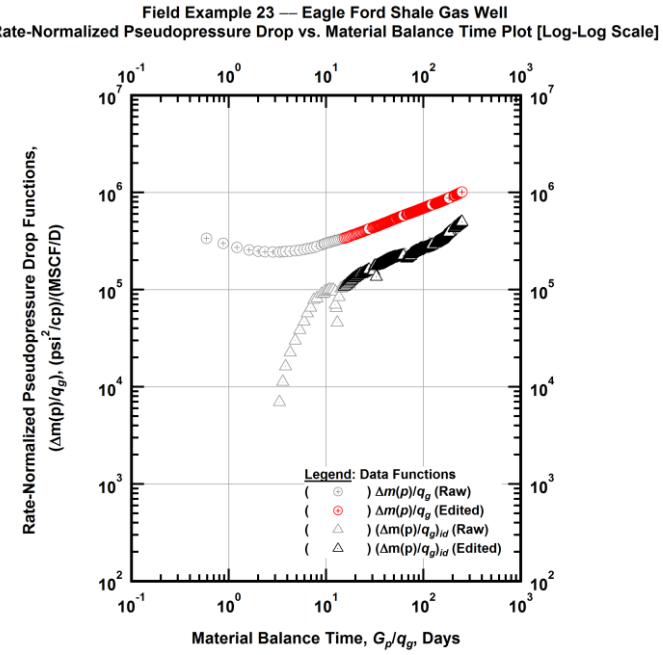

Figure A.672 — (Log-log Plot): "Log-log" diagnostic plot of the filtered production data — rate-normalized pseudopressure drop ($\Delta m(p)/q_g$) and rate-normalized pseudopressure drop integral-derivative $(\Delta m(p)/q_g)_{id}$ versus material balance time (G_p/q_g).

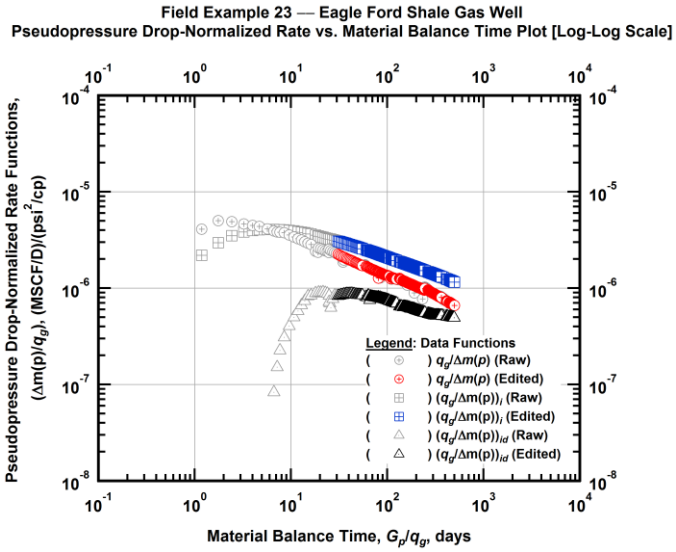

Figure A.673 — (Log-log Plot): "Blasingame" diagnostic plot of the filtered production data — pseudopressure drop-normalized gas flowrate ($q_g/\Delta m(p)$), pseudopressure drop-normalized gas flowrate integral $(q_g/\Delta m(p))_i$ and pseudopressure drop-normalized gas flowrate integral-derivative $(q_g/\Delta m(p))_{id}$ versus material balance time (G_p/q_g).

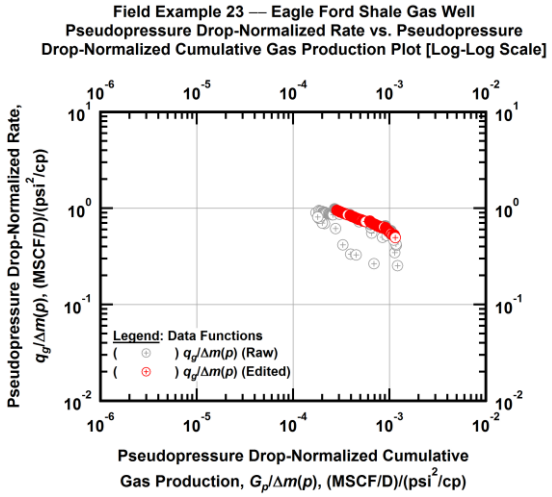

Figure A.674 — (Log-log Plot): Filtered normalized rate with normalized cumulative production plot — pseudopressure drop-normalized gas flowrate ($q_g/\Delta m(p)$) versus pseudopressure drop-normalized cumulative gas production ($G_p/\Delta m(p)$).

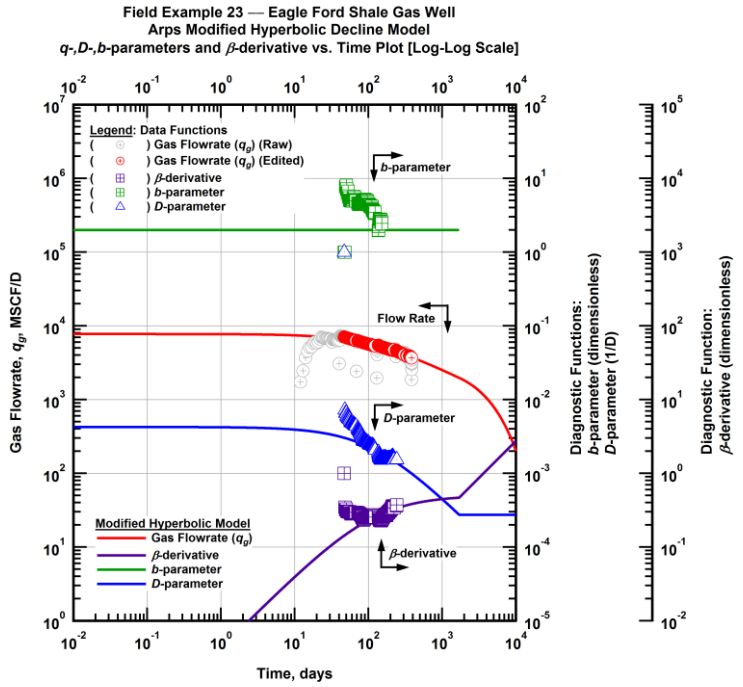

Figure A.675 — (Log-Log Plot): Arps modified hyperbolic decline model plot — time-rate model and data gas flowrate (q_g), *D*- and *b*-parameters and β-derivative versus production time.

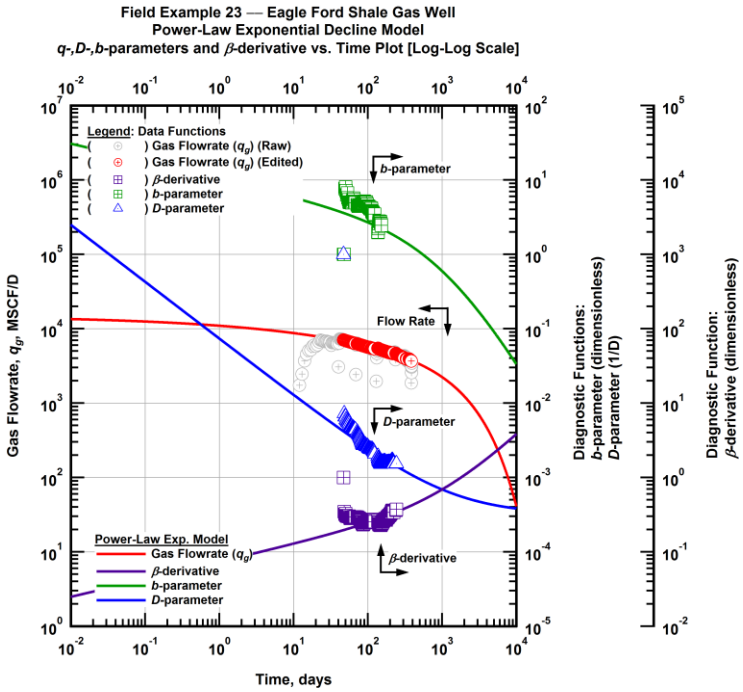

Figure A.676 — (Log-Log Plot): Power-law exponential decline model plot — time-rate model and data gas flowrate (q_g), *D*- and *b*-parameters and β-derivative versus production time.

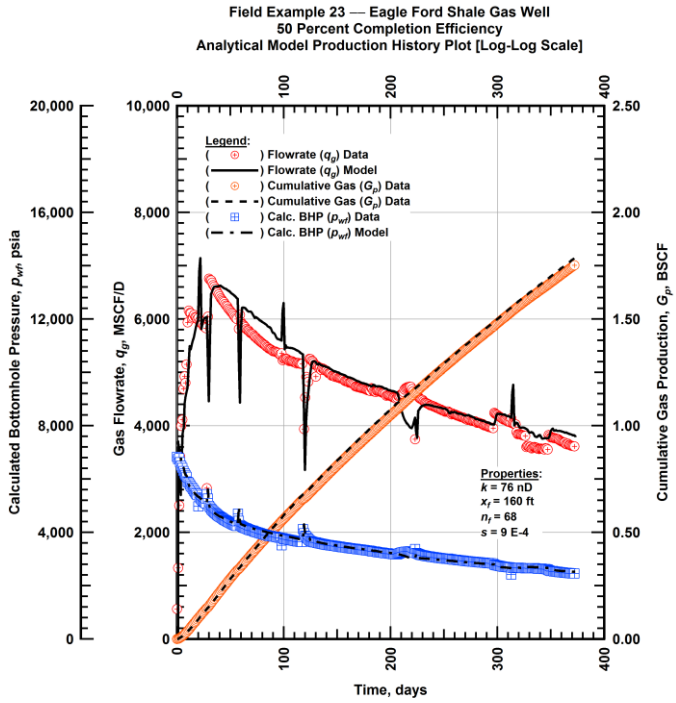

Figure A.677 — (Cartesian Plot): Production history plot — original gas flowrate (q_g), cumulative gas production (G_p), calculated bottomhole pressure (p_{wf}) and 50 percent completion efficiency model matches versus production time.

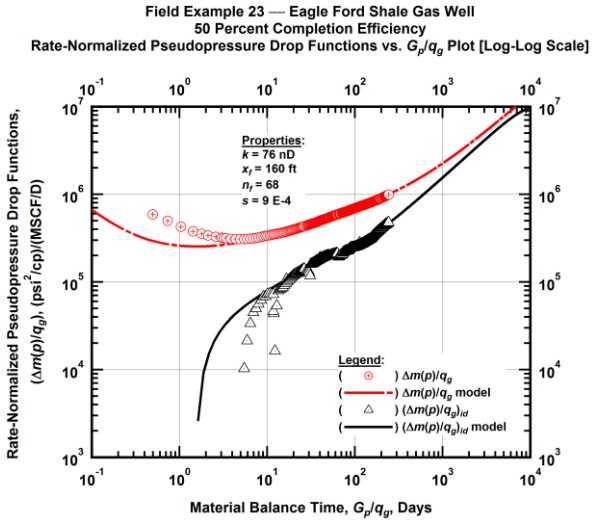

Figure A.678 — (Log-log Plot): "Log-log" diagnostic plot of the original production data — rate-normalized pseudopressure drop ($\Delta m(p)/q_g$), rate-normalized pseudopressure drop integral-derivative $(\Delta m(p)/q_g)_{id}$ and 50 percent completion efficiency model matches versus material balance time (G_p/q_g).

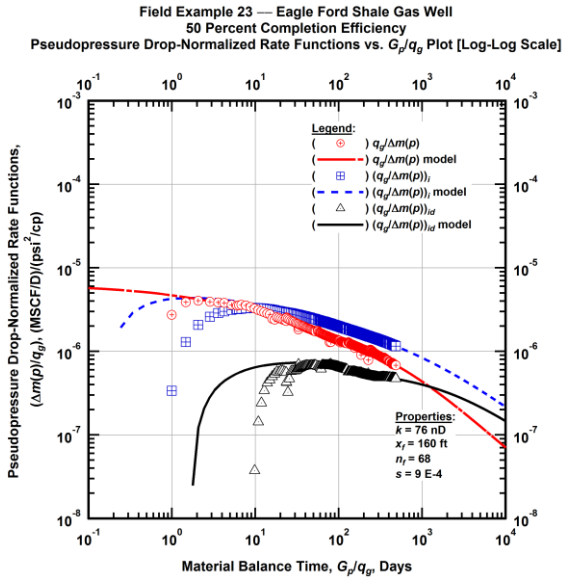

Figure A.679 — (Log-log Plot): "Blasingame" diagnostic plot of the original production data — pseudopressure drop-normalized gas flowrate ($q_g/\Delta m(p)$), pseudopressure drop-normalized gas flowrate integral ($q_g/\Delta m(p))_i$, pseudopressure drop-normalized gas flowrate integral-derivative ($q_g/\Delta m(p))_{id}$ and 50 percent completion efficiency model matches versus material balance time (G_p/q_g).

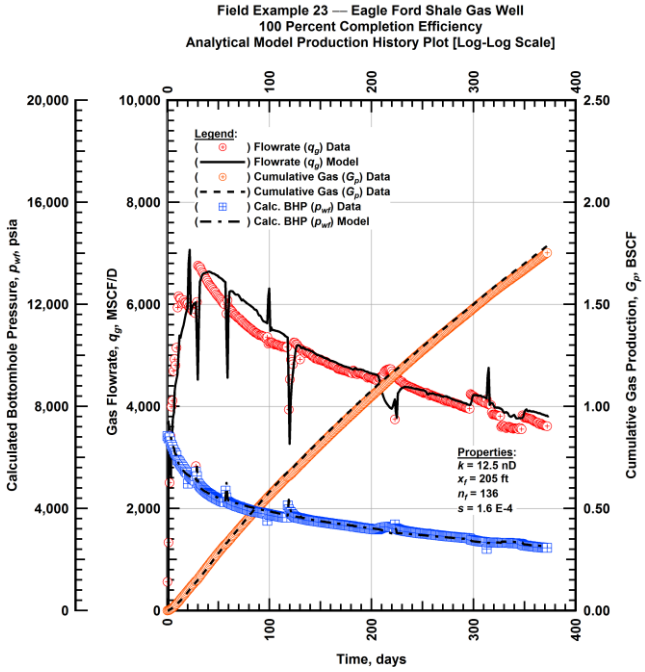

Figure A.680 — (Cartesian Plot): Production history plot — original gas flowrate (q_g), cumulative gas production (G_p), calculated bottomhole pressure (p_{wf}) and 100 percent completion efficiency model matches versus production time.

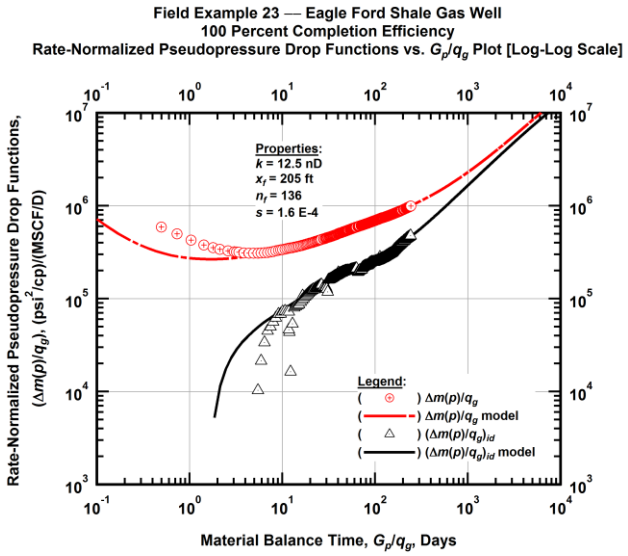

Figure A.681 — (Log-log Plot): "Log-log" diagnostic plot of the original production data — rate-normalized pseudopressure drop ($\Delta m(p)/q_g$), rate-normalized pseudopressure drop integral-derivative $(\Delta m(p)/q_g)_{id}$ and 100 percent completion efficiency model matches versus material balance time (G_p/q_g).

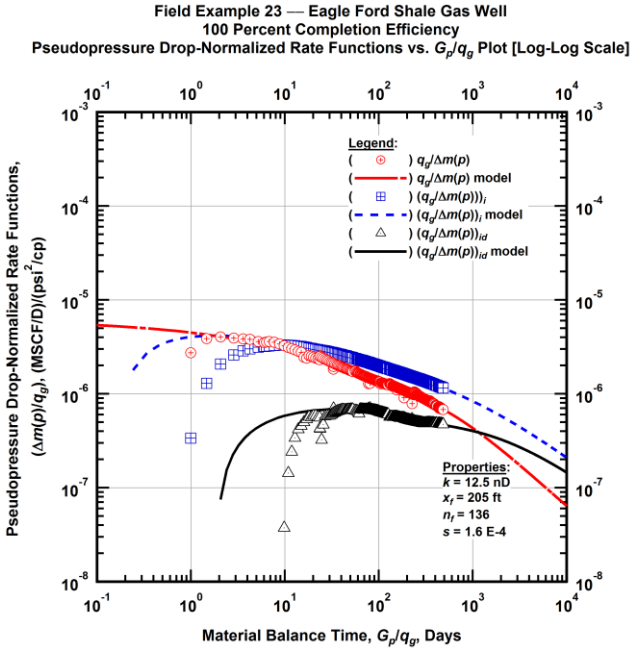

Figure A.682 — (Log-log Plot): "Blasingame" diagnostic plot of the original production data — pseudopressure drop-normalized gas flowrate ($q_g/\Delta m(p)$), pseudopressure drop-normalized gas flowrate integral $(q_g/\Delta m(p))_i$, pseudopressure drop-normalized gas flowrate integral-derivative $(q_g/\Delta m(p))_{id}$ and 100 percent completion efficiency model matches versus material balance time (G_p/q_g).

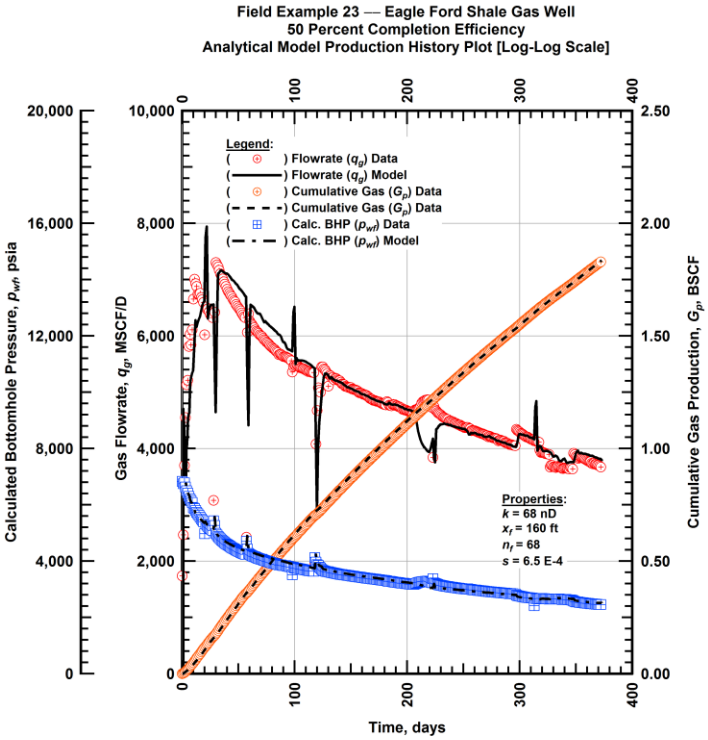

Figure A.683 — (Cartesian Plot): Production history plot — revised gas flowrate (q_g), cumulative gas production (G_p), calculated bottomhole pressure (p_{wf}) and 50 percent completion efficiency model matches versus production time.

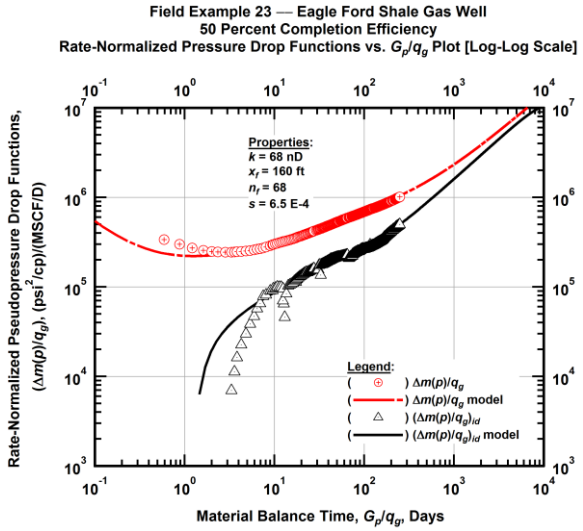

Figure A.684 — (Log-log Plot): "Log-log" diagnostic plot of the revised production data — rate-normalized pseudopressure drop ($\Delta m(p)/q_g$), rate-normalized pseudopressure drop integral-derivative $(\Delta m(p)/q_g)_{id}$ and 50 percent completion efficiency model matches versus material balance time (G_p/q_g).

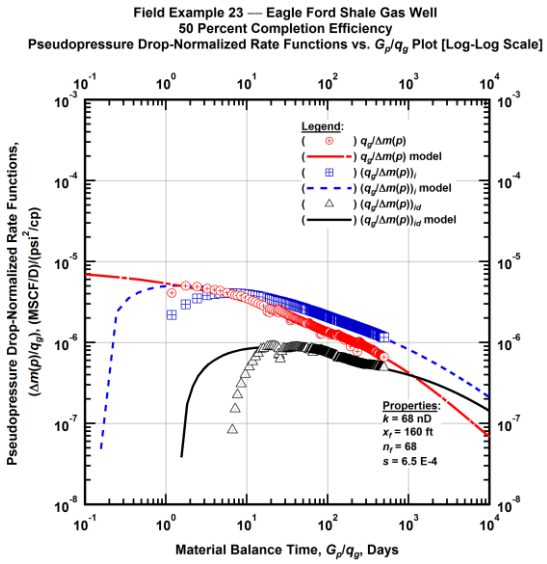

Figure A.685 — (Log-log Plot): "Blasingame" diagnostic plot of the revised production data — pseudopressure drop-normalized gas flowrate ($q_g/\Delta m(p)$), pseudopressure drop-normalized gas flowrate integral $(q_g/\Delta m(p))_i$, pseudopressure drop-normalized gas flowrate integral-derivative $(q_g/\Delta m(p))_{id}$ and 50 percent completion efficiency model matches versus material balance time (G_p/q_g).

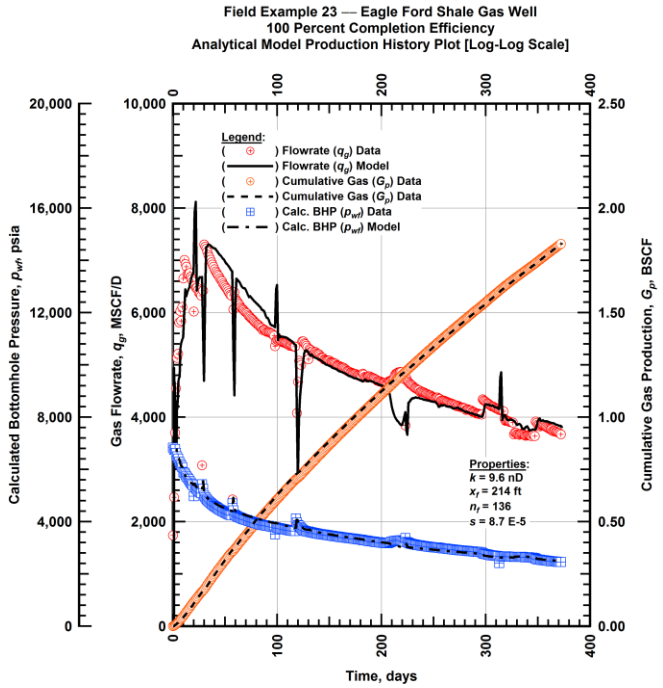

Figure A.686 — (Cartesian Plot): Production history plot — revised gas flowrate (q_g), cumulative gas production (G_p), calculated bottomhole pressure (p_{wf}) and 100 percent completion efficiency model matches versus production time.

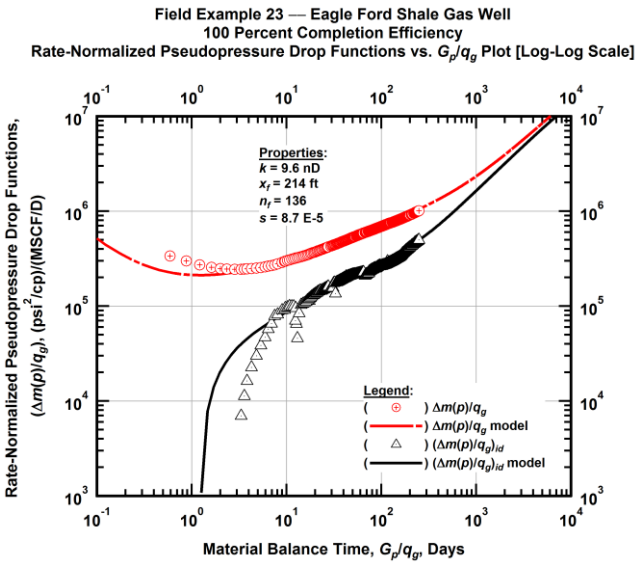

Figure A.687 — (Log-log Plot): "Log-log" diagnostic plot of the revised production data — rate-normalized pseudopressure drop ($\Delta m(p)/q_g$), rate-normalized pseudopressure drop integral-derivative $(\Delta m(p)/q_g)_{id}$ and 100 percent completion efficiency model matches versus material balance time (G_p/q_g).

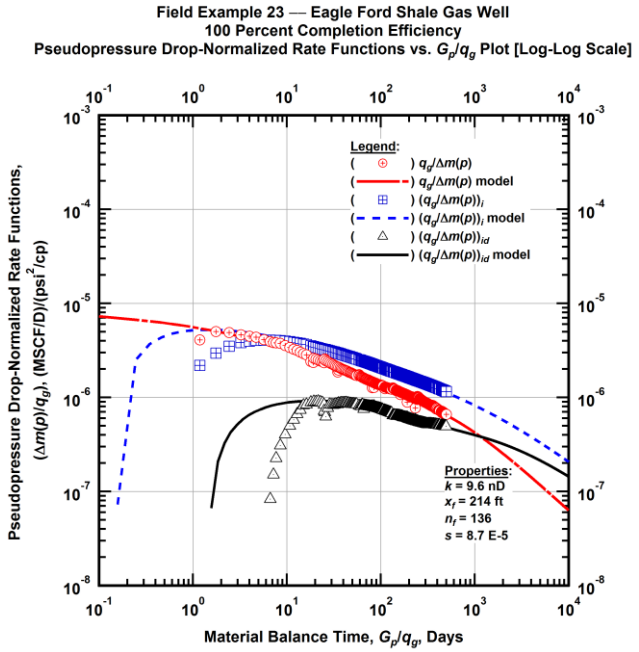

Figure A.688 — (Log-log Plot): "Blasingame" diagnostic plot of the revised production data — pseudopressure drop-normalized gas flowrate ($q_g/\Delta m(p)$), pseudopressure drop-normalized gas flowrate integral $(q_g/\Delta m(p))_i$, pseudopressure drop-normalized gas flowrate integral-derivative $(q_g/\Delta m(p))_{id}$ and 100 percent completion efficiency model matches versus material balance time (G_p/q_g).

Field Example 23 — 30-Year EUR Model Comparison

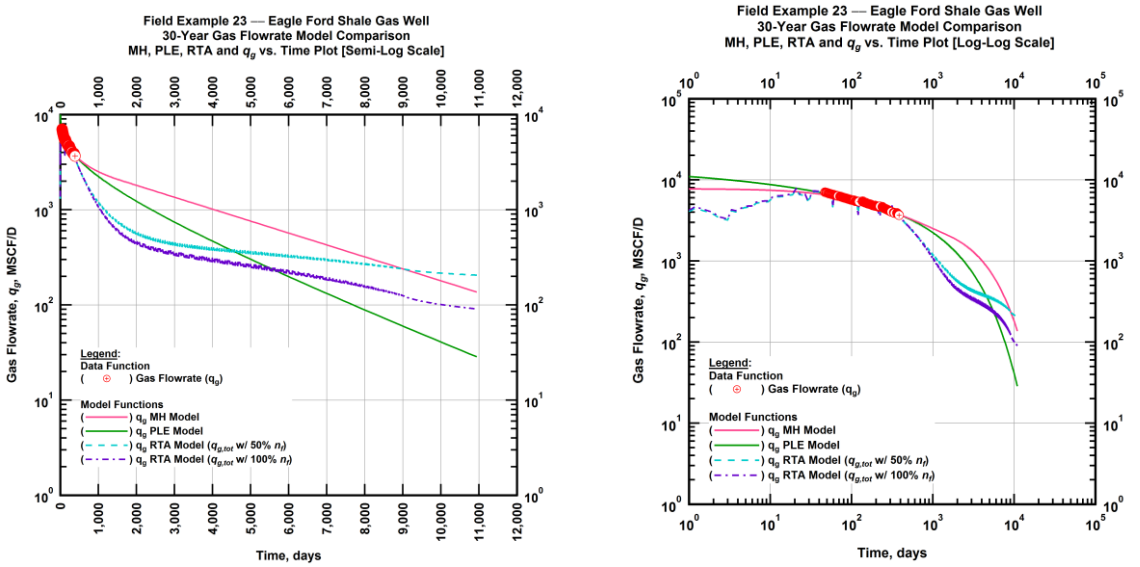

A **B**

Figure A.689 — (A — Semi-Log Plot) and (B — Log-Log Plot): Estimated 30-year revised gas flowrate model comparison — Arps modified hyperbolic decline model, power-law exponential decline model, and 50 percent and 100 percent completion efficiency RTA models revised gas 30-year estimated flowrate decline and historic gas flowrate data (q_g) versus production time.

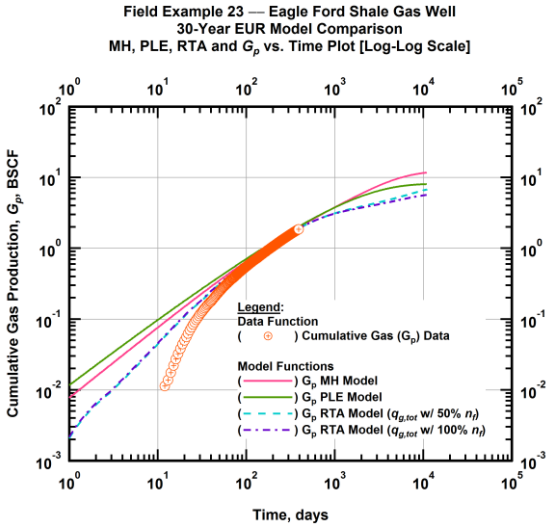

Figure A.690 — (Log-log Plot): PVT revised gas 30-year estimated cumulative production volume model comparison — Arps modified hyperbolic decline model, power-law exponential decline model, and 50 percent and 100 percent completion efficiency RTA model estimated 30-year cumulative gas production volumes and historic cumulative gas production (G_p) versus production time.

Table A.23 — 30-year estimated cumulative revised gas production (EUR), in units of BSCF, for the Arps modified hyperbolic, power-law exponential and analytical time-rate-pressure decline models.

Arps Modified Hyperbolic (BSCF)	Power-Law Exponential (BSCF)	RTA Analytical Model ($q_{g,tot}$ w/ 50% n_f) (BSCF)	RTA Analytical Model ($q_{g,tot}$ w/ 100% n_f) (BSCF)
11.89	7.87	6.84	5.70

Field Example 24 — Time-Rate Analysis

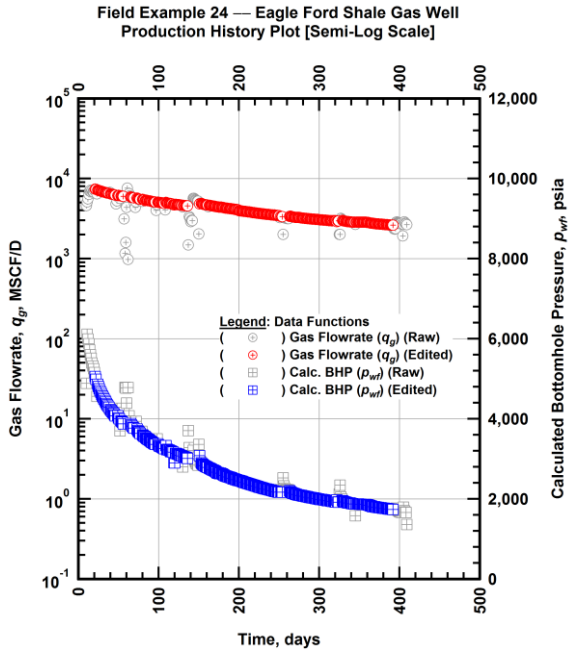

Figure A.691 — (Semi-log Plot): Filtered production history plot — flowrate (q_g) and calculated bottomhole pressure (p_{wf}) versus production time.

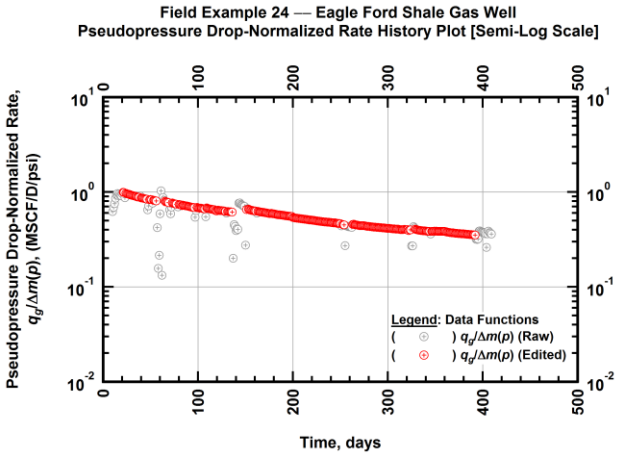

Figure A.692 — (Semi-log Plot): Filtered normalized rate production history plot — pseudopressure drop-normalized gas flowrate ($q_g/\Delta m(p)$) versus production time.

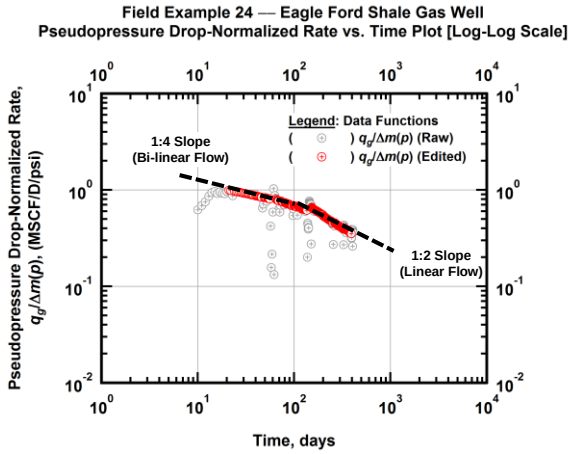

Figure A.693 — (Log-log Plot): Filtered normalized rate production history plot — pseudopressure drop-normalized gas flowrate ($q_g/\Delta m(p)$) versus production time.

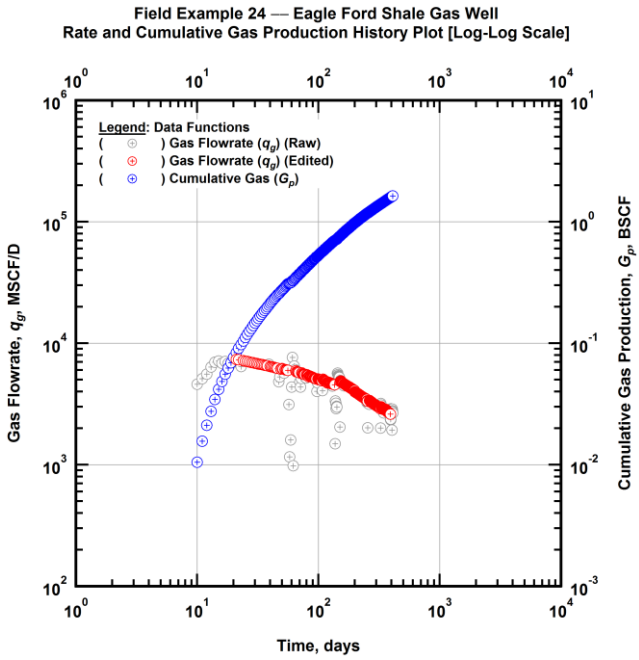

Figure A.694 — (Log-log Plot): Filtered rate and unfiltered cumulative gas production history plot — flowrate (q_g) and cumulative production (G_p) versus production time.

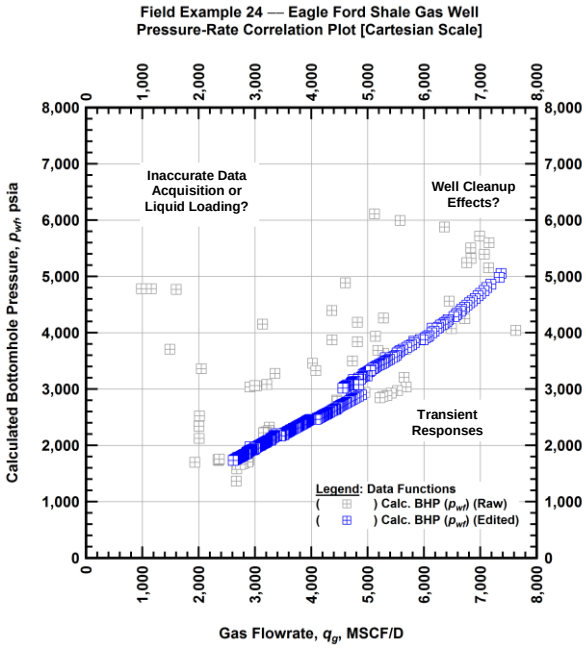

Figure A.695 — (Cartesian Plot): Filtered rate-pressure correlation plot — calculated bottomhole pressure (p_{wf}) versus flowrate (q_g).

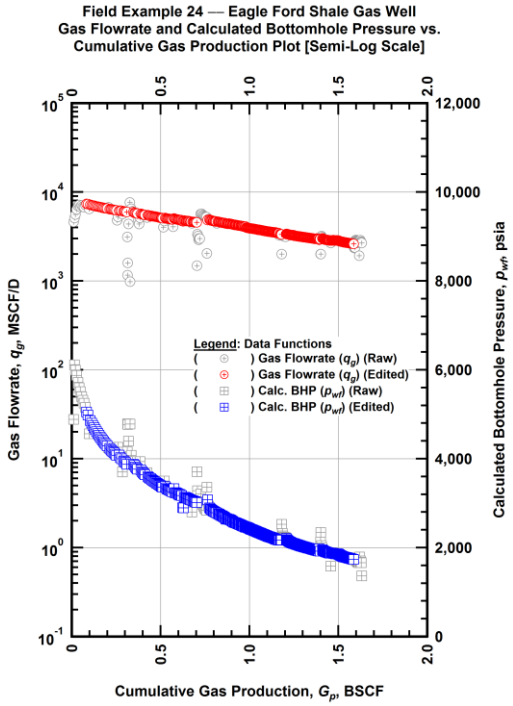

Figure A.696 — (Semi-log Plot): Filtered rate-pressure-cumulative production history plot — flowrate (q_g) and calculated bottomhole pressure (p_{wf}) versus cumulative production (G_p).

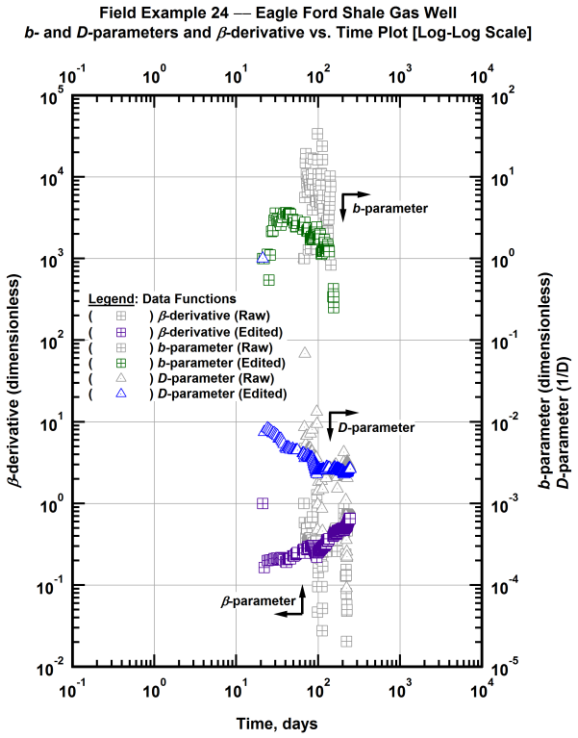

Figure A.697 — (Log-Log Plot): Filtered b, D and β production history plot — b- and D-parameters and β-derivative versus production time.

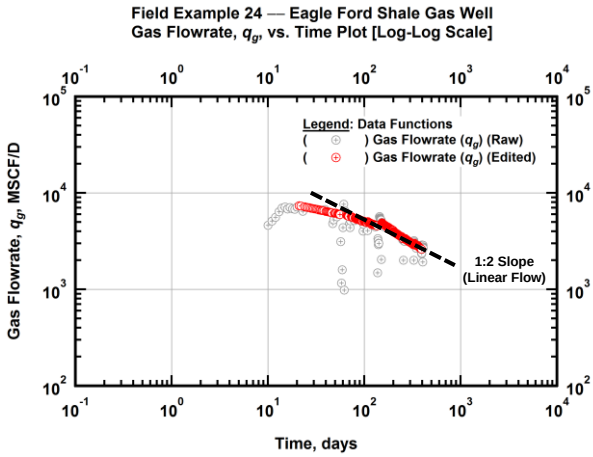

Figure A.698 — (Log-Log Plot): Filtered gas flowrate production history and flow regime identification plot — gas flowrate (q_g) versus production time.

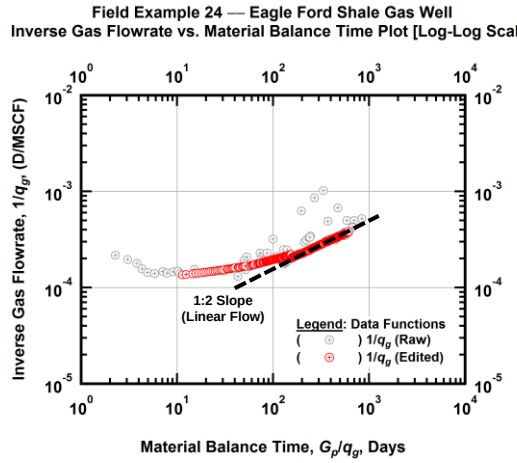

Figure A.699 — (Log-log Plot): Filtered inverse rate with material balance time plot — inverse gas flowrate ($1/q_g$) versus material balance time (G_p/q_g).

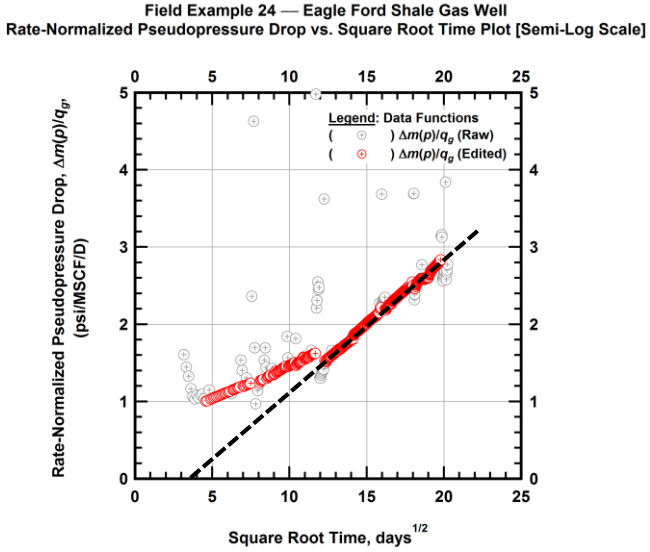

Figure A.700 — (Semi-log Plot): Filtered normalized pseudopressure drop production history plot — rate-normalized pseudopressure drop ($\Delta m(p)/q_g$) versus square root production time ($\sqrt{t}$).

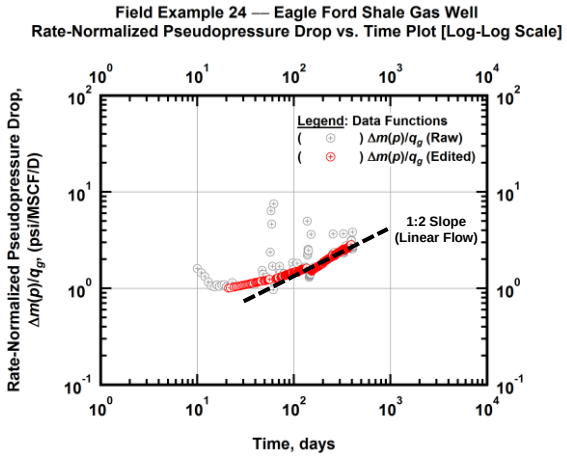

Figure A.701 — (Log-log Plot): Filtered normalized pseudopressure drop production history plot — rate-normalized pseudopressure drop ($\Delta m(p)/q_g$) versus production time.

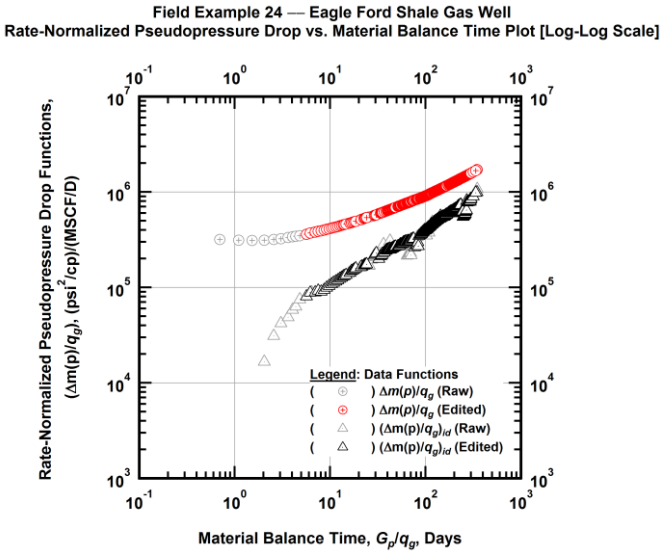

Figure A.702 — (Log-log Plot): "Log-log" diagnostic plot of the filtered production data — rate-normalized pseudopressure drop ($\Delta m(p)/q_g$) and rate-normalized pseudopressure drop integral-derivative $(\Delta m(p)/q_g)_{id}$ versus material balance time (G_p/q_g).

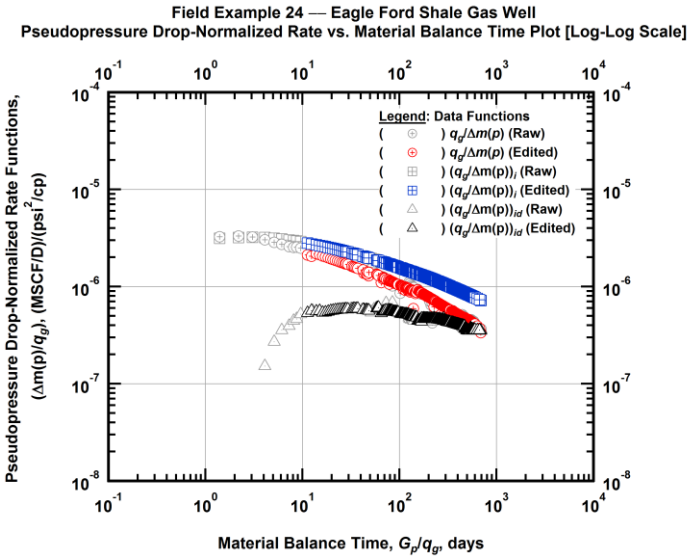

Figure A.703 — (Log-log Plot): "Blasingame" diagnostic plot of the filtered production data — pseudopressure drop-normalized gas flowrate ($q_g/\Delta m(p)$), pseudopressure drop-normalized gas flowrate integral $(q_g/\Delta m(p))_i$ and pseudopressure drop-normalized gas flowrate integral-derivative $(q_g/\Delta m(p))_{id}$ versus material balance time (G_p/q_g).

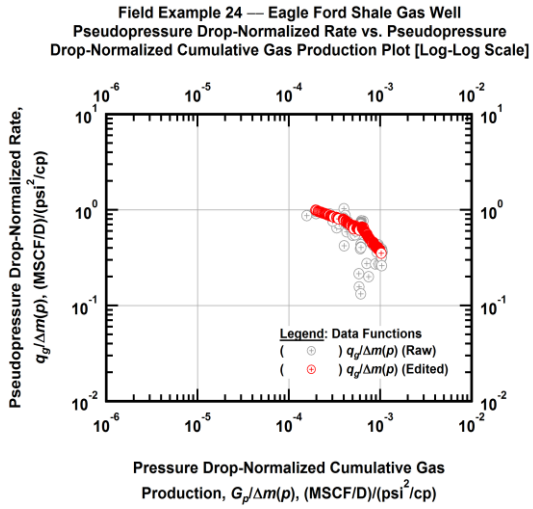

Figure A.704 — (Log-log Plot): Filtered normalized rate with normalized cumulative production plot — pseudopressure drop-normalized gas flowrate ($q_g/\Delta m(p)$) versus pseudopressure drop-normalized cumulative gas production ($G_p/\Delta m(p)$).

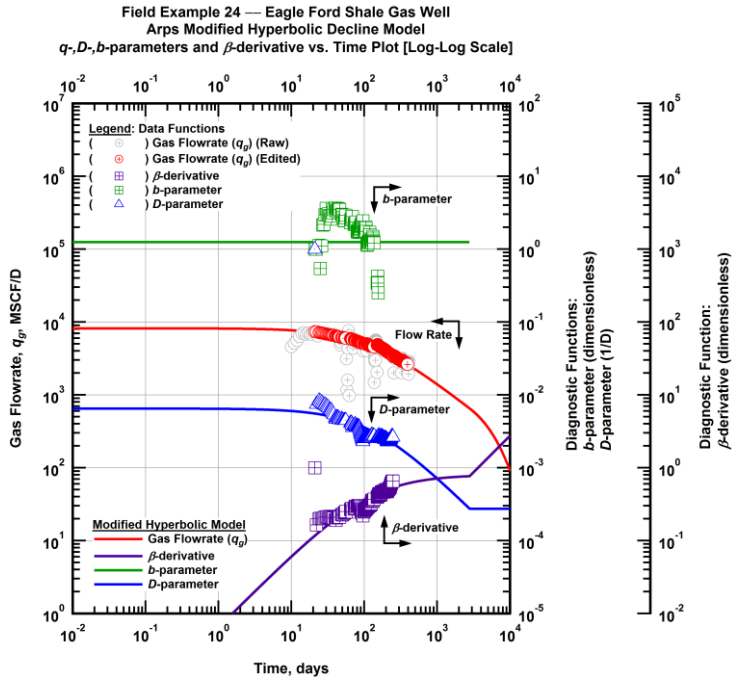

Figure A.705 — (Log-Log Plot): Arps modified hyperbolic decline model plot — time-rate model and data gas flowrate (q_g), *D*- and *b*-parameters and β-derivative versus production time.

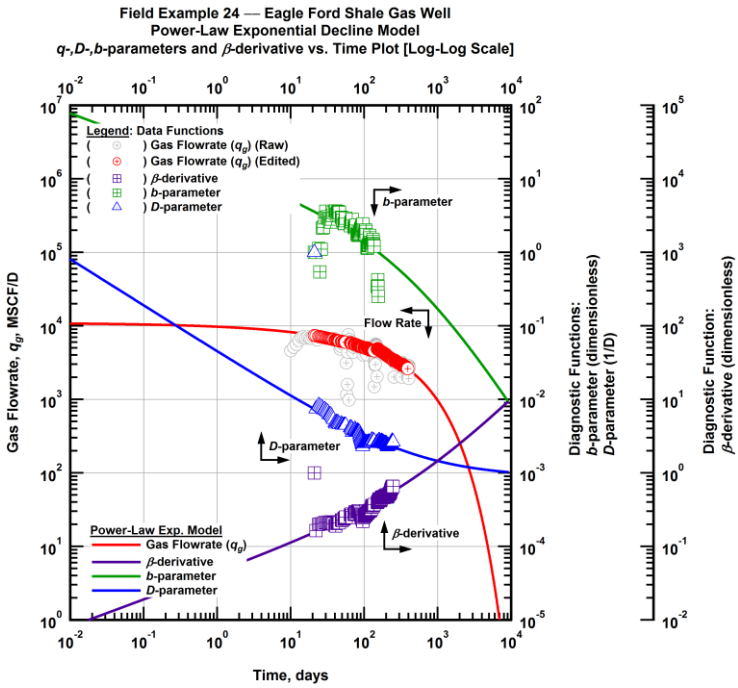

Figure A.706 — (Log-Log Plot): Power-law exponential decline model plot — time-rate model and data gas flowrate (q_g), *D*- and *b*-parameters and β-derivative versus production time.

Field Example 24 — Model-Based (Time-Rate-Pressure) Production Analysis

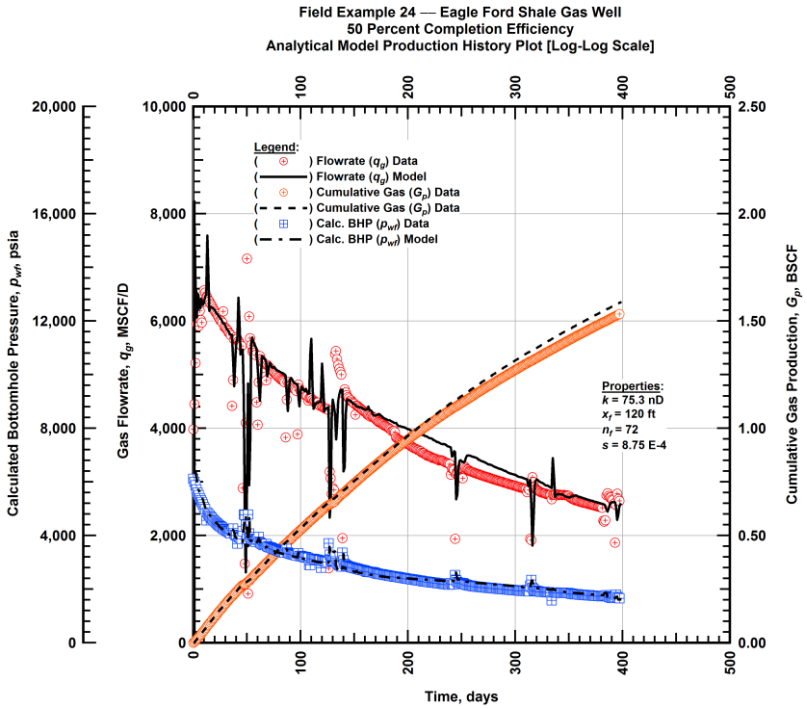

Figure A.707 — (Cartesian Plot): Production history plot — original gas flowrate (q_g), cumulative gas production (G_p), calculated bottomhole pressure (p_{wf}) and 50 percent completion efficiency model matches versus production time.

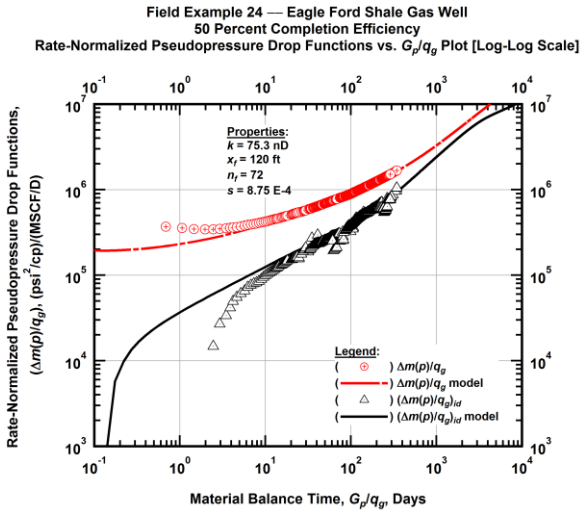

Figure A.708 — (Log-log Plot): "Log-log" diagnostic plot of the original production data — rate-normalized pseudopressure drop ($\Delta m(p)/q_g$), rate-normalized pseudopressure drop integral-derivative $(\Delta m(p)/q_g)_{id}$ and 50 percent completion efficiency model matches versus material balance time (G_p/q_g).

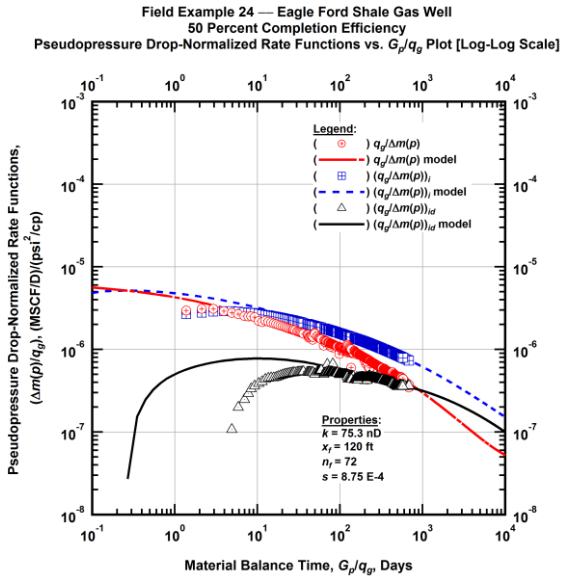

Figure A.709 — (Log-log Plot): "Blasingame" diagnostic plot of the original production data — pseudopressure drop-normalized gas flowrate ($q_g/\Delta m(p)$), pseudopressure drop-normalized gas flowrate integral ($q_g/\Delta m(p))_i$, pseudopressure drop-normalized gas flowrate integral-derivative ($q_g/\Delta m(p))_{id}$ and 50 percent completion efficiency model matches versus material balance time (G_p/q_g).

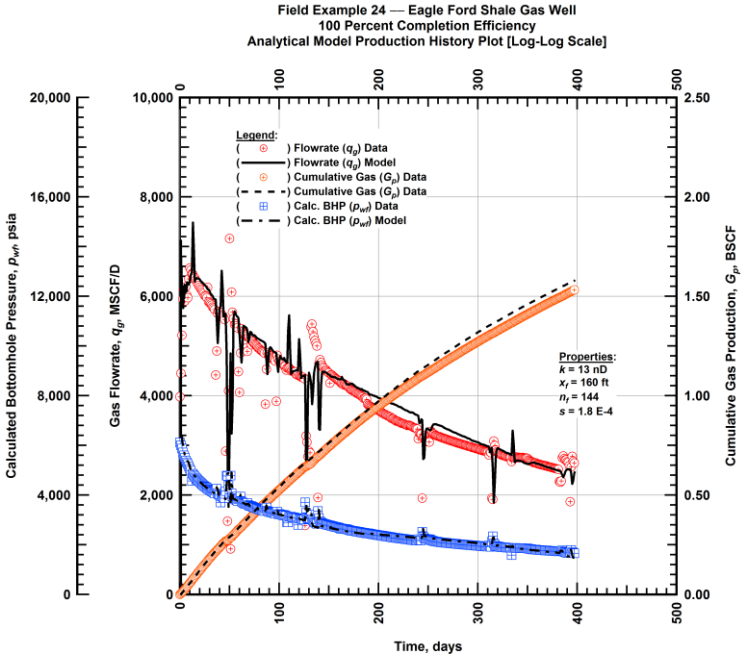

Figure A.710 — (Cartesian Plot): Production history plot — original gas flowrate (q_g), cumulative gas production (G_p), calculated bottomhole pressure (p_{wf}) and 100 percent completion efficiency model matches versus production time.

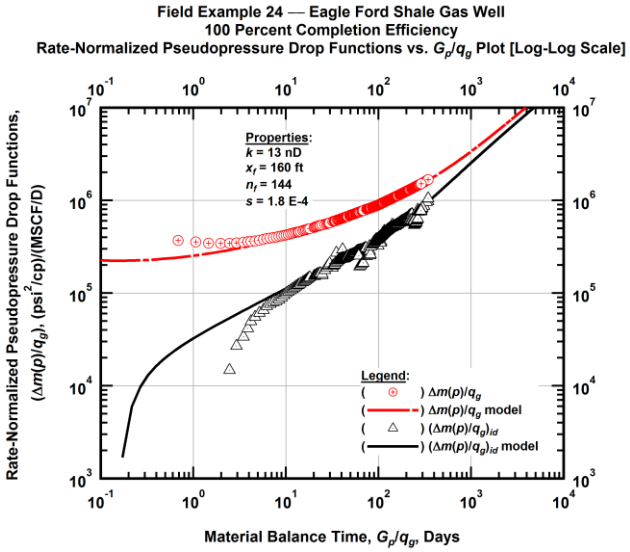

Figure A.711 — (Log-log Plot): "Log-log" diagnostic plot of the original production data — rate-normalized pseudopressure drop ($\Delta m(p)/q_g$), rate-normalized pseudopressure drop integral-derivative $(\Delta m(p)/q_g)_{id}$ and 100 percent completion efficiency model matches versus material balance time (G_p/q_g).

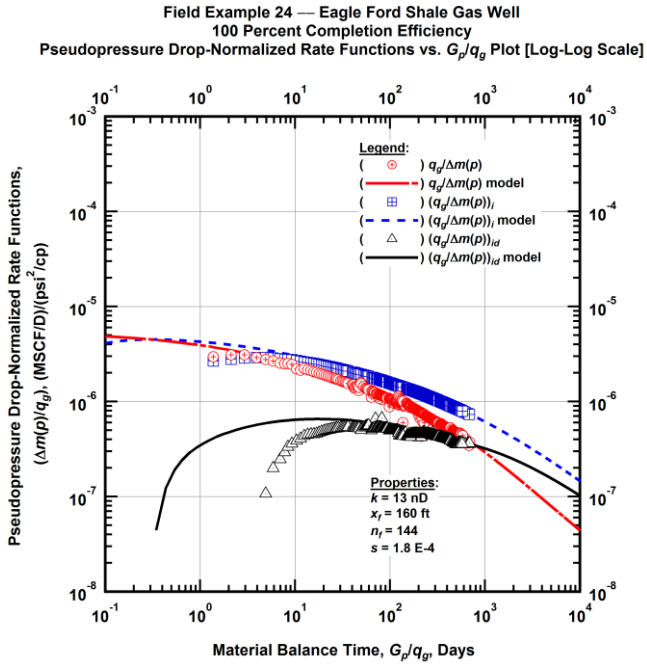

Figure A.712 — (Log-log Plot): "Blasingame" diagnostic plot of the original production data — pseudopressure drop-normalized gas flowrate ($q_g/\Delta m(p)$), pseudopressure drop-normalized gas flowrate integral $(q_g/\Delta m(p))_i$, pseudopressure drop-normalized gas flowrate integral-derivative $(q_g/\Delta m(p))_{id}$ and 100 percent completion efficiency model matches versus material balance time (G_p/q_g).

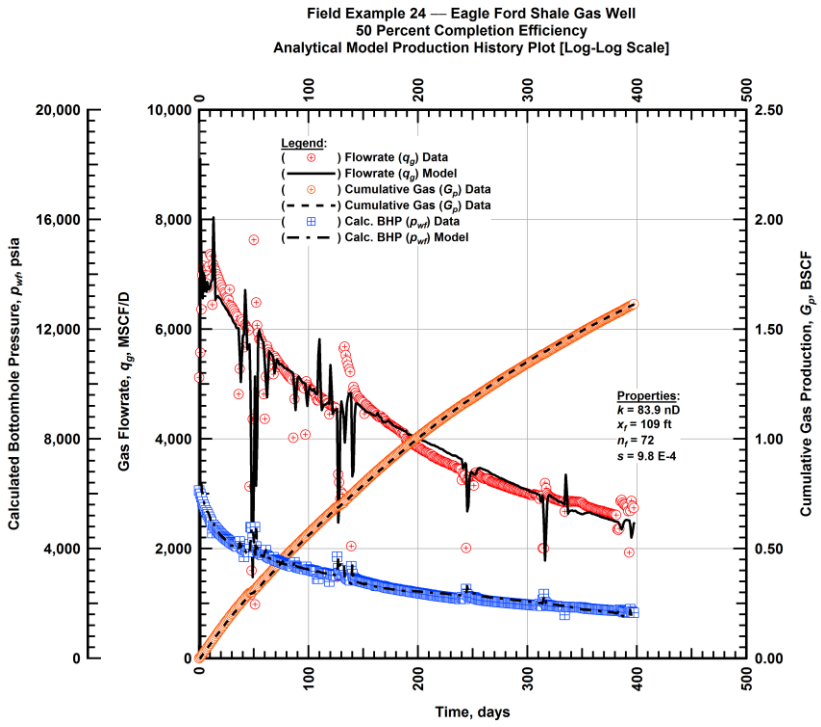

Figure A.713 — (Cartesian Plot): Production history plot — revised gas flowrate (q_g), cumulative gas production (G_p), calculated bottomhole pressure (p_{wf}) and 50 percent completion efficiency model matches versus production time.

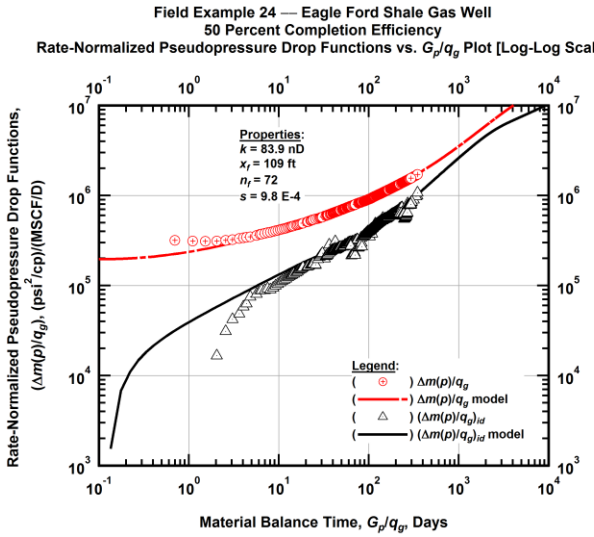

Figure A.714 — (Log-log Plot): "Log-log" diagnostic plot of the revised production data — rate-normalized pseudopressure drop ($\Delta m(p)/q_g$), rate-normalized pseudopressure drop integral-derivative $(\Delta m(p)/q_g)_{id}$ and 50 percent completion efficiency model matches versus material balance time (G_p/q_g).

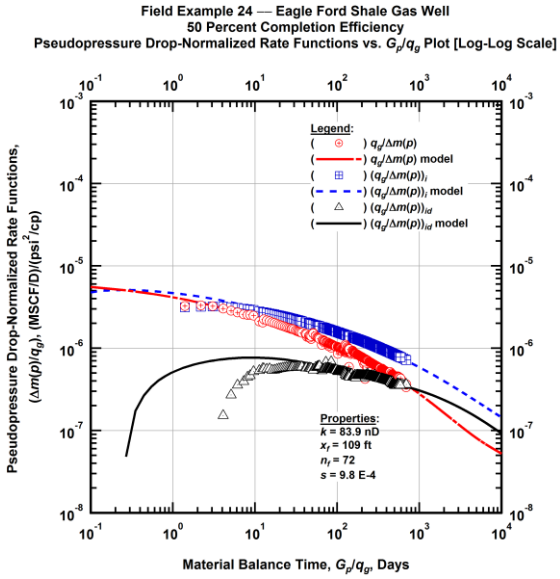

Figure A.715 — (Log-log Plot): "Blasingame" diagnostic plot of the revised production data — pseudopressure drop-normalized gas flowrate ($q_g/\Delta m(p)$), pseudopressure drop-normalized gas flowrate integral ($q_g/\Delta m(p))_i$, pseudopressure drop-normalized gas flowrate integral-derivative ($q_g/\Delta m(p))_{id}$ and 50 percent completion efficiency model matches versus material balance time (G_p/q_g).

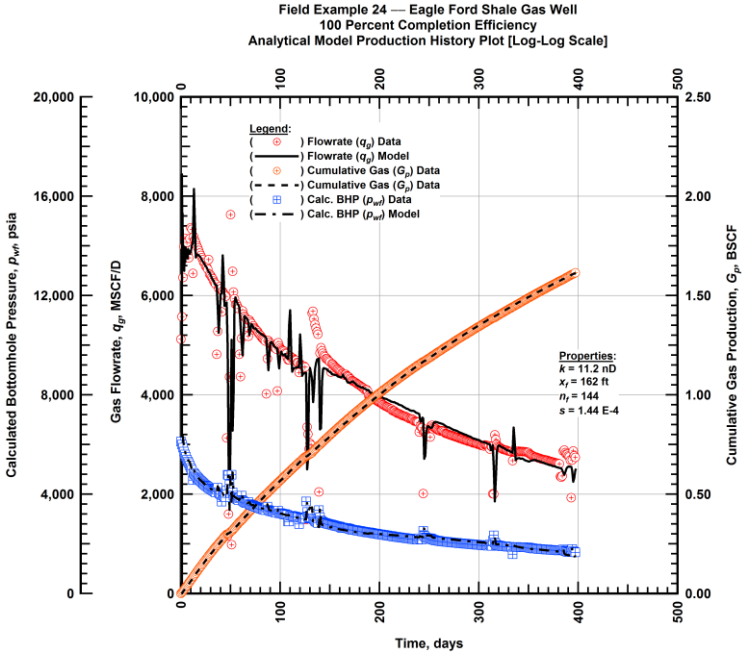

Figure A.716 — (Cartesian Plot): Production history plot — revised gas flowrate (q_g), cumulative gas production (G_p), calculated bottomhole pressure (p_{wf}) and 100 percent completion efficiency model matches versus production time.

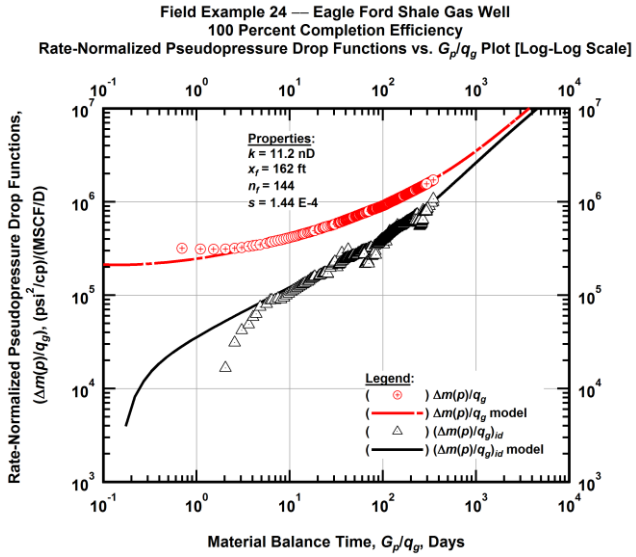

Figure A.717 — (Log-log Plot): "Log-log" diagnostic plot of the revised production data — rate-normalized pseudopressure drop ($\Delta m(p)/q_g$), rate-normalized pseudopressure drop integral-derivative $(\Delta m(p)/q_g)_{id}$ and 100 percent completion efficiency model matches versus material balance time (G_p/q_g).

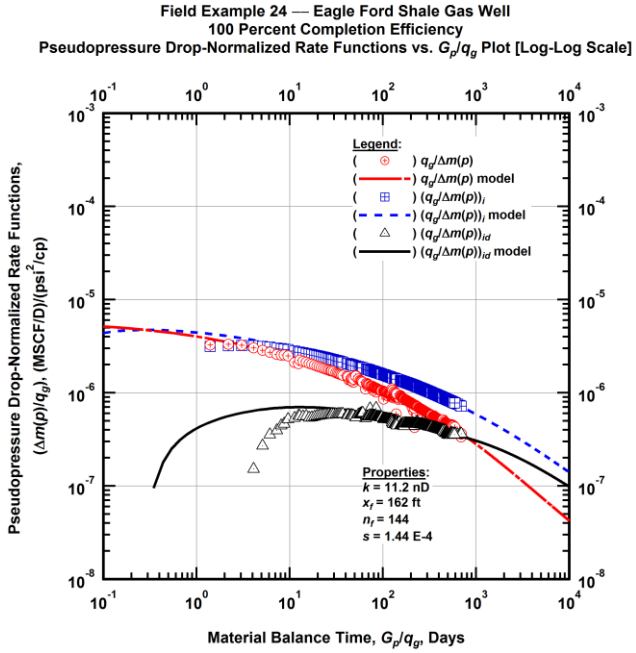

Figure A.718 — (Log-log Plot): "Blasingame" diagnostic plot of the revised production data — pseudopressure drop-normalized gas flowrate ($q_g/\Delta m(p)$), pseudopressure drop-normalized gas flowrate integral $(q_g/\Delta m(p))_i$, pseudopressure drop-normalized gas flowrate integral-derivative $(q_g/\Delta m(p))_{id}$ and 100 percent completion efficiency model matches versus material balance time (G_p/q_g).

Field Example 24 — 30-Year EUR Model Comparison

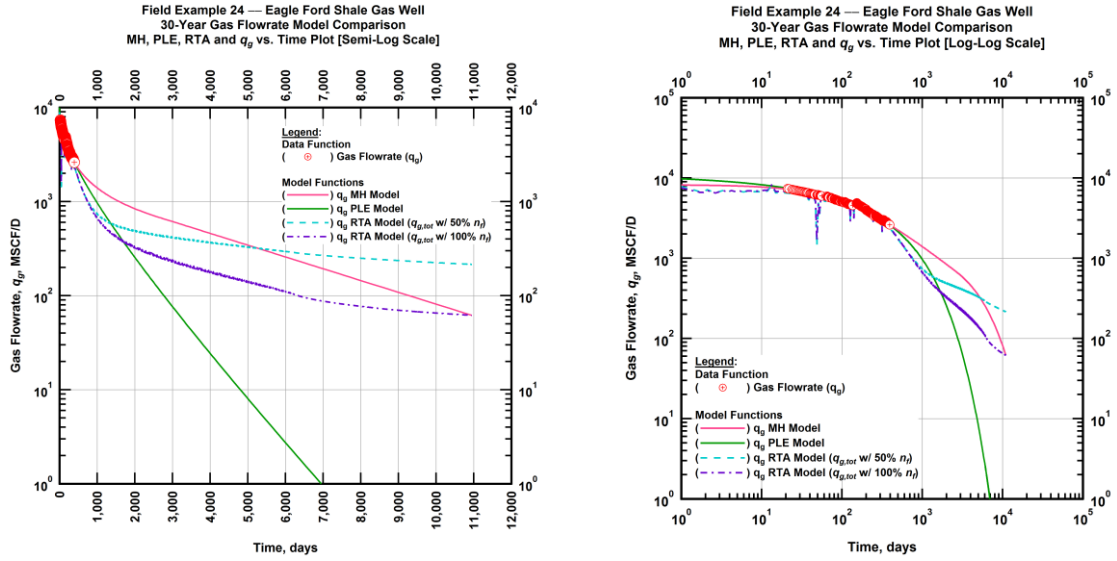

A **B**

Figure A.719 — (A — Semi-Log Plot) and (B — Log-Log Plot): Estimated 30-year revised gas flowrate model comparison — Arps modified hyperbolic decline model, power-law exponential decline model, and 50 percent and 100 percent completion efficiency RTA models revised gas 30-year estimated flowrate decline and historic gas flowrate data (q_g) versus production time.

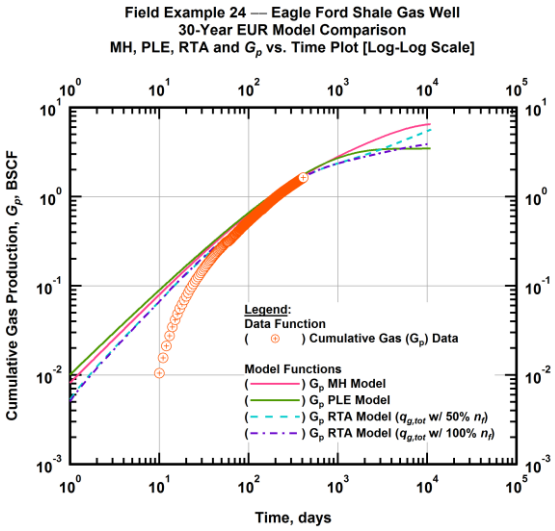

Figure A.720 — (Log-log Plot): PVT revised gas 30-year estimated cumulative production volume model comparison — Arps modified hyperbolic decline model, power-law exponential decline model, and 50 percent and 100 percent completion efficiency RTA model estimated 30-year cumulative gas production volumes and historic cumulative gas production (G_p) versus production time.

Table A.24 — 30-year estimated cumulative revised gas production (EUR), in units of BSCF, for the Arps modified hyperbolic, power-law exponential and analytical time-rate-pressure decline models.

Arps Modified Hyperbolic (BSCF)	Power-Law Exponential (BSCF)	RTA Analytical Model ($q_{g,tot}$ w/ 50% n_f) (BSCF)	RTA Analytical Model ($q_{g,tot}$ w/ 100% n_f) (BSCF)
6.51	3.30	5.73	3.96

Field Example 25 — Time-Rate Analysis

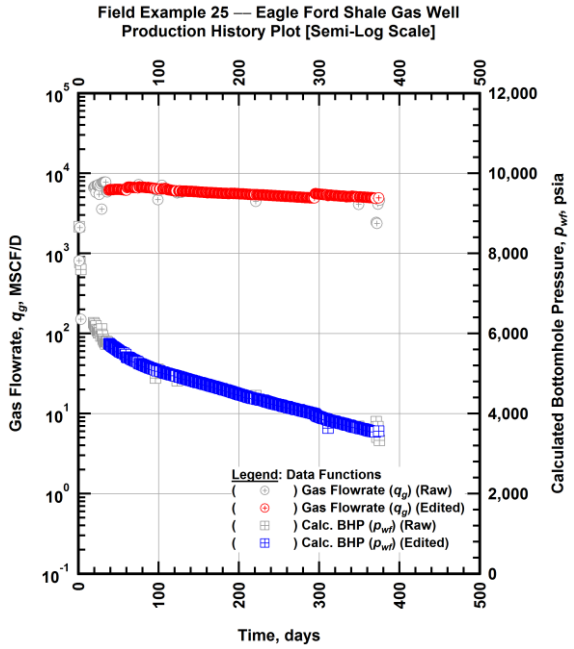

Figure A.721 — (Semi-log Plot): Filtered production history plot — flowrate (q_g) and calculated bottomhole pressure (p_{wf}) versus production time.

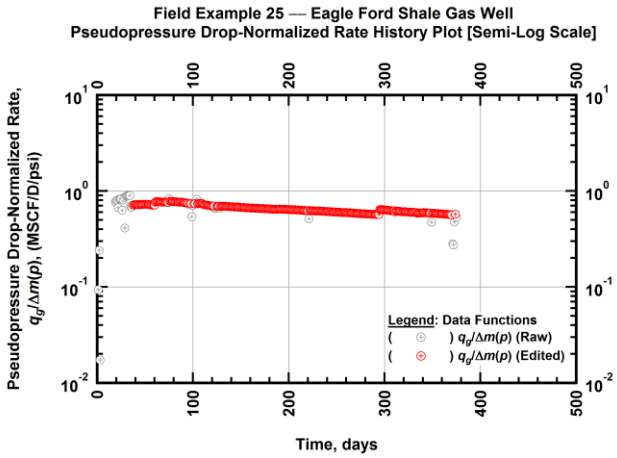

Figure A.722 — (Semi-log Plot): Filtered normalized rate production history plot — pseudopressure drop-normalized gas flowrate ($q_g/\Delta m(p)$) versus production time.

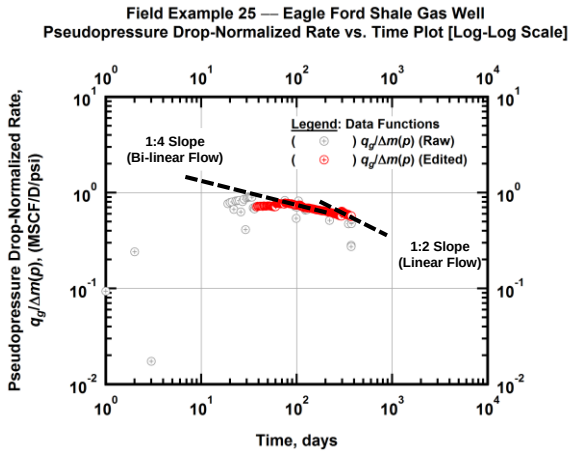

Figure A.723 — (Log-log Plot): Filtered normalized rate production history plot — pseudopressure drop-normalized gas flowrate ($q_g/\Delta m(p)$) versus production time.

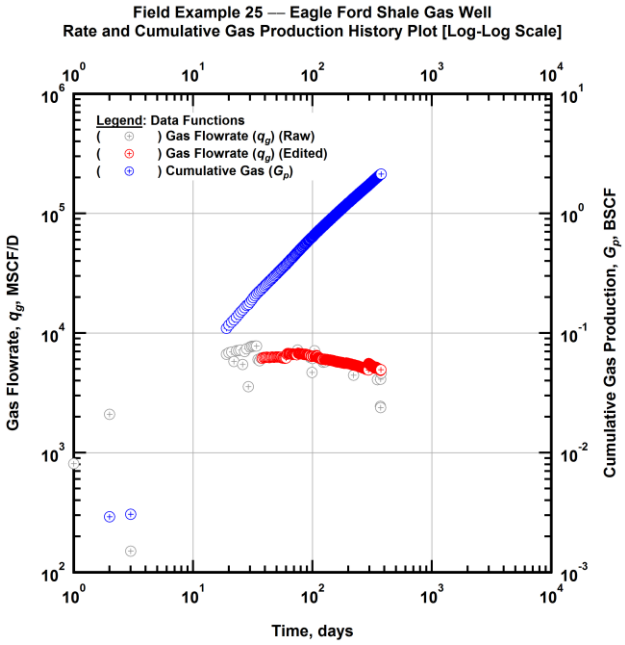

Figure A.724 — (Log-log Plot): Filtered rate and unfiltered cumulative gas production history plot — flowrate (q_g) and cumulative production (G_p) versus production time.

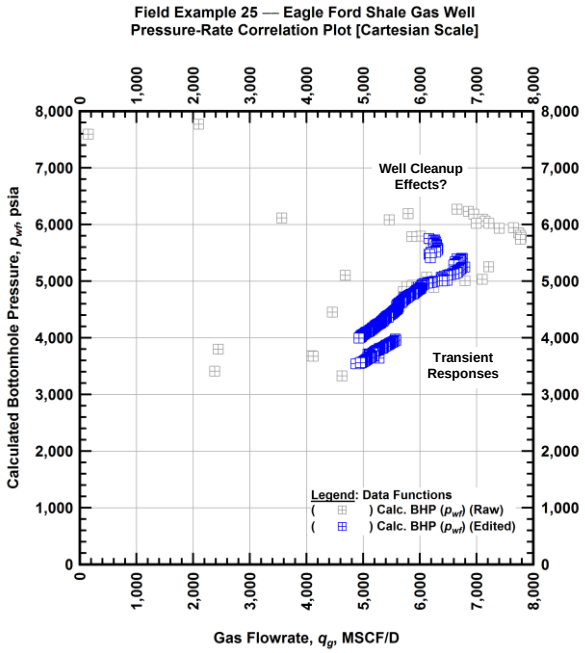

Figure A.725 — (Cartesian Plot): Filtered rate-pressure correlation plot — calculated bottomhole pressure (p_{wf}) versus flowrate (q_g).

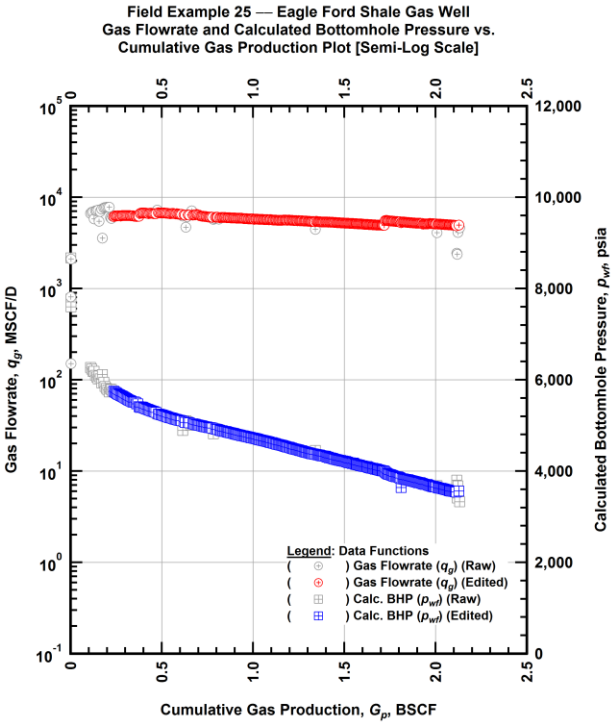

Figure A.726 — (Semi-log Plot): Filtered rate-pressure-cumulative production history plot — flowrate (q_g) and calculated bottomhole pressure (p_{wf}) versus cumulative production (G_p).

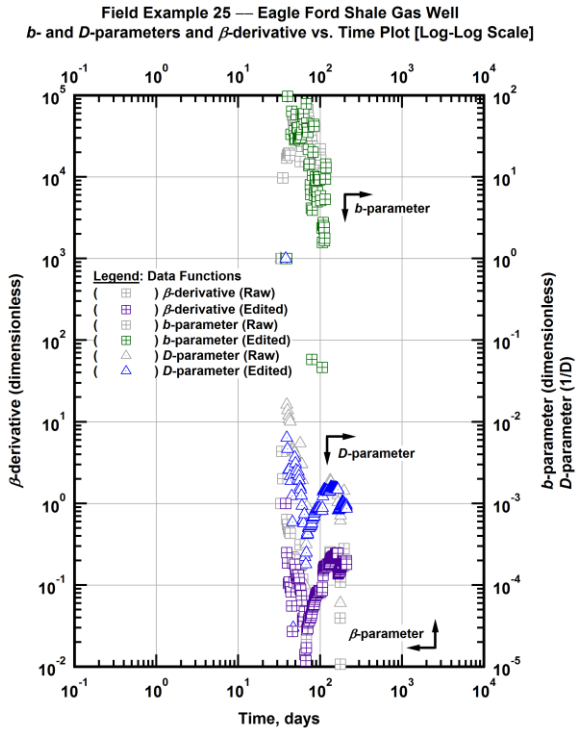

Figure A.727 — (Log-Log Plot): Filtered b, D and β production history plot — b- and D-parameters and β-derivative versus production time.

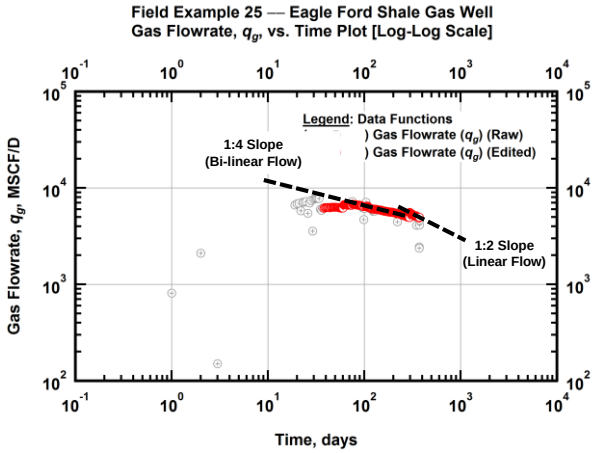

Figure A.728 — (Log-Log Plot): Filtered gas flowrate production history and flow regime identification plot — gas flowrate (q_g) versus production time.

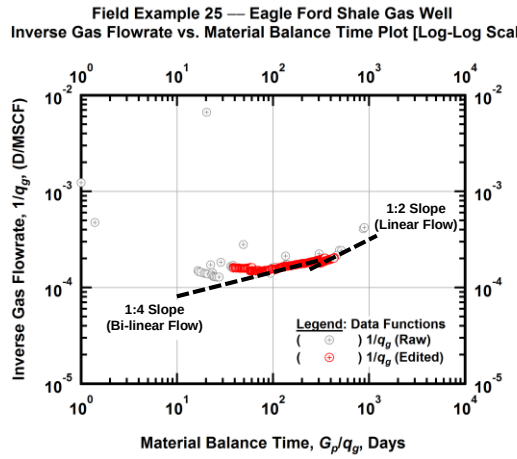

Figure A.729 — (Log-log Plot): Filtered inverse rate with material balance time plot — inverse gas flowrate ($1/q_g$) versus material balance time (G_p/q_g).

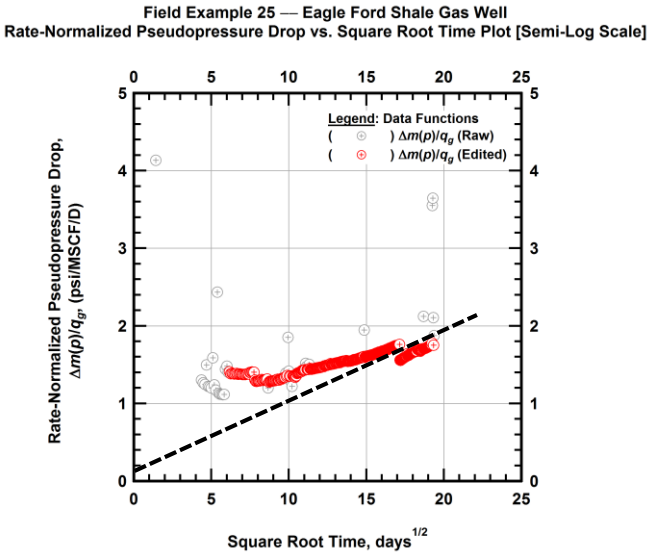

Figure A.730 — (Semi-log Plot): Filtered normalized pseudopressure drop production history plot — rate-normalized pseudopressure drop ($\Delta m(p)/q_g$) versus square root production time ($\sqrt{t}$).

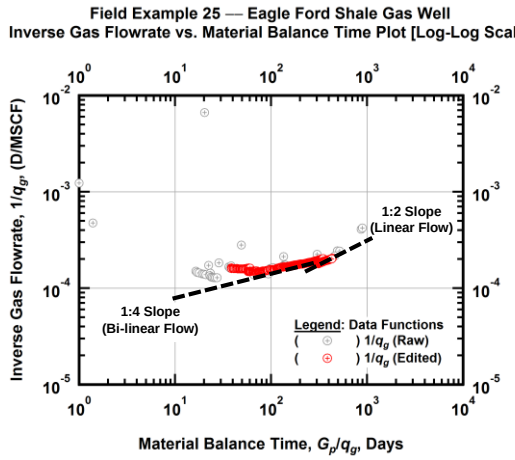

Figure A.731 — (Log-log Plot): Filtered normalized pseudopressure drop production history plot — rate-normalized pseudopressure drop ($\Delta m(p)/q_g$) versus production time.

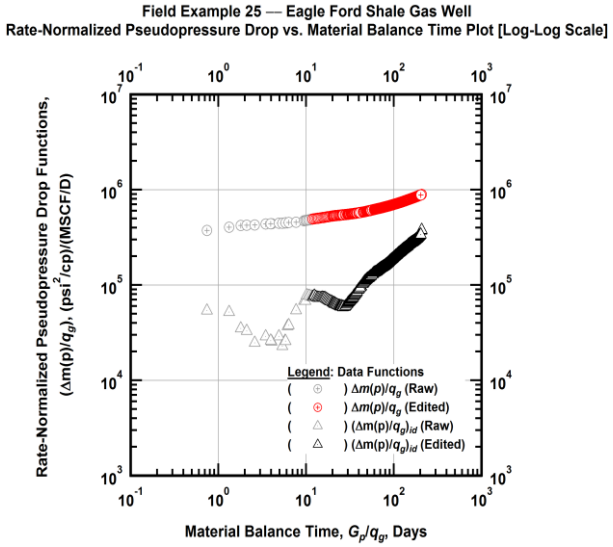

Figure A.732 — (Log-log Plot): "Log-log" diagnostic plot of the filtered production data — rate-normalized pseudopressure drop ($\Delta m(p)/q_g$) and rate-normalized pseudopressure drop integral-derivative $(\Delta m(p)/q_g)_{id}$ versus material balance time (G_p/q_g).

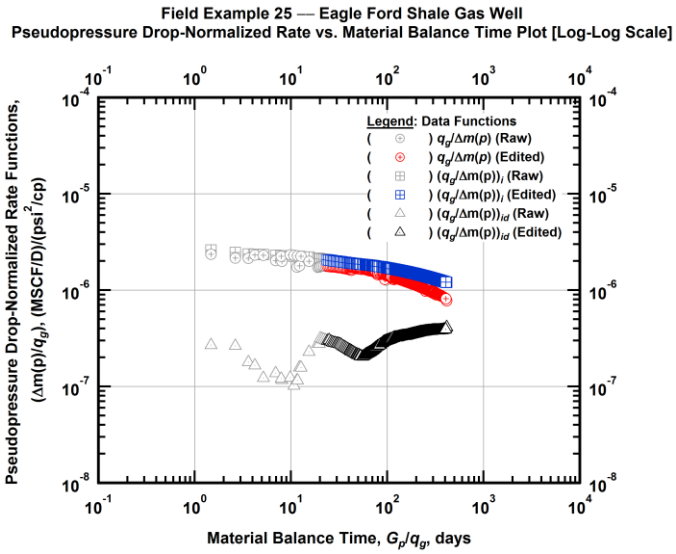

Figure A.733 — (Log-log Plot): "Blasingame" diagnostic plot of the filtered production data — pseudopressure drop-normalized gas flowrate ($q_g/\Delta m(p)$), pseudopressure drop-normalized gas flowrate integral $(q_g/\Delta m(p))_i$ and pseudopressure drop-normalized gas flowrate integral-derivative $(q_g/\Delta m(p))_{id}$ versus material balance time (G_p/q_g).

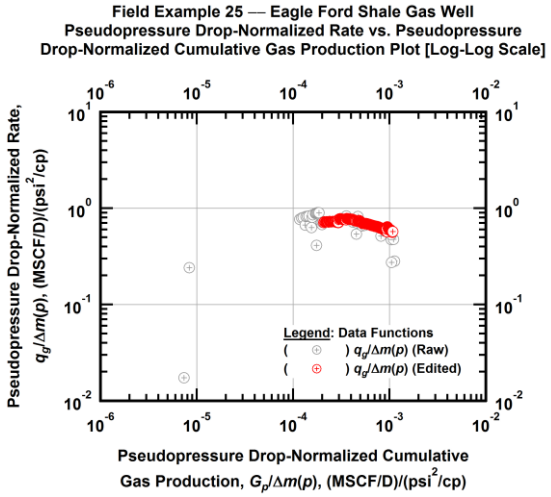

Figure A.734 — (Log-log Plot): Filtered normalized rate with normalized cumulative production plot — pseudopressure drop-normalized gas flowrate ($q_g/\Delta m(p)$) versus pseudopressure drop-normalized cumulative gas production ($G_p/\Delta m(p)$).

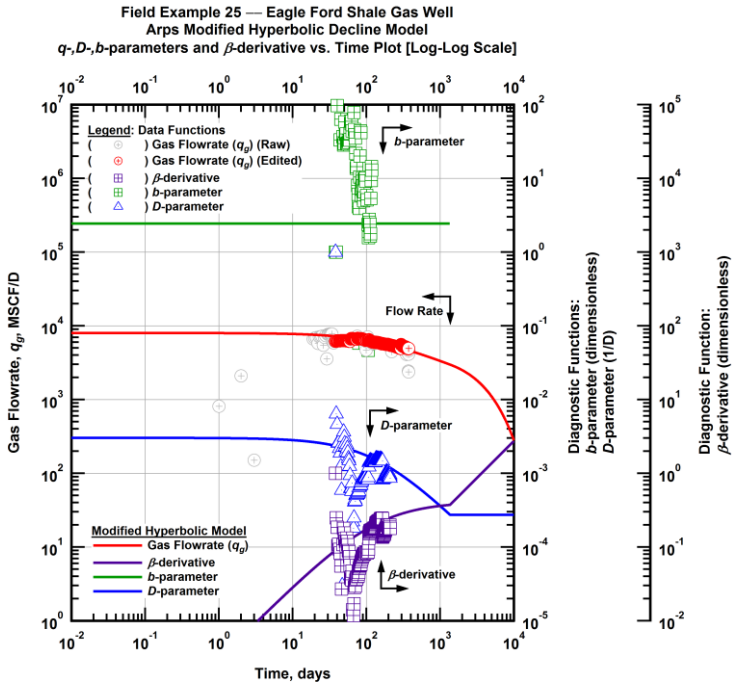

Figure A.735 — (Log-Log Plot): Arps modified hyperbolic decline model plot — time-rate model and data gas flowrate (q_g), *D*- and *b*-parameters and β-derivative versus production time.

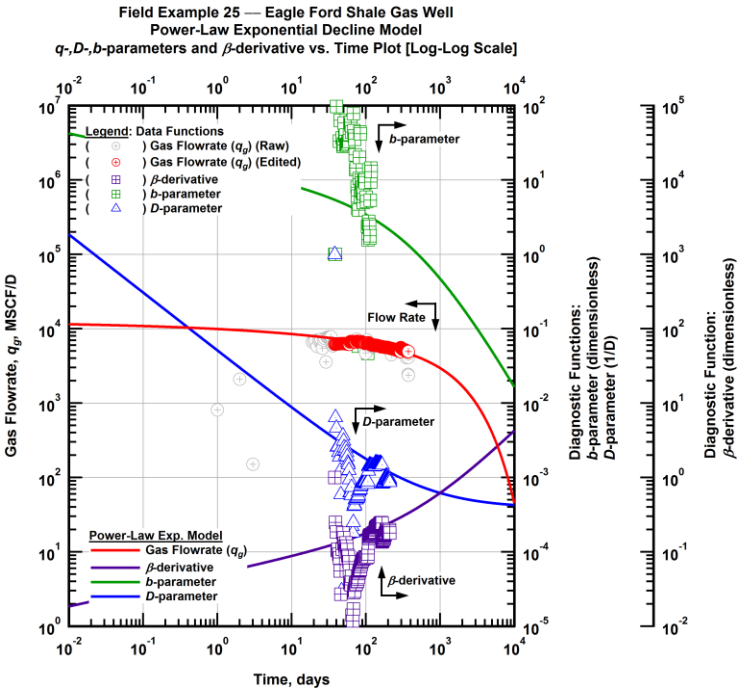

Figure A.736 — (Log-Log Plot): Power-law exponential decline model plot — time-rate model and data gas flowrate (q_g), *D*- and *b*-parameters and β-derivative versus production time.

Field Example 25 — Model-Based (Time-Rate-Pressure) Production Analysis

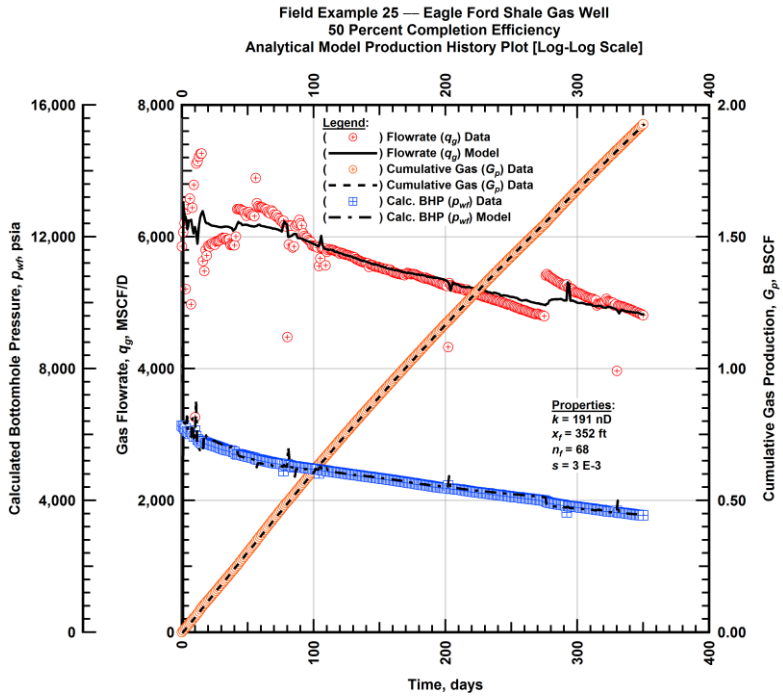

Figure A.737 — (Cartesian Plot): Production history plot — original gas flowrate (q_g), cumulative gas production (G_p), calculated bottomhole pressure (p_{wf}) and 50 percent completion efficiency model matches versus production time.

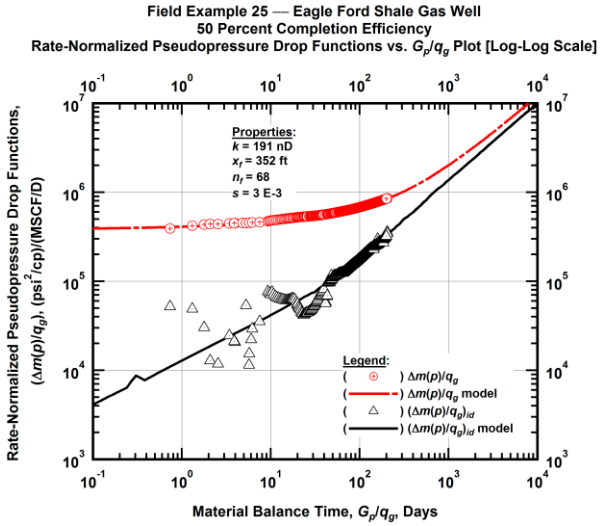

Figure A.738 — (Log-log Plot): "Log-log" diagnostic plot of the original production data — rate-normalized pseudopressure drop ($\Delta m(p)/q_g$), rate-normalized pseudopressure drop integral-derivative $(\Delta m(p)/q_g)_{id}$ and 50 percent completion efficiency model matches versus material balance time (G_p/q_g).

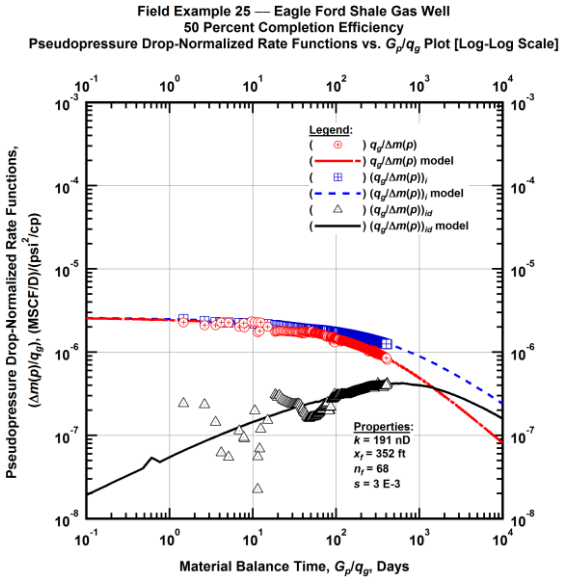

Figure A.739 — (Log-log Plot): "Blasingame" diagnostic plot of the original production data — pseudopressure drop-normalized gas flowrate ($q_g/\Delta m(p)$), pseudopressure drop-normalized gas flowrate integral $(q_g/\Delta m(p))_i$, pseudopressure drop-normalized gas flowrate integral-derivative $(q_g/\Delta m(p))_{id}$ and 50 percent completion efficiency model matches versus material balance time (G_p/q_g).

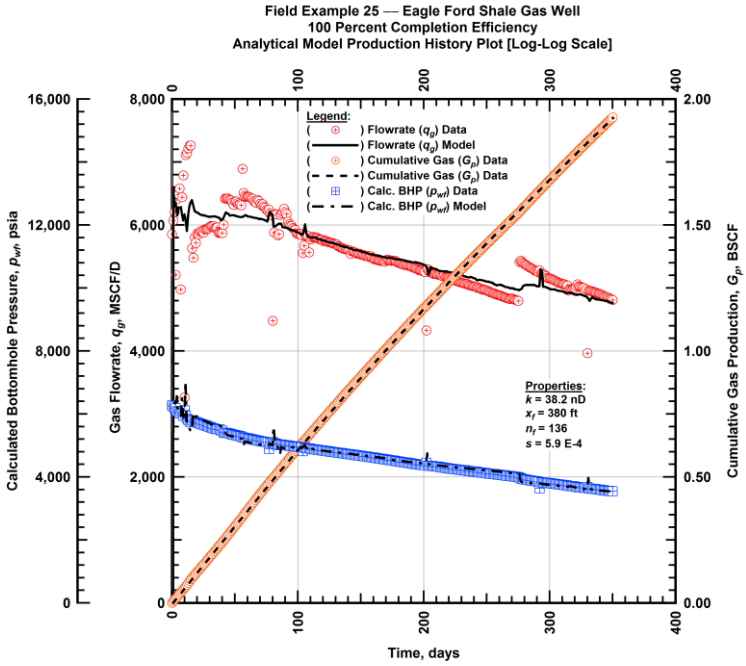

Figure A.740 — (Cartesian Plot): Production history plot — original gas flowrate (q_g), cumulative gas production (G_p), calculated bottomhole pressure (p_{wf}) and 100 percent completion efficiency model matches versus production time.

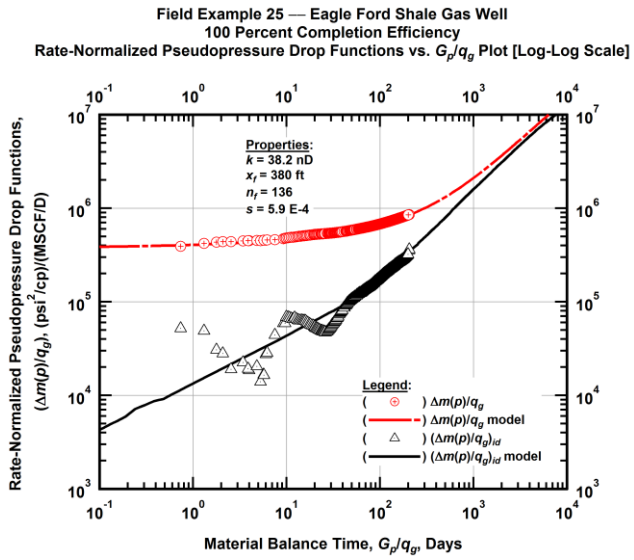

Figure A.741 — (Log-log Plot): "Log-log" diagnostic plot of the original production data — rate-normalized pseudopressure drop ($\Delta m(p)/q_g$), rate-normalized pseudopressure drop integral-derivative $(\Delta m(p)/q_g)_{id}$ and 100 percent completion efficiency model matches versus material balance time (G_p/q_g).

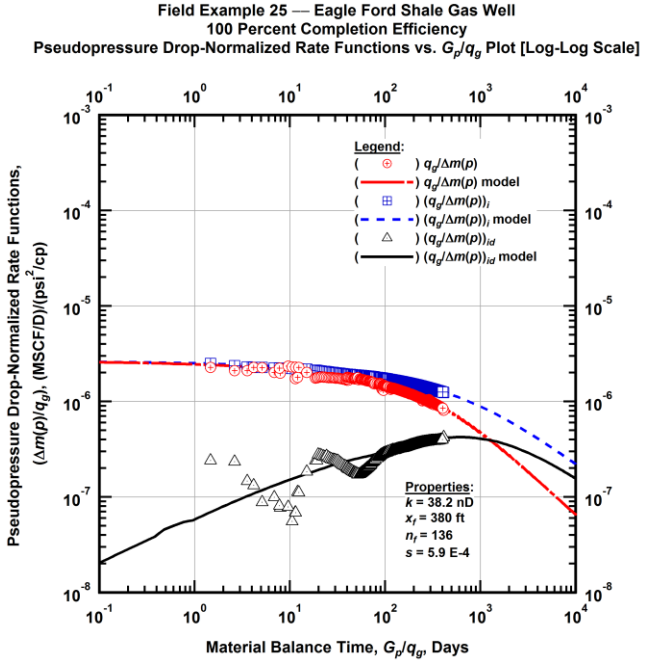

Figure A.742 — (Log-log Plot): "Blasingame" diagnostic plot of the original production data — pseudopressure drop-normalized gas flowrate ($q_g/\Delta m(p)$), pseudopressure drop-normalized gas flowrate integral $(q_g/\Delta m(p))_i$, pseudopressure drop-normalized gas flowrate integral-derivative $(q_g/\Delta m(p))_{id}$ and 100 percent completion efficiency model matches versus material balance time (G_p/q_g).

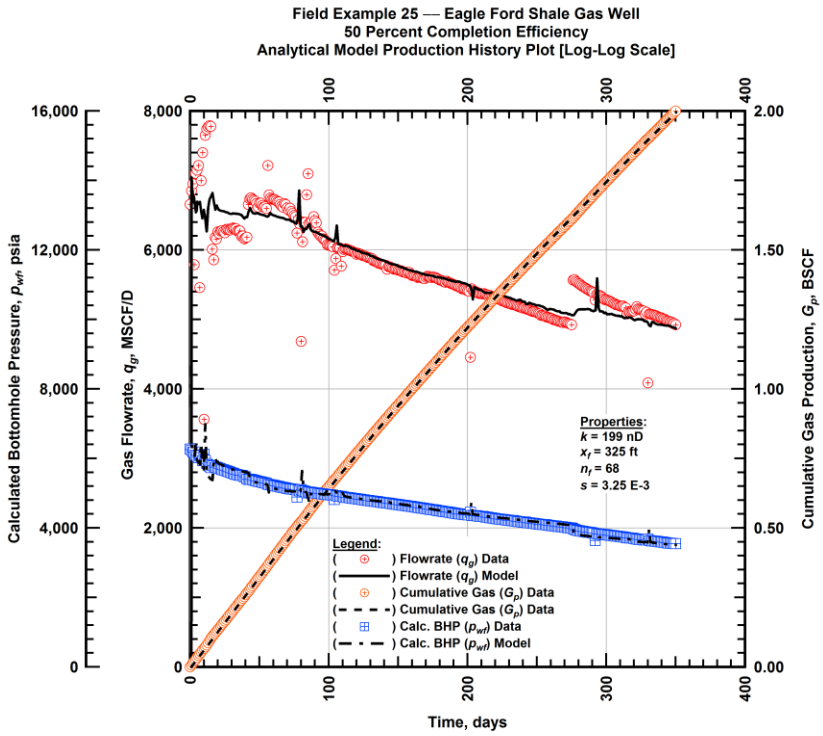

Figure A.743 — (Cartesian Plot): Production history plot — revised gas flowrate (q_g), cumulative gas production (G_p), calculated bottomhole pressure (p_{wf}) and 50 percent completion efficiency model matches versus production time.

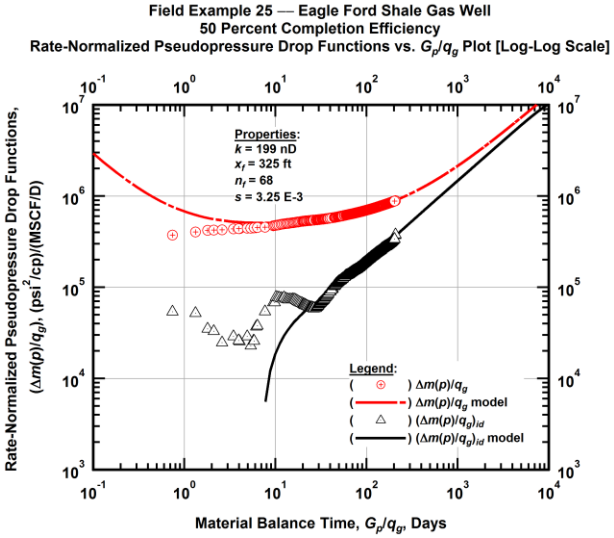

Figure A.744 — (Log-log Plot): "Log-log" diagnostic plot of the revised production data — rate-normalized pseudopressure drop ($\Delta m(p)/q_g$), rate-normalized pseudopressure drop integral-derivative $(\Delta m(p)/q_g)_{id}$ and 50 percent completion efficiency model matches versus material balance time (G_p/q_g).

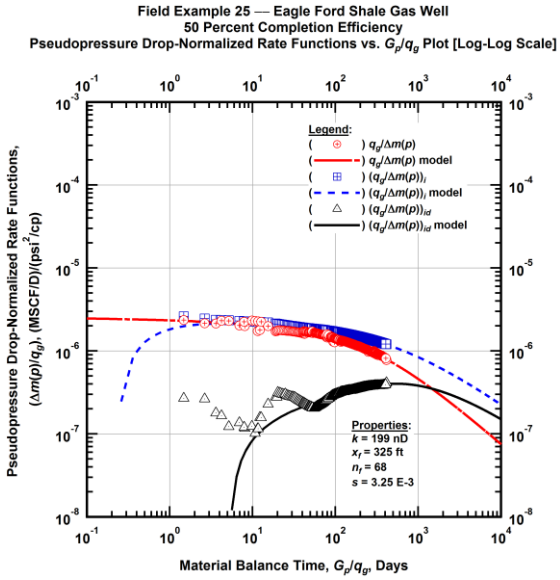

Figure A.745 — (Log-log Plot): "Blasingame" diagnostic plot of the revised production data — pseudopressure drop-normalized gas flowrate ($q_g/\Delta m(p)$), pseudopressure drop-normalized gas flowrate integral $(q_g/\Delta m(p))_i$, pseudopressure drop-normalized gas flowrate integral-derivative $(q_g/\Delta m(p))_{id}$ and 50 percent completion efficiency model matches versus material balance time (G_p/q_g).

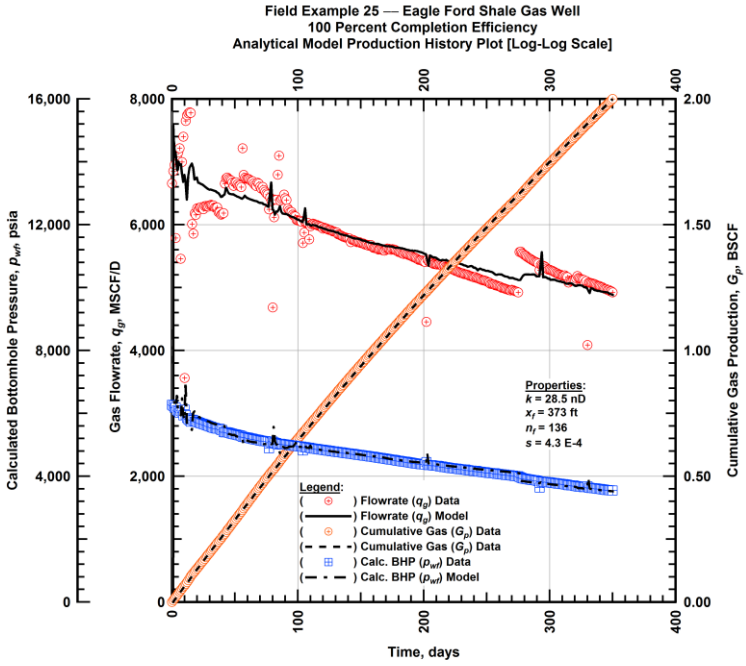

Figure A.746 — (Cartesian Plot): Production history plot — revised gas flowrate (q_g), cumulative gas production (G_p), calculated bottomhole pressure (p_{wf}) and 100 percent completion efficiency model matches versus production time.

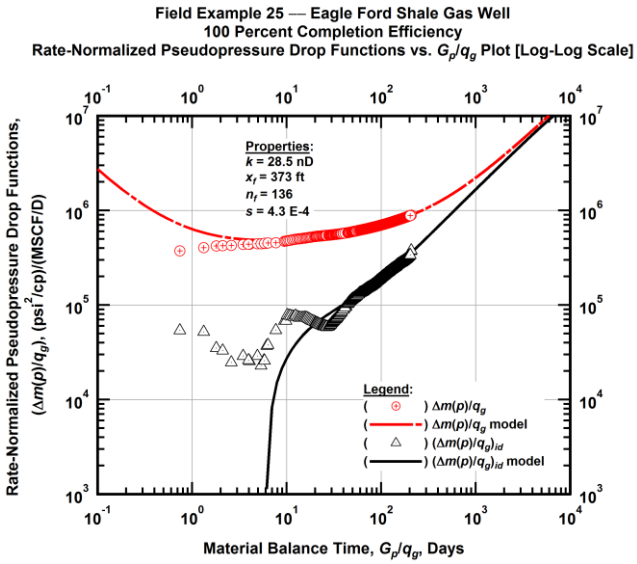

Figure A.747 — (Log-log Plot): "Log-log" diagnostic plot of the revised production data — rate-normalized pseudopressure drop ($\Delta m(p)/q_g$), rate-normalized pseudopressure drop integral-derivative $(\Delta m(p)/q_g)_{id}$ and 100 percent completion efficiency model matches versus material balance time (G_p/q_g).

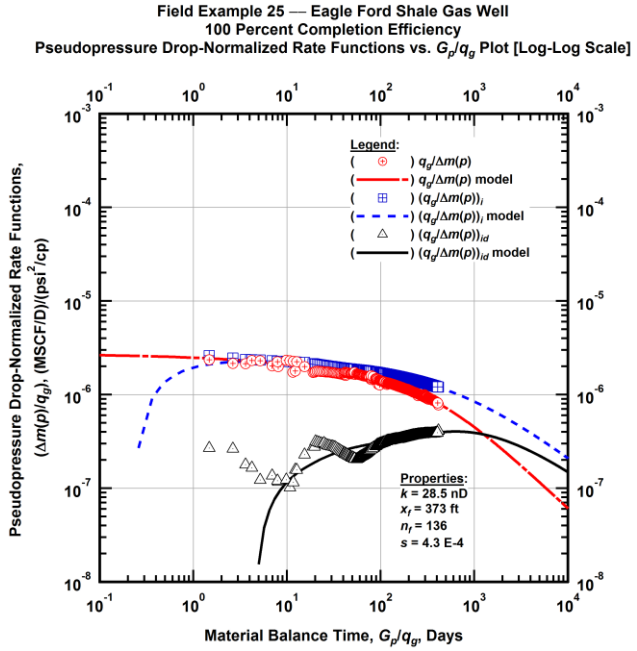

Figure A.748 — (Log-log Plot): "Blasingame" diagnostic plot of the revised production data — pseudopressure drop-normalized gas flowrate ($q_g/\Delta m(p)$), pseudopressure drop-normalized gas flowrate integral $(q_g/\Delta m(p))_i$, pseudopressure drop-normalized gas flowrate integral-derivative $(q_g/\Delta m(p))_{id}$ and 100 percent completion efficiency model matches versus material balance time (G_p/q_g).

Field Example 25 — 30-Year EUR Model Comparison

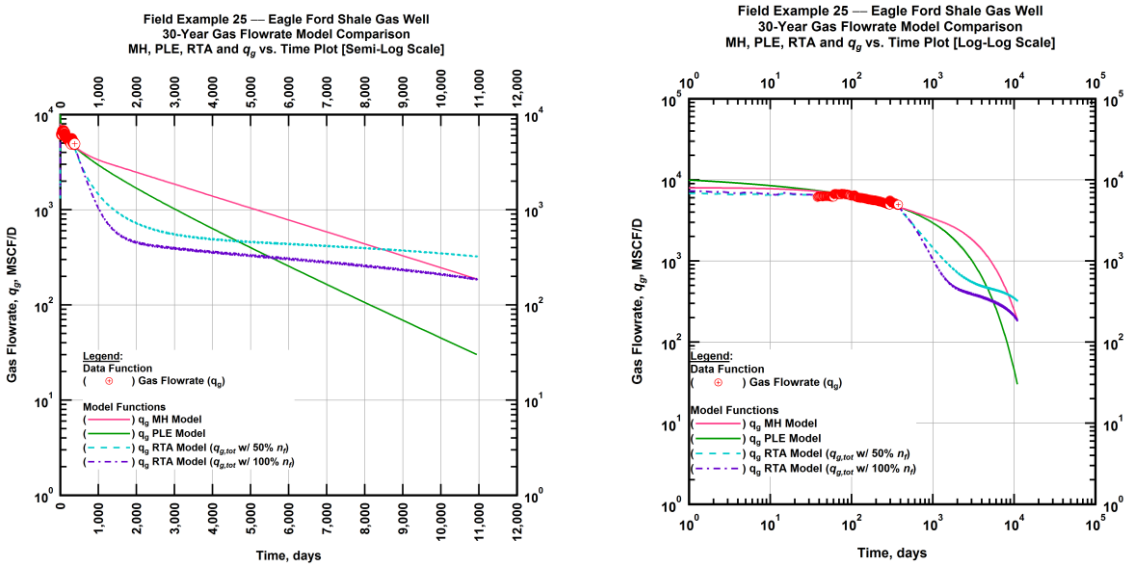

A **B**

Figure A.749 — (A — Semi-Log Plot) and (B — Log-Log Plot): Estimated 30-year revised gas flowrate model comparison — Arps modified hyperbolic decline model, power-law exponential decline model, and 50 percent and 100 percent completion efficiency RTA models revised gas 30-year estimated flowrate decline and historic gas flowrate data (q_g) versus production time.

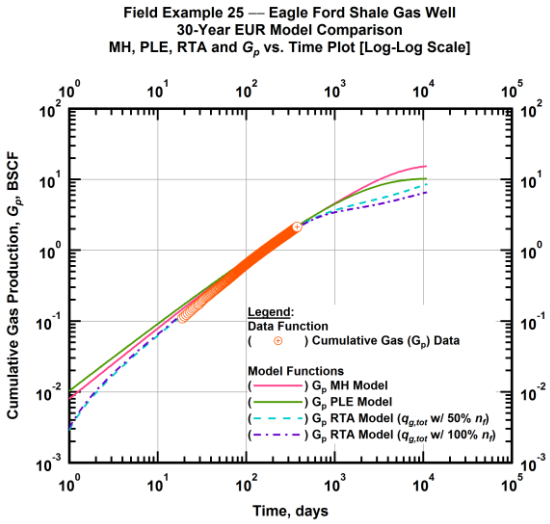

Figure A.750 — (Log-log Plot): PVT revised gas 30-year estimated cumulative production volume model comparison — Arps modified hyperbolic decline model, power-law exponential decline model, and 50 percent and 100 percent completion efficiency RTA model estimated 30-year cumulative gas production volumes and historic cumulative gas production (G_p) versus production time.

Table A.25 — 30-year estimated cumulative revised gas production (EUR), in units of BSCF, for the Arps modified hyperbolic, power-law exponential and analytical time-rate-pressure decline models.

Arps Modified Hyperbolic (BSCF)	Power-Law Exponential (BSCF)	RTA Analytical Model ($q_{g,tot}$ w/ 50% n_f) (BSCF)	RTA Analytical Model ($q_{g,tot}$ w/ 100% n_f) (BSCF)
15.82	10.13	8.71	6.73

Field Example 26 — Time-Rate Analysis

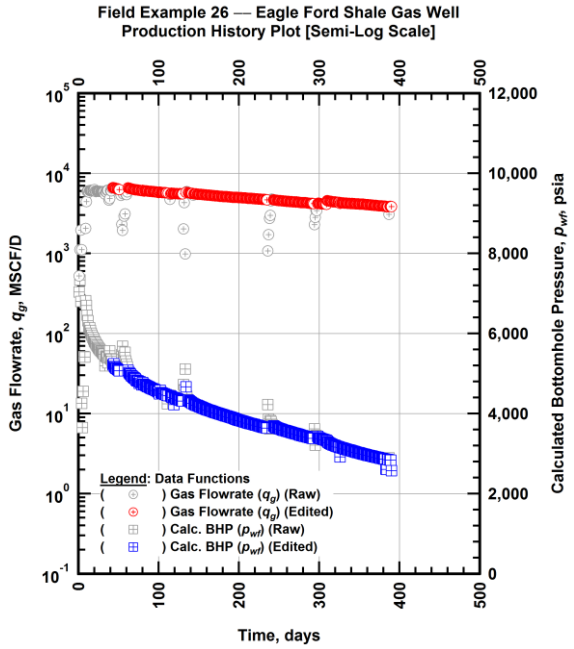

Figure A.751 — (Semi-log Plot): Filtered production history plot — flowrate (q_g) and calculated bottomhole pressure (p_{wf}) versus production time.

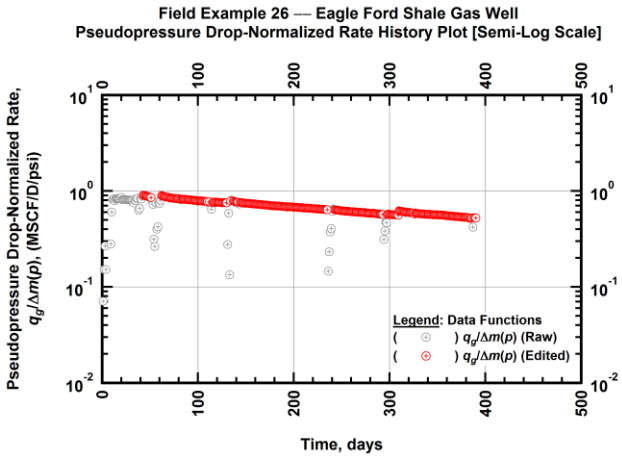

Figure A.752 — (Semi-log Plot): Filtered normalized rate production history plot — pseudopressure drop-normalized gas flowrate ($q_g/\Delta m(p)$) versus production time.

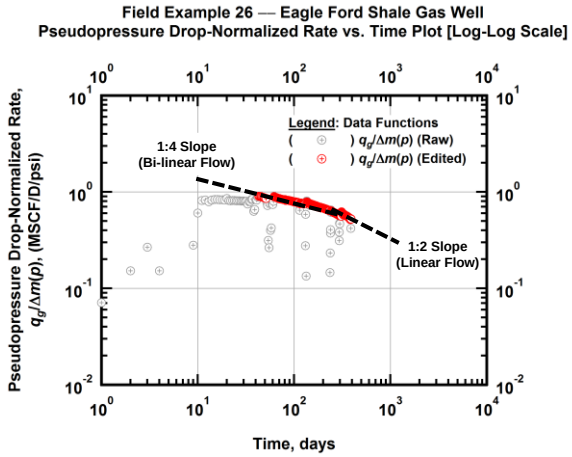

Figure A.753 — (Log-log Plot): Filtered normalized rate production history plot — pseudopressure drop-normalized gas flowrate ($q_g/\Delta m(p)$) versus production time.

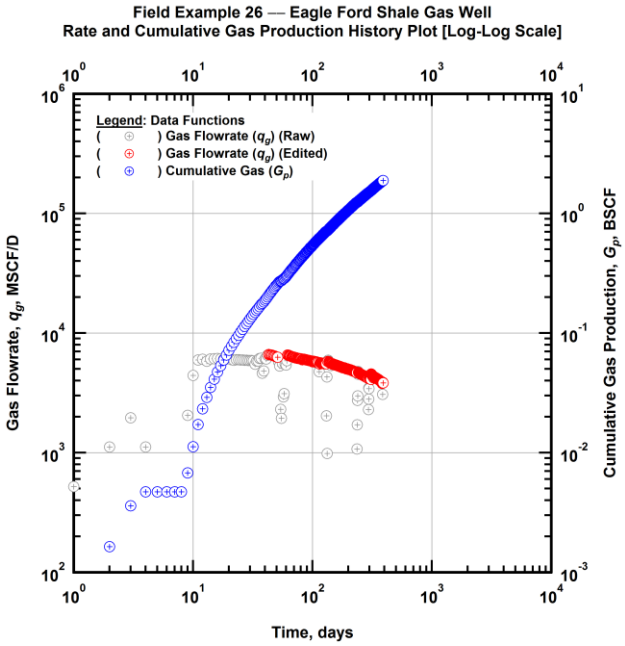

Figure A.754 — (Log-log Plot): Filtered rate and unfiltered cumulative gas production history plot — flowrate (q_g) and cumulative production (G_p) versus production time.

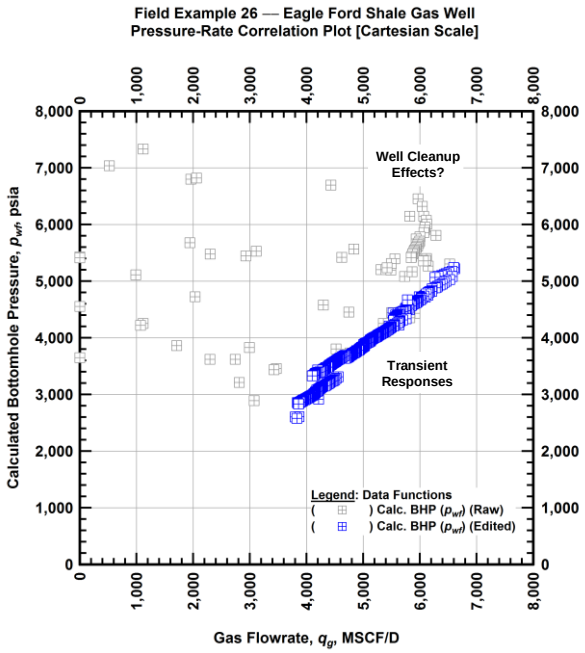

Figure A.755 — (Cartesian Plot): Filtered rate-pressure correlation plot — calculated bottomhole pressure (p_{wf}) versus flowrate (q_g).

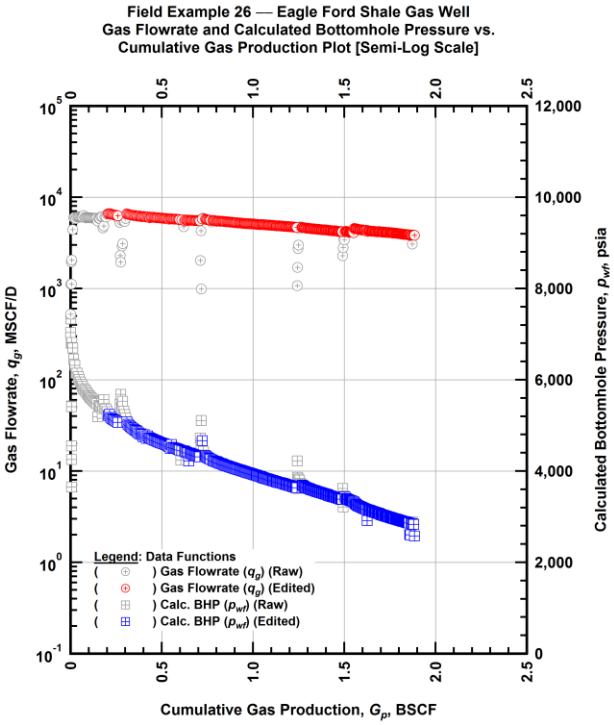

Figure A.756 — (Semi-log Plot): Filtered rate-pressure-cumulative production history plot — flowrate (q_g) and calculated bottomhole pressure (p_{wf}) versus cumulative production (G_p).

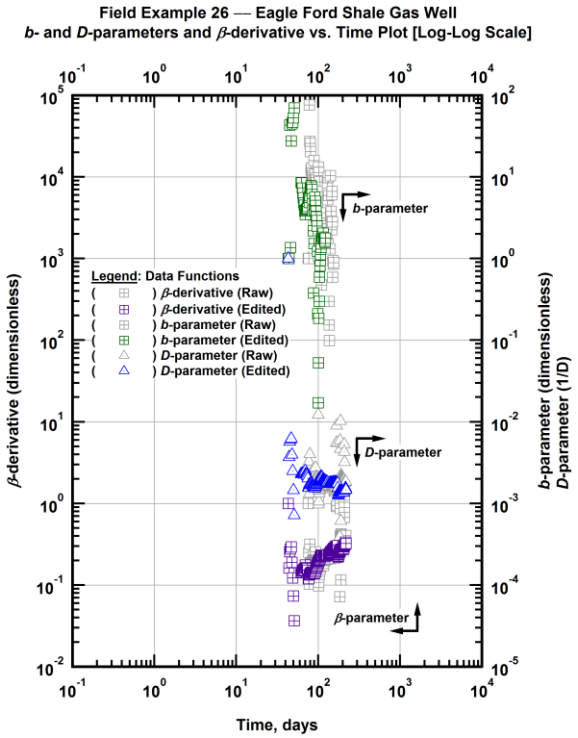

Figure A.757 — (Log-Log Plot): Filtered b, D and β production history plot — b- and D-parameters and β-derivative versus production time.

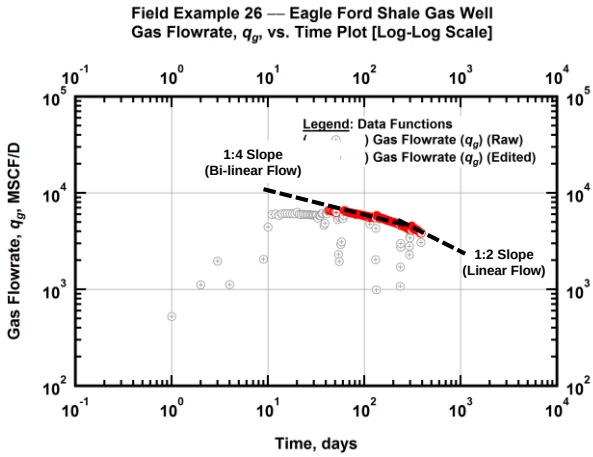

Figure A.758 — (Log-Log Plot): Filtered gas flowrate production history and flow regime identification plot — gas flowrate (q_g) versus production time.

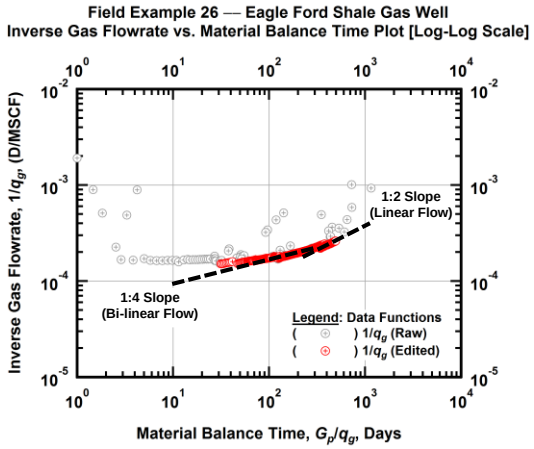

Figure A.759 — (Log-log Plot): Filtered inverse rate with material balance time plot — inverse gas flowrate ($1/q_g$) versus material balance time (G_p/q_g).

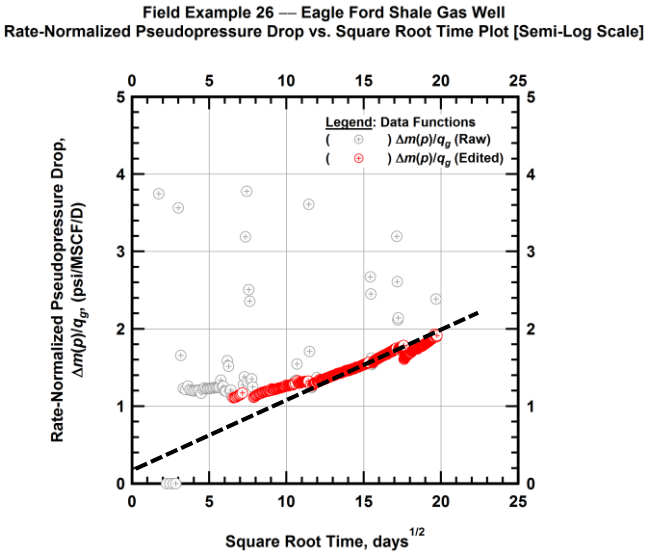

Figure A.760 — (Semi-log Plot): Filtered normalized pseudopressure drop production history plot — rate-normalized pseudopressure drop ($\Delta m(p)/q_g$) versus square root production time ($\sqrt{t}$).

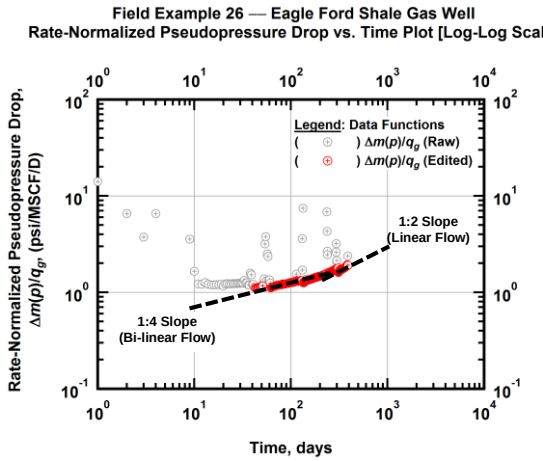

Figure A.761 — (Log-log Plot): Filtered normalized pseudopressure drop production history plot — rate-normalized pseudopressure drop ($\Delta m(p)/q_g$) versus production time.

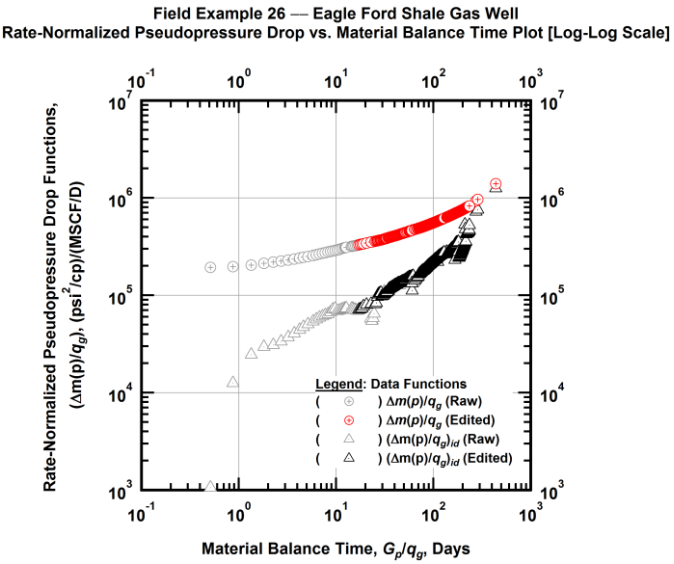

Figure A.762 — (Log-log Plot): "Log-log" diagnostic plot of the filtered production data — rate-normalized pseudopressure drop ($\Delta m(p)/q_g$) and rate-normalized pseudopressure drop integral-derivative $(\Delta m(p)/q_g)_{id}$ versus material balance time (G_p/q_g).

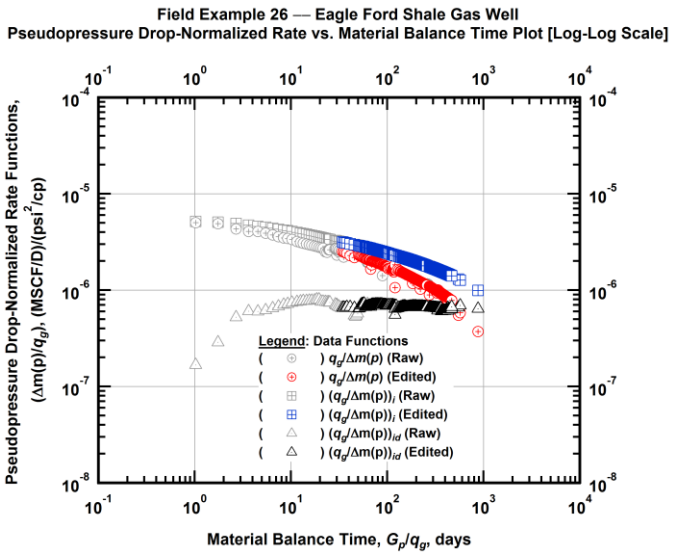

Figure A.763 — (Log-log Plot): "Blasingame" diagnostic plot of the filtered production data — pseudopressure drop-normalized gas flowrate ($q_g/\Delta m(p)$), pseudopressure drop-normalized gas flowrate integral $(q_g/\Delta m(p))_i$ and pseudopressure drop-normalized gas flowrate integral-derivative $(q_g/\Delta m(p))_{id}$ versus material balance time (G_p/q_g).

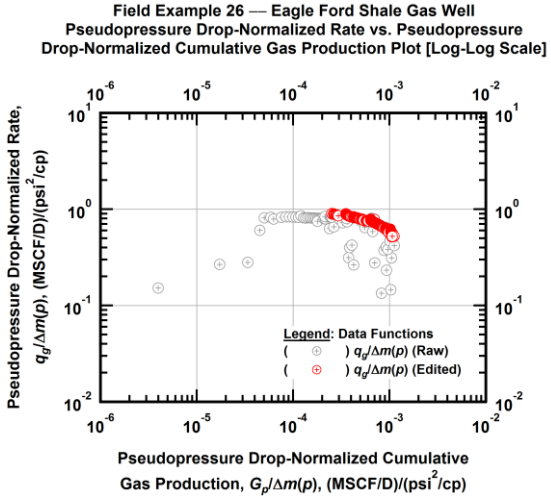

Figure A.764 — (Log-log Plot): Filtered normalized rate with normalized cumulative production plot — pseudopressure drop-normalized gas flowrate ($q_g/\Delta m(p)$) versus pseudopressure drop-normalized cumulative gas production ($G_p/\Delta m(p)$).

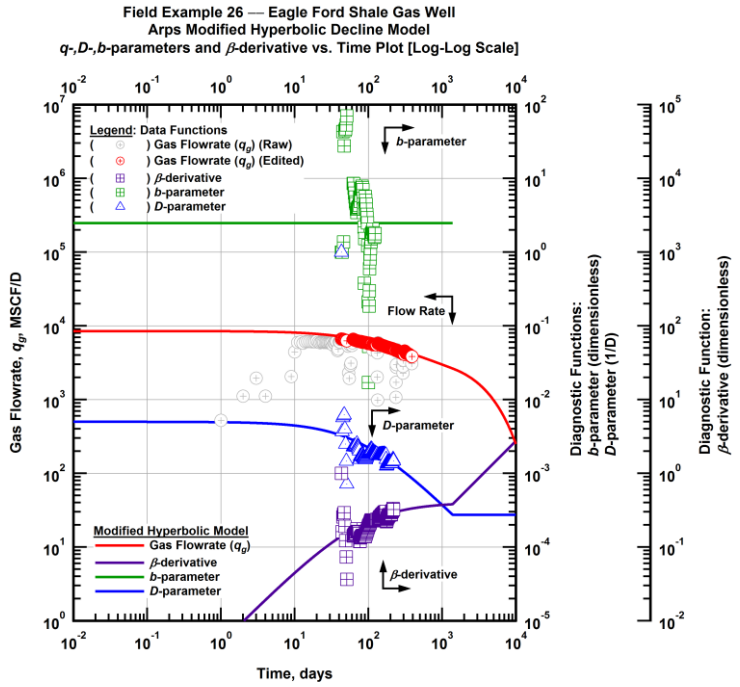

Figure A.765 — (Log-Log Plot): Arps modified hyperbolic decline model plot — time-rate model and data gas flowrate (q_g), *D*- and *b*-parameters and β-derivative versus production time.

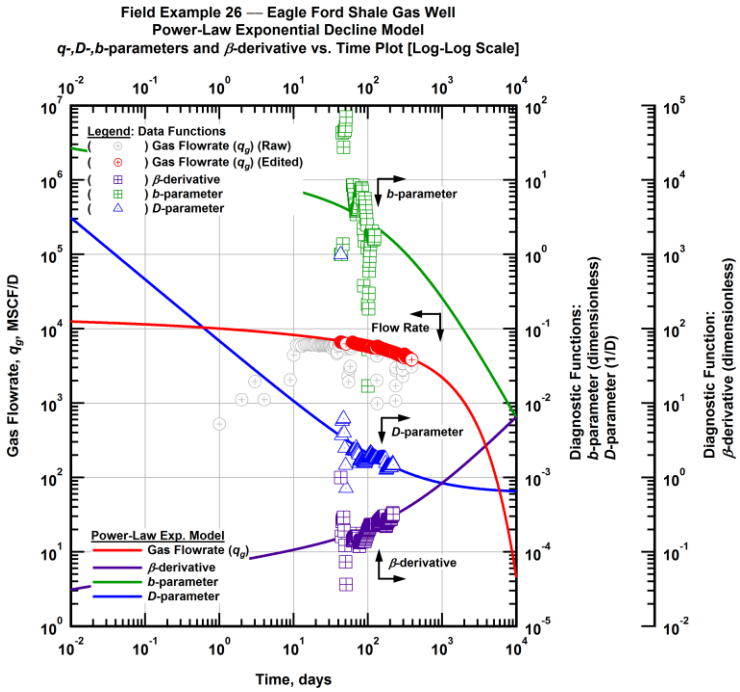

Figure A.766 — (Log-Log Plot): Power-law exponential decline model plot — time-rate model and data gas flowrate (q_g), *D*- and *b*-parameters and β-derivative versus production time.

Field Example 26 — Model-Based (Time-Rate-Pressure) Production Analysis

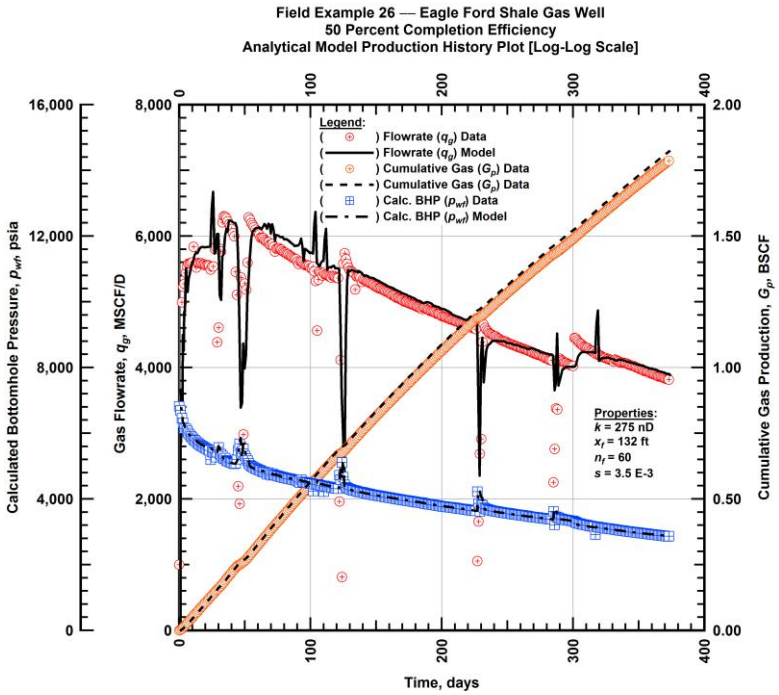

Figure A.767 — (Cartesian Plot): Production history plot — original gas flowrate (q_g), cumulative gas production (G_p), calculated bottomhole pressure (p_{wf}) and 50 percent completion efficiency model matches versus production time.

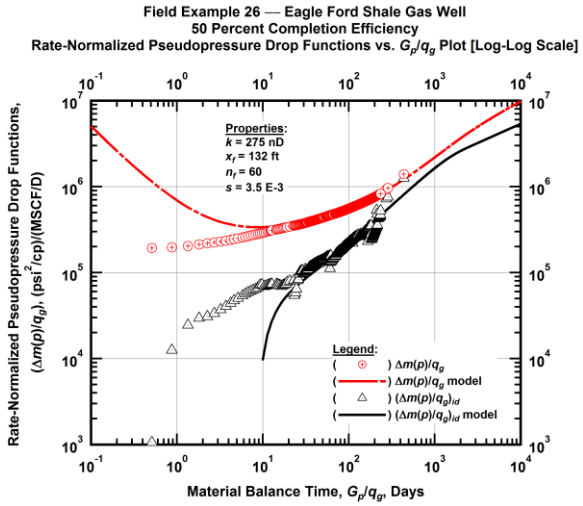

Figure A.768 — (Log-log Plot): "Log-log" diagnostic plot of the original production data — rate-normalized pseudopressure drop ($\Delta m(p)/q_g$), rate-normalized pseudopressure drop integral-derivative $(\Delta m(p)/q_g)_{id}$ and 50 percent completion efficiency model matches versus material balance time (G_p/q_g).

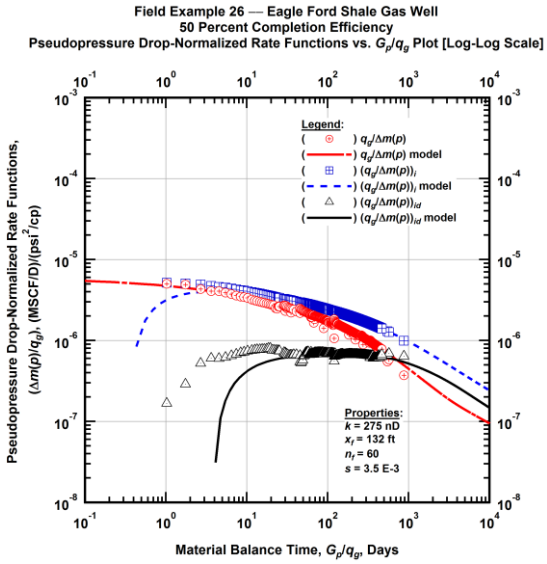

Figure A.769 — (Log-log Plot): "Blasingame" diagnostic plot of the original production data — pseudopressure drop-normalized gas flowrate ($q_g/\Delta m(p)$), pseudopressure drop-normalized gas flowrate integral $(q_g/\Delta m(p))_i$, pseudopressure drop-normalized gas flowrate integral-derivative $(q_g/\Delta m(p))_{id}$ and 50 percent completion efficiency model matches versus material balance time (G_p/q_g).

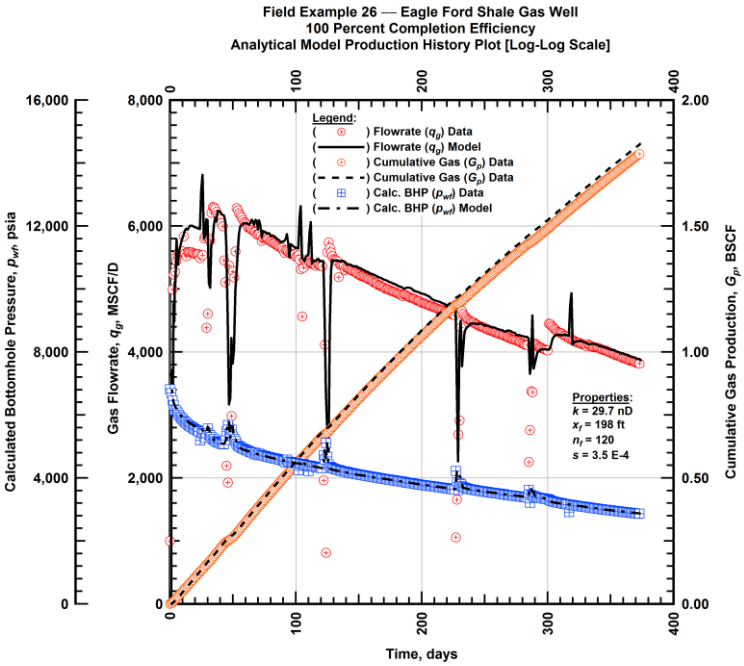

Figure A.770 — (Cartesian Plot): Production history plot — original gas flowrate (q_g), cumulative gas production (G_p), calculated bottomhole pressure (p_{wf}) and 100 percent completion efficiency model matches versus production time.

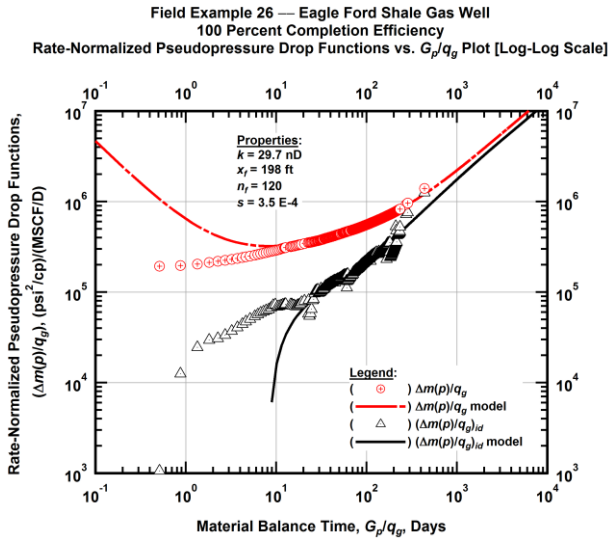

Figure A.771 — (Log-log Plot): "Log-log" diagnostic plot of the original production data — rate-normalized pseudopressure drop ($\Delta m(p)/q_g$), rate-normalized pseudopressure drop integral-derivative $(\Delta m(p)/q_g)_{id}$ and 100 percent completion efficiency model matches versus material balance time (G_p/q_g).

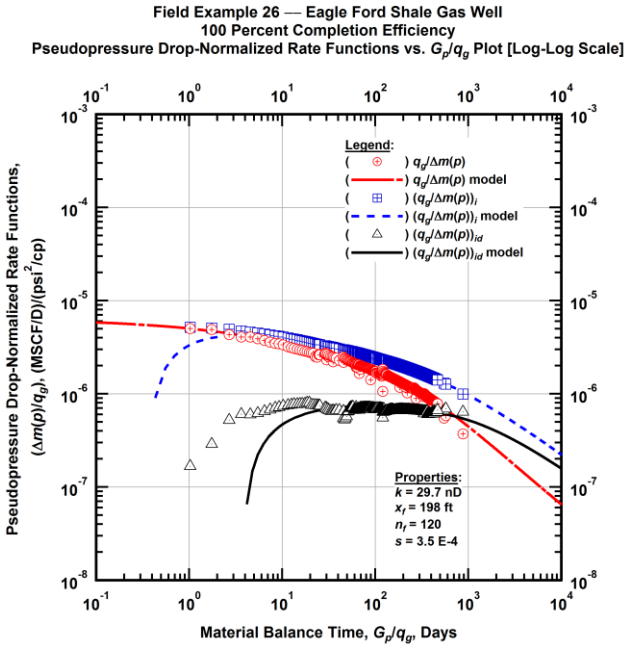

Figure A.772 — (Log-log Plot): "Blasingame" diagnostic plot of the original production data — pseudopressure drop-normalized gas flowrate ($q_g/\Delta m(p)$), pseudopressure drop-normalized gas flowrate integral $(q_g/\Delta m(p))_i$, pseudopressure drop-normalized gas flowrate integral-derivative $(q_g/\Delta m(p))_{id}$ and 100 percent completion efficiency model matches versus material balance time (G_p/q_g).

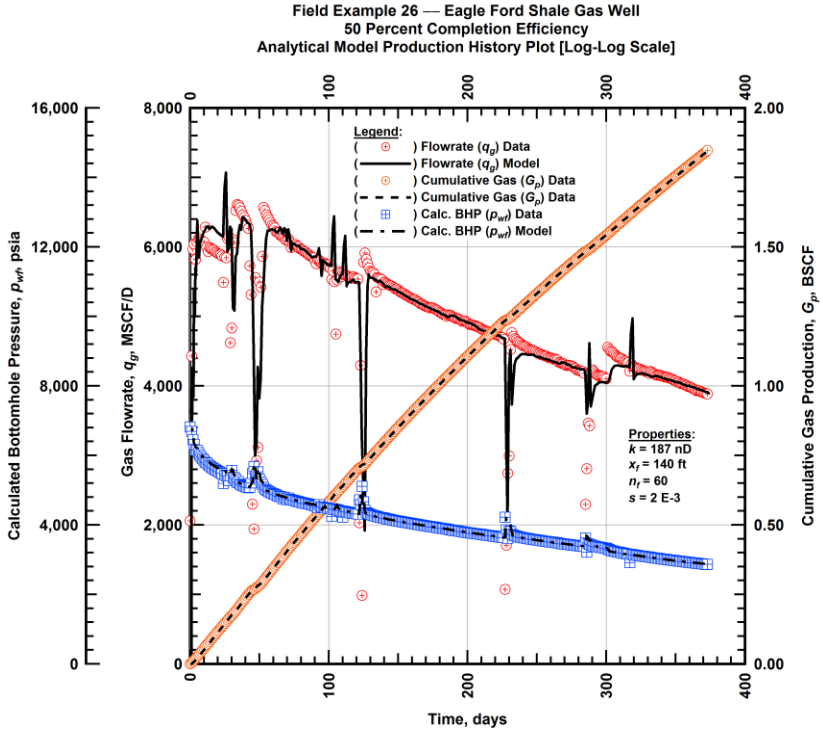

Figure A.773 — (Cartesian Plot): Production history plot — revised gas flowrate (q_g), cumulative gas production (G_p), calculated bottomhole pressure (p_{wf}) and 50 percent completion efficiency model matches versus production time.

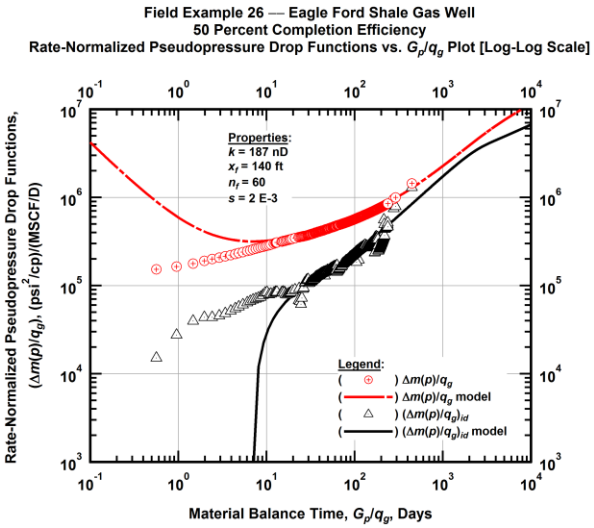

Figure A.774 — (Log-log Plot): "Log-log" diagnostic plot of the revised production data — rate-normalized pseudopressure drop ($\Delta m(p)/q_g$), rate-normalized pseudopressure drop integral-derivative $(\Delta m(p)/q_g)_{id}$ and 50 percent completion efficiency model matches versus material balance time (G_p/q_g).

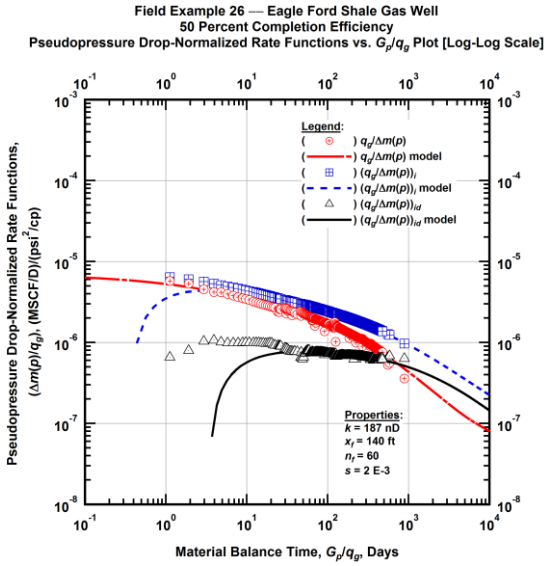

Figure A.775 — (Log-log Plot): "Blasingame" diagnostic plot of the revised production data — pseudopressure drop-normalized gas flowrate ($q_g/\Delta m(p)$), pseudopressure drop-normalized gas flowrate integral $(q_g/\Delta m(p))_i$, pseudopressure drop-normalized gas flowrate integral-derivative $(q_g/\Delta m(p))_{id}$ and 50 percent completion efficiency model matches versus material balance time (G_p/q_g).

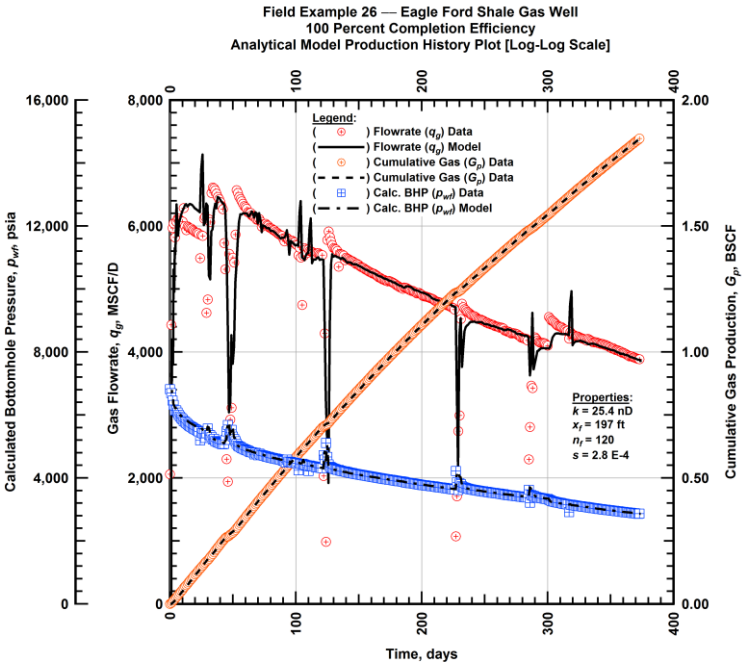

Figure A.776 — (Cartesian Plot): Production history plot — revised gas flowrate (q_g), cumulative gas production (G_p), calculated bottomhole pressure (p_{wf}) and 100 percent completion efficiency model matches versus production time.

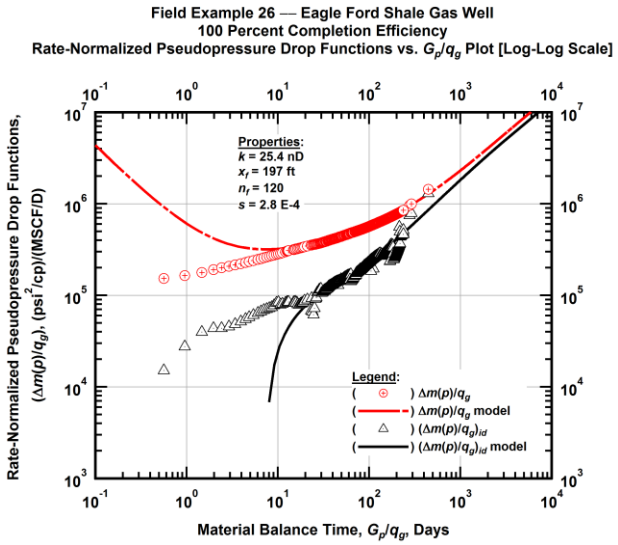

Figure A.777 — (Log-log Plot): "Log-log" diagnostic plot of the revised production data — rate-normalized pseudopressure drop ($\Delta m(p)/q_g$), rate-normalized pseudopressure drop integral-derivative $(\Delta m(p)/q_g)_{id}$ and 100 percent completion efficiency model matches versus material balance time (G_p/q_g).

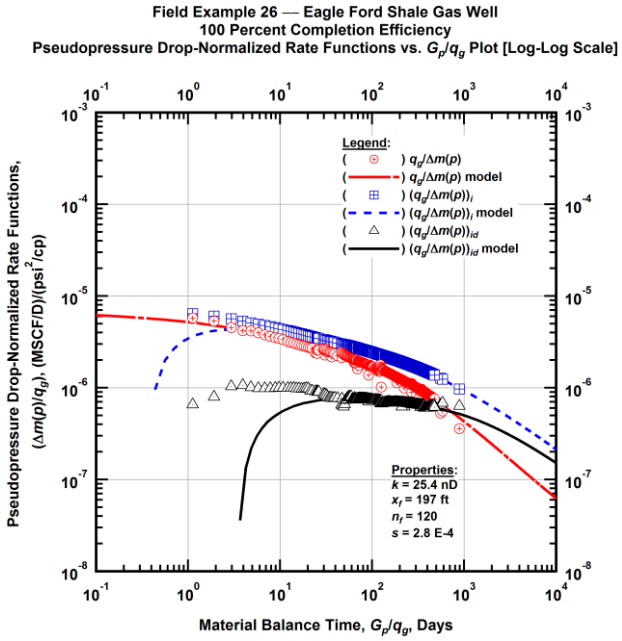

Figure A.778 — (Log-log Plot): "Blasingame" diagnostic plot of the revised production data — pseudopressure drop-normalized gas flowrate ($q_g/\Delta m(p)$), pseudopressure drop-normalized gas flowrate integral $(q_g/\Delta m(p))_i$, pseudopressure drop-normalized gas flowrate integral-derivative $(q_g/\Delta m(p))_{id}$ and 100 percent completion efficiency model matches versus material balance time (G_p/q_g).

Field Example 26 — 30-Year EUR Model Comparison

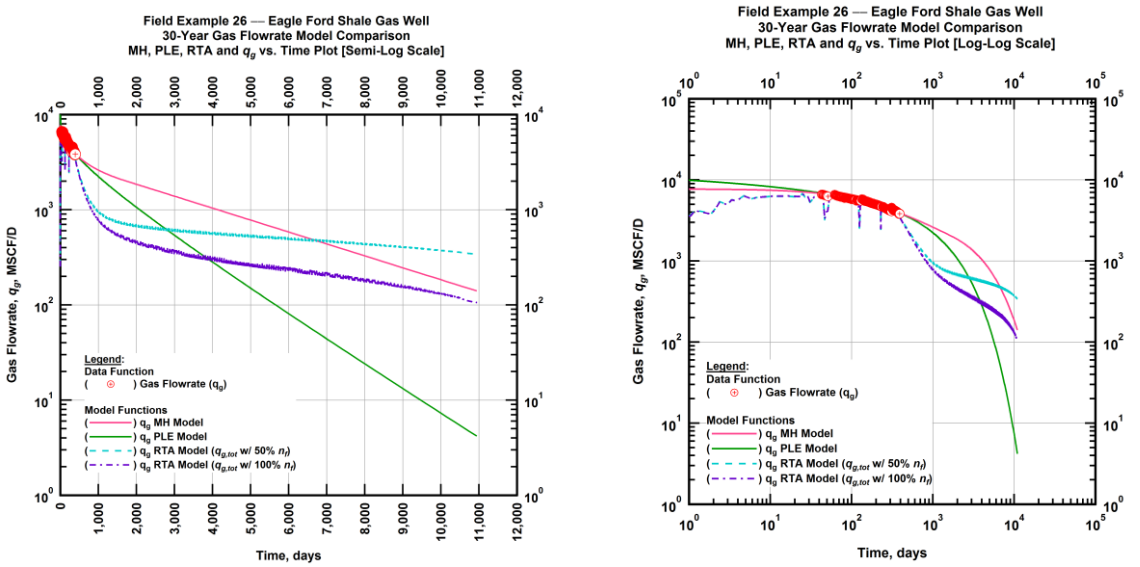

A **B**

Figure A.779 — (A — Semi-Log Plot) and (B — Log-Log Plot): Estimated 30-year revised gas flowrate model comparison — Arps modified hyperbolic decline model, power-law exponential decline model, and 50 percent and 100 percent completion efficiency RTA models revised gas 30-year estimated flowrate decline and historic gas flowrate data (q_g) versus production time.

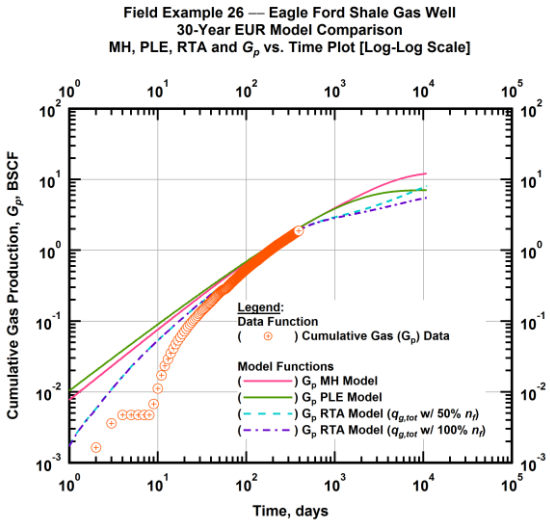

Figure A.780 — (Log-log Plot): PVT revised gas 30-year estimated cumulative production volume model comparison — Arps modified hyperbolic decline model, power-law exponential decline model, and 50 percent and 100 percent completion efficiency RTA model estimated 30-year cumulative gas production volumes and historic cumulative gas production (G_p) versus production time.

Table A.26 — 30-year estimated cumulative revised gas production (EUR), in units of BSCF, for the Arps modified hyperbolic, power-law exponential and analytical time-rate-pressure decline models.

Arps Modified Hyperbolic (BSCF)	Power-Law Exponential (BSCF)	RTA Analytical Model ($q_{g,tot}$ w/ 50% n_f) (BSCF)	RTA Analytical Model ($q_{g,tot}$ w/ 100% n_f) (BSCF)
12.20	6.84	8.17	5.55

Field Example 27 — Time-Rate Analysis

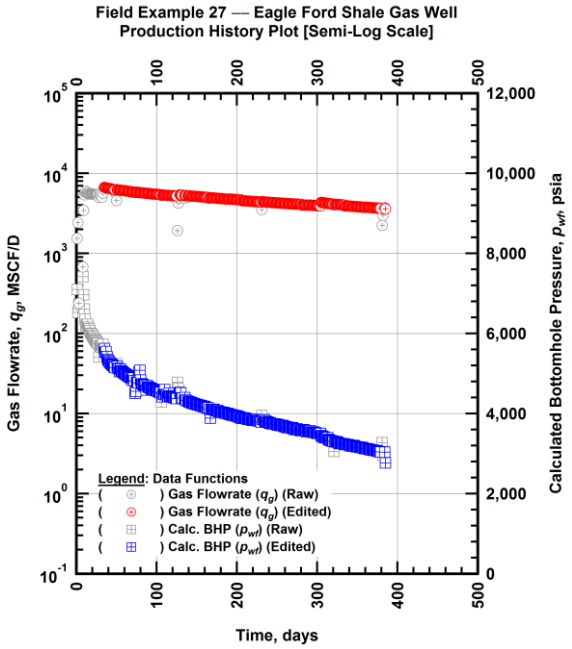

Figure A.781 — (Semi-log Plot): Filtered production history plot — flowrate (q_g) and calculated bottomhole pressure (p_{wf}) versus production time.

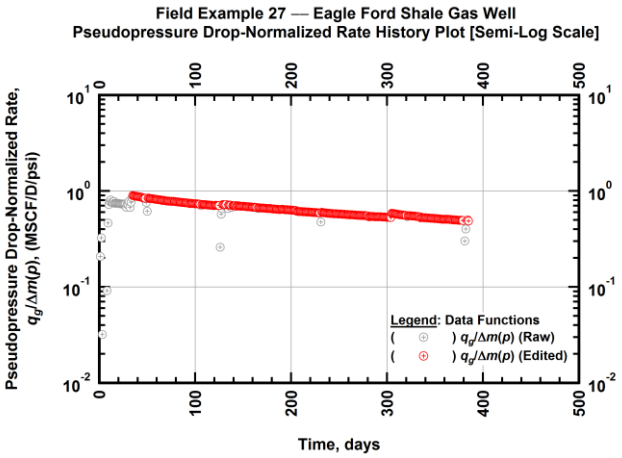

Figure A.782 — (Semi-log Plot): Filtered normalized rate production history plot — pseudopressure drop-normalized gas flowrate ($q_g/\Delta m(p)$) versus production time.

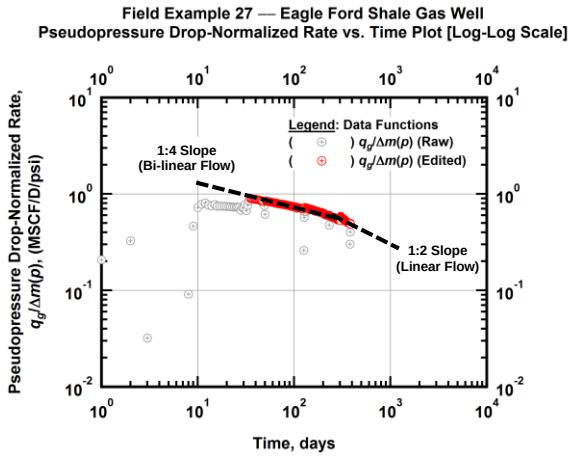

Figure A.783 — (Log-log Plot): Filtered normalized rate production history plot — pseudopressure drop-normalized gas flowrate ($q_g/\Delta m(p)$) versus production time.

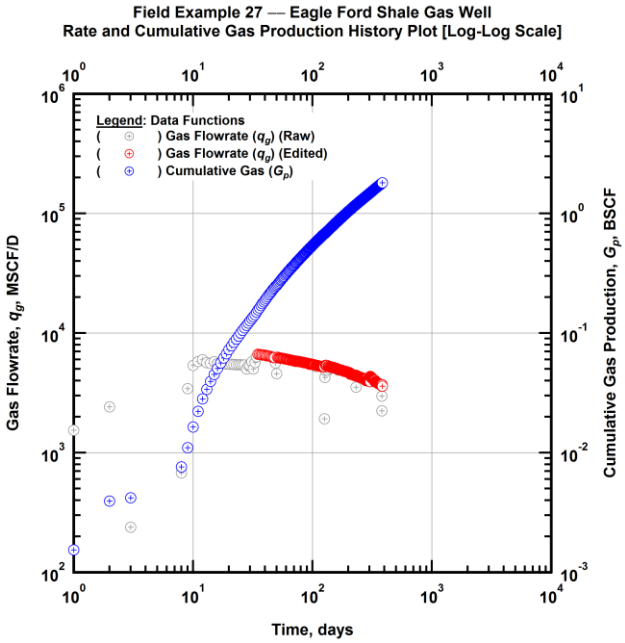

Figure A.784 — (Log-log Plot): Filtered rate and unfiltered cumulative gas production history plot — flowrate (q_g) and cumulative production (G_p) versus production time.

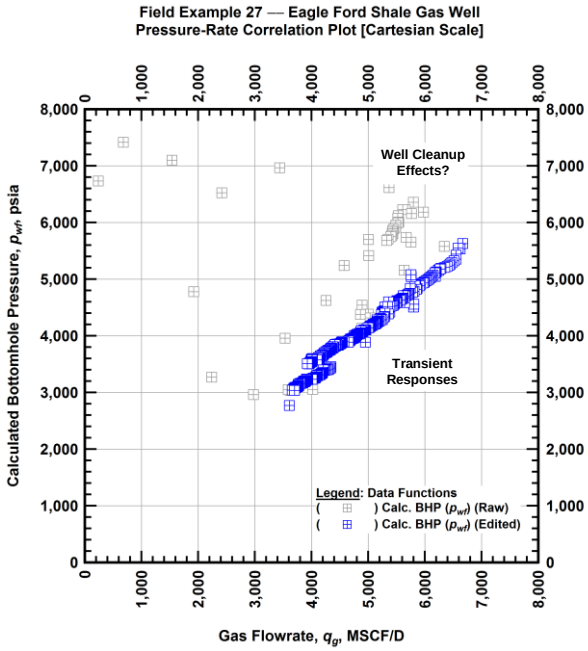

Figure A.785 — (Cartesian Plot): Filtered rate-pressure correlation plot — calculated bottomhole pressure (p_{wf}) versus flowrate (q_g).

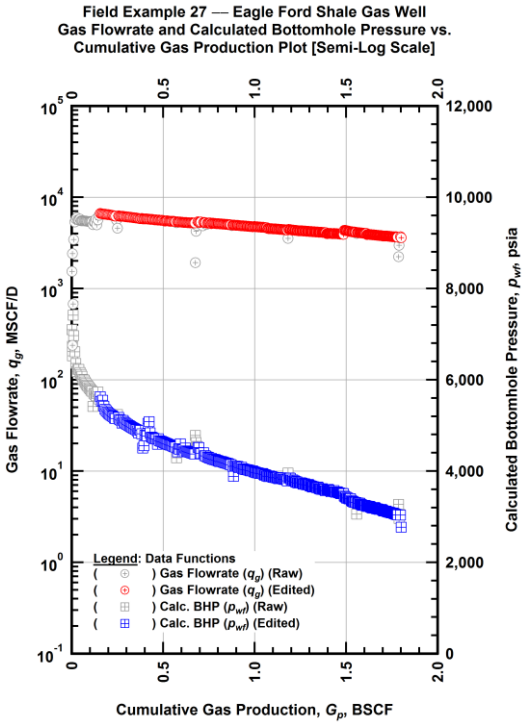

Figure A.786 — (Semi-log Plot): Filtered rate-pressure-cumulative production history plot — flowrate (q_g) and calculated bottomhole pressure (p_{wf}) versus cumulative production (G_p).

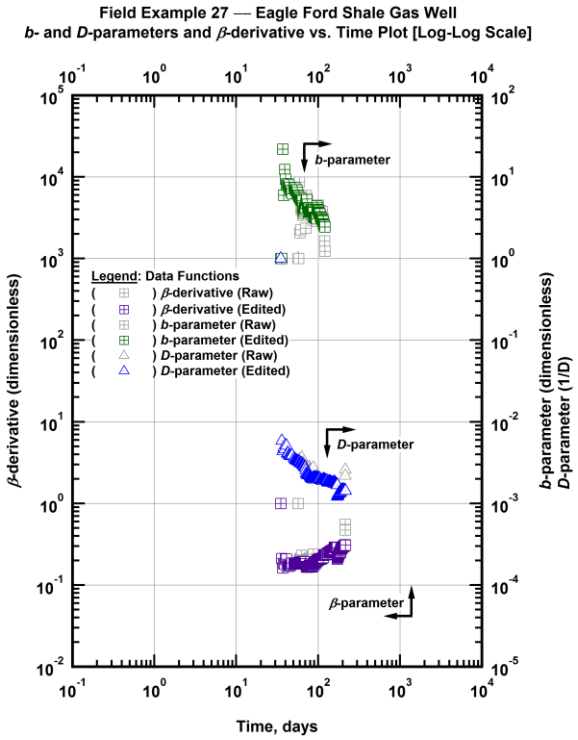

Figure A.787 — (Log-Log Plot): Filtered b, D and β production history plot — b- and D-parameters and β-derivative versus production time.

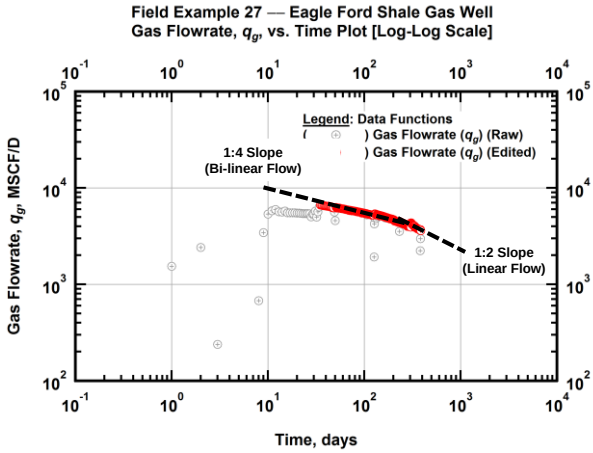

Figure A.788 — (Log-Log Plot): Filtered gas flowrate production history and flow regime identification plot — gas flowrate (q_g) versus production time.

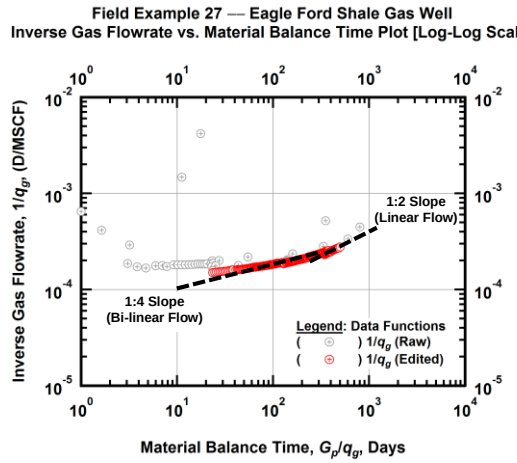

Figure A.789 — (Log-log Plot): Filtered inverse rate with material balance time plot — inverse gas flowrate ($1/q_g$) versus material balance time (G_p/q_g).

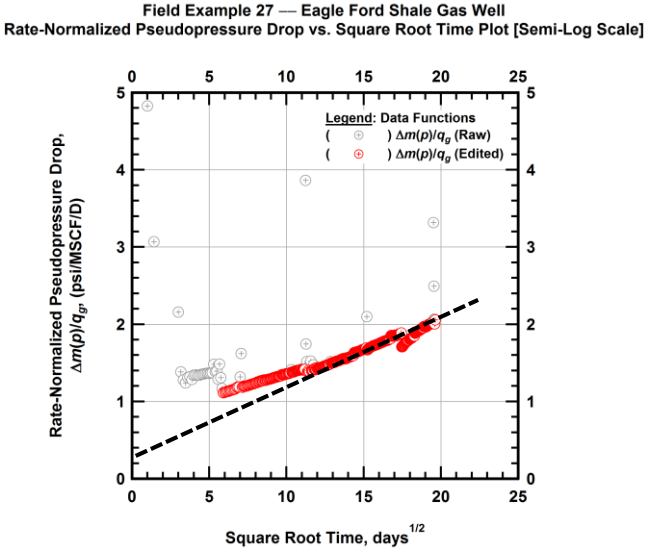

Figure A.790 — (Semi-log Plot): Filtered normalized pseudopressure drop production history plot — rate-normalized pseudopressure drop ($\Delta m(p)/q_g$) versus square root production time ($\sqrt{t}$).

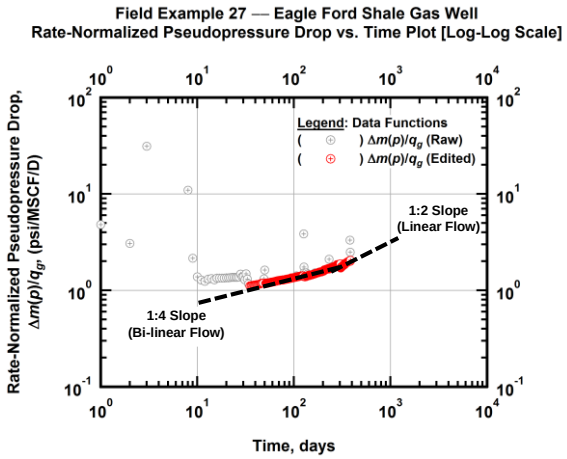

Figure A.791 — (Log-log Plot): Filtered normalized pseudopressure drop production history plot — rate-normalized pseudopressure drop ($\Delta m(p)/q_g$) versus production time.

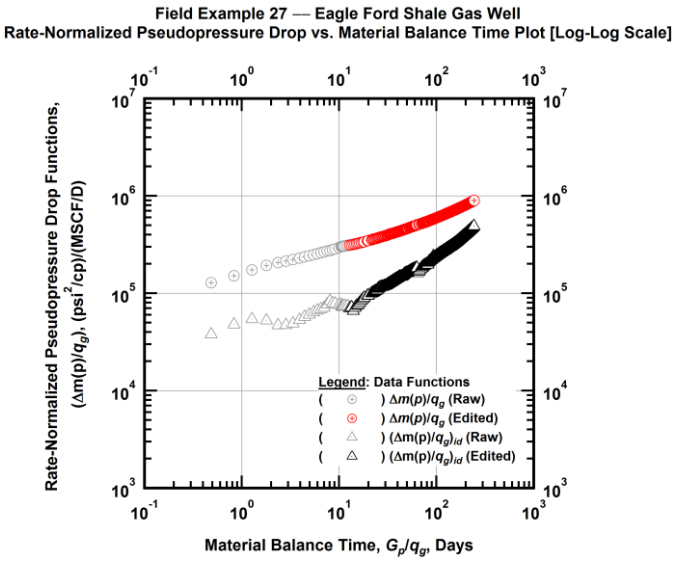

Figure A.792 — (Log-log Plot): "Log-log" diagnostic plot of the filtered production data — rate-normalized pseudopressure drop ($\Delta m(p)/q_g$) and rate-normalized pseudopressure drop integral-derivative $(\Delta m(p)/q_g)_{id}$ versus material balance time (G_p/q_g).

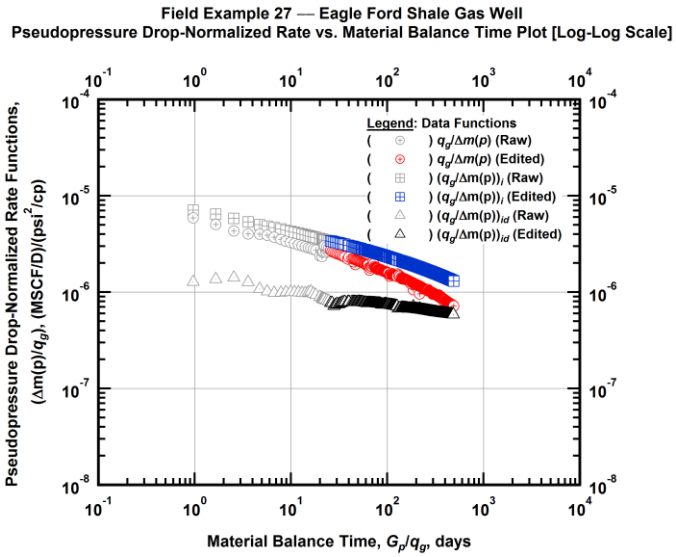

Figure A.793 — (Log-log Plot): "Blasingame" diagnostic plot of the filtered production data — pseudopressure drop-normalized gas flowrate ($q_g/\Delta m(p)$), pseudopressure drop-normalized gas flowrate integral $(q_g/\Delta m(p))_i$ and pseudopressure drop-normalized gas flowrate integral-derivative $(q_g/\Delta m(p))_{id}$ versus material balance time (G_p/q_g).

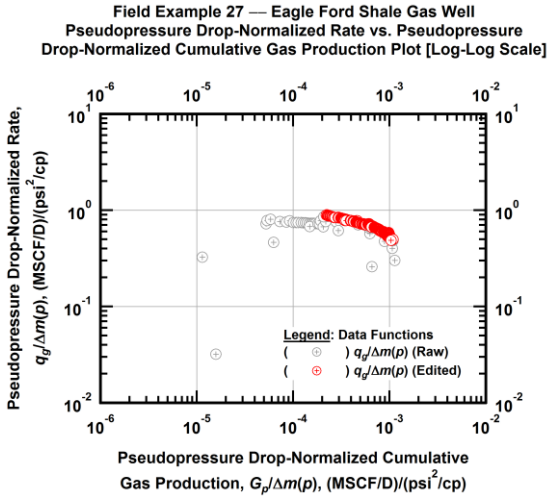

Figure A.794 — (Log-log Plot): Filtered normalized rate with normalized cumulative production plot — pseudopressure drop-normalized gas flowrate ($q_g/\Delta m(p)$) versus pseudopressure drop-normalized cumulative gas production ($G_p/\Delta m(p)$).

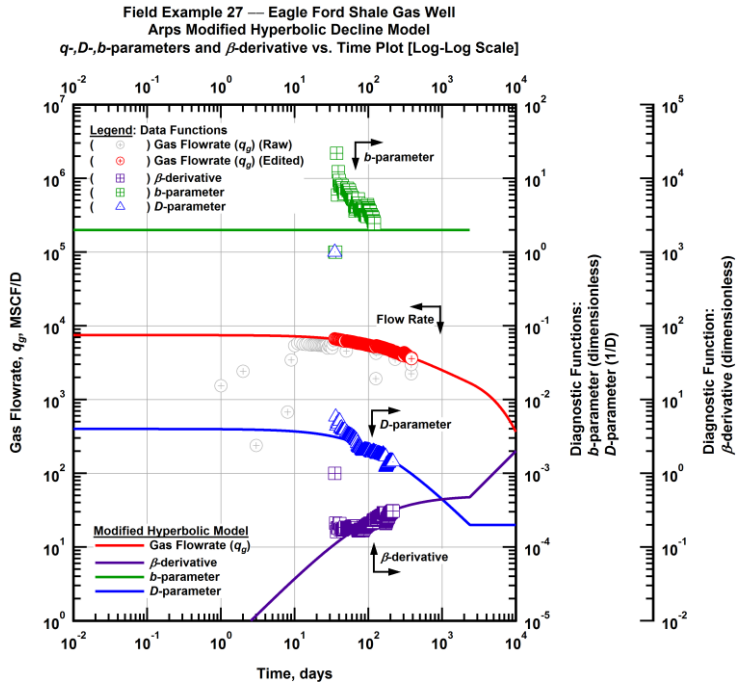

Figure A.795 — (Log-Log Plot): Arps modified hyperbolic decline model plot — time-rate model and data gas flowrate (q_g), *D*- and *b*-parameters and β-derivative versus production time.

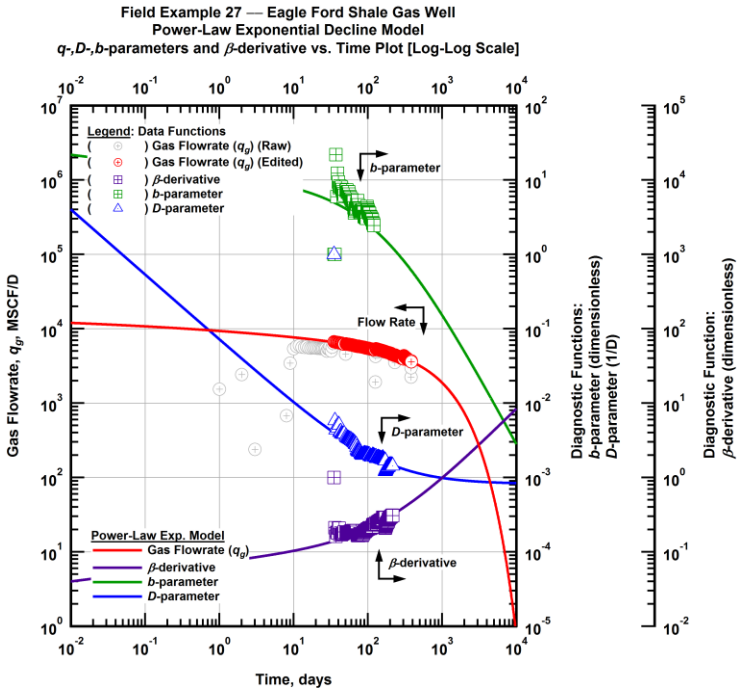

Figure A.796 — (Log-Log Plot): Power-law exponential decline model plot — time-rate model and data gas flowrate (q_g), *D*- and *b*-parameters and β-derivative versus production time.

Field Example 27 — Model-Based (Time-Rate-Pressure) Production Analysis

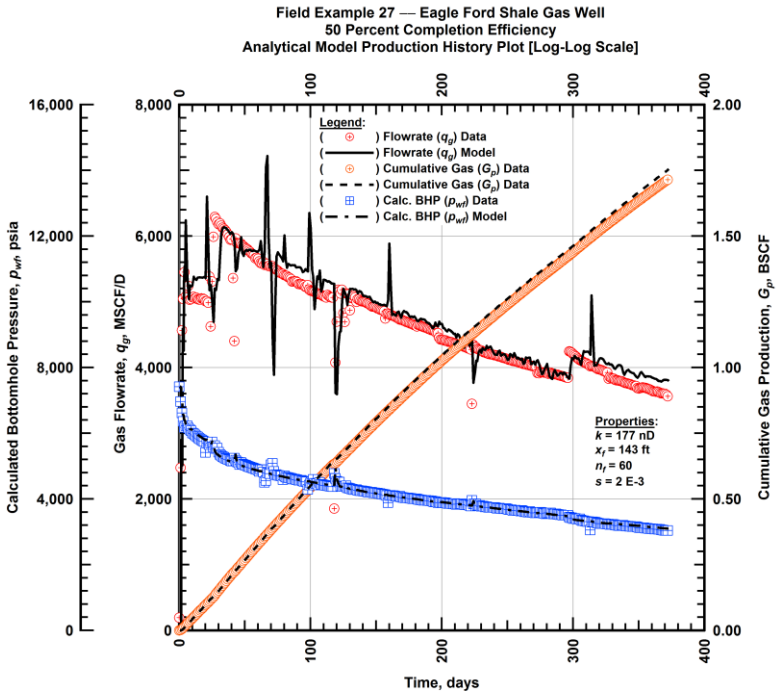

Figure A.797 — (Cartesian Plot): Production history plot — original gas flowrate (q_g), cumulative gas production (G_p), calculated bottomhole pressure (p_{wf}) and 50 percent completion efficiency model matches versus production time.

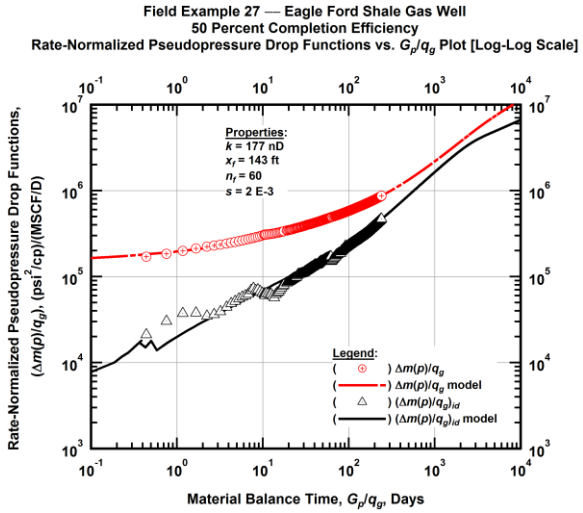

Figure A.798 — (Log-log Plot): "Log-log" diagnostic plot of the original production data — rate-normalized pseudopressure drop ($\Delta m(p)/q_g$), rate-normalized pseudopressure drop integral-derivative $(\Delta m(p)/q_g)_{id}$ and 50 percent completion efficiency model matches versus material balance time (G_p/q_g).

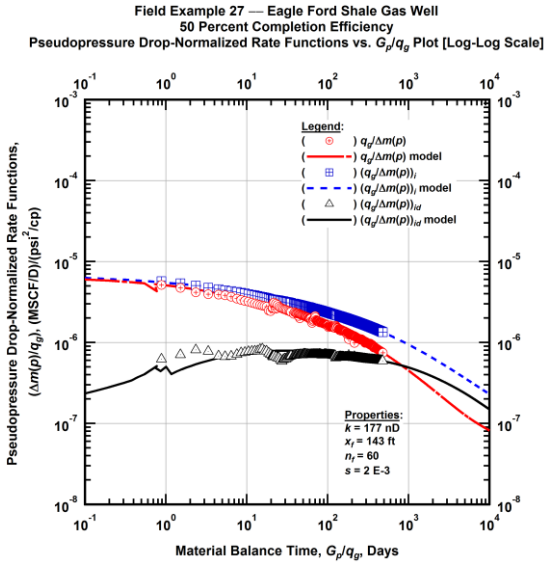

Figure A.799 — (Log-log Plot): "Blasingame" diagnostic plot of the original production data — pseudopressure drop-normalized gas flowrate ($q_g/\Delta m(p)$), pseudopressure drop-normalized gas flowrate integral $(q_g/\Delta m(p))_i$, pseudopressure drop-normalized gas flowrate integral-derivative $(q_g/\Delta m(p))_{id}$ and 50 percent completion efficiency model matches versus material balance time (G_p/q_g).

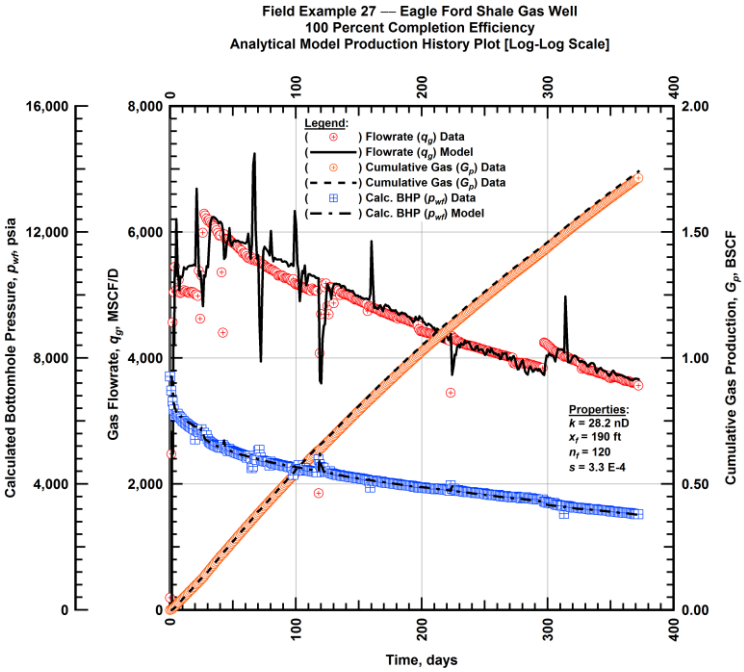

Figure A.800 — (Cartesian Plot): Production history plot — original gas flowrate (q_g), cumulative gas production (G_p), calculated bottomhole pressure (p_{wf}) and 100 percent completion efficiency model matches versus production time.

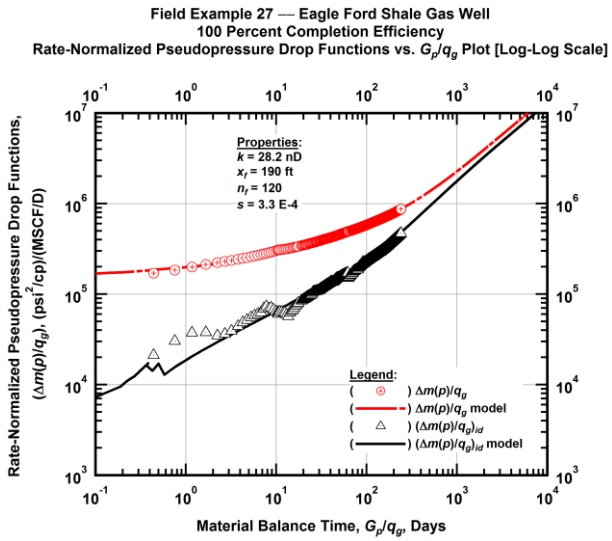

Figure A.801 — (Log-log Plot): "Log-log" diagnostic plot of the original production data — rate-normalized pseudopressure drop ($\Delta m(p)/q_g$), rate-normalized pseudopressure drop integral-derivative $(\Delta m(p)/q_g)_{id}$ and 100 percent completion efficiency model matches versus material balance time (G_p/q_g).

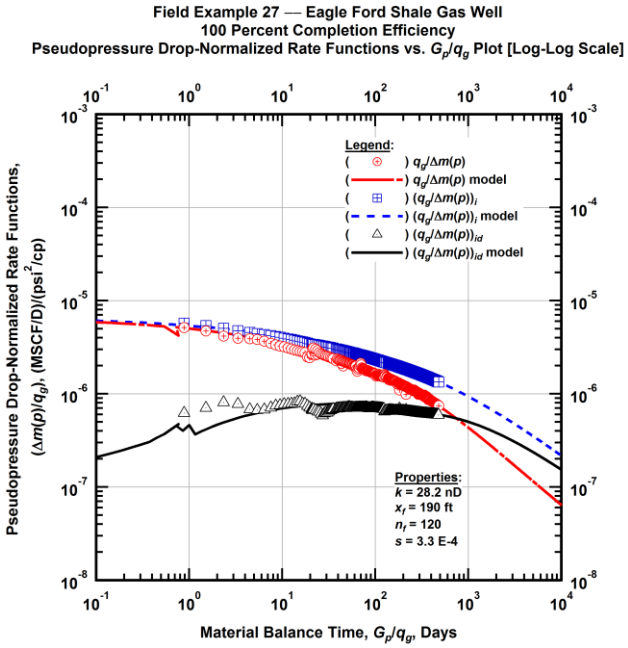

Figure A.802 — (Log-log Plot): "Blasingame" diagnostic plot of the original production data — pseudopressure drop-normalized gas flowrate ($q_g/\Delta m(p)$), pseudopressure drop-normalized gas flowrate integral $(q_g/\Delta m(p))_i$, pseudopressure drop-normalized gas flowrate integral-derivative $(q_g/\Delta m(p))_{id}$ and 100 percent completion efficiency model matches versus material balance time (G_p/q_g).

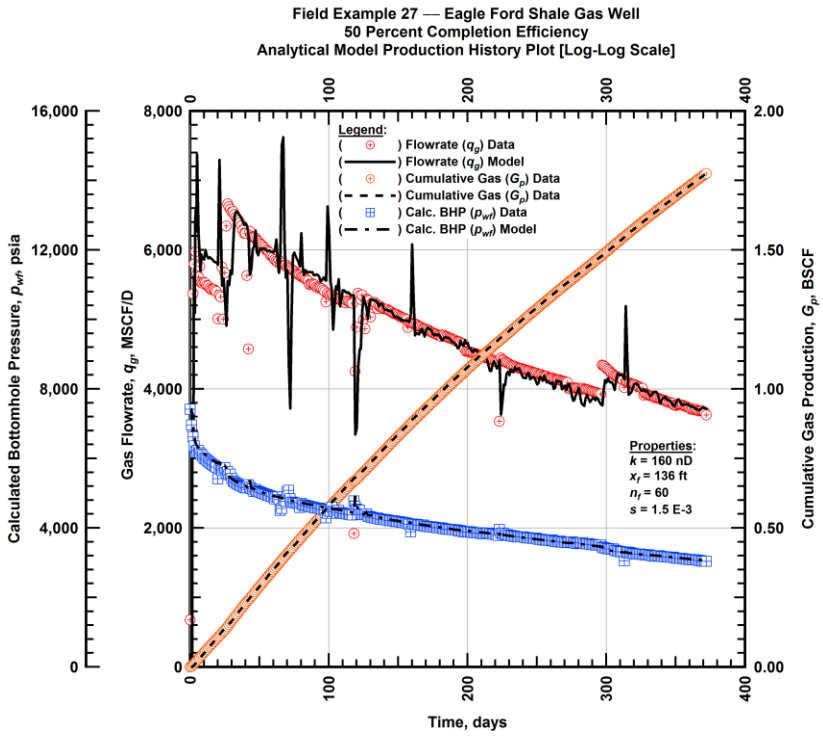

Figure A.803 — (Cartesian Plot): Production history plot — revised gas flowrate (q_g), cumulative gas production (G_p), calculated bottomhole pressure (p_{wf}) and 50 percent completion efficiency model matches versus production time.

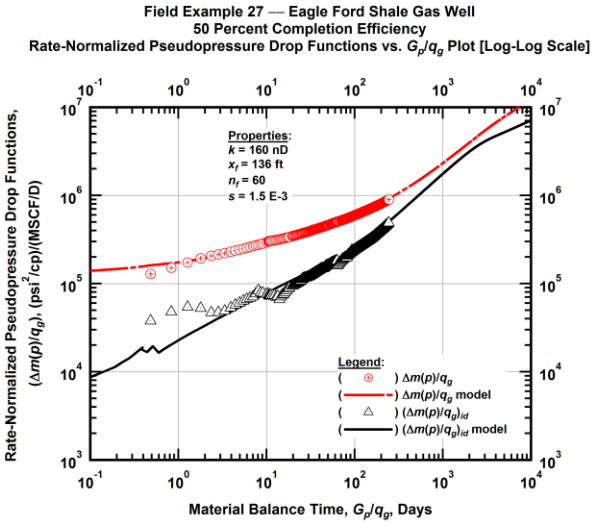

Figure A.804 — (Log-log Plot): "Log-log" diagnostic plot of the revised production data — rate-normalized pseudopressure drop ($\Delta m(p)/q_g$), rate-normalized pseudopressure drop integral-derivative $(\Delta m(p)/q_g)_{id}$ and 50 percent completion efficiency model matches versus material balance time (G_p/q_g).

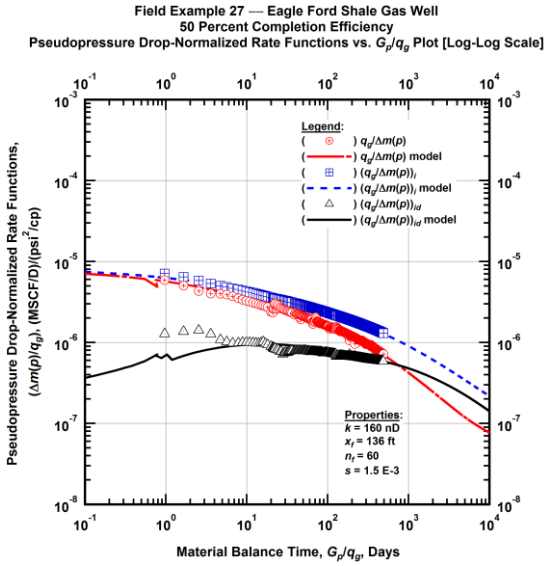

Figure A.805 — (Log-log Plot): "Blasingame" diagnostic plot of the revised production data — pseudopressure drop-normalized gas flowrate ($q_g/\Delta m(p)$), pseudopressure drop-normalized gas flowrate integral $(q_g/\Delta m(p))_i$, pseudopressure drop-normalized gas flowrate integral-derivative $(q_g/\Delta m(p))_{id}$ and 50 percent completion efficiency model matches versus material balance time (G_p/q_g).

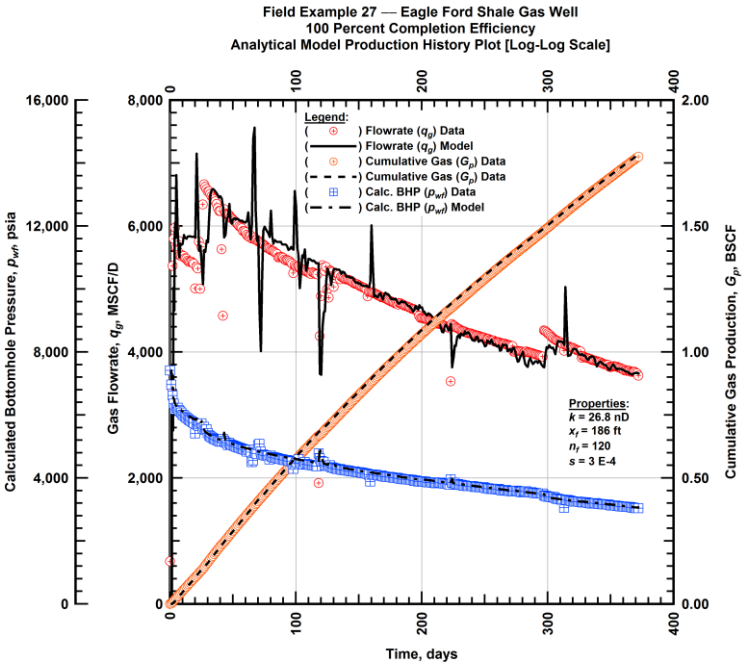

Figure A.806 — (Cartesian Plot): Production history plot — revised gas flowrate (q_g), cumulative gas production (G_p), calculated bottomhole pressure (p_{wf}) and 100 percent completion efficiency model matches versus production time.

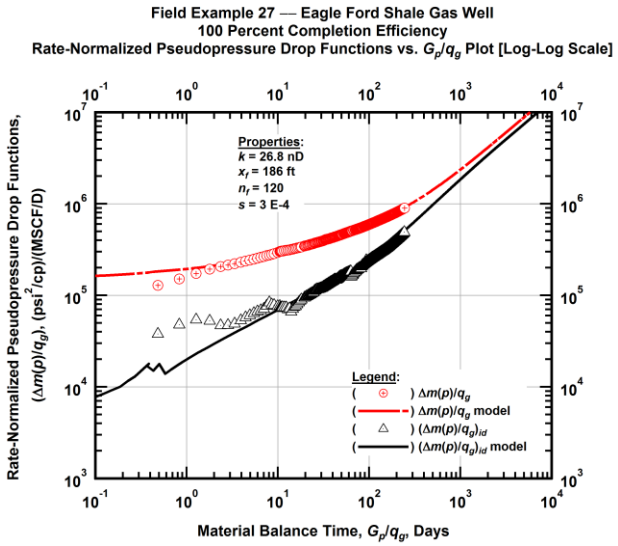

Figure A.807 — (Log-log Plot): "Log-log" diagnostic plot of the revised production data — rate-normalized pseudopressure drop ($\Delta m(p)/q_g$), rate-normalized pseudopressure drop integral-derivative $(\Delta m(p)/q_g)_{id}$ and 100 percent completion efficiency model matches versus material balance time (G_p/q_g).

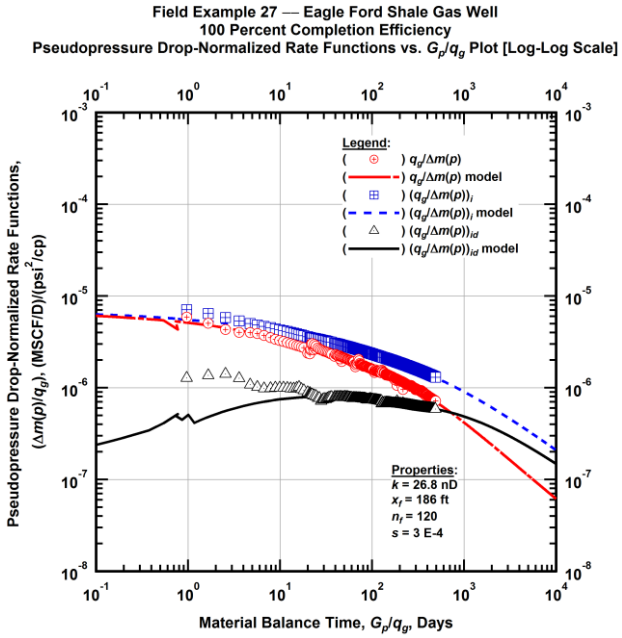

Figure A.808 — (Log-log Plot): "Blasingame" diagnostic plot of the revised production data — pseudopressure drop-normalized gas flowrate ($q_g/\Delta m(p)$), pseudopressure drop-normalized gas flowrate integral $(q_g/\Delta m(p))_i$, pseudopressure drop-normalized gas flowrate integral-derivative $(q_g/\Delta m(p))_{id}$ and 100 percent completion efficiency model matches versus material balance time (G_p/q_g).

Field Example 27 — 30-Year EUR Model Comparison

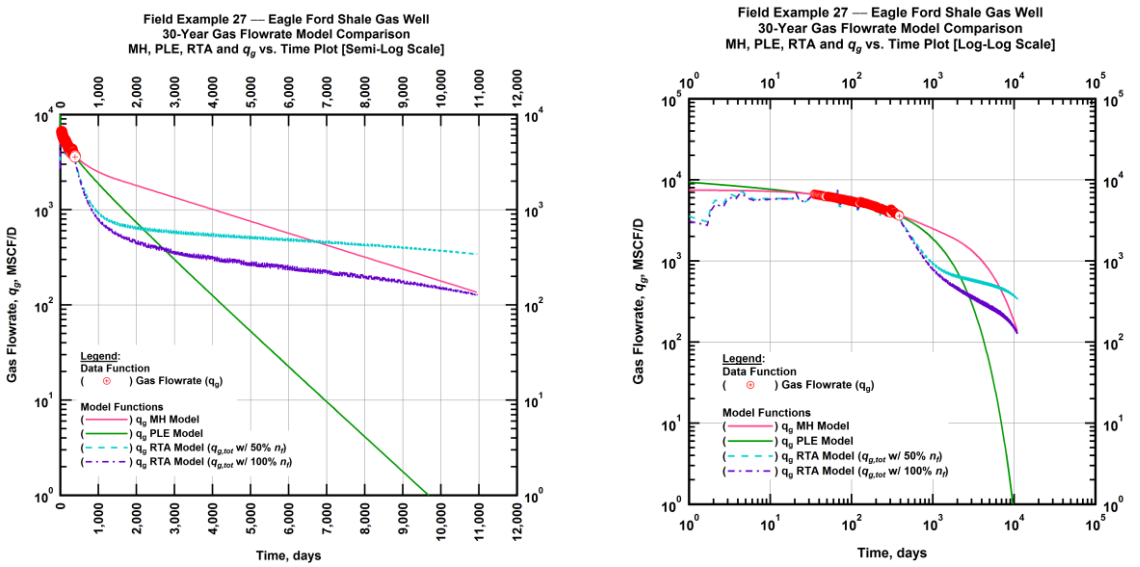

A **B**

Figure A.809 — (A — Semi-Log Plot) and (B — Log-Log Plot): Estimated 30-year revised gas flowrate model comparison — Arps modified hyperbolic decline model, power-law exponential decline model, and 50 percent and 100 percent completion efficiency RTA models revised gas 30-year estimated flowrate decline and historic gas flowrate data (q_g) versus production time.

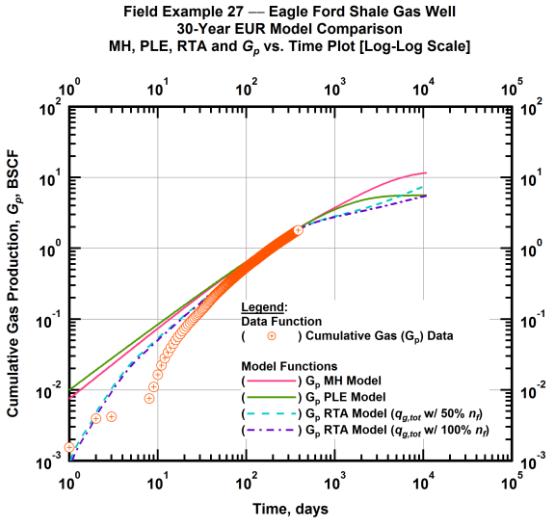

Figure A.810 — (Log-log Plot): PVT revised gas 30-year estimated cumulative production volume model comparison — Arps modified hyperbolic decline model, power-law exponential decline model, and 50 percent and 100 percent completion efficiency RTA model estimated 30-year cumulative gas production volumes and historic cumulative gas production (G_p) versus production time.

Table A.27 — 30-year estimated cumulative revised gas production (EUR), in units of BSCF, for the Arps modified hyperbolic, power-law exponential and analytical time-rate-pressure decline models.

Arps Modified Hyperbolic (BSCF)	Power-Law Exponential (BSCF)	RTA Analytical Model ($q_{g,tot}$ w/ 50% n_f) (BSCF)	RTA Analytical Model ($q_{g,tot}$ w/ 100% n_f) (BSCF)
11.79	5.44	7.90	5.56

Field Example 28 — Time-Rate Analysis

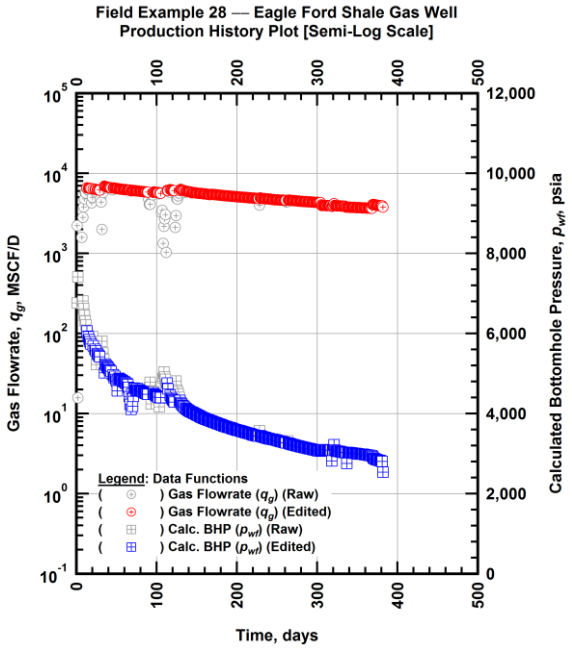

Figure A.811 — (Semi-log Plot): Filtered production history plot — flowrate (q_g) and calculated bottomhole pressure (p_{wf}) versus production time.

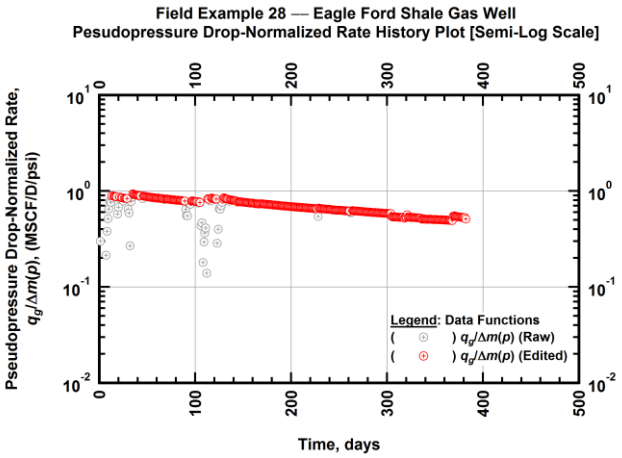

Figure A.812 — (Semi-log Plot): Filtered normalized rate production history plot — pseudopressure drop-normalized gas flowrate ($q_g/\Delta m(p)$) versus production time.

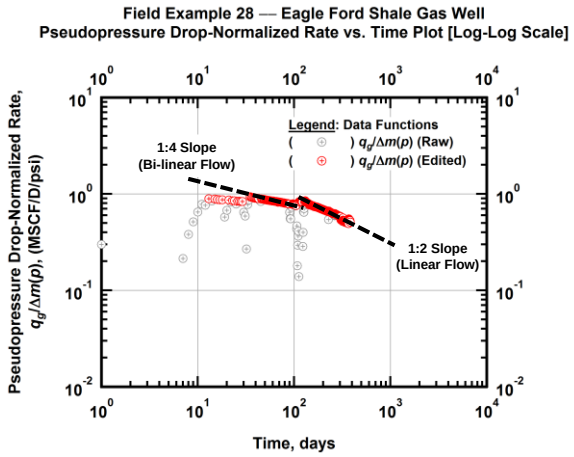

Figure A.813 — (Log-log Plot): Filtered normalized rate production history plot — pseudopressure drop-normalized gas flowrate ($q_g/\Delta m(p)$) versus production time.

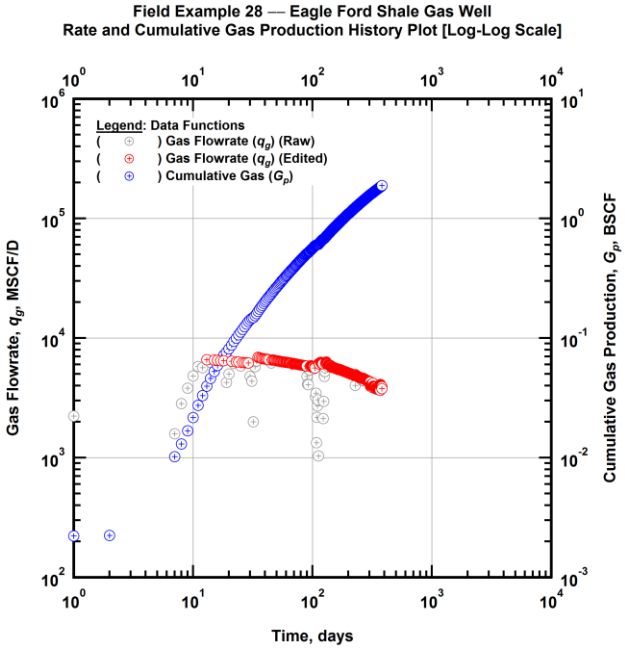

Figure A.814 — (Log-log Plot): Filtered rate and unfiltered cumulative gas production history plot — flowrate (q_g) and cumulative production (G_p) versus production time.

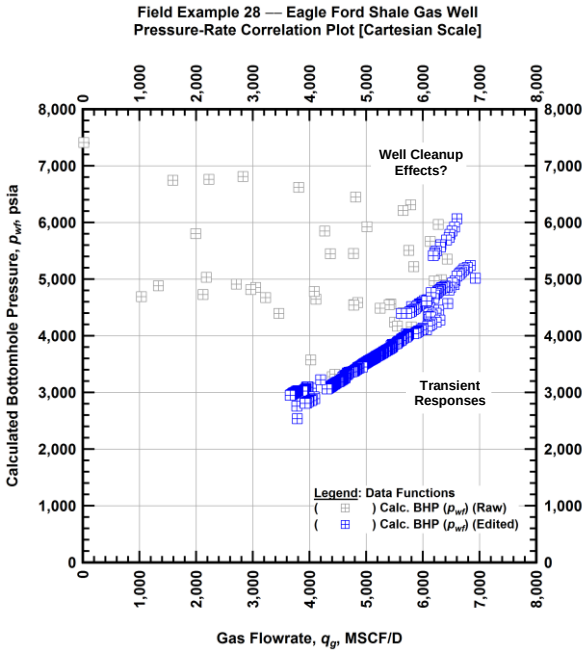

Figure A.815 — (Cartesian Plot): Filtered rate-pressure correlation plot — calculated bottomhole pressure (p_{wf}) versus flowrate (q_g).

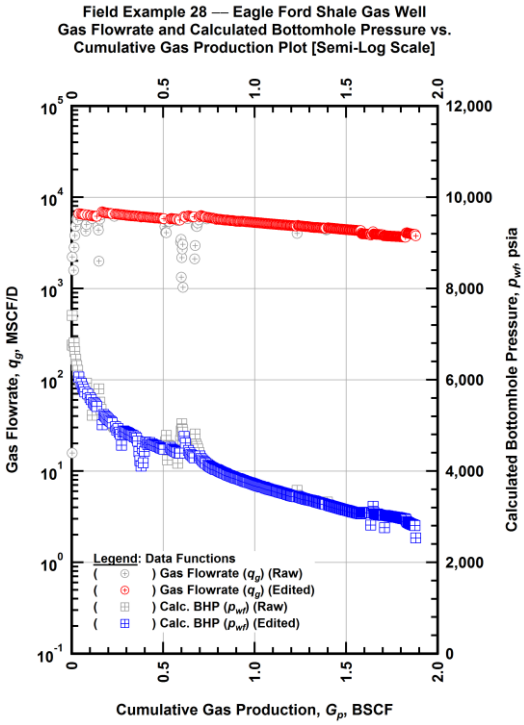

Figure A.816 — (Semi-log Plot): Filtered rate-pressure-cumulative production history plot — flowrate (q_g) and calculated bottomhole pressure (p_{wf}) versus cumulative production (G_p).

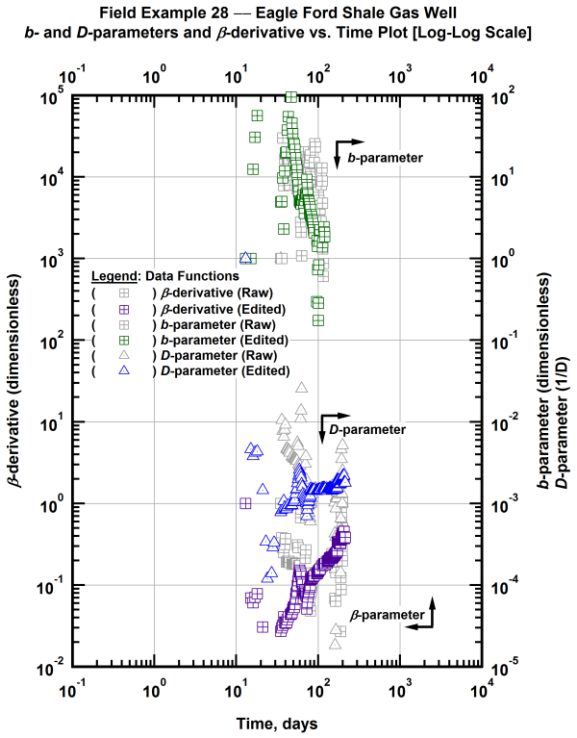

Figure A.817 — (Log-Log Plot): Filtered b, D and β production history plot — b- and D-parameters and β-derivative versus production time.

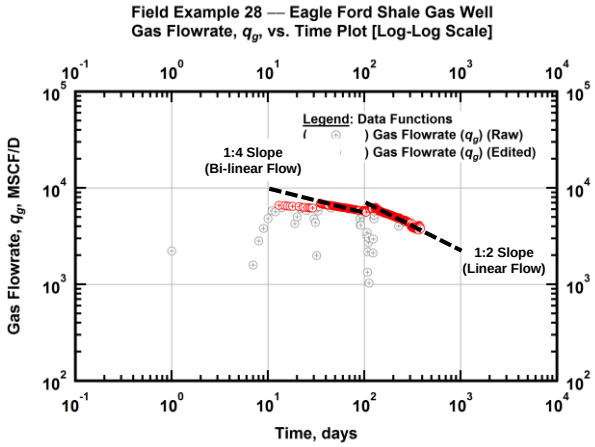

Figure A.818 — (Log-Log Plot): Filtered gas flowrate production history and flow regime identification plot — gas flowrate (q_g) versus production time.

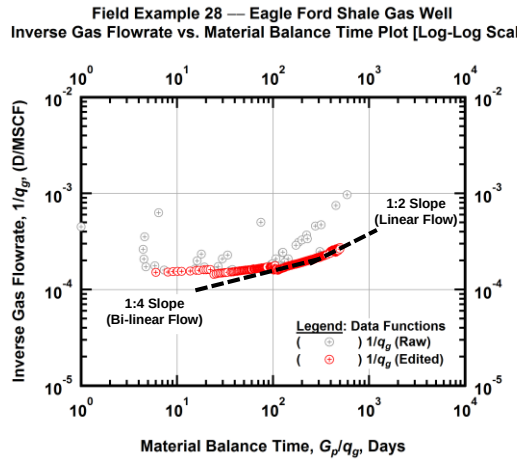

Figure A.819 — (Log-log Plot): Filtered inverse rate with material balance time plot — inverse gas flowrate ($1/q_g$) versus material balance time (G_p/q_g).

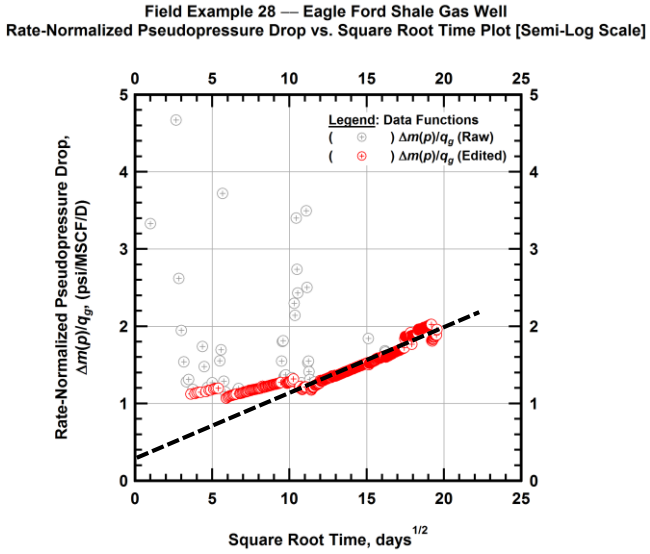

Figure A.820 — (Semi-log Plot): Filtered normalized pseudopressure drop production history plot — rate-normalized pseudopressure drop ($\Delta m(p)/q_g$) versus square root production time ($\sqrt{t}$).

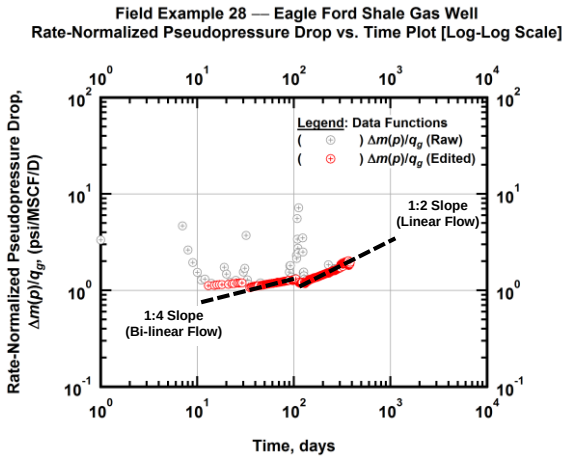

Figure A.821 — (Log-log Plot): Filtered normalized pseudopressure drop production history plot — rate-normalized pseudopressure drop ($\Delta m(p)/q_g$) versus production time.

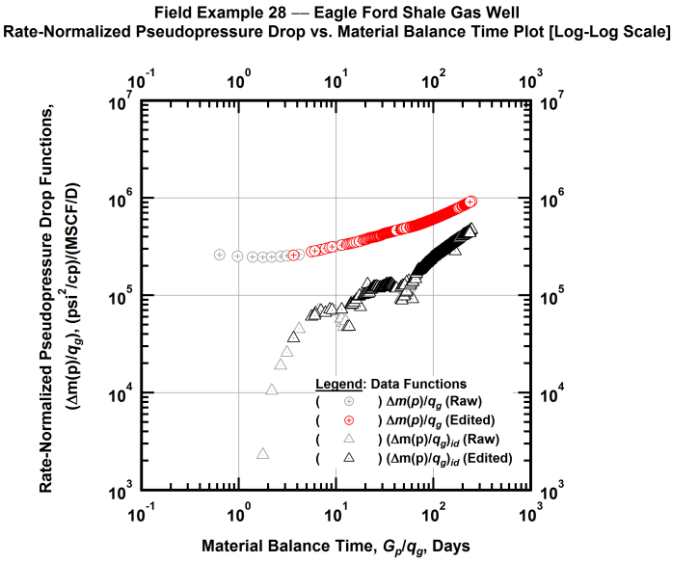

Figure A.822 — (Log-log Plot): "Log-log" diagnostic plot of the filtered production data — rate-normalized pseudopressure drop ($\Delta m(p)/q_g$) and rate-normalized pseudopressure drop integral-derivative $(\Delta m(p)/q_g)_{id}$ versus material balance time (G_p/q_g).

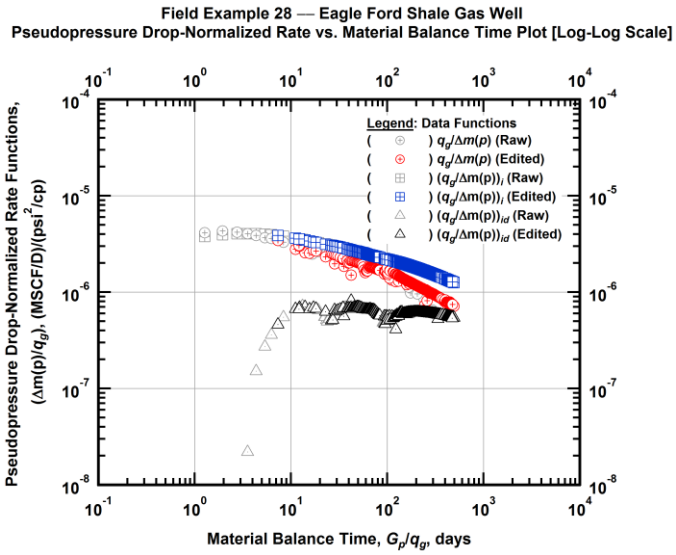

Figure A.823 — (Log-log Plot): "Blasingame" diagnostic plot of the filtered production data — pseudopressure drop-normalized gas flowrate ($q_g/\Delta m(p)$), pseudopressure drop-normalized gas flowrate integral $(q_g/\Delta m(p))_i$ and pseudopressure drop-normalized gas flowrate integral-derivative $(q_g/\Delta m(p))_{id}$ versus material balance time (G_p/q_g).

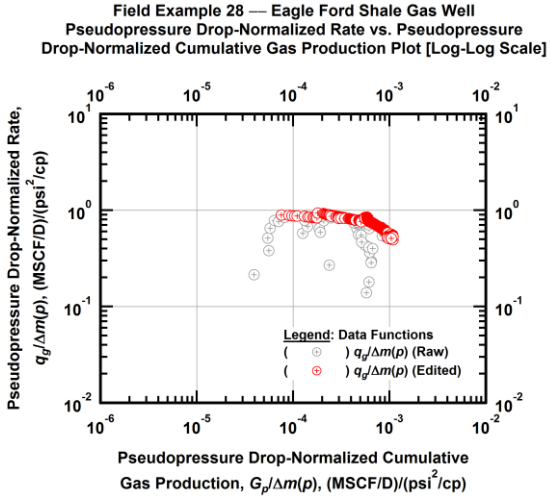

Figure A.824 — (Log-log Plot): Filtered normalized rate with normalized cumulative production plot — pseudopressure drop-normalized gas flowrate ($q_g/\Delta m(p)$) versus pseudopressure drop-normalized cumulative gas production ($G_p/\Delta m(p)$).

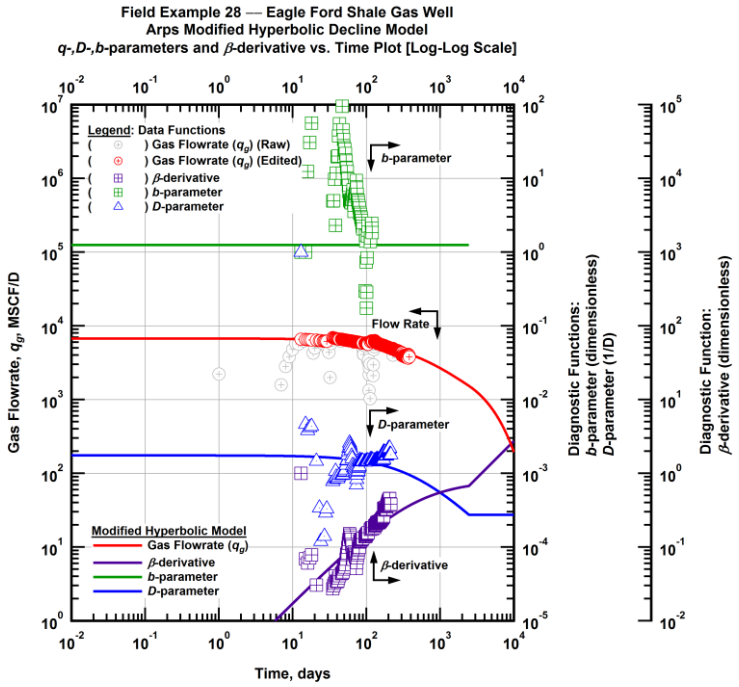

Figure A.825 — (Log-Log Plot): Arps modified hyperbolic decline model plot — time-rate model and data gas flowrate (q_g), *D*- and *b*-parameters and β-derivative versus production time.

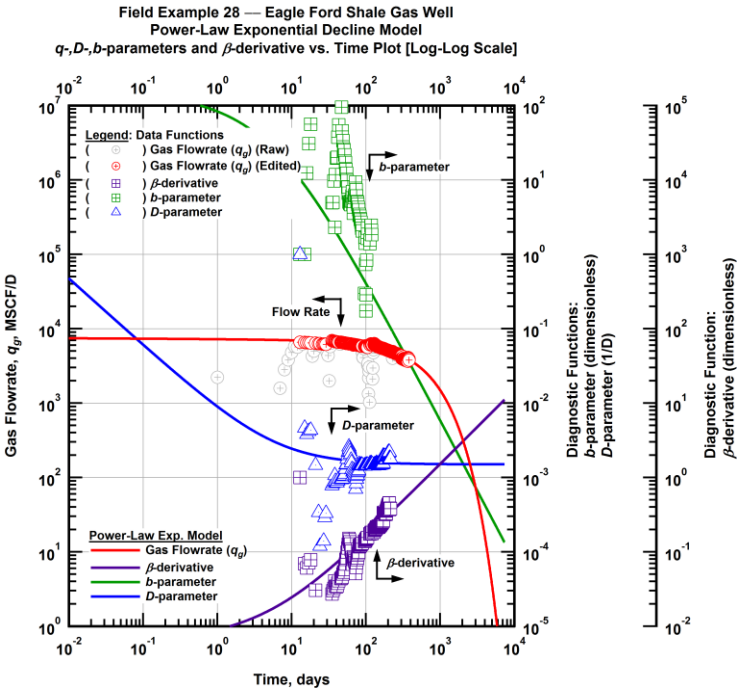

Figure A.826 — (Log-Log Plot): Power-law exponential decline model plot — time-rate model and data gas flowrate (q_g), *D*- and *b*-parameters and β-derivative versus production time.

Field Example 28 — Model-Based (Time-Rate-Pressure) Production Analysis

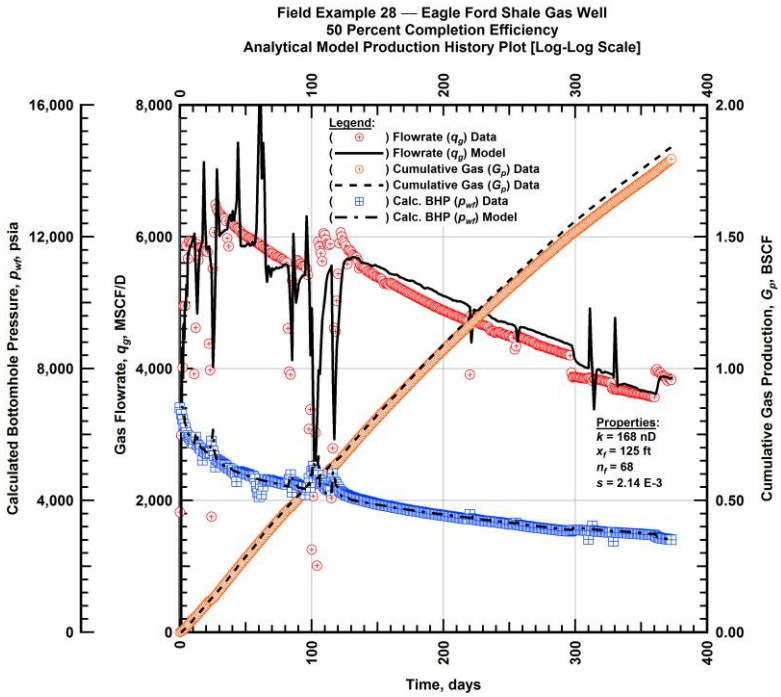

Figure A.827 — (Cartesian Plot): Production history plot — original gas flowrate (q_g), cumulative gas production (G_p), calculated bottomhole pressure (p_{wf}) and 50 percent completion efficiency model matches versus production time.

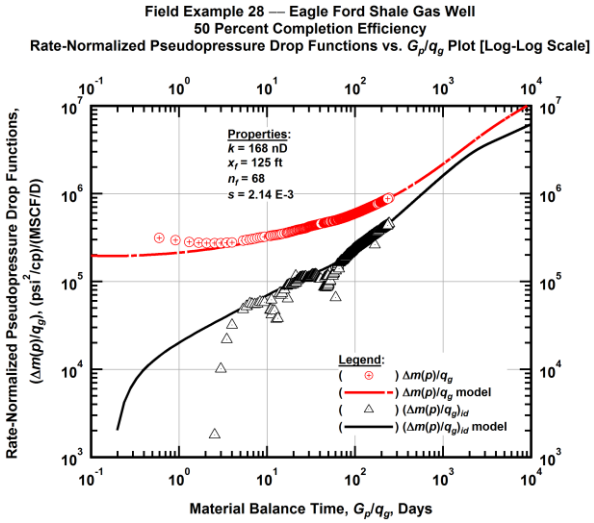

Figure A.828 — (Log-log Plot): "Log-log" diagnostic plot of the original production data — rate-normalized pseudopressure drop ($\Delta m(p)/q_g$), rate-normalized pseudopressure drop integral-derivative $(\Delta m(p)/q_g)_{id}$ and 50 percent completion efficiency model matches versus material balance time (G_p/q_g).

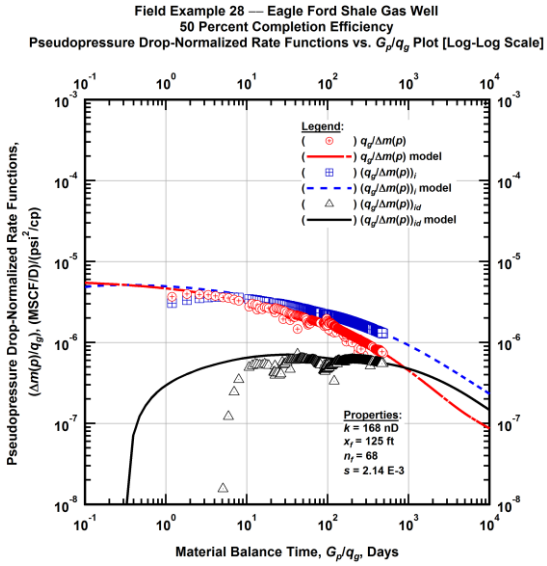

Figure A.829 — (Log-log Plot): "Blasingame" diagnostic plot of the original production data — pseudopressure drop-normalized gas flowrate ($q_g/\Delta m(p)$), pseudopressure drop-normalized gas flowrate integral $(q_g/\Delta m(p))_i$, pseudopressure drop-normalized gas flowrate integral-derivative $(q_g/\Delta m(p))_{id}$ and 50 percent completion efficiency model matches versus material balance time (G_p/q_g).

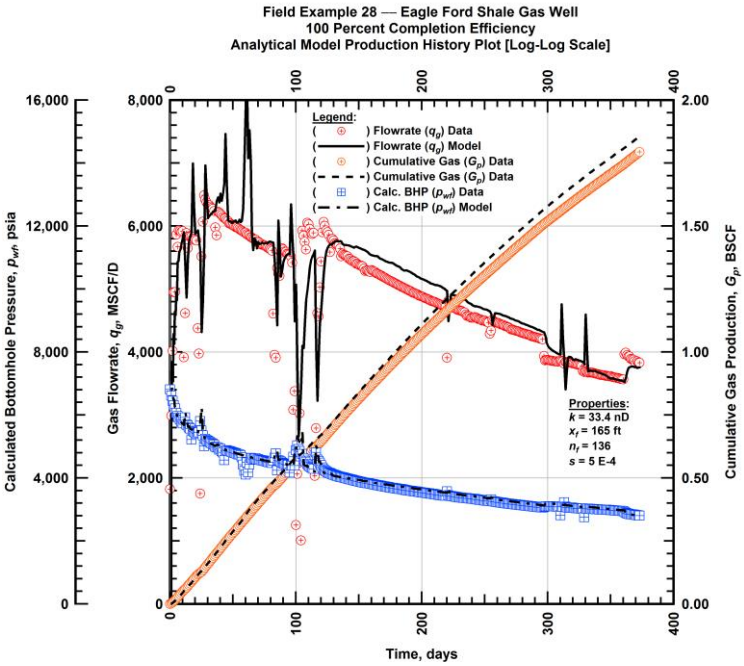

Figure A.830 — (Cartesian Plot): Production history plot — original gas flowrate (q_g), cumulative gas production (G_p), calculated bottomhole pressure (p_{wf}) and 100 percent completion efficiency model matches versus production time.

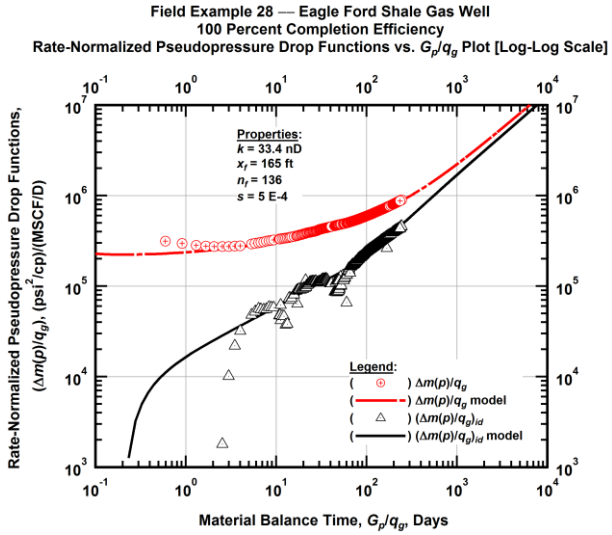

Figure A.831 — (Log-log Plot): "Log-log" diagnostic plot of the original production data — rate-normalized pseudopressure drop ($\Delta m(p)/q_g$), rate-normalized pseudopressure drop integral-derivative $(\Delta m(p)/q_g)_{id}$ and 100 percent completion efficiency model matches versus material balance time (G_p/q_g).

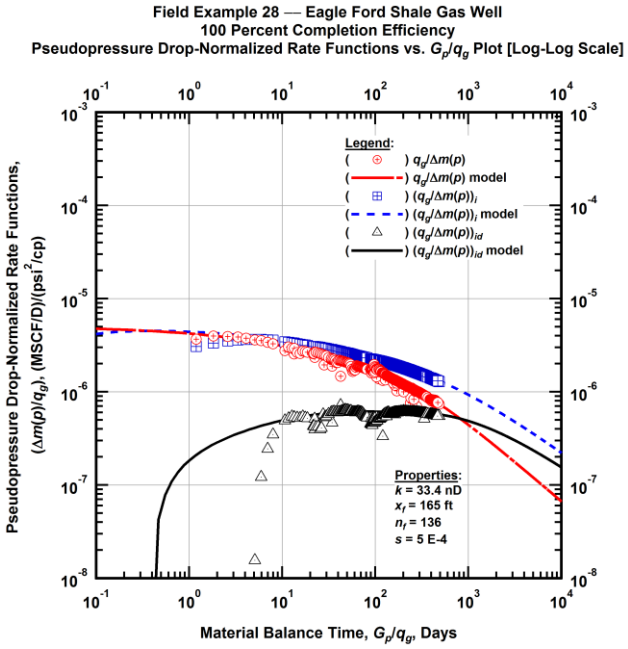

Figure A.832 — (Log-log Plot): "Blasingame" diagnostic plot of the original production data — pseudopressure drop-normalized gas flowrate ($q_g/\Delta m(p)$), pseudopressure drop-normalized gas flowrate integral $(q_g/\Delta m(p))_i$, pseudopressure drop-normalized gas flowrate integral-derivative $(q_g/\Delta m(p))_{id}$ and 100 percent completion efficiency model matches versus material balance time (G_p/q_g).

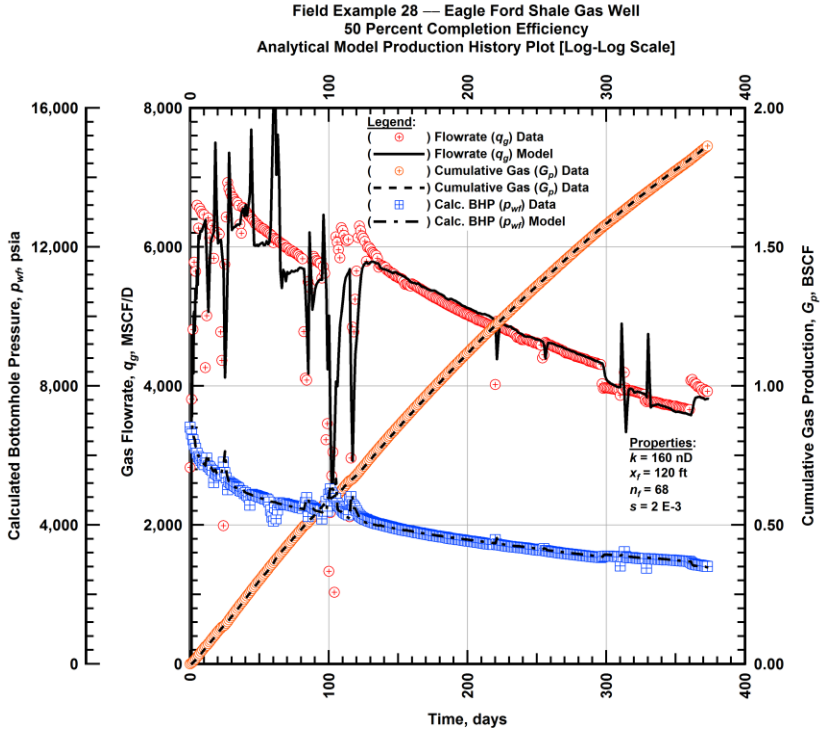

Figure A.833 — (Cartesian Plot): Production history plot — revised gas flowrate (q_g), cumulative gas production (G_p), calculated bottomhole pressure (p_{wf}) and 50 percent completion efficiency model matches versus production time.

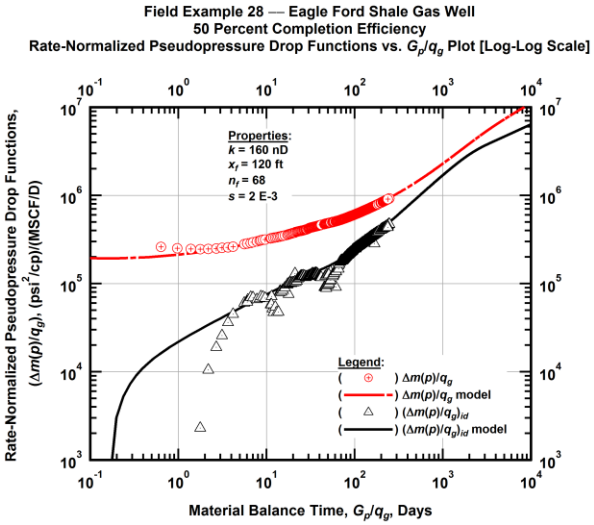

Figure A.834 — (Log-log Plot): "Log-log" diagnostic plot of the revised production data — rate-normalized pseudopressure drop ($\Delta m(p)/q_g$), rate-normalized pseudopressure drop integral-derivative $(\Delta m(p)/q_g)_{id}$ and 50 percent completion efficiency model matches versus material balance time (G_p/q_g).

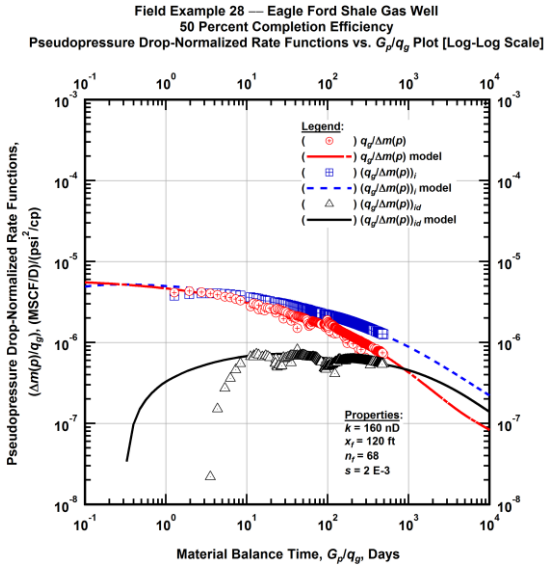

Figure A.835 — (Log-log Plot): "Blasingame" diagnostic plot of the revised production data — pseudopressure drop-normalized gas flowrate ($q_g/\Delta m(p)$), pseudopressure drop-normalized gas flowrate integral $(q_g/\Delta m(p))_i$, pseudopressure drop-normalized gas flowrate integral-derivative $(q_g/\Delta m(p))_{id}$ and 50 percent completion efficiency model matches versus material balance time (G_p/q_g).

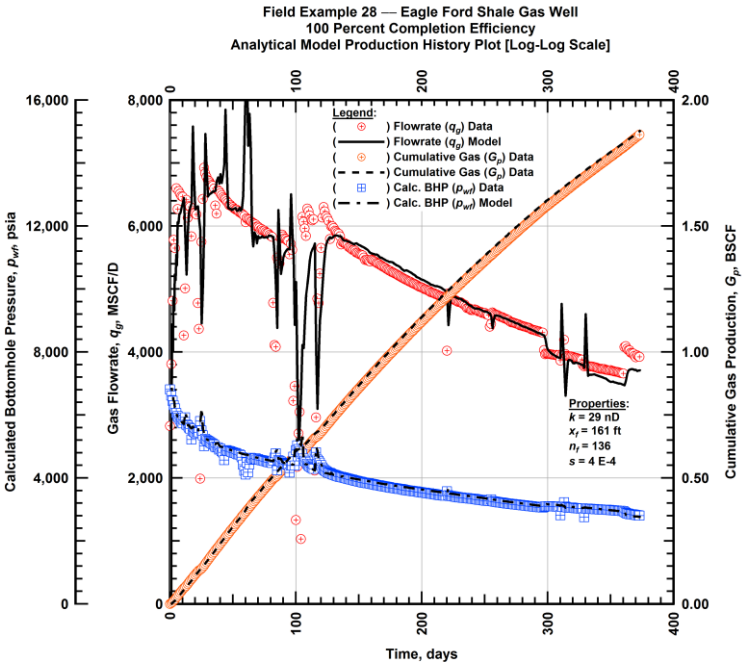

Figure A.836 — (Cartesian Plot): Production history plot — revised gas flowrate (q_g), cumulative gas production (G_p), calculated bottomhole pressure (p_{wf}) and 100 percent completion efficiency model matches versus production time.

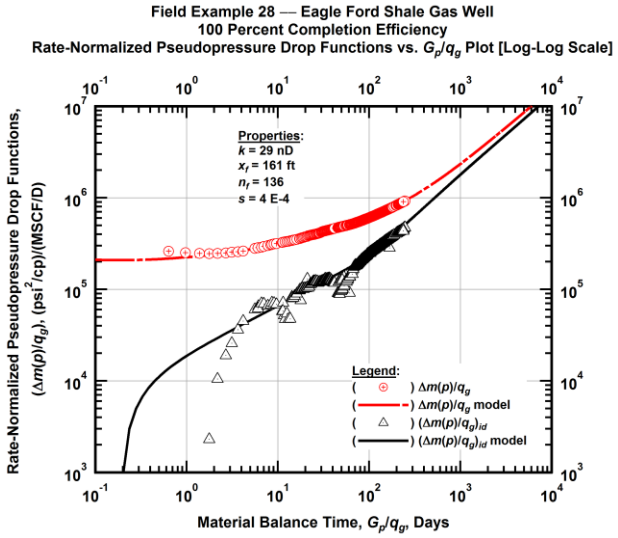

Figure A.837 — (Log-log Plot): "Log-log" diagnostic plot of the revised production data — rate-normalized pseudopressure drop ($\Delta m(p)/q_g$), rate-normalized pseudopressure drop integral-derivative $(\Delta m(p)/q_g)_{id}$ and 100 percent completion efficiency model matches versus material balance time (G_p/q_g).

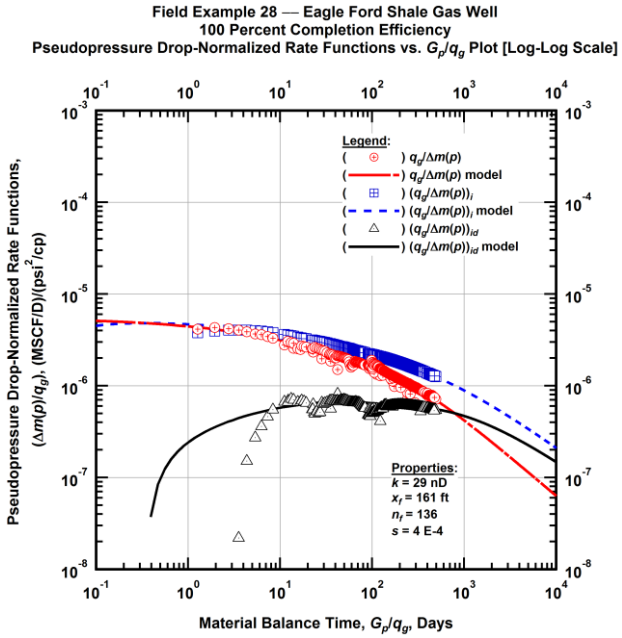

Figure A.838 — (Log-log Plot): "Blasingame" diagnostic plot of the revised production data — pseudopressure drop-normalized gas flowrate ($q_g/\Delta m(p)$), pseudopressure drop-normalized gas flowrate integral $(q_g/\Delta m(p))_i$, pseudopressure drop-normalized gas flowrate integral-derivative $(q_g/\Delta m(p))_{id}$ and 100 percent completion efficiency model matches versus material balance time (G_p/q_g).

Field Example 28 — 30-Year EUR Model Comparison

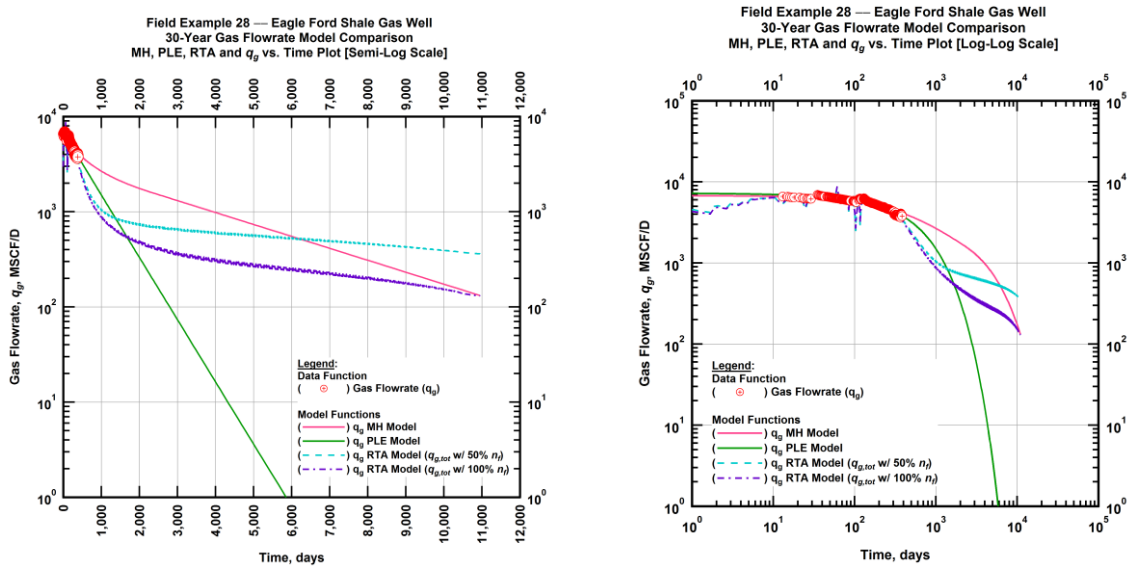

A **B**

Figure A.839 — (A — Semi-Log Plot) and (B — Log-Log Plot): Estimated 30-year revised gas flowrate model comparison — Arps modified hyperbolic decline model, power-law exponential decline model, and 50 percent and 100 percent completion efficiency RTA models revised gas 30-year estimated flowrate decline and historic gas flowrate data (q_g) versus production time.

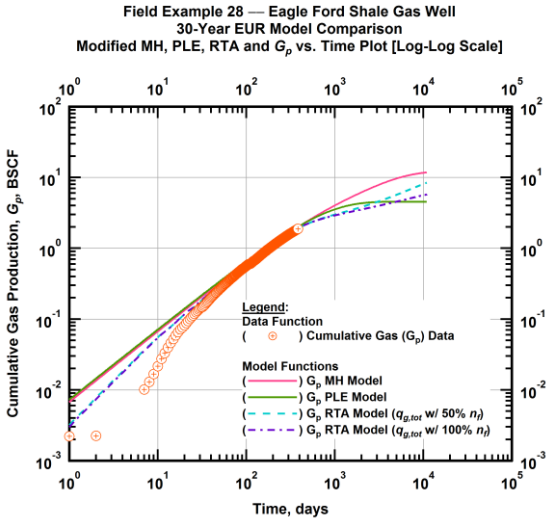

Figure A.840 — (Log-log Plot): PVT revised gas 30-year estimated cumulative production volume model comparison — Arps modified hyperbolic decline model, power-law exponential decline model, and 50 percent and 100 percent completion efficiency RTA model estimated 30-year cumulative gas production volumes and historic cumulative gas production (G_p) versus production time.

Table A.28 — 30-year estimated cumulative revised gas production (EUR), in units of BSCF, for the Arps modified hyperbolic, power-law exponential and analytical time-rate-pressure decline models.

Arps Modified Hyperbolic (BSCF)	Power-Law Exponential (BSCF)	RTA Analytical Model ($q_{g,tot}$ w/ 50% n_f) (BSCF)	RTA Analytical Model ($q_{g,tot}$ w/ 100% n_f) (BSCF)
11.87	4.40	8.57	5.79

Field Example 29 — Time-Rate Analysis

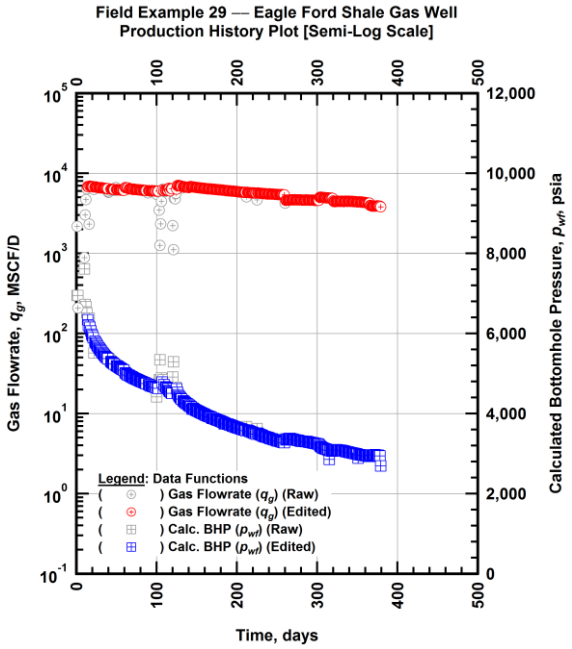

Figure A.841 — (Semi-log Plot): Filtered production history plot — flowrate (q_g) and calculated bottomhole pressure (p_{wf}) versus production time.

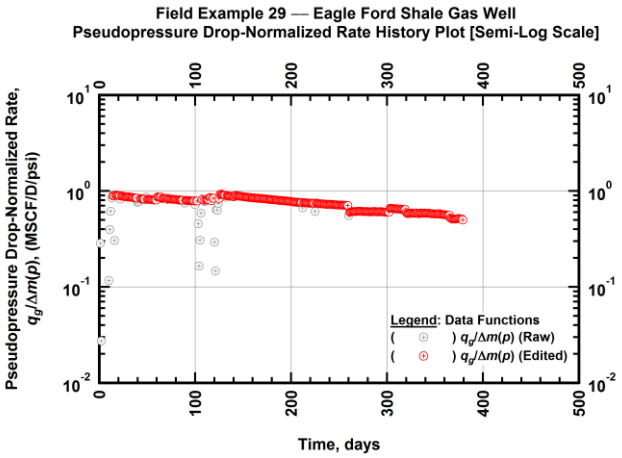

Figure A.842 — (Semi-log Plot): Filtered normalized rate production history plot — pseudopressure drop-normalized gas flowrate ($q_g/\Delta m(p)$) versus production time.

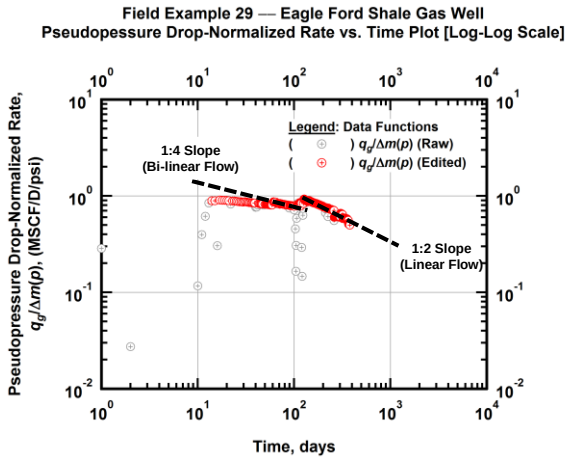

Figure A.843 — (Log-log Plot): Filtered normalized rate production history plot — pseudopressure drop-normalized gas flowrate ($q_g/\Delta m(p)$) versus production time.

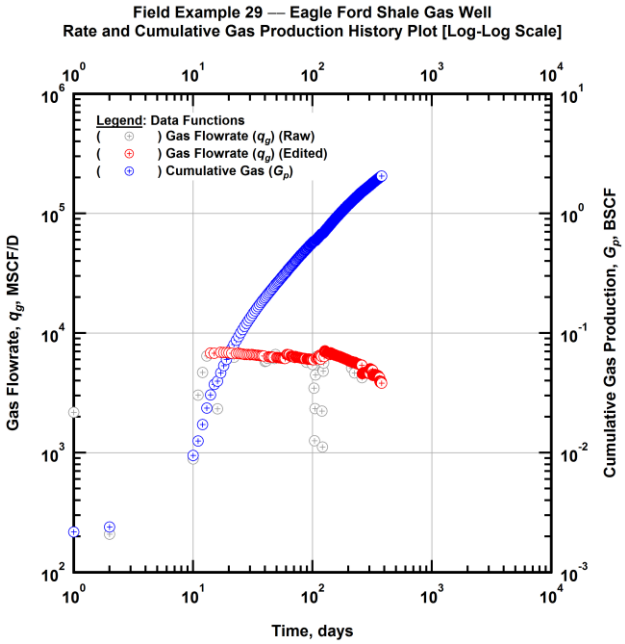

Figure A.844 — (Log-log Plot): Filtered rate and unfiltered cumulative gas production history plot — flowrate (q_g) and cumulative production (G_p) versus production time.

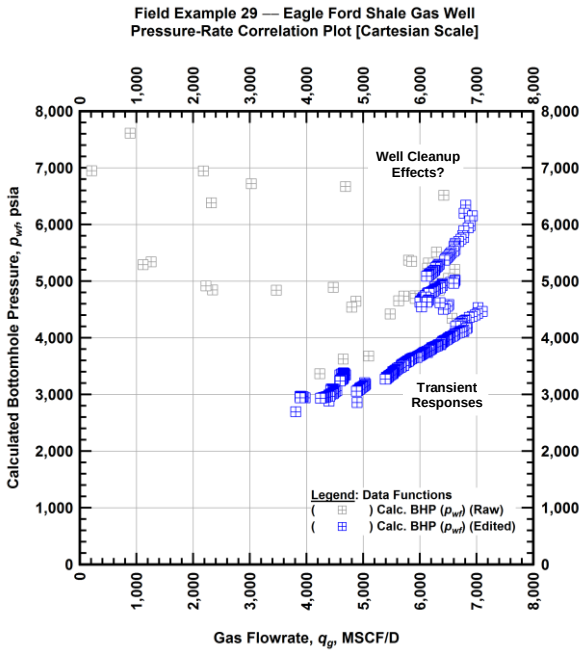

Figure A.845 — (Cartesian Plot): Filtered rate-pressure correlation plot — calculated bottomhole pressure (p_{wf}) versus flowrate (q_g).

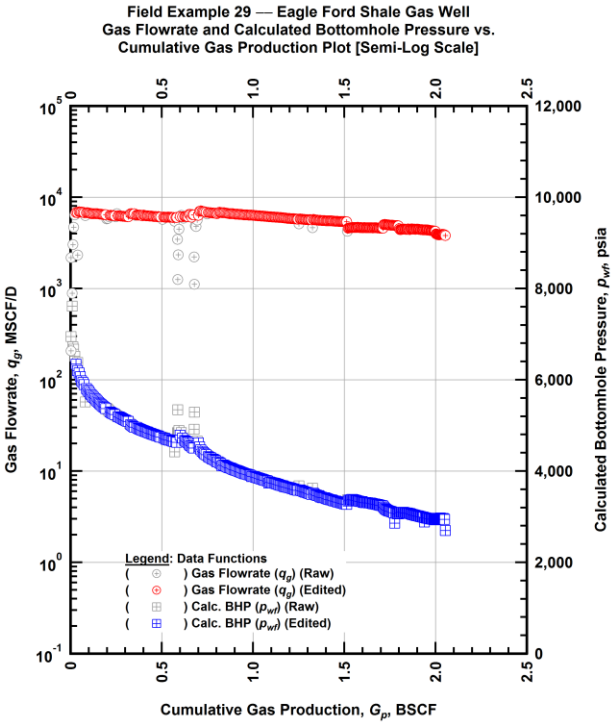

Figure A.846 — (Semi-log Plot): Filtered rate-pressure-cumulative production history plot — flowrate (q_g) and calculated bottomhole pressure (p_{wf}) versus cumulative production (G_p).

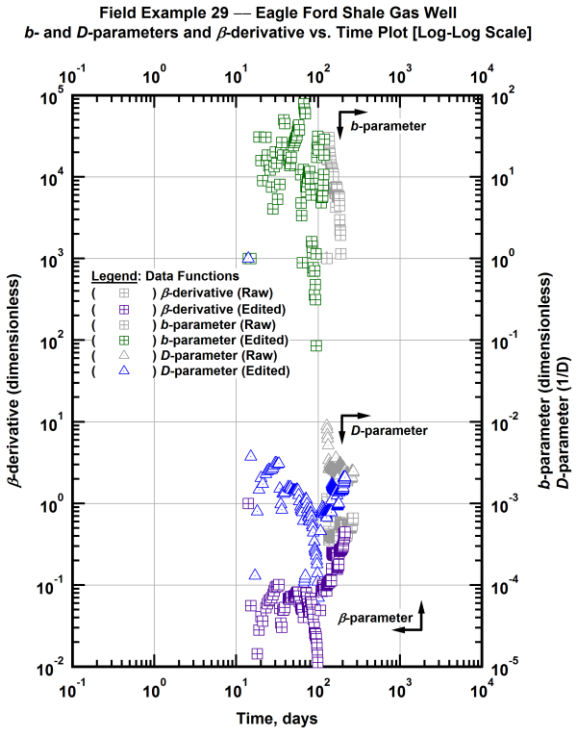

Figure A.847 — (Log-Log Plot): Filtered b, D and β production history plot — b- and D-parameters and β-derivative versus production time.

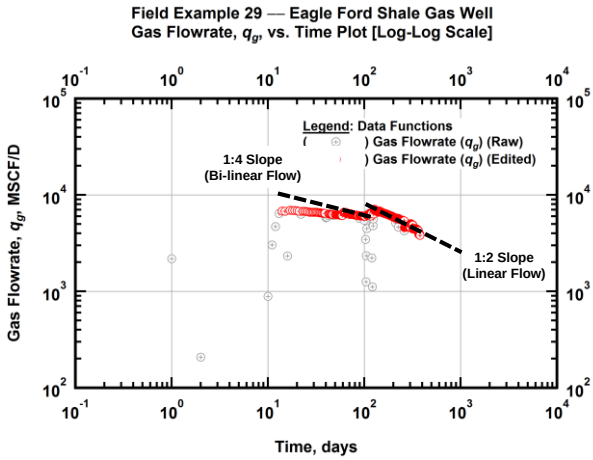

Figure A.848 — (Log-Log Plot): Filtered gas flowrate production history and flow regime identification plot — gas flowrate (q_g) versus production time.

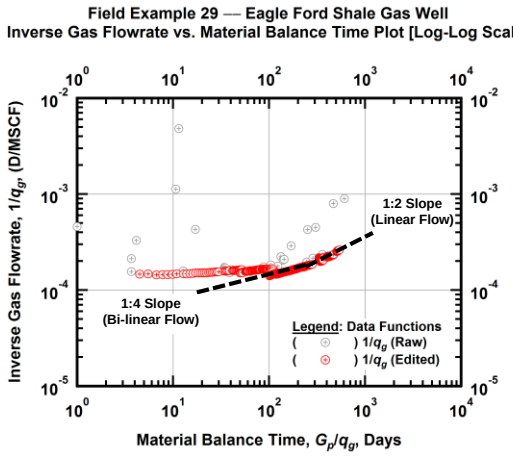

Figure A.849 — (Log-log Plot): Filtered inverse rate with material balance time plot — inverse gas flowrate ($1/q_g$) versus material balance time (G_p/q_g).

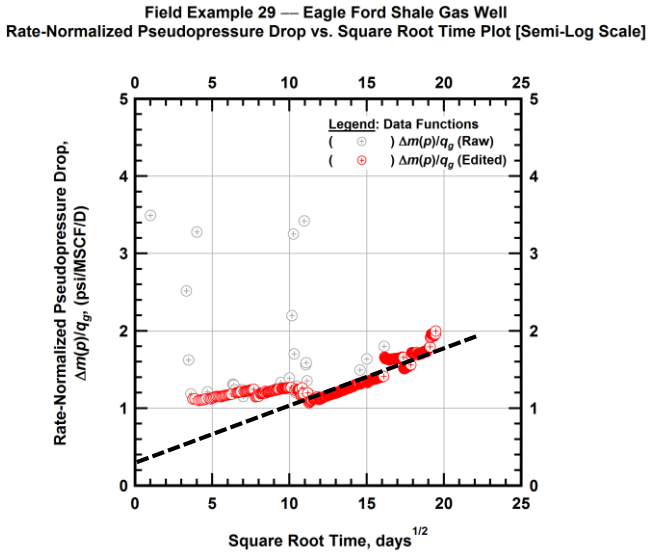

Figure A.850 — (Semi-log Plot): Filtered normalized pseudopressure drop production history plot — rate-normalized pseudopressure drop ($\Delta m(p)/q_g$) versus square root production time ($\sqrt{t}$).

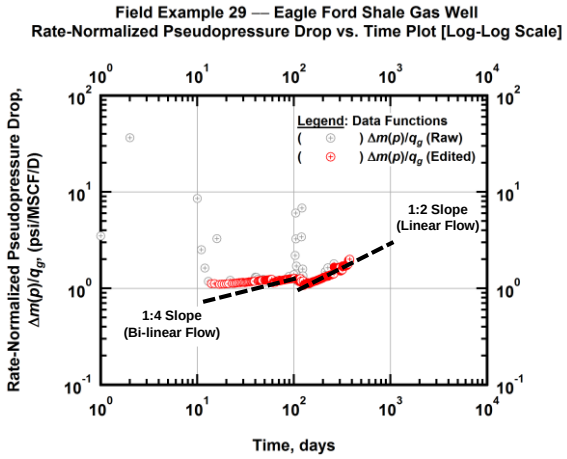

Figure A.851 — (Log-log Plot): Filtered normalized pseudopressure drop production history plot — rate-normalized pseudopressure drop ($\Delta m(p)/q_g$) versus production time.

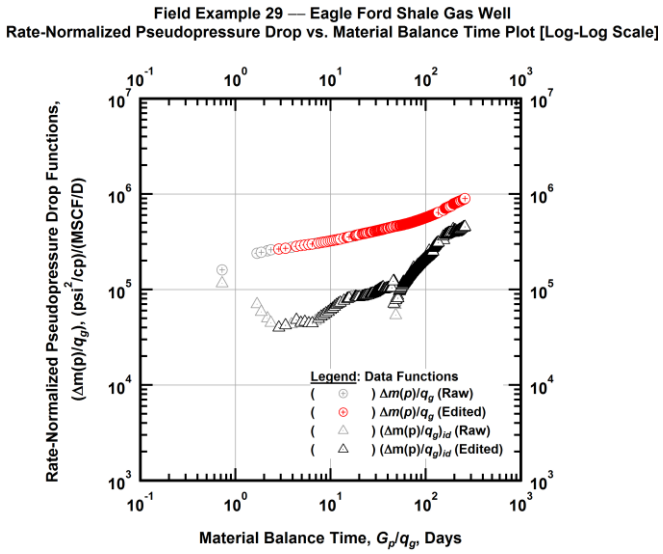

Figure A.852 — (Log-log Plot): "Log-log" diagnostic plot of the filtered production data — rate-normalized pseudopressure drop ($\Delta m(p)/q_g$) and rate-normalized pseudopressure drop integral-derivative $(\Delta m(p)/q_g)_{id}$ versus material balance time (G_p/q_g).

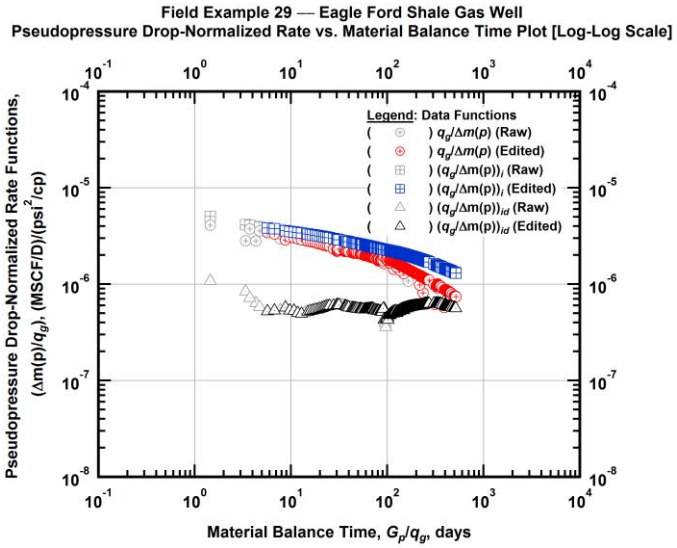

Figure A.853 — (Log-log Plot): "Blasingame" diagnostic plot of the filtered production data — pseudopressure drop-normalized gas flowrate ($q_g/\Delta m(p)$), pseudopressure drop-normalized gas flowrate integral $(q_g/\Delta m(p))_i$ and pseudopressure drop-normalized gas flowrate integral-derivative $(q_g/\Delta m(p))_{id}$ versus material balance time (G_p/q_g).

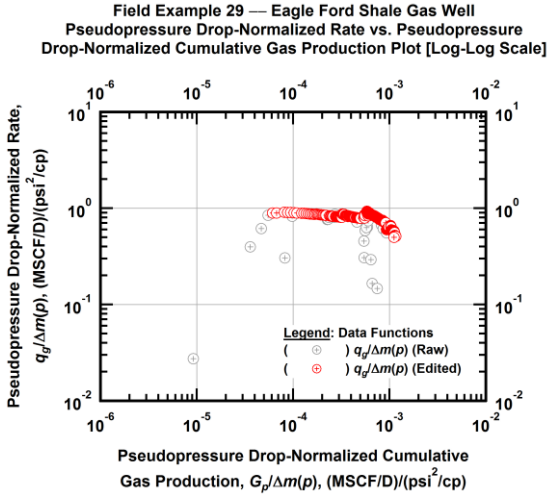

Figure A.854 — (Log-log Plot): Filtered normalized rate with normalized cumulative production plot — pseudopressure drop-normalized gas flowrate ($q_g/\Delta m(p)$) versus pseudopressure drop-normalized cumulative gas production ($G_p/\Delta m(p)$).

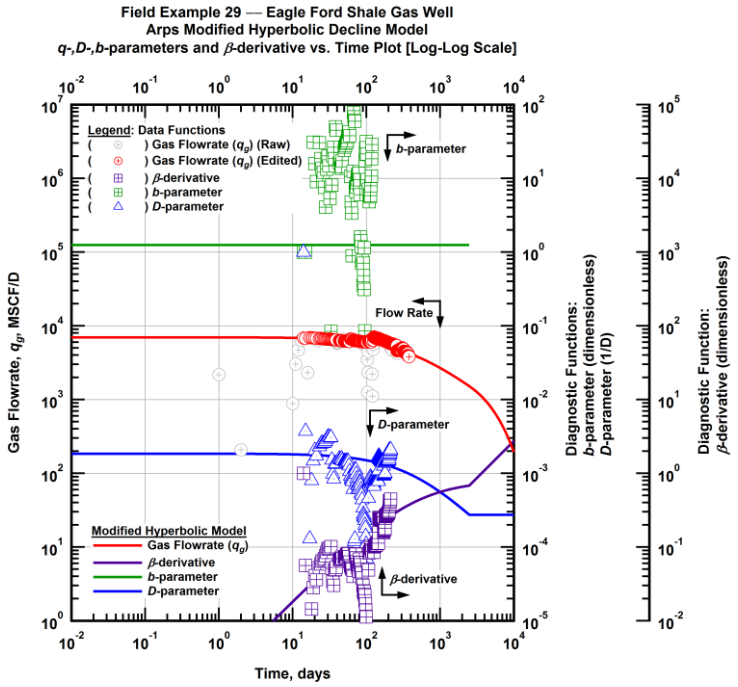

Figure A.855 — (Log-Log Plot): Arps modified hyperbolic decline model plot — time-rate model and data gas flowrate (q_g), *D*- and *b*-parameters and β-derivative versus production time.

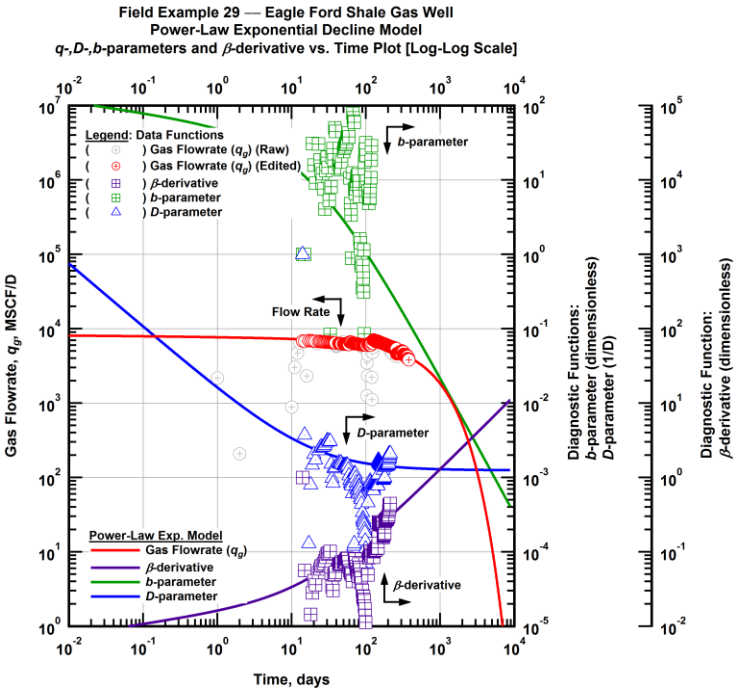

Figure A.856 — (Log-Log Plot): Power-law exponential decline model plot — time-rate model and data gas flowrate (q_g), *D*- and *b*-parameters and β-derivative versus production time.

Field Example 29 — Model-Based (Time-Rate-Pressure) Production Analysis

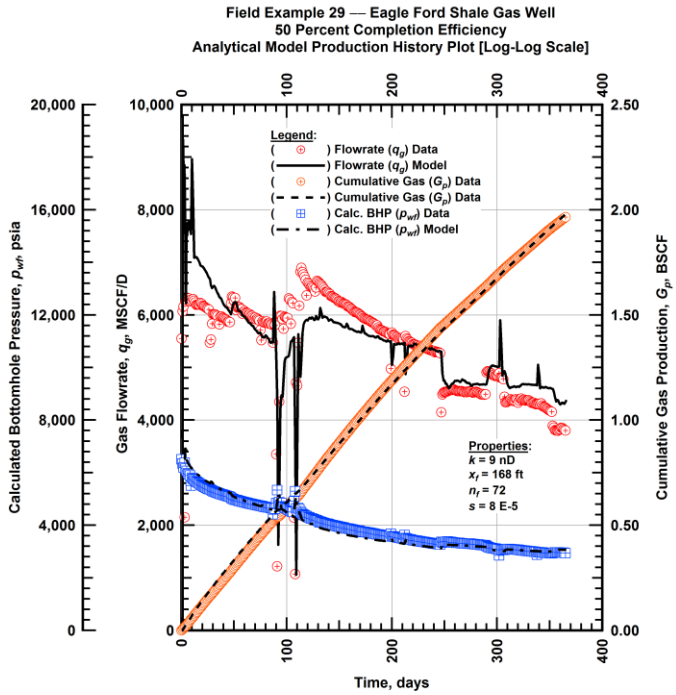

Figure A.857 — (Cartesian Plot): Production history plot — original gas flowrate (q_g), cumulative gas production (G_p), calculated bottomhole pressure (p_{wf}) and 50 percent completion efficiency model matches versus production time.

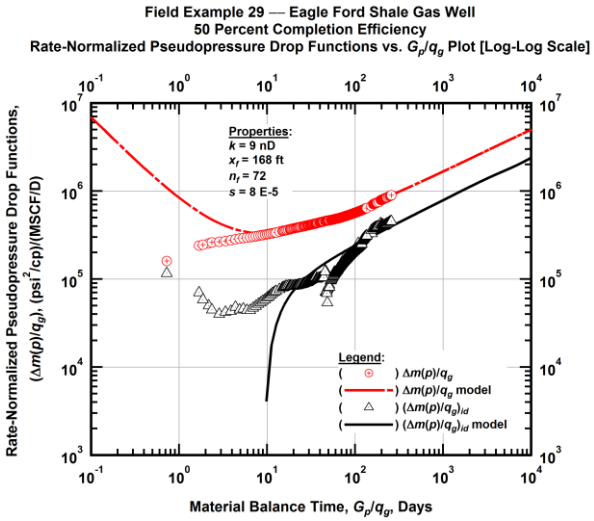

Figure A.858 — (Log-log Plot): "Log-log" diagnostic plot of the original production data — rate-normalized pseudopressure drop ($\Delta m(p)/q_g$), rate-normalized pseudopressure drop integral-derivative $(\Delta m(p)/q_g)_{id}$ and 50 percent completion efficiency model matches versus material balance time (G_p/q_g).

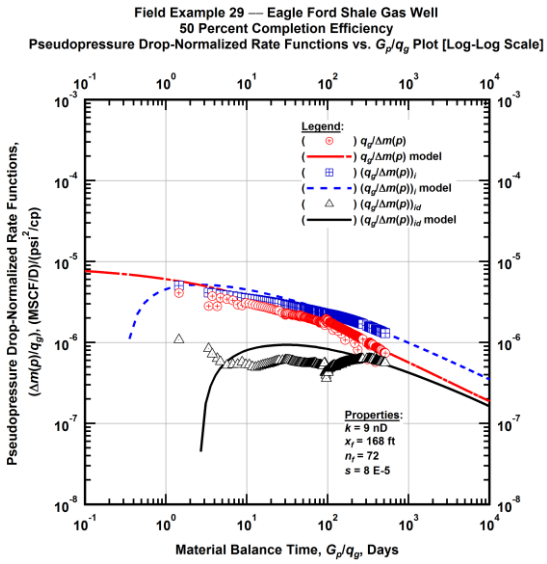

Figure A.859 — (Log-log Plot): "Blasingame" diagnostic plot of the original production data — pseudopressure drop-normalized gas flowrate ($q_g/\Delta m(p)$), pseudopressure drop-normalized gas flowrate integral $(q_g/\Delta m(p))_i$, pseudopressure drop-normalized gas flowrate integral-derivative $(q_g/\Delta m(p))_{id}$ and 50 percent completion efficiency model matches versus material balance time (G_p/q_g).

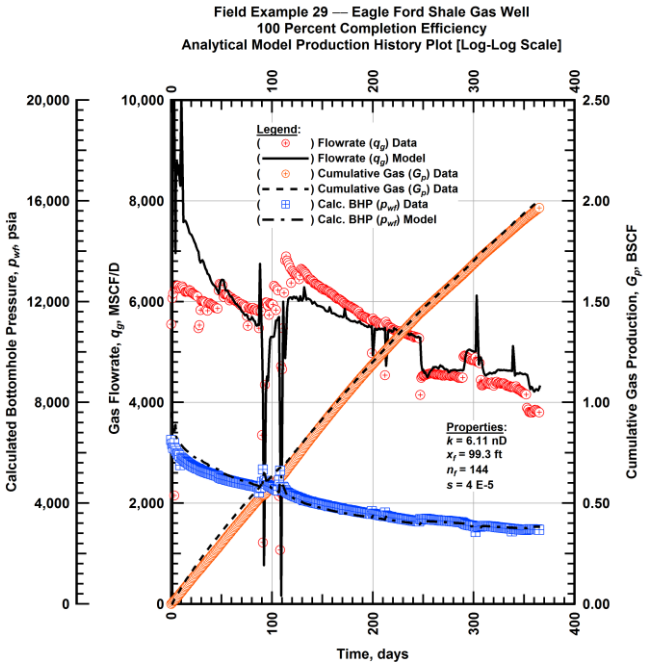

Figure A.860 — (Cartesian Plot): Production history plot — original gas flowrate (q_g), cumulative gas production (G_p), calculated bottomhole pressure (p_{wf}) and 100 percent completion efficiency model matches versus production time.

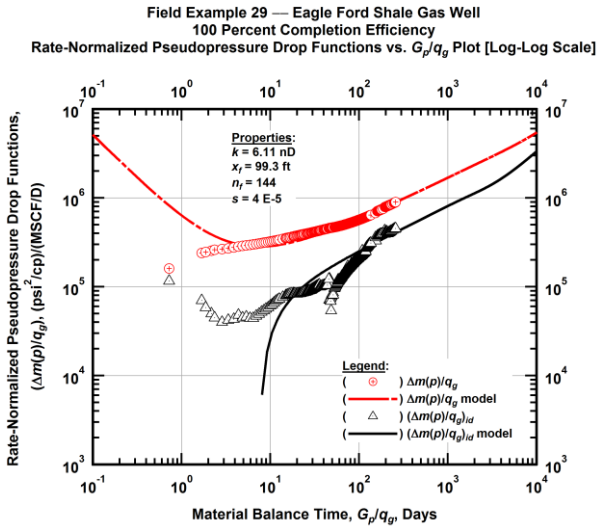

Figure A.861 — (Log-log Plot): "Log-log" diagnostic plot of the original production data — rate-normalized pseudopressure drop ($\Delta m(p)/q_g$), rate-normalized pseudopressure drop integral-derivative $(\Delta m(p)/q_g)_{id}$ and 100 percent completion efficiency model matches versus material balance time (G_p/q_g).

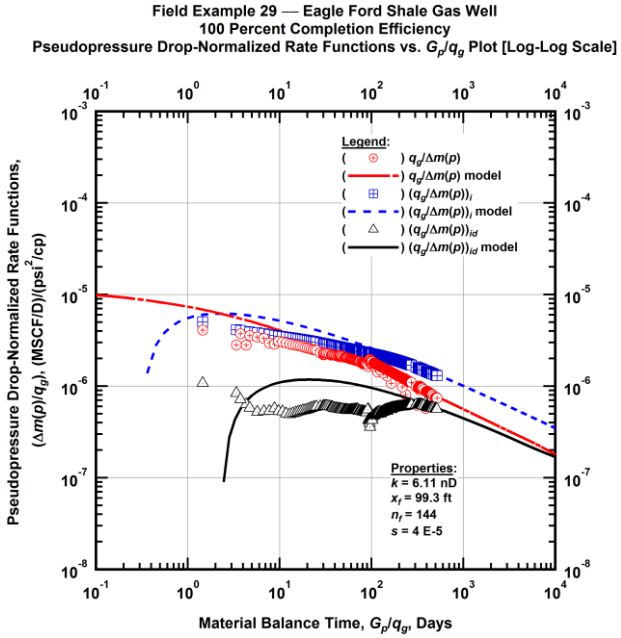

Figure A.862 — (Log-log Plot): "Blasingame" diagnostic plot of the original production data — pseudopressure drop-normalized gas flowrate ($q_g/\Delta m(p)$), pseudopressure drop-normalized gas flowrate integral $(q_g/\Delta m(p))_i$, pseudopressure drop-normalized gas flowrate integral-derivative $(q_g/\Delta m(p))_{id}$ and 100 percent completion efficiency model matches versus material balance time (G_p/q_g).

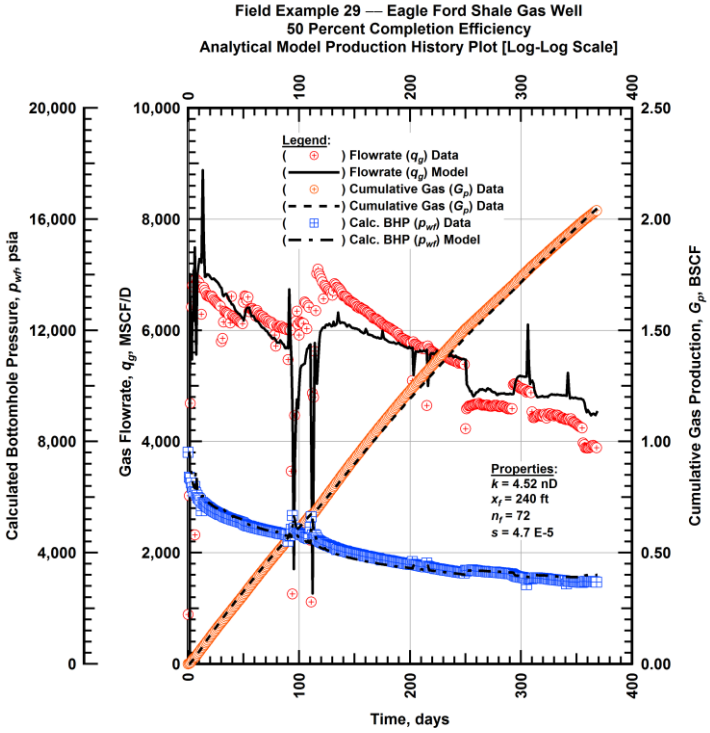

Figure A.863 — (Cartesian Plot): Production history plot — revised gas flowrate (q_g), cumulative gas production (G_p), calculated bottomhole pressure (p_{wf}) and 50 percent completion efficiency model matches versus production time.

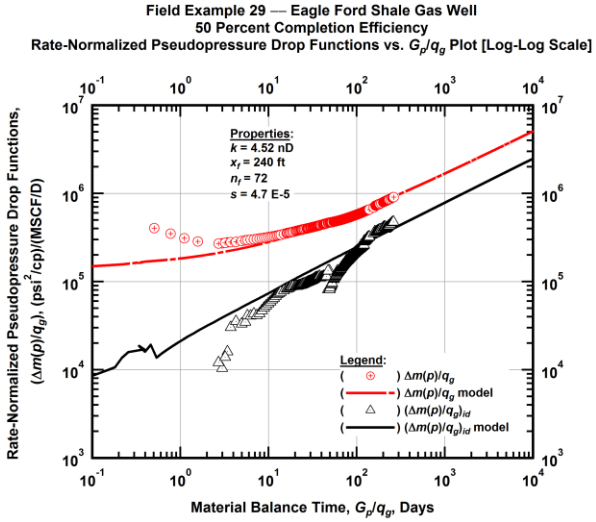

Figure A.864 — (Log-log Plot): "Log-log" diagnostic plot of the revised production data — rate-normalized pseudopressure drop ($\Delta m(p)/q_g$), rate-normalized pseudopressure drop integral-derivative $(\Delta m(p)/q_g)_{id}$ and 50 percent completion efficiency model matches versus material balance time (G_p/q_g).

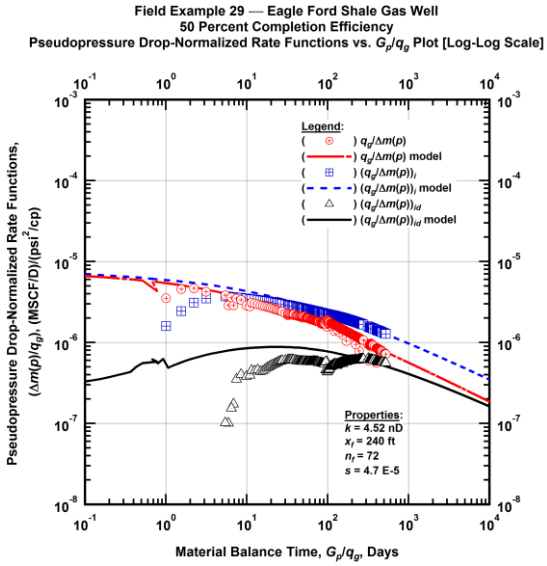

Figure A.865 — (Log-log Plot): "Blasingame" diagnostic plot of the revised production data — pseudopressure drop-normalized gas flowrate ($q_g/\Delta m(p)$), pseudopressure drop-normalized gas flowrate integral $(q_g/\Delta m(p))_i$, pseudopressure drop-normalized gas flowrate integral-derivative $(q_g/\Delta m(p))_{id}$ and 50 percent completion efficiency model matches versus material balance time (G_p/q_g).

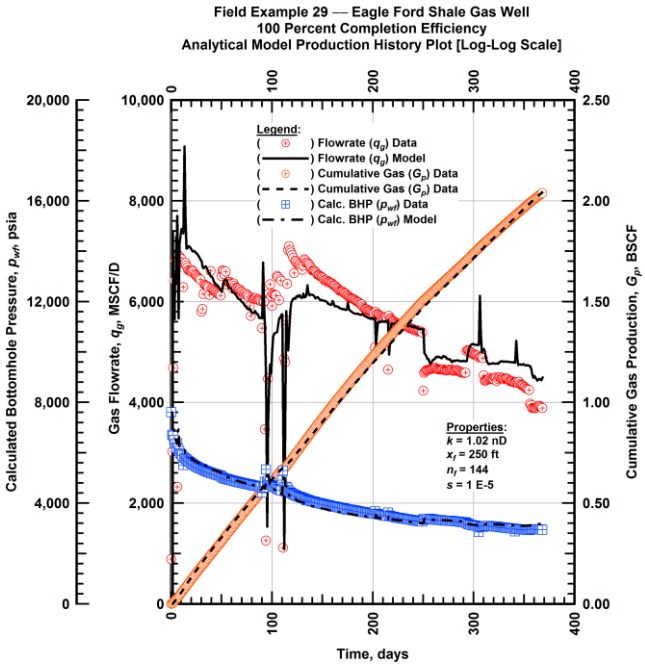

Figure A.866 — (Cartesian Plot): Production history plot — revised gas flowrate (q_g), cumulative gas production (G_p), calculated bottomhole pressure (p_{wf}) and 100 percent completion efficiency model matches versus production time.

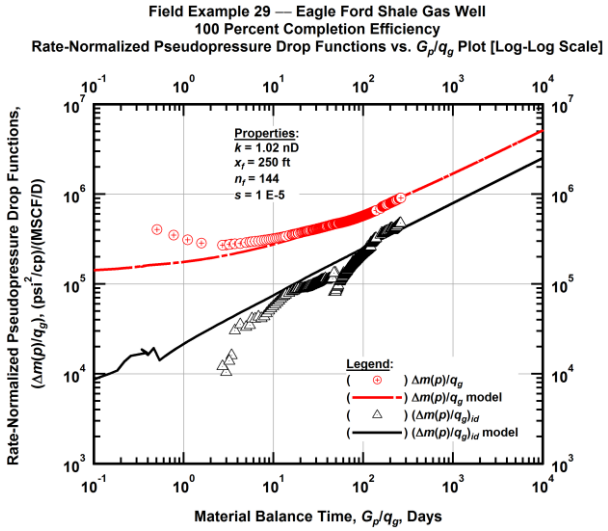

Figure A.867 — (Log-log Plot): "Log-log" diagnostic plot of the revised production data — rate-normalized pseudopressure drop ($\Delta m(p)/q_g$), rate-normalized pseudopressure drop integral-derivative $(\Delta m(p)/q_g)_{id}$ and 100 percent completion efficiency model matches versus material balance time (G_p/q_g).

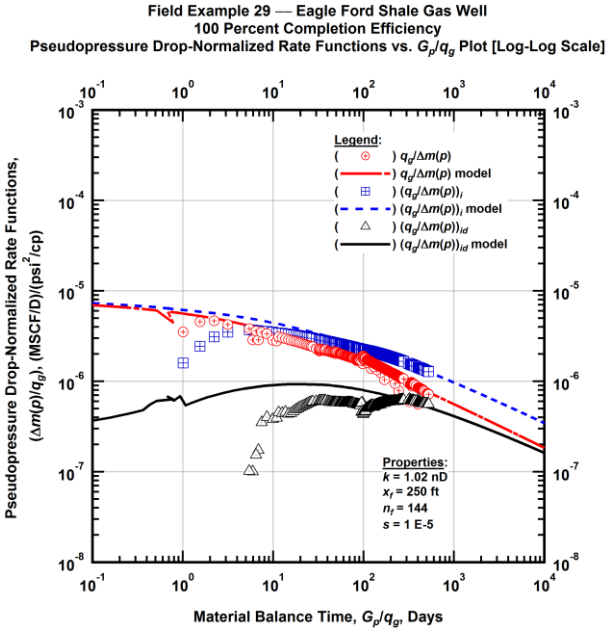

Figure A.868 — (Log-log Plot): "Blasingame" diagnostic plot of the revised production data — pseudopressure drop-normalized gas flowrate ($q_g/\Delta m(p)$), pseudopressure drop-normalized gas flowrate integral $(q_g/\Delta m(p))_i$, pseudopressure drop-normalized gas flowrate integral-derivative $(q_g/\Delta m(p))_{id}$ and 100 percent completion efficiency model matches versus material balance time (G_p/q_g).

Field Example 29 — 30-Year EUR Model Comparison

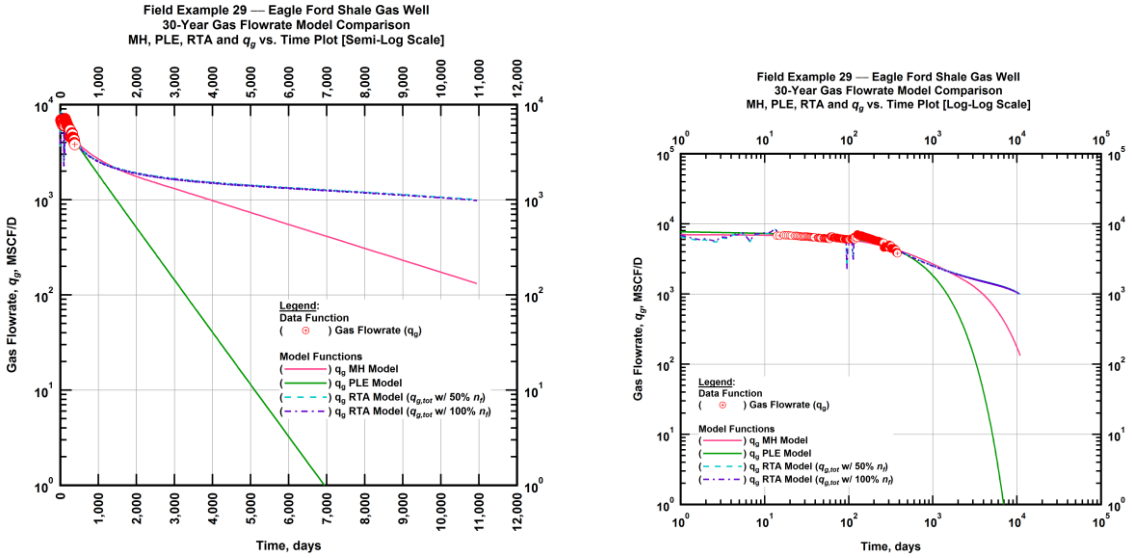

A **B**

Figure A.869 — (A — Semi-Log Plot) and (B — Log-Log Plot): Estimated 30-year revised gas flowrate model comparison — Arps modified hyperbolic decline model, power-law exponential decline model, and 50 percent and 100 percent completion efficiency RTA models revised gas 30-year estimated flowrate decline and historic gas flowrate data (q_g) versus production time.

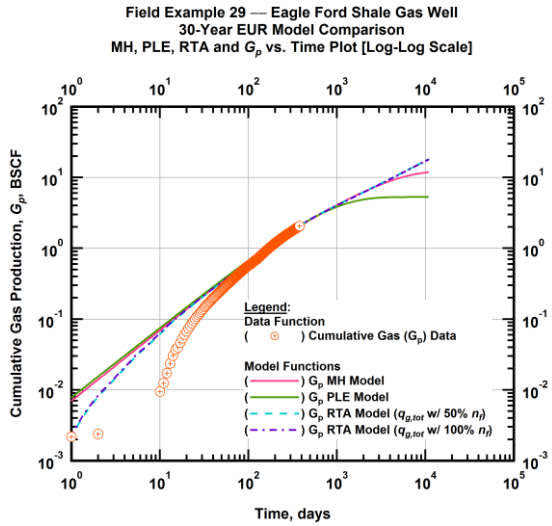

Figure A.870 — (Log-log Plot): PVT revised gas 30-year estimated cumulative production volume model comparison — Arps modified hyperbolic decline model, power-law exponential decline model, and 50 percent and 100 percent completion efficiency RTA model estimated 30-year cumulative gas production volumes and historic cumulative gas production (G_p) versus production time.

Table A.29 — 30-year estimated cumulative revised gas production (EUR), in units of BSCF, for the Arps modified hyperbolic, power-law exponential and analytical time-rate-pressure decline models.

Arps Modified Hyperbolic (BSCF)	Power-Law Exponential (BSCF)	RTA Analytical Model ($q_{g,tot}$ w/ 50% n_f) (BSCF)	RTA Analytical Model ($q_{g,tot}$ w/ 100% n_f) (BSCF)
12.08	5.23	18.53	18.34

Field Example 30 — Time-Rate Analysis

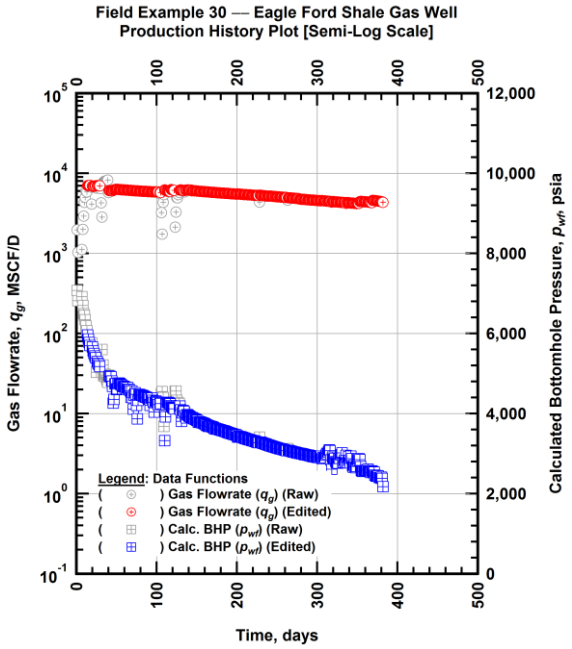

Figure A.871 — (Semi-log Plot): Filtered production history plot — flowrate (qg) and calculated bottomhole pressure (pwf) versus production time.

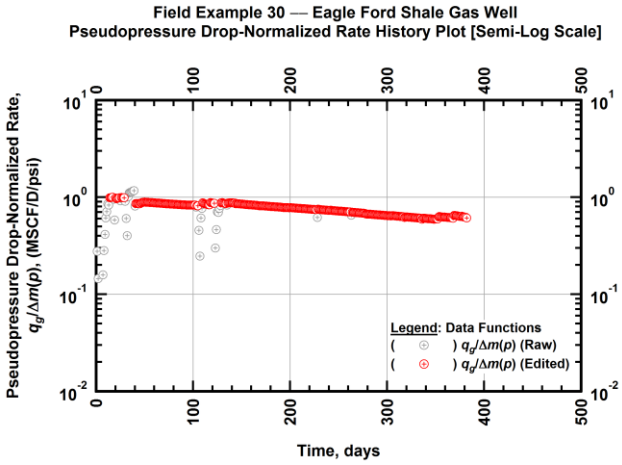

Figure A.872 — (Semi-log Plot): Filtered normalized rate production history plot — pseudopressure drop-normalized gas flowrate ($q_g/\Delta m(p)$) versus production time.

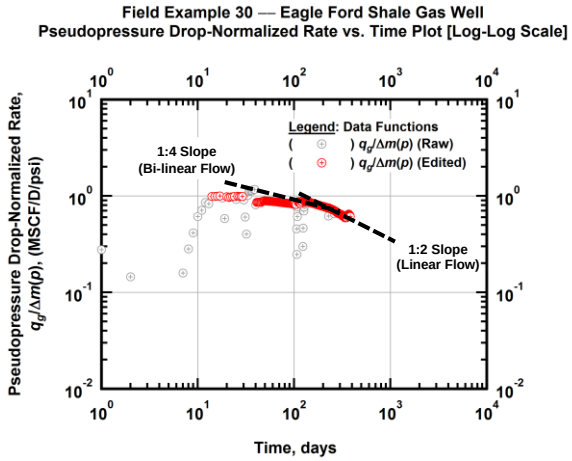

Figure A.873 — (Log-log Plot): Filtered normalized rate production history plot — pseudopressure drop-normalized gas flowrate ($q_g/\Delta m(p)$) versus production time.

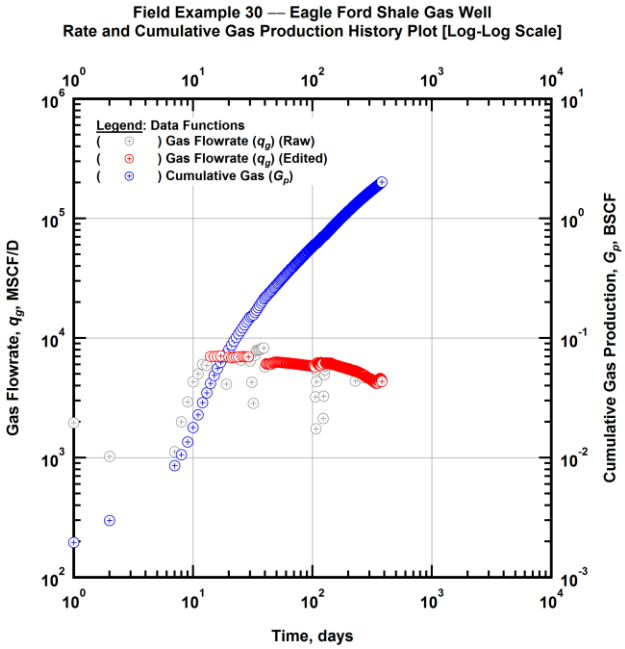

Figure A.874 — (Log-log Plot): Filtered rate and unfiltered cumulative gas production history plot — flowrate (q_g) and cumulative production (G_p) versus production time.

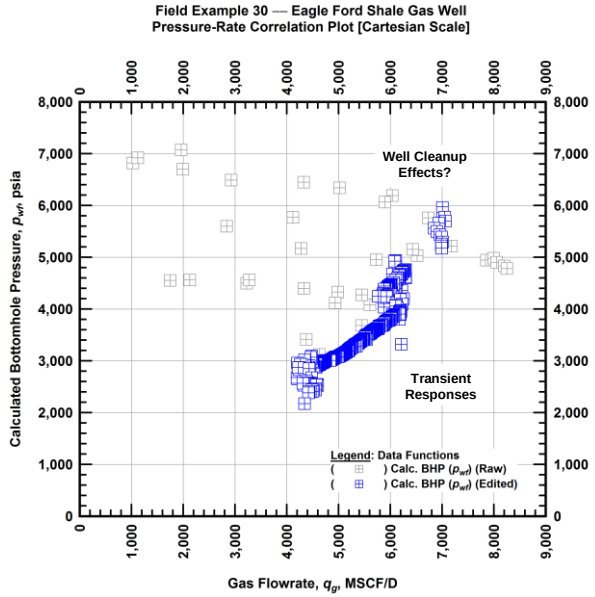

Figure A.875 — (Cartesian Plot): Filtered rate-pressure correlation plot — calculated bottomhole pressure (p_{wf}) versus flowrate (q_g).

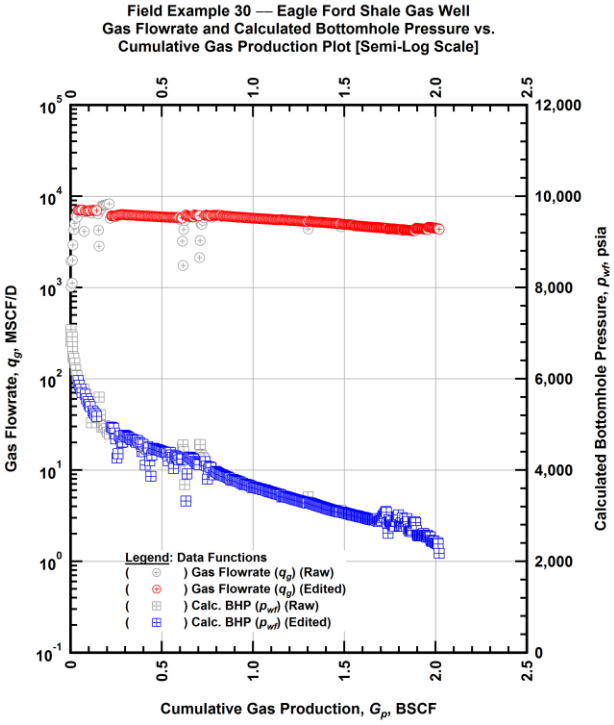

Figure A.876 — (Semi-log Plot): Filtered rate-pressure-cumulative production history plot — flowrate (q_g) and calculated bottomhole pressure (p_{wf}) versus cumulative production (G_p).

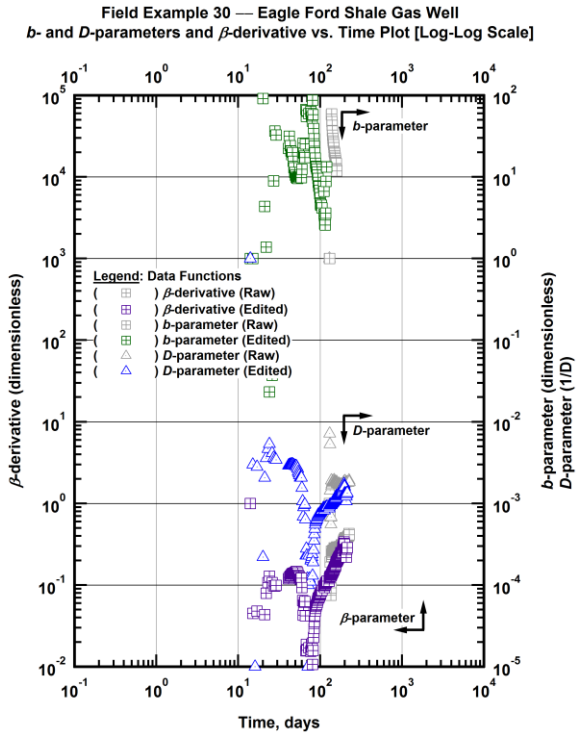

Figure A.877 — (Log-Log Plot): Filtered b, D and β production history plot — b- and D-parameters and β-derivative versus production time.

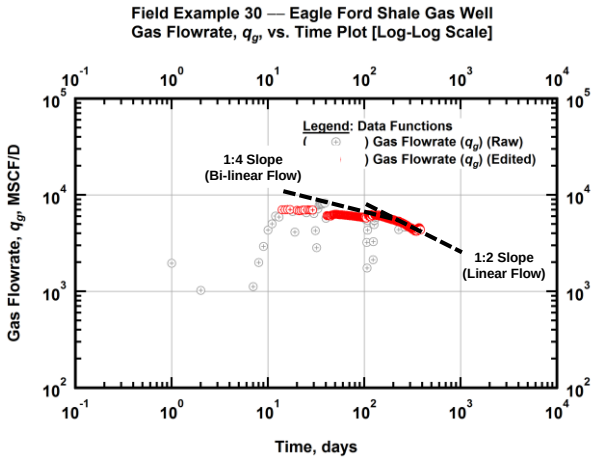

Figure A.878 — (Log-Log Plot): Filtered gas flowrate production history and flow regime identification plot — gas flowrate (q_g) versus production time.

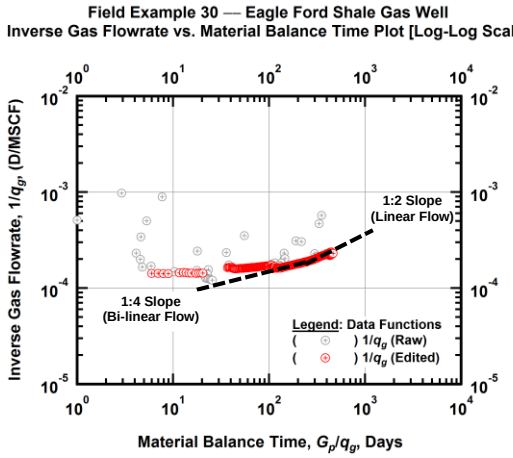

Figure A.879 — (Log-log Plot): Filtered inverse rate with material balance time plot — inverse gas flowrate ($1/q_g$) versus material balance time (G_p/q_g).

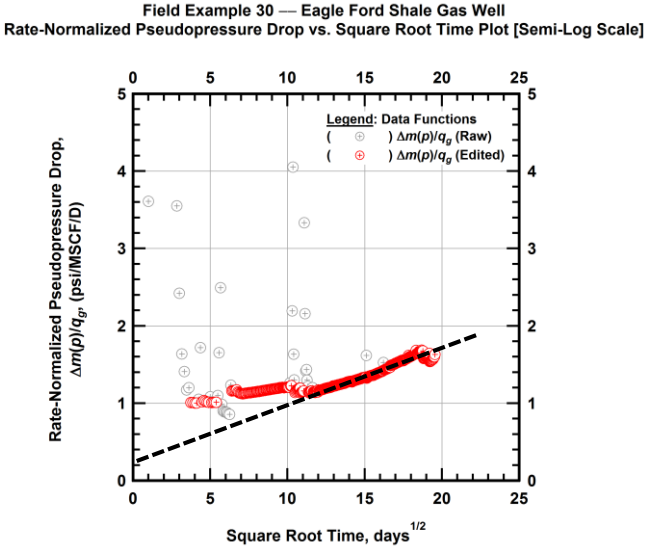

Figure A.880 — (Semi-log Plot): Filtered normalized pseudopressure drop production history plot — rate-normalized pseudopressure drop ($\Delta m(p)/q_g$) versus square root production time ($\sqrt{t}$).

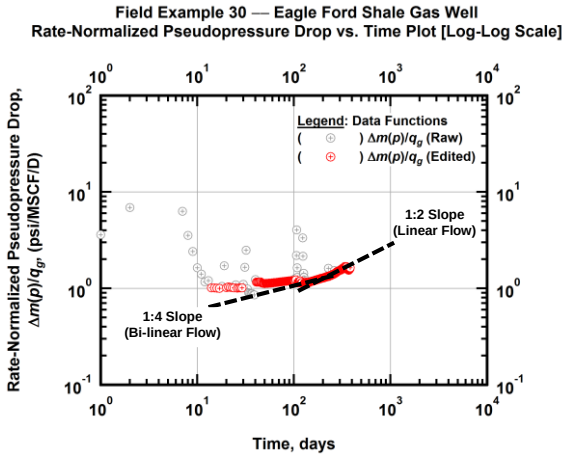

Figure A.881 — (Log-log Plot): Filtered normalized pseudopressure drop production history plot — rate-normalized pseudopressure drop ($\Delta m(p)/q_g$) versus production time.

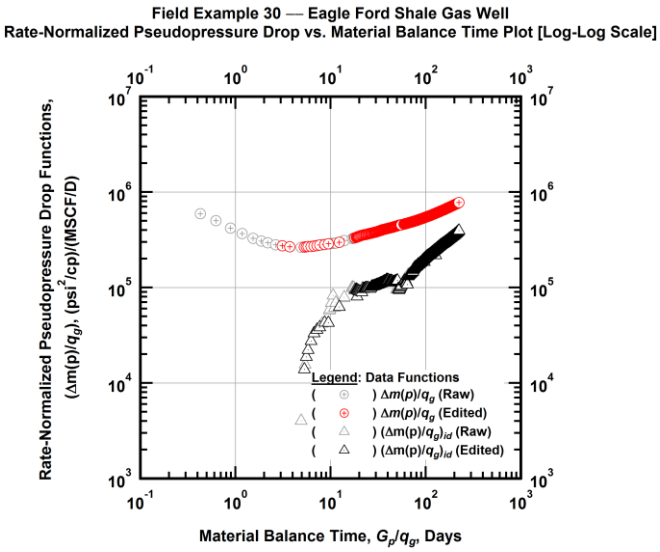

Figure A.882 — (Log-log Plot): "Log-log" diagnostic plot of the filtered production data — rate-normalized pseudopressure drop ($\Delta m(p)/q_g$) and rate-normalized pseudopressure drop integral-derivative $(\Delta m(p)/q_g)_{id}$ versus material balance time (G_p/q_g).

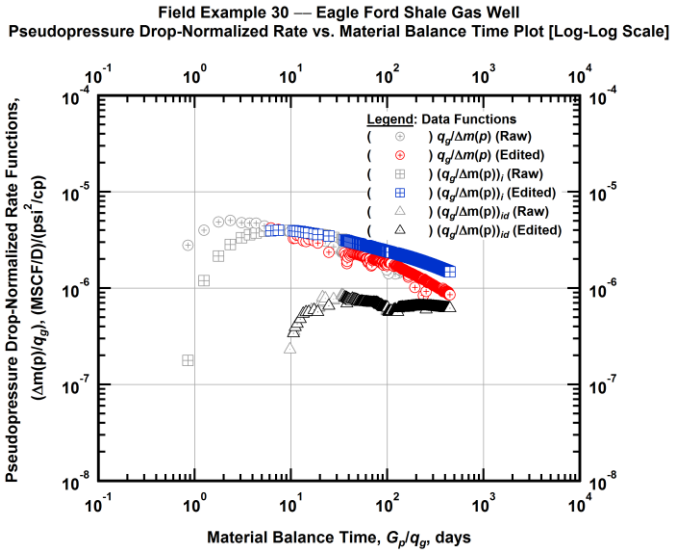

Figure A.883 — (Log-log Plot): "Blasingame" diagnostic plot of the filtered production data — pseudopressure drop-normalized gas flowrate ($q_g/\Delta m(p)$), pseudopressure drop-normalized gas flowrate integral $(q_g/\Delta m(p))_i$ and pseudopressure drop-normalized gas flowrate integral-derivative $(q_g/\Delta m(p))_{id}$ versus material balance time (G_p/q_g).

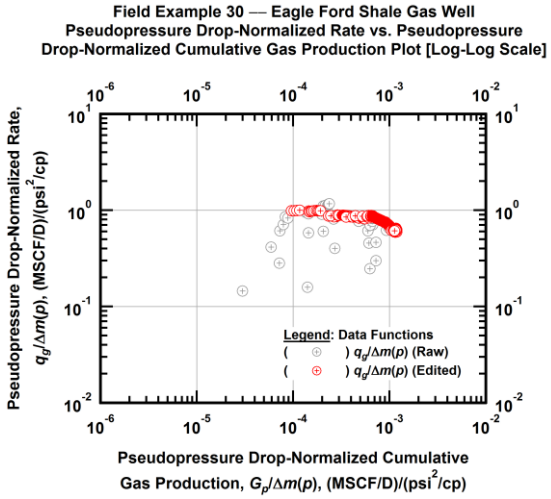

Figure A.884 — (Log-log Plot): Filtered normalized rate with normalized cumulative production plot — pseudopressure drop-normalized gas flowrate ($q_g/\Delta m(p)$) versus pseudopressure drop-normalized cumulative gas production ($G_p/\Delta m(p)$).

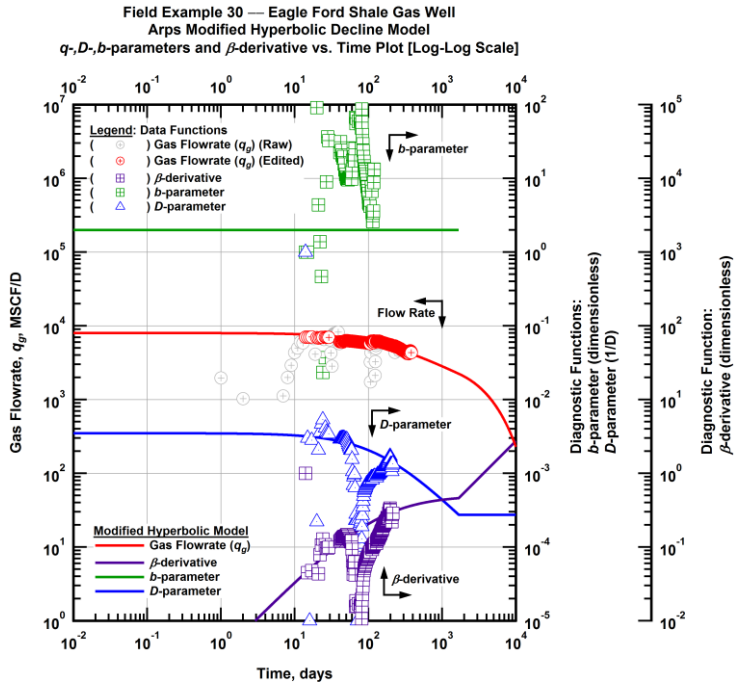

Figure A.885 — (Log-Log Plot): Arps modified hyperbolic decline model plot — time-rate model and data gas flowrate (q_g), *D*- and *b*-parameters and β-derivative versus production time.

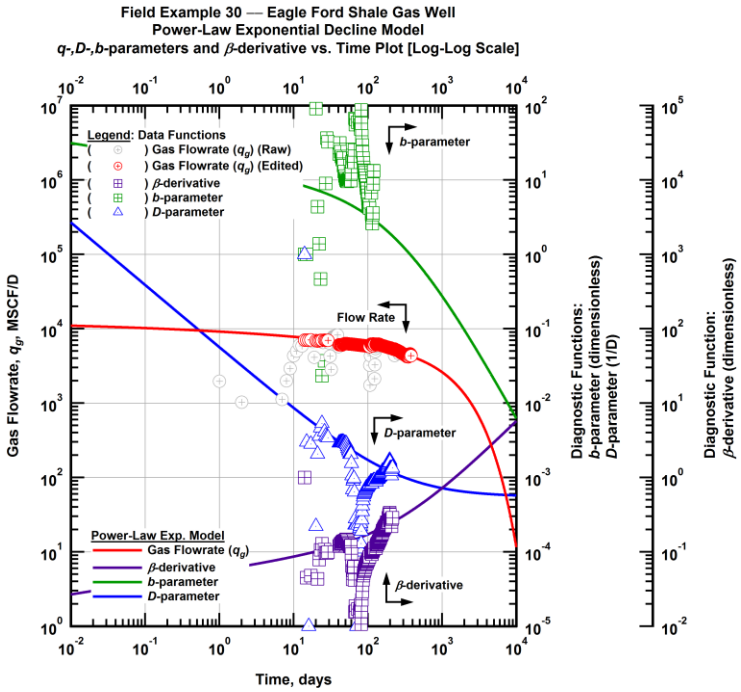

Figure A.886 — (Log-Log Plot): Power-law exponential decline model plot — time-rate model and data gas flowrate (q_g), *D*- and *b*-parameters and β-derivative versus production time.

Field Example 30 — Model-Based (Time-Rate-Pressure) Production Analysis

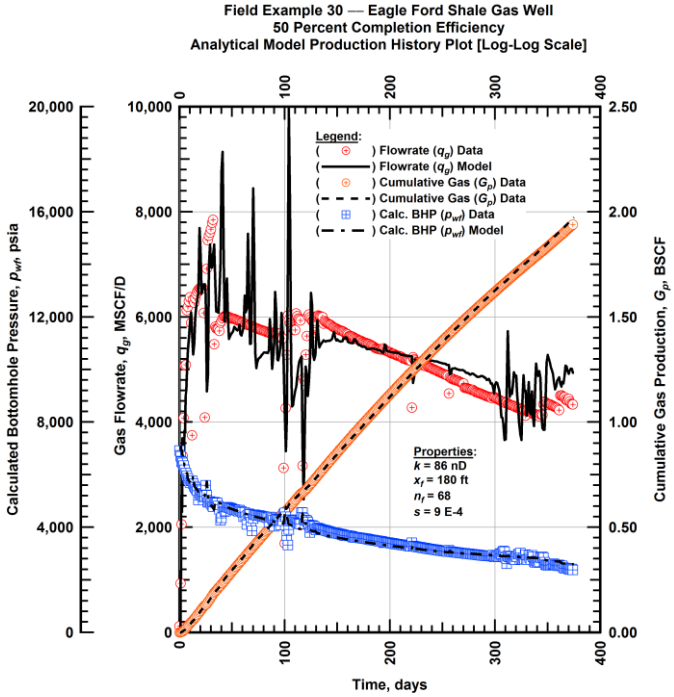

Figure A.887 — (Cartesian Plot): Production history plot — original gas flowrate (q_g), cumulative gas production (G_p), calculated bottomhole pressure (p_{wf}) and 50 percent completion efficiency model matches versus production time.

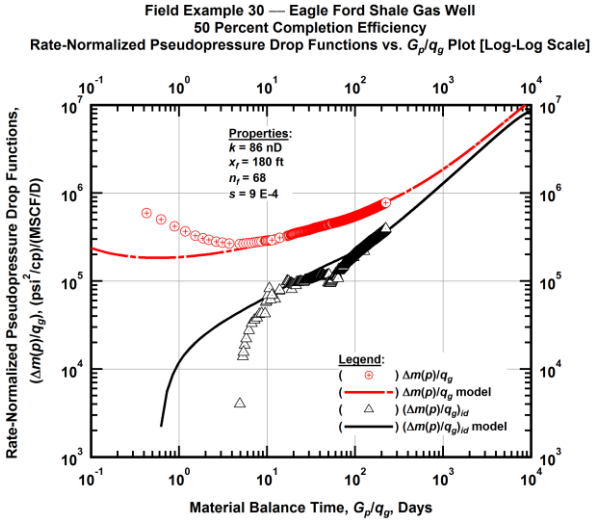

Figure A.888 — (Log-log Plot): "Log-log" diagnostic plot of the original production data — rate-normalized pseudopressure drop ($\Delta m(p)/q_g$), rate-normalized pseudopressure drop integral-derivative $(\Delta m(p)/q_g)_{id}$ and 50 percent completion efficiency model matches versus material balance time (G_p/q_g).

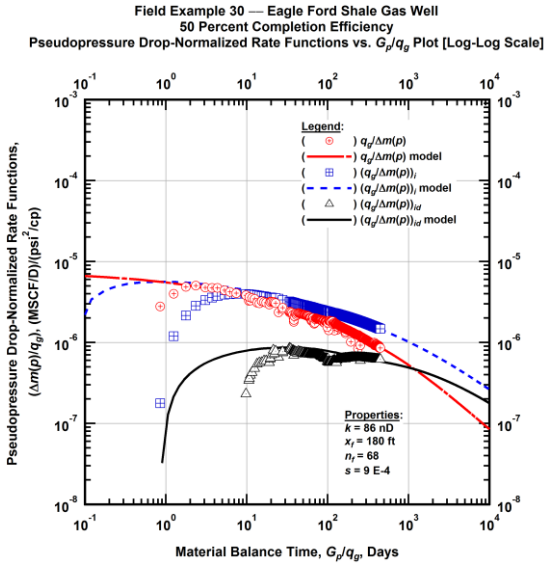

Figure A.889 — (Log-log Plot): "Blasingame" diagnostic plot of the original production data — pseudopressure drop-normalized gas flowrate ($q_g/\Delta m(p)$), pseudopressure drop-normalized gas flowrate integral $(q_g/\Delta m(p))_i$, pseudopressure drop-normalized gas flowrate integral-derivative $(q_g/\Delta m(p))_{id}$ and 50 percent completion efficiency model matches versus material balance time (G_p/q_g).

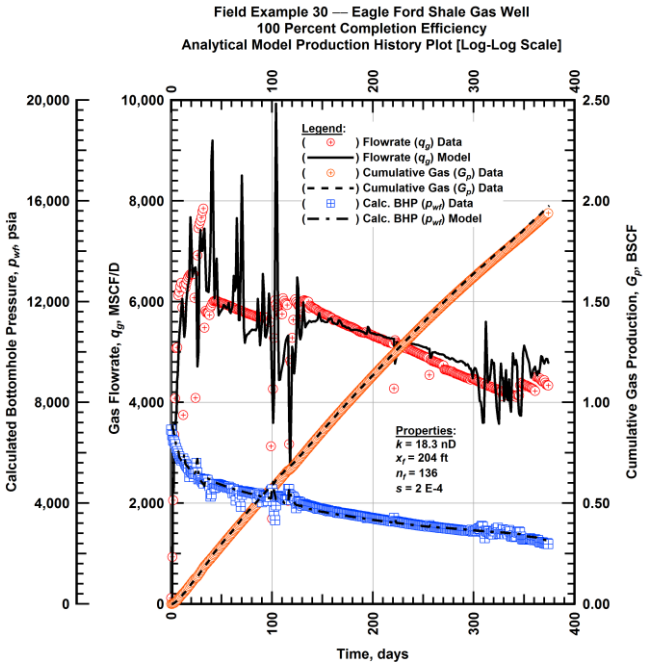

Figure A.890 — (Cartesian Plot): Production history plot — original gas flowrate (q_g), cumulative gas production (G_p), calculated bottomhole pressure (p_{wf}) and 100 percent completion efficiency model matches versus production time.

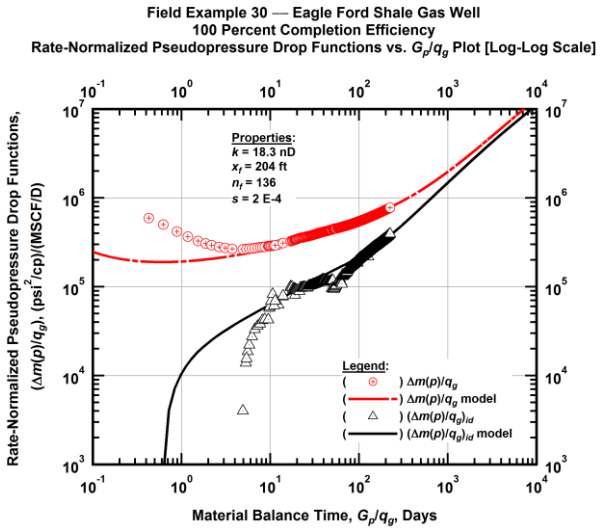

Figure A.891 — (Log-log Plot): "Log-log" diagnostic plot of the original production data — rate-normalized pseudopressure drop ($\Delta m(p)/q_g$), rate-normalized pseudopressure drop integral-derivative $(\Delta m(p)/q_g)_{id}$ and 100 percent completion efficiency model matches versus material balance time (G_p/q_g).

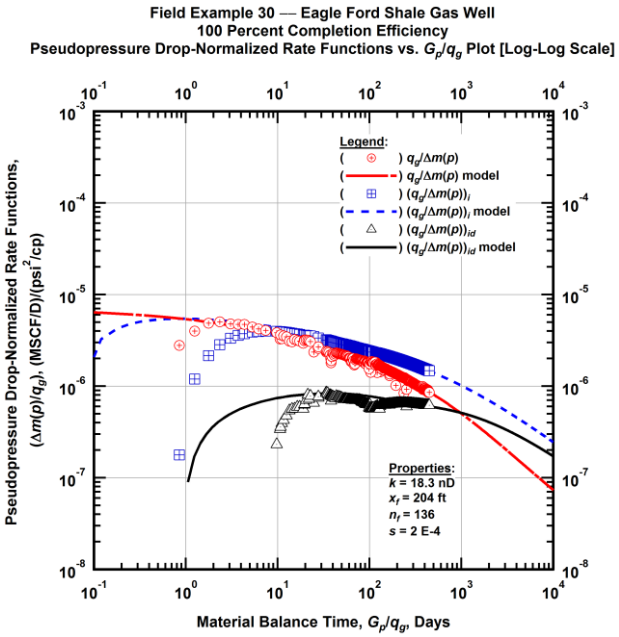

Figure A.892 — (Log-log Plot): "Blasingame" diagnostic plot of the original production data — pseudopressure drop-normalized gas flowrate ($q_g/\Delta m(p)$), pseudopressure drop-normalized gas flowrate integral $(q_g/\Delta m(p))_i$, pseudopressure drop-normalized gas flowrate integral-derivative $(q_g/\Delta m(p))_{id}$ and 100 percent completion efficiency model matches versus material balance time (G_p/q_g).

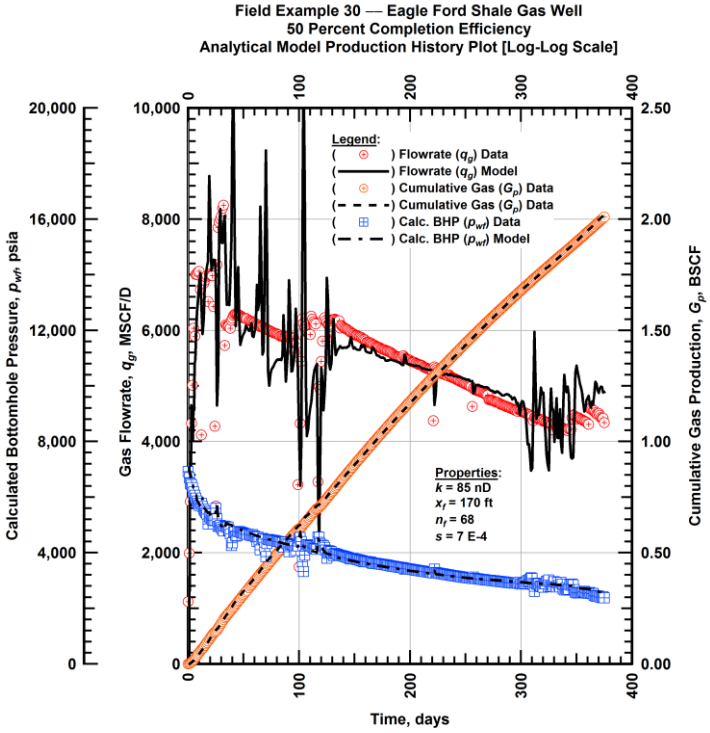

Figure A.893 — (Cartesian Plot): Production history plot — revised gas flowrate (q_g), cumulative gas production (G_p), calculated bottomhole pressure (p_{wf}) and 50 percent completion efficiency model matches versus production time.

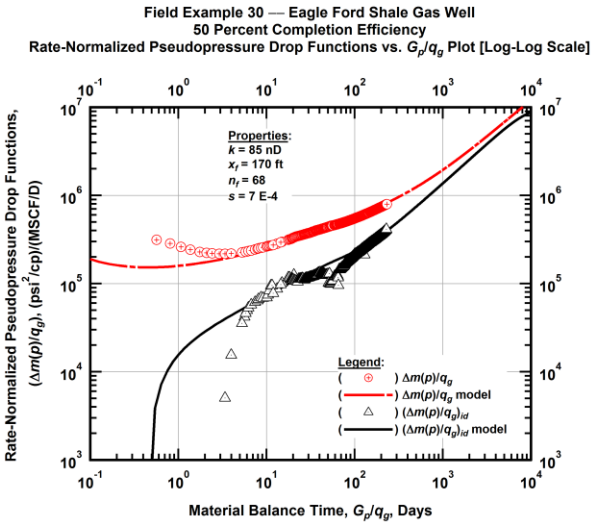

Figure A.894 — (Log-log Plot): "Log-log" diagnostic plot of the revised production data — rate-normalized pseudopressure drop ($\Delta m(p)/q_g$), rate-normalized pseudopressure drop integral-derivative $(\Delta m(p)/q_g)_{id}$ and 50 percent completion efficiency model matches versus material balance time (G_p/q_g).

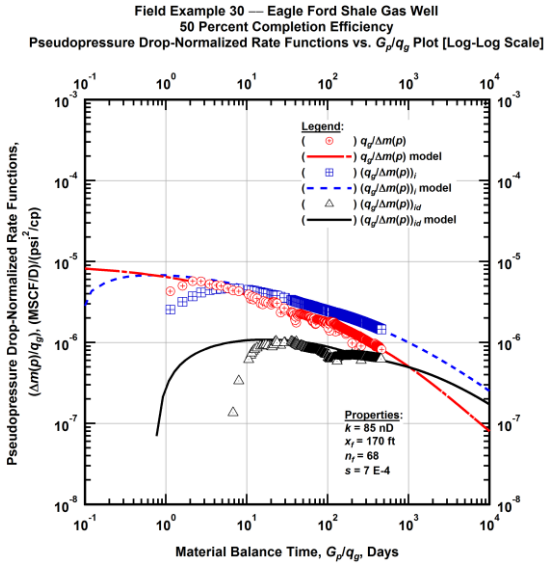

Figure A.895 — (Log-log Plot): "Blasingame" diagnostic plot of the revised production data — pseudopressure drop-normalized gas flowrate ($q_g/\Delta m(p)$), pseudopressure drop-normalized gas flowrate integral $(q_g/\Delta m(p))_i$, pseudopressure drop-normalized gas flowrate integral-derivative $(q_g/\Delta m(p))_{id}$ and 50 percent completion efficiency model matches versus material balance time (G_p/q_g).

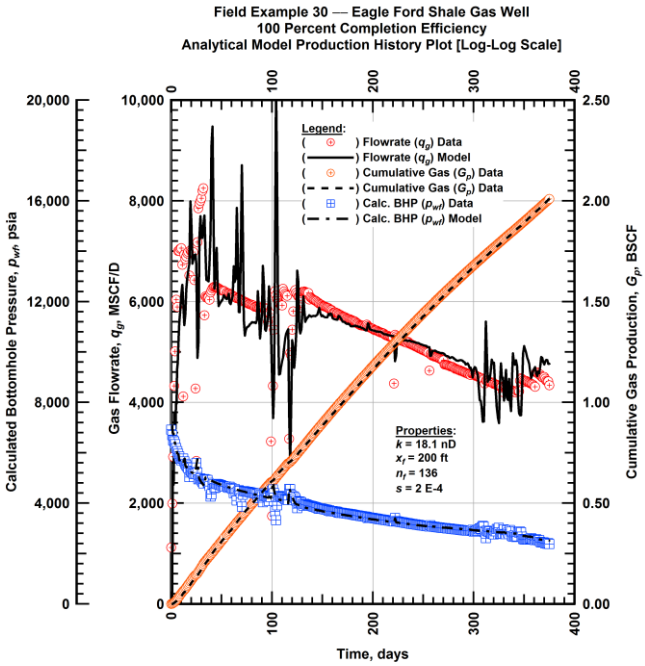

Figure A.896 — (Cartesian Plot): Production history plot — revised gas flowrate (q_g), cumulative gas production (G_p), calculated bottomhole pressure (p_{wf}) and 100 percent completion efficiency model matches versus production time.

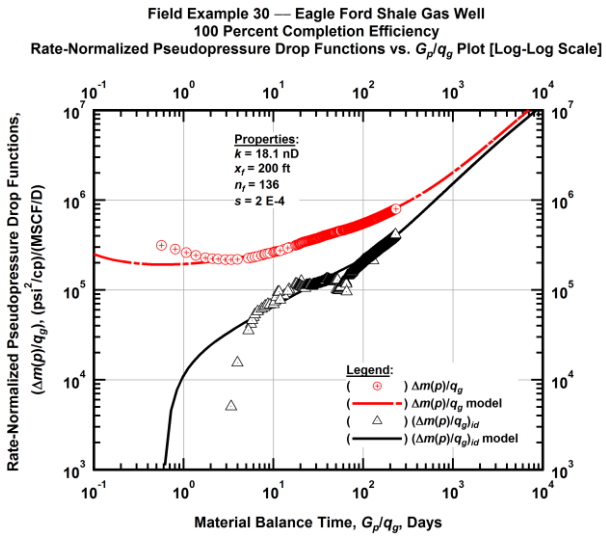

Figure A.897 — (Log-log Plot): "Log-log" diagnostic plot of the revised production data — rate-normalized pseudopressure drop ($\Delta m(p)/q_g$), rate-normalized pseudopressure drop integral-derivative $(\Delta m(p)/q_g)_{id}$ and 100 percent completion efficiency model matches versus material balance time (G_p/q_g).

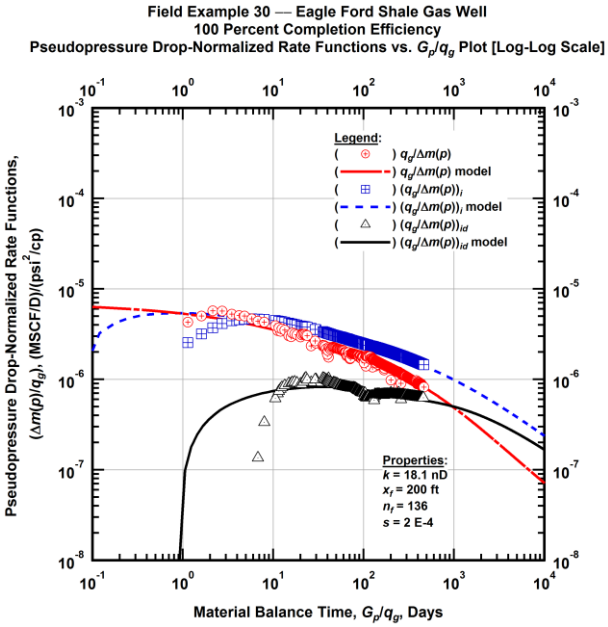

Figure A.898 — (Log-log Plot): "Blasingame" diagnostic plot of the revised production data — pseudopressure drop-normalized gas flowrate ($q_g/\Delta m(p)$), pseudopressure drop-normalized gas flowrate integral $(q_g/\Delta m(p))_i$, pseudopressure drop-normalized gas flowrate integral-derivative $(q_g/\Delta m(p))_{id}$ and 100 percent completion efficiency model matches versus material balance time (G_p/q_g).

Field Example 30 — 30-Year EUR Model Comparison

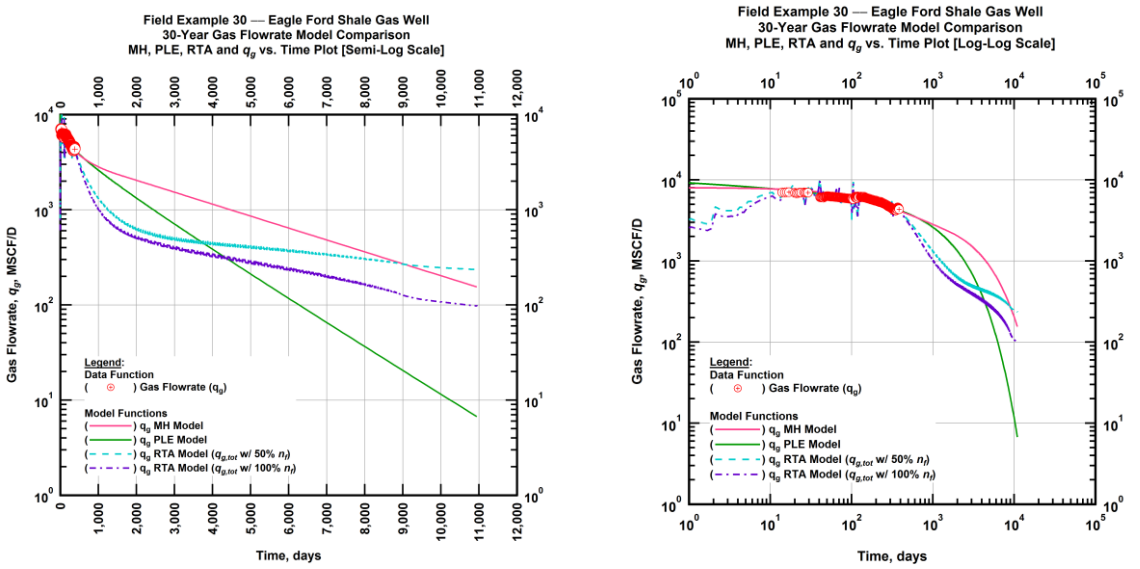

A **B**

Figure A.899 — (A — Semi-Log Plot) and (B — Log-Log Plot): Estimated 30-year revised gas flowrate model comparison — Arps modified hyperbolic decline model, power-law exponential decline model, and 50 percent and 100 percent completion efficiency RTA models revised gas 30-year estimated flowrate decline and historic gas flowrate data (q_g) versus production time.

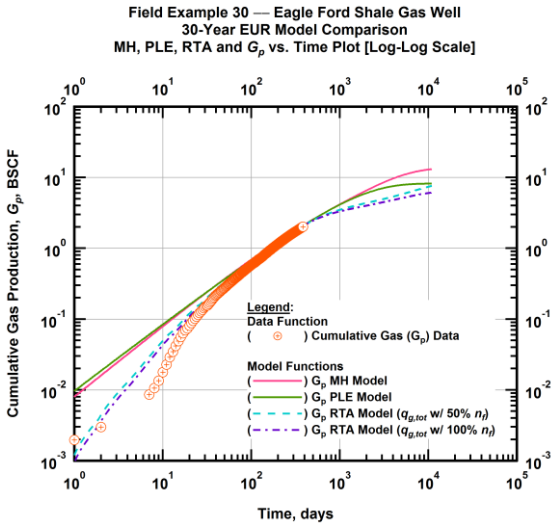

Figure A.900 — (Log-log Plot): PVT revised gas 30-year estimated cumulative production volume model comparison — Arps modified hyperbolic decline model, power-law exponential decline model, and 50 percent and 100 percent completion efficiency RTA model estimated 30-year cumulative gas production volumes and historic cumulative gas production (G_p) versus production time.

Table A.30 — 30-year estimated cumulative revised gas production (EUR), in units of BSCF, for the Arps modified hyperbolic, power-law exponential and analytical time-rate-pressure decline models.

Arps Modified Hyperbolic (BSCF)	Power-Law Exponential (BSCF)	RTA Analytical Model ($q_{g,tot}$ w/ 50% n_f) (BSCF)	RTA Analytical Model ($q_{g,tot}$ w/ 100% n_f) (BSCF)
13.36	8.09	7.70	6.15

APPENDIX B

PRESSURE TRANSIENT ANALYSIS

Field Example 7

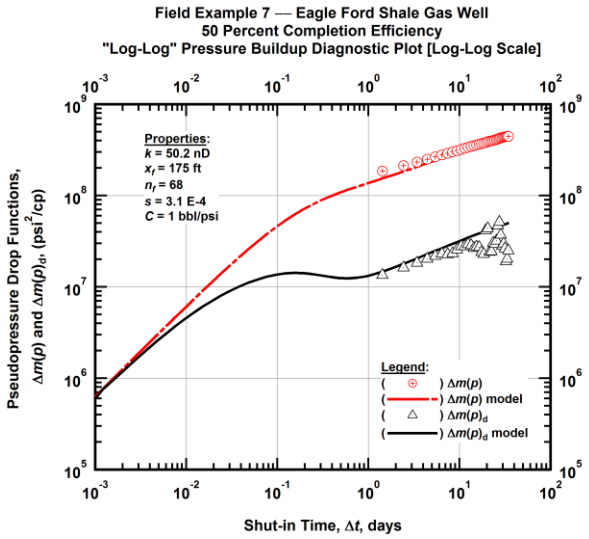

Figure B.1 — (Log-log Plot): "Log-log" pressure buildup diagnostic plot of the revised production data — pseudopressure drop ($\Delta m(p)$) and pseudopressure drop derivative ($\Delta m(p)_d$) and 50 percent completion efficiency model matches versus shut-in time (Δt).

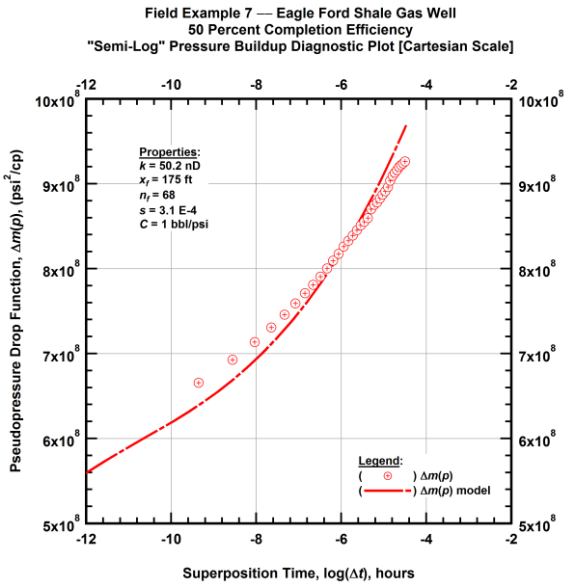

Figure B.2 — (Cartesian Plot): "Semi-log" pressure buildup diagnostic plot of the revised production data — pseudopressure drop ($\Delta m(p)$) and 50 percent completion efficiency model match versus superposition time ($\log(\Delta t)$).

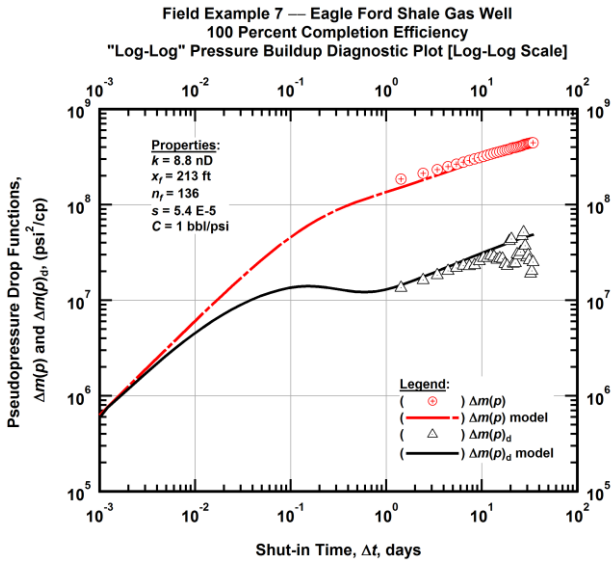

Figure B.3 — (Log-log Plot): "Log-log" pressure buildup diagnostic plot of the revised production data — pseudopressure drop ($\Delta m(p)$) and pseudopressure drop derivative ($\Delta m(p)_d$) and 100 percent completion efficiency model matches versus shut-in time (Δt).

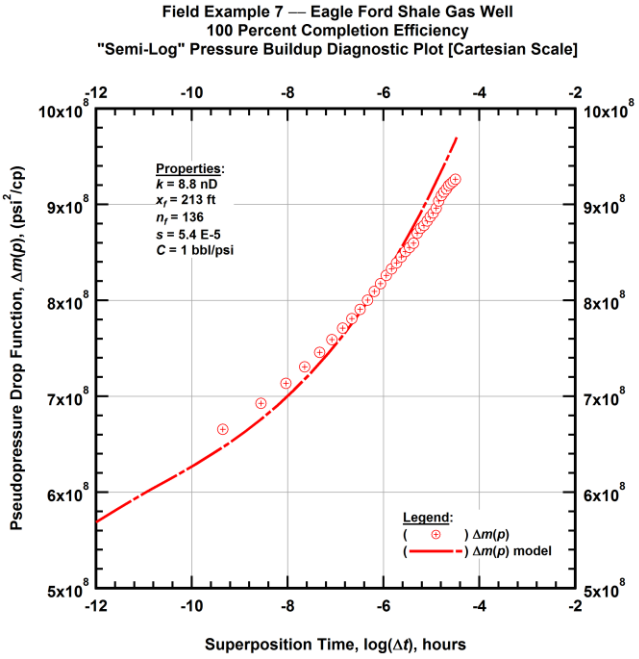

Figure B.4 — (Cartesian Plot): "Semi-log" pressure buildup diagnostic plot of the revised production data — pseudopressure drop ($\Delta m(p)$) and 100 percent completion efficiency model match versus superposition time ($\log(\Delta t)$).

Field Example 8

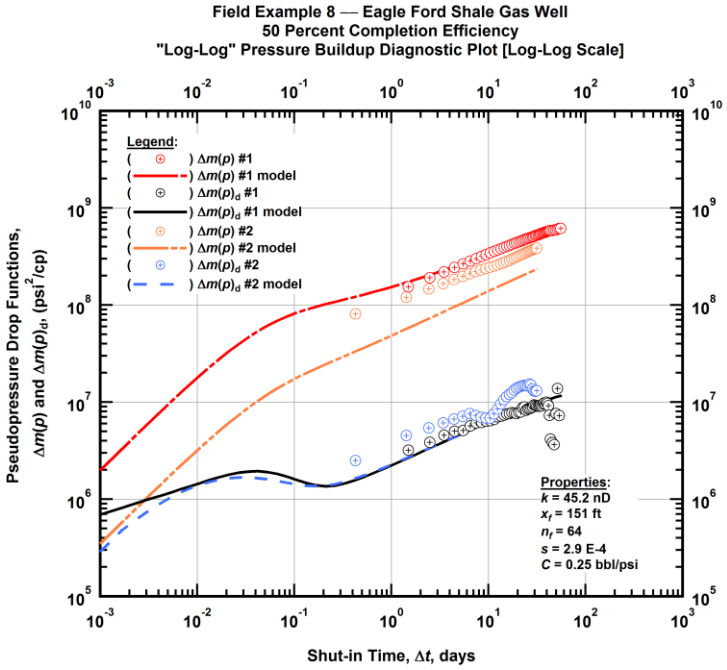

Figure B.5 — (Log-log Plot): "Log-log" pressure buildup diagnostic plot of the revised production data — pseudopressure drop ($\Delta m(p)$) and pseudopressure drop derivative ($\Delta m(p)_d$) and 50 percent completion efficiency model matches versus shut-in time (Δt).

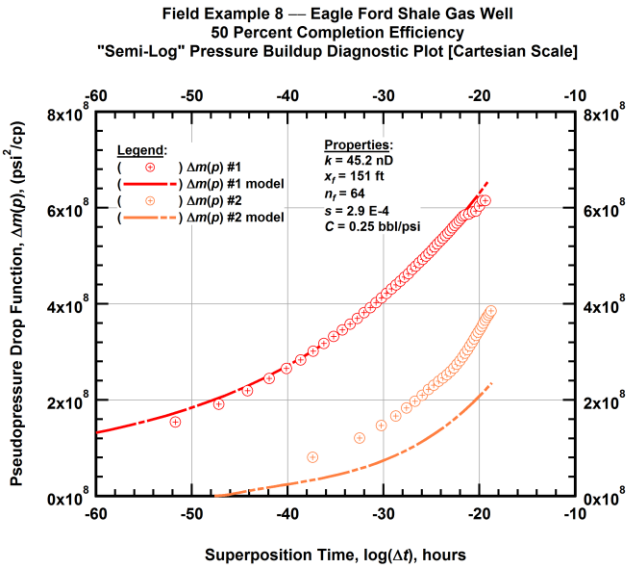

Figure B.6 — (Cartesian Plot): "Semi-log" pressure buildup diagnostic plot of the revised production data — pseudopressure drop ($\Delta m(p)$) and 50 percent completion efficiency model match versus superposition time ($\log(\Delta t)$).

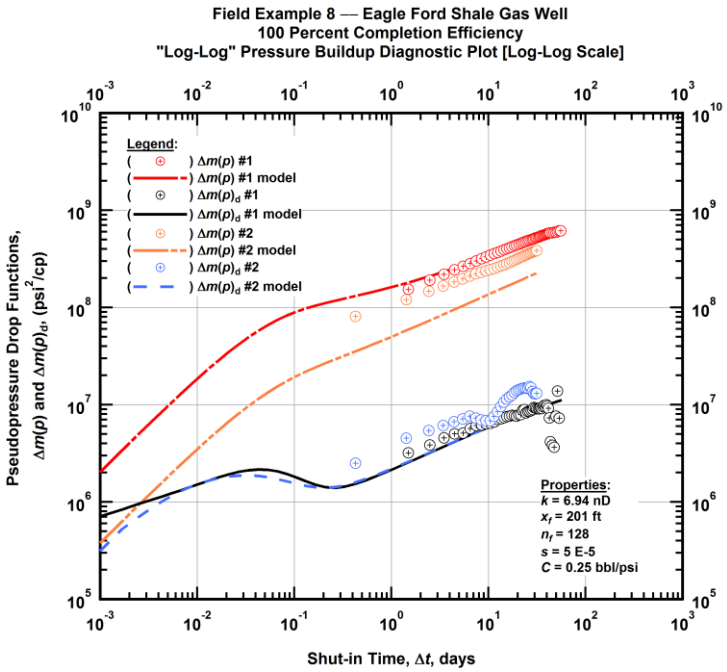

Figure B.7 — (Log-log Plot): "Log-log" pressure buildup diagnostic plot of the revised production data — pseudopressure drop ($\Delta m(p)$) and pseudopressure drop derivative ($\Delta m(p)_d$) and 100 percent completion efficiency model matches versus shut-in time (Δt).

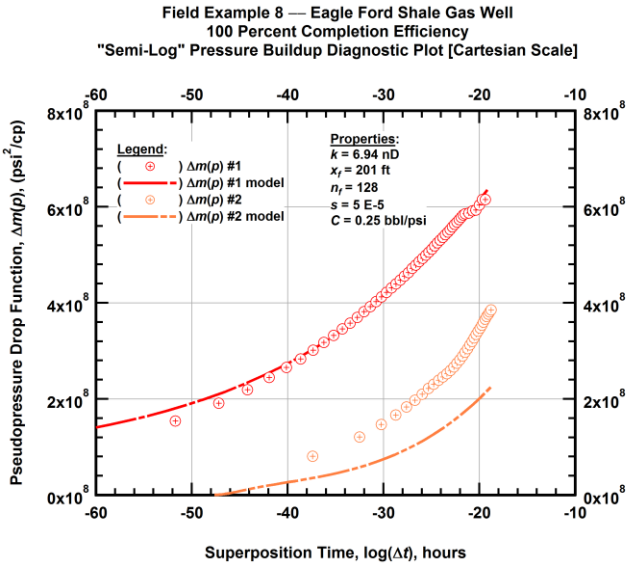

Figure B.8 — (Cartesian Plot): "Semi-log" pressure buildup diagnostic plot of the revised production data — pseudopressure drop ($\Delta m(p)$) and 100 percent completion efficiency model match versus superposition time ($\log(\Delta t)$).

Field Example 9

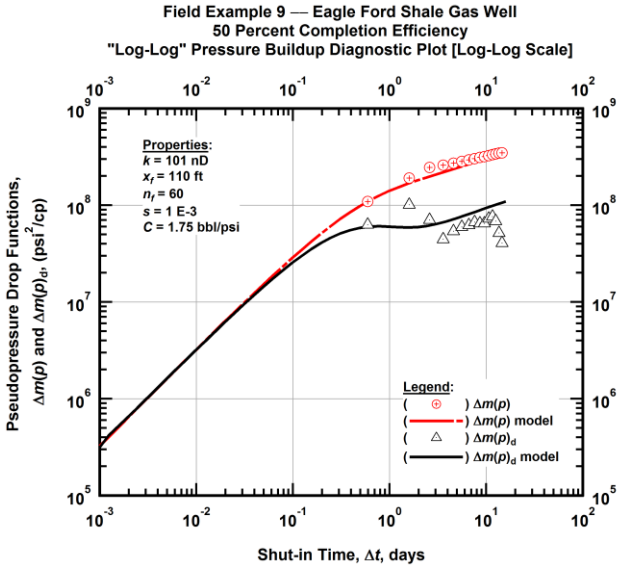

Figure B.9 — (Log-log Plot): "Log-log" pressure buildup diagnostic plot of the revised production data — pseudopressure drop ($\Delta m(p)$) and pseudopressure drop derivative ($\Delta m(p)_d$) and 50 percent completion efficiency model matches versus shut-in time (Δt).

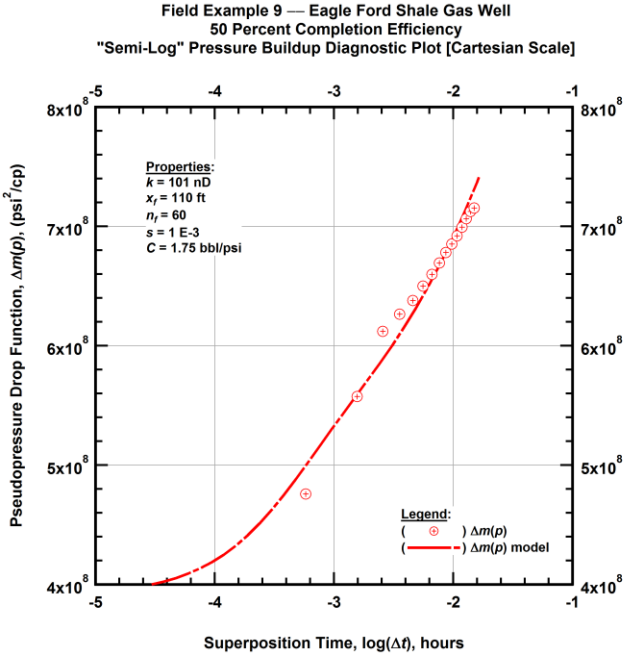

Figure B.10 — (Cartesian Plot): "Semi-log" pressure buildup diagnostic plot of the revised production data — pseudopressure drop ($\Delta m(p)$) and 50 percent completion efficiency model match versus superposition time ($\log(\Delta t)$).

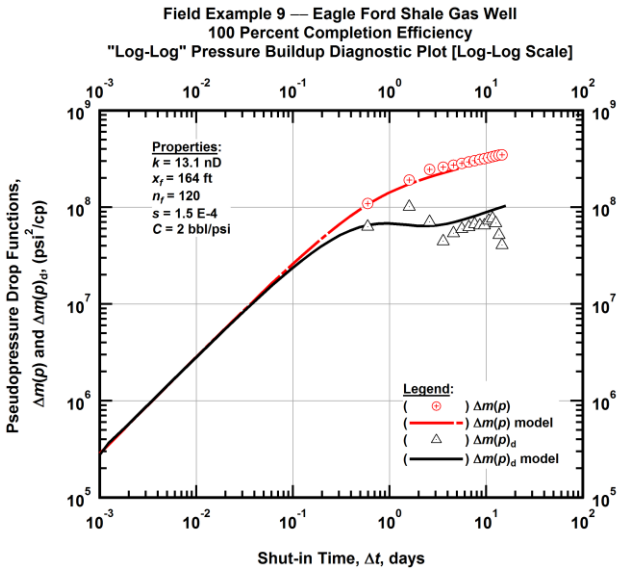

Figure B.11 — (Log-log Plot): "Log-log" pressure buildup diagnostic plot of the revised production data — pseudopressure drop ($\Delta m(p)$) and pseudopressure drop derivative ($\Delta m(p)_d$) and 100 percent completion efficiency model matches versus shut-in time (Δt).

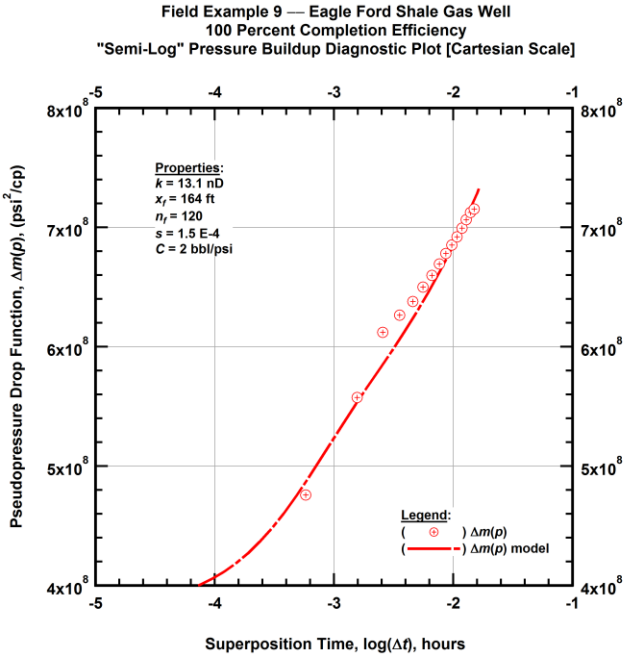

Figure B.12 — (Cartesian Plot): "Semi-log" pressure buildup diagnostic plot of the revised production data — pseudopressure drop ($\Delta m(p)$) and 100 percent completion efficiency model match versus superposition time ($\log(\Delta t)$).

Field Example 10

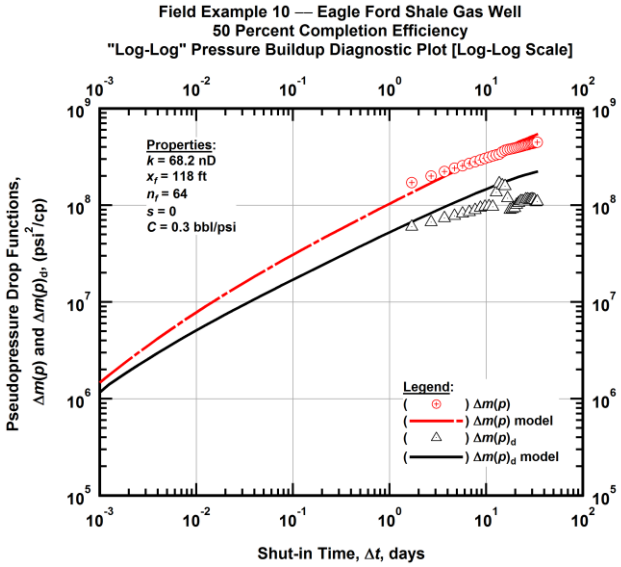

Figure B.13 — (Log-log Plot): "Log-log" pressure buildup diagnostic plot of the revised production data — pseudopressure drop ($\Delta m(p)$) and pseudopressure drop derivative ($\Delta m(p)_d$) and 50 percent completion efficiency model matches versus shut-in time (Δt).

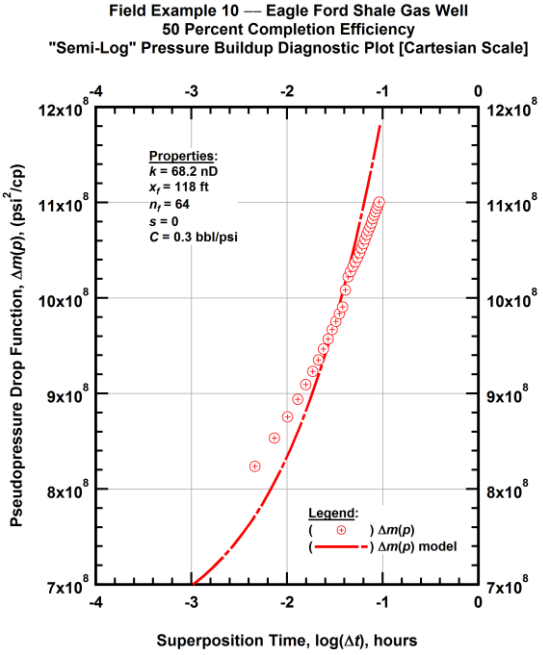

Figure B.14 — (Cartesian Plot): "Semi-log" pressure buildup diagnostic plot of the revised production data — pseudopressure drop ($\Delta m(p)$) and 50 percent completion efficiency model match versus superposition time ($\log(\Delta t)$).

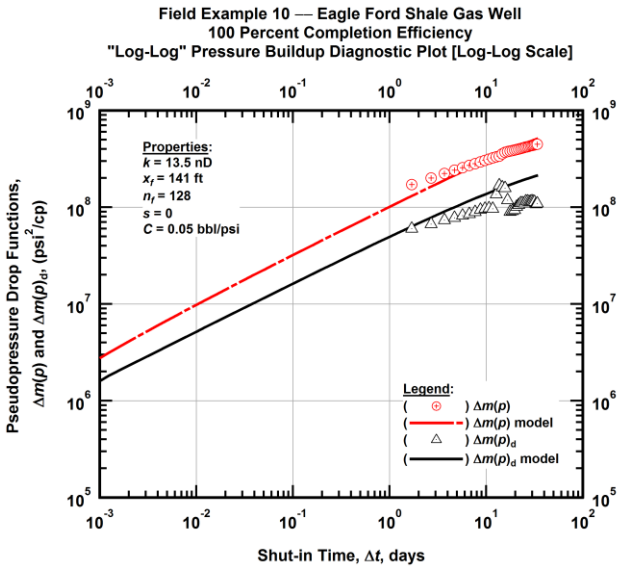

Figure B.15 — (Log-log Plot): "Log-log" pressure buildup diagnostic plot of the revised production data — pseudopressure drop ($\Delta m(p)$) and pseudopressure drop derivative ($\Delta m(p)_d$) and 100 percent completion efficiency model matches versus shut-in time (Δt).

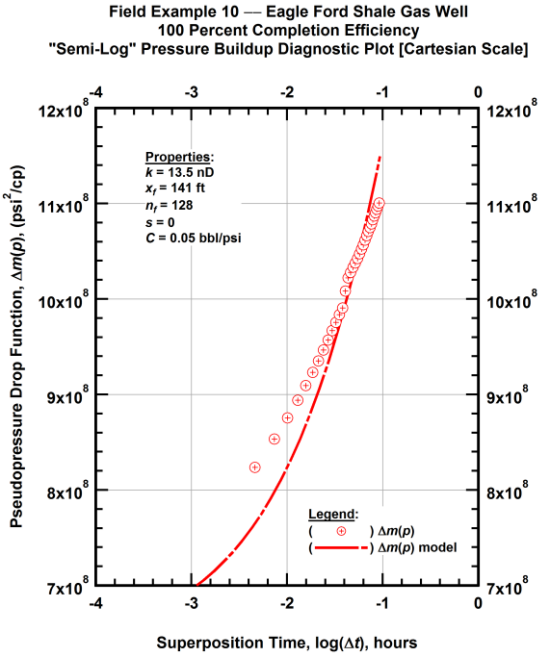

Figure B.16 — (Cartesian Plot): "Semi-log" pressure buildup diagnostic plot of the revised production data — pseudopressure drop ($\Delta m(p)$) and 100 percent completion efficiency model match versus superposition time ($\log(\Delta t)$).

Field Example 11

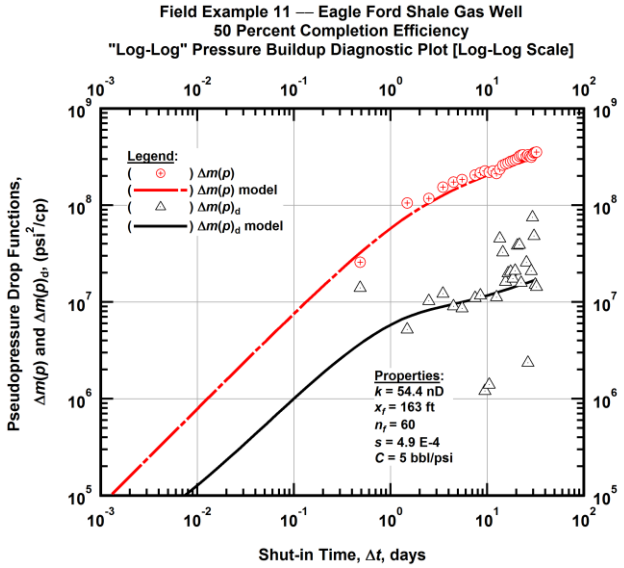

Figure B.17 — (Log-log Plot): "Log-log" pressure buildup diagnostic plot of the revised production data — pseudopressure drop ($\Delta m(p)$) and pseudopressure drop derivative ($\Delta m(p)_d$) and 50 percent completion efficiency model matches versus shut-in time (Δt).

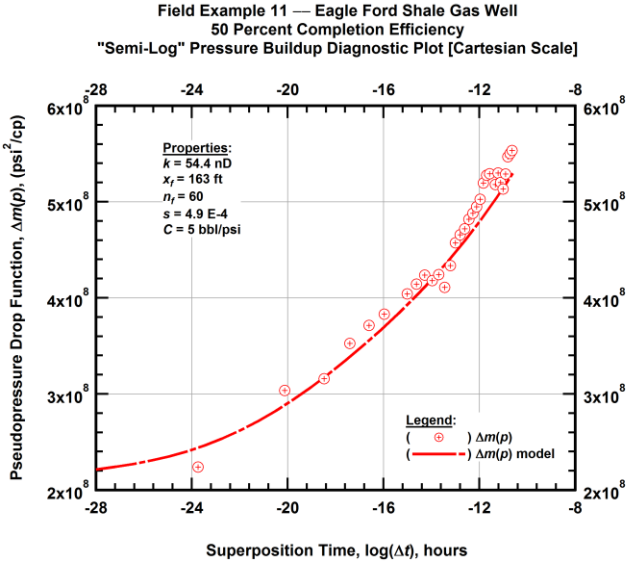

Figure B.18 — (Cartesian Plot): "Semi-log" pressure buildup diagnostic plot of the revised production data — pseudopressure drop ($\Delta m(p)$) and 50 percent completion efficiency model match versus superposition time ($\log(\Delta t)$).

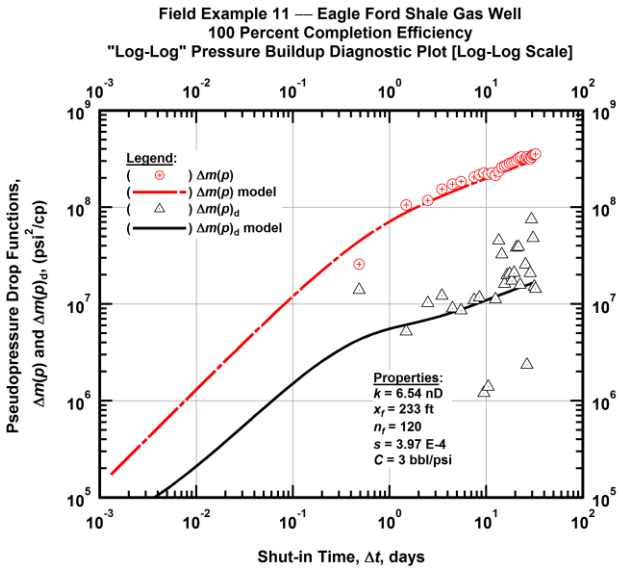

Figure B.19 — (Log-log Plot): "Log-log" pressure buildup diagnostic plot of the revised production data — pseudopressure drop ($\Delta m(p)$) and pseudopressure drop derivative ($\Delta m(p)_d$) and 100 percent completion efficiency model matches versus shut-in time (Δt).

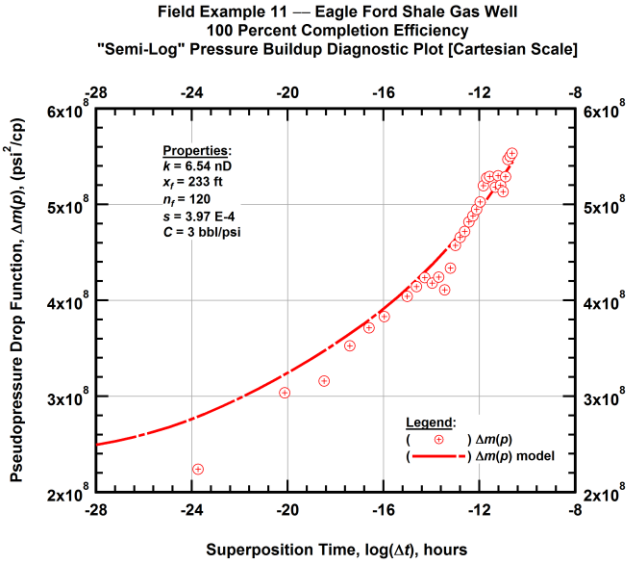

Figure B.20 — (Cartesian Plot): "Semi-log" pressure buildup diagnostic plot of the revised production data — pseudopressure drop ($\Delta m(p)$) and 100 percent completion efficiency model match versus superposition time ($\log(\Delta t)$).

Field Example 14

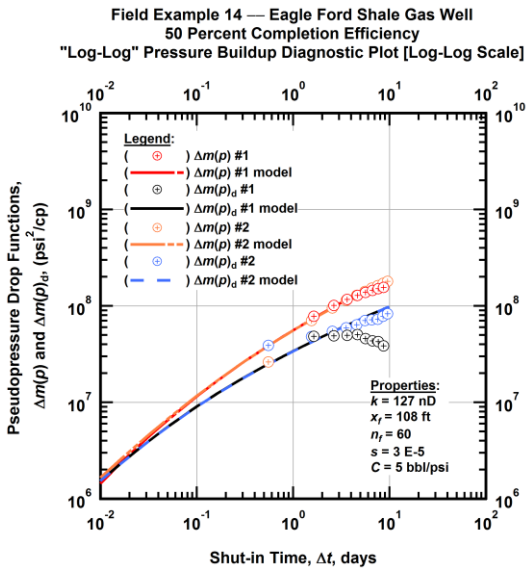

Figure B.21 — (Log-log Plot): "Log-log" pressure buildup diagnostic plot of the revised production data — pseudopressure drop ($\Delta m(p)$) and pseudopressure drop derivative ($\Delta m(p)_d$) and 50 percent completion efficiency model matches versus shut-in time (Δt).

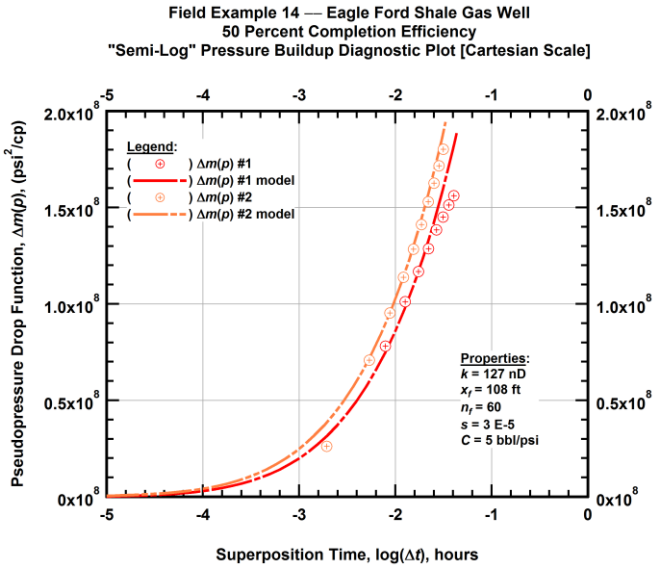

Figure B.22 — (Cartesian Plot): "Semi-log" pressure buildup diagnostic plot of the revised production data — pseudopressure drop ($\Delta m(p)$) and 50 percent completion efficiency model match versus superposition time ($\log(\Delta t)$).

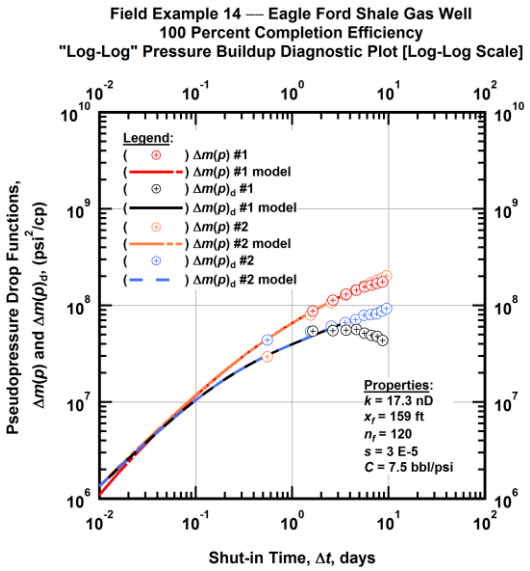

Figure B.23 — (Log-log Plot): "Log-log" pressure buildup diagnostic plot of the revised production data — pseudopressure drop ($\Delta m(p)$) and pseudopressure drop derivative ($\Delta m(p)_d$) and 100 percent completion efficiency model matches versus shut-in time (Δt).

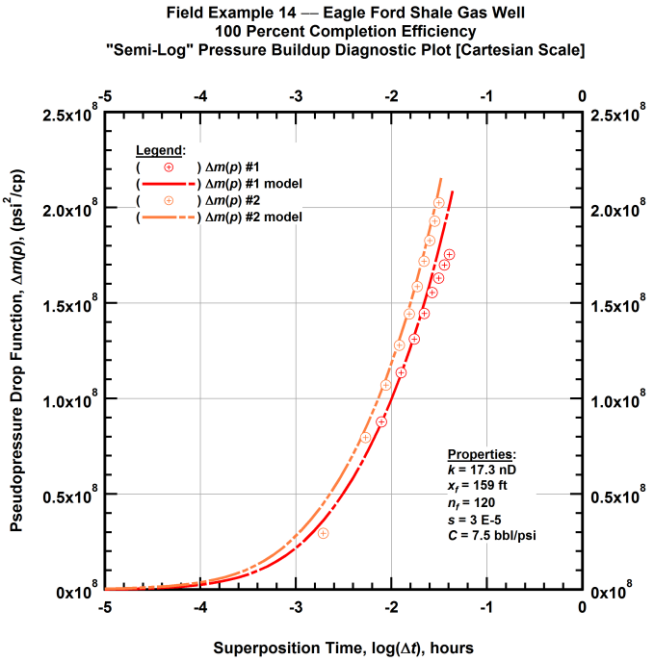

Figure B.24 — (Cartesian Plot): "Semi-log" pressure buildup diagnostic plot of the revised production data — pseudopressure drop ($\Delta m(p)$) and 100 percent completion efficiency model match versus superposition time ($\log(\Delta t)$).

Field Example 15

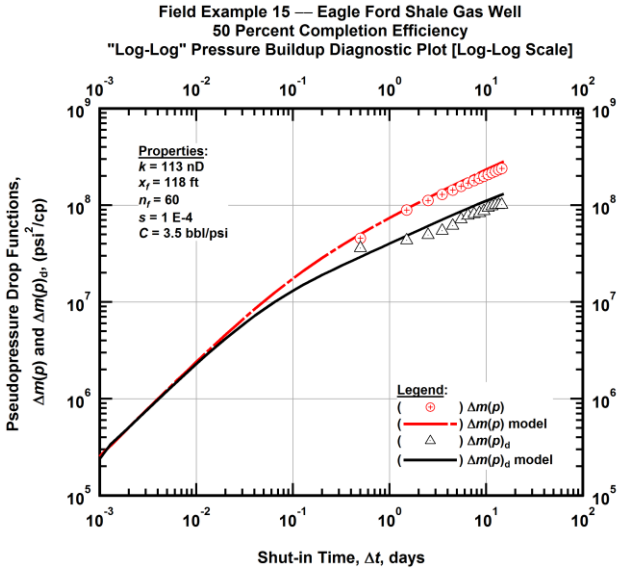

Figure B.25 — (Log-log Plot): "Log-log" pressure buildup diagnostic plot of the revised production data — pseudopressure drop ($\Delta m(p)$) and pseudopressure drop derivative ($\Delta m(p)_d$) and 50 percent completion efficiency model matches versus shut-in time (Δt).

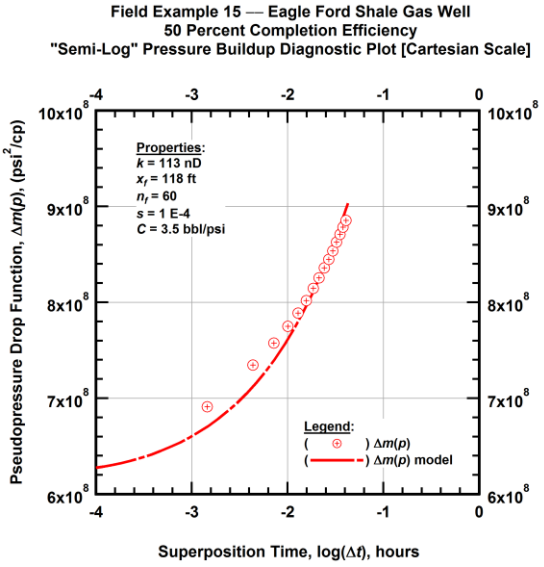

Figure B.26 — (Cartesian Plot): "Semi-log" pressure buildup diagnostic plot of the revised production data — pseudopressure drop ($\Delta m(p)$) and 50 percent completion efficiency model match versus superposition time ($\log(\Delta t)$).

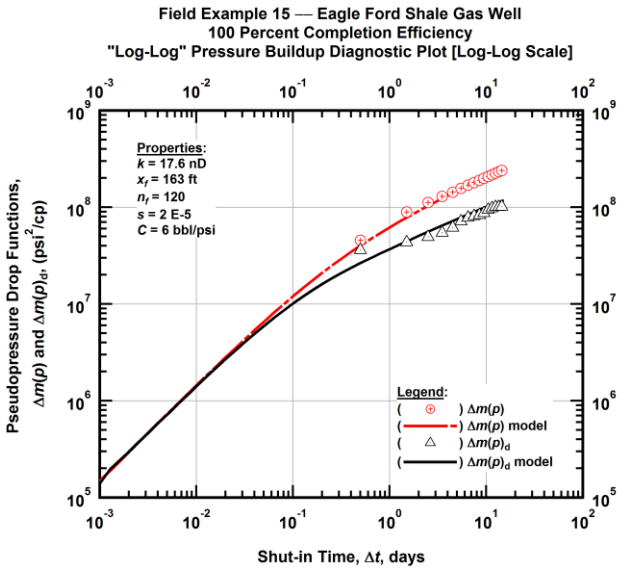

Figure B.27 — (Log-log Plot): "Log-log" pressure buildup diagnostic plot of the revised production data — pseudopressure drop ($\Delta m(p)$) and pseudopressure drop derivative ($\Delta m(p)_d$) and 100 percent completion efficiency model matches versus shut-in time (Δt).

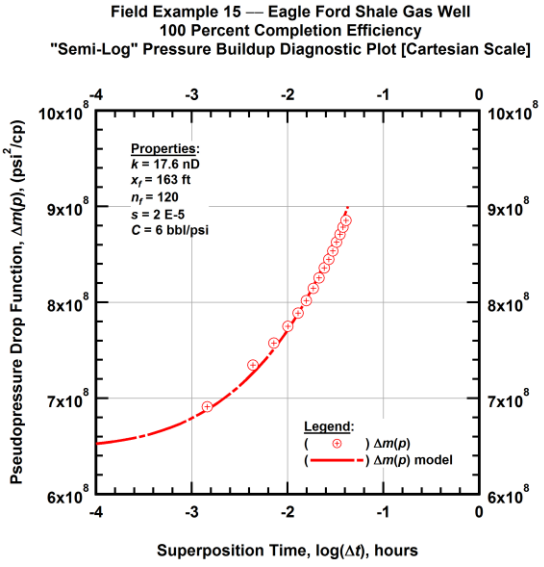

Figure B.28 — (Cartesian Plot): "Semi-log" pressure buildup diagnostic plot of the revised production data — pseudopressure drop ($\Delta m(p)$) and 100 percent completion efficiency model match versus superposition time ($\log(\Delta t)$).

Field Example 16

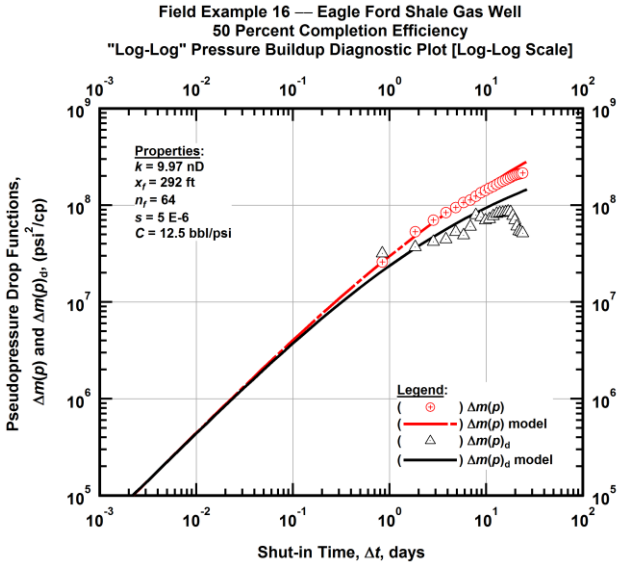

Figure B.29 — (Log-log Plot): "Log-log" pressure buildup diagnostic plot of the revised production data — pseudopressure drop ($\Delta m(p)$) and pseudopressure drop derivative ($\Delta m(p)_d$) and 50 percent completion efficiency model matches versus shut-in time (Δt).

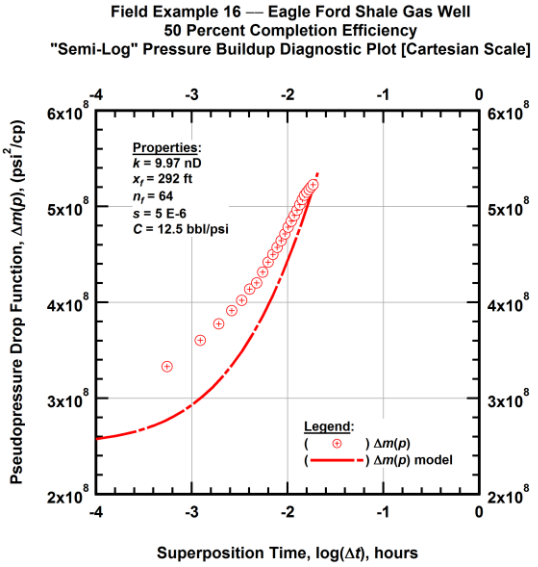

Figure B.30 — (Cartesian Plot): "Semi-log" pressure buildup diagnostic plot of the revised production data — pseudopressure drop ($\Delta m(p)$) and 50 percent completion efficiency model match versus superposition time ($\log(\Delta t)$).

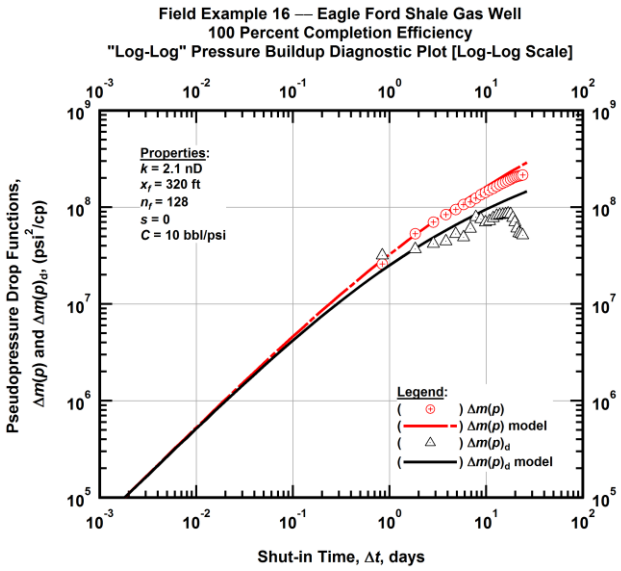

Figure B.31 — (Log-log Plot): "Log-log" pressure buildup diagnostic plot of the revised production data — pseudopressure drop ($\Delta m(p)$) and pseudopressure drop derivative ($\Delta m(p)_d$) and 100 percent completion efficiency model matches versus shut-in time (Δt).

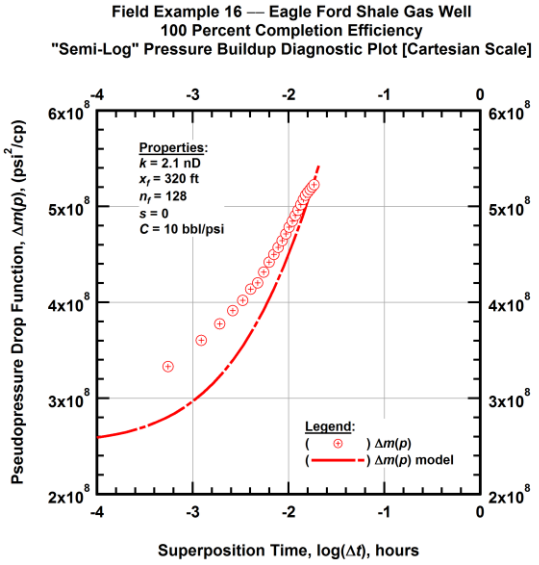

Figure B.32 — (Cartesian Plot): "Semi-log" pressure buildup diagnostic plot of the revised production data — pseudopressure drop ($\Delta m(p)$) and 100 percent completion efficiency model match versus superposition time ($\log(\Delta t)$).

Field Example 17

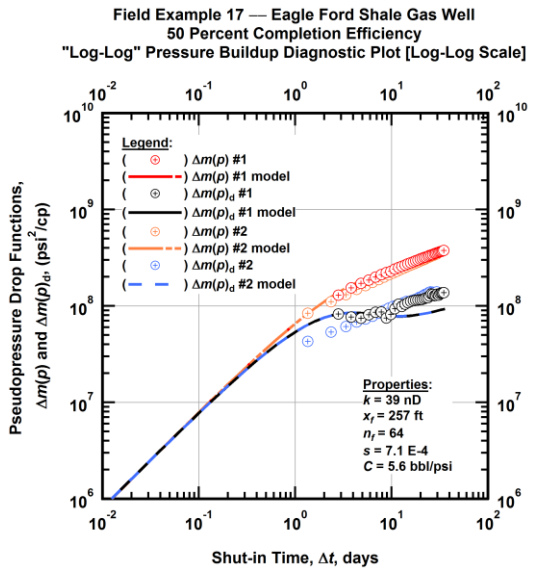

Figure B.33 — (Log-log Plot): "Log-log" pressure buildup diagnostic plot of the revised production data — pseudopressure drop ($\Delta m(p)$) and pseudopressure drop derivative ($\Delta m(p)_d$) and 50 percent completion efficiency model matches versus shut-in time (Δt).

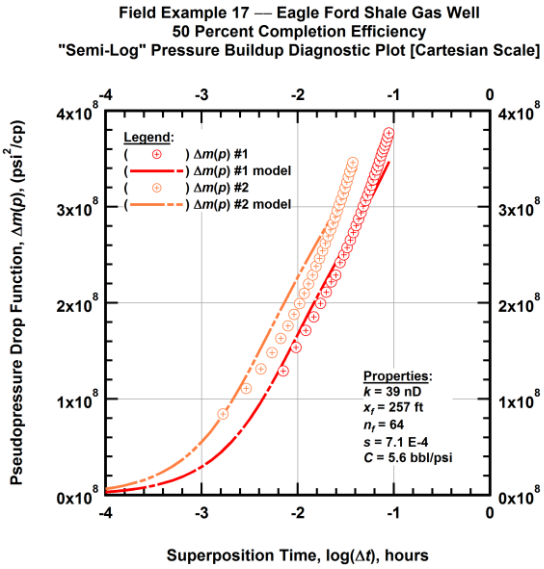

Figure B.34 — (Cartesian Plot): "Semi-log" pressure buildup diagnostic plot of the revised production data — pseudopressure drop ($\Delta m(p)$) and 50 percent completion efficiency model match versus superposition time ($\log(\Delta t)$).

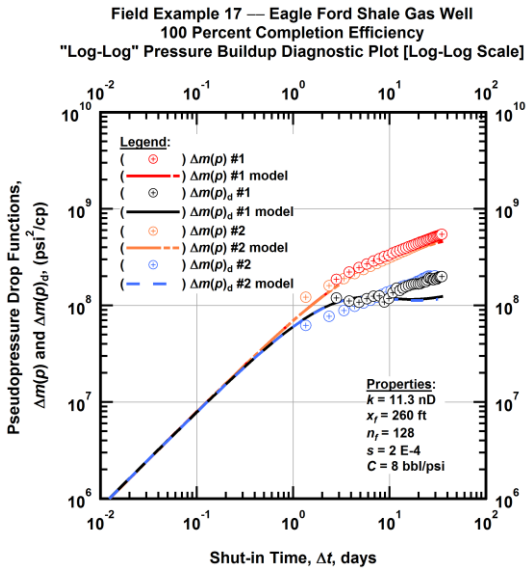

Figure B.35 — (Log-log Plot): "Log-log" pressure buildup diagnostic plot of the revised production data — pseudopressure drop ($\Delta m(p)$) and pseudopressure drop derivative ($\Delta m(p)_d$) and 100 percent completion efficiency model matches versus shut-in time (Δt).

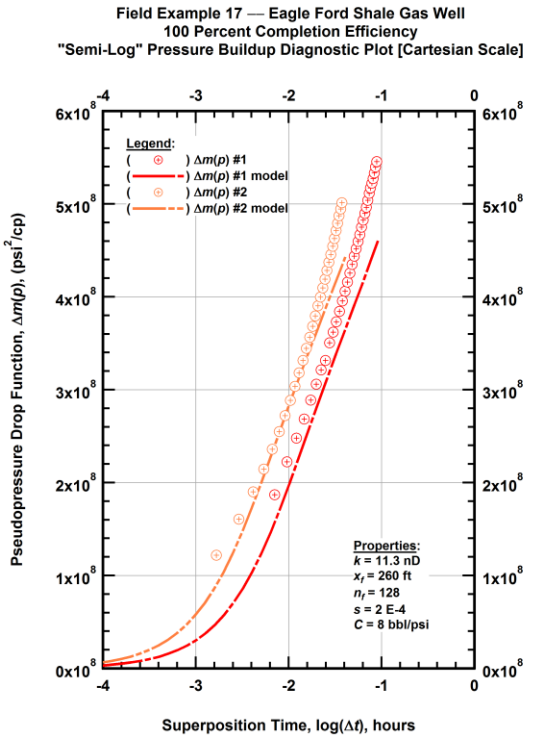

Figure B.36 — (Cartesian Plot): "Semi-log" pressure buildup diagnostic plot of the revised production data — pseudopressure drop ($\Delta m(p)$) and 100 percent completion efficiency model match versus superposition time ($\log(\Delta t)$).

Field Example 18

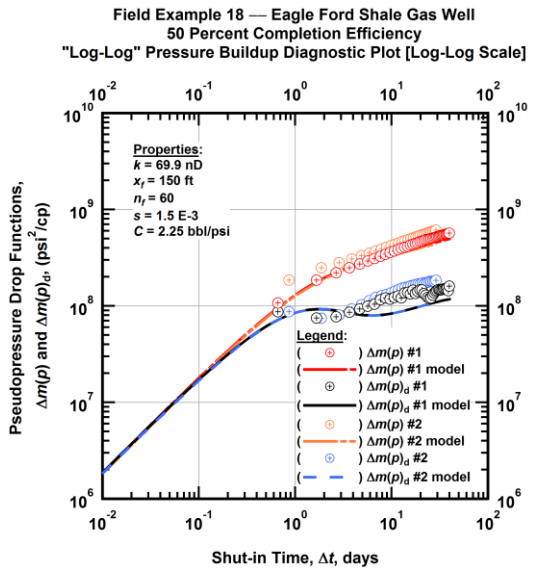

Figure B.37 — (Log-log Plot): "Log-log" pressure buildup diagnostic plot of the revised production data — pseudopressure drop ($\Delta m(p)$) and pseudopressure drop derivative ($\Delta m(p)_d$) and 50 percent completion efficiency model matches versus shut-in time (Δt).

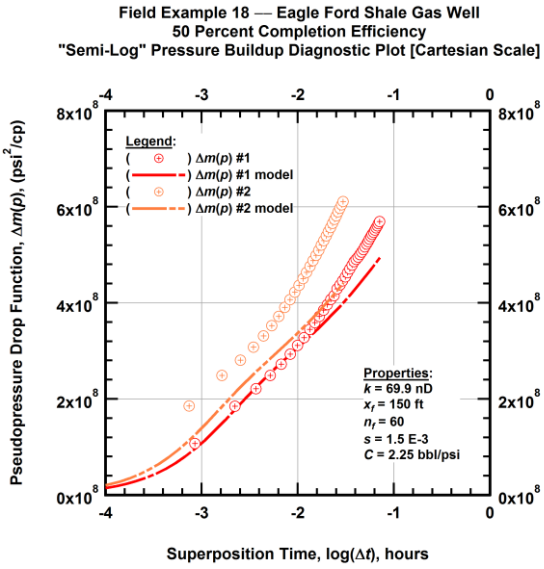

Figure B.38 — (Cartesian Plot): "Semi-log" pressure buildup diagnostic plot of the revised production data — pseudopressure drop ($\Delta m(p)$) and 50 percent completion efficiency model match versus superposition time ($\log(\Delta t)$).

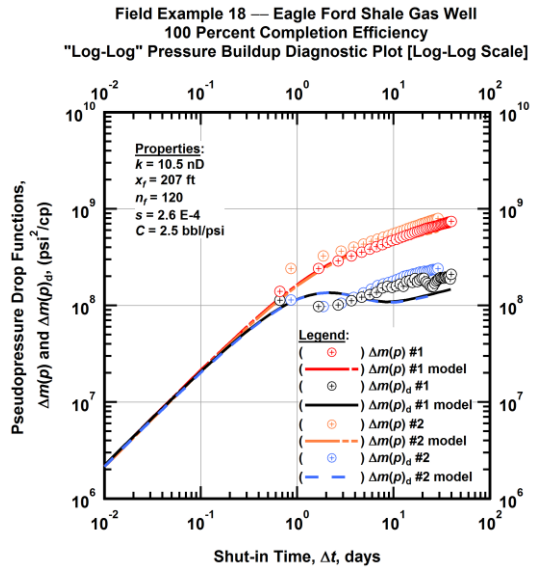

Figure B.39 — (Log-log Plot): "Log-log" pressure buildup diagnostic plot of the revised production data — pseudopressure drop ($\Delta m(p)$) and pseudopressure drop derivative ($\Delta m(p)_d$) and 100 percent completion efficiency model matches versus shut-in time (Δt).

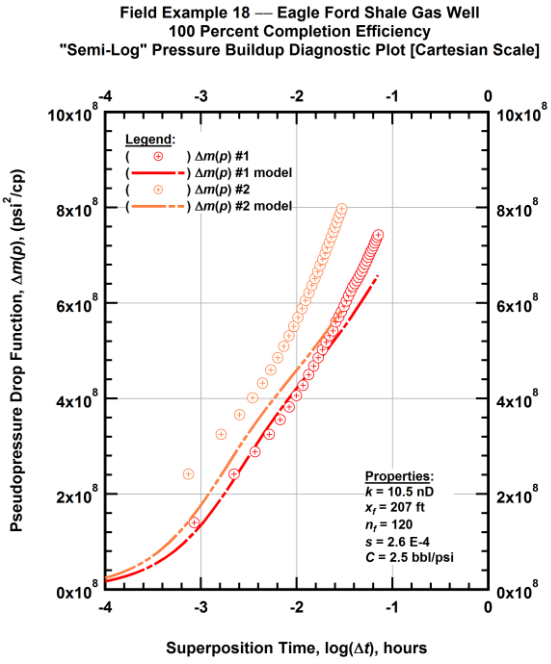

Figure B.40 — (Cartesian Plot): "Semi-log" pressure buildup diagnostic plot of the revised production data — pseudopressure drop ($\Delta m(p)$) and 100 percent completion efficiency model match versus superposition time ($\log(\Delta t)$).

Field Example 19

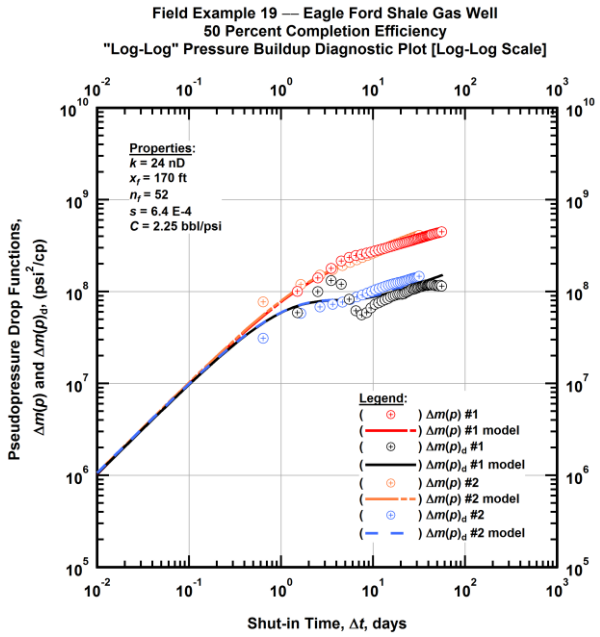

Figure B.41 — (Log-log Plot): "Log-log" pressure buildup diagnostic plot of the revised production data — pseudopressure drop ($\Delta m(p)$) and pseudopressure drop derivative ($\Delta m(p)_d$) and 50 percent completion efficiency model matches versus shut-in time (Δt).

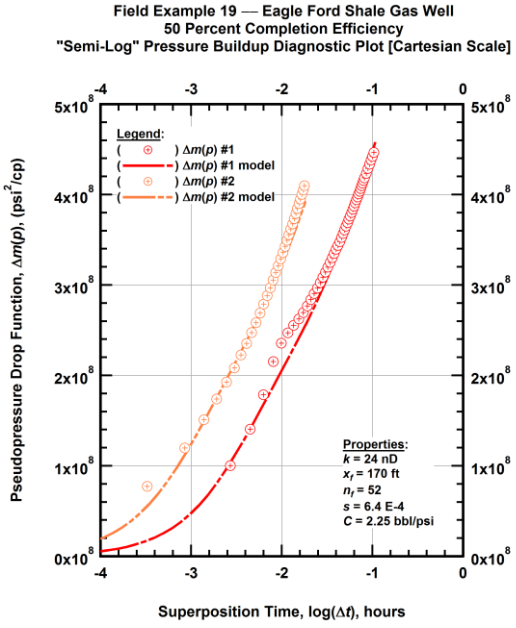

Figure B.42 — (Cartesian Plot): "Semi-log" pressure buildup diagnostic plot of the revised production data — pseudopressure drop ($\Delta m(p)$) and 50 percent completion efficiency model match versus superposition time ($\log(\Delta t)$).

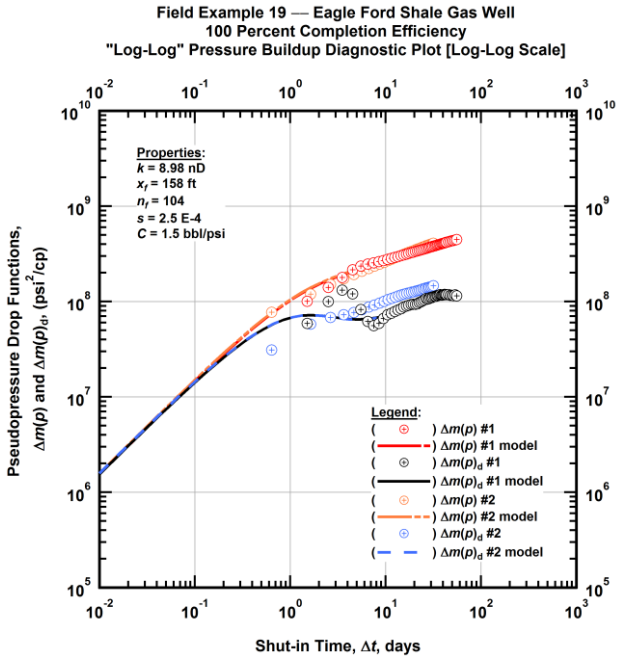

Figure B.43 — (Log-log Plot): "Log-log" pressure buildup diagnostic plot of the revised production data — pseudopressure drop ($\Delta m(p)$) and pseudopressure drop derivative ($\Delta m(p)_d$) and 100 percent completion efficiency model matches versus shut-in time (Δt).

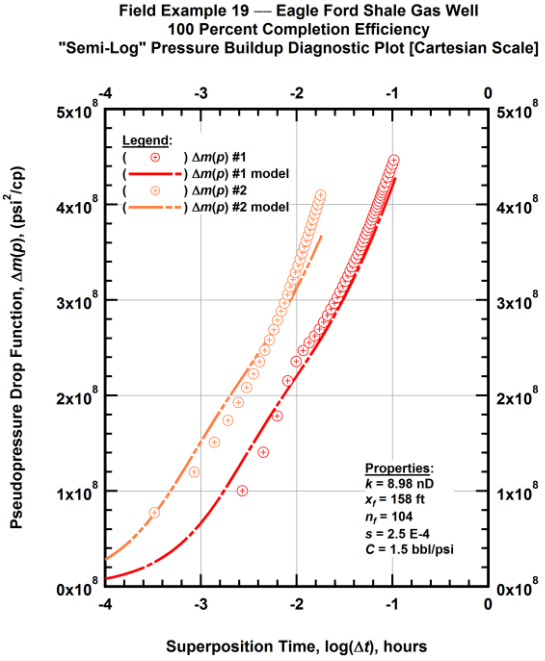

Figure B.44 — (Cartesian Plot): "Semi-log" pressure buildup diagnostic plot of the revised production data — pseudopressure drop ($\Delta m(p)$) and 100 percent completion efficiency model match versus superposition time ($\log(\Delta t)$).

Field Example 21

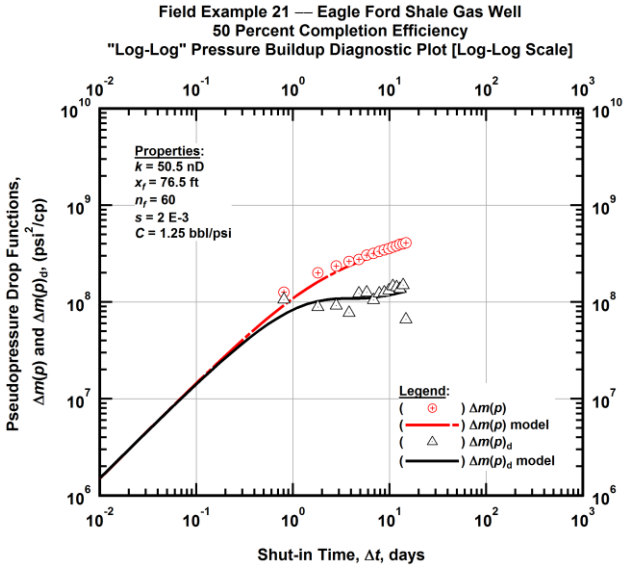

Figure B.45 — (Log-log Plot): "Log-log" pressure buildup diagnostic plot of the revised production data — pseudopressure drop ($\Delta m(p)$) and pseudopressure drop derivative ($\Delta m(p)_d$) and 50 percent completion efficiency model matches versus shut-in time (Δt).

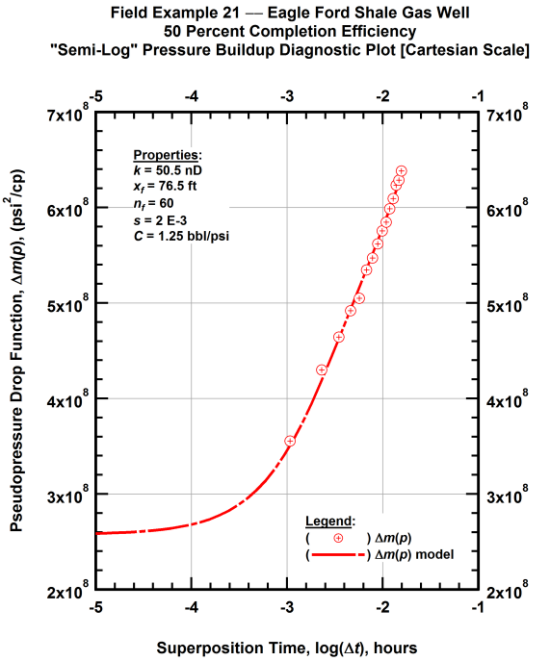

Figure B.46 — (Cartesian Plot): "Semi-log" pressure buildup diagnostic plot of the revised production data — pseudopressure drop ($\Delta m(p)$) and 50 percent completion efficiency model match versus superposition time ($\log(\Delta t)$).

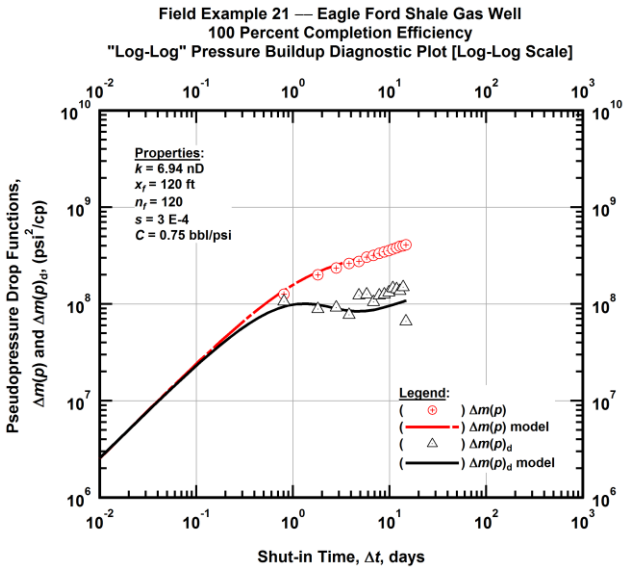

Figure B.47 — (Log-log Plot): "Log-log" pressure buildup diagnostic plot of the revised production data — pseudopressure drop ($\Delta m(p)$) and pseudopressure drop derivative ($\Delta m(p)_d$) and 100 percent completion efficiency model matches versus shut-in time (Δt).

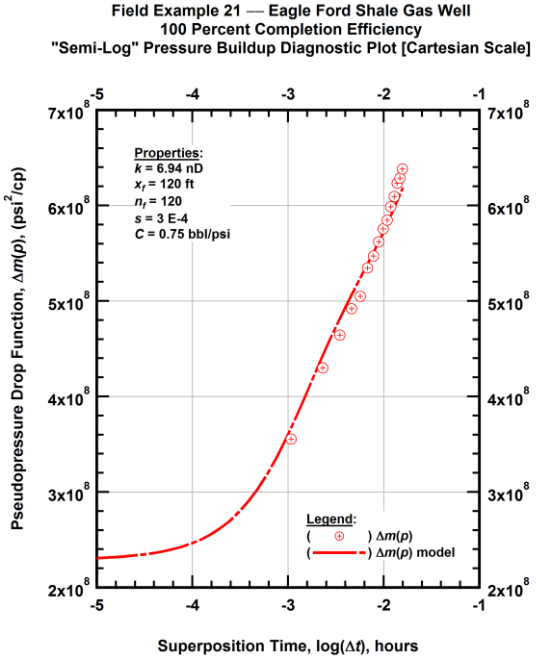

Figure B.48 — (Cartesian Plot): "Semi-log" pressure buildup diagnostic plot of the revised production data — pseudopressure drop ($\Delta m(p)$) and 100 percent completion efficiency model match versus superposition time ($\log(\Delta t)$).